ΔΕΛΤΙΟ ΤΗΣ ΕΛΛΗΝΙΚΗΣ ΓΕΩΛΟΓΙΚΗΣ ΕΤΑΙΡΙΑΣ
Τόμος XLIII, *No* 1

BULLETIN OF THE GEOLOGICAL SOCIETY OF GREECE
Volume XLIII, *No* 1

ΕΙΚΟΝΑ ΕΞΩΦΥΛΛΟΥ - COVER PAGE

Γενική άποψη της γέφυρας Ρίου-Αντιρρίου. Οι πυλώνες της γέφυρας διασκοπήθηκαν γεωφυσικά με χρήση ηχοβολιστή πλευρικής σάρωσης (EG&G 4100P και EG&G 272TD) με σκοπό την αποτύπωση του πυθμένα στην περιοχή του έργου, όσο και των βάθρων των πυλώνων. (Εργαστήριο Θαλάσσιας Γεωλογίας & Φυσικής Ωκεανογραφίας, Πανεπιστήμιο Πατρών. Συλλογή και επεξεργασία: Δ.Χριστοδούλου, Η. Φακίρης).

General view of the Rion-Antirion bridge, from a marine geophysical survey conducted by side scan sonar (EG&G 4100P and EG&G 272TD) in order to map the seafloor at the site of the construction (pylons and piers) (Gallery of the Laboratory of Marine Geology and Physical Oceanography, University of Patras. Data acquisition and Processing: D. Christodoulou, E. Fakiris).

ΔΕΛΤΙΟ ΤΗΣ ΕΛΛΗΝΙΚΗΣ ΓΕΩΛΟΓΙΚΗΣ ΕΤΑΙΡΙΑΣ
Τόμος XLIII, *No* 1

BULLETIN OF THE GEOLOGICAL SOCIETY OF GREECE
Volume XLIII, *No* 1

12ο ΔΙΕΘΝΕΣ ΣΥΝΕΔΡΙΟ
ΤΗΣ ΕΛΛΗΝΙΚΗΣ ΓΕΩΛΟΓΙΚΗΣ ΕΤΑΙΡΙΑΣ

ΠΛΑΝΗΤΗΣ ΓΗ:
Γεωλογικές Διεργασίες και Βιώσιμη Ανάπτυξη

12th INTERNATIONAL CONGRESS
OF THE GEOLOGICAL SOCIETY OF GREECE

PLANET EARTH:
Geological Processes and Sustainable Development

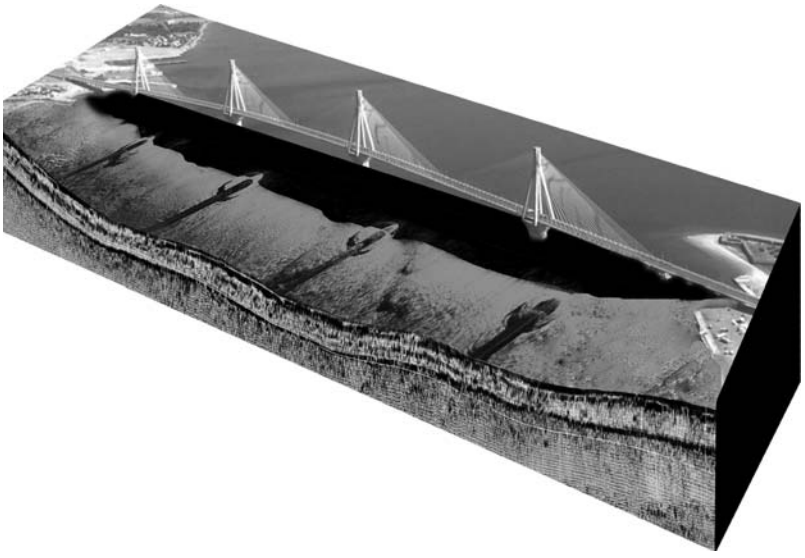

ΠΑΤΡΑ / PATRAS 2010

ISSN 0438-9557

12ο ΔΙΕΘΝΕΣ ΣΥΝΕΔΡΙΟ
ΤΗΣ ΕΛΛΗΝΙΚΗΣ ΓΕΩΛΟΓΙΚΗΣ ΕΤΑΙΡΙΑΣ

ΠΛΑΝΗΤΗΣ ΓΗ:
Γεωλογικές Διεργασίες και Βιώσιμη Ανάπτυξη

Υπό την Αιγίδα του
Υπουργείου Περιβάλλοντος, Ενέργειας και Κλιματικής Αλλαγής

12th INTERNATIONAL CONGRESS
OF THE GEOLOGICAL SOCIETY OF GREECE

PLANET EARTH:
Geological Processes and Sustainable Development

Under the Aegis of the
Ministry of Environment, Energy and Climate Change

ΠΡΑΚΤΙΚΑ / PROCEEDINGS

ΕΠΙΜΕΛΕΙΑ ΕΚΔΟΣΗΣ

Γ. ΚΟΥΚΗΣ
Πανεπιστήμιο Πατρών

Α. ΖΕΛΗΛΙΔΗΣ
Πανεπιστήμιο Πατρών

Ι. ΚΟΥΚΟΥΒΕΛΑΣ
Πανεπιστήμιο Πατρών

Γ. ΠΑΠΑΘΕΟΔΩΡΟΥ
Πανεπιστήμιο Πατρών

Μ. ΓΕΡΑΓΑ
Πανεπιστήμιο Πατρών

Β. ΖΥΓΟΥΡΗ
Πανεπιστήμιο Πατρών

EDITORS

G. KOUKIS
University of Patras

A. ZELILIDIS
University of Patras

I. KOUKOUVELAS
University of Patras

G. PAPATHEODOROU
University of Patras

M. GERAGA
University of Patras

V. ZYGOURI
University of Patras

PATRAS, May 2010

ΕΛΛΗΝΙΚΗ ΓΕΩΛΟΓΙΚΗ ΕΤΑΙΡΕΙΑ

ΔΙΟΙΚΗΤΙΚΟ ΣΥΜΒΟΥΛΙΟ

(που εξελέγη στη Γενική Συνέλευση των μελών της Εταιρίας το Μάρτιο του 2010)

ΠΡΟΕΔΡΟΣ
Απόστολος ΑΛΕΞΟΠΟΥΛΟΣ

ΑΝΤΙΠΡΟΕΔΡΟΣ
Αλεξάνδρα ΖΑΜΠΕΤΑΚΗ-ΛΕΚΚΑ

ΓΕΝ. ΓΡΑΜΜΑΤΕΑΣ
Ευγενία ΜΩΡΑΪΤΗ

ΕΙΔ. ΓΡΑΜΜΑΤΕΑΣ
Δημήτριος ΓΑΛΑΝΑΚΗΣ

ΤΑΜΙΑΣ
Ασημίνα ΑΝΤΩΝΑΡΑΚΟΥ

ΕΦΟΡΟΣ
Χαράλαμπος ΚΡΑΝΗΣ

ΜΕΛΗ
Κωνσταντίνος ΒΟΥΔΟΥΡΗΣ
Χρυσάνθη ΙΩΑΚΕΙΜ
Αθανάσιος ΓΚΑΝΑΣ

GEOLOGICAL SOCIETY OF GREECE

BOARD OF DIRECTORS

(elected at the General Assembly of the members of the Society on March 2010)

PRESIDENT
Apostolos ALEXOPOULOS

VICE-PRESIDENT
Alexandra ZAMBETAKIS-LEKKAS

GENERAL SECRETARY
Evgenia MORAITI

EXECUTIVE SECRETARY
Dimitrios GALANAKIS

TREASURER
Asimina ANTONARAKOU

TRUSTEE
Charalambos KRANIS

MEMBERS
Konstantinos VOUDOURIS
Chyssanthi IOAKIM
Athanasios GANAS

ΟΡΓΑΝΩΤΙΚΗ ΕΠΙΤΡΟΠΗ 12ου ΔΙΕΘΝΟΥΣ ΣΥΝΕΔΡΙΟΥ

ΠΡΟΕΔΡΟΣ
Γεώργιος ΚΟΥΚΗΣ, Καθηγητής Πανεπιστημίου Πατρών

ΑΝΤΙΠΡΟΕΔΡΟΣ
Αβραάμ ΖΕΛΗΛΙΔΗΣ, Καθηγητής Πανεπιστημίου Πατρών

ΓΕΝΙΚΟΣ ΓΡΑΜΜΑΤΕΑΣ
Ιωάννης ΚΟΥΚΟΥΒΕΛΑΣ, Αν. Καθηγητής Πανεπιστημίου Πατρών

ΕΙΔΙΚΟΣ ΓΡΑΜΜΑΤΕΑΣ
Γεώργιος ΠΑΠΑΘΕΟΔΩΡΟΥ, Αν. Καθηγητής Πανεπιστημίου Πατρών

ΤΑΜΙΑΣ
Μαρία ΓΕΡΑΓΑ, Λέκτορας Πανεπιστημίου Πατρών

ΜΕΛΗ

Νικόλαος ΚΟΝΤΟΠΟΥΛΟΣ, Καθηγητής Πανεπιστημίου Πατρών

Νικόλαος ΛΑΜΠΡΑΚΗΣ, Καθηγητής Πανεπιστημίου Πατρών

Νικόλαος ΣΑΜΠΑΤΑΚΑΚΗΣ, Αν. Καθηγητής Πανεπιστημίου Πατρών

Ευθύμιος ΣΩΚΟΣ, Επ. Καθηγητής Πανεπιστημίου Πατρών

Δημήτριος ΠΑΠΟΥΛΗΣ, Λέκτορας Πανεπιστημίου Πατρών

Μιχαήλ ΣΤΑΜΑΤΑΚΗΣ, Καθηγητής Εθνικού και Καποδιστριακού Πανεπιστημίου Αθηνών

Απόστολος ΑΛΕΞΟΠΟΥΛΟΣ, Καθηγητής Εθνικού και Καποδιστριακού Πανεπιστημίου Αθηνών, Πρόεδρος Ε.Γ.Ε.

Κωνσταντίνος ΠΑΠΑΒΑΣΙΛΕΙΟΥ, Αν. Καθηγητής Εθνικού και Καποδιστριακού Πανεπιστημίου Αθηνών, Γενικός Δ/ντής Ι.Γ.Μ.Ε.

Κωνσταντίνος ΜΑΚΡΟΠΟΥΛΟΣ, Καθηγητής Εθνικού και Καποδιστριακού Πανεπιστημίου Αθηνών, Δ/ντής Γεωδυναμικού Ινστιτούτου Ε.Α.Α.

Εμμανουήλ ΜΑΝΟΥΤΣΟΓΛΟΥ, Αν. Καθηγητής Πολυτεχνείου Κρήτης

Σπυρίδων ΠΑΥΛΙΔΗΣ, Καθηγητής Αριστοτελείου Πανεπιστημίου Θεσσαλονίκης

Κωνσταντίνος ΠΑΠΑΚΩΝΣΤΑΝΤΙΝΟΥ, Πρόεδρος ΕΛ.ΚΕ.Θ.Ε.

Γραμματεία Συνεδρίου
Συνέδρα
Ηρ. Πολυτεχνείου 92, 26442 Πάτρα • Τηλ.: 2610 432.200 • Fax: 2610 430.884
URL: www.synedra.gr • E-mail: synedra@synedra.gr

ORGANIZING COMMITTEE OF THE 12th INTERNATIONAL CONGRESS

PRESIDENT
George KOUKIS, Professor, University of Patras

VICE-PRESIDENT
Abraham ZELILIDIS, Professor, University of Patras

GENERAL SECRETARY
Ioannis KOUKOUVELAS, Assoc. Professor, University of Patras

EXECUTIVE SECRETARY
George PAPATHEODOROU, Assoc. Professor, University of Patras

TREASURER
Maria GERAGA, Lecturer, University of Patras

MEMBERS

Nikolaos KONTOPOULOS, Professor, University of Patras

Nikolaos LAMBRAKIS, Professor, University of Patras

Nikolaos SABATAKAKIS, Assoc. Professor, University of Patras

Eythimios SOKOS, Assist. Professor, University of Patras

Dimitrios PAPOULIS, Lecturer, University of Patras

Michael STAMATAKIS, Professor, National and Kapodistrian University of Athens

Apostolos ALEXOPOULOS, Professor, National and Kapodistrian University of Athens. President of G.S.G.

Constantinos PAPAVASSILEIOU, Assoc. Professor, National and Kapodistrian University of Athens, Gen. Director of I.G.M.E.

Konstantinos MAKROPOULOS, Professor, National and Kapodistrian University of Athens, Director of Institute of Geodynamics, N.O.A.

Emmanouil MANOUTSOGLOU, Assoc. Professor, Technical University of Crete

Spyridon PAVLIDES, Professor, Aristotle University of Thessaloniki

Konstantinos PAPACONSTANTINOU, President of H.C.M.R.

Congress Secretariat

Synedra

Iroon Polytechneiou 92, GR 26442 Patras • Ph.: +302610 432.200 • Fax: +302610 430.884
URL: www.synedra.gr • E-mail: synedra@synedra.gr

ΧΟΡΗΓΟΙ
ΤΟΥ 12ου ΔΙΕΘΝΟΥΣ ΣΥΝΕΔΡΙΟΥ ΤΗΣ ΕΛΛΗΝΙΚΗΣ ΓΕΩΛΟΓΙΚΗΣ ΕΤΑΙΡΕΙΑΣ

Υπό την Αιγίδα του
ΥΠΟΥΡΓΕΙΟΥ ΠΕΡΙΒΑΛΛΟΝΤΟΣ, ΕΝΕΡΓΕΙΑΣ & ΚΛΙΜΑΤΙΚΗΣ ΑΛΛΑΓΗΣ

και τη Συμβολή των
ΤΜΗΜΑ ΓΕΩΛΟΓΙΑΣ ΠΑΝΕΠΙΣΤΗΜΙΟΥ ΠΑΤΡΩΝ
ΙΝΣΤΙΤΟΥΤΟ ΓΕΩΛΟΓΙΚΩΝ ΚΑΙ ΜΕΤΑΛΛΕΥΤΙΚΩΝ ΕΡΕΥΝΩΝ
ΓΕΩΤΕΧΝΙΚΟ ΕΠΙΜΕΛΗΤΗΡΙΟ ΕΛΛΑΔΑΣ

ΚΟΙΝΩΦΕΛΕΣ ΙΔΡΥΜΑ
ΙΩΑΝΝΗ Σ. ΛΑΤΣΗ

ΠΑΝΕΠΙΣΤΗΜΙΟ ΠΑΤΡΩΝ

ΟΡΓΑΝΙΣΜΟΣ ΑΝΤΙΣΕΙΣΜΙΚΟΥ
ΣΧΕΔΙΑΣΜΟΥ ΚΑΙ ΠΡΟΣΤΑΣΙΑΣ

ΑΚΤΩΡ Α.Τ.Ε.

ΕΜΒΕΛΕΙΑ Α.Ε.

ΕΛΛΗΝΙΚΑ ΛΑΤΟΜΕΙΑ Α.Ε.

ΟΜΙΛΟΣ ΤΕΧΝΙΚΩΝ ΜΕΛΕΤΩΝ
(ΟΤΜ) Α.Τ.Ε.

ΓΕΦΥΡΑ Α.Ε.

ΓΕΝΙΚΗ ΜΕΛΕΤΩΝ Ε.Π.Ε. «ΙΣΤΡΙΑ»

ΣΥΝΔΕΣΜΟΣ ΜΕΤΑΛΛΕΥΤΙΚΩΝ
ΕΠΙΧΕΙΡΗΣΕΩΝ

ΔΕΛΦΟΙ-ΔΙΣΤΟΜΟΝ Α.Μ.Ε.

ΓΕΩΜΗΧΑΝΙΚΗ Α.Τ.Ε.

Α.Ε. ΤΣΙΜΕΝΤΩΝ ΤΙΤΑΝ

ΕΔΑΦΟΣ ΣΥΜΒΟΥΛΟΙ
ΜΗΧΑΝΙΚΟΙ Α.Ε.

ΓΕΩΣΚΟΠΙΟ Α.Τ.Ε.

Η Οργανωτική Επιτροπή του 12ου Διεθνούς Συνεδρίου της Ελληνικής Γεωλογικής Εταιρίας ευχαριστεί θερμά τα ανωτέρω Ιδρύματα, Ινστιτούτα Ερευνών, Οργανισμούς, Τεχνικές και Μελετητικές Εταιρίες για την οικονομική υποστήριξη και συμβολή τους στην οργάνωση και υλοποίηση του Συνεδρίου.

SPONSORS
OF THE 12th INTERNATIONAL CONGRESS OF THE GEOLOGICAL SOCIETY OF GREECE

Under the Aegis of the

MINISTRY OF ENVIRONMENT, ENERGY AND CLIMATE CHANGE

and the Contribution of the

DEPARTMENT OF GEOLOGY, UNIVERSITY OF PATRAS
INSTITUTE OF GEOLOGY AND MINERAL EXPLORATION
GEOTECHNICAL CHAMBER OF GREECE

JOHN S. LATSIS, PUBLIC BENEFIT FOUNDATION

UNIVERSITY OF PATRAS

EARTHQUAKE PLANNING AND PROTECTION ORGANIZATION

AKTOR S.A.

EMBELIA S.A.

HELLENIC QUARRIES S.A..

CONSULTING ENGINEERING COMPANY (OTM) S.A.

GEFYRA S.A.

GENERAL CONSULTING LTD "ISTRIA"

GREEK MINING ENTERPRISES ASSOCIATION

DELFI-DISTOMON BAUXITE S.A.

GEOMECHANIKI S.A.

TITAN CEMENT COMPANY S.A.

EDAFOS ENGINEERING CONSULTANTS S.A.

GEOSCOPIO S.A.

The Organizing Committee of the 12th International Congress of the Geological Society of Greece expresses its grateful thanks to the above Foundations, Institutes, Organizations, Construction and Consulting Companies for their substantial support.

ΕΠΙΣΤΗΜΟΝΙΚΗ ΕΠΙΤΡΟΠΗ – SCIENTIFIC COMMITTEE

Η Οργανωτική Επιτροπή ευχαριστεί θερμά τους κριτές για τη συμβολή τους στην κρίση όλων των εργασιών. Κάθε εργασία κρίθηκε από δύο κριτές για την απόκτηση Πρακτικών υψηλού επιστημονικού επιπέδου. Η Οργανωτική Επιτροπή δεν έχει ευθύνη για το περιεχόμενο και τις απόψεις που εκφράζονται στις εργασίες από τους συγγραφείς.

The Organizing Committee expresses sincere thanks to the reviewers for their contribution in evaluating and approving of the submitted papers. Each paper has passed through two reviewers, producing Proceedings of high scientific level. The Organizing Committee is not responsible for the content and the views expressed by the authors in the papers.

Alexopoulos A., Alexopoulos I., Alexouli A., Anagnostou C., Antonarakou A., Argyraki A., Avramidis P., Bersezio R., Bogdanov K., Caputo R., Christanis K., Christaras B., Christidis G., Depountis N., Drakatos G., Dresnier Th. Drinia H., Economou G., Fassoulas C., Ferentinos G., Fermeli G., Filippidis A., Fountoulis I. Frey M.L., Gaki – Papanastassiou K., Ganas A., Georgakopoulos A., Geraga M., Godelitsas A., Hatzipanagiotou K., Iliopoulos I., Ioakim C., Kalavrouziotis I., Kaleris V., Kallergis G., Kamberis E., Karakaisis G.F., Karakitsios V., Karastathis V., Karipi S., Katagas C., Kati M., Katsonopoulou D., Kilias A., Kiratzi A., Kitsou D., Kokkalas S., Kollaman H., Kondopoulou D., Konispoliatis N., Konstantinou C., Kontopoulos N., Koroneos A., Koukis G., Koukouvelas I., Lambrakis N., Laskou M., Lekkas E., Loupasakis C., Lykousis V., Magganas A., Manoutsoglou E., Marinos P.V., Markopoulos Th., Migiros G., Mladenova Th., Mountrakis D., Mposkos E., Mylonakis G., Nakov R., Nikolaou N., Oprsal I., Papadimitriou E., Papadimitriou P., Papadopoulos T., Papaioannou Ch., Papamarinopoulos S., Papanastassiou D., Papanikolaou D., Papatheodorou G., Papazachos C.B., Papoulis D., Paraskevopoulos P., Parcharidis I., Pavlides S., Pavlopoulos A., Pe – Piper G., Perdikakis V., Perrakis M., Perraki Th., Petalas C., Pomoni – Papaioannou F., Pomonis P., Ritolo S., Rokka A., Rondoyanni Th., Roumelioti Z., Rozos D., Ruiz – Ortiz P.A., Sabatakakis N., Sachpazi M., Sakellariou D., Scordilis Em., Seifert Th., Skarpelis N., Skias S., Sokos E., Soulios G., Soupios P., Stamatakis M., Stamatelopoulou - Seymour K., Stamatis G., Stiros S., Stournaras G., Syrides G., Theodorou G., Theodosiou I., Torok A., Tranos M., Triantafyllou M.V., Tsapanos T.M., Tselentis G-A., Tsiambaos G., Tsikouras B., Tsipoura – Vlahou M., Tsirambides A., Tsokas G., Tsolis–Katagas P., Tsombos P., Tsourlos P., Tucker M.E., Tulipano L., Tzanis A., Varnavas S., Vavelidis M., Voudouris K., Voulgaris N., Xypolias P., Zagana E., Zambetakis – Lekkas A., Zelilidis A., Zouros N., Zygouri V.

ΔΟΜΗ ΤΩΝ ΠΡΑΚΤΙΚΩΝ / SCHEME OF THE PROCEEDINGS

ΤΟΜΟΣ 1 / VOLUME 1

Εναρκτήρια Ομιλία / Opening Lectures
Κεντρικές και Θεματικές Ομιλίες / Special and Keynote Lectures
Γενική και Τεκτονική Γεωλογία / General and Structural Geology
Νεοτεκτονική και Γεωμορφολογία / Neotectonics and Geomorphology

ΤΟΜΟΣ 2 / VOLUME 2

Παλαιοντολογία, Στρωματογραφία και Ιζηματολογία /
Palaeontology, Stratigraphy and Sedimentology.
Γεωαρχαιολογία / Geoarchaeology
Γεώτοποι / Geosites
Διδακτική των Γεωεπιστημών / Teaching of Earth Sciences
Θαλάσσια Γεωλογία και Ωκεανογραφία / Marine Geology and Oceanography

ΤΟΜΟΣ 3 / VOLUME 3

Τεχνική Γεωλογία και Γεωτεχνική Μηχανική /
Engineering Geology and Geotechnical Engineering
Φυσικές Καταστροφές / Natural Hazards
Αστική Γεωλογία / Urban Geology
Γ.Σ.Π. στις Γεωεπιστήμες / G.I.S in Earth Sciences

ΤΟΜΟΣ 4 / VOLUME 4

Υδρογεωλογία και Υδρολογία / Hydrogeology and Hydrology
Γεωφυσική / Geophysics
Σεισμολογία / Seismology

ΤΟΜΟΣ 5 / VOLUME 5

Ενεργειακές Πρώτες Ύλες και Γεωθερμία / Energy resources and Geothermics
Γεωχημεία και Κοιτασματολογία / Geochemistry and Ore Deposit Geology
Βιομηχανικά Ορυκτά και Πετρώματα / Industrial Minerals and Rocks
Ορυκτολογία και Πετρολογία / Mineralogy and Petrology

ΤΑ ΣΥΝΕΔΡΙΑ ΤΗΣ Ε.Γ.Ε.

1ο ΔΙΗΜΕΡΟ, ΑΘΗΝΑ, 1983, Δελτίο XVII
2ο ΔΙΗΜΕΡΟ, ΑΘΗΝΑ, 1984, Δελτίο XIX
3ο ΣΥΝΕΔΡΙΟ, ΑΘΗΝΑ, 1986, Δελτίο XX
4ο ΣΥΝΕΔΡΙΟ, ΑΘΗΝΑ, 1988, Δελτίο XXIII
5ο ΣΥΝΕΔΡΙΟ, ΘΕΣΣΑΛΟΝΙΚΗ, 1990, Δελτίο XXV
6ο ΣΥΝΕΔΡΙΟ, ΑΘΗΝΑ, 1992, Δελτίο XXVIII
7ο ΣΥΝΕΔΡΙΟ, ΘΕΣΣΑΛΟΝΙΚΗ, 1994, Δελτίο XXX
8ο ΣΥΝΕΔΡΙΟ, ΠΑΤΡΑ, 1998, Δελτίο XXXII
9ο ΣΥΝΕΔΡΙΟ, ΑΘΗΝΑ, 2001, Δελτίο XXXIV
10ο ΣΥΝΕΔΡΙΟ, ΘΕΣΣΑΛΟΝΙΚΗ, 2004, Δελτίο XXXVI
11ο ΣΥΝΕΔΡΙΟ, ΑΘΗΝΑ, 2007, Δελτίο XXXX

THE CONGRESSES OF G.S.G.

1st MEETING, ATHENS, 1983, Bull. XVII
2nd MEETING, ATHENS, 1984, Bull. XIX
3rd CONGRESS, ATHENS, 1986, Bull. XX
4th CONGRESS, ATHENS, 1988, Bull. XXIII
5th CONGRESS, THESSALONIKI, 1990, Bull. XXV
6th CONGRESS, ATHENS, 1992, Bull. XXVIII
7th CONGRESS, THESSALONIKI, 1994, Bull. XXX
8th CONGRESS, PATRAS, 1998, Bull. XXXII
9th CONGRESS, ATHENS, 2001, Bull. XXXIV
10th CONGRESS, THESSALONIKI, 2004, Bull. XXXVI
11th CONGRESS, ATHENS, 2007, Bull. XXXX

ΠΡΟΛΟΓΟΣ

Η Γη είναι ένας πλανήτης με συνεχή και δυναμική εξέλιξη στην ιστορία του. Η γνώση και κατανόηση από τον άνθρωπο της εξέλιξης αυτής είναι μεγάλης σημασίας για τον εντοπισμό, την εκμετάλλευση και τη χρήση των φυσικών πόρων, καθώς και για την ανάδειξη και αντιμετώπιση των περιβαλλοντικών προκλήσεων-προβλημάτων από τη χρήση των πόρων αυτών.

Η περιβαλλοντική αυτή διάσταση απαιτεί μια ολοκληρωμένη, πολυ-επιστημονική θεώρηση του Πλανήτη, που θα περιλαμβάνει τη μελέτη όλων των παραγόντων, όπως της λιθόσφαιρας, της υδρόσφαιρας, της ατμόσφαιρας και της βιόσφαιρας, οι οποίοι συνδέονται μεταξύ τους σε πολύ σημαντικά συστήματα. Τα συστήματα αυτά απαιτούν τη συνεργασία, χωρίς σύνορα και περιορισμούς, των φυσικών επιστημών, όπως η Γεωλογία, η Βιολογία, η Χημεία και η Φυσική. Έτσι μόνο θα κατανοήσουμε τον Πλανήτη μας, θα αναδείξουμε τα περιβαλλοντικά προβλήματα και θα δημιουργήσουμε ενημερωμένες-ευαισθητοποιημένες κοινωνίες, οι οποίες θα μπορούν να αποφασίσουν για το παρόν και το μέλλον του.

Σήμερα είναι γεγονός ότι υπάρχει μια εμπεριστατωμένη άποψη σχετικά με την εξελικτική πορεία της Γης στη διάρκεια των 4,6 δισεκατομμυρίων ετών της ύπαρξής της. Παράλληλα αποτελεί κοινή συνείδηση ότι η ισορροπία του πλανήτη από την καθημερινή πίεση των έξι (6) περίπου δισεκατομμυρίων ανθρώπων που φιλοξενούνται σε αυτόν, είναι πλέον εύθραυστη. Ειδικότερα όσον αφορά στις Γεωεπιστήμες, υπάρχει σοβαρή γνώση σχετικά με τις **Γεωλογικές Διεργασίες**, που έχουν λάβει χώρα στα πλαίσια της ιστορίας αυτής με τη δημιουργία των ορέων και των ωκεανών, τους σεισμούς, την ηφαιστειακή δραστηριότητα, καθώς και την εκδήλωση εξωγενών φαινομένων, όπως οι κατολισθήσεις, οι πλημμύρες, οι ξηρασίες, τα τσουνάμι.

Όσον αφορά στη **Βιώσιμη Ανάπτυξη**, είναι γνωστό ότι τις τελευταίες δεκαετίες η τεχνολογική εξέλιξη και η πληθυσμιακή έκρηξη επέβαλαν μια αλόγιστη και χωρίς σχεδιασμό υπερεκμετάλλευση των φυσικών πόρων, με αποτέλεσμα την υποβάθμιση του περιβάλλοντος για πρώτη φορά στην ιστορία του Πλανήτη μας.

Έτσι, μερικά από τα ερωτήματα που τίθενται επιτακτικά και αναμένουν απαντήσεις από την επιστημονική κοινότητα, δεδομένου ότι εκφράζουν την αγωνία όλης της ανθρωπότητας, είναι τα εξής: α) Οι ανθρώπινες δραστηριότητες έχουν προκαλέσει πράγματι επικίνδυνες τροποποιήσεις του περιβάλλοντος και μάλιστα μη αναστρέψιμες ή οι κλιματικές μεταβολές που παρατηρούνται σήμερα αποτελούν φυσικές διακυμάνσεις; β) Ειδικότερα η βιομηχανική ανάπτυξη και η υπερκατανάλωση ενεργειακών πρώτων υλών αποτελούν κίνδυνο για το περιβάλλον ή θεωρούνται μηδαμινής επίδρασης σε σχέση με τις ηφαιστειακές εκρήξεις και τις αλλαγές των ρευμάτων στους ωκεανούς, οι οποίες προκαλούν δραματικές αλλαγές στο περιβάλλον;

γ) Είναι ακόμα δυνατή μια Βιώσιμη Ανάπτυξη και εάν ναι, ποιο είναι το είδος αυτής στα όρια αντοχής και αποδοχής του πλανήτη μας;

Στα παραπάνω ερωτήματα και προβληματισμούς η επιστήμη της Γεωλογίας έχει να προσφέρει πολλά, δεδομένου ότι οι φυσικές διεργασίες κατά τη διάρκεια της εξέλιξης της Γης έχουν καταγραφεί στους εδαφικούς και βραχώδεις γεωλογικούς σχηματισμούς, χωρίς επηρεασμούς από τις παρεμβάσεις του ανθρώπου. Έτσι οι ανθρώπινες παρεμβάσεις της σύγχρονης εποχής μπορούν να διαχωριστούν και να επισημανθούν, ώστε να αντιμετωπιστούν σωστά. Γενικότερα, η γνώση και κατανόηση της εξέλιξης της Γης μέσα από τις φυσικές διεργασίες μπορούν να συμβάλουν στην αποτύπωση των ρυθμών αλλαγής της Γης στο γεωλογικό χρόνο. Επιπλέον οι ρυθμοί αλλαγής και οι διεργασίες, που είναι υπεύθυνες για αυτούς, μπορούν παράλληλα να αποτελούν δείκτες πρόγνωσης για την πορεία του πλανήτη στο μέλλον. Με άλλα λόγια, το παρελθόν και γενικότερα η γεωλογική ιστορία του Πλανήτη μπορεί να αποτελέσει το «κλειδί» για το παρόν και το μέλλον αυτού.

Συμπερασματικά, η συμβολή της Γεωλογίας και γενικότερα των Φυσικών Επιστημών στην κοινωνία μας είναι πολύ σημαντική για τη γνώση της εξέλιξης της Γης, την έρευνα και αξιολόγηση των φυσικών πόρων, την εκτίμηση των περιβαλλοντικών επιπτώσεων λόγω εκμετάλλευσης των πόρων αυτών, καθώς και την πρόγνωση-αντιμετώπιση των διάφορων φυσικών επικινδυνοτήτων από γεωλογικές διεργασίες και καταστροφικά καιρικά φαινόμενα.

Το 12ο Διεθνές Συνέδριο της Ελληνικής Γεωλογικής Εταιρίας με τίτλο **«Πλανήτης Γη: Γεωλογικές Διεργασίες και Βιώσιμη Ανάπτυξη»** διοργανώνεται από το Τμήμα Γεωλογίας του Πανεπιστημίου Πατρών και πραγματοποιείται στο Συνεδριακό και Πολιτιστικό Κέντρο του Πανεπιστημίου από τις 19 έως 22 Μαΐου 2010. Το Δελτίο της Ελληνικής Γεωλογικής Εταιρίας περιλαμβάνει τα Πρακτικά του Συνεδρίου σε πέντε (5) τόμους των 2.992 σελίδων συνολικά. Οι τόμοι αυτοί καλύπτουν όλο το φάσμα των Γεωεπιστημών σε θέματα της βασικής και εφαρμοσμένης έρευνας. Στα πρακτικά περιλαμβάνονται 267 συνολικά εργασίες από 605 συγγραφείς, όλες στην Αγγλική γλώσσα, δίνοντας έτσι τη δυνατότητα διεθνούς προβολής και χρήσης του επιστημονικού Δελτίου της Εταιρίας. Οι επίσημες γλώσσες του Συνεδρίου είναι η Ελληνική και η Αγγλική.

Στο Συνέδριο υπάρχει σημαντικός αριθμός εργασιών από τον ευρύτερο γεωγραφικό μας χώρο, έχουν δε δηλώσει συμμετοχή πολλοί αξιόλογοι επιστήμονες από την Ελλάδα και το εξωτερικό, καθώς και νέοι ερευνητές και φοιτητές.

Όλες οι εργασίες που δημοσιεύονται, υπεβλήθησαν σε επιστημονική κρίση από εξωτερικούς κριτές, ακολουθώντας τη διαδικασία που είναι διεθνώς καθιερωμένη στα επιστημονικά περιοδικά. Πολλοί αναγνωρισμένοι επιστήμονες, Έλληνες και ξένοι, όλων των ειδικοτήτων, συμμετείχαν στη διαδικασία αυτή. Εκ μέρους της Οργανωτικής Επιτροπής τους ευχαριστώ για τη συμμετοχή και τη συμβολή τους με το σοβαρό έργο που προσέφεραν στην απόκτηση Πρακτικών υψηλού επιπέδου.

Οι επιστημονικές εργασίες εντάχθηκαν σε επιμέρους θεματικές ενότητες, στις οποίες διαχωρίστηκαν τα Πρακτικά και αποτέλεσαν αντικείμενο στις αντίστοιχες Συνεδρίες. Τα κείμενα των ειδικών και προσκεκλημένων ομιλιών, που καλύπτουν το ευρύτερο αντικείμενο της κάθε ενότητας και παρουσιάζουν υψηλού επιπέδου θεώρηση σχετικά με την υφιστάμενη γνώση, τις νέες απόψεις και τάσεις της έρευνας, αποτέλεσαν ιδιαίτερη ενότητα.

Στο Συνέδριο αυτό δίνεται ιδιαίτερη έμφαση στις Γεωλογικές Διεργασίες και τη Βιώσιμη Ανάπτυξη. Όπως αναφέρθηκε διεξοδικά παραπάνω, η κατανόηση της εξέλιξης του πλανήτη Γη μέσα από τις γεωλογικές διεργασίες επιτρέπει στον άνθρωπο να αξιολογήσει τις διάφορες δραστηριότητές του, όπως την αναζήτηση, εκμετάλλευση και χρήση των φυσικών πόρων, καθώς και την κατασκευή διαφόρων έργων υποδομής, χωρίς να προκαλεί επικίνδυνες μεταβολές στο φυσικό και το ανθρωπογενές περιβάλλον. Έτσι μόνο μπορεί να εξασφαλιστεί η Βιώσιμη Ανάπτυξη και να προβλεφθεί η πορεία του Πλανήτη.

Η έγκαιρη εκτύπωση και παράδοση των τόμων του Συνεδρίου στους συνέδρους και στην επιστημονική κοινότητα, καθώς και η γενικότερη οργάνωση του Συνεδρίου γίνεται με την οικονομική στήριξη πολλών φορέων, δημόσιων και ιδιωτικών. Εκφράζονται θερμές ευχαριστίες στο Υπουργείο Περιβάλλοντος, Ενέργειας και Κλιματικής Αλλαγής, που έθεσε το Συνέδριο υπό την αιγίδα του, καθώς και στο Τμήμα Γεωλογίας του Πανεπιστημίου Πατρών, το Ι.Γ.Μ.Ε., και το ΓΕΩΤ.Ε.Ε. Θερμές ευχαριστίες εκφράζονται επίσης στο Κοινωφελές Ίδρυμα Ιωάννη Σ. Λάτση, το Πανεπιστήμιο Πατρών, αλλά και σε ιδιωτικές Τεχνικές και Μελετητικές Εταιρίες, που με τόση προθυμία ανταποκρίθηκαν στην πρόσκλησή μας.

Τέλος, θα ήθελα να εκφράσω τις προσωπικές μου ευχαριστίες στους συναδέλφους της Οργανωτικής Επιτροπής για την αμέριστη βοήθειά τους και την άριστη συνεργασία στη συλλογική αυτή προσπάθεια, καθώς και στο Γραφείο Οργάνωσης Συνεδρίων *«Συνέδρα»*, όπως επίσης στους φοιτητές του Τμήματος Γεωλογίας, που αγκάλιασαν και βοήθησαν στην οργάνωση του Συνεδρίου με απαράμιλλο ζήλο.

Πάτρα, 14 Απριλίου 2010

Γεώργιος Χρ. Κούκης
Πρόεδρος
της Οργανωτικής Επιτροπής

PROLOGUE

Earth is a dynamic Planet that has been continuously changing and evolving throughout its whole history. Knowledge and understanding of the evolution processes is of crucial importance not only to explore and take advantage of the natural recourses that our planet provides, but also to access the degree of environmental impacts that the exploitation of these causes.

This environmental aspect demands to consider a comprehensive and multi-scientific view of our Planet, which involves the study of lithosphere, hydrosphere, biosphere and atmosphere. All the above are closely connected together to form very important and complex natural systems, which need the close cooperation of all sciences involved, such as Geology, Biology, Chemistry and Physics. This is the most effective way to understand our Planet, to consider the environmental problems and enforce societies to become informed and conscious of its present and future.

Nowadays an almost complete and comprehensive knowledge about the evolution of Earth during the 4.6 billion years of its age has been gained. In parallel, it is common sense that our Planet's equilibrium is fragile due to environmental pressures that human causes, since Earth's population exceeds 6 billion people.

In the field of Geo-Sciences, in special, there has been gained sufficient experience about the **Geological Processes** that have been taken place during Earth's history and are evident in the formation of mountains and oceans, by the manifestation of earthquakes, by volcanic activity, as well as in natural phenomena as landslides, floods, droughts and tsunamis.

Concerning **Sustainable Development**, it is well known that during the last decades technological evolution and population growth have imposed an unreasonable and sometimes without design overconsumption of natural resources, which leads to gradual degradation of the environment for the first time in our Planet's history.

Thus, some of the "hot" questions that have been arisen and need to be answered by the Scientific Community, since they express the concern of the whole humanity, are: a) Human activities have indeed caused dangerous and non-reversible modifications of the environment or present climatic changes are a result of normal and natural fluctuations? b) Industrial development and overconsumption of natural recourses are a "red flag" for the environment or they can be considered as of minor effect when compared with volcanic eruptions and changes in the regime of ocean current circulation, which cause dramatic environmental changes? c) Is Sustainable Development still achievable and, if yes, in which form and within our Planet's bearing thresholds?

In the above questions Scientific Community can offer a lot, regarding that natural processes

during Earth's evolution have been imprinted on soil and rock geological formations, without any influence by human activities. Present human actions can be clearly distinguished and identified in order to be treated in the right way. The deep knowledge and understanding of Earth's evolution though natural processes can contribute to imprint the rates of Earth's changes through geological time. The changing rates and the processes responsible for them also contribute to obtain indices to predict similar phenomena for the future. In other words the Past and, generally, the geological history of our Planet is the "key" for the Present and Future.

In conclusion, the contribution of Geology and generally of Natural Sciences in our society is very important to understand Earth's evolution, to assist the research and assessment of natural resources, as well as to estimate the environmental impacts from their exploitation. Furthermore, they can provide solutions to the direction of the prevention and confrontation of natural hazards that are triggered by Geological Processes and catastrophic climatic events.

The 12th International Congress of the Geological Society of Greece entitled **"Planet Earth: Geological Processes & Sustainable Development"** is organized by the Department of Geology of the University of Patras in Greece and is held at the Conference and Cultural Center of the University between the 19th and 22nd of May 2010. The *Bulletin of the Geological Society of Greece* includes the Congress's Proceedings in 5 Volumes of 2.992 pages. These volumes cover the whole spectrum of Geo-Sciences in themes of basic and applied research. They include 267 research papers by 605 authors, all written in English making them easily accessible and promoted internationally. Official languages of the Congress are Greek and English. Many renowned scientists from Greece and abroad participate, covering scientific issues from our broad geographic region, as well as new researchers and students.

All submitted papers were reviewed by external reviewers, following the procedure that is established in scientific magazines. Many renowned scientists, Greek and foreigners, of all specialties, participated in this process. On behalf of the Organizing Committee I would like to thank them for their participation and contribution to acquire Proceedings of high quality.

The research papers were included in specific thematic units to which the Proceedings were divided and covered each Congress's session. Special and Keynote lectures about currently acquired knowledge, new insights and modern research trends for each area of interest comprised a special thematic unit.

This Congress focuses on Geological Processes and Sustainable Development. As it was mentioned above, the understanding of Earth's evolution though geological processes allows human to assess his activities, such as investigation and exploitation of natural resources and construction of Infrastructure Works, without causing serious and dangerous damages to the natural and human environment. This is the only way to secure sustainable development and forecast Earth's future.

The on-time production and delivering of the proceedings to the participants and scientific community, as well as the organization of the Congress is sponsored by many public and pri-

vate Organizations, Services and Companies. I would like to express my special thanks to the Ministry of Environment, Energy and Climate Change, which held the Congress under its aegis, as well as to the Department of Geology of the University of Patras, the Institute of Geology and Mineral Exploration (I.G.M.E.) and the Geotechnical Chamber of Greece for their contribution to organize this Congress. Special thanks are also expressed to the Public Benefit Foundation "John S. Latsis", to the University of Patras and to many private technical and consulting companies which willingly accepted our invitation.

Finally, I would like to personally thank the colleagues of the Organizing Committee for their generous help, support and cooperation to this teamwork, the Congress Organizing firm "*Synedra*", as well as the students of the Department of Geology for their precious contribution.

Patras, 14 of April 2010

George Ch. Koukis
President
of the Organizing Committee

ΠΕΡΙΕΧΟΜΕΝΑ / CONTENTS

ΤΟΜΟΣ 1 / VOLUME 1

Εναρκτήρια Ομιλία / Opening Lectures
Κεντρικές και Θεματικές Ομιλίες / Special and Keynote Lectures
Γενική και Τεκτονική Γεωλογία / General and Structural Geology
Νεοτεκτονική και Γεωμορφολογία / Neotectonics and Geomorphology

ΕΝΑΡΚΤΗΡΙΑ ΟΜΙΛΙΑ / OPENING LECTURE

ΚΕΝΤΡΙΚΕΣ ΟΜΙΛΙΕΣ / SPECIAL LECTURES

ΘΕΜΑΤΙΚΕΣ ΟΜΙΛΙΕΣ / KEYNOTE LECTURES

ΓΕΝΙΚΗ ΚΑΙ ΤΕΚΤΟΝΙΚΗ ΓΕΩΛΟΓΙΑ / GENERAL AND STRUCTURAL GEOLOGY

ΝΕΟΤΕΚΤΟΝΙΚΗ ΚΑΙ ΓΕΩΜΟΡΦΟΛΟΓΙΑ / NEOTECTONICS AND GEOMORPHOLOGY

ΤΟΜΟΣ 2 / VOLUME 2

Παλαιοντολογία, Στρωματογραφία και Ιζηματολογία /
Palaeontology, Stratigraphy and Sedimentology
Γεωαρχαιολογία / Geoarchaeology
Γεώτοποι / Geosites
Διδακτική των Γεωεπιστημών / Teaching Earth Sciences
Θαλάσσια Γεωλογία και Ωκεανογραφία / Marine Geology and Oceanography

ΠΑΛΑΙΟΝΤΟΛΟΓΙΑ, ΣΤΡΩΜΑΤΟΓΡΑΦΙΑ ΚΑΙ ΙΖΗΜΑΤΟΛΟΓΙΑ / PALAEONTOLOGY, STRATIGRAPHY AND SEDIMENTOLOGY

ΓΕΩΑΡΧΑΙΟΛΟΓΙΑ / GEOARCHAEOLOGY

ΓΕΩΤΟΠΟΙ / GEOSITES

ΔΙΔΑΚΤΙΚΗ ΤΩΝ ΓΕΩΕΠΙΣΤΗΜΩΝ / TEACHING EARTH SCIENCES

ΘΑΛΑΣΣΙΑ ΓΕΩΛΟΓΙΑ ΚΑΙ ΩΚΕΑΝΟΓΡΑΦΙΑ / MARINE GEOLOGY AND OCEANOGRAPHY

ΤΟΜΟΣ 3 / VOLUME 3

Τεχνική Γεωλογία και Γεωτεχνική Μηχανική /
Engineering geology and Geotechnical Engineering
Φυσικές Καταστροφές / Natural Hazards
Αστική Γεωλογία / Urban Geology
Γ.Σ.Π. στις Γεωεπιστήμες / GIS in Earth Sciences

ΤΕΧΝΙΚΗ ΓΕΩΛΟΓΙΑ ΚΑΙ ΓΕΩΤΕΧΝΙΚΗ ΜΗΧΑΝΙΚΗ / ENGINEERING GEOLOGY AND GEOTECHNICAL ENGINEERING

ΦΥΣΙΚΕΣ ΚΑΤΑΣΤΡΟΦΕΣ / NATURAL HAZARDS

ΑΣΤΙΚΗ ΓΕΩΛΟΓΙΑ / URBAN GEOLOGY

Γ.Σ.Π. ΣΤΙΣ ΓΕΩΕΠΙΣΤΗΜΕΣ / G.I.S. IN EARTH SCIENCES

ΤΟΜΟΣ 4 / VOLUME 4

Υδρογεωλογία και Υδρολογία / Hydrogeology and Hydrology
Γεωφυσική / Geophysics
Σεισμολογία / Seismology

ΥΔΡΟΓΕΩΛΟΓΙΑ ΚΑΙ ΥΔΡΟΛΟΓΙΑ / HYDROGEOLOGY AND HYDROLOGY

ΓΕΩΦΥΣΙΚΗ / GEOPHYSICS

ΣΕΙΣΜΟΛΟΓΙΑ / SEISMOLOGY

ΤΟΜΟΣ 5 / VOLUME 5

Ενεργειακές Πρώτες Ύλες και Γεωθερμία / Energy resources and Geothermics
Γεωχημεία και Κοιτασματολογία / Geochemistry and Ore Deposit Geology
Βιομηχανικά Ορυκτά και Πετρώματα / Industrial Minerals and Rocks
Ορυκτολογία και Πετρολογία / Mineralogy and Petrology

ΕΝΕΡΓΕΙΑΚΕΣ ΠΡΩΤΕΣ ΥΛΕΣ ΚΑΙ ΓΕΩΘΕΡΜΙΑ / ENERGY RESOURCES AND GEOTHERMICS

ΓΕΩΧΗΜΕΙΑ ΚΑΙ ΚΟΙΤΑΣΜΑΤΟΛΟΓΙΑ / GEOCHEMISTRY AND ORE DEPOSIT GEOLOGY

ΒΙΟΜΗΧΑΝΙΚΑ ΟΡΥΚΤΑ ΚΑΙ ΠΕΤΡΩΜΑΤΑ / INDUSTRIAL MINERALS AND ROCKS

ΟΡΥΚΤΟΛΟΓΙΑ ΚΑΙ ΠΕΤΡΟΛΟΓΙΑ / MINERALOGY AND PETROLOGY

12ο ΔΙΕΘΝΕΣ ΣΥΝΕΔΡΙΟ ΤΗΣ ΕΛΛΗΝΙΚΗΣ ΓΕΩΛΟΓΙΚΗΣ ΕΤΑΙΡΙΑΣ
ΠΛΑΝΗΤΗΣ ΓΗ: Γεωλογικές Διεργασίες και Βιώσιμη Ανάπτυξη

12th INTERNATIONAL CONGRESS OF THE GEOLOGICAL SOCIETY OF GREECE
PLANET EARTH: Geological Processes and Sustainable Development

ΕΝΑΡΚΤΗΡΙΑ ΟΜΙΛΙΑ
OPENING LECTURES

Δελτίο της Ελληνικής Γεωλογικής Εταιρίας, 2010
Πρακτικά 12ου Διεθνούς Συνεδρίου
Πάτρα, Μάιος 2010

Bulletin of the Geological Society of Greece, 2010
Proceedings of the 12th International Congress
Patras, May, 2010

THE "ANTHROPOCENE" IN THE MEDITERRANEAN

Zerefos C.S.

Academy of Athens

President, International Ozone Commission (ICSU)

There is ample evidence by now that climate is changing not only by natural causes but by man-made changes in the overall bio and physico-chemical balance of our planet (IPCC, 2007). This balance is maintained by interactions between the biosphere, the atmosphere, the hydrosphere and the geosphere. These four "spheres" are continuously interacting in such ways and at such rates that quasi-ensure ecological equilibrium and adaptation of humans and the ecosystems to new equilibrium states. But in the past decades, during the period called "the anthropocene", man is also contributing to climate change in a number of activities notable of which are man-made global emissions of greenhouse gases.

The man-made climate change is part of an overall global change caused by human's intervention with nature. This has significant impacts on the biological, physico-chemical systems and to the humans. The effects can be found globally distributed and they are expected to have important consequences not only to humans but to the ecosystems as well. Among the most prominent of these changes are the changes in the hydrological cycle on both global and regional scales, changes in the intensity of extreme weather events and changes in rainfall characteristics and patterns. These changes are expected to affect the incidence and severity of droughts and floods making problematic in some cases even the availability of water.

Global changes provide challenges for health and many aspects of human societies, industry and the overall wealth and security. Notable are the foreseen effects in economies, in agriculture and in food and water security. The list of negative consequences from man-made global change is indeed large. From sea level rise with severe effects on human settlements to the observed effects on biological systems. There is indeed evidence of changes and shifts in the range of plant and animal species to higher latitudes and altitudes and changes in the timing of many life-cycle events, such as flowering. This variability will affect the ecosystems and biodiversity in general. Many of these impacts, especially when operating in synergy, are expected to cause additional threats to humans, to our resources and to the ecosystems.

The year 2008 has been dedicated to Planet Earth by UNESCO and the International Union of Geological Sciences. It is a land mark year that follows the Stern review, the IPCC assessments on climate change and important international research activities in Global Change. The interactions between the hydrosphere, the atmosphere, the biosphere, the cryosphere and the geosphere have been operating on earth for millions of years in the past. Recent concerns on the effects of human activities that intervene with natural globally changing processes are based on observational, modelling and statistical analysis results. Important international efforts aim to integrate observations and coordinate international networking of modellers and experimentalists in Global Change research.

EU and ESA have initiated the Global Monitoring of the Environment and Security (GMES) activity, recently named Kopernikus, aiming to provide to EU countries an operational service for studying man-made changes in the Environment and their related impact concerning the security of the citizens. However, the synergy between the slowly and the fast varying components of geophysical extremes, enhanced by the man-made change on the environment, is an issue of urgency, having several missing links, not considered in such an operational activity. This is particularly important when we investigate the synergistic effects of disasters resulting from nature and accelerated by man and their effects on humans, the society and the ecosystems. For example, earthquakes can be linked with landslides and tsunamis in coastal areas. The synergistic effects of these natural disasters under a manmade, globally changing environment are today mostly unknown and worst of all, there is no existing European infrastructure dealing with interactions between different types of extreme events operating in synergy under the laws of probability. The Mediterranean region is vulnerable to natural and manmade disasters. Natural disasters have always occurred in this part of the world but manmade changes to our environment have worsened the effects on humans and on the ecosystems of natural disasters.

The Mediterranean is already under pressure from global stresses and is highly vulnerable to the impacts of climate change. Floods and droughts can occur in the same area within months of each other. These events can lead to famine and widespread disruption of socio-economic well-being, particularly in the north African shore. Many factors contribute to the impacts of man-made climate variability in the Mediterranean and will have negative effects on its ability to cope with these changes. The overexploitation of land resources including forests, increased population, desertification and land degradation provide additional threats in this area (UNDP 2006). In parts of the Mediterranean and over the north Africa's shore, dust and sand storms have negative impacts on agriculture, infrastructure and health. The Mediterranean is also expected to face increasing water scarcity and stress. Agricultural production relies mainly on rainfall for irrigation and will be severely compromised. Under climate change some agricultural land will be lost, with shorter growing seasons and lower yields. Rising temperatures are changing the geographical distribution of disease vectors which are migrating to new areas and to higher altitudes and latitudes (WHO, 2004).

Climate change is an added stress to already threatened habitats, fragile ecosystems and species in the Mediterranean and is likely to trigger species migration and lead to habitat reduction. Land use changes due to agricultural expansion and subsequent destruction of habitat; pollution; high rates of land use change; population growth and the intrusion of exotic species. In addition, climate change is altering weather and climate patterns that previously have been relatively stable. Climate experts are particularly confident that climate change will bring increasingly frequent and severe heat waves and extreme weather events, as well as a rise in sea levels. These changes have the potential to affect human health in several direct and indirect ways, some of them severe.

Heat exposure has a range of health effects, from mild heat rashes to deadly heat stroke. Heat exposure can also aggravate several chronic diseases, including cardiovascular and respiratory disease. The results can be severe and result in both increased illness and death. Heat also increases ground-level ozone concentrations, causing direct lung injury and increasing the severity of respiratory diseases such as asthma and chronic obstructive pulmonary disease. Higher temperatures and heat waves increased demand for electricity and thus combustion of fossil fuels, generating airborne particulates and indirectly contributing to increased respiratory disease.

Hot days and heat waves present another hazard that can act in synergy with other events. This happened for example, during the heat wave in Europe of August 2003. There were totally 40,000 deaths and this heat wave was created by meteorology; you can see the weather patterns creating extreme heat in Europe and you can see the number of deaths that were reported in Paris, Torino and Barcelona as time is proceeding and there was a very high correlation between the heat wave air temperatures and the number of deaths. The situation here was a common experience in a period of about two to three weeks and most people were elderly people that were not prepared. Usually elder people take drugs which dehydrate them. So without any signal or any information on them being dehydrated, they have been exposed to a heat wave and unintentionally of course they have been exposed to great danger for death. This can be one of the extreme or worst examples of dangers induced by synergistic effects (heat wave, high ozone levels, high dehydration, poor knowledge).

A model that has been prepared by the University of East Anglia, which shows that the heat wave of 2003 will be considered as a cooling event when compared to the year 2060 or beyond. This is because the temperature anomalies are expected to exceed about 6 degrees from now and the 2003 event was about 3 degrees above normal in the observations that have been made.

There were two more heat waves that struck our region in 2007. These heat waves (two small and one large) have set up the scene also for high risk of forest fires. Talking for the summer time, one can see that the area is also extremely vulnerable to very high levels of ozone, which is an aspiratory threat. So oxidants in the atmosphere, in addition to dehydration, in addition to the heat stress have resulted to deaths which could have been prevented; they have resulted also to setting up the scene of rare conditions for the reoccurrence of forest fires, which also operate in synergy threatening humans and the ecosystems.

Over longer time periods, increased temperatures have other effects ranging from drought to ecosystem changes that can affect health. Droughts can result in shortages of clean water and may concentrate contaminants that negatively affect the chemistry of surface waters in some areas. Drought may also strain agricultural productivity and could result in increased food prices and food shortages, worsening the situation of those affected by hunger and food insecurity. Ecosystem changes include migration of the vectors. The dynamics of disease migration are complex and temperature is just one factor affecting the distribution of these diseases.

Increased concentrations of ground-level carbon dioxide and longer growing seasons could result in higher pollen production, worsening allergic and respiratory diseases. Increased carbon dioxide concentrations in sea water may cause oceans to become more acidic and is likely to contribute to adverse ecosystem changes in the Mediterranean Sea and in the world's tropical oceans. This would have potentially dramatic implications for fisheries and the food supply in certain regions of the world.

The direct effects of extreme weather events include drowning from floods, injuries from floods, and structural collapse. Indirect effects outnumber the direct effects and likely will be more costly. Potential indirect effects include aggravation of chronic diseases due to interruptions in health care service, significant mental health concerns both from interrupted care and geographic displacement, and socioeconomic disruption resulting from population displacement and infrastructure loss.

Sea level rise increases the risk from extreme weather events in coastal areas, threatening critical

infrastructure and worsening immediate and chronic health effects. Salt-water entering freshwater drinking supplies is also a concern for these regions, and increased salt content in soil can hinder agricultural activity in coastal areas.

Most of my examples on the effects of climate change were focused on the Mediterranean. An area of high vulnerability following the recent findings from the IPCC reports. An area where the most vulnerable populations (children and elder and particularly those suffering from other causes) are at particular risk. The Mediterranean is threatened not only by man-made and natural extreme climate and weather phenomena. It is vulnerable also to the synergy of such phenomena in case they coincide. The Mediterranean environment is by its nature fragile and vulnerable (alternating drought / floods, heat waves, seismic activity land slide threats etc.). It is fortunate that IPCC is now preparing a report on extreme phenomena and their relation to climate change. Let me express my hope that the international scientific community will also concentrate to the synergy of events and their amplified effects on humans and the ecosystems.

12ο ΔΙΕΘΝΕΣ ΣΥΝΕΔΡΙΟ ΤΗΣ ΕΛΛΗΝΙΚΗΣ ΓΕΩΛΟΓΙΚΗΣ ΕΤΑΙΡΙΑΣ
ΠΛΑΝΗΤΗΣ ΓΗ: Γεωλογικές Διεργασίες και Βιώσιμη Ανάπτυξη

12th INTERNATIONAL CONGRESS OF THE GEOLOGICAL SOCIETY OF GREECE
PLANET EARTH: Geological Processes and Sustainable Development

ΚΕΝΤΡΙΚΕΣ ΟΜΙΛΙΕΣ
SPECIAL LECTURES

Δελτίο της Ελληνικής Γεωλογικής Εταιρίας, 2010
Πρακτικά 12ου Διεθνούς Συνεδρίου
Πάτρα, Μάιος 2010

Bulletin of the Geological Society of Greece, 2010
Proceedings of the 12th International Congress
Patras, May, 2010

CLIMATIC CHANGES: ANTHROPOGENIC INFLUENCE OR NATURALLY INDUCED PHENOMENON

Foscolos A.E.

Technical University of Crete, Department of Mineral Resources Engineering, 731.00 Chania, Greece, foscolos@mred.tuc.gr

Abstract

By the end of the 18th century eminent scientists explained the climatic changes on the basis of temperature and the ensuing glacial retreat. This disturbing observation led many prominent scientists to send air balloons equipped with special devices to trap air from the lower atmosphere in order to measure CO_2 concentrations. Ninety thousand (90,000) measurements were carried out at 138 locations in 4 continents between 1810 and 1961. The data indicated that atmospheric CO_2 concentrations, during the 19th century varied between 290 and 430 ppm (with an average of 322 ppm for the pre-industrial period). For the 20th century, the average concentration is 338 ppm when combined with comparable CO_2 measurements carried out by Mauna Loa Observatory, Hawaii, USA (1958-2000). Measurement precision is ±3%.

Based on thermometric measurements, the mean average temperature increase from 1850 to the present is 0.75°C (0.44°C/100 years) with the following fluctuations. From 1850 to 1940 the temperature increased by +0.6°C, while from 1941 to 1975 temperature dropped by -0.2°C. From 1976 to 1998, the temperature rose by +0.35°C. From 1999 to 2006 temperature increase was nil. Finally, since 2007 the Mean Annual Temperature of Earth's surface has substantially decreased.

As far as CO_2 concentration in the air's atmosphere is concerned, it has been well documented that during the Holocene Epoch there is a substantial time lag between maximum temperatures recorded during the Interglacial periods and maximum CO_2 concentrations in the atmosphere. Moreover, the same time lag is documented between 1850 and 1980, where CO_2 concentrations in the atmosphere lag behind the increase of temperature for more than 100 years. A parallel increase of CO_2 concentrations in the atmosphere and temperature increase is observed only between 1981 and 1995. No correlation is seen thereafter. The divergence is substantial from 2003 to the present where CO_2 concentrations are increased while temperatures are decreased. These interpretations exclude any correlation between atmospheric CO_2 concentrations and temperature fluctuations. Hence, in order to explain the well documented climatic changes the influence of many natural climate drivers should be accepted.

Key words: *climatic changes, temperatures, CO_2 concentrations.*

1. Introduction

Climatic changes have been the subject of intensive research since the late 18th century by eminent scientists (Franklin, 1784; Fourier, 1824; 1827; Agassiz, 1840; Tyndal, 1861; 1863; Croll, 1864; Köppen, 1873; Czerney, 1881; Arrhenius, 1896; 1901). They developed theories to link the presence of erratic boulders in various places in the world to action of former glaciers as well as to explain the temperature rise.

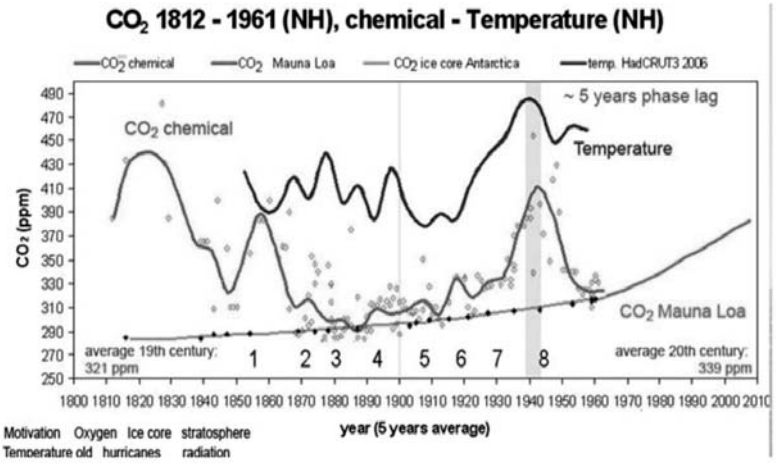

Fig. 1: Evidence of variability of atmospheric CO_2 concentration during the 20th century in the Northern Hemisphere (Beck, 2007).

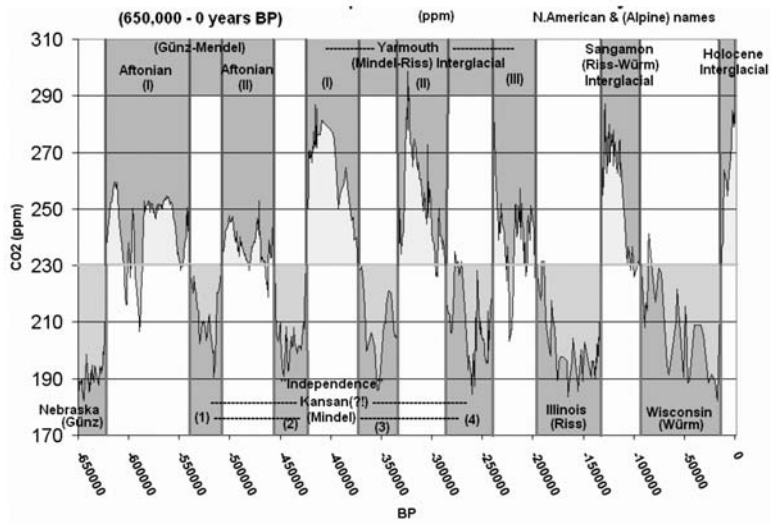

Fig. 2: Late Pleistocene Epoch: Atmospheric CO_2 and the Glacial Cycles. Time Line Glaciations, 2009. Pleistocene Climate Cycles. www.en.Wikipedia.org/wiki/Timeline-of-glaciation.

In addition to the various theories and observations, air balloons equipped with special devices to trap air from the lower atmosphere were sent from a number of European scientists (de Saussure, Bunsen, Pettenkoffer, Kroch[1] and Warburg[1]) in order to measure CO_2 concentrations (Beck, 2007). Ninety thousand (90,000) measurements were carried out at 138 locations in 4 continents between 1810 and 1961. The data indicated that atmospheric CO_2 concentrations varied between 290 ppm and 430 ppm during the 19th century (with an average for the pre-industrial period of 322 ppm), (Fig. 1).

[1] Nobel Prize Winners in Science, 1920 and 1931, respectively.

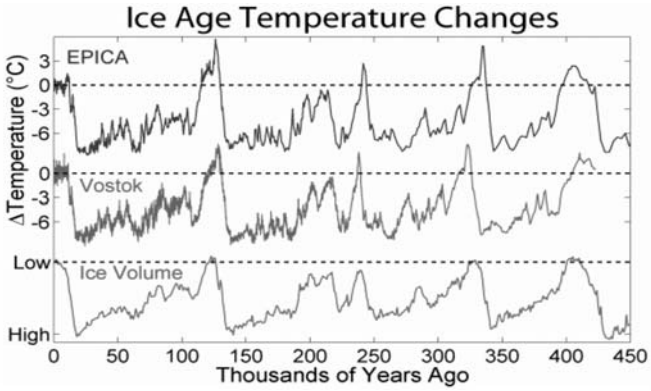

Fig. 3: Climatic changes as documented from Vostok-1 ice-core data (Petit et al., 1999) and EPICA ice-core data (EPICA, 2004), for the last 450,000 years. Worth noticing is the rise of temperature well above the today's one during the long interglacial periods without the complete melting of the ice caps.

For the 20th century, the average concentration is 338 ppm when combined with comparable CO_2 measurements carried out by Mauna Loa Observatory (1958-2009) (Atmospheric CO_2 at Mauna Loa Observatory, Hawaii, USA, 2009). Measurement precision was of the order of ±3%.

In addition to this intense research work, field geologists have mapped the Quaternary glaciations extent and their chronology in Europe as well as in North and South America. Altogether, it took several decades until the ice age theory was fully accepted. This happened on an international scale in the second half of the 1870's (Krüger, 2008). This work is summarized in Figure 2.

2. Analysis of existing climatic changes data

2.1 Middle Pleistocene to Holocene Epochs

Recent ice coring data from Vostok-1 (Petit et al., 1997; 1999) and EPICA (European Project for Ice Coring in Antarctica, Epica 2004) not only have concurred about the climatic changes but also show interglacial temperatures of 1°C to 2.5°C higher than the present Mean Annual Temperature of the Northern Hemisphere of 15°C, for thousands of years (Fig. 3). Since proxy temperature measurements of $\delta^{18}O$ were carried out on ice core samples, it means that even at temperatures well above those prevailing today's, polar ice caps did not melt. These large climatic changes were theoretically attributed to the eccentricity, tilting and wobbling of the earth (Milankovitch, 1940). Finally after three decades this theory was scientifically accepted (Hayes et al., 1974).

Geomagnetic polarity technique along with appropriate sampling has provided a direct assessment of glacial and interglacial environments (Barendregt and Duk-Rodkin, 2004). Through these studies, and $\delta^{18}O$ paleotemperature record from Site 607 in North America, over 100 glacial and interglacial periods were identified (Ruddiman et al., 1989; Raymo, 1992) (Fig. 4). Therefore, it is seen that from the Pliocene till the Holocene Epoch, climatic changes were the norm.

2.2.1 Holocene Epoch. Last Interglacial period

i. 12000 BC to 1850 AD

Climatic changes during this period are very well documented by Dansgaard et al. (1969) and Schon-

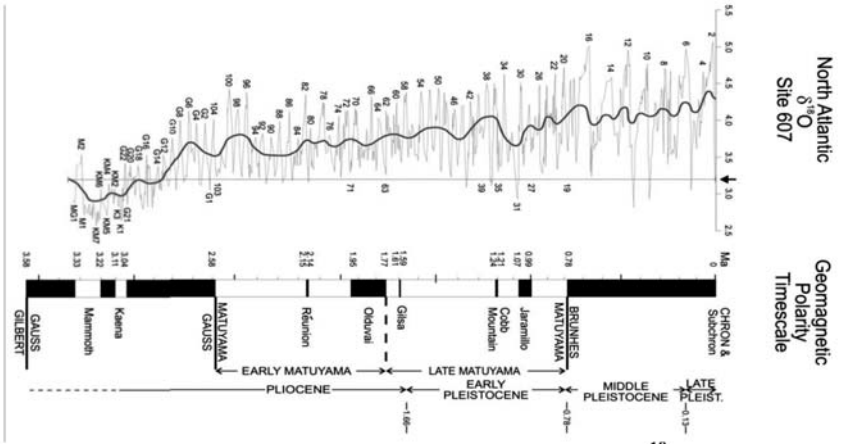

Fig. 4: Geomagnetic polarity scale (Candle and Kent, 1995) and $\delta^{18}O$ paleotemperatures record from Site 607 in the North Atlantic (Ruddiman et al., 1989; Raymo, 1992).

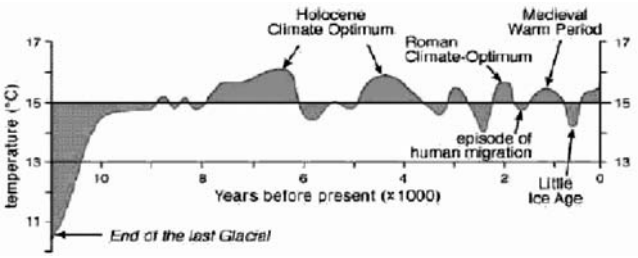

Fig. 5: Average near surface temperatures of the northern hemisphere during the past 11000 years (Dansgaard et al., 1969; Schonwiese 1995).

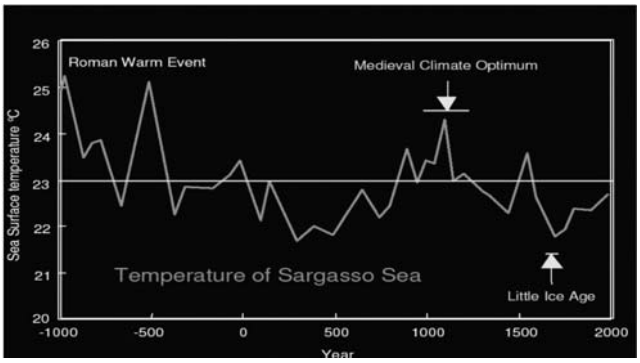

Fig. 6: Sea surface temperatures from the Sargasso sea during the last 3000 years based on oxygen isotopic ratios of *Globigerinoids rubber* (plankton) collected from a box core through 50 cm of bottom sediment (Keigwin, 1996).

wiese (1995), (Fig. 5). The recent glacial retreat began about 14000 years ago (12000 BC). This warming period was shortly interrupted by a sudden cooling, known as Younger Dryas, at about 10000 to 8500 BC. From 8000 BC to about 4000 BC the average global temperature reached its maximum level during the Holocene Epoch and was 1 to 2°C warmer than today's Mean Annual Temperature of the Earth's Atmosphere of 15°C (Pidwirny, 2006). Climatologists call this period the Climatic Optimum.

Worth noticing is that polar ice caps did not vanish between 8000 BC to 4000 BC, since ice core samples were recently collected and CO_2 concentrations were measured in air bubbles which were

Fig. 7: 2000 years of global temperatures based upon 30 year averages (Spencer, 2007).

trapped in the ice cores. Between the span of 4000 years, 2 minor cooling events took place, while a substantial cooling trend took place between 3500 BC and 2000 BC.

From 450 BC to 150 AD, Northern Europe was subjected to another warm period the so-called Roman Warm Period with average temperatures of 2.5°C higher than today's temperature (Keigwin, 1996; Holmgren et al., 1999; 2001; Idso and Idso, 2000; Olafsdottir et al., 2001; Grudd et al., 2002; Jiang et al., 2002; Berglund, 2003; Munroe 2003; D' Arrigo et al., 2004; Loehle, 2004; Fleitman et al., 2004; Hormes et al., 2004; Blundel and Barber, 2005; Linderholm and Gunnarson, 2005; Allen et al., 2007; Mariolakos, 2008) (Fig. 6). Again worth noticing is the fact that polar ice caps did not vanish during the 600 years time span since, again, temperatures were measured in ice core samples and CO_2 concentrations were measured in air bubbles trapped within the ice cores, as well. Subsequently, a cooling period has begun; the last one was until about 900 AD. At its height, the cooling caused the Nile River and the Black Sea to freeze, 829 AD and 800 AD to 801 AD respectively (Pidwirny, 2006).

The period from 900 to 1350 is called the Medieval Warm Period (MWP). During this period, temperatures fluctuated from +0.4°C above the today's (Soon and Baliunas, 2003; Moberg et al., 2005; Viau et al., 2006; Loehle, 2007; Loehle and Mc Culloch, 2008), (Fig. 7), to +0.8°C higher than today's (Seppa and Birks, 2001, 2002; Heikkila and Seppa, 2003). Their estimate was based on pollen data in order to reconstruct past climate thus studying Fennoscandian tree-line fluctuations. The existence of Medieval Warm Period was challenged by Mann et al. (1998; 1999) (Fig. 8) based upon proxy measurements of temperatures from the width of tree rings. However, tree ring data may not capture long-term climate changes (100+ years) because tree size, root/shoot ratio, genetic adaptation to climate, and forest density can all shift in response to pro- longed climate changes, among other reasons (Broecker, 2001; Falcon-Lang, 2005; Loehle, 2005; Moberg et al., 2005).

Most seriously, typical reconstructions assume that tree ring width is linearly related to temperature, but trees may be related in an inverse parabolic manner to temperature, with ring width rising with temperature to an optimal level and then decreasing with further temperature increase (Kelly et al., 1994; D'Arrigo et al., 2004). This response is most likely due to water limitation at higher temperatures due to increase of the evaporation rates. The result of this violation of linearity is to introduce tremendous uncertainty or bias into any reconstruction, particularly for temperatures outside the calibration range. For example, tree rings in many places show recent divergence from observed warming trends, even showing downward trends (Briffa et al., 1998a, 1998b; Pisaric et al., 2007). Other important facts that support the existence of a Medieval Warm Period are archaeological and agricultural data. It is well documented that Greenland was settled from 900 AD till 1350 AD and farming took place due to milder weather than today's (Brown, 2000).

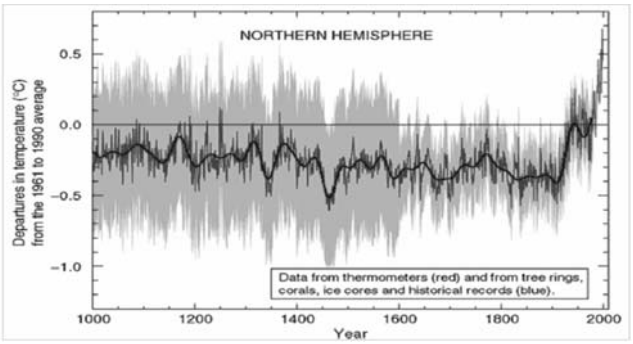

Fig. 8: Millennial Northern Hemisphere (NH) Temperature Reconstruction (blue line) and Instrumental Data (red line from 1000 to 1999 AD, Mann et al., 1999). The graph, "Hockey Stick" relies mainly on tree-rings studies which are annual cycles (high frequency). It is known from geophysics that it is difficult to obtain low frequency (centurial change) data where low frequency is filtered. This graph denies historical records of Medieval Warm Period and Little Ice Age well described by historians (Le Roy Ladurie, 1988; Lamb, 1995).

Also the mere fact that vineyards were extended to North and South England (Schmidt, 2006) during this period indicates, beyond any shadow of doubt, that the climate was much warmer at that time by at least +0.4°C. To have vineyards extending 450 km north of their present northerly growing limit, the climate had to be similar to the one we have today in Southern California, Greece, Italy, Spain etc. Hence, the Hockey Stick diagram (Mann et al., 1998) showing that the +0.4°C during the MWP is well below the acceptable Mean Annual Temperature of 15°C and more or less equivalent to the Little Age Temperatures while the today's +0.35°C is well above the acceptable Mean Annual Temperature of 15°C (Fig. 8), is completely unacceptable. Also unacceptable is the correlation of the proxy measurements of temperatures based on tree rings, 1000 AD to 1850 AD, with those obtained from thermometers, 1850 AD to 2008 AD.

From the above it is concluded that climatic changes were taking place in the past regardless the presence or absence of human beings on Earth, irrespective of atmospheric CO_2 concentrations and without the use of hydrocarbons. An excellent scientific review of thousands of papers along with new scientific data which refutes the alarmist mantra is presented by Singer and Idso (2009).

ii. 1850 AD to 2008 AD

From 1850 thermometric data indicating the Average Mean Annual Temperature of Earth's Surface become available (Jones, 2008; Hadley Meteorological Station, 2008) (Fig. 9). From 1850 to 1910 temperatures were more or less stable fluctuating between -0.4°C and -0.6°C below the optimum average of 15°C. Since 1910, temperatures increased by +0.6°C to reach the optimum of 15°C in 1940. According to NASA's newly published data the hottest year on record in the USA is 1934 and not 1998; three of the hottest years on record occurred before 1940 and six of the top 10 hottest years occurred before 1960[2]. Afterwards temperatures dropped by -0.2°C and stayed at this level, from 1940 to 1980. Subsequently, from 1980 to 1998 the Mean Annual Temperature increased by +0.35°C and remained at this level till 2007. From that date till January 2008 temperature dropped by -0.1°C (Fig. 9). One wonders if this temperature increase, few tenths of a degree, from either 1940 or from 1980 can be considered alarming when in the past much higher temperatures were noticed for extremely long periods without any real damage to either Earth or its inhabitants.

[2] http://data.giss.nasa.gov/gistemp/graphs/ Fig.D.Irg.gif

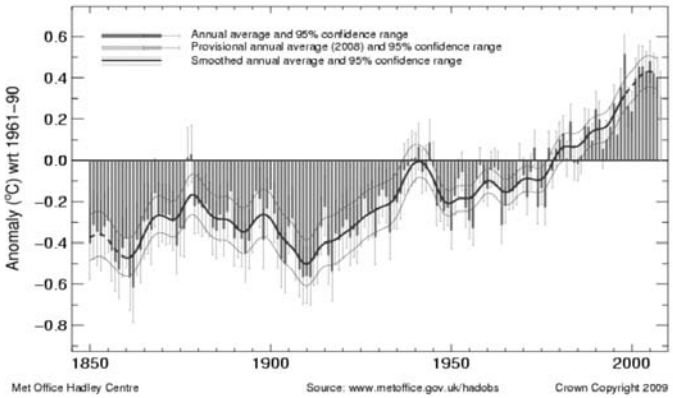

Fig. 9: Global temperature record 1850-2008 (Jones, 2008; http://hadobs.metoffice.com/hadcrut3/diagnostics/global/nh+sh/).

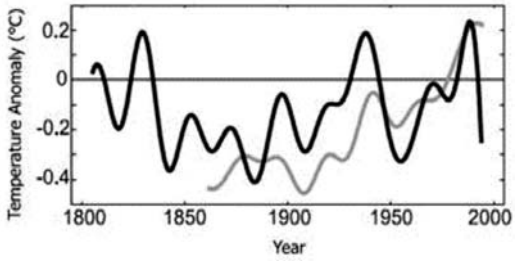

Fig. 10: A 200 year long Antarctic temperature reconstruction (dark line) based upon 200 years sub-annually resolved $\delta^{18}O$ and δD records from precisely dated ice cores obtained from Low Dome Station, Siple Station, Droning Maud Land Station and 2 West Antarctica Sites of the US component of the International Trans-Atlantic Scientific Expedition vs. Mean Temperature of the Southern Hemisphere (lighter line) (Schneider et al., 2006).

Recently (Schneider et al., 2006; see Fig. 10) a series of data suggested that temperatures in Antarctica were colder near the end of the 20th century than it was in the early decades of the 19th century when atmospheric CO_2 concentration was about 100 ppm less than it is currently. This is in agreement with a number of other analyses of Antarctic instrumental surface and air temperature data which also indicate the continent has recently experienced a net cooling, which likely began as early as the mid-1960s (Comiso, 2000; Doran et al., 2002; Thompson and Solomon, 2002).

3. Measurements of atmospheric CO_2 concentrations

Proxy measurements

Proxy measurements of atmospheric CO_2 are carried out using two methods: The first one relies on the relation between the density of stomata in leaves and atmospheric CO_2 concentrations. Paleobotanists can take fossilized leaves and count the number of stomata and therefore get a fairly good picture of how much carbon dioxide was in the atmosphere at the time the leaves died (Kurshner et al., 1996; Beerling et al., 1998; Wagner et al., 1999; 2004; Kouwenberg et al., 2003; Kouwenberg, 2004; Kouwenberg et al., 2005), (Figs 11, 12). The second one assumes that, over time, the concentrations of the various atmospheric gasses are locked when the air bubble is "trapped" in ice.

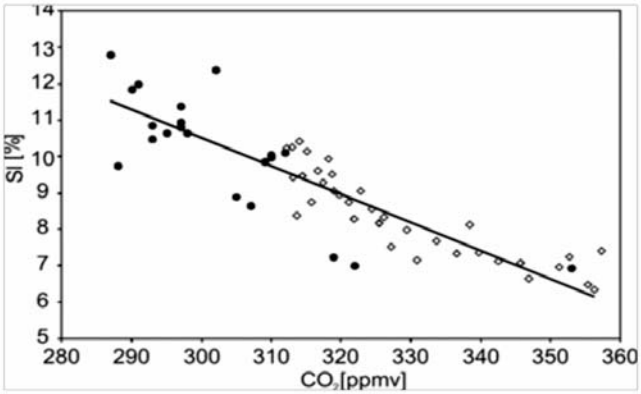

Fig. 11: Correlation of stomata frequency (stomata index=SI) to atmospheric CO_2 from fossil leaves of *B. pendula* (black circles) and *B. pubenscens* (white circles) in lake Little Grisbe, Danemark (Wagner et al., 2004).

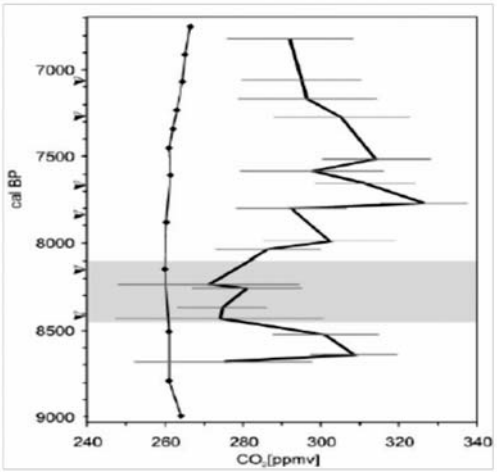

Fig. 12: Reconstruction of Holocene atmospheric CO_2 values from 8700 BC to 6800 BC based upon measurements a) in air bubbles inclusions from Taylor Dome ice core samples (www.ngdc.noaa.gov/paleo/ taylor.html) and b) stomata indices (SI) from fossilized leaves of *B. pendula* and *B. pubescens* (Wagner et al., 2004).

And therefore, as long as it can be determined when the air bubble was trapped, the concentration of CO_2 therein and state can be measured, with confidence, that the atmosphere itself had that same concentration at the time the air bubble was trapped.

However there are two wrong assumptions. Ice, though composed mainly of solid water, does still have some molecules that are in a liquid state. Whether a given molecule is in a solid or liquid (or even gaseous) state, at a given time, depends on how much energy that molecule has at that time. As a result, even at low temperatures, among the three main components of the atmosphere, carbon dioxide is seventy (70) times more soluble than nitrogen and thirty (30) times more soluble than oxygen. This means that, when an air bubble is trapped in ice, not only does the liquid in the ice continue to absorb gasses, but it does so selectively, favouring carbon dioxide, by a huge margin, over the other common gasses in the air bubble. Of course, every molecule of carbon dioxide that passes into a solution is removed from the air within the air bubble.

And therefore, since more carbon dioxide is removed, less carbon dioxide will appear in the re-

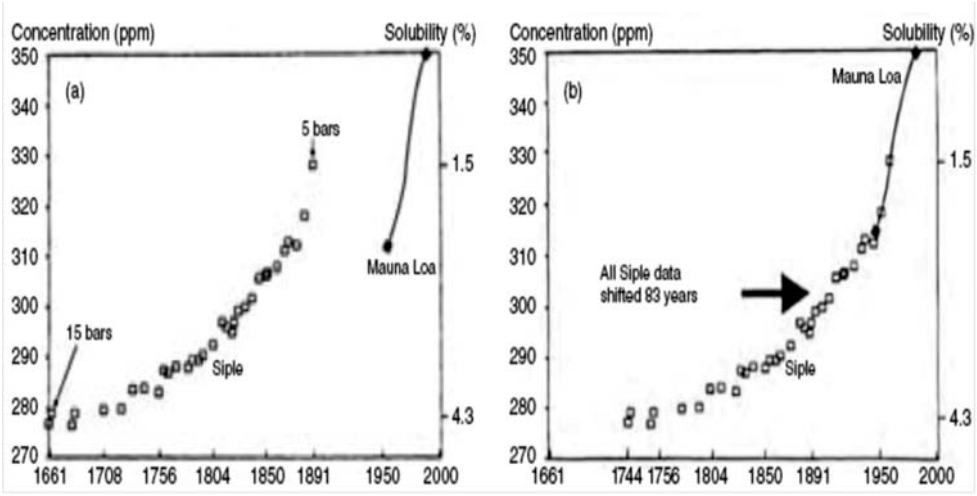

Fig. 13: Concentration of CO_2 in air bubbles from Siple ice core samples, Antarctica (open squares) and in the atmosphere, 1958-1986, Mauna Loa Observatory (solid line), In a) the original Siple data are given assuming an 83 years younger age of the air bubbles in respect to enclosing ice. In b) The same data after arbitrary shifting/correction of the air bubble age (Neftel et al., 1985; Friedli et al., 1986).

maining air. After thousands or millions of years, when that air bubble is tapped, and the gasses within it measured, the concentrations of the various gasses can no longer said to be the same as when that air bubble was trapped, all those years ago (Wiki, Answers, 2009).

Another problem with air bubbles is their dating with respect to the age of ice where trapped in. The consolidation of snow to ice necessary to trap the air takes place at a certain depth (the 'trapping depth') once the pressure of overlying snow is great enough. Since air can freely diffuse from the overlying atmosphere throughout the upper unconsolidated layer (the 'firn'), trapped air is younger than the ice surrounding it. Trapping depth varies with climatic conditions, so the air-ice age difference could vary between 2500 and 6000 years (Barnola et al., 1983; 1987; 1991). This has been acknowledged even by the IPCC scientists by transposing the proxy CO_2 measurements from 1809 to 1892, to read concentrations from 1892 to 1975 (Neftel et al., 1985; Friedli et al., 1986), (Fig. 13). The transposed time was 83 years.

This raises the issue of how the pre-industrial background concentration of CO_2 at 280 ppm has been established (Callendar, 1958). Figure 13 indicates that CO_2 concentration in the atmosphere was not 292 ppm, as stated, but 335 ppm if all the data are considered (Slocum, 1955; Jaworowski et al., 1992). The same background concentration (332 ppm) for the pre-industrial period, is reported by Beck (2007) and Rutledge (2007). Calendar was prejudice in selecting from all his data roughly 30%, which showed concentration around 290 ppm, leaving the remaining 70% which showed concentrations over 300 ppm (Fig. 14).

It must be noted that the mixing of data from ice-core measurements with the direct and actual atmospheric measurements are questionable because the data obtained from the ice-core measurements are unreliable and they do not reflect paleoatmospheric CO_2 concentrations.

Another inconsistency is the past relation between CO_2 concentrations and temperatures based on the today's existing and very accurate data. Currently, atmospheric CO_2 concentration measurements from Mauna Loa Observatory indicate that CO_2 concentrations increased from 315ppm to

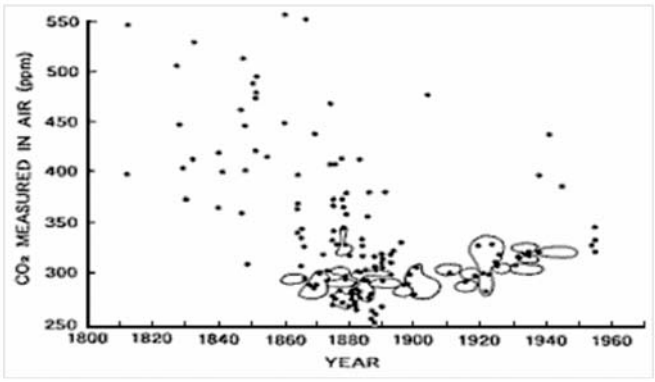

Fig. 14: Average atmospheric CO_2 concentrations measured in the 19th and 20th centuries (Calendar 1958). Calendar rejected both higher and lower values to arrive at the desired background CO_2 value of 290 ppmv. If he had considered all CO_2 values the concentrations would have been 320 ppmv for the 19th century (Jaworowski et al., 1992; Slocum, 1995).

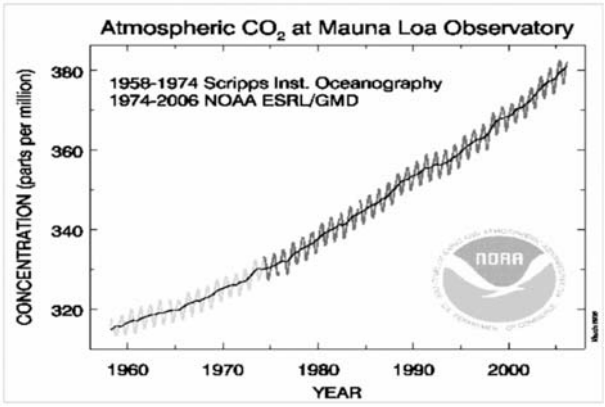

Fig. 15: Atmospheric CO_2 concentration from 1958, 315 ppmv, to 2008, 385 ppmv (Atmospheric CO_2 at Mauna Loa Observatory, Hawaii, USA, 2009).

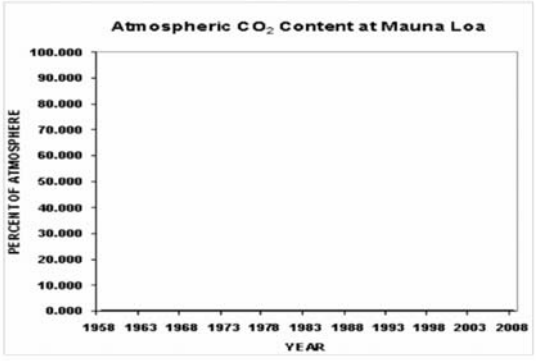

Fig. 16: Atmospheric CO_2 increase during the last 50 years expressed as a percent of the total air composition. It is the, non-discernible, blue line in the bottom (Spencer, 2007) www.jbs.org/jbs-news-feed/4333-fifty-years-of-hot-air-. When comparing the 2 proxy methods it seems that stomata indices (SI), are more reliable as paleoatmospheric CO_2 indicators.

385 ppm (70 ppm) from 1958 to 2008 (Figs 15, 16). From 1940 to date, temperatures, as reported by Jones (2008), increased by +0.35°C above the optimum temperature of 15°C (Fig. 9). One wonders, therefore, if CO_2 concentrations in the atmosphere are the driving force behind temperature in-

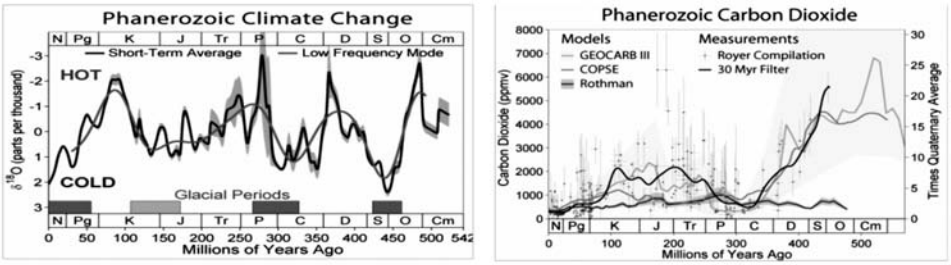

Fig. 17: A. Temperature fluctuation during the Phanerozoic Eon: 500 million years of climate change. en.wikipedia.org/wiki/Geologic-temperature-record. B. Phanerozoic Carbon Dioxide (Royer et al., 2004).

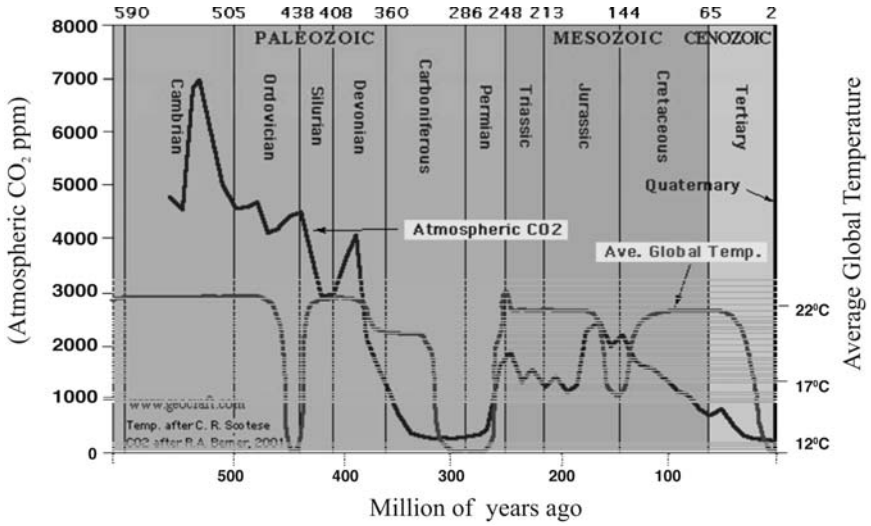

Fig. 18: Correlation of temperature and atmospheric CO_2 concentration over the Phanerozoic time (Berner and Kothavala, 2001; Scotese, 2002).

crease, then why is it that when paleotemperatures, at all interglacial periods, are reported at well over +1°C above the optimum temperature of 15°C, paleo CO_2 concentrations are only 285 ppm. They should have been 460 ppm. Or even higher, if paleotemperatures were +2°C, such as during the Eemian time. The same holds true for the Holocene Epoch period between 8000 AD and 4000 AD when temperatures were +1°C above the optimum temperature of 15°C and the paleoatmospheric CO_2 concentrations were 260 ppm. Henceforth, CO_2 paleoatmospheric concentrations obtained from bubbles yield lower values than stomata indices by 20% (Fig. 12), or by 50% when compared to actual CO_2 measurement concentrations in the atmosphere (Fig. 1).

When comparing the 2 proxy methods it seems that stomata indices (SI) are more reliable as paleoatmospheric CO_2 indicators.

4. The assumed correlation between atmospheric CO_2 and temperature

Examining the possible relationship between CO_2 concentration in the atmosphere, temperatures and presence of Polar ice throughout the Phanerozoic Eon (Fig. 17), it is obvious that such a rela-

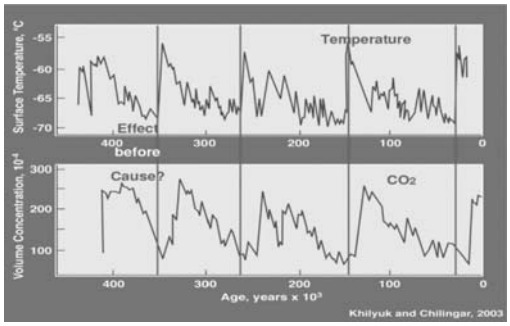

Fig. 19: Time lag between maximum temperatures and atmospheric CO_2 concentration during the Quaternary (Khilyuk and Chiilingar, 2003).

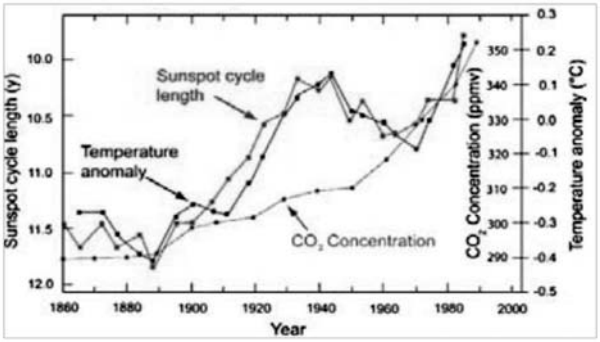

Fig. 20: Correlation between sunspot cycle length, temperature anomalies and atmospheric CO_2 concentration (Friss-Christiensen and Lassen, 1991).

tion does not exist. Polar ice existed from the end of the Silurian Period until the beginning of the Ordovician Period that is for 50 million years, while temperatures were low and the atmospheric CO_2 concentration was close to 4000 ppm, that is 10 times higher than today's (Fig. 18). Examining the relation between atmospheric CO_2 concentrations and temperatures during the Quaternary Period deglaciations periods, it is observed that CO_2 increases lags behind temperature increases by 600±400 years (Khilyuk and Chillingar 2003; 2006), (Fig. 19). The same is also reported by Fisher et al. (1999), Caillon et al. (2003) and Siegenthaler et al. (2005). So it seems that atmospheric CO_2 concentrations are the result of temperature increase rather than the driving force. Exactly the same behaviour is observed between 1850 and 1985 where the increase of atmospheric CO_2 concentration lags behind temperature increase (Friis-Christiensen and Lassen, 1991), (Fig. 20).

Between 1985 and 2000, the atmospheric CO_2 increased along with the temperature which was increased by +0.35°C. This geologically infinitesimal time period, has been used to forecast catastrophic events for mother earth by relating the CO_2 increase in the atmosphere to the rise in temperature. What was omitted was the parallel increase of sunspot numbers which, as will be discussed later, induces temperature increase. However, since 1999, the temperature remained stable until 2006 while CO_2 concentrations increased substantially by 57 billion tons. From 2007 to date, the temperature has been dropping while CO_2 concentrations have risen by an additional 32 billion tons (Fig. 21). An increase of 1 ppmv in the atmosphere requires 2.12 Gt of C. One Gt of C requires 3.667 Gt of CO_2.

Worth mentioning is the fact that during 2008, 35 Gt of CO_2 were emitted from earth (Kahn, 2009; Reuters, 2009), without counting the CO_2 derived from the animal kingdom, while the increase of CO_2 concentration in the atmosphere was only 13 Gt (1.66 ppmv, Mauna Loa Observatory). As a result only 37% of the emitted CO_2 from mother earth stays in the atmosphere. The remaining 22 Gt

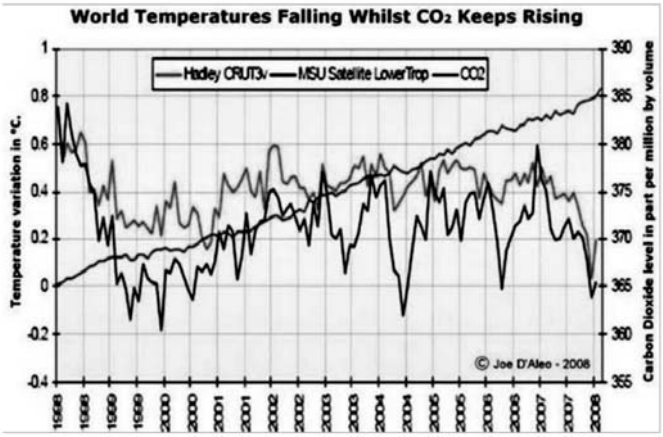

Fig. 21: World temperature is falling while atmospheric CO_2 is rising. Data for a) Average Mean Temperature of Earth's Surface: UK's Hadley Climate Research Unit CRUT3. b) Lower Troposphere Temperature Measurements: NASA's Microwave Sounding Unit (MSU). c) Atmospheric CO_2 concentration: Mauna Loa Observatory, Hawaii, USA (http://icecap.us/images/uploads/Correlation Last Decade pdf).

(63%) returns to earth. And this is done every year. According to NASA (Orbiting Carbon Observatories, OCO) some 66% of the emitted 35 Gt can be attributed to hydrocarbons.

This implies that hydrocarbons contribute roughly 23 Gt of CO_2 every year, roughly the amount that returns back to earth (22 Gt), and hence we have more than one source contributing to the atmospheric CO_2 concentration since the total sum is 35 Gt. The latter could have been easily deduced from the work done by the European scientists from 1812 to 1961 (Beck, 2007). Moreover, it is more than obvious that at least 10 Gt of CO_2 derived from hydrocarbons (43.5%), returns back to earth every year. In reality we do not know the exact CO_2 sources, hence their percent contribution, nor we know where the 22 Gt of CO_2 is disappearing, For this reason, NASA as well as Canada (Spears, 2009) sent, early this year, satellites to resolve these questions.

If we take into account that during the last 50 years, atmospheric CO_2 concentration has increased by 70 ppmv, that is by 0.007%, and that according to NASA OCO 2009 data, 66% of this amount is derived from hydrocarbons, that is 0.0046%[3], then one should wonder if this negligible amount (change of atmospheric air composition in the third decimal point) has caused the climatic change. Is it possible an increase of 2 or even 3 mole, of CO_2 in 100000 moles of other atmospheric gases (currently 39 CO_2 moles in 100000 moles to 41 or 42 CO_2 moles in 100000 moles), to cause a climatic change?

It is therefore seen that there is no relation between atmospheric CO_2 concentrations and small temperature perturbations. But even if there were correlations the influence of CO_2 concentration on temperature is very weak (Lindzen, 2006). Using a logarithmic relationship between the addition of CO_2 to the atmosphere and radiative heating, Lindzen estimated that the 100 ppm post industrial increase in CO_2 concentration (280 ppm pre-industrial to today's 380 ppm) has already caused about 75% of the anticipated I K (+0.37°C) warming, and finally an additional warming of few tenths of a degree occurs.

[3] CO_2 contribution from solid fuels is 40% of the 0.0046% that is less than 0.002%. The carbon capture sequestration (ccs) aims at reducing this 0.002% to 0.001%.

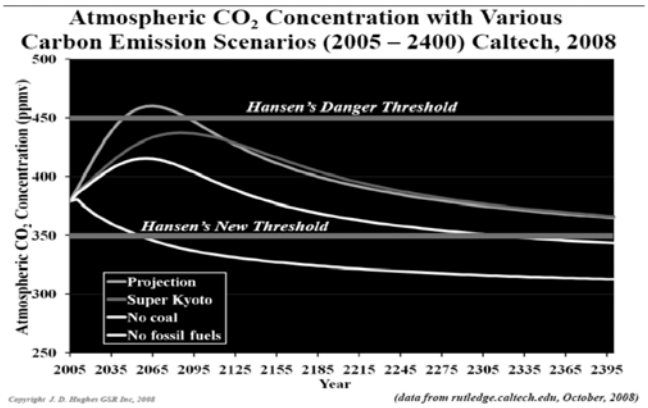

Fig. 22: Atmospheric CO_2 concentrations with various carbon emission scenarios from 2005 AD to 2400 AD, Caltech 2008. Data from rutledge.caltech.edu, October 2008. (Copyright, Hughes, 2009) Worth noticing is the background of 325 ppmv atmospheric CO_2 concentration without the use of hydrocarbons, the same as Beck (2007) and the same if all Calendar's, 1985, data are taken into account.

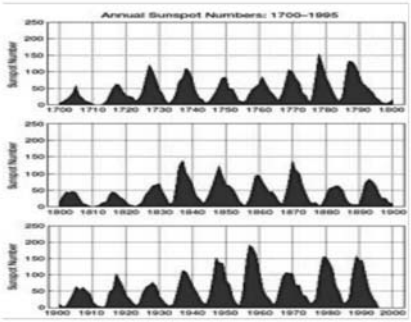

Fig. 23: Sun spot number variations from 1700 AD to 1995 AD (www.ngdc.noaa.gov/stp/SOLAR/SSN/ssn.html).

Sorokhtin et al. (2007) tried to explain the so called "Green House Effect" using the adiabatic theory. This theory is based on the observation that in the troposphere the heat transfer is mainly carried out by convection and the temperature distribution is close to adiabatic. Their reasoning is that air masses expand and cool while rising and compress and heat while descending. As a result, even if the CO_2 concentration in the atmosphere is doubled, that is going from 350 ppm to 700 ppm, the temperature at sea level will increase by 0.01°C.

However, Rutledge (2007) as shown in Figure 22, calculated that of CO_2 concentrations derived from burning fossil fuels cannot exceed 450 ppm. An excellent discussion on the non existing relation between CO_2 concentration in the atmosphere and temperature is presented by Florides and Christodoulides (2009).

5. Relation of Temperature to Solar Activity

The question still remaining is how the small temperature perturbations can be explained when fluctuating between -0.5°C, "The Little Ice Age", to +0.35°C, today's increase. The answer can be found in the Sun's activity, the so called sunspots and solar winds (Svensmark and Friss-Christensen, 1997; Svensmark, 1998; 2007) (Fig. 23).

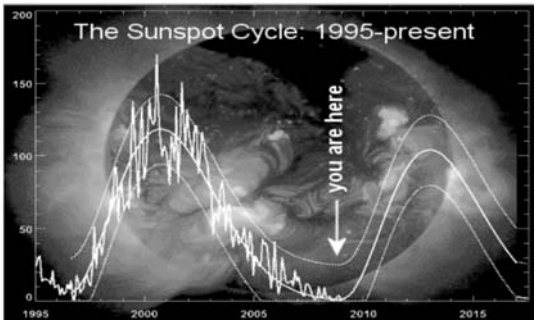

Fig. 24: Eleven (11) year sunspot cycle from 1995 to present. The fluctuation of sunspot numbers is characteristic, (Hathaway, 2008). The correlation with temperature drop Is characteristic (see Fig. 20).

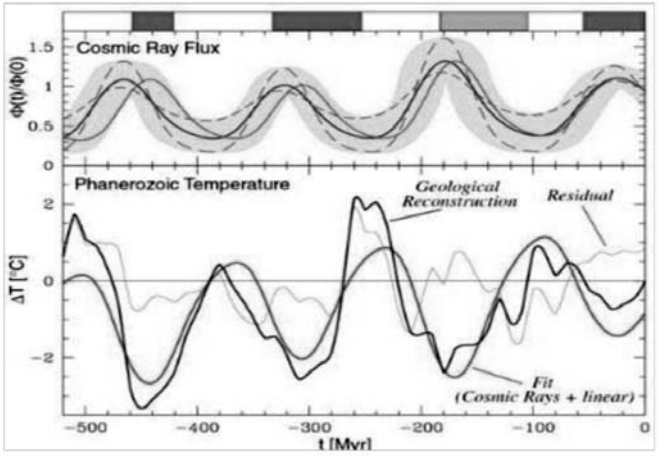

Fig. 25: Celestial drive of Phanerozoic Eon climate? The influence of cosmic ray flux related to temperature change for the last 500 million years with a cycle of about 200 million years, Wilson's cycles (Shaviv and Weiser, 2003).

Sunspots are storms on the sun's surface that are marked by intense magnetic activity and host solar flares and hot gassy ejections from the sun's corona. The number of spots on the sun cycles over time, reaching a peak, the so-called Solar Maximum, every 11 years, Figure 24. Solar winds, according to NASA's Marshall Space Flight Center, consist of magnetized plasma flares and in some cases are linked to sunspots. They emanate from the sun and influence the amount of galactic dust (Murad and Williams, 2002; Landgraf, 2003), which may in turn affect atmospheric phenomena on Earth, such as cloud cover.

It is calculated that when Solar activity is at a minimum, such as in 2009, 40000 tons of galactic dust/space debris (ESA/NASA mission Ulysses) reach the Earth's atmosphere inducing thecondensation of water vapours which leads to clouds formation (Svensmark et al., 2007). Clouds in turn affect the variations seen in temperatures (Shaviv and Weizer, 2003), (Fig. 25).

So the emphasis is on water vapour, which is the number one greenhouse gas, and not CO_2 whose concentration in the atmosphere is 100 times less than water vapour, H_2O. The correlation between sunspot number, the solar activity proxies and the ^{10}Be isotope concentration, which is an indicator of the amount of the galactic dust reaching earth, from 1600 AD until 2000 AD, is presented in Figure 26 (Beer et al., 1994; Hoyt and Schatten 1998a;b).

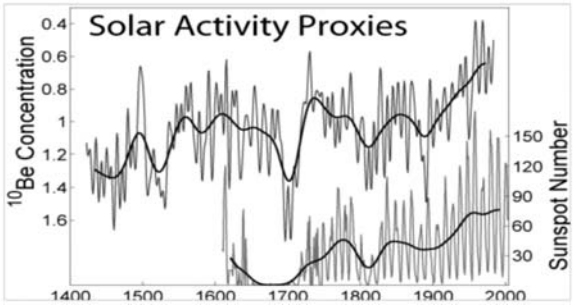

Fig. 26: Solar proxy activities based upon ^{10}Be concentration found n Dye-3, Greenland ice core (Beer et al., 1994). ^{10}Be originates from the incoming galactic dust. Relation to Sunspot number from 1600 AD to 2000 AD (Hoyt and Schatten, 1998a,b).

Another research work by McLean et al. (2009), shows that the surge in global temperature since 1977 can be attributed to a climate shift in the Pacific Ocean that is the relationship between El Nino South Oscillation (ENSO) effect and global temperature. The available data strongly suggests that future global temperatures will continue to change in response to ENSO cycling, solar radiation and volcanic activities.

6. Other Climatic anomalies

Various climatic changes such as the Dansgaard-Oeschger (DO) event have been recognized from ice cores taken from Greenland (GRIP/GISP2) which go back to the end of the last interglacial period, the Eemian Interglacial time. These events seem to have been globally synchronous, and they lasted 1500 years (Voelker, 2003). A lower frequency Bond cycle (Bond et al., 1999; Schulz, 2002; Braun et al., 2005) is characterized by unusually cold conditions that take place during the cold DO phase, the subsequent Heinrich event and the rapid warming phase that follows each Heinrich event (Heinrich 1988; Bond et al., 1992; Grousset et al., 2000). During each Heinrich event, massive fleets of icebergs are released into the North Atlantic, carrying rocks picked up by the glaciers far out to sea. Heinrich events are marked in marine sediments by conspicuous layers of iceberg-transported rock fragments.

Many of the transitions in the DO and Bond cycles were rapid and abrupt, and they are being studied intensively by paleoclimatologists and Earth system scientists to understand the driving mechanisms of such dramatic climatic variations that are not CO_2 driven. These cycles now appear to result from in- teractions between the atmosphere, oceans, ice sheets, and continental rivers that influence thermohaline circulation (the pattern of ocean currents driven by differences in water density, salinity and temperature rather than wind). Thermohaline circulation, in turn, controls ocean heat transport, such as the Gulf Stream which affects the climate of Northern Europe.

Table 1. Major glacial periods in earth's history Glaciations Periods During Paleoproterozoic and Neoproterozoic Ages and the Phanerozoic Eras (www.en.Wikipedia.org/wiki/Timeline-of-glaciation).

Name	Period (Ma)	Period	Era
Quaternary	30 - present	Neogene	Cenozoic
Karoo	360 - 260	Carboniferous and Permian	Paleozoic
Andean-Saharan	450 - 420	Ordovician and Silurian	Paleozoic
Cryogenian (or Sturtian-Varangian)	800 - 635	Cryogenian	Neoproterozoic
Huronian glaciation	2100 - 2400	Siderian and Rhyacian	Paleoproterozoic

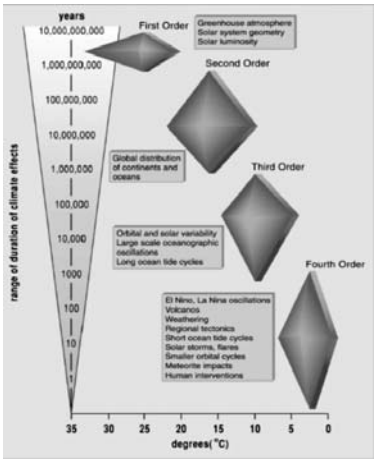

Fig. 27: Geologic constraints on global climate variability. Natural climate drivers ranked by intensity and duration. Human interventions meteorite impacts, volcanic eruptions, El Nino and others are considered the 4th Order affecting climatic variability (Gerhard, 2004).

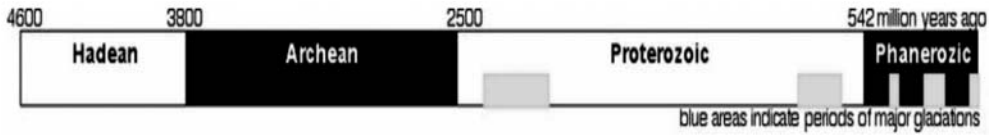

Fig. 28: Major glacial periods in earth's history (www.en.Wikipedia.org/wiki/Timeline-of-glaciation).

Climate, therefore, is driven by many natural processes which operate at many time scales with many scales of influence (Gerhard 2001), (Fig. 27). The mere fact that during the Huronian Glaciation, 2.4 billion years to 2.1 billion years, Paleoproterozoic Era and during the Cryogenian Period, 800 million years to 635 million years ago, Neoproterozoic Era, Earth was totally covered by snow (Tjeerd, 1994; Rieu et al., 2007; Table 1, Fig. 28), while atmospheric CO_2 concentrations were 10 times (Kan and Riding, 2007) to 200 times (Kaufman and Xiao, 2003) higher than today's, and the fact that during the Phanerozoic Era we have glaciations periods irrespective of atmospheric CO_2 concentrations, proves that there are many more natural drivers, besides the miniscule increases of atmospheric CO_2, sunspots and solar winds and Milankovitch cycles, that influence Earth's climate.

7. Conclusions

I. Climatic changes have been the subject of detailed studies for the last 200 years that is since the1800s and not only in the last 20 years.

II. Climatic changes were the norm throughout the Phanerozoic Era.

III. At least 100 glacial and interglacial periods have been measured during the Quaternary Period using Geomagnetic Polarity data.

VI. Climatic Changes during the Quaternary Period were not caused by *Homo sapiens* but by natural climate drivers.

V. During the Holocene Epoch and prior to 1850 AD many climatic changes were identified: The Climatic Optimum from 8000 BC to 4000 BC, with temperatures 1°C to 2°C above the optimum Mean Annual Temperature of 15°C; The Roman Warm Period from 450 BC to 150 AD with temperatures over 2.5°C above the optimum Mean Annual Temperature; and the Medieval

Warm Period from 900 AD to 1400 AD with temperatures over 0.4°C above the optimum Mean Annual Temperature. Homo sapiens who appeared 60000 years ago did not influence these climatic changes. The recent temperature Increase of +0.35°C above the optimum Mean Annual temperature of 15°C from 1980 to 1998 cannot be used to forecast catastrophic events, since from 1999 to date temperatures show a decreasing tendency. In addition, much higher temperatures have been recorded for longer time during the Holocene period without any damage to either earth or its population.

VI. The data, so far, do not support the relation between atmospheric CO_2 and temperature or other climatic changes. By looking into the more reliable and thus far overlooked chemical CO_2 methods for determining atmospheric concentrations one cannot be positive about a relationship between temperature difference and CO_2 concentration. The adiabatic theory suggests that global warming, and hence climatic changes, due to atmospheric CO_2 concentrations is impossible.

VII. Climatic changes are very difficult to assess because there are many natural climate drivers with various intensities and different durations. So, earth's climate system cannot be a function of one and only one factor, namely atmospheric CO_2 concentration.

8. References

Agassiz, L. 1840. Etude sur les glaciers, Nauchatel. Digital book on Wikisource. en. wikipedia. org/wiki/Louis_Agassiz

Allen, J.R.M., Long, A.J., Ottley, C.J., Pearson, D.G., Huntley, B., 2007. Holocene climate variability in northernmost Europe. *Quaternary Science Reviews* 26: 1432-1453.

Arrhenius, S., 1896. On the Influence of Carbonic Acid in the Air Upon the Temperature of the Ground. *Philosophical Magazine* 41: 237-76.

Arrhenius, S., 1901. Über die Wärmeabsorption Durch Kohlensäure und Ihren Einfluss auf die Temperatur der Erdoberfläche. *Förhandlingar Svenska Vetenskapsakademiens* 58: 25-58.

Atmospheric CO_2 at Mauna Loa Observatory, 2009. Scripps Institute of Oceanography and US Department of Commerce, National Oceanic and Atmospheric Administration, Earth System Research Laboratory, Gas Monitoring Data (NOAA ESRL/GMD). Http.//en.wikipedia.org/wiki/File: CO_2-Mauna-Loa.png

Barnola, J.-M., Raynaud, D., Korotkevich, Y.S., Lorius, C., 1987. Vostok ice core provides 160,000-year record of atmospheric CO_2. *Nature* 329: 408-14.

Barnola, J.-M., Raynaud, D., Neftel, A., Oeschger, H., 1983. Comparison of CO_2 measurements by two laboratories on air from bubbles in polar ice. *Nature* 303: 410-13.

Barnola, J.-M., Pimienta, P., Raynaud, D., Korotkevich, Y.S., 1991. CO_2-climate relationship as deduced from the Vostok ice core: A re-examination based on new measurements and on a re-evaluation of the air dating. *Tellus* 43(B):83- 90.

Barendregt, R.W., Duk-Rodkin, A., 2004. Chronology and Extent of Late Cenozoic Ice Sheets in North America: A magnetostratigraphic Assessment" in Quaternary Glaciations-Extent and Chronology, Part II, editors, J. Ehlers and P.L. Gibbard. *Quaternary Science Reviews*, p. 1-7.

Beck, E.G., 2007. 180 years of atmospheric CO_2 gas analysis by chemical methods. *Energy and Environ*., 18, 259-282.

Beer, J., Baumgartner, St., Dittrich-Hannen, B., Hauenstein, J., Kubik, P., Lukasczyk, Ch., Mende, W., Stellmacher, R., Suter, M., 1994. Solar Variability Traced by Cosmogenic Isotopes in The Sun as a Variable Star: Solar and Stellar Irradiance Variations (eds. J.M. Pap, C. Fröhlich, H.S. Hudson and S.K. Solanki), Cambridge University Press, 291-300.

Beerling, D.J., McElwain, J.C., Osborne, C.P. 1998. Stomatal responses of the 'living fossil' *Gingo biloba L.* to changes in atmospheric CO_2 concentrations. *Journal of Experimental Botany* 49, 1603-1607.

Berglund, B.E., 2003. Human impact and climate changes — synchronous events and a causal link? *Quaternary International* 105, 7-12.

Berner, R.A., Kothavala, Z. GEOCARB III: 2002. A revised model of atmospheric CO_2 over Phanerozoic time. IGBP PAGES/World Data Center for Paleoclimatology, Data Contribution Series #2002-051. NOAA/NGDC Paleoclimatology Program, Boulder CO, USA; 2001. bhttp://www1.ncdc.noaa.gov/pub/data/paleo/climate_forcing/trace_gases/phanerozoic

Blundell, A., Barber, K., 2005. A 2800-year palaeoclimatic record from Tore Hill Moss, Stratspey, Scotland: the need for a multi-proxy approach to peat-based climate reconstructions. *Quaternary Science Reviews* 24, 1261-1277.

Bond, G., Heinrich, H., Broecker, W., Labeyrie, L., Mcmanus, J., Andrews, J., Huon, S., Jantschik, R., Clasen, S., Simet, C., 1992. Evidence for massive dis- charges of icebergs into the North Atlantic ocean during the last glacial period. *Nature* 360, 245–249.

Bond, G.C., Showers, W., Elliot, M., Evans, M., Lotti, R., Hajdas, I., Bonani, G., Johnson, S., 1999. The North Atlantic's 1–2 kyr climate rhythm: relation to Heinrich events, Dansgaard/Oeschger cycles and the little ice age. In Clark, P.U., Webb, R.S., Keigwin, L.D. Mechanisms of Global Change at Millennial Time Scales. Geophysical Monograph. American Geophysical Union, Washing- ton DC. pp. 59–76. ISBN 0-87590-033-X.

Braun, H., Christl, M., Rahmstorf, S., Ganopolski, A., Mangini, A., Kubatzki, C., Roth, K., Kromer, B., 2005. Possible solar origin of the 1,470-year glacial climate cycle demonstrated in a coupled model. *Nature*, 438, 208-211.

Briffa, K.R., Osborn, T.J., Schweingruber, F.H., Harris, I.C., Jones, P.D., Shiyatov, S.G., Vaganov, E.A., 1998a. A low-frequency Temperature Variations from a Northern Tree Ring Density Network. *Journal of Geophysical Research*, 106 D3 pp. 2929-2941.

Briffa K.R., Jones, P.D., Schweingruber, F.H., Osborn, T.J., 1998b. Influence of volcanic eruptions on northern hemisphere summer temperature over the past 600 years. *Nature*, 393, 450-455.

Broecker, W.S., 2001. Was the Medieval Warm Period global? *Science*, 291, 1497-1499.

Brown, Dale Mac Kenzie, 2000. The fate of Greenland's Viking. Time-Life's Book.www.archaelogy.org/online/features/Greenland/-Caillon N, Severinghaus J.P., Jouzel J., Barnola, J. M., Kang, J., Lipenkov, V.Y., 2003. Timing of atmospheric CO_2 and Antarctic temperature changes across termination III. *Science*, 299, 1728–1731.

Caillon, N., Severinghaus, J.P., Jouzel, J., Barnola, J.M., Kang, J., Lipenkov, V.Y., 2003. Timing of atmospheric CO_2 and Antarctic temperature changes across termination III. *Science*, 299, 1728–1731.

Callendar, G.S., 1958. On the amount of carbon dioxide in the atmosphere. *Tellus*, 10, 243-248.

Cande, S.C., Kent, D.V., 1995. Revised calibration of the geomagnetic polarity timescale for the Late Cretaceous and Cenozoic. *Journal of Geophysical Research*, B100, 6093-6095.

Comiso, J.C., 2000. Variability and trends in Antarctic surface temperatures from in situ and satellite infrared measurements. *Journal of Climate*, 13, 1674-1696.

Croll, J., 1864. On the Physical Cause of the Change of Climate During Geological Epochs. *Philosophical Magazine*, 28, 121-37.

Czerney, Franz von 1881. Die Veränderlichkeit des Klimas und Ihre Ursachen. Vienna.

Dansgaard, W., Johnsen, S.J., Moller, J., 1969. One thousand centuries of climatic record from the Camp Century on the Greenland Sheet. *Science*, 166, 377-381.

D' Arrigo, R., Mashig, E., Frank, D., Jacoby, G., Wilson, R., 2004. Reconstructed warm season temperatures

for Nome, Seward Peninsula, Alaska. *Geophysical Research Letters*, 31, 10.1029/2004GL019756.

Doran, P.T., Priscu, J.C., Lyons, W.B., Walsh, J.E., Fountain, A.G., McKnight, D.M., Moorhead, D.L., Virginia, R.A., Wall, D.H., Clow, G.D., Fritsen, C.H., McKay, C.P., Parsons, A.N., 2002. Antarctic climate cooling and terrestrial ecosystem response. Nature advance online publication, 13 January 2002 (DOI 10.1038/nature710).

EPICA community members 2004. Eight glacial cycles from an Antarctic ice core. *Nature* 429, 623-628, doi:10.1038/nature02599.

Falcon-Lang, H.J., 2005. Global climate analysis of growth rings in woods, and its implications for deep-time paleoclimate studies. *Paleobiology*, 31, 434-444.

Fisher, H., Wahlen, M., Smith, J., Mastoianni, D., Deck, B., 1999. Ice core records of atmospheric CO2 around the last three Glacial terminations. *Science*, 283, 1712-1714.

Fleitmann, D., Burns, S.J., Neff, U., Mudelsee, M., Mangini, A., Matter, A., 2004. Palaeoclimatic interpretation of high-resolution oxygen isotope profiles derived from annually laminated speleothems from Southern Oman. *Quaternary Science Reviews*, 23, 935-945.

Florides, G.A., Christodoulides, P., 2009. Global warming and carbon dioxide through sciences. *Environmental International*, 35, 390-401.

Fourier, J., 1824. Remarques Générales sur les Températures Du Globe Terrestre et des Espaces Planétaires. Annales de Chemie et de Physique 27: 136-67. Translation by Ebeneser Burgess, "General Remarks on the Temperature of the Earth and Outer Space," *American Journal of Science* 32, 1-20.

Fourier, J., 1827. Mémoire sur les Températures du Globe Terrestre dt des Espaces Planétaires. *Mémoires de l'Académie Royale des Sciences*, 7, 569-604.

Franklin, B., 1784. Meteorological Imaginations and Conjectures (Paper Read 1784). Memoirs of the Literary and Philosophical Society of Manchester 2nd ed., 1789: 373-77. *Reprinted Weatherwise* 35, 262 (1982).

Friedli, H., Lotscher, H., Oeschger, H., Siegenthaler, U., Stauffer, B., 1986."Ice core record of the 13C/12C ratio of atmospheric CO_2 in the past two centuries." *Nature*, 324, 237-238.

Friss-Christiensen, E., Lassen, K., 1991. Length of the solar cycle: An indicator of solar activity closely associated with climate. *Science*, 254, 698-700.

Galaxy M104. Hubble Heritage Gallery Images, 2009. www. Heritage.stsci.edu/…./galindex.html

Gerhard, L.C., 2001. Natural processes are the most significant climate drivers. www.geocraft.com/VW-Fossills/.../Gerhard-Climate-Change. pdf

Grousset, F.E., Pujol, C., Labeyrie, L., Auffret, G., Boelaert, A., (2000-02-01). "Were the North Atlantic Heinrich events triggered by the behaviour of the European ice sheets?" (abstract). Geology, 28(2): 123–126. doi:10.1130/0091-7613(2000)28<123:WTNAHE>2.0.CO;2. http://geology.geoscienceworld.org/cgi/content/abstract/28/2/123

Grudd, H., Briffa, K.R., Karlen, W., Bartholin, T.S., Jones, P.D., Kromer, B., 2002. A 7400-year tree-ring chronology in northern Swedish Lapland: natural climatic variability expressed on annual to millennial timescales. *The Holocene*, 12, 657-665.

Hadley Meterological Center, 2008. HadCRUT 3. Global temperature record. Met Office Hadley Center for Climatic Prediction and Research. www.metoffice.gov.uk/corporate/pressoffice/ 20081216 html-27K

Hathaway, D., 2008. What is wrong with the Sun? (Nothing). science.nasa.gov/…./11 Jul- solarcycle-update.html

Hayes, J.D., Imbrie, J., Shackleton, N.J., 1976. Variations in the Earth's Orbit: Pacemaker of the Ice Ages. *Science*, 194, 1121-1132.

Heikkila, M., Seppa, H., 2003. A 11,000-yr palaeotemperature reconstruction from the southern boreal zone in Finland. *Quaternary Science Reviews*, 22, 541-554.

Heinrich, H., 1988. Origin and consequences of cyclic ice rafting in the Northeast Atlantic Ocean during the past 130,000 years. *Quaternary Research*, 29, 142-152.

Holmgren, K., Karlen, W., Lauritzen, S.E., Lee-Thorp, J. A., Partridge, T. C., Piketh, S., Repinski, P., Stevenson, C., Svanered, O., Tyson, P.D., 1999. A 3000-year high-resolution stalagmite-based record of paleoclimate for north- eastern South Africa. *The Holocene*, 9, 295-309.

Holmgren, K., Tyson, P.D., Moberg, A., Svanered, O., 2001. A preliminary 3000-year regional temperature reconstruction for South Africa. *South African Journal of Science*, 99, 49-51.

Hormes, A., Karlen, W., Possnert, G., 2004. Radiocarbon dating of palaeosol components in moraines in Lapland, northern Sweden. *Quaternary Science Reviews*, 23, 2031-2043.

Hoyt, D.V., Schatten, K.H., 1998a. Group sunspot numbers: A new solar activity reconstruction. Part 1. *Solar Physics*, 179, 189-219.

Hoyt, D. V., Schatten K.H., 1998b. Group sunspot numbers: A new solar activity reconstruction. Part 2. *Solar Physics*, 181, 491-512.

Hughes, J. D., 2009. The energy sustainability dilemma: Powering the future in a finite world. Global Sustainability Research, Inc. Contact: dave-hughes@xplornet.com

Idso, C.D., Idso, K.E., 2000. The Greening of the American West. Center for the Study of Carbon Dioxide and Global Change, Tempe, AZ, USA.

Jaworowski, Z., Segalstad, T.V., Ono, N., 1992. Do glaciers tell a true atmospheric CO_2 story? *The Science of the Total Environment*, 114, 227-284.

Jones, P., 2008. Global temperature record. www.cru.uea. ac.uk/cru/info/warming/ and Brohan, P., J.J. Kennedy, I. Harris, S.F.B. Tett and P.D. Jones, 2006: Uncertainty estimates in regional and global observed tem- perature changes: a new dataset from 1850. *J. Geophysical Research* 111, D12106.

Jiang, H., Seidenkrantz, M-S., Knudsen, K.L., Eiriksson, J., 2002. Late-Holocene summer sea-surface temperatures based on a diatom record from the north Icelandic shelf. *The Holocene*, 12, 137-147.

Kah, L.C., Riding, R., 2007. Mesoproterozoic carbon dioxide levels inferred from calcified cyanobacteria. *Geology*, 35, 799-802.

Kahn, M., 2009. Forests absorb 20% of fossil fuel emissions: study. www.reuters.com/article/ …../idUSTRE 5IH5KE 20092018

Kaufman, A.J., Xiao, S., 2003. High CO_2 levels in the Proterozoic atmosphere estimated from analyses of individual microfossils. *Nature*, 425, 279-282.

Keigwin, L.D., 1996. The Little Ice Age and Medieval Warm Period in the Sargasso Sea. *Science*, 274, 1504-1508.

Kelly, P.F., Kobes, R., Kunstatter, G., 1994. Parametrization invariance and the resolution of the unitary gauge puzzle. *Phys. Rev.* D 50, 7592-7602.

Khilyuk, K., Chillingar G.V., 2003. Global warming: are we confusing cause and effect. Energy Sources, 25, 357-370.

Khilyuk, K., Chillingar, G.V., 2006. Global forces of nature driving the Earth's climate. Are humans involved? *Environmental Geology*, 50, 899-910.

Krüger, T., 2008. Die Entdeckung der Eiszeiten. Internationale Rezeption und Konsequenzen für das Verständnis der Klimageschichte, Basel 2008, ISBN 978-3-7965-2439-4, pp.220-223, pp. 223-224, pp. 540-542.

Köppen, W., 1873. Über Mehrjährige Perioden der Witterung, Insbesondere Über die 11jährige Periode der Temperatur. *Zeitschrift der Osterreichischen Gesellschaft für Meteorologie*, 8, 41-48, 141-50.

Kouwenberg, L.L.R., McElwain, J.C., Kurschner, W.M., Wagner, F., Beerling, D.J., Mayle, F.E., Visscher, H., 2003. Stomatal frequency adjustment of four conifer species to historical changes in at-

mospheric CO_2. *American Journal of Botany*, 90, 610-619.

Kouwenberg, L., 2004. Application of Conifer Needles in the Reconstruction of Holocene CO_2 Levels. PhD Thesis, University of Utrecht; 2004. bhttp://www.bio.uu.nl/~palaeo/Personeel/ Lenny/artikellinks/full.pdfN

Kouwenberg, L., Wagner, R., Kurschner, W., Visscher, H., 2005. Atmospheric CO_2 fluctuations during the last millennium reconstructed by stomatal frequency analysis of *Tsuga heterophylla* needles. *Geology*, 33, 33–36.

Kurschner, W.M., Burgh, van der, J., Visscher, H., Dilcher, D.L., 1996. Oak leaves as biosensors of late Neogene and early Pleistocene paleoatmospheric CO_2 concentrations. *Marine Micropaleontology*, 27, 299-312.

Lamb, H.H., 1995. *Climate, History and the Modern World*. Publisher: Routledge, 464 pp. ISBN: 13: 9780415127356.

Landgraf, M., 2003. *Galactic dust storm enters Solar System*. www.Mewscientist.com/.../dn4021-galactic-dust-storm-enters-solar-system.html

Le Roy Ladurie, E., 1988. *Times of feast, times of famine: a history of climate since the year 1000*. Farrar-Straus and Giroux, Publisher, ISBN: 13: 9780374521220.

Loehle, C., 2004. Climate change: detection and attribution of trends from long-term geologic data. *Ecological Modelling*, 171, 433-450.

Loehle, C., 2005. Estimating climatic timeseries from multi-site data afflicted with dating error. *Mathematical Geology*, 37, 127-140.

Loehle, C., 2007. A 2000 Year Global Temperature Reconstruction based on Non-Tree ring Proxy Data. *Energy & Environment*, 18, 1049-1058.

Loehle, C., McCulloch, J.H., 2008. Correction to: A 2000-year global temperature reconstruction based on non-treering proxies. *Energy & Environment*, 19, 93-100.

Linderholm, H.W., Gunnarson, B.E., 2005. Summer temperature variability in central Scandinavia during the last 3600 years. *Geografiska Annaler*, 87A, 231-241.

Lindzen, R., 2005. Understanding common climate claims. International Seminar on Nuclear War and Planetary Emergencies—34th Session, Erice, Italy, 19–24 August, 2005. Proceedings World Federation of Scientists; 2006. bhttp://www.worldscibooks.com/environsci/ 6076.htmlN

Mann, M.E., Bradley, R.S., Hughes, M.K., 1998. Global-scale temperature patterns and climate forcing over the past six centuries. *Nature*, 392, 779-787.

Mann, M.E., Bradley, R.S., Hughes, M.K., 1999. Northern hemisphere temperatures during the past millennium: inferences, uncertainties, and limitations. *Geophysical Research Letters*, 26, 759-762.

Mariolakos, I.D., 2008. Water and Environment. A Geo-Mythological Approach. AQUA 2008. 4th Intl. Exhibition of Water and Environment. www.mio-ecsde.org/filemgmt/visit. php2?lid= 364

Milankovitch, M., 1940. *Mathematische Klimalehre und Astronomische Theorie der Klimaschwankungen*. In Handbuch der Klimatologie, edited by W. Köppen and R. Geiger, Vol. 1, Pt. A, pp. 1-176. Berlin: Borntraeger.

Moberg, A., Sonechkin, D.M., Holmgren, K., Datsenko, N.M., Karlén, W., 2005. Highly variable Northern Hemisphere temperatures reconstructed from low- and high resolution proxy data. *Nature*, 433, 613-617.

Munroe, J.S., 2003. Estimates of Little Ice Age climate inferred through historical rephotography, Northern Unita Mountains, U.S.A. Arctic. *Antarctic and Alpine Research*, 35, 489-498.

Murad, E., Williams, I.P., 2002. Meteors in the Earth's Atmosphere: Meteoroids and Cosmic Dust and their Interaction with Earth's Upper Atmosphere. Cambridge Univ. Press 322p. ISBN-13: 9780521804318, ISBN: 10: 0521804310 NASA's OCO satellite. Aims to Solve a Climate Change. Scientific American 2009 www.scientificamerican.com/article.cfm?id= nasas...satellite

Neftel, A., Moor, E., Oeschger, H., Stauffer, B., 1985. Evidence from polar ice cores for the increase in atmospheric CO_2 in the past two centuries. *Nature*, 315, 45-47.

Olafsdottir, R., Schlyter, P., Haraldsson, H.V., 2001. Simulating Icelandic vegetation cover during the Holocene: Implications for long-term land degradation. *Geografiska Annaler*, 83A, 203-215.

Petit, J.R., Basile, I., Leruyuet, A., Raynaud, D., Lorius, C., Jouzel, J.M., Stievenard, M., Lipenkov, V.Y., Barkov, N.I., Kudryashov, B.B., Davis, M., Saltzman, E., Kotlyakov. V., 1997. Four climate cycles in Vostok ice core. *Nature*, 387, 359-360.

Petit, J.R., Jouzel, J., Raynaud, D., Barkov, N.I., Barnola, J.-M., Basile, I., Benders, M., Chappellaz, J.,Davis, M., Delayque, G., Delmotte, M., Kotlyakov, V.M., Legrand, M., Lipenkov, V.Y., Lorius, C., Pépin, L., Ritz, C., Saltzman, E., Stievenard, M., 1999. Climate and atmospheric history of the past 420,000 years from the Vostok ice core, Antarctica. *Nature*, 399, 429-436.

Pidwirny, M., 2006. Earth's Climatic History. Fundamentals of Physical Geography, 2nd Edition. Date Viewed. http://www.physicalgeography.net/fundamentals/7x.html

Pisaric, M., Carey, S., Kokelj, S., Youngblut, D., 2007. Anomalous 20th century tree growth, Mackenzie Delta, Northwest Territories, Canada. *Geophysical Research Letters*, 34, doi:10.1029/2006GL029139

Raymo, M.E., 1992. Global climate change: a three million year perspective. In: Kukla, G. and Went, E. (eds.), Start of a Glacial, Proceedings of the Mallorca NATO ARW, NATO ASI Series I, Vol. 3, Springer-Verlag, Heidelberg, p. 207-223.

Reuters, 2009. Orbital Set to Launch Orbiting Carbon Observatory Earth Sci- ence Satellite Aboard Taurus Rocket for NASA, Monday February 23, 2009.

Rieu, R., Allen, P.A., Plotze, M., Pettke, T., 2007. Climatic cycles during a Neoproterozoic "snowball" glacial epoch. *Geology*, 35, 299–302.

Royer, D.L., Berner, R.A., Montañez, I.P., Tabor, N.J., Beerling, D.J., 2004. CO_2 as a primary driver of Phanerozoic climate. GSA Today 2004; 14(3). doi:10.1130/1052-5173.<http://www.soest.hawaii.edu/GG/FACULTY/POPP/Royer%20et%20al.%202004%20GSA%20Today.pdf>.

Ruddiman, W.F., Raymo, M.E., Martinson, D.G., Clement, B.M., Backman, J., 1989. Mid-Pleistocene evolution of Northern Hemisphere climate. *Paleoceanography*, 4, 353-412.

Rutledge, D., 2007. Hubbert's Peak, the coal question and climate change. http;//www.aspousa.org/ proceedings/Houston/presentations/talk 20% for 20% ASPO % from Dave%20 Rutledge pdf

Schönwiese, C., 1995. Klimaänderungen: Daten, Analysen, Prognosen, Springer, Heidelberg (Link to Amazon http://www.amazon.com/Klima%C3%A4nderungen-Daten-Analysen-Prognosen- German/dp/354059096X

Schmidt, G., 2006. Medieval warmth and English wine. RealClimate. http://www.realclimate.org/index.php/archives/2006/07/medieval-warmth-and-english-wine/. Retrieved 2006-07-12.

Schneider, D.P., Steig, E.J., van Ommen, T.D., Dixon, D.A., Mayewski, P.A., Jones, J.M., Bitz, C.M., 2006. Antarctic temperatures over the past two centuries from ice cores. *Geophysical Research Letters*, 33, 10.1029/2006GL027057.

Schulz, M., 2002. On the 1470-year pacing of Dansgaard-Oeschger warm events. *Paleoceanography* 17, 1014. doi:10.1029/2000PA000571

Scotese, C. R., 2002. PALEOMAP Project, Arlington, Texas; 2002. http://www.scotese.comN

Seppa, H., Birks, H.J.B., 2001. July mean temperature and annual precipitation trends during the Holocene in the Fennoscandian tree-line area: pollen-based climate reconstruction. *The Holocene*, 11, 527-539.

Seppa, H., Birks, H.J.B., 2002. Holocene climate reconstruction from the Fennoscandian tree-line area based on pollen data from Toskaljavri. *Quaternary Research*, 57, 191-199.

Shaviv, N.J., Weizer, J., 2003.Celestial driver of Phanerozoic climate? *GSA Today*, 13, 4-10.

Siegenthaler, Urs., Stokes, T,F., Monnin, E., Luthi, D., Schwander, J., Stauffer, B., Raynaud, D., Barnola, J.-M., Fischer, H., Masson-Delmotte, V., Jouzel, J., 2005. Stable carbon cycle-climate relationship during the Late Pleistocene. *Science*, 310, 1313-1317.

Singer, F.S., Idso, G., 2009. Climate change reconsidered. The Heartland Institute, 880 p. ISBN-10: 1934791288.

Slocum, G., 1955. Has the amount of carbon dioxide in the atmosphere changed significantly since the beginning of the twentieth century? Month. Weather Rev.,1955 (October): 225-231.

Soon, W., Baliunas, S., 2003. Proxy Climatic and Environmental Changes of the Past 1000 Years. *Climate Research*, 23, 89-110.

Sorokhtin, O.G., Chillingar, G.V., Khilyuk, L.F., 2007. Global warming and global cooling. Evolution of climate on earth. Developments in Earth & Environmental Sciences, 978-0-444-53815-5.

Spears, T., 2009. Canadian mini-satellite may solve carbon puzzle. www2.canada.com/ calgaryherald/news/story.html?id

Spencer, R., 2007. 2000 years of Global Temperatures: The 2007-2008 Global cooling event. www. drroy spencer. com/

Svensmark, H., Friss-Christensen, E., 1997. Variation of cosmic ray flux and global cloud relationships. *J. Atm. Solar-Terrest. Phys.*, 59, 1225-1232.

Svensmark, H., 1998. "Influence of Cosmic Rays on Earth's Climate". *Physical Review Letters*, 81, 5027–5030.

Svensmark, H, Pedersen, J. O. P., Marsh, N.D., Enghoff, M. B., Uggerhøj, U.I., 2007. "Experimental evidence for the role of ions in particle nucleation under atmospheric conditions". Proceedings of the Royal Society A: Mathematical, Physical and Engineering Sciences 463, 385–396.

Svensmark, H., 2007. Astronomy & Geophysics Cosmoclimatology: a new theory emerges. *Astronomy & Geophysics*, 48, 1.18–1.24.

Thompson, D.W.J., Solomon, S., 2002. Interpretation of recent Southern Hemisphere climate change. *Science*, 296, 895-899.

Tjeerd, H. van A., 1994. New Views on an Old Planet: A History of Global Change 2nd ed. Cambridge University Press, Cambridge, UK, p. 457 10: ISBN 0521447550.

Tyndall, J., 1861. On the Absorption and Radiation of Heat by Gases and Vapours. *Philosophical Magazine* ser. 4, 22, 169-94, 273-85.

Tyndall, J., 1863. On Radiation through the Earth's Atmosphere. *Philosophical Magazine* ser. 4, 25, 200-206.

Viau, A.E., Gajewski, K., Sawada, M.C., Fines, P., 2006. Millennial-scale temperature variations in North America during the Holocene. *Journal of Geophysical Research*, 111, D09102, doi: 1029/2005JD006031.

Voelker, A.H.L., 2002. Global distribution of centennial-scale records for Marine Isotope Stage (MIS) 3: a database. *Quaternary Science Reviews*, 21, 1185-1212. doi:10.1016/S0277-3791(01)00139-1.

Wagner, F., Sjoerd J.P., Bohncke, S.J.P., Dilcher, D.L., Kürschner, W.M., Geel, van B., Visscher, H., 1999. Century-Scale Shifts in Early Holocene Atmospheric CO_2 Concentration. *Science*, 284, 1971-1973.

Wagner, F., Lenny, L.R., Kouwenberg, L.LR., van Hoof, T.B., Visscher, H., 2004. Reproducibility of Holocene atmospheric CO_2 records based on stomatal fre- quency. *Quaternary Science Review*, 23, 1947-1954.

Wiki Answers, 2009. How reliable are air bubbles in ice core samples for deter- mining historic levels of Carbon Dioxide in the atomsphere?wiki.answers.com/.../ How_reliable_are_air_bubbles_in_ice_core_samples_for_determining_historic_levels_of_Carbon_Dioxide_in_the...

Δελτίο της Ελληνικής Γεωλογικής Εταιρίας, 2010
Πρακτικά 12ου Διεθνούς Συνεδρίου
Πάτρα, Μάιος 2010

Bulletin of the Geological Society of Greece, 2010
Proceedings of the 12th International Congress
Patras, May, 2010

GEOPHYSICAL STUDIES AND TECTONISM OF THE HELLENIDES

Makris J.

University of Hamburg and GeoPro GmbH, 20457 Hamburg, Germany

Abstract

By constraining gravity modelling by Deep Seismic Soundings (DSS) and the Bouguer gravity field of Greece a 3-D density-velocity model of the crust and upper mantle was developed. It was shown that in the north Aegean Trough and the Thermaikos Basins the sediments exceed 7 km in thickness. The basins along the western Hellenides and the coastal regions of western Greece are filled with sediments of up to 10 km thickness, including the Prepulia and Alpine metamorphic limestones.

The thickest sedimentary series however, were mapped offshore southwest and southeast of Crete and are of the order of 12 to 14 km. The crust along western Greece and the Peloponnese ranges between 42 and 32 km thickness while the Aegean region is floored by a stretched continental crust varying between 24 to 26 km in the north and eastern parts and thins to only 16 km at the central Cretan Sea. The upper mantle below the Aegean Sea is occupied by a lithothermal system of low density (3.25 gr/cm^3) and Vp velocity (7.7 km/s), which is associated with the subducted Ionian lithosphere below the Aegean Sea.

Isostasy is generally maintained at crustal and subcrustal levels except for the compressional domain of western Greece and the transition between the Mediterranean Ridge and the continental backstop. The isotherms computed from the Heat Flow density data and the density model showed a significant uplift of the temperature field below the Aegean domain. The 400°C isotherm is encountered at less than 10 Km depth. Tectonic deformation is controlled by dextral wrench faulting in the Aegean domain, while western Greece is dominated by compression and crustal shortening. Strike-slip and normal faults accommodate the western Hellenic thrusts and the westwards sliding of the Alpine napes, using the Triassic evaporates as lubricants.

1. Introduction

In order to protect society from earth hazards and secure the resources for its economic development geologic and geophysical information are basic essentials. In the following, I will present a brief summary of efforts and their results in geophysical mapping the Hellenides by active seismic methods, gravity and geothermal techniques. It will be demonstrated, how the obtained physical parameters can be exploited in producing earth models, needed for understanding the seismicity and the present tectonic activity. It is obvious that the limited space does not permit a thorough discussion. My report therefore has to be understood as the intention to show the road ahead rather than claim completeness.

2. Active seismic experiments for crustal studies

In figure one, two colours, red and white, indicate the distribution of seismic profiles that have provided crustal information. White lines are the seismic profiles collected in the 70s and early 80s. They have been presented in several papers by Makris 1978, Makris and Vees 1977, Makris et al. 1977, Ginzburg et al.

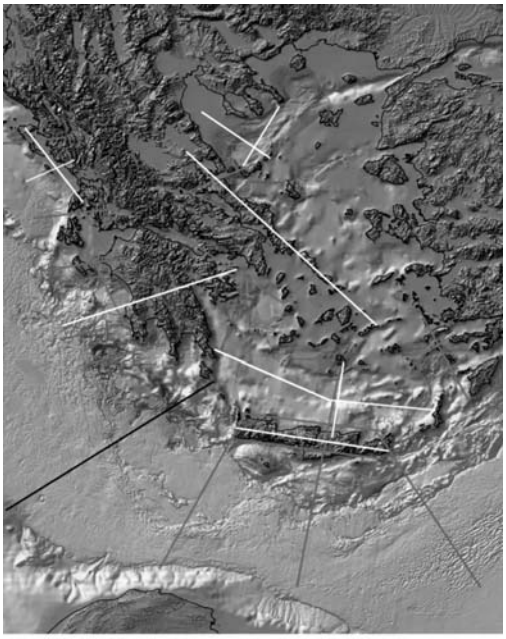

Fig. 1: Location of seismic lines recorded in 1971-1974 and 1982-1984 in white. Red are 2D-lines mapped in 1994 to 2008. In black is a composite line that has been obtained from 2 ships experiments and published by De Voogd et al. in 1992.

1987, Makris and Thiessen 1983. The paper published by Makris 1978 in Tectonophysics gives a summary of these early results. The main shortcoming of those experiments was the limited availability of seismic mobile stations. In most experiments we used 30 MARS 66, 4 channel stations (Berckhemer 1970) that were recording on analogue magnetic tape and were digitized for further processing. The advantage of those days was the use of explosives in generating seismic energy. Up to 1 ton of explosives were fired at sea and the quarry shots recorded from the Mandouthi mines (North Evia) were up to 4 tons large. Seismic signals of very good quality were recorded up to 380 km distance. Seismic models were computed by forward modelling of two-point ray tracing. These experiments were performed in cooperation and with the support of the Seismological Laboratory of the University of Athens, Prof. A. Galanopoulos, and were funded by the Deutsche Forschungsgemeinschaft (German Research Society).

After a period of experimental inactivity, mainly used in developing new instruments, field operations were resumed from the mid 90s till 1998. The seismic lines observed in this period are shown in red (fig. 1). Field operations were conducted in cooperation with the Hellenic Centre for Marine research (HCMR) and the Geodynamic Institute of the National Observatory of Athens. The 1994 program of western Greece was supported by the Public Petroleum Corporation of Greece (PPC). Results have been partially published by Makris and Chonia 2000, Bonhofff et al. 2001, Makris et al. 2001, Makris and Yegorova 2006 and Papoulia and Makris this volume. The projects were funded by the Deutsche Forschungsgemeinschaft, the EU, and the Public Petroleum Cop. Of Greece and GeoPro- Hamburg, Germany.

In figure 2 four seismic lines are presented. Three are results from the latest profiles using Ocean Bottom Seismographs (OBS) at sea and stand alone seismic stations on land. We have used up to 60 land stations and 50 OBSs at the various experiments, provided by GeoPro, Hamburg and 10 OBS provided by HCMR, Anavissos (Dr. Papoulia). The seismic energy was generated using large airgun arrays, tuned to low frequencies and of 40 to 60 lt volume.

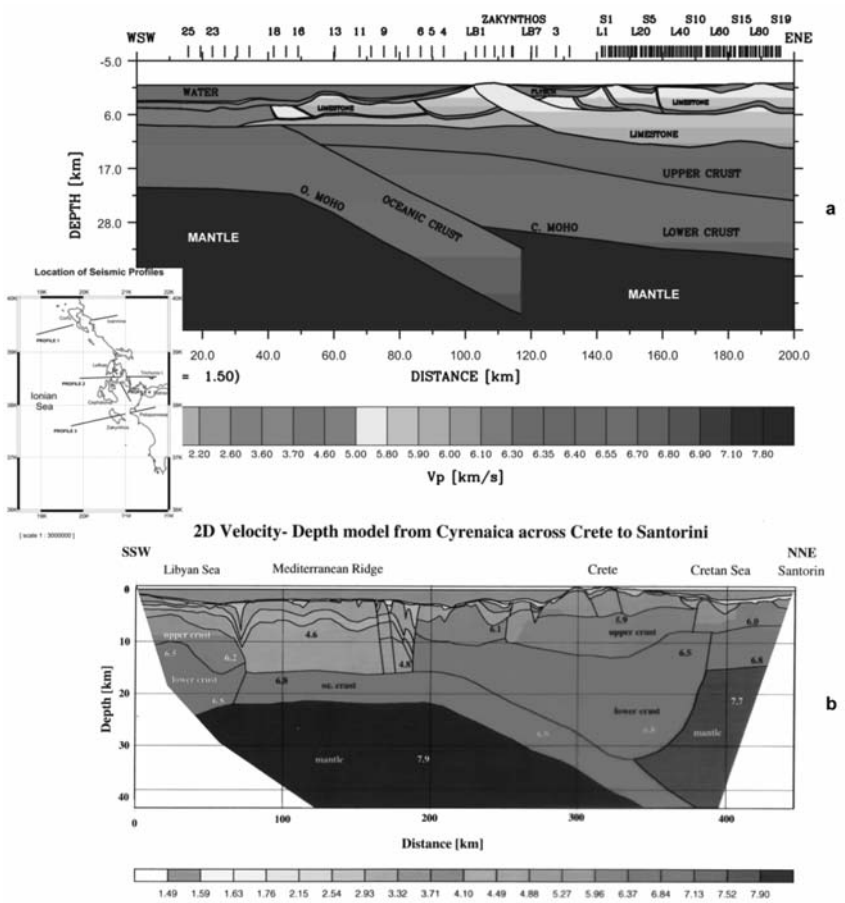

Fig. 2: Examples of crustal cross sections derived by active seismic experiments: a) Makris and Papoulia (2009), b) Makris and Yegorova (2006).

In summary, the crust mapped is very variable in thickness. The western Hellenides on mainland Greece and the Peloponnese exceed 40 km, while the Cretan Sea at its thinnest part is only 16 km thick. The eastern Cyclades are 26 km thick and the crust under north Evia, confirmed also by the Evia experiment of 1996, (Makris et al. 2001) is 30 km thick.

The velocity of the compressional waves Vp at the Moho level is below the Cyclades, Evia and the Cretan Sea 7.7 ± 0.1 km/s and therefore significantly lower then the values obtained below the Peloponnese and Western Greece, where Vp velocity at Moho level is normal with Vp = 8.0 ± 0.1 km/s. The low Vp-velocity below the Aegean Sea is due to the subduction of the oceanic lithosphere of the Ionian plate below the continental domain of the Aegean microplate and the mobilisation of the asthenosphere that has intruded the Aegean region at crustal levels. This is also expressed by the Aegean volcanic activity and its subcrustal seismicity (see e.g. Papazachos and Papazachou 1997, Makropoulos 1978, Galanopoulos 1975). Crete is 32 km thick at the western side, 34 km at its centre, and thins to 26 at the eastern side of the Island. Pn is 7.7 km/s at the eastern side of the Island and 8.0 km/s at the western. Finally, the profile representing the Dodecanese area has crustal thickness of about 23 to 24 km below Rhodes and Nisyros, thinning to the southwest to about 18 km at the eastern Cretan Sea.

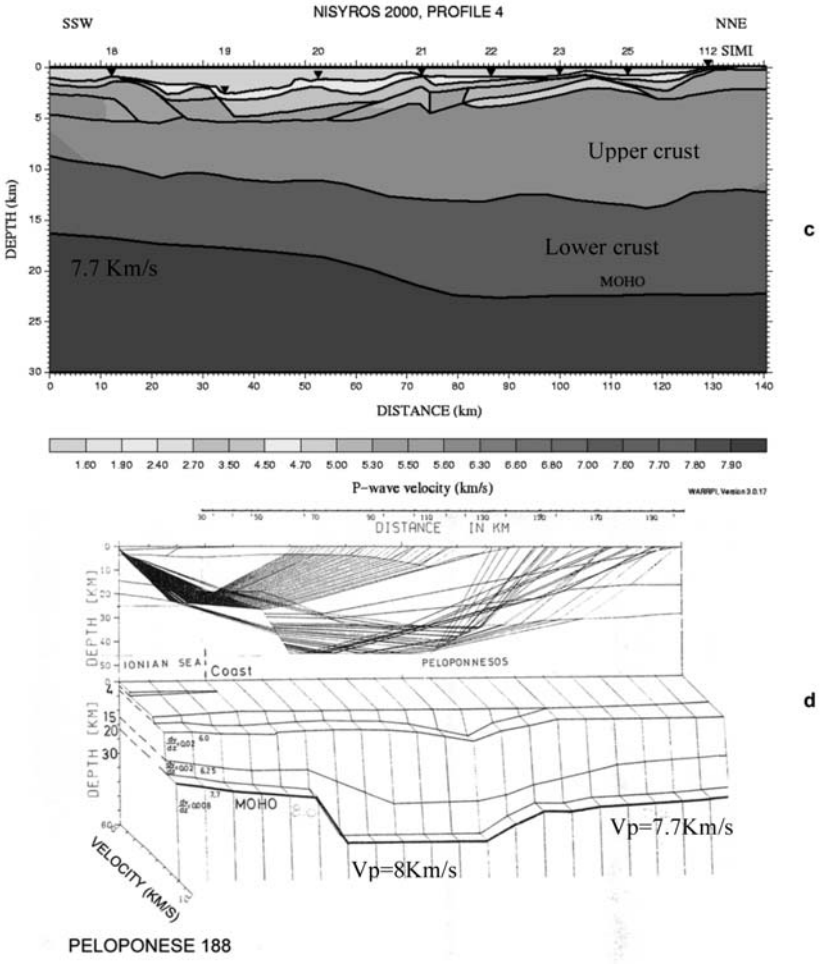

Fig. 2 cont.: Dodecanese, Peloponnese: c) Makris and Chonia (2000), d) Makris (1978).

These seismic crustal profiles were further used to develop a 3-D velocity-density model of Greece by combining them with the gravity field. They have been also exploited to map faults and delineate the tectonic elements that formed the Hellenides. Papoulia and Makris, this volume, present an example of how active seismic data are used to map the main tectonic elements of a region. The procedure followed to obtain 3-D earth models from the 2-D seismic results is schematically presented below:

- 2D-active seismic data provide Vp, Vs and ν models (ν = Poisson ratio).

  Empirical functions between Vp and density ϱ (Birch, 1961, 1962; Nafe and Drake, 1973).

  ↓

- 2D-density models are computed, constrained by 2-D seismic models and the velocity-density empirical functions (2D-gravity modelling).

  Empirical functions between Vp and density ϱ (Birch, 1961, 1962; Nafe and Drake, 1973).

  ↓

- 3D- density models are computed, constrained by the 2-D ρ-models and the Δg''- gravity field (3D gravity modelling).
- 2D and 3D isostatic models are derived from the density model and the g-values of the regional gravity mapping.

↓

- 2D and 3D distribution of the temperature field is computed from the density models and the mapped heat flow density distribution.

↓

The models derived by this procedure can be further used to obtain 3-D velocity models, relocate the regional seismicity and define active faults, permitting to compute seismic hazard reliably.

3. Gravity data and gravity maps of Greece

The regional gravity and magnetic mapping of Greece was accomplished using five to seven crews. Each group consisted of two to three observers and was equipped with: 1 gravity meter (LaCoste and Romberg, Type G), 1 magnetic torsion balance (vertical component, Type Askania), 3 altimeters (Thomen 3 B-4), and 1 aspirated hygrometer. The crews were provided by the following institutions: In 1971: Institute of Geophysics, University of Hamburg (IfG) (Dr. Makris), 3 groups, National Institute of Geology and Mining Researches (IGME), Athens, Greece (Dr. Stavrou), 1 group, Institute of Geodesy, Technical University of Athens (Prof. Veis), 1 group. In 1972: IfG - 4 groups, IGME, Athens, Greece - 1 group, Institute of Physical Astronomy, University of Thessaloniki - 2 groups. In 1973: IfG - 3 groups, IGME, Athens, Greece - 1 group. Officers of the Hellenic Army, Department of Geographic Service (GYS), supported the field parties. Evaluation, reduction and compilation of the data into maps were performed at the University of Hamburg. Gravity data were tight to the first order gravity net established by GYS and the above mentioned institutions and is connected to the European Calibration Line at the Frankfurt Airport. Gravity anomalies are given in form of Bouguer values and presented in a map of 25 mGal isolines (Fig. 3).

The following formulae were used for the reductions and calculation of the free air (Δg') and Bouguer (Δg'') anomalies:

$\Delta g' = g - \gamma + \delta g_F$, $\Delta g'' = \Delta g' + \delta g_T + \delta g_B$

g = measured gravity adjusted to the gravity net which was connected to Athens, East Air Terminal Station A: g = 980,058.28 ± 0.08 mGal.

γ = theoretical gravity according to the International Formula 1967.

δg_F = Free-Air reduction = 0.3086 ($h_s - h_o$) mGal with:

h_s = altitude of the gravity station, h_o = reduction level = $0_m \Rightarrow$

δg_B = Bouguer reduction; the Bouguer masses are reduced spherically to Hayford Zone O_2 (166.7 km), with uniform density of 2.67 gr/cm^3 according the formula given by Cassinis, Dore and Ballarin (1937).

δg_T = topographic reduction, computed with constant density ρ = 2.67gr/cm^3 in a system of geographic coordinates according the equations of Nagy (1966) and Jung (1961).

Reduction techniques for computing gravity anomalies have been described extensively by Makris (1971). The results of the computations are given in Fig. 3. Data at sea were taken from Allan and Morelli (1971) and Finetti and Morelli (1973). The Aegean Sea was mapped by gravity and magnetic surveys in 1982 by the R/V – Sonne and 1983 and 1984 by the R/V-AEGEAO. This was in cooperation between IfG-Hamburg, that provided the instruments and know-how and the HCMR-Athens that provided the R/V-AEGEAO. Crete was resurveyed in 1999 and 1998 by establishing 2000 gravity and

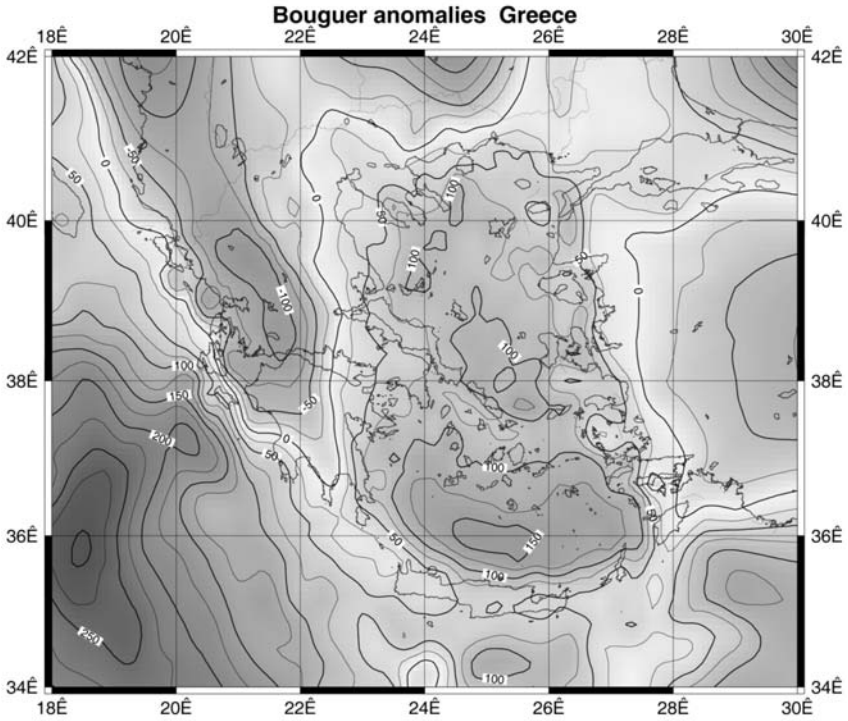

Fig. 3

magnetic stations on the Island by the universities of Hamburg and Bochum. For a discussion of the gravity surveys and their accuracy see Makris and Yegorova 2006, Makris et al. 2001, Makris 1978 and Makris et al. 1973.

A significant number of gravity stations has been additionally mapped by PPC- Athens in western Greece and in the geothermal areas of Lesvos, North Evia, the Serrais basin and the Loutraki-Sousaki zone by IGME in cooperation with the university of Hamburg. The land gravity data exceed 26.000 stations.

4. A qualitative description of the Bouguer gravity field and a 3-D density model

The Hellenic region can be divided into two gravimetric provinces. One is the western Greece with negative gravity values (gravity anomalies refer always to Bouguer gravity). The other is the Aegean region, Crete and the eastern part of Greek Mainland, where the gravity field is positive.

The zone of the negative anomalies of the Hellenides (Fig. 3) has minimum values of -120 mGal with local minima of up to -140 mGal along the Pindos chains. At the northern Peloponnese (Gulf of Patras) we find values of -80 to -120 mGal, which gradually become positive to the south towards the Gulf of Kalamata. The gravity zero line is nearly south north oriented from east Peloponnese to the Olympus Mountains, limiting the Aegean gravity high to the negative gravity low at the west. Eastern Greece, the Aegean Sea and Crete have positive gravity anomalies increasing from +50 mGal in the north to +160 mGal in the south. Maximum values are reached at the Cretan Sea at approximately 36°N between 24 – 26°E ranging locally from +150 to +170 mGal.

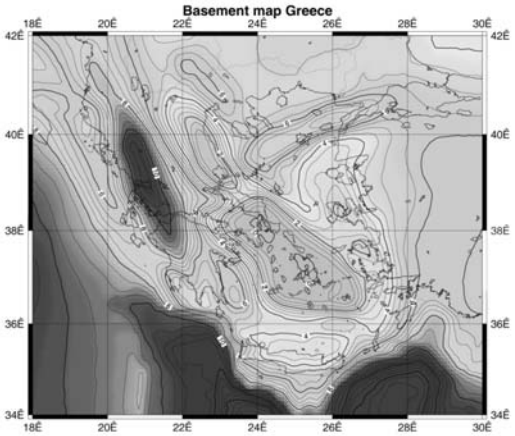
Basement map Greece
18É
20É
22É
24É
26É
28É
30É
42É
40É
38É
36É
34É

a

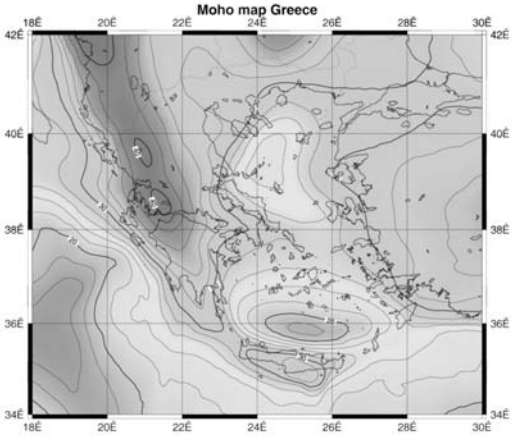
Moho map Greece
18É
20É
22É
24É
26É
28É
30É
42É
40É
38É
36É
34É

b

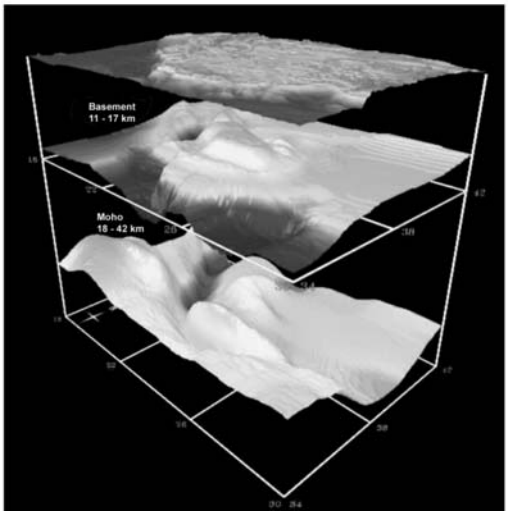
Basement
11 - 17 km
Moho
18 - 42 km

c

Fig. 4

The 3-D density model presented in figure 4 a, b, c is computed by a procedure developed by Tchernysev and Makris (1996), based on the algorithm published by Talwani et al. (1959). The model is discriminated in prisms of 5 x 6 x 0.5 km and the initial geometry and density were constrained by the seismic models located in figure 1. Velocities define the density values using the empirical functions between velocity and density published by Birch (1960 and 1961) and Nafe and Drake (1973). A detailed report on the computation of the 3-D density-velocity model of southern Greece and the Libyan Sea is published by Makris and Yegorova (2006) and a second covering all the country is in preparation by Makris, Yegorova, Papoulia, (2010).

In figure 4 a and b the basement and the Moho maps are presented. Thick sediments, exceeding 6 km were mapped at the North Aegean Trough, the Thermaikos Basin and particularly in western Greece below the external Hellenides, where the sediments are up to 10 km thick. It is also interesting that the largest accumulation of sediments were mapped SE and SW of Crete at two 12 to 14 km deep depressions, separated by a basement high extending south of Crete for more than 100 km.

Crustal thickness has its maximum value with 40 to 42 km below Pindos. The northern and central Aegean Sea is about 24 to 26 km thick and the Cretan Sea 16 to 20 km. Crete is 30 km thick at the west, thickens at the central part of the Island to 34 km and thins again at the east to about 26 km. The crust at Western Turkey thickens to about 30 to 34 km (see also Saunders et al. 1998), while the crust of the Ionian Sea at the backstop, between the western Peloponnese coast and the Mediterranean Ridge is about 24 km thick and floored by thin continental crust. The oceanic part of the Ionian Sea is only 14 km thick, with sediments of more than 6 km (see also Fineti 1982 and Fineti and Morelli 1973). Crustal thickness obtained on continental Greece by Sodouti et al. (2006) from P and S receiver functions are in good agreement with our results. The crustal thickness map (Moho map) however, they published by interpolating isodepth lines between the values obtained at the different stations is very irregular and differs from the Moho map of Makris, Yegorova, Papoulia (2010) of figure 4. The reason is, that they used a very limited number of stations (65 points) and the interpolated lines are inaccurate.

In figures 5a and 5b two crustal cross sections of E-W and N-S orientation were extracted from the 3D-density model. In both sections a low density-velocity body below the Aegean Sea was modelled, extending from Crete to the North-Aegean Trough and from East Peloponnese to western Turkey. This anomalous body, with more than 50 km thickness, is part of the asthenosphere mobilized by the subduction of the Ionian oceanic lithosphere below the Aegean continental domain. It is the source of high heat flow through the Aegean crust and feeds with magma the volcanoes of eastern Greece. The magma generated and mobilized from this low velocity-density intrusion ascends to the surface through zones of crustal weakness. Thus, the volcanoes of Santorini, Colombo and Melos as Makris and Papoulia (2009) showed, are located at the transition of the stretched crust of the Cretan Sea, to the thicker crust of the Cyclades which is build by a series of thrusts, seismically active, as Bonhoff et al. (2006) showed. In the same way the volcanic and the hydrothermal activity at the North Evia Gulf are located at the transition of the thin crust of 20 km in the Gulf (Makris et al. 2001) to the 30 km crust of north Evia (Makris and Vees 1977 and Makris et al. 2001).

The density model presented above can be used for considering the isostatic behaviour of the crust and mantle system and associate it with the tectonic deformation and the seismicity. It can be also used to constrain modelling of the distribution of the isotherms from the heat flow density map, published by Čermak (1979) and presented in figure 7. In figure 6 the pressure in Kbar of the masses that are between 0-20, 0- 40 and 0-60 km depth was calculated. As seen the upper 20 km of the crust and sediments between the Ionian Sea and the Hellenides is not isostatically balanced. The transition between the Ionian Sea and the Peloponnese shows a lateral change from 4.2 to 5.6 Kbar. It is therefore not sur-

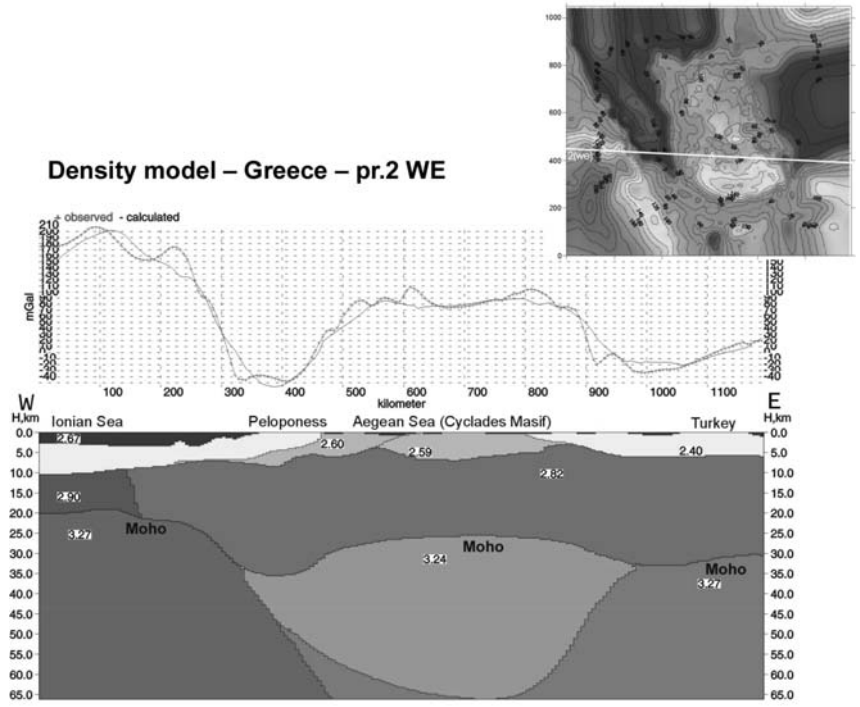

Fig. 5: a. E-W crustal cross section between the oceanic domain of the Ionian Sea and the continental domain of the Aegean microplate.

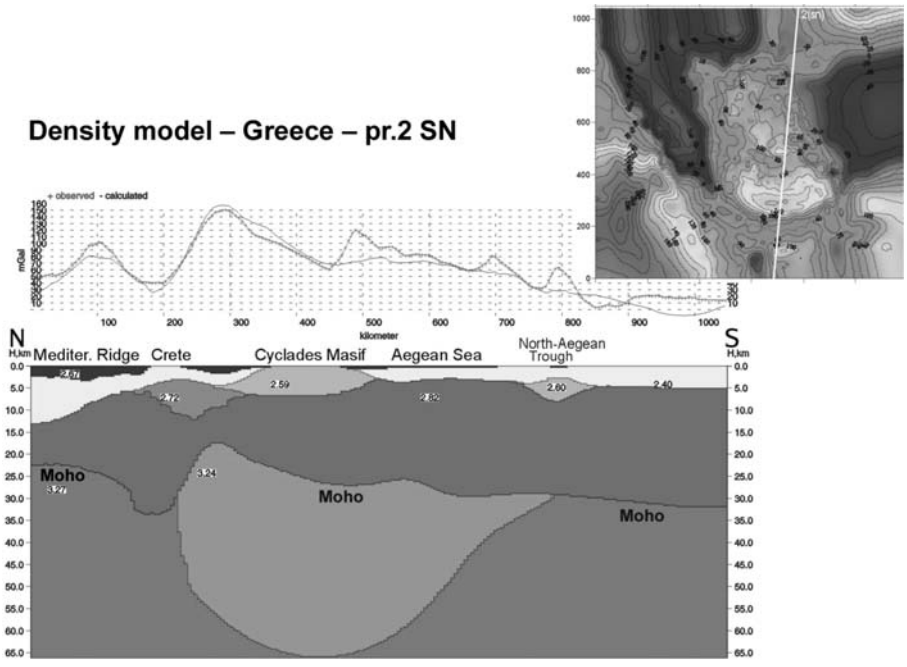

Fig. 5: b. N-S cross section between the Libyan Sea and the northern Aegean Sea.

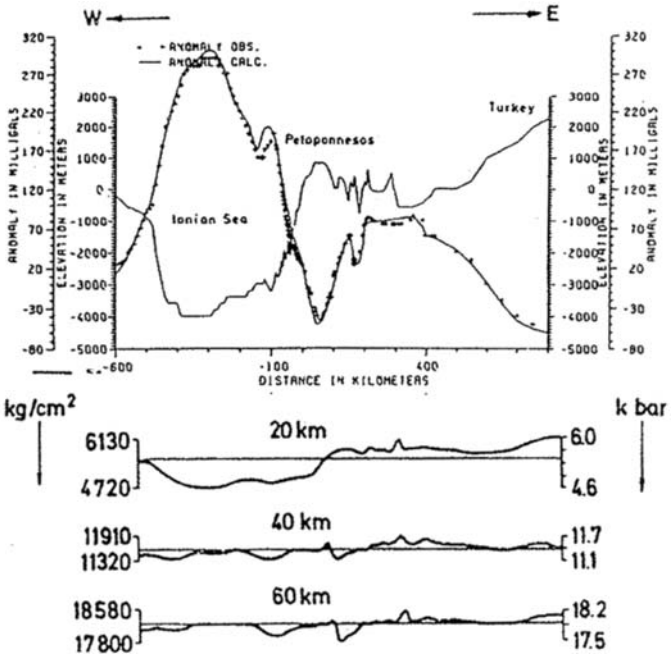

Fig. 6: Mass and pressure distribution at three different levels along an E-W profile between the Ionian Sea and western Turkey (Makris, 1977).

prising that the area with the greatest isostatic disturbance and lateral pressure variation has also significant seismicity at crustal levels. At 40 km and even more so at 60 km depth the regional isostatic balance is established. There are two areas, which remain disturbed. The one is at the transition of the Mediterranean Ridge to the backstop, due to the large difference of the sedimentary thickness. The other is at the central Peloponnese area where the crust is thickened to nearly 40 km and the dense mantle displaced. In both cases we have a significant deficiency of mass.

5. Heatflow density map of the Hellenides and distribution of the isotherms

The heat flow density map presented in figure 7 was compiled by Čermak (1979). Since then only few measurements, mainly concentrated at geothermal areas or boreholes of the oil industry, have been added. The regional features therefore have not changed. The Aegean region including the Saronikos and Evoikos Gulfs are of high heat flow density. The heat flow density values exceed 1.6 HFU (Heat Flow Units) and indicate that the crust alone cannot explain the observed field by the heat generation of the continental crust. The mantle transports heat by conduction and convection of a lithothermal system mobilized by the subduction of the Ionian oceanic lithosphere below the Aegean micro continent. The Aegean Sea, south of the North Aegean Trough and the western part of Turkey are areas of high heat flow. In the contrary, the eastern Mediterranean region and the largest part of the Ionian Sea have HFU < 0.9 and are well below average. The crust is mainly oceanic and therefore of low heat production and the upper mantle is cold and has a small input into the heat flow density field. Using the one dimensional heat conduction equation:

$$T(z) = T(o) + Qo/k * z - A/2k * z^2$$

where "Q_o" is the heat flow density value through the earth surface, "k" is the thermal conductivity and

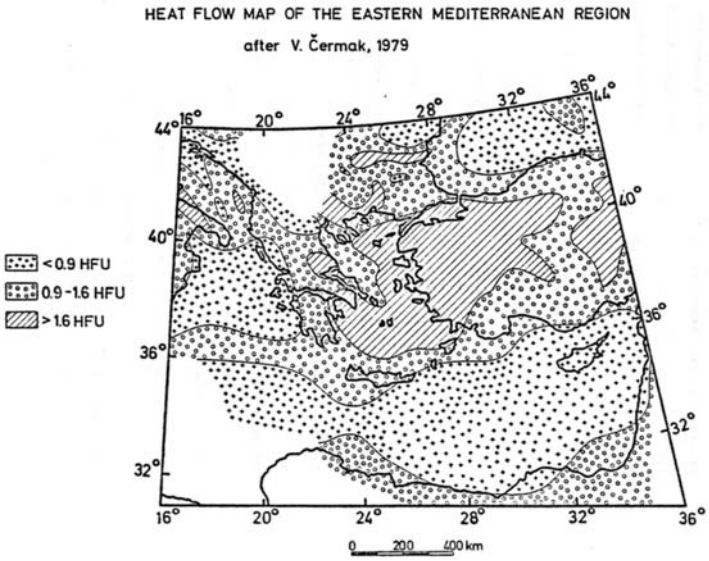

Fig. 7

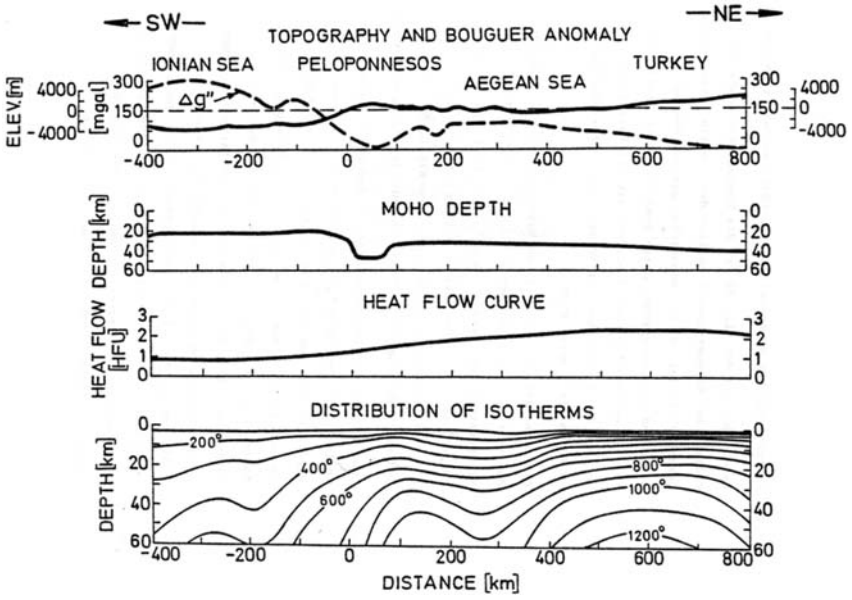

Fig. 8: Calculated isotherms in °C. For further explanations see text.

"A" is the heat production, we can compute the temperature distribution as a function of depth constrained by the density models.

In figure 8 the distribution of the isotherms between the Ionian Sea and western Turkey are presented. In the figure the crustal thickness along the profile, the smoothed heat flow density curve and the corresponding distribution of the isotherms are presented. It is interesting to see that e.g. the 400°C isotherm, which at the deep part of the Ionian Sea is between 40 to 60 km depth below the Aegean

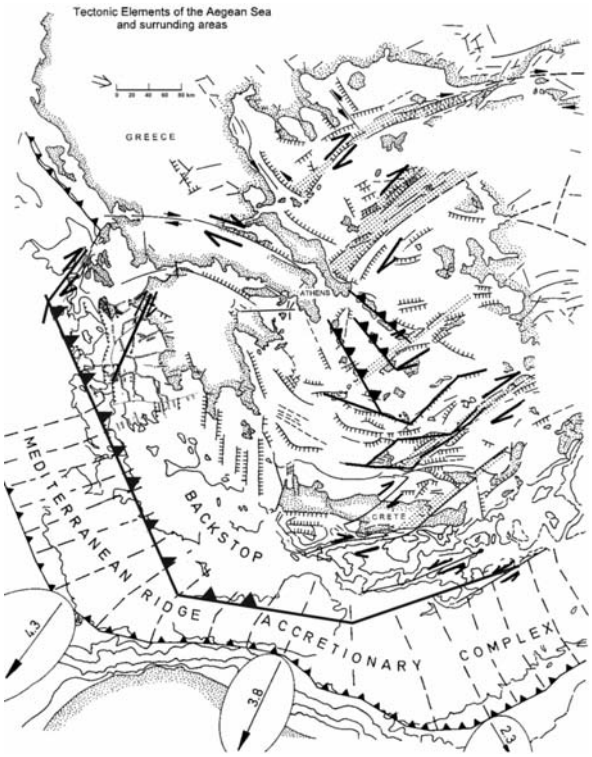

Fig. 9: Simplified schema of the dominant tectonic regions in the Aegean Sea and the western Hellenides.

Sea, is encountered at only 10 km depth. It is therefore not surprising, that all thermal phenomena either in form of volcanoes or as hydrothermal systems are confined within the Aegean region and western Turkey. As stated previously, the volcanoes are linked with deep-sited faults and are confined at the transition of thin to thick crust. The hydrothermal systems are either linked to volcanoes and their magma intrusions or to deep faults that permit penetration of to surface waters to the heated rocks. Heated fluids of various temperatures are transported back to the surface by convection.

6. The main tectonic elements mapped by active seismic profiles

The simplified schema of the main tectonic elements as were mapped by the active and passive seismic data, delineate two different tectonic regions. The eastern north Aegean Sea is directly associated with the dextral wrench fault system of north Anatolia. Seismicity is extremely intense along the strike-slip faults and earthquake magnitudes can obtain destructive values. All this activity is linked to crustal deformation by transtension and transpression accompanied mainly by normal faulting. The same is valid for the Cretan Sea and part of the Dodecanesse, although the seismicity is less intense than that of the north Aegean area. It is only south of Crete at the Ptolemeus, Pliny and Stravo trenches that the strike-slip processes become sinistral in order to accommodate the northeastern motion of the African Plate that is subducted below southwestern Turkey. Crustal seismicity dominates also the western Hellenides. We could map the extension of the continental Aegean microplate to the west, up to the eastern limit of the Mediterranean Ridge. This is also the location where the Ionian Oceanic lithosphere is subduced below continental Hellenides. Thrusting and crust shortening is the dominant tectonic process, accompanied by normal faulting that accommodates the westwards thrusted crustal units. Dextral strike-slip is dominant along the Cephalonia and Andravida Faults, displacing the Hellenides to the

west. Deep seismicity is mapped only below the Aegean volcanoes, due to subduction of the Ionian oceanic lithosphere. Shallow seismicity mapped at the Cyclades on the other hand, is linked to the crustal deformation that created the Cyclades by thrusting and regional upcoming due to isostatic buoyancy caused by the low velocity-density mantle below the central Aegean Sea. The exhumed HP-rocks at the Cyclades developed as a consequence of the small-scale Mediterranean region subduction of an inhomogeneous incoming lithosphere, causing chaos in the subduction process with subsequent retreat of the subduction front (see Husson et al. 2009, Royden and Husson 2006 or Jolivet at al. 2008).

7. Acknowledgements

I want to thank Mrs. J. Mertins and Mrs. M. Toma for their help in the preparation of the text and figures. Dr. J. Papoulia (HCMR) read the manuscript critically and her help and remarks are highly acknowledged.

8. References

Allan, T.D., Morelli, C., 1971. A geophysical study of the Mediterranean Sea, *Boll. Geofis. Teor. Ed. Appl.*, 13, No.50, pp. 99-141, Triest.

Berckhemer, H., 1970. MARS 66- a magnetic tape recording equipment for deep seismic sounding, *Zeitschrift f. Geophys.* 36, 501-518.

Birch, F., 1960/61. The velocity of compressional waves in rocks to 10 kilobars, *J. Geophys. Research* 56, 66.

Bonhoff, M., Makris, J., Papanicolaou, D., Stavrakakis, G., 2001. Crustal Investigations of the Hellenic Subduction Zone Using Wide Aperture Seismic Data. *Tectonophysics* 343, pp. 239 – 262.

Bonhoff, M., Rische, M., Meier, T., Becker, D., Stavrakakis, G., Harjes, H.P., 2006. Microseismic activity in the Hellenic Volcanic Arc, Greece, with emphasis on the seismotectonic setting of the Santorini- Amorgos zone. *Tectonophysics* 423, pp. 17-33.

Cassinis, G., Dore, P., Ballarin, S., 1937. Fundamental tables for reducing gravity observed values. R. Commissione Geodetica Italiana Pubblicazioni, Nuove serie, n. 13.

Čermák, V., 1979. Heat flow map Europe. In: V. Čermák and L. Rybach (Editors), *Terrestrial Heat Flow in Europe*. Springer Verlag, Berlin, Heidelberg, New York, pp. 3-40.

De Voogd, B., Truffert, C., Chamot-Rooke, N., Huchon, P., Lallement, S., Le Pichon, X., 1992. Two ship seismic soundings in the basins of the Eastern Mediterranean Sea (Pasiphae Cruise). *Geophys J. Int.*, 109, 536-552.

Finetti, I., 1982. Structure stratigraphy and evolution of the central Mediterranean Sea. *Boll. Di Geofisica Teorica ed Appl.* XV, 60.

Finetti, I., Morelli, C., 1973. Geophysical exploration of the Mediterranean Sea. *Boll Geof. Teor. Appl.*, 15, 263-344.

Galanopoulos, A.G., 1975. A new model accounting for the intermediate earthquakes at the convec. side of the Hellenic arc, *Ann.Geol.d.Pays Hellen.*, 27, 355-370.

Ginzburg, A., Makris, J., Hirschleber, H.B., 1987. Geophysical Investigations in the North Aegean Trough. *Annales Geophysicae*, 5B, 167-174.

Husson, L., Brun, J-P., Yamato, Ph., Faccenna, C., 2009. Episodic slab rollback fosters exhumation of HP-UHP rocks. *Geophys. J. Int.* 179, 1292-1300.

Jolivet, L. et al., 2008. Subduction, convergence and the mode of backarc extension in the Mediterranean region. *Bull. Soc. Geol. France*, 179, 525-550.

Jung, K., 1961. Schwerkraftverfahren in the Angewandten Geophysik. Akademische Verlagsgesellschaft Geest & Portig KG.

Makris, J., 1978. The Crust and Upper Mantle of the Aegean Region from Deep Seismic Soundings.

Tectonophysics 46, 251-268.

Makris, J., 1978. A Geophysical Study of Greece based on Deep Seismic Studies, Gravity and Magnetics. in Alps, Appenines, Hellenides (ed. H.Closs, D.Roeder, K.Schnüdt): 415-423, Stuttgart Schweitzerbart'sche Verlagsbuchhandlung.

Makris, J., Chonia, T., 2000. Active and Passive Seismic Studies of Nisyros Volcano - East Aegean Sea. Communications of the Dublin Institute of Advanced Studies. Series l, *Geophysical Bulletin Nr 4*.

Makris, J., Mavrides, L.N., Menzel, H., Stavrou, A., Veis, G., 1973. The Gravity Field of Attika, the Peloponnesos and Kithira. *Z.f.Geophys*., 39, 929-936.

Makris, J., Papoulia, J., Papanikolaou, D., Stavrakakis, G., 2001. Thinned continental crust below northern Evoikos Gulf, central Greece, detected from deep seismic soundings. *Tectonophysics,* 341, 225-236.

Makris, J., Papoulia, J., 2009. Tectonic Evolution of Zakynthos Island from deep Seismic Soundings: Thrusting and its Association of the Triassic Evaporites. Intl. Symposium and Field trip Evaporites: Sedimentology, Evaluation and Economic Significance, Zakinthos, Greece, 47-54.

Makris J., Papoulia, J., 2009. The Thera Volcano at the transition between the Cycladic thrust belt and the stretched continental crust of the Cretan Sea. The Atlantis Hypothesis: Searching for a Lost Land. 2nd International Conference, Athens, November 2008. Proceedings of the ATLANTIS 2008 International Conference.

Makris, J., Thiessen, J.,1983. Offshore Investigations of the Sedimentary Basins with a newly developed Ocean Bottom Seismograph. In Expanded Abstracts, 53rd Annual International SEG Meeting, Las Vegas: 470-473.

Makris, J., Vees, R., 1977. Crustal Structure of the Central Aegean Sea and the Islands of Evia and Crete, Greece, obtained by Refraction Seismic Measurements. *J.Geophys*, 42, 329-341.

Makris, J., Weigel, W., Koschyk, K., 1977. Crustal Models of the Cretan Sea deduced from Refraction Seismic Measurements and Gravity Data. In Meteor Forschungsergebnisse Reihe C, 27.

Makris, J., Yegorova, T., 2006. A 3-D density-velocity model between the Cretan Sea and Libya. *Tectonophysics*, 417, 201-220.

Makris, J., Yegorova, T., Papoulia, J., 2010. A 3-D density-velocity model of Greece deducted from gravity and active seismic data. To be submitted to *Geoph.J. Int*.

Makropoulos, K.C., 1978. The statistics of large earthquake magnitude and an evaluation of Greek seismicity, "PhD. Thesis", Edinburg University, 193 pp.

Nafe, J.E. and Drake, C.L., 1973. Physical properties of marine sediments in: The Sea, Vol. 3, Ed. M.N. Hill. Interscience, pp. 794-814.

Nagy, D., 1966. The gravitational attraction of a right rectangular pris. *Geophysics VXXXI*.

Papazachos, B., Papazachou, C., 1997. The earthquakes of Greece. P.Ziti & Co, Thessaloniki, Greece.

Papoulia, J., Makris, J., 2010. Tectonic processes and crustal evolution on/offshore western Peloponnese derived from active and passive seismics. *Bull. Geol. Soc. Greece* 2010, submitted.

Royden, L., Husson, L., 2006. Trench motion, slab geometry and viscous stresses in subduction systems. *Geophys. J. Int*., 167, 881-905.

Saunders, P., Priestley, K., Taymaz, T., 1998. Variations in the crustal structure beneath western Turkey. *Geophys. J. Int.,* 134, 373-389.

Sodouti, F., Kind, R., Hatzfeld, D., Priestley, K., Hanka, W., Wylegalla, K., Stavrakakis, G., Vafidis, A., Harjes, H.P., Bonhofff, M., 2006. Lithospheric structure of the Aegean obtained from P and S receiver functions. *J. Geophys. Res*., Vol. 111.

Talwani, M., Sutton, G.H., Worzel, J.L., 1959. A Crustal Section across the Puerto Rico Trench, I. *Geophys. Res*., 64/10.

Tchernychev, M., Makris, J., 1996. Fast Calculation of Gravity and Magnetic Anomalies Based on 2-D and 3-D Grid Approach. Extended Abstract of the 66th SEG-Meeting. Denver.

Δελτίο της Ελληνικής Γεωλογικής Εταιρίας, 2010
Πρακτικά 12ου Διεθνούς Συνεδρίου
Πάτρα, Μάιος 2010

Bulletin of the Geological Society of Greece, 2010
Proceedings of the 12th International Congress
Patras, May, 2010

INTERMEDIATE TERM EARTHQUAKE PREDICTION BASED ON INTEREVENT TIMES OF MAINSHOCKS AND ON SEISMIC TRIGGERING

Papazachos B.C., Karakaisis G.F., Papazachos C.B. and Scordilis E.M.

Department of Geophysics, School of Geology, Faculty of Science, Aristotle University, GR54124, Thessaloniki, GREECE, karakais@geo.auth.gr, kpapaza@geo.auth.gr, manolis@geo.auth.gr

Abstract

Two models, which contribute to the knowledge on intermediate term earthquake prediction are further examined, improved and applied. The first of these models, called Time and Magnitude Predictable (TIMAP) regional model is based on repeat times of mainshocks generated by tectonic loading on a network of faults which are located in a certain seismic region (faults' region). The second model, called Decelerating-Accelerating Strain (D-AS) model, is based on triggering of a mainshock by its preshocks.

Parameters of the TIMAP model have been specified for the Aegean area and applied by a backward test in 86 circular faults' regions of this area. The test shows the validity of this time dependent model with 29% false alarms.

Data concerning decelerating and accelerating seismic (Benioff) strain, which preceded 46 strong (M≥6.3) recent mainshocks in a variety of global seismotectonic regimes, show that the generation of a mainshock is triggered by quasi-static stress changes due to accelerating preshocks which occur in a broad (critical) region and by static stress changes due to the large number (frequency of occurrence) of small preshocks generated in a narrow (seismogenic) region. Retrospective predictions (postdictions) of these 46 mainshocks by the D–AS model confirms previous results concerning the prediction uncertainties (2σ) of the model in the origin time (± 2.5 years), epicenter location (≤ 150 km) and magnitude (± 0.4) of an ensuing mainshock with a probability ~ 80%. Information is also given on the successful prediction by the D-AS model of: 1) the Cythera strong (M = 6.9) earthquake which occurred on 8 January 2006 in the southwestern part of the Hellenic Arc and 2) of the Rhodes strong (M = 6.4) earthquake which occurred on 15 July 2008 in the Eastern part of this Arc.

A backward combined application of both models in the Aegean area shows an uncertainty ≤120km in the epicenter location of an ensuing mainshock.

1. Introduction

Seismic hazard assessment currently applied is mainly based on the spatial distribution of the mean seismicity because knowledge of the time variation of seismicity is considered insufficient for such practical application. This is due to the fact that prediction of individual strong earthquakes, which are those that cause damage, is a very difficult scientific problem. The solution of this problem can contribute significantly to the development of techniques for time dependent seismic hazard assessment. For this reason prediction of individual strong earthquakes is one of the most important problems of seismology from the social point of view.

Decades of research work on short term prediction (time uncertainty of days to weeks) led to the conclusion that such prediction is not possible with the present scientific knowledge (Wyss, 1997). Long – term earthquake prediction (uncertainty of the order of decades) is also not possible. This is due to the fact that the physical process of generation of a strong earthquake in a fault is characterized by properties of deterministic chaos that require very accurate knowledge of this process in order to predict the next strong earthquake in the fault (Jaumé and Sykes, 1999). Obtaining such knowledge is also not feasible at present. It seams, however, that there is much hope for intermediate-term earthquake prediction (uncertainty of the order of a few years) by the use of seismological observations related to: a) the time variation of stress due to tectonic loading (repeat times of mainshocks, etc) and b) seismic triggering due to precursory stress fluctuations (precursory change of seismicity).

Time variation of stress due to both physical causes (tectonic loading, triggering) has been considered for improving knowledge on earthquake prediction because both contribute to earthquake generation. Thus, long-wavelength stresses associated with the relative motion of major tectonic plates accumulate relatively slowly (~ 10^{-5} MPa per year) while typical frictional strength of seismic faults is relatively high (1 to 10 MPa) (Hill and Prejean, 2006). For this reason, regional stress may remain below the frictional strength of faults for a long time. Therefore, short–term and short–wavelength fluctuations in both the stress field and fault strength are needed in order the local stress state to exceed local failure threshold and contribute to earthquake generation. That is, in addition to tectonic loading, some kind of triggering mechanism is necessary to explain generation of strong earthquakes. Sources of short-term stress fluctuations can be other earthquakes in the crust (Freed, 2005; Steacy et al., 2005), other physical factors (magmatic intrusions, earth's tides, etc) and anthropogenic activities (reservoir filling, etc). Local fluctuation of fault strength results usually from changes in the fluid pore pressure within the fault.

Quantitative information on tectonic loading can be obtained by using data from several sources (seismological, geological, geodetic, etc) but for seismological purposes (seismicity, seismic hazard, earthquake prediction) seismological data (instrumental, historic) are the most proper ones because such data give direct information on the seismic effect of tectonic loading and are easily quantified. Seismological data useful for improving knowledge on earthquake prediction can be the repeat times of large earthquakes (Fedotov, 1965; Shimazaki and Nakata, 1980). There is, however, a limited number of strong earthquakes which occurred on a particular seismic fault for which quantitative information (size, origin time) is available for reliable statistical treatment. For this reason, a seismic region, which includes "a network of neighboring seismic faults" must be considered to increase available repeat times. On this idea it is based the "Time and Magnitude Predictable Regional" model (Papazachos, 1989; Papazachos et al., 1997) in which a large sample of interevent times of strong earthquakes is available in the region for a reliable study of time dependent seismicity.

Stress change in the focal region of a triggering earthquake is transferred in the focal region of a triggered earthquake in three main modes: the static, quasi-static and dynamic.

Static stress change is the perturbation of the static stress field from just before an earthquake to shortly after the generation of seismic waves by elastic dislocation models (Das and Scholz, 1981; King and Cocco, 2001). Static stress changes decay relatively rapidly with distance, Δ, from the epicenter of the triggering earthquake (as Δ^{-3}) and for this reason their triggering potential is limited to one or two source dimensions from the focus of the triggering earthquake.

Quasi-static stress change is the gradual stress perturbations caused by the viscous relaxation of the plastic lower crust and upper mantle in response to the sudden generation of the triggering earthquake across the fault in the overlying brittle crust (Pollitz and Sacks, 2002). Quasi-static stress changes propagate as a two dimensional stress change and thus decays more slowly with distance (as

~Δ^{-2}) and their triggering potential extends to greater distances than static stress changes. On the other hand, the relatively low speed of viscoelastic propagation results in delayed triggering. Both static and quasi-static stress transfer cause permanent stress change in the vicinity of the fault of the triggered earthquake, which shifts the stress state incrementally to the Coulomb failure threshold on the fault.

Dynamic stress propagates as seismic waves and for this reason its amplitude decreases relatively slowly with distance (as Δ^{-2} for body waves and $\Delta^{-3/2}$ for surface waves) and their triggering potential extends from near field to much greater distances than static or quasi-static stress changes (Kilb et al., 2002). Dynamic triggering potential can be further enhanced by amplification of radiation directivity or by stimulating aseismic process (creep, fluid activation) which contribute to triggered seismicity. Dynamic stress is oscillatory and for this reason leaves no permanent stress to overcome Coulomb failure stress in a fault.

Fluctuation of stress is expressed by corresponding deviations of seismicity from the background one caused by tectonic loading. Such seismicity deviations can be positive (seismic excitation) or negative (seismic quiescence). Several precursory seismicity patterns based on such seismicity deviations have been proposed for improving knowledge on earthquake prediction. One of the most distinct such patterns is formed of a precursory seismic excitation in a broad region and of reduced seismicity in the narrow focal region of an ensuing mainshock, originally proposed by Mogi (1969) who called it "doughnut pattern".

Significant additional research by several workers has shown that seismic excitation in the broad (critical) region is characterized by an accelerating generation of intermediate magnitude preshocks (Tocher, 1959; Varnes, 1989; Sykes and Jaumé, 1990; Knopoff et al., 1996; Brehm and Braile, 1998, 1999; Papazachos and Papazachos, 2000, 2001; Robinson, 2000; Tzanis et al., 2000; Tzanis and Makropoulos, 2002; Ben-Zion and Lyakhovsky, 2002; Scordilis et al., 2004; Papazachos et al., 2005b; Mignan et al., 2006, among others). Bufe and Varnes (1993) have shown that the cumulative Benioff strain (sum of square root of seismic energy), S(t), for the accelerating pattern is expressed by relations of the form:

$$S(t) = A + B(t_c - t)^m \tag{1}$$

where t_c is the origin time of the mainshock and A, B, m parameters calculated by the available data with m<1 and B negative.

Intermediate – term quiescence of seismicity of small shocks in the focal region has been also observed before many strong earthquakes and was attributed to stress relaxation due to aseismic sliding (Wyss et al., 1981; Kato et al., 1997). Some researchers (Evison and Rhodes, 1997; Rhoades and Evison, 1993; Evison, 2001) have observed that a seismic excitation phase can be found in the narrow (seismogenic) region preceding seismic quiescence. Papazachos et al. (2005a) used global data to show that intermediate magnitude preshocks in the seismogenic region form a decelerating pattern and the time variation of the cumulative Benioff strain up to the mainshock also follows a power–law (relation 1) but with a power value larger than one (m>1). That is, this pattern of decelerating strain in the focal (seismogenic) region is formed of a transient excitation, followed by a decrease of seismicity of intermediate magnitude shocks.

Papazachos et al. (2006), taking into consideration the above mentioned published information on the observed accelerating and decelerating precursory seismicity and based on such seismicity which preceded globally occurred strong mainshocks (M≥6.0) developed the Decelerating-Accelerating Strain (D-AS) model for intermediate term earthquake prediction. This model is based on empirical relations and parameters most of which have been also derived theoretically and can be physically interpreted.

These constraints relate parameters of a decelerating and an accelerating preshock sequence with the main parameters (origin time, magnitude, epicenter geographic coordinates) of the ensuing mainshock, hence they can, in principle, be used to perform intermediate term prediction of mainshocks.

A goal of the present work is to further develop the time and magnitude predictable (TIMAP) regional model by performing a backward test of this model on strong (M≥6.0) shallow (h≤100km) mainshocks generated in circular faults' regions of the Aegean area (34^0N-43^0N, 19^0E-30^0E). Another goal is to further study properties of the space, time and magnitude distributions of already occurred decelerating and accelerating preshock sequences of 46 recently occurred (since 1980) strong (M≥6.3) shallow (h≤100km) mainshocks in a variety of global seismotectonic regimes. We also show how these properties have been used to form the Decelerating-Accelerating Strain (D-AS) model which is applied in a backward test to estimate its time, space and magnitude uncertainties. Properties of preshocks are also used to give reasonable physical explanations for triggering of a mainshock by its preshocks.

2. The Time and Magnitude Predictable (TIMAP) Model

The TIMAP model is based on the interevent times of mainshocks generated on a network of faults which are located in a seismic region (faults' region). That is, the original catalogue of the region is declustered so that preshocks which trigger a mainshock and postshocks which are triggered by the mainshock are excluded. Thus, seismic triggering is removed and the finally employed catalogue includes only mainshocks caused mainly by tectonic loading. Also, the interevent time considered in this model is the time between mainshocks generated in different faults of the region.

Papazachos et al. (1997) used a large sample of global data (1811 interevent times of mainshocks which occurred in 274 regions located in different seismotectonic regimes) to define the relations:

$$\log T_t = 0.19M_{\min} + 0.33M_p + Q \tag{2}$$

$$M_f = 0.73M_{\min} - 0.28M_p + W \tag{3}$$

where T_t (in years) is the interevent time, M_{min} is the minimum mainshock magnitude considered, M_p is the magnitude of the previous mainshock in the seismic region and M_f is the magnitude of the following mainshock in the region. Q and W are constants which depend on the long-term seismicity level of the seismic region and their mean values (as well as their standard deviation σ_q and σ_w) are calculated by the available data for each region.

Relations (2) and (3) have been derived by using a moment magnitude based on the total seismic moment released by the mainshock and its preshocks and postshocks. This is also done in the present work to calculate Q and W by considering as preshocks and postshocks those events which occurred in a time window ±8.5 years from the origin time of the mainshock. It must be noticed, however, that the differences between the mainshock magnitudes calculated in this way and the observed ones are within the errors' window.

It has been further shown (Papazachos and Papaioannou, 1993; Papazachos et al., 1997) that the ratio T/T_t of the observed interevent time, T, to the calculated, T_t, by relation (2) follows a lognormal distribution, with a mean value equal to zero and a standard deviation, σ_q, which varies from region to region. It means that we can calculate the probability, P, for the occurrence of a mainshock with $M \geq M_{min}$ during the next Δt years, when the previous such mainshock ($M_p \geq M_{min}$) occurred t

years ago, by the relation:

$$P(\Delta t) = \frac{F\left(L_2/\sigma\right) - F\left(L_1/\sigma\right)}{1 - F\left(L_1/\sigma\right)} \tag{4}$$

where, $L_2 = \log\frac{t+\Delta t}{T_t}$, $L_1 = \log\frac{t}{T_t}$ and F is the complementary cumulative value of the normal distribution with mean equal to zero and standard deviation, $\sigma(=\sigma_q)$, where $\sigma_q(=0.15)$ is the average value of the standard deviations calculated for 218 regions in the Aegean area. T_t is calculated by relation (2) since M_{min}, M_p and Q are known.

2.1 Application of the TIMAP model in the Aegean area

Karakaisis et al., (2010) used the catalogue of instrumental (M≥5.2, 1911-2008, h≤100km) data (Papazachos et al., 2008) and of historical (M≥6.0, 464BC-1910) data (Papazachos and Papazachou, 2003) for earthquakes in the Aegean area (34^0N-43^0N, 19^0E-30^0E) to define circular focal regions, (C,r). Center, C, of a circular region is the epicenter of the largest known earthquake ever occurred with this epicenter and with magnitude M_{max} (≥6.0). The radius r (= L/2) is equal to the half fault length of this largest earthquake. For the whole Aegean area (Aegean sea and surrounding lands) 223 such circular focal regions have been defined. Karakaisis and his colleagues (2010) also developed and applied a declustering procedure to exclude associated shocks (preshocks, postshocks) that occurred in the focal region and in a time window ±8.5 years from the origin time of each mainshock. The mainshocks (with M≥5.2) have been identified in each circular focal region and a catalogue of mainshocks has been formed for the whole Aegean area. Furthermore, they defined completeness of mainshocks in each circular region (C, R = 100km). Thus, in each of the 223 such circular regions there is available not only the complete sample of instrumental data (M≥5.2, 1911-2008) but corresponding complete samples of historical mainshocks too.

These complete samples of mainshocks in each of the 223 circular regions of the Aegean area are used in the present work to define 218 circular (C, R≤100km) regions where the TIMAP model holds. For these regions there are calculated the constants Q and W of relations (2) and (3) and the corresponding standard deviations, σ_q and σ_w. A backward test of the model is applied for 86 of these circular regions which include the epicenters of the last two mainshocks with M≥6.0 and the latest (target mainshock) is different in these 86 cases and is retrospectively predicted, as it is explained in the following.

The values of the scaling coefficients (b = 0.19, c = 0.33) of relation (2) and (B = 0.73, C = -0.28) of relation (3) have been calculated by the use of a very large sample of global data, while the corresponding sample for the Aegean area is much smaller. For this reason, the global values of these scaling coefficients are adopted for the Aegean area too. To further support this approach the following test was also performed: By using a sample of 161 interevent times of mainshocks in the Aegean area with a constant M_{min} = 6.0±0.2 (where ±0.2 is the error window) a mean value c^* = 0.47 was determined for the scaling coefficient of the relation $logT_t = c^*M_p + Q$. On the other hand, c^* for the global data is approximately equal to $b+c$ = 0.52, which is in good agreement with the value determined by data in Aegean. This supports the adoption of the scaling coefficients of relation (2), which is the most important one of the TIMAP model.

For each of the 218 centers, C, circles are defined, (C, R), with $R_1 \le R \le R_2$ and a step δR (e.g. R_1 =

20km, R_2 = 100km, δR = 5km). Then, relation (2) is applied to calculate the constant Q by using all available sets ($M_{min} \geq 5.2$, M_p, $logT_t$) in each such circle. As best solution we considered that one for the circle (C, R_σ) for which the number, N_σ, of sets (interevent times) is larger than a certain value, $N_\sigma \geq N_{min}$ (e.g. N_{min} = 4), and the standard deviation, σ_q, takes its smallest value (σ_q = minimum). For each of these regions the values of R_σ and N_σ, the average value of Q and the corresponding standard deviation, σ_q, are determined. Also, the available sets ($M_{min} \geq 5.2$, M_p, M_f) of data for each of the circular regions have been used to define a circle (C, $R_w \leq 100$km) for which the standard deviation takes its smallest value. The complete mainshock data for this circle are used to define the average value of W of relation (3) for each circular region, with a standard deviation σ_w. The average values of the standard deviations for all 218 regions are $\sigma_q = 0.15 \pm 0.06$ and $\sigma_w = 0.21 \pm 0.08$.

A backward test of the TIMAP model is performed to examine its prediction potentiality, that is, to get an idea about the range of uncertainties of the retrospectively predicted by this model epicenters and magnitudes of strong ($M \geq 6.0$) mainshocks. For this purpose, a "target mainshock" is retrospectively predicted on the basis: of the parameters of a previous known mainshock (location, origin time, magnitude) and of known parameters (C, R_σ, Q, σ_q, R_w, W, σ_w) of circular faults' regions where the epicenters of both mainshocks are located. There are 86 such circular seismic regions in the Aegean area which include at least two strong ($M \geq 6.0$) mainshocks with different last mainshocks. These 86 last mainshocks are taken as "target mainshocks" which have been estimated (predicted) retrospectively.

Such retrospective predictions have been made for each one of the 86 target mainshocks. Usually more than one faults' centers, $C(\phi,\lambda)$, are clustered near the epicenter of the mainshock. Thus, the predicted epicenter, $E_t(\phi,\lambda)$, is the geographic mean of the clustered centers, $C(\phi,\lambda)$. In particular, the backward test shows that the distance between the epicenter, E_t, defined by the TIMAP model and the observed epicenter, E, is given by the relation $(EE_t) = 90 \pm 40km$, where $40km$ is one standard deviation, σ. This backward test also shows that the magnitude predicted by the TIMAP model, M_t, for each center, $C(\phi,\lambda)$, is equal to $M_f+0.3$ for $M_f \leq 6.4$, to $M_f+0.2$ for M_f between 6.5 and 6.9 and to $M_f+0.1$ for $M_f \geq 7.0$, where M_f is given by the relation (3). In case of clustered centers, the adopted magnitude is the average of the M_t magnitudes calculated for each center of the cluster. The uncertainty of the magnitude M_t estimated this way is $\sigma = 0.21$. Figure (1) shows the cumulative frequency distribution of the probabilities P_t (Δt = 10years) defined by the TIMAP model on the basis of the available data 2 years before the generation of the 86 target mainshocks with $M \geq 6.0$, of the 66 mainshocks with $M \geq 6.5$ and of the 38 mainshocks with $M \geq 7.0$.

A backward test has been also performed to define the percentage of false alarms. For this purpose, it has been attempted a retrospective prediction of the strong ($M \geq 6.0$) mainshocks which occurred in the whole Aegean area during the time period 1981-2008 when a dense network of seismographic stations has been in operation in this area. The test is based on these data of strong mainshocks and on the 218 circular faults' regions (C, R$\leq$100km) in which the epicenters of corresponding mainshocks are located. The test is also based on the observation that the rate of mainshocks with M$\geq$6.0 in the whole Aegean area is r = 12.6 (with σ = 2.6) earthquakes per decade during the period 1966-2008 when networks of seismic stations were in operation in Greece. That is, the maximum number of expected mainshocks per decade is r+2σ = 18.

The TIMAP model has been applied separately for each one of the nineteen decades, 1981-1990, 1982-1991, …, 1999-2008 and for each of the 218 circular faults' regions. Probabilities, P_t(δt = 10years) have been calculated using relations (2) and (4) with σ = 0.15, which is the average of the calculated σ_q values and by selecting the highest P_t from its values calculated for M_{min} equal to 6.0, 6.5 and 7.0.

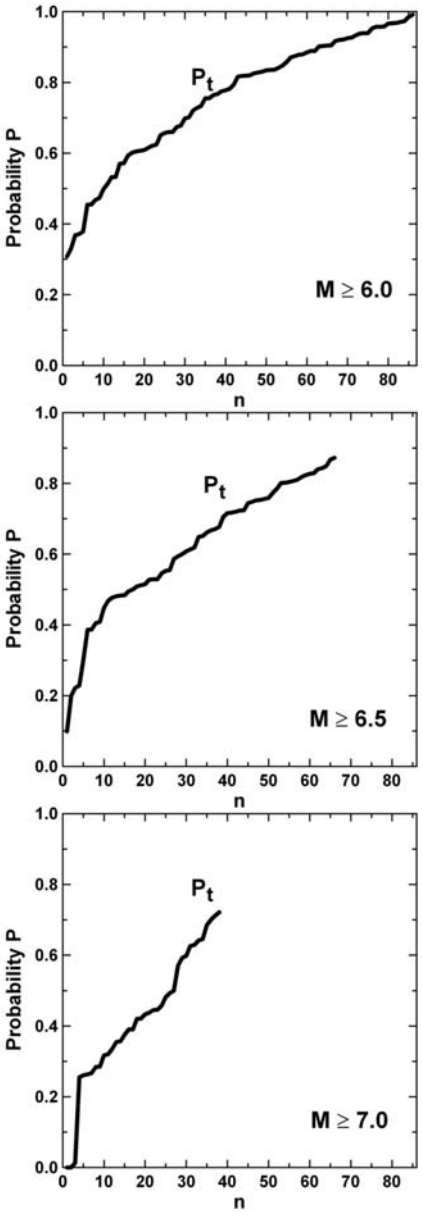

Fig. 1: The probability P(Δt = 10years), as a function of the cumulative frequency, n, of occurrence for the generation of a strong mainshock (M≥6.0 upper part, M≥6.5 middle part and M≥7.0 lower part) in circular faults' regions (C, R≤100km) of the Aegean sea and surrounding lands. Distribution of Pt comes from calculations based on the time dependent (TIMAP) model for a 10 years period which started two years before the generation of each one of the already occurred strong mainshocks.

Thus, for each decade a probability was calculated for each one of the 218 circular faults' regions. Of those, the 18 regions with the eighteen highest probabilities were considered and their locations in respect to the epicenters of the mainshocks occurred in this decade were examined. A faults' re-

gion is considered as "predicting" if it includes the epicenter of at least one strong ($M \geq 6.0$) mainshock of the decade, otherwise the region is considered as "false alarming". This procedure has been repeated for each one of the nineteen decades.

The result of this test is that 243 of the examined regions have been characterized as predicting and 99 as false alarming, that is, the false alarming percentage is 29% for the TIMAP model in the Aegean area. This percentage can be attributed to the non strong triggering of these faults' regions due to absence of seismic excitation.

This test also suggests that the percentage of the false alarms by the TIMAP model is relatively large, which means that this model can be used as complementary of the D-AS model for which false alarms (from tests in random catalogues) are only 10%.

3. The Decelerating-Accelerating Seismic Strain (D-AS) Model

The D-AS model is defined by the power-law relation (1), as well as by other relations which have been derived by Papazachos et al. (2006). In the present work using additional recent global data these relations have been tested and in some cases were slightly modified. These refined relations are presented here for accelerating and decelerating preshock sequences.

3.1 Relations for accelerating preshocks

For accelerating preshocks the model is based on relation (1) and on the following semi-empirical constraints:

$$\log R = 0.42M - 0.30 \log s_a + 1.25, \quad \sigma = 0.15 \tag{5}$$

$$\log\left(t_c - t_{sa}\right) = 4.60 - 0.57 \log s_a, \quad \sigma = 0.10 \tag{6}$$

$$M = M_{13} + 0.60, \quad \sigma = 0.20 \tag{7}$$

where R (in km) is the radius of the circular (critical) region (or the radius of the equivalent circle in the case of an elliptical critical region), s_a (in Joule$^{1/2}$/yr.10^{4}km^2) is the rate of the long term Benioff strain per year and 10^{4}km^2 in the critical region, t_{sa} (in yrs) is the start time of the accelerating sequence, t_c is the origin time of the mainshock, M is the magnitude of the mainshock and M_{13} is the mean magnitude of the three largest preshocks (Papazachos et al., 2006).

In order to compare the obtained results regarding the R, M, t_{sa} values (estimated for each mainshock with the relations (5), (6), (7)), the probability of each obtained parameter was calculated. For this reason each model parameter was estimated with respect to its expected value, assuming that its deviations follow a Gaussian distribution. The average, P_a, of these probabilities is used as a measure of agreement of the determined parameters with those calculated by these global relations (Papazachos and Papazachos, 2001). Furthemore, for each point of the investigated area a "quality index", q_a, has been defined (Papazachos et al., 2002a) by the formula:

$$q_a = \frac{P_a}{mC} \tag{8}$$

where C is the curvature parameter (Bowman et al., 1998) and m is the parameter of relation (1). On the basis of a large sample of data concerning accelerating preshock sequences of mainshocks which

occurred in a variety of seismotectonic regimes and had magnitudes between 5.6 and 8.3 (Papazachos and Papazachos, 2000, 2001; Scordilis et al., 2004; Papazachos et al., 2005b) the following cut off values have been proposed:

$$C \leq 0.60, \quad P_a \geq 0.45, \quad 0.25 \leq m \leq 0.35, \quad q_a \geq 3.0 \tag{9}$$

Worldwide observations show that a mean value of m is 0.30, which is in agreement with theoretical considerations (e.g. Rundle et al., 1996; Ben-Zion et al., 1999). For these reasons, this value was adopted as fixed throughout the present work. The geographic point, Q, for which relations (9) are fulfilled and where the quality index, q_a, has its largest value is considered as the geometrical center of the critical region. The magnitude, M_{min}, of the smallest preshock of an accelerating preshock sequence for which relations (9) applies and q_a has its largest value is given by the relation:

$$M_{\min} = 0.46M + 1.91 \tag{10}$$

where M is the magnitude of the mainshock (Papazachos, 2003; Papazachos et al., 2005b). Thus, for mainshock magnitudes 6.0, 7.0 and 8.0 the corresponding minimum magnitudes of accelerating preshock sequences are 4.7, 5.1 and 5.6, respectively.

The accelerating seismic strain which complies with the constraints of relations (9) cannot be identified until a time, t_{ia}, before the generation of the mainshock, which is called "identification time". In practice, this is the earliest time for which the available data give a valid solution, assuming that the accelerating preshock sequence ends at the (true) origin time, t_c, of the mainshock. From global data concerning accelerating preshock sequences the following relation is derived:

$$\log\left(t_c - t_{ia}\right) = 2.51 - 0.30 \log s_a, \quad \sigma = 0.16 \tag{11}$$

Thus, for $logs_\alpha$ equal to 4.5 and 6.2, which correspond to the smallest and largest usually observed values of strain rate in our data-set, the identification time interval t_c-t_{ia} is equal to 14 years and 4 years, respectively.

The origin time, t_c, and the magnitude, M, of the mainshock depend also on the average origin time, t_a, and average magnitude, M_a, respectively, of the corresponding accelerating preshock sequence. Available data for estimating (predicting) t_c and M from equations (10) and (11) are those which concern accelerating preshocks which have occurred when such prediction is made, that is, a few years before the generation of the mainshock. Taking this into consideration and using the data of accelerating preshock sequences of the mainshokes listed on table (1) the following relations have been derived:

$$\log(t_c - t_a) = 3.11 - 0.36 \log s_a, \quad \sigma = 0.07 \tag{12}$$

$$M = 1.43M_a - 0.60, \qquad \sigma = 0.25 \tag{13}$$

where t_a and M_a is the average origin time and average magnitude, respectively, for the accelerating preshocks which occurred up to three years before the generation of the mainshock (Scordilis, 2010).

Accelerating preshocks are strong (see relation 10) and the largest of these can have magnitude larger than 6.0 and may cause damage. For this reason it is necessary to be able to estimate (predict) the largest accelerating preshock which occur, after the identification time which is given by relation (11) because an accelerating precursory sequence is recognizable after this time. Therefore, the time interval before the generation of the mainshock when the largest accelerating preshock is expected is given by relation (11). Thus, for the Aegean area, where $\log s_a \simeq 5.8$, this time interval is about 6 years. The

epicenter of the maximum accelerating preshock is in the region of the physical center, P_q, and in a maximum distance of 150km from the center. The magnitude, M_{ai}, of this shock is given by the relation;

$$M_{ai} = 0.68M + 1.60, \quad \sigma = 0.30 \tag{14}$$

where M is the mainshock magnitude, as it comes out from the data concerning accelerating preshock sequences of mainshocks listed on table (1). Thus, for mainshock magnitudes 6.5, 7.0, 7.5 and 8.0, the magnitudes of the largest accelerating preshocks are, on the average, 6.0, 6.4, 6.7 and 7.0, respectively.

3.2 Relations for decelerating preshocks

Decelerating seismic strain (Benioff strain) released by intermediate magnitude preshocks in the seismogenic region follows a power-law (relation 1 with m>1) and the relations:

$$\log a = 0.23M - 0.14 \log s_d + 1.40, \quad \sigma = 0.15 \tag{15}$$

$$\log\left(t_c - t_{sd}\right) = 2.95 - 0.31 \log s_d, \quad \sigma = 0.12 \tag{16}$$

where α (in km) is the radius of the circular seismogenic region, M is the magnitude of the mainshock, t_{sd} (in yrs) is the start time of the decelerating preshock sequence, and s_d (in Joule$^{1/2}$/yr.10^{4}km^2) is the long-term seismic strain rate (long-term seismicity) of the seismogenic region (Papazachos et al., 2006). A quality index, q_d, can be also defined by the relation:

$$q_d = \frac{P_d m}{C} \tag{17}$$

where P_d is defined for decelerating seismicity on the basis of quantities a, M, t_{sd} and relations (15, 16). The following cut-off values have been calculated by the use of data for decelerating preshock sequences of corresponding strong mainshocks which occurred in a variety of seismotectonic regimes (Papazachos *et al*., 2006):

$$C \le 0.60, \quad 2.5 \le m \le 3.5, \quad P_d \ge 0.45, \quad q_d \ge 3.0 \tag{18}$$

From relations (6) and (16) it is evident that the duration of accelerating and decelerating sequences is equal for strain rate $\log s_a = \log s_d = 6.35$. Since for most studied areas the strain rate is smaller, the accelerating sequence starts usually earlier than the corresponding decelerating sequence. Thus, for $\log s_d = \log s_a = 4.5$ (low seismicity areas) the duration of the decelerating and accelerating sequences is 36 and 108 years, respectively, while for $\log s_d = \log s_a = 6.2$ (very high seismicity regions) the two durations are almost equal (11 and 12 years, respectively).

Using global data it has been shown (Papazachos et al., 2006) that the minimum magnitude, M_{min}, of decelerating preshocks for which the best solution (smallest C value) is obtained, is given by the relation:

$$M_{\min} = 0.29M + 2.35 \tag{19}$$

where M is the magnitude of the mainshock. Thus, for mainshock magnitudes 6.0, 7.0 and 8.0 the corresponding values of M_{min} are 4.1, 4.4 and 4.7, respectively, which are much smaller than the corresponding minimum values (4.7, 5.1 and 5.6) for accelerating preshocks. It is interesting to note that decelerating seismicity which precedes strong mainshocks ($M \ge 6.0$) is also pronounced for intermediate magnitude ($M \ge 4.0$) preshocks. Data for such shocks are easily available.

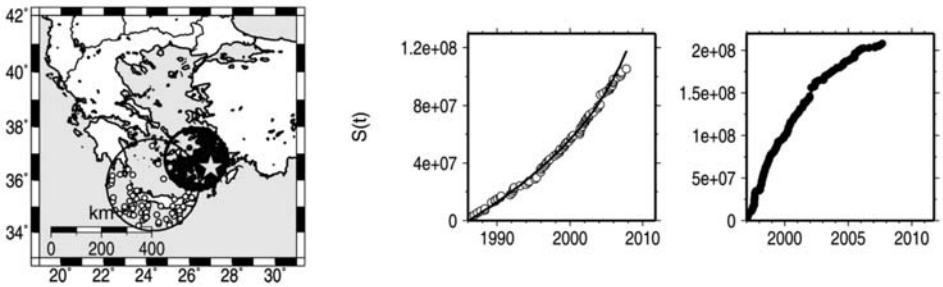

Fig. 2: Space and time variation of decelerating and accelerating preshocks observed (in 2007) before the generation of the strong (M = 6.4) 2008 earthquake near Rhodes island. Left: epicenters of decelerating preshocks (dots in the smaller of the two circles) and of accelerating preshocks (small white circles in the larger circle). The star is the predicted epicenter of the ensuing mainshock. Right: time variation of the Benioff strain, S(t), for decelerating preshocks (dots) and for accelerating preshocks (small white circles). The curves fit the data by a power-law (relation 1). The earthquake occurred (15 July 2008, M = 6.4, 36.0^{0}N, 27.9^{0}E, h = 60km) within the predicted time, magnitude and space windows (Papazachos and Karakaisis, 2008; Papazachos et al., 2009).

An "identification time" is also defined for each decelerating preshock sequence. Similarly to accelerating sequences, this is the earliest time, t_{id}, for which the available data fulfill constraints imposed by relations (18) and the end of the sequence coincides with the origin time of the mainshock. It has been shown that the logarithm of the difference between the origin time of the mainshock, t_c, and the identification time, t_{id}, of the decelerating preshock sequence scales negatively with the strain rate, s_d (Papazachos et al., 2005a). A revised form of this relation based on new additional data is:

$$\log\left(t_c - t_{id}\right) = 2.07 - 0.20 \log s_d, \quad \sigma = 0.15 \tag{20}$$

Thus, for logs_d equal to 4.5 and 6.2, t_c-t_{id} is equal to 15 years and 7 years, respectively.

From relations (11) and (20) it comes out that for $s_d = s_a$ the identification time of the decelerating sequence of a mainshock occurs earlier than the identification time of its accelerating sequence, although the accelerating sequence starts earlier (see relations 6 and 16).

The first part in the time variation of the Benioff strain graph appears to be almost linear for both accelerating and decelerating strain (see fig. 2) and the pattern can be identified after the time when it exceeds the background seismicity level. In a region of low background seismicity this "exceedance" and recognition will occur earlier than in a region of higher background seismicity, suggesting that the difference between the recognition time and the mainshock origin time decreases with increasing background seismicity. This explains why the difference between the origin time of the mainshock and the identification time, t_c-t_i, as well as between the origin time of the mainshock and the calculated start time, t_c-t_s, scale negatively with the long term strain rate, s, for precursory accelerating (relations 6, 11) and decelerating (relations 16, 20) seismic strain.

3.3 Additional predictive properties of the D-AS model

Relations presented in paragraphs (3.1) and (3.2) express predictive properties concerning the time and magnitude of an ensuing mainshock. In the present paragraph revised relations for the prediction of the mainshock epicenter are given. These relations concern the geographic distribution (with respect to the expected mainshock epicenter) of the quality indexes q_d and q_a (relations 8 and 17)

and of six distinct geographic points defined by the geographic distribution of decelerating and accelerating preshocks. An observed time variation of q_d and q_a, which is a qualitative predictive property of the model, is also presented. Uncertainties are also properties of the model and for this reason are examined in this work and are given in this section.

The curvature parameter, C, which qualifies the deviation of the Benioff strain from linearity, takes its smallest value at the center, F, of the decelerating preshocks, C_{df}, and at the center, Q, of the accelerating preshocks, C_{aq}. At other geographic points, including the epicenter, E, of the ensuing mainshock, the values of the curvature parameters are larger. Thus, the mean values of the curvature parameter for preshocks of the mainshocks listed on table (1) are $C_{df} = 0.32$, $C_{aq} = 0.42$ and the corresponding values for the mainshock epicenter are $C_{de} = 0.64$ and $C_{ae} = 0.71$. The larger values of the curvature parameters at the mainshock epicenter result in smaller values of the quality indexes (q_{de}, q_{ae}) at the actual mainshock epicenter with respect to the corresponding optimal values (q_{df}, q_{aq}) at the geometrical centers (F and Q). This is expressed by the following relation, which has been derived by using all available data for the preshock sequences of the mainshocks listed on table (1):

$$\frac{q_{de} + q_{ae}}{q_{df} + q_{aq}} = 0.45 \pm 0.13 \tag{21}$$

This relation applies at the vicinity of the mainshock epicenter and can be used as a constraint in estimating (predicting) this epicenter, as it is explained later.

The locations of three geographic points (F, P_f, V_f) defined by the space distribution of decelerating preshocks and of three corresponding points (Q, P_q, V_q) defined by the space distribution of accelerating preshocks can contribute to the prediction of the mainshock epicenter. F and Q are the geometrical centers of the circular regions of decelerating and accelerating preshocks. P_f and P_q are the physical centers of the two sequences where the density of decelerating and accelerating preshocks, respectively, is highest (Karakaisis et al., 2007). V_f and V_q correspond to the mean geographic center (mean latitude, mean longitude) of the epicenters of decelerating and accelerating preshocks, respectively. There are several ways in which these six points can be used to define the epicenter of the ensuing mainshock. A simple way is to separate the points into two groups and define the geographic mean (mean latitude and mean longitude) of each group. The first group is formed of the points (F, V_f, P_f) which are located in a relatively short distance from the mainshock epicenter and the distance of their geographic mean, D, from the mainshock epicenter, E, is:

$$\begin{aligned} (ED) &= 0.3(DA) + 35.0 \pm 40km, \quad for\ (DA) \le 250km \\ (ED) &= 120 \pm 50km, \qquad\qquad for\ (DA) > 250km \end{aligned} \tag{22}$$

The second group is formed of the three points (Q, V_q, P_q) which are located at relatively large distances from the mainshock epicenter and the distance of their geographic mean, A, from the mainshock epicenter is:

$$(EA) = 0.85(DA) + 50 \pm 80km \tag{23}$$

The available data for the preshock sequences considered in the present work show that the forty–six mainshock epicenters, E, have a tendency to delineate along the line AD and to distribute symmetrically with respect to this line. Thus, the mean distance, x, of E from DA is almost equal to zero

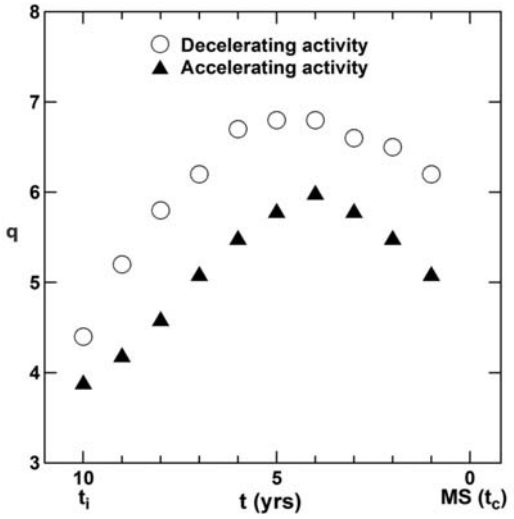

Fig. 3: Variation with the time, t (years), to the mainshock of the quality index, qd, for decelerating preshocks (open circles) and of the corresponding quality index, qa, for accelerating preshocks (black triangles) during the period between the identification time, ti, and the origin time, tc, of the mainshock.

(considering positive the distances of the points, E, which are in one side of DA and negative the distances of these points which are in the other side) with a standard deviation 80 km. That is,

$$x = 0 \pm 80km \tag{24}$$

The line DA intersects the circle (D, R = 120 km) in two points (D_1, D_2). D_1 is closer to the mainshock epicenter (from data of preshock sequences of mainshocks listed on table 1, $ED_1 = 80\pm40$ km and $ED_2 = 180\pm60$ km). Although D_1 is usually between D and A, we are not sure during the pre-mainshock period which of the two intersection points is closer to the epicenter of the ensuing mainshock. For this reason additional independent information is used, such as mean level of time dependent seismicity (e.g. the epicenter, E_t, defined by the TIMAP model in section 2.1) to resolve this ambiguity. Thus, if L_d is one of the points D_1 and D_2 which is in a higher seismicity level (closer to E_t), we can use the following relation as the fifth constraint for the location of the epicenter of the ensuing mainshock:

$$(EL_d) = 80 \pm 40km \tag{25}$$

The estimation (prediction) of the epicenter of an ensuing mainshock is based on constraints defined by relations (21, 22, 23, 24 and 25). That is, for each geographic point of a grid where the mainshock epicenter is expected (typically 2^ox2^o) a probability is calculated for each of these relations by assuming a normal (Gaussian) distribution for the observed deviations and the average of the five probabilities is considered as the representative value of probability for each grid point. The three points with the three highest such probabilities are defined and their geographic mean (mean latitude, mean longitude) is considered as the predicted epicenter. The retrospectively predicted parameters, t_c^*, $E^*(\phi,\lambda)$, M^* by the D-AS model of the 46 strong (M≥6.3) mainshocks are listed in table (1).

One should also consider variation with time to the mainshock of both quality indexes q_d and q_a. This variation is observed during the time period between the identification time (t_{id} or t_{ia}) and the origin time, t_c, of the mainshock (fig. 3). This allows a qualitative continuous inspection (monitoring) of the decelerating, $q_d = q_d(t)$, and accelerating, $q_a = q_a(t)$, preshock sequences with the time to the mainshock. Thus, both indexes increase from the corresponding identification times (t_{id}, t_{ia}) up to about the 60% of the time interval t_c-t_i and both decrease during the rest 40% of the time t_c-t_i. This suggests that during this last time interval before the mainshock, seismic excitation of preshocks declines in the broad (critical) region and is enhanced in the narrow (seismogenic) region.

Table 1. Observed origin time, t_c, epicenter coordinates, $E(\phi,\lambda)$, and moment magnitude, M, of the forty-six mainshocks and corresponding retrospectively predicted values, t^*_c, $E^*(\phi,\lambda)$, M^* for these parameters.

Area		t_c	$E(\phi,\lambda)$	M	t^*_c	$E^*(\phi,\lambda)$	M^*
Mediterranean	1	10.10.1980	36.2, 01.4	7.1	1981.9	36.2, -0.2	7.2
	2	23.11.1980	40.8, 15.3	6.9	1981.1	41.6, 14.0	6.8
	3	21.05.2003	36.9, 03.8	6.8	2001.6	36.0, 3.6	6.8
	4	24.02.2004	35.1, -04.0	6.4	2004.3	35.5, -4.9	6.3
Aegean	1	09.07.1980	39.3, 22.9	6.5	1980.4	39.0, 21.4	6.5
	2	24.02.1981	38.1, 23.0	6.7	1979.3	39.1, 24.1	6.8
	3	19.12.1981	39.0, 25.3	7.2	1982.6	38.4, 24.0	7.3
	4	17.01.1983	38.1, 20.2	7.0	1985.5	38.2, 20.4	6.7
	5	13.05.1995	40.2, 21.7	6.6	1994.3	39.9, 21.2	6.7
	6	13.10.1997	36.4, 22.2	6.4	1997.8	36.7, 22.3	6.4
	7	18.11.1997	37.5, 20.7	6.6	1997.8	36.9, 20.8	6.5
	8	26.07.2001	39.1, 24.4	6.4	2000.9	39.0, 23.6	6.6
	9	14.08.2003	38.7, 20.5	6.3	2003.8	38.7, 20.1	6.5
Anatolia	1	05.07.1983	40.2, 27.3	6.4	1983.3	39.9, 28.5	6.3
	2	13.03.1992	39.7, 39.6	6.6	1991.2	39.2, 38.4	6.5
	3	01.10.1995	38.1, 30.2	6.4	1996.7	39.1, 30.2	6.5
	4	09.10.1996	34.5, 32.1	6.8	1996.8	35.5, 32.0	7.0
	5	17.08.1999	40.8, 30.0	7.5	1993.3	39.6, 30.5	7.1
California	1	08.11.1980	41.1, -124.6	7.3	1981.1	41.6, -124.3	6.9
	2	02.05.1983	36.2, -120.3	6.4	1979.5	35.5, -119.1	6.4
	3	24.11.1987	33.0, -115.9	6.6	1986.7	33.2, -117.2	6.7
	4	18.10.1989	37.1, -121.9	6.9	1990.0	37.1, -122.3	6.8
	5	25.04.1992	40.3, -124.2	7.1	1991.9	39.5, -123.7	7.0
	6	28.06.1992	34.2, -116.4	7.3	1991.8	35.9, -116.2	7.4
	7	17.01.1994	34.2, -118.5	6.6	1993.4	34.5, -118.7	6.3
	8	22.12.2003	35.7, -121.1	6.5	2004.3	36.5, -120.3	6.4
Japan	1	12.07.1993	42.9, 139.2	7.7	1994.6	42.0, 139.5	7.8
	2	04.10.1994	43.7, 147.4	8.3	1995.6	43.3, 147.0	8.3
	3	16.01.1995	34.6, 135.0	7.0	1995.5	35.0, 134.7	7.2
	4	26.05.2003	38.8, 141.6	7.0	2003.0	39.3, 142.3	6.7
	5	25.09.2003	41.8, 143.9	8.3	2004.0	40.7, 144.0	8.3
	6	11.10.2003	37.8, 142.6	7.0	2003.8	36.6, 142.5	6.9
	7	05.09.2004	33.2, 137.1	7.4	2003.1	34.1, 137.5	7.6
	8	16.08.2005	38.3, 142.0	7.2	2004.6	39.4, 141.7	7.1
Central Asia	1	20.06.1990	37.0, 49.3	7.4	1990.6	36.1, 48.7	7.5
	2	19.08.1992	42.1, 73.6	7.2	1993.0	42.1, 72.7	7.1
	3	27.02.1997	30.0, 68.2	7.0	1998.0	30.3, 68.1	6.8
	4	10.05.1997	33.9, 59.8	7.3	1997.8	33.5, 59.8	7.3
	5	08.11.1997	35.1, 87.4	7.5	1996.1	34.6, 87.2	7.4
	6	06.12.2000	39.6, 54.8	7.0	2001.2	40.2, 53.5	7.2
	7	26.01.2001	23.4, 70.2	7.6	2001.2	23.1, 69.3	7.8
	8	14.11.2001	35.9, 90.5	7.8	2004.6	37.2, 91.1	7.7
	9	08.10.2005	34.5, 73.6	7.5	2007.2	35.7, 72.4	7.5
S. America	1	09.10.1995	19.1, -104.2	7.9	1991.9	19.8, -104.5	8.1
	2	13.01.2001	13.0, -88.7	7.7	1998.6	13.2, -88.3	7.9
	3	23.06.2001	-16.3, -73.6	8.3	2001.6	16.5, -74.6	8.2

To define the model uncertainties of the D-AS model with respect to: the origin time, magnitude and epicenter of an ensuing mainshock, a backward test was performed by applying the model to the already occurred preshock sequences of the 46 strong mainshocks listed in table (1). This postdiction resulted in uncertainties: $\pm$2.5 years for the origin time of the mainshock, $\pm$0.4 for its predicted magnitude and $\leq$150km for its epicenter with a probability 90%. Since the probability of the D-AS model for false alarms is of the order of 10%, the total probability for these time, magnitude and space windows is reduced to 80%. This result confirms previous similar results (Papazachos et al., 2006).

When the epicenter, E_t, estimated by the TIMAP model is known (see section 2.1) the finally predicted by both models epicenter is based on relations (21), (22), (23), (24) and (25) and on the relation:

$$(EE_t) = 90 \pm 40km \tag{26}$$

Also, the finally adopted magnitude is the average of the three magnitudes defined by the D-AS model and of the M_t magnitude defined by the TIMAP model. The 2σ uncertainties when estimations are based on both models are: $\pm$2.5 years for the origin time, $\leq$120 km for the epicenter and $\pm$0.4 for the magnitude of the ensuing mainshock with a probability about 80%.

3.4 Physical explanation of accelerating and decelerating precursory strain

Decelerating and accelerating precursory seismicity, the relative relations and values of parameters are mainly results of seismological observations. These empirical results, however, need physical explanation to support their scientific validity. Several such attempts have been already made but there are usually more than one proposals for possible physical models and interpretations. The results of the present work allow the resolutions of such ambiguities.

3.4.1 Physical explanation of accelerating strain

Accelerating precursory Benioff strain has been physically explained by principles of the critical point dynamics, that is, by considering the process of generation of the moderate magnitude accelerating preshocks as a critical phenomenon, culminating in a large event (mainshock) considered as a critical point (Allègre and Mouël, 1994; Sornette and Sammis, 1995; Rundle et al., 2003). We are presenting in this section additional observational information which supports critical triggering of mainshocks by accelerating preshocks and that this triggering is associated with quasi–static stress changes.

Accelerating strain observed for the forty six accelerating preshock sequences considered in the present work occurred at relatively large and much variable distances from the mainshock epicenter ($EQ = 270\pm120$ km). For this reason it is not possible that pre-mainshock static stress changes trigger accelerating preshocks or that static stress change produced by such preshocks trigger the mainshock.

Therefore, critical triggering of the mainshock by accelerating preshocks through a physical process with gradual stress changes and viscous relaxation of the lower crust and upper mantle can explain observed properties (long distances and delay times) of accelerating preshocks. That is, quasi–static stress change explains contribution to triggering of the mainshock by accelerating preshocks because such stress change decays slowly with distance, which means that their triggering potential extends to greater distances than static stress change and because the relatively low speed of viscoelastic propagation results in delayed triggering.

Critical triggering predicts increase of the maximum magnitude of accelerating preshocks with the time to the mainshock. To test it, we divided the total duration of each of the examined 46 acceler-

ating preshock sequences into ten equal time intervals and for each interval the difference of the maximum preshock from the corresponding mainshock was calculated. Then, the mean of these 46 differences for each interval was calculated and the time variation of this mean difference was defined. It was observed that this difference decreases with the time to the mainshock, which means that the magnitude of the largest accelerating preshock increases with the time to the mainshock. This observational result shows that accelerating seismic strain is mainly due to an increase of the magnitude of accelerating preshocks and supports critical triggering of mainsocks by accelerating preshocks. In the same way it has been shown that the frequency (number) of accelerating preshocks also increases with the time to the mainshock.

In the accelerating preshock sequences considered in the present work, there are several cases where a critical region overlaps partly with another which means that an accelerating shock can be preshock of more than one ensuing mainshocks. This observation supports the idea that accelerating preshocks affect the generation of mainshocks by critical triggering.

A power- law for the time variation of accelerating preshock strain, such as relation (1), which has been derived on the basis of damage mechanics theory (Bufe and Varnes, 1993), is also expected if seismic cycle is modeled as a critical phenomenon (Sornette and Sammis, 1995; Saleur at al., 1996). Furthermore, the mean of the observed values of m for this relation is equal to 0.3 (Papazachos and Papazachos, 2001; Ben-Zion and Lyakovsky, 2002) in agreement with values of this parameter determined theoretically on the basis of the critical point dynamics (Rundle et al., 1996; Ben-Zion et al., 1999).

3.4.2 Physical explanation of decelerating strain

Decelerating seismic strain is composed of two main phases. The first is a phase of excitational seismic strain which ends at the identification time (t_{id} in relation 20). The second phase follows and covers a period of decrease (quiescence) for the seismic strain.

Relations (6) and (16) show that increase of precursory strain in the critical region starts before the increase of precursory strain in the seismogenic region. This observation suggests that the first (excitational) phase of precursory strain in the seismogenic region can be a result of contribution of critical (quasi–static) triggering in addition to tectonic stressing. It has been further examined: what is the cause of the following deceleration of seismic strain in the seismogenic region and how the mainshock is triggered by preshocks which occur in the seismogenic region during the phase of decelerating strain.

Decelerating preshocks are generated close to the mainshock epicenter ($FE = 130 \pm 40$ km) and relatively shortly before the mainshock. These observations indicate that changes of static (Coulomb) stress caused by preshocks in the seismogenic region during the decelerating phase contribute to triggering of the mainshock. It must be also taken into account that decelerating preshocks considered in the present work have magnitudes larger than a certain value (see relation 19), which means that there is a finite number of faults where shocks of a decelerating preshock sequences occur.

A frictional stability model (Gomberg et al., 1998) where a seismic fault obeys rate–and–state frictional constitutive relations (Dieterich, 1992, 1994) can explain seismic quiescence that follows a seismic excitation. Thus, this model predicts that, if triggering results from advancing the failure time of inevitable earthquakes and if the population of the available faults is finite, a static load results in seismic excitation followed by seismic quiescence, as it occurs with decelerating preshocks considered in the present work. That is, the seismic excitation in a finite number of faults of the seismogenic region leaves fewer faults available for failure and thus quiescence follows the seismic excitation.

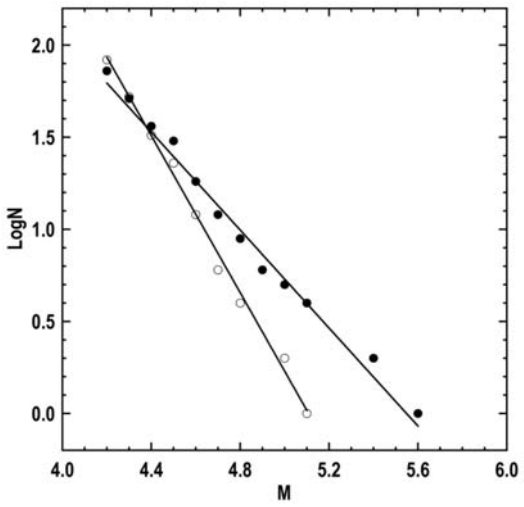

Fig. 4: Cumulative distribution of preshocks in the narrow (seismogenic) region of the mainshock with M = 6.2 which occurred on 6 November 1992 in eastern Aegean (38.1^{0}N, 27.0^{0}E). Dots refer to preshocks which occurred in the seismogenic region before the identification time, when the slope is b = 1.3. Small open circles refer to preshocks occurred in the same region after the identification time when b = 2.1.

Decelerating preshocks are relatively small (see relation 19) and their individual effect on static stress changes is also small because this change increases with the magnitude, M, of the triggering earthquake as $\sim 10^{aM}$. It has been shown, however, that if triggering earthquakes follow the Gutenberg–Richter law with $b>a(= D/2$, where D is the fractal dimension), small earthquakes dominate in stress transfer and earthquake triggering because their high frequency overcomes their small individual triggering potential (Helmstetter, 2003; Helmstetter et al., 2005). For earthquake triggering due to static stress we have $D\sim 2$, which is also interpreted as the fractal dimension of an active fault network. Therefore, seismic sequences with $b>1$ have an increased triggering potential. Such seismic sequences can also trigger strong mainshocks because in static triggering the magnitude of the triggered earthquake is independent of the magnitude of the triggering earthquake (Helmstetter, 2003).

Therefore, it is of importance to calculate the b value of preshocks in the seismogenic region during the time of decelerating strain (second phase) and compare b values with $D/2$. For this purpose, we considered the decelerating preshock sequences of all 12 mainshocks which occurred in the Aegean between 1980 and 2004 and have magnitudes $M \geq 6.1$ (Papazachos et al., 2006). The b value has been calculated by least-squares for the first phase of each decelerating sequence (excitational phase), as well as for its second (later) phase. For the first twelve phases b values between 0.8 and 1.9 have been calculated with a mean and corresponding standard deviation 1.3 ± 0.3. For the twelve late phases b values between 1.1 and 2.1 have been calculated with a mean and corresponding standards deviation 1.6 ± 0.3. That is, all late decelerating preshock sequences, which occurred shortly before the corresponding mainshocks, have high b values and their triggering potential is high. It is, therefore, reasonable to assume that small preshocks which occur in the seismogenic region during the second phase contribute to triggering of the mainshock by increasing static stress.

Figure (4) shows a representative case of variation of the cumulative frequency, N, of decelerating preshocks with their magnitude, M, which started on 4.1.1982 and lasted till the generation of their mainshock (6.11.1992, M = 6.2, 38.1^{o}N, 27.0^{o}E, east Aegean). The first (excitational) phase lasted till 27.10.1984 (~2.7 years) and the frequency distribution (dots in fig. 4) of preshocks of this phase is fitted (in the least-square sense) by the relation:

$$\log N = 7.4 - 1.3M \tag{27}$$

with a high correlation coefficient (r = -0.99). The second (quiescence) phase lasted till the generation of the mainshock (~8.0 years) and the frequency distribution (small open circles in fig. 4) of preshocks of this phase is fitted by the relation:

$$\log N = 10.9 - 2.1M \tag{28}$$

with also a high correlation coefficient (r = -0.99). It is observed (fig. 4, relations 27, 28) that for intermediate magnitude preshocks (4.4–5.6) the frequency in the seismogenic region is high during the excitational phase and is much reduced during the quiescence phase. This explains the corresponding reduction of the calculated Benioff strain and its deceleration with the time to the mainshock. It is also observed that the frequency of the small preshocks in the seismogenic region is high during the second period of the sequence, as it is shown by the increase of the b value, that is, the frequency of small (M<4.4) preshocks is high in the seismogenic region during the whole preshock time period (t_c-t_{sd}).

3.5 Successful predictions by the D-AS model

In addition to backward tests of the D-AS model to estimate its uncertainties, forward tests have been also performed by attempting prediction of future strong (M≥6.3) earthquakes to evaluate its prediction ability in a more objective way. By such forward tests, two strong earthquakes which occurred recently (2006, 2008) in the Aegean area have been successfully predicted. The first of these mainshocks occurred on 8 January 2006 in southwestern Aegean, near the Cythera island, with epicenter coordinates ($\phi = 36.2^0$N, $\lambda = 23.4^0$E), focal depth h = 65km and moment magnitude M = 6.9. The second earthquake occurred on 15 July 2008 in southeastern Aegean, near the Rhodes island ($\phi = 36.0^0$N, $\lambda = 27.9^0$E, h = 60km), with moment magnitude M = 6.4.

Identification of an accelerating pattern of intermediate magnitude preshocks in southwestern Aegean was initially made by using data up to 1 July 2000 and resulted in the estimation (prediction) of epicenter coordinates $\phi = 36.4^0$N, $\lambda = 23.0^0$E, h≤100km, M = 6.8 and time window 2001.3-2004.3 (Papazachos et al., 2002a). Estimation was repeated by the use of additional data collected during the next two years and the prediction based on data up to 1 July 2002 was: epicenter coordinates ($\phi = 36.5^0$N, $\lambda = 23.7^0$E with uncertainty ≤120km), h≤100km, M = 6.9±0.5, origin time t_c = 2006.4±2.0years. That is, the earthquake occurred within the predicted space, magnitude and time windows with a high probability (~80%), while the probability for random occurrence is about 4% (Papazachos et al., 2002b, 2007).

Identification of a decelerating and an accelerating pattern of intermediate magnitude preshocks in southeastern Aegean was made by using data up to 1 October 2007 and resulted in the estimation (prediction) of epicenter coordinates: $\phi = 36.5^0$N, $\lambda = 27.0^0$E with an uncertainty ≤150km, focal depth h≤100km, magnitude $M = 6.5\pm0.4$ and time $t_c = 2010.5\pm2.5$years (Papazachos and Karakaisis, 2008; Papazachos et al., 2009), with a probability of 80% while the probability for random occurrence of the earthquake in these space, magnitude and time windows is much smaller (~36%).

4. Conclusions and Discussion

1. Mainshocks generated by tectonic loading in a network of main faults located in a zone of lithospheric interaction have a quasi-periodic behavior. This is the basic property of the Time and Magnitude Predictable (TIMAP) regional model which is expressed by relation (2). This property, combined with the observation that the ratio T/T_t of the observed repeat times, T, to that, T_t, given by relation (2) follows a lognormal distribution, allows the estimation of the probability for the occurrence of a mainshock in this predefined mainshocks' regions during the next Δt years.

2. The second property of the TIMAP model is expressed by relation (3) which allows the estimation (prediction) of the magnitude, M_f, of the following mainshock in a faults' region. An interesting property expressed by this relation is that the magnitude, M_f, of the ensuing mainshock in the region is negatively related with the magnitude, M_p, of the previous mainshock of the region. It means that the break of a large fault in the region at the start of a period is followed by the break of a smaller fault in this region at the end of the period and vice versa.

3. A backward test of the TIMAP model by attempting retrospective prediction (postdiction) of the last strong ($M \geq 6.0$) mainshock in 86 circular faults' regions of the Aegean area during a period Δt = 10 years, which starts 2 years before the mainshock, gave reasonable results. Also, the mean difference of the observed magnitude and the estimated (predicted) magnitude, M_t (see section 2.1), is almost zero with a standard deviation equal to 0.21.

The Decelerating – Accelerating Strain (D-AS) model, which has been further developed in the present paper by the use of recent global data, has characteristics and predictive properties which are summarized and discussed in the following paragraphs.

4. The D–AS model is based on precursory seismicity change formed of two patterns. The first one is a precursory accelerating generation of the intermediate magnitude shocks which has been observed in a broad region (called in the present work "critical region"). The second pattern is a precursory decelerating generation of intermediate magnitude shocks which is observed in the narrow focal region (called in the present work "seismogenic region"). Both patterns are results of observations made by many workers, by several techniques and in various seismotectonic regimes (see section 3). For this reason these two patterns can be considered as distinct precursory seismicity patterns.

5. The model has been developed on the basis of precursory seismicity of many complete samples of mainshocks which occurred in the Aegean area, western Mediterranean, Anatolia, California, Japan, Central Asia and in south and Central America. The D–AS model is also tested in the present work by recent data concerning preshock sequences of 46 mainshocks which form 7 complete samples and occurred in corresponding seven seismotectonic regimes (see table 1). The validity of the model for all preshock sequences of so many mainshocks which form complete samples and occurred in corresponding different seismotectonic regimes is a very strong evidence that these two seismicity patterns precede systematically strong ($M \geq 6.3$) mainshocks and the D–AS model is of general validity.

6. The D–AS model has been also tested by synthetic but realistic catalogues which show that the probability for false alarms is low (~10%). This is not surprising because the model is based on many properties of a large number of real preshock sequences that put important observational constraints which cannot be easily fulfilled randomly.

7. Although the relations and parameters of the model are based mainly on observations, there are several of them which have been derived theoretically or have been interpreted physically. Thus, relation (1) has been derived on the basis of principles of damage mechanics, as well as on the basis of the critical point dynamics. The mean value of m (= 0.3) of relation (1) which has been calculated observationally by several investigators has been also derived theoretically. Relation (5) and the values of its scaling coefficients (0.42, –0.30) which are based on observations have been also derived theoretically. Relations (11, 20) which predict smaller identification period (t_c–t_{ia}, t_c–t_{id}) for regions of higher seismicity are physically explained because Benioff strain graphs cut high levels of background seismicity closer to the origin time of the mainshock than low levels of background seismicity.

8. Most of the relative published works consider accelerating precursory strain as a result of criticality and that the generation of the mainshocks is due to stress change by critical triggering. Observations made in the present work on 46 accelerating preshock sequences support this idea because the maximum magnitude of preshocks increases with the time to the mainshock as it is predicted by the

critical point theory. Evidence is also presented in the present work that during this physical process stress is transferred in a quasi–static mode and contributes to triggering of the mainshock. The total duration, t_c–t_{sa}, of an accelerating seismic sequence includes two phases. During the first phase, which lasts from the start (t_{sa}) of the sequence till its identification time (t_{ia}), the time variation of the cumulative Benioff strain is almost linear (see fig. 2). During the second phase, which lasts from the identification till the origin time, t_c, of the mainshock, the Benioff strain is accelerating. In most of the sequences the second phase starts with a period of accelerating strain which covers about 60% of the phase (increase of q_a in fig. 3) followed by a period of strain decrease (decrease of q_a in fig. 3), which lasts till the mainshock and is probably due to a return of seismicity to its background level.

9. Precursory seismic quiescence near the focus of many ensuing mainshocks has been observed by several seismologists. In most of these cases it concerns decrease of the frequency of small earthquakes and in others decrease of seismic deformation. By using data concerning the 46 decelerating preshock sequences studied in the present work we have shown that it is the frequency of intermediate magnitude preshocks (M>4.0) in the seismogenic region which increases originally (excitational phase) and then decreases (seismic quiescence phase), that causes corresponding changes in the Benioff strain. The first phase (excitational) which lasts from the start time, t_{sd}, of the sequence till the identification time, t_{id}, is attributed to critical triggering and tectonic stressing. In the second phase, which lasts between t_{id} and t_c, the Benioff strain declines due to decrease of the frequency of the intermediate magnitude preshocks, while the frequency of small shocks (M<4.0) continues to be high during this phase as it comes out from the observed high b value. Decrease of the frequency of the intermediate magnitude preshocks in the seismogenic region (and corresponding quiescence of strain) in the second phase is attributed to the fact that many faults of the seismogenic region were broken during the first (excitational) phase and few left available for failure during the second phase. The triggering ability of the small shocks which occur in the seismogenic region during the second phase is high due to their very large number (b>D/2). This observation and the fact that these small earthquakes occur close to the mainshock (in space and time) suggest that their generation transfer static stress which contributes to triggering of the mainshock. Usually, the second phase is formed of two periods. During the first period, which covers about 60% of the total duration of the phase, the Benioff strain decelerates (increase of q_d in fig. 3). During the second period the Benioff strain increases (decrease of q_d in fig. 3), which means a return of seismicity in the seismogenic region to its background level.

10. Neither the center of the seismogenic region (point F of decelerating preshocks) nor the center of the critical region (point Q of accelerating preshocks) coincides with the mainshock epicenter. However, the center, F, of the seismogenic region is at a relatively short distance from the mainshock epicenter and thus the generation of a very large number of small preshocks (indicated by an increase of the b value) is able to increase static stress and contribute to the triggering of the mainshock. On the contrary the center, Q, of the critical region is at large and variable distances from the mainshock epicenter but due to the large magnitudes of accelerating preshocks (see relation 10) and to the increase of their magnitude and of their frequency with the time to the mainshock, accelerating preshocks can also contribute to the triggering of the mainshock but by quasi–static stress transfer.

11. Another strong evidence for the scientific validity of the D–AS model is that properties of this model have been already applied for intermediate–term successful prediction of two recent strong earthquakes in the Aegean area. The first of these earthquakes, which occurred on 8 January 2006 near the Cythera island (southwest Aegean) with M = 6.9, has been successfully predicted (time, space and magnitude within the predicted windows) in 2002 by the use of data concerning precursory accelerating strain (Papazachos et al., 2002b). The second earthquake, which occurred on 15 July 2008 near Rhodos island (southeast Aegean) with M = 6.4 has been also successfully predicted (on April 2008) by application of the D–AS model (Papazachos and Karakaisis, 2008; Papazachos et al., 2009).

12. Estimation (prediction) of the origin time, t_c, magnitude, M, and epicenter coordinates, $E(\phi, \lambda)$, of an ensuing mainshock is based on empirical relations which express predictive properties of the D–AS model. Thus, the origin time, t_c, is calculated by relations (6), (12) and (16), the magnitude, M, by relations (5), (13) and (15) and the geographic coordinates of the epicenter of the mainshock by constraints put by relations (21), (22), (23), (24) and (25). Retrospective "predictions" (postdictions) of the 46 mainshocks listed on table (1) and comparison of the predicted values with the observed ones confirm that uncertainties are: $\pm$2.5 years for the origin time, $\pm$0.4 for the magnitude and less than 150km for the epicenter, with a probability 80% if we take into consideration false alarms estimated by application of the model in random but realistic catalogues. The error in the epicenter is reduced to $\leq$120 km if results of the TIMAP model are also considered.

5. References

Allègre, C.J. and Le Mouël, J.L., 1994. Introduction to scaling techniques in brittle failure of rocks. *Phys. Earth Planet. Inter.* 87, 85-93.

Ben-Zion, Y., Dahmen, K., Lyakhovsky,V., Ertas, D. and A. Agnon, 1999. Self-driven mode switching of earthquake activity on a fault system. *Earth Planet. Science Lett.* 172, 11-21.

Ben-Zion, Y. and V. Lyakhovsky, 2002. Accelerated seismic release and related aspects of seismicity patterns on earthquake faults. *Pure appl. Geoph.* 159, 2385-2412.

Bowman, D.D., Quillon, G., Sammis, C.G., Sornette, A. and D. Sornette, 1998. An observational test of the critical earthquake concept. *J. Geophys. Res.* 103, 24359-24372.

Brehm, D.J., and L.W. Braile, 1998. Intermediate-term earthquake prediction using precursory events in the New Madrid seismic zone. *Bull. Seism. Soc. Am.* 103, 24359-24372.

Brehm, D.J., and L.W. Braile, 1999. Refinement of the Modified Time-to-failure Method for Intermediate-term Earthquake Prediction. *J. Seismology* 3, 121-138.

Bufe, C.G., and D.J. Varnes, 1993. Predictive modeling of seismic cycle of the Great San Francisco Bay Region. *J.Geophys. Res.* 98, 9871-9883.

Das, S. and C. Scholz, 1981. Off-fault aftershock clusters caused by shear stress increase. *J. Geophys. Res.*, 71, 1669-1675.

Dieterich, J.H., 1992. Earthquake nucleation on faults with rate and state dependent strength, *in Earthquake Source Physics and Earthquake Precursors, edited by T. Mikumo et al., Elsevier, NY,* 115-134.

Dieterich, J.H., 1994. A constitutive law for rate on earthquake prediction and its application to earthquake clustering. *J. Geophys. Res.*, 99, 2601-2618.

Evison, F.F., and D.A. Rhoades, 1997. The precursory earthquake swarm in New Zealand. *N.Z.J. Geol. Geophys.* 40, 537-547.

Evison, F.F., 2001. Long-range synoptic earthquake forecasting: an aim for the millennium. *Tectonophysics* 333, 207-215.

Fedotov, S.A., 1965. Regularities of the distribution of strong earthquakes in Kamchatka, the Kurile Islands and Northeastern Japan (in Russian), *Tr. Inst. Fiz. Zemli, Akad. Naua SSSR,* 36, 66-93.

Freed, A.M., 2005. Earthquake triggering by static, dynamic and postseismic stress transfer. *Ann. Rev. Earth Planet. Sci.*, 33, 335-367.

Gomberg, J., Beeler, N.M., Blanpied, M.L. and Bodin, P., 1998. Earthquake triggering by transient and static deformations. *J. Geophys. Res.*, 103, 24411-24426.

Helmstetter, A., 2003. Is earthquake triggering driven by small earthquakes?. *Physical Review Letters*, 91, 058501-4.

Helmstetter, A., Kagan, Y.Y. and Jackson, D.D., 2005. Importance of small earthquakes for stress transfers and earthquake triggering. *J. Geophys. Res.*, 110, B05508, doi: 10.1029/2004JB003286.

Hill, D.P. and Prejean, S.G., 2006. Dynamic triggering. *Treatise on Geophysics*, 4, 1-52.

Jaumé, S.C. and L.R., Sykes 1999. Evolving towards a critical point: a review of accelerating seismic moment/energy release rate prior to large and great earthquakes. *Pure Appl. Geophys*. 155, 279-306.

Karakaisis, G.F., Papazachos, C.B., Panagiotopoulos, D.G., Scordilis, E.M. and B.C. Papazachos, 2007. Space distribution of preshocks. *Boll. Geof. Teor. Aplic*. 48, 371-383.

Karakaisis, G.F., Papazachos, C.B. and E.M. Scordilis, 2010. Seismic sources and main seismic faults in the Aegean and surrounding area. *Bull. Geol. Soc. Greece*, (submitted).

Kato, N., Ohtake, M. and T. Hirasawa, 1997. Possible mechanism of precursory seismic quiescence: Regional stress relaxation due to preseismic sliding. *Pure Appl. Geophys*. 150, 249-267.

Kilb, D., Gomberg, J. and Bodin, P., 2002. Aftershocks triggering by complete Coulomb stress changes. *J. Geophys. Res*., 107, doi: 10.1029/2001JB000202.

King, G.C.P. and M. Cocco, 2001. Fault interactions by elastic stress changes: new clues from earthquake sequences. *Advances in Geophysics*, 44, 1-38.

Knopoff, L., T.Levshina, V.J. Keillis-Borok and C. Mattoni, 1996. Increased long-rang intermediate-magnitude earthquake activity prior to strong earthquakes in California. *J.Geophys. Res*. 101, 5779-5796.

Mignan, A., D.D. Bowman, and G.C. King, 2006. An observational test of the origin of accelerating moment release before large earthquakes. *J. Geophys. Res*. Doi:10.1029/2006JB004374.

Mogi, K., 1969. Some features of the recent seismic activity in and near Japan.II. Activity before and after great earthquakes. *Bull. Earthquake Res, Inst. Univ.Tokyo* 47, 395-417.

Papazachos, B.C., 1989. A time predictable model for earthquakes in Greece. *Bull. Seism. Soc. Am*., 79, 77-84.

Papazachos, B.C. and Ch.A. Papaioannou, 1993. Long term earthquake prediction in the Aegean area based on the time and magnitude predictable model. *Pure Appl. Geophys*., 140, 593-612.

Papazachos, B.C., Papadimitriou, E.E., Karakaisis, G.F. and Panagiotopoulos, D.G., 1997. Long-term earthquake prediction in the Circum-Pacific convergent belt. *Pure Appl. Geophys*., 149, 173-217.

Papazachos, B.C. and C.B. Papazachos, 2000. Accelerated preshock deformation of broad regions in the Aegean area. *Pure Appl. Geophys*. 157, 1663-1681.

Papazachos, B.C., Karakaisis, G.F., Papazachos, C.B., Scordilis, E.M. and A.S. Savvaidis, 2002b. Space and time variation of seismicity in the region of Greece. *Final report to the Greek Earthquake Planning and Protection Organization (OASP) under project 20242, Aristotle University of Thessaloniki, Research Committee (3 December 2002)*, 21pp.

Papazachos, B.C. and Papazachou, C.B., 2003. The earthquakes of Greece. *"Ziti Publications, Thessaloniki"*, 273pp.

Papazachos, B.C., Karakaisis, G.F., Papazachos, C.B. and E.M. Scordilis, 2007. Evaluation of the results for an intermediate term prediction of the 8 January 2006 M_W = 6.9 Cythera earthquake in southern Aegean. *Bull. Seism. Soc. Am*. 97, 1B, 347-352.

Papazachos, B.C. and G.F. Karakaisis, 2008. Present space-time evolution of seismicity in the region of Greece. *Official Report to the Minister of Public Works of Greece*, 7pp, 30 June 2008.

Papazachos, B.C., Comninakis, P.E., Scordilis, E.M., Karakaisis, G.F. and Papazachos, C.B., 2008. A catalogue of earthquakes in Mediterranean and surrounding area for the period 1901-2008, *Publ. Geoph. Laboratory, University of Thessaloniki*.

Papazachos, B.C., Karakaisis, G.F., Papazachos, C.B., Panagiotopoulos, D.G. and E.M. Scordilis, 2009. A forward test of the Decelerating-Accelerating Seismic Strain Model in the Mediterranean. *Boll. Geofis. Teor. Applic*.,50, 3, 235-254.

Papazachos, C.B., 2003. Minimum preshock magnitude in critical regions of accelerating seismic crustal deformation. *Boll. Geof.Teor. Aplic*. 44, 103-113.

Papazachos, C.B. and B.C. Papazachos, 2001. Precursory accelerating Benioff strain in the Aegean area. *Ann. Geofisica* 144, 461-474.

Papazachos, C.B., Karakaisis, G.F., Savaidis, A.S., and B.C. Papazachos, 2002a. Accelerating seismic crustal deformation in the southern Aegean area. *Bull. Seismol. Soc. Am.* 92, 570-580.

Papazachos, C.B., Scordilis, E.M., Karakaisis, G.F. and B.C. Papazachos, 2005a. Decelerating preshock seismic deformation in fault regions during critical periods. *Bull. Geol. Soc. Greece* 36, 1491-1498.

Papazachos, C.B., Karakaisis, G.F., Scordilis, E.M. and B.C. Papazachos, 2005b. Global observational properties of the critical earthquake model. *Bull. Seismol. Soc. Am.* 95, 1841-1855.

Papazachos, C.B., Karakaisis, G.F., Scordilis, E.M. and B.C. Papazachos, 2006. New observational information on the precursory accelerating and decelerating strain energy release. *Tectonophysics* 423, 83-96.

Pollitz, F.F. and Sacks, I.S., 2002. Stress triggering of the 1999 Hector Mine earthquake by transient deformation following the 1992 Landers earthquake. *Bull. Seism. Soc. Am.*, 92, 4, 1487-1496.

Robinson, R., 2000. A test of the precursory accelerating moment release model on some recent New Zealand earthquakes. *Geoph. J. Int.* 140, 568-576.

Rhoades, D.A. and F.F. Evison, 1993. Long-range earthquake forecasting based on a single predictor. *Geophys. J. Int.* 113, 371-381.

Rundle, J.B., Klein, W. and S. Gross, 1996. Dynamics of a traveling density wave model of earthquakes. *Phys. Rev. Lett.* 76, 4285-4288.

Rundle, J.B., Turcotte, D.L., Shecherbakov, R., Klein, W. and C. Sammis, 2003. Statistical physics approach to understanding the multiscale dynamics of earthquake fault systems. *Rev. Geophys.*, 41, 5/1-5/30.

Saleur, H., Sammis, C.G. and D. Sornette, 1996. Discrete scale invariance, complex fractal dimensions and long-periodic fluctuation in seismicity. *J. Geophy. Res.* 101, 17661-17678.

Scordilis, E.M., 2010. Correlations of the Mean Time and Mean Magnitude of Accelerating Preshocks with the Origin Time and Magnitude of the Mainshock. *Bull. Geo. Soc. Greece*, (submitted).

Scordilis,E.M., Papazachos,C.B., Karakaisis,G.F. and V.G. Karakostas, 2004. Accelerating seismic crustal deformation before strong mainshocks in Adriatic and its importance for earthquake prediction. *J. Seismology* 8, 57-70.

Shimazaki, K. and Nakata, T., 1980. Time predictable recurrence model for large earthquakes. *Geophys. Res. Lett.*, 7, 279-282.

Sornette, D., and C.G. Sammis, 1995. Complex critical exponents from renormalization group theory of earthquakes: implications for earthquake predictions. *J.Phys. I.France* 5, 607-619.

Steacy, S., Gomberg, J. and Cocco, M., 2005. Introduction to special section: Stress transfer, earthquake triggering and time-dependent seismic hazard. *J. Geophys. Res.,* 110, doi: 10.1029/2005JB003692.

Sykes, L.R., and S.C. Jaumé, 1990. Seismic activity on neighboring faults as a long term precursor to large earthquakes in the San Francisco Bay area. *Nature* 348, 595-599.

Tocher, D., 1959. Seismic history of the San Francisco bay region. *Calif. Div. Mines Spec. Rep.* 57, 39-48.

Tzanis, A., F. Vallianatos, and K. Makropoulos, 2000. Seismic and electric precursors to the 17-1-1983, M7 Kefallinia earthquake, Greece: signatures of a SOC system. *Phys. Chem. Earth* 25, 281-287.

Tzanis, A., and K. Makropoulos, 2002. Did the 7/9/1999, m5.9, Athens earthquake came with a warning?. *Natural Hazards* 27, 85-103.

Varnes, D.J., 1989. Predicting earthquakes by analyzing accelerating precursory seismic activity. *Pure Appl. Geophys.* 130, 661-686.

Wyss, M., 1997. Cannot earthquakes be predicted?. *Science* 278, 487-488.

Wyss, M., Klein, F. and A.C. Johnston, 1981. Precursors of the Kalapana M = 7.2 earthquake. *J. Geophys. Res.* 86, 3881-3900.

Δελτίο της Ελληνικής Γεωλογικής Εταιρίας, 2010
Πρακτικά 12ου Διεθνούς Συνεδρίου
Πάτρα, Μάιος 2010

Bulletin of the Geological Society of Greece, 2010
Proceedings of the 12th International Congress
Patras, May, 2010

GROUNDWATER RESOURCES MANAGEMENT IN ARID COUNTRIES

Rausch R.[1], Schüth C.[2] and Kallioras A.[2]

[1] *GTZ-IS, Riyadh, Kingdom of Saudi Arabia, randolf.rausch@gtzdco-ksa.com*

[2] *Technische Universität Darmstadt, Germany, schueth@geo.tu-darmstadt.de, kallioras@geo.tu-darmstadt.de*

Although "arid hydrogeology" is a rather controversial term, the thorough investigation of current groundwater resources potential of arid regions is a key issue not only for the development of these countries but more importantly for the sustainability and preservation of available water resources for domestic use today and in the future. Most of groundwater aquifers in arid regions were recharged many thousands years ago (during wet climatic periods); hence their resources potential is mainly composed of fossil groundwaters. The majority of these aquifers appear in a state of constant depletion as outflow over-exceeds recent groundwater recharge. A prerequisite for the smart management of such groundwater resources is a sound understanding of the aquifer system based on reliable data and robust simulation models.

A brief description of groundwater resources investigations in the Kingdom of Saudi Arabia is presented here, in order to illustrate the current state of the most important groundwater aquifer systems of that arid country. The geological environments are analysed, as well as the hydrologic and climatic regime of different regional aquifer systems throughout the Arabian Peninsula.

The water resources of Saudi Arabia are made up of groundwater, surface water, desalinated seawater, and treated wastewater. The actual total water consumption for 2009 was about 19.3 BCM/a (611 m^3/s) where about 14 BCM/a (444 m^3/s) are taken from non-renewable groundwater resources. This amount equals about 73% of the total water consumption. Most of these fossil groundwater resources are stored in huge sandstone and limestone aquifers on the Arabian Platform in the eastern part of the Kingdom.

In the seventies and eighties of the last century a first countrywide assessment of the water resources was carried out, which was the basis for the national water master plan of the Kingdom. With growing water demand, a reassessment was necessary. Therefore, in 2002 the Ministry of Water & Electricity launched a project to investigate all aquifers in the Kingdom. Since then several aquifer studies were carried out or are in progress. Today, the Saq-, Umm Er Radhuma-, Wajid-, Wasia-Biyadh-Aruma-study are already finished. In the near future, the Dhruma-Minjur-, the Rub' Al Khali-, the Tihama-, and the Arabian-Shield-study including the Harrats will be finalized. The main objectives of all these studies are the assessment of the groundwater resources, and the assessment of the groundwater budget.

The questions to be answered are: how much groundwater is still available, what is its quality, and what are the in- and outflows to the aquifers? To answer these questions, robust and reliable data are needed, which can only achieved by applying the latest technologies in groundwater sciences. Furthermore, research is needed for a better understanding and quantification of special features. The research topics focus on estimation of groundwater recharge, large scale groundwater modeling, and smart groundwater mining. All these investigations are the prerequisite for the smart and efficient managing of the groundwater resources and central part of the future water strategy of the Kingdom of Saudi Arabia. Furthermore, the results of the studies will serve as a blueprint for other arid countries over the world.

12ο ΔΙΕΘΝΕΣ ΣΥΝΕΔΡΙΟ ΤΗΣ ΕΛΛΗΝΙΚΗΣ ΓΕΩΛΟΓΙΚΗΣ ΕΤΑΙΡΙΑΣ
ΠΛΑΝΗΤΗΣ ΓΗ: Γεωλογικές Διεργασίες και Βιώσιμη Ανάπτυξη

12th INTERNATIONAL CONGRESS OF THE GEOLOGICAL SOCIETY OF GREECE
PLANET EARTH: Geological Processes and Sustainable Development

ΘΕΜΑΤΙΚΕΣ ΟΜΙΛΙΕΣ
KEYNOTE LECTURES

Δελτίο της Ελληνικής Γεωλογικής Εταιρίας, 2010
Πρακτικά 12ου Διεθνούς Συνεδρίου
Πάτρα, Μάιος 2010

Bulletin of the Geological Society of Greece, 2010
Proceedings of the 12th International Congress
Patras, May, 2010

MAJOR PALEOGEOGRAPHIC, TECTONIC AND GEODYNAMIC CHANGES FROM THE LAST STAGE OF THE HELLENIDES TO THE ACTUAL HELLENIC ARC AND TRENCH SYSTEM

Papanikolaou D.

[1] *University of Athens, Department of Dynamic, Tectonic, Applied Geology, Panepistimioupoli 15784, Athens, Greece, dpapan@geol.uoa.gr*

Abstract

Present day location and geometry of the Hellenic arc and trench system is only a small portion of the previously developed Hellenic arc that created the Hellenides orogenic system. The timing of differentiation is constrained in Late Miocene, when the arc was divided in a northern and a southern segment. This is based on: a) the dating of the last compressive structures observed all along the Hellenides during Oligocene to Middle-Late Miocene, b) on the time of initiation of the Kephalonia transform fault, c) on the time of opening of the North Aegean Basin and d) on the time of opening of new arc parallel basins in the south and new transverse basins in the central shear zone, separating the rapidly moving southwestwards Hellenic subduction system from the slowly converging system of the Northern Hellenides. The driving mechanism of the arc differentiation is the heterogeneity produced by the different subducting slabs in the north (continental) and in the south (oceanic) and the resulted shear zone because of the retreating plate boundary producing a roll back mechanism in the present arc and trench system. The paleogeographic reconstructions of the Hellenic arc and surrounding areas show the shortening of the East Mediterranean oceanic area, following the slow convergence rate of the European and African plates plus the localised shortening following the rapid Hellenic subduction rate. The result is that the frontal parts of the accretionary prism developed in front of the Hellenic arc have reached the African continent in Cyrenaica whereas on the two sides the basinal parts of the Ionian and Levantine basins are still preserved before their final subduction and closure. The extension produced in the upper plate has resulted in the subsidence of the Aegean Sea and the creation of several neotectonic basins in southern continental Greece in contrast to the absence of new basins in the northern segment since Late Miocene.

Key words: *oceanic subduction, continental subduction, upper plate extension, orogenic arc evolution, arc parallel structures, arc transverse structures.*

1. Introduction

The Hellenides are a segment of the Tethyan Alpine Orogenic Belt developed along the European active margin, resulted from plate convergence between the Eurasian plate in the north and the African plate in the south, with longlasting subduction of the Tethyan basins and platforms underneath the European margin (e.g. Papanikolaou et al, 2004; Van Hinsbergen et al, 2005). Convergence between the two plates has started since Jurassic and produced successive orogenic arcs that gave birth to the orogenic systems of the Hellenides until Miocene (e.g. Aubouin, 1974; Jacobshagen et al, 1978; Papanikolaou 1986;

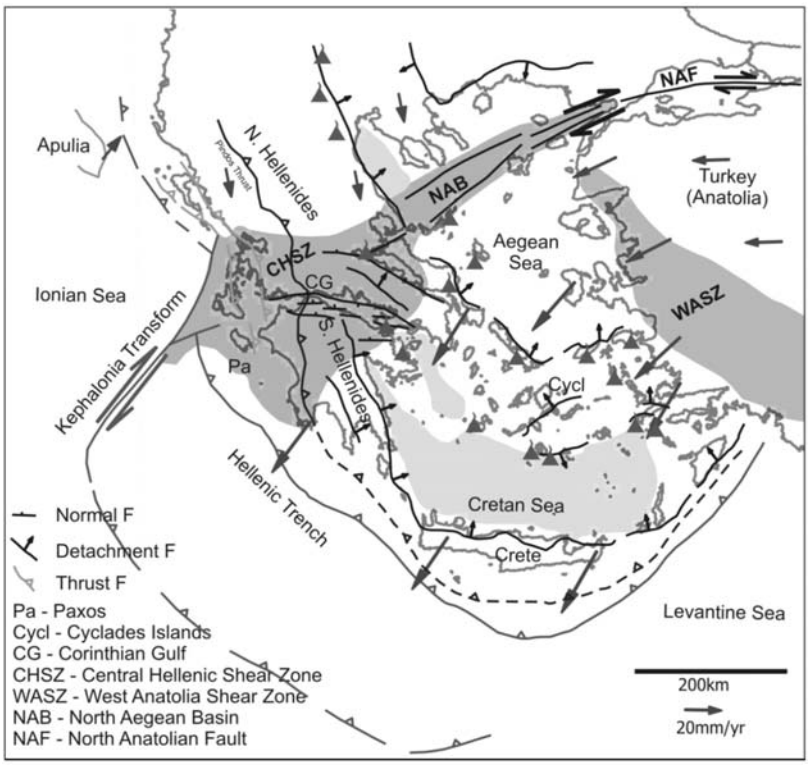

Fig. 1: Tectonic sketch of the Hellenides and the actual Hellenic arc and trench system. Bending of the thrusts in the southern segment is shown by the Pindos thrust and Late Miocene thrusts within the Ionian unit. The Late Miocene volcanic arc is shown in comparison to the Quaternary volcanic arc, developed only in the southern segment. Representative GPS rates are included together with the CHSZ and WASZ. Major detachments and normal faults of Late Miocene – Present are indicated.

1993). However, convergence is still going on today with an average rate of 1 cm/year (e.g. Reilinger et al, 1997; Kahle et al, 2000) in the eastern Mediterranean, including the Hellenides, whereas collision has occured at the western Mediterranean since early Miocene and at the Arabia – Caucasus transcet since middle Miocene (e.g. Cavazza et al, 2004). Thus, subduction of the last remnant of the oceanic basin of the Eastern Mediterranean, developed at the northern part of the African plate, occurs along the actual Hellenic arc and trench system, which is limited between the Amvrakikos Gulf in the northwest and the Rhodos transect in the southeast, forming the Aegean microplate (Fig. 1). The differentiation of the present day Hellenic Arc and trench system from the previous structure of the Hellenic fold and thrust belt necessitates the distinction of the Northern Hellenides and the Southern Hellenides on both sides of the Amvrakikos Gulf (Papanikolaou & Royden, 2007).

Convergence rate between the present day Hellenic arc and Africa, expressed by the ongoing Hellenic subduction, is about 4 cm/year (e.g. Reilinger et al, 1997; Kahle et al, 2000; Hollenstein et al, 2008), which is several times more than the convergence rate between Europe and Africa. This difference between the Africa – Eurasia plate convergence rate and the Hellenic subduction rate is producing extension in the Aegean upper plate and opening of the North Aegean Basin (Papanikolaou & Royden 2007). North of the Amvrakikos Gulf the convergence rate between Apulia (part of the Adria plate) and

the Northern Hellenides is around 8 mm/year and there is no arc and trench system developed other than a compressional seismically active thrust belt (Baker et al, 1997). The lateral differentiation of more than 30 mm/year convergence rate north and south of Amvrakikos is accommodated by the Kephalonia transform fault. In the area of continental Greece and the Aegean the different kinematic motion between the Aegean microplate in the south and the European plate in the north produces a vertical shear zone – the Central Hellenic Shear Zone (CHSZ) (Papanikolaou & Royden 2007) comprising strike-slip, oblique-slip and normal faults (Fig. 1). Another shear zone - the West Anatolian Shear Zone (WASZ) - is developed at the eastern boundary of the Aegean microplate along the western coastline of Minor Asia, because of its differential motion with respect to the Anatolian microplate.

This paper is focused on a review and discussion concerning: 1) The timing of initiation of the present day geometry, from a previous homogeneous geodynamic regime along the Hellenides across the Kephalonia transform, the CHSZ and the North Aegean Basin. 2) The different tectonic and paleogeographic elements, that are considered as key points for understanding the complex evolution of the area. 3) The driving mechanism(s), that produced the observed present day differentiation of the Aegean microplate from the rest European margin. 4) A synthesis, where the overall conclusions are displayed in a series of paleogeographic sketches of the area over the last 34 million years (Oligocene – Present).

2. Timing of differentiation of the Hellenic Arc

The data regarding the timing of differentiation of the Hellenic arc can be grouped in four sets: 1) At the front of the fold and thrust belt along the subduction zone on either side of the Kephalonia transform. 2) Along the CHSZ and on either side of it in the continental part of Greece. 3) In the North Aegean Basin between the northern margin of the Aegean Sea at Macedonia and Thrace and the central and southern Aegean Sea. 4) An overall study of the arc geometry in different periods, before and after the differentiation.

The migration of the Hellenic thrust and fold belt from the internal part of the Hellenides in the Aegean Sea to the external part in the Ionian Sea throughout Eocene – Miocene is well known longtime ago (Philippson, 1959; Aubouin, 1959; 1965; Jacobshagen et al, 1978; Papanikolaou, 1986). The last compressional structures related to the front of the Hellenic fold and thrust belt have been reported from the Ionian islands of Kephalonia and Zakynthos, involving Pliocene or even Early Pleistocene sediments (Mercier et al, 1972; 1979; Underhill, 1989). However, the above structures are localised and rather exceptional with respect to the dating of the latest structures all along the western coast of continental Greece and the rest Ionian Islands, where the latest sediments involved in the compressional structures are of Late Miocene – Early Pliocene age (around 5 million years) including also the well known, all over the Mediterranean Basin, Messinian evaporites (e.g. Zakynthos and Parga) (IGSR & IFP, 1966; B.P. 1971; Hsu et al, 1978). North of the Amvrakikos Gulf there is no evidence of Plio-Quaternary compressional structures and the tectonic trend of the Miocene folds and thrusts is dextrally offset by several tens of km with respect to its location south of the gulf. The overall dextral offset of the Kephalonia transform fault is about 100 km, judging from the location of the northern edge of the Hellenic trench/plate boundary south of the Kephalonia transform and its approximate location north of the Kephalonia transform in the area west of the Paxos and Corfu islands, determined on the basis of bathymetric and geophysical data (e.g. Monopolis & Bruneton, 1982).

In continental Greece, the difference of the distribution of Plio-Quaternary basins north and south of the CHSZ is impressive, with almost no Plio-Quaternary basin formed in the Northern Hellenides in contrast to five basins developed in the southern Hellenides along the transect from Western Messinia in southwestern Peloponnese to southern Evia in the central Aegean (Fig. 2). These basins form neotec-

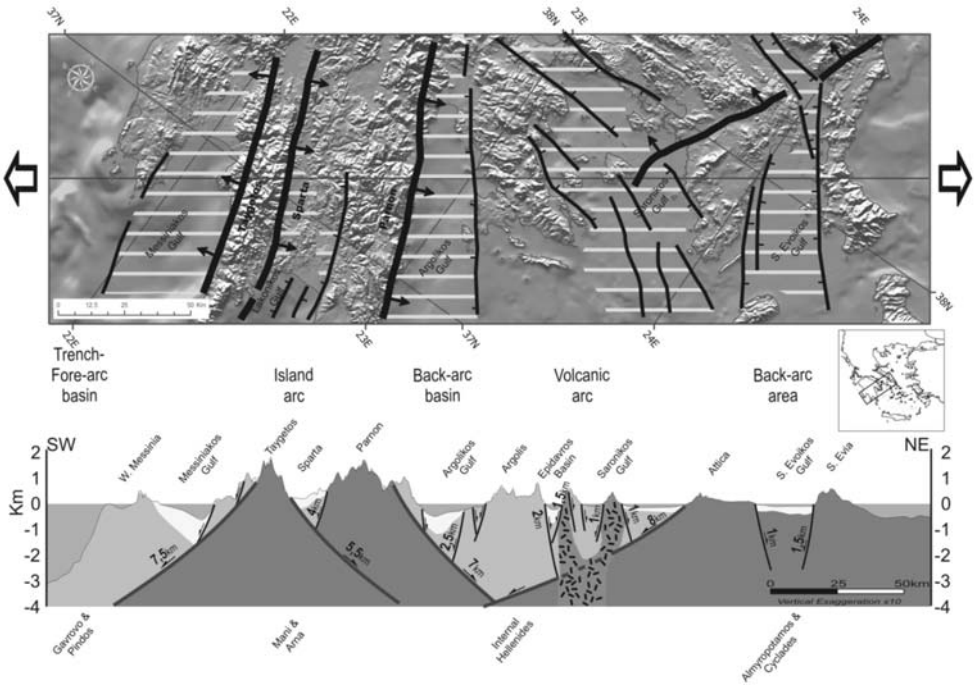

Fig. 2: Schematic neotectonic map and profile across the arc parallel basins/grabens of the Southern Hellenides, developed within Late Miocene – Present under an extension in the ENE-WSW direction (modified after Papanikolaou et al, 1988). A decrease of the deformation is shown by the estimated magnitude of fault throw along the profile.

tonic grabens filed with marine and/or continental sediments onshore and actual marine sedimentary basins offshore, developed within the successive gulfs of Messiniakos, Lakonikos, Argolikos, Saronikos and Southern Evoikos. These basins correspond to neotectonic grabens bounded by neotectonic horsts forming the mountainous regions of Western Messinia, Taygetos/Mani, Parnon, Argolis, Attica and Southern Evia. This alternation of neotectonic horsts and grabens in the NNW-SSE direction shows a WSW-ENE directed extension that forms arc-parallel structures within the Aegean upper plate. The intensity of deformation as expressed by the topographic relief, the sedimentary thickness and the fault displacement values shows a decrease from the external part of the arc in the southwest towards the internal part in the northeast (Papanikolaou et al, 1988). The minimum extension estimated across the above profile is 35 km, considering a mean 45° dip of the normal faults forming the marginal faults of the basins. Within the CHSZ the accomodating structures are mainly the basins of Northern Evoikos Gulf, Beotikos Kiffissos and Corinth Gulf. These basins are transverse or oblique with respect to the arc geometry, with prevailing E-W trend controlled by normal faults which are seismically very active. They are filled with continental sediments mainly of Late Miocene – Pliocene age with some marine influence only during Middle - Late Pleistocene. North of the CHSZ, the latest neotectonic basins / grabens occur east of the Mesohellenic molassic basin with Late Miocene – Pliocene continental deposits. The latest sediments in the continuous molassic sequence of the Mesohellenic basin are of Late Miocene (Tortonian) age marking the end of marine sedimentation in central-northern continental Greece.

The opening of the North Aegean Basin has occurred sometime in Early Pliocene judging from its geometry, sedimentary thickness, fault displacements and differences in the present day GPS rates observed

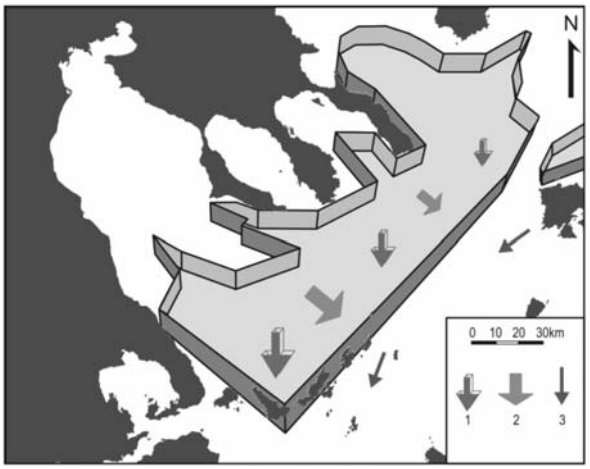

Fig. 3: Block stereo-diagram showing the overall geometry and kinematics of the North Aegean Basin (after Papanikolaou et al, 2002). 1: vertical subsidence, 2: horizontal opening, 3: GPS slip vectors.

on both sides of its margins (Lalechos & Savoyat, 1979; Le Pichon et al, 1984; Armijo et al, 1999; Papanikolaou et al, 2002; 2006). The opening of the basin is more pronounced in the western part (40 km) than in the eastern (20 km) and so is the depth (1600 m in the west and 950 m in the east) (Fig. 3). The location of the basin at the western prolongation of the North Anatolian Fault and its seismotectonic characteristics, implying a dextral strike-slip motion, have been the main argument for an induced basin because of wrench tectonics along the European margin, following the continental collision in the Caucasus area during the Middle Miocene and the subsequent lateral escape of Anatolia (Brunn, 1976; Dewey & Sengor, 1979; LePichon & Angelier, 1979; Armijo et al, 1999; McNeill et al, 2004; Kreemer et al, 2004).

The understanding of the transition period between the last stage of the Hellenides, viewed as a continuous orogenic arc involving all the characteristic parts, and the present day geometry of the Hellenic arc and trench system was based on an analysis of the paleogeographic position of the arc segments by comparing the geometry of the Burdigalian period with that of the Messinian and of the Plio-Quaternary period (Papanikolaou & Dermitzakis, 1981; Dermitzakis & Papanikolaou, 1979; 1981) (Fig. 4). The main features of the arc that have changed in Messinian are: 1) The uplift and ending of marine sedimentation in the Mesohellenic and the Cycladic molassic basins. 2) The opening of a new molassic basin in the area of the Cretan Sea between the Cyclades and Crete. 3) The termination of the volcanic arc activity in the segment of the Northern Hellenides and the continuation of the arc volcanism only in the segment of the Southern Hellenides. During the Plio-Quaternary, the volcanic arc continued its migration towards the more external zones of the Hellenic arc until its present location along the southern margin of the Cycladic plateau at a 60-80 km distance away from the location of the Late Miocene volcanic arc (see also Fig. 1). 4) The initiation of opening of the North Aegean Basin in the North Aegean Sea at the western prolongation of the newly formed North Anatolian Fault (see also Fig. 3). 5) The beggining of subduction of the last remnant of the Tethyan oceanic crust of the Eastern Mediterranean Basin along the arcuate segment formed between the Amvrakikos Gulf and Rhodes. 6) The initiation of the Kephalonia transform fault at the level of the Amvrakikos Gulf. 7) The migration of the fold and thrust belt towards the Ionian islands south of the Kephalonia transform fault, with Plio-Quaternary compressional structures at a distance of several tens of km away from the Late Miocene structures. 8) The disruption of the Late Eocene - Miocene fold and thrust belt and the relative westward displacement of the Hellenides nappes in the southern segment. Thus, the Pindos thrust is observed today at the front of the nappe system in southwest Peloponnese and Kythira Island up to Gavdos Island south of Crete, adjacent to the trench, whereas in the Northern Hellenides it rests along the western slopes of the Pindos chain at a distance of 90-120 km away from the

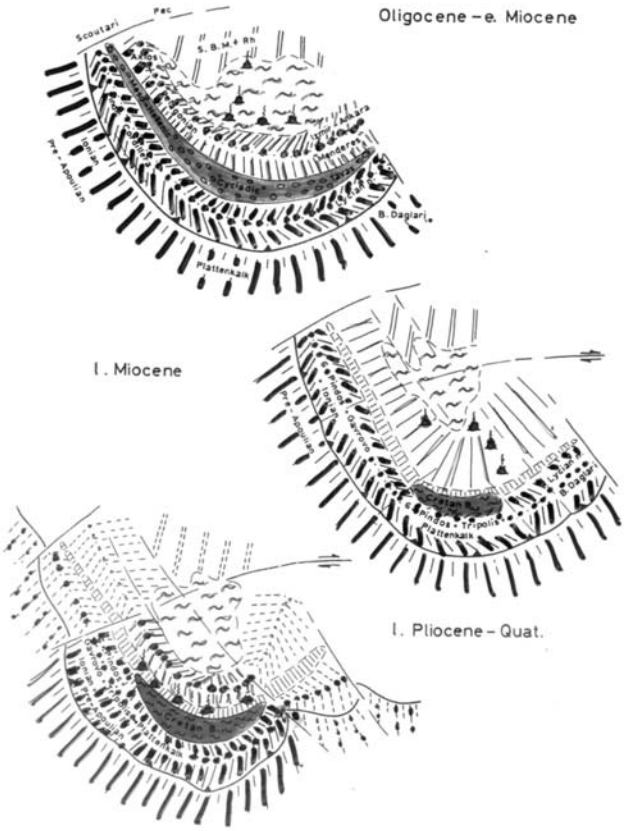

Fig. 4: Paleogeographic and paleogeodynamic sketches of the Hellenic arc from the last stage of the Hellenides (Oligocene – Early/Middle Miocene to a reorganisation period in Late Miocene and to the actual Hellenic arc and trench system (Plio-Quaternary) (after Papanikolaou & Dermitzakis, 1981).

plate boundary (see also Fig. 1). 9) The maximum uplift of the nappe pile in the southern Hellenides, producing the arrival at the surface of the higher mountains of south Peloponnese of the basal metamorphic unit of Mani and of the overlying metamorphic unit of Arna. 10) The development of a number of arc-parallel extensional neotectonic basins in the Southern Peloponnese and of transverse neotectonic basins in the Northern Peloponnese and Sterea Hellas (see also Fig. 2).

In conclusion, the timing of differentiation of the Hellenic arc and its subdivision in the Northern and the Southern Hellenides is constrained in Late Miocene. Tortonian is the last period of the previous uniform Hellenic arc and Messinian is the re-organization period whereas already by the beginning of Pliocene the new subdivision and arc geometry has been established.

3. Sedimentary basins and tectonics

The post-Oligocene sedimentary basins and associated neotectonic structures developed within the upper plate during the migration of the Hellenic orogenic arc can be distinguished in the following three categories.

1) The first category concerns all the arc parallel structures occurring within the orogenic arc from the

front of the fold and thrust belt at the fore-arc basin, to the back-arc area behind the volcanic arc. This category involves compressive structures developed from Late Eocene - Oligocene (e.g. Pindos and Tripolis units) to middle - late Miocene (e.g. Ionian and Paxos units) all along the frontal zone of the Hellenic arc in the paleo-trench and the external zone of the paleo-island arc. It also involves extensional structures related to the opening of the molassic Mesohellenic Basin and its probable continuation in the Cycladic molassic basin to the south. The tectonic trend remains constant in the NNW-SSE direction for both compressive and extensional structures. The sedimentary sequences deposited in the above structures are deep marine clastic sediments of flysch type in the frontal compressional zone and of molassic type in the internal extensional zone. Continental sedimentation is generally rare, such as the Early Miocene Aliveri basin in central Evia and the Strymon basin in Eastern Macedonia.

2) The second category concerns the arc parallel structures occuring within the Late Miocene to Plio-Quaternary Hellenic arc and trench system in the Southern Hellenides. The Parnon and Taygetos extensional detachments in Peloponnese are characteristic arc parallel features together with the other NNW-SSE trending normal faults, described earlier along the transverse profile of Fig. 2. The dominant facies of these basins involve deep marine clastic sedimentation of molassic type, such as the Cretan Basin, and less deep marine sedimentation in the other neotectonic basins. In the case of the Itea – Asmfissa detachment the extensional deformation started in Middle Miocene (Papanikolaou et al, 2009). A middle Miocene age of the detachment faulting resulting in the opening of the Cretan Basin in the north and the Messara Basin in the south was also reported from Crete (Papanikolaou & Vassilakis, 2009). The orientation of the detachments in Crete is following the arc curvature and the general trend is E-W. In the Northern Hellenides the Plio-Quaternary neotectonic basins occur at the previously existing NNW-SSE oriented Late Miocene basins with lignite bearing continental deposits (Burchfiel et al, 2008). No new Plio-Quaternary basins were formed within the Northern Hellenides.

3) The third category concerns the arc transverse structures within the CHSZ developed since Late Miocene. These structures show strike-slip motions combined with normal and oblique faulting (Pavlides et al, 1990; Sokoutis et al, 1993; Koukouvelas & Aydin, 2002), related to the strike-slip faults of the Northern Aegean Sea, where oblique extension can describe better the overall tectonics (Papanikolaou et al, 2002; 2006) (Fig. 2). The dextral strike-slip motion of the CHSZ is expressed mainly by two transverse fault zones with structural trend in the ENE-WSW direction. These strike-slip fault zones are crossing the North Aegean Sea and enter mainland Greece along the Maliakos Gulf and along the Skyros – Aliveri – Northern Attica lineament (Papanikolaou & Royden, 2007). The middle Miocene age of the Kymi Basin and the Oxylithos volcanic rocks (Xypolias et al, 2003) imply the beginning of transverse strike-slip tectonics earlier in the internal part of the Hellenic arc. The general trend of the Plio-Quaternary transverse structures is E-W, overprinting the previous NNW-SSE tectonic trend of the arc parallel structures. The different fault pattern of the Plio-Quaternary neotectonic structures and basins in the CHSZ and south of it in the Southern Hellenides was described by Mariolakos & Papanikolaou (1981, 1987) and Mariolakos et al (1985) who emphasized also the fact that the E-W younger faults are seismically active structures in contrast to the NNW-SSE faults, which are less active (Fig. 5). Within the CHSZ the new structures developed during Plio-Quaternary disrupt the previous arc parallel structures as this is shown on both sides of the Corinth Gulf (Papanikolaou & Royden, 2007). In the case of the Itea – Amfissa detachment, the NNW-SSE oriented arc parallel structure has been active throughout Middle – Late Miocene and was disrupted by the Late Pliocene – Pleistocene E-W faults, bordering the northern margin of the Corinth Gulf (Papanikolaou et al, 2009). The same pattern was observed in the Northern Evoikos Gulf, where the NNW-SSE Aghios Konstantinos detachment was disrupted by the E-W normal faults of the Arkitsa system (Papanikolaou & Royden, 2007).

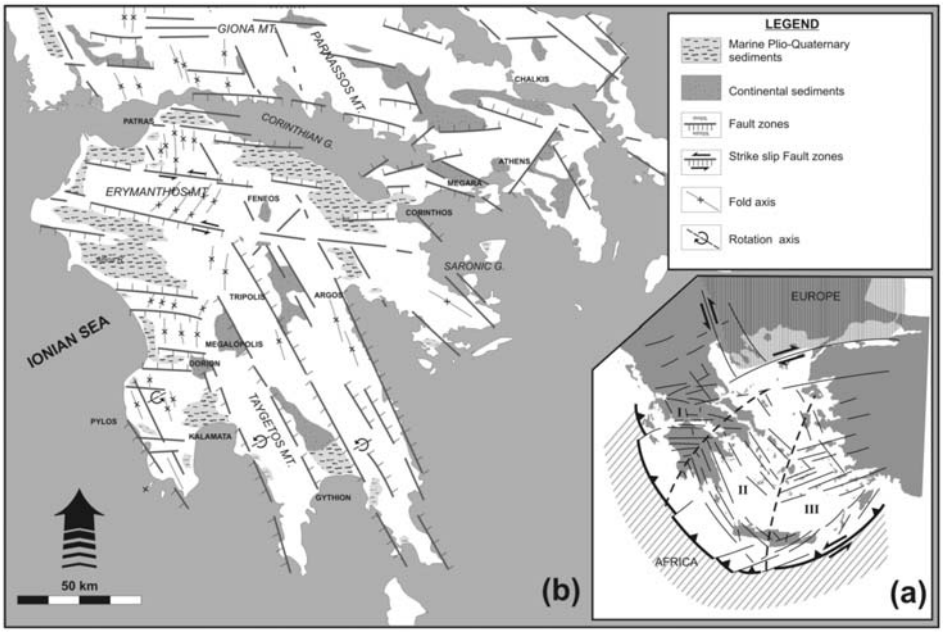

Fig. 5: Neotectonic sketch map of Sterea Hellas and Peloponnese (a) and of the Hellenic arc (b) (after Mariolakos & Papanikolaou, 1981). The distribution of the E-W oriented transverse faults within the CHSZ is confronted to the NNW-SSE arc parallel faults in the Southern Hellenides. The distribution of marine and continental sediments within the neotectonic basins helps to differentiate vertical motions with subsidence during the Pliocene and uplift during the Quaternary around the Peloponnesian coast.

In conclusion, the Hellenic arc exhibits a well pronounced arc parallel structure comprising compressive structures at the frontal zone and extensional structures at the back – arc zone throughout its tectonic evolution since Oligocene times. This arc parallel structure has been disrupted during Late Miocene – Present by transverse and oblique to the arc structures, involving dominantly strike-slip and normal faulting within the CHSZ, that separates the Northern Hellenides from the Southern Hellenides.

4. Driving mechanism(s)

Plate convergence between Africa and Europe has been the main driving force of the ongoing Hellenic subduction and related geodynamic features of the migrating orogenic arc throughout Late Cretaceous – Present. However, this subduction process has been interrupted by some distinct periods of micro-collision of the intermediate continental tectono-stratigraphic terranes of the Hellenides (Papanikolaou, 1989; 1997). Judging from present day GPS rates in the northern Hellenides and the southern Hellenides we can estimate a rate of convergence during the microcollision periods of 5-10 mm/year, similar to the rates observed today between Apulia and the Northern Hellenides and subduction rates of oceanic basins around 40 mm/year. Subduction rates may increase up to 70-80 mm/year judging from other actual subduction zones whereas rates of continental convergence seem to be of the order of a few mm/year worldwide (Sella et al, 2002; Funiciello et al, 2003; Lallemand et al, 2005; Royden & Husson, 2006).

In the case of the Hellenides, the difference between the northern segment and the southern segment corresponds to the ongoing microcollision and continental subduction of the Apulia shallow-water carbonate platform, developed over the Adria continental crust, beneath the external Hellenides nappes

in the north against the subduction of the oceanic crust of the East Mediterranean Basin beneath the southward continuation of the same external Hellenides nappes. The change of the southern segment from continental subduction to oceanic subduction occured sometime in Late Miocene, when the last marginal parts of the External Platform of the Hellenides, known as the Paxos Unit, were subducted. The external carbonate platform of the Hellenides constitutes the external terrane H_1 (Papanikolaou, 1989; 1997) separating the Pindos oceanic basin (terrane H_2) in its internal margin from the East Mediterranean basin (terrane H_0) in its external margin. Subduction of the external platform started in Late Eocene, when flysch sedimentation started in the more internal parts of the platform, comprising the tectonic units of Olympos, Amorgos, and Gavrovo – Tripolis and ended in Late Miocene when the more external parts, represented by the Paxos (known also as Pre-Apulian) unit, have been deformed and uplifted at the front of the Hellenic belt. North of the Kephalonia transform fault the external parts of the external carbonate platform are detected offshore in the Ionian Sea and continue up to the outcrops of the recently uplifted Apulia peninsula.

In conclusion, the creation during Late Miocene and the following evolution up to the present day Hellenic arc and trench system is the result of lateral inhomogeneity of the Hellenic subduction system with continental subduction and micro-collision in the north against oceanic subduction in the south. This produced a very slow convergence in the north, with a rate of 5-10 mm/year, without developing the characteristics of an arc and trench system and a rapid subduction with a rate of 40 mm/year, that created the Hellenic arc and trench system. The transition from slow continental subduction in the late Miocene to rapid oceanic subduction in the Plio-Quaternary in the southern Hellenides was driven by a roll back mechanism occuring at retreating plate boundaries, observed when subduction rate is higher than convergence rate (Royden, 1993; Ten Veen & Postma, 1999).

The above conclusion, as far as the mechanism controlling the differentiation of the Hellenides orogenic belt since Miocene times is based on subduction dynamics and confronts previous models proposing a mechanism based on lateral escape of the Anatolian microplate, following continental collision between the Arabian and Eurasian plates in the Caucasus. In this escape model, the Hellenic arc and trench system obtained its differentiated kinematics, curvature, geometry and internal deformation under the push from the Anatolian microplate, itself been pushed away from the collision zone of Arabia and Eurasia (Brunn, 1976; Mercier et al, 1979; LePichon & Angelier, 1981). This model has not taken into consideration the geodynamic situation and changes of the plate boundary at the front of the Hellenic arc in the west but only the plate dynamics in the east. A major point of concern has been the absence of a strike-slip fault zone through central continental Greece as postulated by the early plate tectonics model of the area (McKenzie, 1972). However, the GPS measurements obtained in the area of the Eastern Mediterranean during the 90's showed that the Anatolia rate is much less than the Aegean rate (20 mm/year versus 35-40 mm/year) (e.g. Reilinger et al, 1997). Thus, instead of push, the relation between Anatolia and Aegean is pull! The analysis of the GPS measurements considering the Aegean area as stable showed the existence of two vertical zones of shear along the northern (CHSZ) and the eastern (WASZ) boundaries of the Aegean microplate with a strike-slip and transtentional character (Papanikolaou & Royden, 2007). The E-W oriented transverse to the arc basins of Corinth, Beotikos Kiffissos and Northern Evoikos in central continental Greece are the result of the CHSZ and the E-W oriented basins of Western Anatolia are the result of the WASZ.

5. Paleogeographic synthesis

The paleogeographic reconstruction of the Hellenic arc during the last 34 million years (Eocene/Oligocene boundary to present) can be understood by taking into account:

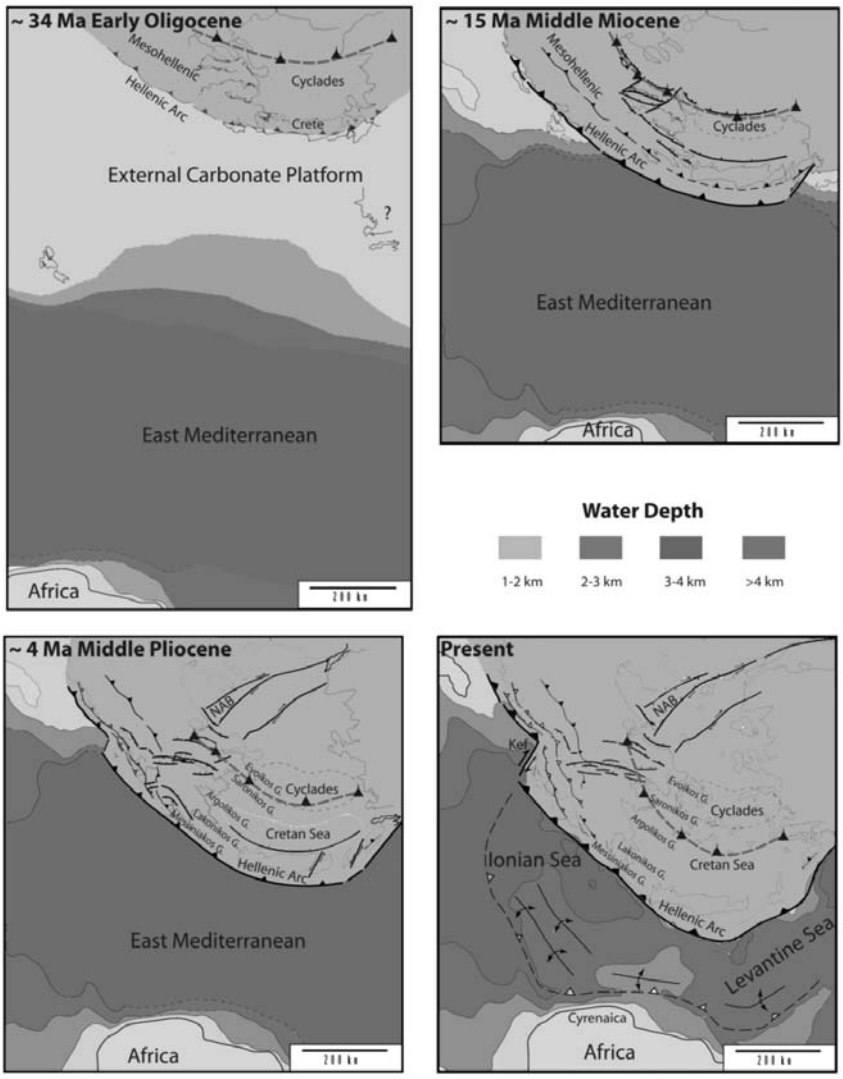

Fig. 6: Paleogeographic sketches of the Hellenic arc and its evolution to the present day Hellenic arc and trench system (modified after Royden & Papanikolaou, manuscript).

1) The estimated average Africa – Europe convergence rate (10 mm/year).

2) The Hellenic subduction rate (at present 35-40 mm/year), after its differentiation from the convergence rate of the rest European margin with an important increase during Late Miocene.

3) The internal deformation of the Aegean microplate, undergoing arc parallel extension at its central segment and horizontal shear with strike-slip faulting along the two marginal zones (CHSZ and WASZ).

4) The migration of the Hellenic arc and its internal subdivision together with the major paleogeographic changes, based on the dictribution and facies of the sedimentary basins (see for Dermitzakis & Papanikolaou, 1979).

The above computations resulted in four paleogeographic sketches corresponding to 34, 15, 4 and 0 million years given in Fig. 6. The northern boundary of the area, approximately along the North Aegean coastal zone was considered stable in the frame of reference. Thus, the difference of the distance from the North Aegean to the coast of the Cyrenaica peninsula in Africa in each sketch shows the amount of convergence between Africa and Europe. The Kephalonia transform fault, separating the Northern from the Southern Hellenides, is shown to increase in the two younger sketches. The opening of the Cretan Basin in the south is shown to develop as an arc parallel extensional basin in late Miocene whereas the North Aegean Basin is shown in the north along the new microplate boundary separating the Aegean from northern continental Greece. The other minor basins (Corinth, Evoikos, Maliakos etc) are developed within the CHSZ. The external carbonate platform of the Hellenides enters the subduction zone 34 million years ago, after the closure of the Pindos basin. At the 15 million years period the more external parts of the external platfrom are shown during their final stage of subduction in the Ionian islands when oceanic subduction of the East Mediterranean basin was established in the southern part of the arc in Crete. The bending of all previous structural trends (pre-Late Miocene) on both sides of the Kephalonia transform is depicted in the last two sketches (e.g. the Pindos thrust). The formation of the east Mediterranean rise is shown at the last sketch, when the Hellenic subduction zone has approached the African passive margin of Cyrenaica and collision is under way at the frontal part whereas subduction pertains in the Ionian and Levantine basins (Finetti et al, 1991).

6. Conclusions

The differentiation of the Hellenic arc occured in Late Miocene separating a northern segment where continental subduction continued from a southern segment where oceanic subduction started. The development of the present Hellenic arc and trench system is the result of oceanic subduction of the East Mediterranean Basin. The geometry of the Hellenic arc has been characterised by arc parallel structures both compressive at the front and extensive in the back throughout its evolution since early Tertiary. The subdivison in Northern and Southern Hellenides was accompanied by the development of the CHSZ, which created strike-slip faults and oblique to normal faults transverse to the arc with a general E-W direction in continental Greece. The extension of the Aegean upper plate produced the subsidence of the Aegean area and the creation of the North Aegean Basin and the arc transverse basins of Corinth, Beotikos Kiffissos, Northern Evoikos and other minor neotectonic basins.

7. Acknowledgments

Long discussions with L. Royden and C. Burchfiel during my visits to MIT in Boston within the MEDUSA project have been very fruitfull and contributed to my better understanding of the Hellenic arc evolution. I wish to thank Ioannis Papanikolaou and Emmanuel Vassilakis for their comments on an early draft of this manuscript and for technical assistance.

8. References

Armijo, R., Meyer, B., Hubert, A., & Barka, A., 1999. Westward propagation of the North Anatolian fault into the northern Aegean: Timing and kinematics. *Geology*, 27, 267-270.

Aubouin, J., 1959. Contribution a l'etude geologique de la Grece septentrionale: Les confins de lÉpire et de la Thessalie. *Ann. Geol. Pays Hellen.*, 10, 1-483.

Aubouin, J., 1965. Geosynclines. *Developments in Geotectonics*, 1, 335p, Elsevier.

Aubouin, J., 1974. Des tectoniques superposees et leur signification par rapport aux modeles geophy-

siques. L'exemple des Dinarides, paleotectonique, tectonique, tarditectonique, neotectonique. *Bull. Soc. Geol. France*, XV, 426-460.

Baker, C., Hatzfeld, D., Lyon-Caen, H., Papadimitriou, E. & Rigo, A., 1997. Earthquake mechanisms of the Adriatic Sea and Western Greece: implications for the oceanic subduction-continental collision transition. *Geophysical Journal International,* 131**,** 559-594.

B. P. Co, 1971. The geological result of petroleum exploration in western Greece. *I.G.R.S. Geology of Greece*, 10, 73p.

Brunn, J., 1976. L'arc concave zagro-taurique et les arcs convexes taurique et egeen: collision et arcs induits. *Bull. Soc. Geol. France*, 18,2, 481-497.

Burchfiel, B.C., Nakov, R., Dumurdzanov, N., Papanikolaou, D., Tzankov, T., Serafimovski, T., King, R.W., Kotzev, V., Todosov, A., & Nurce, B., 2008. Evolution and dynamics of the Cenozoic tectonics of the South Balkan extensional system. *Geosphere*, 4, 6, 919-938.

Cavazza, W., Roure, F. & Ziegler, P., 2004. The Mediterranean area and the surrounding regions: active processes, remnabts of former Tethyan oceans and related thrust belts. In: *The TRANSMED Atlas*, Springer.

Dermitzakis, M. & Papanikolaou, D., 1979. Paleogeography and Geodynamics of the Aegean Region during the Neogene. VII Int. Congress Medit. Neogene, Athens 1979. *Ann. Geol. Pays Hellen.*, hors serie, IV, 245-289.

Dewey, J.F. & Sengor, C.A.M., 1979. Aegean and surrounding regions: complex multiplate and continuum tectonics in a convergent zone. *Geol. Soc. Amer. Bulletin*, 90, 84-92.

Finetti, I., Papanikolaou, D., Del Ben, A. & Karvelis, P., 1991. Preliminary geotectonic interpretation of the East Mediterranean Chain and the Hellenic Arc. Bull. Geol. Soc. Greece, XXV/1, 509-526.

Funiciello, F., Faccenna, C., Giardini, D. & Regenauer-Lieb, K., 2003. Dynamics of retreating slabs: 2. Insights from three-dimensional laboratory experiments. *Journal of Geophysical Research-Solid Earth,* 108**.**

Hollenstein, C., Móller, M.D., Geiger, A. & Kahle, H.G., 2008. Crustal motion and deformation in Greece from a decade of GPS measurements, 1993-2003, *Tectonophysics,* 449**,** 17-40.

Hsu, K. Et al, 1978. History of the Mediterranean salinity crisis. Init. Rep. D.S.P.D., XIII/1, 1053-1078.

I.G.S.R. & I.F.P. 1966. Etude geologique de l'Epire. *Technip*, 306 p.

Jacobshagen, V. Et al, 1978. Structure and geodynamic evolution of the Aegean region. In: *Alps, Apennines, Hellenides*, 537-564, Stuttgart.

Kahle, H.G., Cocard, M., Peter, Y., Geiger, A., Reilenger, R., Barka, A. & Veis, G., 2000. GPS-derived strain rate field within the boundary zones of the Eurasian, African, and Arabian Plates. *Journal of Geophysical Research,* 105**,** 23353-23370.

Koukouvelas, I.K., & Aydin, A., 2002. Fault structure and related basins of the North Aegean Sea and its surroundings. *Tectonics*, 21, 1046, doi:10.1029/2001TC901037.

Kreemer, C., Chamot-Rooke, N., & Le Pichon, X. 2004. Constraints on the evolution and vertical coherency of deformation in the Northern Aegean from a comparison of geodetic, geologic and seismologic data. *Earth and Planetary Science Letters*, 225, 329-346.

Lalechos, N., & Savoyat, E. 1979. La sédimentation Neogene dans le Fosse Nord Egeen. *6th Colloquium on the Geology of the Aegean region,* 2, 591-603.

Lallemand, S., A. Heuret, & Boutelier, D., 2005. On the relationship between slab dip, back-arc stress, upper plate absolute motion, and crustal nature in subduction zones. *Geochemistry Geophysics Geosystems*, 6, Q09006, doi:10.1029/2005GC000917.

Le Pichon, X. & Angelier, J., 1979. The Hellenic arc and trench system: a key to the neotectonic evolution

of the eastern Mediterranean area. *Tectonophysics,* 60**,** 1-42.

LePichon, X., Lyberis, N., & Alvarez, F., 1984. Subsidence history of the North Aegean Trough. *Geological Society of London Special Publication,* 17, 727-741.

Mariolakos, I. & Papanikolaou, D., 1981. The Neogene basins of the Aegean Arc from the Paleogeographic and the Geodynamic point of view. *Proc. Int. Symp. H.E.A.T.*, 383-399.

Mariolakos, I., Papanikolaou, D. & Lagios, E., 1985. A neotectonic geodynamic model of Peloponnesus based on morphotectonics, repeated gravity measurements and seismicity. *Geol. Jahrbuch*, B-50, 3-17.

Mariolakos, I. & Papanikolaou, D., 1987. Deformation pattern and relation between deformation and seismicity in the Hellenic Arc. *Bull. Geol. Soc. Greece*, 19, 59-76.

McKenzie, D., 1972. Active tectonics of the Mediterranean region. *Geophys. J. R. Astron. Soc.* 30, 109-185.

McNeill, L.C., Mille, A., Minshull, T.A., Bull, J.M., Kenyon, N.H., & Ivanov, M., 2004. Extension of the North Anatolian Fault into the North Aegean Trough: Evidence for transtension, strain partitioning and analogues for Sea of Marmara basin models. *Tectonics,* 23, TC2016, doi:10.1029/2002TC001490.

Mercier, et al, 1972. Deformations en compression dans le quaternaire de rivages ioniens (Cephalonie, Grece). Donnes neotectoniques et sismiques. *C. R. Acad. Sciences, Paris*, 175, 2307-2310.

Mercier, J. et al, 1979. La neotectonique de l'arc egeen. *Rev. Geol. Dyn. Geogr. Phys.*, 21, 1, 67-92.

Monopolis, D. & Bruneton, A., 1982. Ionian Sea (Western Greece): its structural outline deduced from drilling and geophysical data. *Tectonophysics*, 83, 227-242.

Papanikolaou, D. & Dermitzakis, M., 1981. Major changes from the last stage of the Hellenides to the Actual Hellenic Arc and Trench system. *Int. Symp. H.E.A.T.*, Athens 1981, Proceedings, II, 57-73.

Papanikolaou, D. & Dermitzakis, M., 1981. The Aegean Arc during Burdigalian and Messinian: A comparison. *Riv. Ital. Paleont.* 87, 1, 83-92.

Papanikolaou, D., 1986. *Geology of Greece* (in Greek). Eptalofos Publications, Department of Geology, University of Athens, 240pp.

Papanikolaou, D., Lykoysis, V., Chronis, G., & Pavlakis, 1988. A comparative study of neotectonic basins across the Hellenic arc: the Messiniakos, Argolikos, Saronikos and Southern Evoikos gulfs. *Basin Research*, 1, 167-176.

Papanikolaou, D., 1989. Are the Medial Crystalline Massifs of the Eastern Mediterranean drifted Gondwanan fragments? *Geol. Soc. Greece Spec. Publ.*, 1, 63-90.

Papanikolaou, D., 1993. Geotectonic evolution of the Aegean. *6th Congress of the Geological Society of Greece*, Athens 1992, *Bull. Geol. Soc. Greece*, 28/1, 33-48.

Papanikolaou, D., 1997. The tectonostratigraphic terranes of the Hellenides. Final volume of IGCP 276, *Ann. Geol. Pays Hellen.*, 37, 495-514.

Papanikolaou, D., Alexandri M, Nomikou, P., & Ballas, D., 2002. Morphotectonic Structure of the Western part of the North Aegean Basin based on swath bathymetry. *Marine Geology*, 190, 465-492.

Papanikolaou, D., Bargathi, H., Dabovski, C., Dimitriu, R., El-Hawat, A., Ioane, D., Kranis, H., Obeidi, A., Oaie, G., Seghedi, A. & Zagorchev, I., 2004. TRANSMED Transect VII: East European Craton – Scythian Platform – Dobrogea – Balkanides – Rhodope Massif – Hellenides – East Mediterranean – Cyrenaica.In: The TRANSMED Atlas. The Mediterranean Region from Crust to Mantle. W.Cavazza, F. Roure, W. Spakman, G. Stampfli, P. Ziegler (eds), Spinger.

Papanikolaou, D., Alexandri, M., & Nomikou, P., 2006. Active faulting in the North Aegean basin. *In* Dilek, Y., and Pavlides, S., eds., Postcollisional tectonics and magmatism in the Mediterranean region and Asia: *Geological Society of America Special Paper*, 409, 189-209, doi:10.1130/2006.2409 (11).

Papanikolaou, D. & Royden, L., 2007. Disruption of the Hellenic Arc: Late Miocene Extensional De-

tachment Faults and steep Pliocene-Quaternary Normal Faults – or – What Happened at Corinth ? *Tectonics*, 26, TC5003, doi:10.1029/2006TC002007.

Papanikolaou, D. & Vassilakis, E., 2009. Thrust faults and extensional detachment faults in Cretan tectonostratigraphy: Implications for Middle Miocene extension. *Tectonophysics*, doi: 10.1016/j.tecto.2009.06.024.

Papanikolaou, D., Gouliotis, L. & Triantaphyllou, M., 2009. The Itea – Amfissa detachment: a pre - Corinth rift Miocene extensional structure in central Greece. *Special Publ. Geol. Soc. London*, "Collision and collapse at the Africa-Arabia-Eurasia subduction zone" vol. 311, 293-310.

Pavlides, S., Mountrakis, D., Kilias, A., & Tranos, M., 1990. The role of strike slip movements in the extensional area of Northern Aegean (Greece). A case of transtensional tectonics. *Annales Tectonicae*, 4, 196-211.

Philippson, A., 1959. Die griechischen Landschaften. Volumes I-V. Klostermann, Frankfurt.

Reilinger, R.E., McClusky, S.C., Oral, M.B., King, R.W., Toksoz, M.N., Barka, A.A., Kinik, I., Lenk, O., & Sanli, I., 1997. Global Posisioning System measurements of present-day crustal movements in the Arabia-Africa-Eurasia plate collision zone. *Journal of Geophysical Research*, 102, 9983-9999.

Royden, L.H., 1993. Evolution of retreating subduction boundaries formed during continental collision, *Tectonics,* 12**,** 629-638.

Royden, L. & Husson, L., 2006. Trench motion, slab geometry and viscous stresses in subduction systems, *Geophysical Journal International,* 167**,** 881-905.

Royden, L. & Papanikolaou, D. Slab segmentation and Late Cenozoic disruption of the Hellenic arc. Manuscript.

Sella, G. F., T.H. Dixon, & Mao, A.L., 2002. REVEL: A model for recent plate velocities from space geodesy. *Journal of Geophysical Research*, 107, 2081, doi:10.1029/2000JB000033.

Sokoutis, D., Brun, J.P., Van den Drissche, J., & Pavlides, S., 1993. A major Oligo-Miocene detachment in southern Rhodope controlling north Aegean extension. *Journal of the Geological Society of London,* 150, 243-246.

ten Veen, J.H. & Postma, G., 1999. Roll-back controlled vertical movements of outer arc-basins of the Hellenic subduction zone (Crete, Greece). Basin Research, 11, 223-241.

Underhill, J.R., 1989. Late Cenozoic deformation of the Hellenide foreland, western Greece. *Bulletin Geological Society of America*, 101, 613-634.

van Hinsbergen, D., Hafkenscheid, E., Spakman, W., Meulenkamp, J. & Wortel, R., 2005. Nappe stacking resulting from subduction of oceanic and continental lithosphere below Greece. *Geology,* 33**,** 325-328.

Δελτίο της Ελληνικής Γεωλογικής Εταιρίας, 2010
Πρακτικά 12ου Διεθνούς Συνεδρίου
Πάτρα, Μάιος 2010

Bulletin of the Geological Society of Greece, 2010
Proceedings of the 12th International Congress
Patras, May, 2010

THE STATUS OF STRATIGRAPHY IN THE 21ST CENTURY

Dermitzakis M.D.[1]

[1] *Department of Historical Geology and Palaeontology, Faculty of Geology and Geoenvironment, University of Athens, Panepistimiopolis 15784, Athens, Greece, mdermi@geol.uoa.gr*

Abstract

The 21st century geological time scale (GTS) will comprise an internationally agreed chronologic hierarchy. Correlation of events into the GTS will be undertaken using a wide variety of methods, including numeric dating, fossil occurrence, physical and chemical properties, tephrochronology and astrochronologic retrodictions. Chronostratigraphic subdivision of the sedimentary rock record should proceed in a bottom up hierarchical manner with lower units defining the boundaries of stratigraphically higher units. A moderate amount of work is required to improve the basis of the hierarchical subdivision of some Cenozoic series boundary subdivisions and to bring them in line with recommendations by the Stratigraphic Guide and recommendations by the International Committee of Stratigraphy (ICS).

Key words: *stratigraphic classification, chronostratigraphy, geochronology.*

1. Introduction

Stratigraphy provides the time frame and descriptive background against which all geology is undertaken, including particularly the description of fossil organisms, the deciphering evolutionary patterns and the reconstruction of geological paleo- environments. The advanced stratigraphic techniques underpin the discovery and exploitation of sedimentary mineral and energy resources. In addition stratigraphy has a part to play in the understanding of dangerous natural hazards and climate change.

During the Italian renaissance, stratigraphy was marked especially by Leonardo's recognition that marine fossil shells represented the remains of animals that formerly lived on ancient seabeds, and Steno's elucidation of the time significance of stratification. Afterwards, the scene shifted to post-Enlightenment western Europe. There, in late 18th century Scotland, James Hutton generalized Leonardo's earlier insights by applying them to igneous rocks and geological observation in general. Then, in early 19th century England, William Smith laid the foundations of geological mapping and biostratigraphy, work that led to the recognition and naming of the Periods of the geological time scale by stratigraphic pioneers such as Sedgwick, Lapworth and Murchison. Meanwhile, Charles Lyell wove the gold thread of uniformitarian interpretation into geological study in his book Principles of Geology, thereby allowing the previous 400 years of insight to be summarized by the pithy aphorism - "the present is the key to the past", (Lyell, 1833). The development of the geological time scale and all preceding geological studies, largely had their basis in observational field evidence. By the late 19th century with the increasing specialization of different branches of geology and the widespread adoption of the petrographic microscope, the need arose for a more systematic approach to the naming and classification of different types of strata, which led into the codex age of stratigraphy. The

demand for more organized codifications of sedimentary rocks was reflected in the distinction drawn at the 2nd International Geological Conference at Bologna (1881) between those terms to be used for past geological time periods (Era, Period. Epoch and Age) and the distinct hierarchy of-terms that were then concerned with the naming of rock bodies (Group, System. Series, Stage).

2. Post Hedberg stratigraphic classification: order or chaos?

Since the First International Geological Congress (IGC, 1878) one of the main issues for global geology was to achieve some order in Stratigraphic Classification and Terminology. Only in 1952 (19th International Geological Conference) the International Subcommission on Stratigraphy was created, under the leadership of H. Hedberg, to produce an International Stratigraphic Guide (ISG). The Guide, published in 1976 (Hedberg, 1976), was the result of an international consensus on a set of principles embodied in a simple and readily usable classification and was soon to become a model for most National and Regional Stratigraphic Codes. After one hundred years of work it seemed that the original goal had been achieved. However, already in 1977 oil geologists introduced "sequence stratigraphy", and the 1983 North American Stratigraphic Code included several new categories. Meanwhile, a number of other stratigraphic methodologies began to be applied, e.g. astronomical calibration in sedimentary cycles. In spite of all that, the ISG second edition was still restricted to the classical categories accepted in 1976, although with the addition of Magnetostratigraphic and Unconformity-Bounded Units (UBUs). The so called "Lithodemic Units" prompted the use of different terminology for non sedimentary rock bodies. "Allostratigraphic units" resulted in a still unsettled discussion on their relationship to UBUs and Sequence Stratigraphy. Chronostratigraphic, Chronometric and Geochronologic units were used in the Geologic Time Scale. These developments were paralleled by the work done by the International Commission on Stratigraphy aimed to achieve a world-wide "chronostratigraphic standardisation" based on "Global Stratotype Sections and Points" (GSSP) for which priority as well as permanence is considered as irrelevant. This resulted in a series of GSSPs defining a scale where the classical time-rock concept becomes redundant and its application represents a practical problem to be solved.

Geologic Time Sca1e 2004 (Gradstein et al., 2004) integrated all the available stratigraphic and geochronology information. The construction of Geological Time Scale 2004 (GTS2004) incorporated different techniques depending on the data available within each interval. Construction involved a large number of specialists, including contribution by past and presents subcommissions officers of the International Commission on Stratigraphy (ICS), geochemists working with radiogenic and stable isotopes, stratigraphes using diverse tools from traditional fossils to astronomical cycles to data base programming, and geomathematicians.

3. Simplifying the Stratigraphy of Time: Implications and practical consequences

Stratigraphy, originally restricted to the study of stratified rocks (e.g., Dunbar and Rodgers, 1957), now has come to encompass all rocks on Earth (e.g., Salvador 1994; Rawson et al., 2002). Three forms of chronology are currently used in the definition of Phanerozoic time scales (Hedberg, 1976; Whittaker et aI., 1991; Salvador, 1994; Rawson et aI., 2002).

The present international nomenclature in English/American recommends a dual hierarchy for the stratigraphical units: rock-units (Erathem, System, Series, Stage) and time units (Era, Period, Epoch, Age) with formal subdivisions into Lower/Upper and Early/Late subunits respectively; the corresponding disciplines are respectively called chronostratigraphy and "geochronology".

By definition, a chronostratigraphic unit consists of all strata formed during the time span of a funda-

mental geochronological unit. However, making practical distinctions between chronostratigraphy and geochronology is often problematic. In particular the distinction between the two parallel hierarchies of chronostratigraphy (time-rock) and geochronology (geologic time) is subtle, and, not clear to the greater part of the geological community. The distinction is normally only encountered when correct terminology (e.g., period versus system, lower versus early) needs to be used in writing or editing scientific papers. Terms such as e.g. Early Jurassic and Lower Jurassic are often used interchangeably.

Chronostratigraphic units currently refer to stratified rocks only. However, geologic time is of wider applicability than the time-rock classification, and of more use in the kind of cross-disciplinary studies that now increasingly characterize geology.

The distinction between geologic time and time-rock classifications, and their distinction from numerical time, blurs the essential simplicity of stratigraphic classification, and is a significant barrier to understanding, not least as regards extending the messages within stratigraphy (biotic evolution; environmental and climatic change) to the lay public. It is important to preserve this fundamental simplicity today, when the main stratigraphic features of rock, time, and fossils have been joined by numerous other types of stratigraphy, such as those employing paleomagnetic reversals, or the sedimentary signature of Milankovitch climatic cycles.

The term "geochronology" as applied to periods, epochs, and so on does not reflect its mainstream vernacular use (e.g., Bates and Jackson, 1987). Isotope geologists working with radiometric dating generally consider themselves to be geochronologists (not geochronometricists) working on problems of geochronology; they do not use the term geochronometry (and neither do mainstream geologists) in everyday work.

In a discussion paper of the Stratigraphy Commission of the Geological Society of London (Zalasiewicz et al., 2004; elaborating an earlier concept of Harland et al., 1990), the following proposals were made:

- ending the distinction between the dual stratigraphic terminology of time-rock, units (of chronostratigraphy) and geologic time units (of geochronology), on the basis that the long-held, but widely misunderstood distinction between these two essentially parallel time-scales in stratigraphy has been rendered unnecessary by the widespread adoption of the GSSP (=golden spike) principle, in defining intervals of geologic time within rock strata.
- using the name "chronostratigraphy" for the definition and application of a hierarchy of eons, eras, periods, epochs and ages. The time units defined by chronostratigraphy in this sense may be qualified by "early" and "late", but not by "lower" and "upper". Although found within strata, they encompass all rock on Earth.
- making the terms eonothem, erathem, system, series and stage formally redundant.
- allowing the term "geochronology" to revert to its mainstream vernacular use of referring to dating and ordering geological events, particularly by obtaining numerical estimates of time, through radiometric dating, the counting of Milankovitch cycles etc.

It was argued that these suggested changes should simplify stratigraphic practice, encompass both stratified and non-stratified rocks, and help geologic understanding, while retaining precision of meaning. What would be the practical consequences of implementing such changes? In the short term, there would certainly be reluctance by many working stratigraphers, possessing long familiarity with the dual terminology, to abandon terms such as "systems" and "series", which are convenient shorthand for referring to the depositional ages of strata. Longer-term, and, more widely, there may be considerable advantages in operating a unified geological time-scale: this would facilitate the correlation of diverse geological phenomena in the construction of increasingly sophisticated (and societally relevant) models of earth history, and aid research between geologist and scientists of other disciplines.

4. Status of the hierarchical subdivision of higher order marine Cenozoic chronostratigraphic units

Chronostratigraphy remains at the center of the science of Stratigraphy. It provides the conceptual framework in which a hierarchical subdivision of the passage of time is recorded in the rock record. International committees have consistently recommended that this subdivision should proceed in a bottom-up succession, beginning with the stage as the fundamental unit in global chronostratigraphy except where this procedure is not possible owing to inadequately documented lower rank (stage) units.

The following represent the recent developments in the status of the hierarchical subdivision of Cenozoic chronostratigraphic units (Berggren, 2007):

- The base of the Pleistocene has been redefined as Gelasian Stage. The placement of the base Pleistocene equivalent to the base Calabrian at Vrica is a convoluted matter as explained in Van Couvering (1997) and Aubry et al. (1999).The GSSP for the Pliocene/Pleistocene boundary was placed at the base of the Pleistocene Series at Vrica (Calabria, Italy) by the joint Working Group of IGCP-4l and the INQUA Subcommission on the Neogene/Quaternary boundary, submitted to, and approved by, the International Commission on Stratigraphy (ICS) in 1983. The proposal was published by Aguirre and Pasini (1985), and accepted by the International Union of Geological Sciences (lUGS) at the 27th International Geological Congress (IGC) in Moscow (Bassett 1985). The GSSP lies at the base of uniform marls just above sapropel bed "e", within the uppermost part of the Olduvai Magnetozone (C2n) (Zijderveld et al. 1991) with a currently estimated astronomical age of 1.806 Ma (Lourens et al. 2004). However, Quaternary geologists have refused the ICS proposal in 2005, to decouple the Pleistocene (base 1.8Ma) and Quaternary (base 2.6 Ma), and to reinstate the Quaternary at the Suberathern/Subera level in the chronostratigraphic hierarchy. In June 2009, the Executive Committee of the International Union of Geological Sciences (IUGS) formally ratified a proposal by the International Commission on Stratigraphy to lower the base of the Quaternary System/Period to the Global Stratotype Section and Point (GSSP) of the Gelasian Stage/Age at Monte San Nicola, Sicily, Italy. The Gelasian until then had been the uppermost stage of the Pliocene Series/Epoch. The base of the Gelasian corresponds to Marine Isotope Stage 103, and has an astronomically tuned age of 2.58 Ma. A proposal that the base of the Pleistocene Series/Epoch be lowered to coincide with that of the Quaternary (the Gelasian GSSP) was also accepted by the IUGS Executive Committee. The GSSP at Vrica, Calabria, Italy, which had hitherto defined the basal boundary of both the Quaternary and the Pleistocene, remains available as the base of the Calabrian Stage/Age (now the second stage of the revised Pleistocene). In ratifying these proposals, the IUGS has acknowledged the distinctive qualities of the Quaternary by reaffirming it as a full system/period, correctly complied with the hierarchical requirements of the geological timescale by lowering the base of the Pleistocene to that of the Quaternary, and fully respected the historical and widespread current usage of both the terms 'Quaternary' and 'Pleistocene' (Gibbard et al., 2009).
- The base Oligocene was defined with no mention of the constituent stages concerned (Priabonian and Rupelian); the base Oligocene has since been found to lie at a level stratigraphically within the upper third of the Priabonian Stage, effectively decapitating the upper part of the Priabonian Stage and at a level - 0.4 my younger than the currently recognized GSSP for the base of the Eocene.
- The base/GGSP of the Eocene was placed at a stratigraphic level nearly 1 my older than the accepted base of the Ypresian Stage s.s.; the Ypresian Stage was simply lowered by this amount, effectively decapitating a significant part of the underlying Thanetian Stage which has been considered of Paleocene age for over a century, and transferring rocks belonging to the upper/late

Thanetian to the lower/early Eocene; the insertion of the "Sparnacian Stage"-which has been shown to span the chronostratigraphic/geochronologic interval from base Eocene to base Ypresian s.s as the basal stage of the lower Eocene –has been suggested.

- The base Pliocene Series was correctly based on a GSSP for the base of its lowest component, the Zanclean Stage, in the Eraclea Minoa section of the composite Rossello section, in south coast of Sicily. The Subcommision on Neogene Stratigraphy (SNS) recommended that the base (GSSP) of the Zanclean Stage (and base Pliocene Series) be placed at the base of the carbonate bed of small-scale cycle 1 in the Trubi Marl Formation in the Eraclea Minoa section (itself a component subsection of the Capo Rossello Composite Section), southern coast of Sicily, corresponding to insolation cycle 510 from the present with an estimated astrochronologic age of 5.33 Ma (Van Couvering et al. 2000). In a recent study of the stratigraphically continuous Miocene-Pliocene Loulja marine section of Atlantic facies (Bou Regreg area, NW Morocco) Van Der Laan et al. (2006) have shown that the Miocene/Pliocene boundary may not coincide with isotope stage TG5 but rather with an "extra (weak) obliquity-controlled cycle between TG 7 and TG5. If true, the authors point out that the boundary would not coincide with a major deglaciation event and associated glacio-eustatic sea-level rise as generally believed; tectonics, rather, are thought to have played a significant role. Earlier, Krijgsman et al. (2001) have shown that the initiation of the Messinian Salinity Crisis at - 6 Ma was not related to a glacio-eustatic event either.

5. Conclusions

After 200 years of discussion, two editions of the International Stratigraphic Guide and with the forthcoming completion of definition of GSSP at all Period boundaries, the stratigraphic community is well prepared to contribute to dealing with mankind's needs and problems. During the 21st century, stratigraphers will continue to provide both the time skeleton and the environmental flesh for imaginative reconstructions of the history of planet earth. Stratigraphers will also remain deeply involved in the search for earth resources, especially sedimentary-based energy resources such as coal, petroleum and uranium, and will help to provide high resolution histories of the occurrence of earthquakes, tsunami, volcanic eruptions and floods.

However 21st century Stratigraphy must conform to criteria of usefulness -both scientific and politicaI. At the same time, the discipline will need to remain true to its historic scientific roots, of which the most important is the application of a strong principle of priority of nomenclature to preserve the value of order observations and literature.

Impediments which today remain to ready and consistent communication of stratigraphic information include differences in approach, and sometimes nomenclature, between different national or regional geological communities; and a number of minor inconsistencies in stratigraphic usage that need to be tidied up. Stratigraphy should add value by providing concise and clear nomenclatural schemes, not subtract value by interminable arguments, or by introducing unnecessary complexity of classification.

6. References

Aguirre, E., Pasini, G., 1985. The Pliocene-Pleistocene boundary. *Episodes*, 8, 116-120.

Aubry, M.-P., Berggren, WA., Van Couvering, JA., and Steininger, E, 1999. Problems in chronostratigraphy: Stages, series unit and boundary stratotypes, global stratotype section and point and tarnished golden spikes. *Earth-Science Reviews*, 46, 99-148.

Bassett, M. G., 1985. Towards a "common language" in stratigraphy. *Episodes*, 8, 87-92.

Bates, R.L., Jackson, lA, 1987. *Glossary of geology*. (third edition), Alexandria, Virginia, American Geological

Institute, 788 p.

Berggren, W.A., 2007. Status ofthe hierarchical subdivision of higher order marine Cenozoic chronostratigraphic units. *Stratigraphy*, 4, 99-108.

Dunbar,C.O., Rodgers, L, 1957. *Principles of stratigraphy*. New York, John, Wiley, 356 p.

Gibbard, PL., Head, M.J., Walker, M.J.C. & the Subcommission on Quaternary Stratigraphy, 2009. Formal ratification of the Quaternary System/Period and the Pleistocene Series/Epoch with a base at 2.58 Ma. *Journal of Quaternary Science*. (in press).

Gradstein, F.M., Ogg, J.G., Smith, A.G., Agterberg, F.P., Bleeker, W., Cooper, R.A., Davydov, V., Gibbard, P., Hinnov, L., House, M.R., Lourens, L. Luterbacher, H-P., McArthur, J., Melchin, M.J., Robb, L.J., Shergold, J., Villeneuve, M., Wardlaw, B.R., Ali, J., Brinkhuis, H., Hilgen, F.J., Hooker, J., Howarth, R.J., Knoll, A.H., Laskar, J., Monechi, S., Powell, J.,

Plumb, K.A., Raffi, I., Röhl, U., Sanfilippo, A., Schmitz, B., Shackleton, N.J., Shields, G.A., Strauss,H., Van Dam, J., Veizer, J., van Kolfschoten, Th., Wilson, D., 2004. *A Geologic Time Scale 2004*. Cambridge University Press, ~500 p.

Harland, W.B., Armstrong, R.L., Cox, A.V., Craig, L.A., Smith, AG., Smith, D.G., 1990. *A geologic time scale 1989*. Cambridge, Cambridge University Press, 263 p.

Hedberg, RD., 1976. *International stratigraphic guide*. New York, John Wiley, 200 p.

Krijgsman, W., Fortuin, A.R., Hilgen, F.J., Sierro, F.J., 2001. Astrochronology for the Messinian Sorbas basin (SE Spain) and orbital (precessional) forcing for evaporite cyclicity, *Sedimentary Geology*, 140, 43–60.

Lourens, L., Hilgen, F., Shackleton, N. J., Laskar, J., Wilson, J., 2004. The Neogene period. In F. M. Gradstein et al. (eds), *A Geologic Time Scale 2004*, p. 409-440, Cambridge University Press.

Lyell, C., 1833. *Principles of Geology, Being an Attempt to Explain the Former Changes of the Earth's Surface by Reference to Causes Now in Operation*, vol. III, John Murray, London p. 398.

Rawson, P.E, Allen, P.M., Bevins, R.E., Brench1ey, P.J., Cope, J.C.W., Evans, JA., Gale, AS., Gibbard, P.L., Gregory, E.J., Hesse1bo, S.P., Marshall, J.E.A, Knox, R.W.O.B., Oates, M.J., Riley, N.J., Rushton, A.W.A, Smith, A.G., Trewin, N.H., Zalasiewicz, J.A, 2002. *Stratigraphical procedure*. Geological Society of London Professional Handbook, 57 p.

Salvador, A., 1994. *The International Stratigraphic Guide: A guide to stratigraphic classificationterminology,and procedure*. New York, John Wiley, 214 p.

Van Couvering, J., 1997. Preface, the new Pleistocene. In: van Couvering, J. (ed.) *The Pleistocene boundary and the beginning of the Quaternary*. University Press: Cambridge. ii-xvii.

Van Couvering, J.A., Castradori, D., Cita, M.B., Hilgen, F.J., Rio, D., 2000. The base of the Zanclean Stage and of the Pliocene Series. *Episodes*, 23, 179–187.

Van Der Laan, E., Snel, E., De Kaenel, E., Hilgen, F.J., Krijgsman, W., 2006. No major deglaciation across the Miocene-Pliocene boundary: Integrated stratigraphy and astronomical tuning of the Loulja sections (Bou Regreg area, NW Morocco). *Paleoceanography*, 21 (3), art. no. PA3011.

Whittaker, A., Cope, J.C.W., Cowie, J.W., Gibbons, W., Hailwood, E.A., House, M.R., Jenkins, D.G., Rawson, A.W.A., Rushton, A.W.A., Smith, D.G., Thomas, A.T., Wimbledon, W.A., 1991. A guide to stratigraphical procedure. *Journal of the Geological Society*, *London* 148, 813–824.

Zalasiewicz, J., Smith, A., Brenchley, P., Evans, J., Knox, R., Riley, N., Gale, A., Gregory, F.J., Rushton, A., Gibbard, P., Hesselbo, S., Marshall, J., Oates, M., Rawson, P., Trewin, N., 2004. Simplifying the stratigraphy of time. *Geology*, 32, 1-4.

Zijderveld, J.D.A., Hilgen, F.J., Langereis, C.G., Verhallen, P.J.J.M., Zachariasse, W.J., 1991. Integrated magnetostratigraphy and biostratigraphy of the upper Pliocene-lower Pleistocene from the Monte Singa and Crotone areas in Calabria, Italy. *Earth and Planetary Science Letters*, 107 (3-4), 697-714.

Δελτίο της Ελληνικής Γεωλογικής Εταιρίας, 2010
Πρακτικά 12ου Διεθνούς Συνεδρίου
Πάτρα, Μάιος 2010

Bulletin of the Geological Society of Greece, 2010
Proceedings of the 12th International Congress
Patras, May, 2010

THE FORGOTTEN GEOGRAPHIC AND PHYSICAL – OCEANOGRAPHIC KNOWLEDGE OF THE PREHISTORIC GREEKS

Mariolakos I.D.[1]

[1] *National and Kapodistrian University of Athens, Faculty of Geology and Geoenvironment, Department of Dynamic, Tectonic & Applied Geology, Panepistimioupoli, Zografou, 157 84, Athens, Greece, mariolakos@geol.uoa.gr*

Abstract

Many believe that the Greek Mythology is a figment of the vivid imagination of the ancient Greeks. Consequently, the Greek Myths are all fantastic stories. In my opinion, this view is erroneous, at least on the subject concerning the geographic and physical-oceanographic characteristics of the Atlantic Ocean, as these were described mainly by Homer, Hesiod, the Orphics and Plutarch.

In the present paper (i) some of the references made by the above mentioned authors are selectively reported, and (ii) the physical and geological validation is given, based on the present-day scientific views and knowledge.

Namely, the prehistoric Greeks knew about the Hyperboreans, the island of Ierne (Ireland), the British isle etc., by the Orphics.

From the writings of Plutarch, they knew (i) the relative position of the present-day Iceland (Ogygia) and its distance from Britain, (ii) that to the west of Iceland, three other islands are located, where the sun sets for only an hour a day, (iii) that further to the west there is a "great continent", which surrounds the Ocean and more.

Homer and Hesiod wrote that (i) the Ocean is a "river" that flows continuously, (ii) that this river encircles the Earth and (iii) that its flow is turbulent not only on the surface, but in depth as well.

Unfortunately, all this knowledge was gradually forgotten by all. This is the reason why Odyssey is considered just an entertaining poem and Ulysses' nostos a fantastic story, with no trace of historic reality.

Key words: *Greek Mythology, Cronus, Ogygia, Atlantic Ocean, Oceanus, Gulf Stream, Heracles.*

1. Introduction

Many believe that the Greek Mythology is a figment of the vivid imagination of the ancient Greeks. Consequently, until the end of the 19th century, all the experts – scientists and especially the archaeologists and the historians, believed that every writing of the ancient authors, such as Hesiod, Plato, Strabo, Diodorus Sicilus and mainly Homer, connected to mythology, lacked even a seed of truth. Consequently, the Greek Myths were all fantastic stories. It was only after the excavations of Schliemann, that it was proven that all of Homer's writings concerning Troy were true, and not only that, but that in Greece, cities like the Mycenae existed and they were the opponents of the Trojans, etc.

Nevertheless, even nowadays, many believe that all included in these writings do not correspond to the

truth. Our own research, concerning the accuracy of many physical and geological descriptions, given by various ancient authors, and especially by Homer, Hesiod, the Orphics, Diodorus Sicilus, Plutarch and others, has shown that the prehistoric Greeks knew many on the physical-oceanographic characteristics of mainly the Atlantic Ocean. Of course, all the above, for unknown reasons, are not described in a way that are easily understood by everyone, but as a myth, part of the Greek Mythology.

In this paper, the object of the geomythological analysis is the Atlantic Ocean and its relation to the great Titans of Greek Mythology, mainly *Oceanus*, *Atlas*, and *Cronus*.

All these refer to a very old era and in any case, at least to the beginning of the 3nd millennium B.C., until the end of the 2nd one, that is until the end of the Mycenaean period.

2. Mythological period

2.1 General

The long history of the human being, of *Homo sapiens*, is divided into two long periods: the historic period, that starts with the invention of writing, and the prehistoric one. The prehistoric period should be further divided into two sub-periods, specifically during the period when *Homo sapiens* is in the hunting and gathering stage (a food gatherer) and a later one, when *Homo sapiens* is a food producer, i.e. *after the initiation of agriculture* and mainly after the cultivation of wheat.

The Mythological period is the prehistoric period that refers to the acts of Gods, deities and heroes, which have not been written down but have remained in the memory of different people, either through tradition, or as it has later been recorded by various authors, but definitely in a very ancient period. These texts constitute the different Mythologies. Such characteristic texts are the Gilgamesh epic, which refers to the people of the Prehistoric Mesopotamia and Hesiod's "Theogony" that represents the Mythology of the Ancient Greeks.

But when we are speaking about Mythology, which is the mythological period or mythological era?

The mythology is always connected to the human. But to which human, to Homo sapiens and/or to Homo neanderthalensis?

We are going to deal mainly with the era of Homo sapiens – not the Homo neanderthalensis (older).

It is undeniable that the borders between myth and reality are vague. Generally speaking, we can say that some of the mythological heroes are historic persons, some others ARE NOT. But, all, or rather *NEARLY ALL* of them represent something.

I believe that it is a *MISTAKE* to consider the Greek Mythology as a beautiful fairytale. The Greek Mythology is actually the most ancient history of the peoples who have lived at the land which was later named Hellas (Greece). This land is the Aegean and the peri-Aegean area. The Greek Mythology constitutes the Pre-history of the first Hellenes.

2.2 What is Geomythology?

Geo-mythology is a branch of the Geosciences, dealing with the physical-geological conditions during mythological era and, through this to find the interrelation between Geology and Mythology. My experience, as a geologist who has spent his life studying the Geology of Greece, has shown that a great part of the Greek Mythology is indirectly influenced by the physical – geological processes of the Aegean and Peri-Aegean areas.

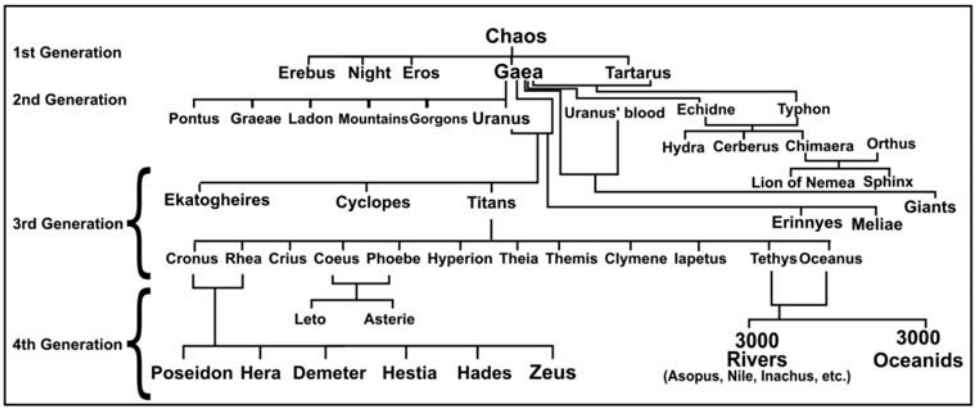

Fig. 1: The genealogy of Gods (4 first generations) according to Hesiod.

The presentation is based on writings of ancient authors *AND ONLY ON THESE* and mainly on the Ilias and Odyssey of Homer, on the "*Theogony*" and "*Works and Days*" of Hesiod, on the *Argonautica* of Orphics, on Plutarch's (*50 – 120 A.D.*) *Moralia* and other well known writers.

The texts of all the above-mentioned authors have been translated, analyzed, commented on, and evaluated mainly by scholars, linguists, poets, historians, archaeologists, art historians, theologists, politicians, both Greeks and foreigners – in other words representatives of humanistic sciences. The result of their efforts? *All or almost all of what is about to be mentioned is fantasy = myth***.**

3. The Genealogy of Gods

3.1 General

According to the genealogy of gods, demigods, heroes, and the other protagonists of the Greek Mythology, mentioned in *Hesiod's Theogeny*, the Titans belong to the third generation and they are the *offsprings of Gaea* (1st generation) and *Uranus I(*Heaven) (2nd generation).

The six Titans and six Titanesses constituted the first *Dodecatheon* (twelve Gods), which was replaced by the 12 well known *Olympian Gods*, the generation of *Zeus* and *Poseidon*. It is widely known that this was not a smooth or peaceful replacement, but the result of a war between the Gods of the Cronuse's generation and the one of Zeus. This battle, referred in the Greek Mythology as *Titanomachy*, resulted in the defeat and the punishment of the Titans, as well as to their exile from Greece, and the Mediterranean Sea, in general.

Three of the most important Titans are *Oceanus*, *Atlas* and *Cronus (Satturn* by the Romans).

Oceanus, according to *Hesiod*, did not take part in the Titanomachy, but he had already left the Mediterranean with his sister and wife, *Tethys*, and had gone to *the place where the sun sets*. This Titan gave his name to the endless sea that surrounds the land of Libya (= Africa) and Europe, e.g. *Ocean = Ωκεανός*.

Atlas, who had lived and had reigned in the central Peloponnesus in Arcadia, and specifically on *Mainalon mt*., was exiled by Zeus at the north-western part of Africa, on *mount Atlas*. He was then punished to carry the *celestial globe* on his shoulders. Atlas gave his name to the neighbouring Ocean, since then known as *Atlantic Ocean*, as well as to the great island "*Atlantis*", mention by

Plato, whose geographical position has been unknown, since it had been destructed by a natural disaster, long before the time of Plato.

Cronus (= Saturn), the third Titan, was also the Titans' leader during the Titanomachy. It is known that Cronus, along with his sister Rhea, who was also his wife, were the parents of the first 6 great Gods of the 4th generation, namely Poseidon, Hades, Demeter, Hera, Hestia and Zeus.

Cronus is widely known for two of his deeds. The first is that he overturned his father, Uranus, and so he became ruler of the world. The second is that, during his reign and because he had been afraid that one of his offspring would overturn him, ordered his wife Rhea to bring to him every newborn child to eat him or her. But Rhea, both in the case of Poseidon and that of Zeus, managed to cheat Cronus, thus saving her two children. When Zeus, Poseidon and the others grew up to be men, doubted the supremacy of Cronus and so, a long war started between the Titans and the Olympians, known as *Titanomachy*. Finally, Zeus and the other Olympians defeated the Titans and exiled them to a far *place of the west*. But where?

3.2 Cronus after the Titanomachy

Cronus on the other hand, initially reached Western Europe, on the coast of the Atlantic Ocean and then it seems that he travelled further, firstly to the north and then to the west.

The final place of exile of the leader of the Titans has been described by Plutarch in such a detail that no doubt remains that the prehistoric Greeks of these ancient times had discovered places, which were unfortunately later forgotten. Worth to note that the hero Herculew visited the place of Cronus exile, but much later.

The original greek text of Plutarch, along with its english translation, are given in Fig. 2.

The texts describing these heroic feats is one of the many texts written by the author in his book, entitled "*Concerning the Face Which Appears in the Orb of the Moon*" and is a part of a great series of texts, know as "*Moralia*"[1].

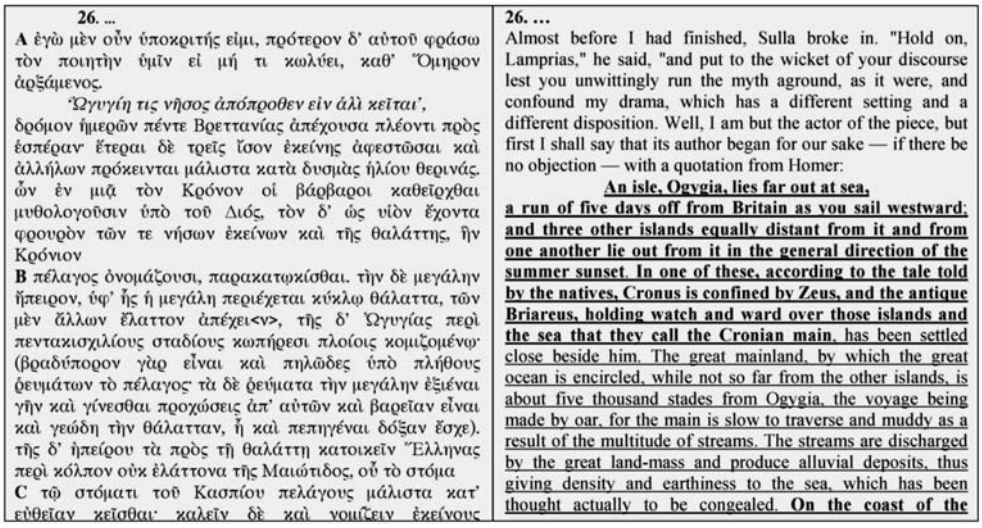

26. …

A ἐγὼ μὲν οὖν ὑποκριτής εἰμι, πρότερον δ' αὐτοῦ φράσω τὸν ποιητὴν ὑμῖν εἰ μή τι κωλύει, καθ' Ὅμηρον ἀρξάμενος.

Ὠγυγίη τις νῆσος ἀπόπροθεν εἰν ἁλὶ κεῖται',

δρόμον ἡμερῶν πέντε Βρεττανίας ἀπέχουσα πλέοντι πρὸς ἑσπέραν· ἕτεραι δὲ τρεῖς ἴσον ἐκείνης ἀφεστῶσαι καὶ ἀλλήλων πρόκεινται μάλιστα κατὰ δυσμὰς ἡλίου θερινάς. ὧν ἐν μιᾷ τὸν Κρόνον οἱ βάρβαροι καθεῖρχθαι μυθολογοῦσιν ὑπὸ τοῦ Διός, τὸν δ' ὡς υἱὸν ἔχοντα φρουρὸν τῶν τε νήσων ἐκείνων καὶ τῆς θαλάττης, ἣν Κρόνιον

B πέλαγος ὀνομάζουσι, παρακατῳκίσθαι. τὴν δὲ μεγάλην ἤπειρον, ὑφ' ἧς ἡ μεγάλη περιέχεται κύκλῳ θάλαττα, τῶν μὲν ἄλλων ἔλαττον ἀπέχει<ν>, τῆς δ' Ὠγυγίας περὶ πεντακισχιλίους σταδίους κωπήρεσι πλοίοις κομιζομένῳ· (βραδύπορον γὰρ εἶναι καὶ πηλῶδες ὑπὸ πλήθους ῥευμάτων τὸ πέλαγος· τὰ δὲ ῥεύματα τὴν μεγάλην ἐξιέναι γῆν καὶ γίνεσθαι προχώσεις ἀπ' αὐτῶν καὶ βαρεῖαν εἶναι καὶ γεώδη τὴν θάλατταν, ἢ καὶ πεπηγέναι δόξαν ἔσχε). τῆς δ' ἠπείρου τὰ πρὸς τῇ θαλάττῃ κατοικεῖν Ἕλληνας περὶ κόλπον οὐκ ἐλάττονα τῆς Μαιώτιδος, οὗ τὸ στόμα

C τῷ στόματι τοῦ Κασπίου πελάγους μάλιστα κατ' εὐθεῖαν κεῖσθαι· καλεῖν δὲ καὶ νομίζειν ἐκείνους

26. …

Almost before I had finished, Sulla broke in. "Hold on, Lamprias," he said, "and put to the wicket of your discourse lest you unwittingly run the myth aground, as it were, and confound my drama, which has a different setting and a different disposition. Well, I am but the actor of the piece, but first I shall say that its author began for our sake — if there be no objection — with a quotation from Homer:

An isle, Ogygia, lies far out at sea,
a run of five days off from Britain as you sail westward;
and three other islands equally distant from it and from one another lie out from it in the general direction of the summer sunset. In one of these, according to the tale told by the natives, Cronus is confined by Zeus, and the antique Briareus, holding watch and ward over those islands and the sea that they call the Cronian main, has been settled close beside him. The great mainland, by which the great ocean is encircled, while not so far from the other islands, is about five thousand stades from Ogygia, the voyage being made by oar, for the main is slow to traverse and muddy as a result of the multitude of streams. The streams are discharged by the great land-mass and produce alluvial deposits, thus giving density and earthiness to the sea, which has been thought actually to be congealed. **On the coast of the**

Fig. 2: Please see next page for continuation and explanation.

[1] (both the original text and the transliteration can be easily found on line (*see References*).

ἠπειρώτας μὲν αὐτοὺς <νησιώτας δὲ τοὺς> ταύτην τὴν γῆν κατοικοῦντας, ὡς καὶ κύκλῳ περίῤῥυτον οὖσαν ὑπὸ τῆς θαλάσσης· οἴεσθαι δὲ τοῖς Κρόνου λαοῖς ἀναμιχθέντας ὕστερον τοὺς μεθ' Ἡρακλέους παραγενομένους καὶ ὑπολειφθέντας ἤδη σβεννύμενον τὸ Ἑλληνικὸν ἐκεῖ καὶ κρατούμενον γλώττῃ τε βαρβαρικῇ καὶ νόμοις καὶ διαίταις οἷον ἀναζωπυρῆσαι πάλιν ἰσχυρὸν καὶ πολὺ γενόμενον· διὸ τιμὰς ἔχειν πρώτας τὸν Ἡρακλέα, δευτέρας δὲ τὸν Κρόνον.

Ὅταν οὖν ὁ τοῦ Κρόνου ἀστήρ, ὃν Φαίνοντα μὲν ἡμεῖς, ἐκείνους δὲ Νυκτοῦρον ἔφη καλεῖν, εἰς Ταῦρον παραγένηται δι' ἐτῶν τριάκοντα, παρασκευασαμένους ἐν

D χρόνῳ πολλῷ τὰ περὶ τὴν θυσίαν καὶ τὸν ἀ... ἐκπέμπειν κλήρῳ λαχόντας ἐν πλοίοις τοσούτοις θεραπείαν τε πολλὴν καὶ παρασκευὴν ἀναγκαίαν μέλλουσι πλεῖν πέλαγος τοσοῦτον εἰρεσίᾳ καὶ χρόνον ἐπὶ ξένης βιοτεύειν πολὺν ἐμβαλλομένους. ἀναχθέντας οὖν χρῆσθαι τύχαις, ὡς εἰκός, ἄλλους ἄλλαις, τοὺς δὲ διασωθέντας ἐκ τῆς θαλάττης πρῶτον μὲν ἐπὶ τὰς προκειμένας νήσους οἰκουμένας δ' ὑφ' Ἑλλήνων κατίσχειν καὶ τὸν ἥλιον ὁρᾶν κρυπτόμενον ὥρας μιᾶς ἔλαττον ἐφ' ἡμέρας τριάκοντα· καὶ νύκτα τοῦτ' εἶναι, σκότος ἔχουσαν ἐλαφρὸν καὶ λυκαυγὲς ἀπὸ δυσμῶν περιλαμπόμενον. ἐκεῖ δὲ

E διατρίψαντας ἡμέρας ἐνενήκοντα μετὰ τιμῆς καὶ φιλοφροσύνης, ἱεροὺς νομιζομένους καὶ προσαγορευομένους, ὑπὸ πνευμάτων ἤδη περαιοῦσθαι· μηδ' ἄλλους τινὰς ἐνοικεῖν ἢ σφᾶς τ' αὐτοὺς καὶ τοὺς πρὸ αὐτῶν ἀποπεμφθέντας. ἐξεῖναι μὲν γὰρ ἀποπλεῖν οἴκαδε τοὺς τῷ θεῷ τὰ τρὶς δέκ' ἔτη συλλατρεύσαντας, αἱρεῖσθαι δὲ τοὺς πλείστους ἐπιεικῶς αὐτόθι κατοικεῖν, τοὺς μὲν ὑπὸ συνηθείας τοὺς δ' ὅτι πόνου δίχα καὶ πραγμάτων ἅφθονα πάρεστι πάντα, πρὸς θυσίαις καὶ χορηγίαις ἢ περὶ λόγους

F τινὰς ἀεὶ καὶ φιλοσοφίαν διατρίβουσι· θαυμαστὴν γὰρ εἶναι τῆς τε νήσου τὴν φύσιν καὶ τὴν πραότητα τοῦ περιέχοντος ἀέρος...

mainland Greeks dwell about a gulf which is not smaller than the Maeotis and the mouth of the Caspian sea [1]. These people consider and call themselves continentals and the inhabitants of this land islanders because the sea flows around it on all sides; and they believe that with the peoples of Cronus there mingled at a later time those who arrived in the train of Heracles and were left behind by him and that these latter so to speak rekindled again to a strong, high flame the Hellenic spark there which was already being quenched and overcome by the tongue, the laws, and the manners of the barbarians. Therefore Heracles has the highest honours and Cronos the second. Now when at intervals of thirty years the star of Cronus, which we call 'Splendent' but they, our author said, call 'Night-watchman,' enters the sign of the Bull, they, having spent a long time in preparation for the sacrifice and the expedition, choose by lot and send forth a sufficient number of envoys in a correspondingly sufficient number of ships, putting aboard a large retinue and the provisions necessary for men who are going to cross so much sea by oar and live such a long time in a foreign land. Now when they have put to sea the several voyagers meet with various fortunes as one might expect; but those who survive the voyage first put in at the outlying islands, which are inhabited by Greeks, **and see the sun pass out of sight for less than an hour over a period of thirty days, — and this is night, though it has a darkness that is slight and twilight glimmering from the west**. There they spend ninety days regarded with honour and friendliness as holy men and so addressed, and then winds carry them across to their appointed goal. Nor do any others inhabit it but themselves and those who have been dispatched before them, for, while those who have served the god together for the stint of thirty years are allowed to sail off home, most of them usually choose to settle in the spot, some out of habit and others because without toil or trouble they have all things in abundance while they constantly employ their time in sacrifices and celebrations or with various discourse and philosophy, for the nature of the island is marvellous as is the softness of the circumambient air. ..

[1] *At this point the correct translation of the ancient text is that* ***the Gulf lies on the same line as the mouth of the Caspian Sea****.*

Fig. 2 cont.: A passage of the original text of Plutarch and its English translation of the book "Concerning the Face which appears in the Orb of the Moon".

From the above mentioned text, anyone can locate the geographical position of the island of Cronus' exile, the travels of the people of Cronus (Cronians), the position of the Gulf of the Great Continent in relation to that of the Caspian Sea, and more.

From this revealing text, we have chosen to present only a few passages, since in such a limited space, it is impossible to refer in detail to all that this great author describes in his book.

Let's see now some of the most important passages of Plutarch's text:

a. "An isle, Ogygia, lies far out at sea, a run of five days off from Britain as you sail westward"

Accepting that vessels similar to Argo (the ship of the Argonauts), could develop speeds approximately 4 – 5 miles/hour, then the distance traveled within 5 days must have been in the order of 5 x 24 = 120 hours, 120 x 4 m/h = 480 miles ≈ 900 km (Fig. 3).

According to these, and using a simple school atlas, *Ogygia* should correspond to the present-day *Iceland*. But, concerning the location of Ogygia, there are various viewpoints, such as: a part of Ice-

land, Greenland, Azores islands (Henriette Mertz), the Bermudas, the small island of Gozo next to Malta, Gavdos isl. south of Crete and Sicily.

Plutarch further informs us:

b. "…three other islands equally distant from it and from one another lie out from it in the general direction of the summer sunset"

Which could these islands be?

If Ogygia corresponds to the present-day *Iceland*, then the 3 islands located to the west, must be *Greenland*, *New Foundland* and *Buffin Isl*. But their distances from Iceland are not equal.

If the name Ogygia corresponds to the present-day *Greenland*, then the 3 islands should be *New Foundland*, *Buffin Isl*. and *Breton Isl***.** In my opinion, this version is not correct.

c. "…In one of these, according to the tale told by the natives, Cronus (Saturn) is confined by Zeus, and the antique Briareus, holding watch and ward over those islands and the sea that they call the Cronian main, has been settled close beside him…"

If this is so, Cronus should have been confined in one of the three above mentioned islands, i.e. Greenland, Buffin Isl. or New Foundland. Concerning the *Cronian main (Sea)*, a name that has been given by the *Hypeboreans*, it should be the *North Atlantic Ocean* (*North Sea*) and mainly the "cold sea", in other words the Sea that is partly, and from time to time, frozen, that is the *Arctic Ocean*.

d. "…The great mainland, by which the great ocean is encircled, while not so far from the other islands, is about five thousand stades from Ogygia, the voyage being made by oar, for the main is slow to traverse and muddy as a result of the multitude of streams."

They knew that, west of these islands a mainland existed. But which could this great mainland be? It is obvious that the only great continent, west of the three great islands, which encircles the great Ocean, is the present-day North America. It is important to underline that Plutarch is not only speaking about a land, but about a *great continental land* (= μεγάλη ηπειρωτική χώρα).

e. "…The streams are discharged by the great land-mass and produce alluvial deposits, thus giving density and earthiness to the sea, which has been thought actually to be congealed."

Plutarch continues:

f. "…On the coast of the mainland Greeks dwell about a gulf which is not smaller than the Maeotis and (*lies on the same line as)* the mouth of the Caspian Sea. These people consider and call themselves continentals and the inhabitants of this land islanders because the sea flows around it on all sides…"

If we take into account that Maeotis is the present-day Azov Sea, and based on a common school geographical atlas, we draw a "straight" line from the "mouth" (that is the northern coast) of Caspian Sea, then we see that the gulf, on the coast of which the Greeks dwell, is the *St. Laurence Gulf*.

g. "…at a later time those who arrived in the train of Heracles…"

Even Heracles, the great hero of the Mycenaean era, visited this great continent, where Greeks continued to inhabit, even at much later time.

h. "…Now when at intervals of thirty years the star of Cronus, which we call 'Splendent' but they, our author said, call 'Night-watchman,' enters the sign of the Bull, they, having spent a long

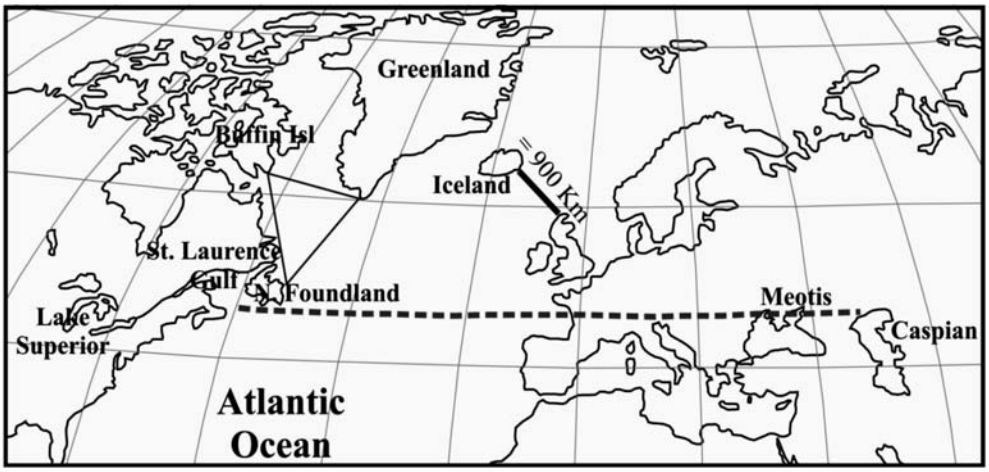

Fig. 3: Map showing the location of the places described in Plutarch's text, the distance between Britain and Ogygia (Iceland), as well as the line (latitude) connecting the entrance of the Caspian Sea and the Gulf of St. Laurence.

> time in preparation for the sacrifice and the expedition, choose by lot and send forth a sufficient number of envoys in a correspondingly sufficient number of ships, putting aboard a large retinue and the provisions necessary for men who are going to cross so much sea by oar and live such a long time in a foreign land. Now when they have put to sea the several voyagers meet with various fortunes as one might expect; but those who survive the voyage first put in at the outlying islands, which are inhabited by Greeks, and see the sun pass out of sight for less than an hour over a period of thirty days, — and this is night, though it has a darkness that is slight and twilight glimmering from the west. …"

After the above-mentioned, two questions rise, namely: (i) "*Where did the prehistoric Greeks know that the sun passes out of sight for less than an hour*?" and (ii) "*Which islands see the sun "passing out" for less than an hour?"*

The answer to the first question is not easy. For sure, Plutarch, who was born in Chaeronia, a small city of the continental Greece, could not have any personal experience. On the other hand, Plutarch later became a priest at the Delphi Oracle. It is throughout possible that he could have been, directly or indirectly, informed by somebody. During these old times, the newly acquired knowledge was restricted mainly among the priests in the temples and in the oracles. The same happened with the priests of Egypt.

But, which are the islands that see the sun "passing out" for less than an hour? It is well known that the Arctic Cycle coincides to the latitude of 66.5° North. Consequently, the areas, and in this case the islands, which "*see the sun passing out for less than an hour" should lie a little to the south of the arctic cycle*.

And another important question: *Why would they go to North America? What were they after*? The answer is that they wanted the *native copper*, which is found in great quantities in the mines around Lake Superior and on Isle Royale (area of present-day U.S.A. - Canadian borders). This view is validated by archaeological excavation and radiodating of findings ranging from 2,450 – 1,050 B.C., i.e. from the beginning of the Proto-Helladic era, until the fall of the Mycenaean Civilization.

4. The knowledge about the Ocean

4.1 General

Let's see now how Homer describes some of the physical and oceanographic characteristics of the Ocean. As it is now accepted, Homer must have lived approximately during the 9th and/or 8th century B.C., while the events he described must have taken place even further in the past, the most recent being the Trojan war and the coming-back of Ulysses.

Homer refers to the Ocean 18 times in the Iliad and 16 times in the Odyssey. Out of all these references, we garner the following:

- "I am going to the world's end to visit oceanus…" (Iliad, XIV) – «…Ο Ωκεανός βρίσκεται στα πέρατα της εύφορης Γης…» (Ξ 201).
- "…the sun's glorious orb now sank into oceanus …" (Iliad, VIII) – «…Εκεί που πέφτει το λαμπρό φως του Ήλιου…» (Θ 485).
- "…as the sun was beginning to beat upon the fields, fresh-risen from the slow still currents of Oceanus…" (Odyssey, XIX) – «…εκ νέου φώτισε τα χωράφια από τον ήσυχο βαθύρροον Ωκεανόν…» (τ 433).

The fact that the sun sets in the Ocean was known, as they have visited again and again the Atlantic Ocean, but how did they know that it also rises from an Ocean? It is well known that to the east of the Aegean area, there are only high mountains. Besides, the Indian Ocean is not located to the east. So, how did they know that the sun rises from the Ocean?

- "(The Earth is surrounded by the) …ever-encircling waters of Oceanus…" (Iliad, XVIII) - Ο Ωκεανός περιβάλλει πανταχόθεν την Γη (Σ 606-607).
- Oceanus is a great river Ωκεανός that stretches to the 4 points of the horizon.
- "…By the flow of the Ocean, towards the west, lies Hades (Odyssey, XIX) and beyond the Elysium plains …" – "…Δίπλα στις ροές του Ωκεανού, προς Δυσμάς, κείται ο Άδης (ω 11) και εντεύθεν κείται το Ηλύσιον Πεδίον…:

Analyzing all the above, we conclude that the Ocean is not a "wide sea", as the Mediterranean or the Red Sea. On the contrary, the Ocean is considered to be a great river, which means that it does not surround the Earth statically, but dynamically, as it flows like a river. Besides, the etymology of the word *Ωκεανός (Oceanus)* in ancient greek, shows this perpetual movement of the river Oceanus. The word Ωκεανός (Oceanus) is the result of the word "*Ωκύς*" which means "*quick*" and "*νάω" which* means *flow*. So, the very word Ωκεανός – Oceanus means *quick flow*.

Another group of texts that refer to the Ocean and its physical and oceanographic characteristics is the Orphic texts. From the Orphics Argonautica and the orphic hymns, we garner the following:

a. "… Hence every river, hence the spreading sea…" - «…από τον Ωκεανό προέρχονται όλοι / οι ποταμοί και όλη η θάλασσα…»

Consequently, the Ocean is compared to the sea. The sea, in this case, is certainly the Mediterranean Sea.

b. "OCEAN I call, whose nature ever flows, From whom at first both Gods and men arose;/ Sire incorruptible, whose waves surround, / And earth's concluding mighty circle bound…" (From the Orphic hymn to the Ocean) - «…αθάνατον πατέρα και αρχή των αθανάτων / θεών και θνητών / ανθρώπων, που κυματίζει γύρω από την / Γη που την περικυκλώνει…»

c. "…Old Ocean too …, / Whose liquid arms begirt the solid land…" (From the Orphic hymn to Pan) - «…Ωκεανός τε πέριξ εν ύδασι γαίαν ελίσσων…» -

The poet Hesiods, in his work "Theogony" refers to the Ocean, as:

d. "…Ocean, the perfect river…" (Hes., 242) - «…Ωκεανοιο, τελήοντος ποτάμοιο…» / «Ωκεανός, ο τέλειος πόταμος» (Ησ. 242) /.

4.2 Characteristics of the Ocean river

Let's see now, how the special characteristics of the flow of the river Ocean, i.e. of the current, are described.

Hesiod refers to the Ocean as *αψόροο* (*back-flowing)*. This characterization has been render as "*swaying*", in modern greek. This means that the ocean water perform a "reversible movement", i.e. a movement along an axis. In my view, this interpretation is not accurate, since the ancient greek word *αψ-ροή* could be rendered as "wild flow", in other words, *turbulent flow*.

Homer refers to the Ocean, using the terms *deep-flowing* (*βαθύροος*) and *deep-vortexed* (*βαθυδίνης*). Deep-flowing means that the river Ocean flows not only on the surface, but also in depth, and this deep flow is not laminar but turbulent, that's why the Ocean is also characterised as *deep-vortexed* (*βαθυδίνης*).

Today, we know that the oceanic currents extend to a depth of about 800 – 1200 m. and that up to that point their flow is turbulent. In recent times, this has been verified with the use of different instruments that allowed the simultaneous measurement of the flow velocity as well as the depth.

But, at the time of Homer, how could anyone know that the river Ocean displays a turbulent flow both on the surface and in depth?

Generally speaking, all the knowledge about the Ocean was forgotten. Even after the discovery of America, nothing is mentioned about the currents, despite the fact that the fishermen of the Ocean must have known them, but for different reasons, they preferred not to speak about them.

5. The forgotten knowledge

All this knowledge was acquired during the time period between the beginning or the middle of the 3rd millennium B.C. and the end of the Mycenaean era, i.e. around the end of the 2nd millennium, about 100 – 150 years after the Trojan War.

This is concluded by the texts left mainly by the Orphics, Homer, Hesiod and Plutarch, who is much younger (50 – 120 AD).

It is well known, the fall of the Mycenaean empire was followed by an era, known as *dark ages*. During this period a lot of the knowledge acquired by the prehistoric Greeks, for unknown reasons, was lost.

Consequently, and despite the fact that the Greeks of the historical times managed to create the well-known Greek Civilisation which peaked during the 5th century B.C., nevertheless they ignored the Ocean. It is strange that, while they created colonies, they developed the commerce and the seafaring, they had conquests, they developed the architecture, the poetry, the theatre etc., they forgot all about the river Ocean, they forgot the Cronian Sea, they forgot about Ogygia and the islands where the sun sets for only an hour per day, for the duration of a month etc.

All these were forgotten, and they were also forgotten by Alexander the Great, by the Romans, but also later by the Christians.

The only exception is Pytheas of Massilia (approx. 380 –310 B.C.), who left Marseille and after

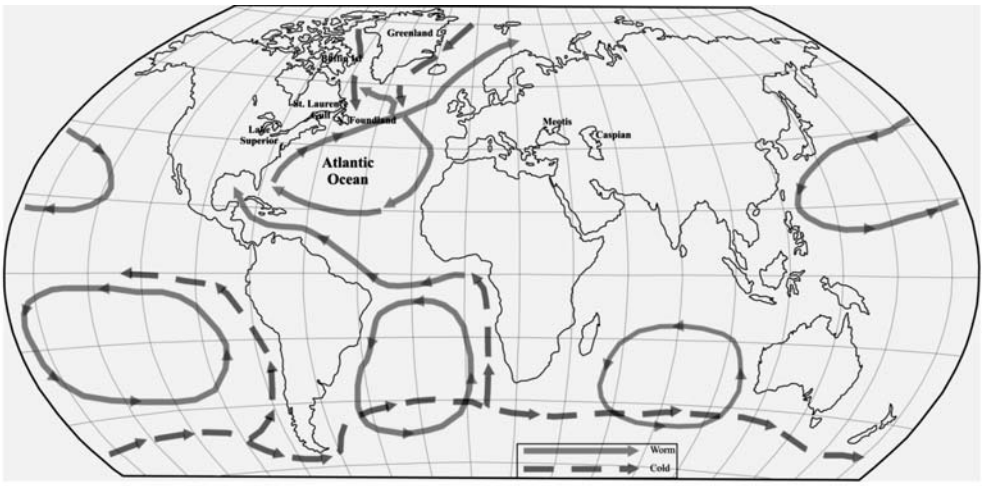

Fig. 4: Generalized map showing the ocean currents circulation (continuous lines: warm currents, dashed lines: cold current).

reaching Britain and Ierne (Ireland), he arrived at *Thule*, which is said to be the present-day Iceland. From there, Pytheas must have arrived in the arctic area and then he must have returned to Massilia.

Consequently, most of the ancient people, including the Phoenicians, must have travelled in the Ocean, but never far from the European coasts. The fact is of course that the book "*About the Ocean*" («*Περί Ωκεανού*»), written by Pytheas around 320 B.C., has been lost and therefore we can't know exactly up to which point he managed to go.

6. The discovery of the Gulf Stream

All the above-mentioned were re-discovered at least 3,000 years later, around the 16th century AD, when *Ponce de Leon* first described the "*Florida Current*" (*1513*).

After this, an effort of studding the Atlantic Ocean currents has started. An intensive study of the Gulf Stream begun during the second half of the 18th century. The occasion was a letter sent by *Benjamin Franklin,* (then Postmaster General of the North American Colonies) to captain *Folger*, asking him to make a chart of Gulf Stream, in order to make the postal delivery from England faster.

By the end of this century, several maps were constructed, among them temperature maps, after detailed and systematic temperature measurements.

The first maps of the area refer to the Gulf Stream as "*Gulf of Florida",* or as *"Florida Straits",* or *"Bahama channel"*. The name "*Gulf Stream*" appeared for the first time in 1842, on a map by *Sydney Morris* and *Samuel Breese*.

The systematic observations begun actually in 1845, while *Mathew Maury*, in his book «*Physical Geography of the Sea*» (*1855*) wrote:

«There is a river in the ocean. In the severest droughts it never fails, and in the mightiest floods it never overflows….Its current is more rapid than the Mississippi or the Amazon…»,

Compare the above passage to that of Homer (8th (?) cent. B.C.):

"*…he set the mighty stream of the river Oceanus…*" *(Iliad,XVIII)* / «*…και έθεσεν επάνω τον μεγαλόσθενο / ποταμό του Ωκεανού…*» (*Ιλιάδα, Σ 607*).

"*…After we were clear of the river Oceanus…*" *(Odyssey, XII)* / «*…αφού κατέλιπε την ροή του ποταμού Ωκεανού…*» *(Οδύσσεια, μ1)*.

From the recent research activity of the scientific community, the results we' re interested in are the ones referring to the meanderisms of the current, as well as the location of gyres and warm core eddies. It's a research effort that begun during the seventies, with the utilization of modern space applications. These applications verify the knowledge – legacy of the Orphics, Homer and Hesiod, Plutarch, Ovid and others. In other words, it is verified that:

- The Ocean is a great river that surrounds the Earth (then considered a disc), as it was depicted on the shields of Hercules and Achilles.
- The Ocean is *back-flowing (αψόροος, οπισθόροος)*.
- The Ocean is *deep-flowing (βαθύρροος)*.
- The Ocean is deep-vortexed (*βαθυδίνης)*.

7. Discussion – conclusions

Summarising all the above mentioned, taken of the writings of two great poets, and mainly (a) Homer's *Iliad* and *Odyssey*, (b) Hesiod's *Theogony* and *Works and Days*, (c) Orphics' *Argonautica* and (d) Plutarch's *Moralia*, we can assert that the prehistoric Greeks, already as far back as the times of Titan Cronus, up until the times of Hercules and Ulysses, should had known plenty of the present-day Atlantic Ocean and its islands, as well as the lands located beyond the Pillars of Hercules.

According to the writings of *Plutarch*, the prehistoric Greeks should have known the following:

(i) Britain and Ierne (Ireland).
(ii) Iceland, which is mentioned as Ogygia, its relative position to Britain and the distance between the two islands.
(iii) The three islands located west of Ogygia (Iceland), which should be the present-day islands of Greenland, Buffin Island and New Foundland.
(iv) That the three above-mentioned islands are equidistant.
(v) He refers to the "Cronian Main (Sea)" that, according to the Orphics, is the name given by the Hyperboreans to the present-day North Atlantic Ocean and a part of the Arctic Ocean.

They also knew:

(vi) That at the west of these three islands there was a great mainland (a great continental country) that encircles the great Sea.
(vii) That the coast of a gulf on this great continent was inhabited by Greeks.
(viii) That the size of the above-mentioned gulf is approximately the same as that of the Maeotian Sea (present-day Azov Sea).
(ix) That this gulf is located "on the same straight line" as the mouth of the Caspian Sea. This means that the northern coast of the Caspian Sea are located on the same latitude as the gulf located on the great mainland (great continent). After this detailed definition, there really must be no doubt that this gulf should be the St. Laurence Gulf of the present-day Canada, and consequently the "great mainland" is North America.
(x) They also knew that sea-currents exiting from the above-mentioned gulf towards the Atlantic carried argillaceous material ("earthiness") that obstructed the sailing of the ships, that's why

the sailors, as they could not use the sails, they sailed by oars.

(xi) That the people that arrived there with Hercules, stayed in an area on one of the three islands, where the sun only set for one hour, for a period of 30 days.

Taking into consideration all the above-mentioned, one can indirectly draw more, concerning the knowledge of the prehistoric Greeks, beyond the confirmation of what is mentioned by Plutarch. These indirect conclusions are the following:

(i) That they knew how to measure great surfaces, i.e. the surface of the Azov Sea (Maeotis) and that of the Gulf of St. Lawrence.

(ii) That the discovery of Iceland, of the three islands and that of the great mainland, must have taken place, according to the most conservative assessment, approx. at the beginning of the 3rd millennium B.C., i.e. at the start of the Proto-Helladic era.

(iii) That they knew the way to determine the latitude of a given area.

(iv) That long before the time of Hercules and the Argonauts, even before the time of Phrixus and Elle, they knew the Caspian Sea, the Hyperboreans, the Rippean mountains, the Sarmatian Sea (Baltic Sea), the different rivers like the Dneiper (which they called Vorysthenis), Don (Tanais) etc., as well as the people who lived in the areas between the Euxenian Pontus and the Baltic Sea (Sarmatian Sea).

Concerning the knowledge about the Ocean, based on Homer's works, Iliad and Odyssey, and those of Hesiod, the conclusions are the following:

(i) Oceanus is a great river that stretches to the four points of the horizon. That means that Oceanus doesn't surround the Earth statically, but dynamically, as it flows like a river.

(ii) The Earth is surrounded by the "*…ever-encircling waters"* of Oceanus (Il., Σ 606-607).

(iii) *"…Old Ocean too …„ / Whose liquid arms begirt the solid land"* (after Orphic Hymn to the god *Pan*).

Based on the above mentioned, it is clear that they knew about the Ocean currents, not only those of the Atlantic Ocean, but of all the Oceans, as "*…the great river stretches to the four points of the horizon…".*

Taking into account all the above mentioned, the following question is posed:

Is it possible for someone (or more) to describe all these places and all these physical and oceanographic characteristics, if they had not visited the area or crossed the Ocean?

Let me remind you that we refer to the time period between the beginning of the 3rd Millennium and the end of the 1st Millennium B.C.

8. References

Hesiod. *Theogony*.

Ησίοδος. *Θεογονία*, *«ΟΙ ΕΛΛΗΝΕΣ»,* Αθήνα, ΚΑΚΤΟΣ, 1992.

Ησίοδος. *Έργα και Ημέραι, «ΟΙ ΕΛΛΗΝΕΣ»,* Αθήνα, ΚΑΚΤΟΣ, 1992.

Homer. *Iliad*.

Homer. *Odyssey*.

Mariolakos, I., 2004. Geomythology. In Birx, J., H. (Ed.)*, Encyclopedia of Anthropology*, vol. 3**,** 1066-1071, New York, SAGE Publ.

Mariolakos, I., Kranioti, A., Marketselis, E., Papageorgiou, M., 2007. Water, mythology and environ-

mental education, *Desalination*, 213/1-3, 141-146.

Maury, M. F., 1855. *The Physical Geography of the Sea*. New York, Harper & Brothers, Publishers. 287pp. Available online at: http://books.google.gr/books?id = Z5jN3YpoOjgC&printsec = frontcover&dq = physical+geography+of+the+sea&cd = 3#v = onepage&q = &f = false

Mertz, H. 1964. *The Wine Dark Sea: Homer's Heroic Epic of the North Atlantic* (*Greek translation by Zairis, NEA THESIS publ., 1995)*.

Mertz, H. 1976. *Atlantis: Dwelling Place of the Gods* (*Greek translation by Zairis, NEA THESIS publ., 1999)*.

Ορφικά. *Αργοναυτικά, Ύμνοι, «ΟΙ ΕΛΛΗΝΕΣ»*, Αθήνα, ΚΑΚΤΟΣ, 1992.

Plato. *Kritias*.

Πλάτων. *Τίμαιος (ή Περί Φύσεως), «ΟΙ ΕΛΛΗΝΕΣ»*, Αθήνα, ΚΑΚΤΟΣ, 1992.

Πλάτων. *Κριτίας (ή Ατλαντικός)*, *«ΟΙ ΕΛΛΗΝΕΣ»*, Αθήνα, ΚΑΚΤΟΣ, 1992.

Πλούταρχος. *Περί του Εμφαινομένου Προσώπου τω Κύκλω της Σελήνης, «ΟΙ ΕΛΛΗΝΕΣ»,* Αθήνα, ΚΑΚΤΟΣ, 1996.

Plutarch. *Moralia, Concerning the Face which appears in the Orb of the Moon*. Available online at: http://www.mikrosapoplous.gr/anc_texts/texts_plut.htm (Greek text), and http://penelope.uchicago.edu/Thayer/E/Roman/Texts/Plutarch/Moralia/The_Face_in_the_Moon*/D.html) (English text).

Δελτίο της Ελληνικής Γεωλογικής Εταιρίας, 2010
Πρακτικά 12ου Διεθνούς Συνεδρίου
Πάτρα, Μάιος 2010

Bulletin of the Geological Society of Greece, 2010
Proceedings of the 12th International Congress
Patras, May, 2010

ATLANTIS IN SPAIN

Papamarinopoulos S.P.

University of Patras, Department of Geology, Patra, Greece

Part I: Plato science and mythology

Abstract

Dealing with Plato's Atlantis one should be aware that its author is the very first person in the world who defined science's and mythology's concepts. However, he introduced several times paramyths in his dialogues and he encrypted in them moral, philosophical, political, mathematical, musicological information and other ideas. Such a person wrote the famous Atlantis story. We shall attempt desipher fully in the successive texts but before we do that we need to familiarize the reader in order to understand the breaking of a 2400 years complexity which will be presented through the Hellenic Geological Society's 12th International Symposium organized by the Patras University Department of Geology.

1. Introduction

Many analysts have entirely rejected Timaeos and Critias as a possible source of any useful historical information. These experts did not really take into account that Plato defined science in his dialogue Phaedros (*Phaedros 277.b.5 - 277.c.3)* and mythology in his dialogue Timaeos (*Criti 110.a.3-110.a.4*.). Besides, he has divided the myths in genuine (*Tim 26.e.4-26.e.5)* and in fabricated ones (*Resp 377.b.5-377.b.6*.). He made great use of the latter in all his dialogues sending messages to his readers for morality, philosophy, politics and sometimes he encrypted, for his own reasons, mathematical theorems or relations within paramythical (fabricated myths) stories. A good example is what Vardulakis and Pugh (2008) found in the Laws in connection with the prime numbers.

2. Plato and Science

Plato initially defined science for first time in the world in Phaedros as follows:

Phaedr 277.b.5-277.c.3

{ΣΩ} Πρὶν ἄν τις τό τε ἀληθὲς ἑκάστων εἰδῇ πέρι ὧν λέγει ἢ γράφει, κατ᾽
αὐτό τε πᾶν ὁρίζεσθαι δυνατὸς γένηται, ὁρισάμενὸς τε πάλιν κατ᾽ εἴδη μέχρι
τοῦ ἀτμήτου τέμνειν ἐπιστηθῇ, περί τε ψυχῆς φύσεως διιδὼν κατὰ ταὐτά,
τὸ προσαρμόττον ἑκάστῃ φύσει εἶδος ἀνευρίσκων, οὕτω τιθῇ καὶ διακοσμῇ τὸν λόγον,
ποικίλῃ μὲν ποικίλους *ψυχῇ* καὶ παναρμονίους διδοὺς λόγους, ἁπλοῦς δὲ ἁπλῇ,

Socrates: "First you must know the truth about the subject that you speak or write about, that is to say, you must be able to isolate it in definition, and having so defined it you must next understand how to divide it into kinds, until you reach the limit of division, secondly, you must have a corresponding discernment of the nature of the soul, discover the type of speech appropriate to each nature, and order and arrange your discourse accordingly, express the nature of the complex and simple *soul* with panarmonic and simple analogies "

Hamilton and Cairns (1980) say that Plato and Descartes, 2000 years apart, expressed almost the same sequential order of mental operations with similar concepts. In Plato's Phaedrus, we find suggestions about the art of speech writing that bear a striking similarity to the four rules of investigation (examination, division, order and enumeration) that are enunciated as the substance of Descartes' Discourse on method.

But Plato does not stop here. Moreover he also defines the concept of mythology in Critias as follows:

Criti 110.a.2-110.a.4

τῶν ἐν τοῖς πρόσθεν καὶ πάλαι ποτὲ γεγονότων ἠμέλουν.
μυθολογία γὰρ ἀναζήτησίς τε τῶν παλαιῶν μετὰ σχολῆς ἅμ᾽ ἐπὶ τὰς πόλεις ἔρχεσθον,

"and their talk was about them; and in consequence they paid no regard to the happenings of bygone ages. For legendary lore and the investigation of antiquity are visitants that come to cities"

He then defines the genuine and fabricated myth's concept respectively. He offers no ambiguity to his reader that he does know what he says and why he describes. He offers the definitions as follows:

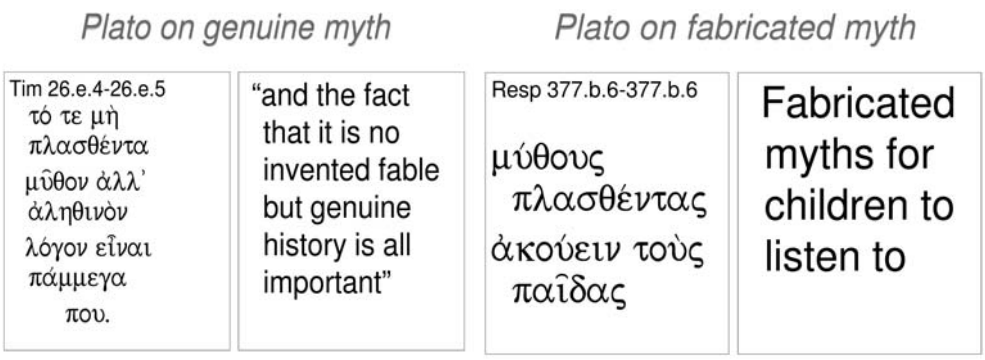

We shall demonstrate to the reader in Part II (Papamarinopoulos, 2010b) that half of Timaeos and Critias in connection with prehistoric Athens was not an imaginary entity but a reality unknown to the historians like Herodotus and Thucydides and yet it was described only by the non-historian Plato. The latter did not have any possibility to know Athens of the 12th century B.C. being a citizen of Athens in the 4th century B.C. of course. Then we shall demonstrate to the reader what, and where and when and how Atlantis was perished in 24 hours in Part III, IV,V and VI.

Figure 1 illustrates how the reader can differentiate geometrically the difference between the genuine and fabricated myth's structure. The genuine myth contains always a kernel of history in its center which can be tested and control-led tran-scientifically. However, it is encapsulated by the successive inventions of the centuries from the initial oral transmitters, from generation to generation, to the time the myth was recorded in a writing system. This spherical sectors does not offer anything reliable to science's scrutiny. The paramyth contains no information in connection with history.

3. Conclusions

Plato's dialogues contain exceptional information in a variety of scientific fields. However, Timaeos and Critias, contains the famous case of Atlantis which is proposed, by the author, to the scientific community as a unique historic reality. Fig. 2 shows the difference of Atlantis' case in comparison to the, historic event, genuine myth and paramyth. To the top (left) the historic event is shown. To the top (right) the genuine myth is shown. To the bottom (left) the paramyth is shown containing no historic information. To the bottom (right) a platonic addition is shown as the most external spherical sector en-

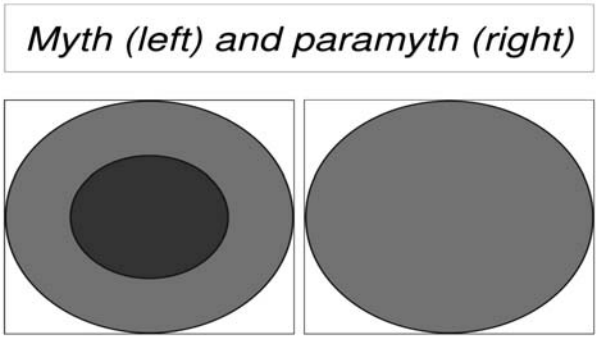

Fig. 1: The genuine myth (left) contains a kernel of historic reality which can be proved scientifically assuming one removes *surgically* the spherical sector which has been added on it through the eons from the oral transmitters of a past physical event from generation to generation. The fabricated myth or paramyth (right) may encrypts interesting information but without containing any historic significance.

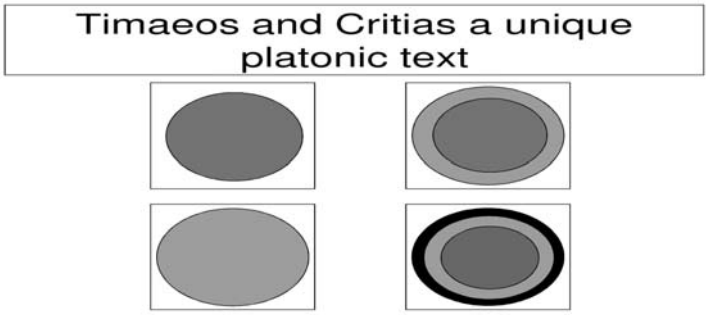

Fig. 2: In top (left) a historic event is shown. Plato knew history but he was not a historian. In bottom (left) a paramyth is shown. Plato made great use of many paramyths which did not contain any historic content. In top (right) a genuine myth is shown containing a historic kernel. In bottom (right) the Atlantis story is shown. It is a genuine myth as in top (right) encapsulated by a platonic black spherical sector containing mathematics.

capsulating an otherwise genuine myth. The platonic addition on Atlantis has been manifested by Brumbaugh (1954) in his famous book on Plato's mathematical imagination.

4. References

Brumbaugh, R.S., 1954. Plato's mathematical imagination."The mathematical passages in the dialogues and their interpretation". Indiana University Press, p.p.302.

Decartes, R., 1967. Le discours de la method. Pataud, J.M. (Ed)., Paris: Bordas.

Hamilton, E., and Cairns, H. (Eds.), 1980. Plato: The Collected Dialogues. Bollingen Series. Princeton: Princeton University Press.

Papamarinopoulos, St.P., 2010b. Atlantis in Spain. Part II: The case of prehistoric Athens Proceedings of the current volume of the 12th International Symposium of the Hellenic Geological Society, May 19-22. Organiser University of Patras.. Department of Geology.

Plato.

Vardulakis,A. and Clive Pugh., 2008. Plato's hidden theorem on the distribution of primes. Springer Science, Volume 30, No 3, p.p. 1-3.

Δελτίο της Ελληνικής Γεωλογικής Εταιρίας, 2010
Πρακτικά 12ου Διεθνούς Συνεδρίου
Πάτρα, Μάιος 2010

Bulletin of the Geological Society of Greece, 2010
Proceedings of the 12th International Congress
Patras, May, 2010

ATLANTIS IN SPAIN

Papamarinopoulos S.P.

University of Patras, Department of Geology, Patra, Greece

Part II: The case of prehistoric Athens

Abstract

Plato, who lived in the 4th century B.C., wrote the dialogue Timaeos and Critias when he was 52 years old. In this he describes a catastrophe in Athens from an earthquake in the presence of excessive rain. He also describes several details, not visible in his century, in the Acropolis of Athens. These details are a spring and architectural details of buildings in which the warriors used to live. In Critias he mentions that the destruction of the spring was caused by an earthquake. The time of the catastrophe of Atlantis was not defined by him but it is implied that it occurred after the assault of the Atlantes in the Mediterranean. Archaeological excavations confirmed the existence of the spring which was about 25 m deep with respect to the present day walking level. Archaeologically dated ceramics, found at its bottom, denote the last function of the spring was in very early 12th century B.C. Plato describes the warriors' settlements which were found outside of the fortification wall in the North East of the Acropolis. The philosopher, who was not a historian, describes a general catastrophe in Greece from which the Greek language survived till his century. Archaeological studies have offered a variety of tablets of Linear B writings which turn out to be the non-alphabetic type of writing of the Greeks up to the 12th century B.C. before the dark ages commence. Modern geoarchaeological and palaeoseismological studies prove that seismic storms occurred in the East Mediterranean between 1225 and 1175 B.C. The result of a fifty-year period of earthquakes was the catastrophe of many late Bronze Age palaces or settlements. For some analysts both Athens and Atlantis presented in Timaeos and Critias are imaginary entities. They maintained that the imaginary conflict between Athens and Atlantis served Plato to produce the first world's "science fiction" and gave the Athenians an anti-imperialistic lesson through his fabricated myth. However, a part of this "science fiction", Athens of Critias, is proved a reality of the 12th century B.C., described only by Plato and not by historians, such as Herodotus, Thucydides and others. Analysts of the past have mixed Plato's fabricated Athens presented in his dialogue Republic with the non-fabricated Athens of his dialogue Critias. This serious error has deflected researchers from their target to interpret Plato's text efficiently.

1. Introduction

Plato at Critias is very specific when he presents the Acropolis of Athens. He describes several architectural elements and a particular spring. He is very clear mentioning an earthquake as the cause of the catastrophe of the spring. Apart of this, isolated event in Athens, he describes a general catastrophe in prehistoric Greece which made its people illiteral. He added the detail of giving Greek names to their off-springs. Undoubtedly he does not know when these events took place. He has the impression that all events are as old as the Egyptian priesthood mentioned to Solon. In other words he connects the assault of the *Atlantes*, the catastrophe of Athens and Greece at a remote time thousands of years before Solon's 6th century B.C. Let us analyze the data and examine all the relevant passages in detail from his dialogues carefully versus the existing past scientific data.

Fig. 1: The North bank of the Acropolis of Athens, (after Broneer, 1939).

2. Plato' s Confirmed Passages I

2.1 Details of prehistoric Athens and its catastrophe

Many analysts of Plato's text in relation to *Atlantis* in the past (Ramage, Fears, Luce and Fredericks, 1978), (Gill, Forsyth-Gordon, 1980) and Vidal-Naquet, 2005) although recognized that Plato in the Republic did indeed present a fabricated myth of prehistoric Athens they did not manage to recognize that in Timaeos and Critias he presented a non-fabricated myth of the prehistoric Athens of the 12th century B.C. The date is obtained from Plato's unique and detailed description of that past Athens. It is highly astonishing because the evidence existed in front of their eyes. They could receive it from Kavadias' (1897), Broneer's (1939, 1948) and Carpenter's (1966) excellent studies. Vidal-Naquet (2005) who was a historian could not understand that Plato played in fact the role of a historian once too, offering unique information, without being able to reach ever the level of the enthusiastic Herodotus or even of the strict and careful Thucydides and the rest of the professional historians. Plato had a genuine interest in prehistory and he expressed it ignoring fully both Herodotus in connection with prehistoric Athens and the world affairs of the 12th century B.C. Vidal-Naquet's model of *imaginary Athens* conflicting with the *imaginary anti-Athens,* in other words *Atlantis*, it does not work at all. Athens of Timaeos and Critias was a proved archaeological reality of the 12th century B.C. completely unknown to the Athenians of the 5th and 4th centuries B.C. Gill's idea (1980) that Timaeos and Critias is a pastiche, in other words a mixture of historic with fictitious information could have a point to build an argument if he had established a rigid set of criteria independent which would allow him to remove fictitious from non-fictitious. But since 1897 we get more additional clarifying proofs for Plato's text. Let us follow these proofs carefully by following Plato's statements step by step. In order to do that, we need to visit Acropolis.

In *Figure 1* the Northern Bank of the Athens Acropolis is shown.

Plato writes as follows in connection with the Acropolis:

Architectural details on Athens's prehistoric Acropolis

Criti 112.b.3-112.b.5
τὰ δ' ἐπάνω τὸ μάχιμον αὐτὸ καθ' αὑτὸμόνον γένος περὶ τὸ τῆς 'Αθηνᾶς 'Ηφαίστου τε ἱερὸν κατῳκήκειν, οἷον μιᾶς οἰκίας κῆπον ἐνὶ περιβόλῳ προσπεριβεβλημένοι

But on the topmost part only the military class by itself had its dwellings round about the temple of Athena and Hephaestus, surrounding themselves with a single ring-fence, which formed, as it were, the enclosure of single dwelling

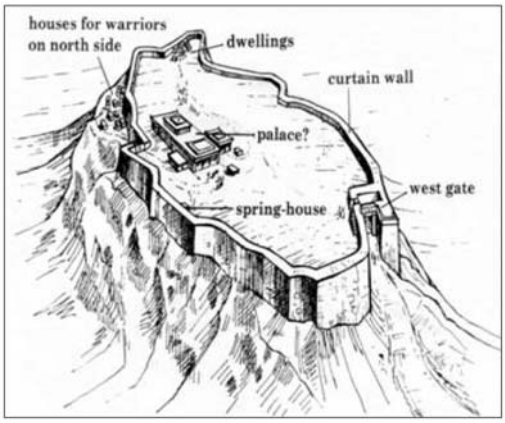

Fig. 2: The outlay of the Acropolis of Athens at the end of the prehistoric period (12th century B.C.). The warriors' houses are in the Northern bank of the Acropolis outside its walls. The spring is also indicated, as Plato describes it (after Castlenden, 1998).

Winter compartments in the north

Criti 112.b.5-112.b.7
τὰ γὰρ πρόσβορρα αὐτῆς ᾤκουν οἰκίας κοινὰς καὶ συσσίτια χειμερινα κατασκευασάμενοι,

on the northward side of it they had established their public dwellings and winter mess-rooms,

Summer compartments in the south

Criti 112.c.6-112.c.7
τὰ δὲ πρὸς νότου, κήπους καὶ γυμνά-σια συσσίτιά τε ἀνέντες οἷα θέρους, κατεχρῶντο ἐπὶ ταῦτα αὐτοῖς.

as for the southward parts, when they vacated their gardens and gymnasia and mess-rooms as was natural in summer

Fig. 3: The spring's entrance (after Travlos, 1971).

In our *project* we would like to send a *visitor* with a *time machine* in prehistoric Athens to climb up and come to the North part of Acropolis. He could see in early 12th century B.C. the buildings of the guardians out side of the wall of the Acropolis as Plato described it in the 4th century B.C. (*Figure 2*).

But if he could continue his tour in a particular sunny day of the summer of 1200 yr B.C. on the Acropolis he would wonder where to find water to drink he would be amazed since on the Acropolis there was a subterranean entrance leading to stairs.

But he had to go down nearly 25 m as *Figure 4* illustrates and there he would find cold water to drink.

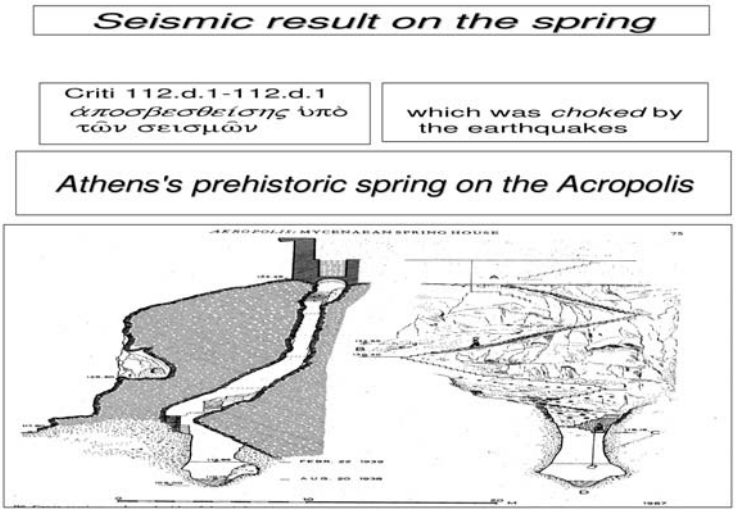

Fig. 4: The vertical section of the spring (after Broneer 1939 and after Travlos, 1971 respectively.

But if the today's visitor had to visit the spring he would realize that it does not function any more. If he had geological knowledge and inspected not only the spring but all the area around Acropolis he would realize that an old earthquake had destroyed it. If by any chance could read Plato's text he would read the following:

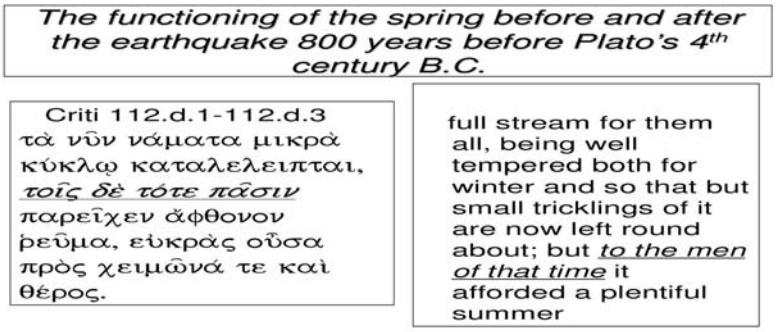

If he was curious enough he would discover in the nearby museum that there is pottery found in the bottom of the old spring. His broken pottery denotes the time of the occurrence of the earthquake which stopped the functioning of the spring. It was the very first part of the 12th century B.C. as Plato once described in Critias 800 years before his period. But continuing reading Plato he would realize that he gives even further details of the functioning of the former spring.

Jordan (2001) uncritically says that Plato saw in the bank of the Acropolis the layer with the Mycenaean blocks and deduced the rest with *the assistance of his fertile imagination!* The question is applicable to Vital-Naquet (2005) as well who in his book said that Plato hated history! We used Jordan's book "The syndrome of Atlantis" which in Vidal-Naquet's opinion is complementary of his own "L'Átlantide" and we say that together with Edwin Ramage, who was editor and one of the authors of the volume of the proceedings of the symposium "Atlantis Fiction or Fact", could not see the following tangible evidence which Kavadias (1897) and Broneer (1939-1948) described. We invite them to read the following passage from Broneer's paper:

"Plato's description of early Athens is highly imaginative, as is the whole background for the dialogue of the Critias with the account of Atlantis and the tale of the war between the two powers. But is the whole story an invention on Plato's part, as modern philologists like to believe, or did he to some extent make use of material handed down by tradition and perhaps recorded by writers whose works are now lost? Whatever view we take of his statement that the account was first recorded by Solon who had received it from Egyptian priests, it must be admitted that if this story is his own invention it was framed as to appear plausible to Critias' interlocutors in the dialogue. We are justified in assuming that the main sketch of his picture of early Athens and of the buildings on the Acropolis is based on tradition and on accounts known to Plato and believed by him to be true. In Plato's days two important but not very copious springs existed on the slopes of the Acropolis, the Klepsydra on the northwest slope, and the spring in the Asklepeion on the south side, and possibly there were others which have since been covered over. It was natural for Plato and his contemporaries to connect these with the tradition of the one large spring in or near the Acropolis which was said to have dried up after an earthquake, and the inference was near at hand that the existing springs came into being as the natural result of this event. Actually there can be no direct connection between the destruction of the one and the origin of the

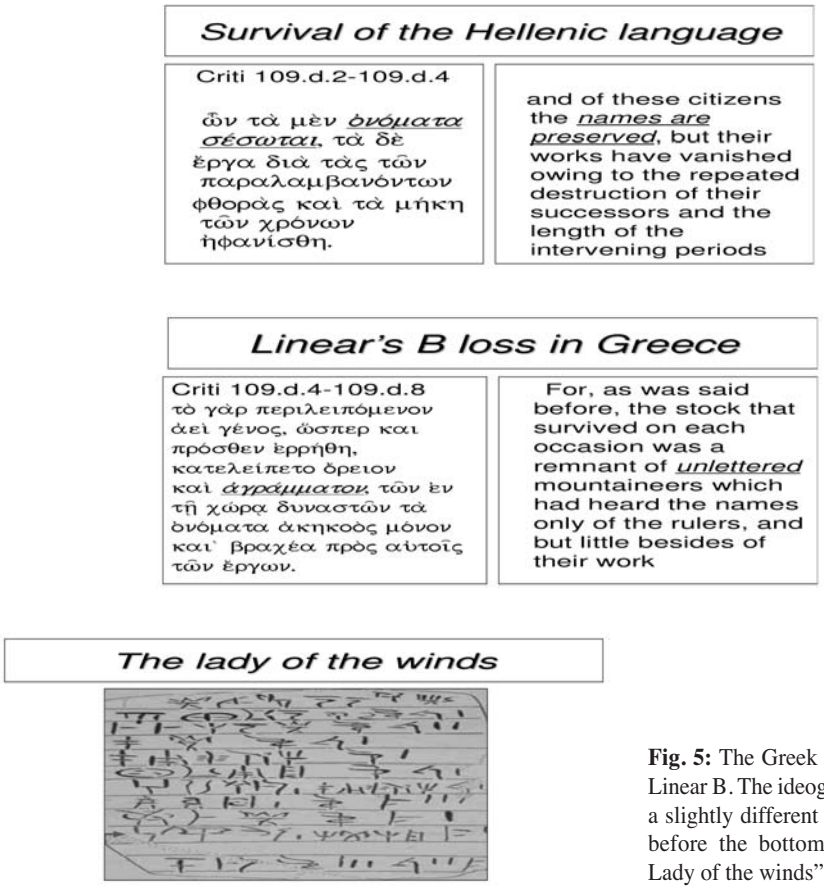

Fig. 5: The Greek writing system of Linear B. The ideographic symbols of a slightly different colour, in the line before the bottom line, mean "the Lady of the winds".

others, for it is likely that the springs on the slopes existed in some form even earlier than the main made fountain on the Acropolis. But tradition centered about the latter, which at one time in the history of the city had been of such importance to the lives of the inhabitants. It can hardly be doubted that this spring, whose existence was all but forgotten to the Athenians of the fifth century B.C. is the very fountain discovered in our excavations. As the earliest artificial water supply of ancient Athens it occupies a unique position among the scanty remains of that remote period."

We wonder what is the syndrome from which Jordan and Vidal-Naquet suffer which did not allow them to see even these unique platonic information about Critias' prehistoric Athens of the 12th century B.C. which are proved historic facts?

3. Plato' s Confirmed Passages II

3.1 The illiteral Greeks and the dark ages

But Plato continues and he describes the end of the Achaean culture in Greece and the consequences of the dark ages. He offers new and unique additional information which both Herodotus and the rest of the historians missed entirely. He says literally that the names of the prehistoric Greeks were saved in spite of the loss of their works!

Plato mentions that the prehistoric Greeks became illiteral.

He also writes that the later Greeks, loving their linguistic heritage, gave Greek names to their children. In *Figure 5*, a Linear B writing example of the Greek language is shown. The symbols at the base of the gray frame, mean the lady *of the winds* in alphabetic Greek.

Plato describes characteristically the Greeks' love in their linguistic heritage with the following way:

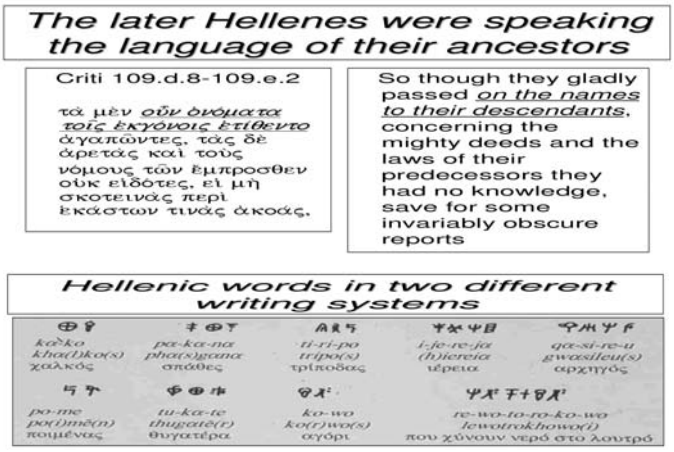

Fig. 6: Common words in Linear B, as found in Greece in the Achaean period (up to the 12th century B.C.) and alphabetic Greek writing symbols (from the 9th century B.C. on wards).

Figure 6 illustrates an example of Greek words in both Linear B and alphabetic Greek writing systems presented in Latin characters.

It is obvious that Carpenter (1966) correctly noted that *Plato was the only one* who described the survival of the Greek language after the catastrophe of the 12th century B.C. Greek language was written in Linear B form, for centuries, before the 12th century B.C. during the Achaean period. It was forgotten during the dark ages every where, except Cyprus, and it was rewritten in alphabetic Greek in the 9th century B.C.

The 9th century B.C. is the century confirmed by Herodotus and by numerous archaeological excavations in Italy, Greece and Asia Minor. We invite the authors of the symposium held at Indiana University in 1978 about *Atlantis* and Jordan and Vidal-Naquet to read Carpenter's publication again who wrote the following statement:

"I am aware that, as F.M. Cornford remarked in his edition of Plato's cosmology, serious scholars now agree that Atlantis probably owed its existence entirely to Plato's imagination".

Carpenter continues further saying the following:

"A remarkable detail that should convince the most skeptical of the genuineness of Solon's conversation with the Saitic priests is the latter's unambiguous statement that the older Greek race had been reduced to an unlettered and uncivilized remnant which, like children, had to learn its letters anew. This claim we know to be entirely exact; but we have no reason to believe that Plato himself was aware of it."

But what was the cause of the catastrophe which made the Achaean culture to vanish? We have presented in these proceedings another cause, one from several in fact, of this destruction Papamarinopoulos (2007a). It is time to present another cause which links us with Plato's text once more. Nur and Cline (2000) have discussed the case of the seismic storms which hit for fifty years Eastern Mediterranean. They present in

Figure 7 a map which exhibits the size of the effect of the seismic storm. They numbered 47 sites starting from Dymaeon Teichos (No1) in Greece and finished with Ashkelon (No47) in Middle East. They claimed that between 1225 and 1175 B.C. the earthquakes destroyed all these late Bronze Age settlements. However, for some reason not understood they missed Athens! In this *Figure* we set Athens with No0 thus making 48 the sites *experienced the seismic storm* and added No35 at the marked point. By doing that we say to the reader that Plato once more writes the truth and in particular he presents part of the turbulent reality of the 12th century B.C. from the standpoint of the Achaean prehistoric Athens. His work was not a small story as Vidal-Naquet (2005) erroneously suggested. The reader may see that in *No13 Troy* is within the list. In other words Homer is justified too saying the following:

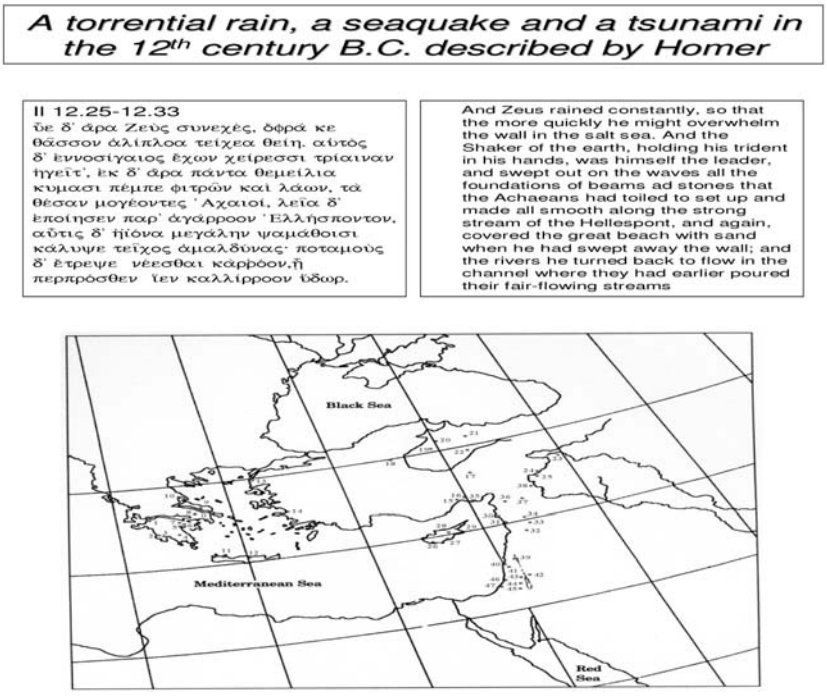

Fig. 7: Both ancient authors, Plato and Homer, retained a different, but complementary, tradition of the 12th century B.C. The author of the present paper has completed Nur's and Cline's (2000) map of the seismic hazards in the East Mediterranean in the 12th century B.C. Modern science offers a full picture of the results of the seismic storms in the East Mediterranean by marking *Athens as 0*. Ancient prehistoric tradition in Greece, originating from the 12th century B.C. has been separately retained for Athens and Troy shown in 0 and 13 respectively.

Homer describes a double event which was expressed initially as exceptional rain followed by a seaquake in the Hellespont producing a tsunami which entered in the Troad and destroyed the Achaean camp. Since we do not know where the Achaean camp was, we observe that 12th century B.C. seismic activity at Troy itself which was most likely close to the Achaean camp. The archaeologically proved seismic event at Troy, mentioned by Nur and Cline (2000), was described by the excavators too in their final report:

"*We feel confident in attributing the disaster to a severe earthquake", "a violent earthquake shock will account more convincingly than any probable human agency for the toppling of the city wall"* Nur and Cline (2000) say that the event has occurred in the period between 1225 and 1175 B.C.

But Plato describes something very similar in connection with Athens as follows:

A torrential rain an earthquake and a land slide described by Plato in connection with Athens in the 12th century B.C.

Criti 112.a.1-112.a.3

νῦν μὲν γὰρ μία γενομένη νὺξ ὑγρὰ διαφερόντως γῆς αὐτὴν ψιλὴν περι-τήξασα πεποίηκε, σεισμῶν ἅμα

For as it is now, the action of a single night of extraordinary rain has crumbled it away and made it bare of soil, when earthquakes occurred simultaneously

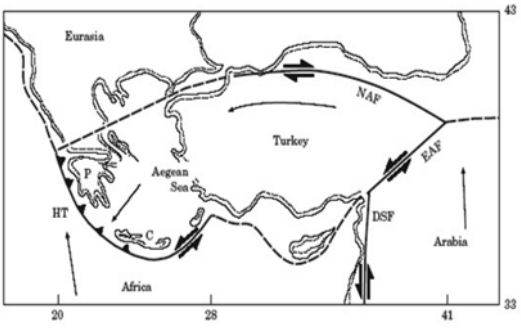

Fig. 8: The major faults of the East Mediterranean which are responsible for the seismic activity (after Nur and Cline, 2000).

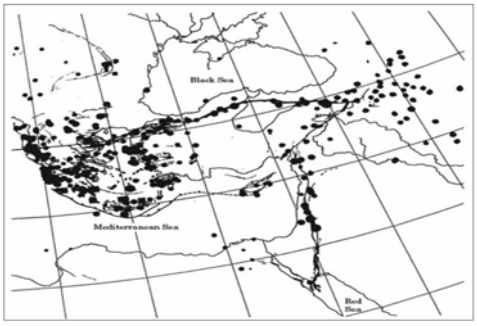

Fig. 9: The seismic epicenters of the East Mediterranean. over the last century. They are produced by earthquakes with a magnitude above 6.5 Richter. They are instrumentally recorded over the twentieth century (after Nur and Cline, 2000).

We know that the seismic event of the Acropolis was recorded because it stopped the subterranean spring in early 12th century B.C. Plato himself does not know the date of the event thus he tries to connect it, convinced by the Egyptian priesthood, with the oldness of Athens, *Atlantis* and Egypt in the range of thousands of years, by putting the Athenian event earlier than occurrence of Deucalion's well known flood. By placing prehistoric Athens in the map, produced by Amos and Nur, we also say that Troy and Athens were destroyed "simultaneously" so to speak in other words due to the seismic storms within the fifty years (1225-1175 B.C.) period. *Figure 8* illustrates the position of the major faults in East Mediterranean.

Figure 9 shows the epicentres of earthquakes with magnitudes 6.5 Richter in East Mediterranean the last 100 years recorded instrumentally.

4. Conclusions

Homer and Plato present seismic catastrophes in Troy and Athens respectively which have been confirmed to have occurred within 12th century B.C.

5. References

Broneer, O., 1939. A Mycenaean fountain on the Athenian acropolis, Hesperia 8, p.p. 317-429.

Broneer, O., 1948. What happened at Athens, American Journal of Archaeology 52, p.p. 111-124.

Carpenter, R., 1966. Discontinuity in Greek civilization. Cambridge University press, p.p. 80.

Castlenden, R., 1998. Atlantis destroyed. Routledge, p.p. 225.

Cornford, F. MacDonald, 1937. Plato's cosmology. (London: Kegan Paul, Trench, Trubner and Co).

Kavadias, P., 1897. Ephemeris, p.28

Homer 8th century B.C. The Iliad. Georgiadis, p.p. 800.

Jordan, P., 2001. The Atlantis syndrome. Sutton publishing, p.p. 308.

Nur, A. and Cline, 2000. Poseidon's horses: Plate tectonics and earthquake storms in the Late Bronze Age Aegean and Eastern Mediterranean, 27, p.p.47-63.

Papamarinopoulos, St. P., 2007a. Phaethon or Phaethousa. A shining comet in the 12th century B.C.? Proceedings of the Melos symposium of 11th-14th of July 2005. The Atlantis Hypothesis: Searching for a Lost land.

Plato 4th century B.C. Critias. Kaktos, p.p. 330.

Ramage, E. S., 1978. Atlantis-Fact or Fiction? Indiana University press.

Travlos, J., 1971. Pictorial Dictionary of Ancient Athens, London, p.72.

Vidal-Naquet, P., 2005. L'Atlantide. Les Belles Lettres, p.p.198.

Zangger, E., 1992. The flood from heaven. Deciphering the Atlantis legend. Sidgwick and Jackson Limited, p.p. 256.

Δελτίο της Ελληνικής Γεωλογικής Εταιρίας, 2010
Πρακτικά 12ου Διεθνούς Συνεδρίου
Πάτρα, Μάιος 2010

Bulletin of the Geological Society of Greece, 2010
Proceedings of the 12th International Congress
Patras, May, 2010

ATLANTIS IN SPAIN

Papamarinopoulos S.P.

University of Patras, Department of Geology, Patra, Greece

Part III: Removing the misunderstandings

Abstract

Plato three times in his text mentioned that the Atlantean events occurred 9000 years before Solon's 6th century B.C. but once he also mentioned 8000 years for the same events. Taking into account the number of the Athenian Kings and the mean span of their successive generations which is more or less 30 years who governed Athens before the 12th century B.C., it is concluded that all of them together span a 350 year period which of course has nothing to do with the 10th millennium claimed by Plato. These Kings together with Theseus the first King of Athens correspond in the 2ed millennium B.C. The archaeological findings in the Acropolis mentioned by Plato, the collapse of the Achaean World, the loss of the writing system in Greece, the assault of the Atlantes have been proved to be of the 12th century B.C. The ancient sources and the archaeological findings in Egypt show a lunar calendrical system practised by the priests who transmitted the story of Atlantis to Solon in the 6th century B.C. Dividing therefore these thousands of years by 12.37 which is the number of the full moon in a year the platonic dates are landing in the end of the 13th to the beginning of the 12th century B.C. Considering the visibility from Atlantis of the celestial bears which are implied as general North indicators Plato himself invalidated the 10th millennium B.C., as the period of the Atlantean events, since no celestial bears can play such a role as celestial North's constellation because the Earth's axis of rotation does not pass through them. This conclusion forces a different interpretation in Plato's thousands of years for the Atlantean events. The only logical explanation is that the thousands of years is moon months understood as years. Plato used the word island for Atlantis which is associated with events belonging in the late Bronze Age in which the word island had the meaning of either promontory or peninsula. The resolution of this major issue removed entirely the 2400 year misunderstanding between the word island and peninsula since Herodotus in the 5th century B.C. added the word peninsula for first time offering to the island today's exclusive meaning. In other words Atlantis was as much an island as Peloponnesus was which an island was never. He also used with the common word Atlantis three different geological entities: a giant island, a horseshow basin and a system of concentric rings associated with geothermal springs and with black, white and red rocks.

1. Intoduction

The story was transmitted to Solon in the 6th century B.C. from the Egyptian priesthood in Sais. The latter is shown in the following Figure 1. At Sais Solon was told that the Atlantean events were realized thousands of years before his period. It is important to analyze this incredible time statement versus our modern scientific knowledge.

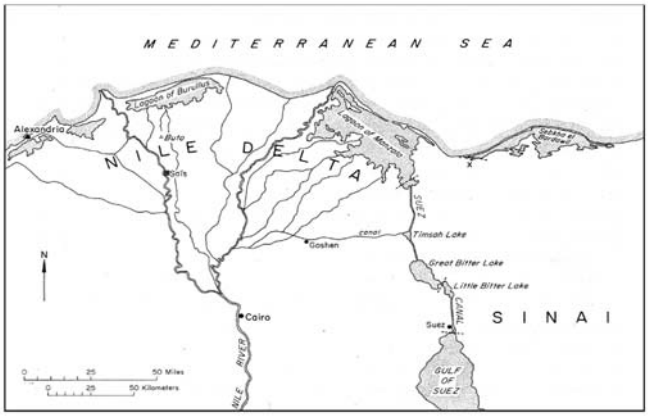

Fig. 1: Sais' location in the Nile's delta is shown.

2. Normalization of the time of the Atlantean and Athenian events

Plato is describing the war of the Atlantes against all nations and then mentions the thousands of years as the years of the Atlantean's events realization. He does it in Criti 109.c.3-109.c.6 as follows:

"Now first of all we must recall the fact that 9000 is the sum of years since the war occurred, as it is recorded, between the dwellers beyond the pillars of Heracles and all that dwelt within them".

In fact he says 9000 years three times in his text and 8000 year one time. He, therefore, gives the impression to the reader of his dialogues of an enormous time span of the Atlantean events. We need to analyze this information properly in order to see if it is correct. Firstly we need to examine the Athenian Kings list which Plato presents since these people, before Theseus' time, were supposed to Atlantis' opponents (Mitropetrou, 2010).

The names were the following *Cecrops, Erechtheus, Erichthonius, Erysichthon,* and others before *Theseus*, (Plato, *Critias,* 10 a 7-8). But these names do not refer to the tenth millennium, but to the second millennium B.C. Combining the traveler Pausanias (*Graeciae Descriptio,* 1, 2, 6) and Apollodorus (*Bibliotheca,* 3, 190), we learn all the kings of Attica before Theseus:

Actaeus, first king of Attica, Cecrops, Erysichthon, Cranaus, Erichthonius, son of Hephaestus and Earth, Pandion, Erechtheus, Cecrops II, Pandion II, Aegeus, Theseus

Therefore, the ten kings of Attica before Theseus cover a time period of 350 years roughly. However, no matter what era, of course before the Trojan War, might Theseus, the patron hero of Athens, be placed in, Actaeus does not exceed chronologically the year 1600 B.C. The most possible chronological period of his reign is the 16th century B.C. (Mitropetrou, 2010). Consequently Plato himself defines the Bronze Age period as the time of the Athenian Kings who faced the Atlanteans. Does he contradict himself with 9000 years he says in his text? The Egyptian priesthood by tradition, and in contract with the civilian pharaonic nomenclature, did not use solar years, but lunar years making practice of two different lunar calendars as Egyptology teaches and as Manetho, the Greek spoken Egyptian mentioned. The latter wrote the following text: *σεληναίους ἐνιαυτούς ἐξ ἡμερῶν τριάκοντα συνεστῶτας* (*fragments* 1 and 2), [that's to say lunar years, each of them consists of 30 days]. Consequently the 9,000 lunar years are equal to 9,000 months *as Diodorus suggested, (The Library of History,* 1, 26, 2, 1 – 4, 3). Based mainly on Manetho and Diodorus and as Egyptology teaches as well –in ancient Egypt, the priests used two different lunar calendars but the pharaonic officials used solar cal-

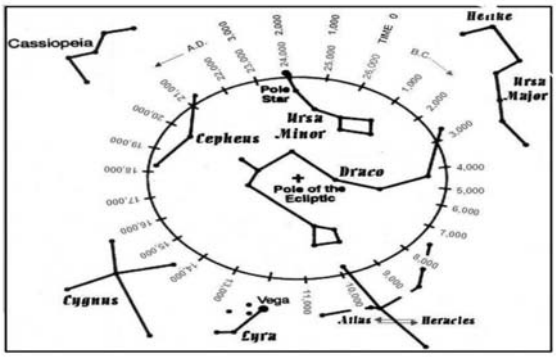

Fig. 2: A unique tran-stellar compass and clock taken from the Hellenic mythology defines constellations which play the role of exact and general celestial North versus time in a 26,000 years time span. It works when the Earth's axis of rotation, in its mode of extension through space, intersects a particular star of one of the constellation shown above. Due to the combined attraction of the moon and the sun on the planet the Earth's axis of rotation scans the celestial sphere in a 26,000 time span. Consequently the 9000 and/or 8000 *assumed solar years* of the Egyptian priests, mentioned to Solon, as the period of the Atlantean' events realization could not be correct because the *celestial bears* could not possibly be visible from an observer on Atlantis within the 10th millennium B.C. This unexpected result was taken from Plato's text. It forces us to accept that 9000 solar years were actually months considered as moon years by the Egyptian priests. Dividing these two numbers with the 12.37, which is the number of the full moons in a year, we land within the end of the 13th and the beginning of the 12th century B.C. In that period *the celestial bears* could be used as general *celestial North indicators*.

endars. Therefore, the possible times of the war against the Atlanteans (Sea Peoples) are within the first quarter of 13th (exactly, 1288 B.C., that is 727.56 plus 561, the year of the Solon's visit in Egypt) and the last quarter of 13th century B.C. (exactly, 1207B.C., that is 646.72 plus 561, the year of the Solon's visit in Egypt), if the time spans are divided by the number 12.37, which is the number of full moons in a year. These time spans (727.56 and 646.72 solar years respectively) are modifications of the Platonic 9,000 and 8,000 years mentioned in *Timaeus* and *Critias,* (Mitropetrou, 2010). If we examine the rest of the information described by Plato analytically we recognise again that the time of all the events he describes in prehistoric Athens and in Greece in general are all proved to be archaeologically within the early 12th century B.C., (Papamarinopoulos, 2010).

But Plato even gives additional information about Atlantis' orientation which by itself offers highly interesting time constraints to the text's analyst. Plato is saying the following:

Criti 118b.1-118b.2

"and this region, all along the *island,* faced towards the *south* and was sheltered from the *northern blasts*"

This description offers Atlantis'orientation and further implies the time in which this observation was done because it involves the *celestial bears*. The latter offers a general indication of the celestial North. We already know that Plato's information in Timaeos and Critias originates in late 12th century B.C. and thus has some Achaean component too in addition to the initial Egyptian one. The celestial *bears* reminds us Homer indicating North who indeed describes North with the *bears*.

If the Platonic information was much older in the range of thousands of years, as he mentions in his text, then the celestial *bears* would not be used. Other constellations offering general or exact North had to be used. For instance the Dragon constellation offers a star as an exact North. It was known to many cultures round about 2.700 yr B.C. The initial transmitter in Plato's text does not use it. The reader can see in Figure 2 periods in the past in which exact North was available. In a circle of

Fig. 3: The Egyptian words meaning coast available in the Egyptian writing system up to the 6th century B.C. are the closer to the case of the island.

roughly 26.000 years various constellations offered a star through which the axis of the earth's extension once passed. Consequently, the *bears* point Atlantis' Bronze Age observation much earlier than Dragon's time and certainly much earlier than Heracles' time, which is in 10.000 yr B.C., presented a star to play the role of an exact North.

It is a further proof, which will be added in those which will be presented in another part of the text, that the text mentioned time spans in *moon years* and therefore the time of the events is not 9.600 yr B.C. in *solar years*. Otherwise North would be a star in *Heracles* constellation and not the constellation of the *bears*. But there is a further implication and this is that the celestial *bears* can not be seen 25 degrees south of the equator. In other words the southern hemisphere, below 25 degrees, can not be the place where the land of Atlantis was located.

3. Island' s evolving meaning versus time

Solon wrote in his notes the case of a giant island which was missed in a single night of misfortune. The case was written down by Plato, since he was Solon's ancestor. The lost island, presented as a paradise, became a source of a large amount of published books with many speculative theories.

Before we examine parts of Plato's text and analyze it we shall attempt to understand the meaning of the word's island from the stand point of the Egyptian and then of the Greek language.

All Egyptologists agree that none of the available words in Egyptian scripts up to the 6th century B.C., shown in Fig.3, in which Solon visited Egypt had the meaning which the word had in Plato's time in the 4th century B.C. In the following Fig.2 the words which the Egyptians used to describe a coast are shown since no other word existed in describing something closer to the 6th century's B.C. Greek meaning of an island.

In the case of the Greek language it is known that the word island got the meaning we have today only in the 5th century B.C. when Herodotus added for first time the word peninsula. Because Atlantis was an old story in accordance with the platonic text then the word island in Greek, before the 5th century B.C., had the possible meanings of promontory or peninsula. Peloponnese is a good example for demonstrating the above mentioned argument because it was never an island but yet it was called as such always from prehistoric to historic times.

Plato describing Atlantis' size says: Tim24.e.6-24.e.7: "the *island* which was larger than Libya and Asia together"

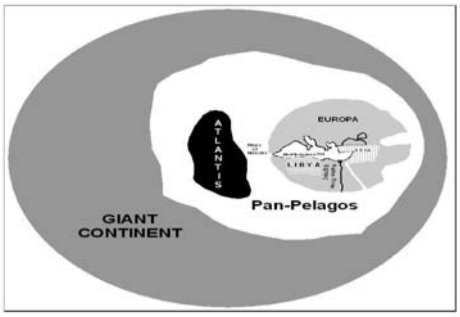

Fig. 4: Plato's world map is shown *with the giant island of Atlantis* in the middle of the Atlantic Ocean in the experts' eyes who concluded what Plato meant.

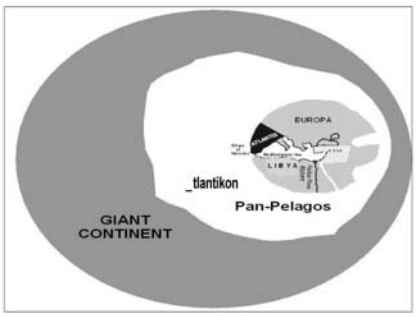

Fig. 5: The map presents Atlantis' *island* with its Bronze Age meaning, in its correct position, in accordance with the platonic text. Atlantis was as much an island as Peloponnesus and Pharos Island in Alexandreia were in prehistoric times. Both they were peninsulae.

We need to define the concepts of Libya and Asia for the Greeks assuming that some parts of the story of Atlantis may come from Greek sources too. In Fig.3 we show the reader Plato's world map. In that Herodotus' map is emplaced. Asia, for the Greeks of 6th and 5th centuries B.C., was only Anatolia and Middle East and not the present day continent of Asia. East of Asia were other countries like Medeia, Persia and India and others. Libya, for the same centuries, was possibly either all today's North Africa minus Egypt or even a smaller part of North Africa. It is unclear from Herodotus' trip who crossed Libya in ten days what Libya's territory was. The term Ri-Bi or Li-Bi was used for first time in Egyptian in the 12th century B.C. In Fig. 4 we demonstrate to the reader how Atlantis' *island* was traditionally conceived both by *experts* and by *romantic* explorers. Libya and Asia are now shown shaded in their correct positions.

That map shown above was a *bitter result* produced by those who did not take into account the word's *island* evolution in the Greek language versus time from the prehistory to the classical period of Greece. They same people did not take into consideration that even in the Egyptian language up to the 6th century B.C. such a meaning did not exist. If Solon's informants were Egyptians they would have had little interest in comparing *areas* of countries. However, they would have been interested in comparing war capacities of the invading Atlantes with those from their traditional enemies the Libyans and Asians who lived in Libya and Asia as Fig.3 shows. In Fig.5 we demonstrate to the reader where Atlantis Island was. Plato describes very clearly Atlantis' position by saying the following statement.

Tim 24.e.5-24.e.6

"island in front of the mouth which you call Heracles' Pillars"

Justifiably Plato calls the sea in front of Atlantis Atlanticon pan-pelagos whereas Herodotus calls it Atlantis Sea. Homer, Herodotus and Plato correctly avoided calling that sea Atlantic Ocean because Ocean was a river and a current. Much later received today's meaning. The word island has been preserved in Linear B because the root of the word *islander's* in genitive has been survived in that ideographic Greek writing system as well. This means that Atlantis was as much as an island as Pharos Island was. Pharos Island was mentioned in Homeric times and in Hellenistic times as well. Chalari et al (2010) with geophysical methods has demonstrated clearly that in the 12th century B.C. Pharos was a peninsula. However, it was called Pharos Island too when the peninsula had been lost even in Alexander's time in the 3ed century B.C. But the reader may say how we know that this pair of Her-

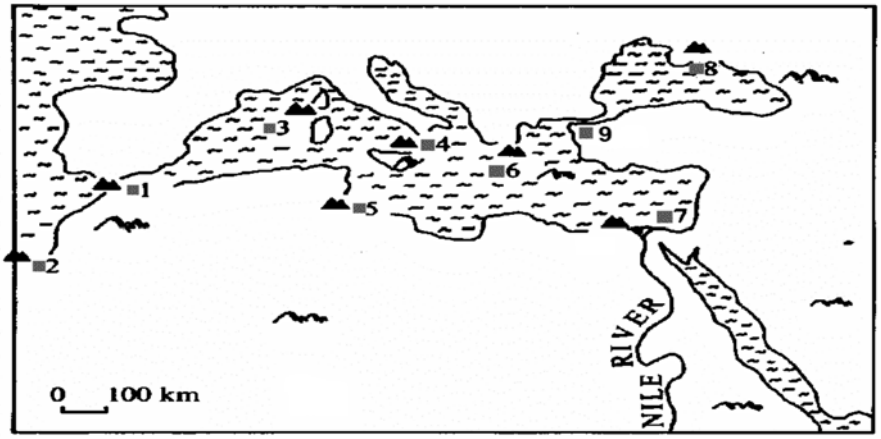

Fig. 6: The distribution of all pairs of Heracles' Pillars (after Zhirov, 1964)

acles' Pillars is definitely the Gibraltar Straits? Did Solon know that these exact pairs were at Gibraltar? The answer is negative. There is not any way of proving historically that he knew but Hesiod who lived earlier, than Solon, in the 7th century B.C. knew. His following passage is very clear proof that the Greeks even before Solon knew where Heracles' Pillars were in connection with Gadeira:

Fragmenta 372.10-372.11 In that Hesiod describes a sea route from Gadeira to Taras city in Italy and the Ionian Islands.

The word (Γαδειρόθεν) means *from Gadeira* demonstrates the case. At first Gadeira is mentioned and then a sea route is mentioned too which connects it with Taras in Italy and the Ionian Sea in Greece respectively. The direction of the sea route is obvious and there is not any confusion whatsoever with other city of Gadeira of the East Mediterranean because Plato called it Gadeiriki meaning, like Chalkidiki, peninsula which does exist only in West Mediterranean. This is an answer to those who attempted to demonstrate that Solon of the 6th century B.C. did not know which pair, from the available nine of Heracles' Pillars, was the one associated with Atlantis' position. According to them, the search for Atlantis had to be sought within the Mediterranean Sea. But on the contrary, the search must be directed within the Atlantic Ocean. Figure 6 shows the distribution of all pairs of Heracles' Pillars. The pair with number 1 is the one Plato meant. Hesiod was the first who gave the answer that the Greeks from the 7th century B.C. knew Cadiz West of Gibraltar. There are, however, also publications corroborating the fact that some contact between Achaean Greeks and Iberians existed even before the 7th century B.C. Martin de La Cruz (1990), studied Mycenaean pottery, dated earlier than the 12th century B.C. found in archaeological excavations in the effluence of Guadalquivir River. This slim, so far, archaeological evidence illustrates that some sort of trade existed between the Achaean Greeks and the Atlantic Ocean Tartessians even before the coming of the Phoenicians.

4. The common name Atlantis

Plato made great use of, the *invented* by him, word Atlantis, for all the three different geological entities shown in Fig.7 producing confusion to careless analysts of his text. This common use of Atlantis' word produced an unwanted confusion because the reader of the platonic text had the impression that Plato meant three different geological entities. The reader also had the impression that a giant island

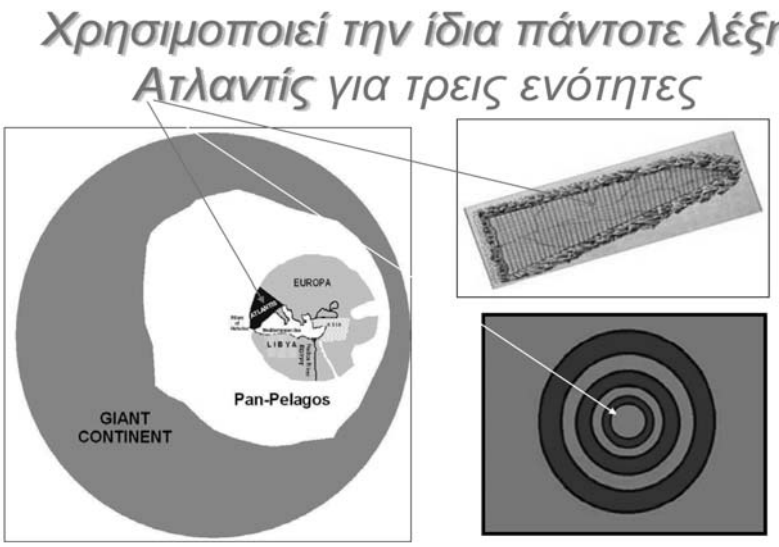

Fig. 7: Plato used the same *word Atlantis*, *invented by him,* for three different geological entities shown above. One of them, the concentric scheme of rings, understood as Atlantis, with the geothermal springs and the black, white and red rocks was lost after earthquakes, floods and a land slide was lost. Matton et al.,(2005) offered a geological analysis of such a concentric system which turned to be a diapeirogenic crater. There are of course other types of diapeirogenic craters than that of Richat's case. (platonic basin as Atlantis was constructed by Zhirov following strictly Plato's text, 1970).

of continental size was lost within one day's and night's duration! Figure 7 serves the purpose of clarifying the complex issue of what exactly the reader expects to understand as the lost Atlantis and not. Atlantis' catastrophe is explained by Papamarinopoulos, (2010 Part VI).

5. Conclusions

The international experts who rejected entirely Atlantis missed the case because they did not consider the evidence presented by Plato himself about the Athenian Kings' and their number and their mean span of their kingship of ancient prehistoric Athens in connection with the time variant (9000 solar years) of his story. They all converged within the 2ed millennium B.C. The evidence of their total span was only 350 years, after Theseus, since the length of each generation is 30 years or so. Their names and their complete sequence originate from the combination of Plato's and other ancient authors' texts. Besides the international experts did not consider the results of the archaeological excavations on the Acropolis of Athens and the mainland of Greece in general and especially of the seismic catastrophes which all converge again within the 12th century B.C. as related to Plato's text!. They also ignored ancient Greek sources and archaeological results in Egypt which all demonstrate in the recognition that the Egyptian priesthood used moon calendars. The same experts did not take into account the meaning's evolution of the word island in Egyptian and in Greek. Finally they did not realised that Plato used the same word Atlantis, invented by him, in order to describe the giant island, a horseshoe shape basin and a concentric ring system with geothermal springs and multicolour rocks. If they had done they would have assisted the resolution of the complexity of Atlantis much earlier than in the end of the last decade of the 21st century.

6. References

Chalari, A., St. P. Papamarinopoulos, G. Papatheodorou and G.Ferentinos., 2010. The Achaeans' coming to Africa and the island of Pharos. Proceedings of the International Conference: The Atlantis Hypothesis: searching for a lost land, Athens 10-11 November 2008, Publisher: Heliotopos, Editor : Stavros Papamarinopoulos, (in print).

Hesiod.

Homer.

Matton, G., Jebrak M., Lee J. K. M., 2005. Resolving the Richat enigma: Doming and hydrothermal karstification above an alkaline complex. Geology, v.35, no 8, p.p. 665-668.

Martin de la Cruz, J.C., 1990. Die erste mykenische Keramik von der Iberischen Halbinsel. PZ 65/1:49-52.

Mitropetrou, H., 2010. The Four Main Questions of the Platonic Logical Myth of Atlantis. Proceedings of the International Conference: The Atlantis Hypothesis: searching for a lost land, Athens 10-11 November, Publisher: Heliotopos, Editor: Stavros Papamarinopoulos, (In print).

Papamarinopoulos, St.P., 2010b. Atlantis in Spain. Part:II The case of prehistoric Athens. Proceedings of the current volume of the 12th International Symposium of the Hellenic Geological Society, May 19-22.

Papamarinopoulos, St. P., 2007c. A Bronze Age catastrophe in the Atlantic Ocean? Proceedings of the International Conference: The Atlantis Hypothesis: searching for a lost land, Melos Island 11-13 July 2005, Publisher: Heliotopos, Editor: Stavros Papamarinopoulos, p.p., 555-571.

Plato.

Zhirov, N., 1970. Atlantis. Atlantology: Basic problems. Progress publishers, Moscow, p.p. 437.

Δελτίο της Ελληνικής Γεωλογικής Εταιρίας, 2010
Πρακτικά 12ου Διεθνούς Συνεδρίου
Πάτρα, Μάιος 2010

Bulletin of the Geological Society of Greece, 2010
Proceedings of the 12th International Congress
Patras, May, 2010

ATLANTIS IN SPAIN

Papamarinopoulos S.P.

University of Patras, Department of Geology, Patra, Greece

Part IV: The concentric city and its geological significance

Abstract

Many analysts in the past faced Atlantis' main city with the same way they faced his idealised concentric cities which he described in his dialogues. However, Atlantis' concentric city has a marked difference which is recognisable if the analyst has geological knowledge. For instance the concentric scheme, the geothermal springs and the black, white and red rocks correspond in volcanogenic, impactogenic and diapeirogenic craters. It is known that building material from rocks existing in the vicinity of the two first, from the three, types of craters have been used in the past. It is also known that cities have been developed both on volcanogenic craters such as Santorin in the Aegean Sea, or on impactogenic craters such as in Nordlichen in Germany and in Yemen's capitol respectively. A simulation experiment was carried out exactly in the platonic geomorphological conditions assuming that the concentric scheme could be of impactogenic origin. The result showed that such multi-ringed crater exhibits the platonic characteristics presented in Critias. However, such solution is not unique because the other two types of craters have not been tested yet. The statistical criterion which may be applied in all three simulations in the described platonic environment will decide by itself which is the most optimal solution between all three. Many experts who know nothing about Plato's views about science and mythology can not differentiate between genuine and fabricated myths utilised by Plato. Most of them do not understand that the multi-ringed crater called Atlantis too by Plato is revealed in the ancient myths prior to Plato and was placed by these writers West of the Gibraltar Straits. Philostratus, in Roman times, is the only Greek writer who described its geological nature in detail and presented its position in Southern Spain. That crater Geryonis was associated with Heracles' visit in Iberia. In the latter's sea environment there are several submerged gigantic diapeirogenic craters and a small one visible even today in Andalucía's. The geological age of the submerged craters, in Cadiz, precedes the prehistoric Greeks' and Iberians' presence in the area. One of them possibly became the object of observations of prehistoric Greek mariners who passed Heracles' Pillars and it was interpreted as Poseidon's act. These Greek mariners were accustomed to interpret craters in the Aegean Sea such the Nisyros', for instance, one as Poseidon's act too.

1. Introduction

Plato in the Laws presented an idealized concentric city shown in Fig. 1. In that city he incorporated his town planning, political, philosophical and mathematical ideas which became known from multiple scientific studies. However, at Critias, Plato presented another concentric city-port with equal and exceptional town planning details. It has been recognized, long time ago, that this particular city associated with the Atlantes' culture had certain distinct geological properties implying a nature born initial structure like a volcanogenic, impactogenic or diapeirogenic crater. On it the Atlantean prehistoric city had been built. Since the experts of the past had "established" that no other ancient author earlier or con-

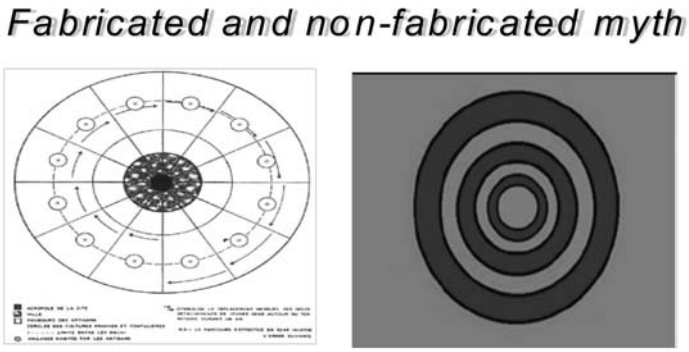

Fig. 1: An idealized concentric city presented by Plato in his dialogue the Laws. It has not any geological significance and consequently it is not an object for further analysis from the standpoint of natural sciences. However, the right picture which is Atlantis' general concentric scheme contains recognizable geological information.

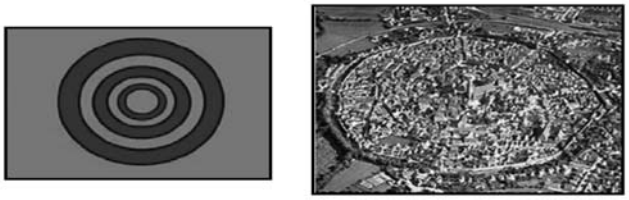

Fig. 2: The platonic concentric scheme versus the Nordlichen medieval city built upon an impactogenic crater.

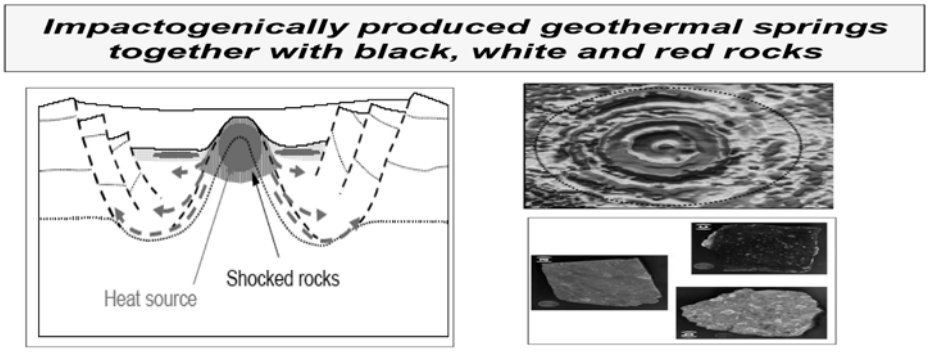

Fig. 3: A schematic presentation of a geothermal field produced by an impactor together with a geophysical image of a concentric scheme of a buried impactor. Black, white and red stones from Rochechouart's impactor in France.

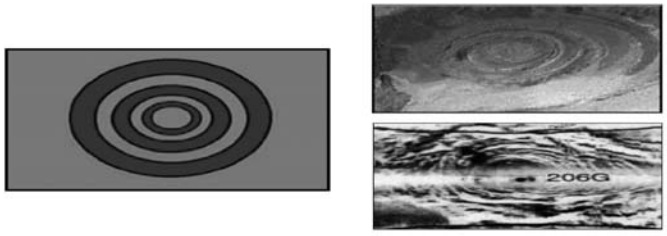

Fig. 4: The platonic concentric scheme and two diapeirogenic concentric (top Richat, Matton et al, 2005) and (bottom Cadiz, after Resbergen et al. 2005).

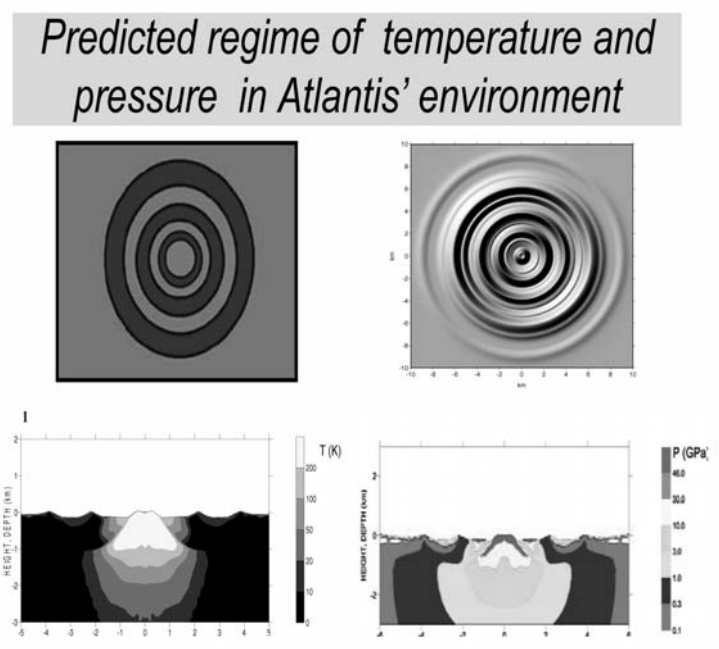

Fig. 5: The result of the arithmetic simulation is to the right of the platonic multi-ringed system. The regimes, produced by a buried impactor, of the temperature and the pressure are below of the two concentric schemes, (after Tsikalas et al, 2007a and 2007b). A similar *simulation study* should be carried out with a diapeirogenic crater.

temporary to Plato mentioned anything about that Atlantean culture and since it was known that Plato had lack of interest about history and moreover he had used many fabricated myths in his dialogues the case was clear for them that Atlantis was a petty fabricated platonic paramyth with no interest to science. We have demonstrated already (Papamarinopoulos, 2010c) that Plato's common use Atlantis' word, which he invented, for three different geological and geographic entities the giant island, the horseshow basin and the concentric scheme produced unwanted confusion. Figure 2 shows Atlantis' general concentric scheme together with Nordlichen the medieval German city which was built upon the impactogenic crater and whose buildings were constructed from impactites. Figure 3 shows a geophysical concentric image produced from a prospected buried impactogenic concentric crater together with the impactogenic regime of geothermal waters and the presence of black, white and red rocks collected from Rochechouart's crater in France. Red suievite prevails in Rochechouart. The impactogenic rocks were used by the Romans to built baths taking energy from warm impactogenic springs which were functioning for thousands of years after the impact.

2. Ancient Greek Sources about Atlantis prior to Plato

We will commence our study with Paul Jordan (2001) who refers to Hellanicus, a 5th century B.C. writer, and interprets the few survived excerpts from his texts in an unscientific way. According to him, Hellanicus who lived some decades prior to Plato did not mention anything about Plato's Atlantis in his lost book. Jordan (2001) believes that Hellanicus described briefly Atlas' daughters, the so called Atlantides. Let us see the text.

Fragmenta 1a,4,F.19a.15

…another one, called Kelaino, whose name means "who is dark in appearance" or darkish in the skin mates with Poseidon and their erotic offspring, Lykos, comes to life. Poseidon places him *in the blessed islands* where he becomes immortal.

Fragmenta 1a,4,F.19b.4

Luce (1978) was the first to find Hellanicus' particular phrase presented below to have an *exceptional similarity* to Plato's phrase. Both of them are presented in italics, firstly that of Hellanicus' and secondly then Plato's.

Fragmenta 1a,4,F.19b.4 – 1a,4,F.19b.6

"Poseidon mated with Kelaeno and their son Lykos was settled by his father in the isles of the blest in order to become immortal".

Plato wrote in Critias something similar to this.

Criti 113.d.4-113.d.5

"and *Poseidon*, being smitten with desire for *her*, *wedded her*".

We observe that *Poseidon* and *Kelaeno* in pre-patonic tradition illustrate *an Earth's circularity* symbolically in the Atlantic Ocean and then in the platonic tradition *Poseidon* and *Cleito* present symbolically the same circularity *in the Atlantic Ocean*. *Hellanicus does not locate however its position*.

We note that Plato immediately after this phrase describes *the elaborated building of Atlantis by Poseidon*. *At this point Plato starts building his paramyth with his mathematical fantasies, (*Brumbaugh, 1954).

According to Hellanicus, Poseidon had intercourse with a woman who is either dark in appearance or her skin is of a darkish type. Then he places the offspring of their love affair in the islands of the blessed. The islands of the blessed are most likely West of Gibraltar, as most ancient Greek authors suggest. According to Plato's version, Poseidon has intercourse with Cleito. One of his descendants is called Azaes whose skin is darkish so to speak. Gill (1980) interprets Azaes as a *parched*, *dark-skinned person*. The reader can now see the double similarity between the two passages. Jordan (2001) missed the point entirely because he saw in that *only* the Atlantide Kelaeno as a star in the constellation of the Pleiades.

Then in accordance with Plato, Poseidon also builds his palace West of Gibraltar. The common elements between the two versions are the erotic act which produces *a "circle" in the woman's body implying the Earth*. The darkish skin in both stories is very relevant in that Eurafrican part of the world. In other words, a nature made circularity in the Earth situated somewhere West of Gibraltar interpreted by the prehistoric Greeks as Poseidon's act became the kernel of the Atlantis case. Unfortunately Hellanicus' entire book, Atlantias, is missing and only some fragments have survived. Let us now consider what Pindar wrote who lived some decades before Plato too. Pindar describes another sacred wedding. *"Somebody"*, whose name is missing, marries a woman, a Nereid, related to the sea as *islander* women in Plato's and Hellanicus' cases related in their respective stories.

Pindar says:

N 4.65-4.70

"He married one of the lofty-throned Nereids. He beheld the line *circle of seats* on which the lords of the sky and sea sat and revealed to him their gifts and his race's power. That which lies to the west of Gadeira cannot be crossed; Turn back again the ship's tackle to the mainland of Europe."

The poet describes a *circular* base where kings of sea and heaven were offering gifts to visitors and

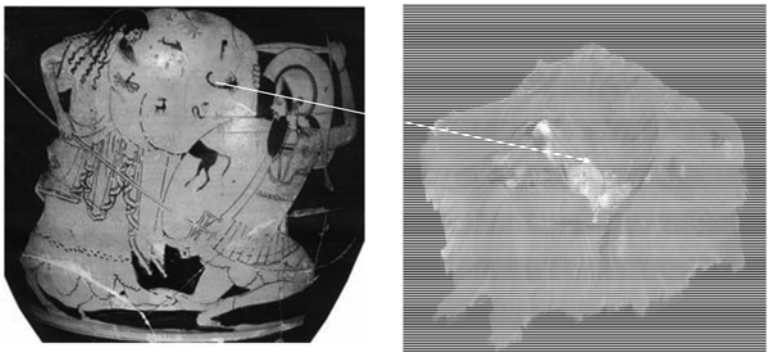

Fig. 6: Poseidon (left) fights with Polyvotis (right). Poseidon had just grabbed a piece of rock from Kos Island and he is ready to drop it against his *enemy*. A huge rock has already *fallen* upon Polyvotis and created Nisyros' crater in other words an *Aegean circularity* similar in shape to an *Atlantic Ocean circularity in the eyes of the prehistoric Greeks*.

speaking to them about their riches. Pindar in the following phrase defines the region of this rich race of kings. It is somewhere round Gadeira.

Let us come now to the 7th century B.C. and examine Hesiod's texts.

Fragmenta 372.10-372.11

Hesiod describes what Poseidon's son, Chryssaor, achieved mimicking his father.

Th 287-290

"But Chryssaor was joined in love to Callirrhoe, the daughter of the glorious Ocean, and begot three-headed Geryones. Him mighty Heracles slew in sea-girt Erytheia."

Poseidon's son, Chryssaor, had an intercourse with the Ocean's daughter Callirrhoe on the land of Erytheia and gave birth to Geryones. Before attempting to interpret what Geryones could be, let us remind the reader that what Hesiod writes is very similar to what Plato describes. Poseidon in Plato's version is replaced by Chryssaor that is Poseidon's son, in Hesiod's version. They both do the same act as Hellanicus and Pindar describe. It is an erotic act at Erytheia somewhere West of Gibraltar. The latter is defined geographically by Stesichoros of the 7th century B.C. to be close to Gadeira. But it is time to leave Hesiod temporarily and show the reader what the impression of the Greeks about Poseidon's act was in producing *circularities* in the Aegean Sea. In Fig.6 Poseidon fights against a warrior *Polybotis*, whose name means "*many bulls*". Polyvotis' name reminds us of Geryones' association with bulls in Erytheia region somewhere West of Gibraltar. Poseidon hits firstly Polyvotis with his trident and then drops a huge rock at him. The result of this action is a *circularity* in the island of Nisyros which is the volcanic crater under which Polyvotis is buried. In other words, he resembles the circularity. Is it possible that Geryones could be something like that?

Polyvotis and Geryones remain *buried* in the Aegean Sea and the Atlantic Ocean respectively. Poseidon is responsible as a warrior and/or a lover respectively. The latter symbolism was Achaeans' common understanding of large circular holes irrespective of the real producing mechanism in our modern science.

Let us come back now to the environment West of Gibraltar and follow what Poseidon himself normally does, apart from producing earthquakes and inducing floods.

Hesiod writes about him:

Th 726-726

“round it runs a fence of bronze”

This *“circular fence of bronze”* is a characteristic example of Poseidon’s building activity which builds round a crater. Furthermore Poseidon does again something similar as Hesiod writes:

Th 732-733

“for Poseidon fixed gates of bronze upon it and a wall runs all round it on every side.”

As the reader observes, Hesiod keeps insisting on describing Poseidon’s capacity that is to build circular walls round Earth’s craters.

However, Geryones’, geological nature is mentioned by Philostratus a writer of 1st century A.D. in his text VA5.4.9-VA5.5.9 in that he says the following among other information in connection with Gadeira and Geryones. Philostratus describes South-west Europe and North-west Africa too.

“They also say that the Islands of the Blessed lie at the extremity of Africa, rising near the deserted promontory.”

“They claim to have seen trees there a kind that exists nowhere else on earth, and are called Geryones’ trees. They are two in number, and grow from the grave that holds Geryones. Each combines the natures of a pine and a fir and drips *blood*, as we are told the Heliad poplar drips *gold*. The island on which the *sanctuary* stands is as large as the temple itself, and is in *no way like a rock*, but resembles a *polished platform*.”

Philostratus described a specific tree characterised by the author as a pine tree uniquely existing in the region which *weeps over* Geryones’ tomb shedding *red tears*. This tree is unique from of an observer’s standpoint coming from the Mediterranean Sea. It is located at Erytheia West of Gibraltar, a region near Gadeira. This tree does not grow within the Mediterranean and consequently it was unique for prehistoric Greeks. It is called a Dragon tree and produces red resin! This is the source of the blood which the legend describes. The legend connects these trees with Geryones because two of them grew on the top of his *tomb*. Philostratus further describes the environment as an island saying that the areas of the island and the temple were the *same*. He also explains that Geryones’ *tomb* had a top where a certain *valvis*, resembling a polished platform, existed. Since Erytheia is a land resembling a *tomb* with a circular flat top, then it is likely to be elevated. Its polished platform *valvis* is always in ancient Greece a point, a line or circle imposing limits on the ground. It has been used by the athletes. A *circular valvis* can be imagined if the reader bears in mind how and where modern athletes throw the discus. Erytheia’s geomorphology, its likely elevated topography, and its flatness implying circular limits reflect an *environmental tomb* and a temple simultaneously. In other words the flat environment described by Philostratus looks likes a *circular perivolos*, as Achaean tombs normally exhibit. The gently hilly like structure of Erytheia’s island could not have been considered as a *tomb* by the ancient Greek observers, if it had not been slightly elevated having a flat top. Thanks to Philostratus we understand that the initial observers interpreted an *earthly natural phenomenon* as a *shouting giant*. The reason was that they saw it as a circular *mouth* giving the impression of somebody *shouting*. We say *shouting*, since Geryones’ name itself means shouting. In Figure 7 we show to the reader, in a sideways view, a small flat topped *Geryones* in Andalusia’s red soil in other words in the legendary *Erythheia*’s (*red land*) environment. In the same Fig.7 we show a set of submerged giant type of Geryones’ structures. Some of them are concentric. They are all in the bottom of Cadiz’s sea.

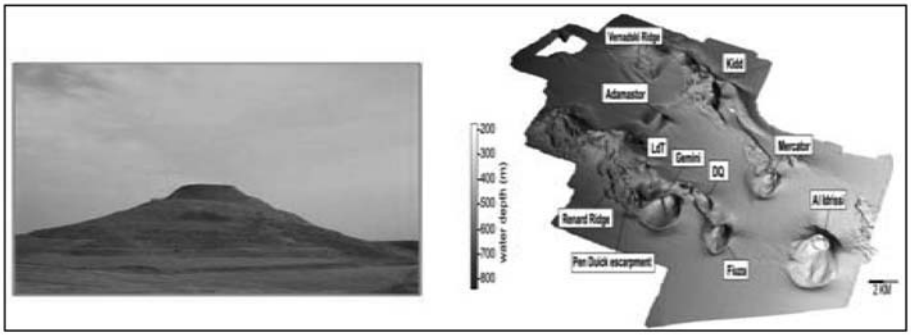

Fig. 7: A diapeirogenic Geryones from Spain in Andalusia with a flat valvis on its top to as Philostratus described it 2000 years ago. It could be interpreted as a *tomb by Greek visiting prehistoric mariners* because it looked like Mycenaean (Achaean) type of tomb, (Photo after Montexano). There are several submerged giant diapeirogenic craters in Cadiz's bay too. Some of them are concentric (map after Resbergen et al, 2005).

Fig. 8: A Dragon Dracaena tree in the Medical school Cadiz (left) is shown. Red resin from a Dragon Dracena and red tears from a tree's trunk, (Papamarinopoulos et al, 2007).

This diapeirogenic crater, shown in Fig.7 resembled what Philostratus described 2000 years ago. It has a flat, circular valvis on the top. But how can one interpret Geryones' *three heads*? The only way to interpret this, as an earthly natural phenomenon, is to imagine three heads one within the other. In other words the *shouting* Geryones exhibited a concentric three-ringed circular crater with a central flat surface on it. It is located somewhere in Erytheia (the red land) close to Gadeira. In that region (Gadeira), thanks to the Atlantic Ocean's climate, there appears the first sign of Dragon's Dracena tree with its westward unique distribution.

Today's observer can find a Dragon tree at Gibraltar and at Cadiz's Medical School along the coast of West Africa, in the Canaries in the Atlantic Ocean and elsewhere, but not within the Mediterranean Sea. It was and continues to be, a characteristic unique tree of the Atlantic Ocean. Figure 8 and illustrate a Dragon tree at Cadiz, *red resin and red tears of a weeping* Dragon tree.

The Atlantic Ocean Dragon tree is at first a short tree and then it grows very slowly. However, it can reach heights up to 19m. It looks like a giant holding the sky with his arms extended upwards.

But can we know anything more about Erytheia? Was it an island or an Iberia's extended land and where was it located exactly? The answer is partly positive. In order to extract some information about it, we have to study Steisichoros' 7th century B.C. fragmented passages carefully and in detail. Let us read the first.

Fragmenta7.1-7.3

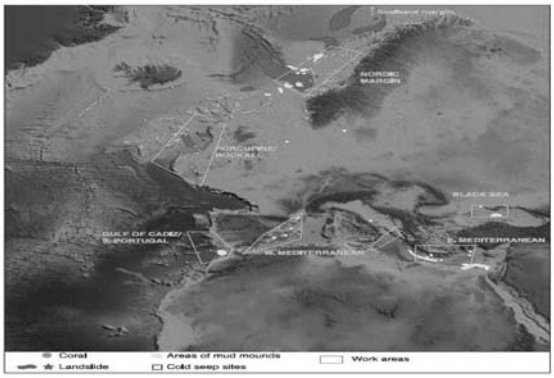

Fig. 9: Giant landslides and diapeirogenic craters (lighter colour perigrammes, dots and letters), (after Rooii, 2005).

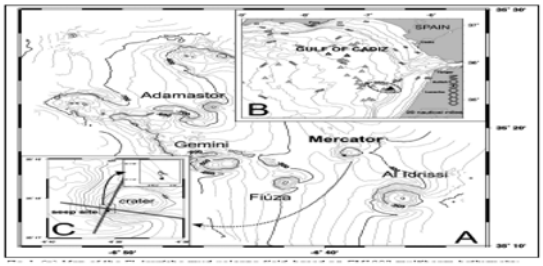

Fig. 10: Giant diapeirogenic craters at Cadiz's bottom in a bathymetric presentation, (after Weaver, 2005).

"Almost *opposite* famous Erytheia… by the limitless silver-rooted waters of the river Tartessus in the hollow of a rock."

Stesichoros describes Erytheia's land as lying opposite a land where the Tartessos River exists close to some *void* associated with silver mines. It is the first time that *a river delta* is mentioned to be located in the land opposite Erytheia's land which is Andalusia of course. Bur a river delta is mentioned by Plato in his Atlantis. The river or channel intersected the concentric multi-ringed scheme.

But this Tartessos River was also Guadalquivir's River older name in southern Spain. The Greeks called Tartessos the Iberian city as well. In other words Andalusia's region is unavoidably described. Steisichoros, however, refers to Geryones too in another excerpt as follows:

Fragmenta S20, col1.2-S20,col2.3 tit102-103

From this particular fragment and from Hesiod's description we deduce that Geryones was on Erytheia's land and additionally that it was located between Gadeira and Iberia! But are we certain that Erytheia was an island with today's meaning or an extend land of Andalusia's basin? The answer is not positive. Erytheia is a word, appearing in the 7th century B.C. In the latter century the concepts of peninsula and island had not been differentiated yet. Eryhteia can not be seen today due to a possible land slide occurred in Andalusia's coast**.** Erytheia's complexity requires another brilliant study similar to that which Chalari et al, 2010 conducted in Alexandreia. In that, Athena Chalari, demonstrated that in prehistoric times Pharos Island was a peninsula! Figure 9 illustrates a map of the distribution of past landslides and diapeirogenic (mud) craters in the Atlantic Ocean (Van Rooij, 2005). As the reader can see the marks of mud craters exist in detail right in the bay of Cadiz (Weaver, 2005). They are shown in Fig.10. The landslide regions are close and within the light colour perigrammes which show dots and letters of diapeirogenic craters.

Since no words of differentiated meanings of islands and peninsula existed before the 5th century B.C.

since Herodotus added for first time the word peninsula in alphabetic Greek, we can deduce that either geological reality could be meaningful. However, it is important to know at some stage in Cadiz's bay and in Andalusia's coast the dates of any possible landslides and the scenario under which they were formed.

But in another fragment Stesichoros continues and states the following:

Fragmenta S20,col2.1-col2.6

"…over the waves of the deep brine they came to the beautiful island of the gods, where the Hesperides have their homes of solid gold;…(buds)".

Stesichoros describes the wonderful island and relates the Hesperides (Pleiades) to it. But the surprise is the case of the Hesperides mentioned again two centuries before Hellanicus' period. In Hellanicus 5th century B.C. Poseidon mates with Kelaeno (*one of the Hesperides*) and their offspring is placed on the islands of the blessed somewhere West of Gibraltar. In the legend of the Hesperides, also called Atlandites, there is an obvious astronomical layer apart from the earthly. The first does not contradict the second. The astronomical layer reflects knowledge of Pleiades' constellation associated possibly with calendrical systems used my mariners. But the case of Hesperid Kelaeno illustrates another earthly layer as a piece of additional information in connection with a particular region West of Gibraltar. This information is the Poseidon's erotic act on Earth as it was conceived by the Greeks somewhere West of Gibraltar. Versions of the Earth having a circular chasm in a marine environment are Calirrhoe in Hesiod, Nereid in Pindar, and Cleito in Plato. These *ladies, representing Earth,* had an erotic contact with Poseidon in an exotic for the prehistoric Greeks environment. The various versions of the legend are multiples attempts of the prehistoric Greeks in the region of Gadeira-Andalousia to interpret a particular circular chasm, once visible. Any of these circular chasms become once a sacred and religious center of Iberians long before the advent of Phoenicians.

But let us go deeper in time and reach Homer's period. Do we have a symbolic presentation of a circularity anywhere? The answer is positive. Let us study the following passages one after the other.

Od13.146-13.152

"Then Poseidon the earth-shaker, answered him:

Quickly should I have close as you say, god of the dark clouds, but always I dread and avoid your wrath. But now I am minded to smite the beautiful ship of the Phaeacians, as she comes back from her convoy on the misty deep, that hereafter they may desist and cease from giving conveyance to men, and to hide their city behind a huge *encircling* mountain".

In the text above Poseidon suggests to Zeus what he is going to do against the Phaeacians describing his threat into two steps. First he means to smite the Phaeacian boat as it approaches the coast of their land with an earthquake and then go to the second realization of his threat which is the *encircling* of their city by dropping on a huge mountain it.

Let us see the realization of his first part of his threat:

Od 13.159-13.164

"Now when the Poseidon the earth-shaker heard this he went to Scheria where the Phaeacians dwell, and there he waited. And she drew close to shore, the seafaring ship speeding swiftly on her way. Then near her came the Earth-shaker and turned her to stone and rooted her far beneath by a blow of the flat of his hand and then he was gone."

After the realization of the first part of his threat the Phaeacians were very afraid. The reader can see what they wanted to do to avoid the imminent catastrophe which was the repetition by Poseidon of the crater's production. *This is a view of the visitors prehistoric Greek in Iberia who interpreted the pre-existing crater there and region's seismicity at the period of their visit but in Homer is reflected upon the Phaeacians*. The latter was possibly visible in the area. In the eyes of prehistoric visiting Greeks, the earthquake activity and the crater were connected directly with Poseidon acts, as they knew from the Aegean Sea, and applied in that area were connected as a severe godly thread against the local peoples. Let us read the next passage:

Od 13.178-13.184

"and now all this is being brought to pass. But now come, as I bid let us all obey. Cease to give convoy to mortals, when anyone comes to our city, and let us sacrifice to Poseidon twelve choice bulls, in hope that he may take pity, and not hide our city behind a huge *encircling* mountain".

Homer keeps repeating the term *encircling mountain* in a marine seismogenous region. This term requires explanation. In order to facilitate ourselves to understand Poseidon's very strange threat we should look in Fig.19. Did Poseidon in the seismogenous marine environment of Nisyros really produce a hole on it by throwing a huge rock or the preexisting crater that was interpreted by the Greeks as been done by Poseidon in the past? Certainly the second case is the correct one. In the light of this question we should see Poseidon's thread against the Phaeacians as a preexisting crater in a seismogenous environment. It has been interpreted as Poseidon's act of the past by the visiting prehistoric Greeks. Since the ongoing seismicity in the area was growing, the interpreters of the circular chasm as Poseidon's first act gave the impression to Phaeacians that he will repeat its act since he was the Earth-shaker. Their fear was based on their interpretation of a preexisting crater in the vicinity of their seismogenous land, as a result of Poseidon's act. Therefore the loss of their boat in the sea, due to an earthquake, increased the observing city's people anxiety of a possible repetition of a Poseidonian worst act since the god of the sea had sent his message. They frightened citizens of Scheria, who lived on or close to a nature made crater believed that Poseidon would throw a huge mountain at them as he did in the past producing the crater. This scenario of course is an impression of the prehistoric Greeks of the events in that region. Scheria of course can not be Corfu as Strabo suggested (Petridis, 1999). It is impossible for the Corfu people not have known the Trojan War when the other Ionian Islands knew it! Scheria, as Depos (1980), Petridis (1999) and Tziropoulou (2008) proposed, is Spain. It is impossible for Scheria to be in the Ionian Sea either since it is not the end of the known world. But Spain, in other words Scheria, was in the end of the known world for the Greeks as Homer and others described it.

3. Conclusions

Figure 11 illustrates Kambanakis' (1892) drawing following Plato's Kritias.

Prior to Plato a nature made either of impactogenic or diapeirogenic origin concentric crater was once visible in Iberia's coast. Ancient authors before and after Plato mentioned it. Plato called it Atlantis and with the same name called a giant island and a horseshow basin. Plato built upon it in other words on pre-existing genuine myth his mathematical fantasies (Brambaugh, 1954). Kritias is the only dialogue which describes a genuine myth and a paramyth together whereas all other dialogues contain only paramyths. The genuine myth reflects the prehistoric and historic contact of the Greeks during the Tartessos and an Atlantic Ocean catastrophe which ruined the elder prehistoric Tartessos. The latter later was rebuilt and smoothly vanished due to Guadalquivir's accumulating sediments.

A platonic mathematical paramyth was built upon an initial prehistoric observation by visiting Greeks of a nature made multi-ringed crater which was preserved by ancient authors as a genuine myth from pre-platonic times and interpreted mythically by the mariners as Poseidon's act in Iberia's palaecoast.

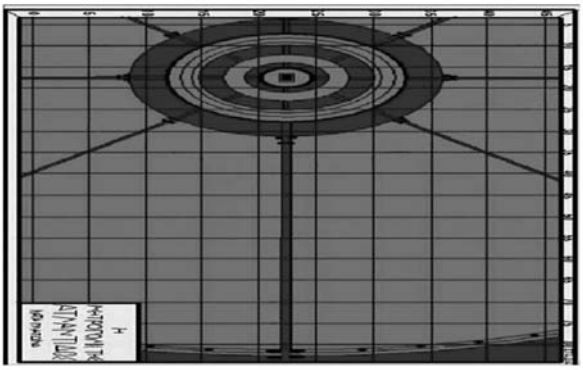

Fig. 11: Pactroclos Kambanakis (1892) was the fist in the modern period who produced Atlantis' picture on a grid. Today there are views on this scheme, shown above, based on differences of various philological elements.

4. References

Brumbaugh, R.S., 1954. Plato's mathematical imagination."The mathematical passages in the dialogues and their interpretation". Indiana University Press, p.p.302.

Chalari, A., St. P. Papamarinopoulos, G. Papatheodorou and G.Ferentinos. The Achaeans' coming to Africa and the island of Pharos. Proceedings of the International Conference: The Atlantis Hypothesis: searching for a lost land, Athens 10-11 November 2008, Publisher: Heliotopos, Editor : Stavros Papamarinopoulos, (in print).

Depos,G. D., 1980. Odyssey "Historical and Geographic verification", Editor Pallas, p.p. 213 (In Greek).

Hellanicus.

Hesiod.

Homer.

Jordan, P., 2001. The Atlantis syndrome. Sutton publishing, p.p. 308.

Kabanakis, P., 1996. The communication, before the deluge, of the two worlds through Atlantis. *A contribution to the study of communication of the prehistoric Greeks with America*. First edition 1892, Second edition Ekate, Athens, (in Greek), 61 pp.

Matton, G., Jebrak M. & Lee J. K. M., 2005. Resolving the Richat enigma: Doming and hydrothermal karstification above an alkaline complex. Geology, v.35, no 8, p.p. 665-668.

Montaxano, D. G. (www.antiguo.com).

Papamarinopoulos, St. P., Drivaliari, N. & Coseyan, Ch., 2007. Red tears in the Atlantic Ocean. Proceedings of the International Conference: The Atlantis Hypothesis: searching for a lost land, Melos Island 11-13 July 2005, Publisher:Heliotopos, Editor: Stavros Papamarinopoulos, p.p. 539-571.

Philostratos (Flavios).

Pindar.

Plato.

Petrides, S.P., 1999. Homer's Odyssey. "America's discovery by the ancient Greeks", Editor D.Tassopoulos, p.p.446.

Resbergen Van, Pieter, Davy Depreiter, Bar Pannemans and Jean-Pierre Henriet., 2005. Sea floor expression of sediment extrusion and intrusion at the El Arraiche mud volcano field, Gulf of Cadiz. Journal of Geophysical Research, Vol.110, FO 2010, doi:10.1029?2004 JF00165, pages 3 from 13.

Rooij, D. Van, 2005. EOS, vol.86, no 49, p.p. 509-511.

Steisichoros.

Strabo.

Tziropoulou, A., 2007. Homer and the so called Homeric problems. Proceedings of the symposium "Homer Science and Technology", Ancient Olympia, (2006). Editor: St. A. Paipetis, p.p. 451-467.

Tsikalas, F., Papamarinopoulos, St. P. & Shuvalov, V. V., 2007a. The origin of the multi-ringed concentric morphology of Atlantis capital and its relation to the Platonic scripts. Proceedings of the International Conference: The Atlantis Hypothesis: searching for a lost land, Melos Island, 11-13 July 2005, p.p. 203-211.

Tsikalas, F., Shuvalov, V. V. & Papamarinopoulos, St. P., 2007b. A new geophysical interpretation of the Platonic multi-ringed concentric morphology of Atlantis capital based on numerical simulations. Proceedings of the International Conference: The Atlantis Hypothesis: searching for a lost land, Melos Island, 11-13 July 2005, p.p.193-202.

Weaver, P. P. E., 2005. Hotspot ecosystem research on the margins of European Seas. EOS, vol.86, no 24, p.p. 226-227.

Δελτίο της Ελληνικής Γεωλογικής Εταιρίας, 2010
Πρακτικά 12ου Διεθνούς Συνεδρίου
Πάτρα, Μάιος 2010

Bulletin of the Geological Society of Greece, 2010
Proceedings of the 12th International Congress
Patras, May, 2010

ATLANTIS IN SPAIN

Papamarinopoulos S.P.

University of Patras, Department of Geology, Patra, Greece

Part V: Atlantis' location

Abstract

Following strictly Plato's information we reach Iberia and there we discovered the basic geomorphological characteristics of a horseshow shape flat and elongated basin which is surrounded by mountains. The basin reaches the Atlantic Ocean. This valley is Andalusia and it was missed by Herodotus and Hecateus, who lived a century earlier than Plato, and constructed North West Europe's map. The Iberian civilization is reflected in the Greek myths prior to Plato too. Atlantis' catastrophe in the shape of the concentric scheme's, being in Iberia's coast, was realized by earthquakes and a tsunami. The discovery of the very first Mycenaean vase's fragment, in Guadalquivir's estuary by Spanish archaeologists in 1990, offered the first archaeological evidence that the prehistoric Greeks had visited Atlantis after all before the 12th century B.C. The recent interest of the Spanish Archaeological Survey in Andalusia initiated because it has been proved geologically that the region had not been submerged since the last ice age. New evidence suggests that the waters may have receded in time for the Iberians in the period Tartesssos to build an urban centre, which was later destroyed by earthquakes and a tsunami as Plato describes in Timaeos and Critias for this region. Although platonic Atlantis could not be considered, as Thucydides would prefer, a historical text but it cannot be considered as a single paramyth either since some parts of his text have been proved already. It can be considered as a genuine myth containing a true prehistoric kernel covered firstly by a layer of inventions produced by transmitting people, the story, from generation to generation between the actual occurrence of the event within the 12th century B.C. and Solon's 6th century B.C. who recorded it and then of the 4th century B.C. when Plato wrote down. Atlantis is also covered by a platonic paramythical layer full of mathematics and musicological information which is recognized and can be removed liberating the genuine myth's kernel from the platonic intervention.

1. Introduction

Plato's text leads the reader to Atlantis' coast since Iberia' Gadeiriki is mentioned. The latter is a small peninsula which today is part of Cadiz bay. Inspecting Herodotus' and Hecateus' of South West Europe maps we find no evidence of a horseshow basin encircled by mountains and yet there Andalusia's basin exists right in Iberia. It has in 90% all the platonic geomorphological characteristics in the exact geographic location and even orientation (Papamarinopoulos, 2010).

2. Approaching Atlantis

Plato (Timaeos 24.e.5-24.e.d) mentioned very clearly Atlantis' position by saying the following statement.

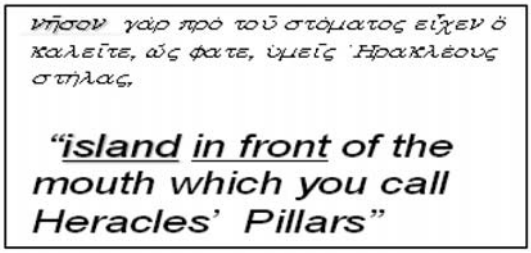

Plato also in addition, described, an *island in front of the mouth and* leads us without any doubt west of Gibraltar. It has been proved that prior of the 6th century B.C., in other words the century in which Solon lived, the prehistoric and historic Greeks knew where exactly the Heracles' Pillars were located in connection with the Atlantic Ocean, (Papamarinopoulos, 2010). But how we could know where exactly, in the Atlantic Ocean, Atlantis was? The following phrase offers the answer completely. In this, not only the name Gadeirus is shown, but also the concept of the small peninsula appears which is Gageiriki (in Greek) implying the peninsula by the ending of Gadeirus which is Gadeiriki. The platonic text (*Tim 24.e.5-24.e.6*) and the map are shown of Fig.1. They both explain clearly the case if the reader adjusts the island's meaning in the pre-Herodotus' time as the case of *Atlantis* is.

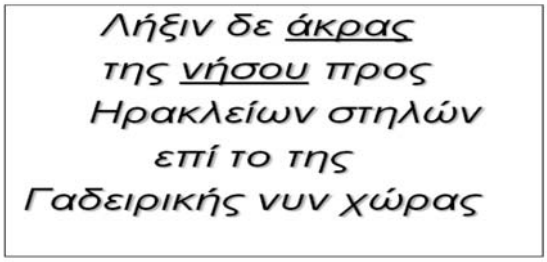

Fig. 1: The extremity of the island, with the meaning of it before Herodotus' 5th century B.C. as peninsula is shown. It without doubt the land Portugal-Spain and its north extend up to Celtia and Germany. The Heracles' Pillars are shown to be close to Cadiz in which the Kingdom of Gadeirus once existed. In that a small or peninsula exists called Gadeiriki by Plato. The word ειλιχότι has been removed because it belongs to just a previous phrase of the platonic text.

In the first part of the phrase the *island* with its pehistoric meaning is presented in connection with the Heracles' Pillars. It is further explained where exactly is t located hat, *in front,* west or east of the Pillars? The *island* is West of the Pillars and furthermore the edge of it is defined fully in the Atlantic Ocean since Gadeirus is mentioned which is Cadiz of course.

The reader now understands that the mysterious Atlantis became visible after all these 2400 years. The Greek word ειλιχότι has been removed from the text since it belongs in the previous platonic phrase. Gill (1980), without comprehending the above mentioned platonic statement, shown in Fig.1, made a very interesting and important observation: He says the expression in Greek "επί το της" means in English "up to the". He finds it odd: it looks as though Plato intended to say facing that part of the land in other words the peninsula of Gadeira. This observation is a golden key in understanding the text because there is only one way for an observer to see Gadeiriki (peninsula), *and the same time to be up to the country in which Gadeiriki belongs to and further to be close to the Pillars.* He has to be west of the Pillars and west of Gadeiriki on Iberia only in order to satisfy the text. The observer had to be placed on Spain's land having his back west in other words on Atlantis itself. Gill (1980) finds it odd because he has in his mind the

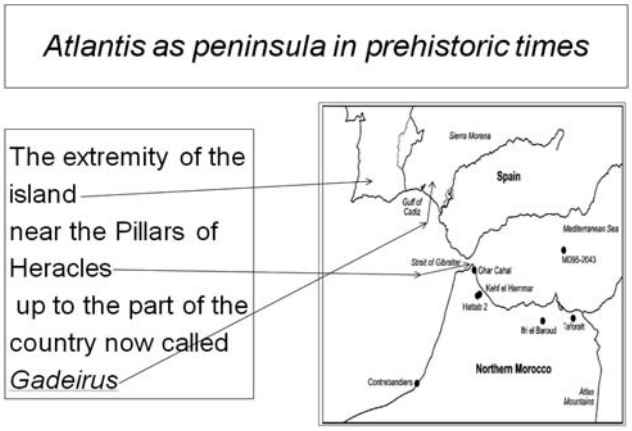

giant nesos in the middle of the Atlantic Ocean. If the observer was placed in the middle of the Atlantic Ocean he could not be *close* to the Pillars and he could not be *close* to Gadeiriki either in order to satisfy the platonic text. The possibility that does not pass through from Gill's mind is that the two concepts of island and peninsula were not differentiated in the Bronze Age up to the 12th century B.C. or even in Homer's time up to the 8th century B.C. but only some decades before Plato's time in Herodotus text when he introduced for first time the word peninsula. Historian Pierre Vidal-Naquet and archaeologist Christos Doumas were victims of the same issue. If, all the above mentioned, had understood this detail they would have immediately realized that the only way to face the peninsula of Gadeiriki, in that specific platonic context, is to be on the giant *island* of Iberonesos exactly in Andalusia in which Cadiz is located, which of course is in the Atlantic Ocean. Another element of interest Richter (2007) identified that Plato´s Atlantis was in a River Delta without locating in Andalusia. He was correct because Plato does describe a river's delta intersecting the famous concentric scheme which calls Atlantis and further the ancient writer Steisichoros who preceded Plato's 4th century B.C. mentioned it too. Steisichoros in the 7th century B.C. described the concentric multi-ringed scheme called Geryonis being on Erytheia's land which was opposite of Tartessos River in other words Andalusia's Guadalquivir River!

That simple! Plato described Atlantis having placed the observer sitting on the land of Iberia at Andalusia without knowing the basin himself! The confusion of 2.400 years is now over.

Plato further describes a horseshow basin and calls it Atlantis too with the following phrase. Figure 2 shows the platonic valley.

This basin-Atlantis is geomorphologically similar with the flat and rectangular valley of Andalusia

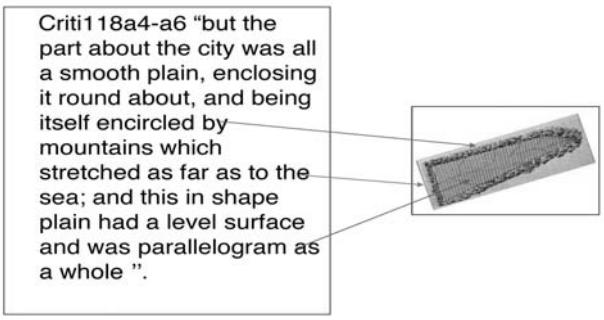

Fig. 2: The platonic text and the accurate geomorphological details of the platonic basin is shown. The concentric feature is in the south of the basin. Today is missing from Andalusia' coast line. (The platonic basin after Zhirov, 1970).

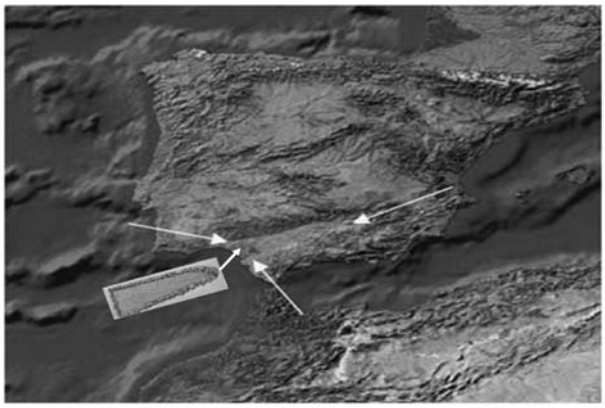

Fig. 3: Plato's basin is compared with Andalusia's basin. All Plato's preceding geographers-historians had no knowledge of its existence and yet the philosopher described it in right position, orientation and shape. The ongoing archaeological studies will tell us if the elaborate system of the internal canals in a chequerboard pattern existed in prehistoric times. Brumbaugh (1954) demonstrated that the size of the platonic valley, the chequerboard pattern in it and the elaborate water canals in connection with the concentric scheme and the geometric details on it were part of Plato's mathematical paramyth. Allen (2010) has other views which lead us to Bolivia in which a chequerboard pattern of canals have been found together with a concentric volcanogenic scheme placed in the middle of the eastern side of the rectangular net. Allen needs to demonstrate the age of that system in order to be taken as another serious candidate of Atlantis' location otherwise it will be interpreted as a mere coincidence if its age is younger than Solon's 6th century B.C.

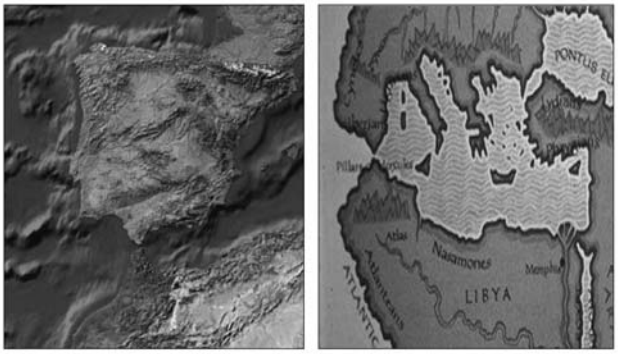

Fig. 4: The comparison between a modern southern European map and that of Herodotus' is shown. In the latter Andalusia's basin is missing.

and the encircling of it by the mountain range of Siera Nevada and Siera Morena as Foliot (1984) correctly had pointed out. The reader can examine in Figure 8 how Plato (Criti 118a4-a6) described its features analytically. Plato himself did not realize that he was describing Iberia. The richness of metal and wood supplies characterizes Andalusia. The following Fig. 3 illustrates the basin of Andalusia and it is compared with the platonic valley shown in the same figure too. The similarity is up to 90%!

In Figure 4 the South west Europe's modern map and Herodotus' 5th century B.C. map are compared respectively. Andalusia's basin is missing from the second.

Figure 5 shows where Atlantis is located in a modern map.

3. The West giant Continent

In Fig. 6 we present world map, to the reader, adjusted to the platonic text. We should explain if ancient

Fig. 5: Atlantis as a major gigantic island has been found. The platonic valley has been found too. What is missing is the concentric feature in the Andalusia's coast.

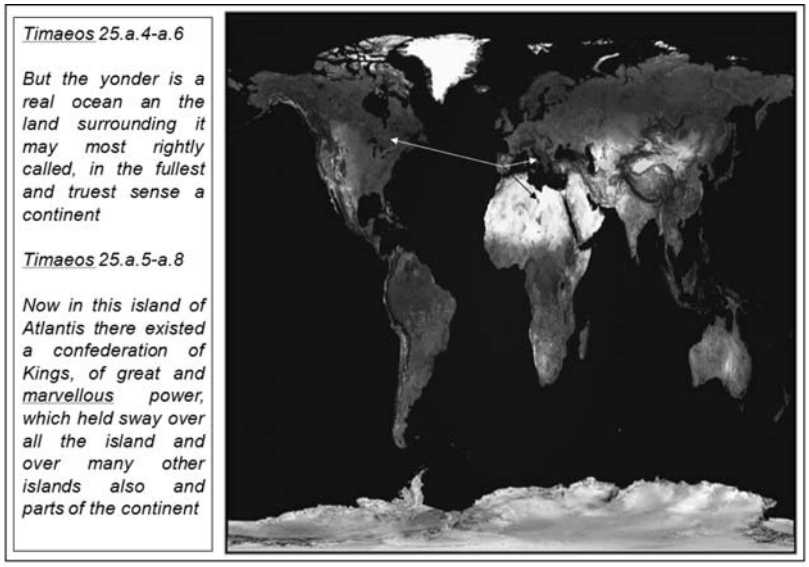

Fig. 6: Plato connects *Iberian Atlantis* with the Americas. It remains to be proved both in Iberia if that Bronge Age Atlantis ever existed through today's advancing Spanish Archaeological Service's studies in Andalusia's Donana region. Then the cultural relation between Bronze Age Iberia and the Americas would be a much harder task to be proved.

prehistoric societies knew about the existence of a giant continent west of Gibraltar in any possible way. In fact the giant platonic mass is a crude presentation of the two Americas and Antarctica together.

Parsche and Nerlich, (1995) demonstrated that the internal tissues of an Egyptian's body were full of three different narcotics. The time span of the dated *naturally mummified Egyptian body* is 1070 yr

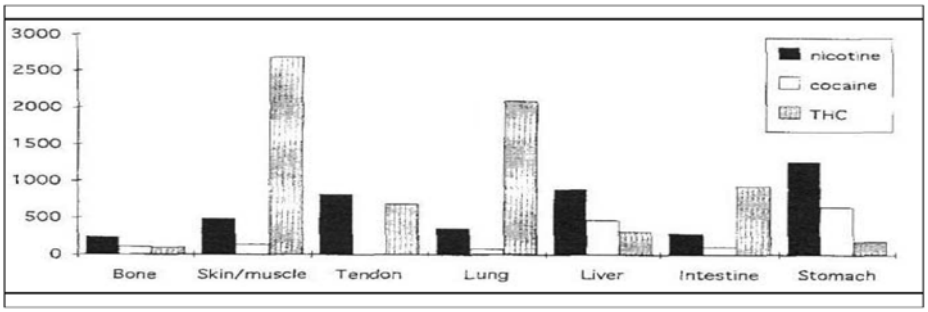

Fig. 7: The ppresence of drugs in different *internal tissues* of an *Egyptian's naturally mummified mummy's of the 10th century B.C,* (after Parsche and Nerlich, 1995) proved the person used these narcotics when he was alive. These results prove beyond doubt of the body's possible contamination at any period that some ancient prehistoric mariners knew Plato's continent long time ago before Plutarch's Greeks in the 1st century A.D., (Kontaratos et al, 2010), the medieval Chinese mariners in 1451 yr A.D., 33 years before Columbus' birth, (Menzies, 2002) and of course Columbus himself in the medieval period who rediscovered it in 1498 yr A.D. It remains a historic enigma how Plato from where received this information in the 4th century B.C.

B.C. This unexpected information illustrates *the prior knowledge* of the giant westerly land by Solon's and/or Plato's *informants*. Their findings demonstrated that the person, when he was alive, made use of these substances since his body was naturally mummified. Consequently there is not possibility of any contamination of any kind at any epoch.

Balabanova's (1997) studies on *naturally mummified bodies from Egypt* demonstrated, further, that they contained nicotine, cotinine and cocaine in the deeper tissues of their bodies like lungs, stomach, intestines, leaver e.t.c. The existence of cotinine means that when those people were alive were using nicotine which had been metabolized into cotinine. Similarly the existence of cocaine means that when they were alive, they used cocaine.

Although one can not exclude the possibility, wild Nicotiana Tombacum's existence outside South America, it is very difficult to accept that Erythroxylon Coca's plant was growing somewhere else *outside* South America *in the same quantities* and further that this information was known to Egyptians. Figure 7 shows the case of the findings in the Egyptian body. It seems that Plato was informed from sources which sciences can not define about the west continent's existence after all.

Another enigma reinforcing the previous statement is the map of Johannes Schöner which appeared out of the blue in Nurenberg in the medieval period. In that the reader can see well mapped South America and Antarctica. The latter's discovery came much later. It is a serious question of how the unknown cartographers managed to do it before the discovery of the longitude's measurement. Who and when was able in the past to map South America with such correctness in terms of latitude and longitude depicting its coast lines without knowing the longitude's measurement?

It is known of course, that thanks to John Harrison an English brilliant engineer in 1773, an instrument was invented allowing a practical way to measure longitude en route in the sea. Nobody of course could assume that cartographers in the medieval period could produce the map shown in Fig. 8 just 35 years after Columbus' assumed official discovery even if *all of them* were able to know to deal with the longitude and further if *they all had agreed to carry together* such as task! It seems after all that Plato had correct information of the giant's continent existence who's Aristotelis, Strabo and others *after him* and the geographers-historians *before him* did not have.

Fig. 8: The Marble Globe of Gotha showing South America and Antarctica produced *at the of blue* in Nuremberg in 1533 by Johannes Schöner has remarkable images of the two continents South America and Antarctica. The first was considered undiscovered prior to Christopher Columbus' "landing" in 1498 in South America. The second was discovered much later (courtesy Dominique Görlitz, unpublished data).

4. Conclusions

1. The word *nesos* had the meaning of peninsula or promontory in prehistoric times but in the 5th century B.C. Herodotus added the word *chersonesos* meaning peninsula (Le Noan, 2005). Therefore it is more than likely that Portugal-Spain land and its northern extend was a giant *nesos (island) in the eyes of prehistoric visiting Greeks*. *An example is* Peloponnesus for instance in prehistoric times for the Achaean observers which was never an *island (nesos)*. A second example is Pharos Island in Alexandria which was peninsula in prehistoric times and yet it was called island from prehistory to the historic period (Chalari, et al, 2010). We have reached Andalusia's coast based *only* and *strictly* on Plato's text. However, we have reached the same region through the study of other ancient texts w3ho mentioned the circularity even prior to Plato.

2. Plato is proved to be correct in West Mediterranean describing Andalusia's horseshoe geomorphological shape with a 90% accuracy. This information could not have been known to him since

the historians had not mentioned of them. Herodotus had described Iberia's map and had mentioned the Pyrenees but he has completely missed the Andalusia's basin and its surrounding mountains. Iberia was known to the Greeks before Solon's 6th century B.C. as Depos (1980), Petrides (1999) and Tziropoulou (2008) say. All the three used entirely different arguments, to the author of this paper, and they equated Scheria with Iberia agreeing with him.

3. From Plato's text there emerges a new window of the 12th century B.C. focusing on the West and is different from Homer's who wrote about the 12th century B.C. which is focused on the East Mediterranean.

4. Pierre Vidal-Naquet's (2005) theory of imaginary Athens and imaginary anti-Athens (Atlantis) has collapsed since prehistoric Athens was real and Atlantis's geomorphology is a real geological reality. They were both unknown to historians.

7. Christos Doumas (2007) opinion that Atlantis is fully utopia crashes on the presented arguments.

5. References

Balabanova, St., 1997. Die Geschichte der Tabakpflanze vor Columbus auβerrhalb Amerikas sowie das Rauchen im Spiegel der Zeien. Innovati-ons-Verlags-Gesellschaft m.b.H..p.p. 112.

Allen, J., 2010. Atlantis: Lost Kingdom of the Andes. Athens. Proceedings of the International Conference: The Atlantis Hypothesis: searching for a lost land, Athens 10-11 November 2008, Publisher: Heliotopos, Editor : Stavros Papamarinopoulos, (in print).

Brumbaugh, R.S., 1954. Plato's mathematical imagination. "The mathematical passages in the dialogues and their interpretation". Indiana University Press, p.p. 302.

Chalari, A., St. P. Papamarinopoulos, G. Papatheodorou and G.Ferentinos. The Achaeans' coming to Africa and the island of Pharos. Proceedings of the International Conference: The Atlantis Hypothesis: searching for a lost land, Athens 10-11 November 2008, Publisher: Heliotopos, Editor : Stavros Papamarinopoulos, (in print).

Depos,G. D., 1980. Odyssey "Historical and Geographic verification", Editor Pallas, p.p. 213 (In Greek).

Doumas, Ch., 2007. The search for Atlantis: The utopia of a utopia. Proceedings of the International Conference: The Atlantis Hypothesis: searching for a lost land, Melos Island 11-13 July 2005, Publisher: Heliotopos, Editor: Stavros Papamarinopoulos, p.p.1-7.

Foliot, K.A., 1984. Atlantis revisited. "A documented account of the fabled island as it was long ago and it is today". Information Printing, Eynsham, Oxford, p.p. 129.

Gill,C., 1980. Plato: The Atlantis story. Bristol classical press. Editor: C.J.Rowe, p.p. 93.

Gorlitz, D., 2007. Personal communication. The Johannes Schöner Globe.

Kontaratos, A., et al., 2010. Rethinking Atlantis**.** Atlantis and the American Connection. "Prehistoric Voyages To America". The team of scientists who worked on Plutarch's passage and proved that Greek mariners knew the Americas and especially the gulf Gulf of St. Lawrence for which Plutarch offers a map's description which demonstrates that St.Lawrence's entrance is in the same parallel as that of Maeotis Lake (Azov Sea) and further that North and South America as one landmass are surrounded by sea were the following: Anthony Kontaratos (Professor of Engineering Administration, University of Patras, Greece), Markos Papadopoulos (Commodore, Hellenic Merchant Marine), Mina Papadopoulou (Historian - Archaeologist.), Stavros Papamarinopoulos (Professor. of Geophysics, University of Patras, Greece), Panagiotis Mitropetros (Scholar - Ancient Greek Expert), Eleni Mitropetrou (Archaeologist) and Paschalia Mitskidou (Senior Research Scientist).

Kraft, J. C., Rapp, G., Kayan, I. & Luce, J., 2003. Harbor areas at ancient Troy: Sedimentology and Geomorphology complement Homer's Iliad. Geology, v.34, no2, p.p. 163-166.

Le Noan, G., 2005. The Ithaka of the sunset. Editions Tremen. "Collection Commentaires". p.p. 126.

Menzies, G., 2002. 1421. The year China discovered the world. Bantam Press, p.p. 520.

Papamarinopoulos, St.P., 2003. Was Plato's Atlantis the island of Santorini? Proceedings of the international symposium, "Extra ordinary machines and structures in antiquity", Ancient Olympia, 19-24 August 2001. Editor: St.A.Paipetis, Peri Tecnon., p.p. 259-265.

Papamarinopoulos, St. P., Drivaliari, N. & Coseyan, Ch., 2007. Red tears in the Atlantic Ocean. Proceedings of the International Conference: The Atlantis Hypothesis: searching for a lost land, Melos Island 11-13 July 2005, Publisher:Heliotopos, Editor: Stavros Papamarinopoulos, p.p. 539-571.

Papamarinopoulos, St.P., 2010. Plato and the seismic catastrophe in the 12th century B.C. Athens. Proceedings of the International Conference: The Atlantis Hypothesis: searching for a lost land, Athens 10-11 November 2008, Publisher: Heliotopos, Editor : Stavros Papamarinopoulos, (in print).

Papamarinopoulos, St. P., 2007c. A Bronze Age catastrophe in the Atlantic Ocean? Proceedings of the International Conference: The Atlantis Hypothesis: searching for a lost land, Melos Island 11-13 July 2005, Publisher: Heliotopos, Editor: Stavros Papamarinopoulos, p.p., 555-571.

Papamarinopoulos, St.P. and Cosegian, Ch., 2007. The ritual of the bull in Atlantis and its basic parallel in Iberia. Proceedings of the International Conference: The Atlantis Hypothesis: searching for a lost land, Melos Island 11-13 July 2005, Publisher:Heliotopos, Editor: Stavros Papamarinopoulos, p.p. 525-538.

Papamarinopoulos, St.P., 2007a. The memory of a comet during the Trojan war. Proceedings of the present symposium. Homer, Science and Technology. Ancient Olympia, (2006). Editor: St.A. Paipetis, p.p. 341-356.

Parsche, F and Nerlich, A., 1995. Presence of drugs in different tissues of an Egyptian mummy. Fresenious J anal Chem, 352, p.p. 380-384.

Petrides, S.P., 1999. Homer's Odyssey. "America's discovery by the ancient Greeks", Editor D.Tassopoulos, p.p. 446.

Plato.

Plutarch.

Richter, U., 2007. Plato´s Atlantis was in a River Delta. Proceedings of the International Conference: The Atlantis Hypothesis: searching for a lost land, Melos island 11-13 July 2005 (in print) Strabo Geog 17.3.4.18-17.3.4.25.

Steisichoros.

Tziropoulou, A., 2007. Homer and the so called Homeric problems. Proceedings of the present symposium. Homer Science and Technology, Ancient Olympia, (2006). Editor: St. A. Paipetis, p.p. 451-467.

Tsikalas, F., Papamarinopoulos, St. P. & Shuvalov, V. V., 2007a. The origin of the multi-ringed concentric morphology of Atlantis capital and its relation to the Platonic scripts. Proceedings of the International Conference: The Atlantis Hypothesis: searching for a lost land, Melos Island, 11-13 July 2005, p.p. 203-211.

Tsikalas, F., Shuvalov, V. V. & Papamarinopoulos, St. P., 2007b. A new geophysical interpretation of the Platonic multi-ringed concentric morphology of Atlantis capital based on numerical simulations. Proceedings of the International Conference: The Atlantis Hypothesis: searching for a lost land, Melos Island, 11-13 July 2005, p.p. 193-202.

Vidal-Naquet, P., 2005. L'Atlantide. "Petite histoire d'un mythe platonicien" Les Belles Lettres. p.p. 198.

Zhirov, N., 1970. Atlantis. Atlantology: Basic problems. Progress publishers, Moscow, p.p. 437.

Δελτίο της Ελληνικής Γεωλογικής Εταιρίας, 2010
Πρακτικά 12ου Διεθνούς Συνεδρίου
Πάτρα, Μάιος 2010

Bulletin of the Geological Society of Greece, 2010
Proceedings of the 12th International Congress
Patras, May, 2010

ATLANTIS IN SPAIN

Papamarinopoulos S.P.

University of Patras, Department of Geology, Patra, Greece

Part VI: The end of Atlantis

Abstract

Plato described the end of Atlantis very vividly in a single day and night due to earthquakes and floods and nobody believed him because all experts imagined the impossibility of the giant island's continental size in the middle of the Atlantic Ocean to vanish in 24 hours. They did not care to understand that Plato meant three different geographic and geological entities all called by him Atlantis which were the giant island, the horseshow basin and the concentric rater. Following Plato's text that giant island was identified as the peninsula of Portugal-Spain and its northern extend. They did not even care to interpret correctly a genuine myth's kernel which belonged in the end of the Bronze Age considering the island's change of meaning versus time from prehistory to history both for the Egyptian and the Greek language up to Solon's visit in Egypt in the 6th century B.C. This, mentioned above negligence, produced delay in understanding a complex problem which required a very good geological background besides other trans-scientific knowledge in archaeology, philology, mythology and mathematics in order to be faced properly. The loss of a nature made multi-ringed crater, which Plato also called Atlantis, in Andalusia's palaecoast in the end of the Bronze Age due to earthquakes, a tsunami and land slide constitutes the end of Atlantis.

1. Introduction

Following the new advances in understanding Plato's text (Papamarinopoulos, 2010a, b, c, d, e) we reached Iberia's coast.

There we identified the horseshow platonic basin as Andalusia's basin. Our working hypothesis based on the homeric and non-homeric mythological tradition in connection with the Tartessian prehistoric culture is that in the river delta described by Plato in the 4th century B.C. as Atlantis's delta which was also described by Steisichoros exactly in the same region in the 7th century B.C. a nature made multi-ringed feature once existed. Pre and post platonic ancient Greek writers presented symbolically as Poseidon's act. Philostratus's text, who lived in Roman times, survived *the geological nature of this concentric multi-ringed feature* in Iberia's coast (Papamarinopoulos, 2010d).

2. Catastrophe by earthquakes and floods

Plato describes a catastrophe in a single night and day of the *island at Gadiz*. How can we explain such rapid catastrophe? If we compare the seismicity of Southern Europe and North West Africa over the last century with the corresponding one of the East Mediterranean and especially the Aegean Sea we can easily conclude that the latter exhibits much higher release seismic energy than the first. Figure 1 illustrates the position of epicenters of earthquakes with magnitude above 6 Richter on both ends of the Mediterranean.

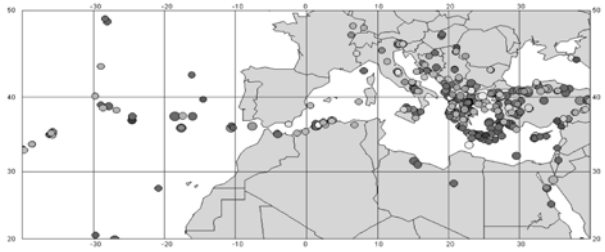

Fig. 1: The distribution of earthquake epicenters above 6.5 Richter (courtesy British Geological Survey).

But then how can we account Atlantis' catastrophe? The answer came at the Melos International Symposium *as thunder* when Gutscher (2005) a C.N.R.S geologist pointed very clearly that the mechanism of Atlantis', which Plato described, can be fully explained in terms of geology and seismotectonics at the bottom of the Atlantic Ocean in the region west of Gibraltar. In his opinion the seismogenous fault called Gorringe Bank, situated about 6 degrees west of Gibraltar, produces earthquakes with a frequency of about 1.200-1.500 years with magnitudes above 8 Richter. The consequent of these giant earthquakes are tsunamis which eventually reach Morocco's and Iberia's coasts simultaneously and hit them with sea waves of 10-15 m heights and with horrible speeds. In Figure 2 the position of Gorringe Bank is shown.

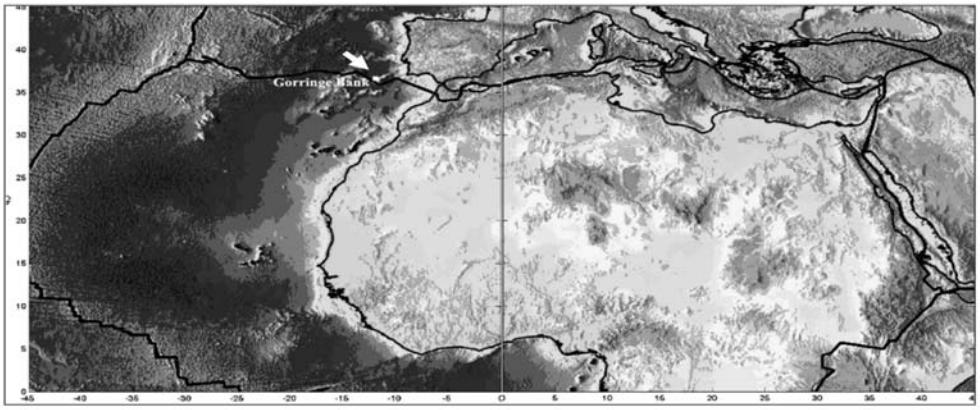

Fig. 2: Gorringe Bank's seismogenous fault (white arrow) position is shown exactly placed on the lithosphaeric contact (black line) between Africa and Eurasia. It is a *possible source* of the prehistoric earthquake which destroyed Atlantis.

Figures 3 and 4 show what Plato wrote about the main seismic event and its aftershocks and the tsunami which produced afterwards. The pictures illustrate what possibly happened in late Bronze Age which destroyed the Iberian culture of prehistoric Tartessos. The geoarchaeological studies in Andalusia's Donana region were initiated recently.

In Figure 5 and 6 Lisbon's (1755 yr A.D.) catastrophe by earthquakes and floods is shown respectively.

In Figure 7 Gutscher's simulation study on the dynamics of a running tsunami in the end of the glaciated period is shown. His simulation is based on the Lisbon 1555 yr A.D. but it can be carried out at any time period based on the consequent chosen palaeocoast.

It shows very clearly what exactly happened in 1755 yr A.D. and is going to happens any time when a tsunami is generated at Gorringe Bank at the Atlantic Ocean's bottom! It seems that Plato led us

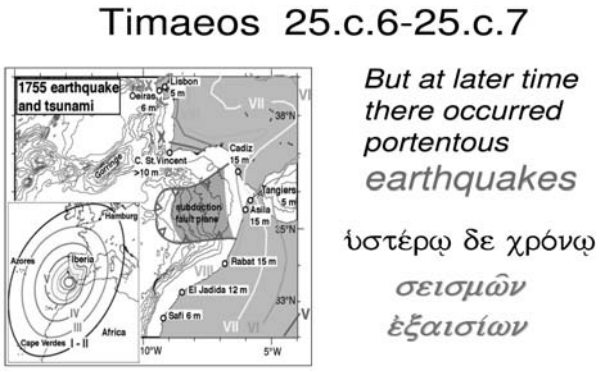

Fig. 3: The Lisbon 1755 yr A.D. earthquake is illustrated in the very region in which the platonic text leads us in the Atlantic Ocean.

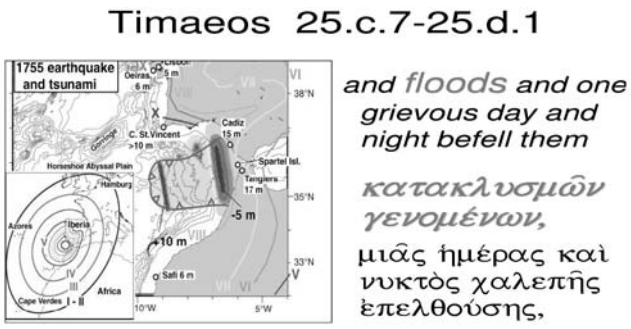

Fig. 4: The Lisbon 1755 yr A.D. advancing tsunami, after simulation, is illustrated in the same region mentioned in Fig.3. The *assumed prehistoric* tsunami of the 12th century B.C. contained *several waves* producing *several floods successively* as the platonic text says in a day and night of misfortune and as the Lisbon 1755 A.D. demonstrated.

Fig. 5: The Lisbon's 1755 yr A.D. seismic catastrophe (after Shrady, 2008).

Fig. 6: Lisbon' 1755 yr A.D. tsunami is shown (after Shrady, 2008).

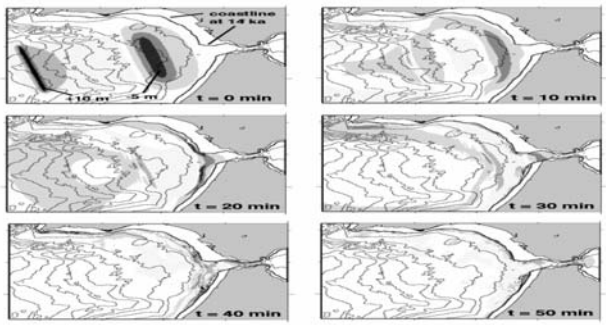

Fig. 7: A simulation study based on of the 1755 yr. A.D. Lisbon's tsunami was conducted by Gutsher (2005).

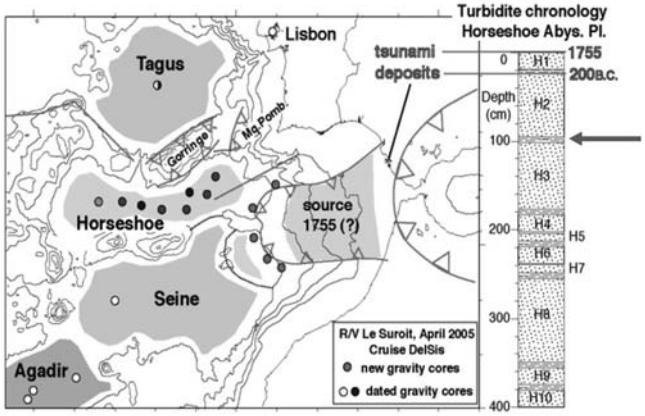

Fig. 8: A *library* of past tsunamis recorded in the sediments of the Atlantic Ocean (after Lebreiro et al, 1997). The first two top tsunamis are recognized and have been proved historically and geologically respectively. If the layer shown, by the author by the arrow, is of the late Bronze Age then the present theory will get its first credit.

to this region round Cadiz in Andalusia and his choice was not fortuitous for the position of his Atlantis because the coast of Andalusia is prone to giant catastrophic phenomena not related with its regular seismicity as Figure 1 clearly illustrates. The danger exists, hidden deeply in the Atlantic Ocean, and any prehistoric city existing in any of the coasts shown above would have been destroyed firstly by earthquakes and then by floods as Plato once described. But do we have any way to know the sequence of these events? The answer is positive and it is shown in Figure 8.

The reader can see two dated events in the stratigraphic column. The first in the top is the historically known 1755 yr A.D. event. Immediately below there is another one of 200 yr B.C. It remains a question if the third turbitide layer, counting from the top, is that which produced the catastrophe of late Bronze Age. Atlantis' catastrophe presents a scenario explaining Troy's, and Athens' catastrophes too in the 12th century B.C. Troy was destroyed, after an extensive rain, by an earthquake. The Achaeans' camp destroyed by a tsunami originating from the sea coast as Homer described. Athens was marked by an extensive rain and by an earthquake and Atlantis was destroyed by earthquakes and a tsunami originating deeply from the Atlantic Ocean in a single night and day. The first two have occurred in the 12th century B.C. and they were confirmed. Troy's and Atlantis' tsunami remains to be proved.

3. The Atlantes

But even the war of the advancing Atlantes as Plato uniquely described was conducted within the late part of the 13th century and the very beginning of the 12th century B.C. It seems that Plato described the second round in which the Sea Peoples attacked Ramses the III Egypt as archaeological

studies have proved without a doubt. All these events are tabulated in the following order.

Plato allows the reader to understand that Solon' initial informants had the strong impression that all attackers entered the Mediterranean basin through the Atlantic Ocean. Today we know that there had been two wars against Egypt and that some of the Atlantes originated from Anatolia. Others originated from Italy and Libya and some others possibly originate from central Europe.

Plato adds another point of interest in connection with Atlantis' influence

Tim25.a.8-25.b.5

"And, moreover, of the lands here within the Straits they ruled over Libya as far as Egypt, and over Europe as far as Tuscany. So this host, being all gathered together, made an attempt one time to enslave by one single onslaught both your country and ours and the whole of the territory within the Straits."

But what is the archaeological opinion about the events and war activities in the specified period toward the beginning of the 12th century B.C.? O'Connor (2000), for instance, discusses the event of 1208 yr B.C. when an aggressive coalition attempted to conquer Egypt in Pharaoh's Menenptah 5th year. Egyptian sources describe the names of the participating coalition being Sherden, Tursha and Shekelesh. These names have been identified as Sardinians, Etruscans and Sicilians all living in the Atlantis' zone of influence which is Tuscany in other words Italy. All these people fought together with Libyans against Egypt. We have *double correspondence* with the Platonic text since these two zones are mentioned in Critias. But there are also *differences*. The Egyptian sources mentioned two more people the Lukki and Ekwesh The first disagreement between archaeology and Plato's account lies with the Lukki which are people living in Lykia in Anatolia. Anatolia was not mentioned as Atlantis' zone of influence. The second possible disagreement in accordance with O' Connor is major because Ekwesh is the name of the Achaeans Greeks! However, Iakovidis (2007) and Sandars (1978) fully disagree with O'Connor. Sandars (1978) in particular wonders how the Ekwesh could be Achaeans when they appeared *circumcised* in accordance with the Egyptian sources. It is a well known fact that Europeans living in Asia or in Europe never practiced circumcision from prehistory to the historic period. The same scientist says that there is not any linguistic relation between the words Ekwesh and Achaeans or even between Ekwesh and Ahiwaya. The latter was the name by which the Hittites called the Achaeans.

Plato continues to describe how the Athenians managed to face the Atlantes alone. He describes it like this Tim25.c.1-25.c.6:

"And acting partly as leader of the Greeks (*meaning the city of Athens*) and partly standing alone by itself when deserted by all others, after encountering the deadliest perils, it defeated the invaders and reared a trophy; where it saved from slavery such as who dwell within the bounds of Heracles it ungrudgingly set free."

Herodotus visited Egypt earlier than Solon but learnt nothing about the two assaults of the Sea Peoples against East Mediterranean. From Plato's text one gets the conclusion that Solon's informants had at least mentioned only one to him and associated it with Athenians. Was it possible that Plato had recorded the second assault of the Sea Peoples? The answer is positive because Achaean mercenaries were not in Egypt before 1208 yr B.C. There is not textual or any archaeological evidence supporting the case. Homer says that the Achaeans arrived to Egypt after the Trojan War in other words after 1184 yr B.C. Consequently there was not any chance to have in Egypt a city such as Sais associated with Achaeans earlier than 1208 yr B.C. Let us examine this second assault which occurred in Pharaoh Rameses the III 8th year. Wachsmann (2000) who studied the Egyptian sources mentioned the names Peleset, Sikala, Sheklesh, Denyen and Weshesh. Sandars (1978) explained in her study that the Deneyn

were not the Achaeans known by a similar name but some peoples living close to Syria at Adana and they had been known to the Egyptians since the 14th century B.C. from the Amarna tablets. The Egyptians called their land Danuna, whereas they called Tanaja the country of the Achaeans which is Peloponnesus of course Banou (2000). We, therefore, conclude that the Achaeans did not contribute to either against or in favour of the Egyptians in the 1176 yr B.C. event. But the Sea Peoples lost the battle. This information is not mentioned in Plato's documents. Consequently how and where did the Greeks manage to defeat the Atlantes since the Atlantes lost the war in Egypt and the Greeks did not face them in Greece or in Egypt? Marinatos (1950) interpreted Plato's Atlantes as a Sea Peoples remote echo. He wrote that a war between Ionian Greeks and the Egyptians' enemies in Sudan 30 years before Solon's visit to Sais in the 6th century B.C., explained, partly the enthusiastic acceptance of Solon by them since was Athenian in other words Ionian. However, Marinatos (1950) said that it is possible that, 600 years earlier than this event of very early 6th century B.C., prehistoric Greeks after Troy's capture, had a war activity outside of Greece against the advancing Atlantes. They did not defeat them entirely but they reduced their initial war capacity and when they reached Egypt, tired, they were defeated completely by Ramses III in the Nile. Both events are lacking historical confirmation in the Greek literature. For instance no celebrations were carried out for these victories in any Ionian city and jet for the 6th century B.C. war victory exists *double archaeological evidence* in Greek and Egyptian languages found in Egypt Gembaza (2010).

Iakovidis (2007) suggested that the Sea Peoples destroyed the prehistoric ports in Greece and Middle East and ruined indirectly the Achaeans' economy. This military action is actually a type of easy looting and not a war strategy but nevertheless was effective. From this looting of the ports many countries suffered in 1176 yr B.C. One of them was Greece. This reminds us the platonic text about common suffering of Egyptians, Greeks and other peoples within the Mediterranean due to pressures by the Atlantes. Although the military victory of the Egyptians is clear the platonic text presents the Greeks as victorious somewhere! Assuming the correctness of the information a possible place where the Greeks could have been victorious is Atlantis itself. Our scenario requires an Achaean leader of the Greeks of Athenian origin to be in Egypt with his companions after the Trojan War. Foliot (1984) says that as we know from Homer Menelaos a warrior of the Trojan War, came to Egypt accidentally due to a storm occurred in the Aegean Sea. It is possible that a part of the victorious Achaeans of Athenian origin in Troy also came to Egypt after the Trojan war of 1184 yr B.C. and remained there at Sais. Zangger (1995) reminds us that Thucydides recounted how the survivors of the Trojan War spread all around the central and eastern Mediterranean. We could add that some of the Mycenaeans went to the West and even passed through the straits into the Atlantic Ocean as Homer says and Tziropoulou (2008) proved in her text. When the Sea Peoples moved against the Eastern Mediterranean in either 1176 or 1177 yr B.C., Athenian warriors, who were already at Sais, decided to go against them one of their own strategic place at Atlantis. This means that Solon was talking to Egyptians through interpreters or to spoken Greek Egyptians. The latter had extracted this information from their own archives as a result of a report of some survivors who had returned to Egypt 600 years before Solon's visit and kept a record of what had happened during the war with the Atlantes in Atlantis. This scenario may explain the friendliness between Gadeirians and Athenians and between the Saitians and Athenians. We would like to clarify the reader that Sais was the city where the story began in the 6th century B.C. and Gadeira is the city which is very close to Andalusia's coast where the story was ended. There, the assumed religious nature made circular center, once was flourishing. It *vanished* in the end of the Bronze Age. Between the two localities the connecting element paradoxically are the Athenians as Plato and Philostratus independently say!

For such a scenario to be proved detailed studies are required both in Sais and the coast of Andalusia. There possibly exists, the multi-ringed nature made religious center, with all possible proofs which

will either support or demolish the presented scenario.

Plato, however, describes the Athenian's victory who built a victorious monument at Atlantis in the following way:

Tim 25.b.7-25.c.4

"For if stood pre-eminent above all in gallancy and all warlike arts, and acting partly as leader of the Greeks, and partly standing alone by itself when deserted by all others, after encountering the deadliest perils, it defeated the invaders and reared a trophy;"

In other words Plato describes Mycenaean Athenians as leaders of the Greeks against Atlantis waging a campaign in which they were victorious. Similarly Mycenaean Peloponnesians being leaders of the Greeks campaigned against Troy. If the reader requests some other sources about what Plato describes he will find nothing among either historians' texts or among any archaeological findings in the Mediterranean countries. It is therefore likely to think that Plato imagined this campaign and the victory of his prehistoric compatriots. The reader, however, knows that Plato described events in Timaeos and Critias for which the historian's silence was characteristic and yet archaeology has proved his writings one by one.

But was it ever possible that Mycenaean Athenians could have been leaders of the Greeks? From the Mycenaean tradition we know King Eurystheus of Tiryns who got killed in a campaign against Mycenaean Athenians. Eurystheus was the king who had demanded from Heracles the realization of the twelve labors. The Mycenaean conflict, between the Peloponnesians and the Athenians which we have just described, is a remote echo of the struggle between tribes of Mycenaeans to impose on each other their will. We can not prove that Mycenaean Athenians were ever leaders of the Greeks but what Plato described seems not to be impossible within the evolution of the Mycenaean world. But Plato does not only describe the victory of the Greeks against the Atlantes but also a double catastrophe in the following way:

Tim 25.c.6- 25.d.3

"But at later time there occurred portentous earthquakes and floods, and one grievous day and night befell them, when the whole body of your warriors was swallowed up by the earth, and the island of Atlantis in like manner was swallowed up by the sea and vanished;"

In other words after the victory of the Mycenaean Athenians against the Atlantes at a region in the Atlantic Ocean there was an unknown time span not defined by Plato. After that there was a catastrophe caused by earthquakes and floods in which the Greeks and the "Atlantes" got lost. Let us examine how Foliot (1984) evaluates these particular platonic events. She judges that the catastrophe was in two different places and not in one, as Plato implies. She explains that due to heavy rain and the occurred earthquake, a part of land at the Acropolis together with the Athenian warriors land slided killing most of them. We do not have any doubt about the severe earthquake. It has been proved and its consequence (broken pots) has precisely been dated as being in early 12th century B.C. For the rest we do not have any findings yet. The catastrophe in Andalusia's coast in 12th century B.C. has not yet been documented.

Plato knew, that when he was 52 years old, Helike vanished in the Corinthian gulf after an earthquake and a tsunami but Peloponnese remained intact. Plato knew what a volcanic catastrophe was because he witnessed himself an Aetna's explosion during the years he was in Italy. Therefore he knew that a giant mass can not easily disappear even if it was connected with either catastrophe mentioned earlier. However, Atlantis' common use for everything in his report induced unwanted confusion which lasted for centuries. But let us go further. Foliot (1984) believes she has the answer of the war of the Atlantes against the Athenians in Greece and she uses the Hellenic mythology to explain it. She mentions Athena's victory against Poseidon in Attica and Hera's victory over the same god in Argos. She identifies the At-

lantes with Poseidon and the Greeks with Athena and Hera respectively. But she fails in this interpretation because the Atlantes, in other words the Sea Peoples, as Marinatos (1950) first proposed they were, did not fight with the Greeks in Greece the way they did in Egypt. No traces of war activity were ever found in Greece in the 12th century B.C. On the contrary we have a very good record of what Ramses the III achieved in Egypt against the Atlantes. Plato's view presents a major difference. Let us further examine Foliot's (1984) view. She reminds us, as Homer says, that the Achaeans reached Egypt after the Trojan War where they were received warmly by the Egyptians. It is very possible that the Egyptians who *felt the pressure* of the Sea Peoples and the Libyans in 1208 yr B.C. received the victors of the Trojan War as mercenaries in order to increase their military capacity against their hostile neighbors. In accordance with Foliot's (1984) scenario the Mycenaean Athenians settled in attractive Sais and organized a type of city. In other words several years before the second assault of 1176 yr B.C. of the Sea Peoples against Egypt, the Mycenaeans warriors had already been there. We remind the reader the Mycenaean Athenians with Menestheus as well as their leader had been at Troy with other Mycenaeans just few years before. We also remind the reader of the fact that Menestheus a hero of the Trojan War was honoured in Gadeira by the *hellenised* Gadeirians as Philostratus has recorded in his text. Foliot's (1984) scenario explains the friendliness of the Saitians to the Athenian Solon of the 6th century B.C. and the similarities between the Egyptian goddess Neith and Athena. In Plato's text it appears that the discussion between Solon and the Saitian priests had no problems of conversation.

It appears that the *priests* knew particular details of the Acropolis of Athens of the 12th century B.C. If the people who discussed with Solon were only Egyptians then clear difficulties would have been in their conversation. However, the text does not mention any difficulty in conversation. We find very strange that *Egyptian priests* had interest for architectural details on the Acropolis of Athens and its eventful history in the 12th century B.C.

But since no war of the Atlantes and the Mycenaeans ever existed within Greece and/or Egypt, then is it possible that such a battle took place at Atlantis? And how the information of the catastrophe reached Egypt? Our scenario assumes a contingent of Mycenaean Greeks under Athenian leadership to travel from Egypt to Andalusia, a place already known to Mycenaean traders, and engaged in a war with the Atlantes. After the natural disaster at Andalusia some of the survivors came back to Sais and kept a record of what had happened there. The archives' content in the 6th century B.C. were made known to Solon a compatriot, so to speak, of theirs. The victory did not remain in the tradition of the Athenians in the main land of Greece not only because there was not any eloquent poet, such as Homer, to write about but also because the informants remained only at Sais. Another Achaean victory which did not interest any poet was that of the first fall of Troy 30 years before the legendary Trojan War. In the Eastern part of Aphaea's temple (490-480 yr B.C.) on the island of Aegina details of that first war against Troy are given with Ajax's father, whereas in its Western part Ajax himself is shown, Kakridis (1986). Yet some tradition remained even in the absence of an epic poem. Although Plato's story is differentiated with respect to the present day archaeological knowledge, we propose that his differentiation signals a parallel history within the turbulent 12th century B.C. unknown to science so far. It is not necessarily diametrically opposed to the existing archaeological knowledge in Egypt of the war of 1176 yr B.C.

However It contains exaggerations, mistakes and anachronisms which can be removed. The origin of the Peoples of the Sea remains enigmatic and the whole issue is still open. Betancourt (2000) for instance, does not accept the simplistic view that the Sea Peoples were Aegean Sea Peoples who left the Aegean Sea due to hardships and, *en route to settle in Palestine*, fought with the Egyptians and then *became* the Philistines of Middle East. Certainly their name is not included in the list of the names that attacked Egypt in 1176 yr B.C.

Wachsmann (2000) mentions the possibility that between the Sea Peoples there were warriors from central Europe! He says that "t*he bird-boat motif is not a symbolic device common to Mycenaean cultural realm. Notable in this regard, therefore, is a bird-boat-like depiction painted on the sherd of Late Helladic IIIC krater sherd found in Tiryns "* Wachsmann (2000) continues saying "*The manner in which the bird-heads are positioned on the stem and stern of the ship form a sea going "bird-boat" As this motif is foreign to the Mycenaean world, we must conclude that the specific ship used by the Medinet Habu artists as a prototype for their five depictions of a Sea Peoples' ship, was manned by a crew that held religious beliefs consistent with those of the Urnfield culture. Or, to put it plainly, the crew was likely to have been composed of Urnfield people*.

In the following Table I the military activities of the Achaeans and of the Atlantes are tabulated versus time. We can not know if there was any military activity between the Achaeans and the Atlantes in Andalusia or even if there was any multi-ringed feature which was destroyed in its coast in the platonic way. However, we know that some of Plato's passages, for which no other independent sources exist, have been confirmed so far one by one by archaeology. Kunhe (2008) concludes that Atlantis is in the same place as the author of this study suggests. He believes that Plato knew the Medinet Habu archives and used them the way *he liked*. Kunhe's (2008) view does not, however, explain the friendliness of the Saitian priests to Solon and the Athenians in general. Neither does he explain the Gadeirian's friendliness toward the Athenians and nor the honoring by them of the Athenian Menestheus a hero of the Trojan War. He does not take into account that Gadeira was part of Atlantis and of course he does not connect it at all with the Athenians.

The same researcher does not take into account Homer who described the Achaeans' arrival to Egypt after the Trojan War. Finally he equates Tartessos with the concentric formation. However, Tartessos, existed up to the Roman period and *vanished smoothly* due to the accumulations of continuous added sediments by Guadalquivir river. Some old authors have reached the same conclusion, as the present author, but without taking into account *all the geomythological and geoarchaeological data* available to them at the period of their publications Schulten (1924), Jessen (1925), Whishaw (1928), Wickboldt (2007), Kunhe (2008).

Table I. Achaean and Atlantean military operations in the 12th century B.C.

1224:	First fall of Troy by Ajax's father and his companions
1208:	First assault of the Sea Peoples (Atlantes) against Egypt
1195:	Beginning of the Trojan War
1184:	Second fall of Troy by Ajax and his companions
1184+:	Achaean's return to Greece.
	General instability is exhibited in Greece. *Agamemnon's murder*
1184+:	Achaean's arrival in Egypt
1176:	Second assault of the Sea Peoples (Atlantes) against Egypt
1177:	Odysseus' return to *Cephalonia* from Atlantis,
	(Papamarinopoulos, 2007a) and (Tziropoulou, 2008)
1177+:	Atlantis' *possible* catastrophe

Odysseus' return from Atlantis in 1177 yr B.C. (Papamarinopoulos, 2007a), in the way Homer described it, indicate Achaean knowledge of the region. However, it illustrates that the sacred coastal cyclic feature was still functioning in spite of the beginning of the seismicity and before its complete annihilation. This means that after Odysseus' return the Athenians got in conflict with the Atlantes. Since we do not have any tradition in Athens as a memory of that victory, we can either accept that Plato

invented the war, the victory and the catastrophe at Atlantis or that a contingent of Achaeans with Athenians from Egypt as leaders did a military operation in Atlantis. The remaining survivors returned to Egypt and kept a record of the events. These *particular archives* remained in Sais for 600 years and were made known to Solon due to his Athenian origin in the 6th century B.C.

4. Conclusions

1. Atlantis' catastrophe by earthquakes (main and aftershocks) and by floods in a day and night is explained in geologic terms fully as a very strong above 8 Richter earthquake which occurred *possibly* in Gorringe Bank's seismogenous fault and a tsunami which followed within the same day. It remains to be proved by the dating of a particular turbidity layer found in cores extracted by marine geologists from the bottom of the Atlantic Ocean.

2. Taking into consideration the Hellenic mythology and an ostrich's shell found in tombs of the Achaean period in Mycenae (Sandars, 1978), it is shown, that Libya was known, independently of Egypt, to the prehistoric Greeks. Similarly taking into consideration the Hellenic mythology and the amber jewelry originating from the Baltic and found in tombs of the Achaean period in Mycenae, it is indicated that Europe's West coast was known. Moran (2003) proved that the Baltic amber was manufactured into jewelry in *Britain*. In addition the discovery of a Linear B tablet in Munich in Germany and the discovery of a Mycenaean sherd in Guadalquivir's estuary indicate again some knowledge of the European Western coast by the prehistoric Greeks mariners. In the pre-cartographic period, before Herodotus world map, some general geographic notes were possibly kept from these areas due to the exchange of trade between Achaeans and Libyans and West and/or central Europeans.

3. Without being a historian Plato uses information originating possibly from Egypt, Greece and Italy. This information was not only confined to the Egyptian priests. He seems to describe the second assault of the Sea Peoples of 1176 yr B.C. in which all participants from different nations were called Atlantes by him. For Plato all originated west of the Gibraltar straits. Today we know that some originated from Anatolia. However, he correctly pinpointed Atlantis' two zones of influence Italy and Libya. He was also correct that some of the Atlantes originated outside of the Gibraltar straits since some of them used boats with the Urnfield's culture symbol which was two birds at each edge of the boat (Wachsmann 2000). The platonic text "ignores" Ramses' the III Egyptian victory against the Atlantes in Egypt and *seems* to know a Greek victory against the Atlantes. The same text describes a lethal end for victors and defeated ones by earthquake and flood. Is it possible that a parallel story was developed in Egypt with the massive part of the Atlantes and another one with the remaining Atlantes in their religious center? The researcher of the future will face three possibilities: Plato either imagined the Atlantes' assault and the war between Achaeans and Atlantes at Atlantis, or knew the Egyptian archives and changed them in order to embellish the Greeks or he described a parallel truth unknown to historians which requires scientific attention and evidence. Marinatos (1950) explained the Egyptian priesthood's enthusiasm when Solon in the 6th Century visited them because he knew that a Greek army composed from mercenaries of Ionian origin hit and destroyed fully the Egyptians enemies in Soudan 30 years before Solon's visit. He proposed that something similar might have occurred with prehistoric Greeks after the Trojan War who fought against the Atlantes (Sea Peoples) outside of Greece and tired then before they reach Egypt in which got annihilated by Ramses the III. Both wars of 12th and 6th century B.C. do not have support of historians. However for the second there is double archaeological evidence in Egypt both in Greek and in Egyptian writings (Gembaza, 2010).

4..Critics who mentioned the antiquity's sole negator, Strabo, with respect Atlantis neglecting to present Plato's supporters in the same issue, like Crantor, Proklos, Poseidonius and others, do not offer service to science. Strabo and Doumas (2007) became victims of not taking into account the island's

meaning evolution versus time in the Greek language, the common name Atlantis given by Plato to the giant island, the horseshow basin and the concentric scheme and of not understanding the tsunami's concept mentioned both by Homer in connection with the Achaean camp's catastrophe in Troad's sea coast in the 12th century B.C. and by Plato in connection with Atlantis catastrophe respectively in Spain in the same 12th century B.C..

Dedication

To Athena, Alexander and Artemis

5. References

Banou, E., 2000. Amenhotep III and his relation with the Aegean. The official trip Crete-Egypt. The official trip catalogue. Ministry of Culture. Editors: Alexandra Karetsou, Maria Andreadaki-Vlazaki and Nikos Papadakis. ISBN 960-7254-93. (In Greek).

Betancourt, P. P., 2000. The Aegean and the origin of the Sea Peoples. The Sea Peoples and their world: A reassessment, E. D. Oren (Editor), University of Pennsylvania Museum, p.p. 360.

Crantor.

Doumas, Ch., 2007. The search for Atlantis: The utopia of a utopia. Proceedings of the International Conference: The Atlantis Hypothesis: searching for a lost land, Melos Island 11-13 July 2005, Publisher: Heliotopos, Editor: Stavros Papamarinopoulos, p.p. 1-7.

Foliot, K.A., 1984. Atlantis revisited. "A documented account of the fabled island as it was long ago and it is today". Information Printing, Eynsham, Oxford, p.p. 129.

Gembaza, T., 2010. Plato's Atlantida nesos as the "Island of Meroe" Part III: Consistency of the "Island of Meroe" with Atlas' kingdomProceedings of the International Symposium: "The Atlantis Hypothesis: searching for a lost land, Athens, 10-11 November, 2008, Publisher: Heliotopos, Editor: Stavros Papamarinopoulos, (In print).

Gutscher, M-A., 2005. Destruction of Atlantis by great earthquake and tsunami? A geological analysis of the Spartel Bank hypothesis. *Geology*, 33, p.p. 685-688.

Kunhe, R.W., 2008. Did Ulysses travel to Atlantis? Proceedings of the present symposium. Homer, Science and Technology. Ancient Olympia, (2006). Editor: St.A.Paipetis, p.p. 509-514.

Iakovidis, S., 2007. Personal communication in Mycenae.

Lebreiro, S.M., McCave, I.N., and Weaver, P., 1997. Late Quaternary turbitide emplacement on the Horseshoe abyssal plain (Iberian margin). *J. Sedimentary Res*. 67, 856-870.

Marinatos, S., 1950. Περί τον θρύλον της Ατλαντίδος, Κρητικά Χρονικά 4, δημοσιευμένες σελίδες, 195-213.

Moran, J., 2003. Personal communication at Tiryns.

O' Connor, D., 2000. The Sea Peoples and the Egyptian Sources. The Sea Peoples and their world: A reassessment, Editor: Elieser D. Oren. Publisher:, University of Pensylvania-The University Museum, p.p. 85-101.

Papamarinopoulos, St.P., 2003. Was Plato's Atlantis the island of Santorini? Proceedings of the international symposium, "Extra ordinary machines and structures in antiquity", Ancient Olympia, 19-24 August 2001. Editor: St.A.Paipetis, Peri Tecnon., p.p. 259-265.

Papamarinopoulos, St. P., Drivaliari, N. & Coseyan, Ch., 2007. Red tears in the Atlantic Ocean. Proceedings of the International Conference: The Atlantis Hypothesis: searching for a lost land, Melos Island 11-13 July 2005, Publisher:Heliotopos, Editor: Stavros Papamarinopoulos, p.p. 539-571.

Papamarinopoulos, St.P., 2010. Plato and the seismic catastrophe in the 12th century B.C. Athens. Proceedings of the International Conference: The Atlantis Hypothesis: searching for a lost land, Athens 10-11 November 2008, Publisher: Heliotopos, Editor: Stavros Papamarinopoulos, (in print).

Papamarinopoulos, St.P., 2007a. The memory of a comet during the Trojan war. Proceedings of the present symposium. Homer, Science and Technology. Ancient Olympia, (2006). Editor: St.A. Paipetis, p.p. 341-356.

Papamrinopoulos, St. P., 2007c. A Bronze Age catastrophe in the Atlantic Ocean? Proceedings of the International Conference: The Atlantis Hypothesis: searching for a lost land, Melos Island 11-13 July 2005, Publisher: Heliotopos, Editor: Stavros Papamarinopoulos, p.p. 555-571.

Papamarinopoulos, St.P., 2010. Atlantis in Spain, Part I: Plato science and mythology. Proceedings of the current volume of the 12th International Symposium of the Hellenic Geological Society, Patra, May 19-22.

Papamarinopoulos, St.P., 2010. Atlantis in Spain, Part II: The case of prehistoric Athens. Proceedings of the current volume of the 12th International Symposium of the Hellenic Geological Society, Patra, May 19-22.

Papamarinopoulos, St.P., 2010. Atlantis in Spain, Part III: Removing the misunderstandings. Proceedings of the current volume of the 12th International Symposium of the Hellenic Geological Society, Patra, May 19-22.

Papamarinopoulos, St.P., 2010. Atlantis in Spain. Part IV: The concentric city. Proceedings of the current volume. of the 12th International Symposium of the Hellenic Geological Society, Patra, May 19-22.

Papamarinopoulos, St.P., 2010. Atlantis in Spain, Part V: Atlantis' location.

Philostratus (Flavios).

Plato.

Poseidonius.

Proklos.

Richter, U., 2007. Plato´s Atlantis was in a River Delta. Proceedings of the International Conference: The Atlantis Hypothesis: searching for a lost land, Melos island 11-13 July 2005 (in print) Strabo Geog 17.3.4.18-17.3.4.25.

Sandars, N.K., 1978. The sea peoples. "Warriors of the ancient Mediterranean 1250-1150 yr B.C., Thames and Hudson, p.p. 223.

Schulten, A., 1922. Tartessos-Ein Beitrag zur altesen Gesschichte des Westerns. Hamburg.

Shrady, N., 2008. The last day. Wrarh, ruinj and reason in the great Lisbon earthquakre of 1755. Viking, p.p. 228.

Steisichoros.

Tziropoulou, A., 2007. Homer and the so called Homeric problems. Proceedings of the present symposium. Homer Science and Technology, Ancient Olympia, (2006). Editor: St. A. Paipetis, p.p. 451-467.

Wachsmann S., 2000. To the Sea of the Philistines. The Sea Peoples and their world: A reassessment, E. D. Oren (Editor), University of Pennsylvania Museum, p.p. 360.

Whishaw, E.M., 1928, Atlantis in Spain. Adventures Lmt, p.p. 284.

Wickboldt,W., 2007. Locating the capital of Atlantis b strict observation of the text by Plato. Proceedings of the International Conference: The Atlantis Hypothesis: searching for a lost land, Melos Island 11-13 July 2005, Publisher:Heliotopos, Editor: Stavros Papamarinopoulos, p.p. 517-523.

Zangger, E., 1995. Who were the Sea Peoples? Aramco World, vol.46, no 3, p.p. 21-31.

Zhirov, N., 1970. Atlantis. Atlantology: Basic problems. Progress publishers, Moscow, p.p. 437.

Δελτίο της Ελληνικής Γεωλογικής Εταιρίας, 2010
Πρακτικά 12ου Διεθνούς Συνεδρίου
Πάτρα, Μάιος 2010

Bulletin of the Geological Society of Greece, 2010
Proceedings of the 12th International Congress
Patras, May, 2010

GEODIVERSITY AND SUSTAINABLE DEVELOPMENT: GEOPARKS - A NEW CHALLENGE FOR RESEARCH AND EDUCATION IN EARTH SCIENCES

Zouros N.[1,2]

[1] *University of the Aegean, Department of Geography, 81100 Mytilene, Greece, nzour@aegean.gr*

[2] *Natural History Museum of the Lesvos Petrified Forest, 81100 Mytilene, Greece – lesvospf@otenet.gr*

Abstract

Recently a new initiative on Geoparks was established in Europe in close synergy with UNESCO aiming at the protection, promotion and rational management of geological landscapes and significant geosites as well as the sustainable development of their hosting territories. Geoparks are broader territories which include a number of geosites linked in a network which recognize these features as key-elements for the development of geotourism through conservation and management.

Greece is characterized by a complex geological setting and evolution and was subjected to a variety of geomorphological processes, resulting in a high level of geodiversity. As a result a large number of spectacular landscapes and outstanding or unique geosites are present in the country, and they are not properly managed and protected. The Lesvos Petrified Forest Geopark, the very first Greek Geopark, already counts one decade of successful operation. In order to protect and efficiently manage the petrified forest, the Natural History Museum of the Lesvos Petrified Forest was founded in 1994 as the management body of the Lesvos Petrified Forest Geopark. Next, a management plan for geological heritage protection as well as the sustainable development of the area was carried out linking the promotion of geosites, environmental education and the development of geotourism.

Key words: *Geodiversity, Geoparks management,, European Geoparks Network.*

1. Introduction

Since 1872 when the first national park was established with the creation of the Yellowstone National Park in the USA, in one of the most attractive and emblematic geological localities in the world, a number of Earth heritage sites and landscapes of outstanding scientific, aesthetic and cultural value have been protected for their unique characteristics by national legislation in several countries. Examples include Mount Vesuvius in Italy, the fjords in Norway, the Verdon gorge in France, the Giant's Causeway in Northern Ireland, the Dorset coast in England, Meteora in Greece, Pamukale in Turkey, Uluru in Australia, Niagara falls in Canada, the Devil's tower and the Grand Canyon in the USA, and the Iguazu falls in Brazil/Argentina.

But although exceptional localities of high geomorphological and geological value gain legal protection by national legislation in several countries, abiotic nature in general as well as specific geosites, failed to gain attention autonomously as elements of value for conservation and management within the nature conservation strategies.

The 1972 UNESCO Convention on the Protection of the World Cultural and Natural Heritage provided

the appropriate framework for the protection of exceptional and unique geological and geomorphological localities. Although UNESCO states that "efforts will be made to balance between the number of cultural heritage and natural heritage properties", the lack of a broader sensitivity on Earth heritage led to a misrepresentation of abiotic nature sites on the World Heritage List. Thus, in spite of its importance for the protection and conservation of some outstanding geosites, it was obvious that the World Heritage Convention was not enough for the protection of the Earth heritage sites around the globe.

The 1991 the Digne conference and the "International declaration of the rights of the memory of the Earth" (Martini 1994) was the starting point for the development of new international initiatives and projects aiming at protecting Earth heritage i.e ProGEO - The European Association for the Conservation of the Geological Heritage or the Malvern International Task Force for Earth Heritage Conservation, (1994).

In 1995 the initiative *Global Geosites* aiming the systematic inventory of the most important geosites was undertaken by the Global Geosites Working Group, set up by the International Union of Geological Sciences (IUGS) with the support of UNESCO. This initiative intended to identify geosites to be included in a global site database and to aid protection projects, but failed to gain the legal support of national governments and was abandoned in 2003.

The Geopark initiative arose in 1996 during the 30th International Geological Congress held in Beijing. During the Symposium on geological heritage issues were discussed dealing with the progress on geoconservation, effectiveness of the existing organizations and the necessity of the creation of new tools which could produce concrete results on Earth heritage protection and management with the strong involvement and participation of the local communities. As a result, during the following years the Geopark initiative was established and the new concept was defined with the support of the European Union and UNESCO. In June 2000 the European Geoparks Network (E.G.N.) was founded by four European territories, each representing a particular geological and geomorphological heritage: the Reserve Geologique de Haute-Provence – France, the Petrified Forest of Lesvos – Greece, Geopark Gerolstein / Vulkaneifel – Germany, and the Maestrazgo Cultural Park –Spain. The four partners signed a convention on Lesvos Island, Greece declaring the creation of the E.G.N and establishing the main characteristics and criteria for the designation of a territory as a "European Geopark", with the main objective being close cooperation in protecting European Earth heritage and promoting a sustainable development of their territories through geotourism (Zouros et al., 2003; Zouros, 2004). During the last decade the Geoparks initiative has expanded globally with 2004 marking the formation of the Global Geoparks Network which operates under the auspices of UNESCO and includes similar regional networks in other continents (UNESCO 2006).

2. International Geopark Networks

Geoparks are territories with a particular geological heritage. They are or include nationally protected areas and a number of internationally important geological heritage sites (geosites and geomorphosites) on any scale, or a mosaic of geological entities of special scientific importance, rarity or beauty. These features are representative of the region's geological history and the events and processes that formed it. Geoparks focus not only on the identification and protection of Earth heritage sites, but join this aim with geosite conservation and rational management, improvement of public understanding on abiotic nature and the sustainable local development through geotourism. Geoparks have well-defined limits and comprise a large enough surface area for it to serve real local economic and cultural development. (Zouros et al., 2003; Zouros, 2004; Eder and Patzak, 2004; UNESCO 2004).

The European Geoparks Network (E.G.N.) operating during the last decade with the support of the E.U. and UNESCO, has expanded to include 35 territories across thirteen European countries (France, Ger-

many, Greece, Spain, Italy, Ireland, U.K., Austria, Romania, the Czech Republic, Portugal, Norway and Croatia) in 2009. The structure of the European Geoparks Network is relatively simple and comprises an Advisory Committee (11 members including representatives of UNESCO, IUGS and IUCN) and a Coordination Committee (comprising of two representatives from each member). Decisions concerning the network are only taken by the Coordination Committee. As part of the Coordination Committee, there is an elected EGN Coordinator and Vice Coordinator to represent the whole Network. They coordinate contacts with other international bodies (E.U., UNESCO, IUGS, IUCN, Council of Europe etc.) and prepare the agenda of the meetings in cooperation with the meeting hosts (Zouros and McKeever, 2009).

Following the successful model of the European Geoparks Network in February 2004, UNESCO established the Global Network of Geoparks (G.G.N.), a global forum of cooperation among National Geoparks worldwide, in order to promote the three goals of conserving a healthy environment, educating the public in Earth Sciences at large, and fostering sustainable economical local development. UNESCO recommends the creation of similar regional networks, reflecting local conditions, elsewhere in the world. Today, besides the European Geoparks Network, the Asia-Pacific Geoparks Network (A.P.G.G.N.) formed in 2007 is also active and other regional networks are under consideration in Latin America, North America and Africa. The Global Geoparks Network consists of regional networks 63 members (1 in Australia, 1 in Brazil, 22 in China, 34 in Europe, 1 in Iran, 3 in Japan, 1 in Malaysia - November 2009).

Protection and sustainable development of Earth heritage and geodiversity through Geopark initiatives contributes to the objectives of Agenda 21, the Agenda of Science for Environment and Development into the twenty-first century adopted by the United Nations Conference on Environment and Development (UNCED, Rio de Janeiro, 1992) and reconfirmed by the World Summit on Sustainable Development 2002 in Johannesburg[1]. In spite of the differences that obviously exist from other protected areas, geoparks meet the general purposes contained in the IUCN - the World Conservation Union definition for protected areas as " an area of land and/or sea especially dedicated to the protection and maintenance of biological diversity, and of natural and associated cultural resources and managed through legal or other effective means" (IUCN 1994). Geoparks as protected territories should not be islands in a sea of development but must be part of every country's national strategy for sustainable management and the wise use of its natural resources, and must be set in a regional planning context, following the declaration of the IV World Congress on National Parks and Protected Areas, in Caracas, Venezuela 1992 (IUCN 1994). The IUCN management categories system provides a common international standard for classifying the many different types of protected area designated in countries around the world, based on primary management objective (Green and Paine 1997). IUCN defined six categories of protected areas. The inclusion of an area in the proposed categories should be assigned on the basis of the primary management objective as contained in the legal definitions on which it was established.

I Strict protection (i.e. Strict Nature Reserve / Wilderness Area).
II Ecosystem conservation and recreation (i.e. National Park).
III Conservation of natural features (i.e. Natural Monument).
IV Conservation through active management (i.e. Habitat/Species Management Area).
V Landscape/seascape conservation and recreation (i.e. Protected Landscape/Seascape).
VI Sustainable use of natural ecosystems (i.e. Managed Resource Protected Area).

[1].The **Johannesburg Declaration on Sustainable Development** was adopted at the World Summit on Sustainable Development (WSSD). The Johannesburg Declaration builds on earlier declarations made at the United Nations Conference on the Human Environment at Stockholm in 1972, and the Earth Summit in Rio de Janeiro in 1992. (Johannesburg Declaration on Sustainable Development, A/CONF.199/20, Chapter 1, Resolution 1, Johannesburg, September 2002).

Within the above mentioned categories, geosites and geological monuments are included in Category III. According to the proposed definition, Category III includes Natural Monuments: protected area containing one, or more, specific natural or natural/cultural feature which is of outstanding or unique value because of its inherent rarity, representative or aesthetic qualities or cultural significance. The area should contain one or more features of outstanding significance (appropriate natural features include spectacular waterfalls, caves, craters, fossil beds, sand dunes and marine features, along with unique or representative fauna and flora; associated cultural features might include cave dwellings, cliff-top forts, archaeological sites, or natural sites which have heritage significance to indigenous peoples). The area should be large enough to protect the integrity of the feature and its immediately related surroundings" (IUCN 1994).

3. Geodiversity in Greece – protection and management

Greece is primarily a mountainous country, with seventy per cent of its territory covered by mountains (42 summits over 2000m) and a very long coastline, with a plethora of peninsulas and islands. The complex geological and geomorphological setting and evolution of the Greek orogen, the Hellenides, resulted to the presence of a high geodiversity. GRAY (2004) defines geodiversity as the natural range of geological (rocks, minerals and fossils), geomorphological (landform, processes) and soil features. The Hellenides consist a variety of imbricated tectonic napes of the Alpine orogeny. The Neogene evolution of the area is related with extensive volcanism and active tectonics. As a result, a large number of spectacular landscapes and outstanding or unique geosites are present in the country.

Since 1937, Greece has started to identify natural areas and place them under special protection. Natural areas are identified as protected areas either according to existing national legislation, or through international conventions and international or European initiatives. Furthermore the sites of the Natura 2000 network are areas of conservation of natural habitats and species of wild fauna and flora of Community interest. In many cases the same area is listed both in national, European and International level. As far as the national legislation is concerned, the declaration of protected areas, in various categories of protection, was based up to 1986 mainly on Forest Law. National Woodland Parks, Aesthetic Forests and Natural Monuments and Landmarks are stipulated by Law No. 996/1971. Wildlife refuges, Controlled Hunting Areas and Game Breeding Stations are stipulated by Law No 177/75, as amended by Law N. 2637/1998. Later on, the Environmental Protection Law was adopted. Law N. 1650/86 following the IUCN definitions further introduced the designation of five categories of protected areas:

- Absolute Nature Reserve Area.
- Nature reserve Area.
- National Park.
- Protected significant natural formation and protected landscape.
- Ecodevelopment Area.

This Law refers clearly to the protection of abiotic components of Nature, but since then very small and timid steps have been taken towards the recognition and protection of the Earth's heritage in Greece.

Some of the most important Greek geosites like the Olympus mount, the Samaria gorge in Crete, the Lavrion ancient mines, the Petrified Forest of Lesvos, the Vikos and Aoos gorges in Epirus, the Vouraikos gorge and the Limnon Cave are included within established protected areas, visited by thousands of visitors each year and benefit from management measures. Others like Meteora – the well known World Heritage site, the Ideon Antron cave, Melidoni and Zoniana caves in Psiloritis Mountain in Crete, the Diros caves in Peloponnesus, the Santorini volcanic caldera, the Nisiros volcano, the Alistrati cave and Aggitis Gorge in Serres etc are established attractions with thousands of visitors each year.

The value of the above mentioned emblematic geosites of Greece is broadly recognized, but the Greek

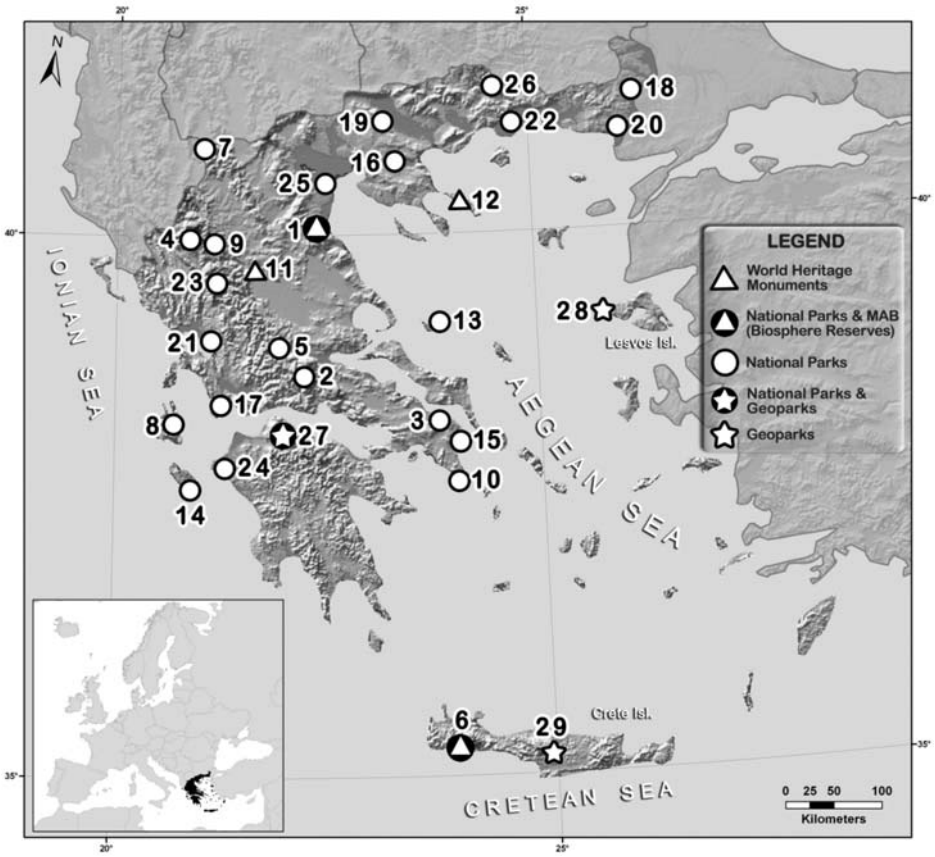

Fig. 1: Protected areas in Greece hosting significant geosites.
(1 – Olympus Mnt. NP, 2 – Parnasos Mnt. NP, 3- Parnitha Mnt. NP, 4 Vikos – Aoos NP, 5 Iti Mnt. NP, 6- Samaria NP, 7-Prespes Lakes NP, 8 Aenos Mnt. NP, 9 N. Pindos NP, 10- Sounion NP, 11- Meteora – WHS, 12 - Mnt. Athos WHS, 13 – N. Sporades Marine Park, 14 – Zakinthos Marine Park, 15 – Schinias – Marathonas NP, 16 – Koronia – Volvi Lakes NP, 17 – Messolongi – Etolikon NP, 18 – Dadia NP, 19 – Kerkini Lake NP, 20 - Evros delta NP, 21 - Amvrakikos NP, 22 – E. Macedonia – Thrace NP, 23 – Tzoumerka NP, 24 – Kotichi – Strofilia NP, 25 – Axios-Ludias-Aliakmon delta NP, 26 – Prodopi Mnt. NP, 27 – Chelmos – Vouraikos NP, 28 - Lesvos Petrified Forest Geopark, 29 - Psiloritis Geopark).

state has not yet recognized geosites autonomously within the protected areas as elements of value for conservation and management. Protection and management of geosites is associated to the legal characterization of their hosting territory, either as natural protected area or as area of archaeological interest thus is related mainly to the conservation of habitats and ecosystems or it is attributed to their cultural value. However many important and even outstanding geosites which are not included within the already existing protected areas remain without protection and management.

In spite of the efforts of the scientific community there is no national inventory of geosites. An attempt to create a working group for the protection of the geological heritage in Greece was formed in 1995 by IGME and was enlarged with the contribution of scientists from the universities and other institutions. In 2004 the Geological Society of Greece formed the Commission for the Enhancement of Geological and Geomorphological Heritage, which is coordinating the scientific efforts in geoconservation.

Several efforts have been made to identify the most important geosites. During the 80's the first attempt was made by the Greek Institute of Geology and Mining Research (IGME) and a list of 50 geosites was submitted to the Ministry of Culture, but without further result. Next, in the frame of the Geosites project, a geosites framework list for South Eastern European countries was prepared (Theodosiou-Drandaki et al., 2003). Aiming to define the most significant geosites of the Greek archipelago was made by the Natural History Museum of the Lesvos Petrified Forest, in collaboration with the Departments of Geology of the Universities of Athens and Thessaloniki and the Department of Geography of the University of the Aegean (1998-2001). This research project aiming at the selection, description and assessment of geosites in the broad Aegean area was financed by the Ministry of the Aegean. The result was the creation of the Atlas of the geological monuments of the Aegean (Velitzelos et al., 2003; Zouros et al., 2004). During 2006-2008 IGME carried out a research project funded by the 3rd Community Support Framework aiming at the selection, description of geosites, the compilation of an inventory of geosites in Greece and the examination of the potential for new Geoparks.

Concrete and viable results in geosite protection geodiversity management in Greece are related to the operation of the first Greek Geoparks. This is a result of the Geoparks management structure operation as well as of the ongoing evaluation procedure which has been established by the European Geoparks Network. In order to achieve high quality standards in Geopark operation and the services provided to visitors, the EGN established an evaluation procedure for all new applicants for membership in the EGN. EGN membership is limited to a period of 4-years after which a revalidation procedure can lead to the renewal of membership. The revalidation follows similar procedures as the evaluation. Greece is represented in both Geopark Networks by three Geoparks: the Lesvos Petrified Forest founding member of the EGN, the Psiloritis Geopark in Crete (2001) and the Helmos–Vouraikos Geopark (2009), which is the youngest member of the EGN. Geoparks should be managed by a clearly defined structure, organised according to the national legislation of each country and with the ability to enforce the protection, enhancement and sustainable development policies within its territory. Management structures in Greek Geoparks do not follow the same structure as they respond to local peculiarities, but they operate in a similar way to achieve their goals. The Lesvos Petrified Forest is managed by the Natural History Museum of the Lesvos Petrified Forest, the Psiloritis Geopark by the Development Company of Psiloritis AKOM and the Helmos-Vouraikos by the Managing Authority of the Helmos-Vouraikos which is a public body of the Ministry of the Environment.

Geoparks are continuously developing, experimenting and enhancing methods for preserving our geological heritage and supporting the development of scientific research in the various disciplines of Earth Sciences. The main purposes of management in Geoparks are the following:

- Scientific research.
- Maintenance of environmental services.
- Protection of specific natural and cultural features.
- Geodiversity and biodiversity protection.
- Tourism and recreation.
- Education.
- Sustainable use of resources from natural ecosystems.
- Sustainable local development.
- Maintenance of cultural and traditional attributes.

4. Geodiversity management in the Lesvos Petrified Forest

The Lesvos Petrified Forest Geopark is used as en example to explore the results of geodiversity management in this protected area. The Petrified Forest of Lesvos is declared a protected natural monument (Pres-

idential Decree 433/1985). With this decree, one marine and four land sections are protected. These sections cover a large area of 150.000 acres in the regions of Sigri, Antissa and Eressos, the marine section around the islet of Nisiopi or Megalonisi and four land regions as well as individual appearances of fossilized trunks.The Barcelona Convention with its attached Protocols was ratified by Greece under Law 855/78 (OG 235/A/1978) and Law 1634/86 (OG 104/A/1986). Under Protocol «On specially protected areas of the Mediterranean» the Lesvos petrified forest and eight other protected areas have been declared as Specially Protected Areas. The greek framework for the protection of natural sites of European Importance through the "Natura 2000 Network" is created, following the E.U. directive (92/43/EC).The area of the Petrified Forest is included among the sites that constitute the National List of the Natura 2000 Network, after it was included in the Western Peninsula Lesvos - Petrified Forest region (code GR 4110003).

The Natural History Museum of the Lesvos Petrified Forest, aiming at protection and efficient management of the Lesvos Petrified Forest, was founded in 1994. It is a non-profit organisation and the management structure of the Lesvos Petrified Forest Geopark. Its seven-member board encompasses representatives of the state (Ministry of Culture, Ministry of Environment), the local authorities, universities and representatives of the local community. Its scientific, technical and administrative staff includes 10 permanent and 25 temporary employees. The Lesvos Petrified Forest Geopark comprises a core zone (15,000 hectares of the petrified forest protected area) and a broad buffer zone (more than 20,000 hectares of the central volcanic terrains).

Geodiversity management is based on a strategic plan for the sustainable development of the area. This plan links the protection, conservation and promotion of geosites with the development of geotourism and educational activities. The Lesvos geopark has also created links with local tourist enterprises, artisans and women's cooperatives producing local food and drinks. Integrating Earth heritage as an integral part of the territorial identity and combining all the existing resources, this strategy creates a new quality offer both for local stakeholders and geopark visitors. The Geopark strategic plan takes into consideration the existing natural and cultural resources, tangible and intangible, in order to attract not only those interested in Earth heritage monuments but also the general public together with certain focus groups. Thus it aims at raising public awareness of abiotic nature and promoting the Geopark as an ideal destination for recreation and education.

In the Lesvos Geopark, the presence of important geosites (i.e. fossil sites, volcanic structures, craters, and thermal springs, tectonic, erosional and coastal geosites) is accompanied by enchanting landscapes, wetlands, sites of natural beauty and ecological value, protected biotopes and biological reserves, archaeological monuments, medieval castles and monasteries, picturesque villages, local traditions and gastronomy. The Geopark area is also the birthplace of famous people of art and literature such as the great poet Sappho and the philosopher Theophrastus of Eressos who is regarded as the father of botany and mineralogy, the singer and citharede Arion, the poet and citharede Terpander of Antissa who lived in about the first half of the 7th century BC and is regarded as the real founder of Greek classical music and of lyric poetry, and the painter G. Iakovidis (1853-1932). The promotion of the interaction between abiotic and biotic nature, geology and life, nature and culture is very important to call attention to the importance of Earth heritage conservation and protection for nature conservation and administration of territorial identity.

Scientific knowledge and research is a prerequisite for successful geodiversity management as it is necessary in all fields of activities i.e. geosite identification and mapping, conservation, exhibition, interpretation, communication and promotion. Thus a research team was formed and five permanent researchers in Earth and environmental sciences were engaged to support the Geopark's operation. The Museum research team has worked in close collaboration with the Universities of the Aegean, Athens and Thessaloniki since its foundation. This collaboration has proved to be essential towards

geosite and fossil identification and interpretation for the public. The Museum also established collaboration agreements with other museums, universities, research institutes and Geoparks in Greece and abroad. Many researchers, PhD, master and undergraduate students have used the opportunity of a placement at the Museum and to collaborate in a variety of research projects in the broader field of Earth and environmental sciences.

The Museum exhibitions, the Aegean geosite inventory, the Lesvos geosite map as well as the creation of installations and activities for geosite protection and interpretation are based on the results of this scientific research. Several geosites were identified within the overland area, along the coast and in the marine zone of the Lesvos Petrified Forest Geopark. Paleontological excavations in the petrified forest area, ongoing since 1997, include systematic excavations within the parks as well as in rescue excavations in sites of public or private construction within the protected area. Geosite protection measures comprise regular maintenance (fencing, cleaning) and janitor services to protect geosites against abuse and vandalism, geosite monitoring providing the necessary measures and protective installations against weathering and erosion, treatment of vulnerable geosites with annual conservation and protective measures (preparation, sealing). Conservation work on fossil plants started in 1998 by the Museum conservation team both for in situ fossil trees located in the parks, and in the conservation labs for smaller objects kept within the museum premises.

The Museum and its exhibitions were designed with two objectives: the first to offer the best conditions for the exhibition and interpretation of the fossil plant exhibits of the Lesvos Petrified Forest and secondly to be a Museum that welcomes and befriends its visitors. Scientific research, mapping and excavations result in the exhibits that constitute the main part of the museum collections while another essential component comes from donations which provide data for the interpretation of the processes and phenomena that form the Earth's crust evolution in the Aegean region.

The creation of the Petrified Forest visiting parks, the creation of geotouristic trails linking sites of interest within the geopark, the placement of geosite interpretation panels and info points are essential elements for the operation of the Lesvos geopark, providing to the Geopark visitors access to the geological heritage and information of the processes that led to the creation of this natural monument 20 million years ago. The main geotouristic infrastructure in the Lesvos geopark are the "lava paths" that lead visitors along the ancient path of the pyroclastic flows from the main volcanoes to the Petrified Forest. These are footpaths that link the various geosites and other sites of interest throughout the geopark. Panels along the footpaths provide information about the different geosites that the visitor will encounter along the way. On entering the Lesvos geopark region, signs along the Mytilene-Kalloni-Sigri road direct the visitor towards the Petrified Forest and demarcate the borders of the protected area. Walking trails start from different points along the main road.

Scientific results are the basis for the development of a broad range of activities for the Lesvos geopark that assist in raising public awareness about the importance of geosites, including guided tours in the petrified forest parks, the development of environmental education programmes on geosites, the organisation of summer schools and field camps for university students, the establishment vocational training seminars for unemployed young people, the publication of books and field guides, the production of CDs and DVDs and the promotion of monumental geosites.

Thus not only the geopark visitors but also the local population and especially the your students living within the geopark realise that certain "rocks" in the vicinity of their houses represent remnants of outstanding phenomena and processes and demonstrate the geological history of their living area. In this way geoforms and rocks gain a new identity for the people and at the same time become objects to be respected and protected.

5. Conclusions

Geology and landscape have profoundly influenced society, civilization, and the cultural diversity of our planet but geosites failed to gain attention autonomously as elements of value for conservation and management within the nature conservation strategies.

The Geoparks Network is a new initiative aiming at geodiversity management and protection adopting a holistic approach in nature conservation. The main goal of geoparks is to improve and augment the recognition, protection, conservation and promotion of their geological and geomorphological features, but their interest also concerns the biological elements and cultural sites they contain. The Geoparks initiative adds a new dimension to the 1972 Convention concerning the Protection of the World Cultural and Natural Heritage by highlighting the potential for interaction between socio-economic and cultural development and conservation of the natural environment (UNESCO, 2006). Geoparks address the strong need for the effective management of important geological sites and for the sustainable economic development of rural areas through the development of geotourism thus enhancing the value of their Earth heritage, landscapes and geological formations. For the effective management of a Geopark it is essential to establish a solid, flexible and powerful management structure that will be able to decide on the protection, promotion, economic development and progress of the geopark.

With the Natural History Museum of the Lesvos Petrified Forest as its management body, the Lesvos Petrified Forest European and Global Geopark can provide a good example of successful geodiversity management in a Geopark territory. The Geopark management plan is based on scientific results and includes a variety of activities aiming at geoconservation, geosite interpretation and promotion, the creation of geotouristic and educational activities and local development in order to raise public awareness of the values of Earth heritage conservation.

6. References

Dudley, N., (Editor), 2008. *Guidelines for Applying Protected Area Management Categories*. Gland, Switzerland: IUCN. x + 86pp.

Eagles, Paul F.J., McCool, Stephen F. and Haynes, Christopher D.A., 2002. *Sustainable Tourism in Protected Areas: Guidelines for Planning and Management*. IUCN Gland, Switzerland and Cambridge, UK. xv + 183pp.

EKBY, 2009. Protected areas in Greece. Available online at: http://www.ekby.gr

European Geoparks Network EGN Magazine. No 1-6. Available online at: http://www.europeangeoparks.org

Eder W., Patzak M., 2004 – Geoparks - geological attractions: a tool for public education, recreation and sustainable economic development. *Episodes*, 27/3, 162–164.

Gray M., 2004 – *Geodiversity, valuing and conserving abiotic nature*. J. Wiley & Sons, Chichester, 434 p.

IUCN, 1994. Guidelines for Protected Area Management Categories. CNPPA with the assistance of WCMC. IUCN, Gland, Switzerland and Cambridge, UK. x + 261pp. Available online at: http://www.unep-wcmc.org/protected_areas/categories/eng/index.html

Mc Keever P. and Zouros N., 2005. Geoparks: Celebrating earth heritage, sustaining local communities. *Episodes* vol. 28, No 4, p. 274-278.

Mac Keever P., Zouros N., Patzak M., 2009. Global Network of National Geoparks. *World Heritage* No 52, 54.

Martini G. (Ed.), 1993 – *Actes du premier symposium international sur la protection au patrimonie géologique* [Proceedings of the First Symposium on Earth Heritage Conservation], Digne, France, 11–16 June 1991. *Mémoires de la Societé géologique de France, numéro spécial* 165, 276 p.

Theodossiou-Drandaki I., Nakov R., Wimbledon W.A.P., Serjani A., Neziraj A., Hallaci H., Sijaric G., Begovic P., Petrussenko Sv., Tchoumatchenco Pl., Todorov T., Zagorchev I., Antonov M., Sinnyovski D., Diakantoni A., Fassoulas Ch., Fermeli G., Galanakis D., Koutsouveli A., Livaditi A., Papadopoulou K., Paschos P., Rassiou A., Skarpelis N., Zouros N., Grigorescu D., Andrasanu Al., Hlad Br., Herlec U., Kazanci N., Saroglu F., Dogan A., Inaner H., Dimitrijevic M., Gavrilovic D., Krstic B., Mijovic D. , 2003 – IUGS Geosites project progress - a first attempt at a common framework list for South Eastern European Countries. Proceedings of the conference *"Natural and cultural landscapes"*. The Geological Foundation, Dublin, Ireland, 9-11/9/2002, 81-89.

UNESCO, 2006 – Guidelines and Criteria for National Geoparks seeking UNESCO's assistance to join the Global Geoparks Network, Paris, January 2006. Internal document, 10 p.

Velitzelos, E., D. Mountrakis, N. Zouros, N. Soulakellis, 2003. Atlas of the geological monuments of the Aegean. Ministry of the Aegean, Adam editions, Athens p.352.

Zouros N., 2004. The European Geoparks Network. Geological heritage protection and local development. *Episodes*, 27/3, 165–171.

Zouros N., 2005. Assessment, protection and promotion of geomorphological and geological sites in the Aegean area, Greece. *Géomorphologie: relief, processus, environnement,* no 3, 227-234.

Zouros N., 2007. Geomorphosite assessment and management in protected areas of Greece. Case study of the Lesvos island coastal geomorphosites. Geographica Helvetica, Jg.62, Heft 3/2007, 169-180.

Zouros N. Martini G. Frey M.L., 2003. P*roceedings of the 2nd European Geoparks Network Meeting*, Lesvos 3-7 October 2001, p. 184.

Zouros, N., N. Soulakellis, D. Mountrakis, E, Velitzelos, 2004. Atlas of the geological monuments of the Aegean. Contribution to the protection and promotion of geological heritage in Greece. 32nd International Geological Congress, 20-30 August 2004, Florence, Abstracts, p. 224.

Zouros N. and McKeever P., 2009. European Geopark Network and Geotourism. The 3rd International Symposium on the Development within Geoparks. Geo-heritage Protection and Cooperation. Aug. 22-25, 2009.Tai'an City, Shandong Province, China.

Δελτίο της Ελληνικής Γεωλογικής Εταιρίας, 2010
Πρακτικά 12ου Διεθνούς Συνεδρίου
Πάτρα, Μάιος 2010

Bulletin of the Geological Society of Greece, 2010
Proceedings of the 12th International Congress
Patras, May, 2010

AN ANALYSIS OF GEOLOGICAL TEXTBOOKS, AT 1830-1930

Makri K.[1], Pavlides S.B.[1], Kastanis N.[2]

[1] *Department of Geology, Aristotle University of Thessaloniki, kmakri@geo.auth.gr, pavlides@geo.auth.gr*

[2] *Department of Mathematics, Aristotle University of Thessaloniki, nioka@math.auth.gr*

Abstract

The geological education in Greece is essentially rooted in the second half of the 19th century. Since 1836, when the Secondary Education was legislated in Greece, in spite of the fact that Geology is referred to all educational programs, geology was not taught before 1880, due to the lack of competent teachers and their books. The deficiency is limited with the first complete edition of the book Geology addressed in Secondary Education. This work presents and analyzes the content of a representative sample of school textbooks of Geology, as the approach of geological theories, including the definition and interpretation of geological phenomena, is the result of the trend, followed by each author.

Key words: *Secondary Education. geological text books.*

1. Introduction

The analysis of school textbooks is based on registering differences, identifying patterns and making comparisons. In this paper, an attempt for the comparison of geological textbooks in Greece is presented. At the present work, two books that were taught at the Secondary Education, "Physical Political Geography" by Con. Mitsopoulos and "Elements of Geology" by Anastasios Megas, and two books that were used at the University of Athens, during the above period, "Elements of Geology" by Con.Mitsopoulos, at 1885, and "Elements of Geology" by the same author, at 1893, are studied. A basic criterion on the selection of the above textbooks is the fact that they were approved by the Ministry of Ecclesiastical Affairs and Public Education, as well as the recognition of their authors. The above academic books are the first complete Greek ones, whose author wrote one of the presented textbooks.

By the comparison of the above books, comments are generated about their compatibility and the uniformity of the level of Geology in Secondary and Academic Education at the University of Athens. The implementation of Geology in Secondary and Academic Education is conducted almost simultaneously, but with significant differences in the content.

2. Geological textbooks

The used school textbooks belong to different time periods from 1885 until 1922. There is no information on the origin and the influences of the books "Elements of Geology" by A. Megas and "Physical and Political Geography" by Con. Mistopoulos. However, it is noted that there is extended literature, mainly German as well as English, French and Italian, at the academic book of the same period, written by the last mentioned author.

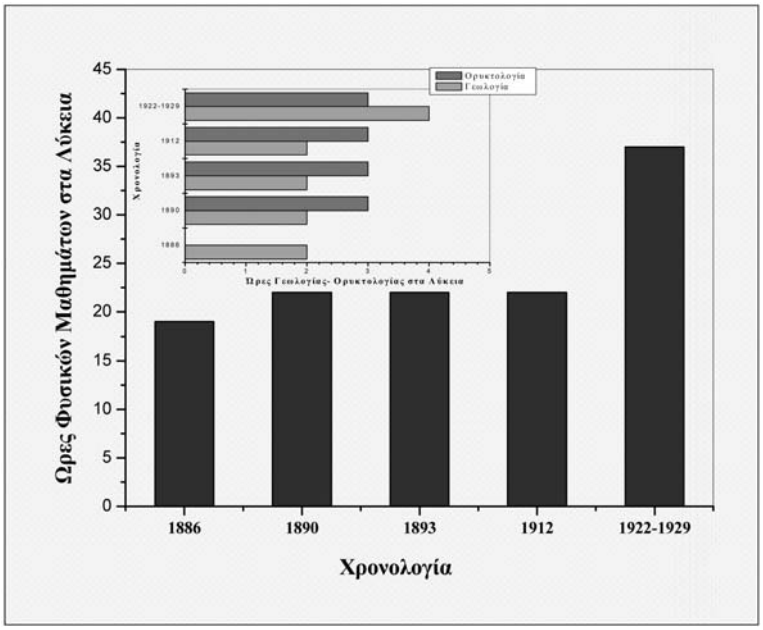

Fig. 1: Development of Natural Sciences in Practical Lyceum (Makri, 2006).

2.1 The appearance of geological education

Since 1836 when the Secondary Education is legislated in Greece, the teaching of Geology is present in all educational programs. Essentially, however, Geology is not taught systematically, due to the lack of competent teachers and validly authorized books. Since 1880, due to the approval of textbooks on Geology by the Ministry of Education, the systematic teaching of Geology is observed, leading to the authorship of new geological textbooks. (Fig. 1).

At the University of Athens, since its establishment in 1839, the seat of Natural History on the subjects Zoology, Mineralogy, Geology and Botany is included at the permanent regular seats. At the schedule study at the University of Athens (*Historical Archives of University of Athens*) since 1864 and until 1911, it is clear that geology was taught daily, while Mineralogy was taught three days per week. Hercules Mitsopoulos (Patras, 1816 – Athens 1892) was the first teacher of Geology until 1890, where he was succeeded by his nephew Constantine Mitsopoulos (Patras, 1846 - Athens, 1911).

2.2 Textbooks of University Education

Con. Mitsopoulos, in his book ***Elements of Geology*** of 1893, cites literature in the preface, mainly from German and English books, by distinguished scientists such as Ch. Lyell, J. Schmidt, and J. Dana (Fig. 2). The self-titled book published in 1885, which is lithograph, the style of content varies slightly from the version of 1893. In particular, the issue of 1893 contained more detailed topics on tectonic structures and seismology. Throughout the book, a narrative structure for natural science subjects, in general, dominates. At the chapter on the utility of Geology, Con. Mitsopoulos refers that peculiar interpretations on Geological phenomena have been attributed at different periods, because Church Authorities did not allow subversive theories and

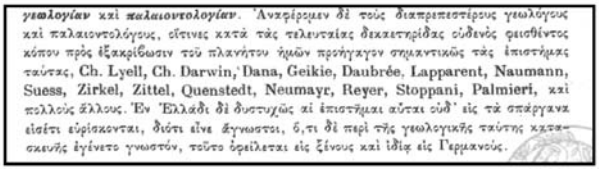

γεωλογίαν καὶ παλαιοντολογίαν. Ἀναφέρομεν δὲ τοὺς διαπρεπεστέρους γεωλόγους καὶ παλαιοντολόγους, οἵτινες κατὰ τὰς τελευταίας δεκαετηρίδας σύδενὸς φεισθέντος κόπου πρὸς ἐξακρίβωσιν τοῦ πλανήτου ἡμῶν προήγαγον σημαντικῶς τὰς ἐπιστήμας ταύτας, Ch. Lyell, Ch. Darwin, Dana, Geikie, Daubrée, Lapparent, Naumann, Suess, Zirkel, Zittel, Quenstedt, Neumayr, Reyer, Stoppani, Palmieri, καὶ πολλοὺς ἄλλους. Ἐν Ἑλλάδι δὲ δυστυχῶς αἱ ἐπιστῆμαι αὗται οὐδ' εἰς τὰ σπάργανα εἰσέτι εὑρίσκονται, διότι εἶνε ἄγνωστοι, ὅ,τι δὲ περὶ τῆς γεωλογικῆς ταύτης κατασκευῆς ἠγένετο γνωστόν, τοῦτο ὀφείλεται εἰς ξένους καὶ ἰδίᾳ εἰς Γερμανούς.

Fig. 2: Details from text book Elements of Geology, 1893.

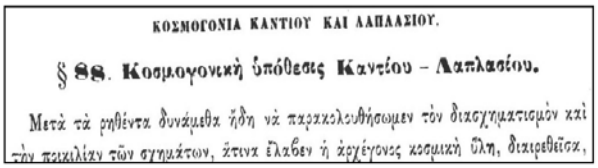

ΚΟΣΜΟΓΟΝΙΑ ΚΑΝΤΙΟΥ ΚΑΙ ΛΑΠΛΑΣΙΟΥ.

§ 88. Κοσμογονικὴ ὑπόθεσις Καντίου – Λαπλασίου.

Μετὰ τὰ ῥηθέντα δυνάμεθα ἤδη νὰ παρακολουθήσωμεν τὸν διασχηματισμὸν καὶ τὴν ποικιλίαν τῶν σχημάτων, ἅτινα ἔλαβεν ἡ ἀρχέγονος κοσμικὴ ὕλη, διαιρεθεῖσα,

Fig. 3: Details from text book Elements of Geology, 1893.

ΚΩΝΣΤΑΝΤΙΝΟΥ ΜΗΤΣΟΠΟΥΛΟΥ

ΣΤΟΙΧΕΙΑ

ΓΕΩΛΟΓΙΑΣ

ΤΟΜΟΣ ΠΡΩΤΟΣ

ΦΥΣΙΚΗ ΓΕΩΛΟΓΙΑ ΚΑΙ ΔΥΝΑΜΙΚΗ ΓΕΩΛΟΓΙΑ

ΕΚΔΟΣΙΣ
ΑΝΕΣΤΗ ΚΩΝΣΤΑΝΤΙΝΙΔΟΥ

ΕΝ ΑΘΗΝΑΙΣ
ΕΚ ΤΟΥ ΤΥΠΟΓΡΑΦΕΙΟΥ ΤΩΝ ΚΑΤΑΣΤΗΜΑΤΩΝ
ΑΝΕΣΤΗ ΚΩΝΣΤΑΝΤΙΝΙΔΟΥ
1893

Fig. 4: Elements of Geology, 1893.

ideas to be taught. Mitsopoulos's view on Geology is clear and he does not hesitate to attack to his criticisers.

Both academic books by Con. Mitsopoulos, there are several references to recognized scientists, of that present time, such as Werner, Lyell and Hutton in geological theories about the creation of the earth. At the above book, two of the opposite theories are presented: the theory which proposed rocks are formed from the crystallisation of minerals in the early Earth's oceans (Neptunism) and the theory which claimed that the volcanic activity was the source of rocks on the surface of the Earth with forms that we see nowadays only arising after erosion or other gradual processes (Ploutonism).

Also Con. Mitsopoulos teaches his students including the cosmogony of Kant and Laplace (Fig. 3) for the gradual creation and evolution of planets due to internal forces of the solar system from an initial cloud, (*αρχέγονος κοσμική ύλη διαιρεθείσα εις διάφορους φωτονεφέλας….αίτινες διαμελισθείσαι εν χρόνω μακρώ*), the alterations in the earth's magnetism, the theory of Isostasy as well as Darwin's theory of Evolution.

2.3 Textbooks of Secondary Education

Anastasios Megas is the author of ***Elements of Geology and Mineralogy*** (Fig. 5). He came from the Siatista and was a teacher and scholar. One of his important studies was the "History of the language issue". He studied literature in Athens, and after his graduation, he worked in Secondary Education (1914 - 20) and then, with an introduction by Nikolaos Politis, he was detached as an editor at the Folklore Archive of the Academy of Athens (1920-27). Anastasios Megas was prominent scholar of his time and experienced teacher, without any academic studies.

At the preface of his book, A. Megas does not allow us to conclude whether the book is a translation or not of a foreign textbook. However, the contained figures as well as the contents, reveal that the author was influenced from the academic book "Elements of Geology" by Con. Mitsopoulos.

The first part states that the Geology studies and describes:


Α. Κ. ΜΕΓΑ

ΣΤΟΙΧΕΙΑ

ΓΕΩΛΟΓΙΑΣ

ΚΑΙ

ΟΡΥΚΤΟΛΟΓΙΑΣ

ΠΡΟΣ ΧΡΗΣΙΝ

ΤΩΝ ΜΑΘΗΤΩΝ ΤΗΣ ΔΕΥΤΕΡΑΣ ΤΑΞΕΩΣ ΤΩΝ ΓΥΜΝΑΣΙΩΝ

ΕΚΔΟΣΙΣ ΤΡΙΤΗ

ΕΝ ΑΘΗΝΑΙΣ

Εκδοσις Ιωαννου Δ. Κολλαρου

1922

Fig. 5: Elements of Geology and Mineralogy, 1922.


ΚΩΝΣΤΑΝΤΙΝΟΥ Μ. ΜΗΤΣΟΠΟΥΛΟΥ

ΓΕΩΓΡΑΦΙΑ

ΦΥΣΙΚΗ ΚΑΙ ΠΟΛΙΤΙΚΗ

ΕΓΚΕΚΡΙΜΕΝΗ

ΠΡΟΣ ΧΡΗΣΙΝ

ΤΩΝ ΕΛΛΗΝΙΚΩΝ ΣΧΟΛΕΙΩΝ

ΕΝ ΑΘΗΝΑΙΣ

1900

Fig. 6: Text book Physical and Political Geography, 1900.

- The changes that still occur today on Earth, due to the uninterrupted operation of wind and water.
- The occurring phenomena until nowadays and reveal the internal structure of Earth.
- The creation and provision of rocks throughout the lithosphere and the formation of mountains, the plains and the sea.
- The different forms or formations existing on Earth and the evolution of organic beings on it.

Mineralogy is the science that studies and describes, respectively:

- The physical properties of minerals.
- The chemical composition and properties of minerals. The usefulness of each one, and mainly the one of the most useful.

Both belong to the science of physiography, which examines and describes everything on Earth, organic and inorganic matter, and across the Earth, as a natural and celestial body.

Of particular interest is the chapter on Geology in the creation of the Earth, which is far from the present data. The description is vivid; it contains scientific terminology and similar myth-making.

At the chapter on Mineralogy, well developed and detailed data crystallography, the planes of symmetry, the Crystallographic axes, the twins, the cracks and fracture, hardness and durability, specific gravity, the electromagnetic properties. More detailed description of the minerals are of economic and scientific interest for the time, that the: Diamond, graphite, the spontaneous sulfur, gold, silver, copper, iron, pyrite, etc.

A particular example is the book ***Physical and Political Geography*** (Fig. 6). by Con. Mitsopoulos. That book was taught in Greek schools, from 1896 to 1901.

Constantine Mitsopoulos followed the footsteps of his uncle, Hercules Mitsopoulos. He studied at the University of Athens, from which he received the first Greek Ph.D in Physics, in 1868, and continued his studies at the University of Freiburg, from where he received the diploma of engi-

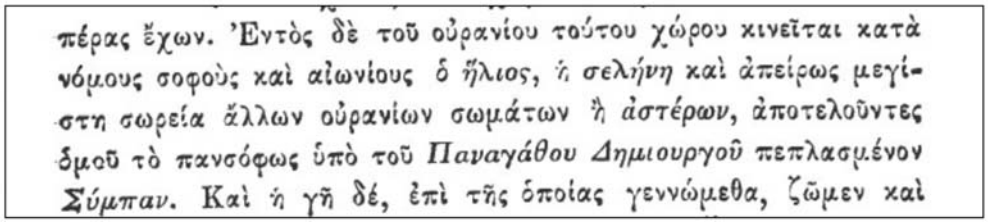

πέρας ἔχων. Ἐντὸς δὲ τοῦ οὐρανίου τούτου χώρου κινεῖται κατὰ νόμους σοφοὺς καὶ αἰωνίους ὁ ἥλιος, ἡ σελήνη καὶ ἀπείρως μεγίστη σωρεία ἄλλων οὐρανίων σωμάτων ἢ ἀστέρων, ἀποτελοῦντες δμοῦ τὸ πανσόφως ὑπὸ τοῦ *Παναγάθου Δημιουργοῦ* πεπλασμένον *Σύμπαν*. Καὶ ἡ γῆ δέ, ἐπὶ τῆς ὁποίας γεννώμεθα, ζῶμεν καὶ

Fig. 7: Details from text book Physical and Political Geography, 1900.

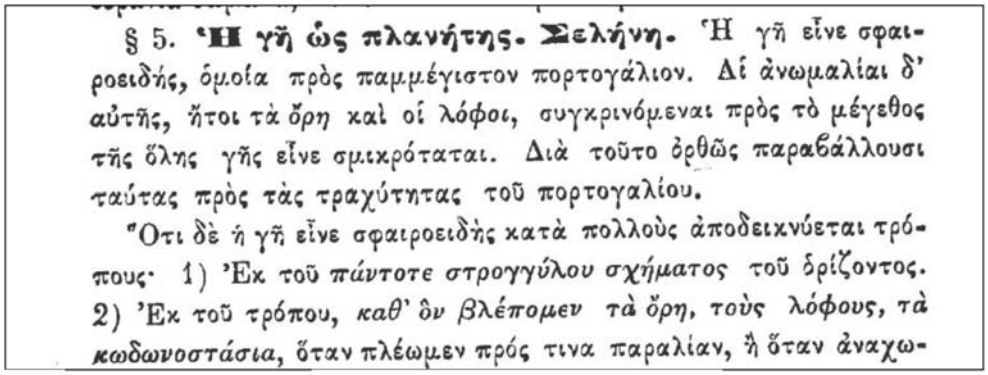

§ 5. **Ἡ γῆ ὡς πλανήτης. Σελήνη.** Ἡ γῆ εἶνε σφαιροειδής, ὁμοία πρὸς παμμέγιστον πορτογάλιον. Δί ἀνωμαλίαι δ' αὐτῆς, ἤτοι τὰ ὄρη καὶ οἱ λόφοι, συγκρινόμεναι πρὸς τὸ μέγεθος τῆς ὅλης γῆς εἶνε σμικρόταται. Διὰ τοῦτο ὀρθῶς παραβάλλουσι ταύτας πρὸς τὰς τραχύτητας τοῦ πορτογαλίου.

Ὅτι δὲ ἡ γῆ εἶνε σφαιροειδὴς κατὰ πολλοὺς ἀποδεικνύεται τρόπους· 1) Ἐκ τοῦ *πάντοτε στρογγύλου σχήματος* τοῦ ὁρίζοντος. 2) Ἐκ τοῦ τρόπου, *καθ' ὃν βλέπομεν τὰ ὄρη, τοὺς λόφους, τὰ κωδωνοστάσια*, ὅταν πλέωμεν πρός τινα παραλίαν, ἢ ὅταν ἀναχω-

Fig. 8: Details from text book Physical and Political Geography, 1900.

neer metallurgist. In 1875 he was appointed as a Temporary Professor of Geology and Mineralogy at the University of Athens; in 1878 as a Temporary Professor of the same courses at the Polytechnic School and in 1880 he was promoted to Ordinary Professor at the University of Athens. He was elected Dean of the University of Athens (1907) and Director of the Technical University (1902-11). The great contribution of Con. Mitsopoulos was the creation of the Mineralogical Museum, at the University of Athens, which is still used until today for the teaching of students on the subjects of Mineralogy and Geology.

The book is consisted of two parts; "General Geography" (Part A) and "Chorogeografia of five continents". (Part B). The first part, which has a geological content, is divided into four separate chapters, Geonomia, Geophysics, Physiographic, Anthropological Geography and Geography.

In the preface of the above book it is mentioned that the universe is a creation of the Wise God and the mankind is the optimum of God's creation, donated with rationality. (Fig. 7).

A typical passage is the description of the shape of the Earth. The round shape of Earth is proven by empirical thoughts, without any mention on the theory of cosmogony (Fig. 8). Throughout the first part there are no references to scientists, both Greeks and Europeans.

Throughout the book, a narrative structure is followed for general issues with simplified physical geography definitions, using simple definitions, without be mentioned on the formation of mankind and Earth. There are not any references on discreet geologists, despite the fact that Con. Mitsopoulos was aware of their work, as it is obvious at his academic books.

At the same time, the content of University textbooks by Con. Mitsopoulos, is of a different style.

The inconsistency between high-school and university textbooks written by Con. Mitsopoulos on the origin of mankind and the creation of the universe is obvious. He is considered as a progressive scientist and one of the early and ardent supporters of the Theory on Evolution. Why did he write in another style for secondary education, while his teaching at the University was dominated by contemporary views. Perhaps the answer lays to the needed approval by the Ministry of Education and Church that had to accompany the school textbook *Physical Geography and Politics*. It is known from the literature that he received severe criticism from Professor of Philosophy S. Lambros and Professor of Mythology and Civil Antiquities N. Politis in 1895, for his, under approval, textbook *Geography,* which was proposed to be taught at the Greek Schools.

3. Conclusions-Results

The content of the textbooks includes knowledge of practical and economic interest (e.g. commercial minerals, exploitable resources). Furthermore, a broad spectrum of subjects such as theories of volcanism, solar activity, and wind and water energy are cited in a descriptive way.

The level and goal of the knowledge on Mineralogy was satisfactory regard to metallic minerals, industrial minerals and valuable stones, since they were relevant to economic and practical applications of Science. On the contrary, the classical taught knowledge on Geology was simply descriptive and, often, the interpretation was conducted using beliefs from mythology and religion.

Essentially, the level of knowledge reflects social and economic needs of the studied period, as well as the need of construction of metal and salt mines.

There is a significant approach to cosmogony in book "Elements of Geology" comparing to the corresponding textbook by the same author, "Physical and Political Geography". In secondary education, the creation of the earth is divine; however, in academic education, the creation and the evolution of Earth is explained by Kant and Laplace.

It is noteworthy that modern scientific concepts, such as the Theory of Evolution, the theory of Isostasy and Cosmogony, arriving on time in Greek books, but only in the University, and therefore the level of geological knowledge in Secondary Education is not consistent with the one of the University.

This conclusion seems inevitable, given that the conservative Greek society of the late 19th century and the beginning of the 20th, the critical theory was not adopted, and contradicted to the well-structured positions and attitudes of that period.

4. References

Αντωνίου Α., 1987. Τα προγράμματα της Μέσης εκπαίδευσης (1833-1925), ΙΑΕΝ, Αθήνα.

Καββάδας Αλ., 1908. Μελέτη επί του "Περί των ημετέρων προγόνων" πονηματίου του κ. Μηλιαράκη (καθηγητού της Βοτανικής εν τω Εθνικώ Πανεπιστημίω) και ανασκευή αυτού. Τύποις Δ. Ευστρατίου και Δ. Δελή, Αθήνα.

Κουλούρη Χρ., 1988. Ιστορία και Γεωγραφία στα Ελληνικά Σχολεία (1834-1914): Γνωστικό αντικείμενο και ιδεολογικές προεκτάσεις. Ιστορικό Αρχείο Ελληνικής Νεολαίας. Γενική Γραμματεία Νέας Γενιάς.

Κριμπάς Κων., 1986. Δαρβινικά, Εκδόσεις Ερμής.

Μακρή Κυρ., 2007. Μελέτη της διδασκαλίας της Γεωλογίας στην Ελλάδα 1830-1930.

Μεταπτυχιακή Διατριβή Ειδίκευσης, Τμήμα Χημείας Α.Π.Θ.

Μακρή Κ, Παυλίδης Σ., 2008. Όταν η Γεωλογία διδασκόταν στη Μέση Εκπαίδευση. Γεωενημέρωση Τεύχος 1, 24-27.

Μέγας Α.Ε., 1922. Στοιχεία Γεωλογίας και Ορυκτολογίας, Κολλάρος Ι., Βιβλιοπωλείο της Εστίας, Αθήνα.

Μητσόπουλος Κων., 1885. Στοιχεία Γεωλογίας Φυσιογραφική Γεωλογια, Τόμος Ά, Αθήνα.

Μητσόπουλος Κων., 1893. Στοιχεία Γεωλογίας Φυσιογραφική και Δυναμική Γεωλογια, Τόμος Ά, Αθήνα.

Παυλίδης Σπ., 2007. Παν-γαία, Εκδόσεις Leader Books, Θεσσαλονίκη.

Σωτηριάδου Α., 1990. Η εμφάνιση της Θεωρίας της εξέλιξης των ειδών, δεδομένα από τον ελληνικό χώρο. Διδακτορική Διατριβή ΑΠΘ.

Ταμπάκης Κ., Σκορδούλης Κ., 2004. Η ιστορική διάσταση της επιστήμης στα εγχειρίδια των Φυσικών Επιστημών. 3ο Διεθνές Συνέδριο: Ιστορίας Εκπαίδευσης, Πάτρα.

Herbert S., 2005. Charles Darwin, geologist, Cornell University Press.

Delo D. M., 1950. Role of the Earth Sciences in General Education, Science, New Series, Vol. 112, No. 2898.

Ιστορικό Αρχείο Εθνικού Καποδιστριακού Πανεπιστημίου: http://pergamos.lib.uoa.gr

Δελτίο της Ελληνικής Γεωλογικής Εταιρίας, 2010
Πρακτικά 12ου Διεθνούς Συνεδρίου
Πάτρα, Μάιος 2010

Bulletin of the Geological Society of Greece, 2010
Proceedings of the 12th International Congress
Patras, May, 2010

THE CONTRIBUTION OF MARINE GEOLOGY TO THE SOCIO-ECONOMIC DEVELOPMENT OF GREECE: MARINE RESOURCES, INFRASTRUCTURE, ENVIRONMENT SUSTAINABILITY, CULTURAL HERITAGE

A BRIEF ACCOUNT OF THE 30 YEARS CONTRIBUTION OF THE LABORATORY OF MARINE GEOLOGY AND PHYSICAL OCEANOGRAPHY

Ferentinos G.

University of Patras, Department of Geology, Laboratory of Marine Geology and Physical Oceanography, 26500 Patras, Greece, gferen@upatras.gr

1. Introduction

Marine geology is one of the core disciplines of Geology dealing with the geology of the oceans. In its broadest sense it includes the following major sub-disciplines:
(i) Marine geophysics and Tectonics,
(ii) Marine stratigraphy and Palaeo-oceanography,
(iii) Marine geochemistry and
(iv) Sedimentology.

Advances made from research in the above mentioned sub-discipline fields in the 2nd half of the 20th century lead to a new view of the earth's dynamics such as: Seafloor Spreading and Plate Tectonics, Tectonic History of the Oceans, Sea-Level History, Palaeo-oceanographic and Palaeoclimatologiec Changes.

Modern societal needs demand the extension of marine geology to new frontiers which would deal with the impact of human activity on the seas as well as with the impact of natural processes (hazards) on human activities.

The aims of this paper are to (i) outline human activity that occur in the oceans, (ii) discuss the impact of this activity on the environment as well as the impact of the marine geological processes on the activity and (iii) to present examples of how marine geology can contribute to the socio-economic development in Greece, through its involvement in the exploration, exploitation, development, management and risk assessment studies of the resources, infrastructure, environment sustainability and protection of the cultural heritage in the Greek Archipelago.

2. The beginning of marine geology in Greece

The "Challenger" expedition (1872-1876) marked the beginning of the systematic study of the oceans and consequently the beginning of "marine geology" as a discipline of geology, all around the world.

During this expedition the first deep soundings and sediment samples on a global scale were taken. The sounding data collected, resulted in the first published bathymetric chart of the Atlantic Ocean whilst the sediment samples collected, contributed to the recognition of the major types of ocean sediments and their distribution patterns.

At about the same time the discovery of telegraphy and the prospect of extending the new means of rapid communication between continents (i.e. Europe-America) by laying submarine telegraph cables, gave the incentive to industry to become involved in the study of the seabed morphology and sediments or rocks lying on it, to ensure safe laying of the cables. This was the first application of marine geology on industrial activity in the seas.

Here in Greece the first surveys directly or indirectly related to the study of geological phenomena occurring under the sea and affecting human activities were carried out by: (i) A. Miaoulis (an officer in the Greek Admiralty) in Amvrakikos Gulf, in 1866, (ii) the Bell telegraph and telephone Company in the Gulf of Corinth between 1897 and 1950 and (iii) Prof. G. Georgalas and N. Liatsikas, both geologists, in the Greek Geological Survey in the Gulf of Santorini in 1930.

The first survey was carried out in Amfilochia (Karvasara) Bay to try to locate a possible underwater volcano, based on information that during the 1847 and 1865 earthquakes, sulfur emanated from the seafloor causing the death of shells and fish.

The second set of surveys was carried out in the Gulf of Corinth for the purpose of laying and repairing submarine telegraph/telephone cables damaged by the occurrence of submarine landslides. The surveys revealed the high frequency occurrence of landslides, on average 2 landslides every 3 years. The third survey was carried out in the Santorini Gulf after the 1925-26 and 1928 eruption of the Santorini Volcano, to examine the occurrence of changes in the morphology of the seafloor caused by the eruptions and to study the composition of the gas and water emanating from the seafloor.

3. Human activity in the seas

Current human activity in the seas are related to: (i) exploitation/exploration of non-living and living resources, (ii) coastal and offshore engineering structures and coastal protection, (iii) wave and wind power driven production, (iv) submarine telecommunication and power connections and (v) marine pollution and waste management (Table 1).

Table 1.

MAN'S ACTIVITIES IN THE OCEANS AND INLAND WATERS				
Exploitation/ exploration of non-living & living resources	***Harbour construction & coastal management***	***Submarine cable connections***	***Marine pollution and waste management***	***Human activity on land which affects the marine environment***
• Oil & Gas • Non-Petroleum Minerals • Benthic Fisheries • Aquaculture	Selection of site • Dredged spoil • Beach protection • Beach nourishment	• Telecommunication links • Power links	Waste Material • Dredged spoil • Sewage sludge • Industrial by-products	• Dams & Reservoirs • Rivers • Deforestration/ Farming

Table 2.

ENVIRONMENTAL IMPACTS OF MAN'S ACTIVITIES IN THE OCEAN RELATED TO GEOLOGICAL PROCESSES			
Type of activity	***Impact***	***Cause***	***Information required for the protection of the marine environment***
Harbour construction	Shoreline erosion and/or accretion	Waves and Currents	• Sediments texture • Rates of erosion / accretion • Waves & Current regime
• Harbour & Channel maintenance dredged spoil • Sewage sludge • Industrial by-products • Marine mining	Changes in the physical, chemical and biological parameters of the particulate matter in the water column and of the sediments on the seafloor	Introduction of • coarse and/or fine material • contaminants 1. heavy metals 2. organic compounds 3. radioactive wastes	• Hydraulic regime • Particulate matter 1. Grain size 2. Composition 3. Density • Physical & mechanical properties of the sediments on the seafloor: • Bedform geometry • Man-made particles: 1. Shape 2. Grain size 3. density 4. composition
Aquaculture	Changes in the physical, chemical and biological parameters of the particulate matter in the water column and of the sediments on the seafloor	• Introduction in the marine environment of waste food and faecal pellets • Direct release of nutrients	• Hydraulic regime • Particulate matter 1. Grain size 2. Composition 3. Density • Physical & mechanical properties of the sediments on the seafloor: • Bedform geometry
Benthic fisheries	Changes in the physical, chemical and biological parameters of the sediments on the seafloor	Trawling and dredging equipment	• Hydraulic regime • Physical & mechanical properties of the sediments on the seafloor • Sediment-Biota interaction
Deforestation & cultivation	Changes in the physical, chemical and biological parameters of the particulate matter in the water column and of the sediments on the seafloor	Anthropogenically mobilized soil	• Hydraulic regime • Particulate matter 1. Grain size 2. Composition 3. Density • Physical & mechanical properties of the sediments on the seafloor:

Table 2. Continued

ENVIRONMENTAL IMPACTS OF MAN'S ACTIVITIES IN THE OCEAN RELATED TO GEOLOGICAL PROCESSES			
Type of activity	***Impact***	***Cause***	***Information required for the protection of the marine environment***
			• Bedform geometry • Sediment-Biota interaction
Dams and reservoirs River diversion	• Shoreline erosion • Changes in the physical, chemical and biological parameters of the particulate matter in the water column and of the sediments on the seafloor	Reduction of sediment supply	• Texture of sediments • Waves & Current regime • Physical & mechanical properties of the sediments on the seafloor: • Bedform geometry • Man-made particles: 1.Shape 2.Grain size 3. density • Sediment-Biota interaction

The above mentioned human activity has as impact on the marine environment (Table 2) like: (i) shoreline modification (erosion and/or accretion) and (ii) modification of the physical, chemical and biological parameters of the sea water and of the particulate matter in it and of the sediments on the sea floor. These changes in turn affect the balance of the biogeochemical processes which operates in the marine environment resulting in its degradation. There is also human activity on land, such as dam and reservoir construction, river diversion, farming and deforestation which affect the mariner environment.

To avoid, mitigate and/or take remedial measures on the impacts imposed to the marine environment by human activity, knowledge of the causal factors is needed as well as how these factors operate (Table 2). Furthermore a detailed knowledge of the physical, chemical and biological parameters which occur in the marine environment is needed (Table 2).

As human activity in the marine environment increases, natural hazards become more frequent and environmental risks more common place (Table 3).

Marine geology, based on the scientific issues that it covers is considered the relevant science to resolve, evaluate, remediate and mitigate man's impact on the marine environment and the natural processes (hazards) impact on man's activity.

4. Case studies

The case studies presented below are based on a 30 year involvement and experience be the Laboratory in natural hazard risk assessment studies, environment assessment studies, vulnerability studies, infrastructure site selection studies related to harbour, pipeline and cable route engineering works, harbour and channel dredging, monitoring of environmental parameters in coastal waters and protection and management of submarine heritage.

Table 3.

ENVIRONMENTAL HAZARDS* TO MAN'S ACTIVITIES IN THE OCEAN RELATED TO GEOLOGICAL PROCESSES			
Type of activity	***Hazard***	***Cause***	***Information required for the safe construction and operation***
• Gas & Oil platforms • Pipilines/ Outfalls • Submarine cables • Harbours	Gravitative Mass Movements: • Slides • Slumps • Sediment flows • Turbidity currents	Static Loading: • Insufficient sediment bearing capacity Cyclic Loading: • Earthquakes • Storms & storm surges • Tsunamis • Structure vibration	• Physical & mechanical properties of sediments • Gas in sediments
• Gas & Oil platforms • Harbours • Pipilines/ Outfalls • Submarine cables	Erosion & Deposition	• Waves & Currents • Storm & Storm surges	• Texture and density of sediments • Bedform geometry • Wave and current regime
Emplacement of nuclear wastes deep in the seafloor for storage	Transport of radionuclides to the seafloor	• Seafloor erosion • Thermal & fluid-mechanical responses of sediment	Physical & mechanical properties of sediments • fine grained clays • low permeability • low shear strength Depositional environment (pelagic) and absence of any erosive episodes by currents or mass wasting

* are defined as the highest values of forces resulting from geological, oceanographical and meteorological phenomena in an area

4.1 A natural hazard risk assessment study in the Corinth Gulf

The Gulf of Corinth is an active half-graben characterized by intense seismic activity. Marine geological surveys were carried out to evaluate: (i) the maximum probable expected offshore earthquake magnitude, (ii) the potential sources of submarine landslides and (iii) the potential tsunami hazard imposed by active offshore faults and submarine landslides.

The surveys showed that:

(i) the fault trace length of the offshore faults is between 5 and 15 km. This suggests that the expected maximum earthquake magnitude would be 6.5 R based on regression equations correlating to fault trace length and seismic moment magnitude. However, it should be noted that the maximum recorded earthquake magnitude in the Gulf on Feb, 24th 1981 was 6.7R.
(ii) the potential maximum seismic fault surface displacement is estimated to be about 1m and therefore the potential maximum wave height in the Gulf above the source would be expected to be approximately the same as the co-seismic vertical displacement.
(iii) the potential maximum tsunami wave height, due to a submarine landslide in the Gulf would be 4.04m above the source, based on the existing knowledge regarding landslide source area, landslide size, slope dip and traveling distance.

4.2 The Navarino naval battle site, Greece: an integrated remote-sensing survey and a rational management approach

Navarino Bay is a natural sheltered anchorage in the southern Ionian Sea, located near the town of Pylos. Navarino Bay has been a haven for ships for thousands of years due to its central location in the Mediterranean Sea. During the Greek war of independence from the Ottoman Empire, one of the most significant battles in European history fought there in 1827. At present oil tankers and large cargo vessels en route from oil-rich Middle East countries to Europe usually stop at Navarino Bay.

The 3.5 KHz seismic and side scan sonar survey in the Bay has shown that:
(i) the floor of Navarino Bay is covered by soft mud more than 25m in thickness and that the seafloor is scoured by the anchors of the moored tankers. The scour marks are up to 2m wide, up to 300m long and up to 2m deep.
(ii) shipwreck remains of the battle lies on the seafloor and possible few shipwrecks are buried under the seabed.
(iii) shipwreck remains are under threat from the heavy anchors of tankers which sink into the seabed and when dragged dig furrows in the seabed, thus disintegrating the shipwrecks.
(iv) the wreckship remains can be protected from further destruction by the construction of permanent offshore anchoring systems away from the shipwreck remains.

4.3 Geological and man-made hazards for laying submarine cable in the Aegean and Ionian Seas

Greece is surrounded by more than one hundred islands scattered throughout the Aegean and Ionian archipelagos. The boom in business and tourism over the last three decades has resulted in the need of laying many submarine power and telephone cables between the Greek mainland and the islands. For the safe laying of the cables and the avoidance of any after laying cable failures, the safest seafloor route must be selected. The route must be as much as possible free from any potential geological and man-made hazards.

The geological and man-made hazards which pose damage to the cables are: (a) active faults and earthquakes, (b) pock-marks and gas charged sediments, (c) salt doming, (d) tsunami, (e) submarine landslides, (f) erosional features on the seabed (canyons, channels), (g) anomalous relief, (h) sediment erosion, transport and deposition and (i) human activity such as fishing, dredging, anchoring and wrecks on the seafloor.

The experience gained by the Laboratory through its involvement in feasibility studies for submarine cable links between the Greek mainland and the islands, suggests that it is essential for a ma-

rine geological survey to be carried out by the governmental organization or the private industry interested in the submarine cable link for the selection of the safest cable route, the feasibility of the cable burial, the degree of difficulty involved in the burial of the cable and the selection of the most efficient burial method. The above studies must be done before the order is given to the cable manufacturer and the cable laying company to ensure that no mistakes are made and also to keep the cost at a minimum.

5. Acknowledgments

I would like to mention that in all this 30 year involvement of the Laboratory in marine geology, the contribution of all the post-graduate students of the Laboratory, who spent days and nights in the sea and some of whom are now scientific personnel in the Laboratory or somewhere else, cannot be underestimated. Their hard work and dedication in the scientific effort of the Laboratory was indeed a very important factor in the success of the Laboratory, which could not have achieved without them.

I refer in particular to:
1. G. Papatheodorou (Associate Professor, Department of Geology, Patras University).
2. N. Kastanos (Secondary School Teacher).
3. P. Achelleopoulos (Secondary School Teacher).
4. I. Zacharias (Assistant Professor, Department of Environment, Ioannina University).
5. G. Gkionis (Marine Geologist, Consultant).
6. M. Geraga (Lecturer, Department of Geology, Patras University).
7. T. Hasiotis (Lecturer, Department of Marine Science, Aegean University).
8. A. Stefatos (Senior Marine Geophysist, Rock Resources, Norway).
9. A. Chalari (Underwater Archaeology, Laboratory of Marine Geology).
10. D. Christodoulou (Research Associate, Laboratory of Marine Geology).
11. M. Iatrou (Post-graduate student).
12. I. Fakiris (Post-graduate student).
13. M. Prevenios (Post-graduate student).

Δελτίο της Ελληνικής Γεωλογικής Εταιρίας, 2010
Πρακτικά 12ου Διεθνούς Συνεδρίου
Πάτρα, Μάιος 2010

Bulletin of the Geological Society of Greece, 2010
Proceedings of the 12th International Congress
Patras, May, 2010

ENGINEERING GEOLOGICAL BEHAVIOUR OF HETEROGENEOUS AND CHAOTIC ROCK MASSES

Tsiambaos G.

National Technical University of Athens, School of Civil Engineering, Department of Geotechnical Engineering, gktsiamb@central.ntua.gr

Abstract

The engineering characterization of heterogeneous and complex geological formations for estimating their rock mass strength and deformability characteristics constitutes a challenge to geo-scientists and engineers dealing with the design and construction of slopes and tunnels. Mélanges and similar heterogeneous mixtures of hard blocks in weaker matrix, known as "bimrocks", present an overall strength significantly greater than the matrix strength, because the presence of rock blocks, above a threshold volumetric proportion, influences the mechanical characteristics and the behaviour of these rock masses. Moreover, recent studies have shown that the strength and mechanical behaviour of heterogeneous and composite rock masses such as flysch and molasses consisting of alternating layers of competent and incompetent rocks are governed by the presence and volumetric percentage of the interlayers of the weaker rocks.

Key words: *heterogeneous rock masses, composite rocks, mélanges, rock strength, laboratory testing.*

1. Introduction

The quantitative description, characterization and classification of heterogeneous and chaotic rock masses, as well as the estimation of their strength and deformability are of great importance for the design of surface and underground engineering woks.

Complex geological mixtures such as melanges, fault rocks, tectonic breccias, pyroclastic rocks and sheared ophiolites can be considered as mixtures of blocks of competent rock embedded within a weaker matrix (block-in-matrix rocks or bimrocks, as introduced by Medley, 1994). The overall uniaxial compressive strength and the shear strength characteristics of these rocks depend on the rock block proportions, taking into account the scale of engineering interest (laboratory to site scale).

Furthermore, heterogeneous and composite rock masses such as flysch and molasses consisting of alternating layers of two or more lithological units (mainly sandstone, siltstone or shale) present a strongly anisotropic behaviour. The first attempt to characterize, from an engineering geological point of view, and to present a methodology for estimating the Geological Strength Index (GSI) of these rock masses was made by Marinos and Hoek (2001) and Hoek et al. (2005).

Recent laboratory studies have indicated that the overall strength and deformability characteristics of layered composite rocks are mainly governed by the relative thickness of competent and incompetent constituents and especially the volumetric percentage of the weaker member.

Fig. 1: Blocks of moderately weathered granite in a completely weathered mass.

Fig. 2: Fault breccia.

Fig. 3: Ophiolitic mélange (blocks of serpentinized peridotites in a volcano-sedimentary matrix).

2. Block-in-matrix rocks (Bimrocks)

2.1 Origin

The term "block-in-matrix rocks" was originally introduced by Raymond (1984) as "blocks of one lithology enclosed in materials of another lithology". This term is applied for heterogeneous, complex geological formations, tectonically deformed and disturbed, containing competent blocks of varied lithologies embedded in weaker bonded matrix rocks of finer texture, such as mélanges, sheared serpentinites, olistostromes, cataclastic fault rocks, weathered rocks and coarse pyroclastics (Figures 1, 2 and 3). The blocks range between several tens to hundreds of meters in size to millimeter-sized fragments within gouge. Medley (1994), suggested the neutral word "bimrocks" in order to characterize these "rock/ soil" mix-

tures and study their peculiar behaviour from an engineering point of view. The same author defined "bimrocks" as "a mixture of rocks composed of geotechnically significant blocks within a bonded matrix of finer texture". The expression "geotechnically significant blocks" means that there is a strength contrast between blocks and matrix, and consequently the volume and size of the blocks greatly influence the rock mass strength and deformability at the scales of engineering interest. Medley (1994) has suggested a threshold value of at least two (2) for the ratio of the uniaxial compressive strength (UCS) of rock blocks to UCS of matrix for a geological rock mixture to be considered as a bimrock.

2.2 Scale effects

The engineering behaviour of these rocks is controlled by the presence both of bocks and matrix. It must be noted that neglecting the presence of rock blocks and considering only the strength of the weak matrix, is too conservative in estimating the overall strength of bimrocks. As rock block proportion increases, strength and stiffness increase and deformability decreases depending on the relative orientation of blocks to applied stresses (Lindquist, 1994; Lindquist and Goodman, 1994). The weakest elements in bimrocks are the contacts between strong blocks and weak matrix, since matrix shear zones generally pass around blocks via the block/matrix contacts with the most intense shearing often present adjacent to the largest blocks.

Stress distributions in bimrocks depend on the lithologies; size distributions; orientations and shapes of blocks; and the orientations of matrix shears. All these factors influence stability of slopes (Medley and Sanz, 2004) and underground excavations (Button et al., 2003; Moritz et al., 2004; Riedmüller and Schubert, 2002).

Block sizes in mélanges can exceed several orders of magnitude, ranging between millimeters and tens of kilometers (Medley, 1994; Medley and Lindquist, 1995) and consequently small blocks at one scale of interest (i.e. laboratory rock specimen) may be part of the matrix at a larger scale (tunnel diameter). In order to study the scale effects in bimrocks, Medley (1994) introduced a "characteristic engineering dimension, Lc" which depends on the volume of blocks relative to the dimensions of an engineering project. According to Medley (1994), Lc may variously be: 1) an indicator of the size of the entire site (i,e, landslide area, A), such as the square root of A ($\sqrt{A}$) or the landslide depth; 2) the size of the largest block (dmax) at the site; 3) the height of a slope or excavation; 4) the tunnel diameter; 5) a footing width or; 6) the dimension of a laboratory specimen.

The smallest geotechnically significant block, as defined above, within a volume of bimrock is about 0.05 Lc, which is the threshold size between blocks and matrix at the chosen scale (Medley, 1994). For any given volume of bimrock, blocks smaller than 0.05 Lc constitute greater than 95 percent of the total number but contribute less than 1 percent to the total volume of bimrock. These blocks smaller than the block/matrix threshold dimension have negligible effect on the bimrock strength and are considered as matrix material. The largest geotechnically significant block is about 0.75 Lc. In the case of the foundation of a bridge pier of 2m diameter (Lc = 200cm), blocks with dimensions smaller than 10cm (0.05 Lc) are consider as matrix. For the same bimrock, where a 20m diameter tunnel excavation is considered, rock blocks with dimensions up to 100cm belong to the matrix of the whole rock mass.

2.3 Estimation of volumetric block proportions

As indicated above, to predict the mechanical properties of bimrocks, the volumetric block proportion must be estimated in the engineering project site. When adequate number of boreholes has been executed in the site, the volumetric block proportion (VBP) of a bimrock can be approximated by measuring lin-

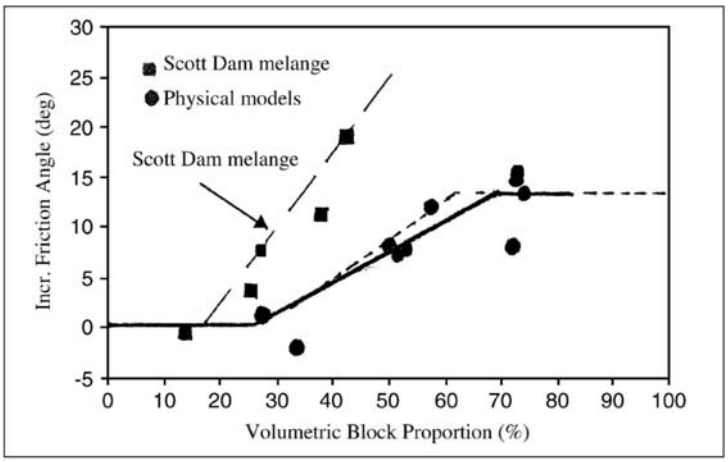

Fig. 4: Strength dependence of bimrocks on volumetric block proportion (after Medley, 1999).

ear block proportions of drilled cores (Medley, 1994). The linear block proportion can be estimated as the ratio of the total length of rock cores to the total length of drilling. The minimum required length of sampling boreholes in total must be at least 10 times the size of the expected largest block in the bimrock (10Lc, or 10dmax). Using the measurement of drilled cores or scanlines on photographs for the VBP estimation are considered as one-dimensional (1-D) methods. Moreover, geological mapping and image analysis on scanned images or photographs from outcrops in the site of the engineering project are examples of two-dimensional (2-D) methods. Sieve analysis of bimrock samples is a three-dimensional (3-D), but can be used only for laboratory investigations of weak rocks, when separation of blocks from matrix is possible. If a significant density contrast between blocks and matrix exists, the overall density of the laboratory cylindrical specimens will vary directly in proportion to VBP.

2.4 Bimrock strength

Irfan and Tang (1993), Lindquist (1994) and Lindquist and Goodman (1994) determined that the overall strength of a bimrock is related to the volumetric proportion of the blocks. Lindquist (1994) suggested that below about 25 percent volumetric block proportion, the strength and deformation properties of a bimrock is that of the matrix; between about 25 percent and 75 percent, the friction angle and modulus of deformation of the bimrock mass proportionally increase (Figure 4). Beyond 75 percent block proportion, the blocks tend to touch each other and there is no further increase in bimrock strength, since the strength of the individual blocks is generally considered to has no effect on the bimrock overall strength (Medley, 1994).

In order to investigate the shear strength characteristics of bimrocks, laboratory specimens could be considered as scale models of the in situ rock masses. Given that the diameter of the laboratory specimens is the characteristic engineering dimension (Lc), blocks included in the specimens are considered to be those with maximum dimensions between about 0.05 (5 percent) and 0.75 (75 percent) of the specimen diameter (in case of cylindrical specimens). The volumetric block proportions of each specimen can be determined after disaggregating them and wash sieving to retrieve the blocks. The volume of blocks (and thence the volumetric block proportion) can also be estimated by measuring the specific gravity of the blocks and weighing the specimens (Lindquist, 1994a). Medley (1994) described methods of approximating block proportions from scanlines drawn on the side of specimens or image analysis of specimen exteriors, although these measures are generally not the same as volumetric proportions.

Fig. 5: Outcrop of volcanic block and tuff mixture (after Sönmez et al., 2004). PA: pink andesite blocks, BA: black andesite blocks; T: tuff.

Laboratory specimens of bimrocks exhibiting a range of volumetric block proportions could be tested using multistage triaxial compression or direct shear tests for measuring effective friction angle and cohesion as a function of volumetric block proportion. The overall volumetric block proportion of the bimrock, as estimated from borehole data, can be used to determine the strength of the bimrock on site.

Sönmez et al. (2004, 2006) studied the mechanical behaviour of Ankara agglomerate, a mixture of volcanoclastic blocks and tuff matrix. The blocks ranged in size from a few centimetres to about one meter (Figure 5). The 2D measurements of blocks in the Ankara Agglomerate revealed that these blocks composed of pink (lighter) and black (darker) andesite ranged between 1 and 70 cm (mean value, 11 cm).

By conducting uniaxial compression tests on specimens of andesite rocks, it was determined that the average values of UCS for pink and black andesite blocks are about 50 and 90 MPa respectively and that of the tuff matrix 10 MPa. The minimum and maximum ratio of UCS of blocks to the UCS of tuff matrix is 2.5 and 19, respectively. The maximum and minimum UCS values of NX-size core specimens of Ankara Agglomerate were 5.7 and 55 MPa, respectively, and the average UCS value was 24.9 MPa.

However, separation of the andesite blocks from weak tuff matrix was impossible by using sieve analysis because of the tuff matrix acting as cementing agent. So, image analysis methods were used to estimate the volumetric block proportions. However, a composite block proportion was used to study the differences in overall UCS due to differences in the proportions of the two different andesite block types. A weighted "equivalent block proportion", or EBP, accommodates two or more types of blocks differing in individual mechanical properties:

$$EBP = \sum_{i}^{n} VP_i \frac{UCS_i}{UCS_{max\_block}}$$

where, VP_i is the volumetric block proportion of ith block, UCS is the uniaxial compressive strength, n is the number of different types of blocks, and $UCS_{max\ \_block}$ is the uniaxial compressive strength of the stronger block type.

The uniaxial compressive strengths of the Ankara Agglomerate specimens were then normalized by dividing them by the average uniaxial compressive strength of the matrix: this parameter is denoted as UCS_N. The relationships of Figure 6 are non-linear, particulary above about 70 % equivalent block proportion, suggesting that the dependence of overall bimrock strength on block proportion is more complex than previously understood and further study is required. The plot also indicates that at high equivalent block porportions the overall bimrock becomes uniformally stronger.

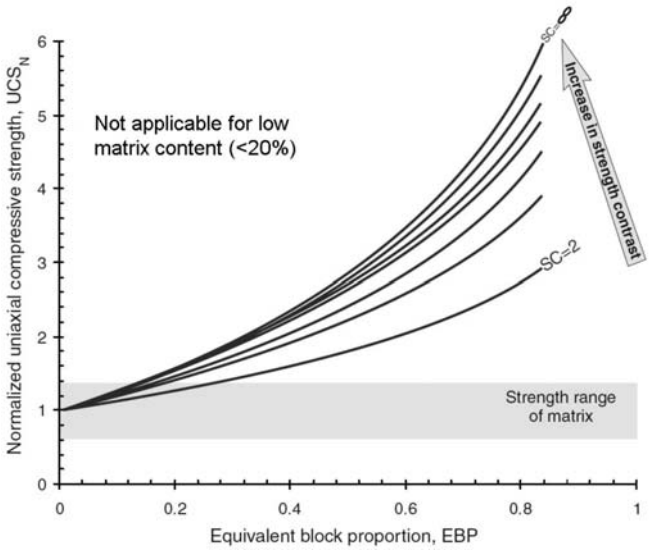

Fig. 6: Relationships between equivalent block portion (EBP) and UCS of Ankara agglomerate, with lines of different strength contrast (ratios) between andesite blocks and tuff matrix (after Sonmez et al., 2006).

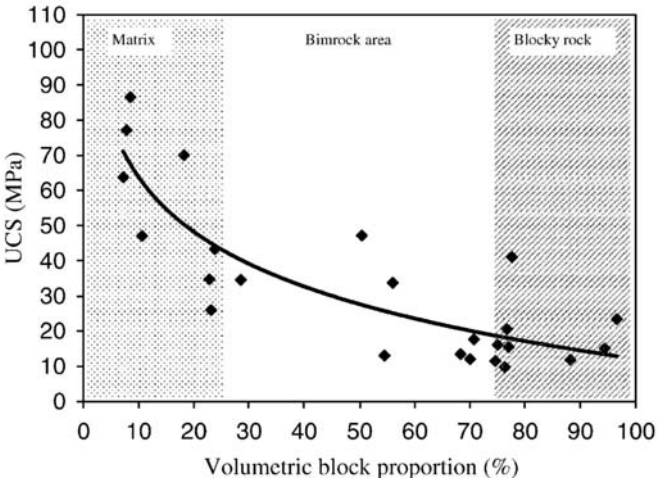

Fig. 7: Volumetric Block Proportion (VBP) versus Uniaxial Compressive Strength (UCS) for a fault cemented tectonic breccia (after Kahraman and Alber, 2006).

This behaviour shows that at high volumetric block proportions (greater than about 70 to 75 %), block/matrix rock mixtures should be considered as very blocky to disintegrated rock masses, according to GSI (Marinos and Hoek, 2000) for which the Hoek-Brown failure criterion (Hoek et al., 2002) should be successfully applied.

Kahraman and Alber (2006) studied the unconfined compressive strength of a fault cemented tectonic breccia consisting of weak, weathered slate components (blocks of various dimensions) and strong matrix consisting of recrystalized limestone. According to the testing results, the UCS of the breccia specimens decreases as the volumetric block proportion, VBP, increases, as shown in Fig-

ure 7. These results are different from the findings of Sönmez et al. (2004, 2006). The difference between the two studies is due to the matrix type. The matrix of Ankara Agglomerate was weaker than the andesite blocks, whereas the matrix of fault breccia studied by Kahraman and Alber (2006) was stronger than the weak blocks of slate.

Karzulovic and Diaz (1994) studied the behaviour of a cemented breccia (Braden Breccia, Chile) for the design of underground openings in this rock. Any attempt to classify the rock mass was unsuccessful due to the presence of only few discontinuities. Therefore, it was decided to treat this rock mass as a weak but homogeneous "almost intact" rock and to determine its properties by means of triaxial tests on 100mm diameter specimens (Hoek, 2007). The in situ GSI value of this breccia was estimated (not measured) close to 75 by a back analysis of the behaviour of underground openings and taking into account the laboratory results of the specimens tested.

Marinos et al. (2005) presented a quantitative description of ophiolitic complex rock masses, using the GSI, and described the effects of serpentinisation and shearing on the mechanical behaviour of these rock masses in underground excavations. They considered low to very low GSI values (10 to 20) for ophiolite melanges and since it is very difficult to obtain σ_{ci} from laboratory tests, they derived values of σ_{ci} and m_i from a back analysis of the behaviour of tunnels excavated in these rock masses. However, when these rocks have a soil-like behaviour the GSI assignment is meaningless.

Carter et al. (2007) stated that, although the Hoek-Brown non-linear criterion (Hoek et al., 2002) for strength estimation of rock masses based on GSI classification system (Marinos and Hoek, 2000) proven in general remarkably successful for defining rock mass behaviour for underground and surface rock excavations, however difficulties have been experienced for very low strength rocks, i.e exhibiting an unconfined compressive strength, UCS = σ_{ci} lower than about 15MPa, because in such cases the rock mass behaviour is less controlled by discontinuities. For these weak rocks Carter et al. (2007) proposed a transition (function of UCS = σ_{ci}) for rock masses and Mohr-Coulomb equivalent strength predictions for soils.

In many cases, mélanges or sheared serpentinites and other weak rocks with similar structure could be considered as bimrocks and their strength and deformation characteristics could be estimated by using the approach mentioned above for these rocks.

It must be noted that all the previous works for bimrocks have not considered their strength anisotropy due to blocks shape and orientation, which is an important factor since foliated and sheared bimrocks could exhibit a high anisotropic behavior.

2.5 Shear strength of tectonically disturbed and weathered flysch

Flysch represents a typical structurally complex formation with a wide distribution in central and western Greece. Heterogeneity of lithology, intense folding, shearing with numerous overthrusts and weathering, are the main reasons of critical slope stability and the activation of large scale landslides in this formation. The study of large landslides in tectonically disturbed and weathered flysch, affecting the road Trikala to Arta, close to the Elati village, showed that the sliding mass had a thickness of about 10m (Christoulas et al., 1988). The characteristic engineering dimension (Lc) for the landslide can be assumed equal to the average thickness of the slide (10m). The block/matrix threshold was thus selected as 0.5m (0.05Lc), whereas the maximum dimension of observed blocks of sandstone or overthrusted limestone in the weathered zone of flysch was 3-5m. The exploration of the landslide area indicated that proportion of rock blocks with dimensions greater than the threshold value of 0.5m is about 20-30% (volumetric block proportion of weathered zone of flysch).

Fig. 8: Alternated layers of sandstones and siltstones of flysch formation (Evinochori region).

The shear strength characteristics of weathered flysch was determined by testing specimens in the large shear box apparatus, 300mm square and about 160mm thick (Christoulas et al., 1988, Kaltezi-otis and Tsiambaos, 1994). The weathered flysch specimens were prepared with different block proportions ("gravels" percentage with dimensions greater than about 8mm, i.e. greater than 5% of the shear box thickness). The determined effective angle of friction was as high as 35^0 - 40^0 for the specimens exhibiting a volumetric block proportion of about 20%, as estimated by sieve analysis. Moreover, the fine grained portion of the flysch was tested in ring shear apparatus in order to estimate the residual shear strength characteristics of fine grained material of weathered flysch. The measured angle of friction of this material, representing the matrix of the weathered flysch, was ranged from 19^0 to 21^0. It is obvious that considering the low values of angle of friction for slope stability analysis can lead to very conservative results. On the contrary, the specimens tested in the laboratory with volumetric block proportions almost the same as those of the in situ weathered flysch gave more representative shear strength characteristics (angle of friction 35^0 - 40^0). These estimated values of friction angle (considering no cohesion of disturbed flysch) can better explain the slope instability after taking into account the role of ground water and the pore pressure developed during the rainy season.

3. Heterogeneous, composite rock masses

Heterogeneous and composite rock masses are those consisting of two or more lithological units exhibiting a structure of alternating layers of competent and incompetent rocks with varying thickness.

Flysch and molasse constitute characteristic examples of such rocks. They are characterized by rhythmic alternations of sandstone and pelitic (fine grained) rocks such as siltstones, marls, shales and clay shales (Figure 8). Conglomerates and limestones can also be present.

For the benefit of the design of a large number of engineering projects in Greece in these rock masses, Marinos and Hoek (2001), Hoek et al. (2005) and Marinos (2010) suggested modified charts for estimating the GSI for these heterogeneous and composite rock masses, based on the lithology, structure and surface conditions (for bedding planes in particular). They excluded from this procedure rock masses with predominant weak planar discontinuities which are probable to cause structurally controlled failures.

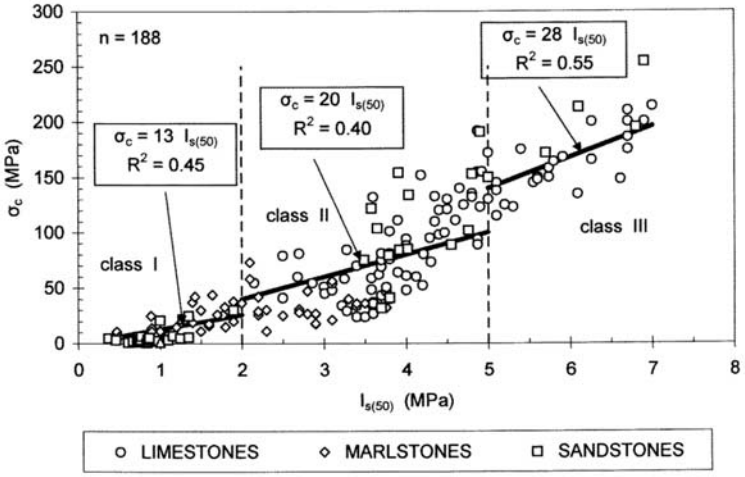

Fig. 9: Conversion factors correlating point loading and uniaxial compressive strength for soft to strong sedimentary rocks (after Tsiambaos & Sabatakakis, 2004).

Regarding the selection of the "intact" rock properties σ_{ci} and m_i, for flysch composite rocks, they suggested proportions of values ("weighted average") for each rock mass type of the proposed modified charts, reducing values of σ_{ci} and m_i of competent rocks (sandstones) up to 40%, when the layers of these rocks are separated from each other by weaker layers of siltstones or shales. Therefore, having defined the parameters σ_{ci}, m_i and GSI, the mechanical properties of the heterogeneous rock mass are estimated by using the Hoek-Brown failure criterion (Hoek and Brown, 1997).

It must be noted that from the weak members of these heterogeneous rock masses it is very difficult to obtain "intact" core samples for determining the uniaxial compressive strength in the laboratory. Moreover, laboratory tests carried out on core samples often result in a lower strength value due to sampling and preparation disturbance. Marinos and Hoek (2001) insist that using the results of such tests in the Hoek-Brown criterion will impose a double penalty on the strength (in addition to that imposed by GSI) and will give unrealistically low values for the rock mass strength.

In such cases, the use of the point load test on samples in which the load can be applied normal to the bedding or any other weakness planes for estimating the uniaxial compressive strength of weak rocks is advisable.

Tsiambaos and Sabatakakis (2004) and Sabatakakis et al. (2008) studied the relationship between the uniaxial compressive strength of intact sedimentary rocks and point load index $Is_{(50)}$ and estimated that the conversion factor k ($\sigma_{ci} = k\ Is_{(50)}$) has no a single value, but varies from 13 for soft sedimentary rocks (i.e. shales and siltstones) exhibiting a value of $Is_{(50)}$ <2 MPa to 28 for harder rocks with values of $Is_{(50)}$ greater than 5 MPa (Figure 9).

The overall strength of heterogeneous and composite rock masses is one of the main research subjects the last decade. Goodman (1993) had emphasized that any combination of more than one lithlogical type of rock exhibiting different properties impose a complex geotechnical engineering problem.

Greco et al. (1993) conducted a study for determining the strength and failure mechanism of composite rocks in the context of the stability analysis of the columns and masonry walls of a Cathedral, built with stones of different rock types. Testing cylindrical specimens made up of disks of various

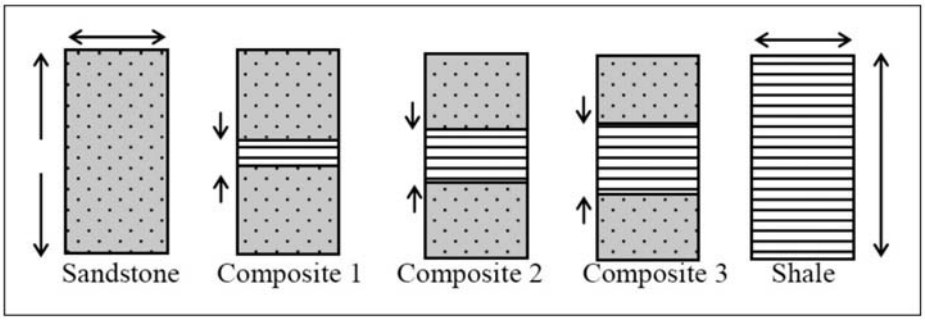

Fig. 10: Different types of composite specimens consisting of sandstone with shale interlayer (after Zainab et al., 2007).

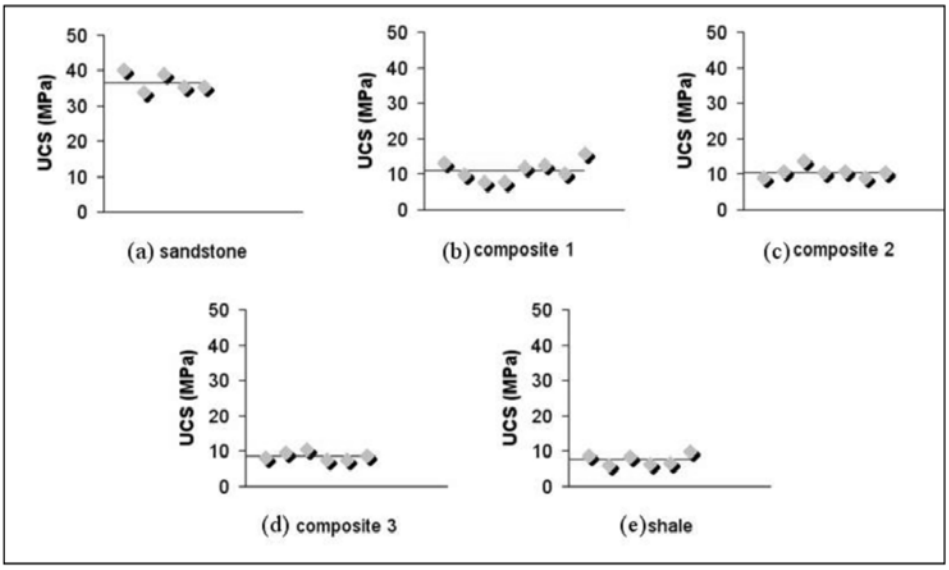

Fig. 11: Uniaxial compressive strength (UCS) of composite specimens illustrated in fig. 10.

rocks, they observed different failure mechanisms for stratified disk specimen from those of single rock, while the loss of compressive strength for composite rock specimens was up to 70 percent in comparison with the uniaxial compressive strength of individual stones.

Zainab et al. (2007) carried out a laboratory study to determine the strength of tropically weathered sandstone and shale in Malaysia. The composite samples were designed into three different thickness ratio of shale to the total height of specimens, H, each having 0.1H, 0.2H and 0.3H of shale.

Each specimen was then marked as composite 1, composite 2 and composite 3 respectively (Figure 10). These composite samples were prepared to simulate the possible geometry profile of the constituents in the interbedded sedimentary formation.

From the analysis of test results, shown in Figure 11, it is concluded that only a low percentage (i.e. 10%) of shale reduces the strength of composite rock specimen drastically by almost 70%.

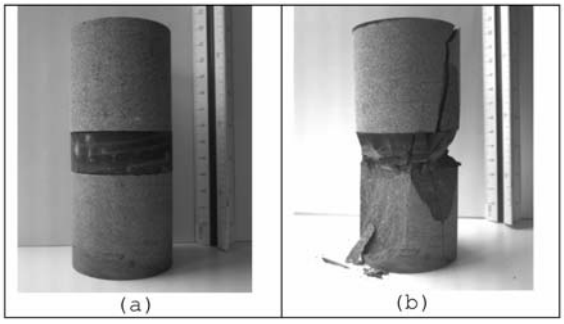

Fig. 12: Cylindrical composite rock specimen made up of sandstone (light grey) with siltstone interlayer (dark grey): (a) pre-failure, (b) post-failure.

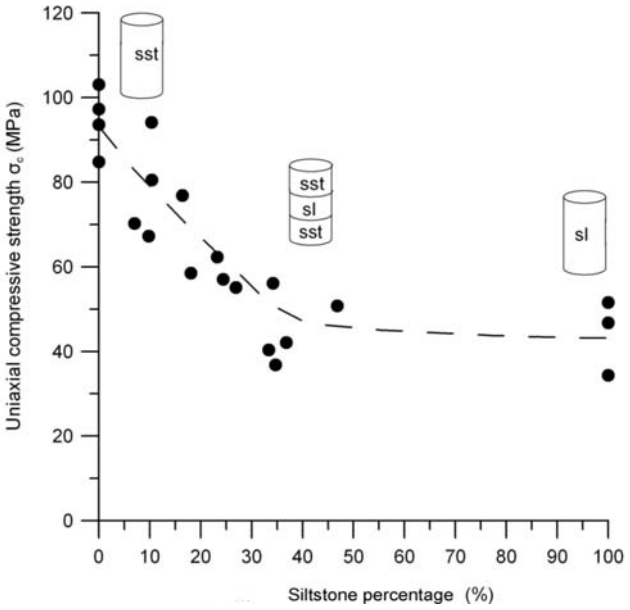

Fig. 13: Uniaxial compressive strength reduction of composite rocks with increasing siltstone volumetric percentage (sst: sandstone, sl: siltstone).

Recent laboratory research for the estimation of the strength and deformability characteristics of heterogeneous rocks is carried out in the laboratory of Engineering Geology and Rock Mechanics, of the Geotechnical Engineering Department, NTUA (Tziallas, 2010). The composite rock specimens tested were made up of disks of sandstone and siltstone which belong to the Ionian flysch formation of Evinochori region (Figure 12). The intermediate siltstone disks were of varying thickness and the volumetric percentage of siltstone for the cylindrical composite specimens ranged from 10 to 50 percent. The uniaxial compressive strength of sandstone specimens ranges from 85 to 105 MPa and of siltstone specimens from 30 to 50 MPa.

According to the preliminary test results, the uniaxial compressive strength of composite specimens is significantly reduced when the siltstone percentage is increased from 10% to 20% (Figure 13). When the siltstone percentage of composite specimens is increased to about 30%, their uniaxial compressive strength is further reduced and becomes almost equal to the siltstone strength.

Further research is necessary to check the validity of these results and to study the deformability characteristics of composite rocks.

4. References

Button E. A., Schubert W., Riedmueller G., Klima K. & Medley E.W., 2003. Tunnelling in tectonic melanges – accommodating the impacts of geomechanical complexities and anisotropic rock mass fabrics. *International Bulletin of Engineering Geology and the Environment*, 63 (2), 109 - 117.

Carter T.G., Diederichs M.S., Carvalho J.L., 2007. A unified procedure for Hoek-Brown prediction of strength and post yield behaviour foe rockmasses at the extreme ends of the rock competency scale. 11th Congress of ISRM, Taylor & francis Group, London, 161-164.

Christoulas S., Kalteziotis N., Gassios E., Sabatakakis N., Tsiambaos G., 1988. Instability phenomena in weathered flysch in Greece. Proc. 5th Intern. Symposium on Landslides, Lausanne, Vol. 1, 103-108.

Goodman R.E., 1993. Engineering Geology - Rock in Engineering Construction. Smith, M.R. and Collis, L.,eds., John Wiley & Sons, Inc., 412 p.

Greco O.D., Ferrero A.M., Ogger C., 1993. Experimental and analytical interpretation of the behaviour of laboratory tests on composite specimens. International Journal of Rock Mechanics & Mining Sciences and Geomechanics Abstracts, 30(7), 1539-1543.

Hoek E., 2007. Rock Engineering. Course notes, 313 p.

Hoek E., Brown E.T., 1997. Practical estimates of rock mass strength. Int. J. Rock Mech. Min. Sci. Geomech. Abstr. 34 (8), 1165-86.

Hoek E., Carranza-Torres C., Corkum B., 2002. Hoek-Brown failure criterion – 2002 edition. In: Proceedings of the fifth NARMS-TAC conference", Toronto, Canada, July 2002, vol I. Balkema, Rotterdam, 267-273.

Hoek E., Marinos P., Marinos V., 2005. Characterization and engineering properties of tectonically undisturbed but lithologically varied sedimentary rock masses. *Int. J. Rock Mech. Min. Sci.*, 42(2), 277-285.

Kahraman S., Alber M, 2006. Estimating the unconfined compressive strength and elastic modulus of a fault breccia mixture of weak rocks and strong matrix. *Int. J. Rock Mech. Min. Sci.* 43, 1277-87.

Kalteziotis N., Tsiambaos G., 1994. Instability phenomena of weathered flysch with reference in the regions of Ag. Dimitrios and Pili Trikala Dams. Proc. Dam Geology and Greek Experiences, Ed. P. Marinos, 169-177.

Karzulovic L., Diaz A.J., 1994. Comprehensive approach to rock mechanics applied = Integral approach to applied mechanics rocks. Assessment of geomechanical properties Gap in El Teniente mine Braden, 2 v.

Lindquist E.S., 1994. The strength and deformation properties of mélange. PhD thesis, Dept. of Civil Engineering, Univ. of California, Berkeley, 264 p.

Lindquist H.S., Goodman R.H., 1994. Strength and deformation properties of a physical model mélange. In: Nelson PP, Laubach SH, editors. Proceedings of the first North American rock mechanics symposium. Rotterdam: Balkema, 843-850.

Marinos P., Hoek E., 2000. GSI: a geologically friendly tool for rock mass strength estimation. In: Proceedings of the GeoEng2000 at the international conference on geotechnical and geological engineering. Melbourne, Technomic publishers. Lancaster, 1422-1446.

Marinos P., Hoek E,. 2001. Estimating the geotechnical properties of heterogeneous rock masses such as fiysch. *Bull. Eng. Geol. Env.*, 60, 82-92.

Marinos V., 2010. New proposed GSI classification charts for weak or complex rock masses. Bulletin of the Geological Society of Greece, Proceedings of the 12th International Congress, Patras (under publication).

Medley E.W., 1994. The engineering characterization of mélanges and similar block-in-matrix rocks (bimrocks). PhD dissertation, University of California, Berkeley, UMJ, Inc., Ann Arbor, MJ, 387 p.

Medley E.W., 1997. Uncertainty in estimates of block volumetric proportion in melange bimrocks. In Proc. Int. Symp. of Int. Assoc. Eng. Geol., Athens, Greece; June 23-27; A.A. Balkema, Rotterdam, vol. 1, 267 - 272.

Medley E.W., 1999. Systematic characterization of mélange bimrocks and other chaotic soil/rock mixtures. *Felsbau-Rock Soil Eng*., 17, 152-162.

Medley E.W., 2001. Orderly characterization of chaotic Franciscan Mélanges. *Felsbau rock Soil Eng*., 19, 20-33.

Medley E., Lindquist E.S., 1995. The engineering significance of the scale-indepedence of some Franciscan Melanges in California, USA. In: Daemen, J.K., Schultz, E.A. (eds.):35th US Rock Mech. Sym. Rotterdam. Balkema, 907-914.

Medley E.W., and Sanz. P.R., 2004. Characterization of Bimrocks (Rock/Soil Mixtures) With Application to Slope Stability Problems. In Schubert, W. (ed), Proc. Eurock 2004 and 53rd Geomechanics Colloquium, Salzburg, Austria, Oct 2004.

Moritz B., Grossaeur K., and Schubert W., 2004. Short Term Prediction of System Behaviour of Shallow Tunnels in Heterogeneous Ground Felsbau. *J. of Engineering Geology, Geomechanics and Tunnelling*. 22 (5/2004), pp. 35-43.

Raymond L.A., 1984. Classification of melanges: in Melanges: Their nature, origin and significance. Special Publication 228, Geol. Soc. of America, Boulder, Colorado; 7-20.

Riedmüller G., Brosch F.J., Klima K. and Medley E.W., 2004. Engineering Geological Classification of Fault Rocks. Poster at Eurock 2004 and 53rd Geomechanics Colloquium, Salzburg, Austria, October 2004.

Sabatakakis N., Koukis G., Tsiambaos G., Papanakli S., 2008. Index properties and strength variation controlled by microstructure for sedimentary rocks. *Engineering Geology*, 97, 80-90.

Sonmez H., Tuncay E., Gokceoglu C., 2004. Models to predict the uniaxial compressive strength and the modulus of elasticity for Ankara Agglomerate. *Int. J. Rock. Min. Sci*., Vol. 41, No.5, 717-729.

Sonmez H., Gokceoglu C., Medley E.W., Tuncay E., Nefeslioglu H.A., 2006. Estimating the uniaxial compressive strength of a volcanic bimrock. *Int. Rock Mech. Min. Sci*., 43, 554-561.

Tziallas G., 2010. Estimation of strength and deformability characteristics of composite rocks. MSc Thesis, Geotecnical Engineering Department, NTUA (in Greek).

Tsiambaos G., Sabatakakis N., 2004. Considerations on strength sedimentary rocks. *Engineering Geology*, 72, 261-273.

Zainab M., Kamaruzaman M., Cho G. C., 2007. Uniaxial compressive strength of composite rock material with respect to shale thickness ratio and moisture content. The Electronic Journal of Geotechnical engineering, 13, 1-10.

Δελτίο της Ελληνικής Γεωλογικής Εταιρίας, 2010
Πρακτικά 12ου Διεθνούς Συνεδρίου
Πάτρα, Μάιος 2010

Bulletin of the Geological Society of Greece, 2010
Proceedings of the 12th International Congress
Patras, May, 2010

SPRINGS (CLASSIFICATION, FUNCTION, CAPTURING)

Soulios G.[1]

[1] *Department of Geology, Aristotle University of Thessaloniki, gsoulios@geo.auth.gr*

Abstract

Todd, K (1980) proposed the following definition for springs: "a concentrated discharge of groundwater that emerges on the ground as a stream of water that flows freely". Spring is distinguished from water leak that is a normally diffused but extended (linear or 2D) slower movement of groundwater towards the ground surface. Uprush is every groundwater emergence on the ground surface or through the bed of water bodies (river, lake, sea).

In the context of hydrogeology springs and uprushes in general are in fact "overflows" of aquifers; hence they serve as aquifer discharge mechanisms. Springs emerge at the cross section of groundwater level with the topographic relief.

Springs are a strong evidence of rich groundwater potential. A big number of small springs emerging at the margins of basins or the hill slopes are an evidence of a shallow aquifer of low hydraulic conductivity. On the contrary, big springs emerging at the bottom of valleys, i.e. the basic geomorphological level, are an indication of a high potential aquifer characterized by considerable values of hydraulic conductivity.

1. Spring classification criteria

Spring classification in categories and types may be performed on the basis of various alternative criteria (several types may be distinguished in each category). Different spring categories occur depending on the criterion selected for classification. Hence, the following criteria may be used for spring classification:

- Mean spring discharge q (may be classified in very low, low, average, large, very large springs).
- Annual fluctuation of spring discharge, i.e. on the basis of the ratio $\omega = \frac{q_M}{q_m}$, where q_M and q_m are the maximum and minimum annual spring discharge, respectively ($\omega < 5$ constant discharge spring, $\omega > 5$ variable discharge spring).
- Discharge regime (perennial, seasonal, intermittent springs).
- Lithology of the recharge basin (karstic, ophiolitic, etc).
- Spring water chemistry and concentration of various ions (bicarbonate, alkaline, magnesium, etc).
- Water temperature (cold, normal, warm springs).
- Location of emergence relative to the seashore (inland, coastal, sub-marine springs).

2. Spring categories with regards to the geological structure

i Contact springs, figure 1. They are formed on the contact of a permeable formation (e.g. lime-

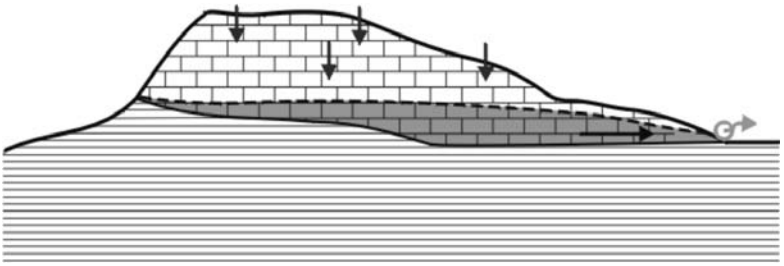

Fig. 1: Contact spring.

stone) that is superimposed on an impermeable formation, such as argillaceous schist. Those springs are related to perched aquifers.

Those springs emerge above the base level and are usually low to average. Their recharge basin is small and discharged volumes are not considerable. Their character is often seasonal and their discharge variable ($\omega>5$).

ii Quasy-contact springs, figure 2. A geological formation is often not characterized by uniform values of hydraulic conductivities throughout its entire vertical extent, either due to minor lithological variations, or mainly due to the development of zones of higher density in cracks and fissures. As a result, zones of higher hydraulic conductivity may exist upon zones of lower hydraulic conductivity. As illustrated in figure 2, in these cases seasonal or permanent perched aquifers of low potential may exist that are discharged at a spring.

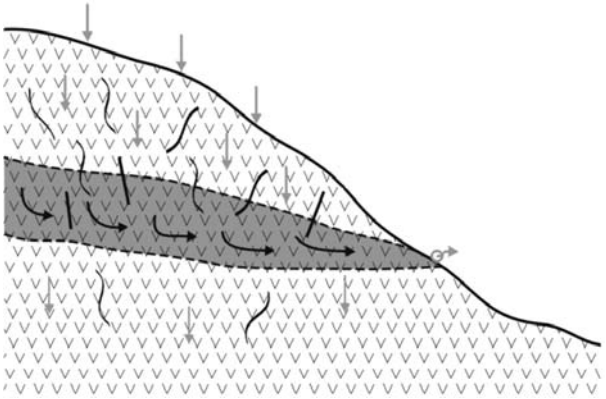

Fig. 2: Quasi-contact spring.

Quasi-contact springs are often seasonal with highly variable low discharge. Discharged volumes are low. Springs of this type emerge above base level.

iii Fault springs, figure 3. Creation of this type of spring is related to a fault that shifts to contact a permeable formation, i.e. an aquifer with an impermeable formation. Hence, the aquifer overflows at the fault. Those springs may be regarded as overflow springs (see below). Springs of this category often emerge close to the base level, may be of either low or high discharge rates whilst their discharge is variable. Recharge basins of those springs are often large and consequently total discharge volumes are high.

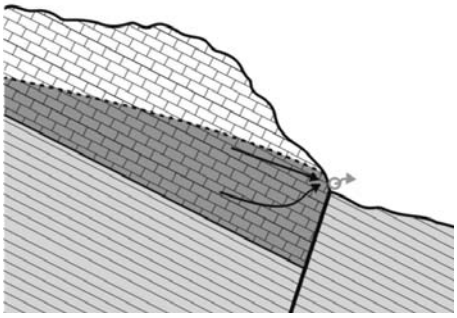

Fig. 3: Fault spring.

iv Overflow springs, figure 4. Several terms exist in the Greek reference literature for this particular category of springs and probably the presented one describes best their characteristics.

Normally those springs emerge at the regional base level. They are perennial, with a constant or at least not highly variable discharge rate and are related to high potential aquifers, which consequently results in large total discharge volumes.

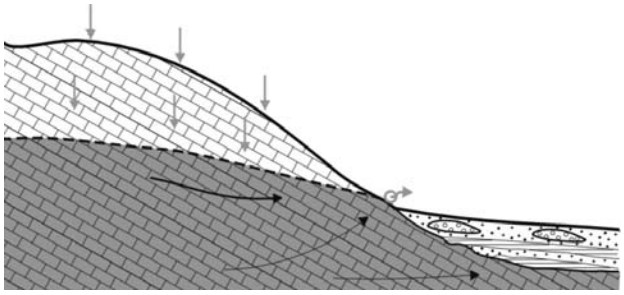

Fig. 4: Overflow spring.

In practice there are numerous combinations of afore presented spring categories which in fact mean that each spring may be considered to form a unique category on its own. Here are some special spring types that may be classified in one of the previously discussed categories.

- Irregular spring, figure 5. Water reaches the emergence point trough a siphon. In order for the spring to discharge water, groundwater level should reach the highest level of the siphon (AA'). If groundwater level falls below level BB' no water will be discharged from the spring, even if BB' level is above the elevation of the emergence point. As a result, the spring cease to discharge suddenly as it starts to discharge again given the right conditions. Hence spring operates at irregular intervals.

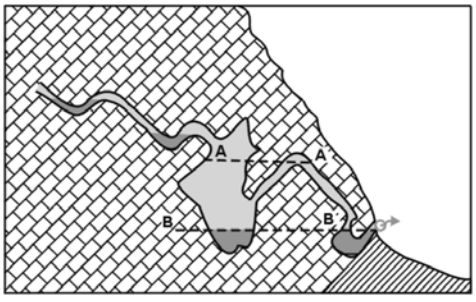

Fig. 5: Irregular spring.

- Vauclusian spring, figure 6. This term originates from the famous spring of Vaucluse, at the region of Avignon (France), which is a large spring with a mean annual discharge in the order of 30-40 m^3/sec. This spring is characterized by the existence of a large and deep conduit through which water emerges at ground surface. Water moves upwards due to hydrostatic pressure since the surrounding rock is solid and impermeable.

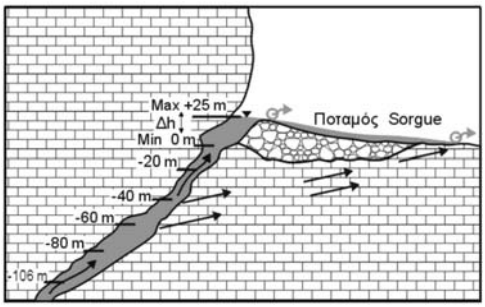

Fig. 6: Vauclusian spring.

- Uplift fault spring, figure 7. Emergence of this spring at the particular point is attributed to a fault that has uplifted an aquifer near ground surface. Hydrostatic pressure forces water to flow upwards through the permeable zone that is created due to fault tectonics and emerge at the fault line on ground surface. At the point of emergence the uplift movement of the water may be seen.

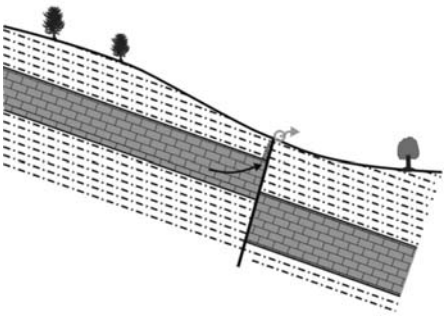

Fig. 7: Uplift fault spring.

- Trop-plein spring. Occasionally, an aquifer that is being discharged to a spring may receive excessive recharge due to heavy rainfalls and groundwater levels may rise considerably. In such cases, it is possible that groundwater levels intersect the topography and a second spring is thus formed, which operates in parallel to the main spring, as illustrated in figure 8. This second spring is seasonal and operates only during periods of highly elevated groundwater levels.

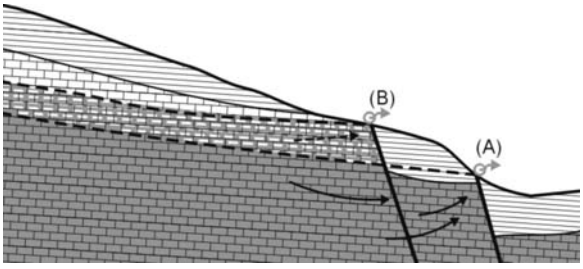

Fig. 8: Uplift fault (A) and Trop-plein (B) spring.

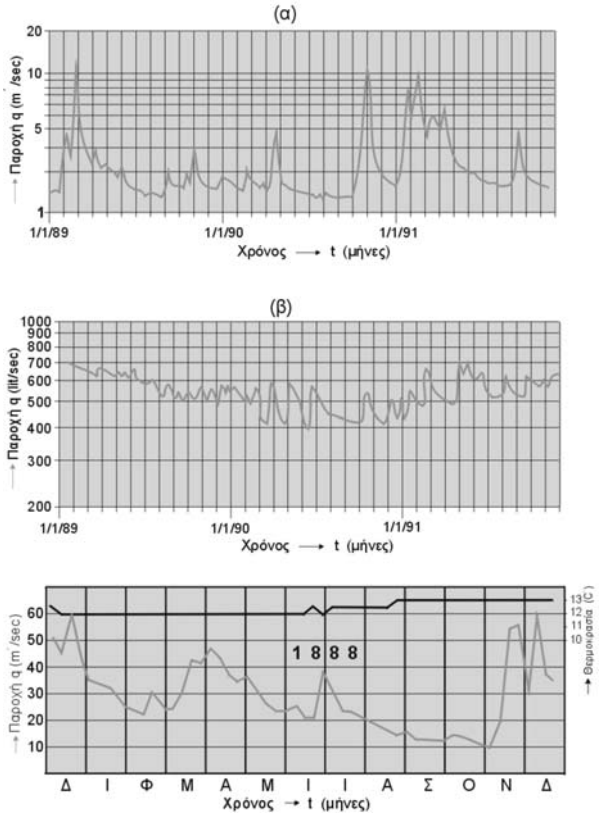

Fig. 9: Spring hydrographs (a) Aghios Nikolaos of Naoussa spring, (b) Aghios Ioannis of Serres spring, (c) Vaucluse (Avignon-France) spring.

Other special types of springs include thermal and coastal and sub-marine springs that will however be discussed on following chapters.

3. Spring function – Hydrographs –Recharge Zone

i It is obvious that every spring is related to an aquifer the groundwater level of which controls its discharge rate: High level corresponds to high discharge and low level corresponds to low discharge. When groundwater level declines below the emergence point the spring ceases to discharge.

ii Figure 9 illustrates the hydrographs of three springs:

(a) Aghios Nikolaos of Naoussa spring, characterized by high discharge variability ($\omega>10$),
(b) Aghios Ioannis of Serres spring characterized by low discharge variability ($\omega<5$),
(c) Vaucluse (Avignon-France) spring, for year 1888, also characterized by high discharge variability ($\omega>5$).

iii Each spring has a corresponding recharge zone, i.e. an area the groundwater of which drains to the spring. The larger the recharge area is the higher the discharge of the spring is. Precipitation depth and infiltration coefficient are also two factors that control the discharge.

4. Spring recession equations

Springs may be considered as a system comprising an "input", (which corresponds to infiltration within the recharge zone, or any other form of recharge), an aquifer (or an aquifer system) which transforms rain to discharge and therefore acts as "transformation function" and an "output" which is the spring discharge, i.e. the system is "Hyetograph – Transformation function – Hydrograph".

At this system, the "rising curve" of the hydrograph that represents the increase of the spring discharge, depends on the characteristics of the aquifer and the rainfall (entrance), while the "recession curve" depends only on the characteristics of the aquifer. Therefore, most of the suggested equations refer to recession curve.

i. Maillet's formula (1905). This formula depends on a conceptual model, according to which, the discharge of an aquifer is accomplished through an opening, like the discharge that takes place in pot through a porous cap. Therefore, the aquifer is simulated as a pot. Based on this correspondence, Maillet concluded to the exponential equation that expresses the exponential reduction of the discharge.

$$q = qoe\text{-}at \qquad (1)$$

where, q_o = is the initial discharge of the spring at starting time t_o,
t = is the time duration, in days, since the time t_o,
q = is the water discharge of the spring at some time t,
e = is the base of the napierian logarithm (= 2.71),
a = is a coefficient, known as recession coefficient or coefficient of tarissement, with dimension T^{-1} and time unit per day.

The recession coefficient is characteristic for each spring. This coefficient depends on the following parameters:

- The aquifer permeability k: the higher the k, the higher the coefficient a.
- The storage coefficient S (or the effective porosity m_e): the higher the S, the lower the coefficient a.
- The size of the aquifer: the bigger the size, the lower the value of coefficient a.
- The shape and the transmissivity coefficient (T) of the aquifer, the presence of relatively impermeable intermediate zones or layers, etc.

The recession coefficient has a physical meaning, since it corresponds to the physical properties of the system "aquifer-spring". Practically, this coefficient represents the daily spring discharge recession rate, during the recession period of the hydrograph.

An application of Maillet's equation at Korisos (Kastoria) spring is shown in Fig. 10. It is observed that the discharge values at the beginning of the depletion curve deviate from the straight line (which corresponds to the recession curve).

It is possible to calculate the effective reserves of a spring at a specific time point "t" during the dry period, if the recession coefficient "a" and the discharge of the spring "q" at the specific time point "t" are known. In fact, if we integrate over time "t" the second part of equation (1), we can calculate them as follows:

$$W = \int_{t=0}^{\infty} q.e^{-at}dt \qquad (2)$$

or $$W = \frac{c.q}{a} \qquad (3) \quad \text{hence} \quad W = \frac{84.660q}{a} \qquad (3)'$$

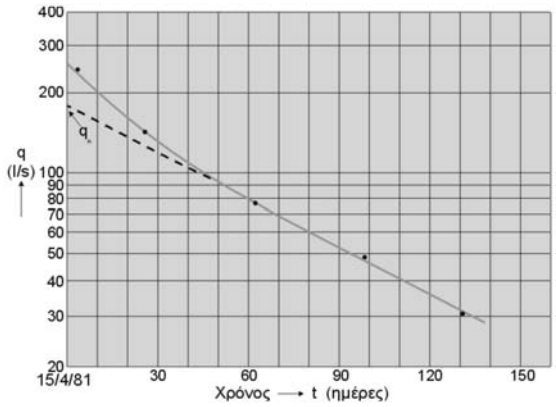

Fig. 10: Application of Maillet's equation in Korisos (Kastoria) spring.

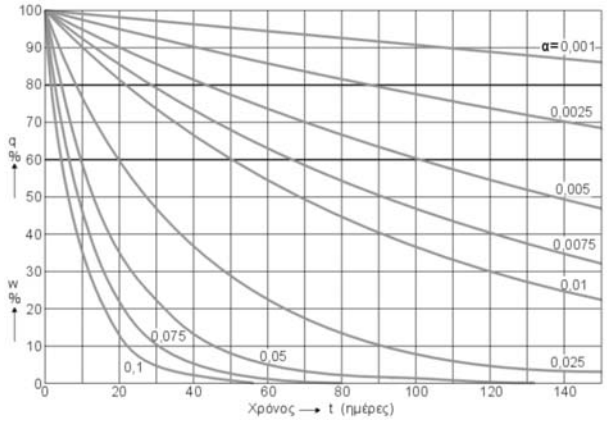

Fig. 11: Reduction of the discharge (q) and of the reserves (W) of a spring over time (t) during the dry period, in relation to the recession coefficient a.

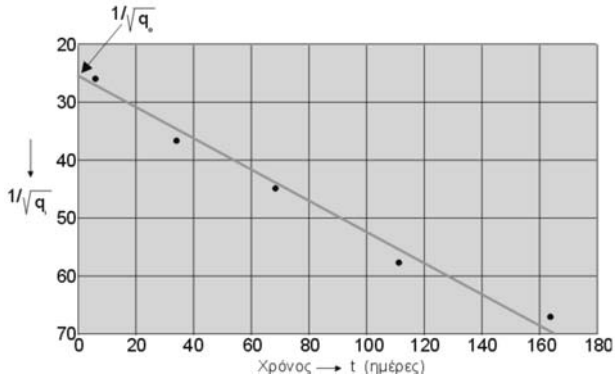

Fig. 12: Application of Tison's formula at the Korisos (Kastoria) spring.

Where c = integration constant; c = 86.400, the seconds of a 24-hour day, since "q" is calculated as volume/sec and a is calculated per day.

The graphs of Fig. 11 show the comparative (percentage) reduction of the discharge rate "q", and the evacuable reserves as a function of the time t (since the beginning of the dry period) and the recession coefficient a.

ii. Tison formula (1960). This formula is also based on a conceptual model. According to Tison, the aquifer discharge is not point but linear, which means that the aquifer is discharged along one side of the aquifer, through several spouts along a line. Therefore, Tison proposed the "hyperbolic formula":

$$q = \frac{q_0}{(1+at)^2} \tag{4}$$

The coefficient "a" in this formula is different from Maillet's formula "a".

Tison's formula (1960) was not widely applied or referenced in the international literature. Figure 12 shows an application of Tison's formula at the Korisos spring (Kastoria), where it was calculated that $a = 1{,}09 \times 10^{-2}\ d^{-1}$ and $q_0 = 0{,}16$.

The evacuable reserves according to Tison (1960) are calculated from the equation

$$W = \frac{86.400 q_0}{a(1+at)} \tag{5}$$

iii. Forkasiewicz-Paloc formula (1967). It is a formula based on an empirical approach. These two researchers observed that Maillet's recession coefficient was not always constant for a spring and that Maillet's formula is valid only for the dry period, for the recession segment of the hydrograph and not for the rising segment. So, they concluded to the formula:

$$\frac{1}{q^2} = \frac{1}{q_0^2} + \beta t \tag{6}$$

where β = discharge recession coefficient, which has no physical meaning nor it corresponds to a property or parameter of "aquifers-spring" system.

This formula was not widely applied or referenced in the international literature. Fig. 13 illustrates an application of this formula, implemented by the above researchers, for a spring in France.

Finally, it is mentioned that the integration of this formula does not provide the volume of the evacuable reserves at a specific time point, but it provides the volume W that will flow out of the spring between time t_1 (q_1) and t_2 (q_2):

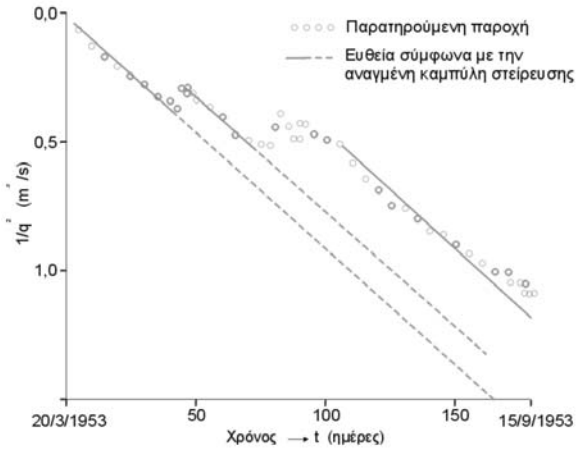

Fig. 13: Application of Forkasiewicz-Paloc equation at the spring of Lez (Montpellier, France).

$$W = \frac{2}{\beta}\left(\frac{1}{q_2} - \frac{1}{q_1}\right) 86.400 \quad (7)$$

iv. Schoeller formula (1967). It is a new approach of the Maillet's formula. Theoretically, it concerns karstic springs, but it may be also applicable in other types of springs. It assumes that inside the karstic mass exist:

- A conduit network of big potholes, fissures etc, through which the circulation of the groundwater towards the spring is rapid.
- A conduit network of medium size fissures and other types of discontinuities, through which the groundwater flows with relatively lower velocity.
- A conduit network of small and fine joints, through which groundwater flows with small velocity.

Therefore, the hydrograph is decomposed into several components (straight lines) from which usually only 2 or 3 contribute significantly to the total discharge of the spring. The formula that describes the hydrograph decomposition is:

$$q = q_{01}e^{-a_1 t} + q_{02}e^{-a_2 t} + q_{03}e^{-a_3 t} \quad (8)$$

Fig. 14 illustrates the application of the above formulas for the springs of Voula, Trikala.

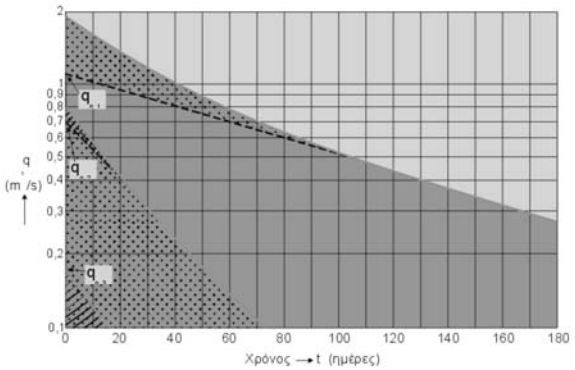

Fig. 14: Application of the Schoeller method at Voula (Trikala) spring.

It is possible for every type of conduits to find the corresponding reserves W_{01}, W_{02}, W_{03}.

It is marked that Schoeller's formula is multiparametric, i.e. it consists of many parameters (α_1, α_2, α_3…) contrary to the previous formulas that are single-parametric.

This formula is regarded as the basis for the simulation of the springs flow and discharge, especially for the karstic springs.

v. Mangin's formula (1974). Mangin considered that the water flows towards the spring from:

- The saturated zone, i.e. the aquifer, which is described by Maillet's formula.
- The unsaturated zone, directly to the spring, without passing through the saturated zone. This type of water reaches the spring certain days "t_i" after the rainfall cessation. After the passage of t_i number of days, the water reaches the spring from the saturated zone only.

The first segment of the hydrograph deviates from the exponential curve, Fig. 14: the water that flows out of the spring comes from both the saturated and the unsaturated zones, while the other segment of the recession curve corresponds to the discharge of the saturated zone only. For this reason, the semi-logarithmic diagram logq-t, Fig. 14, at the beginning, deviates from the straight line. Man-

gin's equation is given by the formula:

$$q = q_0 e^{-at} + q_0^* \frac{1 - nt}{1 + \varepsilon t} \tag{9}$$

The first part is the known Maillet's formula, while the second one is the homographic, bi-parametrical formula of Mangin.

$$q^* = q_0^* \frac{1 - nt}{1 + \varepsilon t} \tag{10}$$

where $n = \frac{1}{t_i}$ is a parameter with dimension [T^{-1}] per day and is related to the number of days, during which the water reaches the spring from the unsaturated zone.
ε = heterogeneity coefficient of the unsaturated zone, which characterize the curvature of the recession curve of the hydrograph.

The Mangin's formula corresponds to the upper dotted part of Fig. 14. The application of this formula is shown at Fig. 15 for the Korisos (Kastoria) spring and the results are n = 0.016 d^{-1} (t_i = 62 days), ε = 0.137, q_0^* = 1.70 m^3/sec.

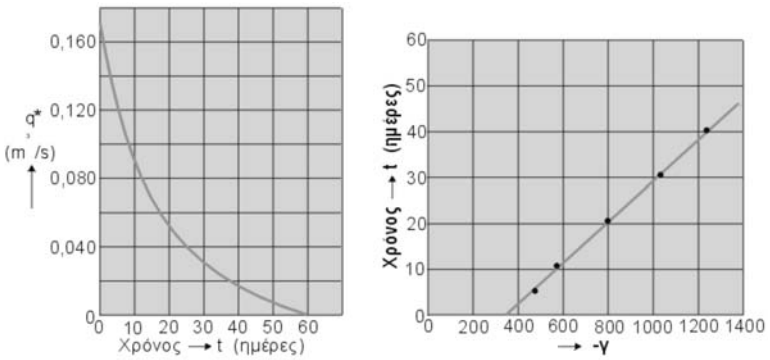

Fig. 15: Application of Mangin's method (1974) at Korisos (Kastoria) spring.

Integration of Mangin's formula (10) provides the reserves of the unsaturated zone.

This formula has significantly contributed to the understanding of the spring mechanism and it is widely used in mathematical simulations.

vi. Finally, it is mentioned that many other formulas have been suggested, mainly tri-parametric, but without significant references in the literature. In addition, many formulas related to the hydrodynamics of the aquifers with specific boundary conditions have been proposed (Berkaloff, 1967, Delhomme, 1971, Tripet, 1969, Galabov, 1972, Burger, 1959 etc.).

5. Boundary conditions of groundwater systems that feed springs

i. A simplified aquifer system, as it mentioned, consists of a single spring and can be simulated with a container that is emptied by a tap (a hole), Figure 16 (a). In this case we have a 'simple', 'normal' unit hydrograph. In this hydrograph, the recession curve will have the following feature: while there is no recharge (i.e. dry period without rainfall), the gradient will decrease continuously with the time t. In

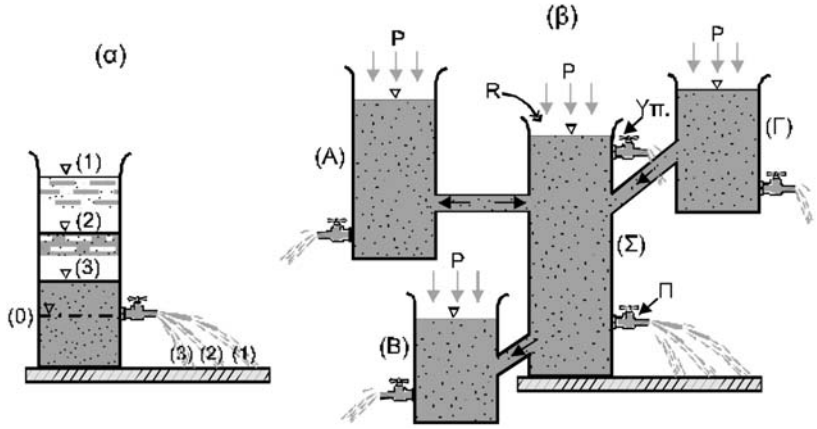

Fig. 16: Spring fed by: (α) «simple», (β) «complex» aquifer system.

practice, although, it happens not always or perhaps not so often. The groundwater system that feed the spring is often "complex", Figure 16 (b) and may have various organization, composition and operation.

All this complex organization and operation of the aquifer system that supplies a spring will be reflected and clearly recorded in its hydrograph and especially in the recession curve. There are other ways and methods, however, to determine the complicacy and complexity of an aquifer system that feeds a spring. We will present some of them.

ii. Discharge correlation method. Two springs that belong to the same aquifer system have common features: boundary conditions, piezometric surface, recharge regime, limits of groundwater flow, unsaturated zone. In other words, they have many common factors that influence their discharge. Thus, their discharge should be correlated, so even more strongly as the aforementioned factors are the main factors that determine it.

The application of the discharge correlation method in three different pairs of springs is presented in figure 17:

The first (α), for the neighbouring springs Aposkepou and Kefalariou: Based on 20 measurements, the correlation coefficient of their discharges was estimated to be r = 96,6%. This indicates that both springs belong to the some aquifer system, as was confirmed later with pumping tests.

The second (β), for the neighbouring springs «Megali Vrisi» and «Aghios Dimitris» Kserovouniou (northwestern part of mountain of Othris): Based on 21 measurements the correlation coefficient of their discharges was estimated to be r = 88.4%. This coefficient neither so big, nor so small, indicates that both springs belong to an united aquifer system, having nevertheless low hydraulic connection.

The third (γ), for the neighbouring springs Korisos and Militsas Kastorias: Based on 25 measurements the correlation coefficient of their discharges was estimated to be r = 81,3%. It is without doubt that both springs are fed from two different aquifer systems, as was confirmed later; the decrease of the discharge of Korisos spring due to pumping, do not significantly influence the discharge of Militsa spring.

Consequently, two neighbouring springs can be:

- completely independent, i.e. being fed from two independent aquifer systems,
- or belong to an aquifer system with a powerless hydraulic connection,

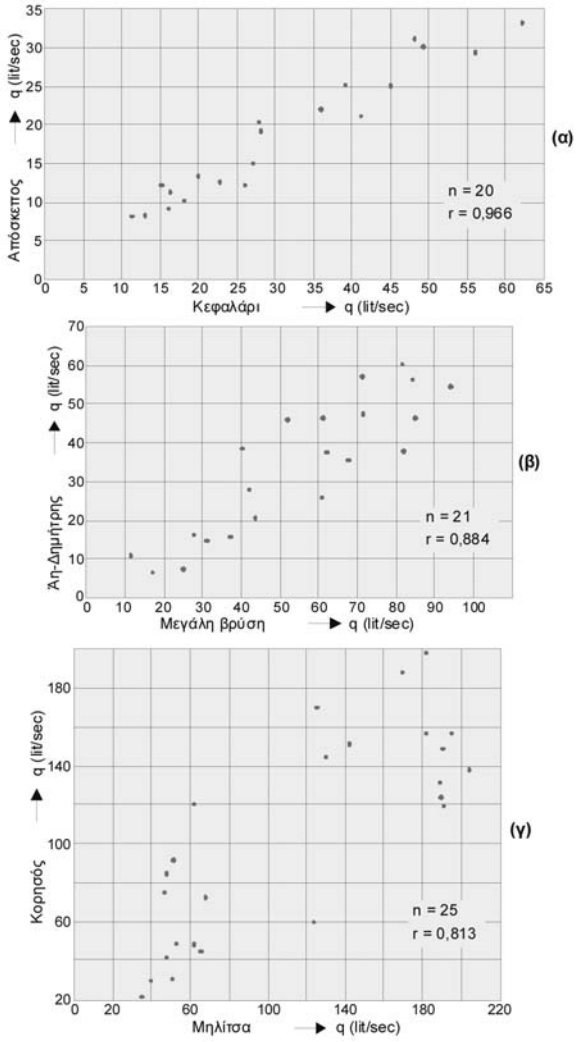

Fig. 17: Discharge correlations from different pair of springs (see the text).

- or, finally, belong to an united aquifer system with a strong hydraulic connection.

Thus, the correlation coefficient r of discharges may take a wide range of values and indicates what happens.

iii. Sorted discharges method. When we have one "simple" aquifer system in which groundwater is discharged by one spring, its discharge follows the law: the number of days with high discharge is relatively small and grows as the discharge diminishes, so the number of days with low discharges in a hydrological year is the largest. Thus, every year is recorded a distribution of discharges, coherent to that of Gauss.

The drawing of a cumulative curve of sorted discharges in a 'simple', 'normal' aquifer system with one spring will be a straight line, while that in a "complex" with "anomalies" and "episodes" will have breaks in the line, up or down in some classes of discharges, which are indicative of the kind of 'anomaly' or 'episode'.

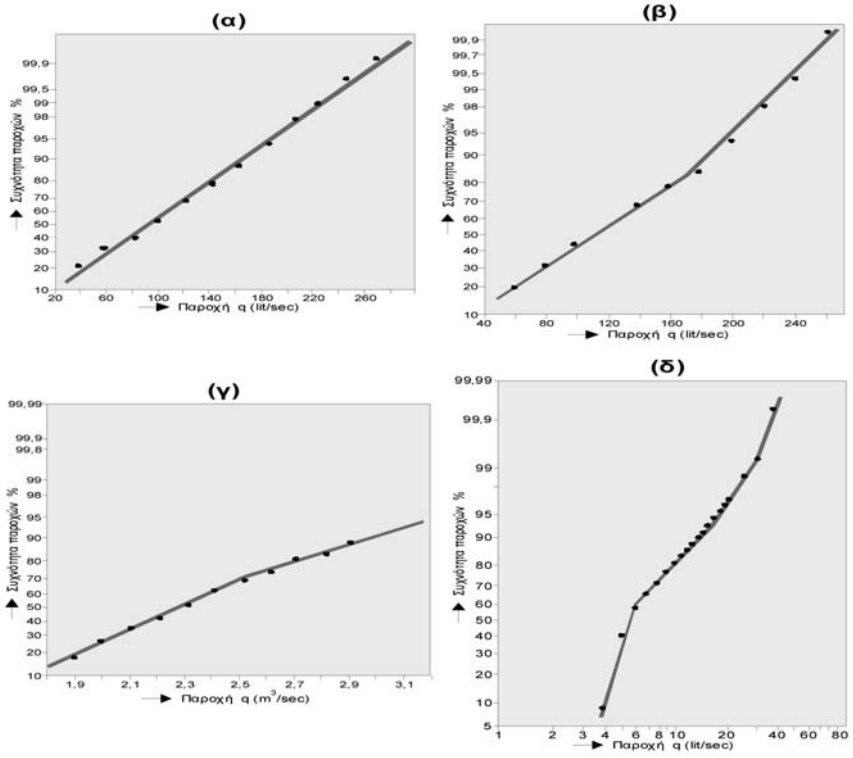

Fig. 18: Cumulative curves of sorting discharges (see the text).

In figure 18, we can see: In fig. 18(α) the case of a "simple" aquifer system (Korisos spring, Kastoria) with one output, that is one spring, without other "losses".

In fig. 18(β) the case of Militsa spring (Kastoria) that apart from the main spring there is an overflow spring, operating seasonal, when the aquifer system recharges strongly (by rainfall) and the discharge of the main spring is above a critical value. In this point, the curve presents a decline, indicating water loss.

In fig. 18(γ) the case of Almiros spring (Aghios Nikolaos, island of Crete); when the rainfall rate is high, the streams formed in non-karst parts of the recharge zone and flow in its karst parts, supply entire groundwater system. So, when the discharge creates a decline in slope (break) of curve (reverse to that of (b) case) that means recharge.

In fig. 18(δ) a complex case with many declines in discharge curve due to "episodes" and organization of aquifer system (Almiros spring, Heraklion, island of Crete) is presented.

iv. Boundary conditions of aquifer system and the recession curve of hydrograph. As mentioned, the shape of the recession curve consists the reflection, "the transfer" of the structure and operation of the entire aquifer system. In this curve depicted quantity data, as well as the whole structure and the boundary conditions of the aquifer system: recharge, losses, "episodes", structure and size of the saturation and the unsaturated zone. The above enter as boundary conditions and form the shape of the recession curve of hydrograph. Any deviation of the general rule that governs the recession curve can be reflected in the hydrograph. In figure 19, six (6) different types of recession curve of spring hydrograph, are presented. Each of which recession curves has special significance:

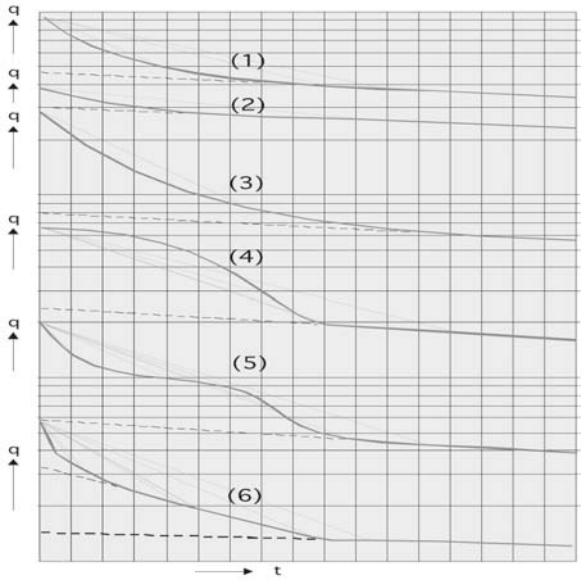

Fig. 19: Different types of recession curves from spring hydrographs (see the text).

The curve (1) from Korisos spring (Kastoria) corresponds to a "simple" and "normal" aquifer system. The saturated zone is "normal" compared to the unsaturated zone.

The curve (2) from Aghios Nikolaos spring (Crete) indicates that the size of the unsaturated zone is small compared to the saturated.

The curve (3) from Stilos-Armeni spring (Crete) indicates that the unsaturated zone is very large compared to the saturated zone.

The curve (4) from Militsa spring (Kastoria) indicates the existence and the seasonal operation of an overflow spring.

The curve (5) from the Mikro Vouno (Chtouri, Thessaly) spring indicates the hydraulic connection between two different semi-independent aquifer systems: one karst system (the principal), and another alluvial system (secondary), which recharge the first one.

The curve (6) from the Maara spring (Aghitis, Drama) means a multiple recharge of the spring: from the main aquifer system, from seasonal lake and from recharge of surface flows.

The first three curves show quantitative differences in the structure of the aquifer system, and the entire range between (1), (2) and (3) is possible and goes back to the relationship between the saturated and the unsaturated zone.

From the other hand, the last three present qualitative differences: different boundary conditions as concerns the recharge, the discharge of the system and the structure-composition and inter-connection of individual components.

v. Cumulative curves of annual precipitation and reduced discharge.When a decrease in discharge of a spring is recorded, it is not obvious from a priori whether is due to any decrease in precipitation or any human intervention, or both. Indeed is possible that human interference with pumping does not happen in the immediate aquifer system that feeds the spring, but in another one that may be located some distance away and has an indirect hydraulic connection with it.

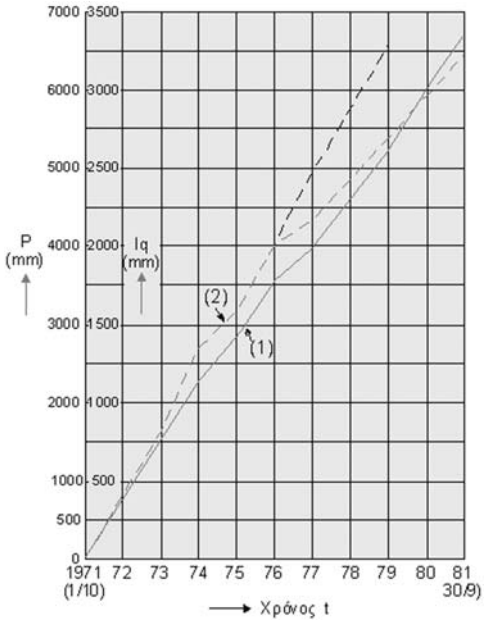

Fig. 20: Cumulative curves of annual precipitation (1) and reduced discharge (2).

The answer can be given with the development of cumulative precipitation curves P and the reduced discharge Iq (Figure 20). Reduced discharge Iq is the quotient of the annual volume of discharge of a spring by the surface area (zone) of recharge. It is estimated as water height (mm) and corresponds to the amount of infiltrated water. The reduced discharge is practically the height (mm) of the water discharge.

If the reduced discharge Iq changes mean slope compared to the slope of precipitation, is observed human intervention. In figure 20, an example from the Voula spring (Trikala) is presented. By 1975, there were no boreholes drilled in the region. Since 1975 began to be drilled and pumped boreholes in the broader alluvial aquifer in contact with the karstic system that feeds the spring. This caused a gradual deviation of Iq in relation to the average initial course.

6. Spring capture

i. One right spring capture to be done the mechanism of discharge must be known, the hydrograph (fluctuation of discharge through time) and the geometry of geological formation. For that reason:

- The exact point of discharge must be known which sometimes does not converge with the point of emerge in the surface, Fig. 21.
- Soil and subsoil must be removed till the point of discharge.
- It must be checked and confirmed if we have a full discharge, or a spout or multiple points of discharge.
- The hydrograph of the spring must be known and the fluctuation of its discharge.

According to these assumptions the planning of the spring capture will be planned. In addition to these we must decide if it is right to be done; but while it decided whether it will be:

- A project of simple spring capture for the total or for a part of its discharge.
- A project of capture and deployment of that spring meaning a project that will aim to the increase of the discharge without modification of the water supplies.
- A project of capture with readjustment of the water supplies.

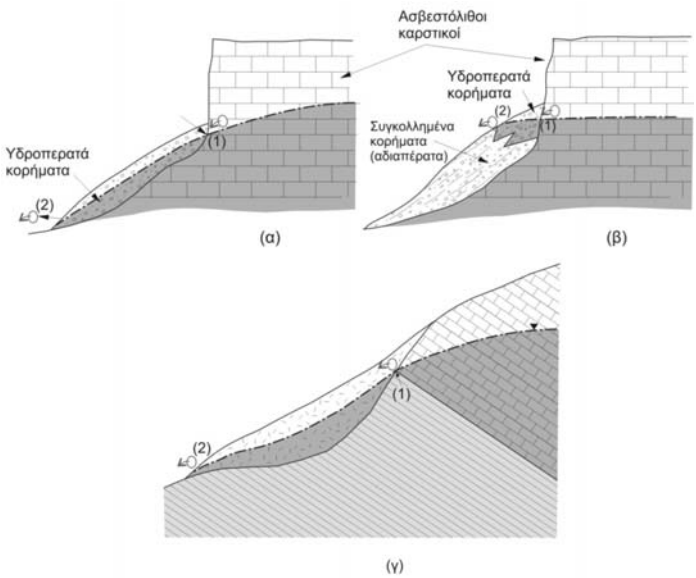

Fig. 21: Some cases with different point of subterrain (1) and terrain (2) point of discharge. (a) and (b) from Kallergis (1999) after Letourneur and Michael, (1979) and (c) from Dimopoulos (1983) redrawn – modified – completed from the author.

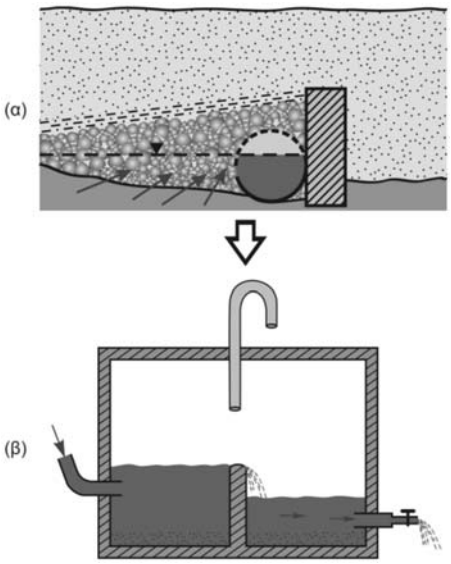

Fig. 22: (a) simple spring capture with perforated pipe vertical to the water direction and waterproofed diaphragm, (b) water capture tank which divert the water in distribution system (see text).

According to the hydrogeological conditions and the pursuing purpose it is possible to develop a water capture of a spring with different projects.

A simple water capture project is shown in Figure 22. This contains a dry wall at the point of discharge (excavation and cleaning already took place), a perforated concrete pipe at the point of spout which is covered with impenetrable clay material or with concrete to its other side.

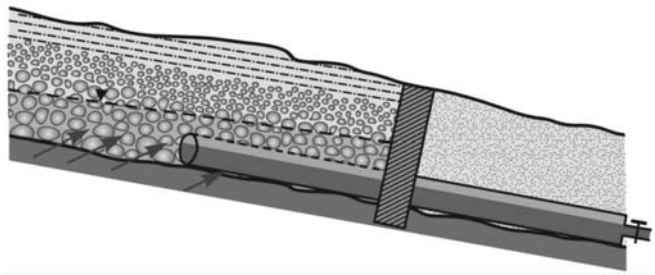

Fig. 23: Spring capture with perforated pipe parallel to the direction of the flow and vertical insulating diaphragm (see text).

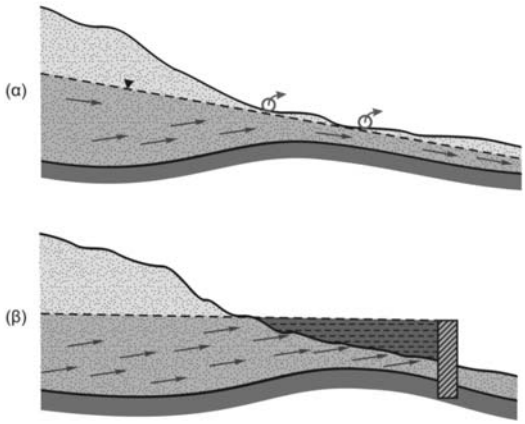

Fig. 24: Capture of spring and shallow aquifer with the construction of vertical sealed underground and above the ground diaphragm.

Another way of simple spring capture is shown in Figure 23.Also there, after the excavation and the cleaning of the soil a pipe is placed (concrete, or PVC or stainless material),also perforated in its half or more covered with rock curb, till the exact length of the allocation, this length is usually up to 2-3 m from this point and then the pipe is not perforated. A while after the point from where the pipe is not perforated an impenetrable diaphragm is placed, pushed in the well to the subsoil which is made by concrete or a clay material.

If it is chosen for the capture to be done with a pipe vertical to the direction of the flow (Fig. 22) or parallel to the direction (Fig. 23) or even at the side, depends from the geometry and the extension of the discharge area.

Another way of spring capture with which its deployment is achievable is with the creation of underground or above the ground diaphragm which will restrain the flow (Fig. 24) and is applicable mainly at contact spring in perched or shallow aquifer and rarely in overflow springs as shown in figure.

In figure 25 there is a spring capture with collective tunnel and discharge control tank. Simultaneously it is made partial or total spring regulation of resources, because the water level of the aquifer from point (1) is moving to point (2) and according to the operations from the control tank it can remain permanently there or rise to a middle level or during the year can achieve its initial level (1).

In figure 26 we have a spring capture with the construction of a well (a) and non collective tunnel (b) from its basement.

Finally figure 27 shows a simple spring capture. After the excavation, the cleaning and also the disclosure of the main water carrying crack in a relative cohesive cracking rock, concrete walls (or from other material) are created with piezometric chamber and chamber with filter and conduit leading in the tank or consumption.

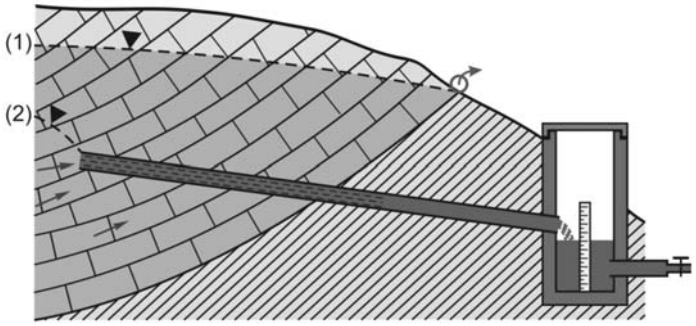

Fig. 25: Spring and aquifer capture with collector trench (1) initial water level, 92) water level during the system operation (Schneider, 1973) redrawn and modified from the author.

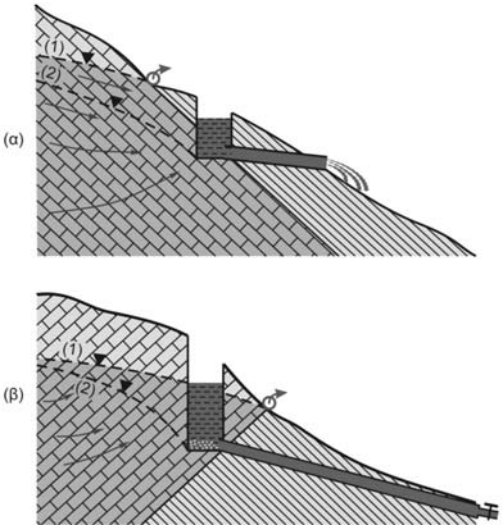

Fig. 26: Spring capture with a well and tunnel aquifer (a) parallel with the impermeable (b) vertical with the impermeable (1) initial water level, (2) water level during the system operation (Schneider, 1973) redrawn, modified and completed by the author.

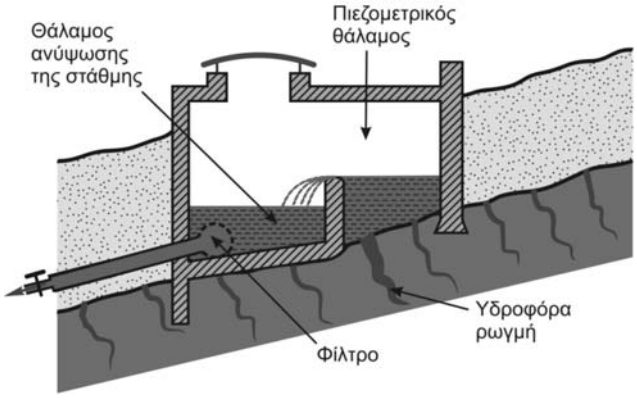

Fig. 27: Spring capture (Kallergis, 1999 after Letourneur and Michel, 1971, redrawn-modified by the author).

Another last case of water capture is shown in figure 28. In this case we have multiple spouts towards a line. Water capture is made with the construction of a water capture trench and tunnel.

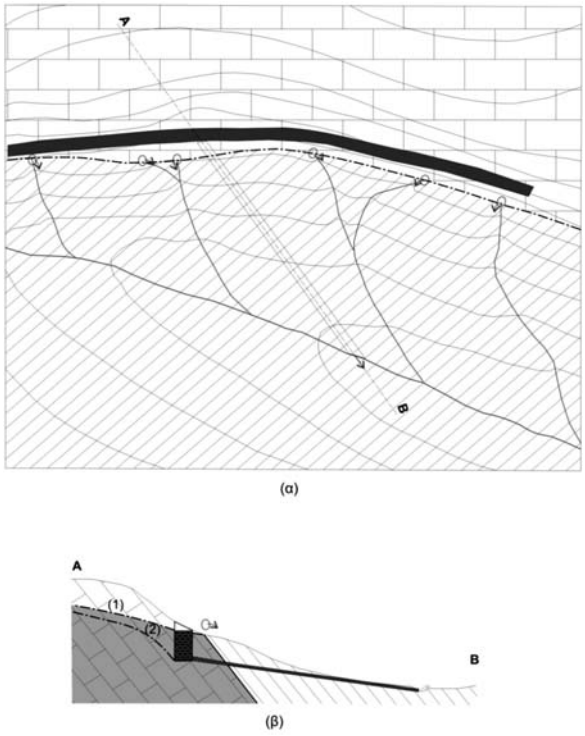

Fig. 28: Aquifer capture with collector trench and collector tunnel (Schneider, 1973) redrawn and modified from the author.

7. References

Algrot, M., 1967. L' ecoulement de la fontaine de Vaucluse. *Travaux du Lab. d' Hydrogeologie-Geochimie, Universite de Bordeaux, t. XV, 97 p.*

Beauregard, J., 1978. Le bas debits des cours d'eau en France. Etiages normaux et exeptionnels. Frequence et repartition. *Hydrog. et Geol. de l' Ing., deuxiere serie, n° 3, p. 215-223, editions B.R.G.M., Orleans (France).*

Bennett, T. W., 1970. On the design and construction of infiltration galleries. *Ground Water, v.8, n° 3, p. 16-24.*

Berkaloff, E., 1967. La limite de validite des formulles courantes de tarrissent du debit. *Chronique d' Hydrogeologie, n° 10, p. 31-41, editions B.R.G.M., Orleans, France.*

Bezes, C., 1976. Contribution a la modelisation des systemes aquifers karstiques. *Memoires du C.E.R.G.H., v. X, fasc. I-II, p. 1-135, Montpellier.*

Boegli, A., 1980. Karst Hydrography and physical Speleologie. *Springer-Verlag, Berlin, 144 p.*

Burger, A., 1959. Hydrogeologie du basin de l' Areuse. *Bul. Soc. Neuchat. Geogr., t. 52, n° 11, fasc. 1, p. 5-304.*

Dimopoulos, G., 1995. Recherce suv la gestion des ressources hydriques -5: Les travaux de captge (en grec). *Ed. du Depart. de Geologie, Univ. De Thessalonique, p. 111-159.*

Drogue, C., 1967. Essai de determination des composantes de l' ecoulement des sources karstiques. *Chronique d' Hydrog., n° 10, p. 43-47, editions du B.R.G.M., Orleans (France).*

Drogue, C., 1969. Contribution a l' etude quantitative des systemes hydrologiques karstiques d' après l' exemple de quelques karst perimediterranees. *These d' etat, Univ. de Montpellier, 482 p.*

Delhomme, J., 1971. Essai de schematization de l' ecoulement de l' eau dans un massif calcaire (determination analytique de la reponse unitaire). *Rapport LHM R/71/1, 7p. Labor. d' Hydrologie mathematique, Ecole de Mines, Paris.*

Galabov, M., 1972. Sur l' expression mathematique des hydrogrammes des sources et le prognostic du debit. *Bul. B.R.G.M. ser. (2), III, nº 2/1972, p. 52-57, Orleáns, France.*

Galabov, M., 2008 Analysis and application of springs time series. *Πρακτικά 8ου Υδρογεωλογικού Συνεδρίου, Τόμος 1, σελ. 17-32.*

Forkasiewicz, J., Paloc, H. 1967. Le regime de tarissement de la Voux de la Vis. *Chronique d' Hydrogeologie, nº 10, kp. 59-73, editions B.R.G.M., Orleans, France.*

Kallergis, G., 1999. Hydrogéologie Appliquée–Environmentale (en grec) Vol. A. *Ed. de Chambre Technique de Grèce, 331 p.*

Letournier, J., Michel, R., 1971. Geologie du genie civil. *Ed. Armand Colin, Paris, 436 p.*

Maillet, E., 1905. Essais d' hydraulique souterraine et fluviale. *Herman, Paris, 218 p+24 fig., 11 graph., h.t.*

Mangin, A., 1974. Contribution a l' etude hydrodynamique des aquifers karstiques, premiere partie. *Ann. Speleol. 29, nº 3, p. 283-332.*

Mangin, A., 1974. Contribution a l' etude hydrodynamique des aquifers karstiques, deuxieme partie. *Ann. Speleol. T. 26, fasc. 2, p. 283-329, Moulis (Ariege), France.*

Mijatovic, B., 1974. Determination de la transmissivite et du coefficient d' emmagasinement par la courbe de tarissement dans les aquifers karstiques. *Mem. A.I.H., Reunion de Montpellier, nº 10, p. 225-230.*

Schneider, H., 1973. Die Wassererchliessung. *Ed. Nulkan – Verlag, 847 p.*

Schoeller, H., 1967. Hydrodynamique dans le karst (ecoulement et emmagasinement). *Chronique d' Hydrogeologie nº 10, p. 7-21, edition B.R.G.M., Orleans, France.*

Soulios, G., 1985. Recherches sur l' unite des systemes aquifers karstiques d' après des exemples du karst hellenique. *Journal of Hydrology, v. 81, p. 333-354.*

SoulioS, G., 1991. Contribution a l' etude des courbes de recession des sources karstiques: exemples du pays helleniques. *Journal of Hydrology, v. 124, p. 29-42.*

Soulios, G., 2008. Hydrogéologie générale. Deuxième volume (en grec). *Ed. Univ. Studio Press, 349 p.*

Tison, G., 1960. Courbe de tarrissement, coefficient d' ecoulement et permeabilite du bassin. *Memoires A.I.H.S., p. 229-243.*

Todd, K.D., 1980. Groundwater Hydrology. *John Wiley & Sons, New York, 2nd ed., 535 p.*

Tripet, J., 1969. Une methode d' approache de l' analyse du tarrissement d' une source karstique. Etude preliminaire. *Mem. B.R.G.M., nº 76, p. 701-709, Orleans, France.*

Welchert, W. T., Freeman, B. N., 1973. Horizontal wells. *Jour. Range Management, v. 26, p. 253-256.*

Δελτίο της Ελληνικής Γεωλογικής Εταιρίας, 2010
Πρακτικά 12ου Διεθνούς Συνεδρίου
Πάτρα, Μάιος 2010

Bulletin of the Geological Society of Greece, 2010
Proceedings of the 12th International Congress
Patras, May, 2010

EARTHQUAKES AND PREVENTIVE MEASURES

Makropoulos K. C.

Department of Geophysics, University of Athens, 157 84 Athens, Greece, kmacrop@geol.uoa.gr

Abstract

The most important natural hazard in Greece is earthquake. The earthquake phenomenon can be explained using the theory of Plate Tectonics. Greece lies in the middle of the collision between two major tectonic plates, the Eurasian and the African, resulting in a very fragmented geotectonic regime. From the point of energy released, half of the European seismic energy is released within the Greek territory. Thus, the ways and means of reducing the seismic risk, that is the consequences from an earthquake, is for Greece of vital importance. The seismic risk is the convolution of the seismic hazard and the vulnerability of the specific area. From those factors, the vulnerability, which expresses the weakness or the sensitivity of the system and the value at risk during an earthquake, is the only parameter that can and should be minimized. The accomplishment of such an important task requires a combination of top-down and bottom-up approaches. In terms of the top-down approach, the Earthquake Planning and Protection Organisation's, (E.P.P.O.), main target is to plan the national policy for earthquake protection, as well as to coordinate the public and private resources for the implementation of this policy, through issuing regulations, guidelines for emergency situation or for strengthening existing buildings including monuments of cultural heritage value e.t.c. EPPO also has a strong educational/training focus, targeting inter alia schools and hospitals. Of importance are also bottom up approaches, often at the personal level, which include useful measures concerning the proper behaviour before, during and after a destructive earthquake. These approaches are also part of the EPPO mandate and focus.

Key words: *Greece, earthquake, seismic hazard, vulnerability, risk, preventive measures, E.P.P.O.*

1. Introduction

Earthquake is a natural phenomenon that occurs without warning and does not respect cities, nations or borders. It is a judge of the efficiency of the antiseismic measures that are applied to each construction, to the planning of a city and to the state level. When a large earthquake occurs, mistakes and incautiousness which were hidden under glamorous building facades are revealed and are, unfortunately, often accompanied by loss of human life. Experience of destructive earthquakes in Greece conforms to its long history, with evidence dating back to 550B.C.

On the other hand, the earthquake is a message of life, a sign that our planet is and will remain alive, keeping mankind alive as well. This is because the earthquakes are the result of the continuous deformation and movement of the earth due to endogenous forces caused by gravity, rotation, and heat from within the Planet. The extraterrestrial forces coming from sources like solar radiation and the gravitational pull of the Moon and the Sun causing the tides etc., try to extinguish all anomalies of the surface of the Earth and, if it weren't for the endogenous forces that cause the earthquakes, the

Fig. 1: The six main tectonic plates.

surface of the Earth would be covered by water of equal depth at all points. Therefore, the earthquake is indeed a message of liveliness for our Earth.

In the present study the effort will concentrate to the, brief, explanation/answer of the following question: why Greece had, has and will continue to have high seismicity. Subsequently, given the intense seismic activity of our country and the lack, to date, of a reliable earthquake prediction model, the attention will focus on measures to reduce the consequences of an earthquake to constructions, environment and, most importantly, to people.

2. Greek seismicity and Plate Tectonics

The main natural hazards are earthquakes, volcanic eruptions, floods, intense meteorological phenomena, fires, desertification phenomena, coastal hazards and landslides. Among these natural hazards, earthquake is the one that causes the most severe destruction in Greece since the antiquity.

The occurrence of an earthquake can be sufficiently explained by the Theory of Plate Tectonics. From the moment we could identify the earthquake by analyzing the seismogram, an effort began to study its origin and answer questions such as: why did it strike in this area and not the other. Such questions were explored by mapping the epicentres, calculated with ever increasing accuracy as the seismographs became more numerous and sensitive. The mapping showed that the distribution of sources on the Earth is not random. They are concentrated on narrow zones dividing the surface of the Earth in six big pieces that comprise the six main lithospheric plates (Fig. 1) namely the Pacific, American, Eurasian, African, Indian, and Antarctic plate.

Greece lies in the middle of the collision between two tectonic plates, the Eurasian and the African, the latter sinking under the former at a rate that exceeds 3-4 cm per year south and east of Crete (Fig. 2). Greece, apart from the collision front, and due to its relatively small size, is broken into pieces, with many seismic zones. As a result of this complex seismo-tectonic regime, Greece has the greatest seismicity in the whole of Europe (Makropoulos and Burton, 1981; Ambraseys & Jackson 1990; Papazachos, 1996; Papazachos and Papazachou, 2003). Half the energy of all the earthquakes occurring in Europe is released in Greece. There is no Greek province that doesn't host seismic sources (Fig. 3). Fortunately, approximately 75% of Greek earthquakes occur either under the sea, away from inhabited areas, or in several kilometres depth and do not cause major disasters.

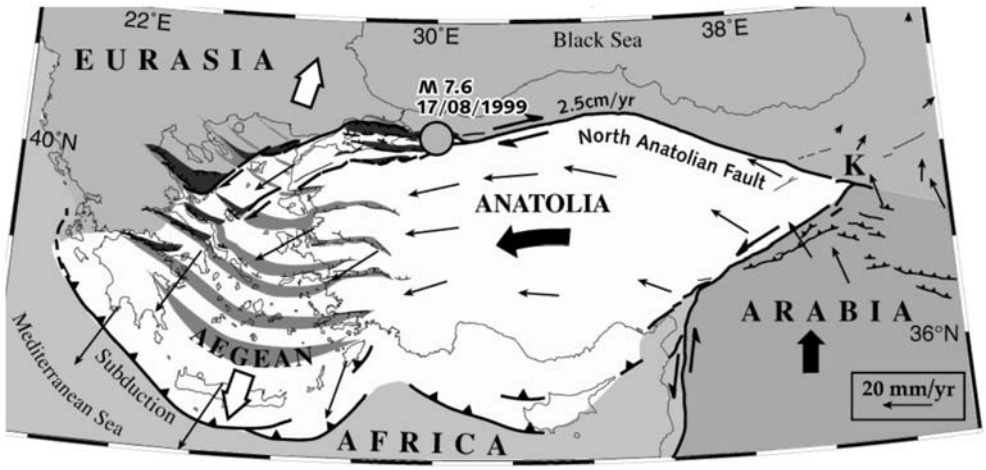

Fig. 2: Tectonic plates in the broader area of Greece (after Armijo et al., 1999).

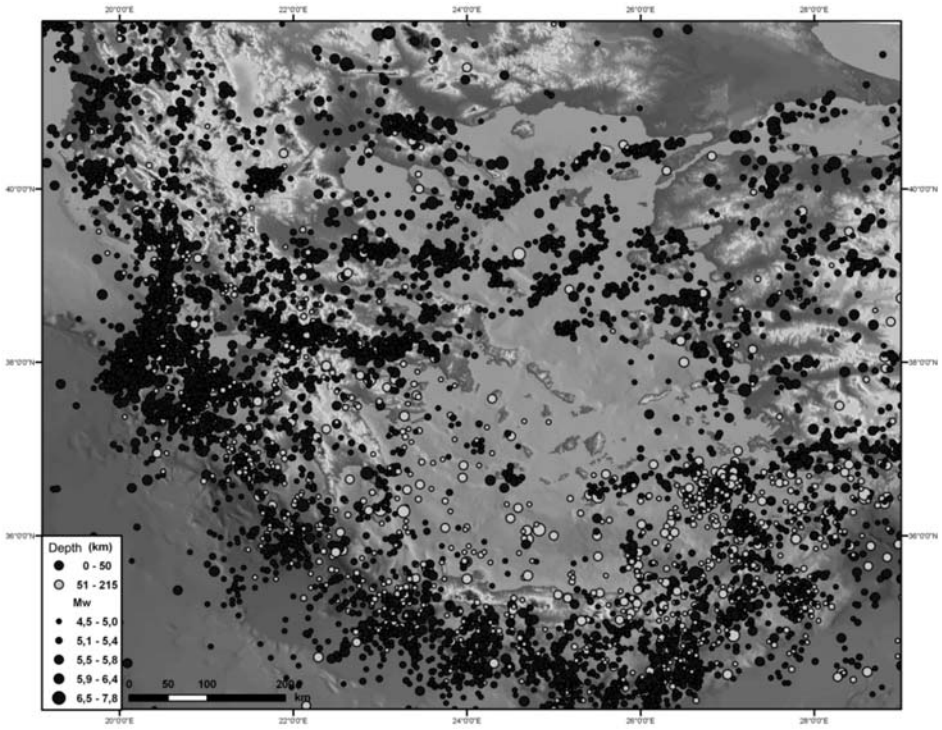

Fig. 3: Seismicity in Greece for the period 1900-2009.

Apart from the high level of seismicity in Greece, due to its position between the Eurasian and African plates, resulting in a very fragmented geotectonic environment, the risk from an earthquake, despite modern technical advances, especially for the big cities, continues to be substantial and even rising. This is because of the overcrowding in large cities and the rising

demand for land development, factors which force construction on inappropriate grounds. Even within the same city, the differences in damages can be huge, since the ground factor plays a decisive role.

Another, equally important reason that today the consequences of an earthquake (risk) are greater than before, is the height of the buildings. Whereas 40 or 50 years ago in Greece there existed primarily low rise houses, today many buildings are multi-store high-rise ones. This fact made our cities more vulnerable to both, local and distant earthquakes. As it is well know, a structure will suffer great damage and may collapse if its eigenperiod becomes equal or very near to the predominant periods of the seismic waves arriving at the foundation of that building (resonance phenomenon). But the more distant the earthquake, the richer its seismic waves are in long periods. Thus, a high-rise building is more at risk by a relatively distant earthquake than by a local event. Example of increasing vulnerability is the case of Athens, our capital city. Most of the apartment buildings (six to eight stories), built after 1960 in Athens have an eigenperiod very close to the periods of the seismic waves arriving at Athens from seismic sources 60 and 70 kilometres away, i.e. from the well know from the antiquity seismic sources of Corinthos and Atalanti. The 1981 Corinth earthquake with an intensity around 7 degrees of MM in Athens, was the undeniable proof of this newly introduced vulnerability.

Since the geological phenomena that cause the earthquakes hardly change within 100 or 200 years, the only certainty is that earthquakes will continue to test man's labors and expose our mistakes or inconsideration.

Before going into specific ways and means of reducing the consequences from an earthquake by introducing certain preventive measures, the definition of the terms involved will, briefly, be described next.

3. Seismic Hazard, Vulnerability and Risk

Seismic risk (R) has been defined as the potential economic, social and environmental consequences of hazardous seismic events that may occur in a specified period of time. It is the combination, the convolution in mathematics (Fig. 4), of the seismic hazard (H) of a region, which is defined as the probability P of an event of certain magnitude M to occur within a specific area in the next T years, and the vulnerability (V), which expresses the weakness or the sensitivity of the system and the value at risk in the area, during an earthquake.

Among the three factors that determine the level of seismic risk and consequently the level of the possible disaster, seismologists and geoscientists try to determine the seismic hazard using the seismic history of the area, its geology and tectonics. This effort aims at providing Engineers with all the data they need for a proper and realistic earthquake resistant design. An earthquake resistant design is crucial, since even if earthquakes could be predicted in the future (which is far from the state of the art today), they cannot be avoided.

Therefore, the reduction of seismic risk is mainly possible through reducing the vulnerability, or the sensitivity of both technical and social structures and of their reinforcement in order to face large earthquake with the least possible damage.

Next, practical measures of strengthening the technical and social structures and thus reducing their vulnerability and consequently the seismic risk, at the national and individual levels will be presented as these emerged from the activities of the Earthquake Planning and Protection Organisation (E.P.P.O. or as is more commonly known, O.A.S.P.).

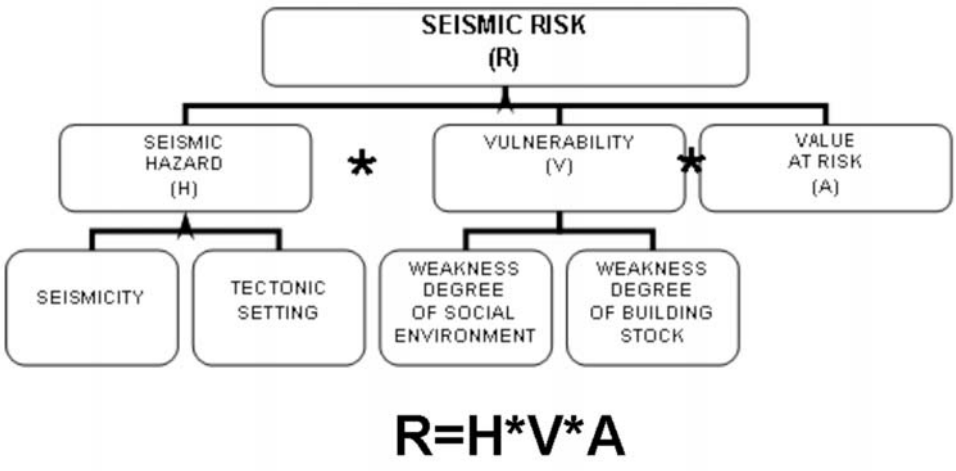

Fig. 4: Definition of Seismic Risk.

4. Protective Measures

4.1 National level

Prevention measures should be taken at both the national (top-down) and individual (bottom-up) levels. Concerning the national level the responsible institutions in Greece are the Secretariat General of Civil Protection (SGCP), and the E.P.P.O. The latter is a legal entity and operates under the supervision of the Ministry for Infrastructure, Transport and Communications.

The aim of E.P.P.O. is to process and plan the national policy for earthquake protection – as well as to coordinate the public and private resources for the implementation of this policy. For this reason E.P.P.O. makes up all the necessary programs, leads and coordinates the earthquake protection policy of the country during the pre-seismic period while the SGCP is responsible for the co and post-seismic period, in close cooperation with other public and private organizations that participate in relevant subjects.

In the prevention sector, E.P.P.O.'s policy mainly aims at five (5) fundamental directions:

1. The prompt and reliable briefing of the State and the citizens from the scientific institutions that study seismic events and the seismic danger, so that planning and confrontation of the danger are feasible.
2. The improvement of regulations for strengthening the antiseismic behaviour and the antiseismic capacity and safety of structures and especially of buildings and bridges, so as to minimize the damage caused by the earthquake.
3. The cultivation of an "earthquake-aware" conscience and behaviour of the citizens through continuous training and briefing, so that they know what to do before, during, and after an earthquake in order to protect effectively their lives and wealth.
4. The prompt and rational planning of the State's readiness to confront emergencies and aid the affected i.e. immediate mobilization, sufficiency of forces and means, co-ordination of all the organizations involved in the case of an earthquake.
5. The production and exploitation of up-to-date scientific knowledge and technology in Greece in subjects that are related with the seismic danger and its confrontation, so that permanent and sufficient scientific support to the State is ensured and the seismic defence of the country is achieved.

The main activities of E.P.P.O. are:

1. Strengthening of the seismic capacity of the structures, through regulations such as the Greek Seismic Design Code (EAK –2004), Greek Design Code of Reinforced Concrete (EKOS – 2000), Regulation of Repair and Strengthening of Buildings, Pre-earthquake Inspection of Public Buildings and Pre-earthquake Inspection of Bridges.
2. Study and estimation of the seismic danger (through the disciplines of seismology and seismotectonics), including ensuring the existence of reliable seismological data, enactment of specifications and recommendations for the elaboration of studies related to seismic hazard and emphasis in the local ground conditions.
3. Briefing of citizens, including School Educational Programs, Educational Seminars to school teachers, briefing of the citizens in subjects related to earthquakes, forming and training of groups of volunteers.
4. Emergency Planning, including the design of the Plan «Xenokratis- Earthquakes» and the Construction of rescue equipment for trapped persons.

4.2 Individual level

Some prevention measures that should be taken at the level of the individual, taken from F.E.M.A. (2010) and E.P.P.O. (2010), are the following:

4.2.1 Check for hazards in the home

Fasten shelves securely to walls. Place large or heavy objects on lower shelves. Store breakable items such as, bottled foods, glass, and china in low closed cabinets with latches. Hang heavy items such as pictures and mirrors away from beds, couches, and anywhere people sit. Brace overhead light fixtures. Repair defective electrical wiring and leaky gas connections. These are potential fire risks. Secure a water heater by strapping it to the wall studs and bolting it to the floor. Repair any deep cracks in ceilings or foundations. Get expert advice if there are signs of structural defects.

4.2.2 Identify safe places in each room

Under sturdy furniture such as a heavy desk or table, against an inside wall. Away from where glass could shatter—around windows, mirrors, pictures, or where book-cases or other heavy furniture could fall over.

4.2.3 Locate safe places outdoors

In the open, away from buildings, trees, telephone and electrical lines, overpasses, or elevated expressways.

4.2.4 Make sure all family members know how to respond after an earthquake

Teach all family members how and when to turn off gas, electricity, and water. Teach children how and when to call emergency services, the police, or fire department and which radio station to tune to for emergency information.

4.2.5 Contact local emergency management office or Red Cross chapter for information on earthquakes

4.2.6 Have disaster supplies on hand

Flashlight and extra batteries, portable, battery-operated radio and extra batteries. First aid kit and manual, emergency food and water, non-electric can opener, essential medicines, sturdy shoes.

4.2.7 Develop an emergency communication plan

In case family members are separated from one another during an earthquake (a real possibility during the day when adults are at work and children are at school), develop a plan for reuniting after the disaster.

Ask an out-of-state relative or friend to serve as the "family contact." After a disaster, it's often easier to call long distance. Make sure everyone in the family knows the name, address and phone number of the contact person.

4.2.8 If indoors

Take cover under a piece of heavy furniture or against an inside wall and hold on. Stay inside. The most dangerous thing to do during the shaking of an earth-quake is to try to leave the building because objects can fall on you.

4.2.9 If outdoors

Move into the open, away from buildings, street lights, and utility wires. Once in the open, stay there until the shaking stops.

4.2.10 If in a moving vehicle

Stop quickly and stay in the vehicle. Move to a clear area away from buildings, trees, overpasses, or utility wires. Once the shaking has stopped, proceed with caution. Avoid bridges or ramps that might have been damaged by the quake.

4.2.11 Stay out of damaged buildings. Return home only when authorities say it is safe

Use the telephone only for emergency calls. Clean up spilled medicines, bleaches or gasoline or other flammable liquids immediately. Leave the area if you smell gas or fumes from other chemicals. Open closet and cupboard doors cautiously. Inspect the entire length of chimneys carefully for damage. Unnoticed damage could lead to a fire.

4.2.12 Be prepared for aftershocks

Although smaller than the main shock, aftershocks cause additional damage and may bring weakened structures down. Aftershocks can occur in the first hours, days, weeks, or even months after the quake.

4.2.13 Help injured or trapped persons

Give first aid where appropriate. Do not move seriously injured persons unless they are in immediate danger of further injury. Call for help.

Remember to help your neighbours who may require special assistance — infants, the elderly, and people with disabilities.

4.2.14 Inspection Utilities in a Damaged Home

Check for gas leaks: If you smell gas or hear a blowing or hissing noise, open a window and quickly leave the building. Turn off the gas at the outside main valve if you can and call the gas company from a neighbour's home. If you turn off the gas for any reason, it must be turned back on by a professional.

Look for electrical system damage: If you see sparks or broken or frayed wires, or if you smell hot insulation, turn off the electricity at the main fuse box or circuit breaker. If you have to step in water to get to the fuse box or circuit breaker, call an electrician first for advice.

Check for sewage and water lines damage: If you suspect sewage lines are damaged, avoid using the toilets and call a plumber. If water pipes are damaged, contact the water company and avoid using water from the tap. You can obtain safe water by melting ice cubes.

5. Concluding remarks

From the above discussion it should be clear that, due to its unique seismotectonic regime, Greece had, has and unfortunately will continue to have earthquakes. However our knowledge about the phenomenon and today's advancements in earthquake engineering, allows us to deal with it more effectively. How?

First of all, by building in such a way, as to minimize the effects of an earthquake, which, even if we could predict it, we cannot prevent it from happening and, second, equally important, a change of culture that can be summarized in the following motto: We have to learn to live with the earthquakes, which means we have to learn as much as we can about the earthquake as a phenomenon, since our understanding of it, as well as the knowledge of practical ways of protection, such as those described above, are decisive factors in mitigating the indirect or secondary effects and panic, which, sometimes, are worse than the disaster caused by the earthquake itself. Thus, education of the citizens, starting from the primary school, is of vital importance and is among the main preparedness measures at both national and individual levels.

Finally, one thing should be clear by now, that earthquakes are unavoidable and certain to recur. Therefore, it is up to us, individual citizens, civil society and the state, to plan ahead and prepare for the unwelcome but inevitable future events, especially in Greece which has such a long experience of building and rebuilding what Poseidon's or Enceladus, wrath has left behind in ruins.

6. References

Ambraseys, N. N. and Jackson, J. A., 1990. Seismicity and associated strain in central Greece be-tween 1890 and 1988. *Geophys. J. Int.,* 101, 663-708.

Armijo R., Meyer B., Hubert A., Barka A., Westward propagation of the North Anatolian fault into the northern Aegean: timing and kinematics, 1999, *Geology*, 27, 267-270.

E.P.P.O., 2010. Earthquake Safety Measures, http://www.oasp.gr/default.asp?l1 = 3&l2 = 2#A, in Greek.

F.E.M.A., 2010. What to Do Before an Earthquake, During an Earthquake, After an Earthquake. http://www.fema.gov/hazard/earthquake

Makropoulos, K. C. and Burton, P. W., 1981. A catalogue of seismicity in Greece and adjacent areas. *Geophys. J. R. Astron. Soc.*, 65, 741-762.

Papazachos, B. C., 1996. Large seismic faults in the Hellenic Arc. *Ann. Geofisica*, Vol. XXXIX, N. 5, 891-903.

Δελτίο της Ελληνικής Γεωλογικής Εταιρίας, 2010
Πρακτικά 12ου Διεθνούς Συνεδρίου
Πάτρα, Μάιος 2010

Bulletin of the Geological Society of Greece, 2010
Proceedings of the 12th International Congress
Patras, May, 2010

ENERGY RESOURCES OF GREECE: FACTS AND MYTHS

Christanis K.

University of Patras, Department of Geology, 26500 Rio, Greece, christan@upatras.gr

Abstract

Energy is essential for human life and civilization being extremely crucial for the continuation of human development. The main concern worldwide is to meet rising demand for energy in a sustainable way and at reasonable cost. Greece has significant lignite and some uranium reserves and remarkable potentials in renewable sources. However, the primary energy mix used in the country today is based on lignite and imported oil and gas, the latter increasing country's dependency on foreign suppliers, while renewable sources play a minor role. The public opinion is misinformed and sometimes confused in respect of some aspects concerning energy issues. This strongly influences important decisions on energy projects and in overall, the energy policy of the country.

Key words: *energy sources, greenhouse gas emissions, Greece, primary energy.*

1. Introduction

Energy is essential for human society and civilization; it is one of the fundamental prerequisites to achieve economic growth, social and cultural development, which by turn are improving our standard of living.

Before the industrial revolution, the energy demands were modest. Man relied on the sun and the biomass for heat, on animal muscles and the wind power for transportation, on own and animal muscles as well as on wind and water power for labour tasks. Over time the energy demands of the mankind were continuously rising. It is estimated that *homo hunter* needed 20 MJ per day, *homo agricola* 40 MJ and *homo industrialis* 175 MJ (Bell, 1995). In 1800 by a global population of around 1 billion, the annual energy use per capita did not exceed some 20 GJ on average. Some 200 years later, the global population has risen by a factor higher than 6, while the per capita annual energy consumption is estimated to have risen by a factor of 20 (Grübler, 2004).

The increase of the world population, the technological and industrial development and the life modernization resulted in the rapid increase of energy demand globally. Among the mineral resources exploited annually worldwide, fossil fuels posses the first places in terms of quantity and economic significance (Fig. 1). Energy became obviously the backbone of every national economy and today the security of energy supply is among the first priorities for all the national governments. The access to reliable energy sources at reasonable cost and the environment-friendly energy generation are essential for future economic growth and the prosperity of the society. The global energy needs are covered to more than 80% by fossil fuels, namely oil, gas and coal, whereas nuclear power and renewable sources contribute to only 6.5% and 13.5%, respectively (Fig. 2a).

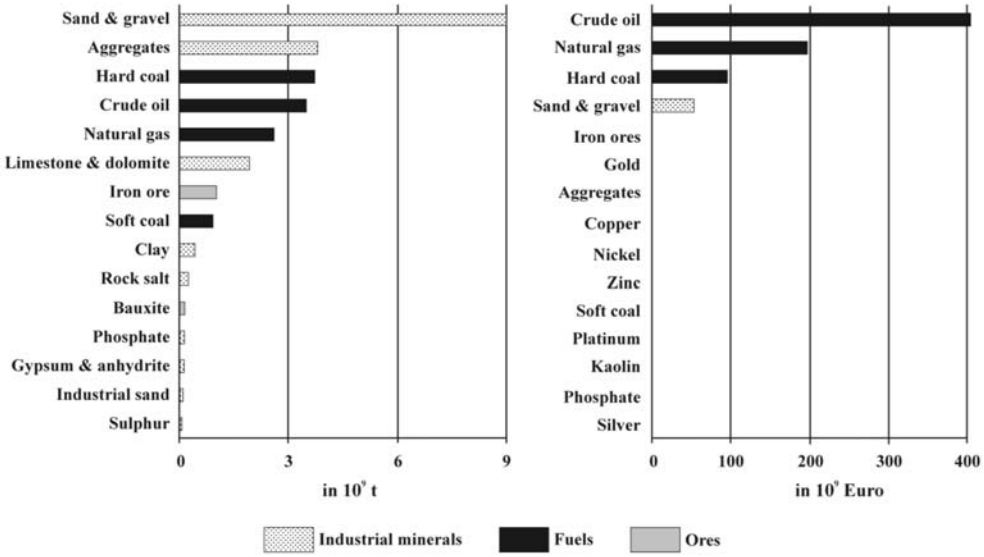

Fig. 1: The top-15 mineral resources globally produced in 2002 ranked by quantity (left) and value (right) (after Lüttig, 2007).

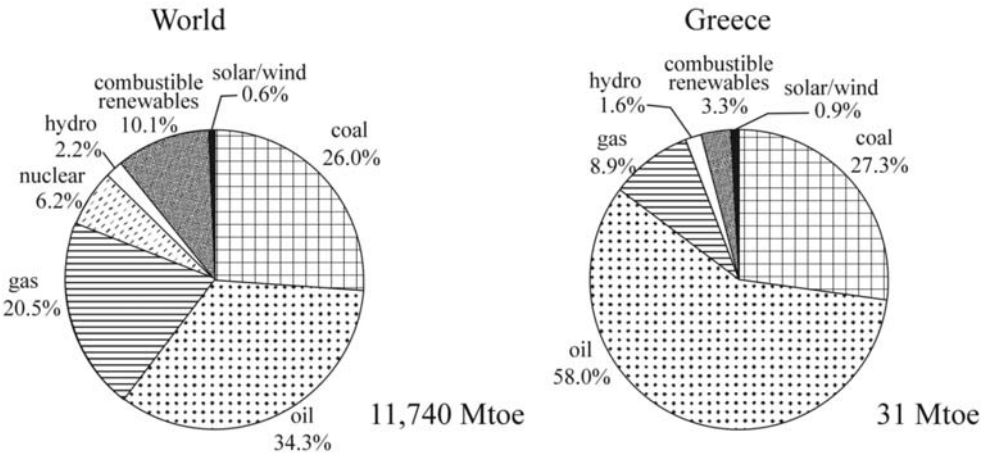

Fig. 2: Share of primary energy production in 2006 in the world (left) and in Greece (right) (IEA, 2008).

2. The primary energy status of Greece

In 2006 Greece relied on energy imports by 72%, being well above the EU average of 54% (EUROSTAT, 2009). The primary energy mix of the country is based to $^2/_3$ on hydrocarbons (IEA, 2008). Coal is a domestic fuel used mainly for electric power generation, while the renewable energy sources cover <6% of the demand (Fig. 2b). Greece does not own nuclear power plants.

2.1 Oil

The crude oil reserves of Greece are estimated to amount some 10 Mbbl (EIA, 2009). Promising oil-

bearing areas might exist. Crude oil resources in Western Greece and the North-Aegean Sea are speculated but further exploration is necessary. The domestic production from Prinos, Northern Greece, amounts c. 1,000 bbl/d, which cover only c. 0.2% of the daily consumption (432,000 bbl). Thus, Greece strongly depends on oil imports, mainly from Iran, Saudi Arabia, Russia, Libya, Egypt and Kazakhstan, with Russia and the Black Sea countries becoming more important after finishing the construction of the Burgas-Alexandroupolis pipeline. Although the demand for oil has increased in the last years, its percentage contribution to total primary energy production is gradually decreasing due to the rising introduction of natural gas (IEA, 2008).

2.2 Natural Gas

With reserves of only 70 Gcf (EIA, 2009), Greece does not produce natural gas. Consumption, however, has increased significantly and this trend is expected to continue and possibly tripling over the next ten years. Despite the recent strong demand growth, the share of natural gas in total energy consumption is still small, reaching 8.9% in 2006 (Fig. 2b). Greece imports c. $^2/_3$ of its natural gas demands from Russia and the remaining $^1/_3$ from Algeria as LNG.

2.3 Coal

Greece relies heavily on domestic lignite reserves amounting 4.3 Gt. Around 63.6% of the exploitable reserves are hosted in the tectonic trench of Western Macedonia (Florina, Amyntaeo, Ptolemais, Kozani), 28.8% in Eastern Macedonia (Drama), Northern Greece, and 7.6% in Megalopolis Basin, on Peloponnese (Kavouridis, 2008). Several lignite deposits are distributed over the country but there are no plans for exploitation. The main production areas are these of Western Macedonia and Megalopolis. With an annual lignite production exceeding 70 Mt in 2006, Greece is the second largest European lignite exploiter after Germany.

The country does not own hard coal reserves; small amounts, c. 0.5 Mt of bituminous coal, are yearly imported from South Africa, Russia, Venezuela, and Colombia (EIA, 2009).

2.4 Nuclear energy

Uranium reserves are known in the areas of Drama and Xanthi, at the North-East part of the country. The reserves could support a nuclear power plant but after a political decision in early 1980's, nuclear energy is not a priority.

2.5 Renewable sources

Due to the geographic position and the geomorphologic conditions, Greece has high solar and wind potentials. Annual solar radiation ranges between 120 kWh/m^2 in the northern part to 150 kWh/m^2 in the southern part (Tsilingiridis and Martinopoulos, 2010) and the average wind energy flux is in excess of 600 W/m^2 per year at 10 m height (Lalas et al., 1983). Both parameters are sufficient to supply large-scale power generation units, which can substitute to a high extent fossil fuel power plants being responsible for 50% CO_2, 80% SO_2 and 33% NO_x of the domestic release (Kaldellis et al., 2008). This could be very well applicable in the case of small-scale industries, as well as in isolated areas like the islands. Wind farms are already installed on the Greek islands of Crete, Evia, Andros, and Samos, whereas Naxos possesses also a high wind potential for large scale-electricity generation (Fyrippis et al., 2010).

Another renewable resource of Greece is geothermal energy. Due to recent volcanism, geothermal fields are located throughout the country; Santorini, Milos and Nissyros Islands are the most prom-

ising high-enthalpy fields for electricity generation. Unfortunately, trials to install a 2-MW geothermal power plant on Milos Island failed in late 1980's (Delliou, 1990), and hence geothermal energy did not recover since, mainly due to social and political reasons.

Hydropower is responsible in a positive way to whatever progress Greece had achieved after World War II. The construction of large dams coupled with hydro-power plants during the 1950's and the 1960's provided electricity to major industries at that time like the aluminium industry and revived the countryside population, especially in the indigent Western Greece. Most of the dams are built along major rivers, especially in Western Greece, where the annual rainfall and water reserves are relatively abundant.

The biomass potential is also significant due to the high agricultural production, which yields high amounts of wastes; recent studies show that the climate is suitable for the cultivation of several plants suitable for bio-fuel production (Tuck et al., 2006).

3. Facts and Myths

After the first oil crisis in 1973, the public awareness on the limitation and the depletion of the fossil-fuel reserves begun to increase steadily. Simultaneously, the environmental aspects of all human activities, particularly the energy generation, attracted increasingly attention. The interrelationship among energy supply and security, economic prosperity and environmental impacts became a favourable topic of the daily discussions in the developed countries. Scientists from irrelevant disciplines, ecologists considering selective data sets only, politicians following advisors with minor knowledge, speculating media, companies with variable interests, lay persons, all following sometimes paths beyond any logic, did and do judgements and statements on related topics resulting in the disinformation of the public opinion and confusing the people. This results in the lack of social concurrence, which is a prerequisite for the implementation of certain energy projects.

The present paper aims to clarify some aspects of the Greek energy sector that are presented to the publicity in a subjective way causing misinterpretations.

3.1 Oil

Although oil combustion is a significant CO_2 emitter, a surprising low publicity is given to this. In fact, oil is emitting only around 20% less CO_2 than coal for the same power generated. In the transport section, however, oil and its derivatives are exclusively used contributing significantly to the greenhouse gas (GHG) emissions. Oil is the main fuel consumed in Greece (58%; see Fig. 2b). According to EUROSTAT (2007) the GHG emissions from transportation sector in Greece reached c. 18% of the total GHG emissions being second after the power generation sector (45%). Additionally, the increased rate of GHG emissions from transport is higher than the respective from power generation during the last decade indicating the increasing environmental impact from oil combustion and vehicle emissions. All these, along with some other activities, requiring oil combustion like building heating systems and private, small-scale power generators particularly used in the agricultural and stock-farming sector, prove that although oil is environmentally friendlier than coal, in terms of absolute values it is also a major greenhouse gas source.

Apart from environmental issues oil is not a domestic energy source meaning that its use requires import from and hence, dependency on other countries. This, in turn, has a direct impact on both the economy and the policy of Greece.

3.2 Natural Gas

The introduction of natural gas into the Greek energy market was advertised in the 1990's as a clean and environmental friendly source. Over the last decade the natural gas contribution to Greece's gross energy generation has increased by an amazing 7,500% (!).

Natural gas consists of methane, which by burning is oxidised to CO_2. Of course, the amount of CO_2 emitted by gas combustion is c. 50% lower than this emitted by oil combustion for the same energy output (IEA, 2009a). In this sense, the truth is that natural gas is, indeed, cleaner and friendlier than oil and coal but not at all 'clean and environmental friendly'. Indisputably natural gas is the least emitting fossil fuel; however, the extraordinary increase in its use over the last years yields considerable amounts of CO_2 released in the atmosphere.

On the other hand, the reliability of the natural gas supply was hardly tested at the time of the conflicts between Russia and Ukraine, particularly in January 2009. The dependence on Russia but also on the countries the pipeline is coming through is a fact. Thus, a major part of Greece's energy sources relies not only upon typical trade rules like price bargain but also on geopolitical scenarios and foreign affairs.

3.3 Coal

Coal is considered the 'dirtiest' fuel contributing significantly to the greenhouse effect, thus being blamed for climatic change.

The fact is that coal combustion really emits huge amounts of CO_2, more than every other fossil fuel used for power generation. CO_2 emitted from hard coal and lignite combustion is c. 1.3 and 1.45 times, respectively, the amount released by oil combustion for the same energy output (IEA, 2009a). Over the last decades it has been told that the human CO_2 footprint, mainly due to coal combustion, causes global warming, which results in melting of polar caps, threatens life on our planet and implies huge social, political and economic impacts. The fact is that fossil-fuel based power generation contributes significantly to the increase of the CO_2 concentration in the atmosphere with coal combustion being the 'champion' followed by oil and gas. Climate change, a more careful expression of global warming transferred to the Greek media as 'over warming', is based on speculative projections.

Additional coal combustion by-products are also SO_2, NO_x, fly ash and volatile trace elements (some of them being hazardous pollutants), which however, do not attract significant attention and remain out of publicity. There are only two thermal power plants (TPPs), these of Meliti and Megalopolis B, which are equipped with desulphurisation plants for SO_2 removal, whereas measures to reduce NO_x, like the installation of fluidised-bed combustion units, have not been adopted in Greece.

Clean Coal Technologies (CCTs) such as Carbon Capture and Storage (CCS), coal gasification and coal liquefaction, provide workable solutions to these problems. However, the electricity cost will be rise as the existing coal-fired power plants cannot easily adapt to the CCTs. On the other hand, investing in the optimization of a domestic power supply will prove for the benefit of the medium and long-term efficiency of both our economy and environment.

In the last years there are suggestions to import hard coal for feeding new coal-fired TPPs. The supply and economic dependence on imports from other countries and the small improvement in the CO_2 emissions do not offer a rigid solution to the energy supply of the country.

3.4 Nuclear power

There are several pro and contra arguments concerning the installation of nuclear fission power plants in Greece.

Nuclear power generation can perhaps be regarded as clean since it has zero emissions. This is true under conditions of safe operation, and without considering the radioactive wastes. However, the accidents at Three Mile Island and Chernobyl, as well as dozens of others with smaller impacts, showed that every human construction, even the safest one, as a nuclear fission power plant, has weak points and a finite duration of life. Therefore, even if there is a very small risk of an accident in a nuclear power plant, in case it happens the damage will be enormous on both population and environment and it will also have long term effects on living organisms.

Greece is characterised by intense seismic activity, which might damage a nuclear power plant with enormous environmental impacts. Nevertheless, seismicity cannot be regarded as a severe threat since countries with essentially higher seismicity, e.g. Japan, successfully apply nuclear power generation already since several decades.

Greece owns domestic uranium reserves capable to support the operation of a 1000-MW nuclear power plant. This is partly true. It is economically not feasible though to operate plants for preparing the fuel rods as well as for re-processing the used fuel rods. This means that the uranium from the Greek deposits should be locally processed to produce the yellow cake, which should be transported abroad, and later the fuel rods should return back to Greece. After the fission in the reactor the used fuel rods have to be sent abroad to a re-treatment plant in order to remove useful elements such as U and Pu, and to isolate the high radioactive substances. All these will increase Greece's dependence on several foreign countries.

Finally, the problems of the final deposition of the radioactive wastes and of the decommissioning and final deposition of the reactor by the end of its life cycle still remain unsolved.

3.5 Renewable sources

Wind and solar potential could substitute a large part of the fossil fuels resulting in a reduction of GHG emissions and a decrease of oil and natural gas dependencies with positive effects on both environment and economy. However, in several cases the geomorphologic conditions of the country impose technical complications in terms of bringing wind and solar power to the grid, as the optimal locations for power generation are in remote areas away from the grid (EUROSTAT, 2009). Of course, the operation of solar and wind units are emission-free with negligible environmental impacts since they do not involve fuel combustion. Despite all these, however, one should see beyond this deceivable inference. Modern technology for the conversion of wind and solar energy to electricity requires the use of special composite compounds, which in turn require the use of expensive raw materials. Although the cost of photovoltaics has fallen during the last decades, it still is 4-6 times higher than the cost of power generation from fossil fuels (Şen, 2004). It is estimated that the photovoltaic modules in a solar power plant account for 50% of the total cost, whereas their efficiency reaches only 10% and the manufacturing of the cells requires primary energy (Afgan and Carvalho, 2002). Moreover, the efficiency of wind and solar systems is relatively low demanding the occupation of vast areas in order to cover the energy needs of a large number of consumers. Thus, the installation of large-scale facilities might be not feasible causing a severe alteration on the landscape, being a weak point, which won broad publicity and caused protests against such installations in several cases. The availability of these systems is also restricted depending strongly on the meteorological conditions; in days of inability to generate power, the demand

has to be covered by other primary energy sources. Overall the major disadvantage that renders wind and solar energy inappropriate for massive application is the inability of storage. Electricity must be consumed whenever it is available or – in other words – demand determines the power generation. Thus, despite the fact that solar and wind energy utilization neither produces GHG nor volatile and toxic compounds, they are not absolutely innocent from environmental point of view as they have been advertised and are also still expensive energy sources compared to the conventional fuels.

Geothermal energy is included in the renewable energy sources, although each geothermal reservoir hosts finite heat reserves. It could significantly contribute to the energy budget of the country. Most of the geothermal fields are of low enthalpy (e.g. Northern Greece) not proper for electricity generation; however, they could very well be exploited for heating purposes contributing to the reduction of oil use and thus, having benefits for both national economy and environment. However, due to inappropriate management of the high-enthalpy geothermal field on Milos Island in the 1980's (Delliou, 1990) this energy source is heavily defamed and the public opinion is negative towards the exploitation of geothermal energy for power generation. Apart from small- or pilot-scale private initiatives the large geothermal potential remains unexploited.

The hydroelectric power plants are always a reliable solution, particularly during periods of high energy demand as in the summer. The water reservoirs of the dams in Greece are also used for irrigation of the adjacent cultivated fields. As the demand for irrigation during summer is also high, both uses for irrigation and power generation are sometimes in conflict. As agriculture has a social advantage, hydropower is far from optimal exploitation. Moreover, the construction of large-size dams bind huge water reserves lowering the water table in the downwards areas and at ecologically sensitive places such as the river deltas. The retention of sedimentary load by the dam seriously affects river mouths or estuaries and the concomitant shoreline (erosion). The construction of new small-scale dams or the modification of the already existing ones could be a feasible solution of all these problems. Although, it has to be kept in mind that hydroelectric energy relies strongly to the climatic conditions, meaning that prolonged dry seasons would minimize any usage of this source.

Although biomass is one of the first energy sources used by humankind, nowadays it is considered not obsolete but promising and environmental friendly. This is due to the fact that it is regarded cleaner and cheaper than fossil fuels. This statement however, is not accurate enough as biomass is a very broad term including various and heterogeneous materials mostly derived from living plants and animals. Having this in mind one cannot argue for or against it as a unique group and compare it to the well-defined and tight group of fossil fuels. Simple burning of biomass for power generation is inefficient, as heat losses are high resulting to the combustion of large amounts in order to obtain the requested energy. Biomass could be economically feasible only in terms of secondary production, i.e. the production of liquid and gas fuels through pyrolysis or of ethanol-based fuels (bio-fuels) through fermentation. The worldwide leading country in this direction is Brazil, which has substituted oil and its derivatives with bio-diesel to a high extent. However, the massive biomass production requires the binding of extended areas (energy farms) either cultivated for crops or forested. This results in either the rise of the crop prices or the diminishing of forestland, respectively. Thus, steps towards biomass production in energy farms require long-term careful planning to reduce the above mentioned impacts.

3.6 Other energy-related aspects

Some further general aspects related to energy and the confused public opinion, are to mention here:

(a) Hydrogen technology: Fuel cell technology offers an alternative to substitute conventional en-

gines, as they convert the energy derived from an oxidized fuel to electricity and water. Several types of fuels are used or tested but the most common is hydrogen with oxygen playing the role of the oxidant. The major disadvantage is still the very high cost of fuel cells, which is unmatchable by the conventional fuels despite the significant decrease being achieved during the last decade (Boudghene-Stambouli and Traversa, 2002). Should their cost become competitive to other energy sources, they could constitute a powerful solution to the GHG emissions, although the disposal of the used cells made from precious but toxic metals (platinum, palladium) would also be an issue of environmental concern. Of course, hydrogen is beyond the frame of the present paper dealing with primary energy sources only. Furthermore, the hydrogen production has to be also considered in the calculation of the efficiency and the emissions of the entire system.

(b) Economic measures to reduce emissions: Carbon tax, a 'green' tax on carbon dioxide emissions, and emission trading, an administrative tool applied since 2005 within EU, are measures aiming to reduce emissions of CO_2 mainly from power generation and other energy-intensive industries like the production cement, iron and steel, glass, ceramics, and the manufacture of vehicles (EU-ETS, 2009). Both measures aim also to increase the competitiveness of the renewable energy sources. They result in an increase of the energy cost, and beyond any positive or negative criticism on the administrative application of these measures, studies reveal that poor consumers spend a greater proportion of their income on energy-intensive goods and fuel, i.e. higher energy cost tends to affect more the poor than the rich people (Neuhoff, 2008).

(c) Carbon dioxide vs climate change: The perspective of Earth's climate change due to fossil fuel combustion accounting for c. 80% of the global GHG emissions (Omer, 2008), dominates in the public opinion today. Every environmentalist and every sensitive citizen on this planet is aware of this as it is stated in the daily discussions, the media, and the policies over and over again. However, Earth's climate was changing significantly and sometimes rapidly in the past before man begun combusting fossil fuels. Earth's climate system is complex and the scientific knowledge about all climatic functions is still poor; thus, science is not at a level to give definite and precise answers for the causes of global warming (Florides and Christodoulides, 2009). Human-induced global warming is an unproven hypothesis derived from speculative projections inside computer programs (Plimer, 2009).

4. Conclusion

The greatest challenge of our society today regarding the energy sector is how to meet rising demand for energy in a sustainable way and at reasonable cost. Greece is facing, of course, the same challenge; the country has significant lignite and some uranium reserves and remarkable wind, solar, hydropower and geothermal potentials. However, the primary energy mix used in the country is based on lignite and imported oil and gas. Renewable energy sources play currently a minor role (<6%). The latter resources are capable to increase their contribution, if the cost of energy generation will become more competitive in comparison to this from fossil fuels; and in fact due to environmental taxation the fossil fuel prices are in an increasing mode.

In many energy aspects policy plays a dominant role. Politicians, environmentalists, journalists, sometimes also scientific groups representing different positions, create confusion in the public opinion. Over-sensationalism leads sometimes to fear without any reason. On the other hand, science offers solutions if facts and figures are examined carefully on a pure scientific basis.

Energy independency should be a key factor for the decisions of the Greek State in order to consolidate a viable economy along with sustainability. We haven't yet exploited the potentialities of the

domestic resources, even in a moderate satisfactory level. Coal reserves are utilized without the mobilization of all the elements that could add value to optimize the benefits, both economic and environmental. Clean coal technologies along with more efficient mining and processing techniques could improve the exploitation of our domestic resources. Geothermal fields are not even part of the discussion, whereas other countries without any high-enthalpy fields are investing significant amounts in hot-rock systems. Oil and coal exploration in Greece are highly 'flammable" topics.

There is a need for a wider cooperation between government, local communities, NGO, academic and research bodies and industries under Research and Technology Initiatives, which will enable us to develop a sustainable energy strategy for short, medium and long-term planning. The challenge for the modern Geoscientists lies exactly there; to provide viable and sustainable solutions to the "Energy Issue".

5. References

Afgan, N.H. & Carvalho, M.G., 2002. Multi-criteria assessment of new and renewable energy power plants. *Energy*, 27, 739-755.

Ayres, R.U., Turton, H. & Casten, T., 2007. Energy efficiency, sustainability and economic growth. *Energy*, 32(5), 634-648.

Bell, A. (ed.), 1995. Physical Resources and Environment: Fossil fuels. The Open University, Milton Keynes.

Boudghene-Stambouli, A., & Traversa, E., 2002. Fuel cells, an alternative to standard sources of Energy. *Renewable and Sustainable Energy Reviews*, 6, 297–306.

Delliou, E.E., 1990. Greece, Milos island geothermal project. Transactions-Geothermal Resources Council, 14(1), 595-600.

Energy Information Administration (EIA), 2009. Country Analysis Briefs: Greece. http://www.eia.doe.gov/emeu/cabs/Greece/Full.html

EU-ETS, 2009. Emission Trading System (http://ec.europa.eu/environment/climat/emission).

EUROSTAT, 2007. http://epp.eurostat.ec.europa.eu

EUROSTAT, 2009. Panorama of energy Energy statistics to support EU policies and solutions (http://epp.eurostat.ec.europa.eu/cache/ITY_OFFPUB/KS-GH-09-001/EN/KS-GH-09-001-EN.PDF).

Florides, G.A. & Christodoulides, P., 2009. Global warming and carbon dioxide through sciences. *Environmental International,* 35, 390-401.

Fyrippis, I., Axaopoulos, P. & Panayiotou, G., 2010. Wind energy potential assessment in Naxos Island, Greece. *Applied Energy*, 87, 577-586.

Grübler, A., 2004. Transitions in energy use. Encyclopedia of energy, vol. 6. Elsevier Academic, London.

International Energy Agency (IEA) 2008. http://www.iea.org/stats/countryresults.asp?COUNTRY_CODE=GR&Submit

International Energy Agency (IEA), 2009a. CO_2 emissions from fuel combustion highlights (http://www.iea.org/co2highlights/co2highlights.pdf).

International Energy Agency (IEA), 2009b. Key world energy statistics (http://www.iea.org/texbase/nppdf/free/2009/key_stats_2009.pdf).

Kaldellis, J.K., Kondili, E.M. & Paliatsos, A.G., 2008. The contribution of renewable energy sources on reducing the air pollution of Greek electricity generation sector. *Fresenius Environmental Bulletin*, 17, 1584-1593.

Kavouridis, K., 2008. Lignite industry in Greece within a world context: Mining, energy supply and environment. *Energy Policy*, 36, 1257-1272.

Lalas, D.P., Tselepidaki, H. & Theoharatos, G., 1983. An analysis of wind power potential in Greece. *Solar Energy*, 30, 497-505.

Lüttig, G., 2007. Die (neue) Rohstoffschlange: Instrument für die Verständlichmachung der sozioökonomischen Bedeutung der mineralischen Rohstoffe. *World of Mining – Surface & Underground*, 1, 50-53.

Neuhoff, K., 2008. Tackling Carbon: How to price carbon for climate policy. Electricity Policy Research Group (http://www.eprg.group.cam.ac.uk/wp-content/uploads/2009/03/tackling-carbon_final_3009082.pdf).

Omer, A.M., 2008. Energy, environment and sustainable development. *Renewable & Sustainable Energy Reviews*, 12, 2265-2300.

Plimer, I., 2009. Heaven+Earth: Global warming, the missing science. Connor Court Publ., Ballan.

Şen, Z., 2004. Solar energy in progress and future research trends. *Progress in Energy and Combustion Science*, 30, 367–416.

Tsilingiridis, G. & Martinopoulos, G., 2010. Thirty years of domestic solar hot water systems use in Greece-energy and environmental benefits-future perspectives. *Renewable Energy*, 35, 490-497.

Tuck, G., Glendining, M.J., House, J.I. & Wattenbach, M., 2006. The potential distribution of bioenergy crops under present and future climate. *Biomass and Bioenergy*, 30, 183-197.

Δελτίο της Ελληνικής Γεωλογικής Εταιρίας, 2010
Πρακτικά 12ου Διεθνούς Συνεδρίου
Πάτρα, Μάιος 2010

Bulletin of the Geological Society of Greece, 2010
Proceedings of the 12th International Congress
Patras, May, 2010

MEDICAL GEOCHEMISTRY A KEY IN THE PRECAUTIONARY MEASURES AGAINST THE DEVELOPMENT OF CANCER AND OTHER DISEASES

Varnavas S.

University of Patras, Department of Geology, 26500 Patras, Greece, s.p.varnavas@upatras.gr

Abstract

A considerable number of diseases are directly related to environmental impact. Toxic metals such as Hg, Pb, Cd, and As may damage significantly the human health when they exceed certain levels in the body. For example specific precautions should be taken for the diet of pregnant women and the children. Lead concentrations exceeding the safe values can cause severe damage to the development of central nervous system, as well as a general developmental delay of fetuses and young children, interfering with the functioning of almost every brain neurotransmitter. In particular for the pregnant women, it has been found that the exposure of the fetus on high lead values may cause, apart from neurological and behavioral problems, low birth weight, pre-term delivery, spontaneous abortion and stillbirth. Organic mercury (methyl mercury) is the most dangerous form of mercury, because it is the most easily absorbed orally and crosses into the brain and fetus so readily. Populations exposed to chemical compounds containing As, Ni, Cr, Cd, etc. are considered of high-risk in developing cancer.

Environmental geochemical studies can help in assessing the quality of the environment as well as the determination of the sources of pollutants, their behaviour and other characteristics. This knowledge is necessary in any application of remediation methodologies and waste management for the prevention of pollutants in getting into the food chain. It is also used in determining safe criteria regarding the quality of soils, drinking water, construction of schools, playgrounds etc. In this work the importance of environmental geochemical research and its applications towards the protection of human health is demonstrated.

Key words: *Medical geochemistry, metals in human health, metals in cancer disease, metals in nervous diseases, Pb in fetus development, remediation methods, job diseases.*

1. Introduction

Results of epidemiological studies and laboratory experiments in combination with environmental geochemical studies have shown the impact of the environment on human health and development of diseases including cancer (Bennet, 1981, Spang, 1988, NIOSH, 1977). Environmental geochemical studies can help in assessing the quality of the environment as well as the determination of the sources of pollutants, their behaviour and other characteristics. In this work the importance of environmental geochemical research and its applications towards the protection of human health is demonstrated. On the basis of the results of geochemical studies remediation methodologies leading to prevention of toxic elements in getting into the food chain are applied,while criteria are put for the quality of soils, water etc. In addition decision makers are helped to make the necessary and right decisions in the management of toxic waste.

2. Health Risks

Populations exposed to chemical compounds containing As, Ni, Cr, Cu, Cd, etc. are considered of high-risk groups in developing cancer(EPA, 1984, Merian, 1991).The above and many other elements may cause various diseases in human beings (Merian, 1991, Nriagu,1984).

High concentrations of manganese in human body can cause parkinson. Research in regard to the presence of Mn and other metals in the environment in relation to human health were carried out in Greece (Kondakis et al. 1989, Leotsinidis and Kondakis 1990). Similarly the levels of As in waters and sediments were investigated (Varnavas and Cronan 1988; 1991, Aloupi et al.,2009).

2.1 Toxic Metals in the Diet of Pregnant Women and the Children

Toxic metals such as Hg, Pb, Cd, and As may damage significantly the human health when they exceed certain levels in the body. Specific precautions should be taken for the diet of pregnant women and the children. During pregnancy, women need additional nutrient constituents in their diet. In an effort to take these with their food, there is a risk to get toxic elements, which may be very harmful for the health of both the pregnant and the fetus. During childhood, children may get toxic metals with their food present either in the preservatives or in the wrappings of the food.

The importance of the proper diet of pregnant women and the children in relation to the presence of toxic metals is given here, so as to avoid health risks. In order to achieve this, the necessary precautions are described, the knowledge of which is very useful for the protection of the health of pregnant women and the children.

Organic mercury (methyl mercury) is the most dangerous form of mercury, because it is the most easily absorbed orally and crosses into the brain and fetus so readily (Lappe and Calfin,2002). The major source of organic mercury exposure is contaminated fish, particularly carnivorous fish such as swordfish, tuna, shark, and pike (Cook, 2001).

High amounts of lead present in the wrappers of food (i.e. sweets), in the printing ink on the surface of the food package, facilitate the uptake of lead by the children during eating sweets etc. In particular, it has been found that poly-vinyl-chloride (PVC) linings used for wrapping food contain lead, which can migrate from PVC to the food (Tarantino,2006). For this reason FDA gives certain instructions to the manufacturers of PVC flexible lunchboxes. Lead concentrations exceeding the safe values can cause severe damage to the development of central nervous system, as well as a general developmental delay of fetus and young children, interfering with the functioning of almost every brain neurotransmitter (Farley,1998). In particular for the pregnant women, it has been found that the exposure of the fetus on high lead values may cause, apart from neurological and behavioral problems, low birth weight, pre-term delivery, spontaneous abortion and stillbirth (Varnavas and Varnavas 2007).

2.2 Specific Environments

2.2.1 Soils Adjacent to Major Roads

Several studies have demonstrated an apparent influence of traffic on both soil and crops grown in close proximity of major roads in Greece. Below two case studies are described one from the are a of Araxos with cultivations of: *Lycopersicum esculentum* and the other one from Lappas area with cultivations of *Solanum melongena*. The concentrations of heavy metals in soils and leaves of the plant species *Lycopersicum esculentum* and *Solanum melongena* at the edge of the road and 10 m from the road were determined. In general, the concentrations of heavy metals were found to be significantly

lower when the plant species were cultivated at a distance 10 m from the major road. This is a result of the impact of road pollution on food-crops. Major sources of metals are the combustion of diesel and/or petrol, the wheels of the cars, as well as the dust from the limestone transported by the trucks.

The Mn concentrations measured in leaves of both species were lower in plants that were cultivated at a distance of 10 m from the major road. The concentration of Mn found in *Lycopersicum esculentum* cultivated at a distance of 10 m from the road was 87 ppm, (reduced by 51%, compared with that of 176 ppm in plants cultivated at the edge of the road). It is interesting to note that the decrease of Mn in the leaves of *Lycopersicum esculentum* is much greater, with regard to its decrease in *Solanum melongena* (Fig. 1). In *Solanum melongena* cultivations, the reduction in Mn for plants at a distance of 10 m to the major road was 4 %. Decreases were observed in Cu concentrations of leaves of all species, when they were cultivated 10 m far from the major road. The percentage decreases of Cu levels in *Lycopersicum esculentum* and *Solanum melongena* were 19% and 2%, respectively. In plant species *Lycopersicum esculentum* and *Solanum melongena* the corresponding decreases of Zn were 7% and 0.3%, respectively.

Table 1. The decreases (%) in trace metal content of soils and leaves, grown 10 m from the road, with regard to samples at 0 m distance (Kalavrouziotis et.al.,2006).

Element	trace element decreases (%) of soils and leaves, 10 m from the road (compared to samples at 0 m)			
	Lycopersicum esculentum		*Solanum melongena*	
	Leaves	Soils	Leaves	Soils
Mn	51	28	4	2
Al	9	17	10	12
Cu	19	47	2	37
Fe	4	25	20	4
Pb	8	7	54	8
Cr	30	23	13	16
Co	39	25	20	12

The decrease of Cr in *Lycopersicum esculentum* leaves was 30 %, but that in *Solanum melongena* leaves only 13%. Decreases in Co levels were observed to be 39% and 20% for *Lycopersicum esculentum* and *Solanum melongena*, cultivated at 10 m from the major road. The concentrations of Al in leaves of *Lycopersicum esculentum* and *Solanum melongena* were reduced by 9 and 10%, when cultivated 10 m far from the major road.

The concentrations of Fe in leaves of all plant species cultivated at a distance of 10 m from the major road were found to be lower than those in plants cultivated at the edge of the major road. In the leaves of *Solanum melongena*, the percentage decrease was found to be 20%, whereas that in *Lycopersicum esculenum* leaves was only 4%. Overall, it is shown that the concentrations of all elements studied in both *Lycopersicum esculentum* and *Solanum melongena* decrease from the edge of the road to 10 m distance. It is noted that the elemental concentrations in both soils and plants further decrease, away from the road edge and with distance from the road (Table 1, Fig. 1). Therefore, it can be clearly deduced that there has been an input of these elements from the traffic. In conclu-

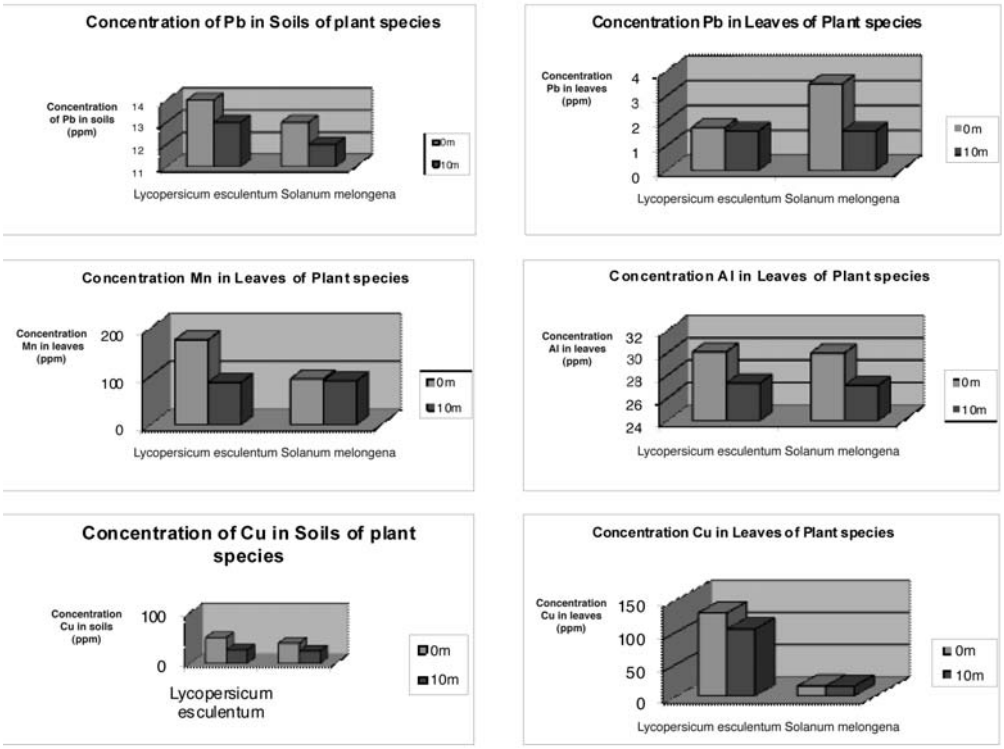

Fig. 1: Concentrations of Mn, Cu, Zn, Fe, Al, Pb,Co and Cr in the soils and leaves of plant species which cultivated at the edge of the road and 10 m from the major road(Kalavrouziotis et.al., 2006).

sion the results demonstrated remarkable decreases in Pb, Zn, Cu, Ni, Cr and Co levels at 10 m distance from the road, compared to the examined samples from the edge of the road (Kalavrouziotis et.al., 2006).Similar studies from other Greek areas such as the Athens Thessaloniki main road and elsewhere have demonsrated severe influence of the traffic on the soils and crops(Kalavrouziotis et.al., 2007a, b, Vissirski et.al., 2008).Other studies have shown increase in the concentrations of the (PGEs) element group both in the soils and crops located in the vicinity of main roads (Kalavrouziotis and Koukoulakis, 2009).Therefore it is necessary that remediation methods should be applied on such soils and other precaution measures should be taken to prevent the pollutants to get into the food chain and protect the human health.

2.2.2 Mining Environments

Toxic solid waste occur in the area of Polis Chrysochous, near the Limni Mine mining area, 5 Km East of the town of Polis in the Paphos District, Cyprus (Fig. 2). It was formed as a result of extended exploitation and mineral processing of sulphide minerals. Although the exploitation of copper deposits started in early times, it was more intensified between 1955 and 1979; then the mine was close down.

During the above period, a total amount of 16,000,000 tons of ore was extracted, with an average content of 1.1% copper and 14.9% sulphur. In addition to the mining tailings present in the area, metal rich solid waste resulted from the mineral processing form distinct mounds. Also, remainings

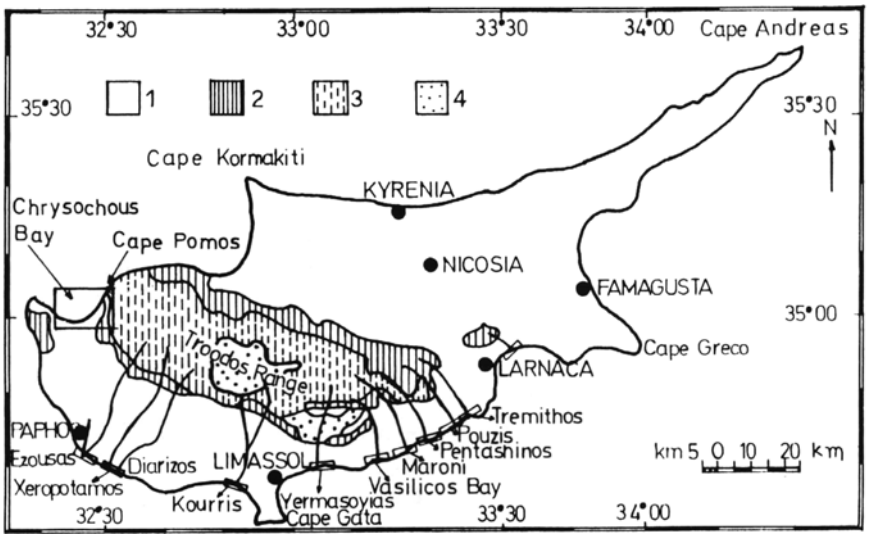

Fig. 2: Map of Cyprus showing the geology of the Troodos massif 1: sedimentary rocks, 2: upper and lower pillow lavas, 3: basal group and diabase, 4: gabbro granophyre suite ultramafic suite (Constantinou 1979) and the location of the area studied.

Fig. 3: Acid drainage related to pyrite oxidation (from Hermioni mining area Greece).

from metallurgical processes such as slags of pebble size are scattered in the area. Such slags occur on the beach investigated here. Environmental geochemical and mineralogical investigations on Chrysochou mining region were carried out by Varnavas et al., 1990, 1994.

The environmental impact of the Limni Mine Cyprus mining activities was assessed on the basis of

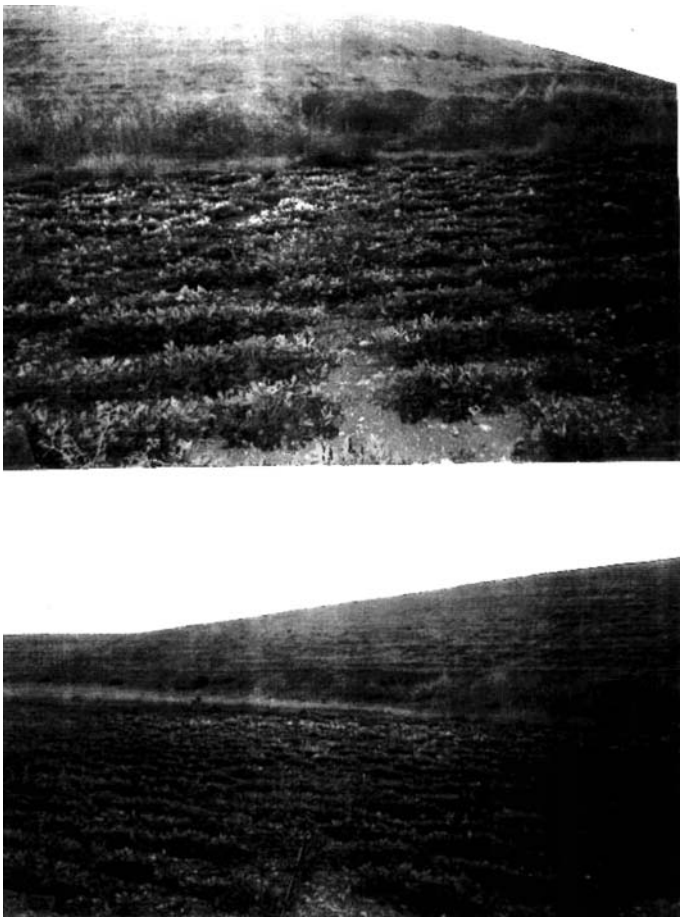

Fig. 4: Peanut plants grown at the edge of pyrite toxic waste (Polis Chrysochous mining area, Cyprus).

a detailed geochemical study. It was revealed that the mounds of toxic solid waste occurring in the area have undergone a high degree of chemical weathering leading to a wide dispersion of metals such as Fe, Cu, Zn, As, Mn in the surrounding area, including the beach. As a result of these processes large quantities of "pyrite sand" and its oxidation products occur on the adjacent beach, being a permanent source of toxic metals for the seawater.

Considering the metal rich dust formed and food production taking place in this highly metal polluted area (Figs 4 and 5) it is suggested that immediate action should be taken towards its remediation for the protection of the human health (Varnavas et al., 2000; 2001). Similar remediation actions should be taken also for other areas such as the Hermioni mining area in Greece (Varnavas et al., 1992; 1994; Fig. 3).

2.2.3 Port Environment and Maritime Transport

Ship emissions derived from the combustion of petroleum products contain harmful organic and inorganic substances that remain in air for a long period of time. Under certain meteorological conditions they can be taken up by human beings via respiratory and other systems. As a result of this, respiratory inflammations and neurological problems, cancer, even death, are caused. (Bailey and Solomon, 2004; Cooper, 2003; Corbett and Fishbeck, 1997; Isakson et al., 2000; Moreno et al., 2004; Saxe and Larsen, 2004; Stone

Fig. 5: Wheat production at the edge of pyrite toxic waste (Polis Chrysochous mining area, Cyprus).

and Donaldson, 1998; Wilson and Spengler, 1996).The impacts of maritime transport activities as well as the environmental conditions occurring in the port of Patras and in the surroundings are the subject of an on going doctoral thesis in the University of Patras (Apostolopoulou, 2010). Preliminary results show that the maritime transport has severely affected the air quality in the area during peak periods.

2.2.4 Wood Production and Management

The production preservation and industrial use of wood has a lot of environmental impacts. In the industrial use of wood, a variety of chemical compounds are used as preservatives of wood against fungi. The chemicals used for the preservation of wood usually are metal rich organic compounds, biokillers, etc. which cause severe environmental impact on the human health as well as on the ecosystems. The most common preservatives are: Chromate- Copper-Arsenate (Cr, Cu, As- CCA) and Cu, Zn, As. These are used under specific directions of Environmental Protection Agency of the United States (EPA), being introduced in the wood under pressure. Additionally, for the same purpose chemicals containing Hg are used against fungi, as well as organic compounds such as pentachlorophenole, Cu- rich napthaline. As a result of this, human health is being influenced on a great extent. For this reason, the World Health Organization, the European Union and the Environmental Protection Agency (EPA) as well as other National and Inter-

national Organizations have put regulations which control the safety of working people during the above processes. More specifically, such criteria give emphasis on the management of wood waste (Table 2).

The conditions in Greece under which all above processes take place need to be investigated in regard to the contaminants released in the environment. Emphasis should be given to the management of wood waste. Considering the fact that the industrial use of wood is increasing with time, it is expected that in the future health damages of human beings associated with wood processing will be more pronounced.

It is advised that the use of chemicals on wood preservation should be avoided and should be used only in the cases where no other possibilities are found. The most commonly used compound is Uera - Formaldehyde (UF). Formaldehyde has the ability to be released with time in the environment and it is responsible for the "syndrome of ill building". The investigation of such buildings showed

Table 2. Chromium, Copper, and Arsenic Concentrations in Treated Wood and Treated Wood Ash Samples. Regulatory Levels Provided for Comparison (EPA, 2002).

Wood Type			Metals Concentration, mg metal per kg of wood or ash		
			Cr	Cu	As
Unburned Wood[a]	Untreated Wood		7.0	3.7	2.0
	CCA-Treated Wood at 0.25 pcf		2,060	1,230	1,850
	CCA-Treated Wood at 0.60 pcf		4,940	2,950	4,435
	CCA-Treated Wood at 2.50 pcf		20,600	12,300	18,500
Ash[b]	Non-CCA-Treated Wood		141	212	28
	CCA-Treated Wood at 0.25 pcf		20,600	11,200	11,400
	CCA-Treated Wood at 0.60 pcf		51,100	32,300	42,800
	CCA-Treated Wood at 2.50 pcf		174,000	104,000	113,500
Regulatory Limits	Federal[c]	Ceiling (mg/kg)	Not Applicable	4300	75
		Pollution (mg/kg)	Not Applicable	1500	41
	Florida[d]	Industrial (mg/kg)	430	12,000	3.7
		Residential (mg/kg)	290	105	0.8

[a] Computed values assuming that retention rating equals amount of chemical in wood.
[b] Measured values.
[c] Federal Register 40 CFR Part 503.13, Standards for the Use or Disposal of Sewage Sludge, Subpart B, Land Application.
[d] Florida Department of Environmental Protection, Proposed Chapter 62-777, F.A.C. Contaminant Target Clean-up Levels.

that the responsible factors controlling the above syndrome include: temperature, humidity, air exchange as well as in-house environment pollutants, like dust, noise, and lighting.

It is seen that during the industrial use of wood, the use of wooden products and the management of wooden waste significant environmental problems are caused. Environmental geochemical research is needed towards the environmental protection by investigating the possibilities of reducing the pesticides used for wood preservation (Karaberou and Varnavas, 2004, 2007).

2.2.5 Wetlands and Lagoons

Wetlands and lagoon environments are important environments, both from economic and tourist point of view. Usually, a large number of human activities take place within or near these areas. Additionally, major natural processes and the results of wetland - land interaction processes lead to environmental changes which have a negative influence on the life of people. Considering the fact that significant fishing activities take place in these environments and the environmental conditions influence the food production special attention should be taken on them.

The Aetoliko lagoon on the west Greek Coasts is an important marine environment(Voutsinou- taliadouri and Satsmatsis, 1987) and the environmental conditions occurring there in relation to the behavior of pollutants are described as an example. Domestic sewage from the town of Aetolikon and from a number of adjacent villages are the main sources of pollutants in the lagoon. Another major source of pollutants is the existing pumping system on the west coast, bringing freshwaters in the lagoon. These are surface waters, which are collected in a pool prior to their discharge in the lagoon. Other sources of pollutants are related to human activities such as olive oil mills, the effluents of which are discharged in the lagoon through streams]. Occasionally significant quantities of toxic gases are released from the seafloor, which escaping through the water column cause fish death and put in danger the health local people. Therefore, the study of the influence of these waters on the lagoon is of great importance. In order to achieve this, the following methodology was used: a) in situ measurements were carried out for pH, conductivity, temperature, b) water sampling was carried out. Both, measurements and sampling were carried out at increasing distance from the site of discharge and at different seasons, c) The quantity of suspended solids in the waters at different sampling sites was measured. It was isolated and analyzed for a number of elements such as Cd, Pb, Cn, Cr, Zn, Mn, Al, Si, Fe and Ca.

An investigation of the fresh water - seawater interaction processes showed that at the transition from the freshwater to the seawater with slight increase of the salinity there is a sudden increase in the phosphorus value. This phenomenon was observed in December, January and May. Under the same conditions there is a tendency for metals to increase in the particulate matter. This is a result of increase of the degree of transfer of the ions from the dissolved to the solid form. The degree of incorporation of the metals studied in the solid form decreases in the following order: Mn>Zn>Cu>Cd>Fe. These are useful observations, which can be used in planning the decontamination of the lagoon.

Dissolved oxygen measurements were carried out in the hot period (June) in the deeper zone of the lagoon, which showed that D.O. decreases from the sea surface down to 8m depth. Just below this depth (8.5m) D.O. is below 1 mg/l, while below 9m down to the seafloor D.O. is zero (Fig. 6b).

2.2.6 Decontamination Methodology

In situ measurements (Fig. 7) and laboratory work allowed the determination of the existing environmental conditions in the Aetoliko lagoon, which are of importance in planning its decontamination and management.

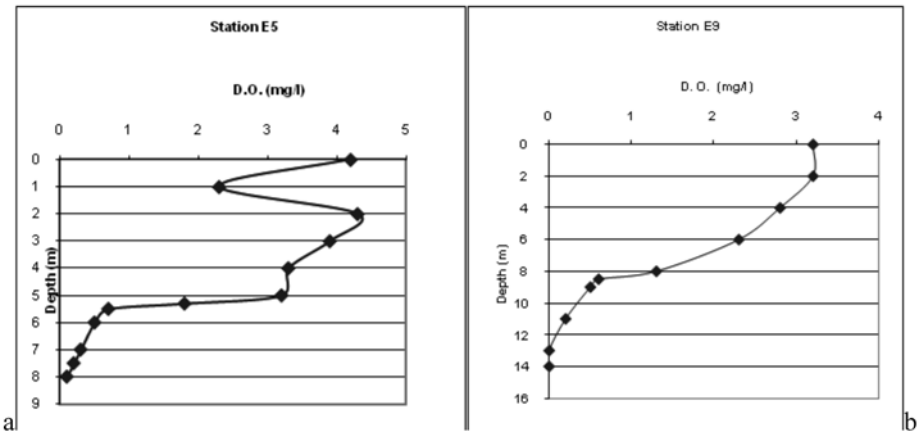

Fig. 6: Vertical variability of dissolved oxygen at different stations (21.6.99, Varnavas, 2005).

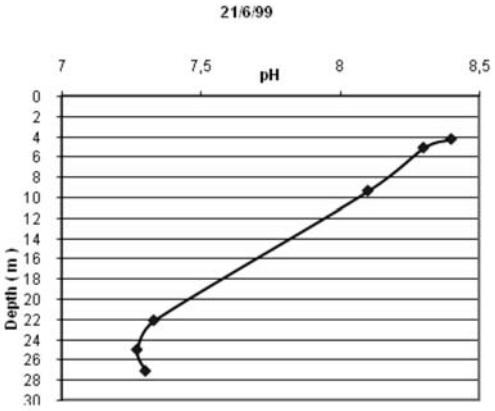

Fig. 7: Vertical variability of pH (21.6.99, Varnavas, 2005).

A major source of contaminants is the fresh water discharged in the lagoon by the pumping system. The study of the behavior of these contaminants, mainly phosphorous and toxic metals (i.e. Pb, Cd, Cr et.) suggests that removal of these contaminants will greatly improve the quality of the freshwater and in turn of the lagoon. The removal of the contaminants can be achieved by planning and construction of an artificial pond for this purpose.

It has been revealed that at intermediate water depths there is a cold layer at the top of which pollutants (i.e. Cd, Pb, Cr, Mn etc.) float in the form of particulate matter. Similar layer rich in pollutants also exists in shallow layers and near the seafloor. These are characterized by sharp peaks in conductivity.

The deep waters, where release of toxic gases takes place, are characterized by low pH relative to the waters of the upper part of the column. Further geochemical study is needed prior to take any action for improving the quality of the seafloor environment.

Below 9m depth dissolved oxygen reaches zero value down the seafloor (32m). It is therefore revealed that a large part of the water masses in the lagoon are under anoxic conditions.

It should be stressed that actions must be taken for decontamination of the lagoon for the following reasons:

(i) The lagoon is a food source environment; fishing of large quantities of fish throughout the year takes place.
(ii) Although it is not known whether toxic metals get into the food chain, their presence in large amounts may affect directly or indirectly the human health (Varnavas, 2005).

3. Acknowledgments

I would like to thank my collaborators Assistant Professor Ioannis Kalavrouziotis, Mrs Georgia Karaberou and Miss Katerina Apostolopoulou for their valuable discussions and help during the writing up of this paper. I also thank Dr Panos Stefanopoulos for his help in putting the text according to the format of the proceedings.

4. References

Ahlgren, S., Holmlund, J., 2002. Outcrop Scans Give New View. American Association of Petroleum Geologists Explorer, July 2002. Available online at: http://www.aapg.org/explorer/geophysical_corner/2002/07gpc.cfm

Aloupi, M., Angelidis, M. O., Gavril, A. M., Koulousaris, M. and Verandas, S.P., 2009. Influence of geology on arsenic concentrations in ground and surface water in central Lesvos, Greece. *Environmental Monitoring and Assessment,* 151,(1-4), 383-396.

Apostolopoulou, K. 2010. Assessment of environmental geochemical conditions in the Patras port area. On going Doctoral thesis, University of Patras.

Bailey, D. and Solomon, G., 2004. Pollution prevention at ports: clearing the air. *Environmental Impact Assessment Review*, 24, (7-8).

Bennett, B.G., 1981. Exposure of man to environment arsenic - an exposure commitment assessment. *Science of the Total Environment*, 20, 99-107.

Cooper, D.A., 2003. Exhaust emissions from ships at Berth, *Atmospheric Environment*, 37, 3817-3830.

Cook, K., 2001. Mercury in your fish, Located at www.mercola.com/2001/apr/25/mercury_fish.htm

Constantinou, G., 1979. Metallogenesis associated with Troodos ophiolite. In: Panayiotou A. (ed) Ophiolites: Proceedings International Ophiolite Symposium, Cyprus Geological Survey Department, Nicosia, Cyprus, 663-674.

Corbett, J.J. and Fishbeck, P., 1997. Emissions from ships, *Science*, 278, 823-824.

EPA (U.S. Environmental Protection Agency), 1984. Health assessments. Document for Chromium Final Report. Washington D.C.

EPA, U.S. Environmental Protection Agency, 2002. What You Need to Know about Wood Pressure Treated with Chromate Copper Arsenate (CCA).

Farley, D., 1998. Dangers of Lead Still Linger, FDA/CFSAN FDA Consumer.

Isakson, J., Persson,T. A., and Selin Lindgren, E., 2001. Identification and assessment of ship emissions and their effects in the harbour of Goteborg, Sweden. *Atmospheric Environment* 35.

Kalavrouziotis, I.K., Carter, J., Mehra, A., Varnavas S.P., Drakatos P.A., 2006, 'Towards an understanding of metal contamination in food and soils related to road traffic', *Fresenius Environmental Bulletin,* 15, (3), 170-175.

Kalavrouziotis, I.K., Carter, J., Varnavas, S.P., Mehra, A., Drakatos P.A., 2007a. Towards an understanding of the effect of road pollution on adjacent food crops: Zea mays as an example. *International Journal Environment and Pollution*, 30, (3-4), 576-592.

Kalavrouziotis, I.K., Jones, P.W., Carter, J., Varnavas, *S.P.,* 2007 b. Uptake of trace metals of *lycopersicum*

esculendum at a site Adjacent to the main road, - Athens-Thessaloniki, Greece. *Fresenius Environmental Bulletin*, 16, (2), 133-139.

Kalavrouziotis I.K. and Koukoulakis P., 2009. The environmental impact of the platinum group elements (Pt, Pd, Rh) emitted by the automobile catalyst converters. *International Journal Water, Air and Soil Pollution*, 196, (1-4), 393-402.

Karaberou, G. and Varnavas, S.P., 2004. an investigation into the possibility of reducing the environmental impacts resulting from the industrial use of wood. 1st National Congress on Green chemistry. February 2004 (p19), Athens.

Karaberou, G. and Varnavas, S.P., 2007. Wood industrial activities as major metal contaminant sources. 2nd National Congress on Green chemistry, March 2007, Patras.

Kondakis, XG., Makris, N., Leotsinidis, M., Prinu, M., 1989. Possible health effects of high Mn concentrations in drinking water. *Archives of Environmental Health,* 44, 175-178.

Lappé, M. and Chalfin, N., 2002. Identifying Toxic Risks Before and During Pregnancy: A Decision Tree and Action Plan. Located at http//www. Cetos. Org/articles/MoDFinalReport.pdf

Leotsinidis, M. and Kondakis, X., 1990. Trace metals in scalp hair of greek agriculture workers, *Science of the Total Environment*, 6, 223-226.

Merian, E., (Edit), 1991. Metals and their compounds in the environment. VCH, Weinheim.

Moreno, T., Jones, T.P. and Richards, R.J., 2004. Characterizations of aerosol particulate matter from urban and industrial environments: examples from Cardiff and Port Talbot, South Wales, UK. *Science of the Total Environment*, 334-335, 337-346.

NIOSH. (National Institute of Occupational Safety and Health), 1977. Criteria for recommended standards: Occupational Exposure to Inorganic nickel, pp. 1-282, U.S. Department of Health, Education and Welfare, Washington, D.C.

Nriagu, J. O. (edit), 1984. Nickel in the environment pp. 1-833, Wiley, New York.

Saxe, H., and Larsen, T., 2004. Air pollution from ships in three Danish ports. *Atmospheric Environment*, 38, (24).

Spang, G., 1988. In vivo monitoring of Cadmium workers in Cadmium 86 Edited. Proceedings pp. 162-164. Cadmium Council New York, IL 2RO Research Triangle Park, North Carolina.

Stone, V. and Donaldson, K., 1998. Small particles big problem. *The Aerosol Society Newsletter* 33, 12-14.

Tarantino, L.M., 2006. Letter to Manufacturers and Suppliers Concerning the Presence of Lead in Soft Vinyl Lunchboxes, US FDA/CFSAN.

Varnavas, S.P. and Cronan, D.S., 1988. Arsenic, antimony and bismuth in sentiments and waters from the Santorini hydrothermal field, Greece. *Chemical Geology*, 67, 295-305.

Varnavas, S.P., 1990. Formation of placer mineral deposits in high energy environments: The Cyprus continental Shelf, *Geo-Marine Letters*, 10, 51-58.

Varnavas, S.P. and Cronan, D.S., 1991. Hydrothermal metallogenetic processes off the islands of Nissiros and Kos on the Hellenic Volcanic Arc. *Marine Geology*, 99, 109-133.

Varnavas, S.P., Kritsotakis, K.G., Panagos, A.G., 1992. Metal pollution offshore Hermioni area, Greece, related to mining activities. In: Proceedings of the 5th International Conference on Environmental Contamination, J. - P. Vernet (edit) C.E.P. Consultants Edinburgh U.K. pp. 78-81.

Varnavas, S.P., Panagos, A.G. and Kritsotakis, G., 1994. Environmental impact of mining activities on the Hermioni area Greece. In: Environmental Contamination, J. - P. Vernet (edit) Elsevier, Amsterdam, pp. 119-145.

Varnavas, S.P. (editor), 1994. Proceedings of Sixth International Conference on Environmental contam-

ination, Delfi, Greece, CEP. Consultants Ltd.

Varnavas, S.P., Forstner, U., Salomons, U., Balopoulos, E., Brill, J., Golik, A., Loizides, L., Zodiatis, G., 2000. Environmental impact of mining activities in the Eastern Mediterranean Sea. Oceanography of the Eastern Mediterranean and Black Sea, European Commission. Energy Environment and Sustainable Development. pp. 412- 413.

Varnavas, S.P., Forstner, U. and Calmano, W., 2001. Environmental assessment and Human Health in a highly metal polluted Coastal Zone Associated with Toxic Solid Waste. The Need of Immediate Action. University of the Aegean, Dept. Environmental Studies. Global Nest, Ermoupolis, Syros island, Greece, 3-6 September 2001. Volume B. T, D. Lekkas (ed). pp. 903- 908.

Varnavas, S.P., 2005. Environmental Conditions in a Polluted Lagoon. Implications for Decontamination Planning and Management. *IASME Transactions*, 2, (5), 764-768.

Varnavas, P.S and Varnavas S.P., 2007. Health risks from toxic metals present in the diet of pregnant women and the children. 2nd National Congress on Green chemistry (P10) March 2007, Patras.

Vissikirsky, V., Stepashko, V., Kalavrouziotis, I., Varnavas, S., 2008. The road pollution impact on Zea Mays: Inductive modeling and Qualitative assessment. *International Journal of Air, Soil and Water Pollution*, 195, 301-310.

Voutsinou-Taliadouri, F., Satsmadjis, J. and Iatridis, B., 1987. Granulometric and metal composition in sediments from a group from Ionian lagoons. *Marine Pollution Bulletin* 18, 49-52.

Wilson, R., and Spengler, J., 1996. Particles in our air: concentrations and health effects, Boston. Harvard University Press.

Δελτίο της Ελληνικής Γεωλογικής Εταιρίας, 2010
Πρακτικά 12ου Διεθνούς Συνεδρίου
Πάτρα, Μάιος 2010

Bulletin of the Geological Society of Greece, 2010
Proceedings of the 12th International Congress
Patras, May, 2010

WANDERING ABOUT MINERALOGY AND PETROLOGY

Katagas Ch.

Department of Geology, Section of Earth Materials, University of Patras, 26500 Rio, Greece; C.Katagas@upatras.gr

Abstract

Over the past few years an intense amount of research on various themes stimulated the development of Mineralogy and all its diversity, and many exciting discoveries have been made. New or technologically developed analytical and experimental methods such as ion microprobe, powerful MAS NMR, LA-ICP-MS, IR, Raman, XAS spectroscopies, beams of high intensity, Synchrotron radiation that enhanced the sensitivity of conventional spectroscopic and XRD techniques, beams of neutrons, widely available information and tremendous computing and modelling facilities have turned out to be excellent tools, promoting the ability of mineralogy in solving global and societal challenges.

Mineralogy today offers insights into important scientific issues, including sustainable development, evolution of the Earth and origins of life, deep Earth processes, physics and chemistry of Earth materials, fluids, magmas, igneous rocks and time scales, archaeomineralogy, nano-, geo-, and bio- environmental sciences.

The mineralogical sciences today are going through a period of rapid expansion and diversification and this trend is going to continue in future. There is now great potential for much interesting work in the latter areas but also the need to somehow protect the coherence of our discipline.

Key words: *Mineralogy, Petrology, Late developments.*

1. Introduction

When the president of this congress did me the honor to invite me as a keynote speaker, I decided to present a journey through the late achievements in the fields of mineralogy and petrology. I soon realized that the presentation of such a topic in a short lecture is a very difficult task but on the other hand I was very pleased because I would have the opportunity to argue on some erroneous comments we usually hear from some other fellow Earth scientists who think that mineralogy and petrology are fading-away.

Time and space restrictions impede this lecture of covering in detail such a huge topic and the progress that was made in all mineralogical and petrological sub-disciplines. What I have dealt with here is what has caught my own attention over the last few years, thus I may not have given due emphasis to some other important fields of mineralogy and petrology. I have undoubtedly been influenced in my choice and emphasis on topics of my own background and this article was written to give my own "snapshot" view rather than a fully academic analysis. It was not possible to mention here all the references I have used to present the progress was made in the various fields of mineralogy and petrology. In presenting the advances in each field I have roughly followed the list of the themes organized by the international program committee for the 2010 Goldschmidt conference. The interested reader

may find authoritative contributions to each of the themes starting from those of the committee leaders for the individual themes (http://www.goldschmidt2010.org/themes).

Taking into account the central theme of the congress, I will start with some thoughts on the theory and practice of sustainable development and mineral resources. Sustainability of the Earth can be defined as the maintenance of the Earth systems and the use of any renewable resources they provide, at rates which guarantee the continuity of their viability. The strongest links between Earth's sustainability issues and mineralogical sciences exist in the areas of mineral- water and mineral-atmosphere interactions, in the role of minerals as economic resources, and in the environmental consequences of mining and the remediation of polluted areas.

Minerals always were and always will be in the service of mankind providing the necessary raw materials that present and future economic activity demands, in order to drive modern or future civilization (Hochella, 2002). There would be some who would argue that the concept of sustainable resources cannot be applied to the non-renewable mineral resources. This matter, however relates both to the discussion of whether the mineral resources should be conserved in some way for the benefit of future generations (intergenerational consideration) and to the environmental consequences of mineral extraction.

Mineral resources may not be essential for simple human survival, but are essential for human well being. Considering the human population dynamics, the availability of these non renewable resources will most likely be in overall decline (Hochella, 2002) unless we find ways to assist the sustainable development by "sustaining the unsustainable" mineral resources. Better knowledge of the understanding and sustainable use of minerals, public pressure to the mineral extracting, processing and using industries to move towards technologies enabling "more to be done with less", are very important issues. Mineralogy, petrology and geochemistry, as well as other geological branches drive our basic understanding of the natural environment. There is now the recognition that if we claim for sustainable development, emphasis must be placed on sustaining the knowledge basis, on which our future strategies for sustainability at all levels must be founded (Cook and Johan, 1994). Progress in our understanding of the processes in systems that support the human habitation of this planet, especially in the interaction of minerals with the hydrosphere, atmosphere and biosphere can play a key role in dictating the sustainability of our planet.

2. Evolution of the Early Earth and origins of life

Progress in understanding the evolution of the Early Earth has been dramatic in the last years. There are recent articles focusing on evidence that the oceans, continental crust and some form of plate tectonics all existed four billion years ago, and possibly even earlier (see Nutman, 2006).

The oldest known rocks are found in Acasta, Canada (4.0 Ga) and recently, isolated detrital zircons, derived from unknown rocks from localities in western Australia, have provided evidence for 4.4Ga. The existence of zircon grains as old as 4.4Ga indicates that small amounts of granitic (sensu lato) protocontinent existed at that time and that the continent building processes were well under way by then.

Recent studies on the three major components of the Archean Greenstone belts, (tonalite-trondhjemite-granodiorite, TTG) and layered anorthosite complexes provide critical information on petrogenetic and geodynamic processes operated in the early Earth. Greenstone belts are dominated by: a) a komatiite-basalt association erupted in the form of intra-oceanic plateaus or alternatively continental flood sequences and b) a bimodal tholeitic to calc-alcaline basalts and dacites association, erupted in a magmatic arc setting. TTGs display diverse geochemical compositions and constitute 70 to 80 % of the surviving Archean crust. Anorthosite complexes are suggested to be a key component of the early crust but their petrogenesis and tectonic setting are poorly constrained.

Contributions that present innovative and integrated micro-analytical approaches to study inclusions in Hadean zircons and chemical and isotopic biosigniatures in Archean and Paleoproterozoic rocks, including iron formations, carbonates, shales, basalts, sulfate and phosphate rich rocks, provide exciting new avenues to reconstruct paleoenvironments.

Mineralogy offers insights into the debate on the origins of life, for various minerals may have played many different roles on the transition from geochemistry to biochemistry (see Hazen, 2005). Laboratory investigations and theoretical modeling explore the potential roles played by interactions between prebiotic molecules and mineral surfaces in promoting the mechanisms whereby molecules such as amino acids and nucleic acid fragments can bind to mineral surfaces leading possibly to the emergence of biological systems.

According to Ferris (2005) montmorilonite may have played a central role in the evolution of life. Ferris and co-workers (1989) have shown experimentally that Na-montmorilonite can adsorb organic compounds and can catalyze the formation of the first self-replicating RNA oligomers required for the origin of the first life in a protective environment. He suggested that life based on RNA preceded current life which is based on DNA and protein molecules.

One of life's most puzzling characteristics is that the basic constituents of the living organisms are chiral, but only L-amino acids (Laevo) are present in proteins and only D-nucleotides (Dextra) are present in nucleic acid. Hazen (2004) suggested that chiral mineral surfaces may have played a key role in separating left-from right-handed molecules or in catalyzing chiral synthesis reactions, since certain crystal faces of common minerals, like quartz and calcite display an aptitude for adsorbing handed molecules.

3. Deep Earth processes: Core and mantle

There has been a tremendous development in our understanding of the processes in the Earth's interior, coming from laboratory and computer experiments. Such experiments try to recreate the enormous P-T conditions which prevail in the deep Earth; measure the properties of minerals under such conditions; and study mantle rocks found at the surface. By comparing mineral properties at high P and T with geophysical observations we acquire information on the mineralogy, composition, temperature, deformation and structure of the Earth from the top of the mantle to the center of the planet.

Understanding of the deep Earth has been aided by new developments in diamond anvil cell and the large volume press technology combined with in situ XRD, spectroscopy and imaging techniques at synchrotron facilities. Recent advances in mass spectrometry, in particular, allow the stable isotope compositions of elements such as Mg, Si, and the transition metals to be determined at unprecedented levels of precision. In trace element research is now possible to measure mobile gas partitioning and trace element partitioning in mineral-water, mineral-melt, metal-silicate and metal-metal systems. Based on these data, quantitative models have been constructed that contribute to our understanding of a wide range of planetary differentiation processes, including crust and core formation, magma generation at ridges and hot spots, and element mobilization in subduction settings.

A phase transition of $MgSiO_3$ perovskite to the higher-pressure form post-perovskite was recently discovered (Murakami et al., 2004) at P-T conditions (120 GPa, ~2500^{o}K) resembling those occurring in the vicinity of the Earth's core-mantle boundary. This phase transformation is considered to be a possible cause for the D$''$ discontinuity, may explain many of the seismic features of the D$''$ layer, and is one of the few available means by which the thermal structure of the deepest mantle can be determined. A review of the early 2009 status concerning the structure, materials and dynamics of the lowermost mantle was presented by Trønnes (2009) and a description of the labora-

tory-based methods used in the discipline of mineral physics may be found in articles by Bass and Parise (2008), Bass et al., (2008), Karato and Weindrer (2008).

The developments in analytical methods provided the means to study composition, textures and microscale mineralogy of lithospheric mantle derived peridotites and eclogites at the micro and nano scale, in addition to what can be learned from whole rock major and trace element or isotopic analyses of the samples. Such studies of mantle rocks and minerals from continental and oceanic environments considerably widened our knowledge about the composition of the Earth's mantle but also about processes that changed its nature through time. Recent geochemical and geophysical studies tend to agree that material injected into the mantle at subduction zones is responsible for the compositional heterogeneity of the mantle and the creation of mantle reservoirs. Geochemical studies have highlighted the need for heterogeneous pyroxenite-peridotite-sediment mixtures to explain magmatism in oceanic and continental provinces. Seismic tomographic studies give evidence for subduction of oceanic lithosphere through the 660 km discontinuity and consequent return flow or upwelling of lower mantle into the upper mantle beneath hot spots and ocean ridges.

It is now generally accepted that oceanic basalts convey information about the chemical composition, thermal structure and dynamics of the mantle. It has been suggested that we can read the mantle signature in basalt compositions. But how mantle properties are translated into basalt compositions? Furthermore, do spatial patterns observed in the composition of oceanic basalts directly reflect mantle heterogeneity or, alternatively, they originate from regional-scale variations in melting behavior? These are issues that remain unresolved.

A number of recent studies focus on fluid-mineral interactions in deep crust and mantle. The quantification of the properties of fluids, particularly C-H-O-Si-bearing fluids, and their interactions with minerals in the deep crust and mantle is very important for understanding processes such as subduction, the generation of metamorphic fluids, the formation of deep mineral deposits and the deep carbon cycle. Field studies of high pressure rocks affected by fluids and experimental and theoretical studies of fluid properties, mineral solubilities and aqueous complexing at high P and T improve our understanding of these interactions.

Contributions to the study of the composition and structure of the continental lithosphere provide growing evidence for the importance of refertilization and deformation for the compositional evolution of the continental lithospheric mantle. Our models for the origin, chemical composition, physical properties and dynamics of the deep continental lithosphere are based mostly on magma-borne mantle fragments; however recent studies suggest that these fragments do not actually represent a mantle region. Combined efforts by petrologists, geochemists, geophysicists and field geologists may contribute in unraveling this and other lithosphere's secrets.

4. Physics and chemistry of Earth materials

Contributions to the study of chemical and biological processes at mineral surfaces have seen an intensive thrust in the last few years, primarily because of the new developments in the instrumental techniques that we can use to study surfaces at the atomic or near atomic level. Recent research of great interest includes fundamental molecular-scale mineral/microbe/water interface processes that impact the speciation, transport and potential bioavailability of the contaminants in our environment.

Of interest are also hydrogeochemical and mineralogical studies on low permeability sedimentary and crystalline rocks that limit fluid flow and solute transport. These rocks are important in the waste management, petroleum exploration and development, carbon dioxide sequestration and in groundwater protection and development.

Uranium in the environment, in natural deposits or in anthropogenic systems (e.g. mine waste receiving areas, radiogenic pollutants), is a concern to humans because of the potential for habitat contamination by radiotoxic constituents and the degradation of ground water quality. One of the key issues in embracing a much-expanded nuclear option for energy production is the safe disposal of the nuclear wastes (Ewing, 2006). Issues such as the basic geochemistry of uranium, the origin of exploitable uranium deposits, the dispersal of mill tailings and the disposal of depleted uranium or the products of multiple reprocessing schemes need basic working knowledge of Earth systems.

Significant knowledge has been acquired on the interactions of metals with clays, including trace metal fate transport and retardation, and in particular issues concerning radioelement (e.g. U) migration in natural systems, in radioactive waste disposal sites or in engineered barriers.

Clays have high specific surface area and reactivity, they are able to efficiently retard metal migration in the geosphere, and to control natural biochemical cycles of many trace elements in soil and freshwaters. Almost universally, bentonite is considered an important component in nuclear waste repositories as part of a multi barrier system (Pusch, 2006). It provides a tertiary engineered buffer by: a) limiting the entry of water into the waste b) contributing to the retention of radionuclide in the case of a leak c) assisting in dissipating heat from radioactive decay and d) protecting the radioactive waste bearing canisters against mechanical shock.

Current efforts in carbon dioxide sequestration through geological storage and mineral carbonation render additional motivation to further our understanding of the mineralization in the carbonate systems. Mineral carbonation could be accomplished by reactions between CO_2 with divalent cations such as Ca^{+2}, Mg^{+2} and Fe^{+2} to form carbonate minerals. Source for the divalent cations could be silicate minerals such as forsterite ($MgSiO_4$) or anorthite ($CaAl_2Si_2O_8$). Basalts are considered to be among rocks with best CO_2 storage capacity providing vast in situ carbon-mineralization sites throughout the world (Goldberg et al., 2008). Large efforts by the scientific community (Mineralogists/Petrologists/Geochemists) are still required to ensure that the in situ CO_2 sequestration in basalt or ultramafic rocks is technologically and economically viable.

Atmospheric dust is generated through a wide range of natural and human activities. Research on the particulate matter (PM) has been focused primarily on organic particles produced through combustion processes (e.g. coal combustion, forest fires). Inorganic dust is also abundant in the atmosphere and has major impacts on e.g. climate, oceanic nutrient levels and even traffic. Recent research focuses on the mineralogical, geochemical and isotopic characterization of both anthropogenic (combustion, abrasion, construction) and naturally occurring inorganic dust (e.g. volcanic eruptions or continental erosion) with contributions on topics such as single particle mineralogical characterization, isotopic tracing, inorganic organic PM interaction (e.g. adsorption), nutrient transport, quantitative distribution and source allocation of various PM types, and the interaction of PM with soils, plants, glaciers, oceans and climate.

5. Evolution of the oceanic crust and its hydrothermal systems

Hydrothermal activity at oceanic spreading centers plays a critical role in the chemical, physical and thermal evolution of the oceanic crust and it is strongly influenced by the dominant tectonic setting. Recent work has highlighted the diversity of hydrothermal systems both in the near ridge high temperature environment and off axis. Research topics such as fluid rock interaction, phase separation, magmatic degassing, the formation of metal-sulfide deposits and metamorphic reactions are now focusing on processes in crust formed at slow spreading rates versus processes at faster spreading rates.

6. Fluids, magmas and hydrothermal ore formation

Fluids and melt inclusions are our best source of information concerning the composition, temperature and

pressure of fluids associated with a wide range of geological processes in various geologic environments and times, including sedimentary basins, hydrothermal ore deposits, volcanic systems, subduction environments the upper mantle and diamond source regions and ultra high pressure metamorphic environments.

Economic geologists are increasingly recognizing that hydrothermal ore forming processes may have their roots in magma chambers in the upper mantle suggesting thus a vertical evolution of hydrothermal ore-forming systems.

Due to the unique role of nanoscale phases as agents of elemental transport and enrichment in ore systems, research on various aspects of nanomineralogy applied to mineral deposits, using all types of high resolution instrumental techniques (and computational methods) including HRTEM, HRSEM, SIMS, synchrotron XAS, XPS, AFM/AST and atomic modeling applications, has been significantly increased.

Microanalytical tools are also increasingly used for in situ microanalysis of single crystals of zircon, titanite, apatite and other accessory phases. The broad scale interest in single crystal mineral analyses stems from the limitations of whole rock trace element analyses in accessing the history of complex processes undergone by a single sample. Analyses of some accessory phases have wide potential applications, providing constraints on time, temperature, elemental and isotopic composition, magmatic oxidation state and fluid-melt evolution, among many others, from that same mineral grain.

7. Metamorphism over multiple length and time scales

Studies on mineralogical, petrological, stable /radiogenic isotope characteristics, microstructures, experimental and numerial modeling related to deeply subducted high and ultrahigh pressure metamorphic rocks, representing both oceanic and continental crusts, and fragments of the deep mantle, provided new insights into the global geodynamic processes operating in Earth's deep interior.

Following the worldwide recognition of UHP metamorphic rocks in more than 25 terranes, UHP metamorphism is no longer considered an "exotic" process; its significance affects all other disciplines of solid earth sciences, particularly petrology, geodynamics, global tectonics, seismology and geochemical cycling. During the last two decades diamond was discovered as micro-inclusions within garnet and zircon in about 10 localities of crustal metamorphic terranes. Due to these discoveries the PT diagram of metamorphic conditions realized by the Earth's crust had to be extended to 40kbar, equivalent with burial depths of about 140km. More recent research, based on modern nanoscale techniques led to the discovery of new indicator phases/associations for UHP-metamorphism (TiO_2, majoritic garnet, supersilisic titanite and clinopyroxene, pseudomorphs after stishovite, high-K clinopyroxene) which require continental subduction of at least 300km. As a result of the increasing role of UHP metamorphism in geosciences, in addition to important contributions on regional UHP-provinces, numerous scientific contributions have focused on topics such as high pressure experiments, computer modeling, geochronology, trace element geochemistry, Raman mapping, using techniques such as synchrotron infrared spectroscopy- nanosecondary ion mass spectrometry and diamond-anvil-cell technology.

Utilization of monazite, xenotime and zircon for dating a series of events considering recrystallization or partial alteration due to fluids and/or melts has gained great strides over the last decade. Complex textures seen in these accessory minerals can now be interpreted in terms of origins, history and chemical nature of the host rock, integrating thus geochronology, petrology and geochemistry. Current developments in zircon research, for example, is of fundamental importance. Based on detailed in situ isotopic, chemical, spectroscopic and microtextural studies of complex zircon crystals at high spatial resolution, or even at the scale of individual growth zones within a single grain, researchers can now link zircon ages to metamorphic or igneous petrogenetic events.

In addition, the oxygen isotope ratio of zircon can be used to discriminate between new crust (mantle derived) and crust that has been reworked (Valley, 2003; Harley and Kelly, 2007). This approach is even more powerful when combined with zircon U-Pb data and Hf isotope information on the same analyzed grains.

Some recent studies link metamorphic and igneous processes at subduction zones. Subduction-related metamorphic rocks from some localities provide petrological and geochemical evidence for large fluxes of aqueous fluids. Arc lavas contain abundant evidence for the involvement of aqueous fluids in their production. Research on eclogite-Arc magma connection by fluid introduction and transport at metamorphic conditions, fluid transport in the mantle wedge and slab-derived fluid contributions (volatiles, trace elements, isotope ratios) to arc magmas, provide new insights into the processes of fluid production, transport and evolution that ultimately lead to the generation of arc magmas.

Recent developments in metamorphic petrology and isotope geochemistry do permit increasingly accurate determinations of PT conditions of metamorphic samples, deformation analysis, geochronological constraints on the rates of orogenetic processes and forward models of orogenesis. However, continuing advances in understanding of the transport of elements and isotopes indicate that it is necessary to focus and move towards a scale heretofore inaccessible to traditional optical microscopy. At the nanometer scale, coupled dissolution/reprecipitation has already emerged as a crucial process. Ongoing research on metamorphism promotes the linkage of different methods to tackle macroscale to microscale issues in topics such as the tectonic affinity of subducted continents, transition from oceanic subduction to continental collision, crust mantle interaction during continental subduction-exhumation, time and duration of HP/UHP metamorphism, fluid effects on phase equilibria and P-T estimates, generation and action of aqueous fluid and hydrous melt, element and isotopic mobility, scale and magnitude of crustal melting, syn- and post-collisional magmatism, accessory minerals and trace elements. Metamorphism retains a dynamic and essential role for understanding the whole Earth from crust to core and it is not restricted solely to experiments! We should bear in mind that, besides the use of various modern techniques, many of these pioneering investigations were only possible through observations using the polarizing microscope, which remains a fundamental tool in geosciences!

8. Global element cycles and climate change

Microorganisms are intimately involved in the biogeochemical cycling of metals and metalloids. Certain microbial processes solubilize metals thereby increasing their mobility, which may increase bioavailability and potential toxicity, whereas other processes result in immobilization and reduce bioavailability.

The nature of microbe-mineral interaction also involves habitat conditions such as nutrient availability, presence or absence of toxic elements or pH buffering that contribute to the success or failure of a microbial consortium. The metabolic processes of the colonizing consortium influence mineral weathering, releasing, for example, limiting nutrients to the microorganisms (Bennet et al., 2002). Research on mineral-microbe interactions is an area of current and future expansion and is of great importance for both the mineralogical community and the advancement of the Environmental sciences.

Biomineralization in the marine realm is also a very interesting topic with implications on the understanding of the mineralization processes in natural systems. Chemical and isotopic signatures within biominerals provide information about the environment in which the minerals areformed. However, the interpretation of these signatures is difficult because the physiological environment of the organism may differ from extracellular conditions. Unraveling these effects requires an understanding of the processes of biomineralization which can be gained by laboratory culturing, investigated by experimental and theoretical techniques.

9. Nano-Geo-Environmental science: A new frontier in mineralogy

Recent contributions reveal a nanotechnology revolution for the geosciences. Reviews of the field and its development may be found in contributions by Wigginton et al., (2007), Navrotsky et al., (2008) and Hochella et al., (2008a). The manipulation of individual atoms and molecules through nanotechnology could have a big impact on alternative energy, resource extraction and pollution control.

Fuel cells are promising alternatives to conventional batteries and ultimately, a great many of aqueous solutions, of both natural and artificial origin, will become nontraditional resources. Waste water, acid mine drainage, seawater or saline lakes, which often are considered as problems, could become potential sources of materials with the help of molecular separation techniques, and as the molecular separation techniques mature, they will blur the distinction between a "pollutant" and a resource (Hochella, 2008b).

Nanoparticles (1 to 100 nanometers) are ubiquitous in the environment and can provide the majority of reactive surface area in many natural systems. They represent a transition phase between dissolved and true particulates. It is believed that they help to control the fate and transport of metals, radionuclides, organic contaminants and the cycling of nutrients showing unique, and sometimes difficult to predict behavior. They still lack a comprehensive description of their environmental functions, and to understand their role in geochemical and environmental processes we need to make progress in isolating them from natural media, analyzing and quantifying their properties, understanding reactions on a nano scale and the role that compositions and structure play in their behavior. Their properties can deviate significantly from those of a larger particle of the same phase and there are cases where bulk analogs to nanomaterials do not even exist. Due to the size of these particles, to look into the nanoworld, we need special techniques. Modeling, electron microscopy, spectroscopy and XRD are techniques that we can use to understand and predict nanoparticle behavior with respect to complex hydro-bio-geochemical processes. Synchrotron radiation based X-Ray techniques with high spatial and spectra resolution are suitable not only for the identification and characterization of nanoparticles on a trace element level, but also to explore and understand their interactions with the environment.

One of the major issues of research in recent years has been the interactions of nanoparticles with environmental pollutants and particularly the retention of radionuclides at the mineral-water interface. Such mineral-water interface reactions lead to the incorporation of radionuclides by solids. Although the reactions are not sufficiently understood, surface-catalyzed condensation processes include formation of nanoparticles, surface precipitates and solid solutions with the reaction host phase and may or may not be triggered by surface redox processes. Field and microscopy/spectroscopy based studies indicate that radionuclides can be transported by groundwater over several kilometers in short periods of time defying thermodynamically based conditions (Hochella, 2008). Novikov et al (2006) showed that 70 to 90% of the plutonium transport in groundwater is accomplished by way of ferric oxides less than 15nm in size. Much remains to be learned from the characteristics and behavior of natural nanoparticles. Nanogeoscience is at a relatively early stage of development but it seems that the near future will be an exciting time of new realizations, discoveries and change.

10. Analytical and experimental techniques

During the last 30 years we see an almost continuous application of new or technologically developed instrumental techniques to mineralogy, petrology and geochemistry. In the study of mineral structures, the X-ray diffraction techniques have been revolutionized by modern computerization and can now be used in combination with other emerging or rejuvenated techniques such as neutron diffraction, Transmission Electron Microscopy and spectroscopic methods (UV, optical, IR, Raman, Mössbauer). Magic

Angle Spinning, Nuclear Magnetic Resonance (MAS NMR) and X-Ray absorption (XAS) spectroscopies, as well as IR and Raman spectroscopies, are also effective with non crystalline materials and have been important techniques for the structural characterization of glasses and melts, providing insights into their short-range order-property relationships (Henderson, 2005, Calas et.al., 2006).

New methods, experimental and theoretical, emerge to provide means for materials synthesis, crystal growth and studies on mineral stabilities, reactions and assemblages at various conditions of pressure, temperature and composition. The conditions prevailed in the Earth's interior can be reproduced in the laboratory using laser-heated diamond anvil cells, which currently permit access to pressure – temperature conditions of 225 GPa and 5000 K, respectively. We now have a better knowledge on the mineralogy of the deep Earth and a better understanding of the behavior of rocks and minerals under extreme P- T conditions.

A major revolution in mineralogy and petrology came from the development and use of the Secondary-Ion Mass Spectrometer (SIMS, Ion microprobe). Ion Microprobe has the ability to analyze samples for trace REE, HFSE, light- lithophile elements and isotopes. It has proven very powerful for high spatial resolution (commonly <30 μm wide and < 1 μm deep) microprobe dating of zoned minerals using radiogenic isotopes and as microprobe for stable isotope systems. The method is relatively non destructive, allowing multiple analyses to be performed within single grains or zones within grains. In addition, isotopes and trace element analysis using nanometer scale ion imaging techniques have been applied to various research areas, including fluid-rock systems, paleoclimate, and biochemistry. ICP-MS (Inductively coupled plasma mass spectrometry) has become one of the standard methods for mineral analysis for measuring isotopes. It utilizes several sample introduction techniques, including laser ablation (LA) and direct introduction of a solution in the ionization region. The LA- ICP–MS method employs a focused laser beam to ablate material from samples. The ejected matter is ionized using an Argon plasma before being passed through to a mass spectrometer.

Mass spectrometric techniques have shed light to many geological problems, including the geochronology of inclusions in a meteorite (4.566± 0.002 billion years); based on W and Hf isotopes it was found that the formation of the core in an iron meteorite took place within 10 million years of the beginning of the solar system. Other isotopic systems indicate that by ~40 million years Earth had differentiated and that by 200 million years melts had crystallized in the crust, forming zircons (See Sutton et al., 2006)

Zircon grains are highly resistant to weathering; they can survive multiple geologic events and can provide a wealth of information regarding the crystal and mantle evolution studies. Zircon, for example in HP rocks, often protects mineral inclusions formed at high pressures from retrogression during exhumation, preserves different growth domains within a single crystal and in this way documents different stages of the subduction-exhumation history, which can now be puzzled out using Zircon U- Pb data (Gebauer et al., 1997) and Hf isotope information. Furthermore, a recently developed geothermometer based on the Ti content of Zircon in equilibrium with rutile is important in relating Zircon growth to temperature (Watson et al., 2006).

A number of contributions emphasize on the covariation of chemical and isotopic tracers in minerals used for geochronology (e.g. zircon) and thermochronologic (e.g. titanite) investigations. However, it is critical to understand which geochemical traits can help us make distinctions such as: when a chronometer becomes a thermochronometer, how can thermochronometers be tied to other minerals in a given metamorphic paragenesis and how can combined isotopic and geochronologic information (e.g. U-Pb, Hf, O in zircon) help us to better understand magmatic and petrogenetic processes.

One of the most remarkable changes that has taken place in the past decade is the development and operation of many technologically advanced research facilities at national or international laboratories focused on synchrotron light source or neutron scattering experiments. The research at these large scale

laboratories has impact in most Earth Sciences disciplines, including mineralogy, petrology and geochemistry. Issue No.1 of the "Elements" magazine (Vol. 2, 2006) provided an overview of these User research facilities and interesting reviews on the capabilities of Synchrotron Radiation, Neutron and Mass Spectrometry techniques in tackling complex scientific problems related to Earth materials and geological processes (Brown et al., 2006 a, b; Sutton et al., 2006; Parise and Brown 2006).

Synchrotrons generate extremely intense radiation in the Infrared to hard X-ray energy range. The average brightness of synchrotron light is six to twelve orders of magnitude greater than that of conventional laboratory x-ray sources, for example. The beams of the high intensity synchrotron radiation can be configured in many ways to perform scattering, spectroscopy or imaging experiments, they greatly enhance the sensitivity of conventional types of studies using IR, UV-visible and X-ray radiation and they reduce the experimental time enormously. Most X-ray based methods can be applied with high spatial resolution, including X-ray diffraction at high P and T, X-ray fluorescence, X-ray absorption fine-structure and computed microtomography. A simultaneous application of the techniques can lead to production of elemental maps with sub ppm sensitivity and determination of the speciation and mineralogy at selected locations of the material. Examples of synchrotron radiation research on geological materials are given in Brown et al., (2006).

Beams of neutrons can be tuned to have wavelengths comparable to typical interatomic spacings while simultaneously having energies that are comparable to the energies of thermal vibrations. Thus neutrons can uniquely give information about both the structure and the dynamics of the matter. Unlike scattering by X-rays, the interaction between neutrons and atomic nuclei is nucleus specific, which means that cations, for example Mg^{2+}, Al^{3+}, Si^{4+}, have distinctly different neutron scattering cross sections, thus neutrons are able to provide direct information about Mg/Al/Si ordering in minerals. Diffractometers and spectrometers have been designed to measure the intensity of the scattered neutron beam as a function of scattering vector, but spectrometers also measure as a function of energy change, at the same time. Diffractometers can be optimized for High resolution or high intensity and for measurements at High P and High T.

Other neutron diffraction methods that are becoming increasingly popular in mineral sciences are: small angle scattering, measurements of texture maps, measurements of strain distributions within mineral assemblages and total scattering. The latter is particularly useful for studies of disordered crystalline materials and glasses. Spectrometers have been designed for different frequency ranges to measure the dynamics of atoms within matter (including excitations such as harmonic lattice vibrations) and spin waves (including sound waves and High Frequency bond-bending vibrations such as O-H stretching vibrations) and even lower frequency diffusion motions (Sutton et al., 2006).

Scientific advances made possible by neutron sources in earth and environmental science research may be found in review articles by Brown et al., (2006 b) and Parise and Brown, (2006).

The latest generation of synchrotron x-ray sources and pulsed neutron sources are getting brighter and there are now new opportunities for scattering, spectroscopy and imaging studies of earth materials that were not possible some years ago. We have now the ability, by using third generation synchrotrons, to obtain element and phase distribution and phase identification at the 5 μm level using a combination of micro- XRF mapping, micro XRD and micro XAFs. Many of these developments are ongoing, and the impacts of the synchrotron and neutron source based methods on their complementarity on earth Science research will be enormous.

11. Thoughts on the near future roles of mineralogy and petrology

The intent of this lecture has been not so much to provide a well- digested review of the state of affairs in a given subdiscipline but, rather, to convey the essence and excitement of research occurring

on the frontiers of our Science. However, the question "Where is the frontier?" is rather naïve as the breadth and diversity of our science impart a very wide range of perspectives. To maintain harmony amongst us I would conclude saying that there are different kinds of frontiers in mineralogy and petrology and the criteria in assessing value and importance are very well known to those working in particular disciplines or subdisciplines.

Mineralogical sciences have undergone several major revolutions in the last two or three decades. They are now broader and more sophisticated sciences that have been benefited a lot from the revolution in experimental technology available to physical, chemical and materials sciences research. Mineralogy has become more quantitative, rigorous and mechanism orientated in terms of concepts taken from other sciences. Earth is now considered to be a materials- processing laboratory operating with time, distance, mass, pressure and temperature on an uncomparable large scale. Many of our strengths are built on the foundations and techniques developed to understand the basic physics, chemistry and biology underlying the Earth's formation and evolution.

We, as mineralogists and petrologists, are now seeing the future of our sciences in the application of innovative technologies and experimental methods in our research to understand many fundamental unsolved problems related to what is going on under our feet, how minerals react with water, how pollutants in groundwater, soil and air are transported and absorbed and how complex geochemical cycling takes place. Characterization of fine-grained materials (clays, amorphous phases) and nanomaterials and research work on reactions and processes such as absorption or dissolution and catalysis at mineral surfaces or at the interface between the solid mineral and the medium of interaction are areas of current and future expansion with fairly obvious impacts on the quality of life and the environment. The potential for biological treatment systems to decontaminate solid or fluid waste is enormous and represents one of the key research thrusts.

Perhaps the most significant technological development for mineralogy and petrology is the microfocus synchrotron beam. With synchrotron beams XAS spectra, XRD patterns and XRF, geochemical data may all be acquired with spatial resolution from micron sized particles. Already this has had a tremendous impact on studies of particular well- constrained mineralogical and petrological problems. We expect to see, in the future, several new facilities opened to ease the access problem. Important technological advances include also ongoing improvements to Scanning Probe Microscopy, Scanning Tunneling Microscopy and Atomic Force Microscopy. The development of STM and AFM surface microscopic techniques has given us the capability to study in depth processes such as crystallization, dissolution, absorption at the atomic level, and in situ.

There is now great potential for much interesting work in these areas. Microbeam analytical methods for trace element and isotopic analysis are now available and we expect that ion microprobes should become more common in small scale university analytical centers. The explosive increase in the use of the method will continue in the years to come, due to its capability of directly connecting petrography with trace element/isotope chemistry and its contribution to U-Pb age determinations. There will be also demand for much work with this instrument applied to environmental specimens.

Of course studies on the particular themes cited earlier in this article will continue to be of critical importance for some years. Other subjects could as well be at the forefront of our scientific endeavours:

- Uptake and long-term sequestration of carbon in stable mineral phases remains of critical importance for study.
- Safe disposal of nuclear waste: the recent economic crisis and the high prices of petroleum and other fossil fuels have resulted to increased pressure on many governments for resurgence of interest in nuclear power or to invest more funds in nuclear power production. One of the key is-

sues in embracing a much-expanded nuclear option for energy production is the safe disposal of the nuclear wastes. Environmental mineralogy has a critical role to play in evaluating the primary nuclear waste (Ewing, 2001, 2006) measuring radionuclide transport in the engineered and geologic portions of the barrier system and evaluating the models of risk that rely on a number of geochemical parameters (Wogelius et al., 2007).

- Study of glasses and melts: spectroscopic techniques, (particularly infrared and Raman, NMR, Mösbauer and X-Ray absorption spectroscopy) have recently begun to be applied to glass structure, as spectroscopic data on silicate glasses and melts are similar. Most work to date has focused on the short range structure of glasses. It is important for this work to continue in the next years with more wide range of glass compositions and the advanced synchrotron and neutron scattering techniques should play increasingly important role, providing important information on this topic. The study of glasses and melts is highly connected with the disposal of the nuclear wastes, as the most common practice has been to immobilize HLW in borosilicate glasses or according to recent work, in phosphates, including monazite, apatite and glasses (Oelkers and Montel, 2008).

12. Mineralogy and petrology in the cross road: Diversification and Expansion or fragmentation?

Environmental mineralogy and geochemistry, nanomineralogy, biomineralogy and mineral physics are intellectually close to the interfaces between Earth sciences and disciplines such as chemistry, materials science, microbiology, physics and structural molecular biology. However in all these areas of research the need for interdisciplinary cooperation between mineralogists and other specialists will continue to grow. Our community has the obligation to contribute our skills towards a better understanding of the issues and mineralogists are committed to enhancing and promoting the role of mineralogy in solving global and societal challenges.

A large amount of mineralogical work occurs in disparate fields, and many of us are not aware of the full range of the subjects because the work done is commonly not visible to the bulk Earth science community (Hawthorne, 1993). Thus, this great diversity has adversely affected the general view of mineralogy and many earth scientists are not conversant with the breadth and intellectual vitality of current work in mineralogy. Works on zeolites and clays are characteristic examples.

Natural zeolites have exciting surface and structural properties, they possess attractive absorption, cation exchange, dehydration - rehydration and catalysis properties, which contribute directly to their use; They are being used for example in construction, as hydroponic substrate for growing plants in space missions, in pollution control, in the handling and storage of nuclear wastes, in biotechnology and in many other applications. (see in Colella and Mumpton, 2000). Their atomic scale structure gives them interesting and useful catalytic properties, therefore, the characterization and synthesis of new zeolites have become of great interest to some sectors of the chemical industry. Thus, although many mineral scientists have played prominent roles in the study and development of the field of zeolites and some still play, most of the important zeolite characterization and synthesis works are now published in the chemistry literature or in specialized journals (e.g. Zeolites) rather than in the mineralogical literature. Almost unknown to all but the zeolite chemists and engineers are also everyday zeolite applications such as: 3-fold increase in yield of gasoline from petroleum using zeolite catalysts, higher octane number and lower pollutants in automobile exhausts, cleaner multi-pane windows from zeolite absorbing vapours, safer brakes in trucks and trains, deodorization of animal litter, barns, ashtrays, refrigerators, and athletic footwear, longer life of refrigerators and selective absorbents in nuclear waste (Smith,1999; Mumpton, 1999). Consequently, although much work by mineralogists, or of interest to mineralogists

is done in this field, most earth scientists are largely unaware of this aspect of mineralogical work because these journals are normally obscure to most Earth Scientists.

Clay minerals are fine grained sheet silicates with extremely diverse chemical composition and structure, made of various configurations of tetrahedrally and octathedrally coordinated layers. They vary in size from amorphous materials to barely recognizable particles under a polarizing microscope. Proper identification of a clay mineral requires X- ray diffraction techniques, and optical microscopy does not really help much for their identification. Clay minerals are of great importance to many areas of Earth sciences, including sedimentology, geological engineering, environmental processes, hydrothermal and weathering processes and industrial mineralogy.

Most undergraduate Earth Science students have a feeling that clays are not "proper" minerals mostly because they cannot see them easily under the microscope. On the other hand clay mineralogy has withdrawn from the rest of mineralogy and now has separate societies, journals and meetings, to the general detriment of Mineralogy as a whole (Hawthorne, 1993). R.L Frost, in the highlights of the July, 2002 issue of Geotimes, wrote:

"*Clay science is alive and well- but perhaps not in the traditional departments of geology and natural resources. In the new millennium, clay science is thriving in schools of Chemistry, departments of Engineering and research programmes of environmental science*".

The following two passages are quoted from the president's of the International Association for study of Clays annual report (Bish, 2009):

"*…As the global scientific Society faces increasing diversification of clay science, it is more important that AIPEA members actively participate in the life of our society. At the same time, there appears to be a renaissance in related sciences wherein clay minerals play an important role, in fields such as chemistry, biological sciences and materials science…*".

"*…Clay mineralogy has been experiencing renewed interest worldwide based on an explosion of activity of a variety of fields outside of traditional clay mineralogy. Perusal of many journals in chemistry, physics and materials sciences reveals significant interest in the fine grained materials that we all study and use…*".

Of course we cannot put limits on what is Mineralogy and we must allow every flower to blossom. With such a cooperative research we will have an enormous impact of our discipline on important highly visible scientific issues that confront society today and on our scientific understanding of the mineralogical, geochemical and biological system we call Earth.

Mineralogy is going through a period of rapid expansion and diversification and the formal Mineralogical community (mineralogical associations and societies) needs bridges for our connection to one another within our broad discipline and for our connection to other fields such as environmental science, material science, solid state physics, biosciences and chemistry. More appreciations of the work done by all sectors of the community working on minerals would pull all these branches back into a coherent discipline. Mineralogists, petrologists and geochemists have to establish a larger collective presence. We all have to help to achieve this goal.

I strongly believe that the future of the Mineralogical sciences is very bright. There will be much research excitement in our fields in the years to come and we must try to attract the attention of talented students wishing really to study Earth sciences. Today, there is probably no standard answer to the question of what constitutes an ideal undergraduate geology curriculum. Nevertheless, the classical fields of Mineralogy and Petrology remain vitally important because they provide essential back-

ground about Earth's materials, the geological processes that produce and affect them and they certainly have a huge impact in the quality of our life. However, we must also create space for the newer ideas and applications of our sciences. Existing courses could be enhanced, for example, by devoting time to discussions on the adsorption, cation exchange, dehydration and catalytic properties of minerals, which are important for the development of their applications. We must encourage the new generations of scientists to follow our field because at no previous time has there been so much excitement in mineralogy and petrology.

13. Acknowledgments

I thank T. Kotopouli and Y. Iliopoulos for reading and commenting on the manuscript.

14. References

Bass, J.D., Parise, J.B., 2008. Deep earth and recent developments in mineral physics. *Elements, 4* (3), 157-163.

Bass, J.D., Sinogeikin, S.V., Li, B., 2008. Elastic properties of minerals: A key for understanding the composition and temperature of earth's interior. *Elements, 4* (3), 165-170.

Benner, S. A., Caraco, M. D., Thomson, J. M., Gaucher, E. A., 2002. Evolution: Planetary biology - paleontological, geological, and molecular histories of life. *Science, 296*(5569), 864-868.

Bish, D., 2009. 2009 President's report. AIPEA Newsletter, 41, 1-3.

Brown Jr., G.E., Calas, G., Hemley, R.J., 2006a. Scientific advances made possible by user facilities. *Elements, 2* (1), 23-30.

Brown Jr., G. E., Sutton, S. R., Calas, G., 2006b. User facilities around the world. *Elements, 2* (1), 9-14.

Calas, G., Henderson, G. S., Stebbins, J.F., 2006. Glasses and melts: Linking geochemistry and materials science. *Elements, 2* (5), 265-268.

Cook, P. and Johan, Z., 1994. Introduction: Mineral resources and sustainable developments: A workshop. Abstracts and background documents. Technical report WF/94/12, British Geological survey, U.K., pp. 10-13.

Colella C. and Mumpton, F.A. (Eds), 2000. *Natural Zeolites for the Third Millennium* De Frede - Editore, Napoli, Italy, 484 pp

Ewing, R.C., 2001. The design and evaluation of nuclear-waste forms: Clues from mineralogy. *Canadian Mineralogist, 39*(3), 697-715.

Ewing, R.C., 2006. The nuclear fuel cycle: A role for mineralogy and geochemistry. *Elements, 2*(6), 331-334.

Ferris, J.P., 2005. Mineral Catalysis and Prebiotic Synthesis: Montmorillonite-Catalyzed Formation of RNA. *Elements*; 1 (3), 145-149.

Ferris, J.P., Ertem, G., Agarwal, V., 1989. Mineral catalysis of the formation of dimers of 5´-AMP in aqueous solution: The possible role of montmorillonite clays in the prebiotic synthesis of RNA. *Origins of Life and Evolution of the Biosphere, 19* (2), 165-178.

Gebauer, D., Schertl, H., Brix, M., Schreyer, W. 1997. 35 ma old ultrahigh-pressure metamorphism and evidence for very rapid exhumation in the dora maira massif, western alps. *Lithos, 41* (1-3), 5-24.

Goldberg, D.S., Takahashi, T., Slagle, A.L., 2008. Carbon dioxide sequestration in deep-sea basalt. *Proceedings of the National Academy of Sciences of the United States of America, 105* (29), 9920-9925.

Harley, S. L. and Kelly, N.M., 2007. The impact of zircon-garnet REE distribution data on the interpretation of zircon U-pb ages in complex high-grade terrains: An example from the rauer islands, east antarctica. *Chemical Geology, 241*(1-2), 62-87.

Hawthorne, F.C., 1993. Minerals, mineralogy and mineralogists: Past, present and future. *Canadian Mineralogist, 31* (2), 253-296.

Hazen, R.M., 2004. Chiral crystal faces of common rock-forming minerals. In G. Palyi, C. Zucchi and L Caggliotti, Eds. *Progress in Biological Chirality*. New York: Elsevier, Chapter 11, pp.137-151.

Hazen, R.M., 2005. Genesis: Rocks, minerals and the geochemical origin of life. *Elements* 1, #3, 135-137.

Henderson, G.S., 2005. The structure of silicate melts: A glass perspective. *Canadian Mineralogist, 43* (6), 1921-1958.

Hochella, M.F., 2002. Sustaining earth: Thoughts on the present and future roles of mineralogy in environmental science. *Mineralogical Magazine, 66* (5), 627-652.

Hochella Jr., M.F., 2008. Nanogeoscience: From origin to cutting-edge applications. *Elements, 4* (6), 373-379.

Karato, S.-I. and Weidner, D.J., 2008. Laboratory studies of the rlheological properties of minerals under deep-mantle conditions. *Elements, 4* (3), 191-196.

Mumpton, F.A., 1999. La roca magica: Uses of natural zeolites in agriculture and industry. *Proceedings of the National Academy of Sciences of the United States of America, 96* (7), 3463-3470.

Murakami, M., Hirose, K., Kawamura, K., Sata, N., Ohishi, Y., 2004. Post-perovskite phase transition in $MgSiO_3$. *Science, 304* (5672), 855-858.

Navrotsky, A., Mazeina, L., Majzlan, J., 2008. Size-driven structural and thermodynamic complexity in iron oxides. *Science, 319* (5870), 1635-1638.

Novikov, A.P., Kalmykov, S.N., Utsunomiya, S., Ewing, R.C., Horreard, F., Merkulov, A., et al., 2006. Colloid transport of plutonium in the far-field of the mayak production association, russia. *Science, 314* (5799), 638-641.

Nutman, A.P., 2006. Antiquity of the oceans and continents, *Elements* 2, pp. 223–227.

Oelkers, E.H. and Montel, J., 2008. Phosphates and nuclear waste storage. *Elements, 4* (2), 113-116.

Parise J.B. and Brown Jr., G.E., 2006. New opportunities at emerging facilities, *Elements, 2,* 37-42.

Pusch, R., 2006. Clays and nuclear waste management. In: F. Bergaya, B.K.G. Theng and G. Lagaly, Editors, *Handbook of Clay Science*, Elsevier, pp. 703–716.

Smith, J.V., 1999. Geology, mineralogy, and human welfare. *Proceedings of the National Academy of Sciences of the United States of America, 96* (7), 3348-3349.

Sutton, S.R., Caffee, M.W., Dove, M.T., 2006. Synchrotron radiation, neutron, and mass spectrometry techniques at user facilities. *Elements, 2* (1), 15-21.

Trønnes, R.G., 2009. Structure, mineralogy and dynamics of the lowermost mantle. *Mineralogy and Petrology,* 1-19.

Valley, J.W., 2003. Oxygen isotopes in zircon. *Reviews in Mineralogy and Geochemistry, 53* (1), 343-385.

Watson, E.B., Wark, D.A., Thomas, J.B., 2006. Crystallization thermometers for zircon and rutile. *Contributions to Mineralogy and Petrology, 151* (4), 413-433.

Wigginton, N.S., Haus, K.L., Hochella Jr., M.F., 2007. Aquatic environmental nanoparticles. *Journal of Environmental Monitoring, 9* (12), 1306-1316.

Wogelius, R.A., Morris, P.M., Kertesz, M.A., Chardon, E., Stark, A.I.R., Warren, M., Brydie, J.R., 2007. Mineral surface reactivity and mass transfer in environmental mineralogy. *European Journal of Mineralogy, 19* (3), 297-307.

12ο ΔΙΕΘΝΕΣ ΣΥΝΕΔΡΙΟ ΤΗΣ ΕΛΛΗΝΙΚΗΣ ΓΕΩΛΟΓΙΚΗΣ ΕΤΑΙΡΙΑΣ
ΠΛΑΝΗΤΗΣ ΓΗ: Γεωλογικές Διεργασίες και Βιώσιμη Ανάπτυξη

12th INTERNATIONAL CONGRESS OF THE GEOLOGICAL SOCIETY OF GREECE
PLANET EARTH: Geological Processes and Sustainable Development

ΓΕΝΙΚΗ ΚΑΙ ΤΕΚΤΟΝΙΚΗ ΓΕΩΛΟΓΙΑ
GENERAL AND STRUCTURAL GEOLOGY

Δελτίο της Ελληνικής Γεωλογικής Εταιρίας, 2010
Πρακτικά 12ου Διεθνούς Συνεδρίου
Πάτρα, Μάιος 2010

Bulletin of the Geological Society of Greece, 2010
Proceedings of the 12th International Congress
Patras, May, 2010

A NEW INTERPRETATION OF THE STRUCTURE OF INTERNAL HELLENIDES

Argyriadis I.[1], Midoun M.[2] and Ntontos P.[3]

[1] *Cabinet de Géologie Argyriadis, 975 chemin du Pré de Caune, 83740 La Cadière d'Azur, France*
E-Mail: ion@argyriadis.net

[2] *Cabinet 2M Conseils, Le Condorcet 18 rue Elie Pelias13016 Marseille*
E-Mail: geode2m@gmail.com

[3] *4 G. Griva st., 21100, Nafplio – Greece E-Mail: ntontos@naf.forthnet.gr*

Abstract

This study is based on some new observations made from Southern and Central Evia, Argolis and North-central part of Pindos. Our observations lead us to adopt a simplified view of the paleogeography of Greek mainland just before the Alpine orogeny. The subsequent varied tectonic units originate mainly from the following paleogeographic areas:

- *A carbonate Arab-African shelf margin which displays several lateral transitions, ridges and basins. In the Greek mainland this margin is represented by the Preapulian, Ionian, Gavrovo-Tripolis, Parnassos zones, Olympus platform and probably the Kavala and Thassos Marbles.*
- *A transition zone from the shelf units to the Tethys ophiolites (Pindos Zone, Styra, Argolis and Hydra, Eretrias new unit).*
- *Tethys ophiolites, which might represent an "ocean" fault zone or subduction of lithosphere along a weak zone.*
- *An Hercynian continental mass (Servomacedonian).*

1. Introduction

New field observations made from Southern (IA) and Central Evia (IA and MM), Argolis (IA and PN) and North-central part of Pindos (IA). The combination of them, leads us to adopt a new aspect of the structure of internal Hellenides. Starting with a briefly description for each area we will pass through the conclusions to the new aspect.

In southern Evia three main tectonic units are exposed, the Almyropotamos unit, Tsakaioi-Ochi unit and Styra unit while in the northern part of the island, we distinguished a new unit consisting of Seta's Paleozoic and Dirfis-Olympus (Eretrias) Mesozoic limestones. This complex is underlying the ophiolitic complex of Central Euboia separated by a thick mylonitic zone.

In the Argolis area, three main units are present: Mesozoic limestones at the bottom, a mylonitized zone consisting of ophiolitic and chert matrix including limestone remnants in the middle and the ophiolitic complex of Eastern Greece at the top of succession.

In northern and central Pindos area, we describe the existence of Late Cretaceous (Campanian) transgressions over ophiolitic bodies indicating the presence of Pindos Zone east of Parnassos Zone, near the ophiolitic complex of Eastern Greece.

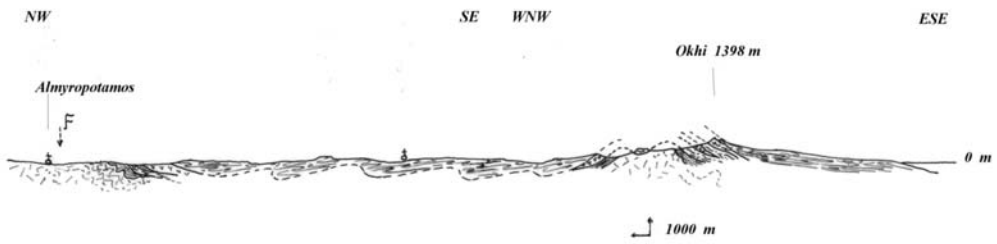

Fig. 1: Geological section of South Evia (I. Argyriadis, 2005).

2. Evia

Evia belongs to the internal Hellenides and for many years many scientists argue for the geological composition. We will consider the south part first and then the central part.

2.1 Southern Evia

Southern Evia constitutes part of Attica-Cyclades massif; a stack of metamorphic formations, which their age and the structure, has been an argument issue since the dues of 19th century. Since 1967 an announcement was made (Argyriadis 1967), according to which Southern Evia is a tectonic window, underlying the units of Central Evia and Northern Attica. This interpretation assumes four (4) units:

- Almyropotamos unit consisting of Mesozoic marbles.
- Tsakaioi unit consisting of schist and amphibolite including large bodies of serpentine.
- Styra unit consisting of thin plate marble, sipoline, quartzite and amphibolitic schist.
- Ochi unit is consists of glaucophane schist, large bodies of amphibolite and manganese microquartzite.

Since then, many researchers (Argyriadis et al 1976, Aubouin 1977, Dubois & Bignot 1979, Gerneut 1971, Katsikatsos 1971, 1977, 1991, Katsikatsos et al 1986, Lensky et al 1997, Maluski et al 1981, Papanikolaou 1987, Shaked et al 2000) adopt that subdivision fulfilling and refining the details: Paleocene's metaflysch over Almyropotamo's marbles, "blue schists" over the other units, adopting also new nomenclature (see Geological Map of IGME). However, this first subdivision contained "errors of youth" that are retracted by the newer observations of the author and thus today, the dominate aspect is that exists only three units which are multiple folded: the Almyropotamos unit at the bottom and the other two units, Styra and Tsakaioi-Ochi, at the top of succession. Depending the later folding the upper unit change. For example, at the site Rouklia-Lala, Styra unit is overthrusted marbles which form an anticline while a thin ophiolitic intercalation exists. Furthermore Styra unit is overthrust over the ophiolitic assemblage of Ochi unit from Platanisto to the Ochi shelter.

2.2 Central Evia

Central Evia is considered as a sedimentary succession consisting by Paleozoic slates and limestone, Mesozoic limestone of Triassic and Jurassic period bearing ophiolites. This succession is «sealed» by transgressive Cenomanian limestone followed by thin bedded Late Campanian limestone where they progressively pass to flysch (Maastrichtian to Paleocene) (Argyriadis 1966, Aubuin 1977, Aubuin et al 1976, Deprat 1904, Guernet 1971, Renz 1940).

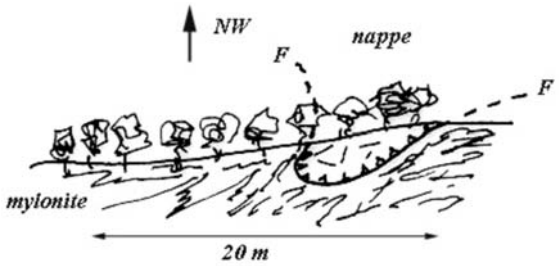

Fig. 2: The contact between Central Evia's unit and mylonite. Position's coordinates 38° 25′54′′ N and 23° 42′30′′E.

Our researches in the region led us to distinguish a new unit. The fossiliferous Mesozoic limestone of Dirfis-Olympus unit is placed tectonically below the Paleozoic Seta's unit although the contact between the two units seems to be a stratigraphic conformity. This conformity can be seen on the section of the road from Eretria to Geronta. In other words the whole system seems to be reversed.

The lineaments that differentiate the new unit from the so far called Central Evia's unit are:

- The unit is intensely folded. The plunge direction of the main fold axes are 90° to 100°, 45° and 300°.
- The folds whose main axis trends to E-W are mainly isoclinals, upright or inclined to NNE while those whose main axis trends to NW-SE are inclined to SW (Dinaric folds).
- The Paleozoic component of the unit is constituted by clastic sediments containing intercalations of limestone. Triassic begins with volcanic rocks and tuffs while Jurassic and probably Early Cretaceous turns to cherts, quartzites and thin plate limestones (J. Deprat in 1904 found Early Cretaceous fossils SW of Dirfi's mountain and M. Lys had mention "ghosts" of Early Cretaceous foraminifera).
- There seems to be no emersion, unconformity or transgression except local "hard ground" of Late Paleozoic

There is tectonic relationship between the new unit and Central Evia's unit with the last one being over the first one. The overthrust plane, folded after the thrust movement, is characterized by the presence of a remarkable broad mylonite, frequently many hundreds meters thick. The new unit is surrounded by that mylonite:

- Westwards, is present from Malakonta surrounding the folded west side of Olympus Mountain (with remnants of gabbros, pillow lavas, radiolarite, which can be seen from Ag. Anna's church near Geronta), covered by newer sediments until Kambia where there is a remarkable zone of fragmented dolomite. The mylonite continues around Dirfi, Steni, Ag. Athanasios, Glyfada (Tserges) to the Aegean Sea. It has to be noticed that the new unit is reversed and that is obvious at Liri (East side of Dirfi's cone) and at Tsougaraki col on the road from Ag. Athanasio to Glyfada, where we can see Paleozoic slates above the Mesozoic limestones.
- From north-eastern the mylonite arises in the land in Metoxi in order to turns to Manikia and Paramerites (tectonic remnants and mylonite of ophiolites) heading towards Aliveri.
- In the southern, the mylonite is present in Oropos region as the last formation towards the sea.

We underline that the new unit includes the mountain range from Dirfi to Xerovouni and Skotini which is constituted by limestone. This limestone pass under Seta's slates and reappears in Olympus region.

It is therefore a unit (paleogeographic area) with many of its constitutive formations been known but

they were consider to be part of Central Evia's ophiolites. Furthermore, remarkable mylonite has not been mentioned before, considering being "schists-chert" formation. We believe that this unit is a completely different paleogeographic area than ophiolitic complex of Eastern Greece which is present northern of Chalkida city. We will call this new unit as Eretria's unit.

3. Argolis

Geological maps of this area suffer from a confusion presenting an extended Late Cretaceous flysch formation of "sediments of passage from Eastern Greece zone to Pindos zone" (Bachmann & Risch 1978, Bannert & Bender 1968, Baumgartner 1985, Clift 1996, Dercourt 1970, Leibundgut et Attinger 1986, Renz 1940). Actually, there are limited occurrences of flysch formation. However the majority of occurrences are a formation that we will refer to as "mélange". It is a thick mylonite zone with intense deformation that includes radiolarite, remnants of serpentine, blocks of limestone usually of Late Cretaceous period and mainly clastic sediments with ophiolite origin. This clastic material is characterized by the presence of roundstones which are strongly orientated and cleaved. Here are some examples:

- **In Tolo city,** geological map presents flysch formation placed tectonically over Late Cretaceous limestone or under Triassic limestone. Actually, mylonite is overthrust recrystallized limestone probably of Triassic age. This can be seen on the road towards Tolo's port. This mass includes blocks of underlying limestone, sandstones with ophiolite origin, fragmented radiolarite and pillow lavas and blocks of black limestone. Moving north-westwards to the waste bank of Tolo, at the col of Seitan-bachtse site we see the tectonic contact between the mylonite and subjacent limestone. Limestone is karstified before upthrust and ophiolitic material seems to be depressed inside karstic cavities. The same mylonite can be seen under the ancient castle of Asini.
- **In the area of Pyrgiotika village,** flysch formation exists but it is under the mylonite with the contact between these two formations being intensely folded. Easternly of the village we observe remnant of serpentine inside the mylonite, covered by white and purple calcschists with *Globotruncana sp*.. Nearby there is a tectonic remnant of white limestone and radiolarite always inside the mylonite.
- **In the area of Marathea village,** peaks of Goumouria and Aetovigla are chisel out in thick bedded limestone in the base of which Lower Triasic lavas exists. Despite what geological map describe, this limestone is not over the flysch formation but below it. Even more this formation is not flysch but mylonite which is overthrust onto the Triassic limestone. This overthrust can be seen clearly near the Ag. Georgios's church which is founded on limestone tectonic remnants inside the mylonite.
- **In Argos city,** Aspida's hill consists of highly altered ophiolite with transgressive bioclastic limestone, probably of Late Cretaceous epoch. Flysch is totally absent and Larrisa's hill consists of radiolarite and thin plate, pink, limestone of Pindos Zone, covered by thick bedded limestones, probably Cretaceous (near Panagias's Monastery).
- **Westwards of Argos City in the area of Ag. Triada's church** there is an extended appearance of highly altered ophiolite which contains old, pedogenetic surfaces covered by lateritic crusts and angeritic dolomites continental or lacustrine origin. On that surface seems to lie in stratigraphic conformity limestone with hornstone intercalations containing ostracodes.
- **In site Akova,** limestone of the eastern front of Loutses Mountain is below tectonically fragmented ophiolite which in turn is below intensely folded sandstone with ophiolitic origin.

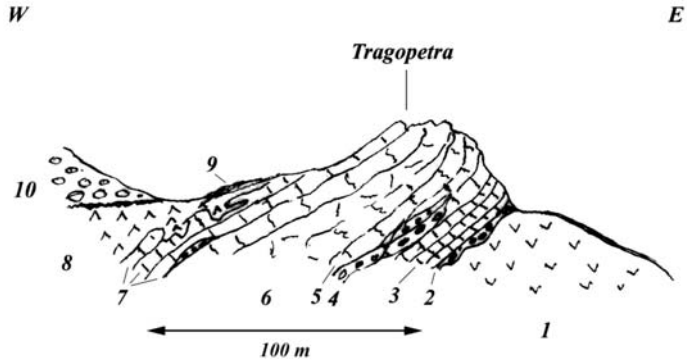

Fig. 3: Tragopetra's geological section (see text for explanation).

Constructively in Argolis area, three paleogeographic areas are present: a carbonate shelf belonging to Paleo-African margin, a continental slope (Pindos Zone) which now forms tectonic slices and the ophiolitic complex of Eastern Greece tectonically placed at the top of succession. The original fingerprint of this research is the recognition of the broad mylonite just like Evia.

4. Pindos

4.1 Northern Pindos

A Late Cretaceous transgression over ophiolitic complex has been described (Argyriadis 2004, 2007). In this region, ophiolitic complex has been tectonically placed over Pindos Zone (Philippson 1890, Reinhardt 1911, Kober 1931, 1952, Renz 1940, Brunn 1956). Inside ophiolitic complex there are limestones of Triassic, Jurassic age, or Upper Cretaceous, even Eocene epoch, embedded or intercalated. An array of limestone outcrops is observed eastern of Katara site. From south to north we meet Tragopetra, Petra Portas, anonymous outcrops and Megali Petra. Common attribute between these outcrops is the Late Cretaceous epoch. Although Brunn (1956), primary, had interpreted these outcrops as tectonically placed, today it has been proved (Argyriadis 2004) that they are transgression's remnants.

The most reachable outcrop is Tragopetra, beside the *National Road 6*, about 2 km eastern of Katara's col. Here, the origin of ophiolite is peridotite and gabbros which fluctuates to doleritic lavas. It is fully serpentinized and has strong tectonic deformation. The columnar section of the specific site is (microfauna determinations by G. Tronchetti, Marseille):

- Ophiolitic lavas at the bottom (1).
- Transgressive conglomerate (2) consisting of ophiolitic rounded shingles mainly peridotite and gabbros and sometimes radiolarite. Conglomerate fulfils concavities on ophiolite's surface. Thickness range from 10 to 100 cm.
- Thin layer (about 10 cm thick) of red coloured limestone.
- White coloured bedded limestone (3) up to 7-8 m thick. At the bottom they contain ophiolitic pebbles same as the previous ones. In the last two calcareous horizons founded Globotruncana linneiana, Gl. bulloïdes, Gl. arca, Contusotruncana fornicata, as well as Rugoglobigerina sp., Heterohelix striata, Pseudotextularia sp., Plassoglobulina sp., Calcisphaerulidae showing Late Campanian age.

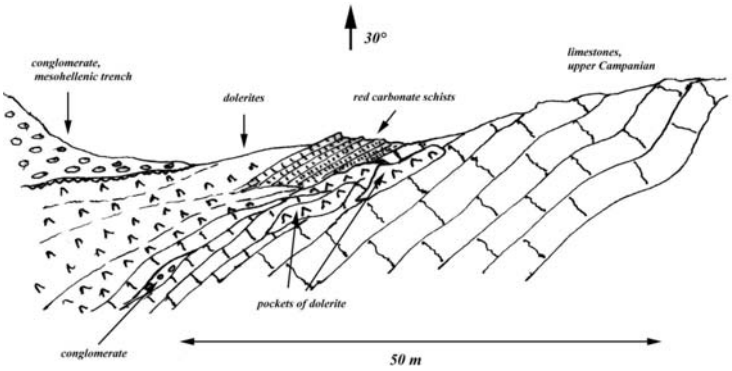

Fig. 4: Detailed view of Tragopetra's limestone outcrop.

- Miscellaneous conglomerate (4) up to 1-2 m thick, containing ophiolitic, quartzite, crystallic rock and limestone pebbles.
- Pink coloured limestone (5), up to 2-3 m thick, with cleavages and lenticular intercalations of conglomerate. It has the same microfauna with layer (3).
- White coloured thick bedded limestone (6) up to 30 m thick. Only small orbicular foraminifera have been founded without key fossils.
- Pink coloured, thin bedded limestone (7), up to few meters thick, with lenticular intercalations of conglomerate same as previous. It has the same Globotruncana microfossils but even more, Globotruncanella havanensis, showing Early Maastrichtian age. The limestone series ends upwards in a karstic surface with big concavities.
- Effusions of doleritic lavas (8), completely different than previous one of ophiolite, also fully alterated. Locally lava penetrates and discharges inside the concavities of subjacent karst. The thickness is estimated to 50 m.
- Superimposed red carbonate schists (9), fulfilling the concavities of subjacent doleritic lavas, up to 1-2 m thick.
- Conglomerate (10), of Auversian age over previous lava formation, in stratigraphic conformity. It is also miscellaneous but different than previous one, consisting of big boulders (up to 20 cm diameter) of crystallic rock. It is the base of MesoHellenic Trench.

About a kilometre north of Tragopetra, in site "Tzina" an array of outcrops begins trending north. The first outcrop is called "Petra Portas" and constitutes of transgressive limestone with Globotruncana, up to 20 m thick, over peridotite. The limestone fluctuates to red coloured, cleavage limestone and then to altered doleritic lavas. A fingerprint of "Petra Portas" is the active karst big enough to supply a spring.

Northernly thus Tzina's col, we can observe other three similar outcrops with reducing thickness of limestone. In the outcrop which is 200 m easternly of the col, above the limestone instead of doleritic lavas there is a series of red, green and white radiolarite, up to 5 m thick. Upwards this series discontinues by tectonic contacts with superjacent ophiolite.

The northern and last outcrop, Megali Petra, is the thickest outcrop of limestone, more than 50 m thick. It is intensively folded, with main axis trending N-S and E-W. Some of them have an intense vertical component. The whole structure forms a rock mass extending for many hundreds meters. The columnar section of the specific site is (microfauna determinations by G. Tronchetti, Marseille):

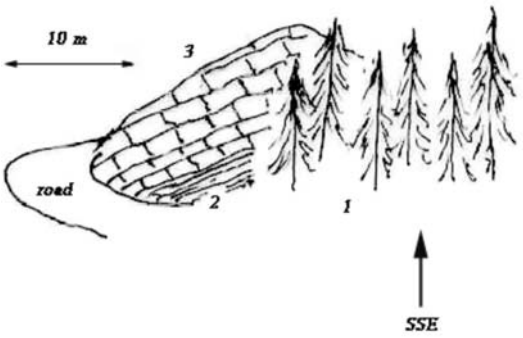

Fig. 5: Outcrop of serpentine in "Melana Litharia". 1: serpentine, 2: pink calcschists, 3: transgressive limestone of Campanian.

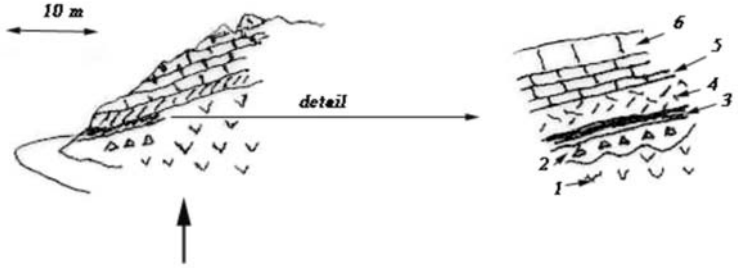

Fig. 6: Outcrop of serpentine in "Melana Litharia" 300 m southernly from previous outcrop. 1: serpentine, 2: breccias up to 20 cm thick, with limestone and ophiolite fragments, 3: Crust up to 5 cm thick of altered volcanic matrix 4: Altered volcanic rock up to 1 m thick, 5: thin plate limestone with Globotruncana arca, 6: white limestone with Gl. Arca and Gl.cf calcarata.

- High altered peridotite (serpentine) at the bottom.
- Coarse-grain arkose of varying thickness (fulfils concavities of subjacent surface).
- Thin bedded, purple coloured limestone, up to 5 m thick. There are signs of intense thermal influence while intrusions of altered lava are present. Many non determinable shells of elasmobranches have been found.
- Red, cleavage limestone, up to 5-6 m thick.
- Thin bedded, white or pink coloured limestone, up to 20 m thick, with Globotruncana fossils just like Tragopetra's outcrop and conglomerates intercalations with boulders and pebbles of peridotite, lavas, radiolarite in a calcareous matrix. In the upper horizons of this formation Globotruncanita cf. Calcarata has been founded showing Upper Campagnian age.
- Succession of sandstone and clastic limestone at the bottom and authentic red radiorarite and plate limestone with Globotruncana upwards.

4.2 Central Pindos

Something similar can be observed at Vardousia Mountain, in the area of Artotina, about 6 km south of the village. In Arenta Mountain (1604 m), in a site, called "Melana Litharia", a serpentinized ophiolitic mass covered northwards by transgressive limestone with Globotruncana, is tectonically placed between flysch formations.

This ophiolitic mass is constituted of serpentines, gabbros, pillow lavas, radiolarite, etc. Transgressive limestone, up to 25 m thick, becomes upwards thin bedded, pink coloured ending up as pink-violet calcschists. This formation is intensively deformed and is under and simultaneously over flysch formation. It is just the case of tectonic insertion defined up and down by tectonic unconformities. The subjacent flysch formation contains clastic material of ophiolitic origin indicate that Pindos Zone and Tethys ophiolites was in direct adjacency. We remind that in Parnassos unit the carbonic sedimentation goes up to Eocene and flysch begins afterwards (Renz 1940, Aubuin 1977).

5. Conclusions

According to Ch. Lyell's principle of "actualism" we can conclude for each studied area:

- **In South Evia,** the lower unit (Almyropotamos) is considering to be a carbonate shelf-margin. This unit is identified as part of the Paleo-African – Arab shelf margin. Styra unit, identified as part of the continental slope from the shelf units to the Tethys ophiolites is overthrust Almyropotamos unit. The contact between the two units is strongly multi-phase folded. At least one folding phase is younger than main thrust movement, trapping Tethys's ophiolite which had to be over Styra unit.
- **In Central Evia,** we describe the Eretria unit identified as part of the same continental slope, also strongly folded with isoclinal or inclined folds but significant less extent of metamorphism. Above Eretria unit we find overthrust Central Evia's unit consisting of ophiolites, transgressive limestone of Late Cretaceous and flysch. This overthrust is characterized by the strong folding of contact's surface and the existence of a broad mylonite.
- **In Argolis,** except the minimal metamorphism (or the lack of it) we have the same situation: a carbonate shelf at the bottom and over that, fragmented, discontinuous wedges of a paleogeographic continental slope (Pindos Zone and relative transition sediments). At the top we find overthrust an ophiolitic complex (SubPelagonian Zone).
- **In Pindos,** our observations answer a question of the classic conception for internal Hellenides: the existence, Easternly from Pindos Zone, Parnassos Zone, namely an insertion of carbonic shelf between Pindos continental slope and Tethys's ophiolites. In Northern Pindos, we have the evidence that ophiolites were deformed and repeatedly had emerged and corroded before the Campagnian (transgression of Late Jurassic in Vermio, Middle Cretaceous westwards from Vourino and Campagnian in the region of Metsovo) and that also the Dinaric thrust movements before Auversian became in sculptural conditions and in no case in depths of subduction zone. In Southern Pindos, the existence of ophiolite wedges - or even olistholites – inside flysch of Late Cretaceous-Paleocene shows obviously that the period before the trust movements of Late Eocene, Pindos continental slope was next Tethys's ophiolites, Easternly of Parnassos shelf, and the overthrust of Parnassos on Pindos became in later phase.

Synthetic interpretation. Our observations lead us to adopt a simplified view of the paleogeography of Greek mainland just before the Alpine orogeny. The subsequent varied tectonic units originate mainly from the following paleogeographic areas:

- A carbonate Arab-African shelf margin which displays several lateral transitions, ridges and basins. In the Greek mainland this margin is represented by the Preapulian, Ionian, Gavrovo-Tripolis, Parnassos zones, Olympus platform and probably the Kavala and Thassos Marbles (Argyriadis & Fourquin, 1987).
- A transition zone (continental slope) from the shelf units to the Tethys ophiolites (Pindos Zone, Styra, Argolis and Hydra, Eretrias new unit.

- Tethys ophiolites, which might represent an "ocean" fault zone or subduction of lithosphere along a weak zone.
- An Hercynian continental mass (Servomacedonian).

Already in Middle Cretaceous or even earlier, Tethys's ophiolite was deformed and at least folded but also was emerged (see laterites, transgressions and disagreements of Middle and Late Cretaceous, etc). This emersion possibly characterizes and certain parts of African shelf. Immediately afterwards ophiolites overthrust on the African shelf in an enormous movement, which drifted, fragment and disintegrated the continental slope, like Pindos. This movement is accompanied also by proportional locomotion of European-Asian mass. It is deformed in the scale of planet. It is obvious that this major movement was followed by a phase of compaction and strongly, isoclinal folding, trending from SSW to NNE (see Southern and Central Evia). Most obvious today (because newest) deformation during Late Eocene and Oligocene are relatively more limited and rather of minor importance if we examine the total area of deformation that is extended from Caribbean to Indonesia.

6. References

Argyriadis I. 1966. La série stratigraphique de l'Eubée moyenne (Grèce). Existence de mouvements intrasénoniens. *C. R. Acad. Sci., Paris*, 262 (D), p. 2427 - 2430.

Argyriadis I. 1966. Sur la tectonique de l'Eubée moyenne. Présence de lambeaux allochtones et raccord probable avec la Macédoine. *C.R. Acad. Sci., Paris*, 262 (D), p. 2577-2580.

Argyriadis I. 1967. Sur le problème des relations structurales entre formations métamorphiques et non métamorphiques en Attique et en Eubée. *C.R. Acad. Sci., Paris*, 264 (D), p. 438-441.

Argyriadis I. 1975. Mésogée permienne, chaîne hercynienne et cassure téthysienne. *Bull. Soc. Géol. Fr.,* (7), p. 56-67.

Argyriadis I. 2000. La tectonique de la Basse Provence: proposition d'une interprétation nouvelle. *C.R. Acad. Sc. Paris*, IIa, vol. 331 n°12, p. 797 – 802.

Argyriadis I. 2004. Ανωκρητιδική επίκλυση στους οφειολίθους Βορείας Πίνδου. Θεωρητικά συμπεράσματα (Upper cretaceous transgression over the ophiolites of northern Pindos). *Bull. Geol. Soc. Greece* vol. XXXVI, 2, 2004, p. 802 – 807.

Argyriadis I. & Fourquin Cl. 1987. La structure du complexe de nappes rhodopien en Grèce: une fenêtre hellénique africaine sous les Balkans. *C.R. Acad. Sci. Paris*, 305, Série II, p. 727-732.

Argyriadis I., Mercier J.L., Vergely P., 1976. La fenêtre d'Attique-Cyclades et les corrélations Hellénides –Taurides. *C.R. Acad. Sci., Paris*, 283, (D), p. 599-601.

Argyriadis I., 1974. Sur l'orogenèse mésogéenne des temps crétacés. *Revue de Géogr. Phys. et Géol. Dyn.*, vol. XVI, 1, p. 23 – 60.

Argyriadis I., Graciansky P.C. (de), Marcoux J., Ricou L.E., 1980. The opening of the Mesozoïc Tethys between Eurasia and Arabia-Africa. 26e CGI, Coll. 5, Eds BRGM, p. 199-214.

Aronis G., 1964. Observations on the coastal karst of Greece. Mémoires A.I.H., t. V, Réunion d'Athènes 1962, p. 256 – 265.

Aubouin J., 1977. Méditerranée orientale et Méditerranée occidentale: esquisse d'une comparaison du cadre alpin. *Bull. Soc. Géol. Fr.*, (7), XIX, n°3, p. 421-435.

Aubouin J., Bonneau M., Davidson J., Leboulenger P. et Matesco S. 1976. Esquisse structurale de l'arc égéen externe: des Dinarides aux Taurides. *Bull. Soc. Géol. Fr.*, (7), XVIII, p. 327-336.

Bachmann, G. and Risch, H., 1978. Late Mesozoic and Paleogene development of the Argolis peninsula

(Peloponesos). In: Closs, H., Roeder, D. and Schmidt, K., (eds). Alps, Apennines and Hellenides. Schweiserbart, Stuttgart, pp. 424-427.

Bannert, D. and Bender, H., 1968. Zur Geologie der Argolis-Halbinsel (Peloponnes, Griechenland). *Geologica et Palaeontologica*, 2, 151-162.

Baumgartner, P., 1985. Jurassic sedimentary evolution and nappe emplacement in the Argolis peninsula (Peloponessus, Greece). Memoire de la Societie Helvetique pour la Science Naturelle.

Bonzanigo, L., 1982. Géologie de l'arrière pays d'Erétrie (Eubée, Grèce). Travail de Diplôme à l'Ecole Polytechnique Fédérale, Zürich.

Brunn, J.H., 1952. Les éruptions ophiolitiques dans le NW de la Grèce et leurs rapports avec l'oro genèse. 19 ème congrès géol. Int.17, 19-27.

Brunn, J.H., 1956. Contribution à l'étude géologique du Pinde septentrional et de la Macédoine occidentale. *Ann. Géol. Pays Hellen.* 7, 410 p.

Brunn, J.H., 1960. Mise en place et différenciation de l'association pluto-volcanique du cortège ophiolitique. *Rev. Géogr. phys. Géol. dyn.*, Sér. 2, 3, 115-132.

Brunn J.H., Argyriadis I. and Braud J. 2001. Magmatic emplacement of northwestern Greece ophiolites. Proccedings of the 9th International Congress of the Geological Society of Greece, 2001, *Bull. Geol. Soc. Greece*, XXIV, vol. 6.

Brunn, J.H., Argyriadis, I., Braud, J., 2004. Μαγματική τοποθέτηση των οφειολίθων της βορειοδυτικής Ελλάδας (Magmatic emplacement of northwestern Greece ophiolites.). *Bull. Geol. Soc. Greece,* XXXVI, 4, 2004, p. 1625 – 1628.

Celet, P. et Ferrière, J., 1978. Les Hellénides internes: le Pélagonien. *Eclogae Geol. Helvetiae* 71/3, 467 - 495.

Clift, P. and Robertson, A., 1990. Deep-water basins within the Mesozoic carbonate platform of Argolis, Greece. *Journal of the Geological Society*, 147, 825-836.

Clift, P., 1992. The collision tectonics of the southern Greek Neotethys. *Geologische Rundschau*, 81/3, 669-679.

Clift, P., 1996. Accretion tectonics of the Neotethyan Ermioni Complex, Peloponessos, Greece. *Journal of the Geological Society*, 153, 745-757.

Degnan, P.J., Robertson, A.H.F, 1991. Tectonic and sedimentary evolution of the Western Pindos Ocean: NW Peloponnese, Greece. *Bull. Geol. Soc. Greece*, 25/1, 263-273.

Degnan, P.J., Robertson, A.H.F., 1998. Mesozoic-early Tertiary passive margin evolution of the Pindos ocean (NW Peloponnese, Greece). *Sedimentary Geology*, 117, 33-70.

Deprat, J., 1903. Sur la structure de l'île d'Eubée. *C.R. Acad. Sci., Paris*, 137, 666 - 668.

Deprat, J., 1903. Notes préliminaires sur la géologie de l'île d'Eubée. B.S.G.F., (4), 3, 229 - 243 et B.S.G.F. (7), 4, 340 - 356.

Deprat, J., 1904. Etude géologique et pétrographique de l'île d'Eubée. Thèse, Besançon 1904. Carte géol.

Dercourt, J., 1970. L'expansion océanique actuelle et fossile: ses implications géotectoniques. *Bull. Soc. Géol. Fr.*, (7), 12, 261-317.

Dubois, R. and Bignot, G., 1979. Présence d'un "hard ground" nummulitique au-delà de la série crétacée d'Almyropotamos (Eubée méridionale, Grèce). *C.R. Acad. Sci., Paris*, 289, 993-995.

Gautier, P. and Brun, J.P., 1994. Crustal-scale geometry and kinematics of late-orogenic extension in the central Aegean (Cyclades and Evvia Island). *Tectonophysics*, 238, 399-424.

Guernet, Cl., 1971. Etudes géologiques en Eubée et dans les régions voisines (Grèce). Thèse, Paris 1971, 395, 50 pl.

Jones, G., Robertson, A., Cann, J., 1990. Genesis and emplacement of the supra-subduction zone Pindos

ophiolite, northwestern Greece. In: Tj. Peters et al., eds., Ophiolite genesis and evolution of the oceanic lithosphere. Ministry of Petroleum and Minerals, Oman, 771-799.

Katsikatsos, G., 1991a. Geological map of Greece, Aliveri sheet. I.G.M.E., Athens, Greece.

Katsikatsos, G., 1991b. Geological map of Greece, Rafina sheet. I.G.M.E., Athens, Greece.

Katsikatsos, G., Migiros, G., Triantaphyllis, M., Mettos, A., 1986. Geological structure of internal Hellenides (E. Thessaly, SW Macedonia, Euboea, Attica, Northern Cyclades islands and Lesvos). I.G.M.E. Geological and Geographical Research, special issue, 191 – 212.

Katsikatsos, G., 1971. L'âge du système métamorphique de l'Eubée méridionale et sa subdivision stratigraphique. Prak. Acad. Athènes, 44, 223-238.

Katsikatsos, G., 1977. La structure tectonique d'Attique et de l'île d'Eubée. Réun. Extraord. Soc. Géol. Fr.et de Grèce en Grèce, 1976, *Bull. Soc. Géol. Fr.*, (7), XIX, 1, 75-80.

Kober, L., 1915. Alpen und Dinariden. *Geol. Rudsch.* 5, 175-204, Leipzig 1915.

Kober, L., 1931. Das alpine Europa. Borntraeger, Berlin.

Kober, L., 1952. Leitlinien der Tektonik Jugoslaviens. Serbische Akad. D. Wiss. Sonderausgabe, 189, Geol. Institut, n. 3.

Koumantakis, J., Matarangas, D., 1980. Geological map of Greece, Panayia sheet.

Laubscher, H.P., Bernoulli, D., 1977. Mediterranean and Tethys. In: Nairn et al. Eds., The Ocean basins and margins. IV, Mediterranean Plenum Publ., New York.Jackson E., Green H., Moores E., 1980. The Vourinos ophiolite, Greece: cyclic units of lineated cumulates overlying harzburgite tectonite. *Geol. Soc. Amer. Bull.*, 86, 390-398.

Leibundgut, Ch. et Attinger, R., 1986. Coastal Region between Argos and Astros. In Karst hydrogeology of central and eastern Peloponnesus (Greece). Morphis M. and Zojer H. Eds.

Lekkas, S. and Lozios, S. 2000. Tectonic structure of Mt. Hymittos. *Ann. Géol. Pays Helléniques.*, 38, C, 47 – 62.

Lensky, N., Avigad, D., Garfunkel, Z., Evans, B.W., 1997. The tectono-metamorphic evolution of blueschists in South Evia, Hellenide Orogenic belt (Greece). Israel Geological Society, Annual Meeting 1997, 66-67.

Lepsius, R., 1893. Geologie von Attika. Ein Betrag zur Lehre vom Metamorphismus der Gesteine; Berlin 1893, 592 p.

Maluski, H., Vergely, P., Bavay, D., Bavay, P., Katsikatsos, G., 1981. 39Ar/40Ar dating of glaucophanes and phengites in southern Euboea (Greece) ; geodynamic implications. *Bull. Soc. Géol. Fr.*, 5, 469-476.

Mavridis, A., Skoyrtsis-Koroneou, V., Tsaila-Monopoli St., 1977. Contribution to the geology of the sub-Pelagonian zone (Vourinos area, West-Macedonia). VI coll. Aegean Region, Athens 1977, v. I, 175-195.

Mercier, J., 1968. Etude géologique des zones internes des Hellénides en Macédoine centrale (Grèce). *Ann. Géol. Pays Helléniques*, 20, 596 p.

Moores, E.M., 1969. Petrology and structure of the Vourinos ophiolite complex of Nothern Greece. *Geol. Soc. Amer., Spec. Paper*, 118, 74 p.

Papanikolaou, D.J., 1984. The three metamorphic belts of the Hellenides: a review and a kinematic interpretation. In The Geological evolution of the Eastern Mediterranean (eds J.E. Dixon and A.H.F. Robertson), 551-560. Geological Society of London, special publication n° 17.

Papanikolaou, D.J., 1986. Late Cretaceous paleogeography of the metamorphic Hellenides. I.G.M.E. Geological & Geographical Research, special issue, 315-328.

Papanikolaou, D.J., 1987. Tectonic evolution of the Cycladic blueschist belt (Aegean Sea, Greece). In Chemical Transport in Metasomatic Processes (ed. H.C. Helgeson) 429-450. NATO ASI series, 218c.

Parrot, J.F., 1977. Ophiolites du Nord-Ouest syrien et évolution de la croûte océanique téthysienne au cours du mésozoïque. *Tectonophysics*, 41, 251-268.

Philippson, A., 1890. Bericht über eine Reise durch Nord- und Mittel-Griechenland. *Zeitschr. D. Ges. F. Erdk*. 25, 331-416.

Piper, D.J.W., Pe-Piper, G., 1980. Was there a western (external) source of terrigenous sediment for the Pindos zone of the Peloponnese (Greece)?. *Neues Jahrbuch für Geologie und Paläontologie, Monatshefte* 1980, 107-115.

Reinhardt, M., 1911. Sur l'existence de la nappe des roches ophiolitiques en Macédoine. *C.R. de Séances de l'Institut géologique de Roumanie*, Bucarest, 19.

Renz, C., 1940. Die Tektonik der griechischen Gebirge. Mém. Acad. Ath. 8, 1-171.

Renz, C. et Reichel, M., 1945. Beiträge zur Stratigraphie und Paläontologie des ostmediterranen Jungpaläozoïkums und dessen Einordnungim Griechischen Gebirgssystem. I und II Teil: Geologie und Stratigraphie. *Eclogae Geol. Helvetiae* 36, Nr 2 (1945), 211 - 313, mit 3 Textfig. und 1 Tafel 'IX).

Ricou, L.E., 1971. Le croissant ophiolitique péri-arabe, une ceinture de nappes mises en place au Crétacé supérieur. *Rev. Géogr. Phys. Géol. dyn*. (2), vol. XIII, 4, 327-350.

Ricou, L.E., Argyriadis, I., Marcoux, J., 1975. L'axe calcaire du Taurus, un aligne‚ent de fenêtres araboafricaines des nappes radiolaritiques, ophiolitiques et, éta‚orphiques. *Bull. Soc. Géol. Fr*., (7), XVII, 1975, n° 6, 1024-1044.

Robertson, A.H.F., Clift, P.D., Degnan, P.J., Jones, G., 1991. Palaeogeographic and palaeotectonic evolution of the Eastern Mediterranean Neotethys. *Palaeogeography, Palaeoclimatology, Palaeoecology,* 87, 289-343.

Seidel, E., Kreuzer, H., Harre, W., 1982. A late Oligocene/early Miocene high pressure belt in the external Hellenides. *Geologisches Jahrbuch*, E23, 165-206.

Shaked Y., Avigad, D., Garfunkel, Z., 2000. Alpine high-pressure metamorphism at the Almyropotamos window (southern Evia, Greece). *Geol. Mag*. 137 (4), 367-380.

Δελτίο της Ελληνικής Γεωλογικής Εταιρίας, 2010
Πρακτικά 12ου Διεθνούς Συνεδρίου
Πάτρα, Μάιος 2010

Bulletin of the Geological Society of Greece, 2010
Proceedings of the 12th International Congress
Patras, May, 2010

THE PELAGONIAN NAPPE PILE IN NORTHERN GREECE AND FYROM. STRUCTURAL EVOLUTION DURING THE ALPINE OROGENY: A NEW APROACH

Kilias Ad.[1], Frisch W.[2], Avgerinas A.[1], Dunkl I.[3], Falalakis G.[1], Gawlick H-J.[4] and Mountrakis D.[1]

[1] *Department of Geology and Paleontology, University of Thessaloniki, GR-54124, Thessaloniki, Greece.*

[2] *Instiute of Geosciences, University of Tuebingen, D-72076, Tuebingen, Germany.*

[3] *Sedimentology and Enviromental Geology Geoscience center, University of Goettingen, D-37077, Goettingen, Germany*

[4] *Department for Applied Geosciences and Geophysics, University of Leoben, A-8700, Leoben, Austria*

Abstract

The geometry of kinematics and the deformation history of the Pelagonian nappe pile during the Alpine orogeny have been studied in Northern Greece and FYROM. Deformation was started in Middle-Late Jurassic time and was initially associated with ocean-floor subduction followed by ophiolites obduction, nappe stacking and duplication of the Pelagonian continent. The footwall Pelagonian segment from top to bottom was metamorphosed under greenschist to amphibolit facies conditions and a relative high pressure (T = 450° to 620° C and P = 12,5 to 8 kb). Blueschist facies metamorphic assemblages of Late Jurassic age are immediately developed between both hanging-wall and footwall Pelagonian segments. Transgressive Late Jurassic-Early Cretaceous neritic limestones and clastic sediments on the top of the obducted ophiolites are maybe related to extension and basins formation simultaneously with the nappe stacking and metamorphism at the lower structural levels of the Pelagonian nappes. Contractional tectonics and nappe stacking continued during the Albian-Aptian time. Simultaneously retrogression and pressure decreasing taken place at the tectonic lower Pelagonian footwall segment. Low grade mylonitic shear zones, possible related to extension, are developed during Late Cretaceous time simultaneously with basins formation and sedimentation of neritic Late Cretaceous to Paleocene limestones and flysch. Intense shortening and imbrication under semi-ductile to brittle conditions occurred during Paleocene to Eocene time resulting the onset of the dome like formation of the footwall Pelagonian segment. The next stages of deformation from Oligocene to Quaternary are related to brittle extension and the final uplift and configuration of the Pelagonian nappe pile.

Key words: *Pelagonian nappe, Vardar/Axios Zone, compression, extension, Hellenides.*

1. Introduction-Geological setting

While the Tertiary structural evolution of the Hellenides has been studied in detail and is satisfactorily understood (Lister et al., 1984, Sfeikos et al., 1991, Doutsos et al., 1993, Schermer 1993, Dinter and Royden 1993, Kilias et al., 1999, Xypolias et al., 2003), the geometry and kinematics of the early stages of the Alpine orogenic cycle in Jurassic and Cretaceous times still remained poorly stud-

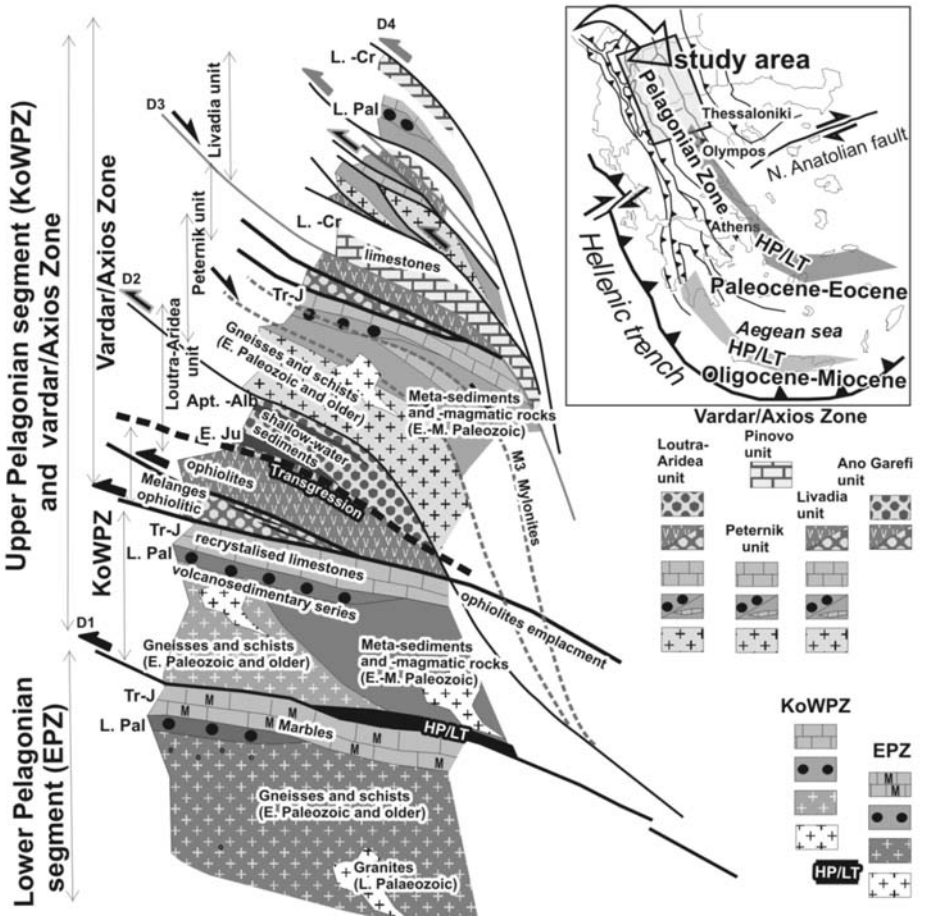

Fig. 1: Alpine architectur and structural evolution of the Pelagonian nape pile and eastern Vardar/Axios Zone.

ied and contradictory. Tertiary deformation in some cases has totally destroyed the older structures.

In order to decipher the deformational processes during the early stages of the Alpine cycle and their migration until Tertiary time, our study focused on the structurally higher Hellenides units, i. e., the Pelagonian nappes (Pelagonian Zone) and the Vardar/Axios Zone in northern Greece and the Former Yugoslavian Republic of Macedonia (FYROM) (Fig. 1,2). The timing of deformation was constrained by radiometric results mainly derived from Most (2003), stratigraphical data from Brown and Robertson (2004) and Sharp and Robertson (2006), as well as cross-cutting relationships of structures on all scales from map to thin section. P-T metamorphic conditions were estimated using metamorphic mineral assemblages and thermobarometric calculations. Shear criteria such as S-C fabrics, shear bands, asymmetric pressure shadows, mica fish, or asymmetric boudins (Simpson and Schmid 1983) have been used in order to study the kinematic history of deformation.

The Pelagonian Zone forms an elongate, NNW-SSE trending nappe pile of continental origin on the top of the External Hellenides extending from FYROM to the south through the central Greek mainland and Evvia into the Cyclades (Attico-Cycladic Massif) (Fig. 1,2). (Jacobshagen et al., 1978,

Mountrakis 1986, Kilias et al., 1991, Doutsos et al., 1993, Schermer 1993, Avgerinas et al., 2001). A different tectono-stratigraphic subdivision is given for the Pelagonian Zone in FYROM, where the Korabi-West Pelagonian Zone (KoWPZ) is distinguished from the East Pelagonian Zone (EPZ) (Medwenitsch 1956, Arsovski & Dumurdzanov 1984) (Fig. 1,2).

The eastern side of the Pelagonian Zone is truncated by the NNW-SSE striking Vardar/Axios Zone (Fig 2) which is particularly very well exposed in the Voras Mountains in northwestern Greece where the tectono-stratigraphic sequence can be best studied. It contains narrow belts of schists, gneisses, granitoides, Paleozoic and Mesozoic metasedimentaty rocks, Neotethyan ophiolites, transgressive Late Jurassic/Early Cretaceous and Late Cretaceous to Paleocene clastic sediments, neritic limestones and flysch (Mercier 1968, Mountrakis 1986, Galeos et al., 1994, Brown and Robertson 2004, Sharp and Robertson 2006). The complicated composition and structures of the Vardar/Axios units are given in detail in Figures 1. To the west of the Pelagonian Zone along its western fringe is evolved the Mirdita/Pindos ophiolites. There is an ongoing discussion about the displacement direction of the obducted ophiolites during Middle to Late Jurassic time on top of the Pelagonian continent, as well as the existence of one or two oceans bothsides of the Pelagonian continent (Jacobshagen et al., 1978, Vergely 1984, Mountrakis 1986, Shallo and Dileck 2003, Brown and Robertson 2004, Rassios and Moores 2006, Sharp and Robertson 2006, Gawlick et al., 2008).

In this paper we rergard the East Pelagonian Zone as an exhumed Pelagonian dome (footwall Pelagonian segment) beneath the overthrust Korabi-West Pelagonian zone (hangingwall Pelagonian segment) and the Vardar/Axios units (Fig. 2).

2. Deformation analysis and kinematics

The geometry and kinematics of deformation, cross cutting relationships, and the syn-kinematic growth of metamorphic mineral assemblages related to a given structure in combination with regional considerations record the progressive activity of seven (D_{HP} to D_6) tectonic events from Middle Jurassic to Neogene time. They document the change from ductile conditions in the early stages of deformation to semi-ductile and eventually brittle conditions in the late stages and are related to plate convergence and the closure of the Tethyan ocean, as well as to orogenic collapse. Shortening and extension alternated.

D_{HP} event

High pressure structures (D_{HP}) are preserved at the boundary between EPZ and KoWPZ on the western limb of the East Pelagonian anticlinorium, and between EPZ and Vardar/Axios Zone at its eastern flank. D_{HP} can be traced on top of the marble cover of the EPZ so that it surrounds the East Pelagonian antictinorium following the tectonic boundary between EPZ and the overlying KoWPZ and Vardar/Axios units (Fig. 1,2).

D_{HP} structures are characterized by the occurrence of a relict S_{HP} foliation associated with an about WNW-ESE trending stretching lineation (L_{HP}). L_{HP} is defined mainly by blue amphibole, white mica and chlorite. Majer and Mason (1983) report also sodic pyroxene related to the high pressure event. Syn-D_{HP} white mica yielded K/Ar ages of ca. 150Ma (Most et al., 2001, Most 2003). D_{HP} is related to subduction, nappe stacking and crustal thickening.

D_1 event

The D_1 event records penetrative ductile structures. They are well preserved in the EPZ and along its top tectonic contact. In the KoWPZ and the Vardar/Axios basement no geochronological or strati-

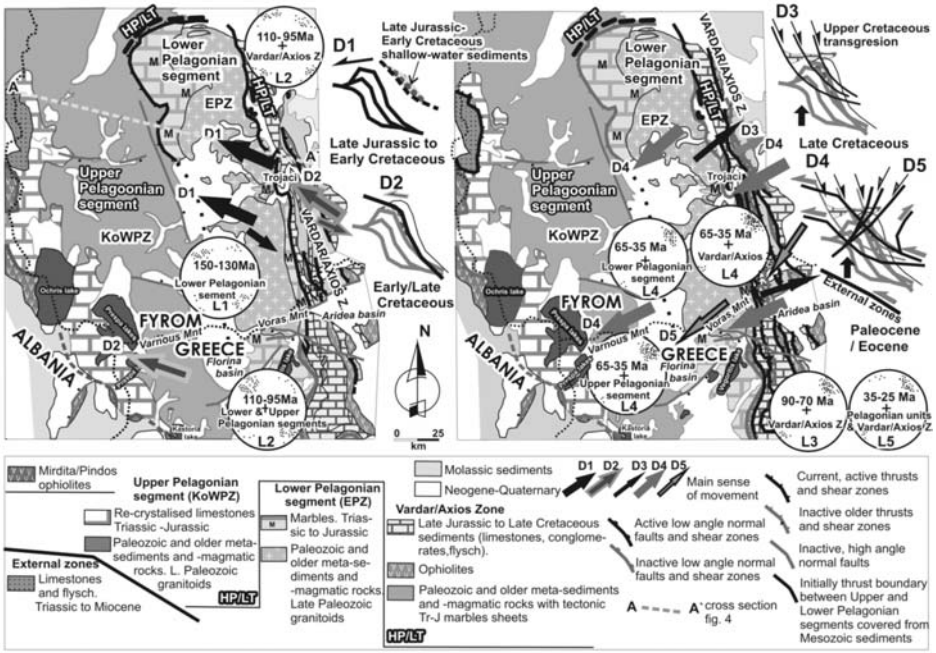

Fig. 2: Tectonic maps of the Pelagonian nape pile and the adjacent Vardar/Axios zone. The main sense of movements during the several stages of the alpine deformation is showed.

graphic data are available to document this event. D1 created a penetrative syn-metamorphic foliation (S_1) with a general NNW-SSE trend. It dips towards the WSW in the western limb of the EPZ culmination and towards the ENE in the eastern limb (Fig. 2).

B_1 folds with S_1 as axial plane foliation are scarce. Only small-scale isoclinal folds were observed (Fig. 3), sometimes also as sheath or intrafolial folds with their axis subparallel to L_1. The L_1 stretching lineation is well developed. Its trend appears not to be constant but mainly NW-SE to WNW-ESE (Fig. 3). NE-SW trending L_1 is also observed in few cases. Chloritoid, white mica, chlorite, feldspar (K-Na-feldspars and/or plagioclase), garnet, quartz ribbons, staurolite, kyanite, and green amphibole are the most common minerals defining S_1 and L_1. Static recrystallisation of quartz created polygonal fabrics and indicate post-kinematic annealing.

The main direction of movement during D_1 appears to be top-to-WNW or NW. In some places deviating directions have been found, e. g., towards SE (Fig. 3). Near Trojaci on the eastern flank of the EPZ, S-C fabrics related to D_1 indicate WNW-ward thrusting of the Paleozoic schists of the Vardar/Axios Zone (Fig. 3). K/Ar, Ar/Ar and Rb/Sr isotopic ages on syn- D_1 white mica and biotite yielded a groop of ages between 150 to 130Ma (Most et al., 2001, Most 2003). Due to attained temperatures duting metamorphism Most (2003) interpreted these ages as being close to crytalisation.

D_2 event

The S_1 foliation became affected by asymmetric, partly isoclinal or recumbent folds during the D_2 event (Fig. 3). The kilometre- scale B_2 folds are associated with small-scale chevron S- and Z- type folds. Fold axes are mainly subhorizontal or slightly plunge towards the NW or SE but in some deviate from this trend.

A pervasive S_2 foliation is axial plane with respect to the B_2 folds and forms the dominant structure of the D_2 event (Fig. 3). Crenulation of S_1 is well developed in the hinge zones of the B_2 folds. Due to intense transposition of S_1, the S_1 and S_2 planes are commonly oriented parallel or subparallel to each other. Like S_1, the S_2 foliation dips towards the SW and NE at the western and eastern limbs of the EPZ, respectively. This geometry of the S_1 and S_2 fabrics defines a clear dome structure (Fig. 1, 2).

S_2 is associated with an L_2 stretching lineation which is mainly defined by the preferred orientation of quartz, feldspar, sericite, chlorite, chloritoid, and actinolite. In the EPZ and the Loutra-Aridea unit of the Vardar/Axios Zone L_2 gently plunges towards the NW or SE. Occasionally, a NE-SW trend is oberserved, which appears to be more common in the tectonically higher metamorphic levels of the Vardar/Axios Zone, e. g., the Peternik and Livadia units, as well as in the KoWPZ (Fig. 2).

Shear sense indicators display a dominant top-to-NW or -WNW transport direction of thrusting. In some cases an opposite, top-to-SE sense of movement is observed. Top-to-SW tectonic transport is mainly recognized in the Peternik and Livadia units of the Vardar/Axios Zone (Fig.1, 2). D_2 appaers to correlate with K/Ar and Ar/Ar ages from syn- D_2 white mica between 110 to 95Ma (Koroneos et al., 1993, Most 2003).

D_3 event

D_3 structures are characterized by discrete mylonitic shear zones with dynamic recrystalisation of quartz. The S_3 mylonitic foliation in general dips to the NE and the associated well developed L_3 stretching lineation plunges downdip (Fig. 2). Shear sense indicators such as S-C fabrics, mica fish, assymetric boudins, and pressure shadows around white mica or feldspar porphyroclasts show a constant downdip (normal) sense of shear. D_3 mylonitic shear zones with opposite top-to-SW sense of shear are observed in few cases only. In contrast to the D_1 and D_2 structures, the D_3 structures show rather constant geometry and kinematics. K/Ar ages of fingrained white mica along the S_3 mylonitic fabric between 90 and 70 Ma (Koroneos et al 1993, Most 2003) report the D_3 evet.

The D_3 mylonitic shear zones are very well developed in the Paleozoic sequences of the Vardar/Axios Zone and the KoWPZ overprinting the penetrative D_2 structures. According to their geometry and kinematics we interpret the D3 mylonitic shear zones as extensional shear zones. They are probably associated with Late Cretaceous basin formation and the sedimentation of Late Cretaceous limestones and Maastrictian to Paleocene flysch. Neubauer et al., (1995) showed that Late Cretaceous extension associated with exhumation of metamorphic rocks and formation of the Gosau basin are also a prominent feature in the highest tectonic unit (the Austroalpine mega-unit) in the Eastern Alps.

D_4 event

D_4 is manifested by open to tight NW-SE trending kink folds, as well as discrete semi-ductile to brittle shear zones indicating constant top-to-SW thrusting (Fig. 2). B_4 folds are generally SW-vergent, in few cases NE-vergence is observed due to backthrusting during the D_4 event. The folds frequenty fold the D_3 shear zones. Locally the folds are associated with a weakly developed crenulation cleavage without significant recrystallization of quartz. The B_4 fold axes did not experience parallel to the transport direction but are still oriented perpendicular to the direction of thrusting as it is typical of a brittle environment of deformation. A penetrative cleavage is also missing. D_4 occurred at lower temperatures and thus in a more shallow crustal level than the previous events.

D_4 structures are mainly exposed in the Vardar/Axios Zone but also occur in the KoWPZ and the EPZ. During D_4 the metamorphic rocks of the Vardar/ Axios Zone overthrust the Maistrichtian/Paleocene flysch of the Late Cretaceous basins causing a local low grade dynamic recrystallisation of

white mica and quartz. K/Ar ages of finegrained sericite of the flysch are ranged between 65 to 50Ma (Most, 2003).

D_5 event

Brittle low angle shear zones with normal displacement are formed during the D_5 event. They cut all previous structures and juxtapose rocks of higher structural levels against rocks of lower tectonic units. Near Agios Athanasios in the Greek part of the study area the Triassic-Jurassic marbles of the EPZ are directly overlying a Late Paleozoic granite along such a shear zone, cutting out a thick metamorphic sequence of gneisses and schists. The NW contact between EPZ and KoWPZ in FYROM has been reworked by a such a D5 shear zone juxtaposing the low grade metamorphic, Paleozoic sequences of the KoWPZ against the Tr-J EPZ marbles cutting out the KoWPZ gneisses and schists (Fig. 4). Omission of several lithologic units is frequently observed along the entire contact between the EPZ marbles and the underlying units. However, the complete sequence is also preserved in some plases. Continuous sedimentation from the underlying metasediments to the Triassic EPZ carbonates is recognized in a few cases, showing the existence of a Permo-Triassic sequence. Meta-ryolites intercalations inbetween these metasediments evidence for a Permo-Triassic volcanosedimentary series under the Triassic-Jurassic EPZ marbles (Figs 1, 4).

D_5 shear zones are best recognized in granites and orthogneisses of the Pelagonian nappes as well as in the Vardar/Axios Zone rocks. They are characterized by ultracataclastic rocks. The narrow and discrete shear zones mostly dip towards the SW. Sense of shear is generally downdip (Figs 2, 3). In some cases a strike-slip sense of displacement along the fault planes is observed. For the D_5 event (normal shear zones and faults) an age between Late Eocene and beginning Miocene is suggested.

D_6 event

D_6 structures overprint all older structures and represent the final deformational stage of the orogen. They are high-angle dip-slip to oblique-slip normal and strike-slip faults related to the Neogene-Quaternary basins development in the study area (Figs 2, 4).

Many of the D_6 faults produce significant tectonostratigraphic gaps juxtaposing higher tectonic units against lower ones. As an example, the E-W to ESE-WNW trending high-angle normal faults along the southern edge of the EPZ schists and gneisses cut their marble cover and the overlying Late Cretaceous to Paleocene limestones and flysch (Fig. 2).

Some of the D_6 faults show recent activity, often associated with impressive fault escarpments as, e.g., the ca. ENE-WSW trending fault along the northern margin of the Almopias basin (Fig. 2, Pavlides et al., 1990).

3 Relationships between deformation and metamorphism

Metamorphic conditions were calculated from mineral assemblages with syn-kinematic growth with respect to the tectonometamorphic events, as well as with the Tweeq method (Bermann 1991), the garnet-biotite (Ferry and Spear 1978), the garnet-muscovite (Hynes and Forest 1988), the garnet-chlorite (Grambing 1990), the muscovite-paragonite (Blencoe et al., 1994), the chloritoid-chlorite (Vidal et al., 1999), and the chlorite (Zang and Fyfe 1995) geothermometers, and the phengite component geobarometer (Massonne and Schreyer 1987). Amphibole and biotite compositions were also used to estimate the P-T conditions (Laird et al., 1984, Schreurs 1985). Mineral chemical analyses were carried out using a JEOV 8900 Superprobe electron microprobe in the Institute of Geosciences of the University of Tübingen.

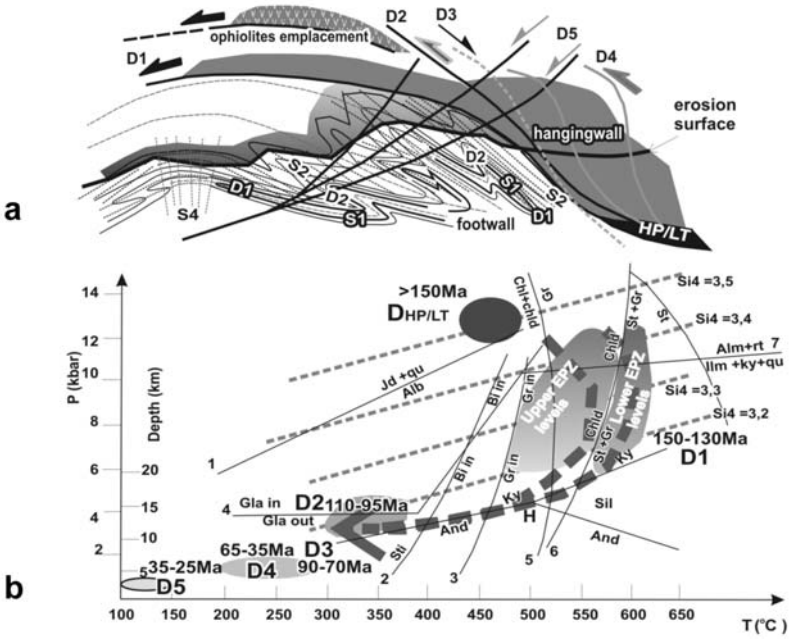

Fig. 3: a. Geometry and kinematics of deformation, b. P-T metamorphic conditions during the several stages of alpine deformation in the study area.

HP event

The occurrence of phengite, glaucophane, barroisitic hornblende, and rutile in the amphibolites, gneisses, and schists along the western, northern, and eastern tectonic boundary of the EPZ testifies to the existence of a HP event (Fig. 2,4). Sodic pyroxene has been found in the boundary zone between EPZ and Vardar/Axios Zone (Majer and Mason 1983).

Phengitic white mica with maximum 3.5 Si atoms per formula unit (apfu) from a glaucophane schist tectonically above the EPZ marble cover near Skopje (Fig. 3) indicates a minimum pressure of 12.5 kb for the D_{HP} (blueschist facies) event (phengite barometer after Massonne and Schreyer 1987), assuming a temperature of 450-500° C (Most 2003).

D_1 event

The critical syn-D_1 mineral assemblages of the EPZ domal structure used for the thermobarometric investigations are as follows. The metapelites are characterized by garnet, white mica, biotite, chlorite, chloritoid, quartz, plagioclase, ilmenite, sphene, kyanite, and epidote. Staurolite appears in the lower structural levels only. Chloritoid and rutile (as a relict HP mineral) are often included in garnet porphyroblasts showing in some cases a well-developed internal foliation. Rutile is often replaced by ilmenite. The amphibolites contain green amphibole, garnet, white mica, epidote, plagioclase, and biotite.

In the upper tectonostratigraphic levels of the EPZ the calculated temperatures range from 450° to 580° C for a pressure of 10 kb. In the lower levels the temperatures vary between 520° and 620° C for the same pressure. The pressures calculated with the Tweeq method range between 8 and 12.5 kb. The Si content of the syn-D_1 white micas varies between 3.2 and 3.4 apfu in average. This indi-

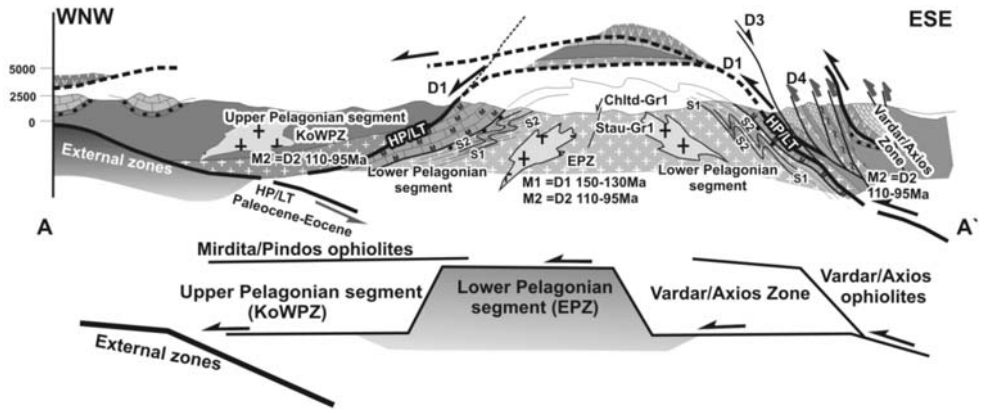

Fig. 4: Cross-section through the Pelagonian nape pile and Vardar/Axios zone.

cates minimum pressures from about 6 to 10 kb for the estimated temperatures (Fig. 3). The decreasing Si content from 3.36 to 3.1 apfu from core to rim in syn-D_1 white mica is ascribed to decreasing pressure during mineral growth.

The changing composition from core to rim of garnet porphyroblasts reflects a change in temperatures during their evolution (Spear et al., 1990). Increasing X_{Alm} and the Mg/(Mg+Fe) ratio as well as decreasing X_{Sps} suggest prograde temperature conditions. Amphibole compositions plot close to the oligoclase isograd in the diagram of Laird et al., (1984). Ti (0.03-0.06 apfu) and Al^{VI} (0.4-0.6) contents in biotite of the lower structural levels point to low to medium amphibolite facies conditions (T = 520° to 600°C) (Table II, Schreurs 1985).

D_2 event

The syn-D_1 greenschist to amphibolite facies mineral assemblages suffered retrograde, lower greenschist facies overprint during the D_2 event, especially well developed in the higher levels of the EPZ. Sericite, actinolite, chlorite, ilmenite, sphene, epidote, and quartz form the critical syn-D_2 mineral paragenesis. Replacement of D_1 minerals is observed: of biotite and garnet by chlorite and of white mica by sericite in the metapelitic rocks, as well as of hornblende by actinolite and chlorite in the amphibolites. Using the chlorite thermometer on syn-D_2 chlorites we estimated a temperature range between 280° to 380° C assuming low-pressure conditions of ca. 4-5 kb (Fig. 3).

Younger events

The low-grade metamorphic mylonites to ultramylonites belonging to the D_3 event are characterized by the dynamic recrystallization of quartz, quartz ribbons, and a strong lattice preferred orientation of quartz. Feldspar clasts may be broken and show subgrain formation. They are embedded in a dynamically recrystallized quartz and sericite matrix. A well developed S-C fabric is shown by the orientation of quartz and mica. Dynamic recrystalisation of quartz and white mica or chlorite is locally observed along the D4 thrust faults and D_5 extensional low angle shear zones and related shear bands.

4. Discussion of the geodynamic evolution - conclusions

Our detailed structural and petrological data combined with geochronological investigation concerning the northern Pelagonian nappe pile and the neighbouring VardarAxios Zone in northern

Greece and FYROM allows us to constrain the geometry and kinematics of deformation, as well as the structural evolution during the Alpine orogeny.

According to our study, the Pelagonian nappe system in northern Greece and FYROM can be divided into two distinct tectonostratigraphic segments, the footwall (EPZ) and the hangingwall (KoWPZ) Pelagonian segments. The KoWPZ is rooted between EPZ and Vardar/Axios Zone, where only intensely imbricated remnants of slices are recognized. The Paleozoic sequence and the gneisses and schists of the Vardar/Axios Zone are considered to represent the equivalents of the KoWPZ, the connection being eroded in the Pelagonian dome structure (Figs 1, 2, 4).

This scenario proves the duplication of the Pelagonian sequence due to Early Jurassic to Early Cretaceous nappe stacking towards WNW to NW (D_{HP} and D_1 event; Figs 3, 4). It can explain the described high grade metamorphism of the footwall segment of the EPZ that was overthrusted of the thick cover of the hangingwall segment of the KoWPZ. Nappe stacking was related to plate convergence and intraoceanic subduction in the Vardar/Axios Zone. Intraoceanic obduction started around 180-170 Ma (Early to Middle Jurassic) as reported by Ar/Ar dating of metamorphic soles and geologic evidence (Roddick et al., 1979, Spray and Roddick 1980, Sharp and Robertson 2006, Gawlick et al., 2008).

Radiolaritic sequences with olistolites, slides and mass flows, described as ophiolitic mélanges, are common in the thrust sheets of the Vardar/Axios and the Mirdita/Pindos Zones. They are overlain by obducted oceanic lithosphere emplaced during the nappe stacking process (Figs 1, 4, Vergely 1984, Brown and Robertson 2004, Sharp and Robertson 2006, Gawlick et al., 2008).

An important point for the reconstruction of the structural evolution of the study area are the late Late Jurassic to Early Cretaceous clastic sediments and neritic limestones transgressively overlying the ophiolites providing an upper limit for ophiolite emplacement. They indicate that the ophiolites were emplaced before the end of the Jurassic period (Figs 1, 2). D1 thrusting and metamorphism in deeper structural levels occurred almost simultaneously with the early sedimentation of this clastic sedimentary sequence, possibly with coeval crustal extension at the top of the nappe pile (Figs 1, 2, 4).

An equivalent sequence of neritic limestones and clastic sediments, the Munella series, is recognized further to the west in Albania, where it seals the Mirdita ophiolitic nappe stack (Gawlick et al., 2008). The Mirdita ophiolites overlie the Triassic-Jurassic carbonate cover of the KoWPZ (Sallo and Dilek 2003, Gawlick et al 2008) (Figs 2, 4).

Plate convergence, thrusting and closure of the Vardar/Axios ocean continued during Aptian to Albian time (ca. 110 to 95 Ma) with the same kinematics as during the D_1 event (D2 event: Figs 1, 2). Apart from the main WNW to NW-ward nappe transport the described scattering of D_1 and D_2 senses of movement may be attributed to strain partitioning and inhomogeneous deformation or to overprinting and rotation during younger tectonic events. Opposite sense of shear can also be produced due at overturned fold limbs and parasitic small-scale drag folds or by a coaxial component of strain as suggested by the occurrence of abundant symmetric structures such as symmetric boudins and symmetrically elongated clasts. SW-ward sense of movement can be explained by transpressional tectonics in an overall oblique plate convergence regime (Kilias 1991, Most 2003, Vamvaka et al., 2006).

D_1 and D_2 nappe stacking was followed by D_3 low angle normal, discrete mylonitic shear zones in Late Cretaceous time. They were associated with basin formation and sedimentation of Late Cretaceous neritic limestones and Maastrichtian to Paleocene flysch (Figs 1, 2, 3). Simultaneously with Late Cretaceous to Paleocene sedimentation on top of the tectonically upper units, thrusting in the tectonically lower and more external (more western) units took place. This thrusting process was associa-

ted with the internal high-pressure metamorphic belt (Fig. 4, Schermer 1993, Kilias et al., 1991). Schermer (1993) relates the formation of the internal HP belt to intra-continental subduction.

The doming of the present antiformal structure of the footwall Pelagonian segment (EPZ) was probably the result of D_4 shortening. D_4 is related to continuous subduction of continental crust beneath the tectonic lower part of the Pelagonian nappe and the creation of the internal HP belt in the Olympos-Ossa area (Kilias et al., 1991, Schermer 1993), on Evvia island (Xypolias et al., 2003), and in the Cyclades (Lister et al., 1984.) (Fig. 1). D_4 is also responsible for the final W- to WSW-ward emplacement of the Internal Hellenides upon the External Hellenides in Eocene-Oligocene time. This means that, from the Late Cretaceous to the Eocene there was a continuous period of deformation prograding from the tectonic top to the tectonic bottom and associated with nappe stacking and HP metamorphism.

Detailed discussion and analysis of paleogeographic settings for the evolution of one or more ocean basins in the Hellenides is outside of the aim of our study. Nevertheless, we like to point out that the suture zone between External and Internal Hellenides is free of ophiolites and all the Pelagonian nappe pile between External Hellenides and the basal ophiolite nappe is continental in origin. Futrhermore, the main NW to WNW directed thrusting during D1 and D2 events, as documented here, indicates that the ophiolitic nappes on top of the Pelagonian nappes should be rooted in the Vardar/Axios ocean basin to the east of the Pelagonian continent. Ophiolite emplacement was consistently towards the west (Figs 3, 4). All this suggests that there was no oceanic realm between External and Internal Hellenides and the Pelagonian continental block was not separated from the External Hellenides by an oceanic lithosphere during Alpine orogeny. Therefore, we do not see an independent Pindos Ocean neither in Triassic nor in Jurassic period.

The same scenario is documented in Albania, where the large Mirdita ophiolites nappes to the west of the KoWPZ are far-traveled parts of the Vardar/Axios (Neotethys) ocean, brought into its present position by W-ward thrusting (Gawlick et al., 2008).

Deformation continued during Oligocene to Early Miocene time (D_5). In higher structural levels of the Pelagonian nappes and the Vardar/Axios Zone brittle conditions prevailed and created cataclasites and ultracataclasites in low-angle extensional shear zones. Simultaneous ductile deformation with mylonites and a constant top-to-the-SW normal sense of shear associated with subhorizontal extension is reported in tectonic deeper levels of the Pelagonian nappe near its contact to the underlying External Hellenides (Kilias et al., 1991, Sfeikos et al., 1991, Schermer 1993). This process is related to Oligocene/Miocene collapse of the Pelagonian nappe pile, tectonic thinning, and unroofing and exhumation of tectonically deeper levels of the External Hellenides (e.g., Olympos-Ossa window). W- to SW-directed thrusting towards the foreland and the most external parts of the Hellenides continued during this period (Sfeikos et al., 1991, Kilias et al., 1991, Schermer 1993).

From Miocene to present time high-angle normal to oblique-normal faults (D_6) affected all units. This extensional event was responsible for the formation of the Neogene basins and steered the unroofing history of the region.

5. References

Arsovski, M. and Dumurdzanov, N., 1984. Recent findings of the structure of the Pelagonian antidinorium and its relation with the Rhodopean and Serbian Macedonian Massif. *Geologica Macedonica,* 2, 15-22.

Avgerinas, A., Kilias, A., Koroneos, A., Mountrakis, D., Frisch, W., Dunkl, I. and Most, T., 2001. Cretaceous

structural evolution of the Pelagonian crystalline in Western Voras Mt. (Macedonia, Northern Greece). *Bulletin of Geological Society of Greece*, 34, 129-136.

Berman, R.G., 1991. Thermobarometry using multiequilibrium calculations: A new technique with petrological applications. *Canadian Mineralogist,* 29, 833-855

Blencoe, J.G., Guidotti, C. V. and Sassi F.P., 1994. The paragonite-muscovite solvus: II. Numerical geothermometers for natural, quasibinary paragonitemuscovite pairs. *Geochim Cosmochim Acta*, 58, 2277-2288.

Brown, S.A.M. and Robertson, A.H.F., 2004. Evidence for the Neotethys ocean rooted in the Vardar zone: evidence from the Voras Mountains, NW Greece. *Tectonophysics*, 381, 143-173.

Catthelineau, M., 1998. Cation site occupancy in chlorites and illites as a function of temperature. *Clay Minerals* 23, 471-485.

Dinter, A.D., and Royden, L., 1993. Late Cenozoic extension in Northeastern Greece: Strymon Valley detachment and Rhodope metamorphic core complex. *Geology*, 21, 45-48.

Doutsos, T., Piper, G., Boronkay, K. and Koukouvelas, I., 1993. Kinematics of the Central Hellenides. *Tectonics*, 12, 936-953.

Ferry, J.M. and Spear, F.S., 1978. Experimental calibration of the partitioning of Fe and Mg between biotite and garnet. *Contributions to Mineralogy and Petrology*, 66, 113-117.

Gawlick, H.J., Frisch, W., Hoxha, L., Dumitrica, P., Krystyn, L., Lein, R., Missoni, S. and Schlagintweit, F., 2008. Mirdita zone ophiolites and associated sediments in Albania reveal Neothethys Ocean origin. *International Journal of Earth Sciences,* 94, 865-881.

Geleos, A., Pamoni-Papaioannou, F., Tsaila-Monopolis, S., Turneek, D. and Joakim, Chr., 1994. Upper Jurassic -Lower Cretaceous "molassic type" sedimentation in the western part of Almopia subzone, Loutra Aridea unit (Northern Greece). *Bulletin of Geological Society of Greece*, 31, 171-184.

Grambling, A.J., 1990. Internaly-consistent geothermometry and H2O barometry in metamorphic rocks: the axample garnet-chlorite-quartz. *Contributions to Mineralogy and Petrology*, 105, 617-628.

Hynes, A. and Forest, R.C., 1988. Empirical garnet-muscovite geothermometry in low-grade petapelites, Selwyn Range (Canadian Rockies). *Journal of Metamorphic Geology*, 6, 297-309.

Jacobshagen, V., Duerr, F., Kockel, K., Kopp, K.O., Kowalczyk, G., Berckhemer, H. and Buttner, D., 1978. Structure and geodynamic evolution of the Aegean region. In: H. Cloos, D. Roeder. and K. Schmidt (eds), Alps, Apennines, Hellenides. *E. Schweizerbart`sche Verlagsbuchhandlung*, Stuttgart, pp. 537-564.

Kilias, A., 1991. Transpressive Tecktonik in den zentralen Helleniden. Aenderung der Translationpfade durch die Transgression Nord-Zentral Griechenland). *Neues Jahrbuch fuer Geologie und Palaeontologie Monatshefte*, 5, 291-306.

Kilias, A., Fassulas, Ch., Priniotakis, M., Frisch, W. and Sfeikos, A., 1991. Deformation and HP/LT metamorphic conditions at the tectonic window of Kranea W. Thessaly, N. Greece). *Zeitschrift der Deutschen Geologischen Gesellschaft*, 142, 87-96.

Kilias, A., Falalakis, G. and Mountrakis, D., 1999. GretaceousTertiary structures and Kinematics of the Serbomacedonian metamorphic rocks and their relation to the exhumation of the Hellenic Hinterland Macedonia, Greece). *International Journal of Earth Sciences,* 88, 513-531.

Koroneos, A., Christofides, G., Del Moro, A., and Kilias, A., 1993. Rb-Sr geochronology and geochemical aspects of the Eastern Varnountas plutonite (NW Macedonia, Greece). *Neues Jahrbuch fuer Mineralogische Abhandlungen*, 165, 297-315.

Laird, J., Lamphere, M.A., and Albee, A.L., 1984. Distribution of Ordovician and Devonian metamorphism in mafic and pelitic schists from northern Vermont. *American Journal of Sciences,* 284, 376-413.

Lister, G.S., Banga, G. and Feenstra, A., 1984. Metamorphic core complex of Cordilleran type in the Cyclades, Aegean Sea, Greece. *Geology*, 12, 221-225.

Majer, V. and Mason, R., 1983. High pressure metamorphism between the Pelagonian Massif and Vardar Ophiolite belt, Yugoslavia. *Mineralogical Magazine*, 47, 139-141.

Massonne, H.J., and Schreyer, W., 1987. Phengite geobarometry based on the limiting assemblage with K-feldspar, phlogopite and quartz. *Contributions to Mineralogy and Petrology*, 96, 212-224.

Medwenitsch, W., 1956. Zur Geologie Vardarisch-Makedoniens (Jugoslawien), zum Problem der Pelagoniden. *Oestereichische Akademie der Wissenschaften, Sitzungsberichte der mathematisch naturwissenschaftlichen Klasse*, Abteilung 1, 165, 397-473.

Mercier, J., 1968. Etude géologique des zones Hellénides en Macèdoine centrale Grece). *Annale Géologique de Pays Hellénique*, 20, 17-92.

Most, T., 2003. Geodynamic evolution of the Eastern Pelagonian zone in Northwestern Greece and the republic of Macedonia. *PhD Thesis,* University of Tuebingen, Tuebingen, 195 pp.

Most, T., Frisch, W., Dunkl, I., Kadosa, B., Boev, B., Avgerinas A. and Kilias, A., 2001. Geochronological and structural investigation of the Northern Pelagonian crystalline zone. Constraints from K/Ar and zirkon and apatite fission track dating. *Bulletin of Geological Society of Greece*, 34, 91-95.

Mountrakis, D. 1986. The Pelagonian zone in Greece: A polyphase deformed fragment of the Cimmerian continent and its role in the geotectonic evolution of the Eastern Mediterranean. *Journal of Geology*, 94, 335-347.

Neubauer, F.,. Dallmeyer, R.D, Dunkl, I. and Schirnik, D., 1995. Late Cretaceous exhumation of the metamorphic Gleinalm dome, Eastern Alps: kinematics, cooling history and sedimentary response in a sinistral wrench corridor. *Tectonophysics*, 242, 79-98.

Pavlides, S., Mountrakis, D., Kilias, A., and Tranos, M., 1990. The role of strikeslip movements in the extensional area of the northern Aegean Greece). *Annale Tectonique*, 4, 196-211.

Rassios, A.H.E. and Moores, E.M., 2006. Heterogeneous mantle complex, crustal processes, and obduction kinematics in a unifield Pinods-Vourinos ophiolitic slab. In: A.H.F. Robertson and D. Mountrakis (eds), Tectonic Development of the Eastern Mediterranean region. *Geological Society of London, Special Publication*, 260, pp. 237-266.

Robertson, A.H.F., Dixon, J.E., Brown S. et al., 1996. Alternative tectonic models for the Late Palaeozoic – Early Tertiary development of Tethys in the Eastern Mediterranean. In: J.E. Dixon and A.H.F. Robertson (eds), The Geological Evolution of the Eastern Mediterranean. *Geological Society of London Special Publications*, 17, pp. 1-74.

Roddick, J., Cameron, W., and Smith, A.G., 1979. PermoTriassic and Jurassic ArAr ages from Greek ophiolites and associated rocks. *Nature*, 279, 788-790.

Schermer, R.E., 1993. Geometry and kinematics of continental basement deformation during the Alpine orogeny, Mt. Olympos region, Greece. *Journal of Structural Geology*, 15, 571-591.

Schreurs, J., 1985. Prograde metamorphism of metapelites garnetbiotit thermometry and prograde changes of biotite chemistry, in high grade rocks of west Unsimae, southwest Finland. *Lithos*, 18, 69-80.

Sfeikos, A., Boehringer, Ch., Frisch, W., Kilias, A. and Ratschbacher, L., 1991. Kinematics of Pelagonian nappes in the Kranea area, North Thessaly, Greece. *Bulletin of Geological Society of Greece*, 25, 101-115.

Shallo, M. and Dilek, Y., 2003. Development of the ideas on the origin of Albanian ophiolites. *Geological Society of America Bulletin, Special Publication*, 373, 351-363.

Sharp, I.R. and Robertson, A.H.F., 2006. Tectonicsedimentary evolution of the western margin of the Mesozoic Vardar Ocean: evidence from the Pelagonian and Almopias zones, northern Greece. In:

A.H.F. Robertson and D. Mountrakis (eds), Tectonic Development of the Eastern Mediterranean Region. *Geological Society of London, Special Publication*, 260, pp. 373-412.

Simpson, C. and Schmid, S.M., 1983. An evaluation of criteria to deduce the sense of movement in sheared rocks. *Geological Society of America Bulletin*, 94, 1281-1288.

Spear, F.S., Hickmott, D.D., and Selverstone, J., 1990. Metamorphic consequences of thrust emplacement. Fall Mountains, New Hampshire. *Geological Society of America Bulletin*, 102, 1344-1360.

Spray, J.G. and Roddick, J.C., 1980. Petrology and $^{40}Ar/^{39}Ar$ geochronology of some Hellenic subophiolitic metamorphic rocks. *Contributions to Mineralogy and Petrology*, 72, 43-55.

Vergely, P. 1984. Tectoniques des ophiolites dans les Hellénides Internes déformation, métamorphisms et phenomenes sédimentaires) Consequences sur l' èvolution des region Téthysiennes Occidentales. *PhD Thesis*, Universite de Paris – Sud, Orsay, 560 pp.

Vidal, O., Goffe, B., Bousquet, R., and Parra, T., 1999. Calibration and testing of an empirical chloritoid-chlorite Mg-Fe exchange thermometer and thermodynamic data for daphnite. *Journal of Metamorphic Geology*, 17, 25-39.

Xypolias, P., Kokkalas, S., and Skourlis, K., 2003. Upward extrusion and subsequent transpression as a possible mechanism for the exhumation of HP/LT rocks in Evia Island (Aegean Sea, Greece). *Journal of Geodynamics*, 35, 303-320.

Yarwood, G.A. and Dixon, J.E., 1977. Lower Gretaceous and younger thrusting in the Pelagonian rocks of the High Pieria, Greece. In: Kallergis (ed). Proceedings of the 6th colloquium on the geology of the Aegean region, Athens, pp. 269-280.

Zang, W. and Fyfe, W.S., 1995. Chloritisation of the hydrothermally altered bedrock at the Igarape Bahia gold deposit, Brazil. *Mineralium Deposita*, 30, 30-38.

Δελτίο της Ελληνικής Γεωλογικής Εταιρίας, 2010
Πρακτικά 12ου Διεθνούς Συνεδρίου
Πάτρα, Μάιος 2010

Bulletin of the Geological Society of Greece, 2010
Proceedings of the 12th International Congress
Patras, May, 2010

GEOLOGICAL AND MAGNETIC SUSCEPTIBILITY MAPPING OF MOUNT GIOUCHTA (CENTRAL CRETE)

Kokinou E.[1], Kamberis E.[2], Sarris A.[3] and Tzanaki I.[1]

[1] *Department of Natural Resources and Environment, Technological Educational Institute Crete, 3 Romanou Str. Chalepa, Chania, Crete, GR 73133 - Greece, ekokinou@chania.teicrete.gr*

[2] *Hellenic Petroleum (Exploration and Exploitation of Hydrocarbons Division), 199 Kifissias Av., 15124 Maroussi, Athens – Greece, ekamperis@hellenic-petroleum.gr*

[3] *Laboratory of Geophysical–Satellite Remote Sensing & Archaeo-environment, Institute for Mediterranean Studies, Foundation for Research and Technology—Hellas, P.O. Box 119, 74100 Rethymnon, Crete - Greece, asaris@ret.forthnet.gr*

Abstract

Giouchta Mt. is located south of Heraklion city, in Crete. It is an N-S trending morphological asymmetric ridge, with steep western slope whilst the eastern slope represents a smoother relief, composed of Mesozoic limestone and Eocene- lower Oligocene flysch sediments of the Gavrovo -Tripolis zone. The present study focuses on the geological structure of Mt. Giouchta. Field mapping and tectonic analysis is performed for this purpose. The dominant structures are contractional in nature, deformed by normal faulting related to the extensional episodes initiated in Serravallian times. The strain pattern in the area is revealed from strain analysis. It is inferred that the orientation of the stress field in the area has changed several times: the N-S, stress field which was dominant during Late Serravallian times changed to NE-SW (in Late Serravallian? - Early Tortonian) and subsequently to WNW-ESE (Early to Middle Tortonian) to become NW-SE in Late Tortonian. This orientation changed also during the Quaternary times trending from NW-SE (Early Pleistocene) to ENE-WSW (Middle Pleistocene-Holocene).

In addition to the above, surface soil samples were collected in the wider area of mount Giouchta and they were analyzed in order to determine the magnetic susceptibility. GIS techniques were used for mapping the spatial distribution of the geological features and the magnetic measurements on the topographic relief of the area. Statistical analysis techniques were also applied in order to investigate the relation of faulting and magnetic susceptibility. Maps representing the spatial distribution of the above measurements were created by using appropriate interpolation algorithms.

Key words: Gavrovo-*Tripolis zone, fault scarp, Heraklion basin, Southern Greece.*

1. Introduction

Crete is situated as an emergent high in the forearc of the subduction system of the African and the Aegean plates. The curved Hellenic outer-arc runs from the Greek mainland to the west towards the western coast of Turkey to the east. Several submarine troughs oriented perpendicular to the arc-parallel plate boundary subdivide the arc into an island chain. Crete is situated in the outermost apex of the outer-arc. The topography of Crete is characterized by a highly mountainous landscape sug-

gesting rather young and rapid uplift. A fast rise of the island is also indicated by Neogene marine deposits of Middle Miocene to early Late Pliocene age that have been uplifted up to several hundreds of meters above the present sea-level (Meulenkamp et al., 1988, 1994). A large number of surface faults underline the essential input of intense tectonic activity on both the surface itself and the landscape evolution (Bonnefont, 1971; Angelier, 1979).

The present work aimed towards a better understanding of the geological conditions in the mountainous area of Giouchta Mt. (Fig.1A) in the Archanes municipality. For this purpose a geological and tectonic survey were conducted in the summer of 2008. Surface soil samples were collected and analyzed in order to determine their magnetic susceptibility and investigate any possible correlation with the geological features. The digital terrain model, structural elements, sedimentary and geophysical data were combined in a GIS. GIS enabled not only the easy visualization of the results but it also contributed to the spatial analysis and correlation among the various geological features.

2. The study area

The study area (Fig. 1B) belongs to the Gavrovo-Tripolis zone. According to Brun (1956) and Aubuin (1959) the External Hellenides s.l. in Western Greece (Pindos, Gavrovo-Tripolis, Ionian and pre-Apulian zones), consist of a series of sub-parallel, north–south trending tectonostragraphic zones including several east–dipping thrust sheets and west verging folds. The Gavrovo-Tripolis zone represents a stable shallow carbonate dominated platform (Dercourt, 1964). The Gavrovo– Tripolis sediments include Middle Triassic to Upper Eocene limestones and Eocene to Lower Oligocene flysch (Fleury, 1980). The permanent shallow–water sediments (Late Jurassic to Latest Cretaceous) appear as a distinct unit affected by successive regressive episodes (Bernier and Fleury, 1980). According to Alexander et al. (1980) this unit structurally underlies Pindos thrust sheets.

The carbonate sequences (Fig. 2) exposed in Giouchta Mt. and located in the northern and southern part of the mountain, comprise Jurassic–Lower Cretaceous (J-K) light grey to grey black, medium bedded to massive, karstic, limestones. The dolomitization decreases from base to top. The central part of Giouchta Mt. is dominated by Upper Cretaceous (Ks.k), grey–black medium–thick bedded, bituminus and dolomitic limestones. Flysch of Upper Eocene–Oligocene belonging to the Gavrovo–Tripolis zone is detected in the northeastern flank of the mountain, comprising alterations of schists and sandstones with small layers of grey calcareous turbidites.

Fassoulas (2001) characterized Giouchtas Mt. as a horst occurred by two antithetic faults that bound the limestones. Based on the slope map presented in Figure 1C, we can further add that this mountain comprise an asymmetric anticline or tectonic horst. This is because slopes of about 80 degrees dominate in the western site of Giouchta Mt. and up to 60 degrees in the eastern part.

3. Methodology

A detailed stratigraphic and tectonic mapping was conducted in the study area (covering about 16 Km^2) in the summer of 2008. Field data was firstly correlated with the Geological map of Greece (1:50000), Epano Archanes Sheet (IGME). Tectonic analysis has been done using FP Tectonics.

Samples were collected from various areas within a depth of 0-15 cm below the surface. GPS coordinates (in EGSA 87 system) were determined at each sampling site in order to be in correlated with the available topographic data. Each of the soil samples was mixed, air-dried, disaggregated and sieved retaining the fraction smaller than 2mm in size in order to reduce the biasing effect of air, water and pebbles. Since our samples were of unknown density, mass specific measurements seemed

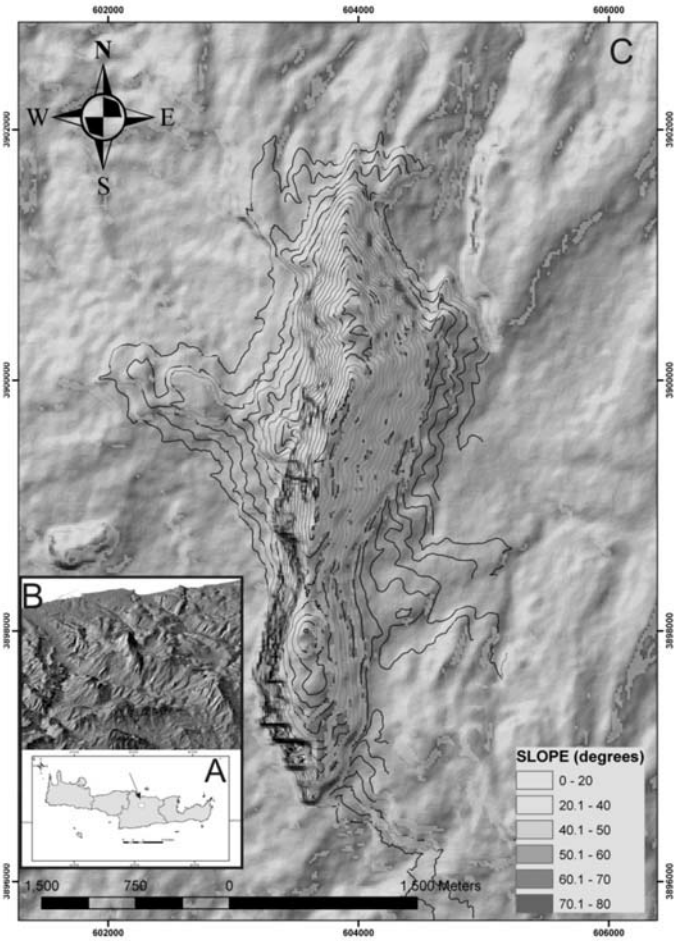

Fig. 1: (A): Location of the study area; (B): Topographic relief showing the wide area of study with the main structural features; (C): a slope map produced from 20 m digital elevation data.

to be more appropriate compared with those based on specific volume. Bartington MS2 susceptibility meter was employed for measuring magnetic susceptibility in two frequencies. A sample of 10 cm^3 tightly packed Manganese Carbonate powder ($\chi = 99.2x10^{-6}$ emu/gr) was used for calibration of the instrument. The consistency of the instrument calibration was checked by measuring the susceptibility of the calibration sample in the beginning and end of the measuring session. Samples were weighted and the subsequent susceptibility measurements in both frequencies were multiplied by a factor w_f = (10/ weight of sample) in order to normalize our measurements for a mass of 10 gr. The contribution of the plastic container was measured for 10 pieces and the average value was subtracted from all measurements.

Digitization techniques and GIS were applied for mapping representation of the data. The digital elevation model was created by the digitization of the topographic map contours (1:5000 scale maps), while the cell size of the digital elevation model was 20 m. Gridding of the magnetic susceptibility was carried out using the inverse distance weighted method. Buffer zones of variable distances were used to calculate the proximity of the particular topographic features with magnetic properties.

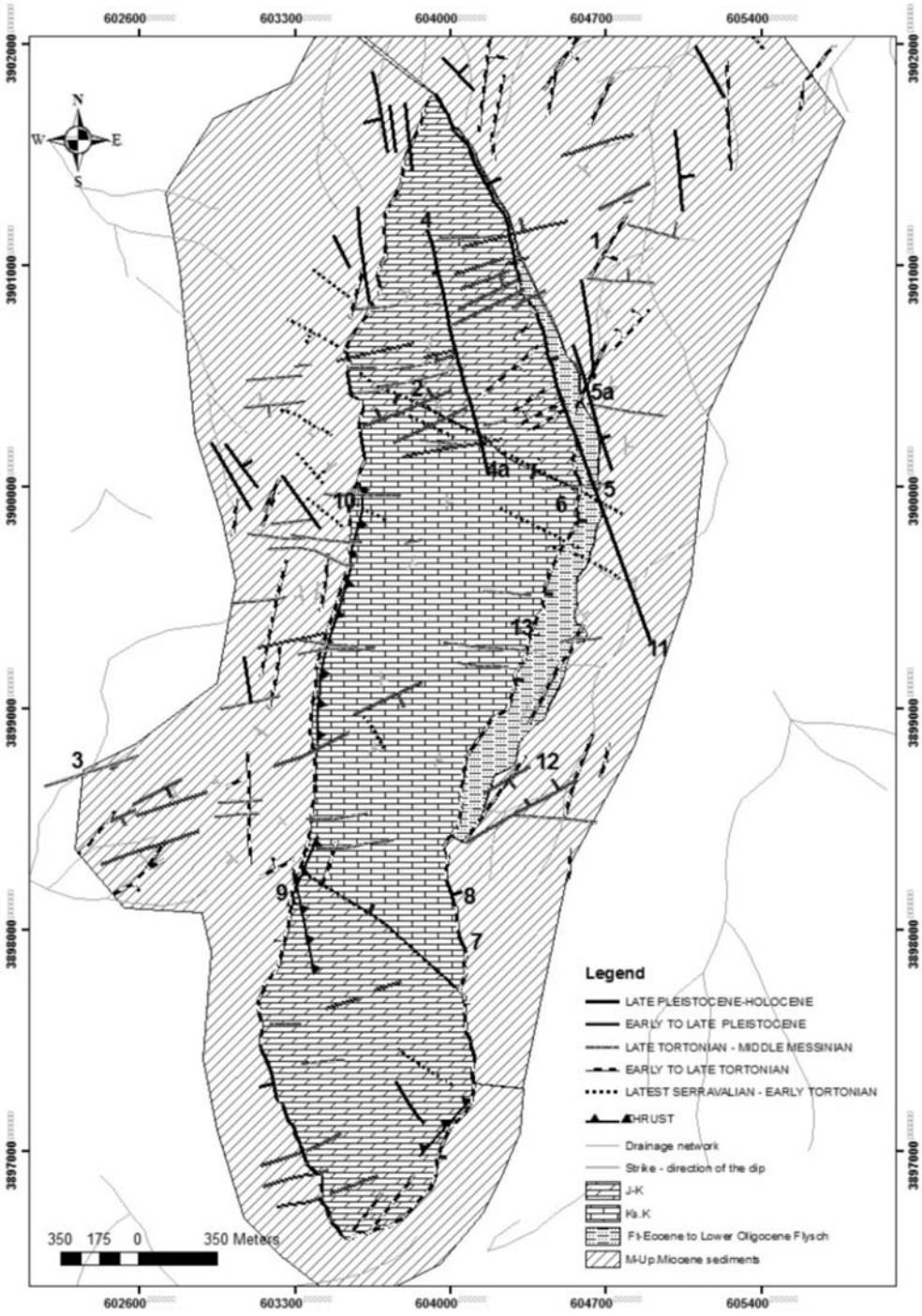

Fig. 2: Geological map of the study area. J-K: Jurassic – Lower Cretaceous limestones, Ks.K: Upper Cretaceous limestones, Ft: Eocene to Lower Oligocene Flysch, M-Up. Miocene sediments. Numbers represent locations of special interest (comments in the text).

4. Results

Structural Data

Cross-cutting relationships between the members of the different fault systems, morphotectonic features and overprinting criteria were used in order to classify, both compressional and extensional structures and related stress field patterns. According to Angelier (1979) reverse and strike slip faults on Crete are rare, small and caused by brief compressional events. In this study compressional structures recorded in J-K present the NE-SW trending general strike of the alpine deformation (southeastern flank of Giouchta Mt), resulting from the NW trending stress field (Figs. 2, 3). Another contraction structure, located in the western flank of Giouchta Mt., witnesses a reverse movement in the Middle (?) - Late Serravallian (about 13.0 Ma) (Figs. 2, 3). This structure might be related to contraction tectonics inferred by Benda et al. (1974) for the eastern Mediterranean and Crete. The above-mentioned stress fields and the related compressional tectonics are also supported by other authors and might be associated to the crustal thickening continued on Crete probably until some weakly-defined time in the middle Miocene (e.g. Mercier et al., 1989; Jolivet et al., 1994, 1996; ten Veen and Postma, 1999). Giouchta Mt. demonstrates a contraction feature (asymmetric anticline) related to the above-mentioned stress fields (Fig. 3). Following the contraction tectonics successive, distinct, extensional episodes took place creating six fault generations considered herein.

Normal fault systems are indicated in Giouchta Mt, i.e. Late Serravallian, Latest Serravallian (?) to Early Tortonian, Early to Middle Tortonian, Late Tortonian, Early Pleistocene and finally Middle Pleistocene to Recent, depicting the above-mentioned tectonic episodes. The results of the tectonic fault plain analysis, the fault strike classification and the correlation to similar studies in the central and eastern Crete, are shown in detail in Figure 3.

The first group includes, roughly E-W trending, in the order km-scale faults active until Late Serravallian times (Fig. 2). Angelier (1979) supported that large normal block faulting probably became in Serravallian times. Fault surfaces and kinematical indicators of these faults are not well preserved. However, overprinting relationships (based on fault intersections and stratigraphic boundaries) indicate that might correspond to the group "A" (Fig. 3, column 3) determined in the central and the eastern part of Crete by Benda et al., (1974), Meulenkamp et al., (1979), Frydas et al., (1998), ten Veen and Postma, (1999).

The second group, belonging to the N120E (to N140E) trending in the order of km-scale faults, presents high angle surfaces and normal dip slip component. These faults mainly cut the older, preneogene and neogene rocks (Fig. 2, Location 10). However, tectonic movements on some fault surfaces may indicate that the corresponding episode started earlier, probably at the Latest Serravallian times. All these faults are intersected by N20-28E fault (Fig. 2, Locations 1, 5, 7) observed in abundance (ten Veen and Postma, 1999) in central Crete at the eastern side of Ida Mountains. Tectonic status at the location (10) corresponds to N222^o extension which is similar to the Earliest Tortonian episode referred by ten Veen and Postma (1999).

The third and the fourth group belong to the N00E-N020E and to the N030-40E trending faults, respectively. Both groups show generally high angle surfaces (70-80^o), except a small number of faults belonging to fourth group that show medium (50-60^o) and normal dip slip component. The differentiation between the two groups is mainly based on the stress field (σ_3 = 97^o to 123^o). These members deformed the older generations of faults (Fig. 2, Locations 1, 8, 9, 10) and are mainly related to the Middle and the Late Tortonian tectonic activity. At this point we have to refer that strike slip motion (Fig. 3) has also been indicated in two members of the third group. Similar strike slip mo-

tion has been reported by ten Veen and Postma (1999) in the same period. These authors referred that the Late Tortonian to Early Messinian episode is marked by important tectonics, related to the beginning of N075E-orientated oblique slip. Faults, belonging to the N020E trending system, are bounding the Giouchta Mt. (Fig. 2, Locations 8, 9) as it is also inferred by Fassoulas (2001). At the location (7) N10-20E fault postdates the older N110-112E trending structure while it is cut by a N160-165E fault (Fig. 2, location 6). It is also noteworthy, that ten Veen and Postma (1999) referred the strong vertical fault movement along N020E, including the Sitia Fault Zone, Ierapetra Fault Zone and the W Dikti Fault Zone.

The reactivation of normal faulting along the older, roughly E-W trending, extensional structures, during Early Messinian, characterized by a roughly dip slip component (close to the locations 2 and 10 in Fig. 2) is also supported by this work.

The fifth group of extensional structures includes the N040E to N060E trending faults showing high angle surfaces and normal dip slip component (Fig. 2, Locations 5, 12). These are moderate-scale NE-SW striking faults (Figure 3, column ¨3¨) associated with the Pleistocene to recent times tectonic activity. At the location (12) in Figure 2, N050E trending faults formed small graben. However, the dextral lateral motion, referred by ten Veen and Postma (1999) for similar structures in the central and the eastern Crete, is not observed in this area.

The sixth group includes the youngest members, belonging to the N160E - N180E trending faults (Fig. 2, locations 4-4a, 5, 7, 8, 11). They present high angle surfaces and normal dip slip component, too. Especially, at the locations (5) and (5a) part of the flysch is trapped between two similar faults with significant vertical throw. Faults belonging to the N160E group intersect all the above-mentioned faults and are probably associated to the radial extension dominating in the southern Aegean area (Angelier, 1982). This group is also indicated in adjacent areas covered by Holocene sediments. Armijo et al. (1982) and Lyon-Caen et al. (1988), however, stated that at present Peloponnesus and Crete are dominated by approximately E-W extension and dip-slip movements along approximately N-S orientated faults. Our work field data is in agreement with this. However, the last two groups could be equivalents to the episode “E” shown in Figure 3.

Moreover, we have no data, concerning the Late Miocene (Messinian) and Early Pliocene times extensional stress patterns, as no outcrops, dated at these time-periods, are present in the study area. Some data about the above-mentioned periods and related extensional stress fields, varying from WNW- ESE to ENE-WSW are indicating in the Figure 3 from adjacent areas (Axos - Anogia basin, paper under preparation).

Additionally, it is noted that our data are also in agreement with kinematics and structural data from the tectonic windows of eastern Crete and Dodecanese Islands (Kokkalas and Doutsos, 2004).

Magnetic Data

Figures 4a,b show the distribution of the mean low frequency measured magnetic susceptibility (LF), mean high frequency measured magnetic susceptibility (HF) and frequency dependent susceptibility (FD) in relation to normal faulting age. Low and high frequency magnetic properties are proportional and correspond to relative greater values for the Latest Serravalian – Early Tortonian faults. The frequency dependent susceptibility shows an inverse proportional relation to the fault age, except for the Early to Late Tortonian faults. At this point we have to refer that the Late Tortonian-Middle Messinian group corresponds to reactivation along the older, roughly E-W trending, extensional structures. The distribution of the low frequency and frequency dependent magnetic susceptibility is shown in the maps of Figures 6 and

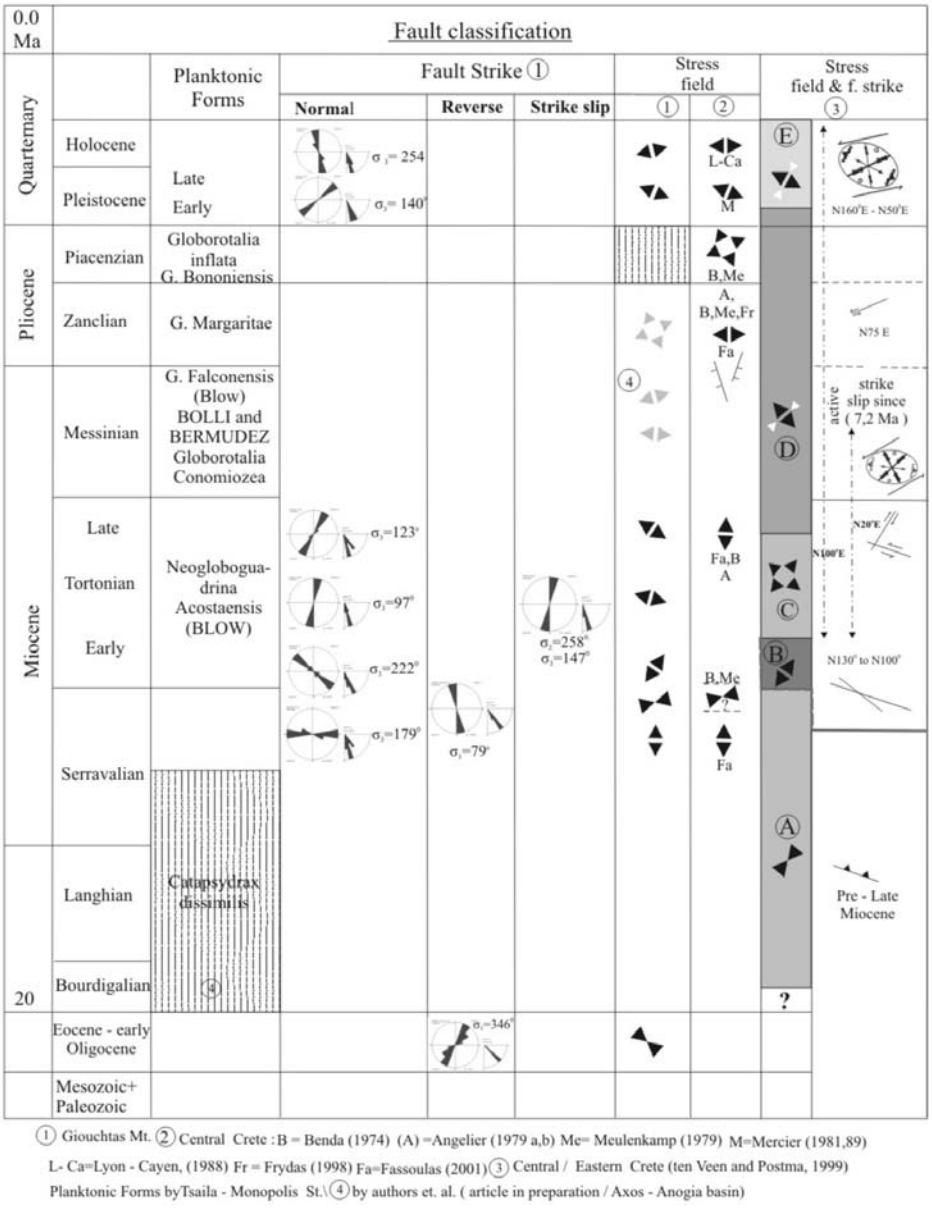

Fig. 3: Fault classification in Giouchta Mt.

7. Relatively high values of the low frequency susceptibility observed in the whole area, demonstrating that the stratigraphy of the study area consists of Miocene sediments and Jurassic-Cretacoeus limestone. It has to be mentioned that at least two regions located in the top of Giouchta Mt. have been recognized as being functioned as sacred places in the ancient times and the corresponding intense anthropogenic activity influenced the distribution of magnetic susceptibility in the corresponding areas. A good correlation between faulting strike and LF as well FD magnetic susceptibility is generally observed (Fig. 5).

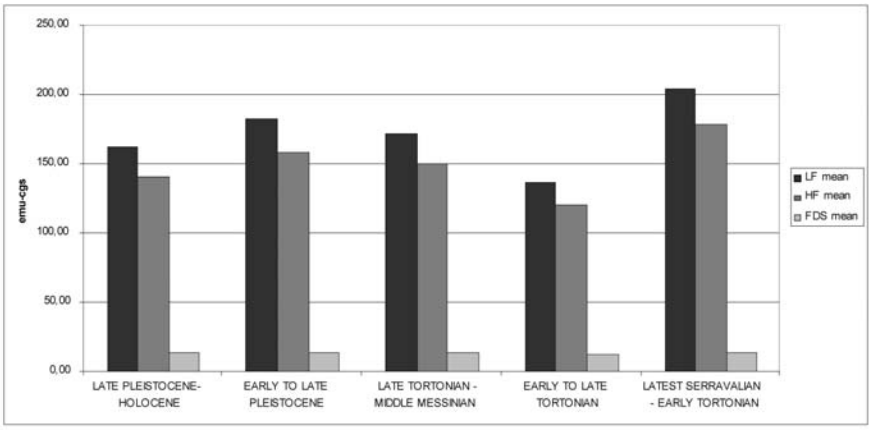

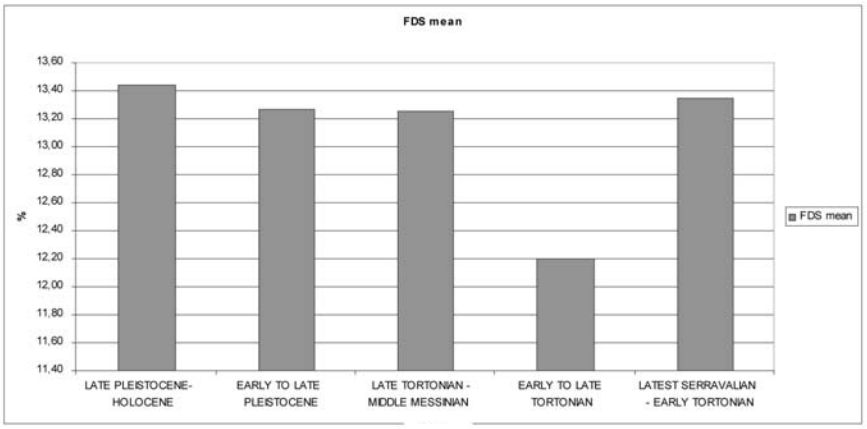

Fig. 4: Classification of the faults in relation to stratigraphy, mean of the magnetic properties, frequency dependent susceptibility.

5. Conclusions

Giouchta Mt. is an example of a pre-existing contraction structure that was deformed in later stages by normal faulting, produced by extensional episodes from latest Serravallian to sub recent times. These episodes indicate stress fields that influenced the area, with N-S trending direction in Late Serravallian times, via NE-SW in Latest Serravallian (?)-Early Tortonian, to WNW-ESE during Early to Middle Tortonian. The stress field changed to NW-SE in Late Tortonian to Early Pleistocene times and finally to ENE-WSW in Middle Pleistocene to sub recent time-period.

Moreover, the reactivation of normal faulting along the older, roughly E-W trending, extensional structures, during Early Messinian, is characterized by a dip slip component. Finally, strain direction changes to ENE-WSW during Middle Pleistocene to Holocene times.

Magnetic susceptibility is proved to be a useful tool for fault zone characterization. As a future work we plan to carry out thermomagnetic runs in air to the surface samples as well palaeomagnetic analyses in cores from holes dug deeply below the weathered crust.

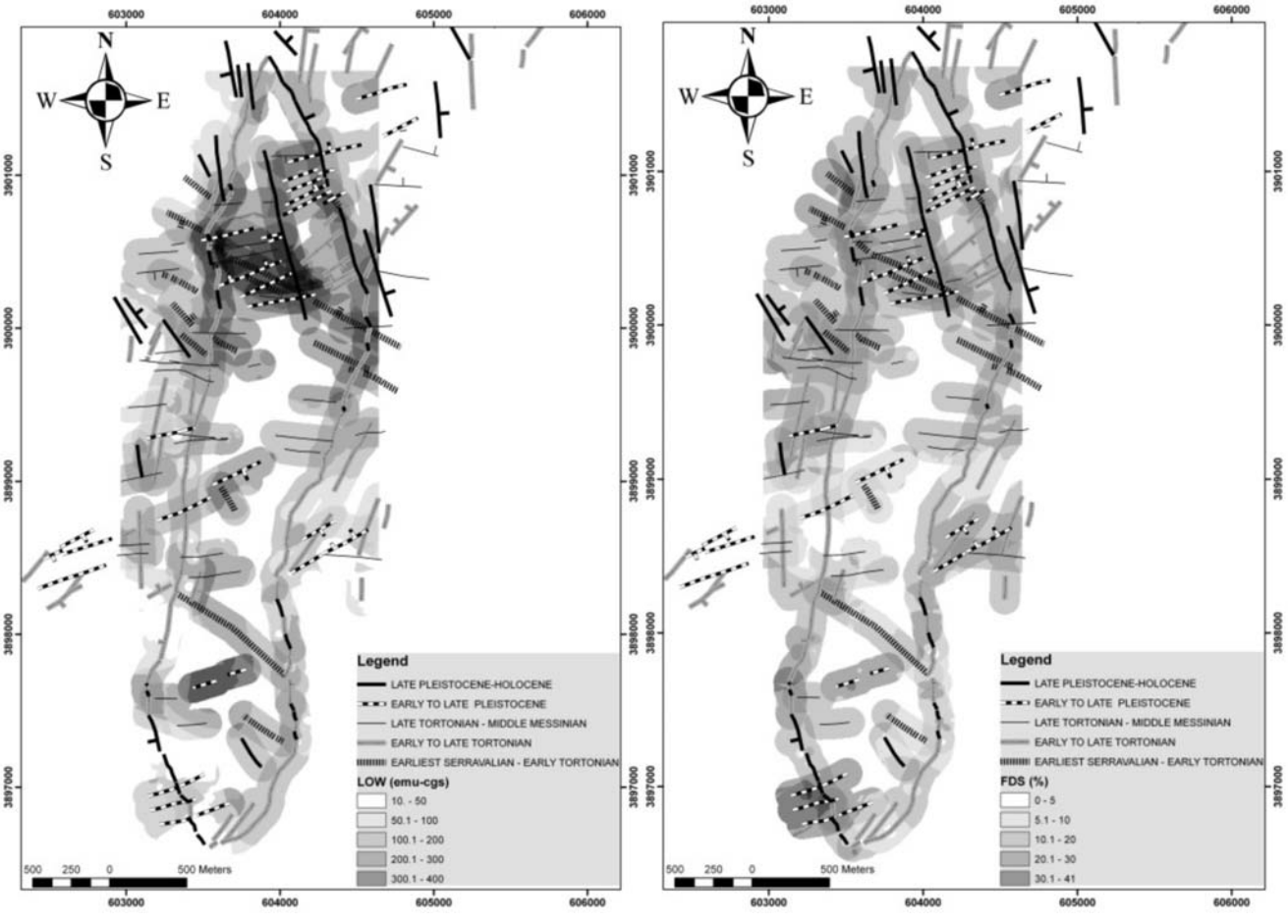

Fig. 5: Distribution of the low frequency (left) and frequency dependent (right) susceptibility in relation to faulting.

6. References

Alexander, J., Nichols, E.G. & Leigh, S. 1990. The origins of marine conglomerate in the Indus foreland basin, Greece. *Sed. Geol*, 66, 243-254.

Angelier, J., 1979. Néotectonique de L'arc Egaen. *Soc. Geol. Nord*, Spec. Publ., 3.

Aubouin, J., 1959. Contribution a l'étude géologique de la Grèce septentrionale: le confins de l'Epire et de la Thessalie. *Ann. Geol. Pays Hellen.*, 10, 1-484.

Armijo, R., Lyon-Caen, H., Papanastassiou, D., 1982. East-west extension and Holocene normal fault – scarps in the Hellenic arc. *Geology*, 20, 491-494.

Benda, L., Meulenkamp, J.E., Zachariasse, W.J., 1974. Biostratigraphic correlations in the Eastern Mediterranean Neogene. 1. Correlation between planktonic foraminiferal, uvigerinid, sporomorphal and mammal zonations of the Cretan and Italian Neogene. *Newsl. Stratigr.*, 3, 205–217.

Bonnefont, J.C., 1977. La néotectonique et sa traduction dans le paysage géomorphologique de l'Ile de Crete (Gre`ce). *Rev. Gjogr. Phys. Gjol. Dyn.*, 14, 93–108.

Brunn, J-H., 1956. Contribution a l'étude géologique du Pinde et d' une partie de la Macédoine occidentale. *Ann. Geol. Pays. Hellen.*, 13, 1-446.

Dercourt, J., 1964. Contribution a l'étude géologique d' un secteur du Péloponnèse occidental. *Ann. Geol. Pays. Hellen.*, 15, 1-418.

Fassoulas, C., 2001. The tectonic development of a Neogene basin at the leading edge of the active European margin: the Heraklion basin, Crete, Greece. *J. Geodyn.*, 31, 49-70.

Fleury, J., 1980. Les zones de Gavrovo - Tripolitsa et du Pinde - Olonos (Grèce continentale et Pèloponnése du Nord). Évolution d'une plateforme et d'un bassin dans leur carde alpin. *Soc. Géol. Nord*, 4, 1-651. Frydas, D. 1998. Plankton-Stratigraphie des Pliozans und unteren Pleistozans des SW-Peloponnes, Griechenland. *Newsletters on Stratigraphy*, 23, 91–108.

Geological map of Greece (1:50000), Epano Archanes sheet, IGME.

Kokkalas, S. and Doutsos, T., 2004. Kinematics and strain partitioning in the southeast Hellenides (Greece). *Geol. J.*, 39, 121-140.

Lyon-Caen, H., Armijo, R., Drakapoulos, J., Baskoutas, J., Delibassis, N., Gaulon, R., Kouskouna, V., Latoussakis, J., Makropoulos, K., Papadimitrou, P., Papanastassiou, D., Pedotti, G., 1988. The 1986 Kalamata (south Peloponnesus) earthquake: detailed study of a normal fault, evidences for east–west extension in the Hellenic arc. *J. Geophys. Res.*, 93, 14967–15000.

Mercier, J.L., 1981. Extensional-compressional tectonics associated with the Aegean Arc: comparison with the Andean Cordillera of south Peru – north Bolivia. *Phil. Trans. R. Soc. London*, A, 300, 337–355.

Mercier, J.L., Sorel, D., Vergely, P., Simeakis, K., 1989. Extensional tectonic regimes in the Aegean basins during the Cenozoic. *Basin Res.*, 2, 49–71.

Meulenkamp, J.E., 1979. Field guide to the Neogene of Crete. *Publishers. Dept. Geol. Pal. University of Athens*, ser. A, 32, 1–31.

Meulenkamp, J.E., Wortel, M.J.R., Van Wamel, W.A., Spakman, W., Hoogerduyn Straating, N.E., 1988. On the Hellenic subduction zone and the geodynamic evolution of Crete since the late Middle Miocene. *Tectonophysics*, 146, 203–215.

Meulenkamp, J.E.,Van Der Zwaan, G.J., Van Wamel, W.A., 1994. On Late Miocene to Recent vertical motions in the Cretan segment of the Hellenic arc. *Tectonophysics*, 234, 53–72.

Ten Veen, J.H. and Postma, G., 1999. Neogene tectonics and basin fill patterns in the Hellenic outer-arc (Crete, Greece). *Basin Research*, 11, 223–241.

Δελτίο της Ελληνικής Γεωλογικής Εταιρίας, 2010
Πρακτικά 12ου Διεθνούς Συνεδρίου
Πάτρα, Μάιος 2010

Bulletin of the Geological Society of Greece, 2010
Proceedings of the 12th International Congress
Patras, May, 2010

CENOZOIC TECTONIC EVOLUTION OF THE EASTERN ALPS – A RECONSTRUCTION BASED ON $^{40}AR/^{39}AR$ WHITE MICA, ZIRCON AND APATITE FISSION TRACK, AND APATITE (U/Th)-He THERMOCHRONOLOGY

Kurz W.[1], Wölfler A.[1] and Handler R.[2]

[1] *University of Graz, Institute of Earth Sciences, Heinrichstrasse 26,A- 8010 Graz, Austria, walter.kurz@uni-graz. andreas.woelfler@uni-graz.at*

[2] *Institut für Geologie und Paläontologie, Universität Salzburg, Hellbrunner Strasse 34, A - 5020 Salzburg, Austria. present address: forstinger + stadlmann ZT-OEG, Achenpromenade 14, A-5081 Anif, Austria, ro-handler@gmx.at*

Abstract

The Cenozoic tectonic evolution of the Eastern Alps is defined by nappe assembly within the Penninic and Subpenninic units and their subsequent exhumation. The units above, however, are affected by extension and related faulting. By applying distinct thermochronological methods with closure temperatures ranging from ~450° to ~40°C we reveal the thermochronological evolution of the eastern part of the Eastern Alps. $^{40}Ar/^{39}Ar$ dating on white mica, zircon and apatite fission track, and apatite U/Th-He thermochronology were carried out within distinct tectonic units (Penninic vs. Austroalpine) and on host rocks and fault- related rocks (cataclasites and fault gouges) along major fault zones. We use particularly the ability of fission tracks to record the thermal history as a measure of heat transfer in fault zones, causing measurable changes of fission track ages and track lengths. Additionally, these studies will provide a general cooling and exhumation history of fault zones and adjacentcrustal blocks.

Key words: *thermochronology, Eastern Alps, Penninic, Austroalpine, Tauern Window, Koralm, faulting.*

1. Introduction

The Cenozoic evolution of the Eastern Alps (Fig. 1) is mainly characterized by the continent-continent collision between the European lower plate in the north and the Adriatic upper plate in the south, subsequent to the consumption of Penninic oceanic domains (for summary, see Neubauer et al., 2000; Schuster and Kurz, 2005). While the external parts of the European plate were deeply subducted and affected by the detachment of crustal slices and nappe stacking (e.g., Kurz et al., 1996; Schmid et al., 2004; Froitzheim et al., 2008), most parts of the Adria- derived units, termed as Australpine and Southalpine, were almost completely exhumed and therefore close to the surface (e.g., Hejl, 1997; Pischinger et al., 2008).

During Cenozoic times the Eastern Alps are therefore characterized by a contrasting evolution of the lower plate units, i.e. the subduction of Penninic and Subpenninic units and their subsequent exhumation (e.g. Kurz and Froitzheim, 2002; Kurz, 2005, 2006) and upper plate units mainly affected by brittle faulting during orogen-parallel escape tectonics (lateral extrusion) (Ratschbacher et al., 1991; Frisch et al., 1998, 2000).

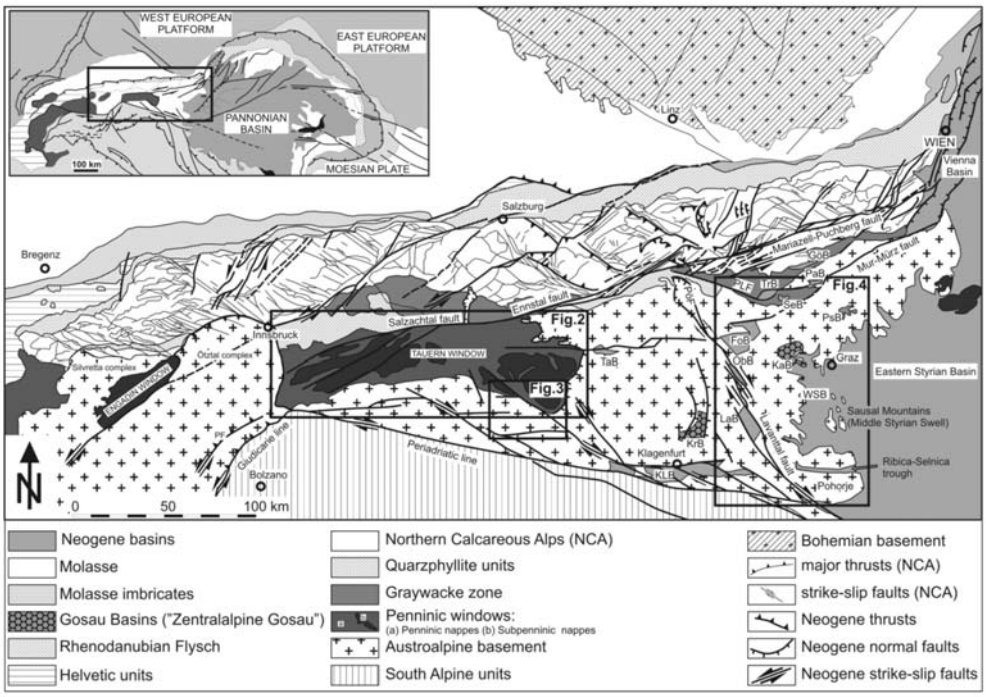

Fig. 1: Tectonic map of the Eastern Alps displaying major and minor Paleogene to Neogene fault systems (after Linzer et al., 2002). PLF = Palten – Liesing fault; PöF = Pöls fault; GöT = Göriach Basin; PaT = Parschlug Basin; SeT = Seegraben Basin; FoT = Fohnsdorf Basin; ObT = Obdach Basin; LaT = Lavanttal Basin; TaT = Tamsweg Basin; TrT = Trofaiach Basin; WSB = Western Styrian Basin; KrT = Krappfeld Gosau Basin; KaT = Kainach Gosau Basin.

By applying distinct thermochronological methods with closure temperatures ranging from ~450° to ~40°C ($^{40}Ar/^{39}Ar$ dating on white mica, zircon and apatite fission track (ZFT, AFT), and apatite U/Th-He) we reveal the thermochronological evolution of distinct tectonic units of the Eastern Alps and provide the reconstruction of their tectonic evolution during Cenozoic times.

2. Geological setting

The Alps (Fig. 1) are the result of the still ongoing convergence between Africa and Europe. Plate tectonic units involved in the Alpine orogen are the European continent, two partly oceanic basins in the Penninic realm, and the Apulian (Adriatic) microcontinent including the Austroalpine and Southalpine units. In the area of the Eastern Alps (Fig. 1) the European continent is represented by the Helvetic Nappes. The European margin is represented by the Subpenninic nappes (in the Tauern Window these are the Venediger Nappe, Eclogite Zone, and Rote Wand – Modereck Nappe) (Fig. 2). Two partly oceanic basins in the Penninic realm (the Northpenninic Valais and the Southpenninic Piemont-Liguria) are represented by the Rhenodanubian Flysch, the Glockner Nappe, the Matrei Zone and the Klammkalk Zone.) The Adriatic (Apulian) microcontinent comprises the Austroalpine and Southalpine units (for review, see Schmid et al., 2004; Froitzheim et al., 2008).

In a geographical sense the Alps are divided into the E-W-trending Eastern Alps (Fig. 1), the Central Alps, and the arc of the Western Alps. Eastern, Central and Western Alps are characterized by a fun-

damentally different geological structure, geological evolution and, in part, a distinct geomorphology. East of the Tauern Window (Figs. 1, 2), the topography gradually changes from high elevations into the Neogene Styrian and Pannonian basin plains (Fig. 1) of a very low elevation above sea level.

The structure of the Eastern Alps is characterized by a system of fault zones (Fig. 1) that developed during late Oligocene to Miocene times. This fault system is related to orogen-parallel escape of Austroalpine units towards east, a process also termed as lateral extrusion (Ratschbacher et al., 1991). In the Eastern Alps this type of escape tectonics resulted in the final exhumation of Penninic and Subpenninic units within distinct tectonic windows (e.g., the Tauern and the Engadine Window) (Fig. 1), and in the subsidence of sedimentary basins along the eastern margin of the Eastern Alps (Styrian Basin) (Fig. 1) and along extrusion-related strike slip faults (Fig. 1) (Decker et al., 1993; Decker and Peresson, 1996). The latter mainly developed as pull-apart basins filled with intramontane molasse deposits. Time constraints on fault activity are mainly defined by the sedimentary deposits along these faults. Sedimentation within the intramontane molasse basins started around 18 Ma (e.g., Sachsenhofer et al., 2000). Another time constraint is given by the exhumation and cooling ages of Penninic and Subpenninic units in the Tauern Window, indicating that lateral extrusion started around 23.5 Ma (Frisch et al., 2000). Geochronological data from extrusion- related fault zones are rare and are only available from exhumed mylonitic shear zones in the vicinity of the Tauern Window (Müller et al., 2000, 2001; Mancktelow et al., 2001). Ages from pseudotachylites in the southwestern part of the Eastern Alps indicate a period of enhanced extrusion-related fault activity between 22 and 16 Ma (Mancktelow et al., 2001; Müller et al., 2001). Farther east, however, only the upper crustal sections affected by cataclastic deformation mechanisms are exposed.

Although the existing data indicate that the main part of orogen- parallel extension occurred during Early to Middle Miocene times (Frisch et al., 2000), seismic events along most of the extrusion- related faults indicate that these are still active (e.g., Reinecker and Lenhardt, 1999; Reinecker, 2000; Lenhardt et al., 2007; Frost et al., 2009) and that a certain amount of displacement should have proceeded from post- Middle Miocene to Recent times.

3. Study areas

In this study we present geochronological ages from: (1) The Subpenninic Eclogite Zone and Rote Wand-Modereck Nappe (Fig. 2) in order to constrain the timing of subduction of the southern European margin and its subsequent exhumation; (2) The southeastern margin of the Tauern Window (Fig. 3) in order to constrain the timing of exhumation of Penninic and Subpenninic units during the formation of the Tauern Window, the timing of faulting along its margins, and the thermochronological evolution of adjacent Austroalpine (upper plate) units; (3) the temporal evolution of the Lavanttal Fault Zone (LFZ) (Fig. 4), being related to the Miocene tectonic evolution of the Eastern Alps. These data provide important information on geochronological dating of faulting and the exhumation and uplift of adjacent Austroalpine basement blocks.

4. Geochronological data from the study areas

4.1 Subpenninic nappes (Tauern Window)

Radiometric $^{40}Ar/^{39}Ar$ ages from the Subpenninic nappes (Eclogite Zone and Rote Wand – Modereck Nappe) (Fig. 2) show that phengites formed under eclogite-facies metamorphic conditions retain their initial isotopic signature, even when associated lithologies were overprinted by greenschist- to amphibolite-facies metamorphism. Different stages of the eclogite-facies evolution can be dated.

An age of 39 Ma from the Rote Wand – Modereck Nappe is interpreted to be close to the burial age of

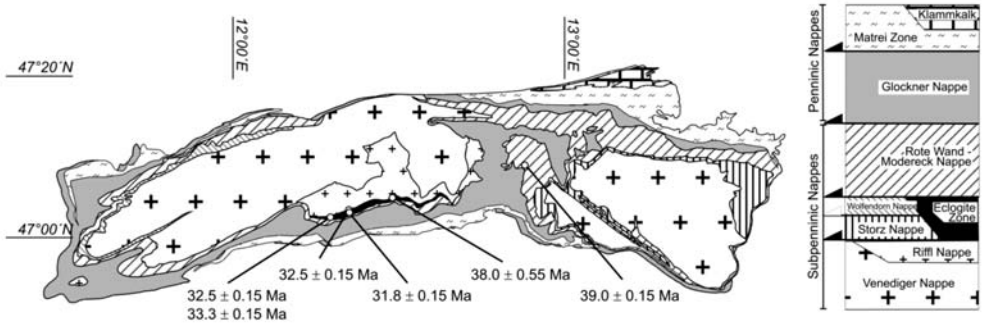

Fig. 2: Tectonic sketch map of the Tauern Window $^{40}Ar/^{39}Ar$- ages and sample locations (after Kurz et al., 2008).

this unit. Eclogite deformation within the Eclogite Zone started at the pressure peak along distinct shear zones, and prevailed along the exhumation path. Ages of *ca*. 38 Ma are only observed for eclogites not affected by subsequent deformation and are interpreted as maximum ages due to the possible influence of homogenously distributed excess argon. During exhumation deformation was localized along distinct mylonitic shear zones. This stage is mainly characterized by the formation of dynamically recrystallized omphacite and phengite. Deformation resulted in the resetting of the Ar isotopic system within the recrystallized white mica. Flat argon release spectra showing ages of 32 Ma within mylonites record the timing of cooling along the exhumation path, and the emplacement onto the Venediger Nappe (European margin). From the pressure peak onwards (*ca*. 25 kbar), eclogitic conditions therfore prevailed for almost 8-10 Ma. Ar-release patterns and $^{36}Ar/^{40}Ar$ vs. $^{39}Ar/^{40}Ar$ isotope correlation analyses indicate no significant ^{40}Ar-loss after initial closure, and only a negligible incorporation of excess argon.

4.2 Southeastern margin of the Tauern Window

Four steep elevation profiles were investigated by zircon and apatite fission track and apatite (U-Th)/He dating, two in the Austroalpine unit and one each in the Subpenninic Hochalm and Sonnblick dome (Fig. 3).

Austroalpine basement units: The Kreuzeck block south of the Polinik fault yields systematically higher ages than the Polinik block north of the Polinik fault (Fig. 3). Two micaschist samples derived from the southernmost part of the Kreuzeck block yield higher ZFT ages (106.7 ± 8.5 and 103.1 ± 7.7 Ma) than previously recognized in this area. These ages are conform to the peak of Eo-Alpine metamorphism in Late Cretaceous times. In the northern part ZFT ages range between 67.8 ± 3.8 and 64.8 ± 3.5 Ma (Fig. 3). AFT ages range from 27.4 ± 2.3 to 19.6 ± 1.6 Ma with a positive relation between age and elevation. The mean track lengths for two apatite samples are 13.3 and 13.6 μm. Cooling rates as determined from zircon/apatite pairs and thermal history modeling demonstrate slow cooling in the order of ~4 °C/Ma between Late Cretaceous and Early Miocene time.

The two ZFT ages from the Polinik block are 39.1 ± 2.3 and 30 ± 1.8 Ma. AFT ages are systematically younger than those from the Kreuzeck block (between 19.4 ± 1.3 and 7.3 ± 0.9 Ma). The unimodal track length distribution indicates a single period of rapid cooling. Apatite (U-Th)/He ages are younger than the apatite fission track ages. The ages vary systematically with elevation.

Tauern Window: ZFT ages from the southeastern Tauern Window are rather uniform and range between 21.5 and 16.3 Ma. AFT ages of both domes show positive age-elevation correlation between 10.6 ± 0.9 and 7.8 ± 0.6 for the Sonnblick dome and 15.2 ± 1.3 and 7.4 ± 0.5 for the Hochalm dome.

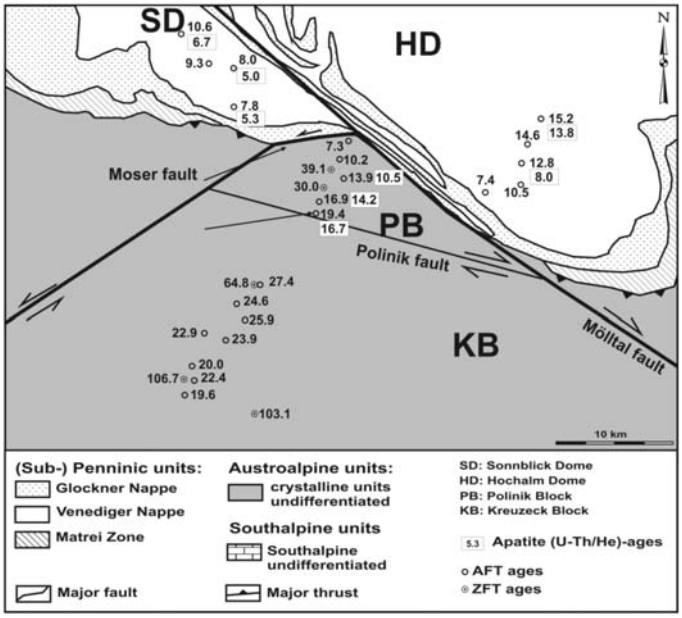

Fig. 3: Fission track (zircon, apatite) and (U-Th)/He ages in Ma from the southeastern Tauern Window and adjacent units (after Wölfler et al., 2008).

The mean track lengths are 14.4 μm and 14.5 μm indicating rapid cooling through the apatite partial annealing zone. Apatite (U-Th)/He ages from the Sonnblick dome range from 6.7 ± 0.4 to 5.0 ± 0.4 and are systematically younger than those from the Hochalm (13.8 ± 1.5 and 8.0 ± 1.1 Ma) (Fig. 3). Both He age sets show positive correlation with elevation. Mean Dpar (mean diameters of etch figures on prismatic surfaces of apatites parallel to the crystallographic c-axis)values of all analyzed samples range from 1.62 to 1.99 μm. They show no variation between different tectonic units and thus indicate uniform chemical composition of the apatite grains.

Within Austroalpine units thermal history modeling reveals tT paths characterized by slow cooling through Late Crateceous and Paleogene time until the Early Miocene, when the region was already near to the surface. In contrast, thermal modeling of the Polinik block demonstrates onset of rapid cooling around 20 Ma, followed by modest decrease in temperature from 12 Ma onwards.

In the Tauern Window the combination of AFT and (U-Th)/He data with ZFT ages from Dunkl et al. (2003) revealed a rapid cooling history (35 °C/Ma) between 20 and 12 Ma, followed by modest cooling until present. Assuming an increased geothermal gradient between 35 and 40 °C for the Tauern Window (Genser et al., 1996; Sachsenhofer, 2001) during Early and Middle Miocene times, this means exhumation rates in the range of 0.9–1 mm/y. This is valid for both the Hochalm and Sonnblick dome. For the latter the thermal model predicts another, short termed accelerated cooling event at 6 Ma, even with reduced initial track length.

The young (U-Th)/He ages between 6.7 and 5.0 Ma indicate that, when the last cooling event occurred, only the samples from the Sonnblick dome were in the apatite He partial retention zone, while the Hochalm dome and Polinik block had already passed through it. This final cooling event is explained as vertical movement of the Sonnblick dome relative to the Polinik block and the Hochalm dome that is accommodated by displacement along its southern and north-eastern margins (Fig. 3).

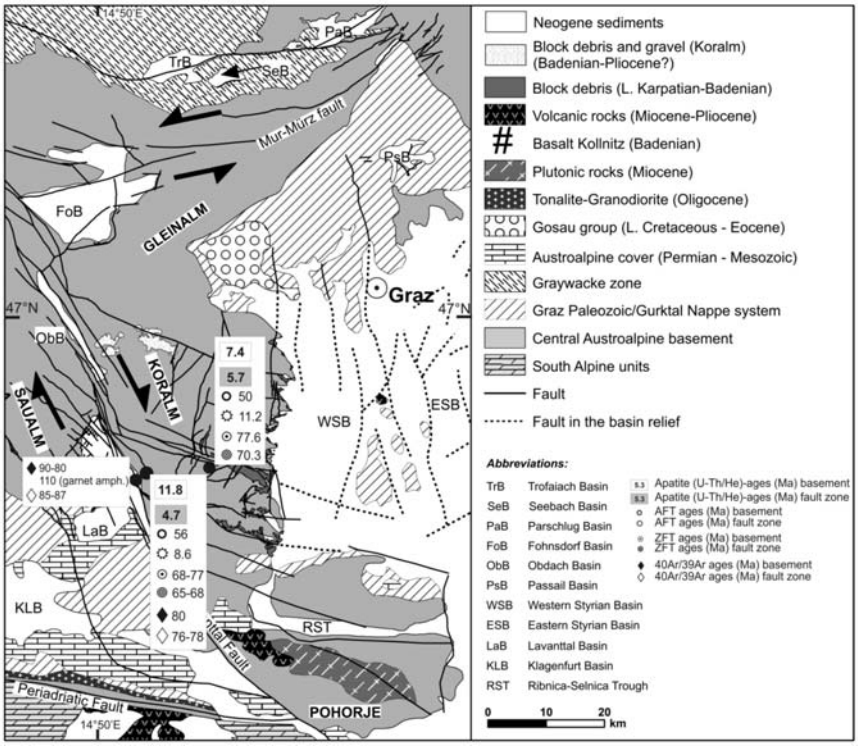

Fig. 4: $^{40}Ar/^{39}Ar$- ages, fission track (zircon, apatite) and (U-Th)/He ages in Ma from the Lavanttal fault zone and adjacent units (after Pischinger et al., 2008).

4.3 Lavanttal fault zone and adjacent Austroalpine units (Koralm massif)

The LFZ is generally described to be related to Miocene orogen-parallel escape tectonics in the Eastern Alps. $^{40}Ar/^{39}Ar$ dating on white mica, zircon and apatite fission track, and apatite U/Th-He thermochronology were carried out on host rocks and fault- related rocks (cataclasites and fault gouges) directly adjacent to the undeformed host rock (Fig. 4).

The main part of $^{40}Ar/^{39}Ar$ muscovite ages provided in this study is in accordance to the ages described from the adjacent Koralm Complex. The related plateau ages are therefore interpreted to represent the cooling of the host rocks below the closure temperature for the Argon isotopic system in muscovite (approximately 400-450° C) during Late Cretaceous times, i.e., between 80 and 90 Ma. Ages of *ca*. 110 Ma from eclogite- amphibolites most likely represent the timing of cooling during exhumation subsequent to eclogite facies metamorphism. Muscovites derived from cataclastic shear zones, however, show Argon release spectra characterized by reduced incremental ages for the first heating steps. This probably indicates Argon loss along the grain boundaries during shearing and lattice distortion, assuming that during stepwise heating Argon will be released from the muscovite rims at first. Samples from fault-related catclasites are characterized by a plateau age of *ca*. 78 Ma and highly reduced incremental ages, respectively, far below the protolith cooling ages described above. This is a strong indication for lattice distortion and related Argon loss during cataclastic shearing, and incomplete subsequent resetting of the argon isotopic system. As the incremental ages are in parts highly erratic, however, statements about the timing of shearing remain speculative.

Zircon fission track ages range between 77.6±5.5 and 64.8±4.6 Ma both within fault- and host rocks. Although all four fault/host rock sample-pair ages do overlap within the 1σ error, there is a clear trend of descending ages to the fault rocks. Track lengths were additionally analyzed and demonstrate reduced mean track lengths of 7.13±1.56 μm and 8.22±1.67 μm in fault core samples. By contrast, the samples from host rocks and damage zones show mean track lengths in the range of 10.00±0.97 μm to 10.42±1.03. Single grain ages are variable within the damage zones and fault core rocks and range between *ca*. 36.6 and 155 Ma.

Apatite fission track protolith ages range between 51.1±2.3 in the central part of the Koralm massif, and 37.7±4.3 Ma along its western margin, ages from fault- related rocks vary between 46.6 ± 4.7 and 43.3 ± 4.2 in the central part, and 43.6 ± 2.1 and 34.3 ± 1.8 Ma along the western margin of the Koralm massif. Single grain ages, however, are variable within all three fault core rocks and range from 76.5±12.3 to 3.6±1.3 Ma. These samples do not pass the chi-square test and can be decomposed into two age clusters. The dominant age components yield a weighted mean of 56.1±4.3 Ma and 8.6±2.6 Ma. Furthermore, the samples from the fault cores show significantly reduced mean track lengths (MTL). There is a clear relationship between single grain ages, MTL and Dpar values. Therefore the smallest Dpar values are associated with the youngest single grain ages and the shortest MTL´s.

Referring to the (U-Th)/He analysis a clear trend of decreasing ages from the host rock toward the damage zones and fault cores can be observed. The weighted mean age from the host rock is 11.8±0.8, from the damage zones 7.4±0.4 and 6.2±0.4 Ma and 4.7±0.3, 5.7±0.5 and 4.8±0.3 Ma from the fault cores.

5. Conclusions - Results

The subduction of the European margin resulted in eclogite facies metamorphism Subpenninic nappes (Eclogite Zone, Rote Wand-Modereck nappe) at about 40-42 Ma (Kurz et al., 2008). The Eclogite Zone ascended towards the surface within the subduction channel (Kurz & Froitzheim 2002; Kurz 2005), while subduction was still active. An age of ca. 38 Ma from undeformed eclogites is assumed to be a maximum age of this cooling event. Cooling of the Rote Wand – Modereck Nappe occurred approximately at the same time (39 Ma). The subsequent emplacement of the Rote Wand – Modereck Nappe along a major out-of-sequence detachment above at mid- to lower crustal levels may be dated at 33-31 Ma, as indicated by the phengite ages from the eclogite mylonites. Subsequently, the Penninic and Subpenninic nappes were emplaced onto the European margin.

Although accompanied by massive crustal thickening, this evolution within the lower plate (at lower crust and upper mantle conditions) is hardly reflected in the upper plate (Austroalpine units). Distinct signatures of faulting, derived from thermochronology, along the LFZ either indicate faulting prior or subsequent to Subpenninic nappe assembly.

The near-surface exhumation of Penninic and Subpenninic units and neighbouring Austroalpine basement units started during Early Miocene times, i.e. 15-20 Ma later. Two Phases are distinguished. Phase 1: Fast exhumation on both sides of the Penninic/Austroalpine boundary conforms with the period of lateral extrusion and tectonic denudation of the Tauern Window contents at 22-12 Ma. The jump to higher ages occurs within the Austroalpine unit along the Polinik fault zone, which therefore defines the boundary between the tectonically denuded units and the rather stationary orogenic lid (Wölfler et al., 2008). Phase 2: According to the occurrence of very young (U-Th)/He ages in the Sonnblick dome we demonstrate a second exhumation pulse at around 6 Ma, which is interpreted as a result of local tectonic complications along an extraction fault (Mölltal fault) (Fig. 3).

Similar to the Kreuzeck block south of the Tauern Window, exhumation and cooling of the Austroalpine units in the eastern part of the Eastern Alps was mainly completed at the end of the Cretaceous, as indicated by $^{40}Ar/^{39}Ar$ white mica and zircon fission track ages from the Koralm basement. During the main phase of lateral extrusion and formation of the Tauern Window, crustal blocks in the eastern parts of the central Eastern Alps therefore do not show significant vertical movement.

The final exhumation and uplift of the Koralm block is most probably related to vertical displacement along the LFZ from 12 Ma onward, as indicated by apatite fission track ages from fault zone cataclasites, and by apatite U/Th-He ages. Continuous displacement along the LFZ until Pliocene times is indicated by single grain apatite and U/Th-He ages. This late phase of fault activity can also be recorded along the southeastern margin of the Tauern Window, particularly along the Mölltal fault, by the final cooling of the Sonnblick dome (Fig. 3).

We therefore conclude that extrusion-related fault activity can be subdivided into three phases:

Phase 1: Formation of the Tauern Window and beginning of lateral extrusion around 23 Ma (e.g., Frisch et al., 1998). This phase, however, is only documented along the margins of the Tauern Window.

Phase 2: Fault activity migrated towards east, accompanied by the formation of intramontane molasse basins (Figs. 1, 2) (approx. 18-16 Ma) (e.g., Sachsenhofer et al, 2000; Pischinger et al., 2008). Vertical movement of Austroalpine units adjacent to these basins can not be resolved by thermochronological methods during this phase.

Phase 3: Final uplift of Austroalpine and (Sub-) Penninic units from 12 Ma onwards, also recorded by a mojor pulse of sedimentary input into the foreland Molasse basins (e.g., Kuhlemann et al., 2006).

6. Acknowledgments

Main parts of this study were carried out during research projects (P-17697-N10) granted by the Austrian Science Fund (FWF) and the German Science Foundation (grant FR 610/22). We gratefully acknowledge the Österreichische Bundesbahnen (ÖBB) (division Infrastruktur Bau) and the 3G Gruppe Geotechnik Graz ZT GmbH for giving access to pilot tunnel excavations, drill core samples, bore hole logs and geological maps acquired during the Koralm tunnel investigation campaign. Hans Genser is thanked for support for argon dating.

7. References

Decker, K., Meschede, M., and Ring, U., 1993. Fault slip analysis along the northern margin of the Eastern Alps (Molasse, Helvetic nappes, North and South Penninic flysch, and Northern Calcareous Alps). *Tectonophysics,* 223, 291-312.

Decker, K. and Peresson, H., 1996. Tertiary kinematics in the Alpine-Carpathian-Pannonian system: links between thrusting, transform faulting and crustal extension. In: Wessely, G. and Liebl, W. (eds.), *Oil and Gas in Alpidic Thrustbelts and Basins of Central and Eastern Europe*. EAGE Special Publication, 69-77.

Dunkl, I., Frisch, W. and Grundmann, G., 2003. Zirkon fission track thermochronology of the southeastern part of the Tauern Window and the adjacent Austroalpine margin, Eastern Alps. *Eclogae geologicae Helvetiae,* 96, 209-217.

Frisch, W., Dunkl, I. and Kuhlemann, J., 2000. Post-collisional orogen-parallel large-scale extension in the Eastern Alps. *Tectonophysics,* 327, 239-265.

Frisch, W., Kuhlemann, J., Dunkl, I. and Brügel, A., 1998. Palinspastic reconstruction and topographic

evolution of the Eastern Alps during late Tertiary tectonic extrusion. *Tectonophysics,* 297, 1-16.

Froitzheim, N., Plasienka, D. and Schuster, R., 2008. Alpine tectonics of the Alps and Western Carpathians. In: McCann, T. (ed.), *The Geology of Central Europe. Volume 2: Mesozoic and Cenozoic*. Geological Society, London, pp. 1141-1232.

Frost, E., Dolan, J., Sammis, C., Hacker, B., Cole, J. and Ratschbacher, L., 2009. Progressive strain localization in a major strike-slip fault exhumed from midseismic depths: Structural observations from the Salzach-Ennstal-Mariazell-Puchberg fault system, Austria. *Journal of Geophysical Research,* 114, B04406, doi: 10.1029/2008JB005763.

Genser, J., Van Wees, J.D., Cloething, S. and Neubauer, F., 1996. Eastern Alpine tectonometamorphic evolution: constraints from two-dimensional P-T-t modeling. *Tectonics,* 15, 584-604.

Hejl, E., 1997. 'Cold spots' during the Cenozoic evolution of the Eastern Alps: thermochronological interpretation of apatite fission-track data. *Tectonophysics,* 272, 159-173.

Kuhlemann, J., Dunkl, I., Brügel, A., Spiegel, C. and Frisch, W., 2006. From source terrains of the Eastern Alps to the Molasse Basin: Detrital record of non-steady-state exhumation. *Tectonophysics,* 413, 301-316.

Kurz, W., 2005. Constriction during exhumation: evidence fro eclogite microstructures. *Geology,* 33, 37-40.

Kurz, W., 2006. Penninic Paleogeography from the Western toward the Eastern Alps - Still Open Questions? *International Geology Review,* 48, 996-1022.

Kurz, W. and Froitzheim, N., 2002. The exhumation of eclogite-facies metamorphic rocks - a review of models confronted with examples from the Alps. *International Geology Review,* 44, 702-743.

Kurz, W., Handler, R. and Bertholdi, C., 2008. Tracing the exhumation of the Eclogite Zone (Tauern Window, Eastern Alps) by $^{40}Ar/^{39}Ar$ dating of white mica in eclogites. *Swiss Journal of Geosciences,* 101 (Supplement 1), S191-S206.

Kurz, W., Neubauer, F. and Genser, J., 1996. Kinematics of Penninic nappes (Glockner Nappe and basement-cover nappes) in the Tauern Window (Eastern Alps, Austria) during subduction and Penninic-Austroalpine collision. *Eclogae geologicae Helvetiae,* 89, 573-605.

Lenhardt, W.A., Freudenthaler, C., Lippitsch, R. and Fiegweil, E., 2007. Focal-depth distributions in the Austrian Eastern Alps based on macroseismic data. *Austrian Journal of Earth Sciences (Mitteilungen der Österreichischen Geologischen Gesellschaft),* 100, 66-79.

Linzer, H.-G., Decker, K., Peresson, H., Dell´Mour, R. and Frisch, W., 2002. Balancing lateral orogenic float of the Eastern Alps. *Tectonophysics,* 354, 211-237.

Mancktelow, N.S., Stöckli, D. F., Grollimund, B., Müller, W., Fügenschuh, B., Viola, G., Seward, D. and Villa, I. M., 2001. The DAV and Periadriatic fault systems in the Eastern Alps south of the Tauern Window. *International Journal of Earth Sciences (Geologische Rundschau),* 90, 593-622.

Müller, W., Mancktelow, N.S. and Meier, M., 2000. Rb-Sr microchrons of synkinematic mica in mylonites: an example from the DAV fault of the Eastern Alps. *Earth and Planetary Science Letters,* 180, 385-397.

Müller, W., Prosser, G., Mancktelow, N.S., Villa, I.M., Kelley, S.P., Viola, G. and Oberli, F., 2001. Geochronological constraints on the evolution of the Periadriatic Fault System (Alps). *International Journal of Earth Sciences (Geologische Rundschau),* 90, 623-653.

Neubauer, F., Genser, J. and Handler, R., 2000. The Eastern Alps: Result of a two-stage collision process. *Mitteilungen der Österreichischen Geologischen Gesellschaft,* 92 (1999), 117-134.

Pischinger, G., Kurz, W., Übleis, M., Egger, M., Fritz, H., Brosch, F. J. and Stingl, K., 2008. Fault slip analysis in the Koralm Massif (Eastern Alps) and consequences for the final uplift of "cold spots" in Miocene times. *Swiss Journal of Geosciences,* 101 (Supplement 1), S235-S254.

Ratschbacher, L., Frisch, W., Linzer, H.-G. and Merle, O., 1991. Lateral Extrusion in the Eastern Alps. Part 2: Structural Analysis. *Tectonics,* 10/2, 257-271.

Reinecker, J., 2000. Stress and deformation: Miocene to present-day tectonics in the Eastern Alps. *Tübinger Geowissenschaftliche Arbeiten, Serie A,* 55, 128 pp.

Reinecker, J. and Lenhardt, W.A., 1999. Present-day stress field and deformation in eastern Austria. *International Journal of Earth Sciences (Geologische Rundschau),* 88, 532-550.

Sachsenhofer, R., 2001. Syn- and post-collisional heat flow in the Cenozoic Eastern Alps. *International Journal of Earth Sciences (Geologische Rundschau),* 90, 579-592.

Sachsenhofer, R.F., Kogler, A., Polesny, H., Strauss, P. and Wagreich, M., 2000. The Neogene Fohnsforf Basin: basin formation and basin inversion during lateral extrusion in the Eastern Alps (Austria). *International Journal of Earth Sciences (Geologische Rundschau),* 89, 415-430.

Schmid, S.M., Fügenschuh, B., Kissling, E., and Schuster, R., 2004. Tectonic map and overall architecture of the Alpine orogen. *Eclogae geologicae Helvetiae,* 97, 93-117.

Schuster, R. and Kurz, W., 2005. Eclogites in the Eastern Alps: High-pressure metamorphism in the context of Alpine orogeny. *Mitteilungen der Österreichischen Geologischen Gesellschaft,* 150, 183-198.

Wölfler, A., Dekant, C., Danišík, M., Kurz, W., Dunkl I., Putiš, M. and Frisch, W., 2008. Late stage differential exhumation of crustal blocks in the central Eastern Alps: evidence from fission track and (U-Th)/He thermochronology. *Terra Nova,* 20, 378-384.

Δελτίο της Ελληνικής Γεωλογικής Εταιρίας, 2010
Πρακτικά 12ου Διεθνούς Συνεδρίου
Πάτρα, Μάιος 2010

Bulletin of the Geological Society of Greece, 2010
Proceedings of the 12th International Congress
Patras, May, 2010

EXHUMATION OF THE HELLENIC ACCRETIONARY PRISM – EVIDENCE FROM FISSION-TRACK THERMOCHRONOLOGY

Marsellos A.E.[1,2], Kidd, W.S.F. [1], Garver, J.I.[2] and Kyriakopoulos, K.G.[3]

[1] *Dept. of Geology, Union College, Schenectady, NY 12308, New York, U.S.A, email: marsellos@gmail.com*

[2] *Dept. of Earth & Atmos. Sciences, State University of New York, Albany NY 12222, New York, U.S.A.*

[3] *Dept. of Geology & Geoenvironment,National & Kapodistrian University of Athens, Panepistimioupolis, GREECE 15784, E.U.*

Abstract

Below the Potamos extensional detachment fault exposed in northern Kythera, the phyllite-quartzite unit (PQU) shows very consistent zircon FT cooling ages of c.11 Ma reflecting the time just after the rapid exhumation through the brittle-ductile transition. In contrast, a wide range of Mesozoic and some Paleozoic zircon FT cooling ages from Eocene-Oligocene Tripolis and Pindos flysch sandstones from above the detachment reflect sedimentary source ages. Early Miocene apatite fission-track cooling ages characterize the flysch sandstones, and show that early Miocene exhumation affected rocks above the detachment.

The thermotectonic evolution of the flysch of Tripolis and Pindos units within the rocks above the Potamos detachment on Kythera is reconstructed using zircon and apatite fission-track (FT) thermochronology. The apatite FT data provide evidence for a burial depth of at least 6km for the samples, which were reset. Burial was not deeper than 11km, since the zircon fission-track system in the same rocks was not reset. The exposed rocks of Tripolis and Pindos flysch on Kythera represent part of an accretionary wedge with a burial shortly after deposition in or near the subduction trench, and a cooling history due to exhumation of the flysch in the early Miocene. The subsequent Mid-Late Miocene exhumation of the PQU unit follows from beneath the (mostly carbonate) Tripolis and Pindos sedimentary rocks.

Key words: *Tripolis and Pindos units flysch, accretionary prism, fission-track thermochronology, Potamos detachment fault, Hellenic forearc.*

1. Introduction

Extensional detachment faulting under both ductile and brittle conditions has been shown to be an important mechanism to bring high-pressure/low-temperature metamorphic rocks to the surface (Platt, 1987). This is common in subduction systems where they experience rollback and slab retreat, such as the Hellenic subduction zone where exhumation of HP-rocks has been confirmed by thermochronology to have been active through detachment faulting from Early to Late Miocene (Thomson et al., 1999; Ring et al., 2001; Brix et al., 2002; Marsellos, 2008; Marsellos et al., 2010). In this setting, some accretionary wedge rocks now in the upper plate of the detachment did not follow the same subducting trajectory as the exhumed HP-rocks. Thermochronological data show that flysch

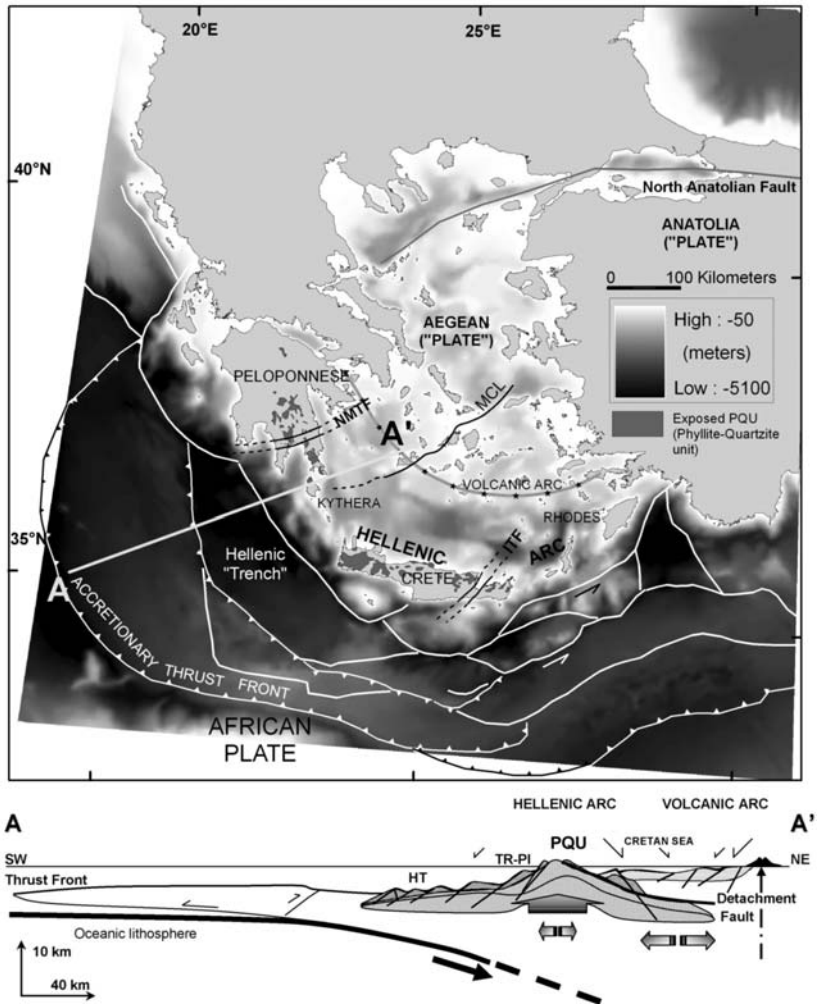

Fig. 1: Tectonic setting of the Hellenic Arc; a representative cross-section line A-A´ shown through Kythera strait. See text for discussion and Marsellos et al., (2010) for reference sources. HT - Hellenic "Trench", TR-PI - Tripolis-Pindos nappe units above extensional detachment; PQU - Phyllite-Quartzite Unit below extensional detachment; NMTF - North Mani Transverse Fault; ITF - Ierapetra Transverse Fault; MCL - Mid-Cycladic Lineament.

turbidites in the Tripolis and Pindos units of Kythera did not become deeply subducted with the HP rocks, but instead they escaped the subduction trajectory in the interval 23 to 15 Ma (Marsellos et al., 2010).

In this paper we attempt to reconstruct the thermotectonic evolution of the flysch of Tripolis and Pindos units within the rocks above the Potamos detachment on Kythera (Marsellos, 2006; Marsellos & Kidd, 2006; 2008) using apatite (Marsellos et al., 2010) and zircon fission-track (FT) thermochronology. We use the thermochronological data to constrain the deformation paths of the Neogene Hellenic orogenic wedge, and discuss possible implications of the rollback and slab retreat which affect the exhumation of HP-rocks and the evolution of the Hellenic orogenic wedge.

2. Tectonic and geological setting

The Hellenic forearc ridge contains substantial exposures of the accretionary wedge of the subduction system uplifted and exposed above sea level (Fig. 1). The pre-Neogene thrust nappes exposed in the Hellenic forearc ridge overlie the young metamorphosed basement of HP rocks. The forearc ridge became emergent in connection with rapid exhumation and uplift of the underlying HP-rocks beginning in Early Miocene in Crete (Fassoulas et al., 1994; Jolivet et al., 1996; Thomson et al., 1999, Brix et al., 2002), in central Peloponnese (Marsellos et al., 2010), and since Middle-Late Miocene in Kythera (Marsellos & Kidd, 2008, Marsellos et al., 2010).

The rocks of the pre-Neogene nappes of the External Hellenides that occur on Kythera Island resulted from northward subduction and late Eocene collision between Apulia and the Pelagonian microcontinent (Mountrakis 1986; Robertson et al., 1991; Doutsos et al., 1993). There are three lithotectonic units exposed in Kythera. The structurally lower metamorphic unit mainly consists of phyllite and quartzites, some mylonitic, with uncommon intercalations of marbles, and blueschists (Lekkas, 1986; Gerolymatos, 1994; Marsellos, 2006), as well as rare, small occurrences of metagranite and gneiss. The protolith of the metamorphic Phyllite-Quartzite unit has been suggested to have formed as a mid-Carboniferous to Triassic rift clastic sequence (Krahl et al. 1983) resulting from the opening of a southern branch of the Neotethyan ocean (Pe-Piper 1982; Seidel et al., 1982; Robertson and Dixon, 1984). The Phyllite-Quartzite unit (PQU) formed from a detrital sequence of Upper Carboniferous to Mid Triassic age (Krahl et al., 1983) with some basement units exposed in eastern Crete and Kithira that provided early Mesozoic, some Paleozoic, and few Precambrian ages (Romano et al., 2004; Xypolias et al., 2006; Zulauf et al., 2007). The Pindos and Tripolis units form the overlying unmetamorphosed lithotectonic units.

The contact of the flysch of the Tripolis and Pindos units with the underlying carbonate rocks of the same units in Kythera has been observed to be mostly tectonic (Theodoropoulos, 1973; Danamos, 1992). The depositional age of Tripolis flysch is mostly Late Eocene-Oligocene, while Pindos flysch is Paleocene (Danamos, 1992). There are a variety of observations concerning whether the flysch in Kythera belongs only to Tripolis unit (Petrocheilos, 1966) or/and to Pindos unit (Theodoropoulos, 1973; Danamos, 1992) or to both of them (Christodoulou, 1967). Apatite fission-track data (Marsellos et al., 2010) show that the flysch rocks from Pindos and Tripolis units left the apatite partial annealing zone (APAZ; c. 120° C) and exhumed at the same time at around 15 Ma. In this paper, we investigate if those rocks approached the zircon partial annealing zone (ZPAZ; c. 240° C ± 50° C) during their subduction or whether they escaped the subduction trajectory before reaching this zone.

2.1 Kythera Detachment Faults

On Kythera Island, a major extensional detachment fault that was active during Middle-Late Miocene (Marsellos, 2006; Marsellos & Kidd, 2006; 2008) separates the metamorphic PQU and the overlying unmetamorphosed units, defining the surface of the domed structure of the metamorphic core complex Zircon fission-track cooling ages indicate that there were two detachment events, one prior to 15 Ma and another starting at ~14 Ma (Marsellos et al., 2010). The first detachment was characterized by arc-normal extension, while the younger ductile and ductile-brittle transitional detachment overprinted earlier structures with arc-parallel extension. Slab retreat and trench rollback, which must have caused the expansion of the Hellenic forearc ridge, may have resulted in the series of detachment faulting and associated sequential exhumation of PQU rocks under arc-normal and subsequent arc-parallel extension (Marsellos et al., 2010).

The Tripolis unit underwent thrust imbrication associated with collision and experienced negligible, very low-pressure and low-temperature metamorphism (average metamorphic temperature of about 260° C according to Rahl and others, 2005). Tripolis flysch was underthrust beneath the Pindos imbricated folded carbonates in the same thrust-imbrication event. These thrust events must predate activity on the extensional detachment now separating the Tripolis and Pindos units from the metamorphic PQU unit.

3. Zircon Fission-Track Ages

3.1 Method

Zircon fission-track data have been obtained from two detrital zircon samples from sandstones above the detachment. The samples are from the flysch of Tripolis unit and Pindos unit in Kythera. Samples were collected from localities close to and farther from the detachment contact between the metamorphic PQU and the overlying unmetamorphosed units. Results and locations are shown in Figure 2 and 3. These zircons, originally detrital grains in sandstones, have a typical range of uranium from 100-300 ppm.

At each locality about 7-10 kg of suitable material was taken and processed for zircon using conventional techniques, specifically crushing with a disk mill, sieving, separation by Rogers table, heavy liquids, Frantz magnetic separator, and final hand-picking from some samples that had pyrite (Naeser, 1976).

Zircon age mounts for fission track analyses were prepared following the techniques outlined by Bernet and Garver (2005). Zircons were mounted in Teflon discs and then polished to expose internal zircon surfaces. The mounted zircons were incrementally etched in a KOH:NaOH eutectic melt at 228° C, between 4-10 hours, until the majority of grains were fully etched. Additionally, multiple mounts from many samples were etched for different times, the total etch time ranging from 9 hr to 24 hr depending on the sample.

Thermal neutron irradiation was performed in the thermal neutron facility at the Oregon State University nuclear reactor, and unknowns were irradiated along with CN glasses and well-calibrated age standards (Fish Canyon Tuff, Buluk Tuff, and Peach Springs Tuff) (Hurford, 1990). All samples were dated using the external detector method (Naeser, 1976; Gleadow, 1981). The detector mica was etched for 15 min in 49% HF at room temperature. All samples were counted at 1250x using a dry 100x objective (10x oculars and 1.25x tube factor) on an Olympus BMAX 60 microscope fitted with an automated stage and a digitizing tablet. All ages with χ^2>5% are reported as pooled ages. Fission track ages ($\pm 1\sigma$) were determined using the Zeta method, and ages were calculated using the computer program and equations in Brandon and Vance (1992). Ages were determined for each sample using the zeta method: ζ values (Hurford and Green, 1983) are listed in table 1. Zeta factor was determined by multiple analyses of zircon standards, using Buluk Member Tuff, Peach Springs Tuff (PST) and Fish Canyon Tuff zircons (Hurford, 1990). Errors were calculated using the "conventional analysis" given by Green (1981). The χ^2 analysis (Galbraith, 1981; Green, 1981) was employed to test the assumption that all analyzed grains are derived from a single population and have a common age with only Poissonian variation.

3.2 Results

Fission track analyses of zircons from rocks above the detachment reveal a significant succession of thermal episodes. Parameters for best-ft peaks, generated from Binomfit program (Brandon, 1996)

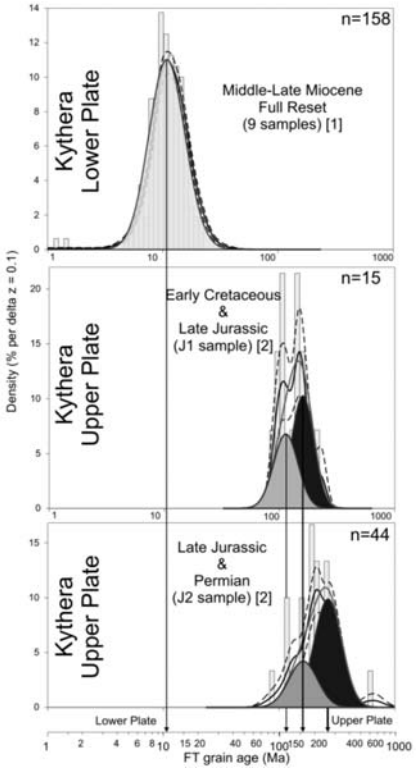

Fig. 2: Results from binomial peak-fitting (Brandon, 1996) represented through the probability density plots. On these plots, the individual histogram bars represent the grain-age components. Thin solid lines represent successive populations identified in the age distributions. Results for first and second population are discussed in text. Zircon fission-track (ZFT) grain ages are from 9 samples from the exposed PQU rocks (lower plate) of [1] Marsellos et al. (2010), and 2 samples from the upper plate ([2] this study).

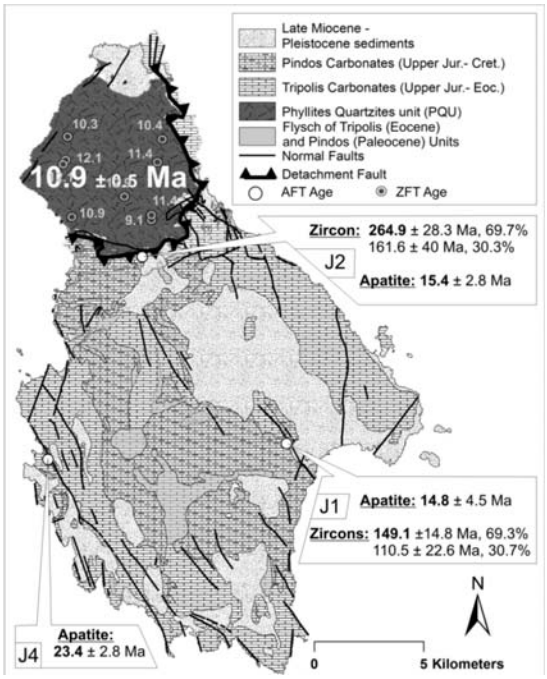

Fig. 3: Sample locations of zircon fission-track (ZFT) and apatite fission-track (AFT) cooling ages from above the detachment (upper plate, Tripolis/Pindos flysch) on Kythera Island (western part of Hellenic forearc). ZFT data from upper plate are reported in this study, ZFT from below the detachment (lower plate, PQ unit) and AFT from upper plate are data first reported in Marsellos et al. (2010). Simplified geological map of Kythera after Petrocheilos (1966) and our observations.

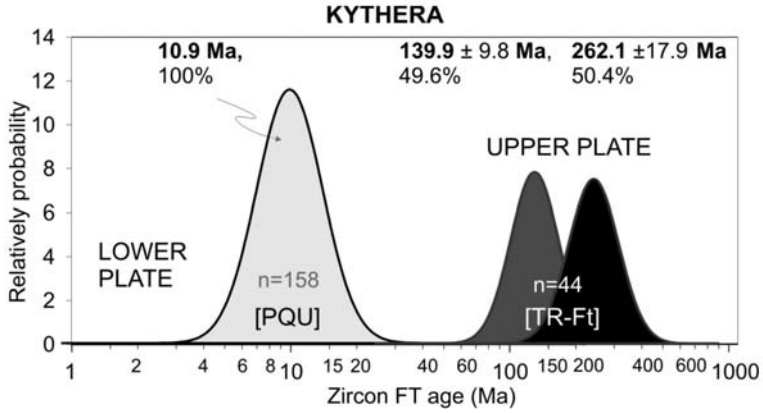

Fig. 4: Results from binomial peak-fitting from Binomfit program (Brandon, 1996) represented through the probability density plots. ZFT grain ages are from nine samples from the exposed PQU rocks (lower plate) from Marsellos et al., (2010), and 2 samples (data of this research) from the flysch of Tripolis and Pindos units (upper plate).

shows for the sample J2 from Pindos flysch a primary population of 149.1 ± 14.8 Ma (69.3% fraction of grains) and a secondary population of 110.5 ± 22.6 Ma (30.7%). Sample J1 from Tripolis flysch shows a primary population of 264.9 ± 28.3 Ma (69.7%) and a secondary population of 161.6 ± 40 Ma (30.3%). Application of Binomfit program to both the flysch samples from above the detachment in Kythera (Fig. 4) gives two distinct population ages of 139.9 ± 9.8 Ma (49.6%) and 262.1 ± 17.9 Ma (50.4%).

4. Discussion

The stratigraphic transition upwards from limestone to flysch is observed on Kythera in the Tripolis unit and Pindos unit (Danamos, 1992; Petrocheilos, 1966) and occurs about the mid-Late Eocene boundary (Petrocheilos, 1966; Fluery, 1980; Thiebault, 1982), which implies proximity to the subduction trench at this time (~37-34 Ma). The Tripolis flysch and underlying carbonates underwent thrust-imbrication associated with collision and experienced negligible, very low-pressure and low-temperature metamorphism (average metamorphic temperature of about 260°C according to Rahl and others, 2005). Tripolis flysch was underthrust beneath the Pindos imbricated folded carbonates in the same thrust-imbrication event. In Kythera (Fig. 3), apatites from the Tripolis flysch (sandstone) cooled through the apatite PAZ at ~15 Ma with evidence of partial resetting at ~23.4 Ma (Marsellos, 2008; Marsellos et al., 2010). Because the Tripolis flysch has not experienced high-pressure metamorphism, then most likely the Tripolis unit escaped the subduction trajectory in the interval 23-15 Ma.

The visual contrast of zircon fission-tracks and associated ages from the detrital grains between the upper plate and lower plate of the detachment in Kythera is very prominent (Fig. 4, 5). Ductile structures are also present in the PQU associated with the exhumation of those HP-rocks (Xypolias & Koukouvelas, 2001; Xypolias & Kokkalas, 2001; Xypolias et al., 2008; Marsellos, 2006; Marsellos & Kidd, 2008; Xypolias et al., 2008; Marsellos et al, 2010) but are missing from the upper plate. The cooling event (9-13 Ma) associated with the detachment activity has been recorded in the fully reset zircons in the Kythera PQU while rocks in the upper plate did not cross the ZPAZ. These data are not compatible with a hypothesis of an overthrusting event placing Tripolis unit above the PQU metamorphics.

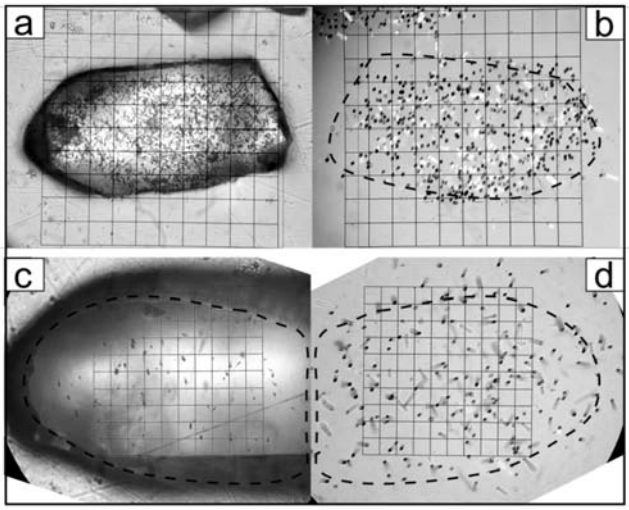

Fig. 5: Photomicrograph of etched zircon grains from (a) upper plate and (c) lower plate under plane transmitted light (100x objective, 1250x total magnification); (b, d) mica print of the zircon after irradiation showing the induced fission tracks in the mica.

Apatite fission track (AFT) ages from the upper plate Tripolis and Pindos flysch older than those from the lower plate PQU also rule this out. AFT ages of ~7 Ma from rocks in the sub-detachment PQU unit of Kythera and the southeastern Peloponnese (Marsellos et al., 2010) represent the time when the Kythera PQU left the apatite PAZ (by exhumation and related cooling) and were tectonically juxtaposed with the Tripolis and Pindos carbonate units. The sub-detachment PQU zircons show cooling ages starting at 12.9 Ma with a peak at 10.9 Ma, while apatites from the rocks above the detachment show cooling below the apatite PAZ at 23.4 Ma and at ca. 15 Ma. The HP-LT rocks below the detachment in Kythera were rapidly exhumed in the interval 13-7 Ma, and while this may have caused local recrystallization in some limestones adjacent to the detachment, our data show that there was no major thermal perturbation caused in the upper plate rocks of the Tripolis unit by this event.

Average cooling rates using both zircon and apatite FT data from Kythera lower plate have been estimated (Marsellos et al., 2010) over the temperature intervals between ZFT and AFT closure, and exhumation to the present surface. The rocks from Kythera (Fig. 6) cooled from ZFT to AFT closure (c. 240° C and 120° C) between ~11 Ma and ~7 Ma, an interval whose range from the FT ages is 1-5.8 Ma (including the ZFT errors), which gives a minimum average cooling rate of 30-50° C/Myr Using apatite FT to the present surface, the rocks in Kythera cooled from 120° C to surface temperature in a maximum duration of 5-9 Myr giving a minimum average cooling rate of 10° C /Myr and a wide potential range up to 30° C/Myr. The time these samples first reached near surface temperatures is uncertain, but cooling ages suggest that there has been overall slower exhumation after ~7 Ma for the PQU on Kythera and southern Peloponnese. This later interval of slower exhumation includes activity on normal faults parallel with the Hellenic Arc some of which cut the detachment and now locally separate the PQU from the unmetamorphosed Tripolis and Pindos units.

Exhumation and cooling, required by the FT ages reported here, can occur either by erosion or by tectonic extension (or a combination of these). Given the temperature constraints on the zircon FT system, with the partial annealing zone maximum temperature not above 280° C, the cooling observed must be largely or entirely from events when the rocks were in the continental crust, and do not, for the metamorphic PQU rocks, necessarily record anything about earlier oblique buoyant exhumation (Thomson et al, 1999) from greater depths in the subduction channel. While the flysch,

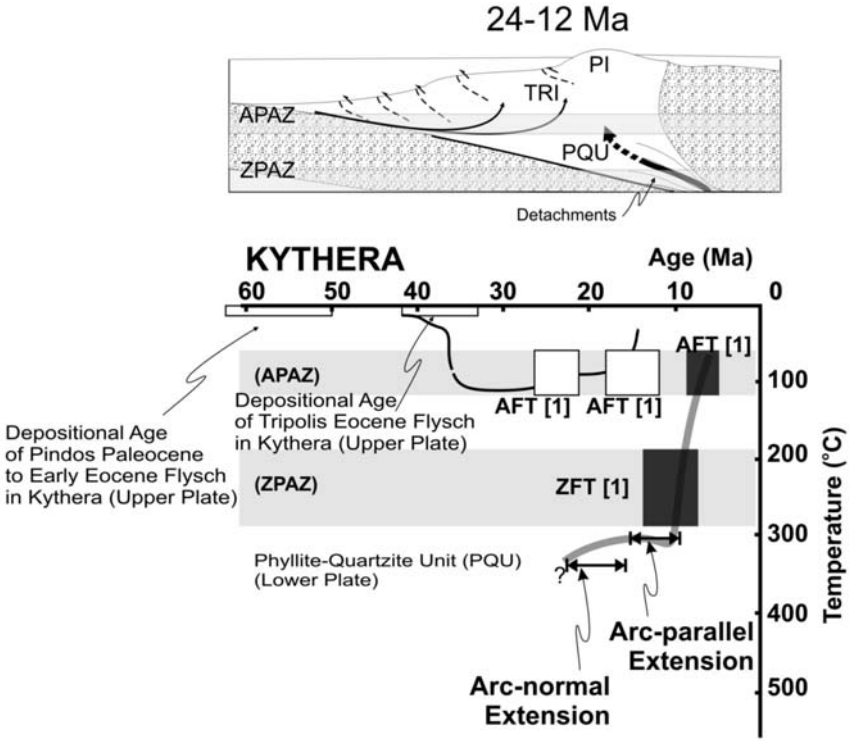

Fig. 6: Temperature-time (T-t) diagram for Kythera (western part of Hellenic Arc) combining: [1] zircon fission-track data of this study, [2] apatite fission-track, and zircon fission-track, of Marsellos et al. (2010). Dark grey boxes and thick grey line are PQU metamorphics of "lower plate" of detachment; white boxes and thin black line are from "upper plate" of detachment. APAZ - Apatite Partial Annealing Zone; ZPAZ - Zircon Partial Annealing Zone.

after incorporation into the thrust accretionary complex, may have been exhumed in significant part by erosion, it is clear from the geological relationships and structures near the detachment fault that exhumation of the PQU in the mid-upper crust through the ZPAZ must have been dominated by tectonic extension. The rapid rates of cooling estimated from the zircon and apatite FT ages in the PQU are consistent with tectonic extension being the dominant exhumation process for these rocks.

In central Peloponnese, we have obtained older zircon FT cooling ages (~21 Ma) from PQU metamorphics compared with those of Kythera, but we have been so far unsuccessful in obtaining apatite FT coling ages from the Tripolis flysch of the Peloponnese. More FT data from the flysch of Tripolis unit and exposed PQU rocks from central or northern Peloponnese are required to extend this study.

Valuable provenance information is retained in these cooling ages. Late Permian to Early Triassic ZFT cooling ages, and Late Jurassic-Early Cretaceous age in the zircons from the Kythera Tripolis and Pindos flysch show the ages of the sediment source rock, which could have been itself sedimentary. The Pindos unit clastic formations of Triassic and Early Cretaceous age correspond to this sedimentary source of Tripolis Unit as Danamos (1992) has independently inferred for the sedimentary source of the Tripolis flysch. Accretion and overthrusting of the Pindos unit to provide a source for the flysch in the late Eocene-Oligocene is plausible in the context of the Apulian-Pelagonian collision.

5. Conclusion

Zircon fission-track ages from Kythera record three thermal episodes. Zircons from the lower plate have Neogene cooling ages associated with the latest exhumation of the HP-LT rocks; the thermal history of these rocks reset and erased sedimentary provenance ages in these zircons. In contrast, zircon grains from the upper plate show Mesozoic and latest Paleozoic zircon fission-track ages that reflect the cooling ages of zircons and thermal evolution in the source region.

Early Miocene apatite cooling ages from above the detachment show when the Tripolis and Pindos units now present on Kythera were exhumed, and perhaps are linked to the earliest activity of the extensional detachment. Apatite FT ages in the PQU metamorphics on Kythera show the-Late Miocene extensional exhumation event of the PQU from beneath the Tripolis (and Pindos) sedimentary rocks.

6. Acknowledgments

Partial funding for field mapping, sample collection, and sample preparation for thermochronology was received from the Geological Society of America (grant to Marsellos). Additional partial funding for sample analysis was provided by the American Chemical Society – Petroleum Research Fund (grant ACS-PRF-47191 to Garver). Neutron irradiation was facilitated by Steve Binney at the Oregon State nuclear reactor as part of the US DOE Reactor Use Sharing Program.

7. References

Bernet, M. and Garver, J.I., 2005. Fission-track Analysis of Detrital Zircon. *Reviews in Mineralogy & Geochemistry 58*, 205-238.

Brandon, M.T., Vance, J.A., 1992. Fission-track ages of detrital zircon grains: implications for the tectonic evolution of the Cenozoic Olympic subduction complex. *American Journal of Science 292*, 565–636.

Brandon, M.T., 1996. Probability density plot for fission-track grain-age samples. *Radiation Measurements 26*, 663–676.

Brix, M.R., Stockhert, B., Seidel, E., Theye, T., Thomson, S.N., Kuster, M., 2002. Thermobarometric data from a fossil zircon partial annealing zone in high pressure-low temperature rocks of eastern and central Crete, Greece. *Tectonophysics 349*, 309-326.

Christodoulou, G., 1966. Some remarks on the Geology of Kythira island and a micropaleontological analysis of its Neogene Formations. *Bull. Geol. Soc. Greece 6*, 385-399.

Danamos, 1992. Contribution to geology and hydrogeology of Kythera Island. *Ph.D. dissertation*, Athens, 330.

Doutsos, T., Piper, G., Boronkay, K., Koukouvelas, I., 1993. Kinematics of the central Hellenides. *Tectonics 12*, 936-953.

Fassoulas, C., Kilias, A., Mountrakis, D., 1994. Postnappe stacking extension and exhumation of high-pressure/low-temperature rocks in the island of Crete, Greece, *Tectonics 13*, 127-138.

Fleury, J.J., 1980. Les zones de Gavrovo-Tripolitza et du Pinde-Olonos (Grece continentale et Peloponedr du Nord): Evolution d'une plateforme et d' un bassin dans leur cadre alpin: *Public. de la Soc. Geol. du Nord, Lille Publication 4*, 651.

Galbraith, R.F., 1981. On statistical models for fission track counts. *Mathematical Geology 13*, 471-488.

Gerolymatos, I. K., 1994. Metamorphose und Tectonik der Phyllit-Quartzit-Serie und der Tyros-Schichten auf dem Peloponnes und Kythira. Berliner Geowissenschaftliche Abhandlungen, *Geologie Palaontologie 164*, 1-101.

Gleadow, A.J.W., 1981. Fission track dating: what are the real alternatives. *Nuclear Tracks 5*, 3-14.

Green, P.F., 1981. A new look at statistics in fission-track dating. *Nuclear Tracks 5*, 77-86.

Hurford, A.J., Green, P.F., 1983. The zeta age calibration of fission-track dating. *Isotope Geoscience 1*, 85-317.

Hurford, A.J., 1990. Standardization of fission track dating calibration: recommendation by the Fission Track Working Group of the I.U.G.S. Subcommission on Geochronology. *Chemical Geology (Isotope Geoscience Section) 80*, 171-178.

Jolivet, L., Goffe, B., Monie, P., Truffert-Luxey C., Patriat, M., Bonneau, M., 1996. Miocene detachment in Crete and exhumation P-T-t paths of high pressure metamorphic rocks. *Tectonics 15*, 1129-1153.

Krahl, J., Kauffmann, G., Kozur, H., Richter, D., Forster, O., Heinritzi, F., 1983. Neue Daten zur Biostratigraphie and zur tectonischen Lagerun der Phyllit-Gruppe und der Trypali-Gruppe auf der Insel Kreta (Griechenland). *Geologische Rundschau 72*, 1147-1166.

Lekkas, Sp., 1986. Les unites structurales dans l'ile de Cythere. *Bul. Geol. Soc. Greece XX*, 159-173.

Marsellos, A.E., 2006. Mapping of the Detachment fault in Kythera Island and study of the related structural shear sense indicators. *Unpublished MS Thesis*, State University of New York Albany, 201.

Marsellos, A.E., Kidd, W.S.F., 2006. Detachment fault and shear zone of the Cretan-Peloponnese ridge in Kythera Island. Geological Society of America, *Abstracts with Programs 38*:7, 238.

Marsellos, A.E., Kidd., W.S.F., 2008. Extension and exhumation of the Hellenic forearc ridge in Kythera. *The Journal of Geology 116*, 640-651.

Marsellos, A.E., 2008. Extension and Exhumation of the Hellenic forearc; and Radiation Damage in Zircon. *Unpublished Ph.D. thesis*, State University of New York Albany, 754.

Marsellos, A.E., Kidd, W.S.F., Garver, J.I., 2010. Extension and exhumation of the HP/LT rocks in the Hellenic forearc ridge. *American Journal of Science, 310, 1-36.*

Mountrakis, D., 1986. The Pelagonian zone in Greece: a polyphase-deformed fragment of the Cimmerian continent and its role in the geotectonic evolution of the eastern Mediterranean. *J.Geol. 94*, 335-347.

Pe-Piper, G., 1982. Geochemistry, tectonic setting and metamorphism of mid-Triassic volcanic rocks of Greece. *Tectonophysics 85,* 253-272.

Petrocheilos, J., 1966. Geological map of Kythera Island, scale 1:50,000. Institute for Geology and Subsurface Research, Athens.

Platt, J.P., 1987. The uplift of high-pressure-low-temperature metamorphic rocks. Phil. Trans.R.Soc.Lond., A321, 87-103.

Robertson, A.H.F., Clift, P.D., Degnan, P., Jones, G., 1991. Paleoceanography of the Eastern Mediterranean Neotethys. *Palaeogeography, Palaeoclimatology, Palaeoecology 87*, 289-343.

Rahl, J.M., Anderson, K.M., Brandon, M.T., Fassoulas, C., 2005. Raman spectroscopic carbonaceous material thermometry of low-grade metamorphic rocks: Calibration and application to tectonic exhumation in Crete, Greece. *Earth and Planetary Science Letters 240*, 339-354.

Ring, U., Brachert, T., Fassoulas, C., 2001. Middle Miocene graben development in Crete and its possible relation to large-scale detachment faults in the southern Aegean. *Terra Nova 13*, 297-304.

Robertson, A.H.F. and Dixon, J.E., 1984. Introduction: aspects of the geological evolution of the eastern Mediterranean. In Dixon, J.E., and Robertson, A.H.F., eds. The geological evolution of the eastern Mediterranean. *Geol. Soc. Lond. Spec.Publ. 17*, 1-74.

Romano, S.S., Dorr, W., Zulauf, G., 2004. Cambrian granitoids in pre-Alpine basement of Crete (Greece): evidence from U-Pb dating of zircon. *Int J Earth Sci (Geol Rundsch) 93*, 844-859.

Seidel, E., Kreuzer, H. and Harre, W., 1982. A Late Oligocene/Early Miocene high-pressure belt in the

extternal Hellenides. *Geol. Jahrb. E23*, 165-206.

Theodoropoulos, D.K., 1973. Physical Geography of the island of Kythira, Athens, 94.

Thiebault, F., 1982. Evolution geodynamique des Hellenides externes en Peloponnese meridional (Grece). *Soc. Geol. du Nord, Publication n.6*, 574.

Thomson, S.N., Stockhert, B., Brix, M.R., 1999. Miocene high-pressure metamorphic rocks of Crete: rapid exhumation by buoyant escape. *in* Ring, U., Brandon, M., Lister, G.S., Willet, S. editors, Exhumation Processes: Normal Faulting, Ductile Flow and Erosion. *Journal of Geological Society of London*, *Special Publication 154*, 87-107.

Xypolias, P., Koukouvelas, I., 2001. Kinematic vorticity and strain rate patterns associated with ductile extrusion in the Chelmos Shear zone (External Hellenides, Greece). *Tectonophysics* 338, 59-77.

Xypolias, P., Kokkalas, S., 2001. Strain-dependent field and plate motions in the south.

Xypolias, P., Koukouvelas, I, Zulauf, G., 2008. Cenozoic tectonic evolution of northeastern Apulia: insights from a key study area in the Hellenides (Kythira, Greece). *Z.dt. Ges. Geowiss*., 159/3, 439-455.

Xypolias, P., Dorr, W., Zulauf, G., 2006. Late Carboniferous plutonism within the pre-Alpine basement of the External Hellenides (Kithira, Greece): evidence from U-Pb zircon dating. *J. Geol. Soc. Lond*., 163, 539-547.

Zulauf, G., Romano, S.S., Dorr, W., Fiala, J., 2007. Crete and the Minoan terranes: Age constaints from U-Pb dating of detrital zircons. *Geol. Soc. Am., Special Paper 423*, 401-411.

Δελτίο της Ελληνικής Γεωλογικής Εταιρίας, 2010
Πρακτικά 12ου Διεθνούς Συνεδρίου
Πάτρα, Μάιος 2010

Bulletin of the Geological Society of Greece, 2010
Proceedings of the 12th International Congress
Patras, May, 2010

TECTONIC SETTING AND DEFORMATION OF THE KALLIDROMO MT, CENTRAL GREECE

Migiros G.[1], Antoniou Vas.[1], Papanikolaou I.[1] and Antoniou Var.[2]

[1] *Laboratory of Mineralogy & Geology, Department of Geological Sciences and Atmospheric Environment, Agricultural University of Athens, 75 Iera Odos Str., 118 55 Athens - GR*
bagm@aua.gr, vantoniou@aua.gr, i.papanikolaou@ucl.ac.uk

[2] *Department of Dynamic, Tectonic and Applied Geology, National and Kapodistrian University of Athens, Faculty of Geology and Geoenvironment, Panepistimioupolis Zografou, 157-84 Athens, Greece, vantoniou@geol.uoa.gr.*

Abstract

Kallidromo Mt. consists of alpine formations which in places are unconformably covered by Neogene and Quaternary sediments. The ophiolites are overthrusted on the massive Mesozoic platform carbonate sequence, which forms the basement unit. The base of the tectonic nappe is characterized by a tectonic melange that consists of sandstones, clay stones, limestones, cherts and basaltic rocks that are mainly observed in pillow forms. Two distinct compressional deformation phases (D1, D2) are traced. Deformation D1 whereas the fold axes, the predominant schistocity planes and shear zones clearly follow a N295°(±10°)-115°(±10°) trend that relates to the Upper Jurrasic-Lower Cretaceous ophiolitic emplacement of the Eo-alpine orogeny and is the predominant feature over the entire study area. Deformation D2 relates to the Cretaceous-Eocene alpine orogeny, follows a N020°(±15°)-N200°(±15°) trend and has a much weaker and secondary imprint in the study area. The tectonic study of the alpine and post-alpine formations shows a complex deformation pattern with a variety of quantitative and qualitative characteristics. These variations can be correlated with different phases and stages of deformation (compressional to extensional) from the timing of the tectonic emplacement of the ophiolites inUpperJurrasic-Lower Cretaceous up to the present-day field.

Key words: *Kallidromo, ophiolites, structural analysis, fault.*

1. Introduction

Mt Kallidromo is an elongated WNW-ESE trending mountain in central Greece and represents a tectonic horst (e.g. Phillip 1974, Goldsworthy and Jackson 2001) between the Sperchios basin northwards and the Beotikos Kifissos basin southwards (Fig.1). The major watershed follows the WNW-ESE elongation of the Kallidromo Mt at 900m elevation. The river network within the alpine rocks is of dendritic type involving mostly small catchments of lower stream order (1-4th based on Strahler classification), whereas within the post-alpine rocks the network is represented by single nodes, involving a more mature network that includes large catchments or small rivers (of 4th and higher stream order), exhibiting a higher hierarchical structure. The Sperchios is a narrow basin trending WNW-ESE, forming the inland prolongation of the Maliakos and Northern Evoikos Gulfs. It is characterized by smoothed landscape with a 50m mean elevation and dips gently towards the south, due to the higher fault slip-rate activity of the faults bordering its southern boundary. The Beotikos Ki-

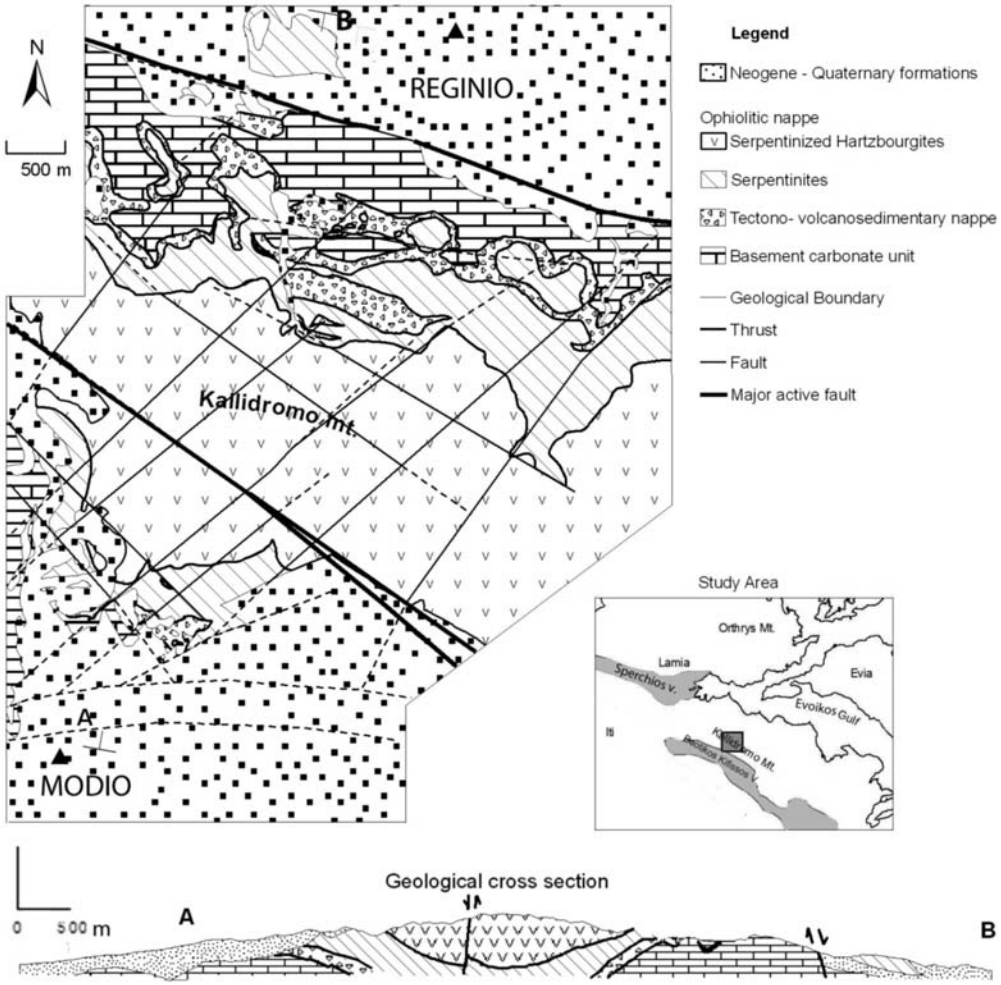

Fig 1: Geological map of the study area.

fissos is a rather shallow basin where the postalpine sedimentary cover is thin, so that the Mesozoic rocks crop at several localities within the basin. It also trends WNW-ESE and has a mean elevation at 150m. This paper examines and presents the lithostratigraphic and tectonic structure of the Kallidromo Mt and analyzes their interrelation.

2. Geological structure

Kallidromo Mt comprises Mesozoic limestones, schist-cherts with basalts, ultramafic rocks and flysch of the Pelagonian zone (Papastamatiou et al., 1962, Celet 1962, Clement 1977, Fleury, 1980, Ferriere 1982, Karipi et al. 2007). It is part of the Internal Hellenides (Brunn, 1956), that has been subdivided by Aubouin (1959) into a non-metamorphic western (Subpelagonian zone e.g. Mountrakis et al. 1983, Papanikolaou 1989) and a metamorphic eastern part (Pelagonian zone s.s.; for an

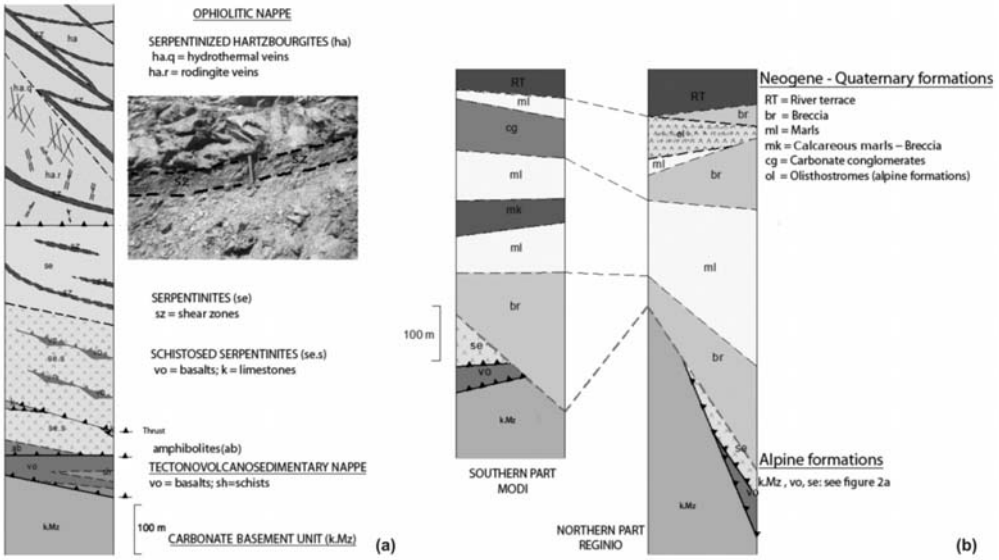

Fig 2: a) Lithostratigraphic column of the Alpine formations of the Kallidromo Mt. b) The post-alpine formations and the alpine basement for the northern (Reginio) and the southern part (Modi) of the study area.

overview see Jacobshagen 1986). Palaeo-geographically, the Pelagonian zone s.l. is considered to be a continental fragment, which was bordered at its internal and external margins by oceanic domains that have been traditionally called the Vardar and Pindos Oceans respectively (Bernoulli and Laubscher, 1972; Jones and Robertson, 1991). The Pelagonian exhibits a complex nappe structure due to repeated thrusting and ophiolite obduction processes from the oceanic realms during the Alpine orogeny. The subduction of the oceanic domains initiated in the Mid-Jurassic and lasted until early Tertiary times and was accompanied by the formation of ophiolite complexes, blueschist belts and ended up by the flysch sedimentation (Smith and Woodstock 1976; Katsikatsos et al. 1986; Jones and Robertson 1991; Faupl et al. 1996). Neogene and Quaternary deposits and sediments rest uncomformably on the alpine rocks both northwards (Reginio into the Sperchios basin) and southwards (Modi into the Beotian basin) and are bounded by active normal faults (Celet 1962, Phillip 1974, Ganas 1997, Kranis 1999, Goldsworthy and Jackson 2001). In the following section a detailed description of the local geological structure is presented regarding the wider Kallidromo Mt.

2.1 Alpine Formations

The Alpine formations are divided into three major units that from lower to upper members consist of: a) the carbonate basement unit, b) the tectonovolcanosedimentary nappe and c) the ophiolitic nappe. Both the ophiolitic and the tectonovolcanosedimentary nappes are thrusted on top of the carbonate basement unit, which represents the Mesozoic neritic platform (Fig.2a).

a) Carbonate basement unit. It comprises fossiliferous Mesozoic carbonate sequence of limestones and dolomites. In a few localities within the limestones, several beds of clay schists intercalations also appear, indicating a temporally deeper sedimentation environment. Towards the northern part of the study area, the limestones appear more crystalline, dolomitised and fragmented. During the prolonged thrusting emplacement several fault planes were developed as documented by the extensive fault zones of various thicknesses (from 5 up to 20m thick) that involve mostly breccia and to

a lesser extend cataclasites.

b) Tectonovolcanosedimentary nappe. This nappe appears always thrusted on top of the carbonate basement unit and below the ophiolitic nappe. It consists of clay-chert and marly limestones formations with basalts of various thicknesses. Basalts are represented by pillow lavas, whose thickness varies from 40 to 100m. The entire formation is highly deformed, folded and fragmented as evidenced by the extensive appearance of thick breccia and other cataclasites.

c) Ophiolitic nappe. The ophiolitic nappe covers the entire central part of the Kallidromo Mountain and has a maximum structural thickness of 900m. Three subunits are defined, that from lower to upper members involve: (a) schistosed serpentinites, (b) serpentinites and (c) serpentinized hartzbourgites. Subunits (a) and (b) form a common mass whose deformation is gradually reduced, up to subunit (c) that is thrusted on top of the others. Towards the base of the ophilitic nappe several amphibolite bodies of various thickness are evident, comprising the so-called "amphibolitic sole". The amphibolites (ab) form discontinuous bodies whose thickness varies from 1 up to 20m. They are often folded and in several cases a cataclastic fabric/texture has been traced (Fig.2a).

Schistosed serpentinites (se.s). Schistosed serpentinites form an heterogenous mass that maintain a highly foliated structure. This foliation was developed due to the intense deformation processes that occurred both during the initial stages of their emplacement as well as during their overthrust on the carbonate basement unit. Such intense deformation processes resulted in internal repetition of the serpentinites. These repetitions that are tectonically controlled can increase locally their thickness up to a significant amount (180m towards the northern part and up to 320m towards the southern part where deformation is more intense). In particular, towards the southern part of the study area, several lenticular bodies of variable sizes of limestones and volcanosedimentary formations are traced along strike these thrusts. Several shear zones of brittle type, whose thickness range from a few cm up to 5m. Finally, in several localities, they appear as a mixture of rocks involving different lithological compounds and forming a mosaic. Such mixtures can locally be characterized as "ophiolitic mélanges". Beyond the serpentinites that dominate mélange, several other rocks such as amphibolites, dolerites, basalts, sandstones, limestones and cherts, do also exist.

Serpentinites (se). The schistosed serpentinites evolve upwards into the serpentinites, which are intensely deformed in a boudinage style. Their boundary with the schistosed serpentinites is often unclear, whereas the intensity of the deformation that have experienced, diminishes towards their upper members. Their thickness is up to 200m, but in a few localities they are absent due to the tectonic wedges between the schistosed serpentinites and the thrusted serpentinized hartzbourgites. Their structure is trending parallel to the approximately E-W trending ophilitic elongated nappe. Shear zones are observed within the serpentinites and particularly as approaching the thrust with the overlying serpentinized hartzbourgites. These shear zones are of brittle type and their thickness varies from a few cm up to 20m.

Serpentinized Hartzbourgites (ha). The serpentinized harzburgites have a thickness up to 500m and are interrupted by various shear zones. These shear zones are either of pure brittle nature or developed on the brittle-ductile boundary and their thickness varies from a few cm up to 50m. The major shear zones follow a mean WNW-ENE direction. Depending on the presence or not of veins they are divided into two main parts, whose boundary, however is in most cases unclear. The body of the serpentinized hartzbourgites that is crosscuted by veins and vents, does not exhibit any petrological differentiation from the body of the serpentinised harzburgite, except from a slightly higher degree of serpentinisation and in places hydrothermal alterations. The circulation of hydrothermal fluids after the rock formation causes serpentinization and alteration of the peridotites, which are converted

to serpentines. During serpentinization ultramafic rocks are oxidized with water into serpentinite. Since during the serpentinization process, rock temperatures can be raised as high as 250°C, formation of non-volcanic hydrothermal vents may take place. The veins are divided into two systems: a) The first system of veins comprise from rodingites and rodingite gabbros (ha.r) (Coleman, 1977) that are intensely deformed and vary in thickness from a few cm up to 4m. b) The second system of veins and vents concerns the hydrothermal processes that occurred following the postgabbro intrusion stage.

2.2 Postalpine formations

The postalpine formations outcrop predominantly towards the northern and southern part of the study area, and cover unconformably the alpine formations. Figure 2b displays the columns including also the basement alpine rocks. Since their features, facies and thicknesses differ significantly between the northern (Reginio) and the southern part (Modi), two separate columns are displayed. They are divided into:

a) Upper Pliocene – Lower Pleistocene Formations

Breccia (br). It is a cohesive formation that consists of various sizes of mostly angular and subangular fragments of rocks and pebbles. They are cemented with finer clastic material mostly sands and clay. They are poorly sorted; however they are rather well stratified. In several localities, several horizons and lenses of redsoil are interfingered as with other sediments as well. They have formed in a continental sedimentary basin that was tectonically controlled, so that in most cases they overlay a thin paleosoil, where a calcite horizon is nicely preserved. Their thickness is up to 250m.

Marls (ml). An unconformity and in places a disconformity separates this formation from the older breccia formation. It is composed mostly of lagoonal type sediments such as clays and marls and locally some lenses and intercalations of gravels, sands and rarely conglomerates appear. Towards the northern part they are characterized by higher homogeneity, having a clear stratification, whereas in the southern part sedimentation processes were more complex and disturbed so that the material is more diverse and several intercalations occur both spatially and temporary. Its maximum thickness is estimated at 260m.

Calcareous marls (mk). It represents a horizon within the marls formation, whose thickness ranges up to 60m. Towards the southern part of the study area, a well developed half a meter thick shear zone, is traced that was formed, due to its gradual sliding on top of the underlying marl formation.

Carbonate conglomerates – Breccia (cg). It is a highly cohesive formation that overlays the marl formation. It outcrops only towards the southern part of the study area and on the upper part of the hilly landscape. It comprises monomict limestone breccia of various sizes with calcitic matrix. This formation has no stratification is poorly sorted and towards its base several coarse, angular fragments and limestone boulders are observed. Towards the northern part of the Kallidromo no similar formation exists. However, in a equivalent stratigraphic locality, several large scale slides of ophiolites are observed within the marl formation. Their presence within this formation north of the Kallidromo fault zone indicates that these sliding processes were related to tectonism that occurred during sedimentation.

b) Upper Pleistocene – Holocene deposits and sediments. They rest unconformably on the previous formations and are of continental origin. They involve, river terraces (RT), talus cones and triangular facets, scree, alluvial fans and deposits. The talus cones, breccia and scree extend along strike and delineate the Kallidromo fault zone. They consist mostly from limestone boulders and fragments and are strictly fault controlled.

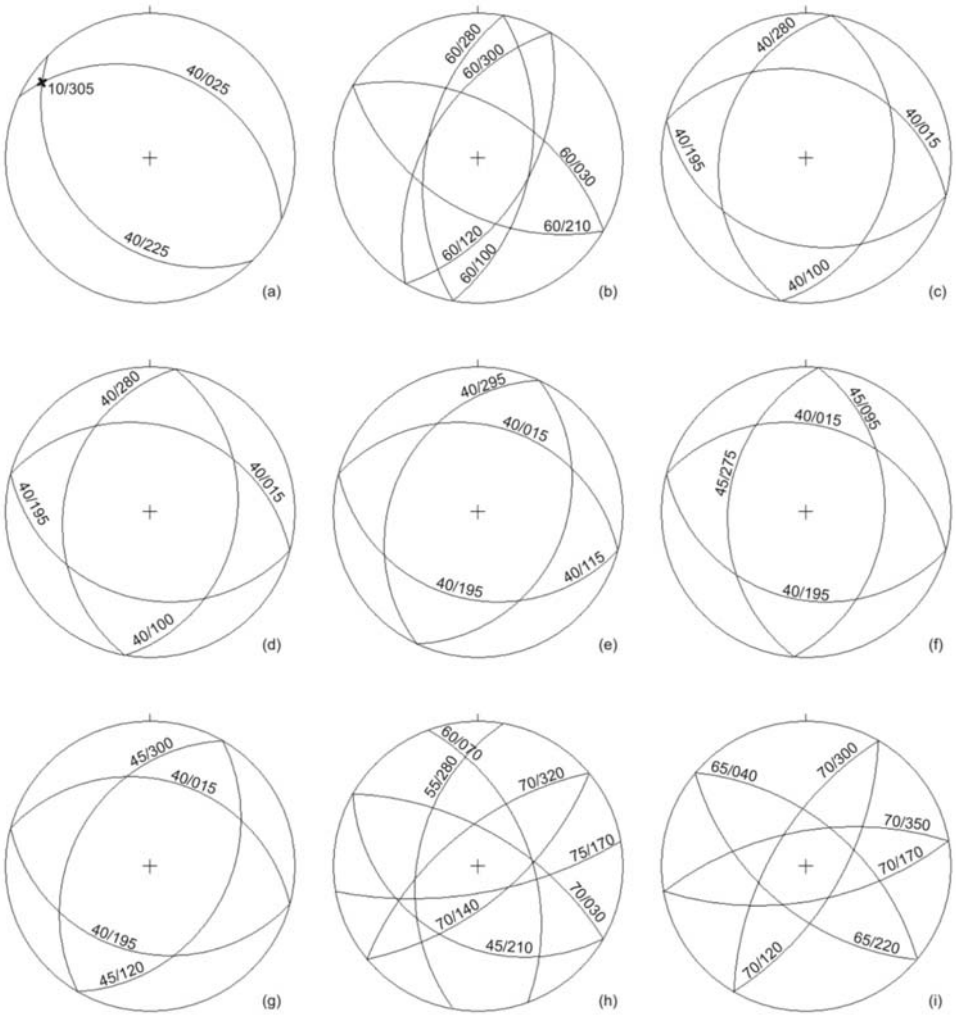

Fig 3: Schmidt stereograms and the mean values for Carbonates: a) The mean bedding planes and the fold axis, b) The three major joint systems. Volcanosendimentary formation: c) Schistocity planes, d) thrusts. Schistosed serpentinites and serpentinites: e) Schistocity. Serpentinized hartzbourgites: f) Schistocity, g) Shear zones, h) joint systems. (i) Faults.

3. Structural Analysis

Detailed structural analysis showed that the study area is characterized by tectonic features that were developed both within a compressive and extensional tectonic environment, including various qualitative and quantitative characteristics that relate to the different deformation phases that these rocks experienced through time. Tectonic analysis defined the directions and dip of the strata or the schistosity, geometric features of folding (fold axis, strike, dip and plunge direction), strike and dip of thrusts and shear zones, joints and faults. Statistical elaboration of the data is presented in the following Schmidt stereograms and the mean values are displayed separately for each alpine formation (Fig. 3).

3.1 Alpine formations

a) Carbonate basement unit. The carbonate basement unit comprises mostly of thick-bedded or non stratified limestones so that no strata are clearly visible at its higher extend. Only towards the northern part of the study area strata dip at approximately 40° both towards NE (N025°) and SW (N225°), due to folding (Fig. 3a). At the same area, strata are intensely folded with inclined folds, whose fold axes plunge 10° towards N305°. Overall, these features imply that the carbonates were deformed during the Eo-alpine orogeny from a NNE up to NE directed compressional field. Three joints systems are recognized (Fig. 3b): a) N030°-N210° that dips 55°-65° both towards NW and SE, b) N010°-N190° that dips 55°-65° towards E and W and c) N300°-N120° that dips 60° towards NE and SW. The joint system that trends at N300°-N120° is developed along strike the major folding axes, whereas the E-W and N030°-N210° striking joint systems are transverse to the axes.

b) Nappe of the tectonovolcanosedimentary formations. This formation and predominantly the cherts are highly folded and fragmented. Only the schistocity could be defined. Two schistocity planes have been extracted (Fig. 3c): a) the primary at N285°-N105°, dipping 40° both towards NNE and SSW, and b) the secondary at N010°-N190° that dips towards 40°-45° both towards NW and SE. The N285°-N105° trending schistocity system is the predominant one covering almost 80% of the measurements, whereas the secondary one left a much weaker imprint. The N285°-N105° trending schistocity system is parallel and in agreement with the thrusts measured within the same formation (Fig. 3d). These imply that the volcanosedimentary formations experienced an intense compressional deformation at NNE direction that is almost parallel and in agreement to their thrusting direction on the underlying carbonate basement unit.

c) Schistosed serpentinites and serpentinites. Measurements delineate two schistocity planes (Fig. 3e): a) is trending N285°-N105°, dips 40° towards NNE and SSW and b) is trending N025°-N205°, dips 40° towards NW and SE. The main thrusts are aligned and parallel to the schistocity planes. Serpentinites are deformed in a boudinage style whose long axis is parallel to the schistocity plane.

d) Serpentinized hartzbourgites. Two main schistocity planes are trending at: a) N005°-N185° and dipping 45° towards W and E and b) N105°-285° dipping 40° towards NNE and SSW (Fig. 3f). Two main directions of shear zones are distinguished (Fig. 3g): a) N030°-N210° that dips 45° towards NW and SE and b) N105°-N285° that dips 40° towards NNE and SSW. Five main joint systems are recognized (Fig. 3h): a) N120°-N300° that dips 70° towards NE and 45° toward SW, b) N050°(±10°)-N230°(±10°) that dips 60°-75° towards NW and SE, c) N010°-N190° that dips 55° towards WSW, d) N340°-N160° that dips 60° towards ENE, e) N080°-N260° that dips 75° towards SSE.

3.2 Faults and Neotectonics

The study area is characterized by three major fault groups (Fig. 3i):

Group 1: It represents faults trending N310°-N130° and dip at 60°-70° towards the NE and SW. They are normal and oblique normal both with sinistral or dextral slip. The rake is higher than 65°.

Group 2: It represents faults trending N030°-N210° and dip at 60°-80° towards the NW and SE. They are normal and oblique normal both with sinistral or dextral slip. The rake ranges between 50°-65°.

Group 3: It represents faults trending approximately E-W (N080°-N260°) that dip 60°-80° towards N and S. These E-W trending steep normal faults bound the postalpine formations and thus the Reginio and Modi basins. They are active and form extensive zones whose thickness ranges from 100 to 500m, within which tens of smaller subparralel faults are developed.

Fault groups 1 and 2 intersect and deform only the alpine basement rocks. Faults of group 2 were initially activated as strike slip during the thrusting emplacement and later were reactivated during the early post-alpine era, whereas with the faults of group 1 controlled the geomorphology creating horsts and grabens. Faults of group 1 are parallel to the major neighboring NW-SE trending detachments of Beotikos-Kifissos and Aghios Konstantinos that outcrop southwards and northwards our study area. These low angle extensional faults were active during Upper Miocene-Lower Pliocene, formed the early postalpine basins and then were crosscut by the Upper Pliocene-Quaternary high angle E-W trending normal faults (Papanikolaou and Royden 2007). Thus, faults of group 3 are the youngest deform both the alpine and postalpine formations crosscut also the faults of groups 1 and 2, and form the present day deformation pattern (Roberts and Ganas 2000).

Towards the northern part of the study area the major Kallidromo fault zone dominates the geomorphological and the geological structure. It trends E-W (±15°) for at least 36km and forms the boundary between the alpine and the postalpine formations. It is an active fault, whose activity is evidenced also by the steep slopes towards the fault plane and the incised catchments that are perpendicular to the fault trace, draining the footwall block. Several breccia of various thicknesses are observed along strike the fault zone as well. Northwards the Kallidromo fault zone, the Reginio basin is developed parallel to the zone at a mean elevation of 150m. This basin northwards is related to the Sperchios basin, through the Kamena Vourla fault. The Kallidromo fault zone has a thickness of 300-500m, separates the alpine and the postalpine formations and comprises of a large number of parallel and subparallel faults. The fault plane dips at 75º to 80º northwards, downthrows the topography for at least 400m (from 700m to 300m elevation). The characteristics of the subparralel faults show that fault activity has now shifted northwards to the lower fault planes following a progressive hanginwall directed migration, which is a common feature in several active normal faults in Greece and elsewhere (e.g. Stewart and Hancock 1994). It displays all characteristics of active faulting such as free face and a cataclastic zone of approximately 5m. It is also probable that the extensive sliding of the ophiolites within the post-alpine formations can be attributed to the initial activity of this fault zone.

The southern part in Modi Basin forms a step-by step monoclinal structure that gradually subsides the area from the 600m to approximately 150m elevation up to the Beotikos Kifissos basin. All faults that are NE-SW trending are considered inactive, except the fringe fault towards the southern part of the Kallidromo Mt. This fault towards its early history bounded the alpine formations. However, it is interesting to note that this structure influenced the conglomerates as well. Indeed, along strike its trace the conglomerates have been ruptured and several small offsets (1-2m) have been observed, followed by a gradual decrease of their thickness. The fault plane dips at 75º towards the SE (150º). The ruptured breccia-conglomerates shows: a) a significant right lateral sense of movement so that the fault can be characterised towards this locality as an oblique normal fault; b) that it is an active structure since these breccia were formed during the Upper Pleistocene. The open fractures that are perpendicular to the fault trace also support the above. Herein, it should be noted that despite their active characteristics, no strong historical events were recorded towards the southern part of the Kallidromo Mt. This implies that the faults are probably of low slip-rate so that their reccurrence intervals have exceeded the length of the historical catalogue.

4. Discussion - Conclusions

A significant mass of ulrtramafic rocks in the Kallidromo Mt, with substantial differentiations both lithological and tectonic has been thrusted on top of the Mesozoic platform, producing an extended

mélange during the Eo-Alpine orogeny. The deformation along this thrust can also be traced through the extensive approximately E-W trending shear zones towards the lower ophiolitic members (schistosed serpentinites). The latter indicates a prolonged emplacement process, and it is highly probable that this boundary was reactivated during the alpine orogeny as well.

Overall, the above measurements clearly show that two distinct deformation phases (D1, D2) are traced. Deformation D1 relates to the Upper Jurrasic-Lower Cretaceous ophiolitic emplacement and is the predominant feature over the entire study area. Fold axes, the predominant schistocity planes and shear zones clearly follow a N295^{o}(±10^{o})-115^{o}(±10^{o}) trend. The approximately 20^{o} difference of the deformation axis between the carbonates (~305^{o}) and the overlying nappes (~285^{o}) demonstrates that an anticlockwise rotation occurred during the ophiolitic emplacement, indicating a prolonged emplacement process, that is also confirmed by the prevailing D1 deformation phase in the deformed rocks. Deformation D2 relates to the Cretaceous-Eocene alpine orogeny and follows a N020^{o}(±15^{o})-N200^{o}(±15^{o}) trend. This deformation has a much weaker imprint in the study area. In particular, it is not traced in the carbonates and the thrusts of the area as the D1 does. Moreover, D2 created the secondary schistocity plane and shear zone directions. The latter are also confirmed in the neighboring Eastern Chlomon locality, whereas the D2 phase clearly affects only the transgressive Cretaceous-Eocene sequence and refolds the E-W trending thrusts and axes of the Eo-alpine phase below the Cenomanian unconformity (Papanikolaou 2009). D2 in Easter Chlomon deforms the Upper Cretaceous and the Paleocene-Eocene flysch and thrusts follow a NNE-SSW to NE-SW trend. Similar D1 and D2 phases are also traced in the neighboring eastern Othris mountain and a similar 10^{o}-15^{o} anticlockwise rotation during the nappe emplacement of the D1 phase has also been observed ((Migiros 1990). This N020^{o}(±15^{o})-N200^{o}(±15^{o}) trend of the Alpine deformation phase D2, is almost perpendicular to the usual NW-SE alpine trend. The latter implies that the entire region from the Chlomon (Papanikolaou 2009), to Kallidromo (current study) and eastern Othris (Migiros 1990) are part of a block that experienced more or less similar post-Eocene rotations.

The post-alpine formations (Upper Pliocene to Holocene) rest uncomformably on the alpine ones and cover the Reginio and Modi basins. The Upper Pliocene-Upper Pleistocene formations comprise mostly clastic sediments of river and lake origin and are characterized by significant lateral changes in composition and thickness, demonstrating that their depositional processes were highly variable. The latter indicates that sedimentation was disrupted and controlled by the tectonic processes that occurred during the formation and initial deepening of the early post-alpine basins. Figure 2b shows this differentiation of the post-alpine sediments between the Reginio and Modi basins, reflecting also the diverse neotectonic environments in both basins.

Three extensional fault groups have been defined. Faults of group 1 (N310^{o}-N130^{o} trending) correlate to the early detachment related extensional phase of Upper Miocene-Lower Pliocene. Faults of group 2 (N030^{o}-N210^{o} trending), were initially acted as strike slip and then reactivated as normal. Finally, group 3 represents the present-day approximately E-W trending (N080^{o}-N260^{o}) high angle active normal faults that express the present-day deformation field, whereas the Kallidromo fault zone that bounds the Reginio basin forms the predominant such active structure in our study area. It is suggested that the Kallidromo is part of an E-W to ENE-WSW trending major structure, whose activity has progressively been shifted northwards towards the Kamena Vourla.

5. References

Aubouin, J., 1959. Contribution a l′etude geologique de la Grece septentrionale: les confins de l'Epire et la Thessalie. *Ann. Geol. Pays Hell.*, 10, 1-484 Athenes.

Bernoulli, D. and Laubscher, H., 1972. The palinspastic problem of the Hellenides. *Eclogae geologicae Helvetiae*, 65, 107-118.

Brunn, J.H., 1956. Contribution à l'étude géologique du Pinde septentrional et d'une partie de la Macédoine occidentale. *Ann. Geol. Pays Hellen.,* 7, 1-358.

Celet, P., 1962. Contribution a l'étude géologique du Parnasse-Kiona et d'une partie des régions méridionales de la Grèce continentale. *Ann. Geol. Pays Hellen.,* 13, 1-446, Athènes.

Clement, B., 1977. Relations structurales entre la zone du Parnasse et la zone Pélagonienne en Béotie (Grèce continentale). VI Colloquium on the Geology of the Aegean Region, Edit. G. Kalergis, IGME, 237-245, Athens.

Coleman, R.C., 1977. Ophiolites-ancient oceanic lithosphere. 229, Springer, Berlin/Heidelberg/New York.

Faupl, P., Pavlopoulos, A., Wagreich, M., Migiros, G., 1996. Pre-Tertiary blueschist terrains in the Hellenides: evidence from detrital minerals of flysch successions. *Terra Nova*, 8, 186-190.

Ferriere, J., 1982. Paléogéographies et tectoniques superposées dans les Hellénides internes au niveau de l' Othrys et du Pélion (Grece). Thèse, sciences, Univ. Lille et Soc. Geol. Nord. Publ. No 8, 970p., Lille.

Fleury, J., 1980. Les zones de Gavrovo-Tripolitsa et du Pindos – Olonos (Grece continentale et Péloponnèse du Nord). Evolution d' une plateforme et d' un bassin dans leur cadre alpin. *Soc. Geol. Nord.*, 4, 651p., Lille.

Ganas, A., 1997. Fault segmentation and seismic hazard assessment in the Gulf of Evía ríft, Central Greece. Unpub1. *PhD Thesis*, Univ. of Reading, 369 p.

Goldsworthy, M. and J. Jackson, 2001. Migration of activity within normal fault systems: examples from the Quaternary of mainland Greece. *J. Struct. Geol.* 23, 489-506.

Jacobshagen, V., 1986. Geologie von Griechenland.Berlint:Gebrüder Borntraeger, 363 p.

Jones, G. and Robertson, A.G.F., 1991. Tectono-stratigraphy and evolution of the Mesozoic Pindos ophiolites and related units, Northwestern Greece. *J. Geol. Soc. London*, 148, 267-288.

Karipi, S., Tsikouras, B., Hatzipanagiotou, K. and Grammatikopoulos, T.A., 2007. Petrogenetic significance of spinel-group minerals from the ultramafic rocks of the Iti and Kallidromon ophiolites (Central Greece). *Lithos* 99, 136-149.

Katsikatsos, G., Migiros G., Triantaphylis M., Mettos A., 1986. Geological structure of Internal Hellenides (E. Thessaly, SW Macedonia, Euboea-Attica-Northern Cyclades Islands and Lesvos). Geol. & Geoph. Res., Special Issue, I.G.M.E., 191-212, Athens.

Kranis, H.D., 1999. Neotectonic activity of fault zones in Lokris, central-eastern mainland Greece. *PhD thesis*, University of Athens, 234p.

Migiros, G., 1990. The lithostratigraphic – tectonic structure of Othris (Central Greece). *Bulletin of the Geological Society of Greece* XXVI, 107-120 (in Greek).

Mountrakis, D., Sapounzis, E., Kilias, A., Eleftheriadis, G. and Christofides, G., 1983. Paleogeographic conditions in the western pelagonian margin in Greece during the initial rifting of the continental area. *Can. J. Earth Sci.*, 20, 1673-1681.

Papanikolaou, D., 1989. Are the Medial Crystalline Massifs on the Eastern Mediterranean drifted Gondwanian fragments? *Sp. Publ. Geol. Soc., Greece*, 1, 63-90.

Papanikolaou, D., 2009. Timing of tectonic emplacement of the ophiolites and terrane paleogeography in the Hellenides. *Lithos* 108, 262-280.

Papanikolaou, D. and Royden, L., 2007. Disruption of the Hellenic arc: Late Miocene extensional detachment faults and steep Pliocene-Quaternary normal faults – or – What happened at Corinth? *Tectonics*, 26, TC5003, doi:10.1029/2006TC002007.

Phillip, H., 1974. Etude néotectonique des ravages egeens en Locride et en Eubée nord-occidentale (Grèce). Thèse de 3o Cycle, Univ. des Sciences et Techniques du Languedoc, Montpellier, 86p.

Papastamatiou, I., Tataris, A., Vetoulis, D., Katsikatsos, G., Lalechos, N., and Eleftheriou, A., 1962. Geological Map of Greece, 1:50.000 scale Amfiklia Sheet, IGME.

Roberts, G.P. and Ganas, A., 2000. Fault-slip directions in central-southern Greece measured from striated and corrugated fault planes: comparison with focal mechanism and geodetic data. *J. Geophys. Res.*, 105, 23,443-23,462.

Smith, A.G. and Woodcock, N.H., 1976. Emplacement model for some "Tethyan" ophiolites. - *Geology*, 4, 653-656.

Stewart, I.S. and Hancock, P.L., 1994. *Neotectonics*. In continental deformation Hancock, P.L. (ed), Pergamon Press, 370-409.

Δελτίο της Ελληνικής Γεωλογικής Εταιρίας, 2010
Πρακτικά 12ου Διεθνούς Συνεδρίου
Πάτρα, Μάιος 2010

Bulletin of the Geological Society of Greece, 2010
Proceedings of the 12th International Congress
Patras, May, 2010

CRUSTAL MOVEMENTS ALONG THE NW HELLENIC VOLCANIC ARC FROM DGPS MEASUREMENTS

Papageorgiou E.,

University of Athens, Department of Geophysics and Geothermy, Zografou 15784, Greece, epapageo@uoa.gr

Abstract

The north-western part of the Hellenic Volcanic Arc was studied by Differential GPS measurements in an attempt to investigate the regional deformation of the area. The GPS network involving stations in Athens, Aegina Island, Methana Peninsula and Soussaki was established in February 2006 and since then it was reoccupied twice. The GPS measurements were primarily referred to World-fixed reference frame (ITRF2000) and then to Europe and Athens as well. The observed velocities for the overall three-year spanning period according to Athens station showed rates at the order of 7-10 mm/yr, while the directions of the displacements tend towards NNW to NNE. The results of the horizontal velocities with respect to Europe indicate rates of SW directions, exhibiting higher magnitudes (25-26±2mm/yr) in the western and southern part of the Saronikos Gulf than in its central part (20±7 mm/yr). The horizontal velocities with respect to ITRF2000 showed consistent SE directions with higher rates in Aegina (12±7 mm/yr) than in Soussaki and Methana (9±3 mm/yr). A kinematic interpretation based on velocity and strain rates is finally attempted on the basis of the regional tectonics in the Saronikos Gulf.

Key words: *NW Volcanic Arc, Saronikos, GPS-velocity, tectonics, kinematics, strain.*

1. Introduction

The NW Volcanic Arc has drawn our attention for research over the last 3 years due to its unique position, as being close to high populated areas, such as Attica, Corinth and Argolida. It is part of the Hellenic Volcanic Arc and has developed in the regional back-arc area of Saronikos Gulf, featuring a variety of volcanic fields. The referring volcanoes of Aegina, Methana and Soussaki (Fig. 1) manifested volcanic activity in Pliocene and Pleistocene times, while historical eruptions were recorded only in Methana (Strabo, Geographica). Submarine volcanic intrusions were also observed in the vicinity of NW Methana, defining the Pavsanias Volcano (Pavlakis et al., 1990). Tensional tectonics and sufficient crustal thickness are the major factors controlling the ascent of the magmas (Dietrich et al. 1988).

Several active faults have been recognized in the regional area of Saronikos (Makris et al., 2004). Yet, the seismicity which follows the main faulting zones is low (Drakatos et al., 2005). On the contrary, strong historical (Papadopoulos et al., 2000) and recent earthquakes (Makropoulos et al., 1989; Papazachos & Papazachou, 1997) have occurred mainly in the western and northern boundaries of the basin, all associated with a roughly N-S extensional tectonic regime.

The crustal deformation in Saronikos Gulf is considered to be fairly complex with block rotations,

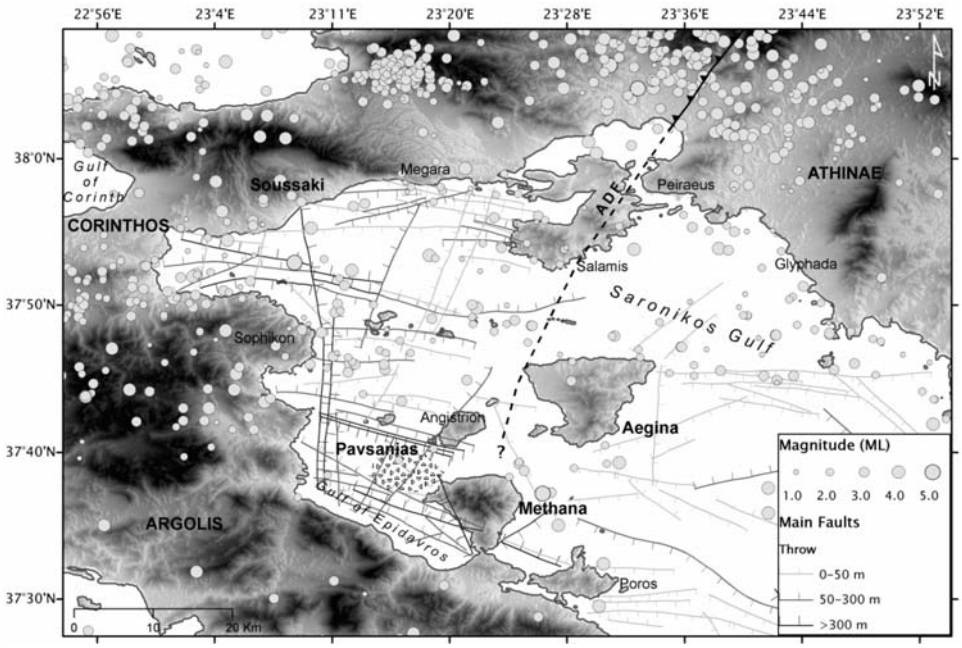

Fig. 1: Seismic activity (1950-2009, AUTH) and major tectonic faults in Saronikos Gulf (from Papanikolaou et al., 1988), at the NW stretch of the Volcanic Arc (Aegina-Methana-Soussaki). ADF: Attica Detachment Fault (Papanikolaou & Royden 2007).

normal faulting and crustal fragmentation (Le Pichon & Angelier 1979; McKenzie 1978; Rotstein 1985). Saronikos Gulf has rather affected by the neotectonic mechanisms acting between the West Hellenic subduction and the Anatolian westward drift. Extensive investigation on the regional deformation of Saronikos Gulf was attempted in this paper. GPS measurements were conducted from 2006 to 2009, in order to provide adequate information on the kinematic characteristics of the studied area. For that reason, a GPS network (SARNET) was established at the volcanic centers of Aegina, Methana and Soussaki as well as in Attica Peninsula. The detection of relative movements was finally allowed as the obtained time series of the measured points provide comparably high accuracy of a few mm/yr.

Therefore, the current kinematic field of crustal motion in Saronikos Gulf, based on repeated GPS observations, is analyzed in terms of velocity and strain rates. From these results a first assessment of the kinematic implications is given in light of tectonic and seismological data.

2. Regional Tectonics

The NW Volcanic Arc lies on Saronikos Gulf with the Pliocene volcanics of Aegina and the Pleistocene of Methana and Soussaki. The neotectonic basin of Saronikos exhibits a tensional regime with the formation of tectonic grabens by normal faulting (McKenzie 1978; Mercier 1979; Le Pichon & Angelier 1979; Dewey & Sengor 1979). In this view, it appears to have a rather complicated structure with different neotectonic styles and the presence of the recent volcanoes in the central part. A western and an eastern part are separated by a very shallow N-S platform at the islands of Methana, Aegina, Angistri and Salamis (Fig. 1). This boundary probably reflects the continuation of

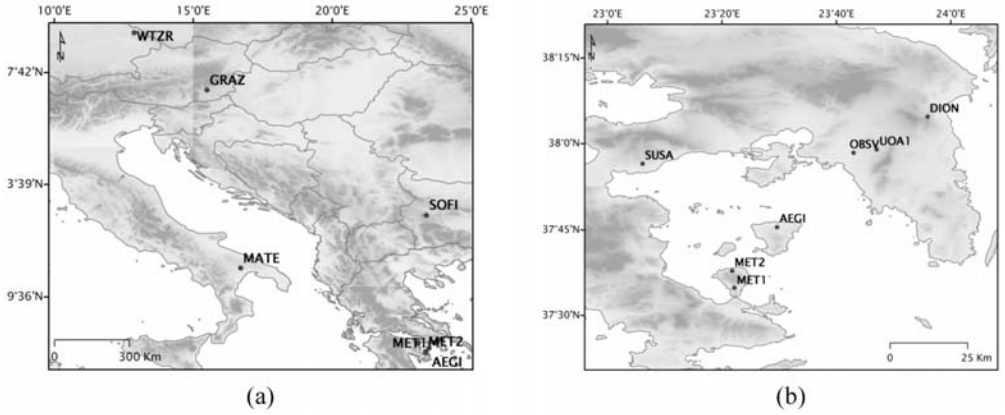

Fig. 2: (a) Locations of IGS and SARNET sites included in the GPS evaluation, (b) Locations of SARNET sites in detail.

the major NNE-SSW trending detachment fault that divides Attica Peninsula to the metamorphic units towards the east from the non-metamorphic units towards the west (Papanikolaou et al., 2009).

Each of the basins developed different fault patterns and displacements, sediment distribution (Papanikolaou et al., 1988) and seismicity (Makropoulos & Burton, 1981; Bath, 1983). Due to the different structure, the western part is characterized by higher seismic activity than the eastern one. Moreover, the Western Saronikos Gulf is divided in a northern and a southern part by a well-defined E-W trending fault zone which seems to be the continuation of the Corinthiakos Gulf fault zone.

At the depth of 17 km the velocity increases considerably and the crustal thickness is restricted up to 20 km. This noticeable low thickness in the region of Saronikos Gulf seems to be the result of the extensional stress field, which dominates the region, as well as of the emergence of mantle material along the NW volcanic arc, which clearly appears at the depth of 12 km (Drakatos et al., 2005).

3. Microseismicity Setting

In order to correlate the seismicity with active faulting in Saronikos Gulf, the seismic information mentioned in this paper is best described by Makris et al. (2004). The earthquake foci are located at two different depths, indicating the existence of two regional stress fields that dominate the Hellenides. The first cluster is concentrated at crustal levels and is related to extensional stresses of the upper crust, while the second concentration of hypocenters is observed at deeper sub-crustal levels. The deeper seismicity is associated with the NE-subduction of Ionian oceanic plate below Greece mainland (Leydecker, 1975; Makropoulos, 1978; Makris & Roever, 1986).

Seismicity in Saronikos Gulf follows distinct tectonic features. Significant seismic activity is observed along the E-W-trending fault which divide Western Saronikos, and in between the Islands of Salamis and Aegina (Fig. 1). In addition, two clusters of epicenters are identified to the NE and east of Aegina, following the NE-SW and E-W orientated faulting structures respectively (Fig. 1). However, below Methana and Aegina volcanic centers deeper events have been registered, implying no evidence of seismic correlation with magmatic and hydrothermal processes (Makris et al., 2004).

Table 1. Site names, coordinates and years of occupation of SARNET (5-8 days per campaing).

GPS Station	Site	Long. (°)	Lat. (°)	Height (m)	Occupation (yr)
AEGI	Aegina	23,49	37,75	234	2006.14, 2007.78, 2008.55
MET1	Methana	23,37	37,58	187	2006.14, 2007.78, 2008.55
MET2	Methana	23,36	37,63	334	2006.14, 2007.78, 2008.55
OBSV	National Observatory of Athens	23,71	37,97	137	2006.14, 2007.78, 2008.55
SUSA	Soussaki	23,10	37,94	241	2006.14, 2007.78, 2008.55
UOA1	University of Athens	23,78	37,98	306	2007.78, 2008.55

Table 2. Site names, coordinates of IGS continuous stations included in GPS evaluation. DION located in Greece was also used as a reference station.

GPS Station	Site	Long. (°)	Lat. (°)	Height (m)
GRAZ	Graz	15.4935	47.0671	538
MATE	Matera	16.7045	40.6491	536
SOFI	Sofia	23.3947	42.5561	1120
WTZR	Wettzell	12.8789	49.1442	666
DION	Dionysos	23.9326	38.0785	515

4. GPS Observations

In order to reveal the kinematic field of the NW Volcanic Arc, Differential GPS measurements were carried out from 2006 to 2009. A GPS network (SARNET) was established for the first time in February of 2006 at the volcanoes of Saronikos (Aegina, Methana and Soussaki) and Attica Peninsula (Fig. 2). Stations were installed by emplacing benchmarks (bronze pins having head-diameter of 2.5 cm) on the ground surface of carboniferous and volcanic rock formations. However, in the absence of bedrock in Soussaki the station was established on the concrete surface of an old construction. The network extending from Athens to the north, Soussaki to the west and Methana to the south was reoccupied two times since 2006, in October of 2007 and August of 2008. All DGPS measurements were made in the static mode using tripods above the benchmarks. Geodetic, dual frequency WILD receivers (SR299 and SR399) were employed for all measurements. Due to the long baselines of the network (30-54 km), all stations operated continuously for nearly a week with a sampling interval of 30 sec.

Stations names, epochs of measurements and approximate site coordinates are listed in Table 1.

To ensure a stable consistent reference frame, the data of Saronikos were evaluated together with those of IGS (*International GPS Service*) sites mainly located in Europe. For this process five IGS

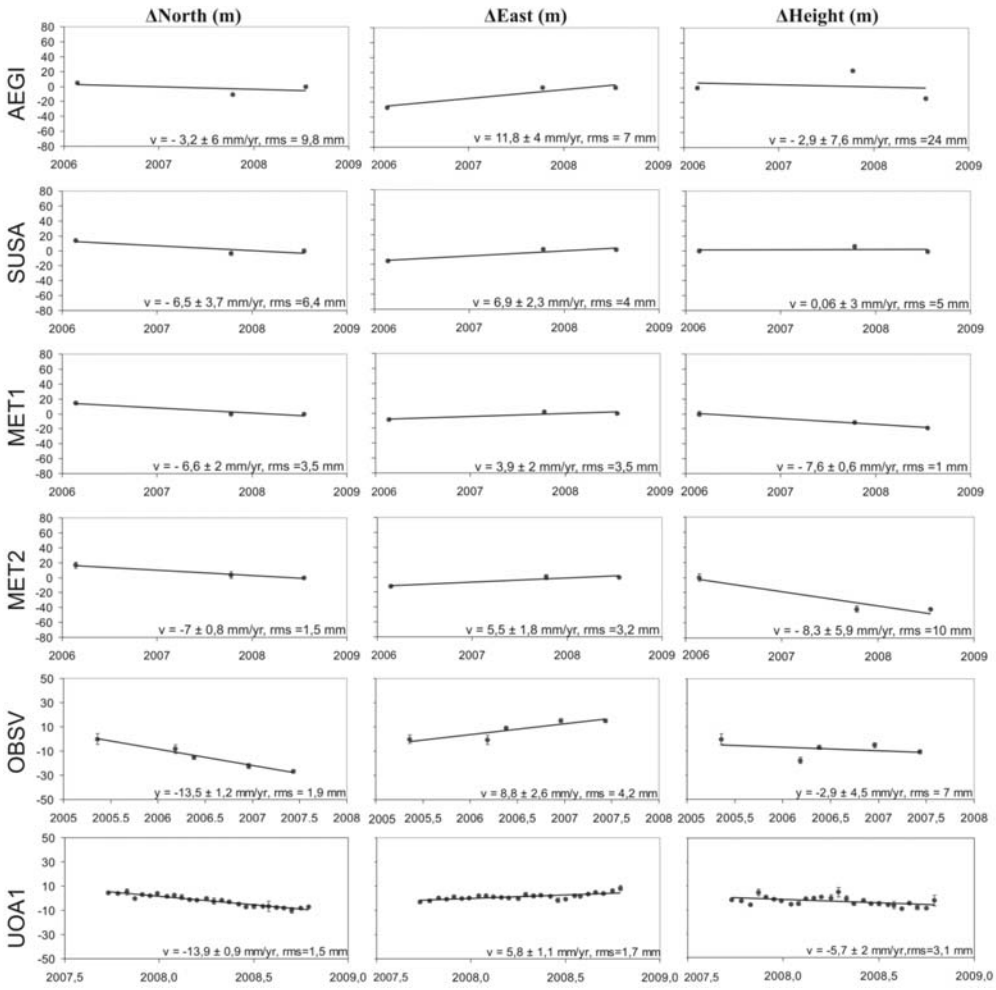

Fig. 3: GPS time series of campaign coordinates (ITRF2000) of Saronikos network.

sites were selected to define the reference frame. The locations of the included IGS sites are shown in Fig. 2. Station names, approximate coordinates are listed in Table 2. The observation data as well as site information (coordinates, receiver and antenna types) were downloaded directly from the IGS server.

The software used for the GPS processing was the *Bernese GPS Software* (BSW) version 4.2, of the Astronomical Institute - University of Berne AIUB (Beutler et al., 2001). An important point of the processing refers to the consistency of the reference frame. In order to obtain really consistent results, site coordinates and velocities, as well as satellite orbits and earth rotation parameters used for the processing were in the same reference frame ITRF2000 (Altamini et al., 2002; Boucher et al., 2004). The final results concerning the overall monitoring period of crustal motion in Saronikos Gulf, are presented below, in terms of velocities with accuracies of a few mm/yr.

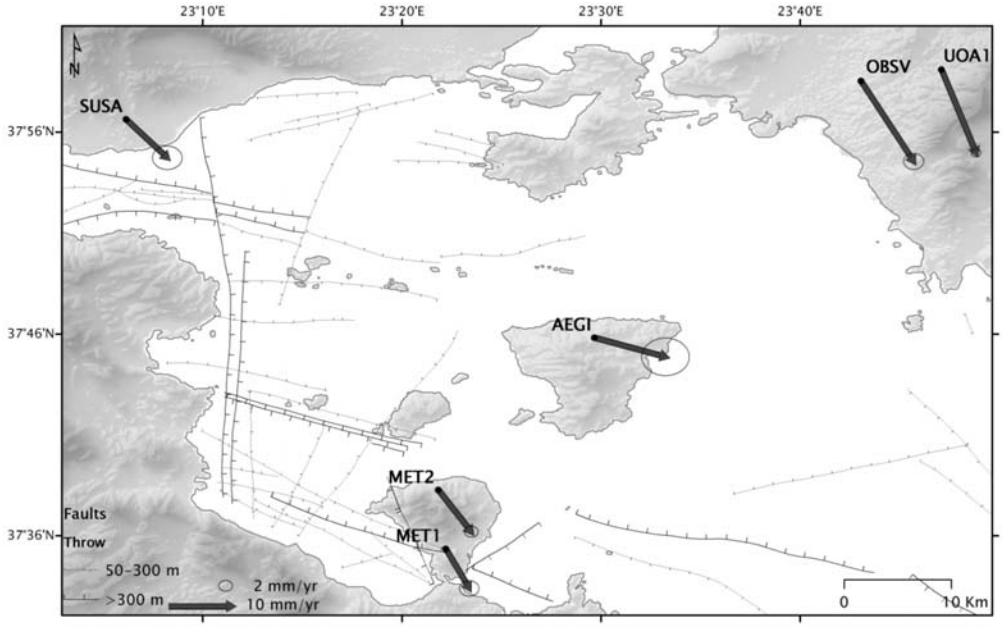

Fig. 4: Velocities with respect to ITRF2000, for the period 2006-2009.

Table 3. Velocities and corresponding precision with respect to World, Europe and Athens, for the period 2006-2009 (in mm/yr).

	ITRF		ETRF		ATHENS					
GPS Station	V_E	V_N	V_E	V_N	V_E	V_N	V_U	σ_E	σ_N	σ_U
AEGI	11.8	-3.2	-11.7	-15	3	10.3	-2.9	4	6	7.6
SUSA	6.9	-6.5	-16.7	-18.3	-1.9	7	0.1	2.3	3.7	3
MET1	3.9	-6.6	-19.7	-18.4	-4.9	6.8	-7.6	2	2	0.6
MET2	5.5	-7	-18.1	-18.8	-3.3	6.5	-8.3	1.8	0.8	5.9
OBSV	8.8	-13.5	-14.8	-25.3	-	-	-2.9	2.6	1.2	4.5
UOA1	5.8	-13.9	-17.8	-25.7	-3	-0.4	-5.7	1.1	0.9	2

The time series of campaign coordinates refer to ITRF2000 (*International Terrestrial Reference Frame, ITRF*). The velocity v of each site, as well as the corresponding coordinate precision (rms) was calculated by weighted linear regression over the campaign coordinates (Fig. 3). The rates of all sites are listed in Table 3, while Fig. 4 displays the horizontal velocities with respect to World. The velocity vectors indicate consistent direction towards the SE for the entirety of the stations. The highest velocity in Saronikos is observed at Aegina Volcano (12.3 ± 7 mm/yr), inasmuch as the lower rates at Soussaki (9.4 ± 4.4 mm/yr) and Methana (8.9 ± 2 mm/yr) volcanic areas. Athens sites display higher rates at the order of 16 ± 3 mm/yr.

Velocities were also computed with respect to Europe, by adding the mean velocity of the European plate (Peter, 2000). The highest velocities are observed yet again in Athens (Table 3), while in Saronikos region, Methana and Soussaki represent higher rates than Aegina. MET1, MET2 and SUSA

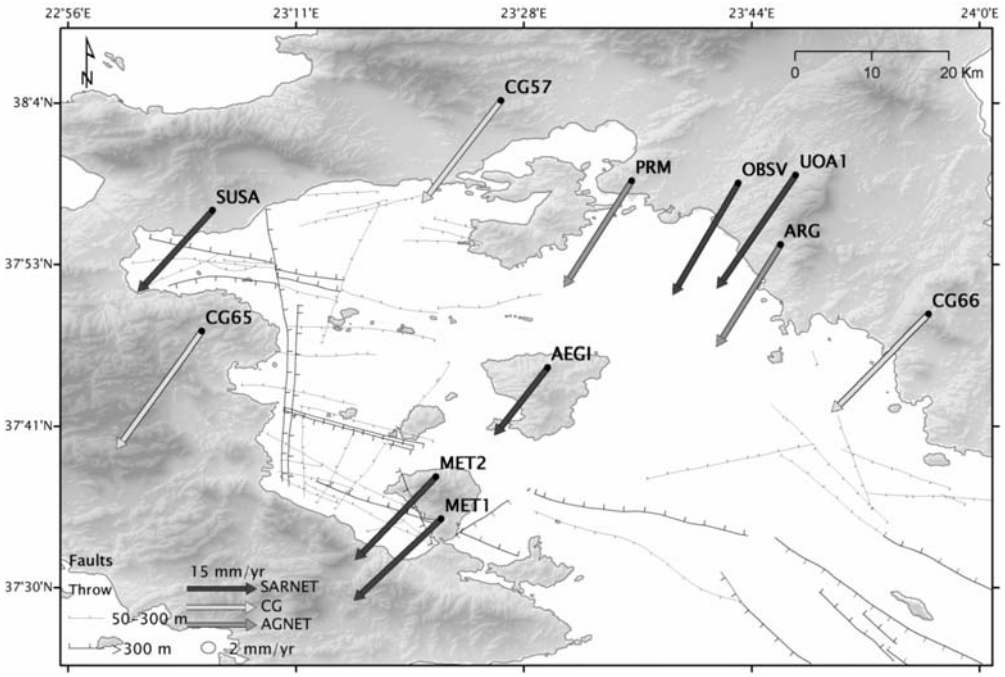

Fig. 5: Velocities with respect to Europe, for the period 2006-2009. Additional velocities used as input for the strain rate calculation are illustrated, belonging to nearby existing networks (CG: Clarke et al., 1998; AGNET: Foumelis, 2009).

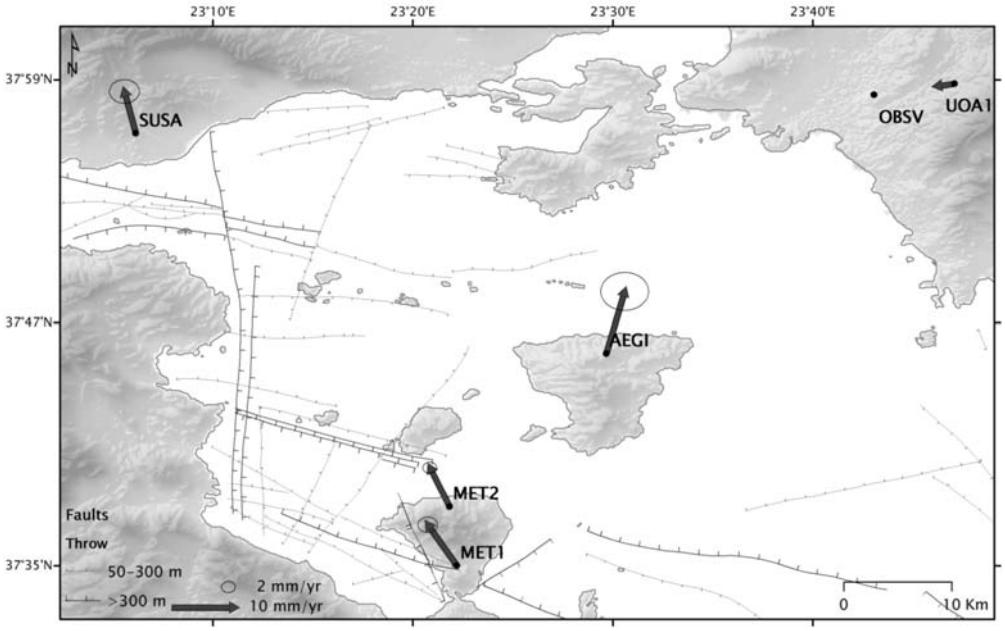

Fig. 6: Velocities with respect to Athens (OBSV), for the period 2006-2009.

sites show almost equal velocities ranging between 25-27 mm/yr. AEGI site deviate from the rest Saronikos network by 6-8 mm/yr, indicating a different motion in the central part of the gulf. The horizontal velocities relative to Europe are shown in Fig. 5, where a general SW-ward direction of motion is observed for the whole network.

The velocities which were calculated with respect to Athens (OBSV site) underline the differentiation of AEGI site among the rest of the network. The southern (MET1-2 sites) and western (SUSA site) borders of the Saronikos Gulf show the same NW trending motion, in contrast to the central part (AEGI site) which exhibits different motion towards the NNE (Fig. 6). Additionally, MET2 and SUSA sites show equal rates of motion (7.3 mm/yr), while AEGI site is moving with higher rates of approx 11 mm/yr (Table 3).

The vertical motion of the network indicates a general subsidence both in Saronikos and Athens regions (Table 3). Southern Saronikos exhibits the highest subsidence with approximate rates -8 mm/yr. AEGI site denote the same velocity with OBSV site (-3 ± 4.5 mm/yr), whereas at the same time SUSA site, bordering the Western Saronikos appears fairly stable with insignificant motion.

5. Strain Rate Field

The strain rate field was based on horizontal velocity rates shown in Fig. 5. For additional constraints, velocity rates belonging to adjacent networks were also included during the strain analysis. Hence, three sites (CG57, CG65 & CG66) of the Central Greece (CG) network determined by Clarke et al. (1998), and two sites (PRM & ARG) of the Athens local network (AGNET) determined by Foumelis (2009) were included. The azimuthal distribution of all sites at the periphery and inward the Saronikos Gulf was appropriate to ensure more accurate results due to the weighted distance between the stations, over and above the network centroid (centre of the mass) used as a reference point in the strain calculation.

In particular, the strain rate calculation was performed by *grid_strain* software package (Teza et al., 2008). It allowed the definition of one single deformation tensor over the whole studied area. Under the hypothesis of a uniform strain field condition, the velocity gradient components with the correspondingly errors were estimated by a least-squares adjustment (Shen & Jackson, 2000). The data affected by larger uncertainties had a smaller effect on the strain computation. Finally, the principal axes of the strain tensor ε_{max} and ε_{min} were estimated, adapting three different scenarios: a) in the first case all sites were involved during the strain computation (Fig. 7), b) in the second case, the strain computation was held independently for western and eastern Saronikos selecting different baselines at each time; therefore, sites AEGI, PRM, SUSA, CG57-65 and MET1-2 were included for the western part-case, and accordingly sites OBSV, UOA1, ARG and CG66 for the eastern one (Fig. 8), and to end with case c) sites SUSA, AEGI and MET1-2 were taking into account for the strain calculation (Fig. 9).

The strain rate results which are presented in Figs. 7-9 mainly confirm the following:

- Along the whole Saronikos Gulf, compression (up to 209 ± 22.6 nstrain/yr) with almost N332° orientation is calculated, and an almost negligible extension along the perpendicular direction. As a result, a dilatation strain (rate) of -203 nstrain/yr and a total shear strain (rate) of 215 nstrain/yr were calculated (Fig. 7).
- Western Gulf shows extension (up to 102 ± 54.8 nstrain/yr) with N67° orientation and compression (up to 155 ± 13.3 nstrain/yr) with 337° orientation. As a result, a dilatation strain (rate) of -53 nstrain/yr and a total shear strain (rate) of 257 nstrain/yr were calculated (Fig. 8).

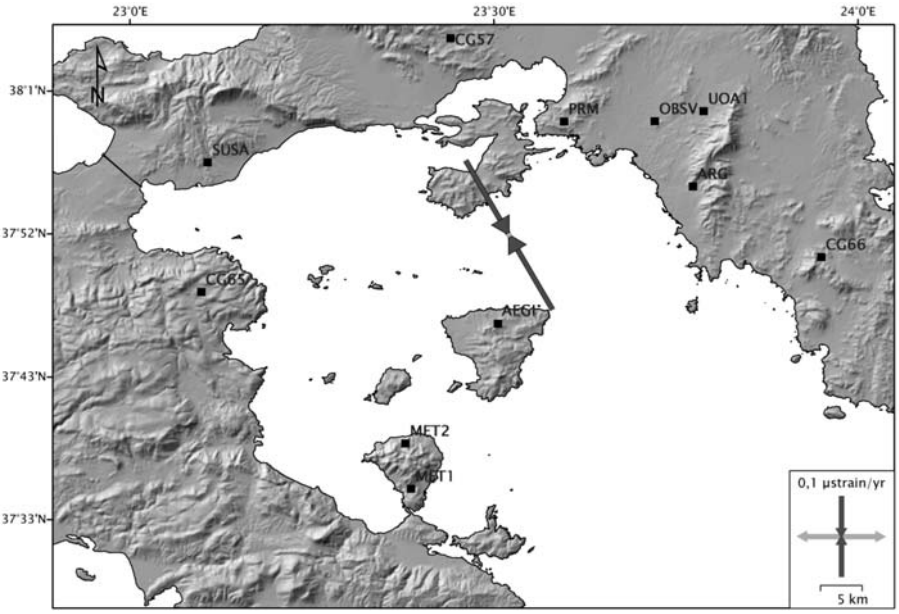

Fig. 7: Principle axes of the strain rate tensor calculated from the velocity field shown in Fig. 5, for Saronikos Gulf on the whole. Dark grey arrows indicate compression, light grey arrows extension.

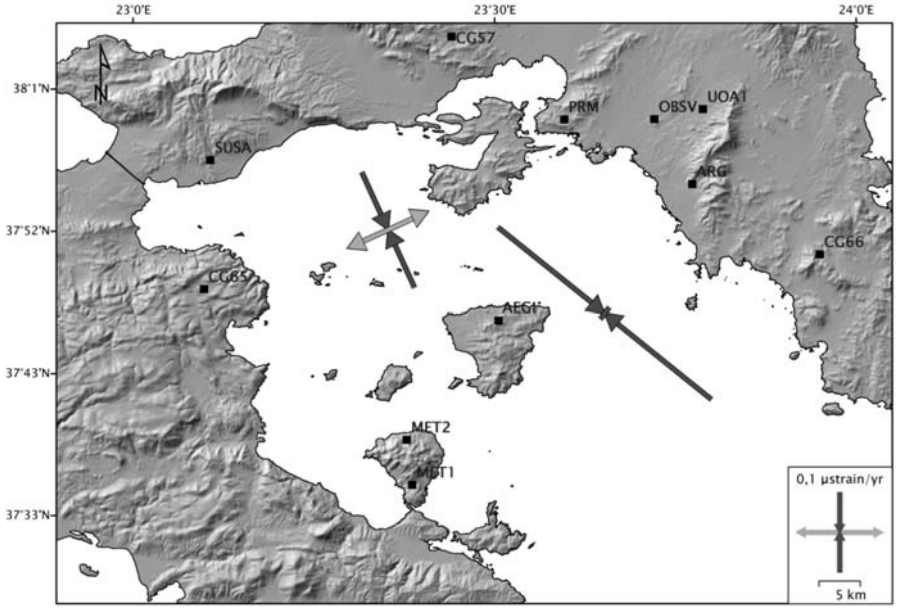

Fig. 8: Principle axes of the strain rate tensor calculated from the velocity field shown in Fig. 5, for the Western and Eastern Saronikos. Dark grey arrows indicate compression, light grey arrows extension.

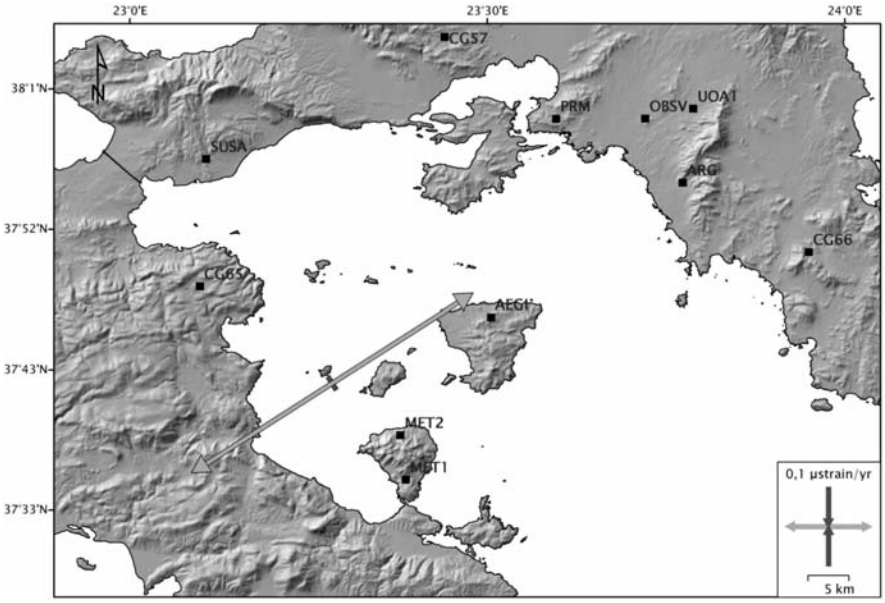

Fig. 9: Principle axes of the strain rate tensor calculated from the velocity field shown in Fig. 5, for the Western Saronikos (sites SUSA, AEGI, MET1, MET2). Dark grey arrows indicate compression, light grey arrows extension.

- Eastern Gulf shows compression (up to 330 ± 3.4 nstrain/yr) with N 311° orientation (Fig. 8).
- Central to South Western Saronikos shows extension (up to 402 ± 36 nstrain/yr) with N59° orientation and secondary compression (up to 20 ± 5 nstrain/yr) along the perpendicular direction (Fig. 9).

The observed compression - extension indicates roughly the same orientation as it is shown in earlier studies (Hollenstein, 2006; Clarke et al. 1998)**.** Still, comparison could be inferred only in the orientation and in the relative motion along the Saronikos Gulf and not to the deformation rates due to the different network spatial extent. Finally, the results indicate both extensional and compressional deformation field along the Saronikos Gulf, whereas higher rates of extension is observed at Western Saronikos, conversely to the compression occurring at Eastern Saronikos.

6. Conclusions-Results

The establishment of a local geodetic network around the Saronikos Gulf enabled the study of its kinematic characteristics based on GPS velocities and strain rate estimation. A first assessment of the kinematic constraints was held, taking into account the tectonic setting and the seismological information of the area.

The results of the DGPS analysis coincide with previous geological (Papanikolaou et al., 1988), seismological and tomographic (Drakatos et al., 2005) findings that divide Saronikos in two different basins. The western part, a region of active tectonic structures, extensional stress field and the presence of current volcanoes, includes MET1, MET2 and SUSA sites, howbeit presents a homogeneous kinematic pattern with consistent motion. The eastern part internally of the current volcanic arc, with volcanoes of Pliocene age, the more solid non-faulting structures and the minor

deformation includes AEGI site, which indicates another trend of motion comparing with the rest of the network. The major detachment fault that cross Attica region to the north, probably continues until Southern Saronikos, differentiating Aegina from Methana and Soussaki volcanoes.

Previous geodetic studies in Saronikos Gulf have not been inferred by GPS measurements. Therefore, velocity results of the western volcanic arc described in this paper cannot be combined directly with other results concerning the same area. Yet, it could be accomplished with the most nearby existing networks (Foumelis, 2009). Finally, an agreement is achieved with the results concerning sites at the southern coast of Attica indicating the same rates of motion.

From the combined velocity field an estimation of the principal strain rates was accomplished. Western Saronikos reveals both extensional and compressional rates, while Eastern Saronikos is dominated by compression. The above mentioned differentiation of western and eastern gulf is also supported by the obtained strain field. The extension which was observed at the western gulf is probably affected by the westward opening of the Corinthiakos Gulf fault system, and its extension to Western Saronikos, retaining its approx E-W-strike, along several well-defined segments (Papanikolaou et al., 1988). The transition from the relative extension to the west gulf to the relative compression at the eastern gulf seems to be controlled so far by the major detachment fault identified to Attica Peninsula and its offshore continuation along the Saronikos Gulf (Papanikolaou et al., 2009). Furthermore, the significant number of faults to the west in contrast with the fewer faults to the east affects to a great extent the above mentioned transition. It may well be assumed that a fault fraction at Eastern Saronikos deform at least partially aseismically, when interpreting the observed strain rate. This could be the reason of the discrepancy between the geodetic results and the seismological findings. In the former both extensional and compressive strain fields are described whereas in the latter extensional tectonic field is reported for the upper crust. This inconsistency seems, to a certain extent, intricate and more extensive investigation is required. However, it is probably associated with the complex geodynamics of the region; extensional stresses due to deformation of the upper crust, as well as subduction of the oceanic Ionian slab below Hellenides (Makris et al., 2004).

The results are considered as a first preliminary step towards a better understanding of the complex present-day dynamics of the Saronikos Gulf. However, to account for the neo- and seismotectonic processes forming the major fault systems is a future work which remains under consideration.

7. Acknowledgments

This work was financed by (i) The European Union (75%), (ii) The General Secretariat for Research & Technology of The Ministry of Development of the Hellenic Republic (25%), and (iii) *Terramentor E.E.I.G.* I would like to thank Professor Evangelos Lagios, Dr. Michael Foumelis for their constructive and critical comments and Dr. Vassileios Sakkas for the production of the time series of UOA1 site (see http://www.remsenslab.geol.uoa.gr/CGPS.html).

8. References

Altamini, Z., Sillard, P. and Boucher, C., 2002. ITRF2000: A new release of the International Terrestrial Reference Frame for earth science applications. *J. Geophys. Res.*, 107(B10):2214, doi:10.1029/2001JB000561.

Bath, M., 1983. The seismology of Greece. *Tectonophysics* 98, 165-180.

Beutler, G., Bock, H., Brockmann, E., Dach, R., Fridez, P., Gurtner, W., Hugentobler, U., Ineichen, D., Johnson, J., Mervart, L., Rothacher, M., Schaer, S., Springer, T. and Weber, R., 2001. Bernese GPS

Software Version 4.2 edited by U. Hugentobler, Schaer, S. and Fridez P., Astronomical Institute, University of Berne, Switzerland.

Boucher, C., Altamini, Z., Sillard, P. and Feissel-Vernier, M., 2004. The ITRF2000. IERS Technical Note 31, Verlag des Bundesamts für Kartographie und Geodäsie, Frankfurt am Main.

Clarke, P.J., Davies, R.R., England, P.C., Parsons, B., Billiris, H., Paradissis, D., Veis, G., Cross, P.A., Denys, P.H., Ashkenazi, V., Bingley, R., Kahle, H-G., Muller, M-V. and Briole, P., 1998. Crustal strain in central Greece from repeated GPS measurements in the interval 1989–1997. *Geophys. J. Int.*, 135, 195– 214.

Dewey, J.F. and Sengor, C.A.M., 1979. Aegean and surrounding regions: complex multiplate and continuum tectonics in a convergent zone. *Bull. Geol. Soc. Am.*, 90, 84– 92.

Dietrich, V.J., Mercolli, I. and Oberhänsli, R., 1988. Dazite, High-Alumina-Basalte und Andesite als Produkte Amphibol-dominierter Differentiation (Aegina und Methana, Aegäischer Inselbogen). *Schweiz. Mineral. Petrogr. Mitt.*, 68, 21-39.

Drakatos, G., Karastathis, V., Makris, J., Papoulia, J. and Stavrakakis, G., 2005. 3D crustal structure in the neotectonic basin of the Gulf of Saronikos (Greece). *Tectonophysics*, 400, 55– 65.

Hollenstein, C., 2006. GPS deformation field and geodynamic implications for the Hellenic plate boundary region, *Ph.D Thesis*, 359 pp.

Le Pichon, X. and Angelier, J., 1979. The Hellenic Arc and trench system: a key to the Neotectonic evolution of the Eastern Mediterranean area. *Tectonophysics*, 60, 1-42.

Makris J., Papoulia J., Ilinski D., Karastathis, V., 2004a. Crustal study of the Saronikos–Corinthiakos basins from wide aperture seismic data: intense crustal thinning below the Saronikos basin. X Conference of the Hellenic geological society, Thessaloniki, Greece. Abstracts.

Makropoulos, K. and Burton, P., 1981. A catalogue of seismicity in Greece and adjacent areas. *Geophys. F. R. Astron. Soc.*, 65, 741-762.

Makropoulos, K., Drakopoulos, J., Latoussakis, J. 1989. A revised and extended earthquake catalog for Greece since 1900. *Geophys. J. Int.* 98, 391–394.

McKenzie, D.P., 1978. Active tectonics of the Alpine Himalayan Belt, the Aegean Sea and surrounding regions. *Geophys. J. R. Astron. Soc.*, 55, 217–252.

Mercier, J.L., Sorel, D., Vergely, P., Simeakis, K., 1989. Extensional tectonic regimes in the Aegean basins during the Cenozoic. *Basin Research*, 2, 49-71.

Papadopoulos, G.A., Drakatos, G., Papanastassiou, D., Kalogeras, I., Stavrakakis, G., 2000. Preliminary results about the catastrophic earthquake of 7 September 1999 in Athens. Greece. *Seismol. Res. Lett.* 17, 318–329.

Papageorgiou, E., 2009. Surface Deformation Study for the Evaluation of Volcanic Hazard Assessment using Geophysical and Space Techniques: The Case of the Hellenic Volcanic Arc. *Doctorate Thesis*, University of Athens (GR).

Papanikolaou, I., Papanikolaou, D., Drakatos, G., 2009. Differentiation of the Fault and Seismicity Pattern on either side of the Major Detachment Fault in the Attica Peninsula and the Saronikos Gulf, Greece. Geophysical Research Abstracts, 11, EGU2009-9494, EGU General Assembly 2009.

Papazachos, B.C. and Papazachou, K., 1997. The Earthquakes of Greece. Zitti Publ., Thessaloniki, p. 304.

Pavlakis, P., Lykousis, V., Papanikolaou, D., Chronis, G., 1990. Discovery of a new submarine volcano in the Western Saronic Gulf: The Paphsanias Volcano. *Bull. Geol. Soc. Greece*, XXIV, 59-70.

Peter, Y., 2000. Present day crustal dynamics in the Adriatic–Aegean plate boundary zone inferred from continuous GPS measurements. *Ph.D. Thesis*, Zurich.

Rotstein, Y., 1985. Tectonics of the Aegean block: rotation, side arc collision on crustal extension, *Tectono-*

physics, 117, 117–137.

Shen, Z.-K., Jackson, D.D., 2000. Optimal estimation of geodetic strain rates from GPS data. *EOS Transactions of the American Geophysical Union* 81, S406.

Strabo. Geographica, Lib. I, 3, 59.

Teza, G., Pesci, A., Galgaro, A., 2008. Grid_strain and grid_strain3: Software packages for strain field computation in 2D and 3D environments. *Computers & Geosciences* 34, 1142–1153.

Foumelis, M., 2009. Surface Deformation Study of the Broader Area of Athens (GR) based on Differential GPS Measurements and Radar Interferometry. *Doctorate Thesis*, University of Athens (GR), 458 p.

Δελτίο της Ελληνικής Γεωλογικής Εταιρίας, 2010
Πρακτικά 12ου Διεθνούς Συνεδρίου
Πάτρα, Μάιος 2010

Bulletin of the Geological Society of Greece, 2010
Proceedings of the 12th International Congress
Patras, May, 2010

DGPS AND MAGNETOTELLURIC CONSTRAINTS ON THE CONTEMPORARY TECTONICS OF THE SANTORINI VOLCANIC COMPLEX, GREECE

Papageorgiou E.[1], Tzanis A.[1], Sotiropoulos P.[1,2] and Lagios E.[1]

[1] *University of Athens, Department of Geophysics and Geothermy, Zografou 15784, Greece, epapageo@uoa.gr*

[2] *TERRAMENTOR E.E.I.G., Sarantaporou Str. & Str. Tompra 10, Ag. Paraskevi, 153 42, Greece, terramen@otenet.gr*

Abstract

The study of vertical and horizontal crustal movements at the Santorini Volcanic Complex (SVC), as deduced by Differential GPS measurements revealed that an intricate pattern of five distinct domains with different horizontal kinematics: The West SVC (Akrotiri peninsula and Therassia) with very significant NNW-ward motion, North Thera with rather significant NW-ward motion, East Thera (Monolithos), with significant SE-ward motion, South Thera with significant NW-ward motion and, finally, central Thera with small westward motion. An apparently dextral, NNW-SSE oblique-to-strike-slip fault emerges as a prominent tectonic structure, separating the West SVC from the rest of the complex; this is the "Santorini Fault Zone". Additional insight is afforded by the results of MT and GDS surveys: a significant NNW-SSE conductive zone was detected, which is collocated with the purported NNW-SSE fault zone indicated by DGPS analysis and may be explained as an epiphenomenal conductivity anomaly. The observed deformation pattern enables the drafting of a qualitative model of contemporary tectonics, which is also presented and discussed. The model is plausible but certainly incomplete and pending verification with numerical modelling and additional observations.

Key words: *Santorini, Differential GPS, Magnetotellurics, tectonic deformation.*

1. Introduction

We report the results of a joint interpretation of Differential GPS (DGPS) and MagnetoTelluric (MT) data, in an attempt to identify and study the contemporary crustal deformation in the area of the Santorini Volcanic Complex (SVC). This multi-centre back-arc volcanic field is located at a break point of the central Hellenic Volcanic Arc (HVA) and comprises a very active locale featuring a large flooded caldera, formed at approx. 1650 B.C.

Ground deformation in back-arc volcanoes is associated with tectonic and volcanic processes, namely regional and local scale faulting and/or magma motion. In the reposed state, ground deformation is primarily a result of tectonic activity. During a paroxysmal period, magma motion assumes the primary role and deformation may serve as a precursor to eruptive activity; in this case the ground surface is expected to dilate (bulge) or contract in response to inflationary or deflationary changes in the magma chamber and the activity associated with the emplacement of dikes at the

upper parts of the volcanic edifice, which is anyway facilitated by the preferential paths created by tectonic activity. The study of ground deformation may assist in understanding the interplay between tectonic and volcanic processes and, in turn provide additional insights into volcanic hazards.

Ground deformation studies at the SVC have been reported by Stiros and Chasapis (2003) and Stiros et al., (2003). Their observational evidence was based on a radial EDM geodetic network comprising 10 stations on the perimeter of the caldera (and in close proximity to the rim), and one central station on Nea Kammeni islet; the particular choice of network layout has not been adequately explained. Based on intermittent observations of radial baseline length changes during the interval 1994-2001, they claim to have detected a phase of temporary dilation with particular expression at North Thera, where a maximum of 9.5 cm was observed. The dilation was attributed magmatic processes (inflation of a small magma chamber under some part of the volcano). These results will be re-evaluated herein, in the light or our new DGPS observations. Ground deformation observations continue at present (e.g. Farmer et al., 2007), but they are based on a single DPGS baseline of only two continuously recording stations, established in 2006. In consequence, hitherto results are neither adequate, nor representative of ground deformation.

DGPS has proven to be an important tool for intermediate and long-term monitoring of active volcanoes, as it provides high resolution 3-D information about the deformation field (e.g. Dvorak and Dzurisin, 1997; Fernandez et al., 1999 and many others). At the SVC, DGPS measurements conducted during the period 1994-2005 have detected non-trivial amounts of ground displacement, in both the horizontal and vertical axes (e.g. Papageorgiou et al., 2007). This enabled the identification of several domains with different kinematic characteristics, which will be further discussed and interpreted herein.

We will argue that the observed differential deformation is primarily the result of differential motion across faulting structures located at the boundaries between the deforming domains. However, the very low seismicity rates, combined with the discontinuous operation of local seismological networks for short exposure periods, does not allow these faulting zones to be directly identified by conventional seismotectonic analysis. Only recently have permanent seismographic networks been installed in the area (see http://ismosav.santorini.net) and the emerging earthquake data set is still incomplete.

As it turns out, there is an opportunity to clarify the situation using magnetotelluric (MT) data, independently collected at Santorini as part of another research project (Lagios et al., 1996). This may provide indirect (geoelectric) albeit well constrained images of the suspected faulting structures and thus assist in their identification.

The reason why observations of the geoelectric structure can image tectonic processes can be traced to the *epiphenomenal* development of electrical conductivity anomalies in response to faulting. Within the *schizosphere,* (brittle upper crust), faulting generates permeable rock, either directly within the fault zone, (fault gouge, breccias and mylonite), or around it as a result of repeated cycles of loading / unloading and elasto-plastic deformation. The presence of water in the immediate neighbourhood of the fault zone is very important factor for tectonic processes, as it influences creep and/or stability. Around the fault, tectonically induced permeability resulting from micro- and meso-scale fracturing, and crack interconnection is generally aligned with the fault. Healing processes are expected to close the cracks and reduce conductivity, unless they are kept open by continuous accumulation of deformation, either seismic or aseismic. Moreover, the more extensive and pervasive the microfracturing, (more heavily deformed the material), the more conductive the rock may be. Geothermal (hydrothermal) areas and volcanic domains in the upper crust are particular environments deserving special attention. The electrical conductivity of near surface rocks arises from the fluid

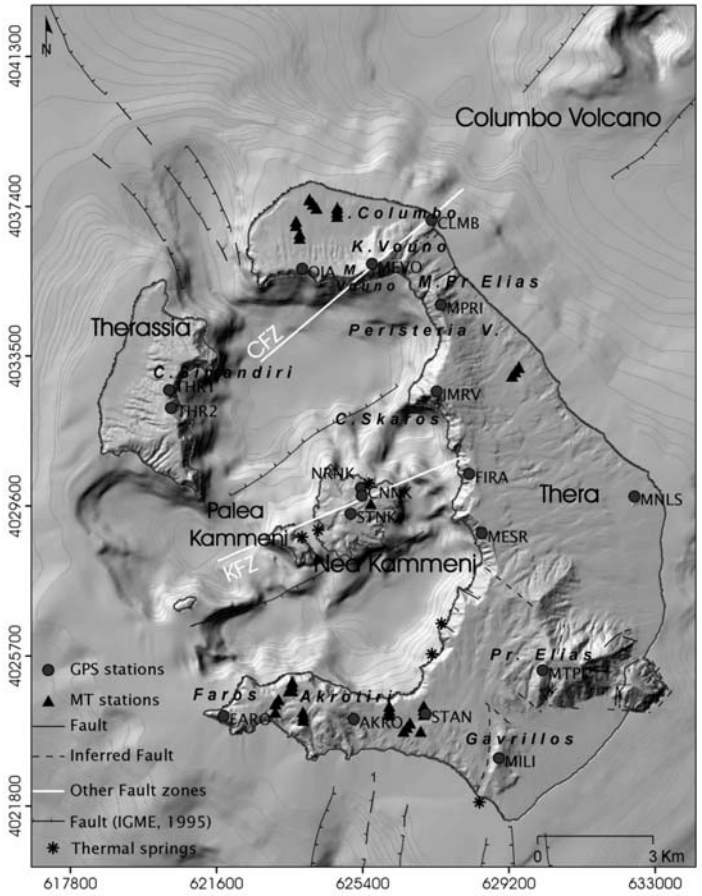

Fig. 1: Simplified map showing the main structural features along the Santorini volcanic complex. Circles represent GPS sites, triangles the MT stations, asterisks the location of thermal springs. CFZ: Columbos Fault KFZ: Kammeni Fault.

content of interconnected pore space (liquid fraction) and depends on the salinity of the pore fluids, the temperature and the presence or absence of clay minerals. Clay minerals may increase the salinity of pore fluids, (hence electrical conductivity), by several orders of magnitude. The liquid fraction will certainly increase in the neighbourhood of fluid circulation conduits, as also will the fraction of clay minerals due to hydrothermal alteration. In convective geothermal systems, especially those controlled by concurrent tectonic activity, circulation conduits are usually identified with the dominant active fault systems through which fluids are transported from the deep feeder reservoirs or heat sources. This is also true for all geological situations associated with active circulation of subterranean waters.

2. Tectonics and volcanism

The SVC (Fig. 1) is part of the HVA developing *ad retro* of the Hellenic Arc and Trench, in an area characterized by extensional regional tectonics which had a profound effect in its evolution. The volcanic activity is dated to at least 1.6 Ma BP (Ferrara et al., 1980). The last significant eruption

has taken place in 1950 and at present, volcanic activity is limited to thermal venting at the locations shown in Figure 1.

The northern part of the island complex lies in a graben, probably the continuation of the Anhydros Basin (Perissoratis 1995). Most of the effusive activity since 530 ka, which includes the Peristeria Volcano, the Simandiri shield, the Skaros shield, the Therassia dome complex, and the Kammeni Volcano has been associated with this feature. The contemporary volcanism is manifested by two major volcanic centres, the Nea Kammeni Volcano rising at the centre of the caldera and the submarine Columbos Volcano, located 7 km NE of Cape Coloumbo (Fig. 1). Their evolution has been affected by two distinct NE-SW tectonic lineaments, the Kammeni and Columbos Fault Zones respectively (Druitt et al., 1989, 1999). These mark the alignment of several eruptive vents and have been interpreted to comprise major normal faults (Pe-Piper & Piper, 2005). Six Plinian eruptions were aligned along Kammeni Fault Zone. Independent volcanic centres at North Thera, as is the Megalo Vouno cinder cone, the Kokkino Vouno cinder cone and the Cape Columbos tuff ring define the Columbos Fault (for details see Fouqué, 1879 and Reck, 1936). In addition, several dykes located at northern Thera, have a NE-SW orientation, as for instance the one between Mikros Profitis Ilias and Megalo Vouno (Heiken & McCoy 1984; Mountrakis et al., 1998). The southern half of the island is situated at the northern flank of a NE-SW-trending basement horst, the Santorini-Amorgos Ridge (Perissoratis 1995). Part of the basement rocks is outcropping at SE Thera (Mt Profitis Elias and Mt Gavrillos).

Direct evidence of faulting at different orientations is found in both geological maps of the SVC (Pichler et al., 1980; Druitt et al., 1999) and is reproduced in Figure 1. The faults comprise short strands with a general NW-SE orientation, observable mainly at South Thera and on the walls of the caldera. A significant NNW-SSE depression between North Thera and Therassia, bears evidence of normal faulting (IGME, 1995; Perissoratis, 1995); the same feature has been interpreted to be, either an extended NW-SE dyke (Pichler and Kussmaul, 1980) or the result of rotational slumping (Heiken and McCoy, 1984). Earthquake activity at and around the SVC is manifested with small magnitude earthquakes and low seismicity rates. The majority of earthquake foci are concentrated around the Columbos volcano, with fairly low activity observed at the rest of the complex (Delibasis et al., 1989; Drakopoulos et al., 1996; Bohnhoff et al., 2006; ISMOSAV, http://ismosav.santorini.net). At present, it is not clear which part(s) of this activity is of tectonic or of volcanic origin.

3. GPS observations and results

A GPS network comprising 18 re-occupiable stations has been established on the SVC (Fig. 1) and was intermittently measured during numerous campaigns during the interval 1994 – 2005. The interested reader may find details about the field measurement and data reduction procedures in Papageorgiou et al. (2007). Herein, the results are presented in terms of average deformation rates (velocities) with accuracies of a few mm/yr. Differences in the vertical motion between stations are better observed and interpreted when referred to a global coordinate system, in this case the ITRF2000 (e.g. Altamini et al, 2002). Conversely, differences in the horizontal motion are overly smoothed when referred to a global reference frame, while they are better resolved and interpreted in local frames. Accordingly, Figure 2 shows the *vertical displacement rates (velocities)* in the ITRF2000 reference frame, while Figure 3 illustrates the *horizontal displacement rates* relative to site MTPI. The selection of the reference station was based on geological criteria, as it is located on the alpine basement, NE of Thera, on apparently stable Upper Triassic limestones.

The vertical velocity results show subsidence at the centre of the caldera, at Nea Kammeni islet, (STNK, -6±2 mm/yr; CNNK, -2.1±0.3 mm/yr) as well as at Southern Thera with maximum rates at

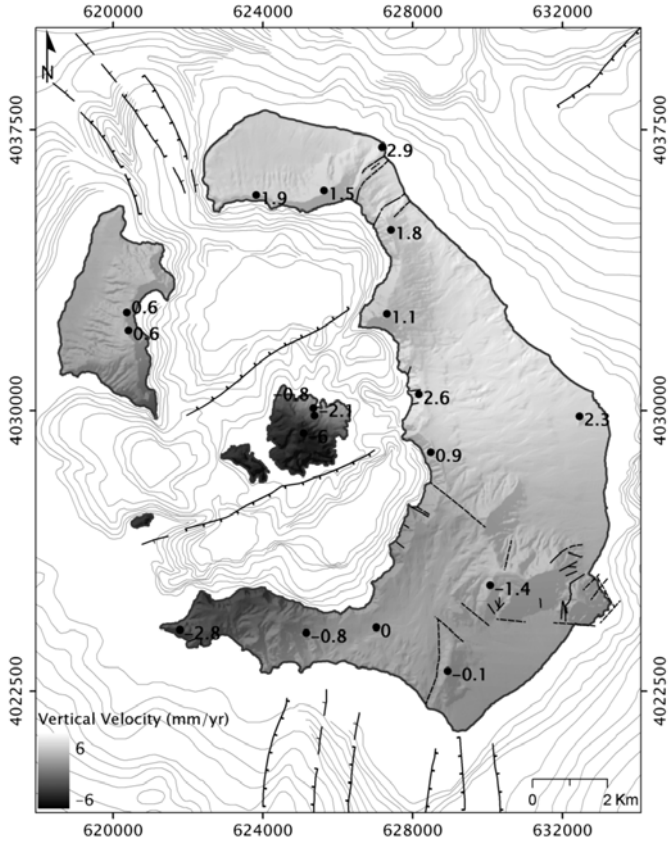

Fig. 2: Vertical deformation rates for the period 1994-2005 in the ITRF2000 reference frame. Dark shades indicate subsidence, bright shades uplift.

the terminus of the Akrotiri peninsula (FARO, -2.8±0.5 mm/yr). Notably, the northernmost station at Nea Kammeni (NRNK) shows a much smaller rate of subsidence (-0.8 ±0.1 mm/yr), possibly related to some interface between the northern-central and southern parts of the islet; this could be the Kammeni Fault. Relative stability is observed at Therassia Island (THR1, 0.6±0.4 mm/yr), while the rest of the network shows uplift with maximum rate at CLMB (2.9±0.1 mm/yr).

In terms of vertical kinematics and at first sight, the SVC would appear to comprise two major domains, NE Thera and Therassia experiencing uplift and SW Thera and the Kammeni islets experiencing subsidence. However, the geometry of the uplift/subsidence distribution is peculiar (arcuate) and the rates of uplift and subsidence are definitely not uniform across each domain – this indicates that the causative mechanisms are much more intricate (and certainly not consistent with explanations involving simple fault geometries).

The horizontal velocity field indicates a very complex kinematic pattern, with *significant* rates for the majority of the stations (see Fig. 3). Very significant NNW – NW-ward motion is observed at the western SVC and specifically at Therassia and Akrotiri Peninsula, with rates in excess of 3mm/yr and an average N340° orientation. North Thera is associated with slightly smaller rates (up to 2mm/yr) and N290° – N310° orientations. The difference in the displacement rate observed between stations OIA, MEVO and CLMB on one hand, and MPRI on the other (~0.7mm/yr), may indicate differen-

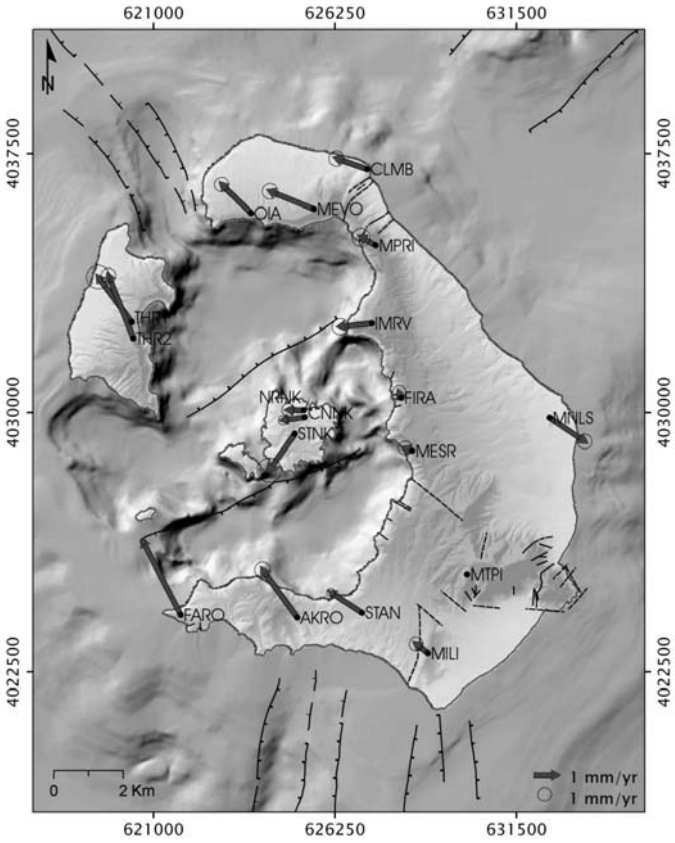

Fig. 3: Horizontal deformation rates relative to MTPI for the period 1994-2005.

tial motion across a normal fault dipping to the SE, which may well be the Columbos Fault. Analogous observations can be made elsewhere: The two southernmost stations, STAN and MILI, exhibit uniform NW direction of motion (N300°) but with quite different rates, possibly indicating the existence of an active discontinuity between them, in a sense analogous to the purported differential displacement across the Columbos Fault. Finally, the station at Monolithos (MNLS) is a *sui generis* beast, exhibiting SE-ward motion at ~N120°, almost exactly *antiparallel* to the motion observed at STAN, MILI and North Thera. Most of the stations located at central Thera, near the rim of the caldera, between Emerovigli (IMRV) and Messaria (MESR), as well as the stations on Nea Kammeni, exhibit altogether different kinematics with low horizontal deformation rates in a west to WSW-ENE direction (N255° – N270°). There are three exceptions: at Fira and Messaria, where the rate is *insignificant* and cannot be appraised, and at south Nea Kammeni (STNK), where it is significant and SSW oriented. These are additional *sui generis* results, further perplexing the interpretation.

It appears that the SVC comprises five distinct domains with different horizontal kinematics relative to station MTPI: The West SVC (Akrotiri peninsula and Therassia) with significant NNW-ward motion, North Thera: with rather significant NW-ward motion, East Thera (Monolithos), with significant SE-ward motion, antiparallel to that of North and South Thera, South Thera with significant NW-ward displacement, sub-parallel to that of North Thera and, finally, Central Thera with westward motion and small displacements. This is a very complex pattern and certainly difficult to interpret.

Nevertheless, it allows two definitive observations to be made:

1. The overall kinematics indicates that in the interval 1994 – 2005, the causative effect is a complex tectonic regime rather than some form of a magmatic process (emplacement). This is consistent with the current reposed state of the SVC, which showed no signs of activity before, during and after the GPS experiment. It is inconsistent with the interpretation of Stiros and Chasapis (2003) and Stiros et al., (2003), reported in Section 1, according to which there has been small scale dilation of a part of the volcano, probably due to minor inflation of a magma chamber. The main line of evidence against this hypothesis comes from the arrangement of the horizontal component of the deformation field, which is certainly not compatible with centrally driven inflation: this would have a distinctive pattern, quite different from the observed. The contribution of magmatic processes cannot be ruled out, but they are not likely to have occurred at an appreciable scale, due to the absence of any companion phenomena (e.g. elevated heat flow, increased hydrothermal activity etc.). The contribution of other volcanic processes cannot be resolved at present; if any, they should be more important in the immediate vicinity of the Kammeni Volcano. It appears that the interpretation of Stiros and co-workers is a consequence of inadvertent bias stemming from the geometry of the network: it was designed to detect radial deformation patterns and so it did, because the relative motion between the different blocks of the SVC is distributed in such a way, that all the radial baselines were bound to change lengths with the observed sign!

2. The differential horizontal motion between the West SVC (Therassia and Akrotiri peninsula) on one hand and the rest of the SVC on the other is very significant. The horizontal kinematics of the former are almost uniform, while in the latter they are intricate and indicative of complex tectonics as discussed above. It is therefore safe to conclude that a major tectonic discontinuity of NNW-SSE orientation (~N340°) exists between the two domains, as shown in Figure 6, this purported fault will henceforth be referred to as the *Santorini Fault Zone* (SFZ).

4. Magnetotelluric Data Analysis and Results

The MagnetoTelluric (MT) survey was conducted during the summer of 1993 (Lagios et al., 1996), providing a total of 34 soundings (Fig. 1). Fairly standard observation procedures were followed, leading to the acquisition of five cartesian components of the natural EM field over the nominal frequency bandwidth 130-0.01 Hz. The data was infested by significant anthropogenic ambient noise, so that advanced processing methods were required (Egbert and Booker, 1986; Tzanis and Beamish, 1988) in order to obtain Earth response functions (MT Tensor Impedances and Magnetic Transfer Functions) with acceptable levels of uncertainty.

The *spatial analysis* of the magnetotelluric Earth response endeavours to extract information about the configuration of the induced natural EM fields, which, in turn, depend on the geometry and configuration of lateral inhomogeneities in the geoelectric structure. The spatial analysis of the impedance tensor used herein is the Canonical Decomposition of Yee and Paulson (1986). It is not possible to show in this thrifty presentation, but it approaches the geoelectric structure as the equivalent of a birefringent material at low frequencies and large scales. In this context, there is a fast – resistive – direction of propagation in which the apparent impedance (resistivity) is maximal, and a slow – conductive – direction in which the apparent impedance is minimal. Given that the local direction of the electric field indicates the local direction of current flow and assuming (quasi) two-dimensional local and regional structures, the spatial analysis of the impedance tensor boils down to the following simple rules (see also Swift,1971):

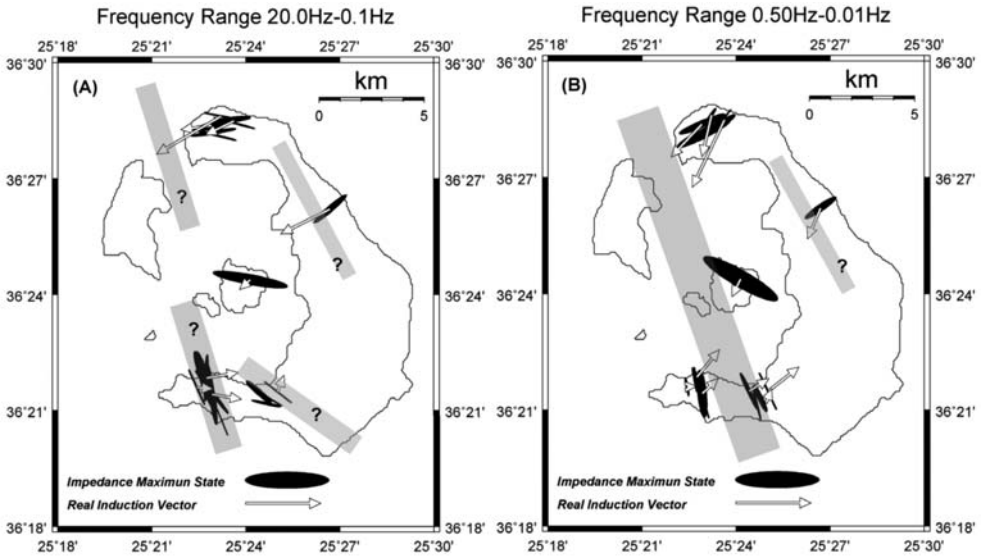

Fig. 4: The maximum characteristic states of the electric field (maximum impedance) and the real induction vectors, averaged (A) over the band 20 – 1 Hz and (B) over the band 0.5 – 0.01 Hz. The thick gray lines represent the approximate location of elongate conductors.

- On the conductive side of a lateral interface, the maximum electric field (maximum state) will be parallel to the strike of the interface and will correspond to the Transverse Electric (TE) mode of EM field propagation.
- On the resistive side of an interface, the maximum electric field will be normal to the strike and will correspond to the Transverse Magnetic (TM) mode of EM field propagation.

The spatial analysis of the MTF is based on the Induction Vector (IV) representation. The IV comprises a magnitude and an azimuth that defines the normal to the local strike of the anomalous concentration of current which produces the anomalous magnetic field. Two such vectors are defined for vertical fields responding in-phase *(real)* and out-phase *(imaginary)* with the horizontal component with which the vertical field exhibits maximum correlation; for 2-D or quasi-2D inhomogeneities they should be parallel or anti-parallel and perpendicular to the strike of the inhomogeneity (e.g. Rokityansky, 1982). Herein we only make use of the real IV for simplicity and brevity. The vector is drawn in the Parkinson convention, so that it will point towards current concentrations, i.e. towards resistivity interfaces.

In a final step and following the above discussion, the properties of the MTTI and the MTF can be combined, leading to the following simple rules for the spatial analysis of 2D structures:

- On the resistive side of a (quasi)2-D interface, the maximum electric field and the real IV are approx. parallel, the IV pointing towards the interface.
- On the conductive side of a (quasi)2-D interface the maximum electric field and the real IV are approx. orthogonal, the IV pointing towards the interface.

The results of the spatial analysis are presented in Figure 4. Figure 4a shows the polarization ellipse of the maximum electric field and the real IV, averaged over the frequency interval 20 – 1 Hz; these frequencies correspond to a relatively shallow part of the geoelectric structure.(see also Fig. 5). The

overall configuration of the electric field and current flow indicates that the shallower part of the geoelectric structure has dominant 2-D attributes with approx. N330°-340° oriented structural trends. At the northern part of Thera, the data indicate TM mode induction over the resistive part of a quasi-2D structure, the interface apparently being located at the area of the channel between Thera and Therassia. At Akrotiri peninsula the data show two distinct domains: The cluster of measurements at the western part of the peninsula, near cape Faros, indicates TE mode induction over the conductive side of a structure; the cluster at the eastern part near Akrotiri town, indicates TE mode as well, albeit driven by a structure and interface with an apparently different configuration of N300°-310°. The geographical distribution of the measurements allows placement of two conductors, one oriented N330°-340° at the western cluster of measurements and one oriented N310°-320°, just east of Akrotiri town. Finally, the sole sounding at Nea Kammeni cannot be interpreted with confidence, as it has attributes of near-filed three-dimensionality.

Figure 4b shows the polarization ellipse of the maximum electric field and the real IV averaged over the frequency interval 0.5 – 0.01 Hz, which corresponds to relatively deep parts of the geoelectric structure (of the order of 2 – 5 km, see also Fig. 5). The overall configuration of the electric field and current flow indicates that the deeper structure also has prevailing 2-D attributes, without being *sensu stricto* 2-D, and appears to be simpler and smoother than the shallower structure indicated by Figure 4a. Only one large scale structural trend with N320°-330° strike is detected and comprises a relatively broad elongate conductor extending between, and inclusive of, the Akrotiri peninsula and the Kammeni islets. This zone is delineated by the TM mode at the N-NW part of Thera and the TE mode at the southern part and Kammeni islets.

Two-dimensional inversion was carried out along a transect of approximately W-E orientation, between Faros and Akrotiri town; this is the only place where MT measurements are available in numbers and spacing sufficient to warrant the exercise. Inversion was performed with the algorithm of Rodi and Mackie (2001), assuming that the maximum electric field represents induction in the TE mode, as concluded by the spatial analysis above. In all cases, a discretized homogenous half-space was used as a starting model; the discretization scheme is apparent in Figure 5. Topography was also taken into consideration. Several inversions with different regularization factors were carried out before a final model was declared. The results are shown in Figure 5, where the approximate location of the interfaces (faults) detected by the spatial analysis are also included in the presentation (dashed lines). The most prominent geoelectric features observable in Figure 5 are two sub-vertical conductive zones, one near Faros at the west and one east of Akrotiri town, which are apparently associated with the conductivity interfaces and are interpreted to be sub-vertical faults or fracture zones of high secondary permeability. These are separated by a relatively resistive zone. Finally, it is apparent that an extensive lateral conductive formation exists at and just below sea level, which is thought to represent sea-water intrusion.

5. Interpretation and Conclusions

We have presented an analysis and joint interpretation of data collected with two methods of geophysical inquiry which, at first sight, might appear to form an unlikely twosome: Differential GPS and Magnetotellurics. Each method has its own means of detecting crustal faulting: GPS relies on kinematics and MT relies on the detection of elongate epiphenomenal conductivity anomalies.

The joint analysis has detected a major structural feature comprising an elongate zone of hefty changes in kinematic characteristics, apparently collocated with an elongate conductivity anomaly. This straddles the entire SVC approximately along the line defined by Akrotiri, the strait between

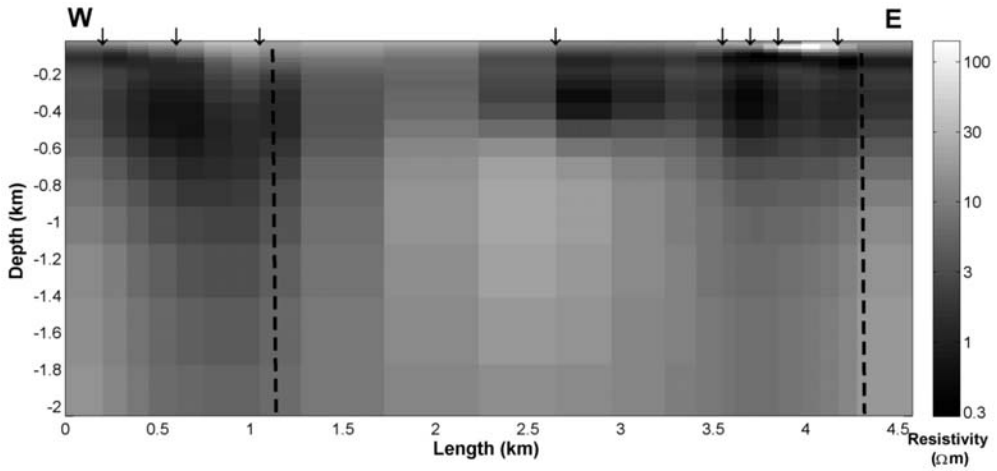

Fig. 5: Geoelectric image of the upper two kilometres of the crust, along the Akrotiri peninsula, obtained with two-dimensional inversion. Depths refer to mean sea level.

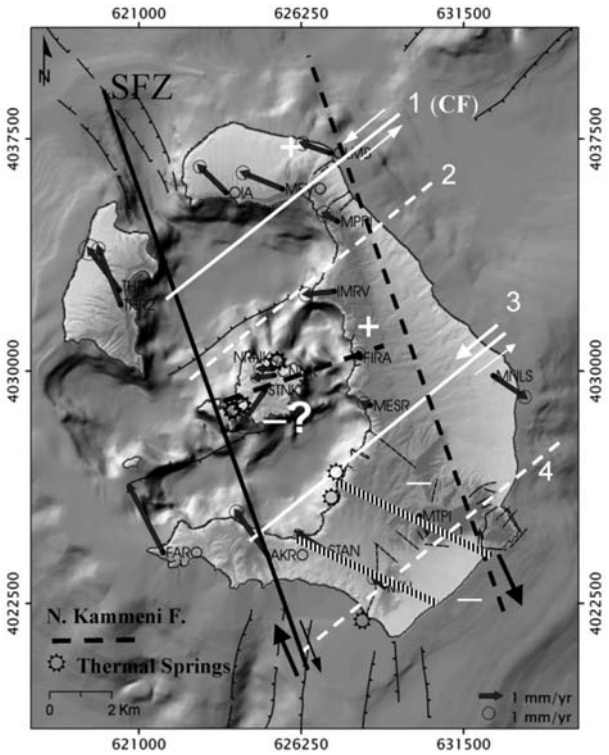

Fig. 6: Tentative interpretation of the DGPS and MT/GDS observations at the Santorini Volcanic Complex.

Palaea and Nea Kammeni islets and the strait between Thera and Therassia (see Fig. 6). This is interpreted to comprise an expression of a major NNW-SSE (~N340°) trending tectonic discontinuity, which we tentatively dub the *Santorini FZ*. Given that at the west SVC the net horizontal

displacement is significantly higher than the net vertical displacement, the SFZ appears to be dextral and oblique-normal to strike-slip. A second expression of the SFZ may separate East Thera from the rest of the SVC; this is tentatively depicted with a dashed line collocated with the conductor detected by the sole MT/GDS sounding measured at the area. The SFZ has not been detected before, although it appears to dominate the tectonics of the SVC.

This major zone aside, the SVC exhibits very complex kinematics, which at its present reposed state is more comfortably understood in terms of tectonics rather than volcanic processes (see discussion in Section 3). A tentative and purely qualitative interpretation is shown in Figure 6.

The numbered white lines represent a system of oblique-normal faults with a rather significant sinistral horizontal slip component. The exact orientation of these faults is not known (and cannot be known without detailed kinematic modelling) but they are tentatively assumed to comprise extensions/ expressions of the Anhydros Basin fault system (ABFS) extending between Amorgos Island and the SVC. Their net horizontal displacement is assumed to be considerably smaller than that of the SFZ, so that their combined action would result in the net NW-ward (N300° - N320°) horizontal motion at North and South Thera and the SE-ward (N120°) motion at East Thera. *Line 1* coincides with the Columbos Fault; extension across this discontinuity may account for the differential motion between stations MFVO and MPRI. *Line 2* has been placed as to separate the NW-ward moving North Thera from the westward moving Central Thira; it is also approximately collocated with a fault of similar orientation, mapped on the caldera walls (Pichler et al., 1980) and the bathymetry (IGME, 1995). *Line 3* is marks the boundary between Central and South Thera. Finally, *Line 4* is tentatively placed to account for the differential displacement between STAN and MILI, in a fashion analogous to the effect observed at North Thera, between MFVO and MPRI. The SFZ is apparently acting as a barrier to the horizontal motion of the ABFS.

The vertically hatched line corresponds to a zone of local extension formed due to the simultaneous action of SFZ and ABFS, which is also hosting an epiphenomenal conductor detected by the MT/GDS data. Together with a second such zone placed just south of MTPI and in association with the thermal springs at the southern perimeter of the caldera, it may form a local graben-like structure with orientation ~N300°, whose NW-ward extension is consistent with a depression observed just south of Therassia. This structure may account for the differences in the subsidence rates observed at South Thera. Nevertheless, it is an apparently shallow and local feature, as it vanishes/ merges with the SFZ at greater depths. Similar zones/ structures may exist elsewhere in the SVC but cannot be detected with the existing MT station layout.

The above interpretation is *far* from being complete or comprehensive. Some major questions still pending are as follows:

- It cannot fully explain the kinematics of Central Thera and the local peculiarities at FIRA and STNK stations. The westward motion there might be due to faster motion of the block defined by Lines 2 and 3 relative to the SFZ; this block includes the Kammeni volcano and the associated special thermal regime, which complicates matters and renders inadequate any attempt to explain the deformation in terms of a simple shearing model. In addition, the role of the Kammeni fault, if any, is still not clear and has not been taken into consideration. In conclusion, the true origin of the observed kinematics at Central Thera is unknown.
- It cannot explain the entire spectrum of observed vertical motions, particularly at Nea Kammeni, presumably for similar reasons.
- It cannot fully explain both the vertical and the SE-ward orientation of the horizontal motion of Monolithos (MNLS) due to the dearth of data in that area and the resulting difficulty to rec-

ognize local peculiarities.

Thus, with the exception of the well defined SFZ, the proposed model of contemporary deformation at the Santorini Volcanic Complex, albeit plausible, should rather be viewed as a basis for discourse and a starting point for future investigations. In fact, its verification relies on future investigations, a cardinal part of which should be quantitative (numerical) modelling in order to reproduce the observed kinematics, as well as additional geological and geophysical observations with an improved GPS network.

6. Acknowledgments

The collection and analysis of MT data was financed by the European Union, through contract EV5V-CT93-0285. The collection and analysis of GPS data was financed by (i) The European Union (75%), (ii) The General Secretariat for Research & Technology (25%), and (iii) *Terramentor E.E.I.G.* The valuable involvement of Dr. Vasileios Sakkas in the GPS field campaigns is dully acknowledged. The knowledgeable advice of Dr. Haralambos Kranis is also cordially appreciated.

7. References

Altamini, Z., Sillard, P. and Boucher, C., 2002. ITRF2000: A new release of the International Terrestrial Reference Frame for Earth Science applications. *J. Geophys. Res.*, 107(B10), 2214, doi:10.1029/2001JB000561.

Bohnhoff, M., Rische, M., Meier, Th., Becker, D., Stavrakakis, G. and Harjes, H-P., 2006. Microseismic activity in the Hellenic Volcanic Arc, Greece, with emphasis on the seismotectonic setting of the Santorini-Amorgos zone. *Tectonophysics*, 423, 17-33.

Delibasis, N., Chailas, S. and Lagios, E., 1989. Surveillance of Thera Volcano-Microseismicity Monitoring. Proc. 3rd Intern. Congress "Thera and the Aegean World", 2, Sept. 3-9, Santorini, Greece, 109-206.

Drakopoulos, J., Makropoulos, C., Stavrakakis, G., Panagiotopoulos, D., Papanastasiou, D., Hatzidimitriou, P., Papazachos, C., Vargemezis, G. and Savvaidis, A., 1996. Seismic monitoring of Santorini Volcano: Seismological network and processing of the seismological data. Santorini Volc. Lab., II, 15.

Druitt, T.H., Mellors, R.A., Pyle, D.M. and Sparks, R.S.J., 1989. Explosive volcanism on Santorini, Greece. *Geological Magazine*, 126, p. 95–126.

Druitt, T.H., Edwards, L., Mellors, R.M., Pyle, D.M., Sparks, R.S.J., Lanphere, M., Davies, M. and Barreiro, B., 1999. Geological Map of the Santorini Islands, 1:20000. *Geological Society of London, Memoir,* 19, 178p.

Dvorak, J.J. and Dzurisin, D., 1997. Volcano geodesy; the search for magma reservoirs and the formation of eruptive event. *Rev. Geophys.*, 35, 343–384.

Egbert, G.D. and Booker, J.R., 1986. Robust estimation of geomagnetic transfer functions. *Geophys. J. R. astr. Soc.*, 87, 173-194.

Farmer, G.F, Newman, A.V., Psimoulis, P., Stiros, S., 2007. Geodetic Characterization of Santorini Caldera from Continuous GPS Measurements. *EOS*.

Fernández, J., Carrasco, J.M., Rundle, J.B. and Arána, V., 1999. Geodetic methods for detecting volcanic unrest: A theoretical approach. *Bull. Volcanol.*, 60, 534–544.

Ferrara, G., Fytikas, M., Guiliano, O. and Marinelli, G., 1980. Age of the formation of the Aegean active volcanic arc. In: Doumas C. (ed). Thera and the Aegean World II, 37-41.

Fouqué, F., 1879. Santorin et ses eruptions. Masson et Cie., Paris, 440p.

Heiken, G. and McCoy, F., 1984. Caldera development during the Minoan eruption, Thera, Cyclades,

Greece. *J. Geophys. Res.*, 89, 8441-8462.

I.G.M.E., 1995. Surficial sediment map of the bottom of the Aegean Sea, Scale 1:200,000: Santorini sheet, IGME, Athens, Greece.

Jackson, J.A., 1994. Active tectonics of the Aegean region. *Annual Reviews of Earth and Planetary Sciences*, 22, 239-271.

Lagios, E., Galanopoulos, D., Sotiropoulos, P. and Vougioukalakis, G., 1996. Audio-Magnetotelluric study of Thera Volcano. Santorini Volc. Lab., II, 10.

Mountrakis, D., Pavlides, S., Chatzipetros, A., Meletidis, S., Tranos, M., Vougioukalakis, G. and Kilias, A., 1998. Active deformation in Santorini. In: Casale R., Fytikas M., Sigvaldarsson G. & Vougioukalakis G. (eds). The European laboratory volcanoes. European Commission, EUR 18161, 13-22.

Papageorgiou, E., Lagios, E., Vassilopoulou, S. and Sakkas, V., 2007. Vertical & Horizontal Ground Deformation of Santorini Island deduced by DGPS measurements. Proceedings of the 11th International Conference Geol. Soc. Greece, Athens, Greece. *Bull. Geol. Soc. Greece*, 40, 1219-1225.

Pe-Piper, G. and Piper, D.J.W., 2005. The South Aegean active volcanic arc: relationships between magmatism and tectonics. *Develop. in Volc.*, 7, 113-133.

Perissoratis, C., 1995. The Santorini volcanic complex and its relation to the stratigraphy and structure of the Aegean Arc, Greece. *Marine Geology*, 128, 37-58.

Pichler, H. and Kussmaul, S., 1980. Comments on the geological map of the Santorini Islands. In: Doumas, C. (ed.). Thera and the Aegean World II. The Thera Foundation, London, 413-427.

Pichler, H., Guenther, D. and Kussmaul, S., 1980. The Geological Map of Greece. Thira Island, Inst. Geol Min. Exploration, Athens 1980.

Reck, H., 1936. Santorini. –Der Werdergang eines Inselvulcans und sein Ausbruch 1925-1928. Dietrich Reimer, Berlin, 3 vols. MANCA.

Rodi, W. and Mackie, R.L., 2001. Nonlinear conjugate gradients algorithm for 2-D magnetotelluric inversion, *Geophysics*, 66, 174–187.

Rokityansky, I.I., 1982. Geoelectromagnetic investigations of the Earth's Crust and Mantle. Springer Verlag.

Stiros, S. and Chasapis, A., 2003. Geodetic monitoring of the Santorini (Thera) volcano. *Survey Review,* 37, 287, 84-88.

Stiros, S., Chasapis, A. and Kontogianni, V., 2003. Geodetic evidence for slow inflation of the Santorini Caldera. Proceedings, 11th FIG Symposium on Deformation Measurements, Santorini, Greece.

Tzanis, A. and Beamish, D., 1989. A high resolution spectral study of audiomagnetotelluric data and noise interactions. *Geophys. J.*, 97, 557-572.

Yee, E. and Paulson, K.V., 1987. The Canonical decomposition and its relationship to other forms of magnetotelluric impedance tensor analysis. *J. Geophys.*, 61, 173–189.

Δελτίο της Ελληνικής Γεωλογικής Εταιρίας, 2010
Πρακτικά 12ου Διεθνούς Συνεδρίου
Πάτρα, Μάιος 2010

Bulletin of the Geological Society of Greece, 2010
Proceedings of the 12th International Congress
Patras, May, 2010

TECTONIC PROCESSES AND CRUSTAL EVOLUTION ON/OFFSHORE WESTERN PELOPONNESE DERIVED FROM ACTIVE AND PASSIVE SEISMICS

Papoulia J.[1] and Makris J.[2]

[1] *Hellenic Centre for Marine Research, Institute of Oceanography, 19013 Anavissos, Attiki, Greece, nana@ath.hcmr.gr*

[2] *GeoPro GmbH, 20457 Hamburg, Germany, info@geopro.com*

Abstract

We developed velocity models of the crust and sediments offshore south western Greece, between the island of Zakynthos and Messinia. Using these velocity models and depth migrating the seismic data we delineated the main faults and associated them with the tectonic processes of western Greece. This active seismic experiment was essential for defining the limits between the continental domain of western Greece and the oceanic one of the deep Ionian Sea.

We successfully linked the onshore with the offshore tectonics and for the first time it was possible to understand how the main dextral fault systems of Cephalonia and Andravida are responsible for the crustal deformation, and its link to the local seismicity. Most of the seismic activity is connected to thrusting, due to crustal shortening or strike-slip faulting that follows the two main dextral wrench faults of Cephalonia and Andravida. It was recognized that the back stop offshore western Peloponnese is floored by thinned continental crust of Preapulia and that the Hellenic Alpine napes do not extend in the back stop domain.

Key words: *crustal structure, Ionian Sea, Hellenides, Mediterranean Ridge.*

1. Introduction

Aim of this study was to map the structure of sediments and crust between Zakynthos and Messinia, southwestern Peloponnese. Particularly the Kiparissiakos gulf and the transition of the continental to the oceanic domains were of special interest. Existing multi channel reflection seismic data, due to the length of the streamer systems used, had never before successfully penetrated at crustal depths, and the crustal thickness had never been uniquely defined (Kamberis et al., 1996; Kokinou et al., 2005). Furthermore, it was our intention to map the main tectonic elements along the crustal models. By connecting the offshore with the onshore tectonic elements we wanted to follow the continuation of the Alpine napes in the offshore. We also intended to locate the continent ocean transition in the offshore and better understand the tectonisation of the backstop and its interaction with the Mediterranean Ridge.

To accomplish this task, we used 60 Ocean Bottom Seismographs (OBSs) and deployed them successively along 5 seismic profiles south of the island of Zakynthos (Fig. 1). In the following we will present the crustal results of this experimental effort and a tectonic map of the Kiparissiakos gulf and the backstop to the west.

2. Geological setting

The area of study is located along the western Peloponnese continental Margin, between the island of Zakynthos to the north and the coast of Messinia peninsula to the south. This segment of the western Hellenic margin is seismically very active (Makropoulos and Burton, 1981; Papazachos and Papazachou, 1997) deforming rapidly with many destructive earthquakes, landslides and a tremendous bathymetric depression of approximately 5000 m in the Matapan basin. Isostasy is also disturbed, and as Makris (1977) showed, at the Peloponnese-Ionian Sea transition the isostatic balance is under compensated.

Onshore western Peloponnese the outcrops of the Gavrovo, Ionian and Preapulia have been mapped by Auboin and Decourt (1962). The Ionian zone is outcropping in the southeastern part of Zakynthos island as intruded Triassic evaporites into Plio-Pleistocene deposits (Underhill, 1989), while pre-Apulian limestones constitute most of the western half of the island. On Strophades island outcrops of salty evaporites have been described as tectonically emplaced diapirs into Pliocene marls, and hypothetically attributed to Messinian deposits (Lyberis and Bizon, 1981). Finally along the Peloponnese coasts of Kyparissiakos gulf outcrops of the Ionian, Gavrovo and Pindos alpine units are known together with continental, marine Pleistocene to Holocene deposits, truncated by E-W trending extensional active faults (Papanikolaou et al., 2007). Offshore only little information is available mainly from seismological and seismic studies. Clement et al., (2000) have investigated the seismic structure of the intra-plate geometry between Cephalonia and Zakynthos. Monopolis and Bruneton (1982) and, more recently, Papanikolaou et al., (2007) have studied the shallow geological structure of this continental margin segment. Aubouin et al., (1976) and Le Pichon et al., (2002) have proposed continuity of the alpine units, and particularly of the Ionian thrusts, beneath most of the area. Papanikolaou et al., (2007) have discussed the various rate of subsidence on the shelf area during Pleistocene to Holocene times and tentatively evidenced a "so-called" coastal fault zone along the Kiparissiakos gulf which they relate to a major change in paleo-geography during Pleistocene times.

3. The seismic experiment

We used 20 to 40 Ocean Bottom Seismographs (OBSs) and observed five 2D profiles in the Kiparissiakos gulf, southwestern Peloponnese, Greece (see Fig. 1).

Inline spacing of the OBSs was 3 to 5 km. Seismic energy was generated by shots fired every 125 m from a tuned air gun array of 2960 cuin. Dominant frequency of the shots was 8 Hz. Data were evaluated by: first break tomography, layered tomography, two point ray tracing forward modeling and depth migration of reflected and refracted arrivals.

Profile P1_2006

This NNW-SSE oriented profile produced important information on the E-W oriented fault systems. It mapped the offshore continuation of several onshore faults of western Peloponnese. For the correlation with the tectonic elements onshore we used three sources: the Seismotectonic map of IGME (1989), Mariolakos et al. (1998) and Papanikolaou et al., (2007). The final velocity model with a tectonic interpretation is presented in Figure 2. The Kiparissiakos basin is separated by a series of faults in three sub basins, which are deforming by extension. The crust below the Basin is relatively thin, approximately 22 km. Between OBS 0 and 1, east of Zakynthos, a major fault was identified separating a thicker continental block to the north from a thinner one to the south. This major fault at the northwestern flank of the Kiparissiakos basin is seismically active and may extend onshore, in the area of Killini. To the south the Basin is terminated by another major normal fault located approxi-

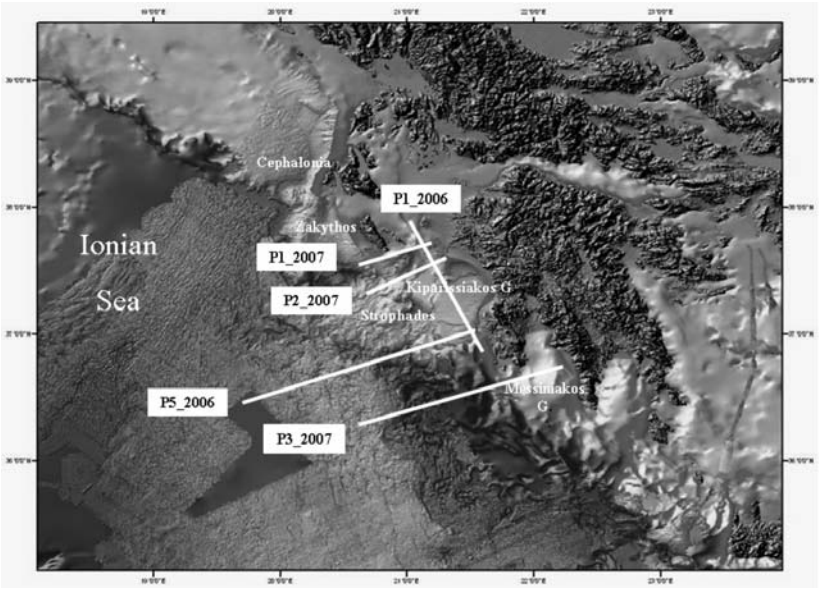

Fig. 1: Location of the five OBS seismic profiles offshore south western Peloponnese.

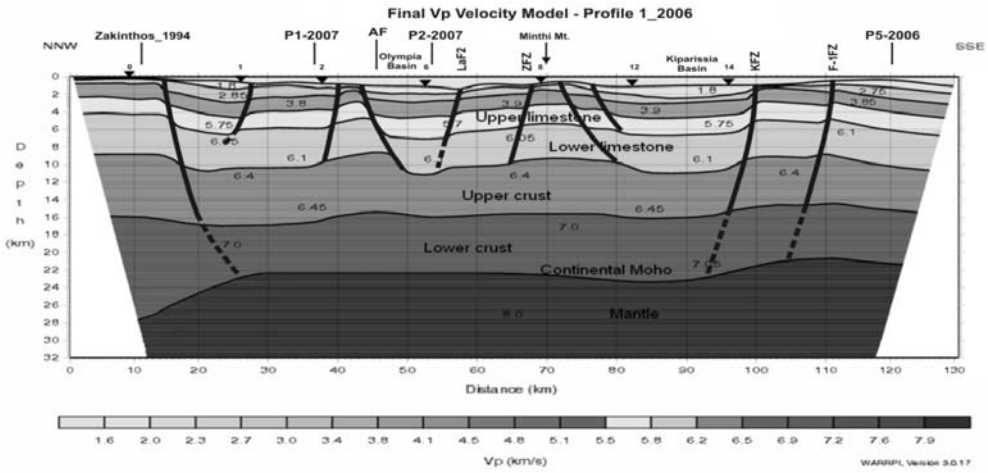

Fig. 2: Velocity Model of profile P1_2006 with tectonic interpretation.

mately 5 km south of OBS 14 and it is the westwards continuation of the Kiparissiakos Fault Zone (KFZ) (see Fig. 3). South of this fault the sedimentary sequences are dipping southwards and the crust is thinned to approximately 21 km. 15 km south of OBS 14 we identified a normal fault dipping northwards, which is the offshore continuation of the onshore mapped fault F-1FZ, north of Filiatra (Mariolakos et al., 1998).

In the central part of the Profile, close to OBS 8, we have mapped an anticline with uplifted sediments deforming also the bathymetry. This anticline is the offshore extension of the Minthi mountain. The normal faults defining the flanks of this anticline correlate with those mapped onshore.

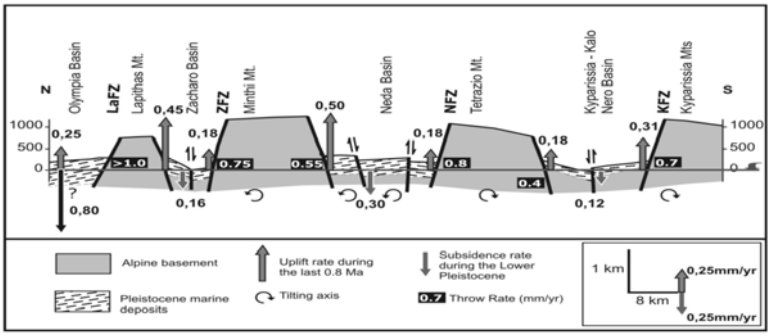

Fig. 3: Schematic cross section from Olympia basin to Kyparissia mountains, western Peloponnese (from Papanikolaou et al., 2007)

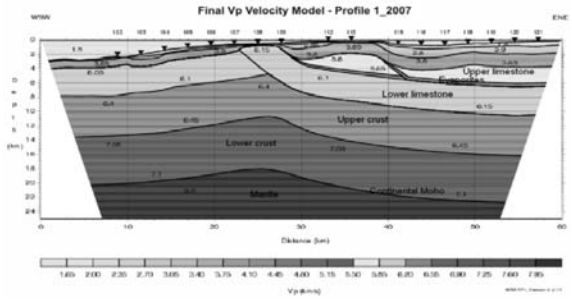

Fig. 4: Velocity Model of profile P1_2007.

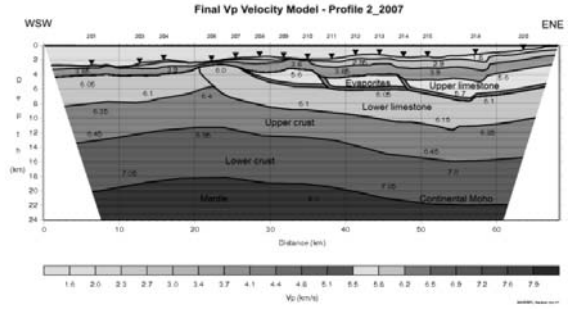

Fig. 5: Velocity Model of profile P2_2007.

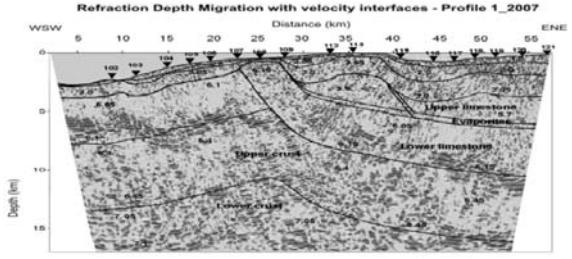

Fig. 6: Depth Migrated seismic data of profile 1_2007 superimposed with velocity interfaces.

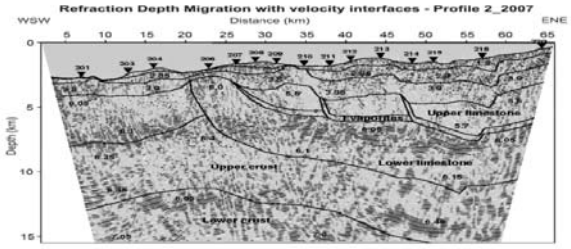

Fig. 7: Depth Migrated seismic data of profile P2_2007 superimposed with velocity interfaces (b).

North of OBS 8 we mapped the offshore continuation of the Lapithas Fault Zone (LaFZ). This fault is the southern flank of the Olympia basin. To the north the Basin is flanked by a normal fault dipping southwards. The continuation of this fault offshore creates a rhombic shape basin, mapped by swath bathymetry (Wardel and Mascle, personal communication, SEAHELLARC technical reports). Significant seismic activity was mapped in this Basin at crustal and sub-crustal levels (Papoulia et al., 2009). Seismicity and focal mechanisms indicate that it has developed by transtensional dextral wrench faulting. We consider this system to be the offshore extension of the Andravida dextral strike slip fault.

Profiles P1_2007 & P2_2007

Both E-W profiles south of Zakynthos have mapped a major thrust, which is the western limit of the Ionian zone of the Hellenic Alpine units to the Preapulia (Figs 4 and 5). Profile 2_2007 shows a significant shift of the Ionian zone and Preapulia thrust to the west; this is due to the influence of the dextral motion along the Andravida strike slip fault. The velocities of 5.6 km/s and 6.1 km/s are assigned to two different metamorphic limestones, an upper and a lower one, which, as we have also seen in previously observed seismic data from the Zakynthos island (Makris and Papoulia, 2009), are separated by evaporites of Triassic age (Nikolaou, personal communication).

In Figures 6 and 7 we present the depth migrated OBS data using the refraction migration technique (Pilipenko and Makris, 1997). The basement geometry is very clearly mapped and it shows the thrusting at the central part of the line and also the tectonized and shortened crustal geometry to the west of the thrusting front. The superimposed interfaces of the velocity model show a good coincidence between the migrated interfaces and those computed by ray tracing. The ray traced structures however are significantly smoothed. The tectonic details and crustal deformation can only be resolved by a reliably applied migration procedure.

Profile P5_2006

Low velocity sediments of Vp values ranging between 2.2 km/s and 3.7 km/s thicken systematically from OBS position 4 to OBS position 19, that is from west to east (Fig. 8). This indicates a gradual subsidence of the oceanic crust towards the collision front, at the Mediterranean Ridge. The western limit of the continental backstop over thrusts the sediments of the Mediterranean Ridge. The subduction of the oceanic slab at this limit is very clearly mapped, following the geometry of the continental Moho. The continental crust thickness at the backstop area to approximately 16 km and was mapped at a depth of 20 km. The oceanic slab below the continental crust was not directly mapped and was assumed as a continuation of the identified oceanic crust below the deep Ionian Sea. We could not resolve any sediments to be involved with the subduction.

The continental part of the profile is covered with thick sediments. We have again identified the exis-

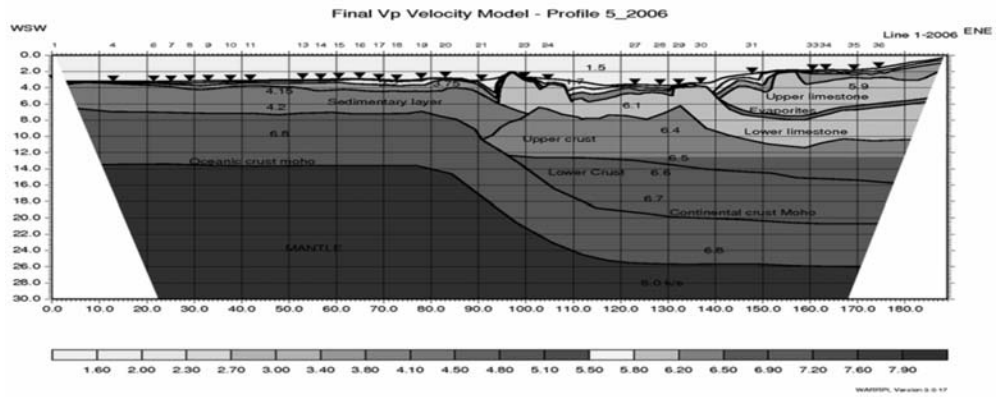

Fig. 8: Velocity Model of profile P5_2006.

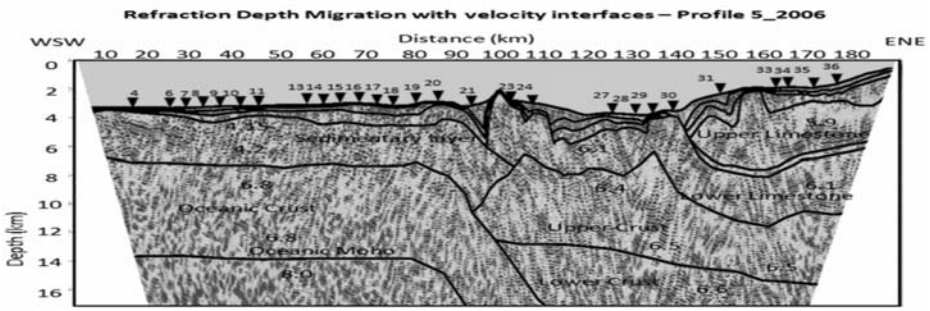

Fig. 9: Depth migrated seismic data of profile 5_2006 superimposed with velocity interfaces.

tence of two high velocity limestone series separated by Triassic evaporites. The upper limestone is terminated at OBS 30, where the uplifted and thrusted lower limestone of Preapulia is nearly exposed to the sea floor. This part of the section coincides with the deepest part of the bathymetry of about 4000 m water depth, and is part of the Hellenic Trench. The backstop area is covered by soft sediments with increasing thickness to the west, deposited on the Preapulia limestone, and is strongly tectonized. The upper limestones representing the Hellenic napes are terminated at the Preapulia thrust (OBS 30).

The migrated section, presented in Figure 9, is limited to the upper 14 km and is overlapped by the velocity interfaces defined by the velocity model of Figure 8. The strongly tectonized upper crustal units are also seen in the migration section. The structural elements mapped by both the velocity modeling and the refraction migration is in good agreement. It is obvious that the eastern part of the profile, to the east of the collision front, is very strongly tectonized by three major thrusts and several normal faults. On the contrary the deep Ionian basin is fairly homogeneous and strong deformation is only observed at the Mediterranean Ridge.

Profile P3_2007

At the western part of the profile, between OBS 341 and OBS 328, we have mapped two high velocity limestone series again separated by the Triassic evaporites, as was identified in all previous lines (Fig. 10). Two main thrusts were mapped in this area. The western one at OBS 335 is within the Hellenic Alpine units and was correlated with the onshore structures of Messinia, specifically lim-

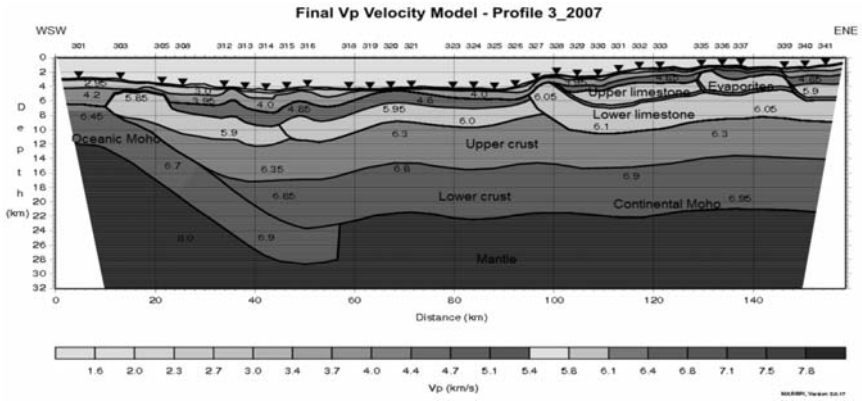

Fig. 10: Velocity Model of profile P3_2007.

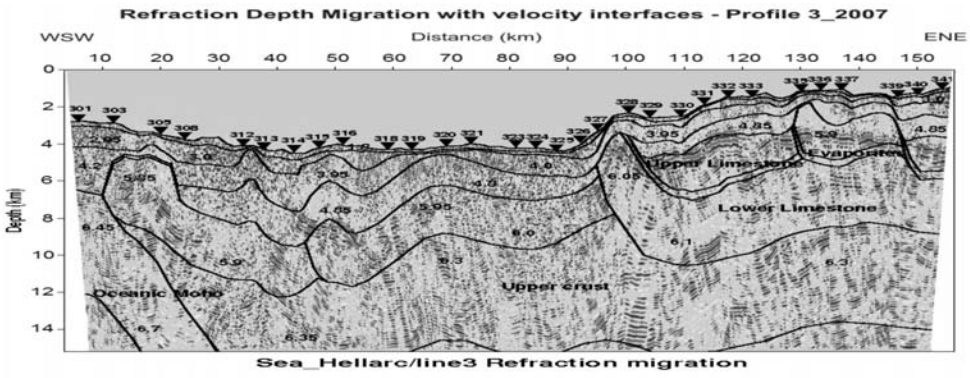

Fig. 11: Depth migrated seismic data of profile 3_2007 superimposed with velocity interfaces

iting the Gavrovo zone to the east from the Ionian zone to the west. The second major thrust is located at OBS 328. The lower limestone of Preapulia is nearly exposed to the surface and defines the western limit of extension of the Hellenic napes. From this thrust front until OBS 303, which is nearly at the western end of the profile, only one high velocity limestone has been identified. All this area is considered to be the continental backstop. The Mediterranean Ridge is clearly marked to the west of this location by a bathymetric uplift and change of the sedimentary structure. The transition zone between the Mediterranean Ridge and the Preapulia backstop is deformed by intense fragmentation of the stretched continental crust of Preapulia and by thrusting of the high velocity limestones over the soft sediments of the Mediterranean Ridge. The sediments at the backstop area thicken from east to west. The thickest part of the post Preapulia sediments is identified below OBS 314 and is about 5 km. Vp velocity of the sediments ranges between 4.0 km/s and 4.85 km/s. We did not follow the oceanic slab below the backstop because energy failed to penetrate below the continental Moho. The later was encountered at a depth of approximately 22 km.

We have again plotted the velocity discontinuities produced by the ray tracing modeling into the depth migrated OBS arrivals of Figure 11. We present only the upper 15 km part of the section in order to obtain a better resolution of the tectonic elements. Two main zones of significant thrusting and crustal shortening were mapped. The eastern one, between OBS 327 and OBS 341, includes

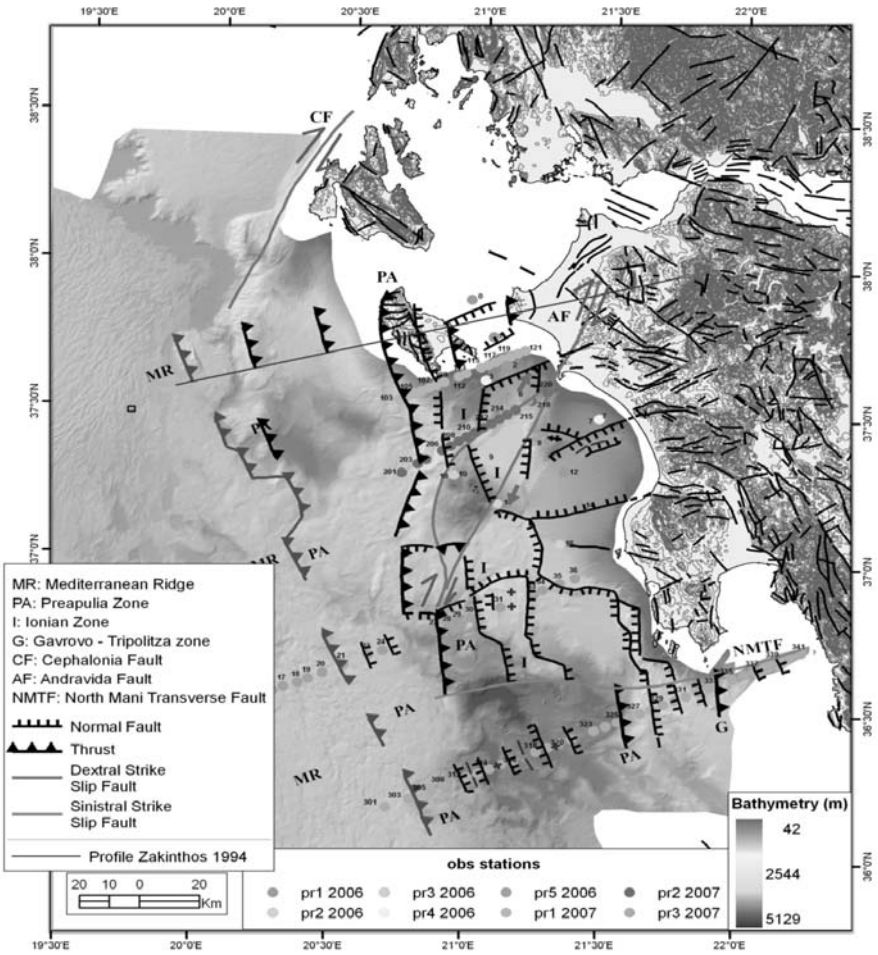

Fig. 12: Simplified structural map of the Kiparissiakos gulf showing the limit of the Mediterranean Ridge, the Hellenic napes edge, and the main tectonic elements.

two main thrusts that have been described in the velocity model of Figure 10. The other thrusted zone at the western part of the section is associated with the uplift of the Preapulia limestones and their westwards thrusting over the oceanic crust domain of the deep Ionian Sea. This is linked with a second thrusting belt close to this compressional front positioned below OBS 312 to OBS 316. It shows that the compression at this front is very intense and is spread over a significant part of the backstop.

4. Conclusions-Results

The active seismic experiment based on the exploitation of OBS technology was performed for the development of high quality crustal velocity models. This was also complemented by a series of multi channel seismic (MCS) lines for the delineation of the shallow sediments and their structure. Five OBS lines were established covering the complete offshore region of western Peloponnese. Our aim in locating the lines was to study the crustal structure of the block between Zakynthos island and the Gulf of Messinia. Particularly we wanted to resolve the westwards continuation of the

Hellenic Alpine units in the offshore region, map the main tectonic elements offshore and link them to the onshore structures.

The NW-SE oriented profile 1_2006 mapped a series of faults of nearly E-W orientation. The crustal thickness in the broader Kiparissiakos area is about 22 km thick and the crust is continental. The sediments range between 8 and 10 km and in their lower part are composed of two high velocity metamorphic limestones (Vp = 5.5 – 6.1 km/s). Triassic evaporites separate the two limestone series, producing salt dome intrusions in several locations, but have not been modelled along this line. The upper sedimentary sequences have Vp velocities between 1.8 and 3.8 km/s. Their thickness varies between 2 and 4 km. The faults mapped along the profile have defined the N-S extension of the Kiparissiakos basin. The master faults at the northern and southern flanks of the Basin are also seismically active and truncate the entire crust. A number of faults were mapped within the Basin that correlate with the onshore fault systems, separating the internal structure of the Basin in a series of sub basins. From south to north, we have the Kiparissia basin, separated from the Olympia basin by the offshore extension of the Minthi mountains. The southern flank of this basin is seismically very active, and associated with sub crustal seismicity that extends to 90 km depth. The northern flank of this basin is linked with crustal seismicity. Fault plane solutions of locally recorded seismicity associated with this area have revealed mainly strike slip faulting of dextral orientation (Papoulia et al., 2009). We consider this fault system to be the offshore extension of the Andravida fault. Further to the north, offshore Katakolo, another sub basin of intense down throw has developed.

Profiles 1_2007 and 2-2007 of ENE-WSW orientation are parallel to the southern coast of Zakynthos and have mapped the northern part of the Kiparissiakos basin and its crust and sediment structure between the coast of western Peloponnese and the Zakynthos and Strophades uplifts. Crustal thickness along both lines varies between 19 and 22 km, always thickening to the east. The thinnest part of the crust coincides with the highest uplift of the Preapulia metamorphic limestone that is thrusted westwards. The continental crust is depressed and the water depth increases systematically up to 3000 m at the western edge of both profiles. To the east of the Preapulia thrust we mapped an upper and a lower limestone series, separated by Triassic evaporites. The lower limestone belongs to Preapulia, and extends also west of the Preapulia thrust. The upper limestone is part of the external Hellenic napes and does not exist west of the Preapulia thrust. The Thrust itself is the limit of the westwards extension of the Hellenides towards the deep Ionian Sea.

The two southern crustal profiles, P5_2006 and P3_2007, have mapped the extension of the continental crust to the west, the western limit of the backstop and its interaction with the Mediterranean Ridge. The crust mapped in the deep Ionian Sea, west of the backstop limit, is oceanic, and has a thickness of approximately 11 km, in a water depth of 3000 m. Sediment thickness varies between 3.2 to 4.5 km, increasing to the east, to the Mediterranean Ridge. The igneous part of the crust with a Vp velocity ranging from 6.45 to 6.8 km/s is about 6.5 km thick and it is part of the Tethys ocean that is now subducting below the Hellenic Arc. East of the collision front, between the continental domain of the backstop and the oceanic one of the deep Ionian Sea, the crust is thickening eastwards. Crustal thickness at the backstop area is about 17 to 18 km. The sediments vary between 4.5 and 8.0 km, depending on the amount of deformation that has affected them. The basic difference between the two lines is the extent of the backstop, between the collision front and the eastward limit of the Hellenic napes. Along the northern profile, the back stop is 40 km wide, while at the southern line it extends for over 80 km. East of the backstop, which is defined at its eastern limit by the Preapulia limestone thrust, the crust thickens, sediment thickness also increases, and two high velocity limestones are mapped, separated by the Triassic evaporites. The lower limestone is the

Preapulia unit, while the upper one is part of the Hellenic napes. Continental crust in this area is approximately 22 km thick and the sediments are strongly deformed.

We have mapped the limit between the Mediterranean Ridge and the backstop, at about 100 to 120 km west of the coast of Peloponnese. We have also identified the Preapulia thrust that terminates the westward extension of the Alpine Hellenic napes. It is interesting that this front is systematically shifted westwards between Zakynthos island and offshore west Messinia, where the backstop has its minimum width of only 40 km. South of the 5_2006 profile the Preapulia thrust is significantly shifted towards Peloponnese by more than 50 km (Fig. 12). This is linked to the left lateral North Mani Transverse Fault (Lallemant, 1984), which is presently inactive.

Correlating the onshore geology and Alpine units with the offshore mapped tectonics, we have placed the limits of the Ionian to the Preapulia zones in the Kiparissiakos area, and the Preapulia, Ionian and Gavrovo zones south of Messinia. Nowhere beyond the Preapulia thrust to the west have we identified the existence of the Hellenic Alpine napes in the backstop area. This observation does not agree with Aubouin et al. (1976) and Le Pichon et al. (2002) who place the limit of western Hellenides deep into the Ionian Sea, extending to the Mediterranean Ridge.

The Kiparissiakos basin is strongly affected by the dextral strike slip fault of Andravida, which is displacing the geological and tectonic elements westwards. This is also responsible for the development of transtensional basins and transpressional uplifts, like the rhombic basin northeast of the Strophades island and the Strophades uplifted block. The tectonic deformation of the Strophades island is also described by Stiros (2005) and is in agreement with the general deformation pattern derived by the present observations.

5. Acknowledgments

Ch. Fasulaka and Th. Patrinos from GEOPRO Hamburg are thanked for seismic modeling. Dr. V. Pilipenko, Academy of Sciences Ukraine is acknowledged for the preparation of the depth migrated sections. The Captain and crew of the R/V AEGAEO HCMR and R/V EXPLORA OGS are acknowledged for their valuable help during the field operations. Dr. D. Ilinski – GEOPRO, MSc A. Tsambas and Mr. P. Pagonis – HCMR participated in field operations and data acquisition.

This study is a contribution to the FP6 EC Project SEAHELLARC.

6. References

Aubouin, J, and Decourt, J., 1962. Zone Preapullien zone Ionienne et zone du Gavrovo en Peloponnese occidentale. *Bulletin de Société Géologique de la France*, 4, 785-794.

Aubouin, J, Bonneau, M., Davidson, J., Leboulenger, P., Matesco, S., Zambetakis, A., 1976. Esquisse structurale de l'arc Egeen externe : des Dinarides aux Taurides, Bull Soc. Geol. France 18, 327-336.

Clément, C., Hirn, A., Charvis, P., Sachpazi, M. and Marnelis, F.: 2000, Seismic structure and the active Hellenic subduction in the Ionian Islands, *Tectonophysics* 329, Issues 1-4, 141-156.

IGME, 1989. Seismotectonic Map of Greece with seismological data, 1:500.000 scale, Athens.

Kamberis, E., Marnelis, F., Louckogiannajis, M., Maltezou, F., Hirn, A., and the STREAMERS Group, 1996. Structure and deformation of the External Hellenides based on seismic data from offshore western Greece. *EAGE Special Publications*, 5, 207-214.

Kokinou, E., Kamberis, E., Vafidis, A., Monopolis, D., Ananiadis, G., and Zelilidis, A., 2005. Deep seismic reflection data from offshore western Greece: a new crustal model for the Ionian sea, *Journal of*

Petroleum Geology, Vol. 28 (2), 185-202.

Lallemant, S., 1984. La Transversale Nord-Mani; Etude Geologique et Aeromagnetique d'une Structure Transverse a l'Arc Egeen Extrerne. Dr. troisieme cycle, University Pierre et Maire Curie, 164 pp.

Le Pichon, X., Lallemant, S.J., Chamot-Rouke, N., Lemeur, D., Pascal, G., 2002. The Mediterranean Ridge backstop and the Hellenic napes, *Marine Geology* 186, 111-125.

Lyberis, N. and Bizon, G. : 1981, Signification structurale des iles Strophades dans la marge Hellénique, *Marine Geology* 39, 57-69.

Makris, J. and Papoulia, J., 2009. Tectonic evolution of Zakynthos island from deep seismic soundings: thrusting and its association with the Triassic evaporites, Intl. Symposium on Evaporites, Zakynthos, pp 47-54.

Mariolakos, I., Sabot, V., Fountoulis, I., Markopoulou-Diakantoni, A., Mirkou, R., 1998. Filiatra. Neotectonic Map of Greece 1:100,000. Earthquake Planning & Protection Org., Athens.

Makris, J., 1977. Geophysical investigations of the Hellenides, Hamburg Geophysical Monographs, Vol. 34.

Makropoulos, C., and Burton, P.W., 1981. A catalogue of the seismicity in Greece and adjacent areas, *Geophys. J. R. astr. Soc*., 65, 741-762.

Monopolis, D. and Bruneton, A.: 1982, Ionian Sea (Western Greece): its structural outline deduced from drilling and geophysical data, *Tectonophysics* 83, 227-242.

Nikolaou, K., 1986. Contribution to the study of the Neogene and the geology and boundaries of Ionian and pre-Apulian isopic zonesin relation to petroleum geology observations mainly in the Islands Strophades, Zante, Cephalonia *PhD Thesis* Univ. of Athens, Athens (in Greek).

Papanikolaou, D., Fountoulis, J., Metaxas, Ch., 2007. Active faults, deformation rates and Quaternary paleogeography at Kyparissiakos Gulf (SW Greece) deduced from onshore and offshore data.

Papazachos, V., and Papazachou, C., 1997. The Earthquakes of Greece, Editions Ziti.

Papoulia, J., Makris, J., Tsambas, A., and Fasulaka, Ch., 2010. Seismic deformation in the southwestern Hellenic arc: Preliminary results from active and passive seismic observations, *Bull. Geol. Soc. Gr.* (in press).

Pilipenko, V. and Makris, J., 1997, Application of migration to the interpretation of WARP data. *Expanded Abstracts of the 69th SEG Meeting*, Dallas.

SEAHELLARC EC FP6 project, Technical Reports, www.seahellarc.gr.

Stiros, S., 2005. Geodetic evidence for mobilization of evaporates during the 1997 Strophades (W Hellenic Arc) 6.5 M_w earthquake, *J. Geophys. Eng*. 2, 111-117.

Underhill, J. R., 1989. Late Cenozoic deformation of the Hellenides foreland, western Greece, *Geological Society of America Bulletin* 101(5), 613-634.

Δελτίο της Ελληνικής Γεωλογικής Εταιρίας, 2010
Πρακτικά 12ου Διεθνούς Συνεδρίου
Πάτρα, Μάιος 2010

Bulletin of the Geological Society of Greece, 2010
Proceedings of the 12th International Congress
Patras, May, 2010

PATTERNS OF DUCTILE DEFORMATION IN ATTICO-CYCLADIC MASSIF

Spanos D., Koukouvelas I., Kokkalas S. and Xypolias P.

University of Patras, Department of Geology, Laboratory of Structural Geology, 26500 Patras, Greece, spanos@upatras.gr

Abstract

The area of Lavrion constitutes the westernmost part of the Attico-Cycladic massif where the allochthonous Cycladic Greenschist-Blueschist unit overthrusts the para-authochthonous Basal unit. The tectonic contact of these units forms a crustal scale thrust zone which is the continuation of the Evia thrust. Our research was focused on quartz-rich schists of the overlying allochthonous unit. Combination of microstructural, finite strain data and quartz and calcite c-axis fabrics analysis was used to characterize the kinematics of rock flow within the thrust zone. The latter was formed under conditions of progressive exhumation and decompression of the high-pressure schists of the Attico-Cycladic massif. A dominant top-to-the-ENE sense of shearing along the thrust zone is inferred by several shear sense criteria. The analysis of several specimens collected from various structural depths manifest that the deformation close to the thrust zone occurred under approximately plane strain conditions and was characterized by an Rxz strain ratio which fluctuates between 3 and 6.5.

Key words: *finite strain, quartz c-axis fabrics, calcite c-axis fabrics, exhumation, Attico-Cycladic massif, Lavrion.*

1. Introduction

Over the last decades, there is a strong debate in the Attico-Cycladic massif (ACM) about the direction of nappes movement that led to the upsurge of the HP/LT rocks from deeper floors of the crust as well as about the prevalent exhumation mechanism. Although numerous studies were done in Evia and the islands of Cyclades, the region of Attica didn't receive similar attention.

In the southern part of Attica (Lavrion area) we implemented a combined analysis consisting of calcite and quartz c-axis fabrics and the evaluation of finite strain data in order to examine the kinematics of rock flow in a crustal scale ductile shear zone. Crystallographic preferred orientation (CPO) of minerals constitutes a widely used criterion for evaluating shear sense in ductile thrust zones (Law, 1990). Identification of kinematic indicators can confirm the results of petrofabric analysis or imply individual deformation events. On the other hand, strain analysis can decipher the conditions that predominate within the deformed rocks of the area. Furthermore, we present first results of calcite c-axis analysis from three representative samples collected from strongly deformed marbles from the thrust zone.

2. Geological setting

The area of Attica comprises the westernmost extension of the Attico-Cycladic Massif (ACM). The

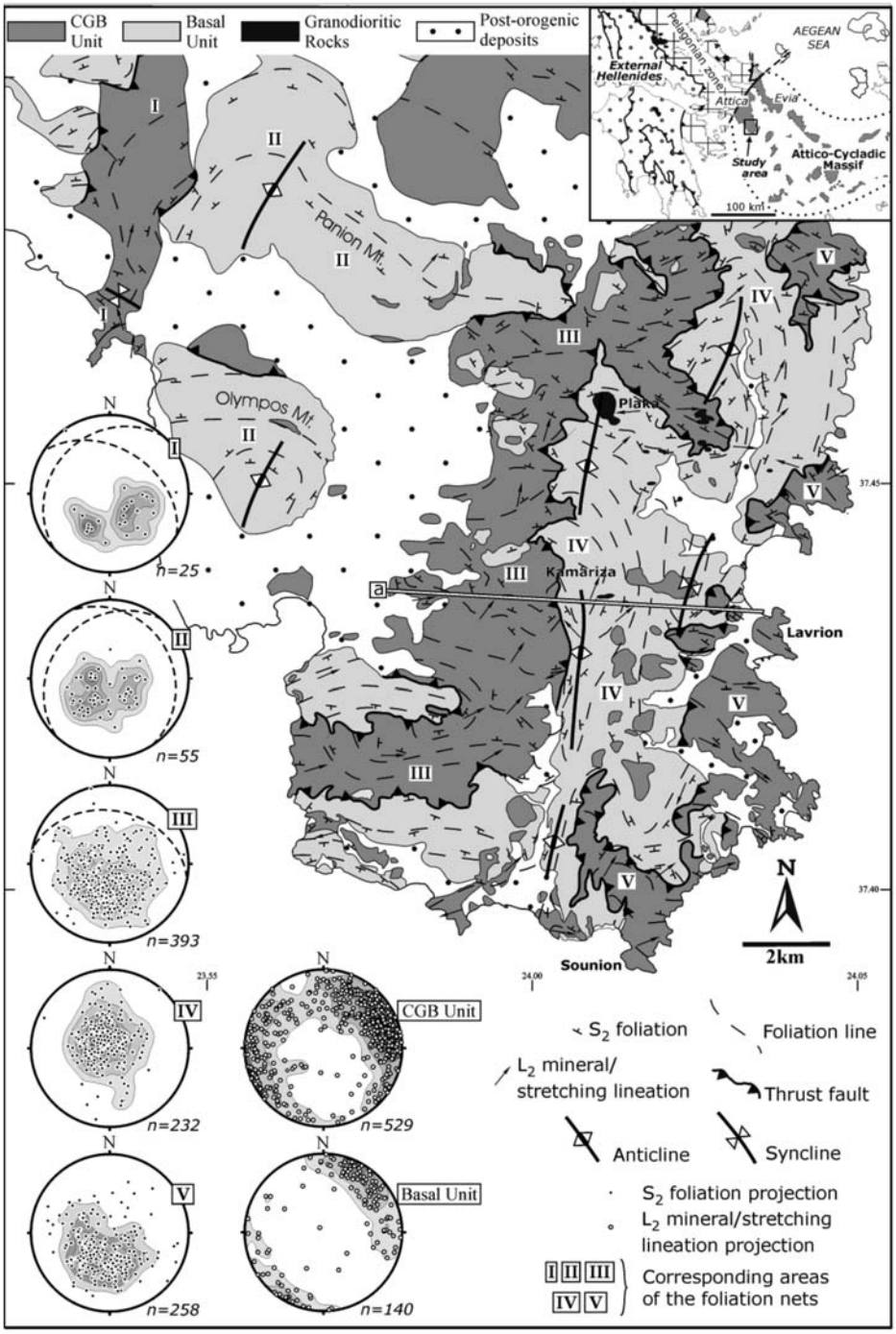

Fig. 1: Simplified geological map showing also foliation trajectories and mineral lineation trends. Lower hemisphere equal-area projections I-V reflect the foliation measurements of the corresponding areas in the map; also quoted the stretching lineation projections of the two main tectonic units; (inset): Generalized tectonic map shows the location of the Lavrion area and the Attico-Cycladic Massif within the Hellenides.

ACM has an internal position within the Alpine orogenic belt of the Hellenides (Fig. 1 inset) and exposes a complex pile of high-pressure (HP) nappes/units, which are tectonically overlain by the Pelagonian zone, a belt of imbricated pre-Alpine crystalline rocks and Mesozoic marbles also belonging to the Internal Hellenides (Mountrakis, 1986; Doutsos et al., 1993; Anders et al., 2007).

In Lavrion area the ACM is divided into two major structural units: the para-authochthonous Basal unit at the bottom, which is considered to be the equivalent of Almyropotamos unit in Evia, and the overlying allochthonous Cycladic Greenschist-Blueschist (CGB) unit (Marinos & Petrascheck, 1956; Katsikatsos et al., 1986). These two units are separated by a major ductile thrust (Kessel, 1990; Avigad et al., 1997; Xypolias et al., 2003). Hereinafter, this zone will be referred as 'Basal thrust'; it is equivalent to the Evia thrust.

The Basal unit is characterised of thick series of Mesozoic marbles and schists with minor lenses of mafic and ultramafic rocks, overlain by a metapelitic sequence, which is interpreted as metaflysch. In Lavrion area the relatively autochthonous Basal unit can be subdivided into: a) the lowermost "Lower Marble", b) the "Kamariza-Kesariani Schists" and c) the uppermost "Upper Marble". This succession of marbles and schists is at least 850m thick and is considered to be of Upper Triassic-Jurassic age according to preserved fossils found in the broad area of Attica (Marinos & Petrascheck, 1956; Photiades & Carras, 2001 and references therein). During the Miocene, an I-type granodiorite (known as "Plaka granodiorite") intruded the Basal unit causing the metamorphism of the adjacent schists (Marinos & Petrascheck, 1956; Skarpelis et al, 2008; Stouraiti, 2009).In Evia, glaucophane relics and Si-rich phengites in the metapelitic sequence were observed impling that the Basal unit underwent HP-metamorphism (~ 350^{o}C / 8-10 kbar; c. 30-35 km depth; Shaked et al., 2000). The possible age of this HP-event is early Miocene (Ring & Reischmann, 2002) or pre-Miocene with early Miocene greenschist-facies overprinting (Bröcker et al., 2004) or late Eocene-Oligocene (e.g. Avigad et al., 1997).

The CGB unit overlies the Basal unit and, apart from the area of Attica, is emerged also in Evia and the islands of Cyclades. In the area of Lavrion, represented by a nappe formed of a thin (up to 250m) metasedimentary succession of schists with quartzites intercalations and calcite-rich marbles, as well as meta-ophiolite mafic bodies. Moreover, this nappe is homologous to the structurally lower Styra nappe of CGB in southern Evia (Katzir et al., 2000; Shaked et al., 2000). The CGB unit includes an epidote - blueschist facies metamorphism (M_1, T_{max} = 450^{o}C; P_{min} = 11 kbar; depth > 40 km) of Eocene age (c. 50-40 Ma), followed by a greenschist to pumpellyite - actinolite facies overprint (M_2, T_{max} = 350^{o}C; P = 4-7 kbar; c. 15-25 km depth) at the Oligocene - Miocene boundary (c. 25 Ma) (Altherr et al., 1979; Bröcker, 1990; Baltatzis, 1996; Shaked et al., 2000; Tomascheck et al., 2003; Bröcker, et al. 2004). Alternatively, Baziotis et al. (2009) calculated lower P-T conditions for M_1 (P~9 kbar, T~350 ^{o}C) and M_2 (P~6 kbar, T~280 ^{o}C) metamorphic events. Research regarding the CGB unit that outcrops in southern Evia, imply that peak metamorphic conditions of the M_1 event slightly increase towards the upper structural levels while the greenschist facies overprint (M_2) was characterized by a decrease in M_2 temperature towards the base of the unit (Shaked et al., 2000; Katzir et al., 2000). The degree of retrogression in the ACM considerably increases downward and pervasively overprinted greenschist facies rocks predominate at the lower structural levels of the CBG unit resulting to the partial or complete effacement of the high pressure M_1 assemblages (Bröcker et al., 2004 and references therein).

3. Main structures and fabrics

The deformed rocks of the CGB nappe preserve proto-mylonitic up to ultra-mylonitic textures. The

second are located at the deeper structural levels of the nappe. The mylonitic foliation (S_m) is defined by planar aggregates of the greenschist facies related minerals such as white mica and albite, and fine grained recrystallized quartz. The S_m bears a well-developed ENE-WSW trending stretching lineation L_m. In low strain domains, an earlier residual S_1 foliation is identified and has been isoclinally folded with contemporaneous development of axial planar foliation (S_2) and an accompanying stretching lineation L_2. The axial planar foliation (S_2) represents the dominant fabric in the area (Fig. 1). In the CGB unit, S_2 generally plunges gently to north and swings to east or west depending the orientation of the contact with the underlying Basal unit. In the Basal unit S_2 trends mostly N-S, dipping west and turning upon east forming N-S to NNE-SSW anticlines. The most representative ones are situated in Panion Mt., Olympos Mt. and southern of Kamariza settlement (Fig. 1). Both, S_2 and the accompanying lineation L_2 are subparallel to S_m and L_m respectively.

Beneath the thrust plane is located a c. 50 m thick zone of strongly foliated to (ultra-) mylonitized marbles of the Basal unit. A shallow ENE-WSW trending stretching lineation (L_m) is defined by micaceous streaks on mylonitic foliation planes of impure marbles. Thin ultramylonites locally display a roughly N-S trending lineation (Fig. 1), which is interpreted to reflect 'rolling' lineation development as described by Passchier (1997). In the deeper structural levels of the Basal unit in Attica, compositional layering (S_1) is strongly deformed by tight to isoclinal, map-scale, ductile folds and a series of east-directed ductile shear zones. The axial-planar foliation (S_2) of these folds as well as the shear zones are sub-parallel or at low angle to the thrust.

4. Microstructural and petrofabric analysis

Microstructural and petrofabric data from 3 oriented calcite-rich and 15 quartz-rich samples that located in the thrust zone are summarized in Figure 2a. Locations of all samples have also been projected on a representative geological cross-section (Fig. 2b). The estimated sampling distances of each sample measured perpendicular to the thrust planes are given in Table 1, where the positive and negative values of depth correspond to samples above (CGB unit) and below (Basal unit) the thrust plane respectively.

All microstructural and crystal fabric data were taken from thin-sections oriented parallel to the stretching lineation (X) and perpendicular to the foliation (XY). Petrofabric analysis of quartz c-axis and calcite c-axis preferred orientation was carried on XZ thin-sections using a Leitz universal stage mounted on an optical microscope.

4.1. Microstructures

In all quartz-rich samples, quartz exceeds 75% of total sample composition and shows evidence of extensive dynamic recrystallization accommodated by either subgrain rotation or low-temperature grain-boundary migration (i.e. transitional between regime 2 and regime 3 of Hirth & Tullis 1992). The volume fraction of quartz recrystallization within samples ranges between 60% and 90%. Highly elongate ribbon grains lying in the plane of foliation (S_m) are locally preserved. Dynamically recrystallized quartz grains are also elongate with their long axes oriented obliquely to the S_m or parallel to it in domains with relatively high phyllosilicate content. Oblique grain-shape fabric (S_q) was locally recognized in 7 of the 18 samples selected for detailed analysis (Fig. 3c). The maximum observed angle between S_m and S_q generally varies from 10^o-20^o (Fig. 2a).

Similar angular relationships have been described elsewhere in quartz-rich tectonites that have undergone non-coaxial deformation (e.g. Law et al. 1986) and the sense of obliquity can be used as a shear sense indicator. A consistent top-to-the ENE shear sense is indicated by all the 7 quartz-rich

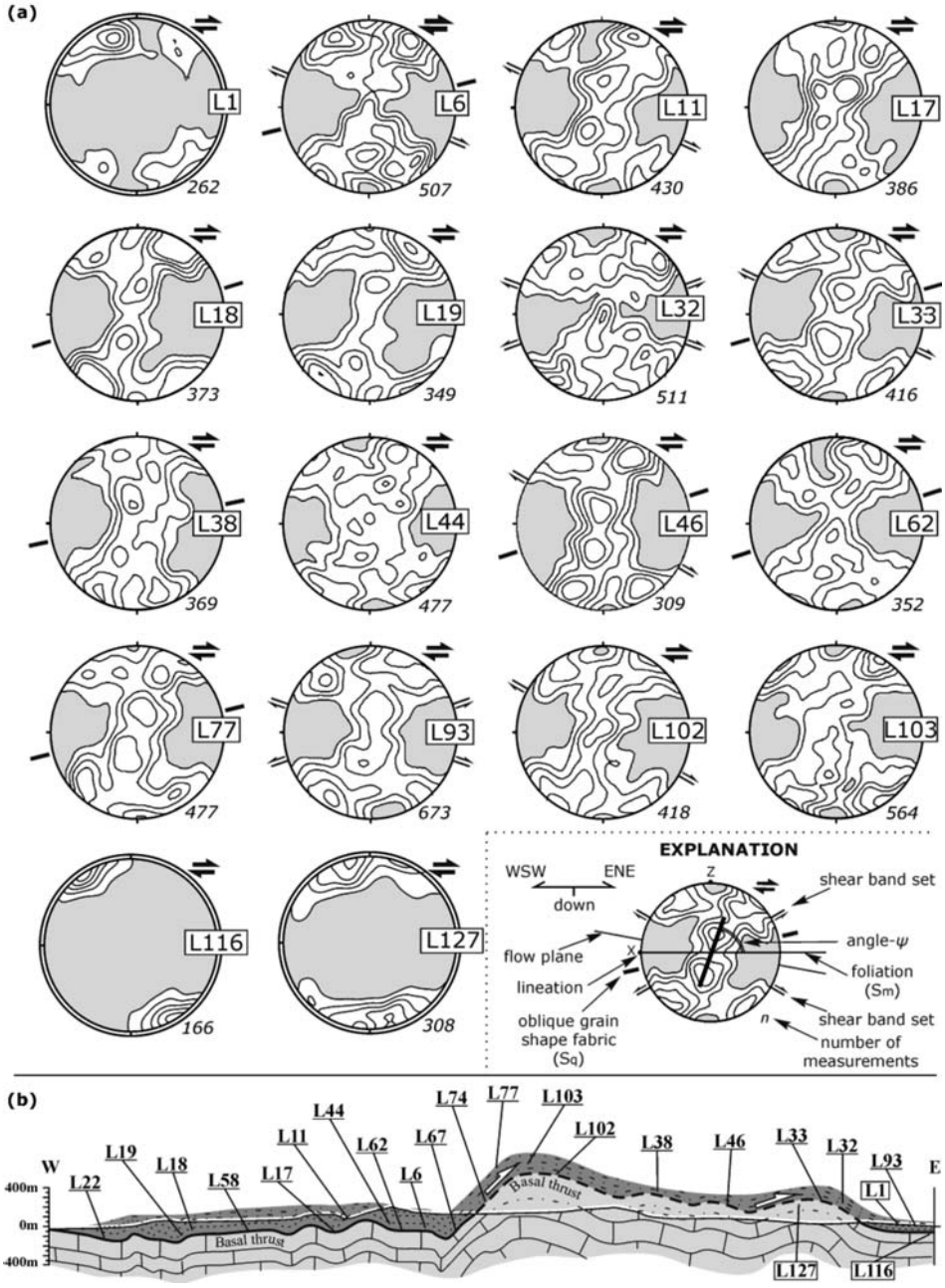

Fig. 2: (a) Contoured diagrams (Lower hemisphere equal-area projections) of optically measured quartz c-axes from 15 samples (after Xypolias et al. 2010) and calcite c-axis from three (L1, L116, L127; nets with double lined periphery) samples; all the XZ section planes are approximately viewed towards the NNW. Samples L116 and L127 were collected from the Basal unit while the rest from CGB unit. Orientations of oblique grain shape fabric (S_q) and shear band sets have been marked for samples where these microstructures were observed. (b) W-E cross-section showing the structural positions of the samples relative to basal thrust while the geographic co-ordinates of each sample locality are given in Table 1.

tectonites displaying an obliquity between S_m and S_q. The same shear sense is inferred from single sets of extensional shear bands (Platt & Vissers 1980) observed in 4 samples containing domains of relatively high phyllosilicate content (Figs. 3a, 2a). The angle of obliquity between shear bands and S_m ranges between 20° and 35°. Weakly developed conjugate shear bands with top-to-the ENE and WSW senses of displacement are locally recorded in 2 samples (Fig. 2a). However, the top-to-the ENE set is dominant in the majority of the samples.

Some samples (e.g. L38, L67) contain rigid feldspar porphyroclasts that are oriented at various angles with respect to S_m. Elongate porphyroclasts oriented at moderate to high angles (>30°) to foliation display δ- or σ-tails and give consistent top-to-the-ENE sense of shear (Figs 3b). In turn, σ-type clasts oriented at low angles to S_m indicate either top-to-the-ENE- or top-to-the-WSW-directed shearing with the direction to be dominant. These microstructural features possibly indicate a component of pure shear during ductile deformation (see also Simpson & DePaor 1997; Klepeis et al. 1999).

4.2 Quartz c-axis fabrics

The majority of analyzed samples are characterized by well-developed quartz c-axis fabrics (Fig. 2a). The intensity of the crystallographic preferred orientation appears to be lower in one sample (L44). This sample contains a relatively high proportion (c. 20-25%) of phyllosilicates and/or other mineral phases. All samples produce fabrics that generally exhibit similar characteristics (Fig. 2a). In terms of density distribution, the standard pattern is type-I cross-girdles (Lister 1977) with discrete and well-developed point maxima at moderate to high angles to the foliation trace.

Among the 15 quartz c-axis fabrics measured close to the thrust zone, 12 are distinctly asymmetrical (in terms of both topology and density distribution) with respect to foliation and lineation, indicating a top-to-the-ENE sense of shear (Fig. 2a). Less clearly defined fabric asymmetry consistent with ENE shear sense was recognized in three samples (L6, L17, L44; Fig. 2a). In all these fabrics, the inferred shear sense is supported by the obliquity (angle ψ) of the central girdle segment, which varies between 70 and 85°, as well as by microstructural shear sense indicators (where observed) described above (Fig. 2a). No unequivocal microstructural shear sense indicators were observed in these samples.

4.3 Calcite c-axis fabrics

The microscopic analysis of calcite has been restricted on determining the crystallographic preferred orientation (CPO) of the optical c-axis of calcite grains in three samples. Sample L1 comes from the CGB unit whilst samples L116 and L127 belong to marble-mylonites of the Basal unit. The objective of the calcite petrofabric analysis is the verification of shear sense via the orientation patterns of calcite grains and the correlation of the exported results with the ones of quartz c-axis. Calcite optical axis measurements were acquired using the procedure introduced by Turner & Weiss (1963). The fabric asymmetry in all three samples documents top-to-the-ENE sense of shear which is concordant with quartz petrofabric analysis. According to the classification from Wenk et al. (1987), c-axis distributions show triclinic symmetry that is characteristic of simple shear deformation. Pole figures of L1 and L127 are characterized by two major and two minor concentrations that imply higher temperatures than L116.

5. Finite strain analysis

Strain analysis was performed on 18 samples including elongate ribbon-like quartz grains. Two mutually perpendicular thin sections were cut from each specimen: one (XZ section) parallel to the lin-

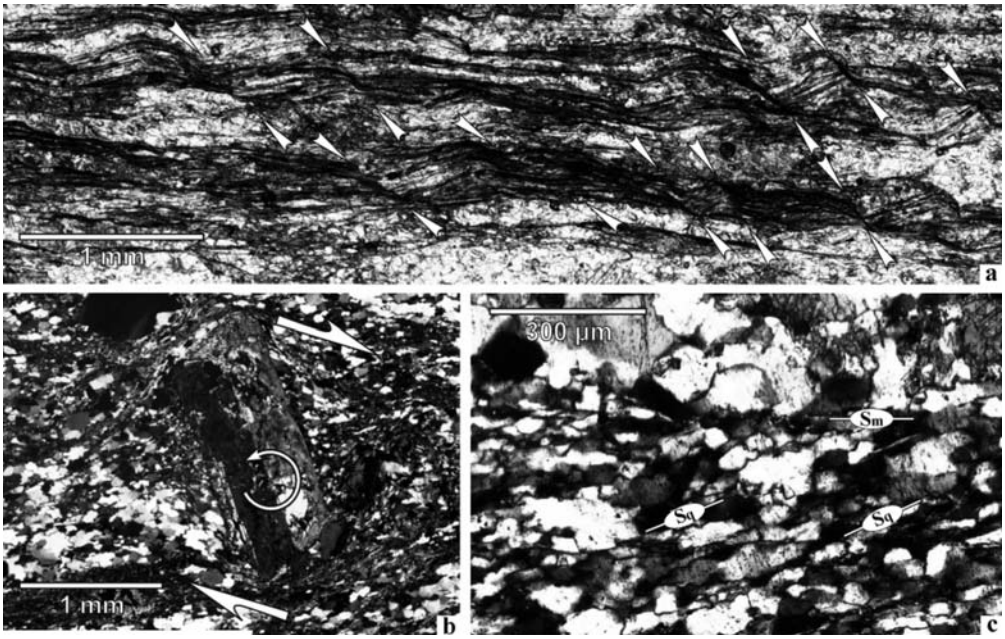

Fig. 3: Photomicrographs of microstructures in the CGB unit shot from thin sections cut perpendicular to foliation and parallel to stretching lineation and viewed towards the NNW; (a) Single set of shear bands in sample L67 indicating top-to-the-ENE sense of shear preferably developed in a phyllosilicate-rich domain inter-bedded in quartz Qtz-rich zones (plane polarized light); (b) Sample L38: backward rotated σ-type plagioclase feldspar porphyroclast. The porphyroclast is embedded in ductily deforming matrix consisting of phyllosilicate and recrystallized quartz and mantled by wedge-shaped recrystallized tails extending from its broad sides indicating top-to-the ENE sense of shear (crossed polarized light); (c) Sample L17: elongate, dynamically recrystallized quartz grains displaying a preferred shape alignment (S_q) oblique to the mylonitic foliation (S_m). The obliquity reflects top-to-the ENE shear sense (crossed polarized light).

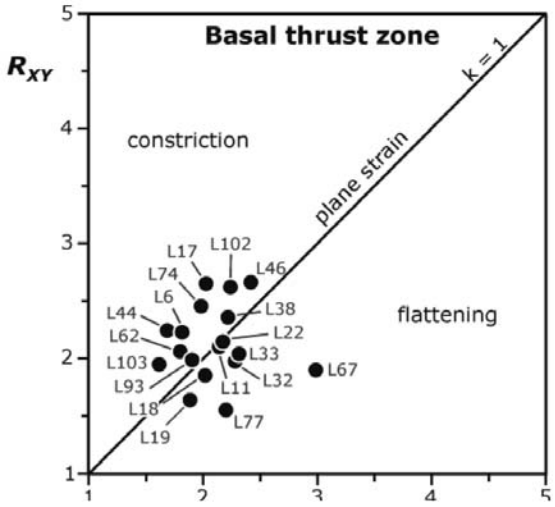

Fig. 4: Flinn diagram showing finite strain data collected from the Basal thrust zone (after Xypolias et al. 2010).

eation and normal to the foliation and one (YZ section) perpendicular to both the lineation and foliation. In each section the traces of 100-150 grain outlines were input into the program SAPE (Mulchrone et al. 2005), which automatically approximates complex grain shapes as ellipses and extracts Rf - ϕ data. The extracted data for each section were analysed using the theta-curve method of Lisle (1985). Calculations of best-fit R_{XZ} and R_{YZ} values were made utilizing the strain analysis program of Mulchrone & Meere (2001). Maximum uncertainty in strain ratio has been estimated to be ± 0.3 (see also Yonkee 2005; Xypolias et al. 2007). Assuming constant volume deformation, the 3D strain was determined by combining 2D data from the assumed R_{XZ} and R_{YZ} principal planes of the strain ellipsoid (Ramsay & Huber, 1987). Results of the strain analysis are presented in Figure 4.

The R_{XZ} strain ratio varies from 3.1 to 6.4 while the determined finite strain data attribute Flinn's parameter (k) values that range between 0.45 (flattening strain) and 1.79 (constrictional strain). Although the values fall in both the apparent flattening and constrictional fields, they generally lie close to the plane strain line (average k = 1.08). This is in agreement with 3D strain data reported from the Evia thrust zone in central Evia area, where an average k = 0.98 has been obtained (Xypolias et al. 2003).

6. Discussion and conclusions

Quartz-rich tectonites above the Basal thrust display a homogeneously developed, greenschist facies foliation (S_m) and an ENE-trending mineral stretching lineation (L_m). The deformation along the Basal thrust zone occurred under approximately plane strain conditions with a dominant top-to-the-ENE sense of shearing along the Basal thrust zone indicated by the asymmetry of quartz and calcite c-axis fabrics with respect to foliation and lineation (Fig. 2). This inferred shear sense is independently supported by the observed sense of obliquity between foliation and shape preferred orientation of recrystallized quartz grains as well as by single sets of normal shear bands. An overall top-to-the-ENE movement sense has been documented in different structural levels of the ACM in central Evia (Xypolias et al., 2003) and neighbouring islands (e.g. Syros and Tinos, Trotet et al., 2001). In contrast, Ring et al. (2007) proposed WSW-directed emplacement of the CGB. Contradicting kinematic evidence for ENE- (e.g. Barton 1976; Doutsos et al. 1993) or WSW- (e.g. Schermer 1993) directed shearing has also been given for the tectonically equivalent nappe contact in the Mt. Olympos region (northern Greece.

The presence of conflicting kinematic indicators may be due to the different rate of emergence within different domains of the CGB unit although the en-

Table 1. Geographical coordinates for samples from the CGB unit.

Sample	Geographical coordinates		D (m)
	Latitude	Longitude	
L77	37°46'41"	24°01'36"	+180
L103	37°47'46"	24°02'03"	+100
L1	37°43'21"	24°04'24"	+75
L32	37°43'12"	24°02'59"	+60
L11	37°43'40"	23°59'13"	+60
L18	37°41'59"	23°57'56"	+50
L19	37°41'57"	23°57'32"	+50
L44	37°41'48"	23°59'46"	+50
L38	37°39'58"	23°59'27"	+40
L67	37°45'56"	24°00'23"	+40
L93	37°44'39"	24°03'46"	+35
L17	37°44'05"	23°59'08"	+30
L6	37°43'13"	24°00'03"	+30
L33	37°41'12"	24°02'43"	+25
L62	37°45'31"	23°59'55"	+15
L102	37°49'06"	24°02'31"	+10
L22	37°41'14"	23°56'17"	+10
L74	37°47'24"	24°01'29"	+10
L46	37°40'25"	24°01'34"	+3
L116	37°47'06"	24°04'24"	-9
L127	37°44'37"	24°03'05"	-38

* For definition see Fig. 2a.
D, distance from the thrust plane;

tire unit had ceaseless ENE movement. In that case, counter sense of shear is observed that testifies a relative movement between adjacent layers of the unit and not the bulk shear sense of CGB unit.

7. References

Altherr, R., Schliestedt, M., Okrusch, M., Seidel, E., Kreuzer, H., Harre, W., Lenz, H., Wendt, I., Wagner, G. A. 1979. Geochronology of high pressure rocks on Sifnos (Cyclades, Greece). *Contributions to Mineralogy and Petrology*, 70, 245-255.

Anders, B., Reischmann, T., Kostopoulos, D., 2007. Zircon geochronology of basement rocks from the Pelagonian Zone, Greece: constraints on the pre-Alpine evolution of the westernmost Internal Hellenides. *International Journal of Earth Sciences*, 96, 639-661.

Avigad, D., Garfunkel, Z., Jolivet, L., Azanon, J.M., 1997. Back arc extension and denudation of Mediterranean eclogites. *Tectonics*, 16, 924-941.

Baltatzis, E., 1996. Blueschist-to-greenschist transition and the P–T path of prasinites from the Lavrion area, Greece. *Mineralogical Magazine,* 60, 551–561.

Barton, C.M., 1976. The tectonic vector and emplacement age of an allochthonous basement slice in the Olympos area, N.E. Greece. *Bulletin de la Société Géologique de France*, 18, 253-258.

Baziotis, I., Proyer, A. and Mposkos, E., 2009. High-pressure/low-temperature metamorphism of basalts in Lavrion (Greece): implications for the preservation of peak metamorphic assemblages in blueschists and greenschists *Eur. J. Mineral. 2009,* 21, 133–148.

Bröcker, M., 1990. Blueschist-to-greenschist transition in metabasites from Tinos Island (Cyclades, Greece): Compositional control or fluid infiltration. *Lithos*, 25, 25–39.

Bröcker, M., Bieling, D., Hacker, B., Gans, P., 2004. High-Si phengite records the time of greenschist facies overprinting: Implications for models suggesting megadetachments in the Aegean Sea. *Journal of Metamorphic Geology,* 22, 427-442.

Doutsos, T., Piper, G., Boronkay, K., Koukouvelas, I., 1993. Kinematics of the Central Hellenides. *Tectonics*, 12, 936-953.

Hirth, G. and Tullis, J., 1992. Dislocation creep regimes in quartz aggregates. *Journal of Structural Geology*, 14, 145-159.

Katsikatsos, G., Migiros, G., Triantaphyllis, M., Mettos, A., 1986. Geological structure of Internal Hellenides. Institute of Geological and Mining Exploration, Athens. *Geological and Geophysical Research, Special Issue*, 191-212.

Katzir, Y., Avigad, D., Matthews, A., Gurfunkel, Z., Evans, B.W., 2000. Origin, HP/LT metamorphism and cooling of ophiolitic mélanges in southern Evia (NW Cyclades), Greece. *Journal of Metamorphic Geology*, 18, 699-718.

Kessel, G., 1990. Untersuchungen zur Deformation und Metamorphose in Attischen Krystallin, Griechenland. *Berliner Geowissenschaftlicher Abhandlungen,* A126, 1–150.

Klepeis, K. A., Daczko, N.R., Clarke, G.L., 1999. Kinematic vorticity and tectonic significance of superposed mylonites in a major lower crustal shear zone, northern Fiordland, New Zealand. *Journal of Structural Geology*, 21, 1385-1405.

Law, R.D., Casey, M., Knipe, R.J., 1986. Kinematic and tectonic significance of microstructures and crystallographic fabrics within quartz mylonites from the Assynt and Eriboll regions of the Moine thrust zone, NW Scotland. *Transactions of the Royal Society of Edinburgh: Earth Sciences*, 77, 99-126.

Law, R.D., Schmid S.M., Wheeler, J., 1990. Simple shear deformation and quartz crystallographic fabrics: a possible natural example from the Torridon area of NW Scotland. *Journal of Structural Geology,* 12, 29-45.

Lisle, R.J., 1985. *Geological Strain Analysis. A Manual for the R_f/j method*. Pergamon Press, New York.

Lister, G.S., 1977. Discussion: Crossed girdle c-axis fabrics in quartzites plastically deformed by plane strain and in progressive simple shear. *Tectonophysics*, 39, 51-54.

Marinos, G.P. and Petrascheck, W.E., 1956. Laurium. Geological and Geophysical Research 4/1, Institute for Geology and Subsurface Research, Athens, 1–247.

Mountrakis, D., 1986. The Pelagonian zone in Greece. A polyphase-deformed fragment of the Cimmerian continent and its role in the geotectonic evolution of the eastern Mediterranean. *Journal of Geology*, 94, 335-347.

Mulchrone, K.F. and Meere, P.A., 2001. Windows program for the analysis of tectonic strain using deformed elliptical markers. *Computers and Geosciences*, 27, 1251–1255.

Mulchrone, K.F., Meere, P.A., Roy Choudhury, K., 2005. SAPE: a program for semi-automatic parameter extraction for strain analysis. *Journal of Structural Geology*, 27, 2084-2098.

Passchier, C.W., 1997. The fabric attractor. *Journal of Structural Geology*, 19, 113-127.

Photiades, A. and Carras, N., 2001. Stratigraphy and geological structure of the Lavrion area (Attica, Greece). Bull. Geol. Soc. Greece. 34/1, 103-109.

Platt, J.P. and Vissers, R.L.M., 1980. Extensional structures in anisotropic rocks. *Journal of Structural Geology*, 2, 397-410.

Ramsay, J.G. and Huber, M.I., 1987. *The Techniques of Modern Structural Geology*, vol. 2. Academic Press, New York.

Ring, U. and Reischmann, T., 2002. The weak and superfast Cretan detachment, Greece: exhumation at subduction rates in extruding wedges. *Journal of the Geological Society, London,* 159, 225–228.

Ring, U., Glodny, J., Will, T., Thomson, S., 2007. An Oligocene extrusion wedge of blueschist-facies nappes on Evia, Aegean Sea, Greece: implications for the early exhumation of high-pressure rocks. *Journal of the Geological Society, London,* 164, 637-652.

Schermer, E.R., 1993. Geometry and kinematics of continental basement deformation during Alpine orogeny, Mt. Olympos region, Greece. *Journal of Structural Geology,* 15, 571-591.

Shaked, Y., Avigad, D., Garfunkel, Z., 2000. Alpine high-pressure metamorphism at the Almyropotamos window (southern Evia, Greece). *Geological Magazine*, 137, 367-380.

Simpson, C. and De Paor, D.G., 1997. Practical analysis of general shear zones using the porhyroclast hyperbolic distribution method: an example from the Scandinavian Caledonides. *In:* SENGUPTA, S. (ed.) *Evolution of Geological Structures in Micro- to Macro-scales*. London: Chapman & Hall, 169-184.

Skarpelis, N., Tsikouras, B., Pe-Piper, G., 2008. The Miocene igneous rocks in the Basal Unit of Lavrion (SE Attica, Greece): petrology and geodynamic implications. *Geological Magazine*, 145, 1-15.

Stouraiti, C., Mitropoulos, P., Tarney, J., Barreiro, B., McGrath, A.M., Baltatzis, E., 2009. Geochemistry and petrogenesis of late Miocene granitoids, Cyclades, southern Aegean: nature of source components.

Tomaschek, F., Kennedy, A.K., Villa, I.M., Lagos, M., Ballhaus, C., 2003. Zircons from Syros, Cyclades, Greece –recrystallization and mobilization of zircon during high-pressure metamorphism. *Journal of Petrology*, 44, 1977–2002.

Trotet, F., Jolivet, L., Vidal, O., 2001. Tectono-metamorphic evolution of Syros and Sifnos islands (Cyclades, Greece). *Tectonophysics*, 338, 179-206.

Turner, F.J. and Weiss, L.E., 1963. *Structural analyses of metamorphic tectonites*.

Wenk, H.R., Takeshita, T., Bechler, E., Erskine, B.G., Matthies, S., 1987. Pure shear and simple shear calcite textures. Comparison of experimental, theoretical and natural data. *Journal of Structural Geol-*

ogy, 9, 731-745.

Xypolias, P., Kokkalas, S., Skourlis, K., 2003. Upward extrusion and subsequent transpression as a possible mechanism for the exhumation of HP/LT rocks in Evia Island (Aegean Sea, Greece). *Journal of Geodynamics*, 35, 303-332.

Xypolias, P., Chatzaras, V., Koukouvelas, I. K., 2007. Strain gradients in zones of ductile thrusting: Insights from the External Hellenides. *Journal of Structural Geology*, 29, 1522-1537.

Xypolias, P., Spanos, D., Chatzaras, V., Kokkalas, S., Koukouvelas, I., 2010. Vorticity of flow in ductile thrust zones: examples from Attico-Cycladic Massif (Internal Hellinides, Greece). In: Law, R. D., Butler, R. W. H., Holdsworth, R., Krabendam, M. & Strachan, R. (eds) *Continental Tectonics and Mountain Building – The Legacy of Peach and Horne, Geological Society, London, Special Publications,* 335, in press.

Yonkee, A., 2005. Strain patterns within part of the Willard thrust sheet, Idaho–Utah–Wyoming thrust belt. *Journal of Structural Geology*, 27, 1315-1343.

Δελτίο της Ελληνικής Γεωλογικής Εταιρίας, 2010
Πρακτικά 12ου Διεθνούς Συνεδρίου
Πάτρα, Μάιος 2010

Bulletin of the Geological Society of Greece, 2010
Proceedings of the 12th International Congress
Patras, May, 2010

A CONTRIBUTION TO THE GEOLOGICAL STRUCTURE OF CHIOS ISLAND, EASTERN AEGEAN SEA

Tselepidis V.[1] and Rondoyanni Th.[2]

[1] *Institute of Geology and Mineral Exploration, Department of Geology and Geological Mapping, vtselepidis@igme.gr*

[2] *National Technical University of Athens, School of Mining and Metallurgical Engineering, Department of Geological Science, rondo@central.ntua.gr*

Abstract

The island of Chios, in the eastern Aegean Sea, is of great geological interest due to the outcrops of the oldest Paleozoic rocks of the Hellenides. Three main geological units of Paleozoic and Mesozoic age dominate, that have a tectonic relationship: the Autochthonous unit is overthrusted by the Parautochthonous unit, which in turn is overthrusted by the Allochthonous unit.

In this work, new geological and tectonic data concerning the Autochthonous unit and especially its part of the Paleozoic - Mesozoic transition are presented and evaluated. Due to the rare outcrops of this transition and the lack of sufficient palaeontological data, there are various and contradictory opinions concerning its normal or discordant character. Based on our field data and lithostratigraphic correlations, we can draw the following main results:

Considering the Autochthonous unit, the transition of the Paleozoic formations to the Mesozoic ones is characterized by an angular unconformity as well as by a basal conglomerate. In some places there is a tectonic contact between them, this of a thrust fault. The Lower Triassic formations of the Parautochthonous unit belong to the Autochthonous unit, since they present similar palaeogeographic conditions. Moreover, the presence of the "Hallstatt" limestones in the Autochthonous unit can be explained by their local deposition in lenticular form.

Key words: *Chios Island, Autochthonous Unit, Parautochthonous Unit, Hallstatt facies, Nagos spring.*

1. Introduction

As the Island of Chios, in the eastern Aegean Sea, has an important geological structure, several geological studies have been conducted there, referring predominantly to the stratigraphic evolution of the Paleozoic and Mesozoic formations. The tectonic structure of Chios is very complicated as a result of several pre-alpine and alpine tectonic phases (Ktenas, 1921; Besenecker, et al. 1968; Herget, 1968; Roth, 1968; Bender, 1970; Assereto et al., 1980; Papanikolaou and Sideris, 1983; Gaetani et al., 1992; Robertson and Pickett, 2000).

According to the geological map of Chios, on a 1:50.000 scale (Besenecker et al., 1971), the greatest part of the island is covered by an Autochthonous unit, the Lower one. It consists of a turbiditic succession including olistoliths of Silurian and Carboniferous rocks, lutites, vulcanites and tuffs of

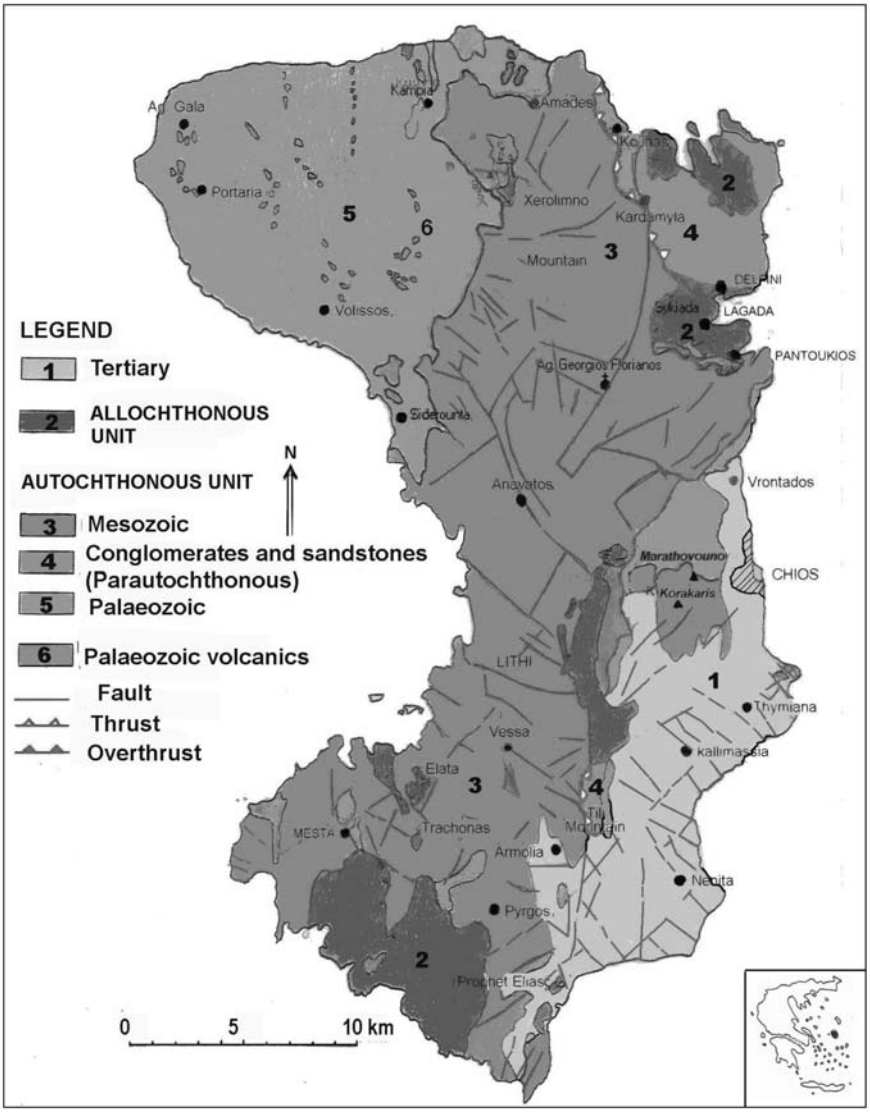

Fig. 1: Structural map of the island of Chios.

the Upper Devonian to Westfalian age, and of a Mesozoic carbonate succession, developed from the base of the Triassic to Lias (Fig. 1). Different tectonic models have been proposed as to the origin of the clastic, chaotic Palaeozoic unit, considered a wildflysch sequence and named Chios melange (Groves et al., 2003). Robertson and Pickett (2000) have interpreted it as a rift setting and a deposition on a deep marine basin. The transition of the Paleozoic formations to the Mesozoic ones is characterized by an angular unconformity as well as by a basal conglomerate.

The Autochthonous unit is overthrusted by the Upper unit (Allochthonous) consisting of a Pensylvanian to Upper Permian sequence, of red siltstones of undetermined age and of Liassic shallow-water carbonates (Kauffman, 1969; Zanchi et al., 2003). Between these two main units, the

Fig. 2: View towards the North of the thrust sheets observed in north-eastern Chios (Ka-Kardamyla village, A.U.-Autochthonous Unit, PA.U.- Parautochthonous Unit, AU-Allochthonous Unit, P-Palaeozoic, L-Lias).

Intermediate unit (Parauthochthonous) cropping out mainly at the north-eastern part of the island (Fig. 2), consists of Upper Palaeozoic and intensively tectonised Liassic carbonate rocks. Due to the lack of sufficient palaeontological data, there are alternative interpretations concerning the origin of this Parauthochthonous unit, mainly based on correlative observations. Besenecker et al. (1968) consider that the Parauthochthonous unit constitutes a fragment of the substratum, carried over with the Allochthonous unit during its emplacement.

The south-eastern part of the island is covered by fluviolacustrine Upper Miocene – Lower Pliocene deposits, consisting of conglomerates, clays and limestones. Miocene and post-Miocene volcanic rocks of limited extension also crop out in different places on the island.

The aim of this paper is to present new data obtained on the Island of Chios, in view of reconsidering the relationship of the tectonostratigraphic units. The study focuses on the Palaeozoic-Mesozoic transition of the Autochthonous unit and the Mesozoic of the Parauthochthonous unit. The results of this work are of a preliminary character because no palaeontological evidence could be found in the collected samples, despite a systematic sampling undertaken. Although lithostratigraphic and tectonic data have led us to propose a different structural model, further research is needed to explain the complicated geological structure of Chios and to interpret the palaeogeographic regime of the broader area.

2. The geological structure of the Autochthonous and Parau-tochthonous units

The Autochthonous unit includes a Palaeozoic sequence uncomfortably overlain by Mesozoic carbonate formations, while transgression conglomerates have developed between them. The lower members of these Mesozoic carbonates show similar lithofacial evolution with the Parautochthonous unit's (Fig. 3). In ascending order, they both consist of:

(a) A basal conglomerate, alternating with coarse-grained sandstones, indication of the alpine transgression on the intensively tectonised Variscan substratum. This formation, constituting the Palaeozoic-Mesozoic boundary, is developed mainly at the northern part of the island, exhibiting its whole thickness in the area of Giossonas.

(b) Thin-bedded, multi-folded limestones of undetermined age, due to the lack of any palaeontological evidence. According to their lithostratigraphic position, a Skythian age could be attributed to them.

(c) The upwards continuity of the Mesozoic sequence differs from place to place. Massive limestones and dolomites of Anisian-Skythian age, dominating in both the Autochthonous and Parautochthonous units, are observed in the northern part of the island. Oolithic limestones are more abundant in the Autochthonous unit. In the southern part outcrop mainly red, micritic limestones of the "Hallstatt" facies and dolomites, dated Upper Scythian to Lower Anisian on the

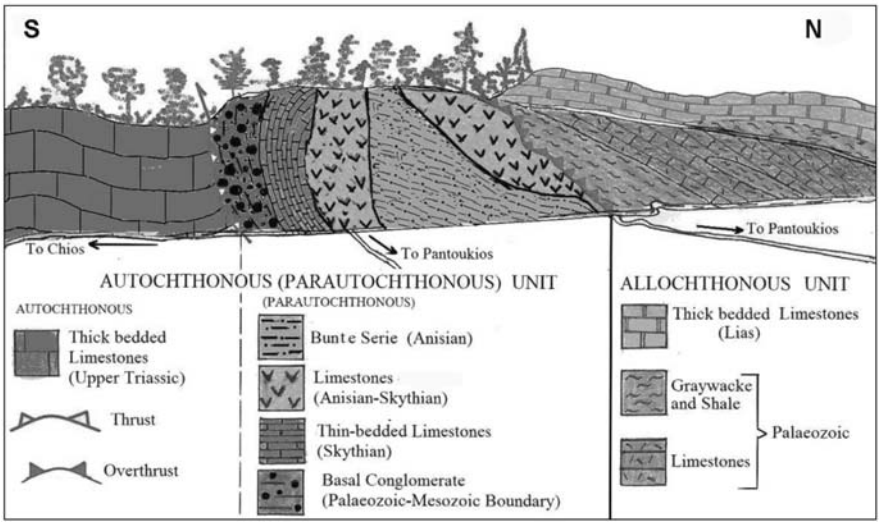

Fig. 3: Schematic geological section along the Vrontados-Pantoukios road (the locations are noted on Fig. 1).

basis of the ammonitic fauna. The characteristic "Hallstatt" limestones which can be easily recognised in the field, have not developed throughout the extent of the Mesozoic sequence and are absent in the northern part of the island.

(d) The "multi-colored sequence" (known as "Bunte Serie") of Anisian age, overlays the above described formations (Figs 4, a and b). It consists of alternating clastic sediments, cherts, radiolarites, limestones, marls, sandy marls, sandstones and conglomerates in the lower part and of well-bedded grey limestones, reddish marly limestones, marls and brecciated horizons in the upper part. According to the included conodonts, these formations are of Anisian age (Kauffman, 1969). The evolution of the Autochthonous Mesozoic sequence on the Autochthonous Palaeozoic substratum can be observed in the region of the mountain Korakaris (Fig. 4a). The Palaeozoic-Mesozoic contact is also observed in this part of the island, to the North of the village Vrontados (Fig. 5a). In some places, the "Bunte Serie" lay directly on the thin-bedded limestones (Fig. 5b), but there is a tectonic contact between them. Such an outcrop can be observed to the North-East of the village Kardamyla.

Although the lack of detailed palaeontological evidence does not allow definitive results concerning the stratigraphic comparison between Autochthonous and Parautochthonous units based on field observations, the lithostratigraphic evolution of these two units presents two differences only. The first is that the "Halstatt" limestones are present in the Autochthonous but not in the Parautochthonous unit. This difference can be explained if we take into account the sedimentation conditions of the 'Hallstatt" facies in the environment of the continental shelf borders. This formation does not have a uniform development throughout its extension, because of its lenticular form; it "disappears" abruptly in the horizontal and vertical sense. It should be noted that in many places in the north-eastern part of Chios Island (e.g. in the area of the village Pantoukios along the coast), we can observe the development of the upper members of the Mesozoic carbonate sequence on the Palaeozoic substratum of both the Autochthonous and Parautochthonous units.

The second difference is that the formations of the Parautochthonous unit are intensively folded and

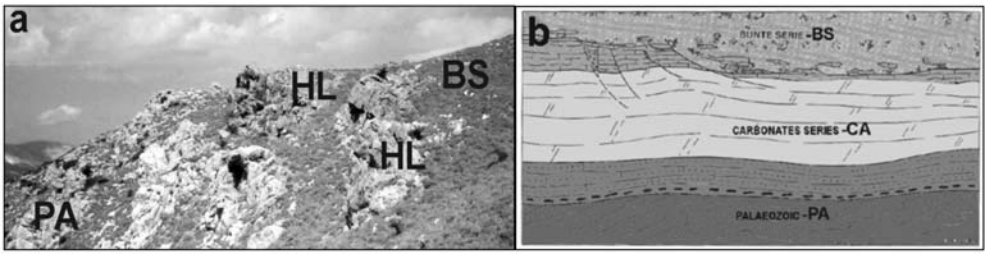

Fig. 4: (a) View of the Authochthonous Mesozoic carbonate series in the Korakaris region. (PA-Palaeozoic, HL-"Hallstatt" limestones, BS- "Bunte Serie") (b) Schematic representation of the same region after Geatani et al. (1992)

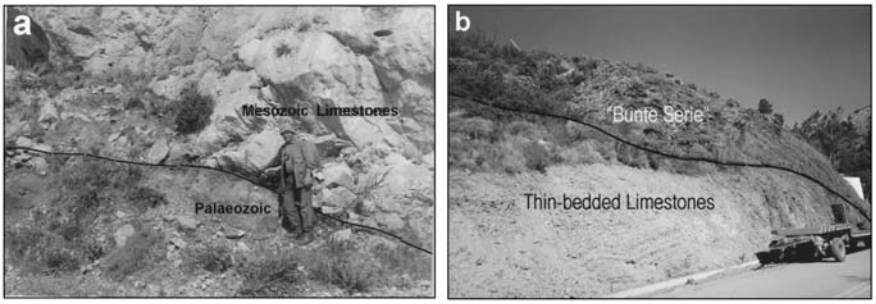

Fig. 5: (a) View of the contact of Authochthonous Palaeozoic with Mesozoic limestones, to the north of the village Vrontados. (b) View of the contact of thin-bedded limestones of the Autochthonous unit with the "Bunte Serie".

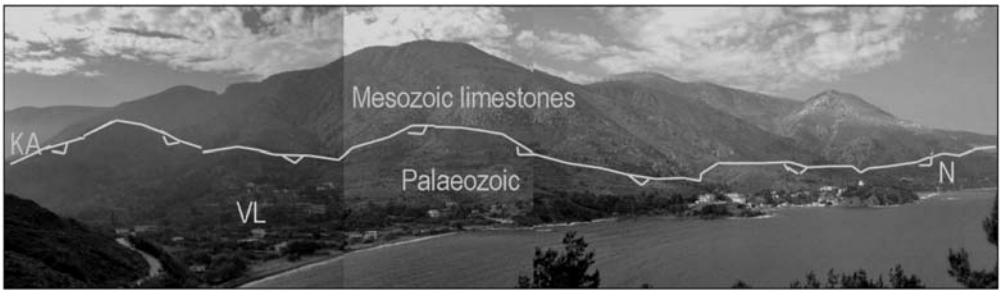

Fig. 6: View of the thrust of the Palaeozoic on the Mesozoic in NE Chios (KA-Kardamyla, VL-Vlychada, N-Nagos).

fractured. This happens systematically only in places where the Allochthonous unit overthrusts the Autochthonous one. Moreover, the Parautochthonous unit only crops out between the other two units and nowhere does it have an independent presence. This fact may also lead to the thought that it does not represent an individual unit deposited onto a different paleogeographic space, but corresponds to the base of the Mesozoic sequence of the Autochthonous unit, thrusted on the Upper Triassic formations of the same unit.

According to recent tectonic observations, the contact between the Palaeozoic and Mesozoic formations of the Autochthonous unit is represented by a thrust structure, observed in north-eastern Chios. This contact has been mapped in the broader area of Vlychada-Nagos, where clastic formations overlay on limestones and dolomites (Fig. 6). This thrust surface has a strike ranging from

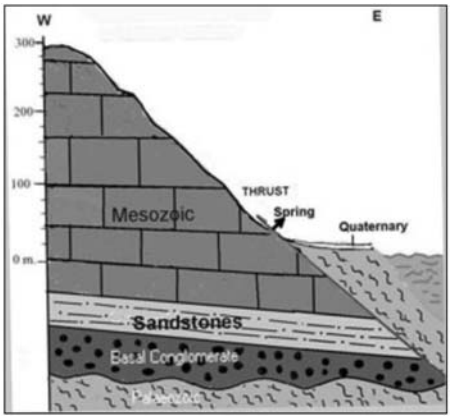

Fig. 7: Schematic geological cross section of the thrust structure at the Nagos spring area.

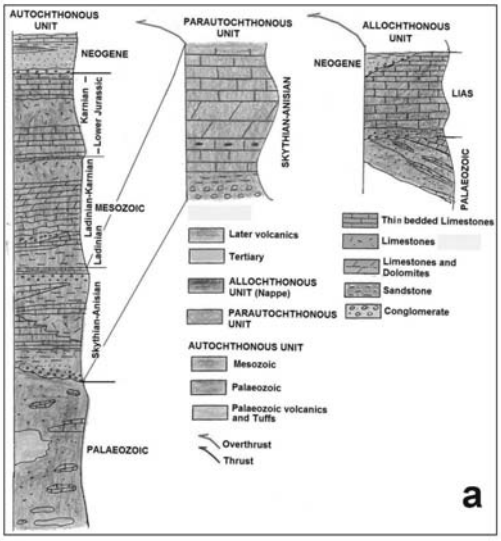

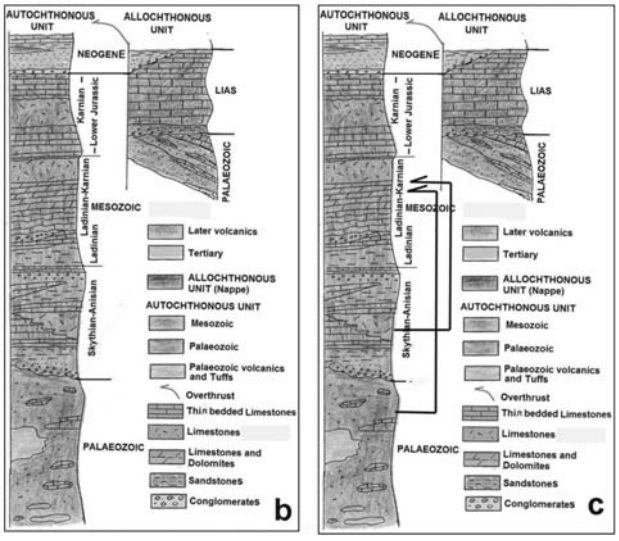

Fig. 8: Schematic lithostratigraphic columns of the Chios structural units (a) and the revised scheme according to the results of this work (b and c).

N5ºW to N5ºE and a dip of 45º to the East, while the tectonic striations observed in some places have a 22º pitch to the North. This tectonic relationship is the origin of the Nagos overflow spring, expressed in the contact of the Palaeozoic and Mesozoic formations (Fig. 7). Geophysical research conducted for hydrogeological purposes by the Institute of Geology and Mineral Exploration of Athens, confirmed the presence of this thrust structure.

Finally, the massive limestones of the Autochthonous Mesozoic series are thrusted either by Palaeozoic clastic formations, or by the basal Mesozoic formations of the same series (Fig. 8c). Following the above data and rationale, a modified structural scheme is proposed for the island of Chios, according to which the Parautochthonous unit is not an individual unit (as in Fig. 8a) but is considered a part of the Autochthonous one (Fig. 8b).

3. Conclusions

According to recent structural observations carried out in Chios Island (more detailed in its north-eastern part), a revised model is proposed for the geological structure. The Parautochthonous unit is not considered an individual unit but constitutes part of the Autochthonous one. Indeed, the geological formations of the Parautochthonous unit, such as the thin-bedded limestones and cherts, have their equivalents in the Autochthonous unit. Comparing these two units from a lithostratigraphic point of view, the major difference between them is the presence of the 'Hallstatt" limestones in the Autochthonous unit. They crop out in the south-western part of the island while they are absent in the north-eastern part. Taking into account the sedimentation conditions of the 'Hallstatt" facies in the environment of the continental shelf borders we can suppose that it has a lenticular form and for this reason a non uniform extension.

The fact that the two units present local lithofacial differentiations does not lead to the conclusion that they have a different palaeogeographic origin, as both are covered by the same formation, the "Bunte Serie". It should be noted that the Bunte Serie is unique in the Greek territory, outcropping only in Chios and the nearby Turkish peninsula of Karaburun. From a tectonic point of view, the thrust of the Parautochthonous unit on the Autochthonous corresponds to a thrust between the formations of the Autochthonous unit that was affected by shearing movements at the base of the Mesozoic.

In conclusion, the Autochthonous unit is presented under three different forms, in Chios: i) as an undisturbed sequence, ii) with a thrust structure between the massive limestones of the Mesozoic series (Upper Triassic) and the base of the Mesozoic and iii) with a thrust structure between the massive limestones of the Mesozoic and the Palaeozoic, as observed in the north-eastern part of the island. Although chronostratigraphic data could not easily be found in Chios, further research is needed for the interpretation of the complicated geological structure of this island, holding a key geodynamic position in the western Palaeotethys.

4. References

Besenecker, H., Durr, S., Herget, G., Jacobshagen, V., Kauffman, G., Ludtke, G., Roth, W. and Tietze, K.V., 1968. Geologie von Chios (Agais). *Geol. Palaeontol.*, 2, 121–150.

Besenecker, H., Durr, S., Herget, G., Kauffman, G., Ludtke, G., Roth, W. and Tietze, K., 1971. Geological map of Greece. Chios, 1:50 000. IGME ed., Athens.

Herget, G., 1978. Die Geology von Nord-chios (Agais).Unpublished *Ph.D. Thesis*, Univ. of Marbrug.

Gaetani, M., Jacobschagen, V., Nicora, A., Kauffmann, G., Tselepides, V., Fantini-Sentini, N., Mertmann, D and Skourtis-Coroneou, V., 1992. The Early-Middle Triassic Boundary st Chios (Greece). *Riv. Ital.*

Paleontol. Stratigraf., 98, 181-204.

Grooves, J., Larghi, C., Nicora, A., Rettori, R., 2003. Mississipian (Lower Carboniferous) microfossils from the Chios Melange (Chios island, Greece). *Geobios*, 36, 379-389.

Kauffmann, G., 1969. Die Geology von Nord-chios (Agais).Unpublished *Ph.D. Thesis*, Univ. of Marbrug.

Ktenas, K., 1921. Sur la decouverte du devonien a l'ile de Chio (Mer Egee). *C.R.somm. Soc. Geol. France*, 170-172.

Papanikolaou, D., Sideris, C.H., 1983. Le Palaeozoique de l'autochtone de Chios: une formation a blocks de type wildflysch d' age Permien. *C.R.A.Sc.*, 297, 603-606.

Robertson, A., Pickett, E., 2000. Palaeozoic-early Tertiary evolution of melanges, rift and passive margin units in the Karaburun peninsula (western Turley) and Chios island (Greece). In tectonics and Magmatism in Turkey and the Surrounding area. *Geological Society of London, Special publication*, 173, 43-82.

Roth, G., 1968. Die Geology von Nord-chios (Agais).Unpublished *Ph.D. Thesis*, Univ. of Marbrug.

Tselepidis, V., 2007. Palaeontological and stratigraphic study of the Epidavros ammonites. Contribution to the knowledge of the "Hallstatt" facies in the Hellenides. *Ph.D. Theseis*, University of Thessaloniki (in Greek)

Zachi, A., Garzanti, E., Larghi, C., Angiolini, L. and Gaetani, M., 2003. The Variscan orogeny in Chios (Greece): Carboniferous accretion along a Palaeotethyan active margin. *Terra Nova*, 15/3, 213-223.

Δελτίο της Ελληνικής Γεωλογικής Εταιρίας, 2010
Πρακτικά 12ου Διεθνούς Συνεδρίου
Πάτρα, Μάιος 2010

Bulletin of the Geological Society of Greece, 2010
Proceedings of the 12th International Congress
Patras, May, 2010

THE NATURE OF DUCTILE DEFORMATION IN THE PHYLLITE-QUARTZITE UNIT (EXTERNAL HELLENIDES)

Xypolias P. and Chatzaras V.

Department of Geology, University of Patras, 26500 Patras – Greece; p.xypolias@upatras.gr

Abstract

This work describes the nature of ductile deformation in the Phyllite-Quartzite (PQ) unit in terms of structural evolution and spatial variation of finite strain and vorticity of flow. The PQ unit is affected by at least three ductile deformation ($D_{1,2,3}$) phases. However, the D_2 is the dominant phase resulting in the formation of a penetrative foliation (S_2) which is by far the most common structural feature in all scales of observation. A stretching lineation (L_2), which trends perpendicular to the structural grain of the belt, is well-developed within the S_2 plane. Numerous kinematic criteria clearly indicate west (or south)-directed transport of the PQ unit during D_2. This phase is also characterized by a systematic non-linear increase of strain ratio (Rxz) with proximity to the Basal thrust. Spatial variation of kinematic vorticity number reveals an increase of pure shear component of D_2 deformation towards the middle structural levels of the unit. These results are used to discuss the validity of various geodynamic models related to the exhumation of the PQ unit.

Key words: *Progressive deformation; finite strain; vorticity; high-pressure rocks; Greece.*

1. Introduction

The metamorphic rocks of the Phyllite-Quartzite (PQ) unit belong to the External Hellenides and constitute a Late Oligocene–Early Miocene high pressure–low temperature (HP-LT) belt, which extends over a distance of 600 km. Over the last two decades, several tectonic models for the exhumation of the PQ unit have been proposed, including underplating with symmetric syn-orogenic (Fassoulas et al. 1994) or asymmetric syn-(or post-) orogenic extension (Jolivet et al., 1996), delamination of the subducting crust followed by buoyancy-driven exhumation (Thomson et al., 1999), solid-state ductile extrusion contemporaneous with continent-continent collision (Xypolias and Doutsos, 2000; Doutsos et al., 2000) as well as gravitational collapse and erosion of a thickened crustal wedge (Zulauf et al., 2008). Each of these models predicts different structural settings and requires different deformation paths for the PQ unit rocks. For example, models of syn-orogenic extension require the creation of large extensional detachments and the formation of extensional sedimentary basins in the upper plate, the model of buoyancy-driven exhumation suggests that the bulk of the PQ unit was escaped upward as a coherent block, unaffected by any pervasive deformation. The ductile extrusion model, in turn, suggests that the exhumation was achieved by upward transport-parallel elongation of the PQ unit rocks and requires penetrative ductile deformation. Therefore, it is clear that despite numerous studies in the area, the mechanism related to the exhumation of the PQ unit is still a matter of debate. Much of the debate stems from the fact that there is also no consensus for the internal structure and tectonic evolution of the PQ unit. This work summarises the results of qualitative and quantitative structural analyses performed in the unit mainly over the last decade and uses these to discuss the applicability of various geodynamic models.

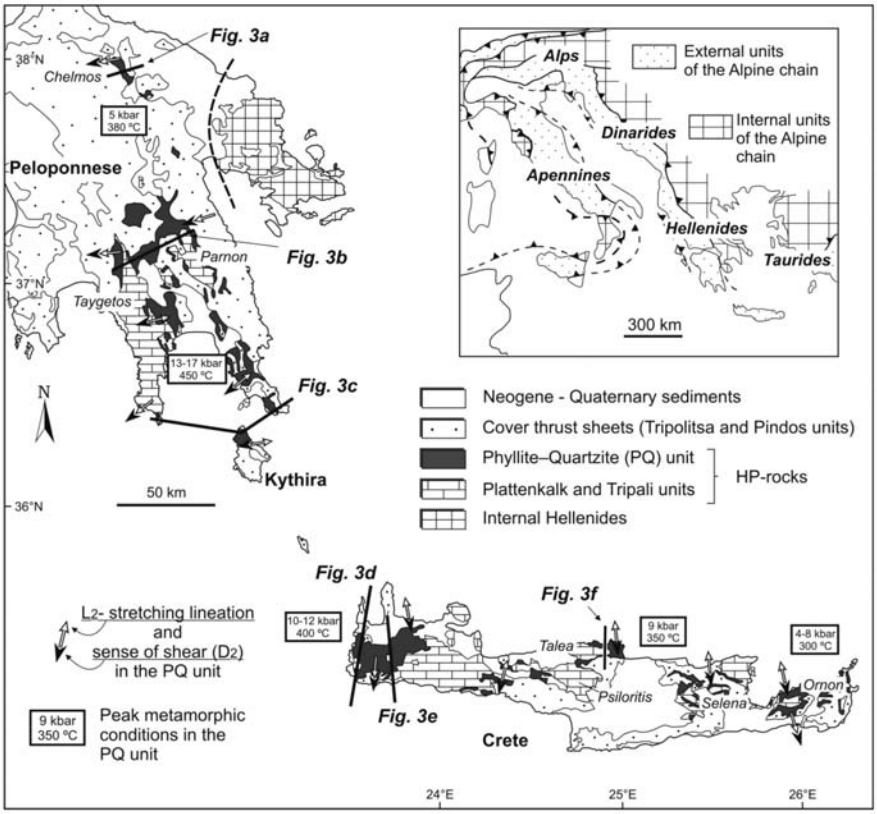

Fig. 1: Simplified geological map of the southwest External Hellenides. L_2 stretching lineation, sense of shear (D_2) and peak metamorphic conditions in the PQ unit are also shown. Metamorphic data after Katagas et al. (1991), Theye et al. (1992), Blumör (1998). Inset: generalized map of the Alpine chain in southeastern Europe (modified after Xypolias et al. 2007).

2. Geological setting

The External Hellenides are part of the Alpine Orogenic belt (Fig. 1a, inset) and form an orocline connecting the Dinarides to the NW with the Taurides to the SE. They mainly consist of Mesozoic and Cenozoic sedimentary rocks that were deposited on the rifted northern margin of the Apulia microcontinent. The present disposition of the External Hellenides is largely the result of progressive southward (in palaeo-coordinates) stacking of nappes/units (Fig. 1). Nappe stacking took place from Eocene to Early Miocene times, following the closure of the Pindos Ocean and the subsequent northward subduction and collision of the Apulia beneath the Pelagonian microcontinent (e.g. Doutsos et al., 1993, Xypolias and Doutsos, 2000).

The PQ unit is considered to be a metamorphosed Late Carboniferouse–Upper Triassic rift sequence consisting of phyllites, quartzites, metaconglomerates and marble intercalations (Robertson, 2006 and references therein). The thickness of the PQ unit is ca. 2 km in the central parts of the HP-belt (Kythira, westernmost Crete; Fig. 1) and decreases systematically towards its lateral tips (north Peloponnese, east Crete; Fig. 1) where it approaches ca. 1 km (Xypolias et al., 2007). Metamorphic conditions in the PQ unit (Fig. 1) decrease systematically in map-view from the central parts to the lateral

tips of the belt (e.g. Theye et al., 1992). Peak P-T conditions have been constrained at 450 ± 30 °C and 13–17 kbar (Theye et al. 1992, Blumör 1998) while the age of the metamorphic peak is constrained at 19–24 Ma (K-Ar and ^{39}Ar-^{40}Ar on white mica; e.g. Panagos et al., 1979, Seidel et al. ,1982). The PQ unit is tectonically emplaced on the Plattenkalk unit by a major ductile thrust (Greiling, 1982; Doutsos et al., 2000; Zulauf et al., 2002; Xypolias and Kokkalas, 2006), the "*Basal thrust*".

The structurally lower Plattenkalk unit is composed of Carboniferous–Eocene carbonate rocks overlain by an Oligocene limy metaflysch with metaconglomerate horizons (e.g. Kowalczyk et al., 1977). Metamorphic index minerals in the Plattenkalk unit have only been found in central Crete at the Talea Window and indicate P-T conditions of 7–10 kbar and ca. 350 °C (Theye et al., 1992). Exceptionally in west Crete, an Upper Triassic–Lower Jurassic carbonate sequence, the Tripali unit, lies tectonically between the Plattenkalk and the PQ units.

The PQ unit is, in turn, overlain by the Tripolitsa and Pindos units representing the cover thrust sheets (Fig. 1). The Pindos and Tripolitsa units are mainly composed of Triassic to Eocene carbonate rocks and an upper Eocene flysch. The Pindos unit tectonically rests on the Tripolitsa unit and both units have a combined structural thickness no greater than 6 km. At the base of Tripolitsa carbonate rocks, a thin Permo-Triassic sequence, referred to as the Tyros Beds, which is in tectonic contact with the underlying PQ unit, has suffered very low-grade metamorphism (200–350 °C, 3–6 kbar; e.g. Thieboult and Triboulet, 1984).

Unconformably above the Cretan nappe pile lies a Neogene sedimentary succession. Data from Crete indicate that sedimentation started with terrigenous deposits of Middle Miocene age, followed by Upper Miocene–Pleistocene fluviolacustrine and open-marine sediments (e.g. Kokkalas et al., 2006).

3. Phases of ductile deformation

Based primarily on overprinting criteria observed in map to outcrop scales as well as on microstructural data, three principal ductile deformation phases (D_1–D_3) have been distinguished to constrain the structural evolution of the PQ unit (Greiling, 1982; Doutsos et al., 2000; Fassoulas et al., 1994; Zulauf et al., 2002; Kokkalas and Doutsos, 2004; Chatzaras et al., 2006; Xypolias et al., 2008). Deformation/metamorphism relationships described below in combination with the proposed P-T-t paths (Fig. 2) imply that these successive phases were coeval with progressive burial and exhumation of the PQ unit rocks.

3.1 D_1 deformation

The older recognized structures (D_1) in the PQ Unit are tight to isoclinal folds with wavelengths ranging from a few mm to about 10 cm. These structures are poorly preserved throughout the area due to intense D_2 ductile deformation and recrystallization. On outcrop scale, the S_1 fabric can be locally recognized mainly within thin competent quartzite layers (Fig. 2a), where it wraps around F_2 fold closures while folded S_1 within the phyllites is mainly visible on the microscale.

3.2 D_2 deformation

Structures and fabrics generated during D_2 deformation are pervasively developed throughout the PQ unit, and are by far the most common structural features observed in the field. This deformation phase is accompanied by a penetrative foliation (S_2) defined by the shape-preferred orientation of glaucophane and chloritoid needles as well as the alignment of micaceous films and elongated quartz aggregates (Fig. 2a). A mineral stretching and clast-elongation lineation (L_2) is well-developed within

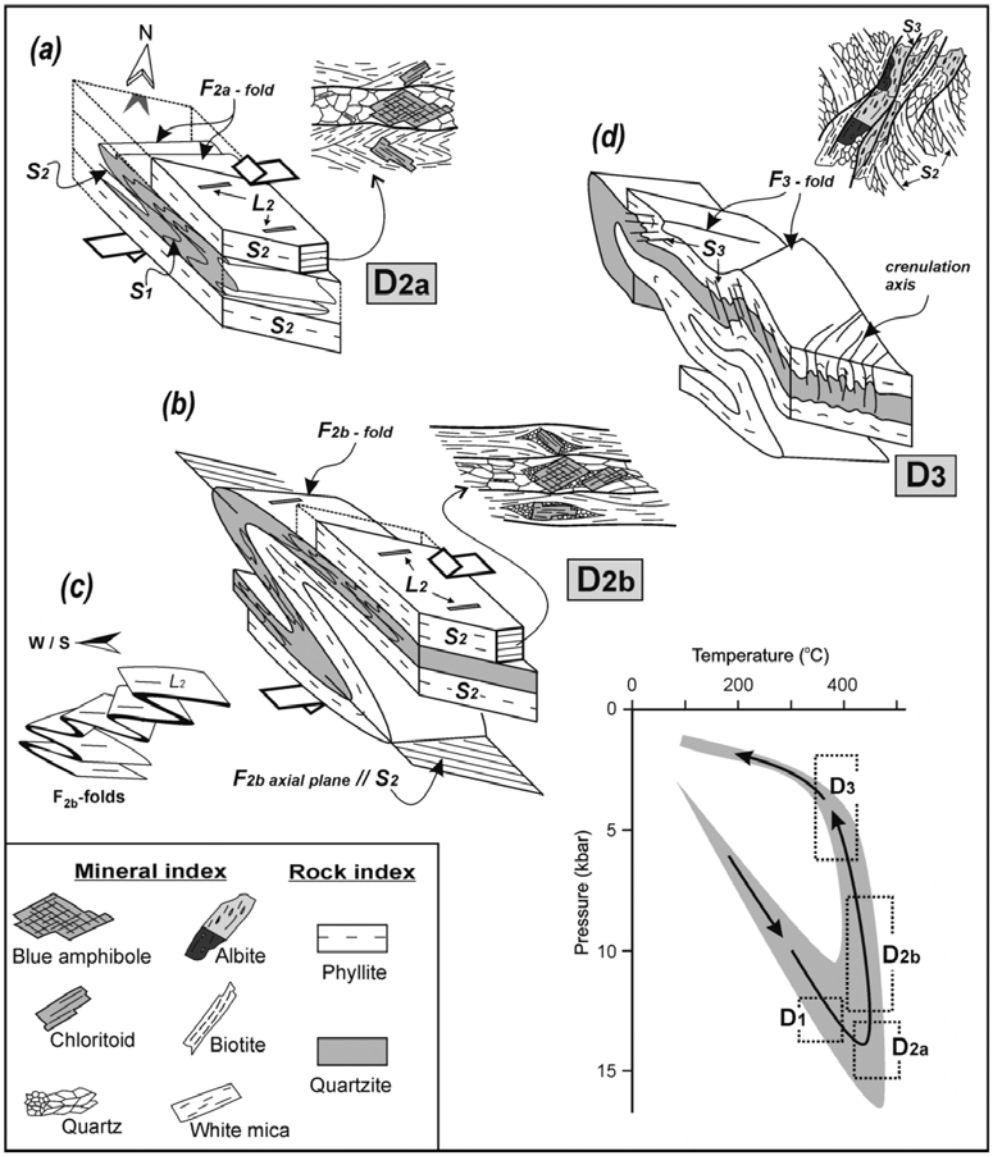

Fig. 2: Deformation/metamorphism relationships and progressive deformation of the PQ unit rocks. Block diagrams showing progressive deformation and associated structures during D_{2a} (a), D_{2b} (b) and D_3 (d) deformation subphases/phases, respectively. Line drawings summarize crystallization-deformation relationships. (c) Block sketch showing the rotation and tightening of F2b folds towards the lower structural levels of the PQ unit. The pressure-temperature path was constructed combining paths proposed by Blumör (1998) and Thomson et al. (1998) for the southern Peloponnese and western Crete, respectively. (Modified after Xypolias et al. 2008).

the plane of S_2 (Fig. 2a). Throughout southwest Hellenides, L_2 systematically trends perpendicular to the structural grain of the belt (Fig. 1).

The D_2 deformation can be subdivided in two successive increments (D_{2a}, D_{2b}) of ductile deformation. The earlier D_{2a} structures appear to be coeval with the main growth of HP-minerals (Fig. 2a) and can be locally recognized in the form of minor isoclinal folds (F_{2a}), which typically trend parallel to the regional L_2 orientation. The second increment of D_2 deformation is accompanied by outcrop-scale F_{2b} folds. As F_{2b} fold axes are sub-parallel or at a small angle to the L_2 lineation and fold axial planes are parallel to the regional S_2 foliation (Fig. 2b), a genetic link between S_2/L_2 and fold development is suggested.

Throughout the PQ unit, it has been recorded a systematic relation between the orientation and style of folds with respect to the structural level in the unit. Specifically, at lower structural levels, the F_{2b} folds are isoclinal with their axes oblique to sub-parallel to the L_2 while at progressively upper structural levels there is an increase in both the apical angle of the folds and the range of divergence between the fold axis and the L_2 orientation (Fig. 2c; e.g. Xypolias and Doutsos, 2000; Chatzaras et al., 2006). This finding is indicative of a progressive rotation of fold axes into the X-axis of finite strain (e.g. Alsop, 1992), resulting from an overall increase in strain magnitude as the contact between the PQ and the Plattenkalk units is approached.

Numerous kinematic indicators such as quartz c-axis fabrics, oblique grain shape fabrics, asymmetric boudins, sigma-shaped porphyroclasts, bookshelf tiling of HP-related minerals, S/C fabrics and single sets C'-type shear bands indicate a clear top-to-the-west (Peloponnese and Kythira) top-to-the-south (Crete) shear sense (Xypolias and Koukouvelas, 2001; Zulauf et al., 2002; Chatzaras et al., 2006). Evidence for top-to-the-east (or north) shearing (backward motion) has been mainly found at the upper structural levels of the PQ unit. Petrofabric data from central Peloponnese also reveals that west-directed ductile shearing in the PQ unit possibly occurred at deformation temperatures of 400–450 °C, while the east-directed movements occurred at lower temperatures (ca. 350 °C). These data imply that backward shearing occurred during the late stages of ductile deformation.

It is semantic to note that throughout the PQ unit quartzites show evidence of dynamic recrystallization accommodated by both subgrain rotation and low-temperature grain-boundary migration. This, in addition to the presence of strong quartz c-axes preferred orientation patterns recorded in Peloponnese and Kythira suggest that dislocation creep was the dominant deformation mechanism during D_2 shearing (Xypolias and Kokkalas, 2006). Evidence for deformation by dissolution precipitation creep is mainly restricted to metasiltstones, where quartz clasts are embedded in a phyllosilicate-rich matrix and occasionally show pressure shadows on both sides of grains (Schwarz and Stockhert, 1996).

3.3 D_3 deformation

The third deformation phase (D_3), is less widely developed than D_2 and is mainly represented by centimetre- to metre scale folds (F_3) and crenulations deforming S_2. The mesoscopic F_3 folds are predominantly open with a gently inclined axial plane cleavage. Microstructural observations from Kythira have shown that discrete S_3 cleavage domains serve as the site for growth of both biotite and albite. Corrosion of quartz and mica along this steeply dipping cleavage has also been recognized indicating that dissolution-mass transfer processes played an important role in their formation. Based on the above mentioned observations, it seems that D_3 deformation commenced under ductile conditions and became progressively more brittle with time.

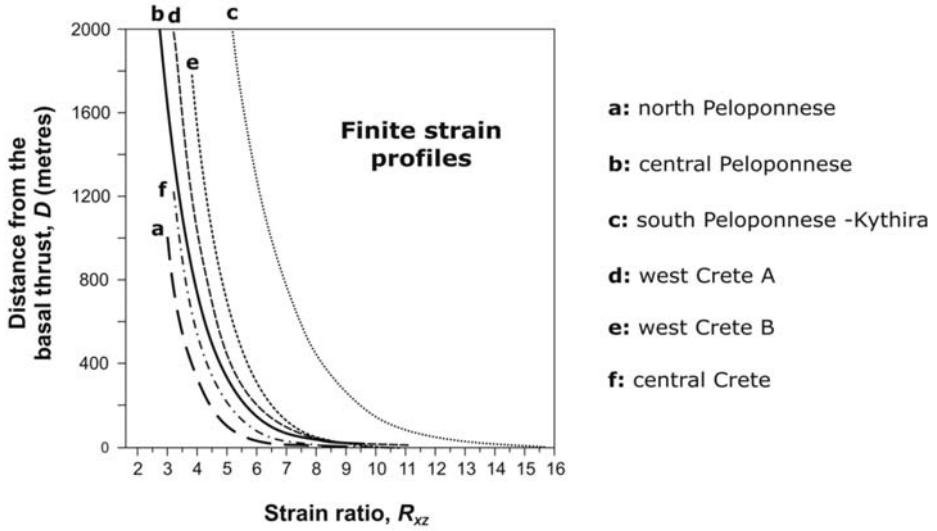

Fig. 3: The best fit curves describing the spatial variation of strain ratio along six traverses in the PQ unit. The location of these traverses is illustrated in Figure 1. (Modified after Xypolias et al. 2007)

4. Finite strain

Systematic analysis of the spatial variation of finite strain associated with D_2 deformation in the PQ unit rocks has been carried out along six traverses (Xypolias et al., 2007 and references therein). The location of these traverses is illustrated in Figure 1. The analysis is based on a total of 200 oriented samples collected from different structural levels above the basal thrust. Finite-strain ratio R_{XZ} was estimated using graphical and algebraic Rf/ϕ methods (Lisle, 1994). Plastically deformed quartz grains and clasts in fine-grained metaconglomerates, metapsammites, metasiltstones and quartzites were used as strain markers. It is emphasized that strain analysis was not carried out in pure quartzites showing extensive dynamic recrystallization because the shape of the most deformed grains may have restored to more equant form. However, analysis was performed in a few quartzites that include slightly recrystallized quartz ribbons embedded in a fine grained matrix. The majority of analysed samples are characterized by the presence of mica aggregates that anastomose around plastically elongated quartz grains or clasts showing evidence of undulose extinction.

Data of the strain ratio (Rxz) were plotted against distance (D) from the basal thrust to examine the variation of R_{XZ} values along the six traverses. The best fit curves describing the spatial variation of strain ratio in the PQ unit are illustrated in Figure 3. As a whole, the profiles show a systematic strain increase with proximity to the basal thrust. However, strain gradient is not constant from the top to the bottom of the shear zone. Specifically, the downward increase in strain ratio is slight at the upper and middle levels of the unit and becomes abrupt at a projected distance of 300 m above the basal thrust (Fig. 3). This progressive non-linear strain increase towards the basal thrust obeys a specific logarithmic function (see Xypolias et al., 2007 for details).

So far, less systematic analytical work about the shape of finite strain ellipsoid has been done. In Crete, the shape of strain ellipsoid varies from flattening via plane to prolate (Fassoulas et al., 1994; Zulauf et al., 2002). 3D strain data from north Peloponnese show slightly constrictional to plane strain conditions, with k being approximately 1.4 (Xypolias and Doutsos, 2000).

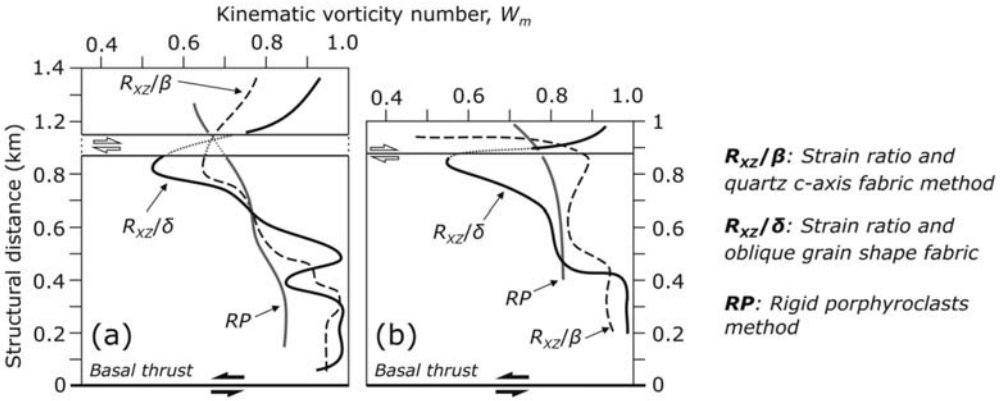

Fig. 4: Graphs (vorticity profiles) illustrating the vertical spatial variation in Wm values within the Phyllite–Quartzite unit in Taygetos (a) and Chelmos (a) areas. (Modified after Xypolias and Koukouvelas 2001; Xypolias 2009).

5. Vorticity and ductile thinning

Quantification of flow vorticity is also critically important for understanding the kinematics of rock flow in deformation zones. Mean kinematic vorticity number (Wm) is the most commonly used numerical measure to specify the shear-induced vorticity caused by the non-coaxial component of deformation. Wm is considered as a non-linear relation between the pure shear and simple shear components of deformation, with Wm = 1 implying simple shear and Wm = 0 implying pure shear flow (Passchier, 1987). Vorticity analyses have been performed in the PQ unit rocks exposed in windows of Peloponnese (Chelmos, Taygetos, Parnon) using a variety of analytical methods such as (a) the rigid porphyroclast method (Passchier, 1987), (b) the finite strain / quartz c-axis fabric method (e.g. Wallis, 1995), (c) the quartz c-axis fabric / oblique grain shape fabric method (Wallis, 1995) and (d) the finite strain / oblique grain shape fabric method (Xypolias, 2009).

Figure 4 illustrates the spatial variation of Wm within the PQ unit in Taygetos and Chelmos areas (Xypolias and Koukouvelas, 2001; Xypolias, 2009). In both vorticity profiles, the general trend observed by 'averaging' the results of these methods is that the Wm value approaches 1 close to the basal thrust and decreases upwards reaching a value less than 0.71 (equal contribution of pure and simple shear) at the middle of the unit, below a zone of backward shearing. Above this zone, the Wm values generally increase.

Deviation from ideal simple shear deformation implies ductile thinning perpendicular to the boundaries of the PQ unit and resultant dip-parallel elongation. For isochoric plane strain deformation, the stretch magnitude both normal and parallel to the flow plane can be calculated, combining strain and vorticity data (e.g. Wallis, 1995). Such calculations in Taygetos area indicate that the average transport-parallel elongation appears to be higher in the middle structural levels of the PQ unit, ranging between 60 and 90%, and lower in the deeper parts of the zone, ranging from 40% to 60%. Less significant variation in ductile thinning normal to the zone has been recorded; it is on the order of 30–45%.

6. Discussion and conclusions

It is clear, from both qualitative and quantitative analyses, that the PQ unit throughout the belt was af-

fected by penetrative deformation during the ductile stage of exhumation. This finding is in constrast to models proposing exhumation of Cretan HP-rocks as a coherent block unaffected by any pervasive deformation (e.g. Thomson et al., 1999). They also propose that during buoyancy-driven exhumation, deformation was restricted to the vicinity of the upper bounding extensional detachment fault. Finite strain profiles, in turn, indicate a systematic non-linear increase of finite strain with proximity to the Basal thrust and do not support strain localization along the upper boundary of the unit. These findings also imply that accumulation of ductile strain was coeval with the emplacement of the PQ on the Plattenkalk units during west (or south)-directed thrusting.

Penetrative ductile deformation in the PQ unit was also associated with ductile thinning and transport-parallel elongation of the material. However, the mechanism by which the ductile thinning and transport-parallel elongation contribute in exhumation of HP-nappes is not unique (e.g. Xypolias et al., 2010). Generally, two major alternative mechanisms have been proposed up to now. According to the first (e.g. Platt, 1993) a component of ductile extensional flow along a shallow dipping mid-crustal deformation zone requires the same component of deformation to be present in the surrounding rocks at the higher structural units. Under this mechanism the exhumation of HP-rocks is achieved by unroofing along the footwalls of low-angle normal faults (syn-orogenic extension). The most reliable indicators of this mechanism are the downward increase in the metamorphic pressure as well as the formation of extensional sedimentary basins in the upper plate (Platt, 1993). Alternatively, the transport-parallel elongation can contribute to the upward ductile extrusion of the HP-rocks (Escher and Beaumont, 1997; Xypolias and Koukouvelas, 2001; Law et al., 2004). In this case, the extruding/exhuming rock unit is modelled to represent a tectonic slice bounded by a basal subduction-related thrust fault and a roof stretching fault. The roof stretching fault may display normal or thrust sense, depending on the motion of the crust above the extruding material (e.g. Godin et al., 2006).

The mechanism of syn-orogenic (asymmetric or symmetric) extension has been adopted by many authors (e.g. Fassoulas et al., 1994; Jolivet et al., 1996) to explain the removal of overburden from above the PQ unit. However, the applicability of this mechanism remains highly questionable since either Oligocene-Early Miocene extensional related basins or normal-sense metamorphic breaks within the PQ unit have been not reported so far. Moreover, it is unclear if a thinning on the order of 30–45% in the upper plate is capable to denudate tectonically the PQ unit rocks. In contrast, several studies have shown that extension lagged behind a significant part of the exhumation process, and is superposed on an orogenic wedge that contains HP-rocks at relatively shallow crustal levels. According to these studies, middle Miocene–Pleistocene extension controlled both the exhumation of HP-rocks from ~10 km to the surface and the initiation of basin formation (Papanikolaou and Vassilakis 2010 and references therein). However, these models seem to underestimate the importance of contraction-related structures deforming Middle Miocene–Early Pleistocene sediments of Crete (Kokkalas and Doutsos, 2001; Kokkalas et al., 2006; Chatzaras et al., 2006; Klein et al., 2008; Tortorici et al., 2010), suggesting that the role of extension is overestimated.

Consequently, solid-state ductile extrusion of PQ unit under continuous compression provides a reasonable explanation for the exhumation of these rocks. According to this mechanism, after peak metamorphism, the PQ unit was detached from its basement and extruded upward to the west (or south) between the basal thrust and the Tripolitsa basement at the top. The effect of this extrusion process was the emplacement of the PQ unit over the Plattenkalk unit bringing it into contact with the overlying cover thrust sheets along a roof stretching fault. The subduction-related basal thrust and roof stretching fault operated contemporaneously in a tectonic setting without any net extension of the overall system. However, as mentioned above the roof stretching fault may display normal (e.g. Crete) or thrust (e.g. Kythira) sense depending on the crust motion above this fault.

7. References

Alsop, G.I., 1992. Progressive deformation and the rotation of contemporary fold axes in the Ballybofey Nappe, north-west Ireland. *Geological Journal* 27, 271-183.

Blumör, T., 1998. Die Phyllit-Qyarzit-Serie SE-Lakoniens (Peloponnes, Griechenland): Hochdruckmetamorphite in einem orogenen Keil. *Frankfurter geowiss. Arb.* A17.1-190.

Chatzaras, V., Xypolias, P., Doutsos, T., 2006. Exhumation of high-pressure rocks under continuous compression: a working hypothesis for southern Hellenides (central Crete, Greece). *Geological Magazine* 143, 859-876.

Doutsos, T., Koukouvelas, I., Poulimenos, G., Kokkalas, S., Xypolias, P., Skourlis, K., 2000. An exhumation model of the south Peloponnesus, Greece. *International Journal of Earth Science* 89, 350-365.

Doutsos, T., Piper, G., Boronkay, K., Koukouvelas, I., 1993. Kinematics of the Central Hellenides.- *Tectonics* 12, 936-953.

Escher, A., Beaumont, C., 1997. Formation, burial and exhumation of basement nappes at crustal scale: a geometric model based on the Western Swiss-Italian Alps. *Journal of Structural Geology* 19, 955-974.

Fassoulas, C., Kilias, A., Mountrakis, D., 1994. Post nappe stacking extension and exhumation of high-pressure/low-temperature rocks in the island of Crete, Greece. *Tectonics* 13, 127-238.

Godin, L., Grujic, D., Law, R. D., Searle, M.P., 2006. Channel flow, ductile extrusion and exhumation in continental collision zones: an introduction, *in* Law, R. D., Searle, M. P., Godin, L. (eds) Channel Flow, Ductile Extrusion and Exhumation in Continental Collision Zones. Geological *Society, London, Special Publications* 268, 1–23.

Greiling, R., 1982. The metamorphic and structural evolution of the Phyllite-Quartzite Nappe of western Crete. *Journal of Structural Geology* 4, 291-297.

Jolivet, L., Goffe, B., Monie, P., Truffert-Luxey, C., Patriat, M., Bonneau, M., 1996. Miocene detachment in Crete and exhumation P-T-t paths of high-pressure metamorphic rocks. *Tectonics* 15, 1129-1153.

Katagas, C., Tsolis-Katagas, P., Baltatzis, E., 1991. Chemical mineralogy and illite crystallinity in low grade metasediments, Zarouchla Group, Northern Peloponnesus, Greece. *Mineralogy and Petrology* 44, 57-71.

Klein, T., Reichhardt, H., Klinger, L., Grigull, S., Wostal, G., Kowalczyk, G., Zulauf, G., 2008. Reverse slip along the contact Phyllite-Quartzite Unit/Tripolitsa Unit in eastern Crete: implications for the geodynamic evolution of the External Hellenides. *in* Xypolias, P., Zulauf, G. (Eds.), Eastern Mediterranean. *Zeitschrift der Deutschen Gesellschaft für Geowissenschaften* 159, 375–398.

Kokkalas, S., Doutsos, T., 2001. Strain-dependent field and plate motions in the south-east Aegean region. *Journal of Geodynamics* 32, 311-332.

Kokkalas, S., Doutsos, T., 2004. Kinematics and strain partitioning in the southeast Hellenides (Greece). *Geological Journal* 39, 121-140.

Kokkalas, S., Xypolias, P., Koukouvelas, I., and Doutsos, T., 2006. Postcollisional contractional and extensional deformation in the Aegean region, *in* Dilek, Y., and Pavlides, S., eds., Post-collisional tectonics and magmatism in the Mediterranean region and Asia: *Geological Society of America Special Paper 409*, p. 97–123.

Kowalczyk, G., Richter, D., Risch, H., Winter, K.P., 1977. Zur zeitlichen Einstufung der tektogenetischen Ereignisse auf dem Peloponnes (Griechenland). *Neues Jahrbuch für Geologie und Paläontologie, Monatshefte* 1977, 549-564.

Law, R.D., Searle, M.P., Simpson, R.L., 2004. Strain, deformation temperatures and vorticity of flow at the top of the Greater Himalayan Slab, Everest Massif, Tibet. *Journal of the Geological Society, London* 161, 305-320.

Lisle, R.J., 1994. Palaeostrain analysis, *in* Hancock, P.L. (Ed.), Continental Deformation. Pergamon Press, Oxford, 28-42.

Panagos, A.G., Pe-Piper, G.G., Piper, D.J.W., Kotopouli, C.N., 1979. Age and stratigraphic subdivision of the Phyllite series Krokee region Peloponnese Greece. *Neues Jahrbuch für Geologie und Paläontologie, Monatshefte* 1979, 181-190.

Papanikolaou, D., Vassilakis, E., 2010. Thrust faults and extensional detachment faults in Cretan tectonostratigraphy: Implications for Middle Miocene extension. *Tectonophysics*, In Press.

Passchier, C.W, 1987. Stable positions of rigid objects in non-coaxial flow-a study in vorticity analysis. *Journal of Structural Geology* 9, 679-690.

Platt, J.P., 1993. Exhumation of high-pressure rocks: a review of concepts and processes. *Terra Nova* 5, 119–133.

Robertson, A.H.F., 2006. Sedimentary evidence from the south Mediterranean region (Sicily, Crete, Peloponnese, Evia) used to test alternative models for the regional tectonic setting of Tethys during Late Palaeozoic–Early Mesozoic time, *in* Robertson, A.H.F., Mountrakis, D. (Eds.), Tectonic Development of the Eastern Mediterranean region. *Geological Society, London, Special Publications* 260, 91-154.

Schwarz, S., Stöckhert, B., 1996. Pressure solution in siliciclastic HP-LT metamorphic rocks - constraints on the state of stress in deep levels of accretionary complexes. *Tectonophysics* 255, 203-209.

Seidel, E., Kreuzer, H., Harre, W., 1982. A late Oligocene/early Miocene high pressure belt in the external Hellenides. *Geologisches Jahrbuch* E23, 165-206.

Theye, T., Seidel, E., Vidal, O., 1992. Carpholite, sudoite, and chloritoid in low-grade high-pressure metapelites from Crete and the Peloponnese. *European Journal of Minerology* 4, 487-507.

Thiebault, F., Triboulet, T., 1984. Alpine metamorphism and deformation in Phyllite nappes (external Hellenides, southern Peloponnesus, Greece): Geodynamic implication. *The Journal of Geology* 92, 185-199.

Thomson, S.N., Stockhert, B., Brix, M.R., 1999. Miocene high-pressure metamorphic rocks of Crete, Greece: rapid exhumation by buoyant escape. In: Ring, U., Brandon, M. T., Lister, G. S., Willet, S. D. (eds) Exhumation Processes: Normal Faulting, Ductile Flow and Erosion. *Geological Society, London, Special Publications* 154, 87-107.

Thomson, S.N., Stöckhert, B., Rauche, H., Brix, M.R., 1998. Thermochronology of the high-pressure metamorphic rocks of Crete, Greece: implications for the speed of tectonic processes. *Geology* 26, 259-262.

Tortorici, L., Caputo, R., Monaco, C., 2010. Late Neogene to Quaternary contractional structures in Crete (Greece). *Tectonophysics* 483, 203-213.

Wallis, S.R., 1995. Vorticity analysis and recognition of ductile extension in the Sanbagawa belt, SW Japan. *Journal of Structural Geology* 17, 1077-1093.

Xypolias, P., 2009. Some new aspects of kinematic vorticity analysis in naturally deformed quartzites. *Journal of Structural Geology*, 31, 3-10.

Xypolias, P., Doutsos, T., 2000. Kinematics of rock flow in a crustal-scale shear zone: implication for the orogenic evolution of the southwestern Hellenides. *Geological Magazine* 137, 81-96.

Xypolias, P., Kokkalas, S., 2006. Heterogeneous ductile deformation along a mid-crustal extruding shear zone: an example from the External Hellenides (Greece), *in* Law, R.D., Searle, M., Godin, L. (Eds.), Channel flow, ductile extrusion and exhumation in continental collision zones. *Geological Society, London, Special Publications* 268, 497-516.

Xypolias, P., Koukouvelas, I.K., 2001. Kinematic vorticity and strain rate patterns associated with ductile

extrusion in the Chelmos Shear Zone (External Hellenides, Greece). *Tectonophysics* 338, 59-77.

Xypolias, P., Chatzaras, V., Koukouvelas, I.K., 2007. Strain gradients in zones of ductile thrusting: Insights from the External Hellenides. *Journal of Structural Geology* 29, 1522-1537.

Xypolias, P., Koukouvelas, I.K., Zulauf, G., 2008. Cenozoic tectonic evolution of northeastern Apulia: Insights from a key study area in the Hellenides (Kythira, Greece), *in* Xypolias, P., Zulauf, G. (Eds.), Eastern Mediterranean. *Zeitschrift der Deutschen Gesellschaft für Geowissenschaften* 159, 439-455.

Xypolias, P., Spanos, D., Chatzaras, V., Kokkalas, S., Koukouvelas, I., 2010. Vorticity of flow in ductile thrust zones: examples from the Attico-Cycladic Massif (Internal Hellenides, Greece), *in* Law, R., Butler, R., Holdsworth, B., Krabbendam, M., Strachan, R. (eds) Continental Tectonics and Mountain Building. *Geological Society, London, Special Publications* 335, In Press.

Zulauf, G., Klein, T., Kowalczyk, G., Krahl, J., Romano, S.S., 2008. The Mirsini Syncline of eastern Crete, Greece: a key area for understanding pre-Alpine and Alpine orogeny in the eastern Mediterranean, *in* Xypolias, P., Zulauf, G. (Eds.), Eastern Mediterranean. *Zeitschrift der Deutschen Gesellschaft für Geowissenschaften* 159, 399–414.

Zulauf, G., Kowalczyk, G., Krahl, J., Petschick, R., Schwanz, S., 2002. The tectonometamorphic evolution of high-pressure low-temperature metamorphic rocks of eastern Crete, Greece: constraints from microfabrics, strain, illite crystallinity and paleodifferential stress. *Journal of Structural Geology* 24, 1805-1828.

12ο ΔΙΕΘΝΕΣ ΣΥΝΕΔΡΙΟ ΤΗΣ ΕΛΛΗΝΙΚΗΣ ΓΕΩΛΟΓΙΚΗΣ ΕΤΑΙΡΙΑΣ
ΠΛΑΝΗΤΗΣ ΓΗ: Γεωλογικές Διεργασίες και Βιώσιμη Ανάπτυξη

12th INTERNATIONAL CONGRESS OF THE GEOLOGICAL SOCIETY OF GREECE
PLANET EARTH: Geological Processes and Sustainable Development

ΝΕΟΤΕΚΤΟΝΙΚΗ ΚΑΙ ΓΕΩΜΟΡΦΟΛΟΓΙΑ
NEOTECTONICS AND GEOMORPHOLOGY

Δελτίο της Ελληνικής Γεωλογικής Εταιρίας, 2010
Πρακτικά 12ου Διεθνούς Συνεδρίου
Πάτρα, Μάιος 2010

Bulletin of the Geological Society of Greece, 2010
Proceedings of the 12th International Congress
Patras, May, 2010

MIDDLE-LATE QUATERNARY GEODYNAMICS OF CRETE, SOUTHERN AEGEAN, AND SEISMOTECTONIC IMPLICATIONS

Caputo R.[1], Catalano S.[2], Monaco C.[2], Romagnoli G.[2], Tortorici G.[2], Tortorici L.[2]

[1] *University of Ferrara, Department of Earth Sciences, via Saragat 1,44122 Ferrara, Italy, rcaputo@unife.it*

[2] *University of Catania, Department of Earth Sciences, Corso Italia 55, 95129 Catania, Italy*

Abstract

In order to characterize and quantify the superficial deformation occurred during Middle-Late Quaternary in the Southern Aegean, we have systematicaly analyzed the major tectonic structures affecting Crete Island. They typically consist of 10 to 30 km-long dip-slip normal faults, separating carbonate and/or metamorphic massifs, in the footwall block, from loose to poorly consolidated alluvial and colluvial materials within the hanging-wall. All these faults show clear evidence of recent re-activation and trend parallel to two principal directions: WNW-ESE and NNE-SSW. Based on all available data for both onland and offshore structures (morphological and structural mapping, satellite imagery and airphotographs remote sensing as well as the analysis of seismic profiles and the investigation of marine terraces and Holocene raised notches along the island coasts), for each fault we estimate and constrain some of the principal seismotectonic parameters and particularly the fault kinematics, the cumulative amount of slip and the slip-rate. Summing up the contribution to crustal extension provided by the two major fault sets (ca. E-W and ca. N-S) we calculate both radial and tangential (i.e. perpendicular and parallel to the Hellenic Arc, respectively) long-term strain-rates. A comparison of these geologically-based values with those obtained from GPS measurements show a good agreement, therefore suggesting that the present-day crustal deformation is probably active since Middle Quaternary and mainly associated with the seismic activity of upper crustal normal faults characterized by frequent shallow moderate-to strong (Mmax = 7.0) seismic events seldom alternating with stronger (Mmax = 7.5) earthquakes occurring along blind low-angle thrust planes affecting deeper and more external sectors of the Hellenic Arc.

Key words: *extensional tectonics, thrust tectonics, regional uplift, fault scarp.*

1. Introduction

The island of Crete in the southernmost sector of the Hellenic Arc is among the most seismically active areas of the whole eastern Mediterranean (Fig. 1). The seismicity is mainly characterized by crustal events, <25-30 km in depth (e.g. Pondrelli et al., 2002; Meier et al., 2004), and both shallow instrumental and historical earthquakes show maximum magnitudes up to 7.0 (Fig. 1; Papazachos and Papazachou, 1997; Papanastassiou et al., 2001; National Observatory of Athens Catalogue, 2009; Kiratzi and Louvari, 2003). The available fault plane solutions (Taymaz et al., 1990; Jost et al., 2002; Pondrelli et al., 2002; Kiratzi and Louvari, 2003) indicate a NNE-SSW direction of compression, close to the Hellenic trench further to the south, but within Crete Island and its surroundings an E(SE)-W(NW) and a roughly N-S extensions prevail associated with ruptures along normal and oblique-slip faults.

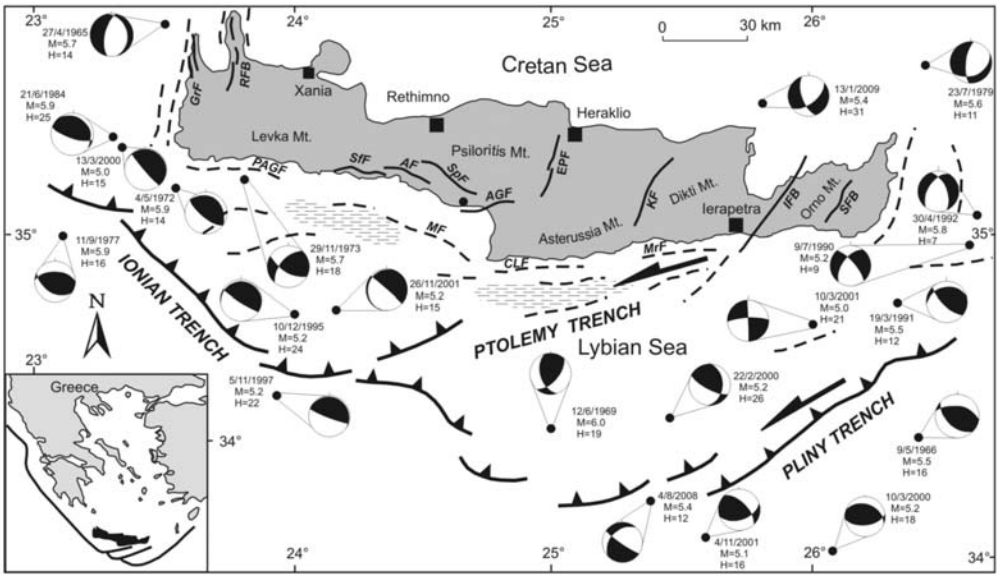

Fig. 1: Simplified tectonic map of the Middle-Late Quaternary active normal faults affecting Crete Island and its surrounding offshore. SfF:Sfakia Fault; AF:Asomatos Fault; SpF:Spili Fault; AGF: Agia Galini Fault; PAGF:Paleochora-Agia Roumeli Fault; MF: Messara Fault; CLF: Cape Lithino Fault; MrF:Mirto Fault; SFB:Sitia Fault Belt; IFB: Ierapetra Fault Belt; KF: Kastelli Fault; EPS: Eastern Psiloritis Fault; RFB: Rodopou Fault Belt; GrF: Gramvousa Fault. Earthquakes and focal mechanisms from Taymaz et al. (1990), Papazachos and Papazachou (1997), Papanastassiou et al. (2001), Jost et al. (2002), Pondrelli et al. (2002), Kiratzi and Louvari (2003) and National Observatory of Athens (2009). Structures located offshore are from Leite and Mascle1 (982), Le Pichon et al. (2002) and Alves et al. (2007).

On the other hand, the rough morphology that characterizes the island also documents the occurrence of an intense Late Quaternary tectonics mainly represented by several hundred meters of regional uplift and at the surface by normal faulting. Indeed, a strong tectonic uplift started about 0.6 Ma ago as recorded by Middle-Late Pleistocene marine terraces (Angelier and Gigout, 1974; Angelier, 1975; 1979; Angelier et al., 1977; Gaki-Papanastassiou et al., 2009) and Holocene raised notches (Pirazzoli et al., 2008; Shaw et al., 2008) as well as by deeply entrenched valleys associated with alluvial and/or transitional coarse-grained sediments along the major depressions.

Crustal scale normal faults affect both offshore (Leite and Mascle, 1982; Le Pichon et al., 2002; Alves et al., 2007) and on land areas (Postma and Drinia, 1993; ten Veen and Mejier, 1998; Fortuin and Peters, 1984; Kokkalas and Doutsos 2001; Monaco and Tortorici, 2004; Caputo et al., 2006), and they consist of 10 to 30 km-long distinct fault segments. These structures generally represent the most impressive morphological features affecting the entire pile of tectonic units of the Alpine orogenic belt (Fassoulas, 1999 and references therein). They run parallel to the principal mountain fronts, commonly bound the major Quaternary basins and show a very young (post-last glacial maximum) morphology documenting their recent activity. On the island of Crete, the Holocene fault-activity is usually easily recognizable when normal fault segments affect hard-rocks because they offset the uniform mountain slopes regularized by the intense Late Pleistocene cryogenetic processes. In several other sectors of the Mediterranean realm, such morphological features have been used to recognise the latest Quaternary tectonic activity along normal faults (Stewart and Hancock, 1991; Armijo et al., 1991;

1992; Caputo, 1993; Piccardi et al., 1999; Benedetti et al., 2002; Monaco and Tortorici, 2004; Palumbo et al., 2004; Roberts and Michetti, 2004; Papanikolaou et al., 2005; Caputo et al., 2006).

A direct association between earthquakes and crustal tectonic structures occurring both on land and offshore have been suggested only for few normal fault segments (Lyon-Caen et al., 1987; Armijo et al., 1992, Fassoulas, 2001; Monaco and Tortorici, 2004; Caputo et al., 2006).

In order to evaluate the Holocene faulting of Crete and to estimate long-term slip-rates and relations with the major seismotectonic parameters a detailed study of several fault scarps has been carried out combining morphological and structural information based on the analysis of satellite imagery, air photographs, topographic maps and field observations and, for the segments extending offshore, by interpreting available seismic profiles. In addition, information regarding the Pleistocene marine terraces and Holocene raised notches deformation along the southern coast of the island have been carried out in order to estimate the long-term throw-rate along the coast-bounding fault segments. Based on all the collected data we could thus reconstruct the Holocene seismotectonic behaviour of Crete in the frame of the geodynamics that governs the frontal segment of the Hellenic Arc.

2. Quaternary normal faulting in Crete and surroundings

Crete Island is characterized by the occurrence of several, mainly dip-slip normal faults bearing evidences of very recent activity. They are typically 10 to 30 km-long and show two major trends: WNW-ESE and NNE-SSW (Fig. 1). These normal faults usually separate Mesozoic carbonate and metamorphic rocks of the Alpine south-verging nappes on the footwall blocks, from coarse-grained alluvial/colluvial Quaternary deposits on the hanging-wall blocks. These structures are characterized by several metres-high and several kilometres-long steeply-dipping scarps that abruptly offset the mountain range (Fig. 2). These features are outstanding in the landscape representing relatively unweathered and vegetation-free zones. Their correlation with recent re-activations of the normal faults is well established worldwide, like in Afar, Greece and Italy and they are interpreted as free faces (Wallace, 1978) due to the cumulative effects of several linear-morphogenic earthquakes (Caputo et al., 2006 and references therein).

During glacial conditions, the weathering and the enhanced sediment mobility along slopes were usually faster than tectonic activity, therefore completely restoring the gradient slope within each interseismic interval. Moreover, glacial climate conditions favoured the formation of the cemented coarse-grained deposits that covered and regularized the mountain slopes continuously burying coseismic surface displacements. Following the last glacial maximum at ca. 18 ka BP, the climate conditions gradually changed and this strongly affected the slope evolution. By reducing the capacity to restore the slope gradient, linear morphogenic earthquakes (i.e. free-faces) could progressively cumulate their effects at the surface (Caputo, 2005). For this reason and according to similar researches carried out along active normal faults within the Mediterranean realm, we conventionally assume a time period of 13 ka for the creation of the fresh tectonic scarps observed in Crete (Benedetti et al., 2002; Papanikolaou et al., 2005; Caputo et al., 2006).

2.1 WNW-ESE trending faults

The WNW-ESE fault trend is mainly concentrated along the southern coast of central Crete where they form a 55 km-long fault belt roughly extending from the villages of Sfakia to the west, and Agia Galini to the east. The fault belt consists of some major segments showing well exposed Holocene scarps entirely developed in bedrock. They are the Sfakia (SfF), Asomatos (AF) and Spili (SpF)

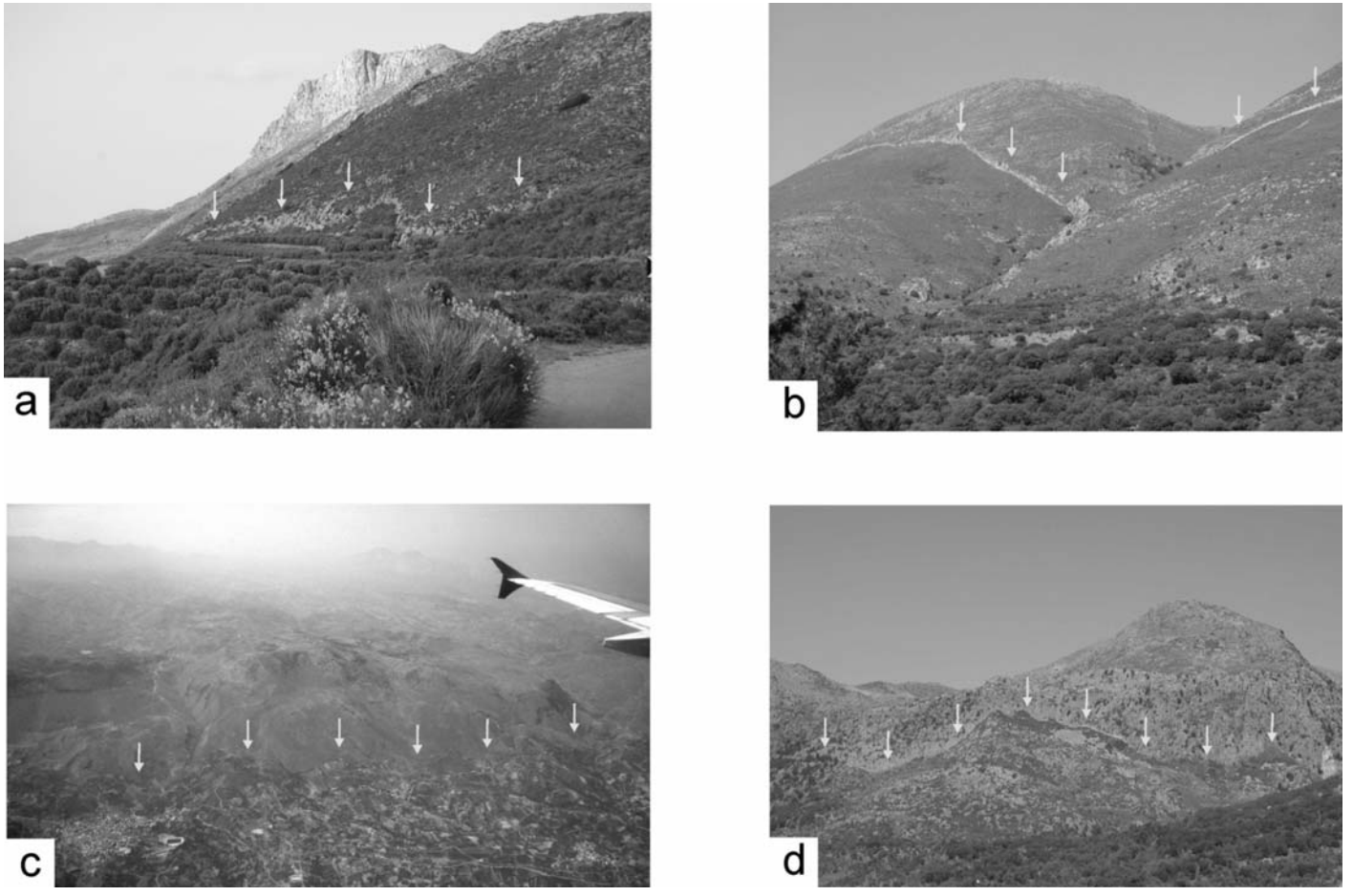

Fig. 2: Examples of cumulative Middle-Late Quaternary morphological escarpements and the post-glacial maximum free-faces (arrows) along the Zou, Lastros, Eastern Psiloritis and Spili faults.

Table 1. Principal seismotectonic parameters of the major active normal faults of Crete and surroundings. L: length of fault segment; D: dip-angle of the fault plane; Tmax: maximum cumulative throw measured along the fault scarp; S: late Quaternary long-term slip-rate; E: long-term extension rate obtained from S and D.

Fault		L (km)	D (°)	Tmax (m)	S (mm/a)	E (mm/a)
WNW-trending fault segments						
	Sfakia (SfF)	16	70S	12	1.0	0.3
	Asomatos (AF)	9	75S	8	0.6	0.2
	Spili (SpF)	16	65S	10	0.8	0.4
NNE-trending fault segments						
SFB	Zou (ZF)	5	65W	8	0.7	0.3
	Kalamavki (KaF)	4	65W	8	0.7	0.3
	Armeni (ArF)	8	70W	6	0.5	0.2
	Lithini (LiF)	5	70W	4	0.3	0.1
IFB	WLastros (LF)	11	60E	15	1.3	0.7
	Sfaka (SF)	9	75W	12	1.0	0.2
	Ha Gorge (HGF)	9	80W	12	0.9	0.2
	Kastelli (KF)	13	70W	6	0.5	0.2
EPFB	Agia Varvara (AVF)	8	70E	8	0.7	0.2
	Kroussonas (KrF)	10	70E	12	1.0	0.3
	Tilissos (TF)	4	70E	10	0.8	0.3
RFB	Gionas (GF)	7	65W	3	0.3	0.1
	Rodopos (RF)	5	70W	4	0.3	0.1
	Kera (KeF)	7	70W	5	0.4	0.1
	Gramvousa (GrF)	10	70W	8	0.7	0.2
Offshore WNW-trending fault segments						
	Paleochora-Agia Roumeli (PAGF)	25	70	-	6.4	2.2
	Messala (MF)	30	70	-	6.1-7.0	2.1-2.4
	Mirto (MrF)	25	70	-	1.4	0.5

faults. Another major structure is represented by the Agia Galini fault (AGF) that borders to the north the Plain of Messara.

All these faults display a very sharp morphology, defined by a steep, linear cumulative scarp reaching heights of several hundred meters and locally exhibiting well developed trapezoidal or triangular facets. The fault traces generally bound a major relief, which represents the footwall block and consists of Mesozoic carbonate or metamorphic rocks, running at the base of the mountain front. Morphotectonic evidences like triangular facets, suspended valleys and thick scarp deposits document a Middle-Late Quaternary activity that can be mapped for several kilometers showing segment lengths between 9 and 25 km. These faults are commonly south dipping with angles of 65°-80°.

As above-mentioned, at the base of the major morphological scarp, these faults show the occurrence of 8 to 15 m-high post-glacial scarps, thus documenting the most recent activity. Within the hanging-wall block, alluvial and colluvial wedges are well developed consisting of calcareous breccias and conglomerates thus confirming the continuous footwall uplift. Antecedent streams forming deeply entrenched channels and scarp-related gullies characterize the uplifted block, whereas a low-energy relief fluvial landscape developed on the hanging-wall block.

Other normal faults exist in the southern offshore part of the island running parallel to the coast line. They are 10 to 25 km-long, WNW-ESE to E-W trending and south-dipping faults. Major evidence of their activity is represented by uplifted Late Quaternary marine terraces and Holocene palaeoshorelines developped in the footwall blocks. Along some of them the seafloor is displaced forming relatively steep scarps reaching heights of about 70-80 m. (Fig. 4 in Alves et al., 2007), thus suggesting that synsedimentary fault activity may have continued up to the present.

2.2 NNE-SSW trending faults

The NNE-SSW trending normal fault segments develop all over the island (Fig. 1) forming well defined and discrete belts that, from East to West, are represented by the Sitia and Ierapetra Fault Belts (SFB and IFB, respectively), the Kastelli Fault (KF), the Eastern Psiloritis Fault (EPF), the Rodopou Fault Belt (RFB) and the Gramvousa Fault (GF).

The SFB forms a 18-20 km-long fault belt separating the carbonate sediments and metamorphic rocks of the Alpine nappes from the Upper Miocene-Pliocene sequences and locally the Holocene (?) lacustrine plain of Handras-Armeni (I.G.M.E., 1959; ten Veen and Postma, 1999). Three major fault segments could be recognized. Single segments are typically characterized by cumulative escarpments up to 200 m and 5-10 m-high fresh (Holocene) scarps at their base. Fault segments are dipping 65°-70° westwards and commonly show dip-slip kinematic indicators. Locally an older oblique-slip (dip-slip and left-lateral) generation of slickenlines is also recorded (Fortuin and Peters, 1984; Kokkalas and Doutsos, 2001).

Also the IFS consists of few major segments for a whole length of 25 km in a NNE-SSW direction separating the Ierapetra-Kavousi alluvial plain, to the west, from the Orno-Tripti massifs, to the east, consisting of carbonate sediments and metamorphic rocks (I.G.M.E., 1959). Single segments are 8.5 to 11 km-long and commonly dip 75°-80° westwards. They are characterized by 300-800 m-high cumulative Quaternary escarpments and at their base 8-14 m-high fresh scarps provide clear evidence of post-last glacial maximum re-activations (Caputo et al., 2006). Dip-slip striations prevail though older sinistral slickenlines have been locally observed. Other morphological features like V-shaped and suspended valleys characterize the footwall block, while syntectonic carbonate breccias widely occur in the hanging-wall.

Similar geological and morphotectonic features can be observed associated with and along the KF, EPF and GF (Fig. 2) documenting their Middle-Late Pleistocene and Holocene activity (Armijo et al., 1996; Fassoulas, 2001; Mouslopoulou et al., 2001).

3. Discussion and conclusions

Based on all available information just briefly described in the previous section, it is thus possible to calculate the slip-rate of the major faults affecting Crete Island. The results show that for the NNE-SSW trending fault segments, slip-rates range between 0.5 and 1.3 mm/a whereas for the WNW-ESE trending normal fault segments the slip-rates vary from 0.8 and 1.2 mm/a. As concerns

the offshore faults, slip-rates have been estimated based on uplifted palaeocoastlinefootwall uplift/hanging-wall downdrop (u/d) ratio . Accordingly, in the eastern sector it is possible to calculate slip-rate 1.4 mm/a. the western offshore we must also consider the uplift contribution the 365 AD thrust-related earthquake (Pirazzoli et al., 1996; Stiros, 2001; Papadimitriou and Karakostas, 2008; Shaw et al., 2008; Ganas and Parsons, 2009). Indeed, in this coastal sector, Early Byzantine palaeocoastlines are found at 9 m-height (Pirazzoli et al., 1996), but the results of numerical models simulating the NE-dipping thrust plane re-activation and associated surface deformation do not fully support such a large uplift. Once separated the regional, thrust-related uplift, it is thus possible to estimate the contribution provided by normal faulting along the western offshore of the island, which is as high as 6 mm/a.

Eventually, by summing up the contribution to crustal extension provided by all normal faults belonging to the two major sets (ca. E-W and ca. N-S), we calculated both radial and tangential (i.e. perpendicular and parallel to the Hellenic Arc, respectively) long-term strain-rates. A comparison of these geologically-based values with those obtained from GPS measurements (Hollestein et al., 2008) show a good agreement, therefore suggesting that the present-day crustal deformation is probably active since Middle Quaternary and mainly associated with the seismic activity of upper crustal normal faults characterized by frequent shallow moderate-to-strong (Mmax = 7.0) seismic events seldom alternating with stronger (Mmax = 7.5) earthquakes occurring along blind low-angle thrust planes affecting deeper and more external sectors of the Hellenic Arc, which now represent the most internal sectors of the Eastern Mediterranean accretionary wedge.

4. References

Alves, T.M., Lykousis, V., Sakellariou, D., Alexandri, S. and Nomikou, P., 2007. Constraining the origin and evolution of confined turbidite systems: southern Cretan margin, Eastern Mediterranean Sea (34°30–36°N). *Geo-Marine Lett*., 27, 41-61.

Angelier, J., 1975. Sur les plates-formes marines Quaternaires et leurs deforamtions: les rivages meridionaux de la Crete orientale (Grece). *C. R. Acad. Sc. Paris*, 281, 1149–1152.

Angelier, J., 1979. Néotectonique de l'Arc égéen. *Soc. Geol. Du Nord*, 3, 418 pp.

Angelier, J., Gigout, M.,1974. Sur les plates-formesmarines et la neotectoniqueQuaternaires de la region d'Ierapetra (Crete, Grece). C. R. Acad. Sc. Paris, 278, 2103–2106.

Angelier, J., Gigout, M. and Hogrel, M.Th., 1977. A propos du gisement tyrrhenien d'Arvi (Crete): Cadre stratigraphique, faune, equisse paleoecologique. *Ann. Geol. Pays Helleniques*, 28, 471-488.

Armijo, R., Lyon-Caen, H. and Papanastassiou, D., 1991. A possible normal-fault rupture for the 464 BC Sparta earthquake. *Nature*, 351, 137-139.

Armijo, R., Lyon-Caen, H., Papanastassiou, D., 1992. East-west extension and Holocene normal-faults scarps in the Hellenic arc. *Geology*, 20, 491-494.

Armijo, R., Meyer, B., King, G.C.P., Rigo, A. and Papanastassiou, D., 1996. Quaternary evolution of the Corinth Rift and its implications for the Late Cenozoic evolution of the Aegean. *Geophys. J.Int.,* 126, 11–53.

Benedetti, L., Finkel, R., Papanastassiou, D., King, G., Armijo, R., Ryerson, F., Farber, D. and Flerit, F., 2002. Post-glacial slip history of the Sparta fault (Greece) determined by 36Cl cosmogenic dating: evidence for non-periodic earthquakes. *Geophys. Res. Lett*., 29, 87-1/87-4.

Caputo, R., 1993. Morphotectonics and kinematics along the Tirnavos Fault, northern Larissa Plain, mainland Greece. *Zeit. Fur Geomorph*., 94, 167-185.

Caputo, R., 2005. Ground effects of large morphogenic earthquakes. *J. Geodyn*., 40, 113-118.

Caputo, R., Monaco, C. and Tortorici, L., 2006. Multiseismic cycle deformation rates from Holocene normal fault scarps on Crete (Greece). *Terra Nova*, 18, 181-190.

Fassoulas, C., 1999. The structural evolution of central Crete: insight to the tectonic evolution of the South Aegean (Greece). *J. Geodyn*., 27, 23-43.

Fassoulas, C., 2001. The tectonic development of a Neogene basin at the leading edge of the active European margin: the Heraklion basin, Crete, Greece, *J. Geodyn*., 31, 49-70.

Fortuin, A.R. and Peters, J.M., 1984. The Prina Complex in eastern Crete and its relationship to possible Miocene strike-slip tectonics. *J. Struct. Geol*., 6, 459-476.

Gaki-Papanastassiou, K., Karymbalis, E., Papanastassiou, D. and Maroukian, H., 2009. Quaternary marine terraces as indicators of neotectonic activity of the Ierapetra normal fault SE Crete (Greece). *Geomorphology*, 104, 38-46.

Ganas, A. and Parsons, T., 2009. Three-dimensional model of Hellenic Arc deformation and origin of the Cretan uplift. *J. Geophys. Res*., 114, doi:10.1029/2008JB005599

Hollestein, C., Muller, M. D., Geiger, A. and Kahle, H. G., 2008. Crustal motion and deformation in Greece from a decade of GPS measurements, 1993–2003. *Tectonophys*, 449, 17-40, doi: 10:1016/j.tecto.2007.12.006

Institute of Geology and Mineral Exploration, 1959. *Geological map of Greece at scale 1:50.000, sheet Ziros*.

Jost, M. L., Knabenbauer, O., Cheng, J. and Harjes, H. P., 2002. Fault plane solutions of microearthquakes and small events in the Hellenic arc. *Tectonophys*., 356, 87-114.

Kiratzi, A. and Louvari, E., 2003. Focal mechanisms of shallow earthquakes in the Aegean Sea and the sourrounding lands determined by waveform modeling: a new database. *J. Geodyn*., 36, 251-274.

Kokkalas, S. and Doutsos, T., 2001. Strain-dependent stress field and plate motions in the south-east Aegean region. *J. Geodyn*., 32, 311-332.

Le Pichon, X., Lallemant, S. J., Chamot Rooke, N., Lemeur, D. and Pascal, G., 2002. The Mediterranean Ridge backstop and the Hellenic nappes. *Marine Geol*., 186, 111-125.

Leite, O. and Mascle, J., 1982. Geological structures on the South Cretan continental margin and Hellenic Trench (eastern Mediterranean). *Marine Geol*., 49, 199-223.

Lyon-Caen, H., Armijo, R., Drakopoulos, J., Baskoutass, J., Delibassis, N., Gaulon, R., Kouskouna, V., Latoussakis, J., Makropoulos, K., Papadimitriou, P., Papanastassiou, D. and Pedotti, G., 1987. The 1986 Kalamata (South Peloponnesus) earthquake: detailed study of a normal fault, evidences for east-west extension in the Hellenic arc. *J. Geophys. Res*., 93, 14967-15000.

Meier, T., Rische, M., Endrun, B., Vafidis, A. and Harjes, H.-P., 2004. Seismicity of the Hellenic subduction zone in the area of western and central Crete observed by temporary local seismic networks. *Tectonophysics*, 383, 149-169.

Monaco, C. and Tortorici, L., 2004. Faulting and effects of earthquakes on Minoan archaeological sites in Crete (Greece). *Tectonophysics*, 382, 103-116.

Mouslopoulou, V., Andreou, C., Atakan, K. and Fountoulis, I., 2001. Paleoseismological investigations along the Kera fault zone, western Crete: implications for seismic hazard assessment. *Bull. Soc. Geol. Greece*, 34, 1531-1537.

National Observatory of Athens, 2009. Earthquake catalogue of Greece, Web site www.gein.noa.gr

Palumbo, L., Benedetti, L., Bourlès, D., Cinque, A. and Finkel, R., 2004. Slip history of the Magnola fault (Apennines, Central Italy) from 36Cl surface exposure dating: evidence for strong earthquakes over the Holocene. *Eart Planet. Sci. Lett*., 225, 163-176.

Papadimitriou, E. E. and Karakostas, V., 2008. Rupture model of the great AD 365 Crete earthquake in

the southwestern part of the Hellenic Arc. *Acta Geophysica*, 56, 293-312.

Papanastassiou, D., Lataoussakis, J. and Stavrakakis, G., 2001. A revised catalogue of earthquakes in the broader area of Greece for the period 1950-2000. *Bull. Soc. Geol. Greece*, 34, 1563-1566.

Papanikolaou, I.D., Roberts, G.P. and Michetti A.M., 2005. Fault scarps and deformation rates in Lazio-Abruzzo, Central Italy: Comparison between geological fault slip-rate and GPS data. *Tectonophys.*, 408, 147-176.

Papazachos, B. and Papazachou, C., 1997. *The earthquakes of Greece*, Editions ZITI, Thessaloniki, 304.

Piccardi, L., Gaudemer, Y. and Tapponnier, P. and Boccaletti, M., 1999. Active oblique extension in the central Apennines (Italy): evidence from the Fucino region. *Geophys. J. Int.*, 139, 499-530.

Pirazzoli, P. A., Laborel, J. And Stiros, S. C., 1996. Earthquake clustering in the Eastern Mediterranean during historical times. *J. Geophys. Res.*, 101, 6083-6097.

Pirazzoli, P. A., Thommeret, J., Thommeret, Y., Laborel, J. and Montaggioni, L. F., 2008. Crustal block movements from Holocene shorelines: Crete and Antikithera (Greece). *Tectonophys.*, 86, 27–43.

Pondrelli, S., Morelli, A., Ekström, G., Mazza, S., Boschi, E. and Dziewonski, A.M., 2002. European-Mediterranean regional centroid-moment tensors: 1997-2000. *Phys. Earth Planet. Int.*, 130, 71-101.

Postma, G. and Drinia, H., 1993. Architecture and sedimentary facies evolution of a marine, expanding outer-arc half-graben (Crete, Late Miocene). *Basin Res.*, 5, 103–124.

Roberts, G. and Michetti, A.M., 2004. Spatial and temporal variations in growth rates along active normal fault systems: an example from The Lazio–Abruzzo Apennines, central Italy. *J. Struct. Geol.*, 26, 2, 339-376.

Shaw, B., Ambraseys, N. N., England, P. C., Floyd, M. A., Gorman, G. J., Higham, T. F. G., Jackson, J. A., Nocquet, J. M., Pain, C. C. and Piggot, M. D., 2008. Eastern Mediterranean tectonics and tsunami hazard inferred from the AD 365 earthquake. *Nature Geoscience*, 1, 268-276.

Stewart, I.S. and Hancock, P.L., 1991. Scales of structural heterogeneity within neotectonic normal fault zones in the Aegean region. *J. Struct. Geol.*, 13, 191-204.

Stiros, S.C., 2001. The AD 365 Crete earthquake and possible seismic clustering during the fourth to sixth centuries AD in the Eastern Mediterranean: a review of historical and archaeological data. *J. Struct. Geol.*, 23, 545-562

Taymaz, T., Jackson, J. and Westaway, R., 1990. Earthquke mechanics in the Hellenic Trench near Crete. *Geophys. J. Int.*, 102, 695-731.

ten Veen, J., Meijer, P., 1998. Late Miocene to Recent tectonic evolution of Crete (Greece): geological observations and model analysis. *Tectonophys.*, 298, 191-208.

ten Veen, J.H. and Postma, G., 1999. Neogene tectonics and basin fill patterns in the Hellenic outer-arc (Crete, Greece). *Basin Res.*, 11, 223-241.

Wallace, R.E., 1978. Geometry and rates of change of fault-generated range fronts, north-central Nevada. *J. Res. U.S. Geol. Survey*, 6, 637-650.

Δελτίο της Ελληνικής Γεωλογικής Εταιρίας, 2010
Πρακτικά 12ου Διεθνούς Συνεδρίου
Πάτρα, Μάιος 2010

Bulletin of the Geological Society of Greece, 2010
Proceedings of the 12th International Congress
Patras, May, 2010

RECENT GEOMORPHIC CHANGES AND ANTHROPOGENIC ACTIVITIES IN THE DELTAIC PLAIN OF PINIOS RIVER IN CENTRAL GREECE

Gaki-Papanastassiou K.[1], Karymbalis E.[2] and Maroukian H.[1]

[1] *University of Athens, Faculty of Geology and Geoenvironment, Department of Geography and Climatology, Panepistimioupolis, 15784 Athens, Greece.*
Emails: gaki@geol.uoa.gr, maroukian@geol.uoa.gr

[2] *Harokopio University, Department of Geography, 70 El. Venizelou Str. 17671 Athens, Greece.*
Email: karymbalis@hua.gr

Abstract

The Pinios river delta is a Late Holocene arcuate type delta, located in the southern Thermaikos gulf (Central Greece). In order to determine the processes which contributed in the recent configuration of the delta, a detailed geomorphic map at the scale of 1:5000 has been prepared showing both the deltaic plain and the coastal zone features using GIS techniques. Comparative examinations of aerial photographs taken in different dates and reliable maps of the last two centuries along with field observations depict recent changes of the delta morphology. The most important factors for the development of the delta are fluvial sedimentation, wave activity and longshore currents in a tectonically active area. Land uses throughout the delta plain have been mapped in an attempt to identify socio-economic activities. The dominant feature in the deltaic plain is the numerous abandoned meandering channels. The delta shoreline is generally retreating due to marine processes especially where former river mouths occur. Finally, various future sea-level rise scenarios have been analyzed and an assessment of the impacts of the potential global future sea-level rise to the delta is estimated.

Key words: *coastal geomorphology, Pinios river delta, geomorphological mapping, Central Greece.*

1. Introduction

A large part of the low lands of mainland Greece are composed of deltaic plains. The Pinios river delta is located in Central Greece in the southern Thermaikos gulf of the north-east Aegean Sea (Fig. 1). It is an arcuate type delta with an area of 69 km^2 and a mean gradient of 0.058%. According to the delta classification proposed by Galloway (1975), the Pinios delta should be classified among those dominated by fluvial sediment supply and wave activity. The combination of suitable conditions for delta formation led to the development of Pinios delta during Late Holocene. Weathering and erosion in the catchment area of the Pinios river has resulted in the production of large quantities of sediments available for transportation. In addition, climate conditions (high mean annual precipitation especially between November and February) and relatively favorable marine characteristics of the receiving basin resulted in the delta formation.

The aim of this study is to determine the processes which contributed in the recent configuration of the delta as well as to assess impacts of the potential future sea-level rise to the delta.

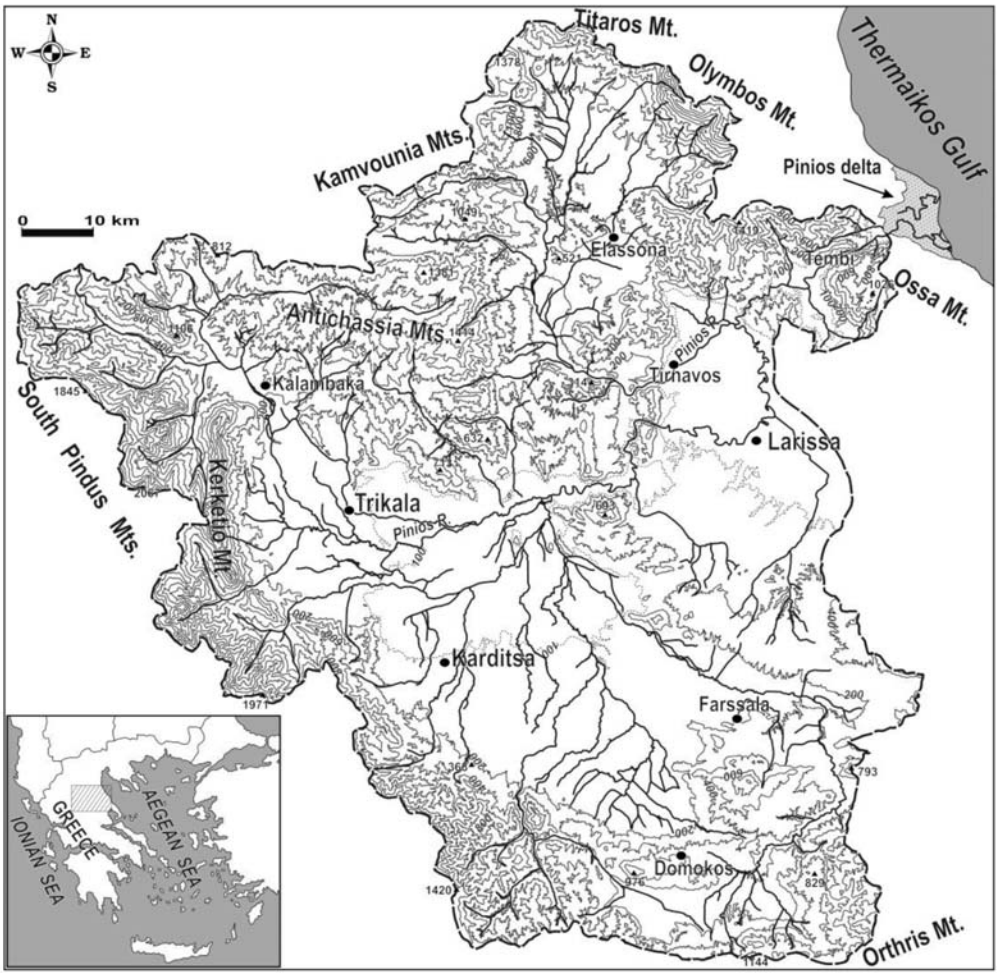

Fig. 1: Topographic map of the Pinios river drainage basin.

2. Drainage basin

The catchment basin of Pinios river has an area of 10704 km^2 flowing into Thermaikos gulf (Fig. 1). Lithologically, it consists of 25,8 % clastic sedimentary rocks, 21.4% metamorphic rocks, 7.1 % calcareous sedimentary rocks, 5.5 % igneous rocks and 40.2 % of unconsolidated fluvial and lacustrine sediments (Fig. 2).

A large amount of riverine sediments has been trapped within the extensive alluvial plain of the river due to the presence of the narrow, hard to erode, gorge of Tembi located between the delta and the alluvial plain acting as a temporary base level for the whole drainage basin of Pinios river. This is the main reason for the limited extension of the delta in relation to the area of the drainage basin.

Mean annual precipitation ranges from 400 mm near the delta to nearly 1600 mm in the highlands (Table 1). Mean annual temperature is about 17^{o}C. Mean annual discharge is 81 m^3/sec ranging between 11 m^3/sec and 176 m^3/sec. The high water period lasts from December till April. Annual sus-

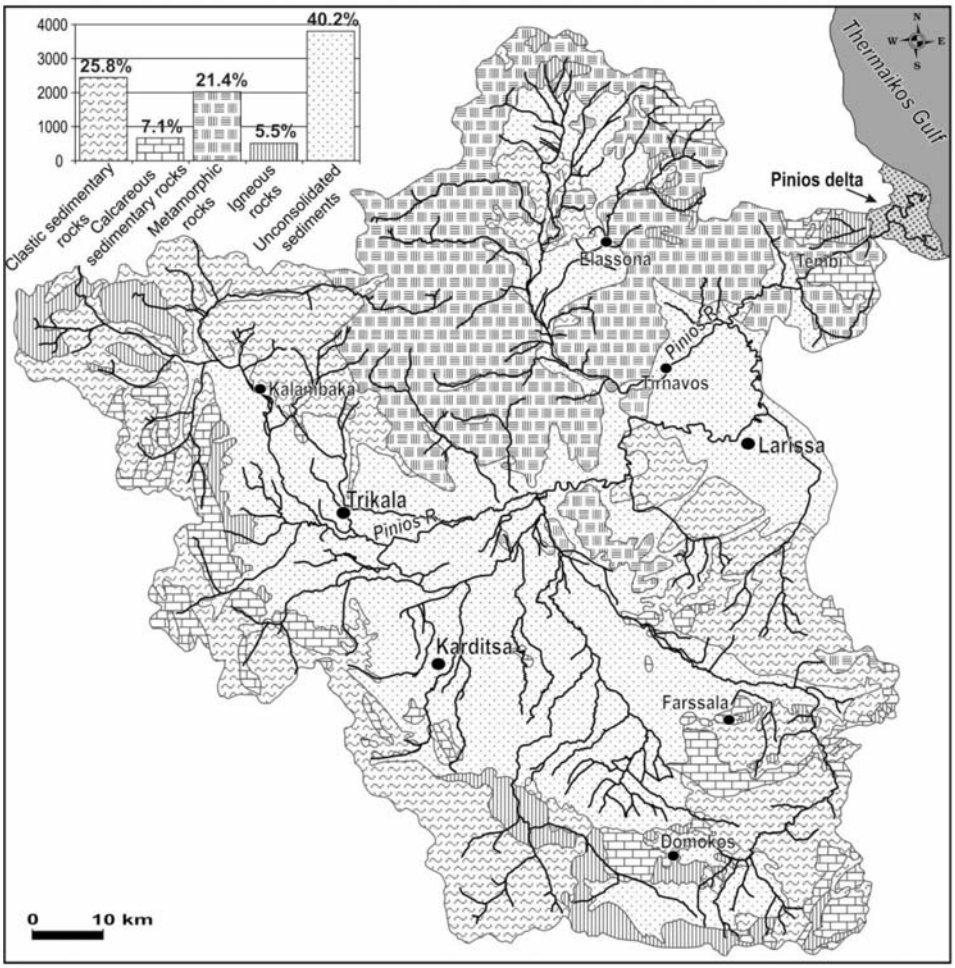

Fig. 2: Lithologic map of the Pinios river drainage basin with a diagram showing the participation of each one of the lithological types in the basin. It is based on the Greek Institute of Geology and Mineral Exloration (IGME) geological map of Greece (2006).

pended sediment load is estimated to be $0.6*10^3$ t/km^2 while annual yield of dissolved load is $0.15*10^3$ t/km^2 (Poulos et. al. 2000).

3. Thermaikos Gulf: the receiving basin

The Pinios delta is located on the western coast of south Thermaikos gulf (Fig. 3) having a microtidal marine environment (mean tidal range about 20 cm) (Hydrographic Service of the Navy, 2005). Coastal drift is towards the south. Surface water circulation is influenced mainly by the prevailing wind conditions. Prevailing N-NW winds move waters south along the coastline while in the case of S-SW winds surface water moves northwards. Wave heights and direction depends on the existing wind regime. Waves related to southerly winds are considered to be the most important in terms of magnitude. Thus high waves of long wavelength are to be expected only from southerly directions. In contrast, winds blowing from the north are more frequent and despite the smaller fetches they gen-

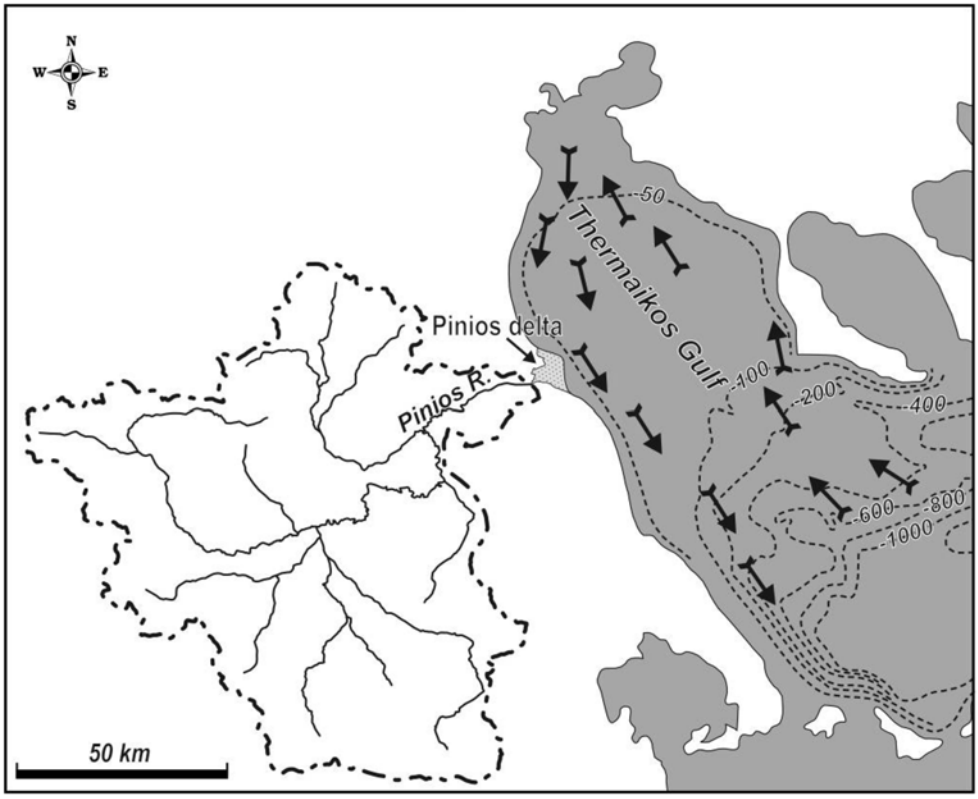

Fig. 3: Location map of the Pinios river drainage basin and delta. Arrows indicate surface waters circulation patterns of Thermaikos gulf.

erate surface gravity waves influencing the general water surface circulation of the gulf.

The Pinios delta is exposed to long wave fetches subjecting the deltaic coastline to a monthly wave power of 70-1454 w/m2 (Poulos et al. 2000). Current speeds are of the order of 5-20 cm/sec near the water surface and up to 9 cm/sec near the seabed.

4. Methodology

In this study topographic diagrams at a scale of 1:5.000 were used in the field to prepare a detailed geomorphological map depicting deltaic features in order to determine the dominant processes responsible for the configuration of the delta. Two series of aerial photographs taken in 1945 and 1995 at scales 1:42000 and 1:33000 respectively were used together with old maps of the previous century in an attempt to determine diachronic shoreline and channel changes along the Pinios river deltaic plain and the coastal zone.

One of the dominant factors for the future evolution of the delta is the expected global sea-level rise. The low-lying areas within the elevation zones of 0-0.5, 0-1, 0-2 and 0-4 m were calculated and land uses for these zones were defined and estimated. Land use were grouped in nine classes including complex cultivation patterns, discontinuous urban fabric, land primarily occupied by agriculture, coastal sands, broadleaf forest, natural grassland, shrub, sclerophyllous vegetation and non

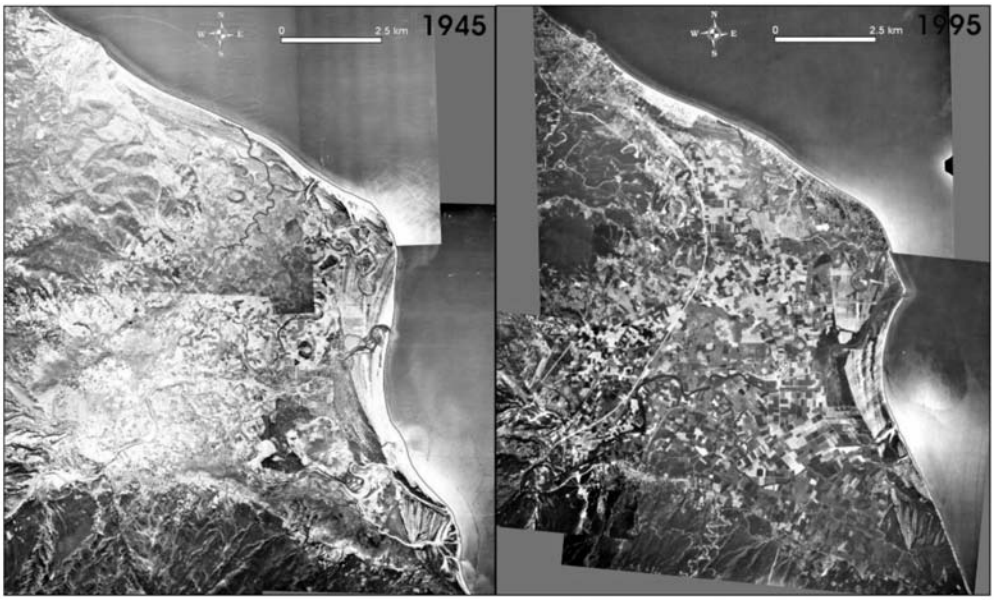

Fig. 4: Aerial photo-mosaic of the Pinios river delta of 1945 and 1995 respectively.

irrigated arable land. A spatial database from analogue maps at various scales, geometrically corrected aerial photographs and field-work data was prepared using GIS.

5. Results

The Pinios river delta is one of the few Greek deltas that have not been affected by human interference like channel alignment or diversion. Abandoned meander channels and oxbow lakes are visible in 1945 aerial photographs (Fig. 4 and 5).

The most recently abandoned distributary is the meandering channel south of the present active one leading to Armira about 4 km south of the present active mouth of the river (Fig. 6a and 5). This channel, which is depicted in 1881, 1910, 1924 and 1935 accurate topographic maps, was partially abandoned naturally in 1955 when the river migrated northwards. Comparable observations of the 1945 and 1995 aerial photographs show that the new course of the active river channel follows a previous abandoned path. A much older group of abandoned channels is located at the northern end of the delta.

The Pinios river deltaic coastal zone is dominated by the abundance of medium to coarse sandy sediments (Fig. 6b). The deltaic coastline has advanced by the gradual accretion of beach ridges. The period of high water discharge (December to March) coincides with that of high wave power. Hence the fluvial sediment input is being reworked by waves and associated longshore currents to form a series of beach ridges (Fig. 6d). At least six beach ridge generations presenting different orientation were recognized and mapped (Fig. 5).

The observation of the georeferenced aerial photographs and the comparable analysis of the digitized shorelines during the period 1945-1995 show that the coastline along the delta south of the present

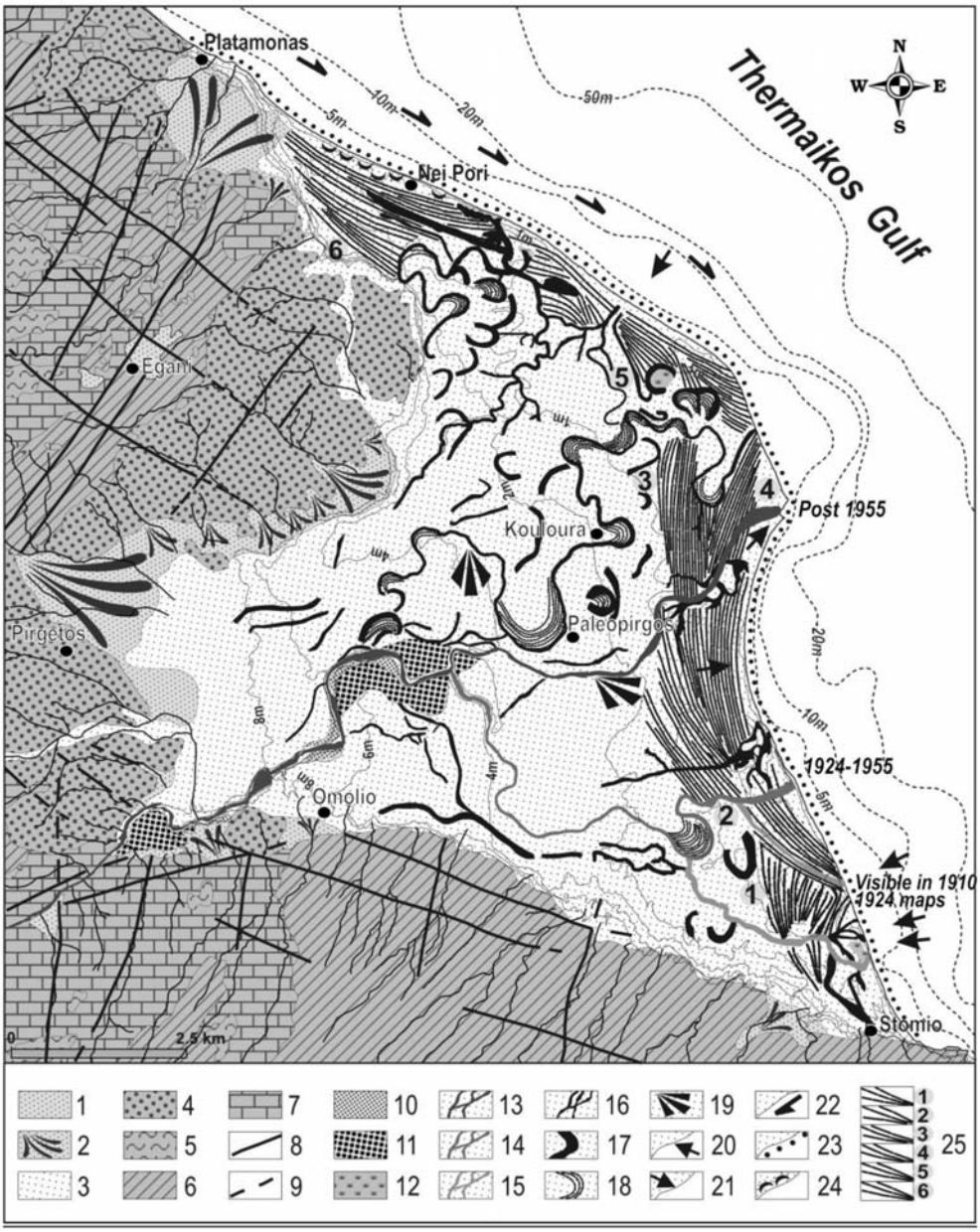

Fig. 5: Geomorphological map of the Pinios river delta. The map was prepared at the scale of 1:5000 based on field observations and the interpretation of aerial photographs. Legend: 1. Alluvial deposits, 2. Alluvial cones, 3. Deltaic plain deposits, 4. Neogene formations 5. Flysch, 6. Schists, gneiss, Amphibolites, 7. Marbles – limestones, 8. Visible fault, 9. Probable fault, 10. Lower fluvial terrace, 11. Higher fluvial terrace, 12. Coastal marsh, 13. Recent channel (active after 1955), 14. Channel before 1955, 15. Channel visible in 1910-1924 maps, 16. Abandoned channels, 17. Abandoned channels, 18. Point bars, 19. Crevasse splays, 20. Retreating coastline, 21. Prograding coastline, 22. Longshore currents, 23. Sandy beaches, 24. Coastal dunes, 25. Beach ridge groups.

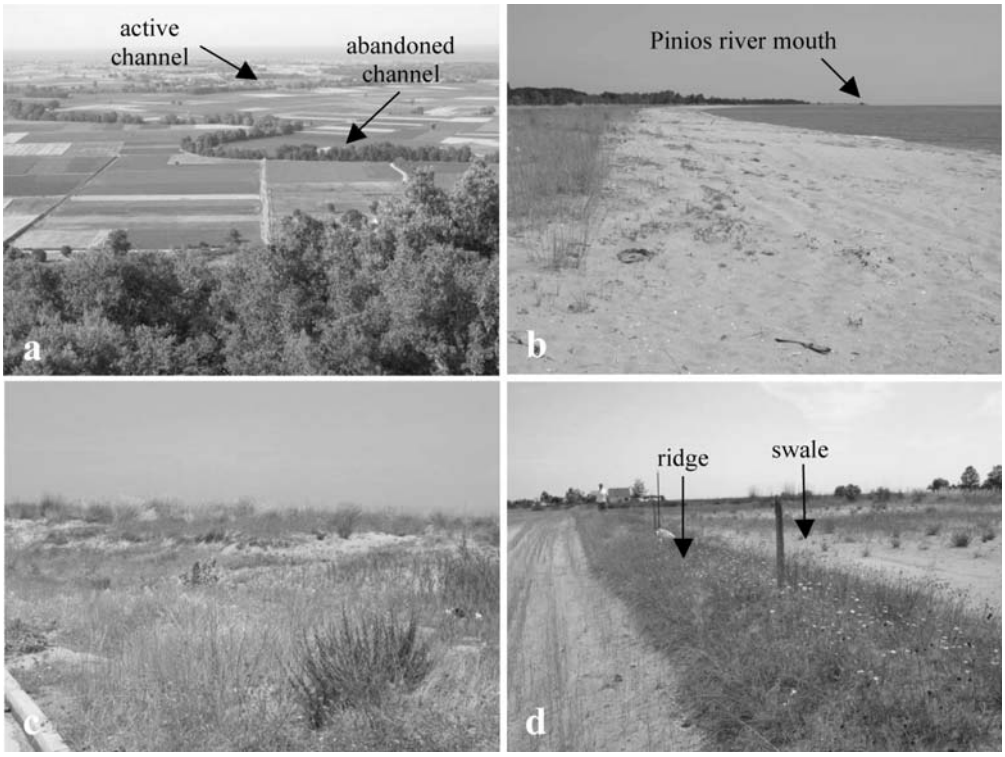

Fig. 6: a) Abandoned and active channel in the deltaic plain of Pinios river. b) Prograding sandy coast near the mouth of Pinios river. c) coastal dunes near Nei Pori. d) ridge and swale topography.

mouth has advanced through beach ridge accretion. The area around the mouth has prograded for about 440 m from 1955 to 1995 (11 m/yr) when the river shifted to its present position. On the contrary, the area of the abandoned mouth to the south (north of Stomio) has retreated for about 180 m corresponding to a maximum erosion rate of 4 m/yr for the 40 year period between 1955 and 1995.

A hazard that is expected to influence the Pinios delta like most of the low-lying coastal areas is the anticipated rapid sea-level rise (Gaki-Papanastassiou et al. 1997). The recent IPCC (2007) reports suggest that sea level will rise from 20 to 50 cm by the year 2100. In the case of deltaic deposits, an additional land subsidence due to sediment compaction should be taken into account. This future sea-level rise will have negative consequences for low-lying deltaic formations (Maroukian and Karymbalis 2004; Karymbalis et al. 2007, Karymbalis and Gaki-Papanastassiou 2008).

Such a rise could enhance the retreat of the Pinios delta coastline. The lying below the contour line of 0.5 m (6.5 km^2) corresponds to 9.5 % of the total area of the delta will face severe problems (Fig. 7). Furthermore, the low-lying area below 1 m is 14. 8 km^2 corresponding to 21.4 % of the delta. It is estimated that an extensive part of the low-lying deltaic coastal zone is occupied by economically important cultivations (4.2 km^2 below 0.5 m and 8.8 km^2 below 1m). The Pinios delta hosts some of the most productive agricultural lands of the broader area. In the early 50's the only settlements along the coast were Platamonas in the north and Stomio in the south. In recent decades these regions have expanded considerably as they have became important resort areas for local and foreign tourists. The most important resort settlement today is Nei Pori southeast of Platamonas.

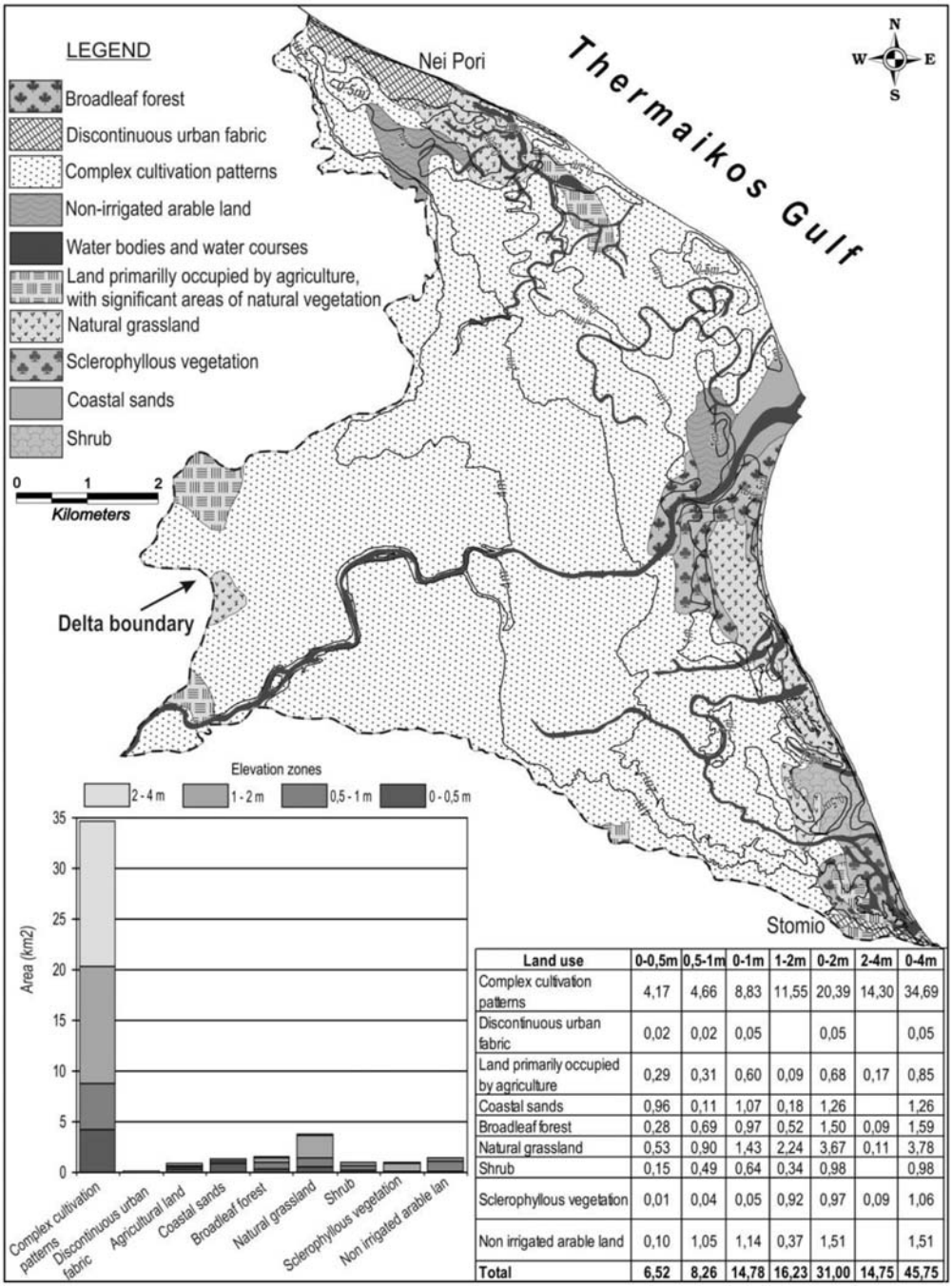

Land use	0-0,5m	0,5-1m	0-1m	1-2m	0-2m	2-4m	0-4m
Complex cultivation patterns	4,17	4,66	8,83	11,55	20,39	14,30	34,69
Discontinuous urban fabric	0,02	0,02	0,05		0,05		0,05
Land primarily occupied by agriculture	0,29	0,31	0,60	0,09	0,68	0,17	0,85
Coastal sands	0,96	0,11	1,07	0,18	1,26		1,26
Broadleaf forest	0,28	0,69	0,97	0,52	1,50	0,09	1,59
Natural grassland	0,53	0,90	1,43	2,24	3,67	0,11	3,78
Shrub	0,15	0,49	0,64	0,34	0,98		0,98
Sclerophyllous vegetation	0,01	0,04	0,05	0,92	0,97	0,09	1,06
Non irrigated arable land	0,10	1,05	1,14	0,37	1,51		1,51
Total	**6,52**	**8,26**	**14,78**	**16,23**	**31,00**	**14,75**	**45,75**

Fig. 7: Map portraying land use of the low-lying area of the delta. The table includes the area of each land use category for each elevation zone (in km^2) and the diagram shows the distribution of the nine land use classes for each elevation zone.

6. Concluding Remarks

- The evolution and the associated morphology of the deltaic plain and coastline results mainly from interaction between the water/sediment discharge and the prevailing wave activity. Abandoned meander channels and beach ridges are the dominant delta landforms. The river has changed its course several times in recent times.
- The region where the delta progrades today is the area around the present mouth where the maximum progradation rate is observed (11 m/yr is estimated between 1955 and 1995) as well as south of it. For the same time period a retreat rate of 4m/yr is estimated north of Stomio where the most recent abandoned mouth is being reworked by marine processes since 1955.
- An increase in mean sea-level by more than 0.5 m, related to a total increase of 2-3^{o}C of air temperature might cause severe erosion, with important economic repercussions. It is estimated that approximately 45.75 km^2 of the deltaic plain lies below the 4 m contour line with 14.8 km^2 located below the absolute elevation of 1 m while the area expected to be covered by the end of this century with a 50 cm sea-level rise is 6.5 km^2. A large part of the potential area to be permanently flooded and/or eroding is occupied by economically important agricultural land and tourist activities.

7. References

Gaki-Papanastassiou, K., Maroukian, H., Pavlopoulos, K. and Zamani, A., 1997. The implications of the expected sea level rise on the low lying areas of continental Greece in the next century. *Proceedings International Symposium on Engineering Geology and the Environment, Athens*, 121-126.

Galloway, W.E., 1975. Process framework for describing the morphological and stratigraphic evolution of deltaic depositional systems. In: Broussard M. L. (Ed.): *Deltas, Models for Exploration*. Houston Geol. Soc., Houston, 87-98.

Hydrographical Service of the Navy, 2005. Tides and tidal data for Greek harbours, 4th edition, Athens (in Greek).

Institute of Geology and Mineral Exploration of Greece (IGME) 2006. *Geological map of Greece, scale 1:500000*.

IPCC 2007. *Climate Change 2007: The physical Science Basis Summary for Policymakers Contribution of Working Group I to the Fourth Assessment Report of the Intergovernmental Panel on Climate Change*, Richard Alley, Terje Berntsen, Nathaniel L. Bindoff, Zhenlin Chen, Amnat Chidthaisong, Pierre Friedlingstein, Jonathan Gregory,Gabriele Hegerl, Martin Heimann, Bruce Hewitson, Brian Hoskins, Fortunat Joos, Jean Jouzel, Vladimir Kattsov, Ulrike Lohmann, Martin Manning, Taroh Matsuno, Mario Molina, Neville Nicholls, Jonathan Overpeck, Dahe Qin, Graciela Raga, Venkatachalam, Ramaswamy, Jiawen Ren, Matilde Rusticucci, Susan Solomon, Richard Somerville, Thomas F. Stocker, Peter Stott, Ronald J. Stouffer, Penny Whetton, Richard A. Wood, David Wratt, Geneva, 18 pp.

Karymbalis, E., Gaki-Papanastassiou, K. and Maroukian, H., 2007. Recent geomorphic evolution of the fan delta of the Mornos river, Greece: Natural Processes and Human Impacts. Bulletin *of the Geological Society of Greece*. *Proceedings of the 11th International Congress*, vol. XXXX, 1538-1551.

Karymbalis, E. and Gaki-Papanastassiou, K., 2008. Geomorphological study of the river deltas of Pinios, Kalamas, Evimos and Mornos. *Proceedings of the 4th Panhellenic Conference on Coastal Zones Management*, Mytilene, Greece, 86-94.

Maroukian, H and Karymbalis, E., 2004. Geomorphic evolution of the fan delta of the Evinos river in western Greece and human impacts in the last 150 years. *Zeitschrift für Geomorphologie N.F.*, 48(2), 201-217.

Poulos, S., Chronis, G., Collins, M. and Lykousis, V., 2000. Thermaikos Gulf coastal system, NW Aegean Sea: an overview of water/sediment fluxes in relation to air-land-ocean interactions and human activities. *Journal of Marine Systems*, 25, 47-76.

Δελτίο της Ελληνικής Γεωλογικής Εταιρίας, 2010
Πρακτικά 12ου Διεθνούς Συνεδρίου
Πάτρα, Μάιος 2010

Bulletin of the Geological Society of Greece, 2010
Proceedings of the 12th International Congress
Patras, May, 2010

GEOMORPHIC EVOLUTION OF WESTERN (PALIKI) KEPHALONIA ISLAND (GREECE) DURING THE QUATERNARY

Gaki - Papanastassiou K.[1], Karymbalis E.[2], Maroukian H.[1] and Tsanakas K.[1]

[1] *University of Athens, Faculty of Geology and Geoenvironment, Department of Geography and Climatologyy, 15771 Athens, Greece*
Emails: gaki@geol.uoa.gr, maroukian@geol.uoa.gr, ktsanakas@geol.uoa.gr

[2] *Harokopio University, Department of Geography, 70 El. Venizelou Str. 17671 Athens, Greece*
Email: karymbalis@hua.gr

Abstract

Kephalonia Island is located in the Ionian Sea (western Greece). The active subduction zone of the African lithosphere submerging beneath the Eurasian plate is placed just west of the island. The evolution of the island is depended mostly on the geodynamic processes derived from this vigorous margin. The geomorphic evolution of the western part of the island (Paliki peninsula) during the Quaternary was studied, by carrying out detailed field geomorphological mapping focusing on both coastal and fluvial landforms, utilizing aerial photos and satellite image interpretation with the use of GIS technology. The coastal morphology of Paliki includes beachrocks, aeolianites, notches and small fan deltas which were all studied and mapped in detail. The drainage systems of the peninsula comprise an older one on carbonate formations in the northwest and a younger Quaternary one in the south and southeast. Eight marine terraces found primarily on the Pliocene marine formations range in elevation from 2 m to 440 m are tilted to the south. In the Late Pleistocene some of the main drainage networks flowed towards the newly-formed gulf of Argostoli to the east.

Key words: *drainage networks, marine terraces, geomorphology, Paliki peninsula, Kephalonia island, Quaternary.*

1. Introduction

The study area, the Paliki peninsula, is located in the western part of the island of Kephalonia which occupies an important position along the Hellenic arc system (Fig. 1). Paliki peninsula exhibits many geomorphic features which reflect the active tectonic regime of the area.

The aim of this work is to examine the geomorphological evolution of the area during the Quaternary based on the study of different geomorphic indicators. The most important among them are a series of uplifted and tilted marine terraces, notches, beachrocks, aeolianites, drainage systems, knickpoints, gorges and fluvial terraces. These geomorphic indicators were studied through detailed geomorphic mapping and extensive field-work.

For this purpose topographic diagrams at a scale of 1:5000 obtained from the Hellenic Military Geographical Service were used in the field. Additionally a spatial database was constructed derived from analogue topographic maps at various scales (1:50000 and 1:5000), geological maps (1:50000 map of IGME and 1:100000 map of BP Co Ltd) aerial photographs and satellite images using GIS

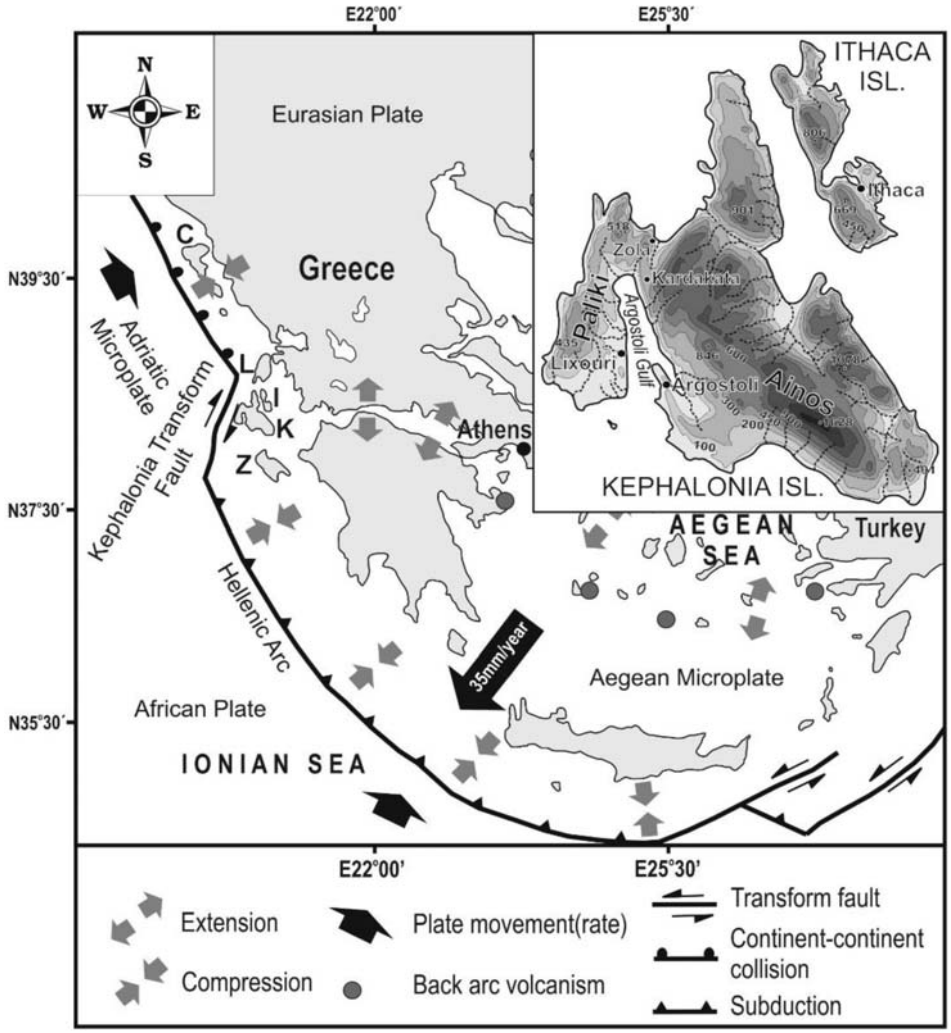

Fig. 1: Location map of the Ionian islands and the geodynamic setting of the broader area of the Aegean. Letters C, L, K, I, and Z stand for the islands of Corfu, Lefkada, Kephalonia, Ithaca and Zakynthos respectively.

techniques. Data procedure in the analytical context of GIS provided data integration including a common geographical reference system, common spatial and temporal coverage with similar scale and quality of the data.

2. Geology, tectonics and seismology of the area

The geodynamic processes in the region are related to the active subduction of the African lithosphere beneath the Eurasian plate, which progressively becomes continental convergence in north-western Greece (Fig. 1). The transition occurs along the Kephalonia Fault Zone (KFZ) a prominent dextral strike slip fault, located offshore west of Kephalonia and Lefkas islands (Scordilis et al., 1985; Louvari et al., 1999).

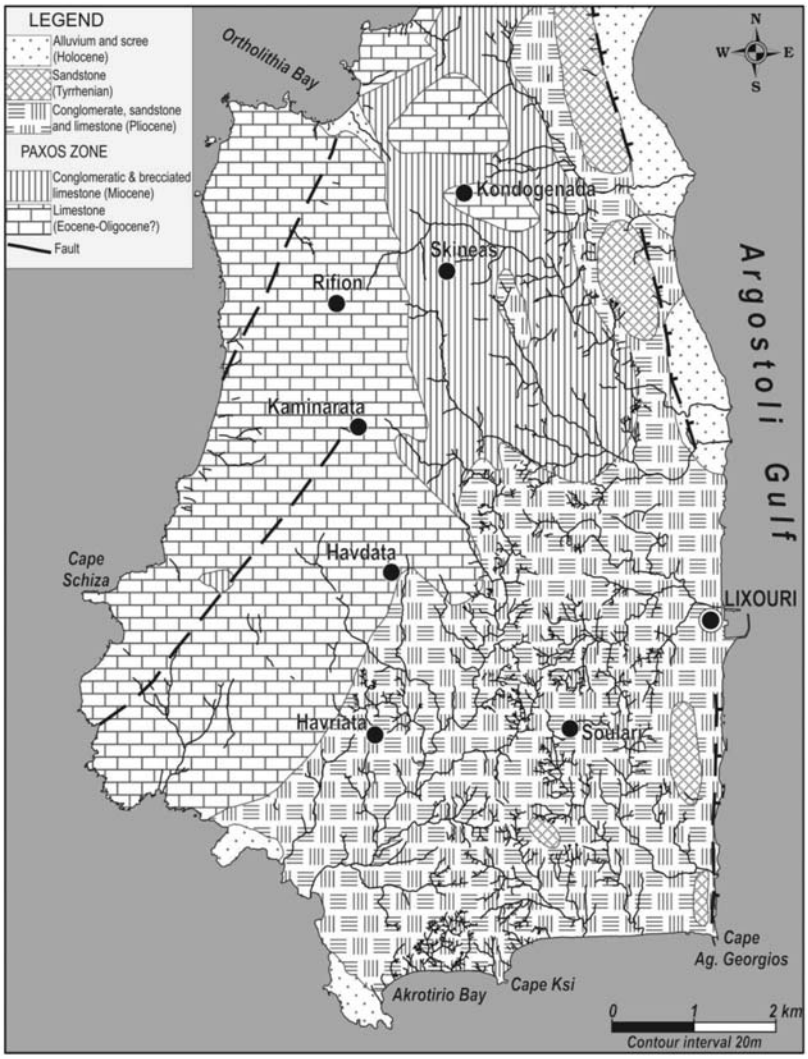

Fig. 2: Simplified geological map of the study area based on the maps by B.P (1971) and IGME, (1985) and detailed field work.

The basement of the island consists of east dipping, NW to NNW striking, thrust sheet fragments of a carbonate platform belonging mainly to the Paxos geotectonic zone (Underhill, 1985, 1989). The Ionian zone is also present occupying a relatively small area in the eastern part of the island.

The alpine basement of the Paliki Peninsula belongs to the Paxos geotectonic zone (BP Co Ltd, 1971; IGME, 1985). The older formations outcropping in the study area are Eocene-Oligocene limestones overlain by conglomeratic and brecciated limestones of Upper Oligocene to Upper Miocene age. The basement is overlain by Pliocene marine deposits. In the Lower Pliocene there is a short stratigraphic hiatus and a transgressive well-bedded conglomeratic facies. Near the base there is a limestone bed passing upwards into sand, sandstone and sandy limestone with layers of marls. Upwards, the blue marls predominate and enclose a rich mollusc fauna while in the uppermost part a

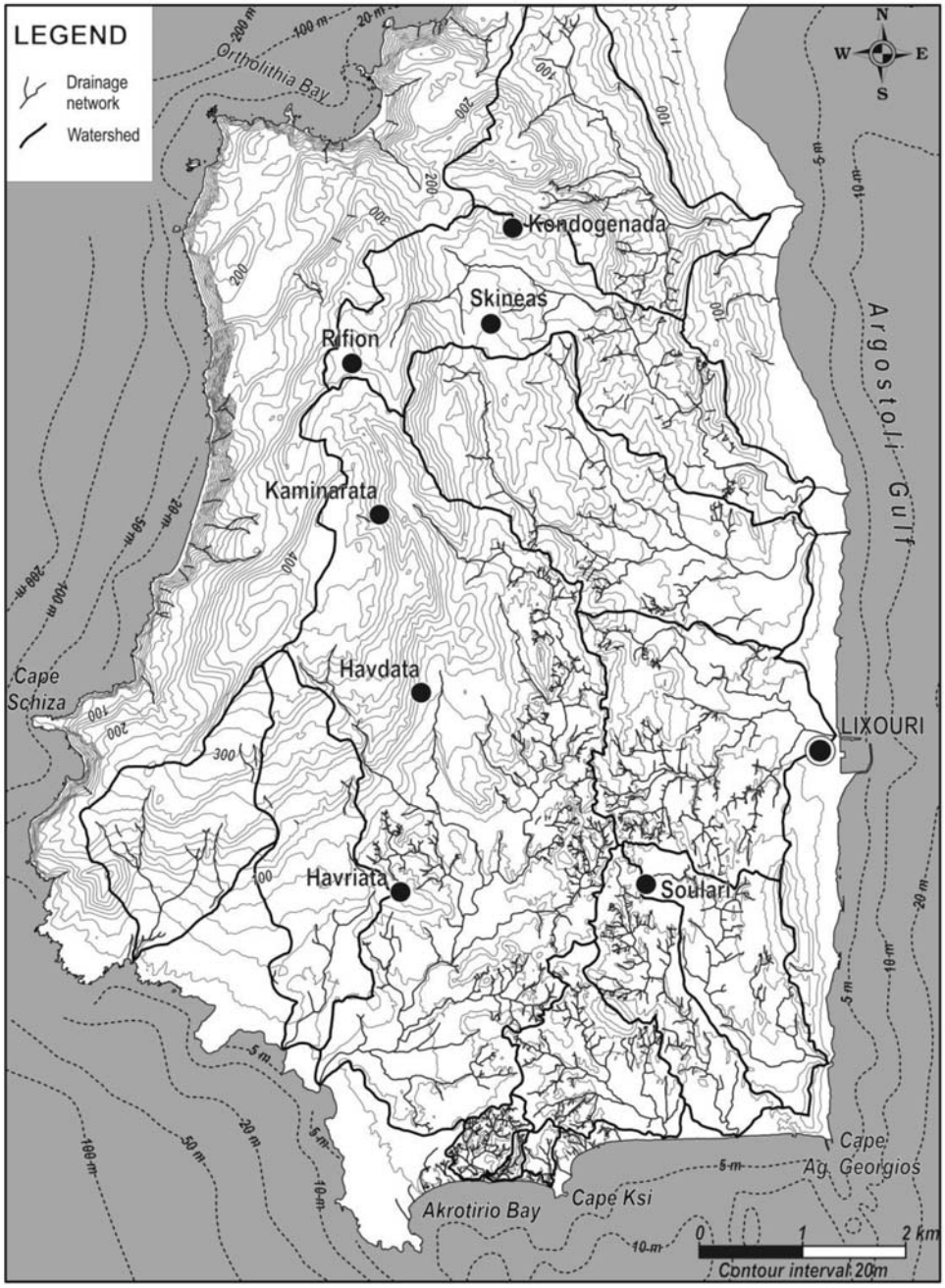

Fig. 3: Topographic map of the study area (Paliki Peninsula).

series of fine-grained sandstones and sandy marls reappear. The Pliocene formations occur in the southern and eastern part of the peninsula (Fig. 2). Along the eastern coast of the peninsula, sandstone formations are observed capping hills whose elevations reach 160 m and according to the ge-

ological map of IGME (1985) their age is Tyrrhenian. Finally, the Holocene deposits are composed of scree, colluvial, fluvio-torrential and coastal sediments. Based on the raised marine deposits of the peninsula it becomes evident that the prevailing tectonic movement is positive (emergence) during the Pleistocene and Holocene periods.

The area is characterized by intense seismicity with strong and frequent earthquakes. During the last millennia two vertical displacements have been verified, which affected most of the island, associated with co-seismic uplift. The first occurred between 350 and 710 AD and the second during the 1953 earthquake, which uplifted mainly the southeastern part of the island by 50 and 70 cm respectively (Pirazzoli et al., 1994; Stiros et al., 1994). Recent precise studies (Cocard et al., 1999; Hollenstein et al., 2006, Lagios et al., 2007) have confirmed the south-westward movement of the Ionian islands with a velocity of 7mm/yr increasing towards the south. A co-seismic horizontal displacement of the area of several cm and interseismic subsidence of up to 4mm/yr has also been found. The latter is in contradiction to the long term geological evidence of uplift, indicating that it is mainly a co-seismic result.

3. Geomorphological analysis

3.1 Drainage systems

The western slopes of the peninsula, where the older limestone formations occur, are drained by a few small, steep streams which flow directly into the Ionian sea. Thus this part of the study area is characterized by coarse drainage density. The northern half of the eastern part of the peninsula is drained by three major drainage networks with the upper reaches of their main channels flowing in a NNW-SSE direction and then turning to the east and emptying into the newly formed gulf of Argostoli. Two knickpoints were identified along the main channels of these three drainage systems. These knickpoints are evidence of two rejuvenation phases of the relief due to the tectonic uplift of the area. The uppermost parts of these drainage networks are the oldest as they have evolved on limestones of Eocene – Oligocene and Miocene age while their lowermost parts passing through the Pliocene deposits are much younger. These drainage networks were tributaries of a much larger drainage system which was active during the last glacial period up until early Holocene. The main channel of this drainage system had an almost N-S direction flowing along the eastern side of the present gulf of Argostoli which was a valley at that period.

At the southern part of the peninsula there are two drainage systems. Their upper parts have developed on limestone formations having a coarse drainage density while the more extensive lower parts drain Pliocene sediments. Additionally some drainage networks drain areas which consist exclusively of Pliocene formations. The main characteristic of these systems is the fine drainage density as a result of the high rainfall and the erodible character of the impermeable Pliocene lithologic sequence. Incision here is intense, especially where marls are present. It is clear that these are the most recent drainage networks of the study area that have evolved during the Quaternary period.

3.2 Marine terraces

Remnants of Quaternary marine terraces have been identified on Paliki peninsula as well as at other locations in the south and southeastern part of the island (Sorel, 1976). Detailed field geomorphological mapping revealed a sequence of eight marine terraces (Photos 1, 2, 3 and 4). The lower two terraces are the most continuous and well preserved and are located at elevations between 2-16 and 18-32 m respectively. They are present along the southern and eastern shoreline of the peninsula.

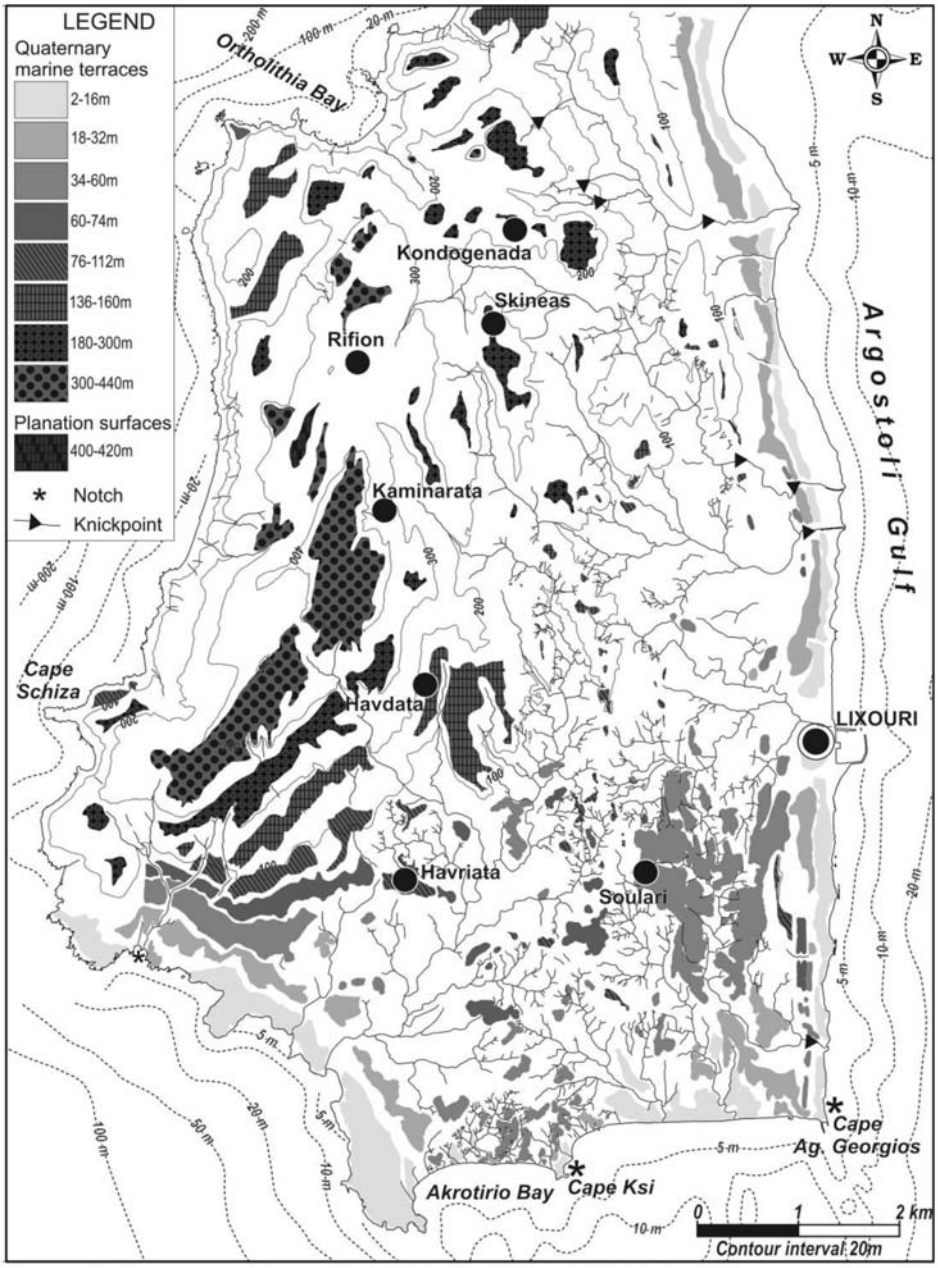

Fig. 4: Map of the Paliki peninsula showing the marine terraces and planation surfaces mapped in the field.

Remnants of higher marine terraces were distinguished at elevations between 34-60, 60-74, 76-112, 136-160, 180-300, 300-440 m respectively. The three higher marine terraces which have developed on Eocene-Oligocene limestones and are tilted to the southeast, seem to represent former shorelines carved during the Pliocene-Pleistocene. All these surfaces are incised by the channels of the drainage

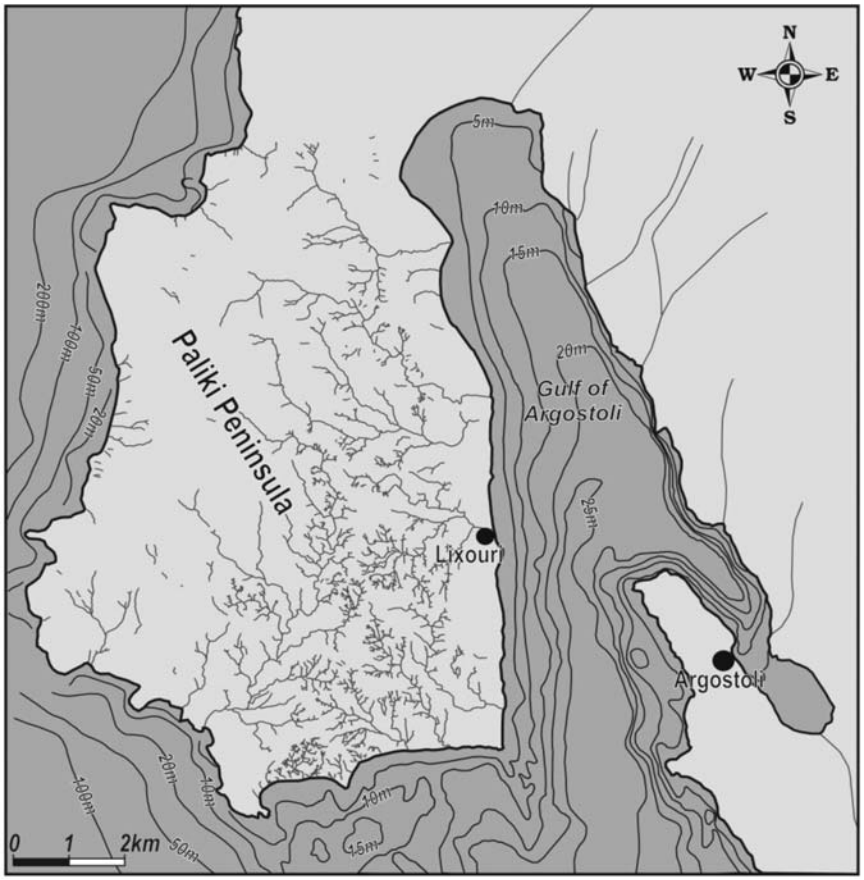

Fig. 5: Bathymetric map of the Argostoli gulf. Drainage networks of the Paliki peninsula are also depicted.

networks. The inner edges of some of the lower platforms were difficult to distinguish mainly due to the erodible lithology of the Pliocece formations.

3.3 Coastal Geomorphology

There are distinctly different geomorphic characteristics as well as geomorphic processes between the eastern and the western shores of the peninsula. The western coast is steep comprising limestone cliffs that reach a maximum height of about 240 m. This part is subject to coastal erosion. On the other hand, the eastern coast is characterized by much lower slopes and sandy beaches. Three small fan deltas have formed at the mouths of the major drainage systems along the western shores of Argostoli gulf. The main reasons for these differences in the coastal geomorphology are the lithology as well as the tectonic regime of the island. The western coasts consist of hard to erode limestone formations while the eastern part is composed of erodible Pliocene formations. The bathymetry of the gulf of Argostoli reveals that it is a shallow submarine valley with a maximum depth of about 25 m east of cape Ag. Georgios, which was active until early Holocene. Its western submarine slopes are less steep than the eastern ones probably due to the deposition of sediments supplied by the drainage networks of the Paliki peninsula.

At the southern and southeastern shores of Paliki the presence of aeolianites and a notch at 1-2 m is

Photo 1. Pleistocene caprock overlying Pliocene blue marls.

Photo 2. Marine terraces at the southwestern edge of the study area.

also noteworthy. Almost the entire length of both the southern and eastern shoreline is made up by the two lower marine terraces.

4. Palaeogeographic evolution – Conclusions

Two generations of drainage systems were identified; an older coarse one which evolved on the carbonate formations and a younger finer one on the more recent Neogene formations. The initial flow

Photo 3. Marine terraces at 90 m.

Photo 4. Raised beach at 3m and marine terrace at 6 m.

direction was to the south but in the Late Quaternary three major drainage systems changed direction towards the east flowing into the newly-formed gulf of Argostoli due to fault tectonism.

Different geomorphological features are observed in the western and the eastern shores of the peninsula mainly due to the lithology and the tectonic regime of the island. The western coasts consist of hard to erode limestone formations comprising steep faulted cliffs subject to intense coastal erosion

while the eastern ones are composed of erodible Pliocene formations characterized by much lower slopes, sandy beaches and small fan deltas at the mouths of the major drainage systems.

Paliki peninsula was almost an island during the Pliocene period. From the beginning of the Pleistocene a gradual uplift of the area started raising the older limestone formations and creating a NNE-SSW slope of the carbonate platform where the first marine terraces were carved.

Eventually, the present Paliki peninsula was formed including the Pliocene formations and having a general N-S slope. The combination of eustatism and vertical tectonic movements has led to the development of eight uplifted marine terraces. A Late Holocene notch was also identified proving that the area is still uplifting. The marine terraces ranging in elevation from 2-16 to 300-440 m with the lower two terraces, at 2-16 and 18-32 m being the most continuous and well preserved. Finally, given that the oldest and highest shoreline is located at an elevation of 440m, and the Quaternary period lasted 2.6 million years the minimum long term uplift rate is estimated to be 0.17 mm/year.

5. References

British Petroleum Co. Ltd., 1971. The geological results of petroleum exploration in western Greece, Athens, Greece. Institute for Geological and Subsurface Research., Report No 10.

Cocard, M., Kahle, H.-G., Geiger, A., Veis, G., Felekis, S., Biliris, H. and Paradissis, D., 1999. New constrains on the rapid crustal motion of the Aegean region: recent results inferred from GPS measurements (1993-1998) across the West Hellenic Arc, Greece. *Earth Planet. Sci. Lett.*, 172, 39-47.

Hollenstein, Ch., Geiger, A., Kahle, H.-G., and Veis, G., 2006. CGPS time-series and trajectories of crustal motion along the West Hellenic Arc. *Geophys. J. Int.*, 164, 182-191.

Institute for Geological and Mining Research, IGME, 1985, Geological map of Kefalonia island. Scale 1:50000.

Lagios, E., Sakkas, V., Papadimitriou, P., Parcharidis, I., Damiata, B.N., Chousianitis, K., Vassilopoulou, S., 2007. Crustal deformation in the central Ionian islands (Greece): Results from DGPS and DInSAR analyses (1995-2006). *Tectonophysics*, 444, 119-145.

Louvari, E., Kiratzi, A.A., and Papazachos, B.C., 1999. The Cephalonia Transform fault and its extension to western Lefkada island (Greece). *Tectonophysics*, 308, 223-236.

Pirazzoli, P.A., Stiros, S.C., Laborel, J., Laborel-Deguen, F., Arnold, M., Papageorgiou and Morhange, C., 1994. Late Holocene shoreline changes related to palaeoseismic events in the Ionian Islands, Greece. *The Holocene*, 4, 397-405.

Scordilis, E., Karakaisis, G., Karakostas, B., Panagiotopoulos, D., Comninakis, P., and Papazachos, B., 1985. Evidence for Transform Faulting in the Ionian Sea: the Cephalonia Island Earthquake Sequence of 1983. *Pure Appl. Geophys.*, 123, 388–397.

Sorel, D., 1976. Etude néotectonique des îles Ioniennes de Céphalonie et de Zante et de l' Elide occidentale (Grèce). These 3e cycle. University Paris Sud. Orsay.

Stiros, S.C., Pirazzoli, P.A., Laborel, J. and Laborel-Deguen, F., 1994. The 1953 earthquake in Cephalonia (Western Hellenic Arc): coastal uplift and halotectonic faulting. *Geophys. J. Int.*, 117, 834-849.

Underhill, J., 1985. Neogene and Quaternary tectonics and sedimentation in Western Greece. *PhD Thesis*. University of Wales.

Δελτίο της Ελληνικής Γεωλογικής Εταιρίας, 2010
Πρακτικά 12ου Διεθνούς Συνεδρίου
Πάτρα, Μάιος 2010

Bulletin of the Geological Society of Greece, 2010
Proceedings of the 12th International Congress
Patras, May, 2010

SEGMENTATION AND INTERACTION OF NORMAL FAULTS IN CENTRAL GREECE

Kokkalas S.

University of Patras, Department of Geology, Laboratory of Structural Geology, 26500 Patras, Greece, skokalas@upatras.gr

Abstract

The aim of this study is to improve our understanding on the mechanical interaction and linkage process between normal fault segments. Faults grow by the process of radial propagation and the linkage of segments, as strain increases, evolving to large fault systems. For this purpose we conducted a combined field and photogeological study on two major segmented fault zones in Central Greece, the Atalanti and Arkitsa fault zones. This approach includes effects of fault size and spatial distribution, scaling laws and footwall-hanginwall topography. Throw distribution and the geometry of the segmented fault arrays were analyzed in order to investigate the complexity of fault zones, the fault linkage process and the geometric characteristics of the relay zones formed between individual segments. The correlation of fault throw with fault length (D-L) and the ratios of overlap-separation (OL-S), separation-fault segment length (S-L) and relay displacement vs. separation (Dr-S) were examined in order to give an insight for fault segment interaction and linkage .

Key words: *fault segmentation, fault geometry, relay zones, Arkitsa-Atalanti fault zones, Evoikos Gulf.*

1. Introduction

Displacements on normal faults are rarely accommodated on a single well-defined slip surface, but are partitioned between interacting fault segments (Walsh and Watterson, 1991; Peacock and Sanderson, 1991; Cartwright et al., 1995; Willemse, 1997). Fault segmentation occurs across a wide range of length scales (Stewart and Hancock, 1991; Trudgill and Cartwright, 1994; Walsh et al., 2003) and faults can be observed as isolated or discontinuing sub-parallel stepping segments with overlapping or underlapping configuration. The transfer of displacement from one fault segment to another, dipping in the same direction, most often occurs through relay structures (Larsen, 1988). These are zones of high fault-parallel shear strain that provide soft linkage (Walsh and Watterson, 1991) between two interacting fault segments (Fig. 1). Breaching occurs when the fault segments are replaced by a single, through-going fault surface. Interaction and linkage between fracture segments have been studied in regimes of thrust and strike-slip faulting (Aydin and Schultz, 1990; Segall and Pollard, 1980; An 1997) and more recently between segments of extension fractures and normal faults in continental areas (Childs et al. 1995; Acocella et al., 2000; Soliva and Benedicto; 2004). All past works aimed to improve comprehension of mechanical interaction and linkage processes between faults, including the effects on scaling laws and growth models of faults as well as in fault size and spatial distribution. The linkage of individual fault segments into faults is critical for understanding the fault array's behaviour. Thus, the degree of fault segment linkage can modify earthquake sequences and

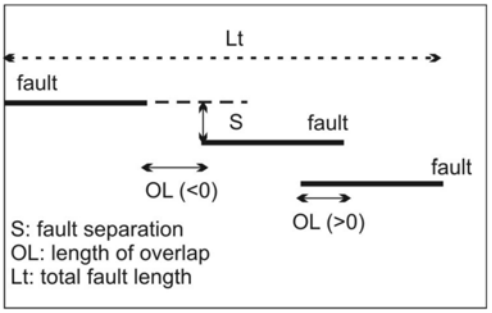

Fig. 1: Simplified illustration showing the main structural features of an interacting fault array and the relay zone terminology used here. S is the width of relay zone or the fault segments separation/overstep, while OL is the length of overlap between them. When OL<0 we have an underlapping configuration while when OL>0 we have an overlapping configuration.

magnitudes because a fault array can possibly act as a single fault (Gupta and Scholtz, 2000; Cowie and Roberts, 2001), indicating in this way its importance in understanding natural seismic hazards.

The purpose of this paper is to shed some light and explore the way in which fault growth by fault linkage influences the development of a fault population that initially has a power-law distribution of lengths.

2. Geological setting

In central Greece, much of the extensional strain is localised into a number of WNW-ESE trending grabens, which are mostly characterised by complex geometries in map view (Fig.1B), and a high degree of segmentation along strike (Doutsos & Poulimenos, 1992; Ganas et al., 1998; Kokkalas et al., 2006). Most of the major range bounding normal faults are thought to have been active in the Pleistocene, but the relative time of their activity is not well constrained.

The study area comprises a series of mainly north-dipping normal fault segments that define the southern boundary of the North Gulf of Evia in central Greece. This graben is one of several seismically active zones of N-S to NE-SW regional extension, with rates on the order of 1-2 mm/yr (Clarke et al. 1998), generally inferred to accommodate mechanical interaction of the North Anatolian–Aegean Trough strike-slip fault system and the Hellenic subduction zone (Doutsos and Kokkalas, 2001; Kokkalas et l. 2006). Basin bounding faults of these grabens are often well exposed where they juxtapose Mesozoic carbonates in their footwalls with Neogene sediments in their hanging walls. Slip on the Arkitsa fault zone, although poorly constrained, is likely to significantly exceed the 300–400 m topographic relief of the associated footwall block, with minimum throw possibly around 500-600 m (Kokkalas et al. 2007). Thus, a slip rate of 0.2-0.3 mm/yr can be calculated for Arkitsa fault zone, taking into account that faults of Evia rift zone started their activity in the last 2-3 My (Ganas et al. 1998). Slip rates for the adjacent Atalanti fault show similar values on the order of 0.27-0.4 mm/yr (Ganas et al. 1998).

The Arkitsa fault zone, together with Ag. Konstantinos fault (AKF) and Kamena Vourla fault (KVF), form a WNW-ESE left stepping, north-dipping fault margin that link with the southern margin of the Almyros-Sperchios graben (Fig.1). The Arkitsa fault zone, which has a length of ~10 km, separates Late Triassic – Jurassic platform carbonates in the footwall from Lower Pliocene to Quaternary sediments in the hangingwall. The geomorphological expression of Arkitsa region, the back-tilted terraces on the hanginwall block of Arkitsa fault, as well as the fresh ~1m band of unweathered limestone at the contact between the scree and fault plane before the quarrying, suggest Holocene seismic activity along this fault. Additionally, the coastline in the region shows evidence of Holocene uplift and subsidence that is controlled by the motion and location of the faults (Roberts & Jackson, 1991; Stiros et al. 1992).

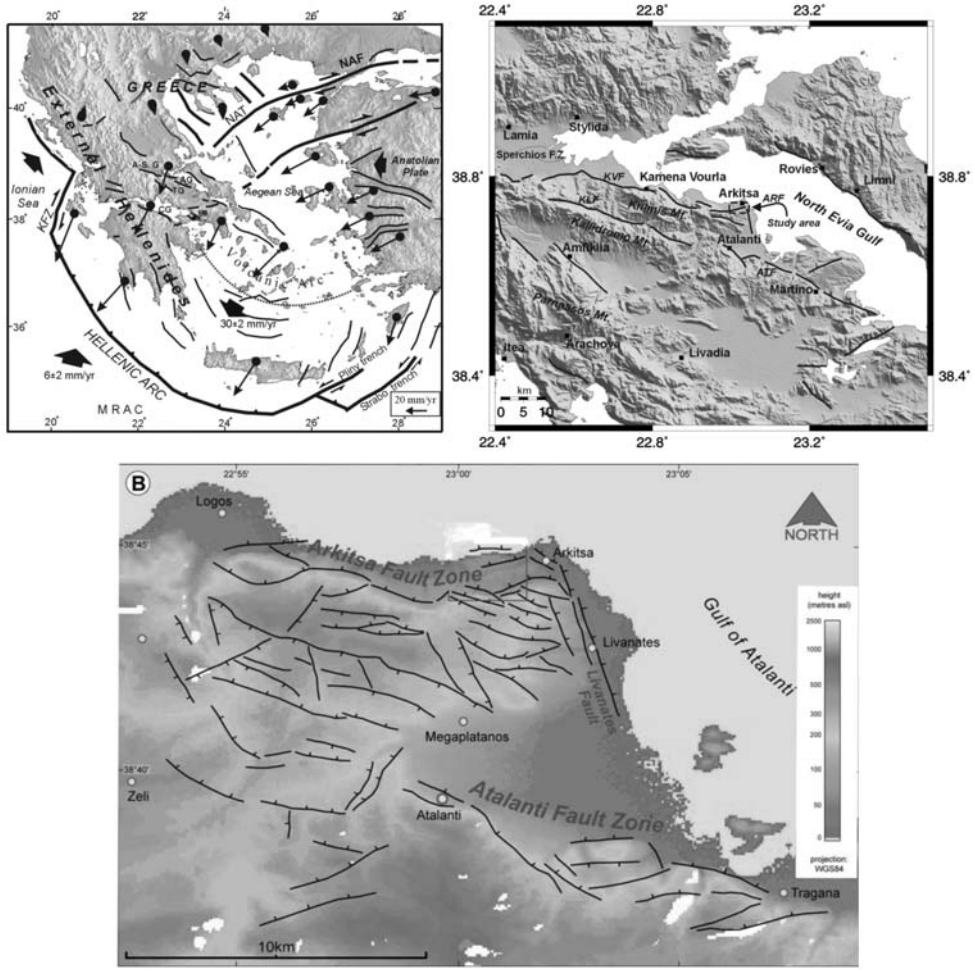

Fig. 2: (up left): Simplified map showing the main structural features along the Hellenic Peninsula, as well as the main active structures. The mean GPS horizontal velocities in the Aegean plate are shown with respect to a Eurasia fixed reference frame. CG: Corinth graben, TG: Tithorea graben, AG: Atalanti graben, A-S.G: Almyros-Sperchios graben, MB: Megara basin. NAT: North Aegean Trough, NAF: North Anatolia Fault, KFZ: Kephalonia transform fault, MRAC: Mediterranean Ridge Accretionary Complex. Map modified from Kokkalas et al. (2006); (up right): Map of central Greece close to the North Evia Gulf showing the main fault traces and the study area (arrow pointing to dashed rectangle). ATF: Atalanti fault, ARF: Arkitsa Fault; KLF: Kallidromo fault, KVF: Kamena Vourla fault. (B. down) Tectonic map of the broader study area. The Arkitsa and Atalanti fault zones are shown on map.

3. Fault zone characteristics

The knowledge of fault dimensions has become a powerful tool on many applications such as the estimation of strain in a region (Marrett and Almendinger 1992, Koukouvelas et al. 1999) and proposing models for fault growth (Walsh et al. 2002; Kim and Sanderson, 2005).

For this purpose we analyzed almost 70 fault traces (Fig. 2B) between Atalanti and Arkitsa fault zones. Beyond the published data, the mapping of faults was derived analysis of aerial photographs

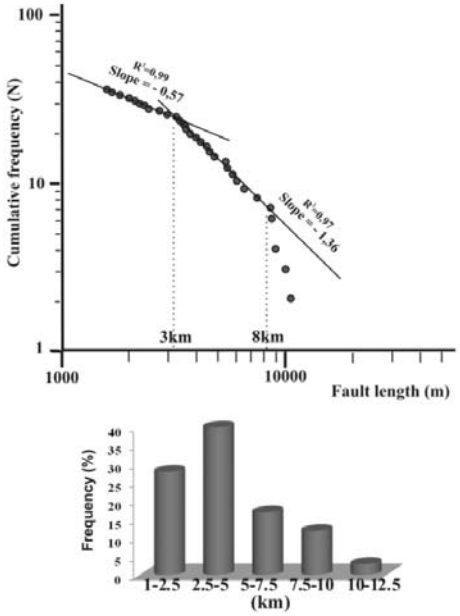

Fig. 3: Log-Log plot of the cumulative frequency with fault length and histogram of frequency with fault length for the faults of the broader study area.

(scale 1:17000) and DTM analysis in areas of poor data collection. Most faults and especially the two studies fault zones of Arkitsa and Atalanti are segmented along strike. Thus, fault segment showing tip areas and maximum throw near to fault center can be regarded as prominent fault segments. From their topographic profiles they appear to have a half spoon footwall shape and display abrupt changes in strike and trend of adjacent segments.

For the histogram of frequency versus fault length, from the studied area, we used data from combined photogeological and field work (Fig. 3). Almost 70% of the fault population is represented by faults with lengths <5 km. Gaps on lengths below 1.5 km can be related to the scale of observation.

3.1 Fault size

Fault size (i.e. displacement and length) has been proposed to be characterized by a power-law distribution (e.g., Marrett and Allmendinger, 1992; Poulimenos, 2000; Walsh et al., 2003). Generally, the population distribution can be expressed as

$$N = c\, U^{-D}, \tag{1}$$

where N is number of faults with a displacement greater than U, c is a constant, and D is the power-law exponent on the cumulative frequency plot. For this equation, an increasing value of D implies a greater number of small faults relative to large faults.

The published values for D of individual datasets ranges from 0.67 to 2.07 (e.g., Cladouhos and Marrett, 1996; Xu et al., 2006). Changes of D-value are due to both measurement and natural process (e.g., Yielding et al., 1996).

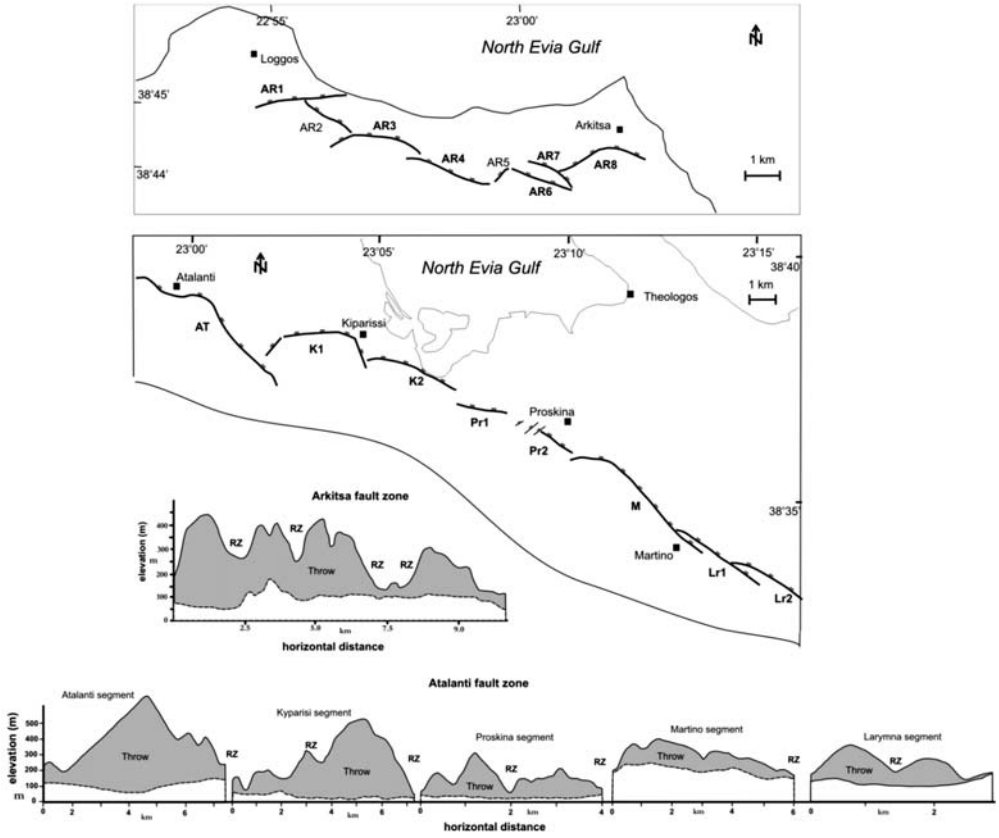

Fig. 4: Simplified maps of the Arkitsa and Atalanti fault zones showing the fault zone segmentation. Below, footwall & hanginwall elevation profiles, derived from DEM's, showing the variation of throw on each fault segment along strikes, are displayed.

For example, if the connectivity of distinct fault trace exposures cannot be observed, the estimated power-law exponents will be higher because the lengths of the faults appear to be smaller. On the other hand, it has been recognized that fault linkage causes the power-law exponent (D) to decrease in progressive deformation (Cladouhos and Marrett, 1996; Wojtal, 1996). This effect is documented by the physical experiments of Mansfield and Cartwright (2001). The systematic variations of the power-law exponent have been explained by strain localization onto progressively fewer and larger faults (Walsh et al., 2003), and have been predicted from physical experiments and numerical models (Cowie et al., 1995; Cladouhos and Marrett, 1996).

Fault length–cumulative frequency data are displayed in log–log graphs in order to identify sampling artifacts that stem from sampling area dimensions and sampling resolution. For the faults in the broader study area a logarithmic plot of the cumulative frequency of faults (N) vs. fault trace length (L) is displayed in Fig.3 Break in the graph indicates that the distribution is multi-fractal with two straight segments fitting the data (bi-fractal), with D-value of 0.57 for fault lengths <3 km and 1.36 for lengths between 3 and 8 km. Frequency distributions comprise the inherent shortcoming of truncation of small-scale features and finite range effect of large-scale features, that were excluded from

our linear relationships (Yielding et al., 1992; Pickering et al., 1995). D value (1.36), for the normal faults with lengths ranging from 3 to 8 km, testifies an increase in the importance of smaller structures contributing relatively more in strain accommodation of the area. Steps on the data-plot presented in Fig.3 subdivide the curve into two distinct sectors and indicate that within fault population there are abrupt increases and decreases in the number of faults at particular length scales (3 km and 8 km). The two sectors of the cumulative distribution may reflect different stages of evolution between fault arrays. Thus, they can be considered to account for fault linkage that replaces two smaller faults within the population with one larger fault (Mansfield and Cartwrigth, 2001).

3.2 Fault throw profiles

The fault zones of Atalanti and Arkitsa, affecting the southern coast of North Evia Gulf were mapped in detail from aerial photography and field observations. Footwall and hanginwall elevation profiles were derived from DEM (SRTM data, 90 m) showing also the variation of fault throw on each fault segment. Depending on scale of observation, these two fault zones are considered to be more or less segmented. For example in the Atalanti fault zone, Pavlides et al. (2004) suggested that this zone comprises five main segments that are also shown in the elevation profile of Fig. 4.

Footwall topography and local highs and lows along strike reveal that some of the main segments are also segmented into smaller segments (Fig. 4). For example, in Atalanti fault zone with the exception of western Atalanti segment, which appears to be a single segment with high amount of displacement, all other fault segments seem to be composed by two smaller segments having various stages of linkage. So, in this study we suggest that Atalanti zone comprises eight segments with a total length of 31.3 km. In a similar way, Arkitsa fault zone is also segmented along strike into five main segments (Ar1-Ar3-Ar4-Ar6-Ar8) with ENE and WNW orientation, while another three segments with NW (Ar2-Ar7) and NE (Ar5) orientations are aligned along the relay zones between the main segments (Fig. 4). More detail studies (i.e. terrestrial laser scanning) on the well-known segment of Arkitsa fault (Kokkalas et al. 2007) showed that this segment is also segmented into another three fault panels, with lengths on the order of 100-300 m and with high degree of curvature (Jones et al. 2009).

From the footwall-hanginwall topographic profiles, a noteworthy characteristic is that fault throw isn't always symmetric and close to fault segment centre as expected in isolated faults but it displays asymmetry towards the tip zone of the neighbouring fault segment, usually towards the west (Fig. 4).

3.3 D/L diagrams

The vertical throw on fault segments is used in this study as a proxy of the displacement, as is suggested also by Anders and Schlische (1994) and Dawers and Anders (1995).

The relationship between maximum displacement and fault length can be described as:

$$d_{max} = cL^n \quad (2)$$

(Cowie and Scholz, 1992; Scholz et al., 1993; Dawers et al., 1993). Attempts to determine the parameter n concluded in n = 2 (Watterson 1986; Walsh and Watterson, 1988), n = 1.5 (Marrett and Allmendinger, 1991; Gillespie et al., 1992) and n = 1 (Gudmundsson, 1992; Dawers et al., 1993). Cowie and Roberts (2001) suggest that the way in which a fault grows is fundamentally denoted by the ratio of maximum displacement to length. During the initial stage of coalescence a linked fault's length is the sum of the lengths of the smaller fault segments, while the maximum displacement remains the greatest value of the individual fault segment. In order for the scaling relationships to be

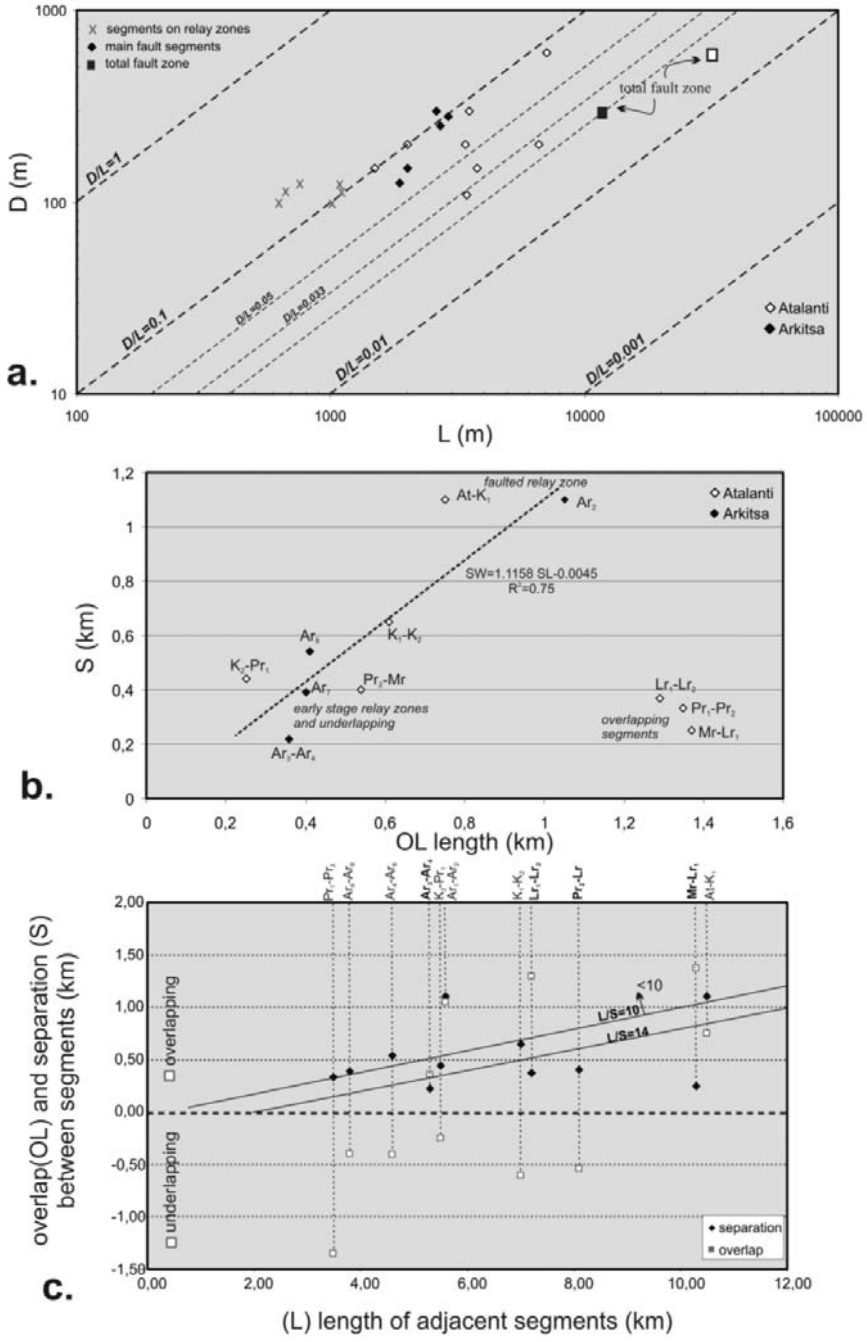

Fig. 5: a) Displacement-length diagram for all fault segments, relay zones as well as for the total length of fault zone b) Separation/overstep versus overlap/underlap length for the studied fault zones and c) Diagram of overlap and separation versus total length of the segments from both sides of the relay zone.

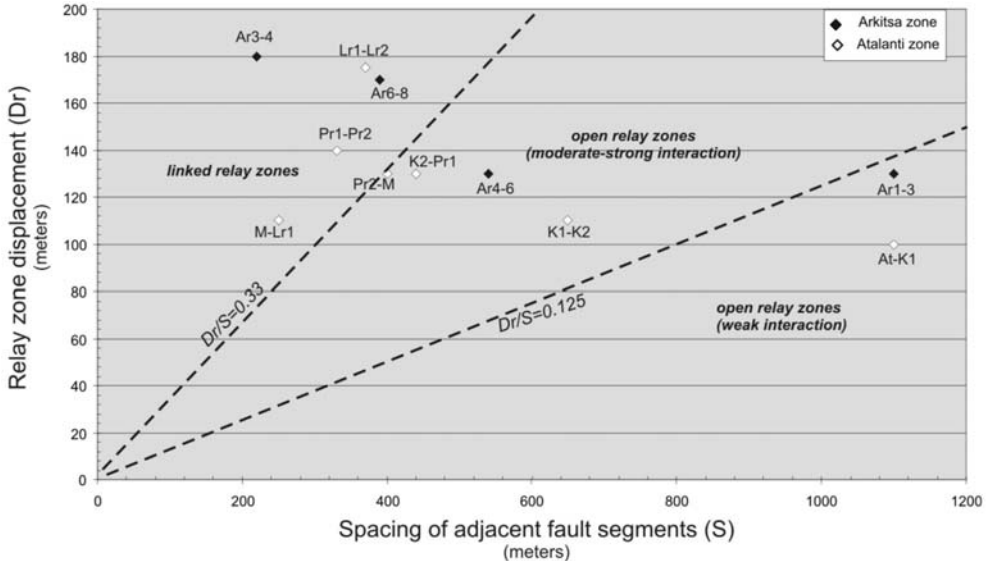

Fig. 6: Graph of relay displacement (Dr) vs. separation (S) of he different types of studied relay zones from Arkitsa and Atalanti. Areas are bounded by specific values of Dr/S.

generally applicable, maximum displacement must be accommodated in large fault structures as a whole because treating fault segments as individual faults generally generates larger dmax/L ratios (Peacock and Sanderson, 1991; Vermilye and Scholz, 1995).

Use of a logarithmic plot of maximum throw vs. fault trace length, for 18 well constrained fault segments (Fig. 5a) shows that the d/L data are bounded between a group of straight lines (Fig. 5a) representing dmax/L ratios between 0.02 and 0.3. Although restrictions such as host lithology and earthquake history must not be disregarded, in general fault populations seem to have similar systematic increase of displacement with length increase. Fault populations suggest that especially for faults <4 km long, throw varies more than one order of magnitude. Since a fault can develop through successive slip events on an individual segment or a group of them, the dmax/L ratio increase depends on the distribution of these events and the rate of fault propagation. Taking into account that segmentation is largely observed within the study area, thereafter, the dmax/L ratio is expected to attain high values in more matured linked faults. The reason why the dmax/L ratios are lower in some cases (i.e. Atalanti fault zone) maybe due to footwall erosion that reduces the displacement. Thus fault populations have d/L values lying beneath the growth line, with growth paths reflecting their own specific history of linkage. It appears that faults lengthen faster at a time, and after evolve their length and throw variably.

Diagram of Fig. 5a shows a general trend towards increasing D with L, but with scatter of about one order of magnitude in D with constant length. The D:L data define a linear band bounded by a pair of parallel straight lines with D/L ratios equal to 0,03 and 0.1. The data from Arkitsa are clustered above a line with a ratio of 0.05 while for Atalanti data are more uniformly distributed to the broad band. Note that the data points for the entire fault length of Arkitsa and Atalanti fall below the data of major fault segments. This can be interpreted as the result of displacement transfer across relay structures, which show higher D/L ratios, (Fig. 5a), which is also associated with steep displacement gradients at segment tips.

D/L systematic displays a change in fault geometry and evolution, where larger strain is represented by incremental increase in displacement than incremental increase in length.

4. Relay zones' geometry

Fracture interaction during propagation of adjacent fracture tips can include several stages. In a first stage underlapping tips of main fractures began to curve outwards from their earlier straight pathway while in a later stage they can develop a hook-shape geometry. In a more progressive stage segments can breach into a single continuous fracture. Relay ramps occur between fault segments that overstep in map view. Characteristic variability in displacement-distance profiles for fault segments and linked faults accompanies the interaction and linkage processes. Displacement transfer by relay ramps is accompanied by steep displacement gradients along fault segments at oversteps. Relay ramps often contribute to a minimum in total fault displacement at a linkage point.

Separation (S) and overlap (OL), the geometric parameters that used to represent relay zone scaling and fault segment interaction are easy to obtain on map views (Aydin and Schultz, 1990). An important measure of the architecture of relay zones is the aspect ratio A = OL/S, where OL is the length of the overlap (or underlap) zone and S is the separation/overstep between fractures (Fig. 5b). The relay zones in the study area display aspect ratios from 0.57 to 5.48 (mean value is 1.99 and s.d. is 1.72). The great majority of values cluster around value 1, while high values (are represented by highly overlapping relay zones (Lr1-Lr2, M-Lr1), as well as by initially collinear fractures (S almost 0; Pr1-Pr2) that show en echelon geometry in the relay zone (see Table 1 and Fig. 4). In general, higher OL/S ratio is consistent with a more evolved stage in fault overlap and linkage. Fault interaction and linkage occur earlier during fault overlap for small values of separation than large ones. Relationship between OL and S from a broad range of scales showed mean values of 4.9 (from normal faults; Acocella et al. 2000) and around 4.7 (for strike slip faults; Aydin and Schultz, 1990).

For a given overstep there is a critical minimum length for the fractures to interact and overlap; below this value interaction and overlap is inhibited. Acocella et al. (2000) suggests that this minimum length appears to be almost 14 times the overstep (S) between fractures, while sandbox models yield similar minimum values (about 10 times the overstep S) in strike-slip settings (An 1997) for linkage to occur. In Fig. 5c, relay zones with higher potential to interact and link are the M-Lr1, Pr2-M and Lr1-Lr2 zones between Martino, Larymna and west Proskina fault segments for the Atalanti zone, while for Arkitsa zone only the Ar3-Ar4 relay zone displays the highest L/S ratio. Great part of the rest of relay zones display values around 10.

We also used a relay displacement-separation diagram in order to define a segment criterion considering that the amount of displacement at relay ramp and fault separation/overstep control the fault's ability to link during overlap (Fig. 6). Relay displacement (Dr), which is the sum of displacement of each fault segment at tip zone, and fault segment separation (S) are measured on the relay ramp on a line normal to the ramp strike and at the centre of the overlap (or underlap) length. The results are presented on Fig. 6 for both the Arkitsa and Atalanti zones. Open relays exhibit low values of ratio Dr/S less than 0.125 and represent relay zones with weak interaction. Open relays with moderate to strong interaction show values between 0.125 and 0.3. Finally, linked relay zones with the highest potential for initiation of linkage and breaching display values above 0.33. Linked relays represent zones in which fault segments link when relay displacement increases during overlap or tip to tip linkage. Results for the linked relay zones fit well with the L/S values mentioned above. None of the studied relay zones display characteristics of fully breaching since they need to display values of Dr/S from a minimum of 0.8 to 1< (see also Soliva and Benedicto, 2004).

Based on the above and according to the segment length of the mapped faults and the potential for interaction and linkage, we used the empirical relationships of Wells and Coppersmith (1994), Ambraseys and Jackson (1998) and Pavlides and Caputo (2004) in order to make a first estimation for the seismic potential magnitude for each fault zone. In table 2, the seismic magnitude is given for each pair of segments with higher potential to interact and link, as well for the whole zone, according to the above mentioned empirical relationships. The Atalanti and Arkitsa Fault zones give a magnitude of 6.82-6.83 and 6.28-6.45 respectively, as is estimated for the worst scenario for total fault length activation, while for all other cases a magnitude between 5.8 and 6.5 is estimated.

5. Conclusions-Results

In cumulative frequency against fault length plots, fault linkage produces shallower slopes near the linked length scales. This effect directly results in fluctuating curves when fault linkage at different length scales occurs. For fault linkage, the size of the linked faults is a fundamental factor that influences the development of a fault population that initially has a power law distribution of lengths. The smallest linked faults result in an increase in the power-law exponent, as seems to be the case for the whole study area, whereas the largest linked faults result in a reduction of the power-law exponent.

A growing fault array characterized by accruing displacement but no significant lateral propagation is "saturated" sensu Wu and Pollard (1995) and in a later stage the increase of d/L suggests the array "matures" sensu Walsh et al. (2002). Multi-fractal properties are observed on well-developed fault networks and are referred to the existence of distinct fault subsets, or reveal fracture mechanism. Our bi-fractal distribution suggests that the two populations are saturated and mature (Fig. 3). Based on the cumulative distribution (Fig. 3), we recognize two characteristic lengths at approximately 3 km and 8 km.

The d/L ratio changes significantly during the fault evolution stages or shows irregularities and scatter due to interaction and linkage between faults, as individual faults grow at different stages of development. The displacement on a particular fault segment or relay zone becomes proportionally larger as interaction increases because fault propagation is inhibited (see also Peacock and Sanderson 1996). Data from Arkitsa show higher values of D/L than Atalanti area and this indicate a more mature stage in the fault array evolution.

Relationships between overlap/underlap, separation, relay displacement and length of the adjacent segments of Atalanti and Arkitsa faults can be used to discriminate relay zones with weak or stronger interaction. The western segments of Atalanti zone (Proskina-Martino and Larymna segments) as well as the central segments of Arkitsa fault (Ar3-Ar4) indicate a stronger interaction and more progressive stage for fault linkage. Additionaly, these segments display the highest value of fault segment length vs. separation (L/S) as well as relay displacement to separation ratio (Dr/S).

In any case of fault rupture scenario an earthquake of magnitude around 6-6.5 is possible in case of reactivation of any pair of these segments, although the study area appears to be in low risk since it displays low strain (Hollenstein et al. 2008) and long recurrence intervals for past strong earthquakes based on paleoseismological studies (Pantosti et al.2004.; Pavlides et al. 2004).

6. Acknowledgments

The author would like to thank the two anonymous reviewers for their suggestions and M. Zambos for discussion on diagram results.

Appendix 1

Table 1. Fault segments and relay zone geometry characteristics.

Fault segment	Length (m)	Throw (m)	Relay displ. (m)	Overlap (m)	Separation (m)	Ratio OL/S
		Atalanti Fault zone				
At	7100	600				
			100	750	1100	0.69
K1	3460	200				
			110	-600	650	0.93
K2	3500	300				
			130	-250	440	0.57
Pr1	1970	200				
			140	-1350	330	4.09
Pr2	1520	150				
			130	-540	400	1.35
Mr	6580	200				
			110	1370	250	5.48
Lr1	3800	150				
			175	1290	370	3.49
Lr2	3400	110				
		Arkitsa Fault zone				
Ar1	2900	280				
Ar2	1700	130	130	1050	1100	0.96
Ar3	2700	250				
			180	360	220	1.64
Ar4	2600	300				
Ar5	660	130	130	-410	540	0.76
Ar6	1970	150				
Ar7	1530	170	170	-400	390	1.03
Ar8	1880	125				

Table 2. Potential magnitudes for fault segment reactivation. Abbreviation of fault segments names same as in Figure 4.

Fault	Length (km)	Wells & Coppersmith (1994)[*1]	Ambraseys & Jackson (1998)[*2]	Pavlides & Caputo (2004)[*3]
Ar_3-Ar_4	5.3	5.81	5.95	6.13
At	7.1	5.98	6.10	6.24
K_1-K_2	7	5.97	6.09	6.24
Ar_3-Ar_4-Ar_6-Ar_8	9.15	6.12	6.22	6.35
Pr_1-Pr_2-M-Lr_1-Lr_2	17.0	6.48	6.53	6.5
Arkitsa F.Z. total	12	6.28	6.36	6.45
Atalanti F.Z. total	31.3	6.83	6.83	6.82

[*1]Wells & Coppersmith (1994): Ms=1.32logL+4.86, L: length of fault
[*2]Ambraseys & Jackson (1998): Ms= 5.13+1.14logL, L : length of fault
[*3]Pavlides & Caputo (2004): Ms=0.9log (SRL)+5.48, SRL=surface rupture length

7. References

Acocella, V., Gudmundsson, A., Funiciello, R., 2000. Interaction and linkage of extensional fractures: examples from the rift zone of Iceland. *J. Struct. Geol.,* 22, 1233–1246.

Ambraseys, N.N. and Jackson, J.A., 1998. Faulting associated with historical and recent earthquakes in the Eastern Mediterranean region. *Geophys. J. Int.*, 133, 390-406.

An, L., 1997. Maximum link distance between strike-slip faults: observations and constraints. *PAGEOPH.,* 150, 19–36.

Anders, M.H., Schlische, R.W., 1994. Overlapping faults, intrabasin highs, and the growth of Normal faults. *J. Geol.* 102, 165–180.

Aydin, A., Schultz, A., 1990. Effect of mechanical interaction on the development of strike-slip faults within echelon patterns. *J. Struct. Geol.,* 12, 123–129.

Cartwright, J.A., Trudgill, B.D., Mansfield, C.S., 1995. Fault growth by segment linkage: an explanation for scatter in maximum displacement and trace length data from the Canyonlands Grabens of SE Utah. *J. Struct. Geol.,* 17, 1319–1326.

Childs, C., Watterson, J., Walsh, J.J., 1995. Fault overlap zones within developing normal fault systems. *J. Geol. Soc., London*, vol. 152, 535-549.

Cladouhos, T.T., Marrett, R., 1996. Are fault growth and linkage models consistent with power-law distributions of fault lengths? *J. Struct. Geol.,* 18, 281-293.

Clarke, P.J., and 13 others, 1998. Crustal strain in central Greece from repeated GPS measurements in the interval 1989–1997. *Geophys. J. Int.*, 135, p. 195–214, doi: 10.1046/j.1365-246X.1998.00633.x.

Cowie, P.A., Scholz, C.H., 1992. Growth of faults by accumulation of seismic slip. *J. Geophys. Res.,* 10, 11085-11095.

Cowie, P.A., Roberts, G.P., 2001. Constraining slip rates and spacings for active normal faults. *J. Struct. Geol.,* 23, 1901–1915.

Cowie, P.A., Sornette, D., Vanneste, C., 1995. Multifractal scaling properties of growing fault population. *Geophys. J. Int.* 122, 457–469.

Dawers, N.H., Anders, M.H., Scholz, C.H., 1993. Growth of normal faults: displacement–length scaling. *Geology* 21, 1107–1110.

Dawers, N.H., Anders, M.H., 1995. Displacement–length scaling and fault linkage. *J. Struct. Geol.,* 17, 607–614.

Doutsos, T., Poulimenos, G., 1992. Geometry and kinematics of active faults and their seismotectonic significance in the western Corinth-Patras rift (Greece). *J. Struct. Geol.,* 14, 689-699.

Doutsos, T., Kokkalas S. 2001. Stress and deformation in the Aegean region. *J. Struct. Geol.,* 23, 455-472.

Ganas, A., Roberts, G., Memou, P., 1998. Segment boundaries, the 1894 ruptures and strain patterns along the Atalanti fault, central Greece. *J. Geodyn*., 26, 461-486.

Gillespie, P.A., Walsh, J.J., Watterson, J., 1992. Limitations of dimension and displacement data from single faults and the consequences for data analysis and interpretation. *J. Struct. Geol*. 14, 1157–1172.

Gudmundsson, A., 1992. Formation and growth of normal faults at the divergent plate boundary in Iceland. *Terra Nova* 4, 464–471.

Gupta, A., Scholz, C., 2000. A model of normal fault interaction based on observations and theory. *J. Struct. Geol.,* 22, 865–879.

Hollenstein, C., Muller, M.D., Geiger, A., and Kahle, H.-G.,2008. Crustal motion and deformation in Greece from a decade of GPS measurements, 1993–2003. *Tectonophysics*, 449, 17–40, doi: 10.1016/j.tecto .2007.12.006

Jones, R.R., Kokkalas, S., McCaffrey, K.J.W., 2009. Quantitative analysis and visualization of nonplanar fault surfaces using terrestrial laser scanning (LIDAR)-The Arkitsa fault, central Greece, as a case study. *Geosphere*, 5, 465-482; doi: 10.1130/GES00216.1

Kim, Y.-S., Sanderson, D.J., 2005. The relationship between displacement and length of faults: a review. *Earth Sci. Rev*. 68, 317–334.

Kokkalas, S., Jones, R.R., McCaffrey, K.J.W., Clegg, P., 2007. Quantitative fault analysis at Arkitsa, Central Greece, using terrestrial laser-scanning ("LiDAR"). *Bull. Geol. Soc. Greece,* XXXVII, 1959-1972.

Kokkalas, S., Xypolias, P., Koukouvelas, I., and Doutsos, T. 2006. Postcollisional contractional and extensional deformation in the Aegean region, *in* Dilek, Y., and Pavlides, S., eds., Post-collisional tectonics and magmatism in the Mediterranean region and Asia: *Geol. Soc. Am. Special Paper 409*, 97–123, doi: 10.1130/2006.2409(06)

Koukouvelas, I.K., Asimakopoulos, M., Doutsos, T., 1999. Fractal characteristics of active normal faults: an example of the eastern Gulf of Corinth, Greece. *Tectonophysics*, 308, 263–274.

Larsen, P.H., 1988. Relay structures in a Lower Permian basement involved extension system. East Greenland. *J. Struct. Geol.,* 10, 3-8.

Mansfield, C., Cartwrigth, J., 2001. Fault growth by linkage: observations and implications from analogue models. *J. Struct. Geol*. 23, 745–763.

Marrett, R.A., Allmedinger, R.W., 1991. Estimates of strain due to brittle faulting: sampling of fault populations, Kinematic analysis of fault-slip data. *J. Struct. Geol.,* 13, 735-738.

Marrett, R., Allmendinger, R.W., 1992. Amount of extension on 'small' faults: an example from the Viking graben. *Geology,* 20, 47–50.

Pantosti, D., De Martini, P.M., Papanastassiou, D., Lemeille, F., Palyvos, N., and Stavrakakis, G., 2004. Paleoseismological Trenching across the Atalanti Fault (Central Greece): Evidence for the Ancestors of the 1894 Earthquake during the Middle Age and Roman Times. *Bull. Seism. Soc. America*, 94, 2, 531-549.

Pavlides, S.B. and Caputo, R., 2004. Magnitude versus fault's surface parameters: quantitative relationships from the Aegean Region. *Tectonophysics*, 380, 3-4, 159-188.

Pavlides S.B., Valkaniotis S., Ganas A., Keramydas D. and Sboras S. 2004 The Atalanti active fault: reevaluation using new heological data. Bull. Geol. Soc. Greece. XXXVI, *Proceedings of the 10th International Congress*, Thessaloniki, 1560-1567.

Peacock, D.C.P., Sanderson, D.J., 1991. Displacements, segment linkage and relay ramps in normal fault zones. *J. Struct. Geol.,* 13, 721-733.

Peacock, D.C.P., Sanderson, D.J., 1996. Effects of propagation rate on displacement variations along faults. *J. Struct. Geol.,* 18, 311-320.

Pickering, G., Bull, J.M., Sanderson, D.J., 1995. Sampling power law distributions. *Tectonophysics* 248, 1-20.

Poulimenos, G., 2000. Scaling properties of normal fault populations in the western Corinth Graben, Greece: implications for fault growth in large strain settings. *J. Struct. Geol.* 22, 307–322.

Roberts, S., and Jackson, J., 1991. Active normal faults in central Greece: An overview, *in* Holdsworth, R.E., and Turner, J.P., compilers, Extensional tectonics: Faulting and related processes: Key Issues in Earth Sciences, Volume 2: London. *Geol. Soc. London*, 151–168.

Scholz, C.H., Dawers, N.H., Yu, J.Z., Anders, M.H., Cowie, P.A., 1993. Fault growth and fault scaling laws: preliminary results. *J.Geophys. Res.*, 98, 21951–21961.

Segall, P., Pollard, D.D., 1980. Mechanics of discontinuous faults. *J.Geophys. Res.*, 85, No B8, 4337-4350.

Soliva, R., Benedicto, A., 2004. A linkage criterion for segmented normal fa*ults. J. Struct. Geol.*, 26, 2251-2267.

Stiros, S.C., Arnold, M., Pirazzoli, P.A., Laborel, J., Laborel, F., and Papageorgiou, S., 1992. Historical coseismic uplift on Euboea Island, Greece. *Earth Plan. Sci. Lett.*, 108, 109–117, doi: 10.1016/0012-821X(92)90063-2

Trudgill, B., Cartwright, J., 1994. Relay-ramp forms and normal ault linkages, Canyonlands national Park, Utah. *Geol. Soc. Am. Bull.*, 106, 1143-1157.

Vermilye, J.M., Scholz, C.H., 1995. Relation between vein length and aperture. *J. Struct. Geol.* 17, 423–434

Walsh, J.J., Watterson, J., 1991. Geometric and kinematic coherence and scale effects in normal fault systems. *Geol. Soc., London, Special Publications*, 56, 193-203.

Walsh, J.J., Nicol, A., Childs, C., 2002. An alternative model for the growth of faults. *J. Struct. Geol.* 24, 1669–1675.

Walsh, J.J., Bailey, W.R., Childs, C., Nicol, A., Bonson, C.G., 2003. Formation of segmented normal faults: a 3-D perspective. *J. Struct. Geol.*, 25, 1251-1262.

Watterson, J., 1986. Fault dimensions, displacements and growth. *Pure Appl.Geophys.* 124, 365–373.

Wells, D.L. and Coppersmith, K.J., 1994. New empirical relationships among magnitude, rupture length, rupture width, rupture area and surface displacement. *Bull. Seism. Soc. America*, 84, 974-1002.

Willemse, E.J.M., 1997. Segmented normal faults: Correspondence between three-dimensional mechanical models and field data. *J. Geophys. Res.*, 102 (B1), 675-692.

Wojtal, S.F., 1996. Changes in fault displacement populations correlated to linkage between faults. *J. Struct. Geol.* 18, 265–279.

Wu, H., Pollard, D.D., 1995. An experimental study of the relationship between joint spacing and layer thickness. *J. Struct. Geol.,* 17, 887-905.

Xu, S.-S., Nieto-Samaniego, A.F., Alaniz-Alvarez, S.A., Velasquillo-Martinez, L.G., 2006. Effect of sampling and linkage on fault length and length–displacement relationship. *Int. J. Earth Sci.* 95, 841–853.

Yielding, G., Walsh, J.J., Watterson, J., 1992. The prediction of small-scale faulting in reservoirs. *First Break* 10, 449-460.

Δελτίο της Ελληνικής Γεωλογικής Εταιρίας, 2010
Πρακτικά 12ου Διεθνούς Συνεδρίου
Πάτρα, Μάιος 2010

Bulletin of the Geological Society of Greece, 2010
Proceedings of the 12th International Congress
Patras, May, 2010

KASTORIA "BLIND" ACTIVE FAULT: HAZARDOUS SEISMOGENIC FAULT OF THE NW GREECE

Ch. P. Metaxas[1], N. S. Lalechos[2] and S. N. Lalechos[1]

[1] *Earthquake Planning and Protection Organization, Xanthou 32, Neo Psykhiko, 15451, Athens, xmetaxas@oasp.gr, slalexos@oasp.gr*

[2] *Former CEO of Public Petroleum Corporation of Greece (DEP – EKY)*

Abstract

The Aliakmon river bed, as well as a series of certain parallel narrow grabens, striking NW-SE are filled with Neogene-Quaternary deposits; thus showing the existence of the covered, "blind", fault zone, which borders the Eastern edge of Meso-Hellenic Trench and passes in close vicinity to the Kastoria town. Distribution of earthquakes epicentres (M≥4.0, for the period of 1930-2009) along this segmented rupture zone, proves the existence at depth of an active seismogenic fault which has generated some strong earthquakes in the past: 1709, M = 6.0; 1812, M = 6.5 and 1894, M = 6.1 (~ 100-year Recurrence Time events). The calculations of Lapsed Rate characterizing the stage of the fault seismic cycle (LR = 115%) show that the active Kastoria fault could be in a pre-seismic stage of its seismic cycle. Applying the seismicity rates model (time-independent Gutenberg-Richter recurrence model) and using the fault seismicity parameters, obtained inside the fault influence zone, as input in EZ-FRISK® software, the Probabilistic Seismic Hazard Analysis has been carried out for the area of Kastoria town. The results show that calculated magnitude for event with 100-year recurrence time is ~6.1, which correspond to the magnitude of three events, occurred at the fault during the last 300 years (corresponding average slip rate . 3 mm/year). As the calculated Hazard Curve shows, the event of that range could give ground shaking in the Kastoria town in the order of 0.625 g at the spectral period of 0.3 sec.

Key words: *seismicity, "blind" seismogenic fault, seismic cycle, Probabilistic Seismic Hazard Analysis, ground shaking, Kastoria town, NW Greece.*

1. Introduction

Vulnerability to earthquakes increases steadily as urbanization and development expand in areas that are prone to significant earthquakes. As the largest earthquakes of the past three decades have demonstrated, the development of large cities in high seismicity areas is often based on an insufficient knowledge of the local seismic hazard, a condition often deteriorated by the construction of seismically unsafe buildings and infrastructures (Boschi et al, 1996).

A "blind fault" should mean a fault plane with its upper limit under the surface of the earth. Blind faulting often induces intense damage owing to unexpected strong shaking. Such blind faults may be accompanied by distributed deformation, the amplitude of which is controlled by the width and the depth of the upper fault limit as well as the amount of the slip on the blind fault plane. Issues on geologically unexpected large earthquakes, wrong long-term forecasts and unknowable earthquakes

are usually related to blind faults.

Papazachos & Papazachou (2003) show the seismogenic fault associated with three historical strong surface earthquakes (1709, M = 6.0; 1812, M = 6.5 and 1894, M = 6.1) in close vicinity to the Kastoria town. No evidence of the surface traces of the fault has been mapped to date along the virtual projection of the fault line at the surface, neither as a result of instant (co-seismic) movements, nor as a result of long-time slip (aseismic creep) on the fault.

The objective of this paper is to define the location of the "blind" active seismogenic fault, to determine its tectonic and seismic activity characteristics as well as the present level of its hazard: seismicity potential, stage of seismic cycle, strong (M>6.0) earthquakes recurrence times and probable values of ground shaking that could be measured in Kastoria town (at the site of Kastoria Strong Motion Station of ITSAK, KAS1, 40.52N, 21.26E) in the case of seismic excitation on above mentioned "blind" active fault.

2. Geological setting

The Meso-Hellenic Trench constitutes a tertiary molassic graben, which has been individualized from middle Eocene. After the major tectonic phase (lower-middle Eocene) of the Pelagonian zone, which is overthrusting the Pindos zone, we observe a transgression in the upper Lutetian within the Pelagonian zone during its fracturing starting from Pindos zone where the sedimentation continues until the upper Eocene (Bizon et al., 1968). The graben formation continues during Oligocene (transgressive and discordant following tectonic movements) with tilting of the basin causing eastward transgressions (Heptakhorio series). Miocene appears to be transgressive on the boundaries of the basin (Pentalofo and Tsotyli series). Generally, the sedimentation is determined by a dissymmetric subsidence of the basin, resulting to tilting phenomena (I.F.P., 1966). The subsidence during Tertiary seems to be discontinuous with alternation of tectonic movements and erosion phases.

Two geodynamic models have been proposed in order to understand the paleogeographic and tectonic evolution of the Meso-Hellenic Trench; it is interpreted either as a back-arc basin (Papanikolaou et al, 1988) or as a piggy-back basin along the eastern flanks of a giant pop-up structure consisting of west-verging, foreland-propagating thrusts within the Apulian plate and of east-verging backthrusts within the Pelagonian plate (Doutsos et al, 1994).

The tectonics of Meso-Hellenic Trench is characterised by two longitudinal deep boundary faults (Fig. 1a) affecting the bedrock (i.e. the Pelagonian and Pindos zone). The fault limiting the NE boundary of the basin seems to increase its activity from Pliocene to date. Thus, Pliocene formations and Quaternary deposits are mainly outcropping along the NE boundary of the basin. In particular, the most recent movements of this normal fault seem to be intensive due to the fact that the western branch of Aliakmon river and all its downstream tributaries are flowing in the SW-NE direction, whereas the main river is thereafter flowing along the NE boundary of the basin, thus covering -with its deposits- the aforementioned fault and making it "blind". In more detail, the NE boundary is not constituted by a single normal fault, but by a series of successive narrow grabens (about 1-2 km wide) developed below the Aliakmon riverbed (Fig. 1b).

The area has been subjected to many deformational events during Alpine times, under both extensional and compressional regimes that reshaped the original structures and changed their relationships until Miocene. Since then, two main neotectonic extensional stages have occurred (Mercier et al., 1993; Mountrakis et al., 1995a); i) a NE-SW extension during upper Miocene - Pliocene that reactivated NW-SE mainly trending normal faults and ii) a NNW-SSE extension during Quaternary

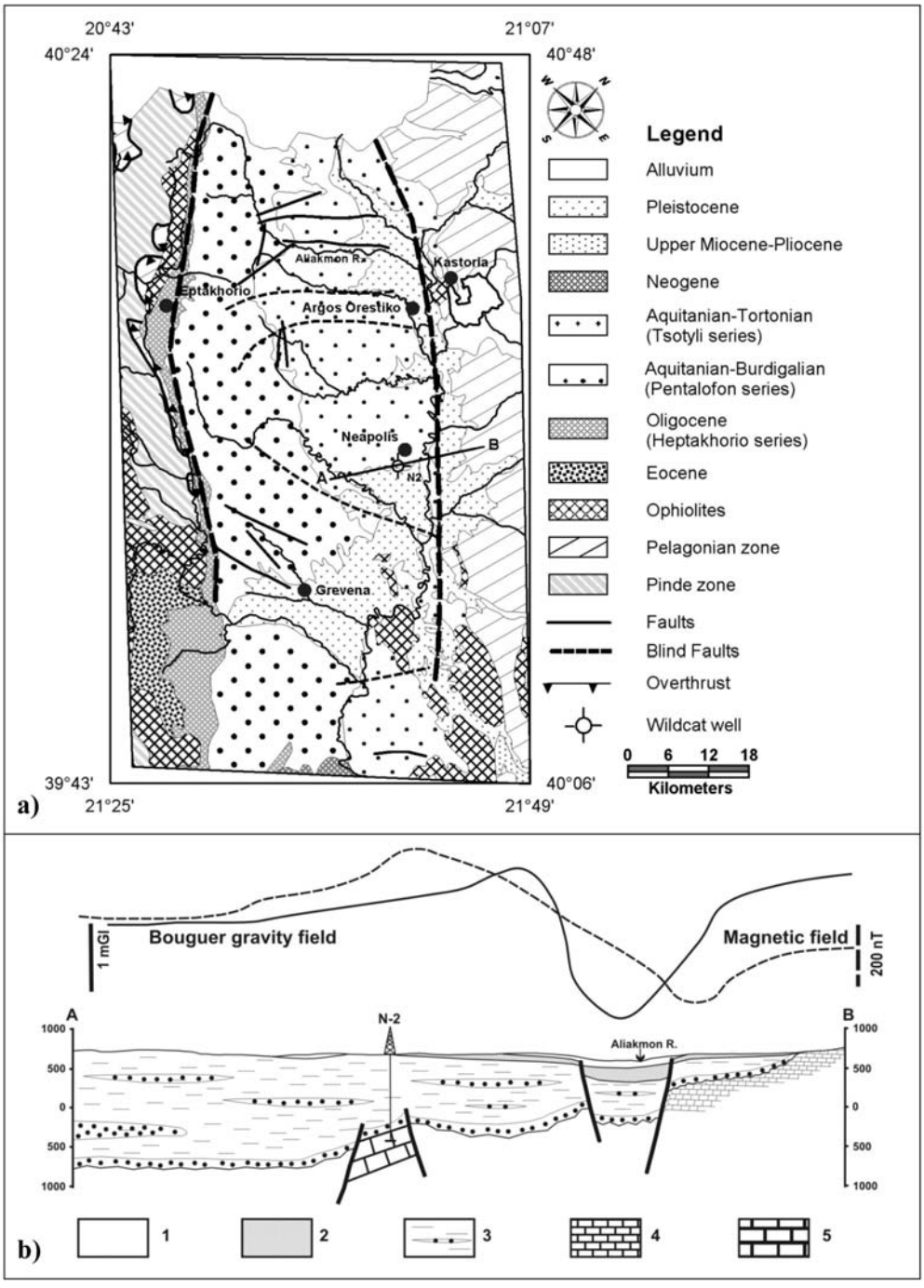

Fig. 1: (a) Map of the Meso-Hellenic Trench (modified after Geological Map of Greece, scale 1/500,000, IGME, 1983). (b) Geological section across the NE boundary; 1: Pleistocene, 2: Pliocene, 3: Marls & conglomerates (Tsotyli series), 4: Pelagonian zone, 5: Pindos zone.

that reactivated NE-SW to E-W trending normal faults, including the fault responsible for the 1995 Kozani-Grevena (M = 6.5) devastating earthquake.

In terms of stress, the activation of the Kastoria fault trending NW-SE appears to be inconsistent with the Mid-Late Pleistocene kinematics of the broader area as well as with the slip-vector of the Grevena seismic fault as shown by the focal mechanism of the 1995 earthquake (Papazachos et al., 1995). Yet, the pitch of the slip-vector on a given fault plane depends not only on the orientation of the principal stress axes but also on a ratio R built on the differences of the principal stress values, such as R = ($\sigma 2-\sigma 1/\sigma 3-\sigma 1$). In an extensional tectonic regime, the azimuth of the slip-vector indicates the direction of extension only if the deviatoric stress $\sigma 2$ value is zero (i.e. R = 0.5). It deviates from the extensional direction when the deviatoric stress $\sigma 2$ value is highly compressional (R<0.5) or extensional (R>0.5) (Mercier & Lalechos, 1993). Thus, the dip-slip kinematics of the Kastoria fault with R>0.5 is compatible with the existing stress field of the area.

3. Seismicity characteristics of the Kastoria fault

Analysis performed in the current study is based on the following recent catalogues: Papazachos et al., 2000 & Papazachos et al., 2009 (completeness 1981-2009 M≥4.0); Papanastasiou et al., 2001 (completeness ≥4.5 for the period 1950-2000); the current catalogue of IG-NOA for the period 1964-2009 (completeness M≥3.5) available on the site www.gein.noa.gr. Joint catalog was constructed for the under study area 39.95N/20.40E - 40.95N/22.00E; all the magnitudes in this catalogue were set equivalent to moment magnitude M_W, in the magnitude range 4.0≤M<8.0.

3.1 Seismic activity

As was mentioned above, three strong earthquakes, occurred in the past at distances than 30 km from Kastoria town (1709, M = 6.0; 1812, M = 6.5 and 1894, M = 6.1), could be related to the same seismogenic fault. Focal mechanism for this fault indicate normal motion on a northwest striking plane: strike -160^{0}N, dip -49^{0}W, rake = -87^0 (Papazachos and Papazachou, 2003).

Distribution of earthquake epicentres in the under study region, shown on Figure 2a (M≥4.0, for the period of 1930-2009), defines some clusters of various shapes. Concentration of earthquakes at the NW corner of the area is apparently associated with the source of Konitsa earthquakes (1996, M = 5.2, 5.3 and 5.5). To the north, in Albania, a prominent concentration of epicentres is forming a N-S seismogenic fault, the source of 1919 earthquake (M = 6.3). Clusters observed at the NW corner appear to be associated with the N-S striking active faults (Aliaj & Dushi, 2007). Relatively sparse, but, in some cases, linear distribution of epicentres, at the NE corner of the study region is forming the borders of Florina Basin, probably controlled by NW-SE active faults, as well as the location of some active faults of NE-SW direction (Mountrakis et al., 1995b). Most of the earthquakes observed at the SE part of the region, define a dense NE directed cluster that represents the 1995 Kozani-Grevena seismic excitation on the trending SW-NE Rimniou-Sarakinas fault zone (main shock M = 6.5).

An area of concentrated seismicity in the centre of Figure 2a, which corresponds with the Greek part of Meso-Hellenic Trench (MHT), shows the relatively high density of epicentres to gravitate towards the NE border of MHT. The Albanian part of MHT, to which the 1960 earthquake source (M = 6.3) is apparently attributed, has exhibited the highest concentration of epicentres in comparison to the Greek part. Moreover, the NE trending aseismic belt can be distinguished along the Greek-Albanian border, which separates the Albanian and Greek clusters of epicentres: no earthquakes have been recorded inside this, about 9-12 km width zone, across the MHT. This picture of

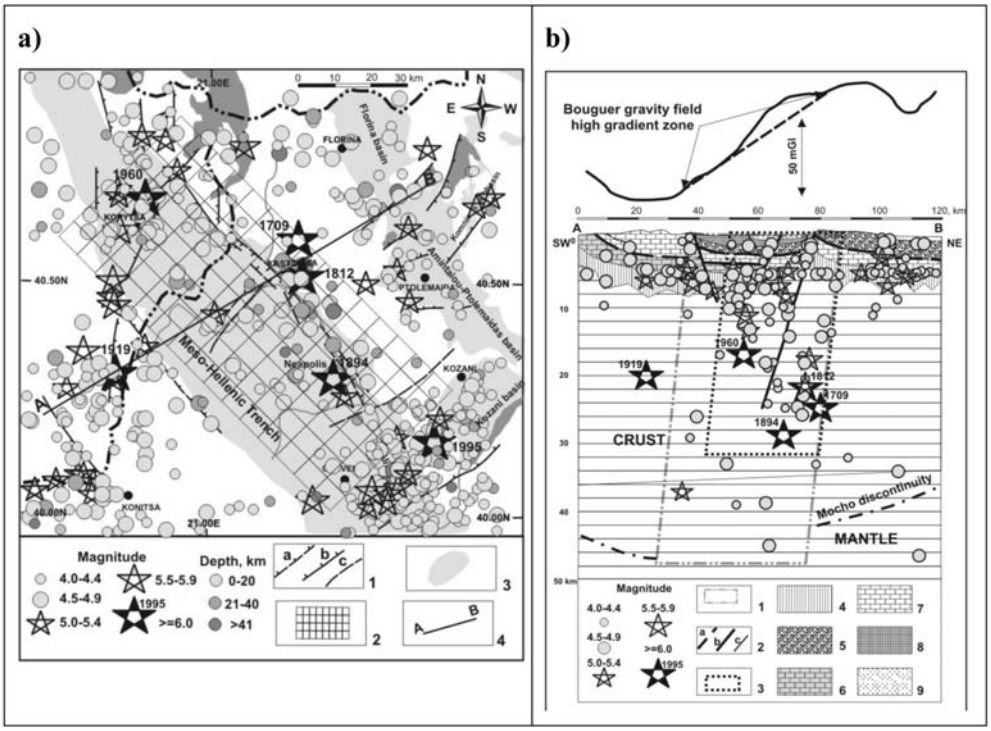

Fig. 2: (a) Distribution of earthquake epicentres vs active faults pattern in NW Greece (West Macedonia). 1: Active faults according to Mountrakis et al. (1995b) and Aliaj & Dushi (2007); 2: Matrix used for epicentre density calculations; 3: Post-alpine basins; 4: Location of profile shown in fig. 2b. (b) Schematic geological-geophysical profile across the Meso-Hellenic Trench. 1: Contours of probable deep-seated crust-mantle structure; 2: Elements of rupture structure: a - nappes; active normal faults: b - main, bordering the MHT, c-secondary; 3: Kastoria fault influence zone according to fault dip, penetration at depth and foci distribution; 4: Pre-alpine basement, 5: Pelagonian zone, 6: Gavrovo zone, 7: Pindos zone; Molassic fill of basins - 8: Mio-Pliocene, 9: Quaternary.

the epicentres distribution along the NE border of the MHT suggests: a) the existence of an active northwest trending seismogenic rupture zone, which is responsible for the seismicity of this area; b) segmentation of this rupture zone into Albanian and Greek segments with length of about 30 and 60 km respectively. The NW elongated belt of epicentres is also forming the SW border of MHT, as in Albania and in Greece, and probably proves that the rupture zone controlling the SW border of MHT is a seismogenic structure.

Analysis of the foci distribution along the schematic geological-geophysical cross-section (Fig 2b) shows that seismicity is involving all the crust, to a depth of approximately 40 km. In the central part of the cross-section related to MHT, earthquakes occur at depths between 1 and 45 km and appear to define a steeply dipping crust-mantle structure beneath the MHT. In the gravity curve (Fig. 2b) this structure is characterized by width zone of Bouguer field high gradient, as it is characteristic for that kind of deep-seated structures (Khesin et al., 1982). To NE and to SW of MHT, the thickness of seismogenic layer does not depasse 12 km. Generally, we observe that outside of MHT zone, the foci are mostly concentrated on faults that border the recent basins, as well as along some crustal discontinuities, as Figure 2b displays.

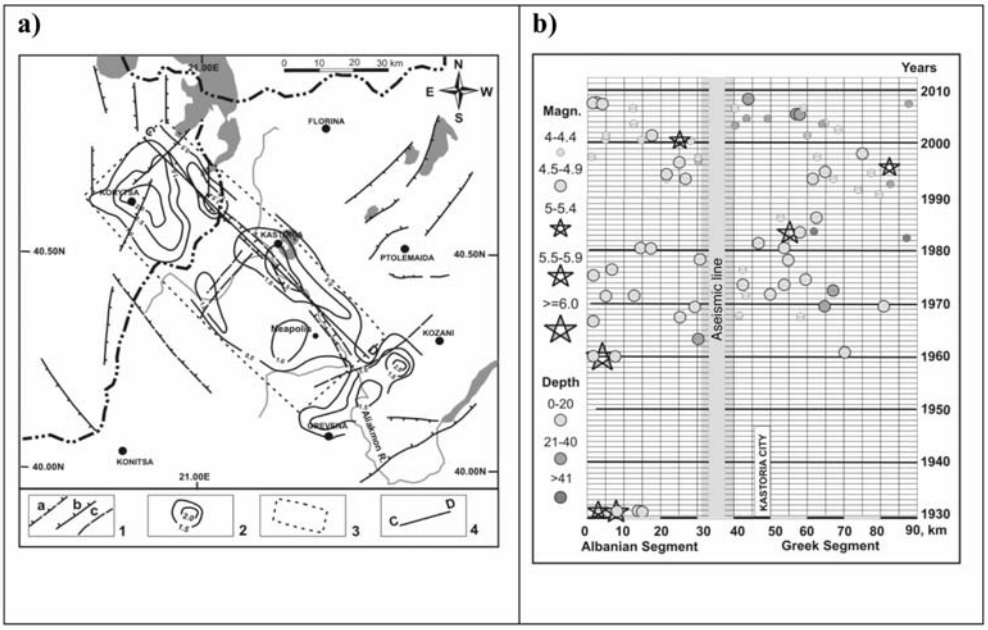

Fig. 3: (a) Density of earthquake epicentres along the Kastoria fault. 1: Active faults according to Mountrakis et al. (1995b) and Aliaj & Dushi (2007); normal faults (barbs towards the subsided block): a- probable, b- mapped, c – faults with undetermined kinematics. 2: Contours of epicentre density, 3: Kastoria fault influence zone, 4: Location of NW-SE profile shown in Fig. 3b.

3.2 Fault Influence Zone

For quantification of the fault recurrence model, we attempted to define earthquake clusters appearing to belong to the Kastoria fault at the NE border of MHT from those corresponding to the surrounding structures. To evaluate the seismic activity along the fault objectively and quantitatively, a simple method has been proposed by Watanabe et al (2006). For each surface fault trace - in our case the area of probable "blind" fault trace - narrow zones Zi are made on the surface, dividing the distance from the fault trace in fixed intervals (i.e. in km). For each Zi, the number of epicentres Ni is counted. Then, the density of earthquake number DNi, can be expressed as DNi = Ni/(Si*P), where Si is the area of zone Zi, and P is the time interval of analysis. DNi generally decreases with the distance from the fault. Thus, the distance where DNi reaches the background level is defined as the fault influence distance FID and the area countered by FIDs can be defined as Fault Influence Zone (FIZ). Because of the lack of evidences about the Kastoria fault surface trace, the grid used in the current study is represented by covering the MHT, NW oriented matrix, of ~50 km*100 km dimension, with similarly elongated narrow cells of size ~6 km * 7 km. For more understandable presentation, the DNi value was calculated as:

DNi = Ni/(Si*P)*100%.

For background level the value 0.5 has been chosen, which means one epicentre inside the cell. The result displayed in the Figure 3a, shows more clearly the faults length and the segmentation of the seismogenic rupture zone along the NE board of MHT; it also allows the contouring of the Fault Influence Zone at surface. The geometry of FIZ defined by seismicity data is in good agreement with the

geometric parameters of FIZ, which were determined, using the fault geometry characteristics, such as fault orientation, length, probable dip angle, penetration at depth (as it can be also seen on Fig. 2b).

It has to be noted that the whole set of epicentres located in the area where the 1995 Kozani earthquake occurred, has not been taken into consideration in the assessment of Kastoria fault seismicity rates.

3.3 Seismic cycle of the fault

The seismic activity cycle along an active fault can be classified in 4 stages, namely the main shock stage, the aftershock stage, the calm stage and the pre-seismic stage (Mogi, 1985). Period of observations for modern seismology is about one hundred years, and it is only a small portion of a cycle that is as long as hundreds to thousands of years. Therefore, it is difficult to recognize the portion of the seismicity cycle corresponding to the current seismic activity. Since there are large variations of recurrence times for each active fault, the concept of Lapsed Rate has been introduced (Itaba and Watanabe, 2005). To assess the Lapsed Rate of an active fault, we have to know Lapsed Time (LT), which is the time interval from the latest major earthquake, occurred on the fault as well as the Recurrence Time (RT), which is the mean recurrence interval of strong events (or events with particular magnitude of interest) for the fault. Therefore, LR is defined from RT and LT of a fault as:

LR = (LT/RT) * 100 [%]

Considering the study of the Kastoria fault (Greek segment) the LR values have been determined for $M \geq 6.0$ earthquakes occurred since 1709; there are 3 events in about 300 years, i.e. 100-year RT events with magnitude M = 6.0-6.5. The calculation performed shows LR = 115%, which allows us to assume that the active Kastoria fault could be in a preparatory stage (pre-seismic according to Mogi, 1985) of the fault seismic cycle.

The space-time distribution of the earthquakes along the Kastoria fault zone (Fig. 3b) displays the fault recent seismic activity. On the Greek segment three periods of activation may be observed. The first occurred the 70's - 80's (17 events with M = 4.2-4.6). The second in the 90's (16 events with M = 4.0-4.7), appears to be the consequence of the 1995 Kozani earthquake (M = 6.5); it was closed with an M = 5.0 event. The third period which has started in 2002 mostly with events at depth >20km is still in progress (to date there are 13 events with magnitude M = 4.0-4.7). It is notable, that each time, during the seismic excitations, the activity has been concentrated at different halves of the Greek segment of the Kastoria fault: during the first period at the NW part of the segment; during the second period at the SE part of the segment and during the period of the last 7 years at the NW part of the segment again (Fig. 3b). The Albanian segment behaves almost in the same way as the Greek one. It is apparently characteristic for solitary fault zones: activation in 90's with main event M = 5.0 in 2001, framed by foreshock and aftershock sequences at the SE part of the segment, then continuous in the 2000's at the NW part of the Albanian segment.

According to Toda, 2002 (in Itaba & Watanabe), the following tendency has been found from the sequences of recent micro and moderate sized earthquake activity on a fault: "When the lapsed time from the most recent event is close to or larger than the recurrence time, seismic activity is comparatively or locally high". Concerning the M~6.0-6.2 event with ~100-year recurrence time (the worst scenario), today's seismic activity of the Greek segment of the Kastoria fault looks to be consistent with the pre-seismic activation stage of the fault.

4. Probabilistic Seismic Hazard Assessment (PSHA)

Analysis of Seismic Hazard that can be due to the Kastoria fault is based on probabilistic concepts,

Table 1.

	Length, km		Dip	M max	Mmin	Seismicity rate, ≥ Mmin	b
	Sur-face	Subsurface					
Kastoria Normal Fault, Greek segment	?	60	~60ºSW	7.0	4.0	2.05	1.08

which allow incorporation of both geological and seismological data. The Cornell-McGuire method (Cornell, 1968; McGuire, 1995, 2004) has proven particularly well suited to calculate expected ground motions for a wide range of seismotectonic environments. The methodology has been realised in EZ-FRISK PC Programme (Risk Engineering, 2005).

4.1 PSHA methodology

Calculation of hazard requires specification of three inputs in EZ F-RISK programme: a) Source geometry, which is the geographic description of the seismic sources. b) Seismicity, which is the rate of earthquake occurrence in particular seismic source and c) Attenuation Equations, which are the relationships that allow the appraisal of ground motion parameters at the site as a function of earthquake magnitude, source-to-site distance and soil conditions at the site.

A seismic source, in our case, is a tectonic fault. Geometry and seismicity parameters of the Kastoria fault, as input for PSH calculations, are shown on the Table 1. Seismic potential of the fault (Mmax) was assessed using Wells and Coppersmith (1994) functions.

The time-independent recurrence model for the Kastoria fault source is based on the observed frequency of occurrence of instrumental seismicity within the above defined Fault Influence Zone. For ground motion parameter calculations, the attenuation equation proposed by Ambraseys et al (1996) for rock conditions was used.

4.2 Results of PSH calculations

The calculations of Kastoria fault activity rates show, that magnitude of event with about 100-year recurrence time, derived using seismicity parameters of the fault, is about 6.1, which is in agreement with the magnitudes of the three events occurred at the fault during the last 300 years (Fig. 4a).

Total Seismic Hazard Curve, a plot of annual probability of exceedance versus a specified ground motion parameter, displaying the 5% damped values of spectral acceleration (Sa) for spectral period T = 0.3 sec, for horizontal component of motion on bedrock, is shown on Figure 4b.

5. Conclusions

The mapping of the Kastoria "blind" fault at the NE border of Meso-Hellenic Trench was performed by using geological data as well as the results of geophysical and seismological observations. The location of the fault zone was defined by the distribution of NW-SE elongated Quaternary basins developed along the bed of Aliakmon River. The existence of such narrow basins below the Aliakmon riverbed is proven by the gravity and magnetic data collected by the Institut Français du Pétrole (1966). The correspondence of elongated gravity minima with elongated in the same direction mag-

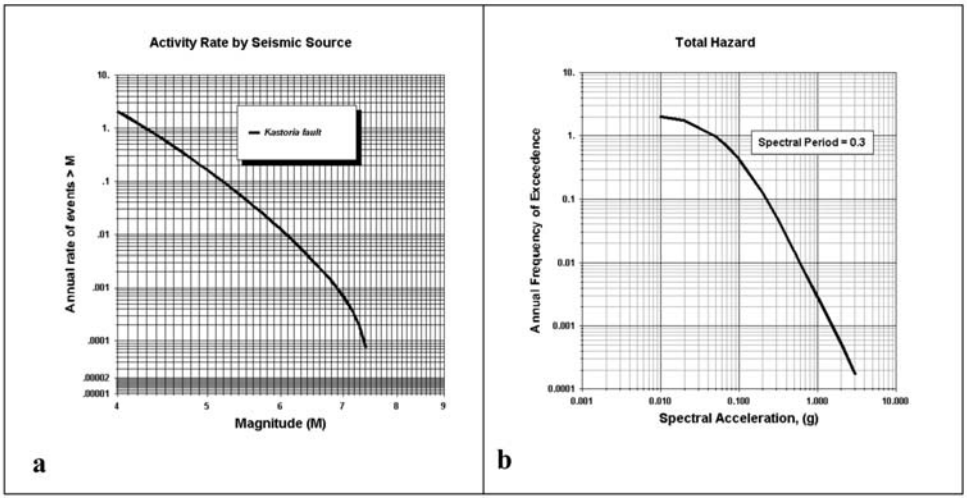

Fig. 4: (a): Activity rates of the Kastoria fault and (b): Total Hazard Curve calculated for bedrock conditions from fault source "Kastoria Fault" at the site "Kastoria town" (Kastoria Strong Motion Station of ITSAK, KAS1, 40.52N, 21.26E, limestone, dolomite limestone).

netic maxima shows the existence of narrow grabens (1-2 km width) filled with Neogene - Quaternary deposits that are characterised by relatively increased magnetic susceptibility (see Table 1 in Metaxas et al, 2001), attributed to effects of ophiolite erosion materials involved in the sedimentation.

The picture of the earthquake epicentre distribution in the area of MHT and particularly along its NE border, proves the existence of an active northwest trending seismogenic rupture zone segmented into two segments (Albanian and Greek) with length of about 30 and 60 km respectively, that are separated by NE trending, 9-12 km wide aseismic belt along the Greek-Albanian border.

The Lapsed Rate of the Kastoria fault Greek segment, calculated for three $M \geq 6.0$ earthquakes occurred since 1709 (100-year Recurrence Time events), shows value of 115%, which allows us to assume that the active Kastoria fault could be in a preparatory stage of the fault seismic cycle.

The result of PSHA shows that the calculated magnitude for event with 100-year recurrence time is ~6.1, which corresponds to the magnitudes of three events, occurred at the fault during the last 300 years. According to Slemmons & dePolo (1986) empirical diagram, the active fault, that gives event of magnitude ~6.1 with recurrence time ~100 years, is characterised by a slip rate of 3 mm/yr. This value corresponds to that of the vertical movements which are shown by the thicknesses of the Holocene deposits (30 - 40 m. for the last 10,000 years) along the Greek segment of the blind Kastoria fault.

As the calculated Hazard Curve is showing, the event of that range could give ground shaking in the Kastoria town of the order of 0.625 g at the spectral period of 0.3 sec.

6. References

Aliaj, S., & Dushi, E., 2007. Seismogenic Models for Albania: Overview of Relevant Data. First Workshop for the NATO Science for Peace, Project No 983054: "Harmonization of Seismic Hazard Maps for the Western Balkan Countries". Ljubliana, Slovenia, 9 November 2007 (Presentation).

Ambraseys, N.N., Simpson, K.A., and Bommer, J.J., 1996. "Prediction of Horizontal Response Spectra

in Europe*", Earthquake Engineering and Structural Dynamics*, Vol.25, p. 371-400.

Bizon, G., Bizon, J.-J., Lalechos, N., Savoyat, E., 1968. Présence d'Éocène transgressif en Thessalie. Incidences sur la paléogéographie régionale. *Bull. Soc. Géol. de France* (7), X, p. 36-38

Boschi, E., Giardini, D., Pantosti, D., Valensise, G., Arrowsmith, R., Basham, P., Burgmann, R., Crone, A., Hull, A., McGuire, R., Schwarts, D., Sieh, K., Ward, S., and Yeats, R., 1996. New trends in active faulting studies for seismic hazard assessment. *ANNALI DI GEOFISICA,* XXXIX, 1301-1307.

Cornell, C.A., 1968. "Engineering seismic risk analysis", *Bull. Seism. Soc. Am.*, 58, 5, 1503-1606.

Doutsos, T., Koukouvelas, I., Zelilidis, A., Kontopoulos N., 1994. Intracontinental wedging and post-orogenic collapse in the Mesohellenic Trough. *Geologische Rundshau*, 83, 257-275.

Institut Français du Pétrole / Branche Recherche et Exploitation du Pétrole 1966. Etude des bassins de Grevena – Thessalie. Rapport pour le Ministère de l'Industrie, Direction Générale des Mines, Grèce.

Itaba, S., and Watanabe, K., 2005. Seismicity cycle and large earthquakes. Pp.4. On-line: http//www.ism.ac.jp/~ogata/Statsei4/abstr/Itaba. pdf

Itaba, S. and Watanabe, K. Seismic activity before and after a large earthquake in seismicity cycle. On line: http://www.rcep.dpri.kyoto-u.ac.jp/~itaba

Itaba, S., Watanabe, K., Nishida, R., Noguchi, T. Change of seismic activity in the cycle of a large earthquake. On-line: http://www.rcep.dpri.kyoto-u.ac.jp/~itaba

Khesin, B., Metaxas, Ch., Alexeev, V., 1982. About the geological nature of large-scale gravity anomaly Taliss-Vandam (On the problem of crustal model of 15 km super-deep well SG-1 in Azerbaijan). VINTI Publishers, No 3680-82, Moscow, 30 pp. (In Russian).

McGuire, R., 1995. Probabilistic seismic hazard analysis and design earthquakes closing the loop. *Bull. Seism. Soc. Am.,* 85, 5, 1275-1284.

McGuire, R., 2004. Seismic Hazard and Risk Analysis. EERI Monograph MNO-10. *Earthq. Eng. Res.* Inst., Oakland, Ca.

Mercier, J-L and Lalechos, S., 1993. The Middle-Late Pleistocene NW-SE extension in Southern Peloponnesus and the kinematics of the seismic fault of the 1986 Kalamata earthquake (Greece). *Proceedings of the 2nd Congress of the Hellenic Geophysical Union*, Florina, 5-7 May 1993, (Seismology), 586-594.

Mercier, J-L., Sorel, D., Lalechos, S., Keraudren B., 1993. The tectonic regimes along the convergent border of the Aegean arc from the late Miocene to the present; southern Peloponnesus as an example. *NATO advanced research workshop on Recent evolution and seismicity of the Mediterranean region*. Erice, Italy, Sept. 18-27, 1992 (In: Recent evolution and seismicity of the Mediterranean region, NATO ASI Series. Series C: Mathematical and Physical Sciences, 402, 141-160, 1993. Boschi-E (editor); Mantovani-E (editor); Morelli-A (editor).

Metaxas, C., Angelopoulos, A., Lalechos, S., Foundoulis, D., 2001. Deep tectonic structure of Northwestern Attica, Greece: Geodynamic Pattern of Athens Earthquake. Proceedings of the 9th International Congress, Athens, September 2001. *Bulletin of the Geol. Soc. of Greece,* XXXIV/1, 259-265.

Mogi, K., 1985. Earthquake Prediction. ACADEMIC PRESS. HBJ Publishers, 382.

Mountrakis, D., Pavlides, S., Zouros, N., Chatzipetros, A., Kostopoulos, D., 1995a. The 13 May 1995 western Macedonia (Greece) earthquake. Preliminary results on the seismic fault geometry and kinematics. *XV Congress of the Carpatho-Balkan Geological Association, September 17-20, 1995, Athens, Greece,* 11.

Mountrakis, D. et al., 1995b. Map of the active faults of Greece, Macedonia area, scale 1:300 000, Thessaloniki University.

Papanastassiou, D., Latoussakis, J., Stavrakakis, J., 2001. A Revised Catalogue of Earthquakes in the

Broader Area of Greece for the period 1950-2000. Proceed. of the 9th International Congress, Athens, September 2001. *Bulletin of the Geol. Soc. of Greece,* XXXIV/4, 1563-1566

Papazachos B.C, Panagiotopoulos, D.G, Scordilis, E.M, Karakaisis, G.F., Papaioannou, Ch.A., Karakostas, B.G., Papadimitriou, E.E., Kiratzi, A.A., Hatzidimitriou, P.M., Leventakis, G.N., Voidomatis, Ph.S., Peftitselis, K.J., Tsapanos, T.M., 1995. Focal properties of the 13 May 1995 large (Ms = 6.6) earthquake in the Kozani area (North Greece). *XV Congress of the Carpatho-Balkan Geological Association, September 17-20, 1995, Athens, Greece,* 13.

Papazachos B. and Papazachou, K., 2003. Earthquakes of Greece. ZITI Publishers,Thessaloniki, 2003, 286. (In Greek).

Papazachos, B.C., Comninakis, P.E., Karakaisis, G.F., Karakostas, B.G., Papaioannou, Ch.A., Papazachos, C.B. and Scordilis, E.M., 2000. A catalogue of earthquakes in Greece and surrounding area for the period 550BC-1999. *Publ. Geophys. Laboratory,* University of Thessaloniki, 1, 333.

Papazachos, B.C., Comninakis, P.E., Scordilis, E.M., Karakaisis, G.F. and Papazachos, C.B., 2009. A catalogue of earthquakes in the Mediterranean and surrounding area for the period 1901 - 2008. *Publ. Geophys. Laboratory*, University of Thessaloniki.

Papanikolaou, D.J., Lekkas, E.L., Mariolakos, I.D., Mirkou, R.M., 1988. Contribution to the geodynamic evolution of the Mesohellenic basin. *Bulletin of the Geol. Soc. of Greece,* XX, 17-36.

Risk Engineering, 2005. EZ-RISK, Software for In-depth Seismic Hazard Analysis. Version 7.01, 272.

Slemmons, D.B. and dePolo, C.M., 1986. Evaluation of active faulting and associated hazards: in Wallace, R.E. (ed.), Studies in Geophysics, Active Tectonics, National Academy Press, 266.

Vergély P., 1984. Tectonique des ophiolites dans les hellénides internes – Conséquences sur l'évolution des régions téthysiennes occidentales. Thèse, Université de Paris-Sud.

Watanabe, K., Itaba, S., Mori, J., Nishida, R., 2006. Quantitative evaluation of seismic activity around active faults and a general seismicity cycle of the fault. *AOGS* 2006, 794/1202

Wells, D., and Coppersmith, J., 1994. New Empirical Relationships among Magnitude, Rupture Length, Rupture Wight, Rupture Area, and Surface Displacement. *Bulletin of the Seismological Society of America*, 84, 974-1002.

Δελτίο της Ελληνικής Γεωλογικής Εταιρίας, 2010
Πρακτικά 12ου Διεθνούς Συνεδρίου
Πάτρα, Μάιος 2010

Bulletin of the Geological Society of Greece, 2010
Proceedings of the 12th International Congress
Patras, May, 2010

SEA LEVEL CHANGES ALONG THE COASTS OF KEA ISLAND AND PALEOGEOGRAPHICAL COASTAL RECONSTRUCTION OF ARCHAEOLOGICAL SITES

Mourtzas N.D.[1]

[1] *Geologist PhD, Gaiaergon Geotechnical Firm., Kefallinias 16-18, 15231 Athens, Greece, gaiaergon@gmail.com*

Abstract

Sea level changes during the Upper Holocene submerged the coasts of Kea in three different phases about 5.50m, 3.90m and 1.50m respectively below the contemporary sea level thus causing sea transgression along the shores of Kea, which varied from 8m to 78m depending on the coastal morphology.

These changes caused the alteration of the earlier morphology at coastal archaeological sites of the Island, as the prehistoric settlement of Ayia Irini and Classical period port of Karthaia, as well as, submerged under the sea areas of coastal human activity during antiquity, as the ancient schist quarry at Spathi bay.

The study of historical, geomorphological and sedimentological data indicative of previous sea levels allow the paleogeographical reconstruction of the coasts during the period of human activities in these areas.

Key words: *sea level change, Kea Island, paleogeographic reconstruction, ancient ports, submerged ancient settlements, ancient quarries.*

1. Introduction: geomorphological features and geological structure of Kea Island

The island of Kea, located at the western side of the Northern Cyclades island complex, has an area of 121km^2 and shores of total length of 86km (Fig. 1). The island's morphology is characterized by its intense topographic relief, which has an average gradient of 28%, while its complex drainage system seems to be the upper part of an older one, broader and today nonexistent; whose greater part now lies under the sea surface. The types of landforms encountered at the coastal zone are Rias with craggy shores which maintain the character of a previous cycle of ground erosion.

The geological formations of the island are part of the "Northern Cyclades" geotectonic unit (Papanikolaou 1986) and include triassic - jurassic limestone and a metamorphic complex of marble, gneiss and schist (Davi 1976).

The triassic - jurassic limestone, located at the northern edge of the island (Fig. 1), have a maximum of thickness 100-150m and they are found up-thrusted, possibly during Cretaceous, on top of the eroded surface of the metamorphic substratum.

Marbles with gneiss-schist intercalations comprises the upper members of the metamorphic system.

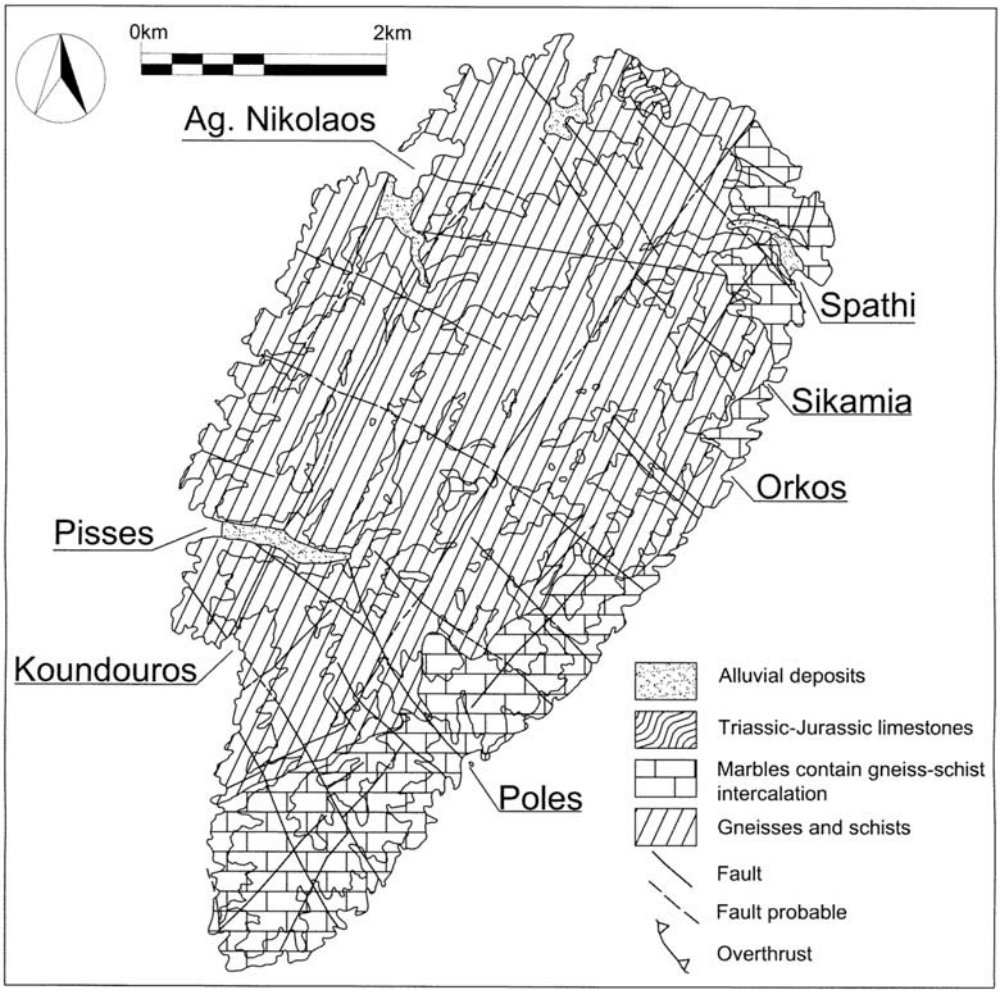

Fig. 1: Simplified geological map of Kea (Davi 1982) showing the position of the areas discussed.

In their contact on the transitional zone of the underlying gneisses and schists as also with the gneiss -schist intercalations, they change into cipolins, often accompanied by calc-schists.

The lower part of the metamorphic system, with a visible thickness more than 1000m, mainly consists of gneisses which often change into schists, therefore an irregularity occurs in their distribution.

The metamorphic complex is found intensely folded by two distinct folding phases, with NE-SW axial direction for the older phase and WNW-ESE for the younger. The main fault lines that cross the island and in some cases shape the morphology of its shores are of NE-SW and NW-SE directions. The NE-SW directed faults were created during a younger phase thus causing the shifting of the NW-SE directed faults of the older phase (Fig. 1).

Table 1.

Beach-rocks characteristics of Kea island									
Site	Width of beach-rock formations			Depth of the base of beach-rock formations			Depth of the top of beach-rock formations		
	younger phase (m)	middle phase (m)	older phase (m)	younger phase (m)	middle phase (m)	older phase (m)	younger phase (m)	middle phase (m)	older phase (m)
Spathi	15.00	-	-	-1.65	-	-	-1.45	-	-
Sykamia	15.00	-	-	-	-	-	-1.95	-	-
Orkos	10.00	43.00	-	-2.05	-3.20	-	-1.90	-2.45	-
Poles	28.20	36.80	55.00	-3.10	-3.80	-5.50	-1.85	-3.40	-4.90
Koundouros	7.50	-	78.00	-0.70	-	-4.60	-1.50	-	-4.10
Koundouros	13.00	17.00	-	-1.35	-3.90	-	-1.90	-2.10	-
Koundouros	10.00	-	-	-0.80	-	-	-1.20	-	-
Koundouros	8.00	-	-	-	-	-	-1.10	-	-

2. Indications of Upper Holocene sea-level changes

Indications of sea-level changes along the shores of Kea are the submerged beach-rock formations, as well as the submerged ancient coastal constructions and settlements of the island. Coastal beach-rock formations are found at the west shores of the island, at Koundouros location, submerged presently under the sea surface (Fig. 1 and table 1). In particular, measurements which were made at four small bays extending south of Koundouros bight revealed that the beach-rocks were deposited during three distinct phases, which all are now found completely submerged under the sea level.

The base and the top of the older phase, which is found at distance 78m from present-day shore, are at depths of -4.10m and -4.60, respectively. The middle phase, which is found at distance 17m from present-day shore, has top and base depths of -2.10m and -3.90m and the younger phase, found at distances ranging from 7.50m to 13m from the shore, have its base and top depths ranging from -0.70m to -1.35m and from -1.10 to -1.90m, respectively.

On the east shores of Kea at Sykamia bay, beach-rock formations, stretching at the entire shoreline, have a width of 15m and reach at a depth of -1.95m. Southerly, at the Orkos bay, the beach-rocks occupy the entire coast and they are developed at two distinct phases. The middle phase, today completely submerged, has a width of 19.50m while the depths of its base and top are -3.20m and -2.45m, respectively, at a distance of 43m from the shoreline. The younger phase of the beach-rocks at Orkos bay has a width of 10m and the depths of its base and top are at -2.05m and -1.90, respectively.

At the SE part of the island, at Poles Gulf, beach-rocks extending along the coasts of the two smaller bays of "Mikres Poles" and "Megales Poles" seem to have been formed during three distinct phases. The older phase was created by cemented deltaic deposits and at a distance of 55m from shoreline the depths of its base and top are at -5.50m and at -4.90, respectively. The middle phase of the beach-rocks, at distances ranging from 13.75m to 36.80m from the shoreline, have the depth of its top from -2.40 to -3.40m and the depth of its base from -2.20m to -3.80m. Finally, the younger phase of the

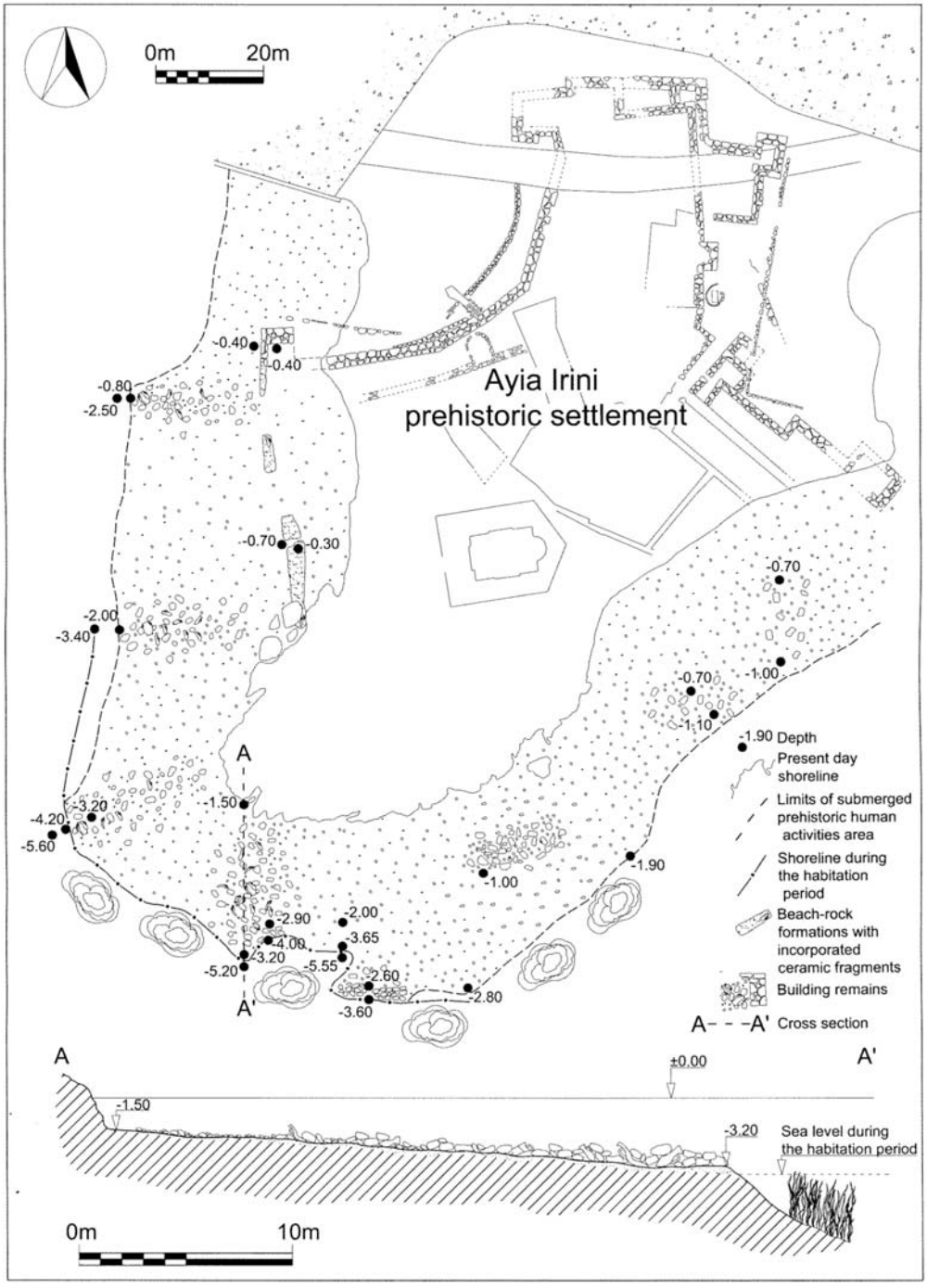

Fig. 2: Paleogeographic reconstruction of the coast of the prehistoric settlement of Ayia Irini.

beach-rocks has its width ranging from 8.50m to 28.20m and the depths of its top are from -0.80m to -1.85m and its base are from -1.35m to -3.10m.

3. Paleogeographic changes of the shores during Upper Holocene

Sea transgression along the shores of Kea, which varied from 15m to 90m depending on the coastal morphology, as a result of changes in sea-level, altered often radically the coastal paleogeomorphology. These changes abolished or degraded the coastal constructions and coastal human activities as well as parts of houses submerged under the sea surface.

3.1 The prehistoric settlement of Ayia Irini

The prehistoric settlement of Ayia Irini is located at the NE part of the shore of Ayios Nikolaos bay. This bay, located at NW shores of the island, is the only natural protected area for the mooring of ships at the north of the island. The natural setting in combination with its geographical location contributed in its development as a naval, commercial and strategic center from Neolithic Age to Classical period (Caskey 1962; Caskey 1964; Caskey 1966; Caskey 1971; Caskey 1972).

This Neolithic settlement was built on a small promontory. The habitation of the area, based on archaeological indications, started during the Neolithic Age. Archaeological research concludes the abrupt ending of the settlement operations and its possible abandonment in the period between the late Neolithic Age and Classical period, while a second period of abandonment took place at late Bronze Age, probably after an earthquake event.

Underwater research around the Ayia Irini promontory revealed that a great part of the settlement is today under the sea-level. The usage area, where the human activities occurred during antiquity, as it is defined by the ancient building ruins, the fragments of terracotta, ancient artifacts etc, surrounds the small promontory. The submerged part of the ancient settlement at the west side of the promontory has a length ranging from 35m to 41m, at the south side from 25m to 32m, while at the southwest side from 27.50m to 33.50m (Fig. 2). In this area, there were found building foundations, walls collapsed on pottery, abundance of terracotta fragments, as well as an accumulation of building stones at the south ending of the submerged part of the settlement, which indicates the construction of a quay wall for the protection of the settlement from sea erosion.

At the characteristic cross-section of the submerged part of the south side of the settlement (Fig. 2) the abrupt morphology as well as the growth of sea vegetation around the usage area is obvious. Based on the above characteristics we conclude at a sea-level lower some 3.40m to 3.60m from today sea-level, during the period that the settlement was active.

This rise of the sea-level is also confirmed by archaeological evidence from the excavations in the east part of Ayia Irini promontory, concerning the so-called “spring room” (Schofield 1998). The room’s floor today lies 3.80m lower than present sea-level. According to archaeological data this area was abandoned between 1450 BC and 1375 BC due to the salinity of the spring’s water.

Finally, the absence of human activities after the Classical period probably is related to the rise of the sea-level and the consequent submergence of a large part of the settlement.

3.2 The submerged schist quarry at Spathi bay

At the south sheer rocky coast of Spathi bay, at a distance of 200m from the sandy beach of the bay, a schist quarry was found. This is the only known quarry of that material in the whole area of the

Cyclades. The traces of quarrying are preserved unaffected, at the terrestrial part of the quarry as well as at the submerged one, which is the larger of the two parts of this ancient quarry site. The quarrying method used doesn't have any particularity and follows the known method used during the antiquity in the Mediterranean basin.

The part of the quarry which lies above the sea-level has a length of 25m and a width of 9.50m, while the submerged part of the ancient exploitation has a length of 25m and the traces of quarrying reach a width of 10m (Fig. 3).

At the front of the submerged part of the quarry, traces of the ancient quarrying activity are preserved, like burnings, grooves, channels, cuts for placing wedges and traces of quarrying equipment. At the bottom of the quarry between depths of -2.50m and -5.00m, traces of detached blocks are found as well as large accumulations of quarrying debris. At the south limit of the quarry the abrupt slope of the bottom reaches a depth of -9.50m and it is covered by quarrying debris.

The layout of the quarrying area indicates a parallel to the sea-level changes evolution of the quarrying activity.

3.3 Paleogeographic reconstruction of Poles Gulf

The Poles golf, in a position sheltered by strong winds and sea waves at Kynthos strait, is delimited at its north and south sides by the craggy shore cliffs of Kafkasos and Pasalimani hill-chains, respectively.

In between, the rocky ramp of Aspri Vigla penetrates in the sea for some 25m, splitting the west sandy coast of the gulf into two smaller bays, "Mikres Poles" (also known as "Ayios Aimilianos") to the South and "Megales Poles" (also known as "Frea") to the North. In the middle of the gulf, aligned with the extension of Aspri Vigla and at a distance of 210m from the shore, a small elongated islet of about 90m length and 40m width is located.

To the west, the hill-chain of "Aspri Vigla" is enclosed by "Eggeriti" and "Kato Meria" mountains; while at north and south it is delimited by two narrow elongated valleys crossed by "Kalamitsis" and "Vathypotamos" torrents whose riverbeds lead to the bays of "Megales" and "Mikres Poles", respectively. Sea-level change indications at Poles gulf are as follow:

- The few historical references on the existence of port installations during antiquity (Thomopoulos 1963; Osborne 1988).
- The engraved inscription on the northern craggy cliff shore of "Megales Poles bay", at a height about 1.00m above the sea-level and a distance of 25m from the sandy beach, today accessible only by the sea, which is dated -based on the type of its letters- at the 3rd century BC (Manthos 1867; Physllas 1921).
- The submersion of the connecting trail between the two bays in front of the "Aspri Vigla" promontory.
- The various carvings on the rocky islet as well as a circular reception of 0.22m diameter and 0.03m depth, found at its northeast side, which could have been used as a supporting base of a small pillar, all presently covered by the sea, even by a slightly intense sea undulation (Manthos 1867).

On the sheer south side of the small projection formed by the eastern edge of "Aspri Vigla" as well as at various points along the craggy N and S rocky coast of the gulf, submerged sea-notches at depths between -1.0m to -1.10m are found. This older sea-notch is recognizable from the horizon-

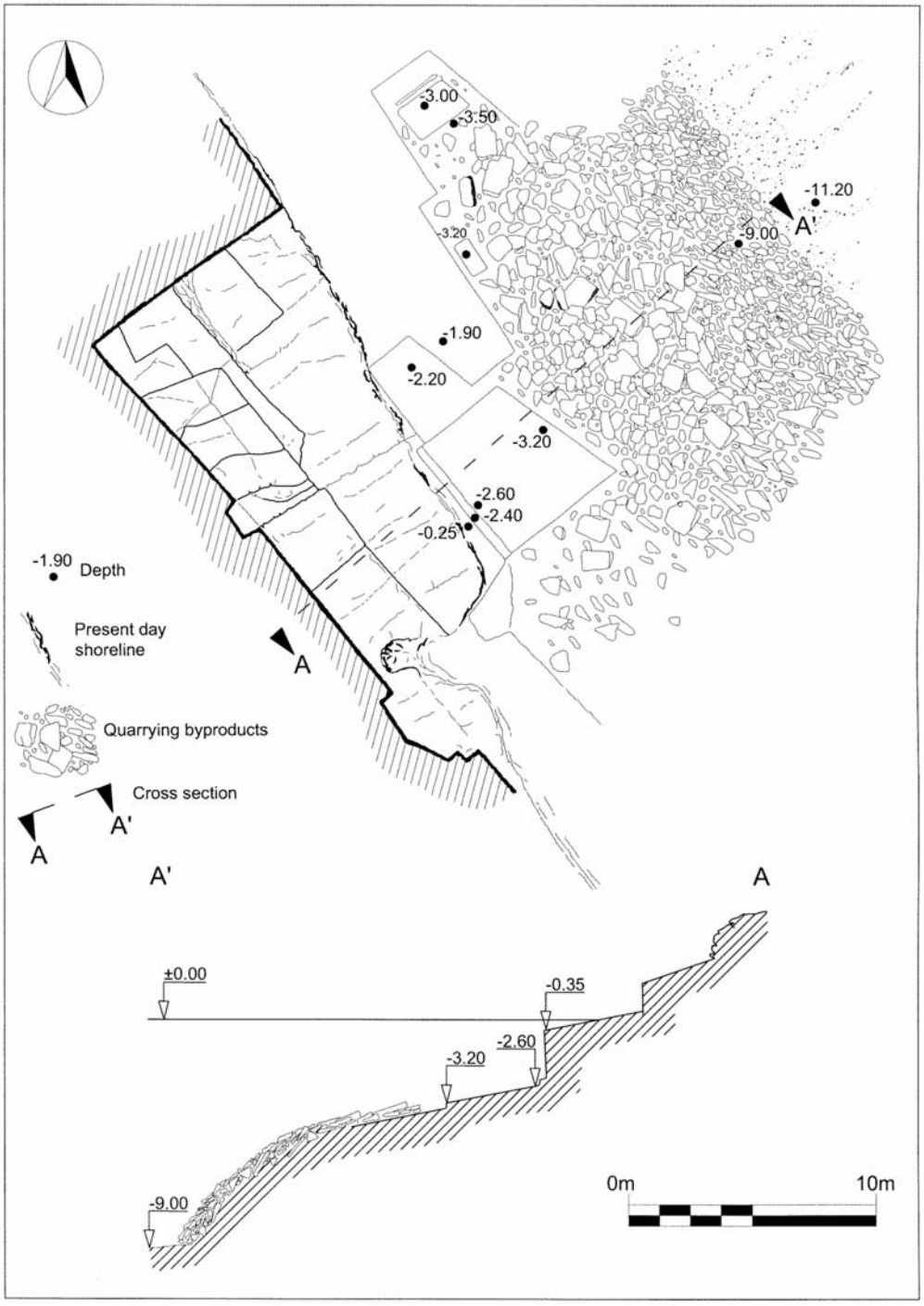

Fig. 3: Plan and charachteristic cross section of the submerged schist quarry at Spathi rocky coast.

Table 2.

Beach-rocks characteristics of the Poles gulf									
Site	Width of beach-rock formations			Depth of the base of beach-rock formations			Depth of the top of beach-rock formations		
	younger phase (m)	middle phase (m)	older phase (m)	younger phase (m)	middle phase (m)	older phase (m)	younger phase (m)	middle phase (m)	older phase (m)
A	8.55	21.20		-1.35	-3.00		-0.90	-2.40	
B	-	22.80		-	-2.50		-	-2.20	
C	10.60	-		-1.60	-		-0.80	-	
D	-	18.20		-2.00	-		-1.60	-	
E	14.30	41.00		-1.75	-4.30		-1.20	-2.40	
F	-	13.75		-	-4.16		-	-2.86	
G	-	26.80		-	-4.10		-	-2.90	
K	-	35.00		-	-4.15		-	-3.40	
L	26.80	31.00		-2.00	-3.30		-1.20	-2.75	
M	28.20	34.00		-2.35	-3.30		-1.20	-2.60	
N	23.00	36.80		-2.38	-3.80		-1.00	-3.05	
O	22.00	-	55.00	-3.10	-	-5.50	-1.85	-	-4.90

tal grooving, with an opening of 0.80m, in the marble layers. The groove is typical asymmetrical cut with a broad slightly inclined base and sheer rough top.

The submerged beach-rocks, which are found along the entire length of the southern (Mikres Poles) and northern (Megales Poles) portions of the bay's western shore, seems to have been formed during two different phases, each of which reflects a period of stability for the two different sea-levels (Fig. 4-left). The presence of sherds and tiles found in the beach-rocks of both two phases are clear indications that were formed after human settlement in the area.

Measurement results showed that the maximum width of the older and deeper phase of the rock formations reaches some 40m, while the maximum depth of the top of the rocks is -3.40m. The most recent phase of the beach-rocks possess a maximum width of 28m, while the depth of their tops coincides with the depth of the ancient shoreline, varying between -0.80m and -1.20m (Table 2).

Measurements which were taken on the north side of "Aspri Vigla" promontory indicate that the beach-rocks in this location were formed during the middle phase, while the younger phase is not apparent due to the disappearance of the sandy shore along the entire length of the promontory, as a consequence of the rise in sea-level.

The parts of the beach-rocks which project from the southern extremities of "Mikres" and "Megales Poles" bays coincides with the points of outflow of the torrents of "Bathypotamos" and "Kalamitsi", which in turn indicates that the beack-rocks are actually the small fossilized deltas of these torrents. The appearance of beach-rocks at the northern extremity of "Megales Poles" bay seems to have been created by fossilized deposits of an older outflow point of "Kalamitsi" torrent.

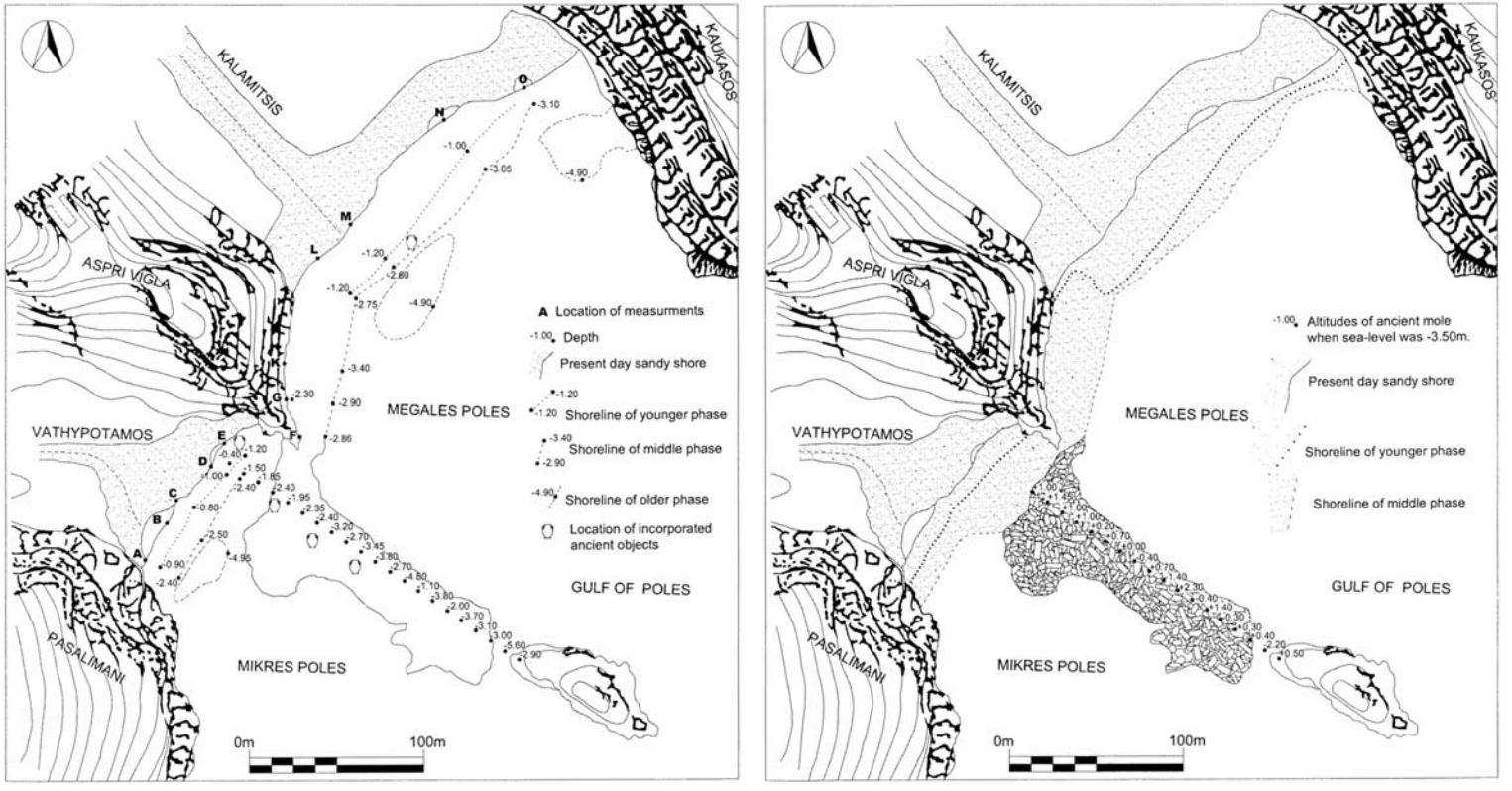

Fig. 4 :(left): Plan of the Poles gulf showing the current coast morphology, the locations of the measurements, bottom depths and limits of the different phases of beach rocks, limits and depths of the submerged ancient breakwater, (right): Paleogeographic reconstruction of Poles gulf showing the different phases of the sandy coast, altitudes and shape of the ancient breakwater.

On the basis of the data obtained from the investigation of the ancient sea notches and the beach-rocks it is concluded that the morphology of the western shore of the bay altered in two separate phases in accordance with the fluctuations of the sea-level in this region. The reconstruction of the coastal morphology during these two phases is attempted in figure 4-right.

During the period when the sea-level was some -3.40m lower than today, as low as the maximum depth of the tops of the older phase of the beach-rocks, the sandy western shore of the bay was wider than the contemporary and extended seawards for some 21m to 40m. During the second and more recent phase when the sea-level was 1.20m lower than present one, as low as the maximum depth of the tops of the second phase of the beach-rocks, and also the depth of the ancient sea notches, the western shore was some 8m to 28m east of its present location; while the narrow sandy beach which existed in the older phase in front of the promontory of "Aspri Vigla", no longer appears.

The small fossilized deltas of the torrents which run into the Poles gulf, the depth of the tops and the bases of which are -4.90m and -5.50m, respectively, were probably formed during an earlier phase than that of the two previous phases, when the sea-level was -4.90m lower than today.

In the course of the underwater investigation of the area between the coast of "Mikres Poles" and the islet, an underwater mound of 160m length and of 30m to 35m width was identified. This underwater mound lies some 40m from the shore in a SE direction and terminates at the islet. The mound is composed of large schist boulders, agglomerated bits of schistolithic rock and schist slabs cemented together with sandy cement containing shell and terracotta fragments. The presence of sherds and tiles, as well as the base of a large bronze vessel struck to the surface of the mound, is evidence of human activity here in the past. Detailed measurements taken along the length of the mound revealed that when sea-level was at -3.40m, the presently submerged mound protruded from the surface some 0.20m to 2.30m (Fig. 4-right).

This morphology constituted a manmade breakwater which further protected from wind and wave an already well-sheltered location and allowed the safe mooring of ships in the harbour. During the second phase, when sea level rose some 2.20m, the breakwater was completely submerged (Fig. 4-right). A channel 8m wide, presently submerged, situated between the eastern end of the breakwater and the islet, allowed for the passage of shipping from one side of the gulf to the other.

Approximately two and a half millennia ago the sea-level in this region was 3.40m lower than today while the sandy beach was wider some 20m to 40m than today at various points. Land communication between the north and south shores of the gulf was possible via the narrow sandy beach which lay before the sheer rocky cliff of the promontory of "Aspri Vigla". Most likely the traces of the ancient path connecting "Mikres" with "Megales Poles" should be sought to the east of the modern animal track, which apparently was formed after the collapse of the east side of the terrace where the Temple of Apollo stood. This collapse brought down the corresponding wall of the temple which stood at the eastern edge of the town (Fig. 4-right). The presently submerged breakwater, stretching between the islet and the sandy coast, which was a rocky ridge partially filled with slabs of marble and schist, stood above the surface of the sea creating the harbour mole of the ancient Karthaia port.

4. Conclusions

Sea-level changes along the shores of Kea during Upper Holocene seem that they have occurred in three distinct phases.

The older phase is defined by a sea-level lower than the contemporary by 4.60m to 5.50m. Indica-

tions of this sea-level are the older beach-rock phase at Koundouros shores as well as the submerged fossilized deltas of the torrents at Poles gulf.

The following middle phase corresponds to a sea-level 3.40m to 3.90m lower than the contemporary. Indications of the middle phase are located at Koundouros shores at the east side of Kea and at Sykamia and Poles gulf at the west side, where beach-rock formations are submerged at related depths. At Ayios Nikolaos, Spathi and Poles gulfs, the middle sea-level is also established by the submerged part of Ayia Irini settlement, the submerged ancient quarry and the harbour installations of ancient Karthaia, respectively. Based on archaeological evidence, this phase of sea-level correlates to the Classical era about two and a half millennia from present day.

The younger phase corresponds to a sea-level 1.10m to 1.50m lower than the contemporary. Indications of the this phase are located at Koundouros shores, at Spathi, Sykamia, Orkos and Poles gulfs, where beach-rock formations and coastal installations are submerged at related depths.

In antiquity, coastal geomorphological features apparently were a major factor in the selection of a coastal location to establish a settlement. People tried to benefit from natural protected coastal morphology, in some cases improve it with small scale interventions, while in only few locations they resorted to extensive harbor projects for the safe access of the ships. Sea-level changes during Upper Holocene altered the paleogeography of the shore and overturned the comparative advantage of a coastal location thus contributing in its decline. Paleogeographic reconstruction of the prehistoric settlement of Ayia Irini and the Classical period port of Karthaia on the island of Kea offer important elements for understanding the selection criteria during antiquity and contribute to the interdisciplinary research.

5. References

Caskey, L.J., 1962. Excavations in Keos 1966-1970. *Hesperia* 31, 1962, pp. 263-283.

Caskey, L.J., 1964. Excavations in Keos 1966-1970. *Hesperia* 33, 1964, pp. 314-335.

Caskey, L.J., 1966. Excavations in Keos 1966-1970. *Hesperia* 35, 1966, pp. 363-376.

Caskey, L.J., 1971. Investigasions in Keos I. *Hesperia* 40, 1971, pp. 358-396.

Caskey, L.J., 1972. Investigasions in Keos II. *Hesperia* 40, 1972, pp. 357-401.

Davi, E., 1972. Γεωλογική κατασκευή της νήσου Κέας. *Bull. Geol. Soc. Greece* 9, 2.

Davi, E., 1982. Geological map of Greece 1:50.000, Kea island, IGME 1982

Manthos, K., 1867. Αρχαιολογία και Ιστορία της νήσου Κέας. Κέα 1867. Unpublished handwritten ms. *In Archives of the BSA*, Athens. N73.

Manthos, K., 1878. Αρχαιολογία και Ιστορία της νήσου Κέας. Κέα 1878. Unpublished handwritten ms. *In Archives of the Greek Historical and Ethnological Society*, nr. 132.

Papanikolaou, D., 1986. The Geology of Greece. 240, Athens.

Physllas, I., 1921. Ιστορία της νήσου Κέας από των αρχαιοτάτων χρόνων μέχρι των καθ' ημάς. Αθήνα 1921, 298.

Schofield, E., 1998. Town planning at Ayia Irini, Kea. Kea-Kythnos: *History and Archaeology Proceeding of an International symposium Kea-Kythnos*, 1994, 117-121.

Thomopoulos, A.J., 1963. Μελέτη Τοπωνυμική της νήσου Κέω. ΕΕΚΜ 3, 193.

Δελτίο της Ελληνικής Γεωλογικής Εταιρίας, 2010
Πρακτικά 12ου Διεθνούς Συνεδρίου
Πάτρα, Μάιος 2010

Bulletin of the Geological Society of Greece, 2010
Proceedings of the 12th International Congress
Patras, May, 2010

A COMPARATIVE MORPHOLOGICAL STUDY OF THE KOS-NISYROS-TILOS VOLCANOSEDIMENTARY BASINS

Nomikou P.[1], Papanikolaou D.[1]

[1] *University of Athens, Department of Geology and Geoenvironment, Panepistimioupoli Zografou, 15784 Athens, Greece, evi@ath.hcmr.gr, dpapan@geol.uoa.gr*

Abstract

A swath bathymetric map of Kos-Nisyros-Tilos Volcanic field was created with 50m grid interval, with 10 m isobaths at a scale 1:100.000 using SEABEAM 1180 (180 kHz) multibeam system for depths <500m and SEABEAM 2120 (20 kHz) multibeam system for depths >500m. Five basins have been distinguished in the circum-volcanic area of Nisyros: 1)Eastern Kos basin, the larger and deeper one, with an average sea-bottom depth of 630m. Submarine canyons within the basin occur along the southern coastline of Kos cutting the isobaths from 150 up to 400m depth. A shallow crater with relative topography of ±70m has been discovered at the bottom of the basin (600-670m) 2)Western Kos basin with average depth of 520m. The basin is separated from the Eastern Kos Basin by a rise between Yali and Kos at 400m depth. This basin is separated from the Western Nisyros basin by the Kondeliousa rise. 3)The Western Nisyros basin is located between Kondeliousa rise and western Kos platform with depths of 550m. 4)The Southern Nisyros basin constitutes the northern end of the large Karpathos basin which reaches more than 2000m depth towards the south. 5)The Tilos basin with depths of 600m occurs southeast of Nisyros Island, separated from South Nisyros Basin through a rise of less than 400m depth. The Pachia-Pergoussa and Yali-Nisyros basins are shallow structures within the intra-volcanic relief of Nisyros and surrounding islets. The geometrty of each basin is discussed in relation to the volcanic and tectonic structure of the graben between Kos and Tilos.The intensity of the active geodynamic acrtivity is demonstrated by the creation of a volcanic relief of 1400m in the Nisyros volcanic field.

Key words: *seabed morphology, multibeam systems, Kos-Nisyros-Tilos Volcanic field, Dodecanese.*

1. Introduction

Systematic research combining onshore and offshore data has been carried out in the area around Kos, Nisyros and Tilos islands in the Dodecanese since the late nineties aiming at a comprehensive view of the geodynamic processes in the area (Papanikolaou et al., 1991; Papanikolaou et al., 1998; Nomikou and Papanikolaou, 2000; Papanikolaou and Nomikou, 2001; Nomikou, 2004; Pe-Piper et al., 2005; Tibaldi et al., 2008). More precisely, the occurrence of the easternmost volcanic activity of the modern volcanic arc in the area gives the possibility of analysing the geomorphology as a result of the ongoing tectonic and volcanic activity. A major point of interest is the understanding of the offshore area and its linkage with the onshore structures.

Our offshore studies including multibeam bathymetric survey have been carried out on the research-vessel R/V AEGAEO of the Hellenic Centre for Marine Research (HCMR), during three successive

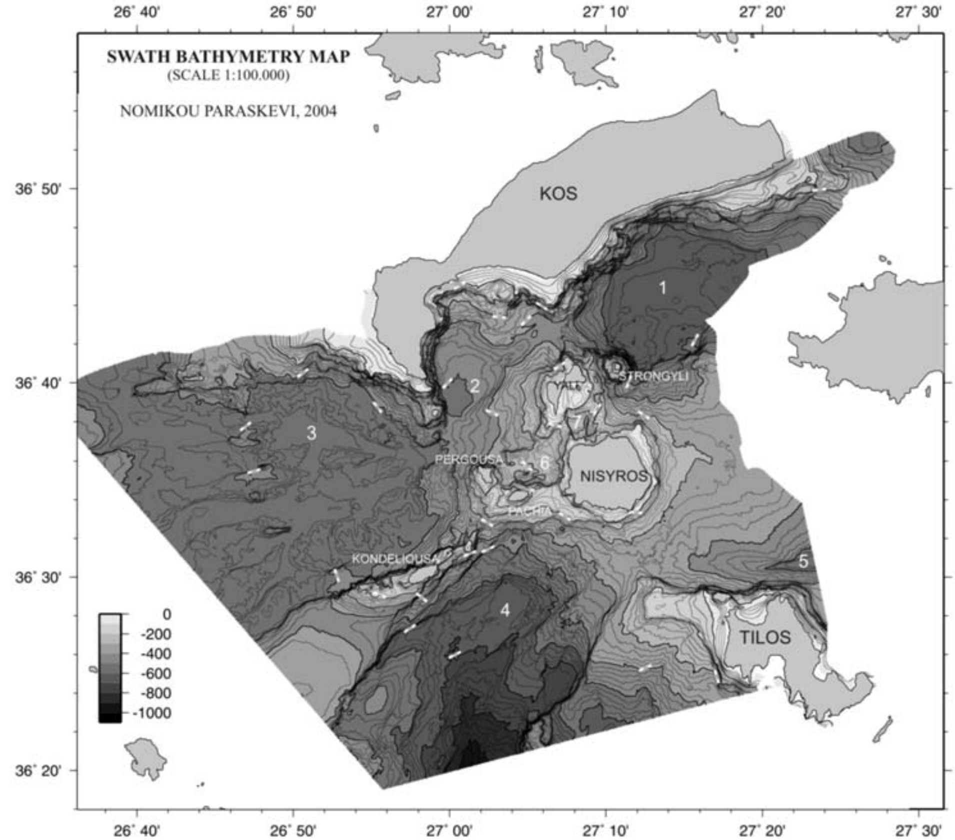

Fig. 1: Multibeam Bathymetric Map of the Kos-Nisyros-Tilos area using 10m isobaths (after Nomikou, 2004) 1: Eastern Kos Basin, 2: Western Kos Basin, 3: Western Nisyros Basin, 4: Southern Nisyros Basin, 5: Tilos Basin, 6: Pachia-Pergousa Basin, 7: Yali-Nisyros Basin.

cruises conducted within the year 2000 in the area of Nisyros–Kos islands. During the first mission, the area of Nisyros Island and the surrounding small islets has been mapped using the SEABEAM 1180 (180 kHz) system, which is suitable for depths <500m. The SEABEAM 1180 is portable, shallow water, compact system integrating transmitter, receiver, interfaces and power stage within a single unit. The other two missions completed the mapping of the whole area of Kos–Nisyros–Tilos using the SEABEAM 2120 (20 kHz) system, which is suitable for depths >500m. The SEABEAM 2120 is arelatively new swath system that has been specifically designed to suit users with survey requirements exceeding 6000m water-depth, accomplishing a satisfactory resolution (up to 1°×1°) without mounting a very large array. By operating the systems for a total of 12 days with an average speed of 10 knots, 3500 km^2 were covered from very shallow depths to depths of 2200m. A swath bathymetric map of Kos–Nisyros Volcanic field was created with a 50m grid interval using 10m isobaths at a scale 1:100.000 (Fig.1). The map is georeferenced to a WGS-84 ellipsoid and a Mercator projection at 38°N (Nomikou, 2004).

The main morphological features of the studied area are three zones of positive relief comprising Kos in the NW (843m elevation in Dikeos Mt), Nisyros (698m in Prophitis Ilias Mt.) and surrounding

islets in the middle and Tilos (654m, Prophitis Ilias) in the SE. These zones subdivide the submarine area between Kos and Tilos in two basins with an average sea bottom depth of 600m. Consequently, the topographic differences between the top of the Mountain ranges and the bottom of the submarine basins are of the order of 1-1.5 km. This topographic difference occurs in some cases like the Dikeos southern slopes within an horizontal distance of 2-4 km with high values of morphological slope both above and below sea-level without the development of continental shelf. On the contrary, the area of the islets around Nisyros is characterized by extended shallow water depths which are occupied by a number of volcanic centers (Nomikou et al., 2004). All these volcanoes have been developed within a neotectonic graben formed by a subsidence of the order of 2.5 Km between the marginal fault zones of Southern Kos and Northern Tilos. The volcanic centers are built up from a base level of -600m, which is the level of the mean sea-bottom of the marine basins up to +700m summit of Prophitis Ilias on the top of the post-caldera volcanic dome of Nisyros Island. Thus, a volcanic relief of more than 1300m has been produced by the geodynamic processes of Upper Pleistocene – Holocene (Papanikolaou & Nomikou, 2001).

2. Submarine Volcano-Sedimentary Basins

The detailed swath bathymetric map permitted the delineation of the following five main marine basins in the circum-volcanic area of Nisyros: 1) Eastern Kos Basin, 2) Western Kos Basin, 3) Western Nisyros Basin, 4) Southern Nisyros Basin and 5) Tilos Basin. Additionally, two smaller basins occur within the shallow-water intra volcanic area of Nisyros: 6) Pachia-Pergousa Basin and 7) Yali-Nisyros Basin (Fig. 1).

2.1 Eastern Kos Basin

Eastern Kos Basin is bordered to the north by the steep southern slopes of Dikeos Mountain whereas towards the south it is separated from the Tilos Basin by the rise connecting Nisyros Island with the Datcha peninsula (Fig. 2). To the east it continues into the basin developed north of Datcha peninsula and south of eastern Kos. This part of the basin was not possible to be charted by our swath bathymetric survey because it belongs to the Turkish coastal area and thus, the conventional hydrographical map of Turkey was used. To the west it is bordered from the Western Kos Basin by the Yali-Kos rise and to the southwest it is bordered by the very steep volcanic cone of Strongyli islet which emerges from 600m of depth to 120m of altitude.The general orientation of the basin is ENE-WSW, parallel to the orientation of Kos Island and of its southern coastline. This orientation is due to a major neotectonic fault running parallel to the coast for more than 20 km, which has subsided the Eastern Kos Basin with respect to the Dikeos mountain of Kos. A number of submarine canyons has been detected from shallow depths of about 150 m to approximately 500 m where the morphological slopes become very small and grade to the sub horizontal basinal part at depths around 640 m.

The morphology of the basinal area is unique in this basin with the geometry of submarine caldera occurring immediately northeast of the base of the Strongyli volcanic cone. This submarine volcanic structure was named Avyssos because of the great depth of its base around 680 m (Fig. 2). The volcanic nature was verified by the analysis of the lithoseismic air-gun profiles showing only very few meters of sediments overlying volcanic formations. The caldera dimensions are 3 km in the NW-SE direction and 4 km in the NE-SW direction. The stereographic diagramme of Avyssos was constructed with 2 m isobaths aiming to demonstrate the geometry of the volcanic structure. At the centre of Avyssos there is a hill of about 1 km length, with a relief of about 60 -70 m, representing later intrusions of volcanic rocks within the almost planar base of the caldera. The peak of the cen-

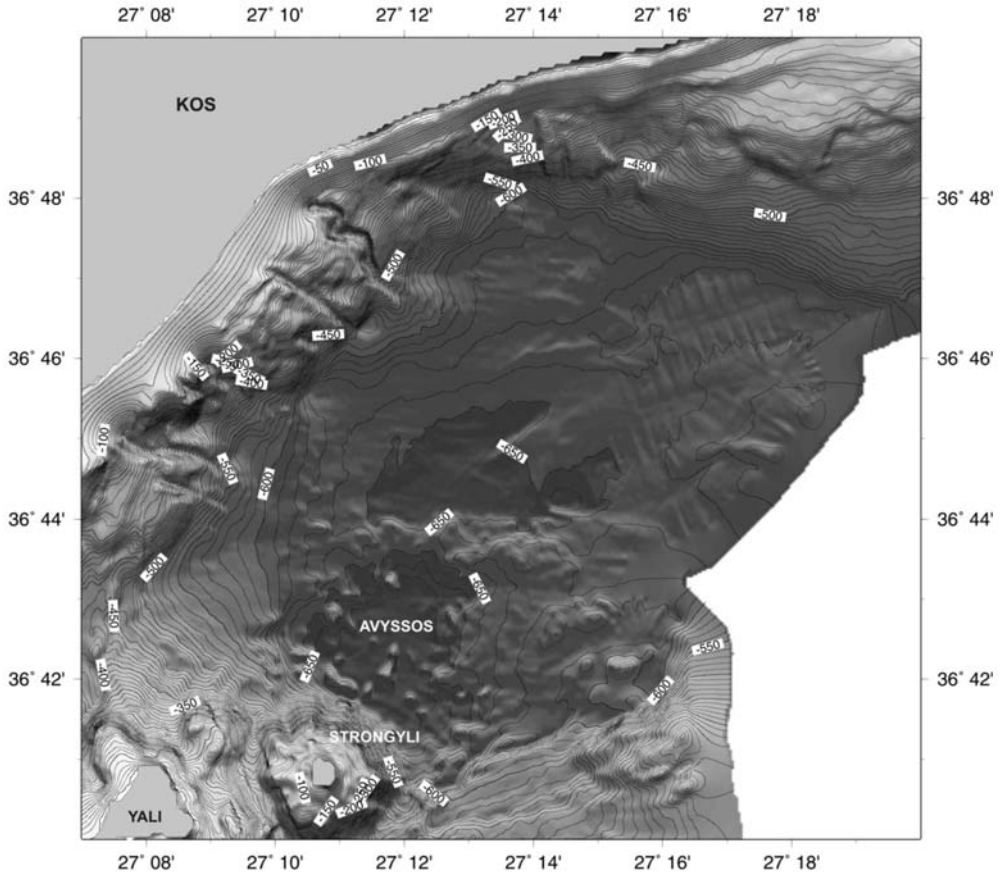

Fig. 2: Detailed bathymetric map of the Eastern Kos Basin using 10m isobaths. Note the canyons along the nortwestern margin and the submarine caldera of "Avyssos" to the northeast of Strongyli islet.

tral volcanic dome lies at 610 m depth, rising 66 m above the planar base of the caldera which is at 676 m depth. The caldera rim lies at about 630 m depth forming a submarine circular cliff of 40-50 m topographic difference.

2.2 Western Kos Basin

Western Kos Basin is bordered to the west by the peninsula of Kefalos and to the north by the southwestern coast of the Antimachia plateau of central Kos. Yali islet occurs to the east and Pergousa islet to the south (Fig. 3). It is open towards Eastern Kos Basin to the east, Western Nisyros Basin to the west and Pachia-Pergoussa Basin to the south. The continental slopes are abrupt almost from all directions but the western margin towards Kefalos Peninsula is very steep and forms an N-S zone of morphological discontinuity.

The deepest part of the basin lies adjacent to the western margin with smooth morphological slopes within the rest of the basinal area which accumulates radialy the sediments towards this subsiding zone. The western margin is controlled by a neotectonic fault of N-S direction which produces up-

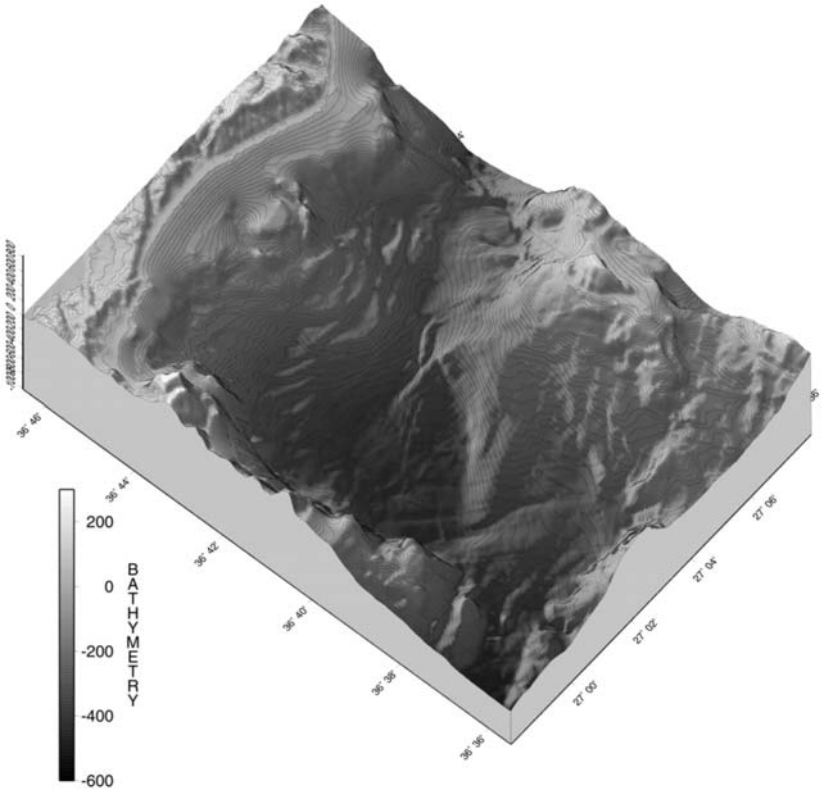

Fig. 3: 3-D view of Western Kos Basin using 10m isobaths.

lift of the western fault-block of the Kefalos Peninsula and subsidence of the eastern fault-block of the Western Kos Basin. The maximum depth of the basin is 530m and only a small horizontal area can be observed around it of about 1 km^2 area. The southeastern and southern slopes of the basin are reflecting the geometry of the lower part of the volcanic cones of the Yali and Pergoussa volcanoes. At the north-western part of the basin is observed half of the Kefalos volcanic structure of Middle Pleistocene age (0.5 myears), while the rest of it is preserved onshore (Dalambakis & Vougioukalakis, 1993) and the rest flowing offshore towards the south. Along the northern slopes of the basin the continental shelf of Kos is observed down to the depth of 150m. Immediately below the edge of the continental shelf there is a graduated arc-shaped form of a mega landslide, exhibiting a type of radial flow to the south with special morphology of arcuate terraces reaching the depths of 400-450m. The toe of the sliding mass to the south is confronted against the base of the north-western part of the Yali volcanic cone.

2.3 Western Nisyros Basin

Western Nisyros Basin is extended to the west of the Pergousa islet and between two shallow water platforms developed towards the west of Kondeliousa islet from the south and west of Kefalos Peninsula from the north. The basin ends towards the west in the area beteen the islands of Syrna and Astypalaia. The overall length of the basin is 40-45 km in the ENE-WSW direction and its width is about 15-20 km. The basinal area is rather flat with maximum depth around 600m (Fig. 4). Its south-

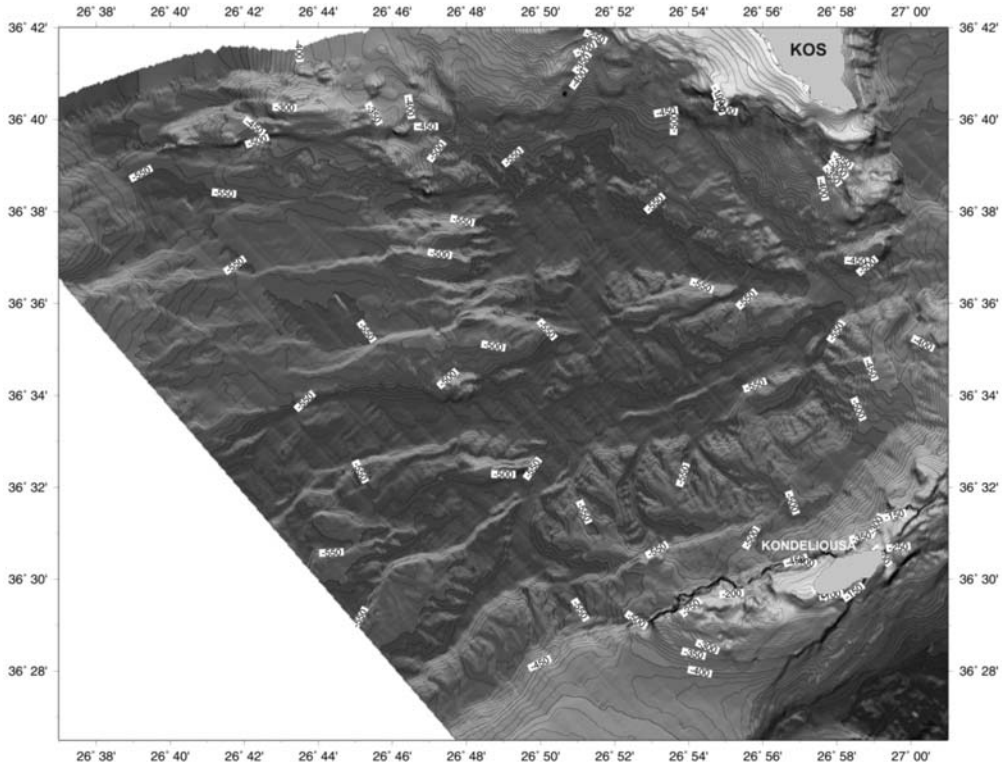

Fig. 4: Bathymetric Map of the Western Nisyros Basin using 5m isobaths. Note the alternation of submarine ridges and channels in the ENE-WSW direction.

ern margin is characterized by abrupt slopes with steep morphological slopes >20% observed between 500m and 200m of depth. This steep morphology is controlled by major fault zone of ENE-WSW direction (Nomikou, 2004) separating the uplifted tectonic horst of Kondeliousa islet to the south, which is made of Mesozoic carbonate rocks, from the subsided basinal area to the north. The topography of the basinal area is characterised by a succession of parallel oblong rises and channels oriented ENE-WSW. The relative topography between these morphological forms is several tens of m with the top of the rises reaching 450m whereas the bottom of the channels reaching 560m. This alternation of rises and channels is probably due to volcanic domes intruding the basinal area which correspond to the rises following the general ENE-WSW trend as this is indicated by the excessive reflections observed on the air-gun litho-seismic profiles (Nomikou, 2004).

2.4 Southern Nisyros Basin

Southern Nisyros Basin is developed to the south of Kondeliousa islet and to the southwest of Nisyros Island. To the east it is bordered by the platform developed along the western margin of Tilos Island (Fig. 5). Towards the southwest it is open to the large basin of Karpathos, which constitutes the eastern segment of the Cretan Basin. The depth of the basin increases towards the southwest up to 970m and further towards the Karpathos Basin it reaches 2200m. The basin is closed towards the northeast by the submarine slopes of the Nisyros volcanic cone. A special morphology of a submarine landslide terrain is observed over a large area of the south-western Nisyros slopes with a vol-

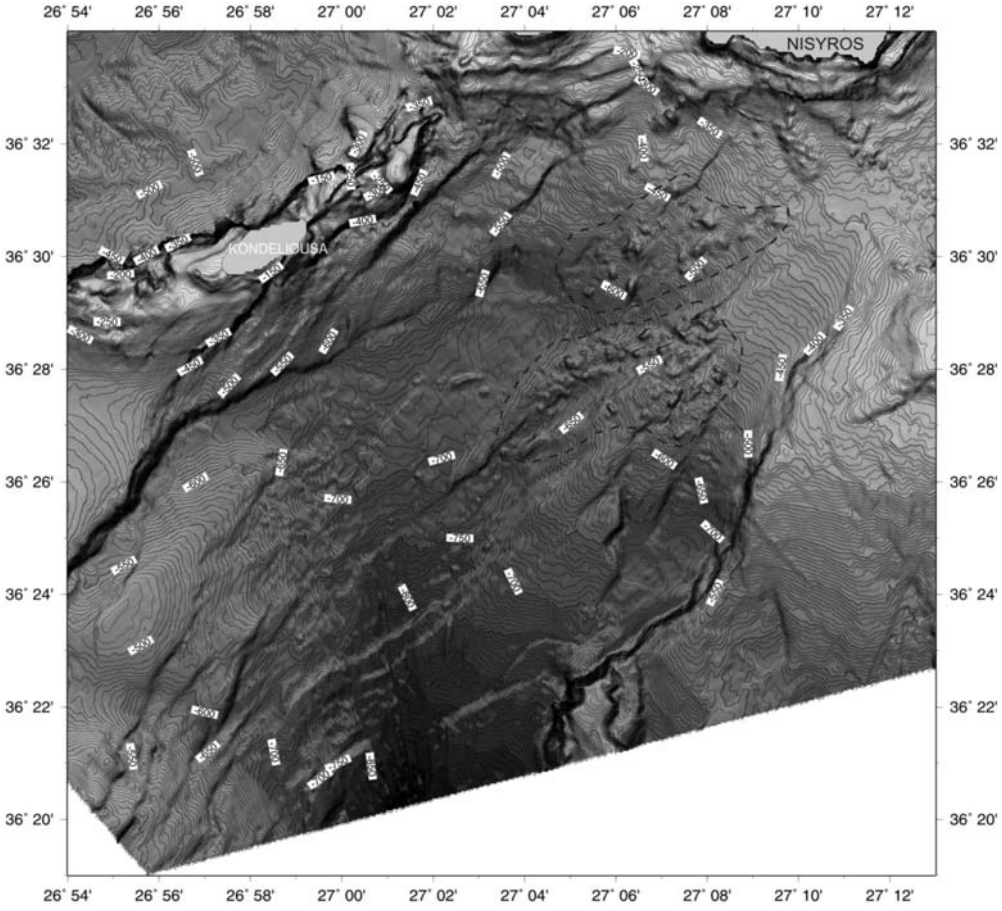

Fig. 5: Bathymetric Map of the Southern Nisyros Basin using 5m isobaths. Note the submarine volcanic landslide south-southeast of Nisyros and the two marginal fault zones in the NE-SW direction.

canic debris avalanche observed between 420-680m of depth (Tibaldi et al., 2008). The relative topography of the slided blocks reaches 80m and their shape varies from circular round geometry to asymmetrical blocks of different orientations. The basin is delimited between two major fault zones of NE-SW direction (Nomikou, 2004) that have caused subsidence of several hundreds of metres. The two fault zones form the two parallel margins of the basin in the NE-SW direction and are characterised by steep slopes. Both marginal faults have produced a strong subsidence of the basin between the uplifted horsts of Kondelioussa in the northwest and Tilos in the southeast. In both horst areas the Mesozoic formations of the Alpine basement are uplifted.

2.5 Tilos Basin

Tilos Basin is developed to the north of Tilos Island and to the southeast of Nisyros Island (Fig. 6). Our map comprises only its western part because of its extension into the Turkish waters towards the east, where it is developed south of the Datcha Peninsula. Towards the southeast it terminates at the area north of Simi Island. Towards the north it is bordered from the Eastern Kos Basin by the E-W

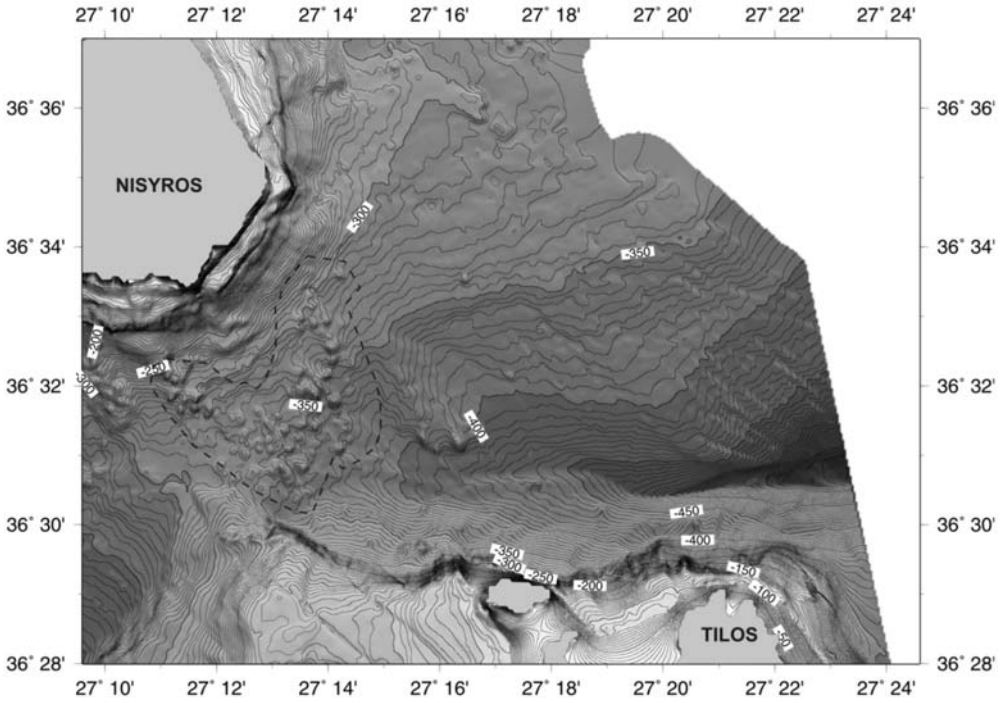

Fig. 6: Bathymetric Map of the Tilos Basin using 5 m isobaths. Note the deposition of the volcanic debris avalanche south of Nisyros.

oriented rise of Nisyros – Datcha. The northern slopes of the basin towards Nisyros Island are smooth with progressive depth increase from 300m to the flat basinal part of the basin at 570m of depth. On the contrary the southern slopes of the basin towards Tilos Island are more abrupt with dense isobaths and steep slopes >20%. This steep morphological zone is due to a major E-W trending fault zone, developed along the northern margin of Tilos Island. The western part of the basin towards its link to the Southern Nisyros Basin is occupied by a special morphology with numerous hills and longitudinal ridges between water depths of 250 and 380m. The overall morphology of this area occurring southeast of Nisyros Island can be viewed as a large deposit of volcanic debris avalanche with a seaward termination displaying an irregular pattern characterized by elongated lobes. These lobes and the elongation of the single elevations might represent a series of aligned ridges emplaced parallel to the flow of the debris avalanches from the Nikia rhyolitic volcanic rocks which predated the Nisyros volcano major caldera explosion (Tibaldi et al., 2008).

2.6 Pachia-Pergousa Basin

Pachia-Pergousa Basin is developed within the intra-volcanic area of the Nisyros volcanic field surrounded by the volcanic islets of Pachia from the west, Pergousa from the south and Yali from the north (Fig. 7). Nisyros Island borders the basin from the east. A number of small fluctuations embossed the seabed likely because of volcanic intrusions. The 300m isobaths to the north of Pachia delimits the flat part of the basin whose maximum depth reaches 345m. The slopes to the east and to the south present abrupt increase of depth shown by dense isobaths due to faults in the N-S and

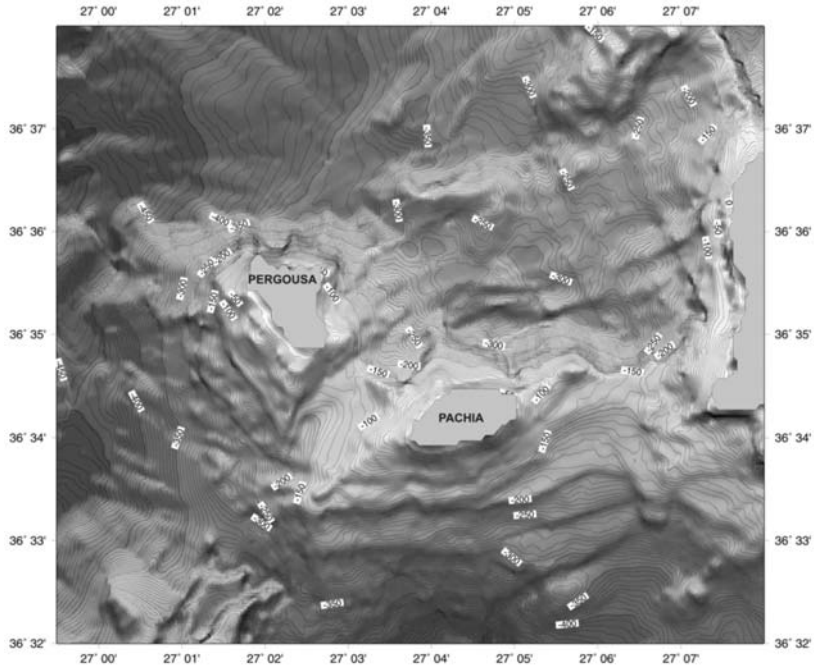

Fig. 7: Bathymetric map of the Pachia-Pergousa Basin using 10m isobaths.

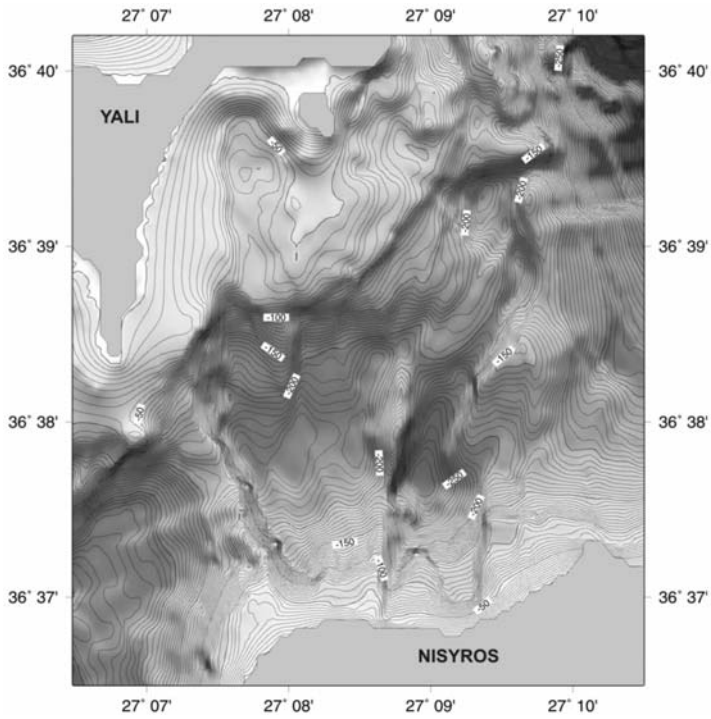

Fig. 8: Bathymetric map of the Yali-Nisyros Basin using 10m isobaths.

E-W direction. The basin is separated from Western Kos Basin towards the northwest by a ridge of 100m hypsometric difference, roughly from the isobath of 300 up to the isobath of 200m. Towards the east and northeast it is separated from the Yali-Nisyros Basin by a small submarine ridge oriented NNW-SSE at 160m of depth.

2.7 Yali-Nisyros Basin

Yali-Nisyros Basin occurs within the intra-volcanic area of the Nisyros volcanic field and is bordered by Nisyros Island in the south and Yali Island in the north (Fig. 8). The basin comprises two sub-basins oriented N-S which are separated by an N-S ridge between Nisyros and Yali islands. The western sub-basin is delimited to the west by the seismic fault zone that was activated in July 1996 and produced extensive damage in Mantraki Town, adjacent to the Panaghia Spiliani Monastery (Nomikou & Papanikolaou, 2000). The submarine survey showed a topographic difference across the fault of about 100m, with the uplifted block to the west at 140 m of depth and the subsided block to the east at 235m depth. The eastern sub-basin is developed also in the N-S direction with deeper maximum depth at 290m.

3. Synthesis-Comparison of Submarine Basins

The Kos-Nisyros-Tilos area comprises three parallel fault zones oriented ENE-WSW between the Kos tectonic horst in the north and the Tilos tectonic horst in the south. The northern zone comprises from west to east the basins of Western Nisyros, Western Kos and Eastern Kos. They are all deep basins with maximum depths between 505m and 670m and they are bordered from the south by volcanic structures of the Nisyros volcanic field. The whole zone represents a northern sub-basin/tectonic graben bordered by the Kos tectonic horst in the north and the Kondelioussa tectonic horst to the south. The middle zone comprises the islands and islets of Kondelioussa, Pachia, Pergoussa, Nisyros, Yali and Strongyli together with the intra-volcanic basins of Pachia-Pergoussa and Yali-Nisyros. The maximum altitude (698m) is observed at Prophitis Ilias on Nisyros Island and the maximum depth of the basins is 290m and 335m for Yali-Nisyros and Pachia-Pergoussa respectively. This middle zone represents a tectonic horst separating the two adjacent grabens to the north (northern zone) and to the south (southern zone) and shows the uplifted above sea-level Alpine basement in Kondelioussa Island together with the thick volcanic rocks of the Nisyros volcanic field. The general trend of this zone from Kondelioussa in the west to Datcha Peninsula to the east is ENE-WSW. The southern zone comprises the basins of Southern Nisyros and Tilos with great depths (570m and more than 1000m). The general trend is NE-SW at the western part and E-W at the eastern part (Nomikou, 2004; Pe-Piper et al., 2005). The northern margin of this southern zone – tectonic graben is made of the volcanic formations of the Nisyros volcanic field, whereas the southern margin is made of the Tilos tectonic horst, with the Alpine basement rocks at maximum altitude of 654m.

In conclusion, the submarine region from Kos to Tilos constitutes a large fault controlled basin with 600m average depth, which is interrupted by a complex volcanic group forming volcanic islands and intra-volcanic basins with less than 350m of depth. The volcanic formations are found at 680m of depth (Avyssos in the Eastern Kos Basin and at the eastern base of the Strongyli volcanic cone) up to 700m of altitude (Rhyolitic domes of Prophitis Ilias on Nisyros) creating a total volcanic relief of more than 1400m. This recent volcanic morphology demonstrates the intense geodynamic processes of the eastern edge of the active Hellenic volcanic arc which can be understood only by the study of the relief both in the offshore and onshore area.

4. References

Dalabakis, P., Vougioukalakis, G., 1993. The Kefalos Tuff Ring (W. Kos): depositional mechanisms, vent position, and model of the evolution of the eruptive activity. *Bull. Geol. Soc. Greece,* 28, 259–273.

Nomikou, P. and Papanikolaou, D., 2000. Active Geodynamics at Nisyros, the eastern edge of the Aegean Volcanic Arc: emphasis on submarine surveys. *Proceedings of the 3rd Int. Conf. Geology East Mediterranean*, Sept. 1998, 97–103.

Nomikou, P., Papanikolaou, D., Alexandri, S., Ballas, D., 2004. New insights on the Kos–Nisyros volcanic field from the morphotectonic analysis of the swath bathymetric map. *Rapp. Comm. Int. Mer. Medit.* 37, 60.

Nomikou, P., 2004. Geodynamic of Dodecanese islands: Kos and Nisyros volcanic field. *PhD Thesis,* University of Athens, Department of Geology.

Papanikolaou, D., Lekkas, E.L., Sakelariou, D., 1991. Volcanic stratigraphy and evolution of the Nisyros volcano. *Bull. Geol. Soc. Greece,* 25, 405–419.

Papanikolaou, D., and collaborators, 1998. Monitoring of Seismic Activity along the Aegean Volcanic Arc: with focus on the eastern part of the arc in Kos and mainly Nisyros Islands. *Newsletter of the European Centre on Prevention and Forecasting of Earthquakes*, 2, 10-35.

Papanikolaou, D. and Nomikou, P., 2001. Tectonic structure and volcanic centres at the eastern edge of the Aegean Volcanic Arc around Nisyros Island. *Bull. Geol. Soc. Greece*, XXXIV/1, 289-296.

Pe-Piper, G., Piper, D.J.W., Perissoratis, C., 2005. Neotectonics of the Kos Plateau Tuff eruption of 161 ka, South Aegean Sea. *J. Volcanol. Geotherm. Res.* 139, 315–338.

Tibaldi, A., Pasquarè, F.A., Papanikolaou, D., Nomikou P., 2008. Discovery of a huge sector collapse at the Nisyros volcano, Greece, by on-land and offshore geological-structural data. *J. Volcanol. Geotherm. Res.* 177, 485-499.

Δελτίο της Ελληνικής Γεωλογικής Εταιρίας, 2010
Πρακτικά 12ου Διεθνούς Συνεδρίου
Πάτρα, Μάιος 2010

Bulletin of the Geological Society of Greece, 2010
Proceedings of the 12th International Congress
Patras, May, 2010

POST- ALPINE LATE PLIOCENE – MIDDLE PLEISTOCENE UPLIFTED MARINE SEQUENCES IN ZAKYNTHOS ISLAND

Papanikolaou M.[1], Papanikolaou D.[2], and Triantaphyllou M.[3]

[1] *University of Cambridge, Department of Geography, Cambridge Quaternary, CB2 3EN, Cambridge, UK, maria.papanikolaou@cantab.net*

[2] *University of Athens,Department of Dynamic Tectonic and Applied Geology, Panepistimioupoli, 15784, Athens, Greece, dpapan@geol.uoa.gr*

[3] *University of Athens,Department of Historical Geology-Paleontology,Panepistimioupoli, 15784, Athens, Greece, mtriant@geol.uoa.gr*

Abstract

Post-orogenic marine sequences crop out in two areas of Zakynthos Island: a) In Gerakas peninsula at the southeastern edge of the island and b) Along the coastal zone of central northern Zakynthos from Alikanas in the west to Zakynthos town in the east.

Detailed stratigraphic analysis of Gerakas area has shown the existence of three formations separated by two unconformities: 1) Gerakas Fm Q_1 comprising marls of Late Pliocene–Early Pleistocene age (2.8 – 0.9 Ma). 2) Kalogeras Fm Q_2 comprising littoral sandstones at the base (Q_{2a}), alternations of sandstones and marls in the middle (Q_{2b}) and marls (e.g. Porto Roma) in the upper part (Q_{2c}). The age of this formation is middle Pleistocene (0,8 – 0,5 Ma). 3) Agios Nikolaos Fm Q_3 comprising littoral sandstones.

Stratigraphic correlations between the two aforementioned areas have been made and equivalent stratigraphic formations, slightly differentiated in the central northern Zakynthos, have been identified. The upper unconformity is well pronounced in the area of Cape Gaidaros whereas the lower unconformity is often masked by debris accumulated along the base of the cliffs produced by the compact sandstones of Q_{2a} above the soft marls of the underlying Q_1. A remarkable increase in the thickness of the middle member Q_{2b} is observed in the northern part with respect to the equivalent Kalogeras Fm in Gerakas area. In contrast, the thickness of the upper member (Q_{2c}) is highly reduced in the limited northern outcrops compared to those of the southeastern exposure.

The Plio-Quaternary post-orogenic marine deposits in both regions represent the creation of the accommodation space formed by the westernmost extensional structure of the Hellenic arc. The two unconformities reflect sea-level changes during the Quaternary within an overall tectonic uplift of Zakynthos Island at the front of the Hellenic arc and trench system, while the entire post-orogenic sequence reflects the intense palaeoclimatic fluctuations of the Quaternary.

Key words: *stratigraphy, Quaternary, stratigraphic correlations, biostratigraphy, palaeoclimate.*

1. Introduction

Zakynthos Island is located at the front of the present-day Hellenic arc and trench system, which is

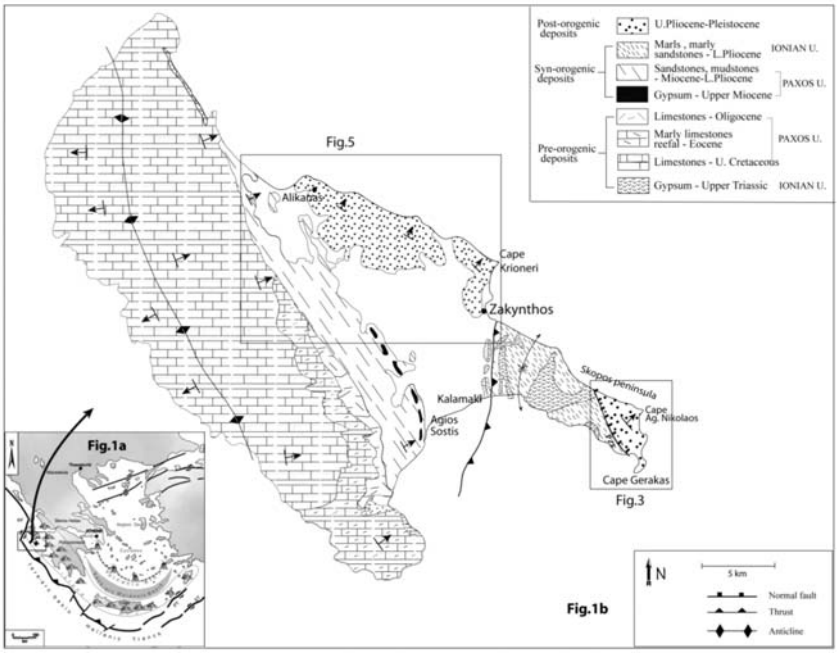

Fig. 1: a) Location of Zakynthos Island within the schematic representation of the Hellenic arc system, b) Geological map of Zakynthos island, modified after Underhill (1989).

formed along the convergent zone of the plate boundaries between the subducting African plate and the overriding Eurasian plate (Fig. 1a). The direction of slip and tectonic transport is trending northeast–southwest as this is deduced from tectonic data both onshore and offshore, from seismotectonic and geodetic data (e.g. McKenzie, 1972; Le Pichon and Angelier, 1979; McClusky *et al.,* 2000; Reilinger *et al.,* 2006). The Hellenic arc shows the characteristics of a thrust and fold belt which has evolved since early Tertiary by migration of the tectonic front from the inner part of the arc in the Aegean area to the more external part in the Ionian Sea. Tectonic units resulting from the different mechanical properties of the stratigraphic successions developed within the palaeogeography of the Hellenides have created nappes with westward tectonic emplacement bringing the more internal tectonic units over the more external (Aubouin et al, 1976). Thus, starting from the Hellenic trench in the west, which occupies depths around 4-5 km, we first observe the tectonic foreland of the Hellenic orogenic system which is known as Paxos unit. This unit is exposed only in the Ionian Islands of Zakynthos, Kephalonia, Lefkada and Paxos. The stratigraphic column comprises Jurassic–Oligocene carbonate rocks of platform and slope facies, followed by Miocene clastic sequences topped by the Messinian evaporites. The tectonism of the Paxos unit occurred during the Messinian–Early Pliocene when the Ionian nappe was emplaced on top of the Messinian evaporites (e.g. Skopos mountain in eastern Zakynthos) (Mercier *et al.,* 1972; Underhill, 1989).

The next eastward tectonic unit is the Ionian nappe, which is observed on top of the Paxos unit in the eastern Zakynthos, eastern Kephalonia and eastern Lefkada. This unit comprises a stratigraphic column of Triassic evaporites, Late Triassic–Early Jurassic shallow-water carbonates, Middle Jurassic–Oligocene pelagic limestones with cherts and Oligocene-Miocene flysch. The sole Ionian formation exposed in Zakynthos, at the southeast part of the island, is the Triassic evaporites.

The geological structure of Zakynhos is rather simple, comprising a geometric anticline affecting all the stratigraphic formations of the Paxos unit in the west and a complex structure of the thrusted Ionian Triassic formations in the east (Fig. 1b). The anticlinal axis of Paxos unit in Western Zakynthos is observed within the Late Cretaceous limestones. The western limp of the fold lies below sea-level towards the deep trench whereas the eastern limp forms the central zone of Zakynthos with a monoclinal structure of an average dip of 40° to the east observed through the Tertiary sequence from the Eocene to the Early Pliocene. The Miocene sedimentary sequence rests unconformably (e.g. Mirkou, 1974; Dermitzakis, 1978) on the underlying platform carbonates along the lower slopes of the Zakynthos anticline with pre-Miocene uplift and erosion of the Eocene and Oligocene formations. The main deformation occurred within the late Miocene – early Pliocene as this is shown by the similar dip of the strata (30° – 45°) both below and above the unconformity. The Ionian thrust has affected the top of the Paxos sequence in the Messinian – Early Pliocene and the syntectonic early Pliocene sediments, at the northern part of the Skopos peninsula, trailed by the Triassic allochthonous formations. The presence of the Triassic evaporites has contributed to the overall complexity with disharmonic deformation (Nikolaou, 1986; Underhill, 1988).

The post-orogenic sediments of Zakynthos are exposed in two areas: (i) In southeastern Zakynthos at the area of Vassilikos, from Cape Gerakas at the south to Cape Agios Nikolaos at the north, at low altitudes below 60 m, and (ii) Along the northern coastal zone from Alikanas in the west to Zakynthos town in the east, where the uplifted marine Plio-Pleistocene sediments form successive hills up to 200 m of elevation.

2. Materials and Methods

During this work the authors carried out geological mapping of the central-northern part of Zakynthos island (Fig. 1) and produced the nannofossil biozonation of ten samples collected from the uppermost beds of the Q_2 Fm marls (Figs 1, 5) (right below the Q_2/Q_3 unconformity) at Cape Gaidaros and Ag. Charalambos sections, probably the only locations where the upper unconformity of the post-orogenic sequence outcrops in the northern part of the island. The nannofossil study was performed on the counts of 300 placoliths using an optical polarizing light microscope and the biozonation was based on the analysis of the biostratigraphically important taxa such as *Pseudoemiliania lacunosa*, *Reticulofenestra asanoi*, *Gephyrocapsa* sp.3, *Gephyrocapsa* spp.>4 etc. Biozones were determined according to the biozonal scheme of Rio et al. (1990). The biostratigraphic analysis allowed lithostratigraphic correlation of the upper unconformity (essentially the topmost marls of the Q_2 Fm) to the equivalent southern post-orogenic outcrops in the Vassilikos area whose extensive published (Triantaphyllou, 1996; Papanikolaou, 2008) biostratigraphic (97 analysed stratigraphic levels) and magnetostratigraphic data (76 analysed stratigraphic levels) render it as a good reference composite sequence, almost 500-metres thick, for the post-orogenic Quaternary deposits of the island.

3. The Quaternary deposits in southeast Zakynthos

The marine Quaternary deposits at the southeast part (Vassilikos area) of the island and the rather conspicuous unconformity separating pelagic marls from the overlying coastal sandstones and calcarenites, e.g. at Gerakas beach, have been known quite a long time ago (e.g. Keraudren, 1970). However, detailed geological mapping by Dermitzakis et al. (1977) proved the existence of two similar unconformities within the Quaternary succession with the distinction of three formations (Figs 2, 3). Later studies (Triantaphyllou, 1993; Triantaphyllou et al., 1997; Duermeijer et al., 1999; Broadley et al., 2006; Papanikolaou, 2008) have better constrained the age of the above stratigraphic succession within the Quaternary and, with the support of biostratigraphy and magnetostratigraphy, have determined with accuracy the chronostratigraphic extension of each formation (Papanikolaou, 2008) (Fig. 4).

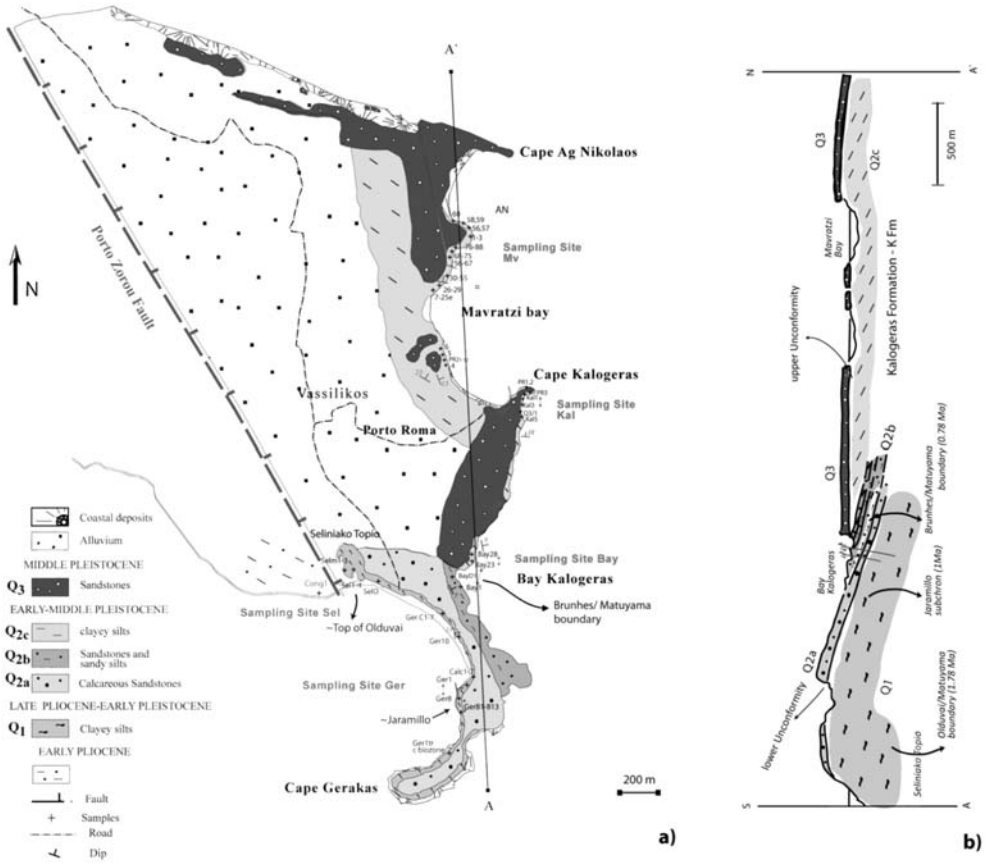

Fig. 2: a) Detailed geological map of southeast Zakynthos peninsula. b) geological section trending N-S (`A-A on the geological map) showing the succession of the three Quaternary post-orogenic formations Q_1, Q_2 and Q_3 and the approximate positions of the magnetostratigraphic events (Papanikolaou, 2008).

Fig. 3: Photo from Bay Kalogeras location showing the two members of Q_2 Formation, that is the alternations of sandstones and silts of Q_{2b} overlain by the silts of Q_{2c}, both unconformably overlain by the calcareous sandstones of Q_3 Formation.

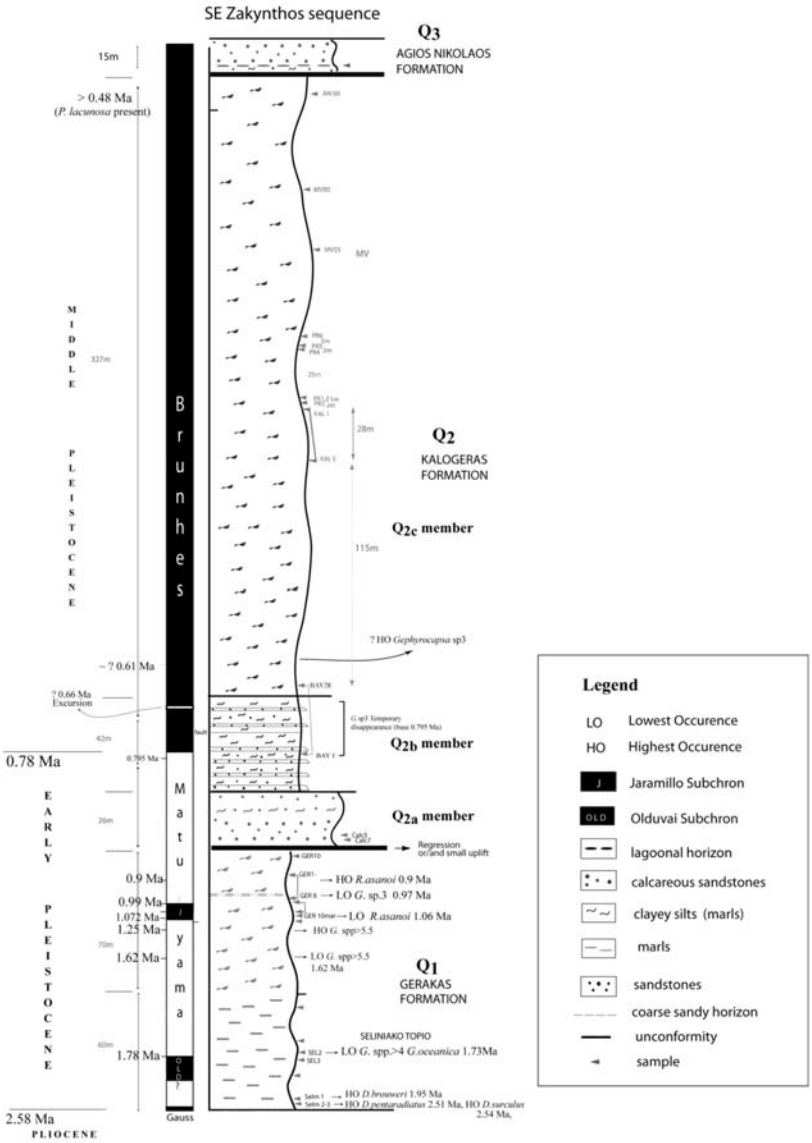

Fig. 4: Composite stratigraphic profile for the southeast peninsula formations. The palaeomagneto-biostratigraphical events are annotated (Papanikolaou, 2008).

In particular, from the bio- and chrono- stratigraphic point of view the southeast Zakynthos provides a composite section (~ 480-metres thick) (Fig.4) starting with Q_1 (Gerakas) Formation exposed at Seliniako Topio and along Gerakas beach at the south comprising 130-metres thick blue marls and clayey silts with the older exposed deposits assigned to nannofossil biozone MNN 16-17, therefore latemost Pliocene in age (~ 2.8 Ma) (Papanikolaou, 2008). The top of the Olduvai Subchron (1.8 Ma) was identified at the middle part of Q_1 Fm while a couple of metres higher the MNN19a/19b nannofossil biozones boundary was recognised.

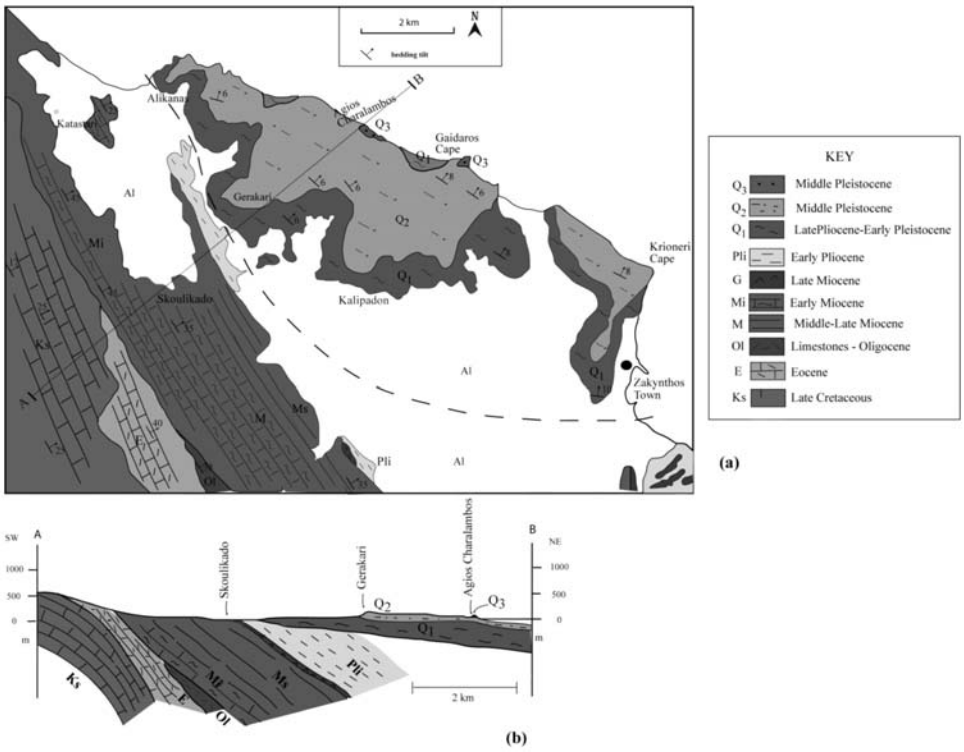

Fig. 5: a) geological map of the central-northern part of Zakynthos and b) geological section SW-NE trending (A-B on the geological map) showing the unconformably overlying post-orogenic deposits of Q_1, Q_2, Q_3 over the carbonate and clastic sequence of Paxos Unit.

The Jaramillo Subchron (1.07-0.99 Ma) was identified at the uppermost part of the formation and the top of the Q_1 Formation has an estimated age of around 0.85 Ma.

The composite section continues northward with Q_2 (Kalogeras) Formation which is initiated at the verge of the latemost Early Pleistocene (~0,8 Ma) and terminates in the Middle Pleistocene (~ 0,5 Ma). This formation consists of three members: a) $Q_{2a,}$ is 40-metres thick and consists of calcareous sandstones and calcarenites, b) Q_{2b} is 25-metres thick and comprises alternations of sandstones and silts, and c) Q_{2c} is around 320-metres thick and consists of silts and intercalations of sandy silts (Fig.3). The Matuyama/Brunhes boundary (0.78 Ma) was identified at the lower beds of the Q_{2b} member and the uppermost beds of the Q_{2c} member, slightly north of Porto Roma, were estimated to be within the nannofossil biozone MNN19f as *P. lacunosa* is present and therefore these beds are older than 0.48 Ma.

The onset of the overlying unconformable Q_3 (Agios Nikolaos) Fm more likely corresponds to the biozone MNN20, thus in the Middle Pleistocene (~ 0,45 Ma), yet its top remains chronologically undetermined (Papanikolaou, 2008).

The entire post-orogenic sequence in SE Zakynthos is bounded by the Porto Zorou fault in the west against the Early Pliocene and Triassic formations of the Skopos mountain, and thus the basal sediments of the post-orogenic series are intangible. On the other hand, the top of the Agios Nikolaos Fm dips under the present-day sea-level to the north extending to the present–day continental shelf of the

island. Thus, the uplifted Middle Pleistocene marine terrace represented by the Agios Nikolaos Fm may be stratigraphically followed by shelf sediments related to the Late Pleistocene and Holocene sea-level changes. This association can only be determined through combined onshore/offshore studies.

4. The Plio-Quaternary deposits of central - northern Zakynthos

The post-orogenic deposits of central-northern Zakynthos are shown in the map of Fig.5 produced during this work. The landscape behind Zakynthos town is a distinctive slightly inclined sedimentary sequence to the north with blue marls at the base capped by brown-reddish sandstones, which form a pronounced marine terrace with steep cliffs and the old castle on top. Biostratigraphic and magnetostratigraphic studies on the popular Citadelle section at Zakynthos town, have shown that it incorporates the Gelasian/Calabrian boundary (until recently Plio/Pleistocene boundary) (Bizon and Müller, 1977; Mirkou, 1987) and the latest Pliocene (Triantaphyllou 1993, 1997; Duermeijer et al., 1999; Suballyova et al., 1999).

In particular, the Citadelle section (Q_1) is more than 200-m thick, while younger beds of the sequence are extended to the north, at the Akrotirio Kryoneri, where the deposition of Q_1 marls persists, at least up to the nannofossil biozone MNN19d (well within the Early Pleistocene) (Triantaphyllou, 1993). The section had been previously studied and was assigned an age of the nannofossil biozone NN19 (Blanc-Vernet and Keraudren, 1969; Kowalcyk et al. 1977). The lower Pleistocene marls are unconformably overlain by around 12-metres thick calcareous sandstones with sandy-marly intercalations (Q_{2a}) which represent the lower unconformity of Gerakas sequence. This unconformity is morphologically apparent all along the southern slopes of the central-northern post-orogenic outcrop, from Zakynthos town in the east to Gerakari and Alikanas in the west, formed by the superposition of the Q_{2a} sandstones upon the Q_1 marls. Thus, the morphology is rather characteristic with the top of the hills being approximately 200 m high, and the geometrical surfaces of the overlying strata of the sandstones dipping with $6^\circ - 8^\circ$ to the north. The most characteristic area occurs near the two settlements of Gerakari village, where the Lower Gerakari is built on the blue marls and the Upper Gerakari on the overlying sandstones (Fig.5). The slightly inclined post-orogenic sedimentary sequence contrasts the structure of the underlying Late Cretaceous to Early Pliocene sedimentary formations which dip $30^\circ - 45^\circ$ to the northeast, as shown in the SW–NE geological section starting from the eastern slopes of the Zakynthos anticline in the southwest to the coastal zone in the northeast (Fig. 5b). The contact between the marls and the sandstones is rarely discernible because it is masked by large blocks and debris fallen from the sandstone cliffs on the underlying soft marls. The change of facies is very abrupt and it may be related to a small disconformity with a minor stratigraphic hiatus.

The upper unconformity (Q_2/Q_3) has been detected during this study in two small outcrops along the coastal zone in the areas of Cape Gaidaros (Fig. 6) and Agios Charalambos. At Cape Gaidaros the upper sandstones (Q_3) overlie, with a small angular unconformity, the alternations of sandstones and marls (Q_{2b}) (Fig.6a). More than 2 meters of marls (Q_{2c}) are missing below the unconformity due to erosion during the chronostratigraphic hiatus between the base of the upper sequence (Q_3) and the top of the middle sequence ($Q_{2b\text{-}c}$). Agios Charalambos section is exposed north of Zakynthos town, at the eastern coast, where the uppermost beds of the exposed 3 metres of marls (Q_{2c}) are correlated with the nannofossil biozone MNN19f (presence of *P.lacunosa*, absence of *Gephyrocapsa* sp. 3) (Middle Pleistocene), and are unconformably overlain by calcarenitic sandstones (Q_3).

The superposition of all three post-orogenic stratigraphic formations in the central-northern Zakynthos can be seen in a few coastal sections as is the case at the western cliffs at Cape Gaidaros where

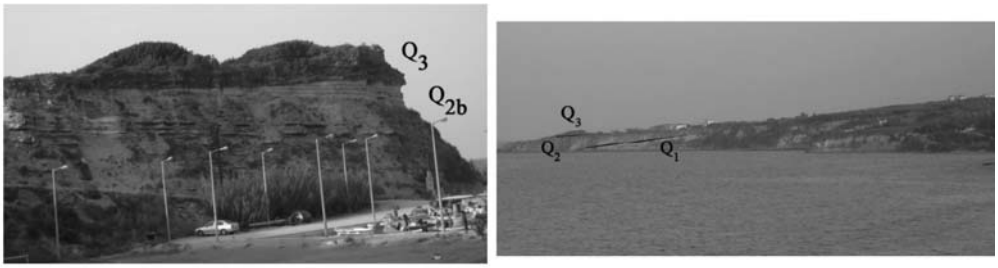

Fig. 6: a) photo showing the sandstones (Q_3) sitting unconformbaly on top of the alternations of marls and sandstones (Q_{2b}) at Cape Gaidaros area. b) photo showing the succession of all three post-orogenic formations at the north coasts of Zakynthos island. The marls of Q_1 Fm are underlain by the alternations of sandstones and marls of Q_2 Fm and the sandstones of Q_3 Fm are clearly overlain on top with an angular unconformity.

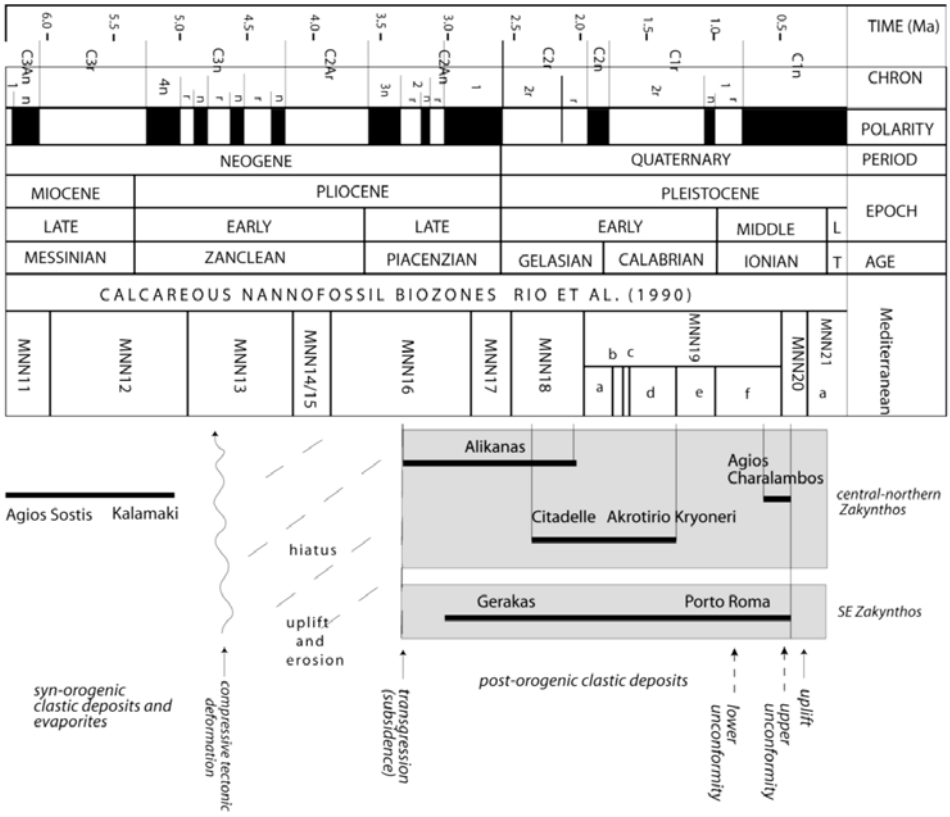

Fig. 7: Stratigraphic table-chart showing the stratigraphic ranges of selected (composite) sections. The chronostratigraphic chart is according to the newly ratified geological time scale (Gibbard et al., 2009).

the blue marls of Q_1 underlie the sandstones and alternations of sandstones and marls of Q_2 as well as some relics of the upper sandstones of Q_3 over Q_2 (Fig. 6b).

5. Discussion and Conclusions

Correlation of the post-orogenic formations of the central-northern part of the island with those of the southeastern part shows a general similarity with only small differences shown on the stratigraphic table-chart of Fig.7. Thus, both unconformities are present with similar characteristics, such as involving dramatic facies changes, except that the lower unconformity is a disconformity, whereas the upper unconformity clearly is an angular unconformity. Both unconformities form marine terraces with contrasting facies below and above.

The main difference between the two post-orogenic outcrop-groups (the south and the north) is the highly reduced thickness in the silts of the Q_{2c} member of only a few metres thick in the central-northern Zakynthos, as opposed to the hundred metres-thick marls in the SE Zakynthos, as seen in the area of Porto Roma. Inversely, the next difference between the two areas refers to the increased thickness of the middle member, $Q_{2b,}$ of the alternations of sandstones and silts, which is almost double in central-northern Zakynthos than that in the southeast. The recorded thickness of Agios Nikolaos Formation is only a few metres in central-northern Zakynthos whereas it exceeds 20 metres in the Agios Nikolaos Cape at southeast Zakynthos.

The compilation of single and composite sections shown in Fig.7 infers that the latest synorogenic deposits in Paxos unit, those of Agios Sostis and Kalamaki sections (Fig.1), are of latest Miocene–earliest Pliocene age (Dermitzakis, 1978; Duermeijer et al., 1999). In particular, these deposits display the Messinian transition from the clastic sequence into evaporitic beds (laminated gypsum, gypsum arenites, balatino, gypsum conglomerates), which are overlain by "trubi" limestones and calcareous marls. Consecutively, compressive deformation and tectonism occurs in the Early Pliocene as a result of the overthrusting Ionian nappe.

The marls sitting on top of the Ionian Triassic evaporites in Skopos peninsula are of Pliocene age, possibly Middle–Late Pliocene (Zellilidis et al., 1998), and are deformed by the evaporitic diapirism (Underhill, 1988). The lack of firm chronologies of these marls, which in this study are characterised as synorogenic deposits during the overthrust of the Ionian nappe, points to the need of further chronostratigraphical study.

The post-orogenic deposits in Zakynthos island are initiated as early as Late Pliocene with the marly deposits at northern Alikanas section being somewhat older (biozone MNN16a according to Triantaphyllou, 1993) than those of Gerakas (Seliniako Topio) (MNN 16-17, latemost Pliocene, Papanikolaou, 2008).

The unconformities of Zakynthos island, at least those at the southeast part of it, seem to reflect eustatic sea-level changes. So, the two unconformities more likely correlate with the sea-level fall of two severe northern hemisphere glaciations, namely the lower unconformity correlates with the cold Marine Isotope Stage (MIS) 22 while the upper unconformity with MIS 12 (Papanikolaou 2008). These eustatic sea-level changes are superimposed on a series of tectonic phases characteristic for this part of the Hellenic arc. Therefore, subsidence during the Late Pliocene-Early Pleistocene and uplift during the Middle Pleistocene is witnessed not only in the Zakynthos sequence but also in the coastal zone of Kyparissiakos Gulf where formations of `Calabrian` marls are unconformably overlain by Pleistocene sandstones. This infers that an extensional depositional centre along the Zakynthos channel and Kyparssiakos Gulf developed during the Late Pliocene–Middle Pleistocene and was

subsequently followed (in the Middle Pleistocene) by stronger uplift of the marine deposits in Western Peloponnesus (Papanikolaou et al., 2007) and weaker in eastern Zakynthos.

6. Acknowledgments

We would like to thank Valia Lianou, Ioanni Dimitriou, Ioanni Papanikolaou and Lena Broadley for their help during fieldwork. Maria Papanikolaou is also grateful to the State Scholarship Foundation (I.K.Y.) which made it possible to fulfil part of this work.

7. References

Aubouin, J., Bonneau, M., Davidson, L., Leboulenger, P., Matesco, S., Zambetakis, A., 1976. Esquisse structurale de l` arc egeen externe: des Dinarides aux Taurides. *Bull. Soc. Geol. France*, XVII, 2, 327-336.

Bizon, G. and Müller, G., 1977. La limite Pliocene-Pleistocene dans l` île de Zante. La coupe de la Citadelle. *C.R. Somm. Soc. Geol. Fr.*, 4, 212-216.

Bizon, G. and Mirkou, R., 1967. Les foraminifères planktoniques du Pliocène de l` île de Zante (Grèce occidentale). *Proc. First. Inter. Conf. Plantk. Microf.*, 1, 188, Genova.

Blanc-Vernet, L. and Keraudren, B., 1969. Sur la présence du Calabrien a Hyalinea balthica dans les Iles de Zakynthos et de Kephallinia (Grèce). *Bull. Musée d` Anthrop. prehist. Monaco*, 15, 91-106.

Broadley, L., Platzman, E., Platt, J., Papanikolaou, M., Matthews, S., 2006. Paleomagnetism and the tectonic evolution of the Ionian zone, northwestern Greece, in Y. Dilek, and S.Pavlides, eds., Postcollisional tectonics and magmatism in the Mediterranean region and Asia: *Geological Society of America Special Paper*, 409.

McClusky, S., Balassanian, S., Barka, A., Demir, C., Ergintav, S., Georgiev, I., Gurkan, O., Hamburger, M., Hurst, K., Kahle, H., Kastens, K., Kekelidze, G., King, R., Kotzev, V., Lenk, O., Mahmoud, S., Mishin, A., Nadariya, M., Ouzounis, A., Paradissis, D., Peter, Y., Prilepin, M., Reilinger, R., Sanli, I., Seeger, H., Tealeb, A., Toksoz, M.N., Veis, G., 2000. Global Positioning System constraints on plate kinematics and dynamics in the Eastern Mediterranean and Caucasus. *J. Geophys. Res.*, 105, B3, 5695–5719.

Dermitzakis, M., 1978. Stratigraphy and sedimentary History of the Miocene of Zakynthos (Ionian island, Greece). *Annales Géologiques des Pays Helleniques*, 29, 47–186.

Dermitzakis, M., Papanikolaou, D., Karotsieris, Z., 1977. The marine quaternary formations of SE Zakynthos island and their Paleogeographic implications. *VI Colloquim on the Geology of the Aegean Region*. Institute of Geological and Mining Research. Reprinted from Proceedings, I, 407–415.

Duermeijer, C.E., Krijgsmana, W., Langereis, C.G., Meulenkamp, J.E., Triantaphyllou, M.V., Zachariasse, W.J., 1999. A Late Pleistocene clockwise rotation phase of Zakynthos (Greece) and implications for the evolution of the western Aegean arc. *Earth and Planetary Science Letters,* 173, 315–331.

Gibbard, P.L., Head, M.J., Walker, M.J.C. and the Subcommission on Quaternary Stratigraphy, 2009. Formal ratification of the Quaternary System/Period and the Pleistocene Series/Epoch with a base at 2.58 *Ma. J. Quaternary Sci.*, ISSN 0267-8179.

McKenzie, D.P., 1972. Active tectonics of the Mediterranean region. *Geophys. J. R. Astron. Soc.*, 30, 109– 185.

Keraudren, B., 1970. Les Formations quaternaires marines de la Grèce. (Premiére Partie). *Bull. De Mus. D`Anthrop. Préhist. de Monaco*, 6–153.

Kowalczyk, G., Muller, C. and Winter, K.-P., 1977. Nannofossils of the Calabrian deposits of Zakinthos (Ionian Islands, Greece). *N. Jb. Geol. Palaont. Mh*, 5, 284-288.

LePichon, C. and Angelier, J. 1979. The Hellenic Arc and trench system: A key to the neotectonic evo-

lution of the Eastern Mediterranean area. *Tectonophysics*, 60, 1-42, 1979.

Mercier, J.L., Bousquet, B., Delibassis, N., Drakopoulos, J., Keraudren, B., Lemeille, F., Sorel, D., 1972. Deformations en compression dans le quaternaire de ravafes ioniens (Cephalonie, Grece). Donnes neotectoniques et sismiques. *C. R. de l` Acad. Sci.*, Paris, 175, 2307–2310.

Mirkou-Peripopoulou, R.M., 1974. Stratigraphie et geologie de la partie septentrionale de l` ile de Zanthe (Grece). *Ann. Geol. Pays Hellen.*, 26, 35-108.

Mirkou, R.-M., 1987. Foraminiferes benthiques plio-pleistocenes de Zanthe. Interpretation paleobathymetrique. *Eclogae geol. Helv.*, 80, 1, 109-125.

Nikolaou, C., 1986. Contribution to the study of Neogene and Geological concepts of the Ionian and Preapulian zone and their boundaries in relation to hydrocarbon exploration mainly on Strophades, Zakynthos and Cephallonia. *PhD thesis,* National and Kapodistrian University of Athens, 350, Athens.

Papanikolaou, D., Fountoulis, I., Metaxas, C., 2007. Active faults, deformation rates and Quaternary paleogeography at Kyparissiakos Gulf (SW Greece) deduced from onshore and offshore data. *Quaternary Int.*, 171–172, 14–30.

Papanikolaou, M.D., 2008. Quaternary palaeoenvironmental analysis of offshore and onshore marine sequences in the Eastern Mediterranean. *PhD thesis*, University of Cambridge.

Reilinger, R., McClusky, S., Vernant, P., Lawrence, S., Ergintav, S., Cakmak, R., Ozener, H., Kadirov, F., Guliev, I., Stepanyan, R., Nadariya, M., Hahubia, G., Mahmoud, S., Sakr, K., ArRajehi, A., Paradissis, D., Al-Aydrus, A., Prilepin, M., Guseva, T., Evren, E., Dmitrotsa, A., Filikov, S.V., Gomez, F., Al-Ghazzi, R., Karam, G., 2006. GPS constraints on continental deformation in the Africa-Arabia-Eurasia continental collision zone and implications for the dynamics of plate interactions. *J. Geophys. Res.*, 111, B05411.

Rio, D., Raffi, I., Villa, G., 1990. Pliocene-Pleistocene calcareous nannofossil distribution patterns in the western Mediterranean. In Kastens, K.A., Mascle, J., et al. (eds), *Proc. Sci. Results ODP*, 107, 513-532, ODP College Station, TX.

Suballyova, D., Tsaila-Monopolis, S., Gautier, F., 1999. Late Pliocene cyclicity on Zakynthos island (Eastern Mediterranean): Palynological evidence; in Wrenn, J.H., Suc, J.P. and Leroy, S.A.G. (eds). The Pliocene: Time of Change; *American Association of Stratigraphic Palynologists Foundation*, 93-101.

Triantaphyllou, M., 1993. Biostratigraphical and ecostratigraphical observations based on calcareous nannofossils of the Eastern Mediterranean Plio-Pleistocene deposits. *PhD thesis*, National and Kapodistrian University of Athens.

Triantaphyllou, M.V., 1998. Revised biostratigraphy based on calcareous nannofossils of the Citadelle section, Zakynthos island, Greece. *J. Nannoplankton Res.*, 20, 31-35.

Triantaphyllou, M., Drinia, H., Dermitzakis, M.D., 1997. The Plio-Pleistocene boundary in the Gerakas section, Zakynthos (Ionian Islands). *N. Jb. Geol. Palaont. Mh*, H.1, 12–30, Stuttgart.

Underhill, J.R., 1988. Triassic evaporites and Plio-Quaternary diapirism in western Greece. *Journal Geological Society of London*, 145, 269–282.

Underhill, J.R., 1989. Late Cenozoic deformation of the Hellenide foreland, western Greece. *Geological Society of America Bulletin*, 101, 613-634.

Zelilidis, A., Kontopoulos, N., Avramidis, P., Piper, D.J.W., 1998. Tectonic and sedimetnological evolution of the Pliocene-Quaternary basins of Zakynthos island, Greece: case study of the transition from compressional to extensional tectonics. *Basin Research*, 10, 393-408.

Δελτίο της Ελληνικής Γεωλογικής Εταιρίας, 2010
Πρακτικά 12ου Διεθνούς Συνεδρίου
Πάτρα, Μάιος 2010

Bulletin of the Geological Society of Greece, 2010
Proceedings of the 12th International Congress
Patras, May, 2010

THE GREEK CATALOGUE OF ACTIVE FAULTS AND DATABASE OF SEISMOGENIC SOURCES

Pavlides S.[1], Caputo R.[2], Sboras S.[2], Chatzipetros A.[1], Papathanasiou G.[1] and Valkaniotis S.[1]

[1] *Aristotle University of Thessaloniki, Department of Geology, Thessaloniki, Greece,*

[2] *University of Ferrara, Department of Earth Sciences, 44122 Ferrara, Italy, rcaputo@unife.it*

Abstract

The new reasearch project to create the Greek Catalogue of Active Faults and Database of Seismogenic Sources has three major goals: (i) the systematic collection of all available information concerning neotectonic, active and capable faults as well as broader seismogenic volumes within the Aegean Region; the search will be mainly based on geological and geophysical data; (ii) the quantification of the principal seismotectonic parameters of the different sources and the associated degree of uncertainty; (iii) to supply an integrated view of potentially damaging seismogenic sources for a better assessment of the Seismic Hazard of Greece. The informatic framework of the database follows that used for the Italian Database of Individual Seismogenic Sources (DISS). In this paper we present the architecture of the new Database of Active faults of the broader Aegean Area relative to Greece, the progress made up to present and the following activities yet to be accomplished.

Key words: *seismogenic fault, seismic hazard, Aegean.*

1. Introduction

The Aegean Region is among the most tectonically active areas of the Mediterranean realm and has the highest seismicity both in terms of frequency of events and magnitudes. It is not always straightforward to correlate seismicity with the causative fault(s). This is mainly due to two reasons: firstly, several crustal sectors of the Aegean, where historical or instrumental epicentres are located, are affected by a dense fault population bearing evidences of recent activity but with badly defined seismotectonic behaviour. Secondly, large sectors of the broader Aegean Region is covered by the sea, therefore lacking crucial field and direct observations. In the latter case, the typical geological approaches are generally replaced with geophysical and seismological investigations (detailed bathymetry, seismic profiles, microseismicity, focal mechanisms, etc), which can be proved very useful.

The principal aim of this research is to create a catalogue as more complete as possible of Greek Active Faults and a Database of Seismogenic Sources within the Aegean Region. Indeed, such data collection, informatization and parametrization of the principal seismotectonic parameters is lacking for the area though it represents the very basics for any realistic seismic hazard assessment.

A first attempt to create a database of Greek seismogenic faults was performed in the frame of the European project FAUST (Faults as a seismological tool; 1998-2000), where ca. 50 sources have been included for the whole Aegean Region. In contrast, the most recent and most complete map of

capable faults in Greece and the broader Aegean Region has been prepared by Pavlides et al. (2007).

Other attempts have been performed in the past, but all of them are lacking in both fault and data completeness. For example, simple map compilations cannot provide much information except the geographical location and a few geometrical characteristics of the faults, like length and dip direction. On the other hand, fault catalogues generally lack important additional data, like geometric, kinematic and seismological ones. In order to bypass the above problems and making the database a continuously updatable open-file, the choice of a GIS software environment was crucial. For our purposes we used the well tested, time-proof, worldwide acknowledged database structure and method proposed by the Istituto Nazionale di Geofisica e Volcanologia (INGV) for the Italian Database of Individual Seismogenic Sources (DISS), which represents the result of almost twenty years research experience of its Working Group (Valensise and Pantosti, 2001). The DISS uses many basic levels of data that can be either independent or directly related. Among the most important ones are the Individual Seismogenic Sources (ISS) and the Composite Seismogenic Sources (CSS) (see Basili et al., 2008, for a more detailed description of the software).

- "Individual Seismogenic Sources" (ISS) are obtained from geological and geophysical data and are characterized by a full set of geometric (strike, dip, length, width and depth), kinematic (rake) and seismological-palaeoseismological parameters (average displacement per event, magnitude, slip rate, return period) and by a rating of the associated uncertainties. ISSs are assumed to exhibit "characteristic" behaviour with respect to rupture length/width and expected mean and maximum magnitude. They are tested against worldwide databases for internal consistence in terms of length, width, average displacement and magnitude. This category of sources favours accuracy of the information supplied over completeness of the sources themselves. As such, they can be used for deterministic assessment of seismic hazard, for calculating earthquake and tsunami scenarios, and for tectonic and geodynamic investigations.

- "Composite Seismogenic Sources" (CSS) are still obtained from geological and geophysical data and characterized by geometric (strike, dip, width, depth) and kinematic (rake) parameters, but their length is more loosely defined and spans two or more Individual Sources. They are not assumed to be capable of a specific earthquake but their potential can be derived from existing earthquake catalogues. A CSS is essentially inferred on the basis of regional surface and subsurface geological data, that are exploited well beyond the simple identification of active faults or youthful tectonic features. Opposite to the previous case, this category of sources favours completeness of the record of potential earthquake sources over accuracy of source description. In conjunction with seismicity and modern strain data, CSSs can thus be used for regional probabilistic seismic hazard assessment and for investigating large-scale geodynamic processes.

Before preparing the catalogue and starting completing the database it is also useful to take into account the fault classification suggested by Pavlides et al. (2007). The major criteria are based on the degree of activity of the tectonic structures, thus allowing to distinguish six fault types:

1. Seismic faults: faults associated with significant earthquakes;
2. Holocene active faults: with documented displacement during the last 10 ka and relatively high slip-rate;
3. Late Quaternary active faults: with documented displacement during the last 40 ka, corresponding to the maximum time interval possibly dated with the 14C method;
4. Quaternary active faults: with documented displacement during the Quaternary (2.6 Ma) and genrally characterized by a low-to-medium slip-rate;
5. Capable faults of uncertain age:with geometrical structure and kinematics favourably oriented

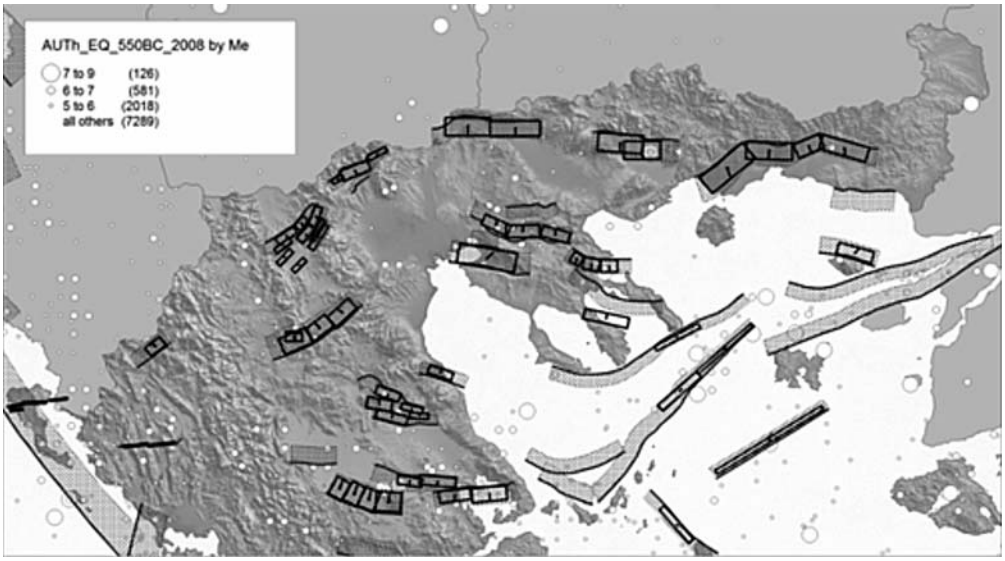

Fig. 1: The Greek Database of Active Faults for the North Aegean area.

in the frame of the present-day stress field, which could be possibly re-activated during a future earthquake;

6. Faults of uncertain activity: possibly inactive.

2. Geological setting

The broader Aegean Region is among the most tectonically active areas of the Mediterranean realm. The tectonic regime is rather complex producing earthquakes with many different orientations of nodal planes and a large variety of fault types both in terms of dimension and kinematics. Three are the dominating large-scale tectonic structures in the area. i) The Hellenic subduction zone, where the African plate is subducted underneath the Aegean; it is associated with a compressive stress field all along the arc. ii) The Inner Aegean region characterized by widespread, mainly N-S trending, crustal extension. iii) The North Aegean Trough (NAT) which represents a transtensional stress regime due to overlapping contribution of the western propagation of the purely strike-slip North Anatolian Fault and the Aegean extension. The combination of all previous tectonic processes produces an intense lithospheric fracturing and the formation of a large number of active faults.

3. Methodology

The procedure follows that proposed for DISS and it is based on MapInfo GIS software. It consists of two correlated software packages: the first is for managing the geometric and kinematic parameters of the ISSs, while the second one is the real core of the database providing the possibility of managing the compelte informatio of each ISS as well as controlling and managing the whole CSS attributes. The most common topographical background we use is a DEM obtained from the SRTM mission with 90x70 m pixel size, while when more detail is required, the 1:50000 scale topographic maps of HMGS or specific satellite imageries are used. For the offshore regions, bathymetric maps and DEMs are used from any available data source (e.g. the Marine Geoscience Data System – MGDS). The whole dataset is referenced to the World Geographical System datum WGS84.

The details about how faults are graphically represented in the database and what are the attributes of every information field can be found in the paper of Basili et al. (2008).

Regarding the qualitative part of the database, all available literature data for each seismogenic source are collected and investigated through a critical revision before entering the many information fields. Original investigations have been also carried out, and will be in the future, for structures with ambiguous or lacking data.

The data included in the database are separated in four major information levels. An interactive selection of a fault allows exploring the data in html formats. The first level of information is the "Source Info Summary" which includes all the parametrized information (geometric, kinematic and seismotectonic) of the fault and information about possibly associated earthquakes. Each of the information field is followed by a short comment concerning the origin of the data. The second level is the "Commentary" that contains comments, open questions and summaries of the considered literature. The third level is the "References", a list of all the related literature used to describe the particular fault. Each reference entry can be also linked with the appropriate electronic document, usually in pdf format. The "Pictures" level is the last one including figures and photographs relevant for the specific fault which can originate either from literature or from any personal collection.

The principal criteria for evaluating the seismogenic potential of a fault are briefly listed in the following.

Geological and morphotectonic features: surface morphology can be strongly affected by active tectonics and hence many such features can be recognized and characterized based on field work and laboratory analyses. Among the most important and commonly used morphotectonic features are fault scarps, triangular facets and the tilting of Quaternary sediments. The age and type of stratigraphic unit(s) affected by a fault scarp or a fault trace are crucial for estimating and constraining the last re-activation of a tectonic structure. The incision and displacement of very recent sediments is a highly important indicator of recent activity. At this regard, the contribution of palaeoseismological investigations is essential (e.g. McCalpin, 1996). A less explicit indicator is the occurrence of a free-face developed in bedrock. In this case, it is not the age of the affected rocks, usually Palaeozoic or Mesozoic in the Greek territory, to be indicative of a recent activity, but the freshness of the morphological feature as well as the geometry and texture of the fault scarp. Steep, sleek and polished surfaces indicate a young fault. Even difference in colour can be a guideline for estimating successive co-seismic re-activations by linear morphogenic events (e.g. Caputo et al., 2004; 2006). On the other hand, metamorphic rocks show poor evidence not only because of their greater erodibility, but also due to the internal fabric, like schistosity, that could generate by simple differential erosion morphological features similar to the tectonic ones. Additionally, with the aid of remote sensing analyses and dedicated software also many qualitative and quantitative morphometric parameters are generally considered, like the drainage pattern, stream orders, etc. (e.g. Goldsworthy and Jackson, 2000; Zovoili et al., 2004).

Seismic activity: it can occur either as localised major earthquakes (moderate to strong) or diffuse microseismicity (e.g. Hatzfeld et al., 1995; 2000; Kementzetzidou, 1996; Pavlides et al., 2007). It is useful to separate the major events as historical or instrumental ones. The former start with the 550 BC event (e.g. Guidoboni et al., 1994; Papazachos and Papazachou, 2003; Ambraseys, 2009) and can be used even for events from the 20th century. The completeness and precision of events before the 19th century is from poor to fair (Pavlides et al., 2007) making often difficult the correlation between earthquakes and causative fault. The instrumental period for the Aegean Region is less than 100 years, but it probably starts to be sufficiently accurate only after the 1970s when the Greek seis-

mographic network was definitely improved. A typical example is the 1954, Sophades earthquake which was produced by a NNE-NE dipping fault according to geological investigations (Ambraseys and Jackson, 1990; Caputo, 1995; Pavlides, 1993) and not by a N-S up to NW-SE trending plane as suggested by the focal mechanism proposed by McKenzie (1972).

Also *geophysical surveys* based on different methodological approaches (electrical resistivity tomographies, ground penetrating radar, high-resolution seismic profiles, etc.) can provide useful information and constraints for characterizing an active fault (e.g. Caputo et al., 2003; Oliveto et al., 2004; Karastathis et al., 2007).

Regional geodynamic setting: the orientation of the fault plane with respect to the active stress field of the broader area is strong evidence (Pavlides et al., 2007). However, this approach could be somehow misleading in specific areas, since the tectonic regime is quite complex showing lateral variations or debated reconstructions by different authors. Areas like the northeastern Aegean or the Ionian Sea belong to this complex regime.

4. Discussion

Within the investigated area we have already recognized, characterized and parametrized almost 40 CSSs and about 60 ISSs. All ISSs show evidences of Late Pleistocene-Holocene activity andsometimes also the occurrence of past 'linear morphogenic earthquakes' (sensu Caputo, 2005) as inferred, for example, from palaeoseismological trenches, archaeoseismological investigations or detailed morphotectonic mapping. In some case, a moderate to strong earthquake has occurred in the last few decades, therefore allowing to investigate the re-activated fault with a great detail, based on a modern scientific approach, and especially generating a rich seismological information associated with the mainshock. In particular, recent instrumental data commonly provide crucial constraints about focal depth, magnitude, focal mechanism (i.e. strike, dip and rake) and aftershock distribution. This additional 'co-seismic' information is obviously not available for all the other geologically-based seismogenic sources (ISSs) where no historical or instrumental earthquakes have been recorded. Accordingly, these faults represent a crucial test for the database and especially for its possible applications in seismic hazard assessment analyses. They have been independently investigated according to the two approaches, in one case the available 'co-seismic' constraints of the principal seismotectonic parameters have been ignored and mainly the cumulative effects of Late Quaternary morphogenic events have been considered; in the other case this additional co-seismic information has been included.

A first comparison shows an important mismatch between the two solutions and a deeper analysis on this difference will suggest a better strategy for the future.

The three following examples can help emphasizing the difference:

1. The Kozani CSS (Western Macedonia) was partly re-activated in 1995 by a Mw = 6.6 event (Papazachos et al., 1995). Using 'only' all geological data, including stratigraphic, structural, morphotectonic and palaeoseismological ones (Pavlides et al., 1995; Mountrakis et al., 1998; Doutsos and Koukouvelas, 1998), three distinct fault segments, each potentially capable of generating moderate-to-strong events, can be recognized (Fig. 2a). In contrast, taking into account the 'co-seismic' information for constraining the principal seismotectonic parameters, a single major ISS can be defined (Fig. 2b). In this specific case, it is obvious that the western segment boundary, which was geologically inferred, was not strong enough to stop the propagation during the 1995 event that eventually re-activated two fault segments. On the other hand,

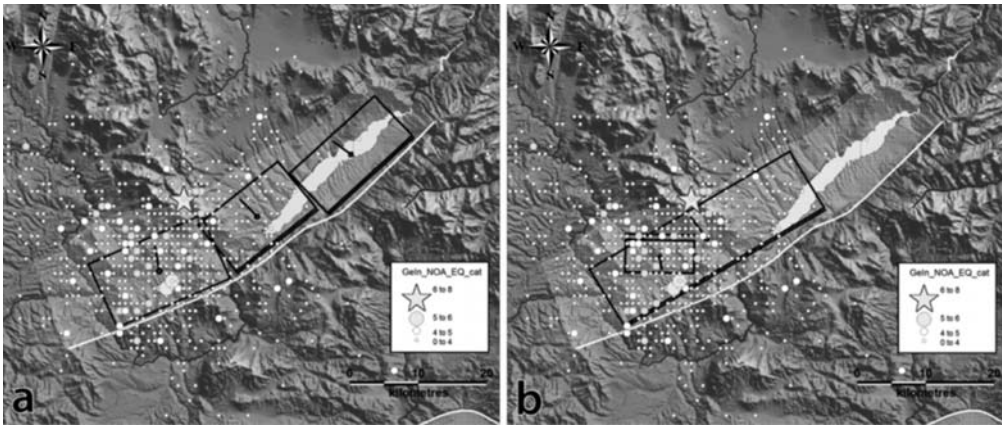

Fig. 2: The Kozani CSS (Western Macedonia) showing the three distinct fault segments, each capable of moderate-to-strong events, recognized based on all geological information relative to the cumulative evidence of Late Quaternary activity (a) and the seismogenic source as constrained considering the 'co-seismic' information associated with the 1995, Mw = 6.6, earthquake (b). See text for further explanations.

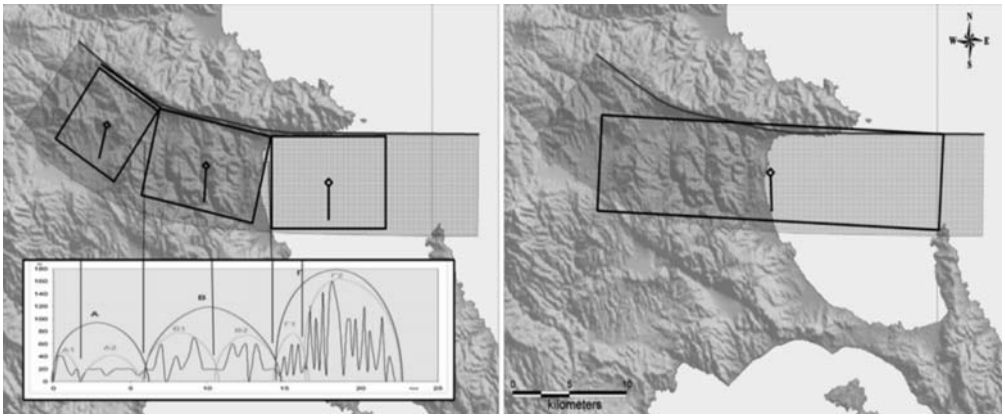

Fig. 3: The Varvara-Stratoni Fault (Chalkidiki peninsula, Central Macedonia) showing the three distinct fault segments, each capable of moderate(-to-strong) events, recognized based on all geological information relative to the cumulative evidence of Late Quaternary activity (a) and the seismogenic source as constrained considering the 'co-seismic' information associated with the 1932, Mw = 7.0, earthquake (b). See text for further explanations.

there is not apparent field evidence for why the third eastern segment did not rupture being separated by a similar segment boundary. It remains an open question whether the earthquake could have ruptured also the third segment or if this occurred in the past (or it will in the future), therefore causing an even more destructive larger magnitude event.

2. The second example is represented by the 1932, Ierissos earthquake (Mw = 7.0) that re-activated the Varvara-Stratoni Fault (Fig. 3). Also in this case, a detailed morphotectonic analysis (Michailidou et al., 2005) suggests the occurrence of three segments characterized by a different cumulative slip history and separated by angular boundaries. Accordingly, whether the geological evidence would suggest three capable faults, the co-seismic information indicates a unique major seismogenic source.

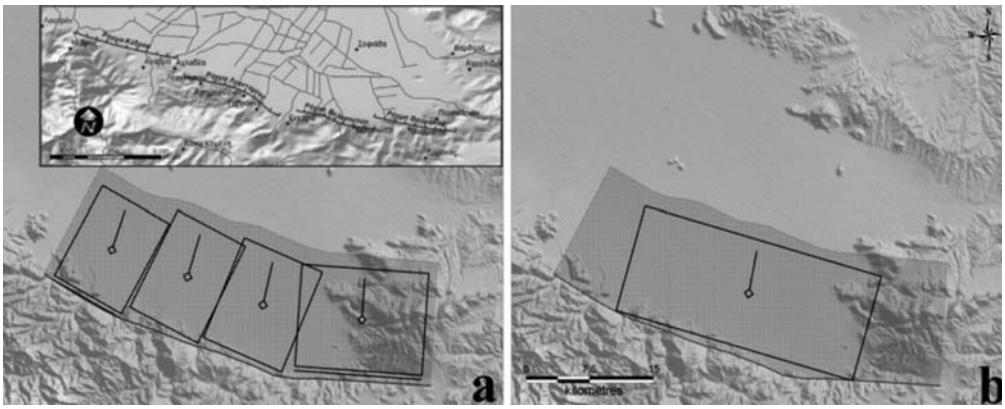

Fig. 4: (a) The Domokos CSS (Southern Thessaly) showing the four distinct fault segments, each capable of moderate-to-strong events, recognized based on all geological information relative to the cumulative evidence of Late Quaternary activity. (b) The seismogenic source as constrained considering the 'co-seismic' information associated with the 1954, Mw = 7.0, earthquake. See text for further explanations.

3. The third case study refers to the 1954, Sophades earthquake (Mw = 7.0), when the Domokos CSS was partly activated (Fig. 4). The field observations documented by Papastamatiou and Mouyaris (1986), the geological and morphotectonic mapping by Caputo (1990; 1995) and Caputo and Pavlides (1993) and the detailed morphotectonic analysis of Valkaniotis (2005) suggest the occurrence of four left-stepping segments forming angular boundaries.

5. Concluding remarks

A large part of the Northern Aegean region has been studied, accomplishing the following targets:

The geographic location of about 40 Composite Seismogenic Sources (CSS) with (almost) complete parametrization ("Source Info Summary" information level) have been already prepared.

The geographic location and further analysis of 60 Individual Seismogenic Sources (ISS), with most of the information fields, comments, open questions, summaries, pictures and references have been completed.

The compilation of the database for the other sectors of the broader Aegean Region is in progress. Many of the faults under investigation and associated with specific historical or instrumental earthquakes (ISS) have been already recognized and mapped.

As far as other Aegean CSSs have geological and tectonic settings comparable to the Kozani and Ierissos case studies, showing the occurrence of geologically distinct fault segments, and reminding that the "characteristic behaviour" of the ISSs is an assumption, it is obvious the importance and need of more specific and careful investigations for improving the database.

6. Acknowledgments

Thanks to Roberto Basili and Gianluca Valensise (INGV, Rome) for providing the DISS software, their continuous assistance and discussions on seismogenic faults issues. Financial assistance provided by the Italian Ministery of University and Research to SS and RC is acknowledged. This is a contribution to the SHARE EU Project (Greek scientific resp. SP).

7. References

Ambraseys, N., 2009. Earthquakes in the Mediterranean and Middle East: A Multidisciplinary Study of Seismicity up to 1900. Cambridge University Press, pp. 968.

Ambraseys, N.N. and Jackson, J.A., 1990. Seismicity and associated strain of central Greece between 1890 and 1988. *Geophys. J. Int.*, 101, 663-708.

Basili, R., Valensise, G., Vannoli, P., Burrato, P., Fracassi, U., Mariano, S., Tiberti, M.M., Boschi, E., 2008. The database of individual seismogenic sources (DISS), version 3: summarizing 20 years of research on Italy's Earthquake Geology. *Tectonophys.*, 453, 20-43.

Caputo, R., 1990. *Geological and structural study of the recent and active brittle deformation of the Neogene-Quaternary basins of Thessaly (Greece)*. Scientific Annals, 12, Aristotle University of Thessaloniki, 2 vol., 5 encl., 252 pp., Thessaloniki.

Caputo, R., 1995. Inference of a seismic gap from geological data: Thessaly (Central Greece) as a case study. *Ann. Geofisica*, 38, 1-19.

Caputo, R., 2005. Ground effects of large morphogenic earthquakes. *J. Geodyn.*, 40(2-3), 113-118.

Caputo, R. and Helly, B., 2005. The Holocene activity of the Rodia Fault, Central Greece. *J. Geodyn.*, 40, 153-169, doi:10.1016/j.jog.2005.07.004

Caputo, R. and Pavlides, S., 1993. Late Cainozoic geodynamic evolution of Thessaly and surroundings (central-northern Greece). *Tectonophysics*, 223(3-4), 339-362.

Caputo, R., Piscitelli, S., Oliveto, A., Rizzo, E., Lapenna, V., 2003. The use of electrical resistivity tomography in Active Tectonic. Examples from the Tyrnavos Basin, Greece. *J. Geodyn.*, 36, 1-2, 19-35.

Caputo, R., Helly, B., Pavlides, S. and Papadopoulos G., 2004. Palaeoseismological investigation of the Tyrnavos Fault (Thessaly, Central Greece). *Tectonophysics*, 394, 1-20, doi:10.1016/j.tecto.2004.07.047

Caputo, R., Monaco, C., Tortorici, L., 2006. Multi-seismic cycle deformation rates from Holocene normal fault scarps on Crete (Greece). *Terra Nova*, 18, 181-190, doi: 10.1111/j.1365-3121.2006.00678.x

Doutsos, T. and Koukouvelas, I., 1998. Fractal analysis of normal faults in northwestern Aegean area, Greece. *J. Geodyn.*, 26, 197-216.

Goldsworthy, M. and Jackson, J., 2000. Active normal fault evolution in Greece revealed by geomorphology and drainage patterns. *J. Geol. Soc. London*, 157, 967-981.

Guidoboni, E., Comastri, A. and Traina, G., 1994. *Catalogue of ancient earthquakes in the Mediterranean area up to 10th century*. ING-SGA, Bologna, 504 pp.

Hatzfeld, D., Kassaras, I., Panagiotopoulos, D., Amorese, D., Makropoulos, K., Karakaisis, G. and Coutant, O., 1995. Microseismicity and strain pattern in northwestern Greece. *Tectonics*, 14, 773-785.

Hatzfeld, D., Karakostas, V., Ziazia, M., Kassaras, I., Papadimitriou, E., Makropoulos, K., Voulgaris, N. and Papaioannou, C., 2000. Microseismicity and faulting geometry in the Gulf of Corinth (Greece). *Geophys. J. Int.*, 141, 438-456.

Karastathis, V.K., Ganas, A., Makris, J., Papoulia, J., Dafnis, P., Gerolymatou, E. and Drakatos, G., 2007. The application of shallow seismic techniques in the study of active faults: The Atalanti normal fault, central Greece. *J. Appl. Geophys.*, 62, 215-233.

Kementzetzidou, D., 1996. *Étude sismotectonique du système Thessalie-îles Sporades (Grèce centrale)*. Ph.D. thesis, Université J. Fourier-Grenoble I, 151 pp., Grenoble.

McCalpin, J.P., (editor) 1996. *Paleoseismology*. Academic Press, 588 pp., San Diego.

McKenzie, D.P. 1972. Active tectonics of the Mediterranean Region. *Geophys. J. Royal astron. Soc. London*, 30, 109-185.

Michailidou, A., Chatzipetros, A. and Pavlides, S., 2005. Quantitative analysis –tectonic geomorfology

indicators of the faults at the region of Stratoni – Varvara Gomati – M. Panagia in the Eastern Chalkidiki. *Bull. Geol. Soc. Greece*, 38, pp. 14-29.

Mountrakis, D., Pavlides, S., Zouros, N., Astaras, T. and Chatzipetros, A., 1998. Seismic fault geometry and kinematics of the 13 May 1995 Western Macedonia (Greece) earthquake. *J. Geodyn.*, 26, 175-196.

Oliveto, A.N., Mucciarelli, M. and Caputo, R., 2004. HVSR prospections in multi-layered environments: an example from the Tyrnavos Basin (Greece). *J. Seismol.*, 8, 395-406.

Papastamatiou, D. and Mouyaris, N., 1986. The earthquake of April 30, 1954, in Sophades (Central Greece). *Geophys. J. R. astron. Soc.*, 87, 885-895.

Papazachos, B. and Papazachou, C., 2003. *The earthquakes of Greece*, Editions ZITI, Thessaloniki, 304.

Papazachos, B.C., Panagiotopoulos, D.G., Scordilis, E.M., Karakaisis, G.F., Papaioannou, Ch.A., Karakostas, B.G., Papadimitriou, E.E., Kiratzi, A.A., Hatzidimitriou, P.M., Leventakis, G.N., Voidomatis, Ph.S., Peftitselis, K.J. and Tsapanos, T.M., 1995. Focal properties of the 13th May 1995 large (Ms = 6.6) Earthquake in the Kozani area (North Greece), XV Congr. Carpatho-Balkan Geological Association, September 17-20, 1995, Athens, Greece, *Proceedings*, 96-106.

Pavlides, S. 1993. Active faulting in multi-fractured seismogenic areas; examples from Greece. *Z. Geomorph. N.F.*, 94, 57-72.

Pavlides, S.B, Zouros, N.C, Chatzipetros, A.A., Kostopoulos. D.S. and Mountrakis, D.M., 1995. The 13 May 1995 western Macedonia, Greece (Kozani Grevena) earthquake; preliminary results, *Terra Nova*, 7, 544-549.

Pavlides, S.B., Valkaniotis, S. and Chatzipetros, A., 2007. Seismically capable faults in Greece and their use in seismic hazard assessment. 4th Int. Conf. Earthq. Geotech. Eng., June 25-28, 2007, Thessaloniki, *Proceedings*, paper n. 1609.

Valensise, G. and Pantosti, D., (Eds) 2001. Database of potential sources for earthquakes larger than M 5.5 in Italy. *Ann. Geofisica*, 44, 797-807.

Valkaniotis, S., 2005. *Active faults investigation of Western Thessaly*. MSc. thesis, Aristotle University of Thessaloniki, pp. 118 [in Greek].

Zovoili, E., Konstantinidi, E. and Koukouvelas, I.K., 2004. Tectonic geomorphology of escarpments: the cases of Kompotades and Nea Anchialos faults. *Bull. Geol. Soc. Greece*, XXXVI, 1716-1725.

Δελτίο της Ελληνικής Γεωλογικής Εταιρίας, 2010
Πρακτικά 12ου Διεθνούς Συνεδρίου
Πάτρα, Μάιος 2010

Bulletin of the Geological Society of Greece, 2010
Proceedings of the 12th International Congress
Patras, May, 2010

FAULTING DEFORMATION OF THE MESOHELLENIC TROUGH IN THE KASTORIA-NESTORION REGION (WESTERN MACEDONIA, GREECE)

Tranos M. D.[1], Mountrakis D. M.[1], Papazachos, C. B.[2], Karagianni, E.[2], and Vamvakaris, D.[2]

[1] *Aristotle University of Thessaloniki, Department of Geology, 54124 Thessaloniki, Greece, tranos@geo.gr, dmountra@geo.auth.gr*

[2] *Aristotle University of Thessaloniki, Department of Geophysics, 54124 Thessaloniki, Greece, cpapazachos@geo.auth.gr, elkarag@geo.auth.gr, dom@geo.auth.gr*

Abstract

The Kastoria-Nestorion region, which belongs to the Tertiary MesoHellenic Trough (MHT), is a low relief NW-SE trending intermountainous basin filled with Tertiary molasse-type sedimentary rocks and nowadays drained by the Aliakmnonas River and its tributaries. In the present work, the large fault zones in the region and the general fault pattern are defined, mapped and described with the aid of satellite images. In addition, a large number of fault-slip data from the mesoscale exposed faults has been recorded, in order to better understand the faulting geometry and kinematics of the region. The stress-inversion analysis of these fault-slip data in comparison with earthquake fault-plane solution information permits us to define the stress regimes imposed to the region from the Late Tertiary up to the present and to correlate them with the late orogenic and post-orogenic deformation of the Hellenic orogen. In particular, five stress regimes have been defined from which the former two (D1 and D2) are related to the late collisional processes between the Apulia and Eurasia plates, the next two events (D3 and D4) are related to the present-day Hellenic subduction zone, whereas the last D5 event which is the active deformation of the region appears as an intra-continental or intra-plate deformation more related with the Adria-Eurasia ongoing convergence rather with the Hellenic subduction zone.

Key words: *stress regime, strike-slip faulting, extension, transpression, neotectonics.*

1. Introduction

The Hellenic orogen constitutes part of the overriding Eurasia plate (Fig. 1) as the latter collided with the Apulia plate during Tertiary and evolved to the present Africa-Eurasia convergent plate system in the eastern Mediterranean (Mountrakis, 2006). Since Serravalian time, it is under a widely distributed extension (Le Pichon and Angelier, 1979) as it is suggested by seismological (McKenzie 1970, 1972; Papazachos et al., 1992) and neotectonic studies (Mountrakis et al. 2006; Kilias et al. 2008) and strain rates estimated by GPS measurements (Reilinger 1997; Kahle et al., 1998; McClusky et al. 2000). The present geotectonic regime, however, is much more complicated since this extension should accommodate: (a) the westward motion of Anatolia, (b) the retreating subduction of the Eastern Mediterranean lithosphere under Eurasia along the Hellenic Trench, and (c) the on-

going continental collision between Adria and Eurasia (north of the Cephalonia Transform Fault), giving rise to the fold mountains of NW Greece and Albania.

Recently, attempts have been made to differentiate the Greek mainland into different domains regarding the stress regime and faulting deformational style (Doutsos and Kokkalas 2001, Papazachos and Kiratzi, 1996, Papazachos et al. 2001), but some of these results are under debate for several areas which are still poorly investigated.

One such area is the Kastoria-Nestorion region in NW-most Macedonia, which lies in the inner part of the Albanian-Pindos cordillera, far from the Hellenic subduction zone, and although it is characterized by low seismicity is crosscut by several big faults. Moreover, the large 1995 Grevena-Kozani earthquake of magnitude M = 6.5 that occurred ca. 55 km SE of the study area as well as historical seismicity of the broader area (Papazachos and Papazachou 2003) verify that this characterization does not preclude the occurrence of large earthquakes in western Macedonia. Therefore, the main target of this paper is to provide the basic information on the faulting deformation and the active stress regime of this area, in order to better understand the neotectonic deformation and processes of the overriding Eurasia plate.

2. Geological setting

The Kastoria-Nestorion region is located in the Western Macedonia and the inner part of the Albanian-Pindos cordillera formed by the west-vergent thrust sheets, driven by the convergence and collision of the Apulia and Eurasia-Pelagonian continental blocks during the Late Cretaceous–Eocene. It is an intermountainous area of low relief with respect to the high mountains in the west (Voios or Grammos Mt) and is drained by the large Aliakmonas River and its tributaries.

In this region, the Pindos cordillera is made up by Pindos and SubPelagonian isopic zones. The former (Crusta-Cukali zone in Albania) is a typical fold-and-thrust-belt of Mesozoic and Early Tertiary sedimentary rocks with successive thrusts and folds that verge towards WSW.

The above mentioned zones are covered in the Kastoria-Nestorion region by the Tertiary sedimentary molasse-type rocks that had filled up the NNW-SSE trending Mesohellenic Trough (MHT) (Fig. 1); a late-orogenic basin of c. 150km length and 30km width formed during the Late Eocene-Miocene, i.e. the late stages of the main Tertiary Alpine orogenic processes. The MHT was developed along the inner slopes of the Albanian-Pindos cordillera over the ophiolites and Cretaceous limestones rocks that placed into the SubPelagonian zone (Mountrakis 1986). It was filled with up to 4 km marine turbidites, siliclastic shelf and terrigenous deposits that grouped into five main formations (Brunn 1956): (a) Krania Fm (of Late Eocene age), (b) Eptachori Fm (of Middle-Late Oligocene age), (c) Pentalofos Fm (of Aquitanian age), (d) Tsotyli Fm (of Late Aquitanian-Burdigalian age) and (e) Ontria Fm (of Burdigalian-Helvetian age). These formations form at a regional scale a homocline sequence that dips gently towards NE with the more to the east formations to be the younger ones.

More precisely, the Kastoria-Nestorion region is made up of molasse-type rocks that form the Pentalofos Fm, Tsotyli Fm and Ontria Fm. The Pentalofos Fm consists of thick (<2500m) marine alternations of turbidite sandstone and shale, with minor conglomerate that divided into the Tsarnos and overlying Kalloni members. The Tsotyli Fm (thickness up to 1500m) rests onto the previous formation, as well as on the basement rocks. Its lower part consists of turbidite conglomerate alternated with sandstones, sandy marls and marlstones, and its upper part is dominated by bluish-grey clayey marlstones with sandy marly limestones interbeds. The Ontria Fm overlying the previous

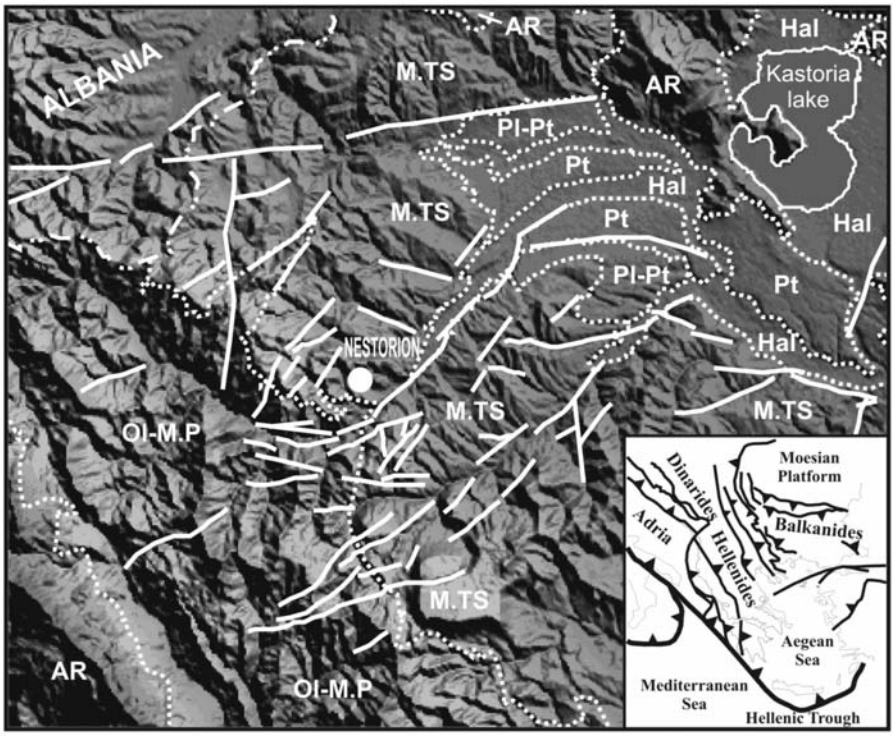

Fig. 1: Shaded relief image of the Kastoria-Nestorion region, Northwestern Macedonia showing the main faults. Geological units are shown as well. Inset map is showing the present-day geotectonic frame of the Southern Balkan. Explanation: Hal: Holocene alluvial deposits, Pt: Pleistocene deposits, Pl-Pt: Pliocene-Pleistocene deposits, M.TS: Tsotili Fm (Miocene), Ol-M.P: Pentalofos Fm (Oligocene-Miocene), AR: Alpine rocks (Sub-Pelagonian zone). Dashed line: geological contact, solid line: Fault-Photolineament.

formation is a shallow clastic sequence (120-150m total thickness) that consists upwards of sandstones, marls and sandy-marly limestones. Its uppermost part is characterised by the presence of some lignite beds.

The Aliakmonas River draining the mountainous area drifts to the SSE, but in the Kastoria-Nestorion region changes its drift towards NE up to the Kastoria Lake and after that point obtains its SE drift again. The latter NE trend is also seen in the drift of other tributaries of the Aliakmonas River, i.e. the Zabourgiantziotikos River, a fact that could imply a tectonic origin.

The region as a part of the Albanian-Pindos cordillera has been subjected to different tectonic events since the main orogenic process that gave rise to the stacking of the units (Kilias et al. 2001). Previous studies have shown that the MHT appears to be a half graben, probably developed in a transtensional stress regime, along the suture zone of the Apulian and Pelagonian basement blocks (Doutsos et al., 1993; Zelilidis et al., 2002). The western margin of the basin has been seen either a steep east-verging thrust (Apulian thrust of Doutsos et al. (1994) or a right-lateral strike-slip fault, i.e., Eptahori fault (Kontopoulos et al. 1999; Vamvaka et al. 2006). In addition, the basin is internally deformed by a series of northwest-striking right-lateral strike-slip faults and east-striking left-lateral strike-slip faults (Doutsos et al., 1994).

Since the late Miocene, the MHT has been mildly deformed by strike-slip motion along major faults along the western margin of the basin such as the Eptachori fault, uplifted, and eroded, with the oldest rocks exposed along the western marginal fault giving rise to the half graben geometry. However, a short period of compression was recognized in Middle-Late Miocene.

Information on the neotectonic regime of the area has been mainly derived by the studies that have been carried out in the region of Ptolemais and Kozani especially after the 1995 Kozani-Grevena earthquake of M = 6.5 (Pavlides and Mountrakis 1987; Mountrakis et al. 1996; Papazachos et al., 1998a; Mountrakis et al. 2006). These studies pointed out that the neotectonic deformation is accommodated through km-long normal faults driven by an NE-SW extension during the Late Miocene-Pliocene and an active NNW-SSE extension since the Quaternary, as also verified by seismological information (e.g. Papazachos et al., 1998b). Due to these stress regimes large fault-bounded Neogene-Quaternary basins have been developed with the most well studied that of Ptolemais-Kozani-Servia basin.

3. Structural data

3.1 Bedding of the molasse-type sedimentary rocks

The bedding of the molasse-type sedimentary rocks in the Kastoria-Nestorion region dips as a rule very gently to the NNE (Fig. 2a). However, it has been found to reveal significant deviations with dips toward the ESE (Fig. 2b), a fact that it is attributed to the tilting of the bedding due more to the NE-SW striking faults that dip mainly towards NW than the folding of the region.

3.2 Faulting

Our study included the satellite interpretation of the landscape of the region in order to define the exposed large fault zones and the field recording of their geometry and kinematics, in order to define the driven stress regime. The fault pattern in the study region is dominated by: (a) NE-SW trending faults that affect mainly the molasse-type sediments. The drift of the Aliakmonas River and its tributaries seems to be controlled by these faults and the valleys formed are filled up only with Holocene alluvial sediments; (b) WNW-ESE to E-W trending faults that crosscut the previous ones and bound basins that are filled up with Pleistocene and Holocene sediments. However, the more precise description of the geometry and kinematics of the faults was based on subdividing the recorded fault-slip data into different groups, considering the orientation of the faults (dip and dip direction), as described by Tranos (1998, 2009). More specifically, the recorded in the field mesoscale faults (Fig. 3a) affecting the molasse-type sedimentary rocks were separated into the following groups according to their strike: 1) WNW-ESE striking faults that form two fault groups with mean dip-direction and dip values of 201-70° and 033-61°, respectively (Fig. 3b, c), 2) NE-SW striking faults that form two fault groups with corresponding mean values 307-81° and 300-58°, respectively (Fig. 3d, e), and 3) NNW to N-S striking faults that form three fault groups with mean values 248-75°, 271-78° and 084-78°, respectively (Fig. 3f, g, h).

WNW-ESE striking faults

The WNW-ESE striking faults include large faults and/or fault zones of width up to 10m that dip either to SSW or to NNE. The NNE-dipping group includes fewer faults, more planar and with larger dispersion in strike with respect to the SSW-dipping group and although, they are also characterized by thinner fault zones they reveal similar multi-deformation history. Indeed, they both exhibit more than one generation of slickenlines that correspond to strike-slip displacements, younger normal dis-

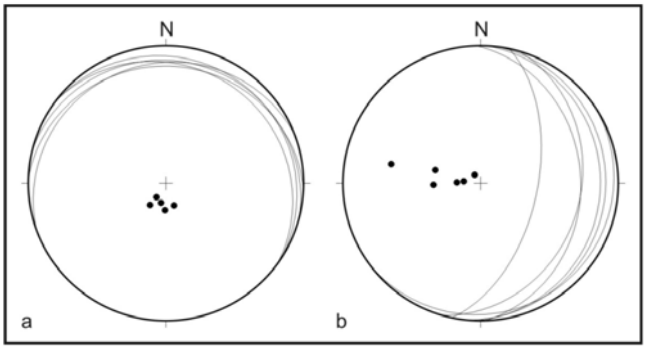

Fig. 2: Primary foliation of the molassic-type sedimentary rocks exposed in Kastoria-Nestorion region. (a) General attitude of the bedding, (b) Bedding attributed to the faulting.

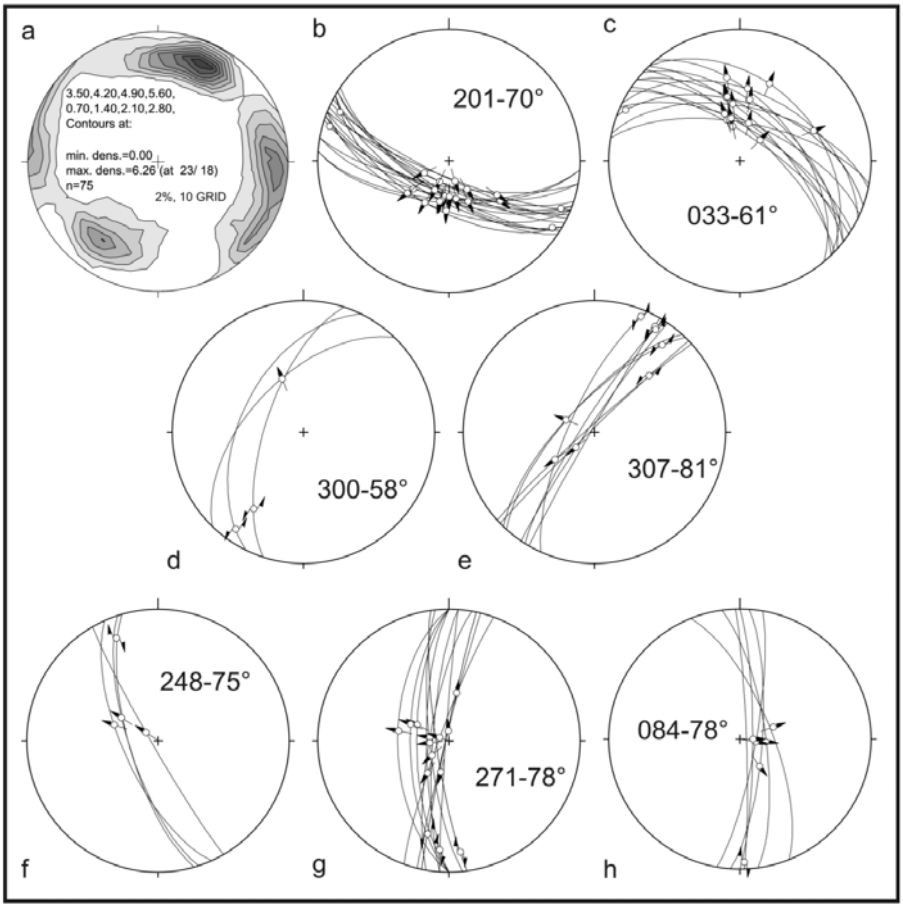

Fig. 3: Stereographic projections (equal area, lower hemisphere) indicating the geometry and kinematics of the mesoscale faults recorded in the Kastoria-Nestorion region. (a) Density diagram of the poles of the mesoscale faults, (b, c) Fault planes and striations of the WNW-ESE striking mesoscale fault groups, (d, e) the NE-SW striking mesoscale faults, and (f, g, h) the NNW-SSE to N-S striking mesoscale faults.

placements that overprinted by left-lateral oblique normal ones. However, the majority of the faults can be fairly described as synthetic or antithetic quasi-Andersonian faults in the field, having as a remarkable feature the drag folding of the bedding of the molasse-type rocks due to their activation.

NE-SW striking faults

The NE-SW striking faults are the longer faults exposed in the region, forming km-long fault zones with a width of several meters. They control the hydrographic network and the recent topography of the region and cut the WNW-ESE striking faults. In particular, faults of this strike control the eastern slopes of the Aliakmonas River (area of Pentavrissos-Omorphoklisia) forming successive fault zones within the bedding of the molasse tilting at various angles. The NE-SW striking faults, which are not prevalent in the mesoscale, exhibit at least two generations of slickenlines, which correspond to strike-slip displacements and younger normal ones. The latter displacements show significant dispersion, but with the clear distinction of the right normal from the left-lateral normal ones.

NNW-SSE to N-S striking faults

These faults form narrow fault zones, the commonest width of which is approximately 30cm. They commonly form splay or bridge faults between the larger NE-SW striking faults and dip at very high angles or are nearly vertical; however along these faults one can hardly see drag folds. The slickenlines of the faults indicate strike-slip displacements overprinted by younger normal ones.

3.3 Fault-slip analysis and stress regimes

The above mentioned fault groups have been studied using the stress-inversion methods of Angelier (1984) and Gephart and Forsyth (1984). For this reason, the fault groups have been separated using field observations, such as overprinting of the slickenlines contained by faults and cross-cutting criteria among the different faults groups. In addition, the fault grouping has also considered the fault type and transport orientation. The stress pattern has been characterized using the type of the most vertical axis and the stress ratio of the resolved stress tensor, following the suggestion of Tranos et al. (2008). The same procedure has been applied for 23 focal mechanisms of earthquakes that occurred in the broader Kastoria-Nestorion region [39.8-40.8^{o}N, 20.8-22^{o}E] within the last 25 years, either compiled for this work from the waveform data of the seismological network of the Aristotle Univ. Thessaloniki (http://seismology.geo.auth.gr) or from various sources (Papazachos and Papazachou, 2003; Mountrakis et al., 2006) in order to assess the active stress field of the region and to compare the stresses defined by fault-slip data and focal mechanisms.

In all cases both applied stress inversion methods provided very compatible results regarding the stress tensor orientation, despite sometimes significant differences regarding the stress ratio value. In the following, the stress pattern for each defined fault group is presented. For the Gephart and Forsyth (1984) approach we also present all compatible solutions within the 95% confidence area, while the final stress solution corresponds to the average (in the least square sense) stress tensor of this confidence area, rather than the optimum solution, which in some cases was located at the border of the confidence area and exhibited negligibly smaller misfit values with respect to the average solution. Therefore, the following stress regimes have been defined:

D1 event (TRP-SS)

This is a transpressional – strike-slip regime associated with NNE-SSW contraction in which the stress tensor has σ_2 vertical axis and stress ratio R = 0.24 (Fig. 4a). It activated NNW-SSE striking faults as right-lateral strike-slip faults and NNE-SSW to NE-SW striking faults as left-lateral strike-

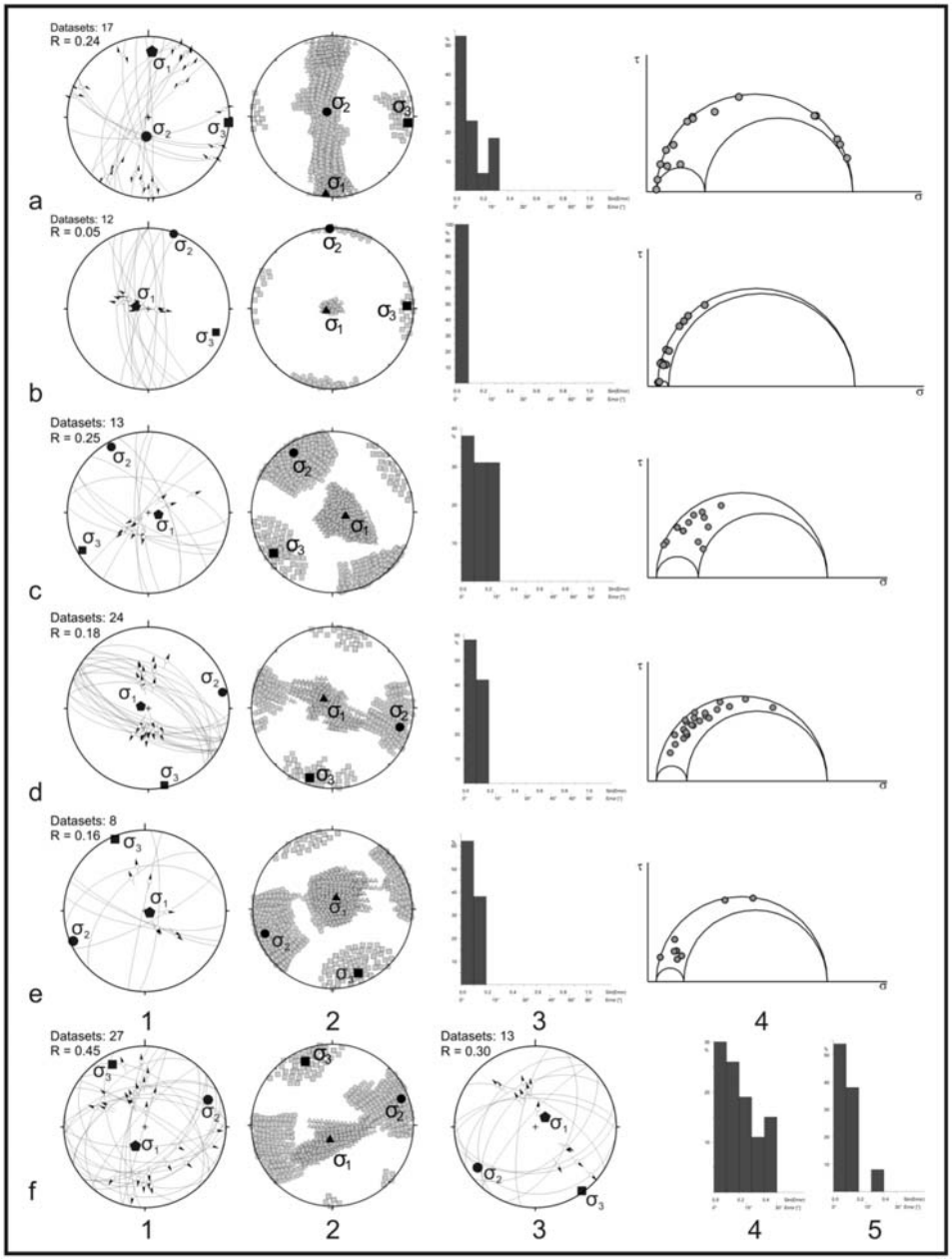

Fig. 4: Stereographic projections (equal area, lower hemisphere) indicating the broader Kastoria-Nestorion area fault-slip and earthquake focal mechanism data activated in the various deformational events: (a) D1 event, (b) D2 event, (c) D3 event, (d) D4 event, (e) D5 event, (f) active stress field from focal mechanisms (see text). Explanation: 1. Fault-slip data and the stress axes from Angelier (1984) method, 2. Average stress axes and 95% confidence area solutions for the Gephart and Forsyth (1984) method, for a, b, c, d, e: 3 & 4. Distribution of the misfit angle between the real and theoretical striae and Mohr diagram from Angelier (1984) method. Only for f: 3. Improved solution with Angelier method (after rejecting those of high misfit angle (>20°), 4 and 5: Misfit angles for f1 and f3 solutions respectively.

slip faults. The small number of the WNW-ESE trending strike-slip faults, the sense of which is not certain from field data, fits well with the stress tensor if they act as right-lateral strike-slip faults, i.e. as R' shears. This event affected the molasse-type sediments of Pentalofos and Tsotyli formations, hence is timely constrained after the Early Miocene (Burdigalian). This stress field does not operate later than the beginning of Late Miocene, considering that Late Miocene and younger sediments have not been affected by similar in geometry and kinematics strike-slip faults.

D2 event (RE)

This event corresponds to an almost radial extension with a vertical σ_1 axis and an extensional stress axis σ_3 oriented subhorizontal along WNW-ESE (Fig. 4b). It activated the previous NNW-SSE to NNE-SSW striking faults as normal faults, with a slip direction trending WNW-ESE. This event should be dated in Middle-Late Miocene, since its corresponding faults have not affected sediments younger than Late Miocene. The fact that the σ_3 axis trends in the same direction as with the previous D1 event suggests that D1 probably evolved progressively to D2, whereas a slip partitioning can be also locally considered, with either normal or strike-slip activation.

D3 event (RE-PE)

This event is defined as a NE-SW extensional stress field with a vertical compression (σ_1) and subhorizontal extension (σ_3) trending NE-SW (Fig. 4c). It activated NNW-SSE striking faults and WNW-ESE striking faults as left-lateral oblique normal faults and right-lateral oblique normal faults, respectively. In addition, NW-SE striking faults were activated as normal faults in this stress field. This deformation event has been very well constrained by several published studies for Northern Greece during the Late Miocene and Pliocene (Pavlides and Mountrakis 1987; Mercier et al. 1989; Mountrakis et al. 2006).

D4 event (RE-PE)

This event is described as an extensional stress regime, associated with N-S to NNE-SSW extension and a vertical σ_1 axis (Fig. 4d). The activated faults are quasi-Andersonian WNW-ESE synthetic and/or antithetic normal faults forming a fault system. During this event, the slip direction, as defined by the fault-slip data, trends N-S. Previously published studies date this event in Quaternary times (Pavlides and Mountrakis 1987; Mercier et al. 1989; Tranos and Mountrakis 1998; Mountrakis et al. 2006), as confirmed by the generally E-W trending basins of the wider area, which are bounded by E-W trending faults and are filled up with Pleistocene and Holocene sediments.

D5 event (RE-PE)

This event is also described by a subhorizontal σ_3 axis trending NNW-SSE and a vertical σ_1 axis mainly activating NE-SW striking faults as normal and right-lateral normal faults (Fig. 4e). From the family of NNW-SSE to NNE-SSW faults, the NNE-SSW ones are also activated during this event as right-lateral oblique faults. More importantly, the WNW-ESE striking faults are also activated in this event, however not as normal faults but as right-lateral oblique ones. The defined extension stress axis (σ_3) is in very good agreement with stress defined using the focal mechanisms of medium (typically M~3.5-4.0) to large (M~5.5-6.5) earthquakes of the broader western Macedonia area (Fig. 4f), including the earthquake activity related with the Grevena-Kozani earthquake (Papazachos et al., 1998a). It should be pointed out that despite the fact that several medium magnitude events in the immediate vicinity of the Kastoria-Nestorion area exhibited even NNE-SSW T-axes, the inverted stress field shows a clear NNW-SSE extensional stress field (in agreement with Fig. 4f), as also confirmed by an independent stress inversion of only these narrower Kastoria-Nestorion area data. We

propose that this D5 event should be dated in Holocene, since the valleys along the corresponding faults are filled up only with Holocene alluvial sediments instead of the WNW-ESE basins that are filled up with both Pleistocene and Holocene sediments.

4. Conclusions-Results

The MHT in the Kastoria-Nestorion region of NW Macedonia indicates a multi-deformed history, not only during its early stages, but also during the Late Tertiary and Quaternary time as herein indicated by the present analysis of faulting. More interest is the fact that the herein described Late Tertiary-Quaternary deformation of the MHT can be correlated with the deformation of North Aegean Trough and the Hellenic hinterland (Tranos 1998, 2009; Georgiadis et al. 2007; Tranos et al. 2008, 2009). In particular, five deformation events have been defined to affect the MHT using the fault-slip data recorded in the Kastoria-Nestorion region and the use of stress-inverse methods of Angelier (1984) and Gephart and Forsyth (1984), respectively. The former three ones, D1, D2 and D3 dominated the region during the Neogene, whereas the last two events D4 and D5 from Quaternary to present. In particular, our analysis suggests that the MHT was initially subjected to a regional transpressional-strike-slip regime in the Miocene times, which can be attributed to the late collision processes between the Eurasia and Apulia plates. The D2 event represents a progressive stage of the D1 event associated with the latest stages of the collision processes. On the other hand, the next faulting deformation (D3 event) was a NE-SW to ENE-WSW extension that relates with the onset of the present-day Hellenic subduction zone and gave rise to the large NW-SE trending fault-bounded basins developed in Macedonia region in the Late Miocene and Pliocene times. More importantly, our analysis suggests that during the Quaternary, probably close to the Late Pleistocene-Holocene boundary, the least principal stress axis of the extensional stress field changed from NNE-SSW (D4 event) to NNW-SSE trend (D5 event). This gradual anticlockwise rotation of the NE-SW extension (D3) to NNE-SSW (D4) and finally NNW-SSE (D5) suggests that the stress regime which is commonly interpreted as a back-arc extension to the present-day Hellenic subduction zone, since it trends orthogonal to it, should have changed to a rather intra-continental or intra-plate deformation. Indeed, the orientation of the least principal contemporary stress axis appears to be more related with the Adria-Eurasia evolved convergence since the former trends along the Dinarides-Hellenides rather the present-day Hellenic subduction zone.

5. References

Angelier, J., and Mechler, P. 1977. Sur une méthode graphique de recherche des contraintes principales également utilisable en tectonique et enséismologie: la methode des diédres droits. *Bull. Soc. Géol. France*, 7(19), 1309–1318.

Angelier, J., 1984. Tectonic analysis of fault slip data sets. *J. Geophys. Res.*, 89, 5835-5848.

Brunn, J. H., 1956. Contribution á l' étude géologique du Pinde septentrionale et d'une partie de la Macédoine occidentale. *Annales Géologiques des Pays Helléniques*, 7, 1–358.

Doutsos, T., and Kokkalas, S., 2001. Stress and deformation patterns in the Aegean region, *J. Struct. Geol.*, 23, 455 – 472.

Doutsos, T., G. Pe-Piper, G., Boronkay, K. and Koukouvelas, I., 1993. Kinematics of the central Hellenides. *Tectonics*, 12, 936–953.

Doutsos, T., Koukouvelas, I., Zelilidis, A. and Kontopoulos, N., 1994. Intracontinental wedging and post-orogenic collapse in the Mesohellenic trough. *Geol. Rundsch.*, 83, 257–275.

Georgiadis, G. A., Tranos, M. D. and Mountrakis, D. M., 2007. Late-and post-Alpine tectonic evolution

of the southern part of the Athos peninsula, northern Greece. *Bull. Geol. Soc. Greece*, 40, 309-320.

Gephart, J. W. and Forsyth, D. W., 1984. An improved method for determining the regional stress tensor using earthquake focal mechanism data: an application to the San Fernando earthquake sequence. *J. Geophys. Res.*, BS9, 9305-9320.

Le Pichon, X., and Angelier, J., 1979. The Hellenic Arc and Trench system: A key to the neotec-tonic evolution of the eastern Mediterranean area. *Tectonophysics*, 69, 1 – 42.

Kahle, H. G., Straub, C., Reilinger, R., McClusky, S., King, R., Hurst, K., Veis, G. and Cross, P., 1998. The strain rate field in the eastern Mediterranean region, estimated by repeated GPS measurements. *Tectonophysics*, 294, 237 – 252.

Kilias, A. A., Tranos, M. D., Papadimitriou, E. E., and Karakostas, V. G., 2008. The recent crustal deformation of the Hellenic orogen in Central Greece; the Kremasta and Sperchios Fault Systems and their relationship with the adjacent large structural features. *Z. dt. Ges. Ge-owiss.*, 159/3, 533-547. DOI: 10.1127/1860-1804/2008/0159-0533.

Kilias, A., Tranos, M., Mountrakis, D., Shallo, M., Marto, A. and Turku, I. 2001. Geometry and kinematics of deformation in the Albanian orogenic belt during the Tertiary. *J. Geodyn.*, 31, 169-187.

Kontopoulos, N., Fokianou, T., Zelilidis, A., Alexiadis, C. and Rigakis, N., 1999. Hydrocarbon potential of the middle Eocene–middle Miocene Mesohellenic piggy-back basin (central Greece): a case study. *Mar. Petrol. Geol.*, 16, 811–824.

McClusky, S., et al. (28 authors) 2000. Global Positioning System constraints on plate kinematics and dynamics in the eastern Mediterranean and Caucasus. *J. Geophys. Res.*, 105, 5695-5719.

McKenzie, D.P. 1970. The plate tectonics of the Mediterranean region. *Nature*, 226, 239-243.

McKenzie, D.P. 1972. Active tectonics of the Mediterranean region. *Geophys. J. R. astr. Soc.*, 30, 109-185.

Mercier, J. L., Simeakis, K., Sorel, D., and Vergely, P., 1989. Extensional tectonic regimes in the Aegean basins during the Cenozoic. *Basin Research*, 2, 49–71.

Mountrakis, D. 1986. The Pelagonian zone in Greece: A polyphase-deformed fragment of the Cimmerian continent and its role in the geotectonic evolution of the eastern Mediterranean. *J. Geol.*, 94, 335-347.

Mountrakis, D., Pavlides, S., Zouros, N., Chatzipetros, A. and Kostopoulos, D., 1996. The 13 May 1995 Western Macedonia (Greece) earthquake. Preliminary results on the seismic fault geometry and kinematics. *Proceedings of the XV Congress of the Carpatho-Balkan Geological Association*, Seismicity of the Balkan region, 112-121.

Mountrakis, D., 2006. Tertiary and Quaternary tectonics of Greece, in Dilek, Y., Pavlides, S., eds., Post-collisional tectonics and magmatism in the Mediterranean region and Asia. *Geological Society of America, Special Paper*, v. 409, p. 125-136. DOI: 10.1130/2006.2409(07).

Mountrakis, D., Tranos, M., Papazachos, C., Thomaidou, E., Karagianni, E., and Vamvakaris, D., 2006. New neotectonic and seismological data about the main active faults and stress regime of Northern Greece. *J. Geol. Soc., London, Sp. Publ.,* 260, 649-670.

Papazachos, B. C., Karakostas, B. G., Kiratzi, A. A., Papadimitriou, E. E. and Papazachos, C. B., 1998a. Basic properties of the faulting which caused the 1995 Kozani-Grevena seismic sequence. *J. Geodyn.*, 26, 217-231.

Papazachos, B.C., Papadimitriou, E.E., Kiratzi, A.A., Papazachos, C.B. and Louvari, E.K., 1998b. Fault plane solutions in the Aegean Sea and the surrounding area and their tectonic implications, *Boll. Geof. Teor. Appl.*, 39, 199-218.

Papazachos, B., Mountrakis, D., Papazachos, C., Tranos, M., Karakaisis, G. & Savvaidis, A. 2001. The faults which have caused the known major earthquakes in Greece and surrounding region between the 5th century BC and today. Proceedings of the 2nd Panhellenic Congress of Earthquake Engineering and

Engineering Seismology, 28–30 September. Technical Chamber of Greece, Thessaloniki, 1, 17–26.

Papazachos, B., and Papazachou, C., 2003. The Earthquakes of Greece. *Editions Ziti*, Thessaloniki, 1-317.

Papazachos, C.B., Kiratzi, A.A. and Papazachos, B.C., 1992. Rates of active crustal deformation in the Aegean and the surrounding area. *J. Geodyn.*, 16, 147-179.

Papazachos, C.B. and Kiratzi, A.A., 1998. A detailed study of the active crustal deformation in the Aegean and surrounding area. *Tectonophysics*, 253, 129-153.

Pavlides, S. and Mountrakis, D., 1987. Extensional tectonics of north-west Macedonia, Greece, since the Late Miocene. *J. Struct. Geol.*, 9, 385–392.

Reiter, F. and Acs, P., 2003. TectonicsFP software. http://www.tectonicsfp.com.

Reilinger, R. E., McClusky, S. C., Oral, M. B., King, R. W., Toksoz, M. N., Barka, A. A., Kinik, I., Lenk, O. and Sanli, I., 1997. Global positioning system measurements of present crustal movements in the Arabia-Africa-Eurasia plate collision zone. *J. Geophys. Res.*, 102, 9983–9999.

Tranos, M. D., 1998. Contribution to the study of the neotectonic deformation in the region of Central Macedonia and North Aegean. *PhD. Thesis*, University of Thessaloniki, (in Greek with extended English abstract).

Tranos, M.D., 2009. Faulting of Lemnos Island; a mirror of faulting of the North Aegean Trough (Northern Greece). *Tectonophysics*, 467, 72–88, DOI: 10.1016/j.tecto.2008.12.018.

Tranos, M. D., Kachev, V. N., and Mountrakis, D. M., 2008. Transtensional origin of the NE-SW Simitli basin along the Strouma (Strymon) Lineament, SW Bulgaria. *J. Geol. Soc. London*, 165, 499-510, doi: 10.1144/0016–76492007–089

Tranos, M. D., Eleftheriadis, G. E., Kilias, A. A., 2009. Philippi granitoid as a proxy for the Oligocene and Miocene crustal deformation in the Rhodope Massif (Eastern Macedonia, Greece). *Geotectonic Research*, 96, 69-85.

Tranos, M. D. and Mountrakis, D. M., 1998. Neotectonic joints of Northern Greece: their signi-ficance on the understanding of the active deformation. *Bull. Geol. Soc. Greece*, 32, 209-219.

Vamvaka, A., Kilias, A., Mountrakis, D. and Papaoikonomou, J., 2006. Geometry and structural evolution of the Mesohellenic Trough (Greece): a new approach. *J. Geol. Soc. London, Sp. Publ.*, 260, 521-538, doi: 10.1144/GSL.SP.2006.260.01.22

Zelilidis, A., Piper, D. J. W. and Kontopoulos, N., 2002. Sedimentation and basin evolution of the Oligocene–Miocene Mesohellenic basin, Greece. *AAPG Bulletin*, 86, 161–182.

Δελτίο της Ελληνικής Γεωλογικής Εταιρίας, 2010
Πρακτικά 12ου Διεθνούς Συνεδρίου
Πάτρα, Μάιος 2010

Bulletin of the Geological Society of Greece, 2010
Proceedings of the 12th International Congress
Patras, May, 2010

GEOMORPHOLOGY AND SEDIMENTOLOGICAL PROCESSES ALONG THE COASTAL ZONE BETWEEN LIVANATES AND AGIOS KONSTANTINOS (N. EVOIKOS GULF, CENTRAL GREECE)

Tsanakas K.[1], Gaki-Papanastassiou K.[2], Poulos S.E.[3] and Maroukian H.[4]

[1] *National and Kapodistrian University of Athens, Faculty of Geology and Geoenvironment, Department of Geography and Climatology, 15784 Athens, Greece, ktsanakas@geol.uoa.gr*

[2] *National and Kapodistrian University of Athens, Faculty of Geology and Geoenvironment, Department of Geography and Climatology, 15784 Athens, Greece, gaki@geol.uoa.gr*

[3] *National and Kapodistrian University of Athens, Faculty of Geology and Geoenvironment, Department of Geography and Climatology, 15784 Athens, Greece, poulos@geol.uoa.gr*

[4] *National and Kapodistrian University of Athens, Faculty of Geology and Geoenvironment, Department of Geography and Climatology, 15784 Athens, Greece, maroukian@geol.uoa.gr*

Abstract

This study deals with aspects of geomorphology and nearshore marine processes in the coastal zone located between Livanates and Agios Konstantinos (North Evoikos Gulf, central Greece). Evoikos Gulf is a tectonic graben bounded by WNW-ESE trending normal faults; it can be further characterized as semi-closed marine basin with water depths exceeding 400m.The Coastal geomorphology is affected by active tectonics with the most prominent morphological features being the uplifted marine terraces and the well-developed deltaic fan of Xerias torrent. In the present investigation, detailed geomorphological mapping at a scale of 1:5000 was performed together with granulometric analysis, while nearshore wave and current activity related to sediment dynamics has been determined on the basis of wind-generated wave regime. The examined coastal zone consists of a series of alluvial cones and fans, Xerias fan being the largest among them, low cliffs, a cuspate foreland and beach zones of limited length, often hosting beachrock formations. The formation and evolution of the study area seems to be controlled by the limited terrestrial influxes, the relatively weak wave regime due to limited wave fetches distances, and the associated longshore currents that induces limited sediment transport.

Key words: *geomorphology, sediment dynamics, coastal erosion, tectonic activity, North Evoikos Gulf, Central Greece.*

1. Introduction

Coastal environments are formed and evolved as the combined effect of endogenic and exogenic processes. This study attempts to invetigate the terrestrial and marine processes combined with the neotectonic acticity that lead to the formation and evolution of the coastal zone between Livanates and Agios Konstantinos that belongs to the North Evoikos Gulf, central Greece (Fig. 1).

The study area lies along the west coast of North Evoikos Gulf and is bounded southwards by Mt. Kserovouni (841m) and Mt. Knimis (726m), and westwards by the delta fan of Xerias torrent. The

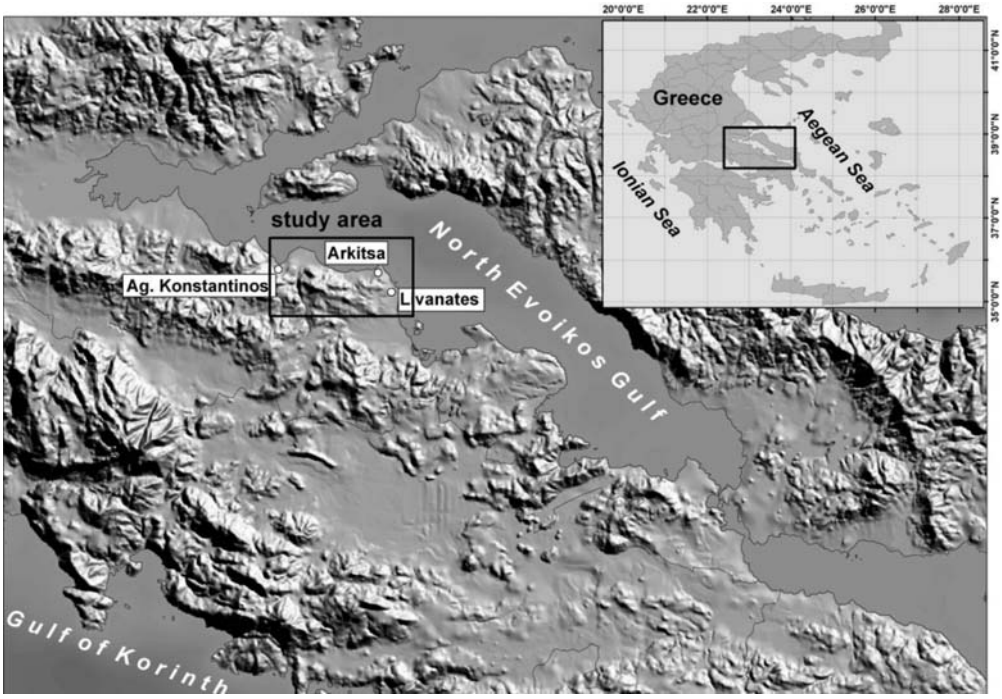

Fig. 1: Location map of the broader region of the study area.

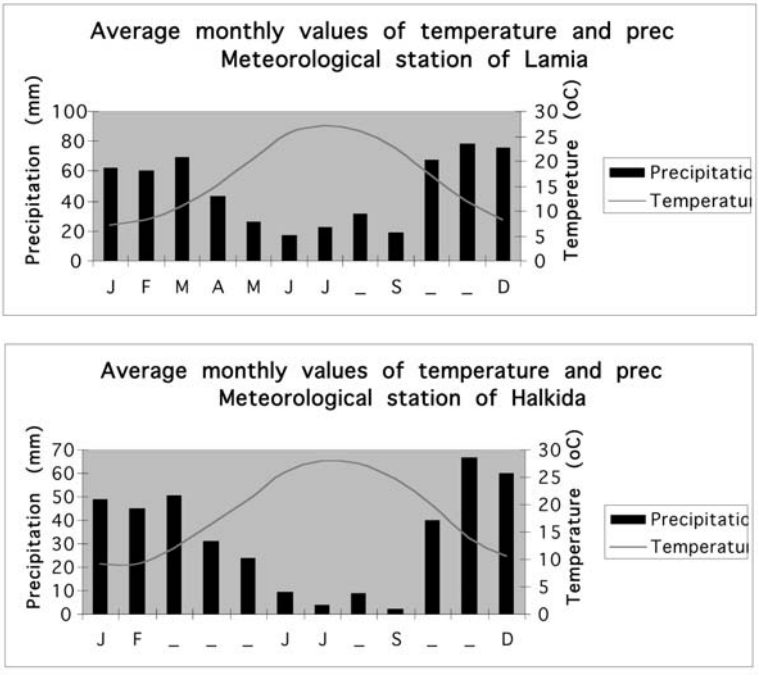

Fig. 2: Average monthly values of temperatures and precipitation (data obtained from Lamia and Halkida meteorological stations, HNMS, 1964-1994).

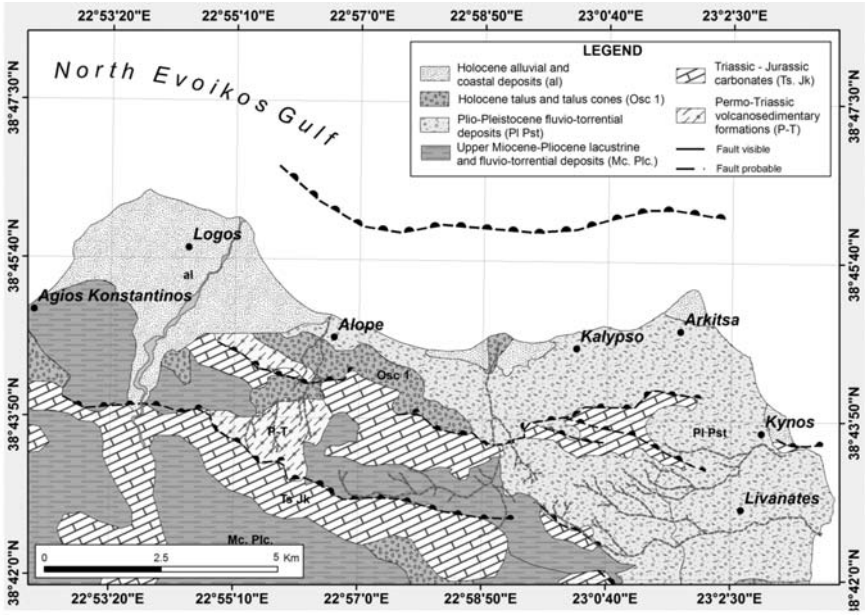

Fig. 3: Geological map of the study area based on the maps by IGME (2006) and field work.

total shoreline length is 25.3 km hosting the mouths of 5 torrents, between them Xerias in the west being the most significant in terms of size and sediment discharge. According to Woodward (1995) the area under investigation undergoes weathering processes that may produce annually 100-200 tn/km^2 of its drainage basin.

Geomorphological and sedimentological processes are related to the prevailing climatological setting. Air temperature as well as precipitation are major factors that designate weathering and erosion rates, while wind speed direction and frequency are the main factors that control the wave regime in a coastal area thus controlling the coastal morphology. Hence, air temperature and precipitation data were obtained from two meteorological stations (Halkida and Lamia) of the Hellenic National Meteorological Service. Data analysis shows an average annual temperature of 16.5 ^{o}C and 573.3 mm of annual precipitation for Lamia station and 18 ^{o}C and 390.2 mm for Halkida station respectively (Fig. 2).

2. Geological and Tectonic setting

Since the Upper Miocene to present, the area of Central Greece has been affected by ongoing active crustal extension in a NNE-SSW direction, mainly by two major mechanisms: the westward motion of the Anatolia plate, and the slab retreat (roll-back) of the African slab under the Hellenic Peninsula (Armijio et al, 1996; Meijer and Wortel 1997; Doutsos and Kokkalas 2001). The structure of this area of Greece is dominated by a series of roughly WNW-ESE-trending extensional faults (accommodating extension of 15-20 mm/y) which have created a series of semi- asymmetric, grabens (Eliet et al, 1995). The most prominent of these extensional structures are the Gulf of Corinth and the Evoikos Gulf, both of which are WNW-ESE trending graben systems about 100 km long, and are bordered by N-dipping master faults, that are usually segmented along their strike giving a step type morphology (Roberts, et al., 1991; Westaway, 1991; Doutsos and Poulimenos, 1992; Roberts and Koukouvelas, 1996; Kokkalas et al., 2006; van Andel et al., 2006).

Table 1. Wave fetch distances (F) and offshore angle of wave crestline with respect to coastline (a_0) for each of the five (A-E) sub-units (positive direction is towards the East).

	UNIT A		UNIT B		UNIT C		UNIT D		UNIT E	
	F (m)	a_0 (º)	F (m)	a_0 (º)	F (m)	a_0 (º)	F (m)	a_0 (º)	F (m)	a_0 (º)
W	4470	40	-	-	-	-	-	-	-	-
NW	7940	5	9050	40	12300	63	12800	35	-	-
N	7300	-50	7070	5	9490	18	14800	-10	12700	65
NE	-	-	14900	-40	13800	-22	15300	-35	16700	20
E	-	-	34000	-85	2300	-67	-	-	26800	-25

The study area belongs to the Pelagonian zone of Central Greece. This unit, lying above a Variscan basement, comprises transgressional clastic and carbonate sediments of Early/Late Permian age and Early to Middle Triassic carbonates (Guernet, 1971; Clément, 1983; Baud et al., 1991). The local lithology (Fig. 3) consists of Permo-Triassic volcano-sedimentary formations, Triassic-Jurassic carbonates and Neogene and Quaternary formations composed of lacustrine, fluvio-torrential and marine deposits.

3. Methodology

In this study topographic maps were obtained at a scale of 1:50.000 and 1:5000 issued by the Hellenic Army Service. In order to examine the influence of the terrestrial and marine processes and to draw conclusions relating to the Quaternary landscape evolution of the study area, detailed geomorphological mapping at a scale of 1:5.000 was performed focusing on the landforms along the coastline. In addition, the coastal slope, sediment size, beachrock formations, coastal stability and longshore drift were also mapped. Data were analysed using GIS technology. A Digital Elevation Model (DEM) of the area was also created from 1:5000 topographic diagrams. The cell size of the grid was 10 m and the software used for this analysis was Arc-GIS v9.3 and Arc Seen v 9.3.

With respect to the coastal wind generated wave regime which governs the nearshore sediment transport and in the absence of wave records, wave characteristics have been estimated at the basis of the prognostic equations of the shore protection manual of the US Army Corps of Engineers (CEM, 1984) utilising the wind data set obtained from the nearby Halkida meteorological station from the Hellenic National Meteorological Service.

Following, the longshore component (onshore to breaking zone) of the wave power per unit length of the shoreline is calculated on the basis of the offshore predicted wave characteristics, assuming a rather uniform nearshore seabed morphology using the equation (CEM, 1994):

$$Pl = 0.058 * \varrho * g^{3/2} * Ho^{5/2} * (\cos a_0)^{1/4} * \sin 2\, a_0 \quad (1)$$

Where, ϱ is the density of seawater (= 1025 kg/m^3), g = 9.81 m/sec^2, Ho the offshore wave height and a_0 the angle of wave crest line with respect to shoreline. The above calculation, due to the variety of coastline orientation has been applied to different units of the coastal area under investigation, as shown in Fig. 6. (for values see Table 1).

The potential rate of longshore sediment transport by volume (Q_l) for sand-sized grains has been determined by the empirically derived equation (Komar, 1978):

$$Q_l = \frac{0.39 \times P_L}{g \times (\sigma - \rho) \times 0.6} \quad (2)$$

Q_l is measured in m^3/s, s and ϱ (kg/m^3) are the densities of sediment (= 2650 kg/m^3) and water (1025 kg/m^3), respectively; P_L is the longshore component of the incoming wave power (Watt/m of wave crest) given by equation 1; 0.39 is a coefficient of efficiency relating to loss of water due to percolation through the sediments, and 0.6 is another coefficient which represents the average proportion of the bulk sediment occupied by particles, rather than pore space. In accordance to the above, Q_l values have been calculated separately for the different sub-units for all the predominant wind/wave directions per each sub-unit.

4. Results and discussion

4.1 Geomorphology

The combination of active tectonics and global variations of sea level during the late Pleistocene has led to the formation of at least three uplifted marine terraces, which correspond to high sea level stands (Fig. 4). The lower and the most recent terrace (A) lies in between 2m and 20m of altitude. The second terrace (B) is found at elevations of 20-40m elevations and the third one (C) at 40-60m. These marine terraces have been formed on Plio-Pleistocene marls. For the lowest (A) and the middle terrace (B) a cap rock formation has been found overlying uncomformaly the Plio-Pleistocene marls; it consist of beach material (sand, pebbles, cobbles and marine fossils). Unbeatably, these coastal landforms indicate Neotectonic activity on the broader study area and could be used as sea level indicators.

The coastline of the investigation area hosts the alluvial fan of the Xerias torrent to the west, another two much smaller cones at its central part and the Arkitsa promontory towards its eastern end. The latter seems to have been formed in earlier stages of sea level stands (as shown by the nearshore bathymetry) and being shaped either by tectonic activity and/or by the operation of a previously active mouth of a torrent.

Furthermore, along the shore zone, a series of coastal landforms has been found that indicate recent (Holocene) tectonic uplift (Pirazzoli, 1996; Gaki-Papanastasiou et al, 1999) as characteristically shown on Figure 5. These include extended and under subaerial erosion beach rock formations (Fig. 5a) marine notches (Fig. 5b) and sea caves (Fig. 5c) along the northern part of the coastal area.

An analogous uplift movement has been denoted at Alope region by the presence of an alluvial cone of Holocene age which lies on top of a layer that consists of beach material (Fig. 5d). This beach material of late Holocene (Roman) age is uplifted at elevations >1 m asl. which suggests significant coastal uplift since Roman times (Cundy et al, 2009).

4.2 Nearshore marine and sedimentological processes

In the microtidal environment of the North Evoikos Gulf the wind generated waves play the main role between the nearshore marine processes. Thus, from the Table 2, where the predicted

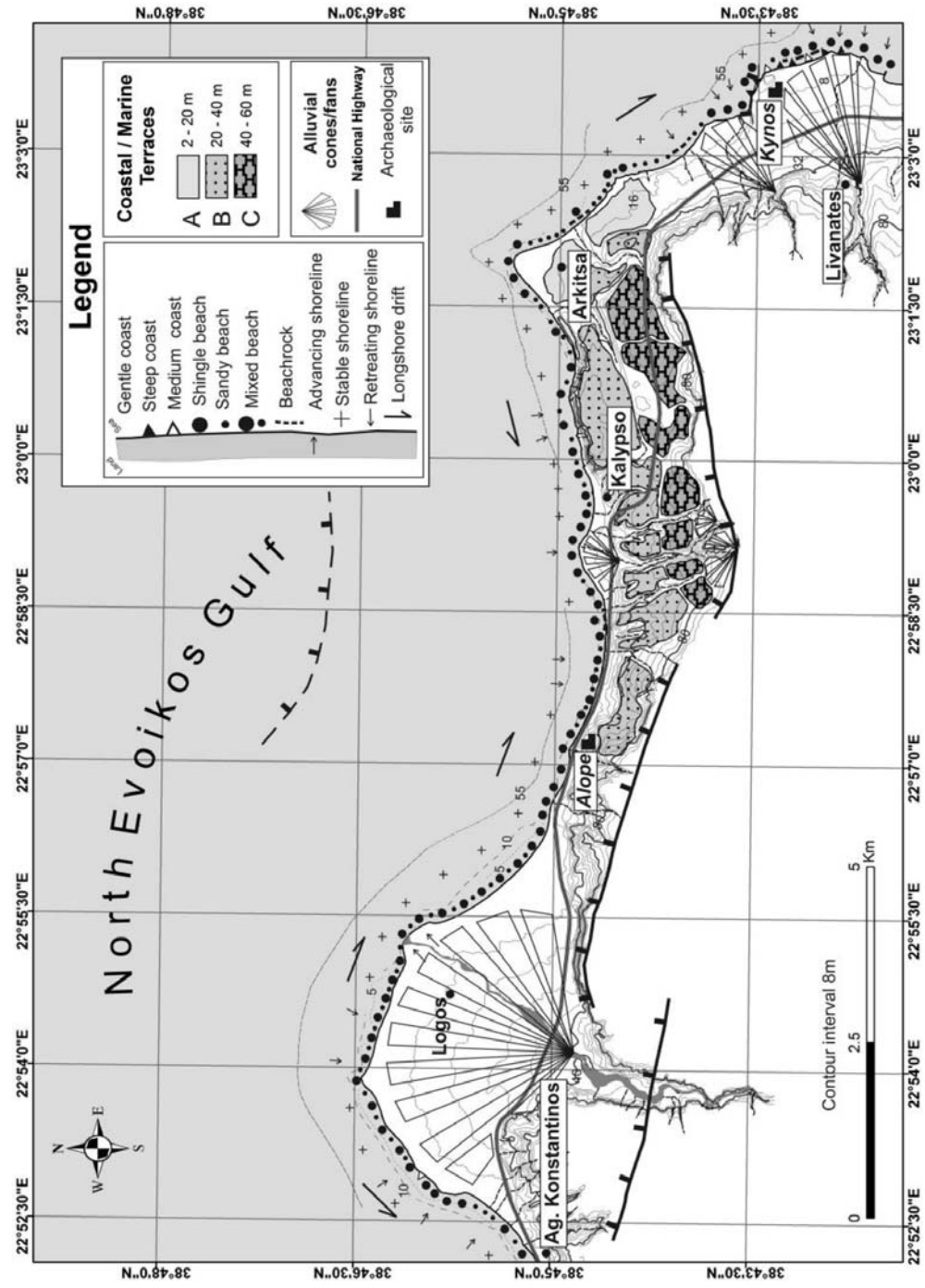

Fig. 4: Gemorphological map of the study area depicting among others, the coastal features along the shoreline, the granulometry as observed on the field and the longshore drift (Cundy et al,, 2009).

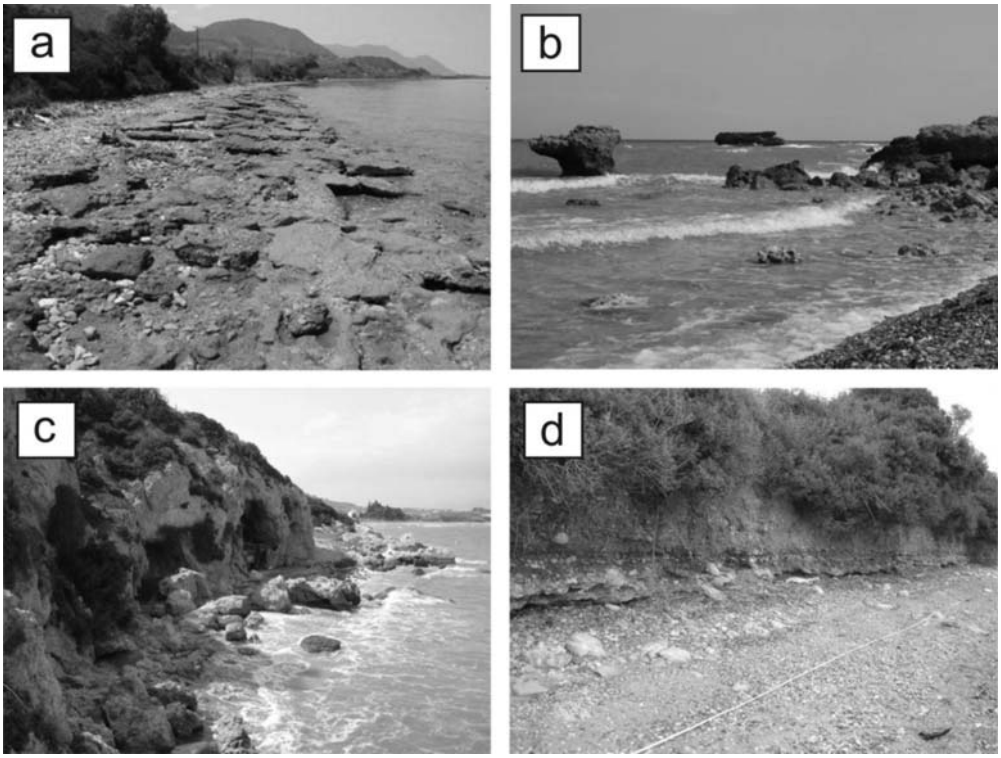

Fig. 5: (a) Uplifted and eroding beachrocks at Kalypso; (b) Uplifted (by 1 m asl) marine notch at Kynos; (c) Uplifted (approx. 2m asl) sea caves at Kynos; and (d) Eroding coastal alluvial cone at Alope. The base of this cliff consists of well cemented beach material, uplifted >1m asl since Roman times.

offshore wave characteristics are presented, it can be seen that the coastal area under investigation undergoes a rather weak wave regime (average wave heights are <0.5 m and periods <3 sec) due to the semi enclosed (restricted wave-fetch distances) character of the North Evoikos Gulf. This nearshore wave climate is associated with a low capability of longshore sediment transport, i.e. the calculated potential annual values are <1200 m^3/yr (Table 3), when those refer to the open Ionian Sea exceeds $2x10^6$ m^3/yr (Poulos et al., 2002). Along the northern part of the coastal area under investigation, the longshore sediment transport is directed towards the east being more pronounced at its western part (units B and C) and induced mostly by the N and NE wind-generated waves (Fig. 6) The highest value belongs to the unit E that presents a NNW-SSE shoreline orientation.

Most of the beach zone consists of mixed material, while relatively higher percentage of sandy material is present in unit E (Fig. 4). Along the shoreline associated with torrential in origin cones, the dominant material consists of shingles and cobbles with the exception of the active mouth of Xerias torrent, where fine-grained sediment is also present. The aforementioned absence of fine-grained material is attributed to low terrestrial influxes and the action of marine processes although are not particularly strong (e.g. wave activity). The latter is in accordance with the overall erosive picture of the beach zone that maybe also attributed (partially) to the continuing rise of sea level during upper Holocene (IPCC, 2007).

Table 2. Weighted average (with respect to frequency of occurrence of each wind direction) of the wind velocity (Ua) and the corresponding prognostic values of significant wave period (Tp) and height (Hs) for the five successive units (A-E) of the coastal area under investigation.

	UNIT A			UNIT B			UNIT C			UNIT D			UNIT E		
	Ua	Tp	Hs	Ua	Tp	Hs	Ua	Tp	Hs	Ua	Tp	Hs	Ua	Tp	Hs
W	2.38	1.33	0.08	-	-	-	-	-	-	-	-	-	-	-	-
NW	4.20	1.85	0.16	3.61	2.59	0.28	3.16	2.13	0.20	2.80	1.97	0.15	-	-	-
N	2.80	1.55	0.10	2.80	1.63	0.12	2.80	1.80	0.14	2.80	1.97	0.15	2.80	1.98	0.16
NE	-	-	-	3.18	2.18	0.20	3.18	2.17	0.20	3.72	2.14	0.27	3.18	2.26	0.21
E	-	-	-	2.16	2.52	0.20	2.79	2.18	0.23	-	-	-	2.16	2.33	0.18

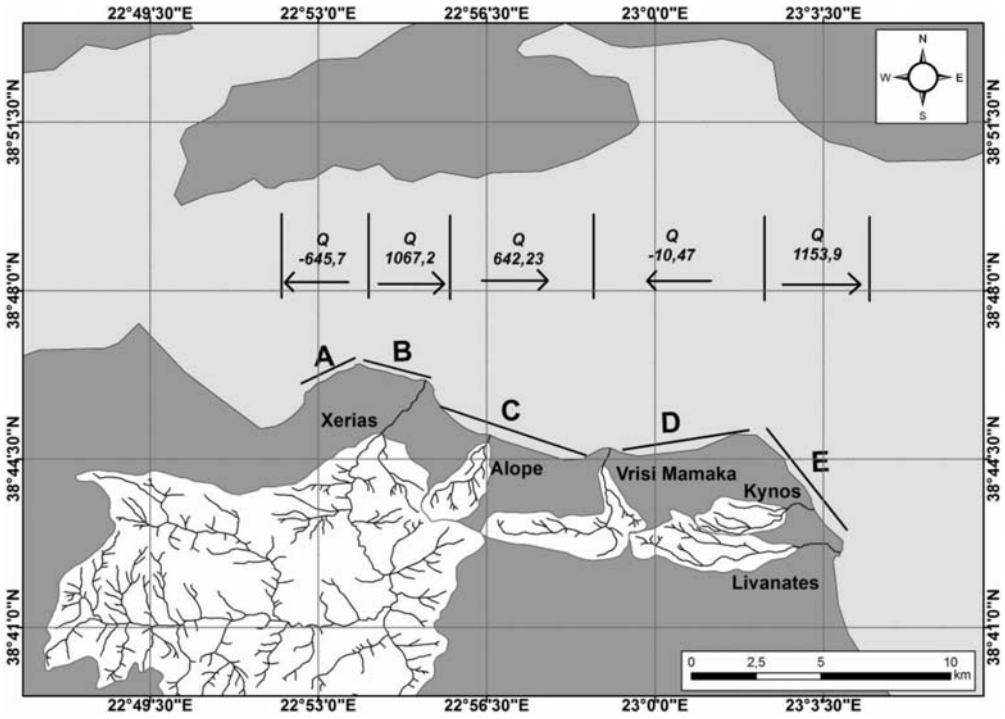

Fig. 6: Map depicting the division of the coastal area into 5 sub-units (A-E) according to their orientation. Q stands for annual potential longshore sediment transport, measured in m^3.

Table 3. Estimated values of potential longshore sediment transport (Q) per wind direction at the different units (A-E).

	UNIT A	UNIT B	UNIT C	UNIT D	UNIT E
W	10.4	-	-	-	-
NW	16.7	1277.5	438.2	611.2	-
N	672.8	127.1	614.3	-624.2	932.4
NE	-	-330.7	-240.5	2.5	260.2
E	-	-6.7	-169.8	-	-38.7
Total	-645.7	+1067.2	+642.2	-10.5	+1153.9

5. Conclusions

The presence of raised coastal landforms such as marine terraces, notches and beachrocks, suggests that the formation and evolution of the coastal zone under investigation is controlled primarily by the endogenic processes and in particular the neotectonic uplift. Nearshore marine processes play a secondary role influencing mainly beach zone shape and granulometry.

6. References

Armijio R., Meyer B., King G.C.P., Rigo A. and Papanastassiou D., 1996. Quaternary evolution of the Corinth rift and its implications for the Late Cenozoic evolution of the Aegean, *Geoph. J. Int*., 126, 11-53

Baud, A., Jenny, C., Papanikolaou, D., Sideris, C., Stampfli, G.M. 1991. New observations on Permian stratigraphy in Greece and geodynamic implication. *Bull. Geol. Soc. Greece*, XXV/1, 187-206.

Carter, R.W.G., 1988. Coastal Environments, London: Academic Press, 617p.

Clement, B. 1983. Évolution géodynamique d'un secteur des Hellénides: l'Attique septentrionale. *Annales Société géologique du Nord*, 101, 87–96.

Cundy, A., Gaki-Papanastassiou, K., Papanastassiou, D., Maroukian, H., Frogley, M. and T. Cane, 2009, Geological and geomorphological evidence of recent coastal uplift along a major Hellenic normal fault system (the Kamena Vourla fault zone, NW Evoikos Gulf, Greece)., *Marine Geology*, (under publication).

Doutsos, T., Kokkalas S. 2001. Stress and deformation in the Aegean region. *J. Struct. Geol*., 23, 455-472.

Doutsos, T., Poulimenos, G., 1992. Geometry and kinematics of active faults and their seismotectonic significance in the western Corinth-Patras rift (Greece). *J. Struct. Geol.,* 14, 689-699.

Eliet, P., and R. Gawthorpe, 1995. Drainage development and sediment supply within rifts, examples from the Sperchios basin, central Greece. *J. Geol. Soc. London*, 152, 883-893.

Gaki-Papanastasiou K., Maroukian H., Papanastassiou D. and Palyvos N., 1999 Geo-archaeology and morphotectonics in the area of Livanates-Kynos-Arkitsa during the Holocene, Proc. 5th National Gongr. of the Geological Society of Greece., 101-111.

Guernet, C., 1971. Etudes géologiques en Eubée et dans les régions voisines (Grèc). Thèse d'Etat Univ. Paris, 395 pp., Paris.

IPCC, 2007. Climate Change 2007: The physical Science Basis Summary for Policymakers Contribution of Working Group I to the Fourth Assessment Report of the Intergovernmental Panel on Climate

Change, Richard Alley et al, Geneva, 18 pp.

Kokkalas, S., Xypolias, P., Koukouvelas, I., and Doutsos, T., 2006. Postcollisional contractional and extensional deformation in the Aegean region, in Dilek, Y., and Pavlides, S., eds., Post-collisional tectonics and magmatism in the Mediterranean region and Asia: *Geological Society of America Special Paper* 409, p. 97–123, doi: 10.1130/2006.2409(06)

Komar, P.D., 1976. Beach Processes and Sedimentation, New Jersey, Englewood Cliffs: Prentice-Hall, Inc., 429pp.

Meijer, P.T., Wortel, M.J.R., 1997. Present-day dynamics of the Aegean region: A model analysis of the horizontal pattern of stress and deformation. *Tectonics* 16, 879-895.

Pirazzoli P., 1996, Sea level changes the last 20000 years. J Wiley p.211

Poulos S.E., Voulgaris G., Kapsimalis V., Collins M. and Evans G., 2002. Sediment fluxes and the evolution of a riverine-supplied tectonically-active coastal system: Kyparissiakos Gulf, Ionian Sea (eastern Mediterranean). (In:) Jones S.J., Frostick L.E. (eds) Sediment Flux to Basins: Causes, Controls and Consequences. *Journal of the Geological Society*, 191: 247-266.

Roberts, S., and J. Jackson 1991. Active normal faulting in central Greece: an overview, in The Geometry of Normal Faults, A.M. Roberts, G. Yielding, and B. Freeman (Editors), *Geological Society Special Publications* 56, Geological Society, London, 125 - 142.

Roberts, G. P. and Koukouvelas, I., 1996. Structural and seismological segmentation of the Gulf of Corinth Fault System: implications for models of fault growth. *Annali di Geophysics* XXXIX, 619-646.

US Army Corps of Engineers, 1984. Shore Protection Manual, Washington DC 21314.

Van Andel, T.H. and C. Perissoratis 2006. Late Quaternary depositional history of the North Evoikos Gulf, Aegean Sea, Greece, *Mar. Geol*., 232, 157-172.

Westaway, R., 1991. Continental extension on sets of parallel faults: observational evidence and theoretical models. In: Roberts, A.M., Yielding, G., Freeman, B. (Eds.), The Geometry of Normal Faults. *Geol. Soc. London Spec. Publ*. 56, 143–169.

Woodward J.C., 1995. Patterns of Erosion and suspended Sediment Yield in Mediterranean River Basins. (In:) Forster I.D.L. Gurnell A.M. & Webb B.W.(Eds), Sediment and water quality in river catchment. Wiley, Chichester, 365-389.

Hellenic Army service, Topographic maps 1:50.000 sheets Pelasgia, Elateia, Livanates, 1979.

Institute of Geology and Mineral Exploration, Geological maps 1:50.000 sheets Pelasgia, Elateia, Livanates, 2006.

Δελτίο της Ελληνικής Γεωλογικής Εταιρίας, 2010
Πρακτικά 12ου Διεθνούς Συνεδρίου
Πάτρα, Μάιος 2010

Bulletin of the Geological Society of Greece, 2010
Proceedings of the 12th International Congress
Patras, May, 2010

MORPHOTECTONIC ANALYSIS OF SOUTHERN ARGOLIS PENINSULA (GREECE) BASED ON GROUND AND SATELLITE DATA BY GIS DEVELOPMENT

Vassilopoulou S.

National and Kapodistrian University of Athens, Faculty of Geology & Geoenvironment, Department of Geophysics-Geothermics, 15784 Athens, Greece, vassilopoulou@geol.uoa.gr

Abstract

Southern Argolis Peninsula is an interesting Geological and Geomorphological area due to the variety of the geological structures and the interchange on the terrain. Ground and remote sensing data, relating to geology and tectonics, were compiled with terrain analysis data in a GIS data base, in order to perform morpho-tectonic analysis in the Southern Argolis Peninsula. Terrain analysis data were automatically produced by the specific software "PROANA" (based on ArcGIS). The main direction of Southern Argolis Terrain is E-W. The same direction is observed from the rose-diagrams of morphological discontinuities. The hydrographic network has a NW-SE main direction. The depositional planation surfaces (0-5%) that are located near the coast are related with neotectonic faults. The direction of the Faulting Zones is mainly ESE-WNW and E-W. The most active tectonic structures were observed to the southern and south-western area of Southern Argolis Peninsula, towards Kranidi and Argolikos Gulf.

Key words: *morpho-tectonic analysis, terrain analysis, GIS, remote sensing data, image processing, image interpretation, Argolis Peninsula, Greece.*

1. Introduction

The morpho-tectonic analysis of Southern Argolis Peninsula (SE Peloponnesus) is the subject of the present research. The variety of the geological structures (Alpine, Post-Alpine and Volcanic formations), as well as the interchange on the terrain (mountains, hills, plains, valleys, morphological discontinuities), are the main reasons that Southern Argolis has great interest not only from the Geological, but also from the Geomorphological point of view.

The linear structures (morphological and tectonic) have not a consistent direction. Different directions are observed in the different parts of the area: Region of Didyma - Iria, Adheres, Kranidi – Ermioni, Porto-Cheli, Poros Island, Methana Peninsula (Fig. 1c). Each region is characterized by different formations and has its own tectonic structure. Terrain's morphological peculiarities, among others, basically depend on tectonic phenomena and geological formations. From attentive study of the terrain, interesting results can be extracted concerning the tectonic – neotectonic – morpho-tectonic e.t.c. characteristics of the area.

Foreign and Greek Scientists have studied the complicated geological structure of Argolis Peninsula since the early of the 20th century. Alpine and Post-Alpine Formations cover the Southern Argolis Penisnsula that are part of the following Geotectonic Units: Sub-Pelagonian (Papanikolaou, 1986,

1989), Arvi-Miamou-Adheres (Papanikolaou, 1989) as well as Akros Unit (Baumgartner 1985, Papanikolaou et al., 1992) including the ophiolite nape of the Ocean Pindos-Cyclades. The formations of Argolis Peninsula are characterized by tectonic facies (thrusts and over-thrusts) of Upper Jurassic - Lower Cretaceus (Vrienlynck, 1978 a, b, 1980, Baumgartner, 1985) as well as Upper Eocene (Vrienlynck, 1978 a, b, 1980, Baumgartner, 1985, Gaitanakis and Photiades, 1989, 1991, 1993, Papanikolaou et al., 1992). Folds follow after thrusts and over-thrusts (Upper Eocene – Oligocene). The last tectonic facies of the region is the faulting tectonics of Neogene-Quaternary as well as the observed volcanicity of Saronikos Gulf (last 5m.a).

2. Methodology

The used methodology in order to perform morpho-tectonic analysis in the Southern Argolis Peninsula will be presented. This work was made within the framework of a Doctorate thesis (Vassilopoulou, 1999), in the Department of Dynamic–Tectonic–Applied Geology, Faculty of Geology & Geoenvironment, University of Athens. The aim of this thesis was to study the recent geodynamic evolution of the Southern Argolis Peninsula based on the terrain analysis by GIS development and the use of remote sensing data.

2.1 Fieldwork

The geological and tectonic data of the area were collected for the compilation of the "Synthetic Geological Map of Southern Argolis Peninsula", as well as "Tectonic map of Southern Argolis Peninsula". Fieldwork also included the checking of the maps of terrain analysis that were automatically produced by the "PROANA" software.

2.2 GIS Development

The GIS methodology was chosen, since there was a large number of data from various sources (thematic maps, satellite images etc.) in different forms (raster, vector) and in different map projections. ArcGIS package was used for the data processing, the map composition, the creation of the relational data-base and the data-base management.

2.3 The Use of Remote Sensing Data

Two digital satellite images LANDSAT 5, TM (16/8/91) and SPOT panchromatic (16/8/94) were processed. The Image Processing was made using the IMAGINE of ERDAS software package. This work can be divided in two steps:

- Image Pre-processing (Geometric Correction and Enhancement).
- Image Interpretation.

Additional processing has been applied to the LANDSAT image concerning the combination of spectral zones, as well as the principal components analysis. The main task was the image interpretation relating to the tectonic features (mainly faults and other tectonic contacts), geological and geomorphological features, based on the main diagnostic characteristics that are used from geo-scientists (Astaras, 1990, 1998, Migiros et al. 1995). The direct recognition of the tectonic features on satellite images, is based on the concept of morpho-structures and mainly on morpho-tectonics. Faults, joints and lineaments most likely have a rectilinear exposure on images and their determination depends on morphological features or in particular patterns. Gupta (1991) describes

the criteria for the recognition of the faults. All the geological morphological and tectonic features were checked in the field and were imported to "PROANA" for the production of the corresponding maps and diagrams.

2.4 The Development of the Specific Software "PROANA"

The specifically developed software (based on ArcGIS), called "PROANA", was named after the Greek initials "Prototype Analysis Anaglyfou (Terrain)". All associated data and maps for the terrain analysis of Argolis Peninsula were automatically produced by "PROANA" (Vassilopoulou 1999, Vassilopoulou 2001). The geological and tectonic data were manipulated and the following maps were compiled (scale 1:50,000): "Synthetic Geological Map of Southern Argolis Peninsula" (Fig. 1a), "Tectonic Map of Southern Argolis Peninsula", "Tectonic Data from Satellite Images" (Fig. 1b). Terrain analysis layers, that have been produced by "PROANA", were related to the geological and tectonic layers, so that new synthetic layers and maps were compiled (scale 1:50,000) with their data base: "Digital Elevation Models (resolution 20m etc.)", "Shaded Relief", "Map of Hydrographic Network and Basins", "Slope and Aspect Map", "Range map" (terrain is divided in categories of elevation zones), "Map of Discontinuities of Morphological Slopes", "Map of Terrain Analysis (Synthetic Map)" (Fig. 2c), "Map of Planation Surfaces Classified in Depositional and Erosional with theirs Slope Direction and Categorized with respect to their Slope" (Fig. 3d), "Planation Surfaces categorized related to their Elevation", etc.

3. Geology and Tectonics

A "Synthetic Geological Map of Southern Argolis Penisula" (Fig. 1a) is given by Vassilopoulou (1999). The following Post-Alpine and Alpine geological formations cover the region:

Post-Alpine Formations:

— Alluvial and Coastal Deposits (Quaternary): Unattached sands, clays, pebbles, breccias and gravels are observed. They are usually developed over the plains that are between the mountains or along water course, coastal areas, river mouth etc.

— Colluvial Deposits and Talus Cone: They consist of pebbles, breccias and congelifracts in different size, either cohesive and agglutinate or unattached. They mainly occur in water course mouth or along faulting zones etc.

— Porto-Cheli - Kranidi Conglomerates - Sandstones - Marls System (Plio-Pleistocene): The system covers the southern region of Argolis Peninsula and is overlaid on the "Kranidi Serpentinites" (in unconformity). It is characterized by small dip to the S-SW. Mainly calcareous but also serpentinites and psammitic pebbles consist the conglomerates. The matrix is calcareous or gridstone and pack sand as well as some times marly. Calcite dykes, calcite fragments and incrustations are observed. The system is overlaid on the lacustrine-terrestrial red pelitic fossil soil in several positions.

— Methana - Poros Volcanic Formations (Pleistocene): They consist of loose volcanic materials, pyroclastic deposits as well as concentrations of volcanic materials, domes and lava flows of dacides and andesites. They cover Methana Peninsula and the southern region of Poros Island.

Alpine Formations: They cover the rest of the region having the major extent. Two units can be distinguished: Argolis Upper Composite Unit which is in tectonic contact with Didyma Unit.

— Argolis Upper Composite Unit (synthetic upper tectonic unit of Southern Argolis Peninsula):

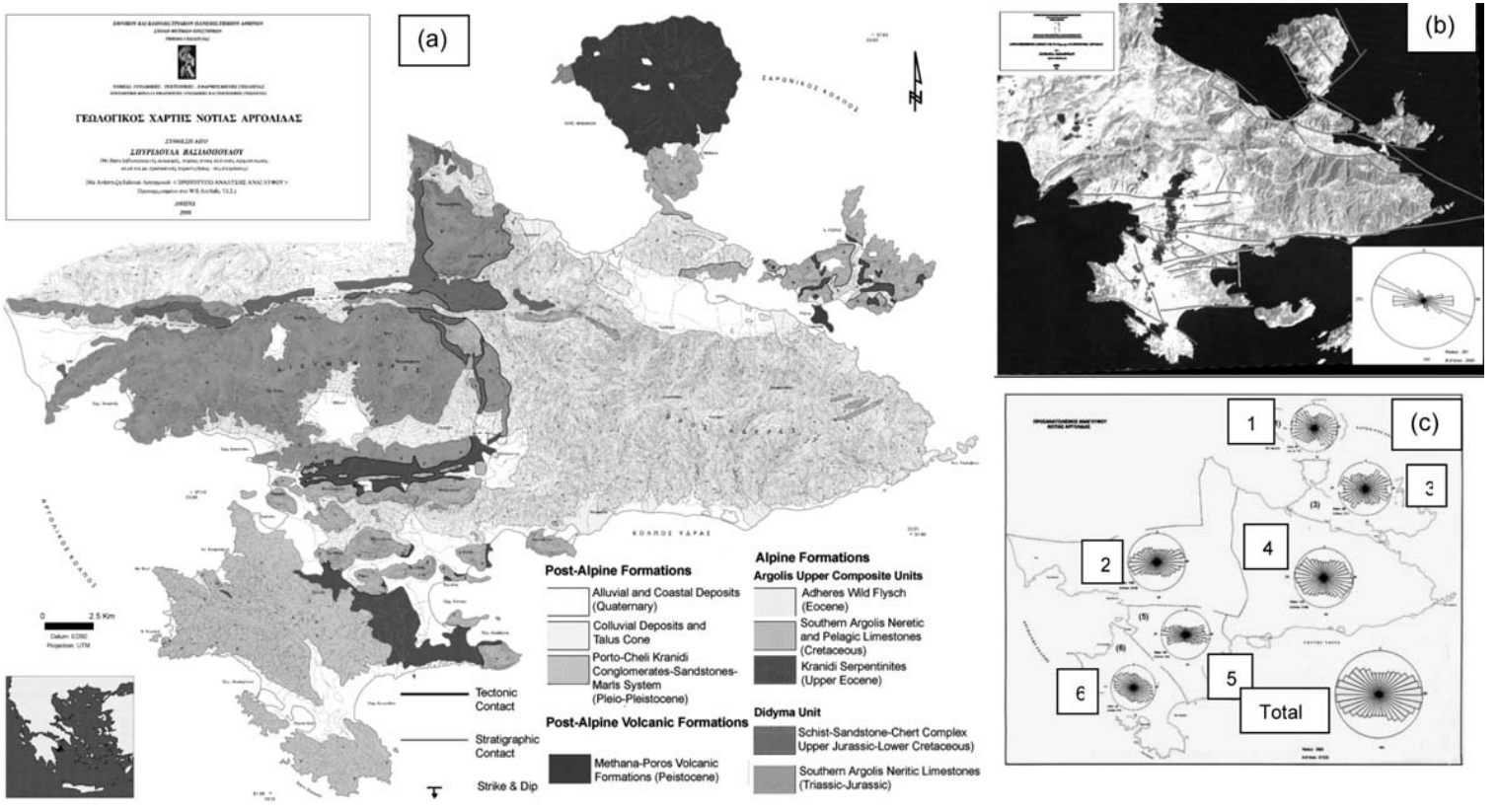

Fig. 1: (a) The Synthetic Geological Map of Southern Argolis Peninsula is presented. b) LANDSAT 5, TM, Satellite Image, false color composite 4-7-2 (RGB), of Southern Argolis Peninsula with Faults (gray line) is given. The directions of the faults appear in the rose-diagram. c) Rose-diagrams of each sub-region (1-6) as well as for the whole region (total diagram) are given and represent the orientation of the Terrain of Southern Argolis Peninsula. For the rose-diagrams creation Arc/Info W/S together with SynArc packages were used.

- Adheres Wild Flysch (Eocene): It belongs to Arvi-Miamou-Adheres Geotectonic Unit. Marls, calcareous-marly and turbidity sandstones, breccias and conglomerates compose the flysch.
- Southern Argolis Neritic and Pelagic Limestones (Cretaceous): Dolomites and quartz conglomerates occur in the base, while neritic, pelagic and intermediate limestones follow.
- Kranidi Serpentinites (Upper Eocene): It is an ophiolitic tectonic melange of serpentinites, hartzburgites, gabbros, amphinolites, andesitic lavas and marbles. This is the lower formation of the unit.

— Didyma Unit (Sub-Pelagonian - neritic basement):

- Schist-Sandstone-Chert Complex (Upper Jurassic - Lower Cretaceous): Schist-sandstone-chert complex with ophiolites are observed. This formation is in tectonic contact with "Southern Argolis Neritic Limestones".
- Southern Argolis Neritic Limestones (Triassic - Jurassic): Fine granular red limestones, neritic limestones of Pantokratoras and Ammonitico Rosso compose this formation.

The "Tectonic Map of Southern Argolis Peninsula" (Fig. 1b) is given by Vassilopoulou (1999). A Rose-diagram of the faults of the Southern Argolis Peninsula (Fig.1b) was created based on the thematic layer of the faults. The directions of the faults appear in the diagram.

4. Terrain Analysis

4.1 Terrain Analysis of Sub-Regions of Southern Argolis Peninsula

The relief of Southern Argolis Peninsula presents various structures. The region was divided in six sub-regions. The deviation of the region was based on the geomorphology, geology and tectonics. The six sub-regions were divided from North to South (Fig. 1c) as follows: (1) Region of Methana, (2) Region of Didyma – Iria, (3) Region of Southern Methana – Poros Island, (4) Region of Adheres, (5) Region of Kranidi-Ermioni, (6) Region of Porto-Cheli.

The qualitative and quantitative terrain analysis of each sub-region as well as of the whole region was based on the terrain analysis data (morphological slopes, morphological discontinuities, hydrographic network, planation surfaces – Figs 2c, 3d). The qualitative terrain analysis was done using the maps of terrain analysis relating to geology and tectonics (Figs 1a, b, 2c, 3d). The quantitative terrain analysis was based on terrain analysis layers, their database and the database management. The statistical analysis of the terrain includes the creation of a rose-diagram that represents the terrain orientation (Fig. 1c) together with diagrams that represent the mean elevation relating to percentage (%) area of the study region (Fig. 2a), the mean elevation of planation surfaces relating to their percentage (%) area (Fig. 3c), etc. A numerous of rose-diagrams for each sub-region and for the whole region (total diagrams) were produced representing the orientation of the linear structures of the terrain: morphological discontinuities, hydrographic network, watersheds (Figs 2b, 3a, b), etc.

The description of the morphological and tectonic features for each of sub-region follows:

(1) Region of Methana: The region includes Methana Peninsula, excluding the southern part of it. Interchanging hills and valleys are observed. The terrain is rough. It is a new structure since is covered from Pleistocene volcanic formations. Methana Peninsula consists the northern part of the Hellenic Volcanic Arc. This region is a neotectonic active block with N-S direction. NW-SE faults of West Saronikos Gulf are the boundaries of this block. The morphology, the structure and all the morphological features of the region, mainly depend on the volcano.

(2) Region of Didyma – Iria: It extends along the north-western margin of the study area, between Argolikos Gulf (eastern) and Adheres Mountain (western). The terrain is characterized as rough (the "areal extend" is decreased when the altitude is increased). The region is covered from Alpine carbonate formations, mainly limestones of Sub-Pelagonian Unit. The fault-block has an E-W direction. It is observed that it is strongly uplifted compare to all the other blocks (planation surfaces are observed at an elevation of 1100m). The morphology of the region depends partially on tectonic activities and on lithology. At present time the erosion controls the terrain, apart from the coastal regions (near to Argolikos Gulf) that they are more active. The residuals planation surfaces, the morphological discontinuities the main branches of the hydrographic network, and the watersheds have a linear expansion in various parts of the region as it appears in the diagrams (Figs 2b, 3a, b). This direction corresponds with the alpine structures (tectonic contacts) and neotectonic structures (faults, etc). Cyclic features are also observed i.e. carbonate basins (Karst Doline of Didyma etc). Contrarily, Iria Plain (western), Loukaiti Plain (eastern) as well as other plains are not karstic and depend on tectonism since they correspond with E-W and NE-SW faults. E-W, NE-SW, NNW–SSE faults are observed while the rest of the tectonic contacts have E-W and N-S directions. The neotectonic fault-block seems to be a tectonic horst since the end of the Alpine Circle until today. Neogene sediments have not been observed. The general geometry of the tectonic structures is mainly according to the West Saronikos Gulf structures.

(3) Region of Southern Methana – Poros Island: The neotectonic fault-block extends at the southern of "Methana Region". It extends from the southern part of Methana Peninsula to the planation surface (southern) which is the northern boundary of Adheres and Poros Island. It is characterized by low elevations, excluding the Asprovouni Mountain (northern of Methana, 335m elevation) and Vigla Mountain (Poros Island, 358m elevation). The fault-block comprises Alpine formations (Eocene flysch, Cretaceous limestones, serpentinites- ultrabasic). The terrain is rough. Faults of E-W and NW-SE directions are observed, while some of them are the boundaries of the region. Tectonism (mainly the tectonic structures of Saronikos Gulf) controls the block. Partially, NW-SE as well as E-W linear expansion of the features is distinguished. Some morphological features are not well formed, since faults with two directions control the terrain.

(4) Region of Adheres: The neotectonic fault-block includes Adheres Mountain (SE Argolis Peninsula) that has a great extent. Adheres Mountain extends in a direction E-W. High altitudes (500-700m) are observed on the ridge of the mountain. Eocene flysch covers the region with the occurrence of limestone rocks. The terrain is characterized by vertical dissection, a N-S dense hydrographic network and intense erosion. N-S linear expansion of the features is observed. The terrain is rough because of the existing steep slopes. The fault block is characterized as a tectonic horst related to Saronikos Gulf (on the North) and Hydra Gulf (on the South) that they are both tectonic grabens. The peculiarity of the relief mainly depends on the lithology since tectonic structures cannot be distinguished interiorly. E-W marginal faults on the North and South control the block and all the morphological features.

(5) Region of Kranidi-Ermioni: This neotectonic fault-block lies south to the "Didyma-Iria Region". Cretaceous limestones, serpentinites-ultrabasic rocks and flysch are observed. It extends from Hydra Gulf (east) to Argolikos Gulf (west) including the villages Fourni, Koilada, Kranidi, Alatovouni, Ermioni, Mouzaki to Petrothalassa (Kranidi Gulf). Small elevation hills are observed together with valleys. Mavrovouni (427m elevation), Profitis Elias (347m) and Asprovouni (396m) have the higher elevation. Alluvial cover the great coastal plains. Many E-W and NW-SE trending faults are observed which are distinguished clearly because of the occurrence of the fault surfaces, morpholog-

ical discontinuities and other morphological and tectonic characteristics. The Fault-block is active and complicated with many faults dividing the region in smaller fault-blocks (horsts and grabens). The directions of the fault-blocks correspond to the directions of the faults. Generally, all the tectonic features are well developed. Linear structures are observed with a general E-W direction. The morphological features of the area as well as the creation of E-W and NW-SE horsts including limestones, grabens including serpentinites and flysch, but also alluvial basins depend on the tectonic activity.

(6) Region of Porto-Cheli: This region is the southern part of Argolis Peninsula. The terrain is hilly. Low and gentle morphological slopes are observed. This morphology is characteristic of the Post-Alpine formations. Porto-Cheli-Kranidi Conglomerates - Sandstones - Marls System (Plio-Pleistocene) cover the region. The higher altitudes (>200m) are observed to the north and the altitude decrease to the south. The main terrain orientation is WNW-ESE and a secondary N-S direction is observed. The main fault direction is NW-SE. Tectonism controls the terrain as well as all the morphological features. Plio-Pleistocene formations indicate that the region was recently under the sea level. At present time the region has been uplifted and some features have not been clearly formed in the region.

4.2 Terrain Analysis of Southern Argolis Peninsula

Southern Argolis Peninsula Terrain is characterized generally smooth, up to elevation of about 200m (Fig. 2a). An anomaly is observed at the diagram of "mean elevation relating to percentage (%) area", because of the "Doline Didyma". The terrain is rough from the elevation of 200m to 700m including some anomalies due to the occurrence of planation surfaces. The terrain is very rough from the elevation above of 700m, where high morphological slopes extend in small area.

4.2.1 Planation Surfaces Classification

The planation surfaces (slope 0-5%) have been classified in four categories according to the diagram "the mean elevation of planation surfaces relating to their percentage (%) area" (Fig. 3c):

a) Planation surfaces with low altitudes 0-30m: They are mainly depositional (apart from the 3% which are erosional) covering the 38% of the total area of all the planation surfaces. They are developed over all the formations of the region. They are coastal having large extent and they are related to the neotectonic faults (Fig. 3c,d).
b) Planation surfaces with altitudes 170-210m: They are mainly depositional covering the 9% of the total area of all the planation surfaces. They are developed over the limestones of Didyma Unit (Didyma-Iria Region) having large extent (but smaller than the previous category). Some of them (having small extent) are developed over flysch (Fig. 3c,d).
c) Planation surfaces with altitudes 70-110m: They are erosional covering the 3% of the total area of all the planation surfaces (Fig. 3c,d). They are mainly developed over the Post-Alpine formations (Porto-Cheli Region). Few planation surfaces are developed over serpentinites and ultrabasic rocks (Ermioni-Kranidi Region).
d) Planation surfaces with altitudes 350-390m: They are depositional and erosional having the 1% extent of the total area of all the planation surfaces (Fig. 3c,d). This category represents mainly the "Doline Malavria" (Didyma-Iria Region) which has been recently created, and the northern boundary of the region, which is covered from schist-sandstone-chert complex (western of Ortholithi).

The rest of the planation surfaces (erosional and depositional) have very small percentage of the total area of all the planation surfaces and extend in a very small area.

The planation surfaces (slope 5-15%) are mainly developed over the Post-Alpine formations having large extent. They have smaller surface extent when they are developed over the talus slope (Didyma Unit). The rest of the planation surfaces cover very small area.

4.2.2 Terrain Orientation

E-W is the main terrain orientation as appears in the rose-diagram (Fig. 1c), while all the other directions are represented with smaller rates to the rose-diagram (Fig. 1c). The N-S direction represents the smaller rate in the diagram.

4.2.3 Morphological Features and Faulting Zones Direction

E-W is the main direction of the morphological discontinuities. The NE-SW direction and the N-S direction have smaller rate of appearance in the rose-diagram (Fig. 2b). Additional, all other directions have also small rates (Fig. 2b).

The hydrographic network has mainly NW-SE direction, and in some areas the directions changes to N-S and E-W. All other directions appear in the diagram with smaller rates (Fig. 3a).

ENE-WSW is the main direction of the watersheds while the N-S direction represents smaller rate in the diagram. All other directions appear in the diagram with smaller rates (Fig. 3b).

The direction of the Faulting Zones is mainly WNW-ESE and E-W. The NW-SE direction and the NE-SW have smaller rates (Fig. 1b).

5. Conclusions

Ground and remote sensing data relating to geology and tectonics were compiled with terrain analysis data (automatically produced by the "PROANA" software) in a GIS data base to perform morpho-tectonic analysis in the Southern Argolis Peninsula.

From "Didyma-Iria" fault-block (North) to "Porto-Cheli" (South), the neotectonic deformation increases. This is expressed by the increase of the morpho-tectonic and tectonic features (planation surfaces, morphological discontinuities, faults) which are more evident at the southern. Also, the faults are related to intense morphological discontinuities, while the faults-mirror, the fault breccia and other tectonic characteristics, are greater in number and clear.

Summarizing, the most active tectonic structures are observed to the southern and south-western area of Southern Argolis Peninsula, towards Kranidi and Argolikos Gulf.

Apart from the general E-W direction of the structures a NW-SE direction is also observed from North to South. The latter happens since the Southern Argolis Peninsula is in between West Saronikos Gulf, which is characterized mainly by E-W faults, and Argolikos Gulf which is characterized by NW-SE faults.

"PROANA" software can be used as a useful tool for various environmental applications, related to the terrain analysis.

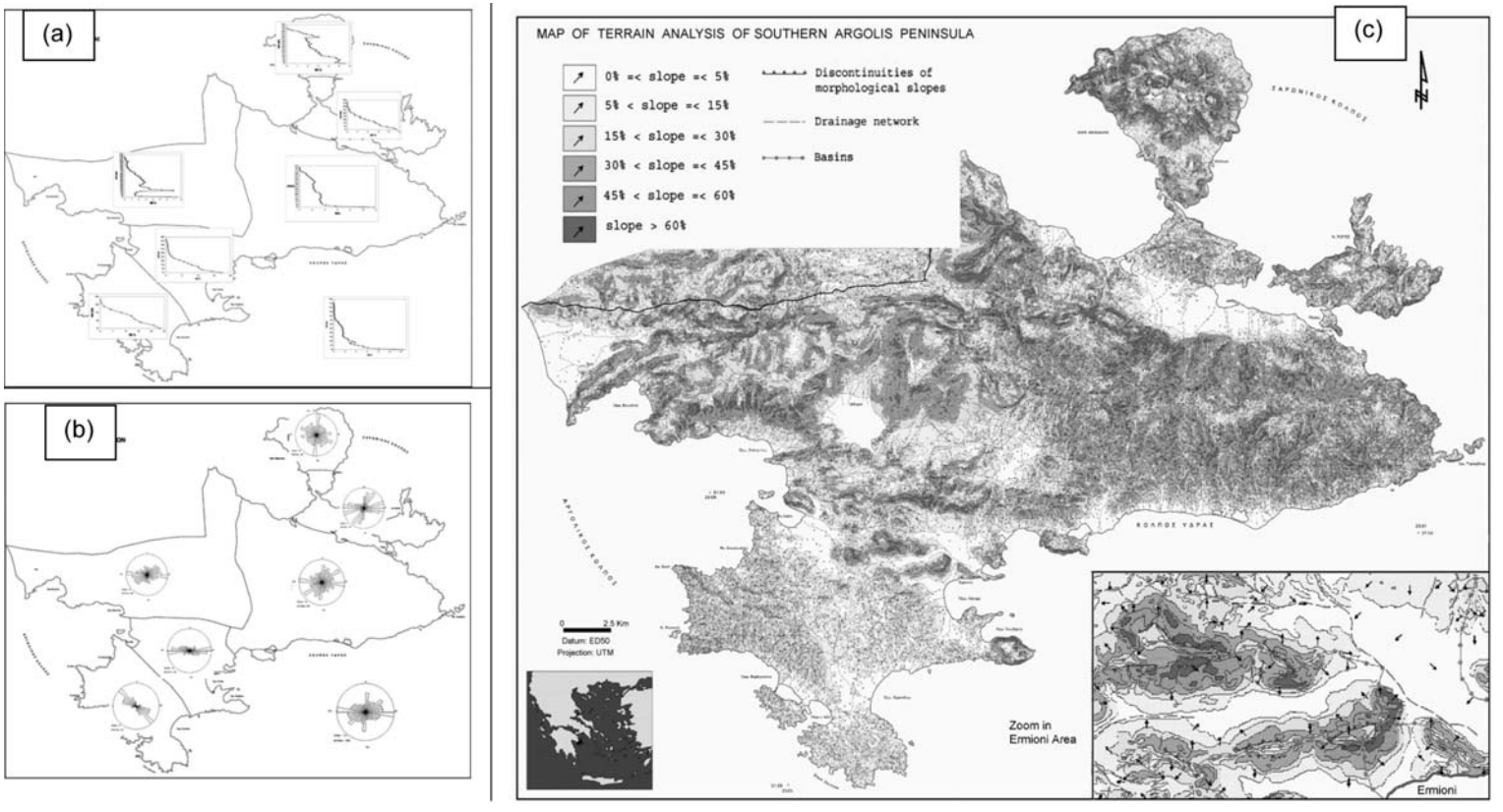

Fig. 2: (a) "The Mean Elevation relating to percentage (%) Area"of Southern Argolis Peninsula is given. The interchanges of the terrain in relation to the elevation can be observed. (b) The Rose-Diagrams of Orientation of Morphological Discontinuities of Slopes is given - These represent the differences in slope more than 10% - This layer is a compilation of the layers of slopes, aspect and range. (c) The "Map of Terrain Analysis" is a synthetic Map. It includes all the features for terrain analysis (slope, aspect, morphological discontinuities, hydrographic network and watersheds), that were automatically produced by "PROANA" software.

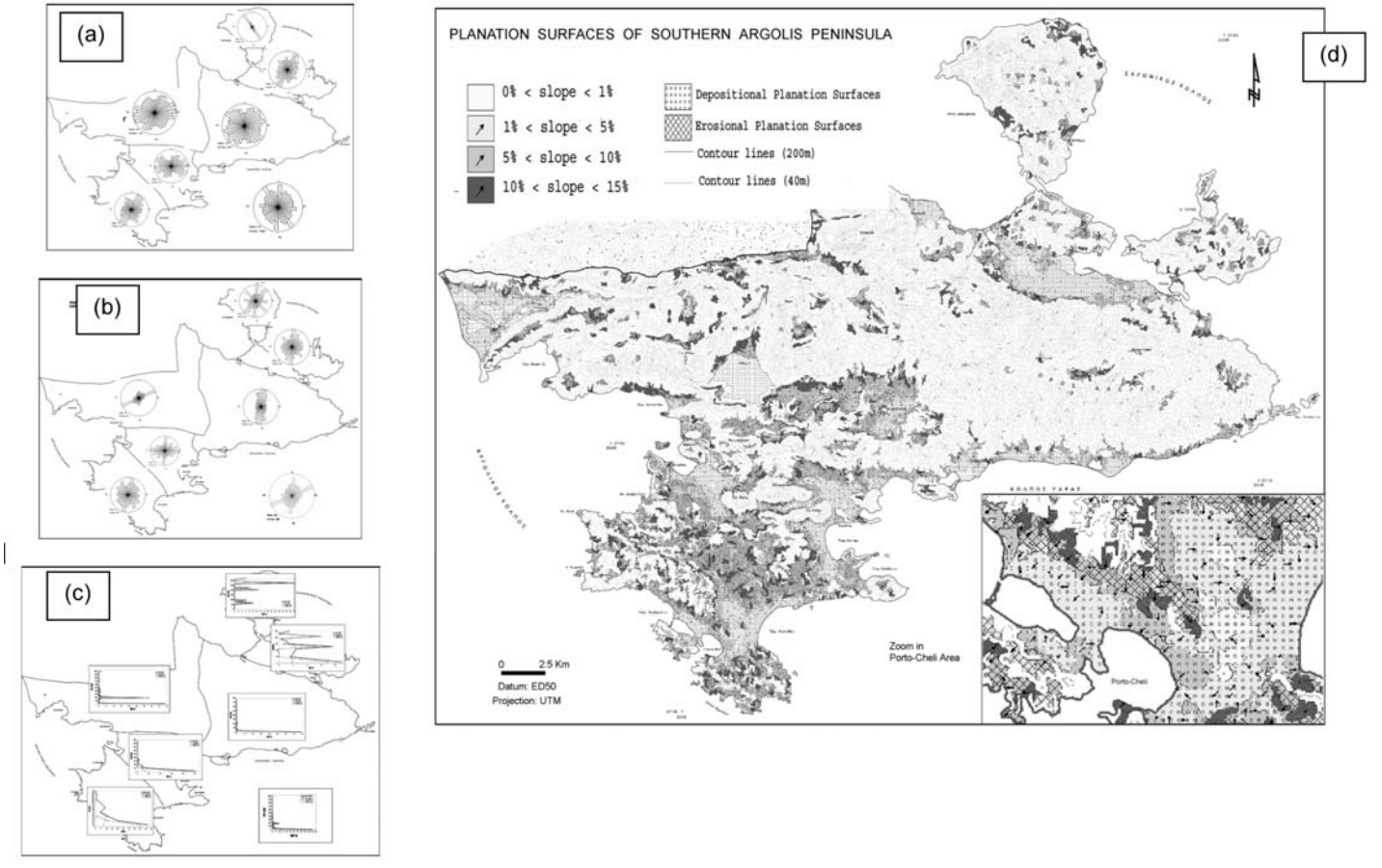

Fig. 3: (a) Rose-Diagrams of Orientation of Hydrographic Network (b) Rose-Diagrams of Orientation of Watersheds (c) "The Mean Elevation of Planation Surfaces relating to their percentage (%) Area" is given. (d) "Map of Planation Surfaces". The planation surfaces are regions of the terrain where their slope has values from 0 to 15%. This synthetic layer is a compilation of the thematic layers of slopes, aspect, range and geology.

6. Acknowledgments

The author would like to thank Prof. D. Papanikolaou, Prof. E. Lagios, Prof. E. Lekkas, Pof. L. Hurni (ETH, Zurich), Prof. Ch. Metaxaki, E. Andoniou, Ass. Prof. S. Lozios, Ass. Prof. Is. Parcharidis, Dr. V. Sakkas and one anonymous referee for their useful comments, as well as MDS Marathon Data Systems Company for their help with ArcGIS s/w package.

7. References

Astaras, Th., 1990. The contribution of Landsat Thematic Mapper Imagery to the Geological and Geomorphological Reconnaissance Mapping in the Mountain Area of Kerkini – SW Part of Rhodope Massif and the Surrounding Plains (Hellenic – Boulgarian Borders). *Geographica Rhodopica*, vol. 2, p.105-114.

Astaras, Th., 1998. Photo-Inerpretation (Remote Sensing) in Geosciences. *Notes,* Aristotle Univ. of Thessaloniki, School of Geology, Dep. of Geology and Phys. Geography.

Baumgartner, P.O., 1985. Jurassic Sedimentary Evolution and Nappe Emplacement in the Argolis Peninsula (Peloponnesus, Greece). Univ. Basel. 137p.

Gaitanakis, P., Photiades, A.D., 1989. Les Unites Ophiolitiques de l' Argolide (Peloponnese, Greece). *Bull. Geol. Soc. Greece*, XXIII /1, 363-380, Athens.

Gaitanakis, P., Photiades, A.D., 1991. Geological Structure of Southern Argolis. *Bull. Geol. Soc. Greece*, XXV /1, 319-338, Athens.

Gaitanakis, P., Photiades, A.D., 1993. New Data on the Geology of Southern Argolis (Peloponnesus, Greece) *Bull. Geol. Soc. Greece*, XXVIII /1, 247-267, Athens.

Gupta, P.R., 1991. Remote Sensing in Geology. *Springer-Verlag*, 356.

Migiros, G., Pavlopoulos, A., Parcharides, Is., 1995. Remote Sensing – Applications in Geosciences. *Notes*, Agricultural Univ. of Athens, Labor. of Oryctology-Geology, Athens.

Papanikolaou, D., 1986. Geology of Greece, p. 240, Athens.

Papanikolaou, D., 1989. Geotectonic map of Greece. Geol. Soc. Of Greece, *Spec. Publ. No 1, IGCP Proj.* No 276, Newsletter No 1.

Papanikolaou, D., Lekkas, E. Logos, E., Lozios, S., 1992. Neotectonic Map of Greece (Lygourion Sheet), Research Project, Nomarchy of Argolis.

Vrielynck, B., 1978a. Donnees nouvelles sur les zones internes du Peloponnese, Grece. Diss. Univ. des Sciences et Techniques Lille, These 3^{o} Cycle, 134p.

Vrielynck, B., 1978b. Donnees nouvelles sur les zones internes du Peloponnese. Les massifs a l' est de la plaine d' Argos (Grece). *Ann. Geol. Pays Hellen.,* 29, 1977, 440-462, Athenes.

Vrielynck, B., 1980. Les tectoniques tangetielles des zones internes du Peloponnese (Argolide, Grece). C.R. Acad. Sci. (Paris) 290, Serie D, 967-970.

Vassilopoulou, S., 1999. Geodynamics of the Argolis Peninsula with GIS development and the use of Remote Sensing Data. PhD Thesis, University of Athens, Faculty of Geology, p. 194.

Vassilopoulou, S., 2001. "PROANA" A Useful Software for Terrain Analysis and Geoenvironmental Applications – Study Case on the Geodynamic Evolution of Argolis Peninsula, Greece. Proc. *20th International Cartographic Conference*, Beijing, China, pp. 3432-344.

Δελτίο της Ελληνικής Γεωλογικής Εταιρίας, 2010
Πρακτικά 12ου Διεθνούς Συνεδρίου
Πάτρα, Μάιος 2010

Bulletin of the Geological Society of Greece, 2010
Proceedings of the 12th International Congress
Patras, May, 2010

PROBABILISTIC HAZARD ASSESSMENT, USING ARIAS INTENSITY EQUATION, IN THE EASTERN PART OF THE GULF OF CORINTH (GREECE)

Zygouri V.

University of Patras, Department of Geology, Laboratory of Structural Geology, 26500 Patras, Greece, zygouri@upatras.gr

Abstract

Shallow earthquakes cause serious damage near the trace of faults. The growth of major cities in hazard prone areas and the public anxiety associated with risks in critical facilities has focused attention to those areas. The Gulf of Corinth constitutes an area prone to high seismicity. During the last 2000 years several strong seismic events have caused extensive collapses, death casualties and widespread landslide phenomena. Strong motion attenuation relationships are considered a significant parameter for any earthquake hazard analysis. Attenuation relationships used in probabilistic hazard assessments predict ground motions components (in this case arias intensity) as a function of source parameters (magnitude and mechanism), propagation path (fault distance) and site effects (site class). In the eastern part of the Gulf of Corinth arias intensity equations were applied for a number of large E-W trending faults dominating the seismic potential of the area. Those faults have already been associated with landslide phenomena according to historic records and by using new methodologies a probabilistic approach of their behaviour has been accomplished for different recurrence intervals.

Key words: *arias intensity, probabilistic hazard assessment, landslide phenomena, eastern gulf of Corinth.*

1. Introduction

The historic seismicity of the Gulf of Corinth is well – described since is responsible for the destruction of ancient cities lying on the northern coasts of Peloponnese. However, the modern seismicity is equal violent and destructive (Ambraseys and Jackson, 1990, Papadopoulos et al., 2000, Papazachos and Papazachou, 2003). These abundant seismically produced hazards are accompanied by serious ground failures as described in the Alkyonides earthquakes (Koukis and Rozos, 1985) and in Pyrgos area (Koukouvelas et al., 1996). The north coast of Peloponnese and especially the eastern part of the Gulf appear a high relief that in combination with the high rate of sedimentation due to the rivers' flow can trigger potential slides and lateral spreads. However, little have been done regarding the estimation of this potential hazard (Koukis et al., 2009).

For this reason we applied strong motion attenuation relationships in the easternmost part of the Gulf of Corinth in order to conduct an earthquake hazard analysis for the most significant almost E – W trending faults. These faults show spectacular exposed surface traces and large cumulative slip.

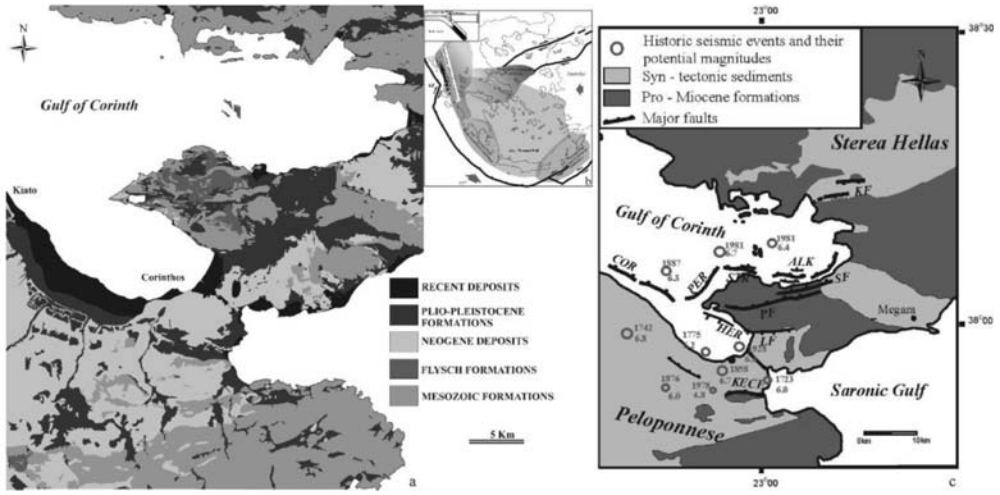

Fig. 1: a) Simplified stratigraphy map of the eastern part of the Gulf of Corinth Greece. b) Geological setting of the study area. c) Simplified map showing the main structural features along the eastern part of the Gulf, as well as the main historical seismic events. COR: Corinthos fault, KECF: Kechriaie fault, LF: Loutraki fault, HER: Heraion fault. PER: Perachora Fault, PF: Pissia Fault, SF: Skinos Fault, STR: Strava fault, ALK: Alkyonides Fault, and KF: Kaparelli Fault.

2. Geological setting

The Gulf trends WNW-ESE across the Hellenic mountain range which reaches an elevation of almost 2km approximately perpendicular to the inherited structural grain of the Alpine orogenesis. Current rates of extension imply that this region is extended in N-S direction up to a rate of 15mm/yr (Briole et al., 2000), while at the eastern end of the Gulf the rate is reduced to a value of 6mm/yr (Avallone et al., 2004). Extensional deformation within the Gulf is inferred initiated in Pliocene and is primarily accommodated by E – W trending faults (Doutsos and Kokkalas, 2001). These major faults have trace length in the order of 15-20 km and are compartmentalized into en-echelon segments, dipping at moderate angles (50-60º) (Koukouvelas and Doutsos, 1996). The sedimentary processes are controlled by the tectonic activity creating high relief through seismic ruptures and suitable conditions for high sediment supply (see Zygouri et al., 2008 and references therein).

In the study area fluvial – lacustrine sediments are recognised in a transect from Kaparelli area through Perachora Peninsula and further south to the Corinthos region (Fig. 1, Collier and Dart, 1991; Bentham et al., 1991). The marine terraces that dominate the coastal zone of north Peloponnese is the result of the sea level changes in combination with the fault activity. At the inner part of the Gulf the sedimentary process consists of turbiditic currents and the development of deltaic fan near the river's mouths.

Historical and instrumental seismic catalogues in the eastern part of the Gulf of Corinth include records of at least twelve rupture events from 426 BC (Ambraseys and Jackson, 1990) up to the last destructive Alkyonides event in 1981 AD (King et al., 1985). In many cases these events triggered large landslides and/or liquefactions in coastal areas recorded in 1858 (Koustas, 1858) and in 1981 event (Koukis and Rozos, 1985). In many cases landslides are responsible for highly variable and significant numbers of casualties and damages after a strong earthquake, therefore, this paper aims to shed some light to the potential distribution of mass wasting induced by the earthquakes of five of main active faults of the eastern part of the Gulf.

Table 1.

Empirical relationships		*Reference*
Rupture Length – Magnitude	$Ms = 1.14\log(L) + 5.27$	Ambraseys and Jackson, 1998
	$Ms = 0.90\log(L) + 5.48$	Pavlides and Caputo, 2004
Magnitude – Distance	$\log(\mathrm{Re}) = -2.98 + 0.75Ms$	Papadopoulos and Plessa, 2000
Arias Intensity	$\ln Ia = 2.8 - 1.98(M-6) + 20.72\ln(M/6) - 1.703\ln(\sqrt{R^2+8.78^2}) + [0.454 + 0.101(M-6)]Sc + [0,479 + 0.334(M-6)]Sd - 0.166Fn + 0.512Fr$	Travasarou et al. 2003
	$\log Ia = -2.663 + 1.125m - 2.332\log(\sqrt{R^2+h^2}) + 0.028S + 0.2F \pm 0.524$	Danciu and Tselentis, 2007

3. Methodology

3.1 General

In recent studies the distribution of mass wasting is recorded only after the strong seismic event occurred. However, recently many studies focus on the prediction of the potential distribution of ground movements induced by earthquakes before such a strong earthquake happens (Capolongo et al. 2002, Wang et al., 2008). For this reason many empirical relationships have been developed in order to describe this distribution (Travasarou et al, 2003, Danciu and Tselentis, 2007), based on worldwide earthquake records. According to Keefer (2002) three types of ground movements can be revealed after a strong motion earthquake: (1) falls and disrupted landslides, (2) coherent slides and (3) lateral spreads and liquefactions, depending on the susceptibility of the material, the slope surface, the distance from the earthquake epicenter and the magnitude of the earthquake. A measure of occurrence of landslides was firstly analyzed by Wilson and Keefer (1985) and modified by Keefer and Wilson (1989) based on the Arias (1970) seismic intensity relationship. According to this threshold intensity values of 0.11m/sec correspond to falls and disrupted landslides, values of 0.32m/sec to coherent slides and values of 0.54m/sec to lateral spreads and liquefactions. These threshold values can be applied to a broad range of geological environments including our study area. To avoid an overestimation of the real conditions corresponding to the area we select the method of logic tree application that is widely used in probabilistic seismic hazard analysis as a flexible tool that can capture the uncertainties included in the determination of seismogenic sources. The assessment of the hazard of earthquakes – induced landslides can be performed at different levels ranging from regional studies to site – specific evaluation of individual slopes.

For this study we used two empirical relationships widely applied in the Greek territory, which correlate the seismic magnitude with the fault rupture (Table 1). Secondly, we apply the relationship of Papadopoulos and Plessa (2000) that correlates the seismic magnitude with the distance in which site effects can be observed (Table 1). Following relationships were parts of a logic tree method applied in each major fault of the eastern domain of the Gulf of Corinth in order to calculate arias intensity as a landslide limit to strong motion attenuation. Despite the widespread use of the methodology especially in probabilistic seismic hazard analysis, guidelines on setting up logic trees and assigning weights to the branches are lacking in the current literature. In our study weights were based on the actual results that in many seismic sequences have been observed.

3.2 Data analysis

The data analysis includes the implementation of the above relationships on four major tectonic

structures dominating the eastern part of the Gulf of Corinth. These are the Kechriaie fault (KECF), the Loutraki fault (LF), the Pissia fault, (PF) the Schinos fault (SF) and the Kaparelli fault (KF) that are associated to strong past earthquakes. These faults have a general WNW-ESE trend and moderate to high dip towards the NNE except from the Loutraki (LF) and the Kaparelli fault (KF) that dip SSW (Fig. 1c). Along their length the faults show spectacular fault scarps, triangular faulted facets and alluvial fans. These faults have been associated with the appearance of long seismic ruptures and they seem responsible of triggering secondary site effects such as landslides and lateral spreads.

The methodology of logic tree diagrams constitutes a visualisation and systematization mean of the estimation process of arias intensity, when the undertaking of many successive decisions is demanded. Each decision appears its own self – determined gravity. The logic tree diagrams include a number of branches representing different conditions or relationships. Thus, they allow a small percentage of uncertainty according to the weight of each decision. The construction of the following logic tree diagrams contains three main branches. At the first branch, there is an estimation of seismic magnitude according to Ambraseys and Jackson (1998) and Pavlides and Caputo (2004) relationships, with the later obtaining greater trust due to the use of only Greek data of extensional related earthquakes. At the second branch the maximum epicentral distance in which landslide effects appear, is estimated according to Papadopoulos and Plessa relationship (2000). At the third branch the relationships of Travasarou et al., (2003) and Danciu and Tselentis (2007) are calculated. This calculation is based on data analysis derived mostly from the Mediterranean region and in currently extending areas (similar geological, climatic and vegetation conditions). Another advantage of these relationships is the introduction of the impact of lithology on the determination of arias intensity.

Applying a logic tree diagram for the 7.8km long KECF (Fig. 2a), the 10.1km long LF (Fig. 2b) the 9.4km long PF (Fig. 2c), the 9.8km long SF (Fig. 2d) and the 9.7km long KF (Fig. 2e) we observe that the relationships of Pavlides and Caputo (2004) and Travasarou et al., (2003) fit best the real ground hazards observed during past strong earthquakes. From the logic tree diagrams the calculated values of arias intensity show that rock falls especially in Mesozoic limestones and lateral spreads in soft sediments are more than expected, while the Neogene formations seem more secure. In the area around KECF, many rockfalls are observed induced by strong seismic events since the orientation and the nature of rocks are not susceptible to falling. Similarly the LF is expected to produce rock falls and slides close to the spectacular uplifted footwall. In addition during the seismic event of 1928 the descriptions suggest a dust cloud generated from the rockfalls from Geraneia mount. At the same time the proximity of the fault to the Vouliagmeni Lake may be responsible for the appearance of lateral spreads over the bankings of the lake in case of seismic loading. The PISF and the SF produce subsidence of the north coast of Perachora Penisnsula. During the seismic sequence of 1981 (Hubert et al., 1996) seismic ground motion contributed to the emergence of rock falls and small in size slides in alluvial cones. At the same seismic sequence few lateral spreads were recorded especially in coastal area due to the activation of SF and KF.

Adapting the calculated values of arias intensity near the fault trace and combining these values with the limits provided by Keefer and Wilson (1989), the surface topography and the lithology formations an estimation of probable areas displaying ground failures can be determined. For this reason we produced in GIS environment theme maps concerning the slope angle and the simplified lithology of the eastern onshore part of the Gulf of Corinth. The lithology structure of the area comprises four main lithotypes. Recent deposits and coastal deltaic deposits are loose sediments, prone to plastic deformation and usually liquefied. Neogene deposits consist of sandstones, conglomerates and marls. They have medium cohesion and are prone to slides in areas of high topography. The fly-

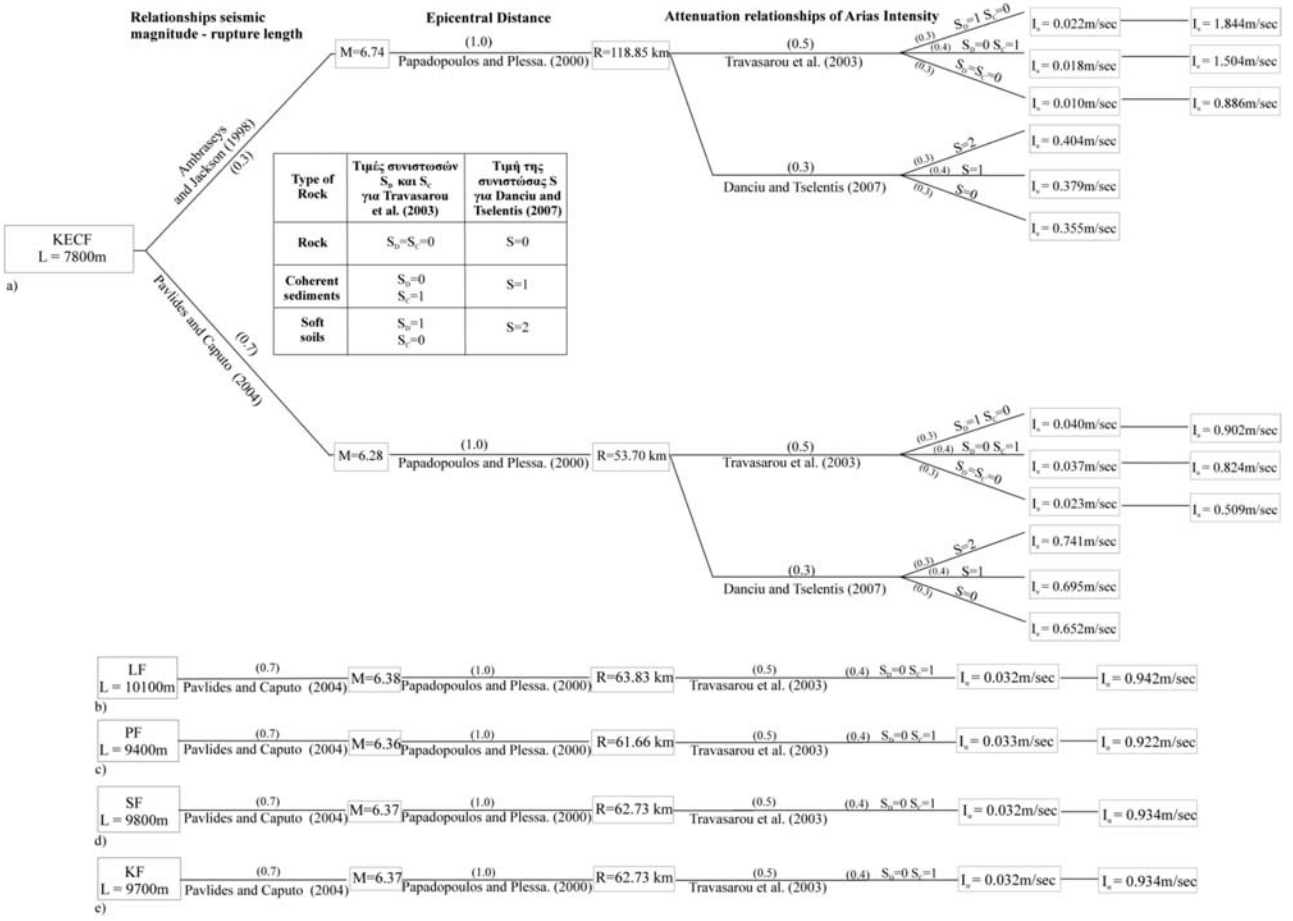

Fig. 2: Logic tree diagram showing the steps for calculating arias intensity in (a) KECF, (b) LF, (c) PF, (d) SF and (e) KF. Small numbers above each line show the implementation of weight on each relationship.

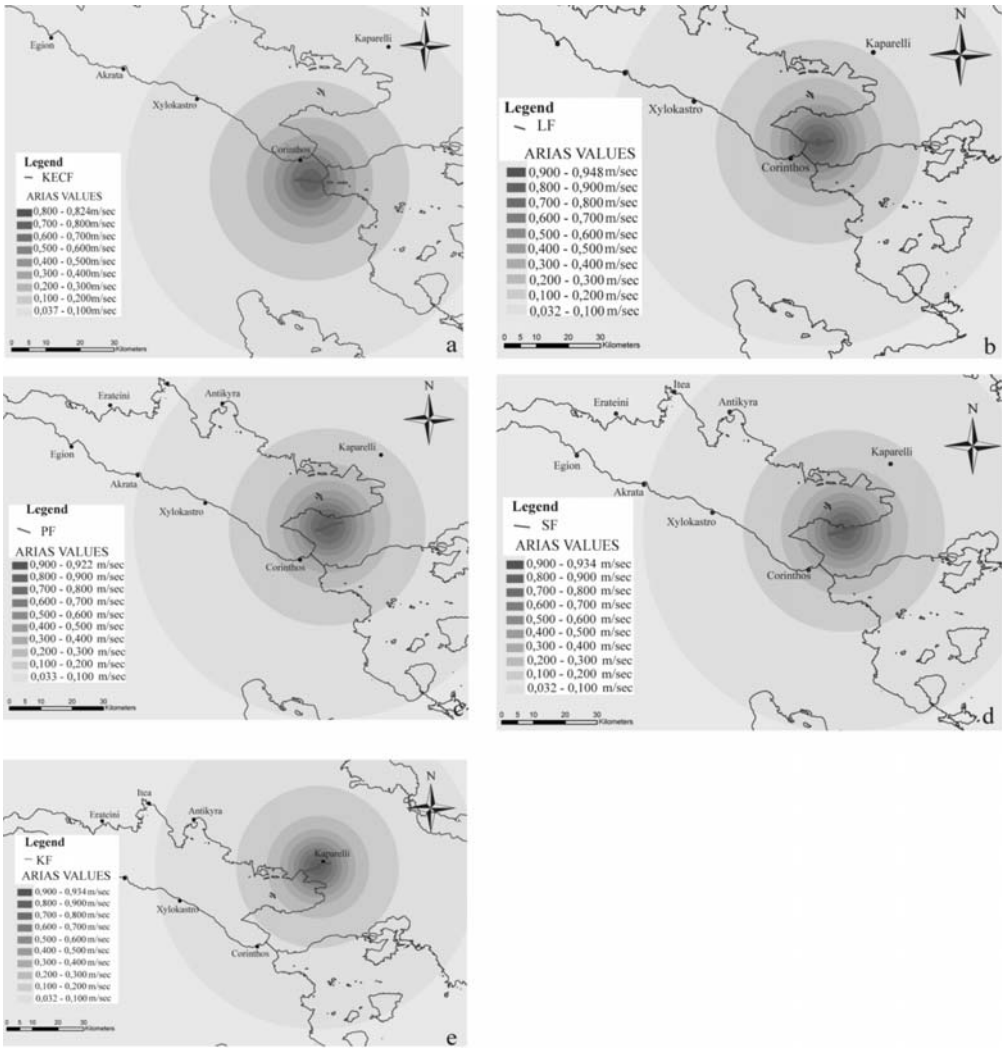

Fig. 3: a) Estimated values for arias intensity of a) KECF, b) LF, c) PF, d) SF and e) KF.

sch deposit characteristics are controlled by the thickness and the interchange between sandstone, conglomerate and clays, usually susceptible to slide. Finally, the Mesozoic formations include limestones, dolomites and ophiolites and they appear adequate geomechanical characteristics.

This kind of approach allows the detailed estimation of seismic hazard due to the motion of a seismic source. The above five faults represent well defined seismic sources with repetitive past activity. The estimation include the interaction between the values within the borders of epicentral area, the values of slope angle exceeding 15-20º and what type of landslides can be triggered by the lithology. In the maps below according to the distribution of arias intensity values (Fig. 3), slope angle (Fig. 4) and lithology (Fig. 1a) the most hazardous areas are underlined according to the expected type of landslides (Fig. 5) derived from the thresholds of arias intensity for each type of landslide.

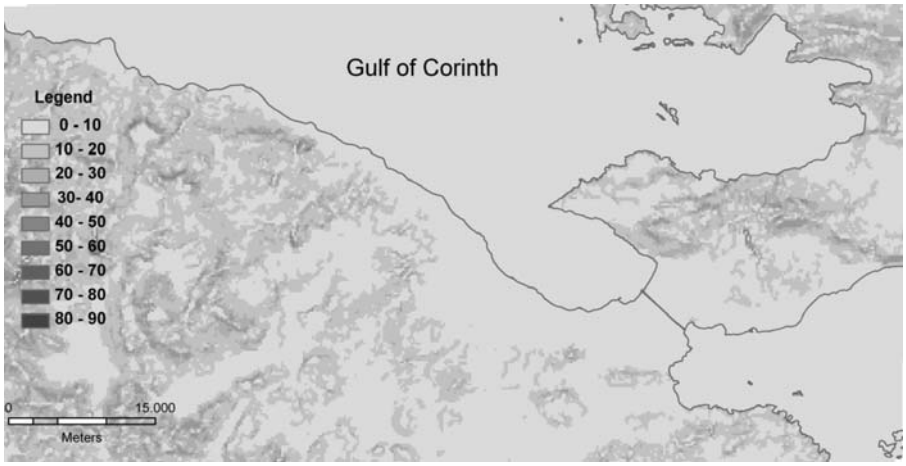

Fig. 4: Slope angle of the Gulf of Corinth.

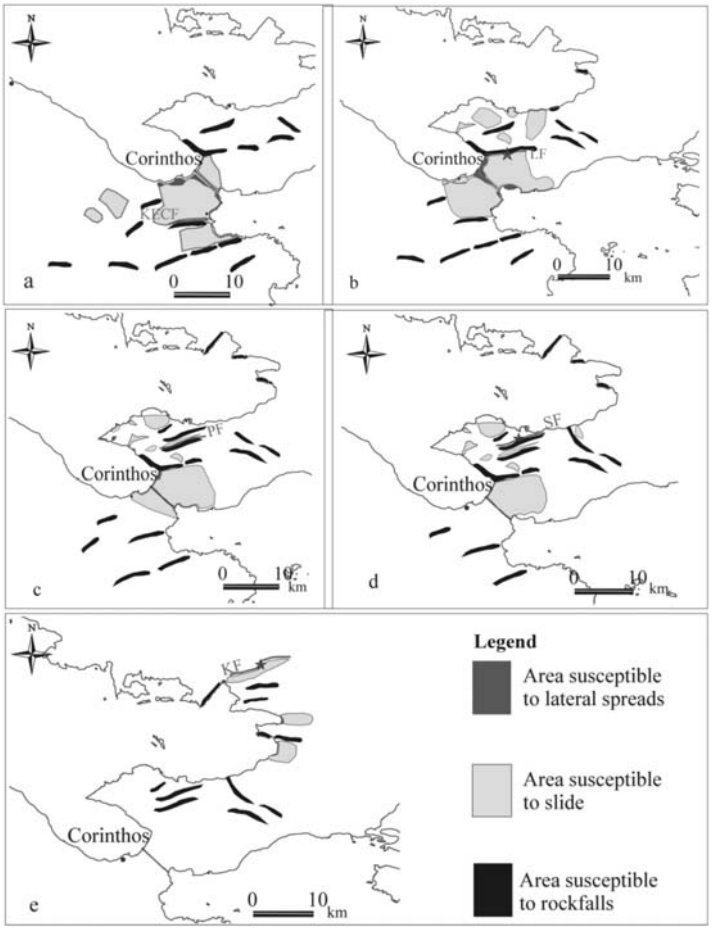

Fig. 5: Areas susceptible to landslide triggered by a) KECF, b) LF, c) PF, d) SF and e) KF seismic activation.

As it can be seen in figure 5, numerous rockfalls are expected during each fault reactivation. The rockfalls occurred usually in highly slope Mesozoic deposits and extend in a large area far away from the epicenter due to the thresholds of arias intensity distribution. Moreover, the historic records confirm that many rockfalls occurred many km away from the actual epicenter. On the contrary the lateral spreads are more restricted in narrow low relief zones near the coastal area and especially in the area of the Isthmus Canal, while the coherent slides are favoured from the slope angle exceeding 15^{o} and the marly composition of lithology.

4. Conclusions-Results

The approaching method of seismic hazard assessment through logic – trees, the application of arias intensity and the selection of arias values as limits representing different types of landslides can be an ideal tool in describing potential ground hazards in areas of significant seismic activity. The interaction between slope angle, lithology and threshold values of arias intensity can define areas showing different types of landslides induced by strong earthquakes. The vast majority of the expected landslides in the eastern part of the Gulf of Corinth is the rockfalls. Most dangerous for provoking serious damages due to landslides are the KECF, the LF and the PF and SF. In those faults the expected damages are extending in a large area exceeding the length of the fault and unfortunately they are traced near significant urban areas and sensitive infrastructures for local economy. The great residential development that takes place in the coastal zone of the eastern part of the Gulf, increases the seismic hazard and at the same time the vulnerability of the constructions. Therefore, such seismic scenarios in a sense of logic - tree diagrams are essential for the estimation of seismic hazard and valuable tools for state decision makers.

5. Acknowledgments

VZ was financially supported by the research project (PENED) that was co – financed by E.U. – European Social Fund (80%) and the Greek Ministry of Development – GSRT (20%).

6. References

Ambraseys, N.N., Jackson J., 1990. Seismicity and associated strain of central Greece between 1890 and 1988. *Geoph. J. Int.* 101, 663-708.

Ambraseys, N.N., Jackson, J.A., 1998. Faulting associated with historical and recent earthquakes in the Eastern Mediterranean region. *Geophys. J. Int.* 133, 390-406

Arias, A., 1970. A measure of Earthquake Intensity, in Seismic Design of Nuclear Power Plants. In Hansen (ed.) the MIT Press, Cambridge, MA, 438-483.

Avallone, A., Briole, P., Agatza-Balodimou, A.M., Billiris, H., Charade, O., Mitsakaki, C., Nercessian, A., Papazissi, K., Paradissis P., Veis, G., 2004. Analysis of eleven years of deformation measured by GPS in the Corinth Rift Laboratory area. *C. R. Geoscience* 336, 301-311.

Bentham, P., Collier, R.E.L., Gawthorpe, R.L., Leeder, M.R., Prosser, S., Stark, C., 1991. Tectono-sedimentary development of an extensional basin: the Neogene Megara Basin, Greece. *J. Geol. Soc. London* 148, 923–934.

Briole, P., Rigo, A., Lyon-Caen, H., Ruegg, J., Papazissi, K., Mistakaki, C., Balodimou, A., Veis, G., Hatzfeld, D., Deschamps, A., 2000. Active deformation of the gulf of Korinthos, Greece: results from repeated GPS surveys between 1990 and 1995. *JGR* 105, 25605-25625.

Capolongo, D., Refice, A., Mankelow, J., 2002. Evaluating earthquake-triggered landslide hazard at the basin scale through GIS in the Upper Sele river Valley. *Surveys in Geophysics* 23, 595-625.

Collier, R.E.L, Dart, C.J., 1991. Neogene to Quaternary rifting, sedimentation and uplift in the Corinth basin, Greece. *J. Geol. Soc. London* 148**,** 1049–1065.

Danciu, L., Tselentis, G.A., 2007. Engineering ground-motion parameters attenuation relationships for Greece**.** *Bull. Seismol. Soc. Am.* 97, 162-183.

Doutsos, T., Kokkalas S. 2001. Stress and deformation in the Aegean region. *Journal of Structural Geology* 23, 455-472.

Hubert, A., King, G., Armijo, R., Meyer, B., Papanastasiou, D., 1996. Fault re-activation stress interaction and rupture propagation of the 1981 Corinth earthquake sequence. *Earth Planet. Sci. Lett.* 142, 573-585

Keefer, D., 2002. Investigating landslides caused by earthquakes – A historical review. *Surveys in Geophysics*, 23, 473-510.

Keefer, D.K., Wilson, R.C., 1989. Predicting earthquake – induced landslides, with emphasis on arid and semi – arid environments. In: Sadler, Morton (eds), Landslides in a semi Arid Environment 2, Inland *Geol. Soc.*, 118-149.

King, G.C.P., Ouyang, Z.X., Papadimitriou, P., Deschamps, A., Gagnepain, L., Houseman, G., Jackson, J.A., Soufleris, C., Virieux, J., 1985. The evolution of the Gulf of Corinth (Greece): an aftershock study of the 1981 earthquakes. *Geophys. J.R. Astron. Soc.* 80, 677-693.

Koukis, G., Rozos, D., 1985. Engineering geological characteristics of the 1981 earthquakes in the Eastern Corinthian Gulf, Greece. *Bull. Int. Assoc. Eng. Geol.* 32, 91-95.

Koukis, G., Sabatakakis, N., Ferentinou, M., Lainas, S., Alexiadou, X., Panagopoulos, A., 2009. Landslide phenomena related to major fault tectonics: rift zone of Corinth Gulf, Greece. *Bull. Eng. Geol. and the Env.*, 215-229

Koukouvelas, I.K., Doutsos, T., 1996. Implications of structural segmentation during earthquakes: The 1995 Egion earthquake, Gulf of Corinth, Greece. *J. Struct. Geol.* 18, 1381-1388.

Koukouvelas, I.K., Mpresiakas, A., Sokos, E., Doutsos, T., 1996. The tectonic setting and earthquake ground hazards of the 1993 Pyrgos earthquake, Peloponnese, Greece. *J. Geol. Soc. London* 152, 39-49.

Koustas, G., 1858. Earthquake of Corinthos. *Pandora* 8, 225-229 (in Greek).

Papadopoulos, G., Plessa, A., 2000. Magnitude – Distance relations for earthquake – induced landslides in Greece. *Eng. Geol.* 58, 251-270.

Papadopoulos, G., Vassilopoulou A., Plessa, A., 2000. A new catalogue of historical earthquakes in the Corinth rift, Central Greece: 480 BC – AD 1910. In: Historical Earthquakes and Tsunamis in the Corinth rift, Central Greece. National Observatory of Athens, Institute of Geodynamics (G. Papadopoulos ed.),Publication No 12, 9-119. National Observatory of Athens, Athens.

Papazachos, B.C., Papazachou, C., 2003. The earthquakes of Greece. Ziti, Thessaloniki.

Pavlides, S., Caputo, R., 2004. Magnitude versus faults' surface parameters: Quantitative relationships from the Aegean Region. *Tectonophysics* 380, 159-188.

Travasarou, T., Bray, J.B., Abrahamson, A., 2003. Empirical attenuation relationship for Arias Intensity. *Earthquake Eng. and Struct. Dynamics* 32, 1133-1155.

Wang, H., Wang, G., Wang, F., Sassa, K., Chen Y. 2008. Probabilistic modelling of seismically triggered landslides using Monte Carlo simulations. *Landslides*, 5, 387-395.

Wilson, R.C., Keefer, D.K., 1985. Predicting Areal Limits of earthquake – induced Landsliding. In: Ziony (ed.) Earthquake Hazards in the Los Angeles region – An earth science perspective *U.S.G.S.* Professional Paper 1360, 317-345.

Zygouri, V., Verroios, S., Kokkalas, S., Xypolias, P., Koukouvelas, I.K., 2008. Scaling properties within the Gulf of Corinth, Greece; comparison between offshore and onshore active faults. *Tectonophysics* 453, 193-210.

ΕΥΡΕΤΗΡΙΟ ΟΝΟΜΑΤΩΝ
AUTHOR INDEX